Advanced Topics of Theoretical Physics II

Advanced Solid-State Theory

Peter E. Blöchl

Caution! This is an unfinished draft version
Mistakes are unavoidable!

Institute of Theoretical Physics; Clausthal University of Technology;
D-38678 Clausthal Zellerfeld; Germany;
http://www.pt.tu-clausthal.de/atp/

don't panic!

[1]

[1] To the title page: What is the meaning of ΦSX? Firstly, it sounds like "Physics". Secondly, the symbols stand for the three main pillars of theoretical physics: "X" is the symbol for the coordinate of a particle and represents Classical Physics. "Φ" is the symbol for the wave function and represents Quantum Physics "S" is the symbol for the entropy and represents Statistical Physics.

Foreword and Outlook

A word of caution, before I start: This book is work in progress. You can use this book as a basis for following through the material presented in the course. But, you should never blindly copy formulas and apply them. The chances that there are still errors is still too large. However, the goal of this lecture is that the reader is able to convince himself, whether it is correct what he learns. For this purpose, I provide explicit derivations of all the material presented in this lecture and I make an effort to provide guidance to make careful reading as easy as possible.

My aim is to include all proofs in a comprehensive and hopefully water-tight manner. I am also avoiding special systems of units. I consider this important in view of a large variety of notations, differing definitions etc. While the proofs have the advantage to train the student to perform the typical operations, it clutters the course with material far from applications. Therefore, I have placed many of the more detailed derivations into appendices. It is strongly recommended to follow through the derivations. On the graduate level, the student should be able to follow the proofs without problem.

This book provides an introduction into the quantum mechanics of the interacting electron gas. It aims at students at the graduate level, that already have a good understanding on one-particle quantum mechanics.

The goal of the lecture is that the student

- understands language of many-particle quantum mechanics using many-particle wave functions, field operators and Green's functions.
- understands the approach to many-particle physics both using Green's functions as well as from the point of view of density-functional theory.
- is familiar with many-electron Green's functions, their meaning and properties
- understands the main theorems underlying the perturbation expansion of Green's functions, including Feynman diagrams.
- understands both time-dependent as well as finite-temperature formulation of Green's functions

In the online version of my lecture notes, there are many hyperreferences that allow one to jump to the relevant information in the book. The hyperlinks do not stand out because they have a different color. Thus, it is important to know where the hyperlinks are. The following items are hyperlinks:

- items in the list of contents will take you to the corresponding section.
- references to equation numbers, figures, tables, sections, appendices, etc. will take you to the indicated object.
- citations will take you to the corresponding position in the list of references

It is recommended that the student is already familiar with the one-particle description of the electronic structure of solids, because the present text implicitly builds on these concepts. These

foundations are provided in the preceding volume of the ΦSX series *"Introduction to solid state theory"*[1].

My lectures do not follow a particular text, but they reflect my personal approach to the problem. Nevertheless it is useful and it will often be necessary to consult other text books. For the section on Green's function, I strongly recommend the book by Stefanucci and van Leeuwen[2]. It makes use of a unified view of zero-temperature, finite-temperature and non-equilibrium Green's functions, which is similar to the present text. A solid, rather detailed, reference employing the more traditional view is the text by Fetter and Walecka [3]. The book of Mattuck [4] presents a very intuitive approach to Feynman diagrams. The book of P. Fulde[5] provides a wealth of physical insight and, in addition, and it connects to the quantum chemical point of view.

Another excellent book on many-particle physics, which, however, concentrates on path integrals, a quite different approach from the one used in my text, is the book by Negele and Orland [6]. A recommended reading are the Lecture notes[7] by Wolf-Dieter Schöne.

With the present lecture notes, I hope to provide a solid ground on the subject of many-electron Green' functions. In order to make use of it it will be necessary to specialize and extend this background. For this purpose, I recommend the lecture notes of the Julich autumn schools on correlated electrons. The lecture notes of these schools are freely available at

`https://www.cond-mat.de/events/correl.html`

0.1 Some Thoughts

Many-particle quantum mechanics comes in several flavors, the most prominent being the following.

- So-called wave function approaches, which directly deal with many-particle wave functions. Wave function approaches are commonly used by quantum chemists.
- Many-particle Green's-function approaches. Green's-function approaches are best known from Feynman diagrams, which are one of the prominent tools in this methodology. Many-particle Green's function are close to spectroscopic measurements of excitations.
- effective independent-particle descriptions such as density-functional theory. Here the physical description is very similar to that of non-interacting electrons, while the interaction are taken into account approximately as in the Hartree-Fock approximation, or exactly as in the density-functional theory. Density-functional theory is the basis of first-principle calculations of solids.

While the focus of this lecture is on Green's functions, the intent of this lecture is to also show the link to other descriptions.

Contents

Part I

Lecture notes

Chapter 1

Non-interacting electrons

In this section, I will remind of some concepts from quantum mechanics and I will introduce my notation. A more detailed coverage is found in Blöchl, *ΦSX: Introduction to Solid State Theory*.[1] While the material in this chapter is rather elementary, I use it to make the reader familiar with the notation and the mathematical language, that will be used in the later chapters.

1.1 One-particle quantum mechanics

1.1.1 One-particle Schrödinger equation

The wave function of a single particle is described by a time-dependent Schrödinger equation.

$$i\hbar\partial_t|\psi(t)\rangle = \hat{h}(t)|\psi(t)\rangle \tag{1.1}$$

where $|\psi(t)\rangle$ is the quantum state and $\hat{h}(t)$ is the time-dependent Hamiltonian.

If the Hamiltonian $\hat{h}$ is time-independent, the problem is invariant under time translations. Time-translation symmetry, in turn, results in energy conservation, which implies that the general solution can be expressed in terms of energy eigenstates $|\varphi_n\rangle$ with arbitrary coefficients c_n.

$$|\psi(t)\rangle = \sum_n |\varphi_n\rangle \mathrm{e}^{-\frac{i}{\hbar}\epsilon_n t} c_n \tag{1.2}$$

The coefficients are determined by the initial conditions as $c_n = \langle\varphi_n|\psi(t=0)\rangle$.

The energy eigenstates $|\varphi_n\rangle$ obey the time-independent Schrödinger equation

$$\hat{h}|\varphi_n\rangle = |\varphi_n\rangle\epsilon_n \tag{1.3}$$

and the orthonormality condition[1]

$$\langle\varphi_m|\varphi_n\rangle = \delta_{m,n} \tag{1.4}$$

To ensure normalization of the wave function $|\psi(t)\rangle$ in Eq. 1.2, the coefficients need to satisfy $\sum_n c_n^* c_n = 1$.

1.1.2 Notation

In my lecture notes, I make an effort to be explicit in notation and units.

[1] The orthogonality of non-degenerate states is automatically satisfied, but the orthogonality between states from the same degenerate multiplet must be imposed.

- vectors are indicated by an upper arrow such as $\vec{r}$.
- matrices are indicated by a bold-face symbol $\boldsymbol{A}$. On the blackboard, I use a double underscore $\underline{\underline{A}}$ instead.
- A quantum state is written in bra-ket notation as $|\psi\rangle$.
- a quantum operator, such as $\hat{A}$, acting on a ket is indicated by a hat. There is a distinction between a quantum operator and a differential operator. Let me demonstrate the difference on the example of a momentum operator.
  - Do not write $\frac{\hbar}{i}\vec{\nabla}|\psi\rangle$, nor $\hat{p}\Psi(\vec{r})$,
  - but

$$\hat{p}|\psi\rangle = \int d^3r|\vec{r}\rangle\frac{\hbar}{i}\vec{\nabla}\langle\vec{r}|\psi\rangle \qquad \text{or} \tag{1.5}$$

$$\frac{\hbar}{i}\vec{\nabla}\langle\vec{r}|\psi\rangle = \frac{\hbar}{i}\vec{\nabla}\psi(\vec{r}) = \langle\vec{r}|\hat{p}|\psi\rangle \tag{1.6}$$

- For the matrix elements of a function of a matrix, taking the inverse as an example for a function, I use

$$A^{-1}_{\alpha,\beta} \stackrel{\text{def}}{=} (A^{-1})_{\alpha,\beta} \neq (A_{\alpha,\beta})^{-1} \tag{1.7}$$

- I do not distinguish between column and row vectors. Rather, I distinguish between two different products, the scalar product and the dyadic product.
  - The **dot product** $\vec{a}\cdot\vec{b} = \vec{a}\vec{b} = \sum_j a_j b_j$ is also called **scalar product** or **inner product**. The dot is often omitted. The dot product of two vectors is a scalar. It corresponds to a product of a row vector on the left with a column vector on the right.
  - **dyadic product** $\vec{a}\otimes\vec{b}$, defined by $(\vec{a}\otimes\vec{b})_{m,n} = a_m b_n$ is also called **outer product**.

1.1.3 Spin orbitals

The electron is properly described by the **Dirac equation**, which is a relativistic equation for spin-$\frac{1}{2}$ particles. The wave function of the Dirac equation has four components, which make up a four-component Dirac spinor. Each component is a complex wave function in real space. The four components describe electrons with two spin directions and positrons with two spin directions. In the non-relativistic limit, the Dirac equation separates into two **Pauli equations**, one for the electron components and one for the positron components. The Pauli equation describes spin-$\frac{1}{2}$ particles with two spin-components.

I will describe electrons here on the level of the Pauli equation: An electron is characterized by a position $\vec{r}$ in space and a spin index σ. The spin index can have the values [2] $\sigma \in \{\uparrow,\downarrow\}$. Often we will refer to the numerical values of σ, namely $\uparrow \mathrel{\hat{=}} +1$ and $\downarrow \mathrel{\hat{=}} -1$.

The wave function of an electron consists of two distinct functions in space and time, namely $\psi(\vec{r},\uparrow,t)$ and $\psi(\vec{r},\downarrow,t)$. The wave function is thus a so-called **spin orbital** or a **two-component spinor**.

[2] The notation using arrows is mathematical slang. It is very intuitive but not according the rules. What it means is that a spin-$\frac{1}{2}$ has a two-dimensional Hilbert space. As basisset for this Hilbert space, I can use the two eigenstates of $\hat{S}_z$

$$\hat{S}_z|\psi_1\rangle = |\psi_1\rangle\left(+\frac{\hbar}{2}\right) \quad \text{and} \quad \hat{S}_z|\psi_2\rangle = |\psi_2\rangle\left(-\frac{\hbar}{2}\right) \tag{1.8}$$

A more pictorial way of distinguishing the two states uses arrows, i.e. $|\uparrow\rangle \stackrel{\text{def}}{=} |\psi_1\rangle$, respectively $|\downarrow\rangle \stackrel{\text{def}}{=} |\psi_2\rangle$. The sum over these two states is written as $\sum_{\sigma\in\{\uparrow,\downarrow\}}$, rather than $\sum_{\sigma=1}^{2}$ or $\sum_{\sigma\in\{1,2\}}$.

REAL-SPACE-AND-SPIN BASISSET

The states $|\vec{r},\sigma\rangle$ form a complete basis for a single electron. The states in this basis are characterized by the eigenvalue equations

$$\begin{aligned}\hat{\vec{r}}|\vec{r},\sigma\rangle &= |\vec{r},\sigma\rangle\vec{r}\\ \hat{S}_z|\vec{r},\sigma\rangle &= |\vec{r},\sigma\rangle\frac{\hbar}{2}\sigma = |\vec{r},\sigma\rangle\begin{cases}+\frac{\hbar}{2} & \text{for } \sigma=+1=\uparrow\\ -\frac{\hbar}{2} & \text{for } \sigma=-1=\downarrow\end{cases}.\end{aligned} \tag{1.9}$$

The states obey the orthonormality condition

$$\langle\vec{r},\sigma|\vec{r'},\sigma'\rangle = \delta(\vec{r}-\vec{r'})\delta_{\sigma,\sigma'} \tag{1.10}$$

and the completeness relation in the one-electron Hilbert space

$$\hat{1} = \sum_{\sigma\in\{\uparrow,\downarrow\}}\int d^3r\ |\vec{r},\sigma\rangle\langle\vec{r},\sigma|\ . \tag{1.11}$$

The one-electron wave function is obtained as

$$\psi(\vec{r},\sigma,t) = \langle\vec{r},\sigma|\psi(t)\rangle \tag{1.12}$$

so that

$$|\psi(t)\rangle = \sum_{\sigma\in\{\uparrow,\downarrow\}}\int d^3r\ |\vec{r},\sigma\rangle\langle\vec{r},\sigma|\psi(t)\rangle = \sum_{\sigma\in\{\uparrow,\downarrow\}}\int d^3r\ |\vec{r},\sigma\rangle\psi(\vec{r},\sigma,t) \tag{1.13}$$

Combined position and spin argument

In order to simplify the notation, we combine the continuous position $\vec{r}$ and discrete spin coordinate σ into a single "four-dimensional" quantity

$$\vec{x} \stackrel{\text{def}}{=} (\vec{r},\sigma) \qquad \text{with } \vec{r}\in\mathbb{R}^3 \text{ and } \sigma\in\{\uparrow,\downarrow\} \tag{1.14}$$

In this notation, the integral is defined as

$$\int d^4x \stackrel{\text{def}}{=} \sum_{\sigma\in\{\uparrow,\downarrow\}}\int d^3r \tag{1.15}$$

and the δ function is

$$\delta(\vec{x}-\vec{x'}) \stackrel{\text{def}}{=} \delta(\vec{r}-\vec{r'})\delta_{\sigma,\sigma'} \tag{1.16}$$

Often, I need to refer to a specific component of $\vec{x}$ such as either the position $\vec{r}$ or the spin index σ. Then, I use the components with the same indices, that is $\vec{x}=(\vec{r},\sigma)$, $\vec{x'}=(\vec{r'},\sigma')$, $\vec{x}_1=(\vec{r}_1,\sigma_1)$, and so on. Let me give a small warning beforehand: I will use the symbol σ also as occupation-number eigenvalues $\sigma\in\{0,1\}$. This notation may be confusing.

1.1.4 Frequently used observables

Let me remind you of the most relevant observables. I will provide here, both, the operator and the corresponding expectation value.

- probability density $n(\vec{r},t)$ for the electron to be at position $\vec{r}$

$$\hat{n}(\vec{r}) \stackrel{\text{def}}{=} \sum_{\sigma\in\{\uparrow,\downarrow\}} |\vec{r},\sigma\rangle\langle\vec{r},\sigma| \tag{1.17}$$

$$n(\vec{r},t) \stackrel{\text{def}}{=} \langle\psi(t)|\hat{n}(\vec{r})|\psi(t)\rangle = \sum_{\sigma\in\{\uparrow,\downarrow\}} |\psi(\vec{r},\sigma,t)|^2 \tag{1.18}$$

The probability density at $\vec{r}$ is sum of the absolute-squared wave-function amplitudes for both spin directions. In one-particle quantum mechanics, the operator $\hat{n}(\vec{r})$ is the real-space projection operator.

- (average) position $\hat{r}$

$$\hat{r} \stackrel{\text{def}}{=} \sum_{\sigma\in\{\uparrow,\downarrow\}} \int d^3r\ |\vec{r},\sigma\rangle\vec{r}\langle\vec{r},\sigma|$$

$$\vec{r}(t) \stackrel{\text{def}}{=} \langle\psi(t)|\hat{\vec{r}}|\psi(t)\rangle = \int d^3r\ \vec{r} \sum_{\sigma\in\{\uparrow,\downarrow\}} |\psi(\vec{r},\sigma,t)|^2 \tag{1.19}$$

The average position is used, for example, to determine the electric dipole $\vec{d} = q\langle\psi|\hat{\vec{r}} - \vec{r}_0\hat{1}|\psi\rangle$ of a molecule, where $q = -e$ is the electron charge. In an optical excitation, the dipole couples to the electric field of the light wave.

- probability P_σ for having spin $\frac{\hbar}{2}\sigma$ along the z-axis. $\hat{P}_\sigma$ is the spin-projection operator.

$$\hat{P}_\sigma = \int d^3r\ |\vec{r},\sigma\rangle\langle\vec{r},\sigma|$$

$$P_\sigma(t) \stackrel{\text{def}}{=} \langle\psi(t)|\hat{P}_\sigma|\psi(t)\rangle = \int d^3r\ |\psi(\vec{r},\sigma,t)|^2\ , \tag{1.20}$$

For example, $P_\uparrow = \int d^3r\ |\psi(\vec{r},\uparrow,t)|^2$.

- Spin along an axis $\vec{e}$ with $\vec{e}^2 = 1$

$$\vec{e}\hat{\vec{S}} \stackrel{\text{def}}{=} \sum_{\sigma,\sigma'\in\{\uparrow,\downarrow\}} \int d^3r\ |\vec{r},\sigma\rangle \sum_{j=1}^{3} e_j \frac{\hbar}{2}\sigma_{j,\sigma,\sigma'}\langle\vec{r},\sigma'|$$

$$\vec{e}\vec{S}(t) = \langle\psi(t)|\vec{e}\hat{\vec{S}}|\psi(t)\rangle = \int d^3r \sum_{j=1}^{3} e_j \frac{\hbar}{2} \sum_{\sigma,\sigma'\in\{\uparrow,\downarrow\}} \psi^*(\vec{r},\sigma,t)\sigma_{j,\sigma,\sigma'}\psi(\vec{r},\sigma',t) \tag{1.21}$$

where the (2×2) matrices $\boldsymbol{\sigma}_j$ are the **Pauli matrices**.

PAULI MATRICES

The Pauli matrices are

$$\boldsymbol{\sigma}_x \hat{=} \begin{pmatrix} 0 & 1 \\ 1 & 0 \end{pmatrix} \quad \text{and} \quad \boldsymbol{\sigma}_y \hat{=} \begin{pmatrix} 0 & -i \\ i & 0 \end{pmatrix} \quad \text{and} \quad \boldsymbol{\sigma}_z \hat{=} \begin{pmatrix} 1 & 0 \\ 0 & -1 \end{pmatrix} \tag{1.22}$$

so that

$$\vec{e}\vec{\boldsymbol{\sigma}} \hat{=} \begin{pmatrix} e_z & e_x - ie_y \\ e_x + ie_y & -e_z \end{pmatrix} \tag{1.23}$$

The most general hermitian 2×2 matrix is $\sum_{j\in\{0,x,y,z\}} a_j\boldsymbol{\sigma}_j$ with a 4-dimensional, real-valued vector $\vec{a}$ with indices $j \in \{0,x,y,z\}$ and the 2-dimensional unit matrix $\boldsymbol{\sigma}_0 = \mathbf{1}$.

I recommend to memorize the Pauli matrices.

- spin density: The spin density $\vec{n}_s(\vec{r},t)$ is defined as the electron density[3] of unpaired electrons.[8].

$$\hat{n}_{s,j}(\vec{r}) = \sum_{\sigma,\sigma'\in\{\uparrow,\downarrow\}} |\vec{r},\sigma\rangle\sigma_{j,\sigma,\sigma'}\langle\vec{r},\sigma'| \qquad \text{for } x\in\{x,y,z\} \tag{1.24}$$

so that

$$n_{s,j}(\vec{r},t) = \sum_{\sigma,\sigma'\in\{\uparrow,\downarrow\}} \psi^*(\vec{r},\sigma,t)\sigma_{j,\sigma,\sigma'}\psi(\vec{r},\sigma',t) \tag{1.25}$$

To avoid ambiguities, let me write down an example, namely the x-component of the spin density:

$$\begin{aligned}\hat{n}_{s,x} &= \begin{pmatrix}|\vec{r},\uparrow\rangle\\|\vec{r},\downarrow\rangle\end{pmatrix}\begin{pmatrix}0&1\\1&0\end{pmatrix}\begin{pmatrix}\langle\vec{r},\uparrow|\\\langle\vec{r},\downarrow|\end{pmatrix} = |\vec{r},\uparrow\rangle\langle\vec{r},\downarrow| + |\vec{r},\downarrow\rangle\langle\vec{r},\uparrow|\\ n_{s,x}(\vec{r},t) &= \psi^*(\vec{r},\uparrow)\psi(\vec{r},\downarrow) + \psi^*(\vec{r},\downarrow)\psi(\vec{r},\uparrow)\end{aligned} \tag{1.26}$$

The spin contribution of the angular-momentum density is obtained from the spin density by multiplication with the spin $\hbar/2$ of the electron

$$\vec{s}(\vec{r},t) \stackrel{\text{def}}{=} \frac{\hbar}{2}\vec{n}_s(\vec{r},t) \tag{1.27}$$

The **magnetization** $\vec{m}(\vec{r},t)$ is obtained from the spin density $\vec{n}_s(\vec{r},t)$ by multiplication with the **electron magnetic moment** $\mu_e = \frac{1}{2}g_e\mu_B$, where $g_e = 2.002319\ldots$ is the electron Landé **g-factor** of the free electron and $\mu_B \stackrel{\text{def}}{=} e\hbar/(2m_e)$ is the **Bohr magneton**.[9]

$$\vec{m}(\vec{r},t) \stackrel{\text{def}}{=} -\mu_e\vec{n}_s(\vec{r},t) \tag{1.28}$$

Because of the negative charge of the electron, its magnetic moment is oriented opposite to the spin direction, which explains the minus sign in the equation Eq. 1.28 above[4].

- momentum: The momentum operator, expressed in a real-space-and-spin basisset, has the following form

[3] According to the definition in the Gold book[8], the spin density would be $|\vec{n}_s(\vec{r},t)|$ rather then the vectorial quantity. I consider this as an oversight, because usually only collinear spin distributions with an axis along the z-direction are considered.

[4] Some caution is needed regarding which quantities carry the minus sign and which do not. This is not always handled on the same way.

MOMENTUM OPERATOR

$$\hat{\vec{p}} = \sum_{\sigma\in\{\uparrow,\downarrow\}} \int d^3r\ |\vec{r},\sigma\rangle \frac{\hbar}{i}\vec{\nabla}\langle\vec{r},\sigma| \tag{1.29}$$

which has matrix elements [a]

$$\langle\vec{r},\sigma|\hat{\vec{p}}|\vec{r'},\sigma'\rangle = \frac{\hbar}{i}\vec{\nabla}_r\delta(\vec{r}-\vec{r'})\delta_{\sigma,\sigma'} = \delta(\vec{r}-\vec{r'})\delta_{\sigma,\sigma'}\frac{\hbar}{i}\vec{\nabla}_{r'} \tag{1.32}$$

where the gradient $\vec{\nabla}$ acts on the spatial argument $\vec{r}$.

[a] Like the δ-function, also $\vec{\nabla}\delta(\vec{r})$ is not a regular function, but a **distribution** (see for example [10]). It is defined by the integral identity

$$\int d^3r\ f(\vec{r})\vec{\nabla}\delta(\vec{r}) = -\vec{\nabla}|_{\vec{r}=\vec{0}}\, f \tag{1.30}$$

where $f(\vec{r})$ can be any differentiable function. One can also construct $\vec{\nabla}\delta(\vec{r})$ as the limit of a sequence of functions, or via the differential quotient from the δ-function

$$\vec{e}\,\vec{\nabla}\delta(\vec{r}) = \lim_{\Delta\to 0}\frac{\delta(\vec{r}+\vec{e}\Delta)-\delta(\vec{r}-\vec{e}\Delta)}{2\Delta} \tag{1.31}$$

where $\vec{e}$ is an arbitrary unit vector. This vector specifies the direction along which the derivative is taken.

The momentum expectation value at time t is

$$\begin{aligned}\vec{p}(t) = \langle\psi(t)|\hat{\vec{p}}|\psi(t)\rangle &\overset{\text{Eq. 1.29}}{=} \sum_{\sigma\in\{\uparrow,\downarrow\}}\int d^3r\ \langle\psi(t)|\vec{r},\sigma\rangle\frac{\hbar}{i}\vec{\nabla}\langle\vec{r},\sigma|\psi(t)\rangle \\ &= \int d^3r \sum_{\sigma\in\{\uparrow,\downarrow\}} \psi^*(\vec{r},\sigma,t)\frac{\hbar}{i}\vec{\nabla}\psi(\vec{r},\sigma,t)\end{aligned} \tag{1.33}$$

- current density: The particle-current density is calculated from the velocity $\vec{v} = \dot{\vec{r}} = \vec{\nabla}_p H(\vec{p},\vec{r})$. For the Hamilton operator $H(\vec{p},\vec{r},t) = \frac{1}{2m}(\vec{p}-q\vec{A}(\vec{r},t))^2 + q\Phi(\vec{r},t)$ of a charged particle with charge q and mass m in an electromagnetic field with an electric potential $\Phi(\vec{r},t)$ and a vector potential $\vec{A}(\vec{r},t)$, the current density is

$$\hat{\vec{j}}(\vec{r}) = \frac{1}{2m_e}\sum_{\sigma\in\{\uparrow,\downarrow\}}\left[\left(\hat{p}-q\vec{A}(\hat{\vec{r}})\right)|\vec{r},\sigma\rangle\langle\vec{r},\sigma| + |\vec{r},\sigma\rangle\langle\vec{r},\sigma|\left(\hat{p}-q\vec{A}(\hat{\vec{r}})\right)\right]. \tag{1.34}$$

Two terms are required to ensure that the observable is represented by a hermitian operator. The charge current is obtained from the particle current by multiplication with the charge q.

1.1.5 Discrete and continuous spectra of quantum states

The spectrum of an operator is the set of its eigenvalues. Quantum states may have discrete and continuous spectra, and, even worse, they may have spectra consisting of discrete eigenvalues and regions, where they are continuous. An example is the hydrogen atom, which has a discrete energy spectrum at negative energies, but a continuous spectrum of scattering states at positive energies. A common mistake is to forget the continuous part of the spectrum.

Rather than dealing with these difficulties, I am avoiding them by introducing what I call a **finite universe**. A continuous spectrum can result, when the norm is defined on an infinite region. When this region is replaced by a finite region, like a very large box, the spectrum becomes discrete. I call this box my finite universe.

As a consequence of the finite extent, all states have the regular normalization and all spectra are discrete. The advantage of this choice is that I can treat localized and extended states on the very same footing. While the spectrum of a finite system is discrete, the eigenvalues may be extremely close. Furthermore, states that extend over the entire box, may have a very small wave function amplitude.

The limit to a truly infinite system, is postponed to the final result, rather than done during the derivations. Given that an infinite system is usually an idealization, I consider this approach appealing.

For infinite periodic systems, which are described with periodic boundary conditions and Bloch's theorem (see below in section 1.1.8), we proceed slightly differently: Rather than choosing a finite volume, we choose a large supercell and require the wave function (not only the potential) to be strictly periodic with the supercell lattice vectors. This requirement leads to a discrete energy spectrum just as in the case described above. The wave functions are normalized within this supercell. Once the final equations have been obtained, we increase the size of the supercell to infinity and normalize within the regular unit cell of the crystal.

1.1.6 Momentum eigenstates

The eigenstates of the momentum are plane waves, which extend over an infinite volume. The momentum eigenvalues are continuous.

I define the basis states as eigenvalues of momentum operator Eq. 1.29 and spin (with $\uparrow \hat{=} 1$ and $\downarrow \hat{=} -1$)

$$\begin{aligned} \hat{\vec{p}}|\vec{p},\sigma\rangle &= |\vec{p},\sigma\rangle\vec{p} \\ \hat{S}_z|\vec{p},\sigma\rangle &= |\vec{p},\sigma\rangle\frac{\hbar}{2}\sigma \end{aligned} \tag{1.35}$$

The eigenvalue equation of the momentum operator Eq. 1.29 and the normalization $\langle\vec{p},\sigma|\vec{p},\sigma\rangle = 1$ define the basis states of the momentum representation as

$$\underbrace{\langle\vec{x}|\vec{p},\sigma'\rangle}_{\langle\vec{r},\sigma|\vec{p},\sigma'\rangle} = \frac{1}{\sqrt{\Omega}} \mathrm{e}^{\frac{i}{\hbar}\vec{p}\vec{r}} \delta_{\sigma,\sigma'} \tag{1.36}$$

where $\Omega = L^3$ is the size of the integration volume, which also defines the periodic boundary condition for the wave function. For periodic boundary conditions in a cubic box of side length L, the set of momentum eigenvalues $\vec{p}_{i,j,k} = (i,j,k)\Delta p$ is discrete with integer i,j,k and the spacing of the momentum eigenvalues is $\Delta p = \frac{2\pi\hbar}{L}$ in each of the three spatial directions.

Note that I define momentum eigenstates which are normalized within a finite, even though very large, box. I name the box jokingly the "finite universe". The consequence of this choice is that the sum over all states is a discrete sum, rather than an integral. This simplifies the notation considerable. The limit to an infinite box needs to be done, but here it is done at the very end of a calculations, or where it becomes convenient, and not right in the beginning. Adopting this style requires that the reader is familiar with executing this limit.[5]

[5] One advantage is that one may capture problems, when another limiting case is to be done, which may not be interchangeable with that to an infinitely large system. In this context is however also important to distinguish between periodic boundary conditions and that of a true finite box.

NORMALIZATION OF MOMENTUM EIGENSTATES

The overlap matrix elements of momentum eigenstates are[a]

$$\langle \vec{p},\sigma|\vec{p'},\sigma'\rangle \overset{\text{Eq. 1.36}}{=} \delta_{\sigma,\sigma'} \int_\Omega d^3r\, \frac{1}{\Omega} e^{\frac{i}{\hbar}(\vec{p}-\vec{p'})\vec{r}} = \delta_{\vec{p},\vec{p'}}\delta_{\sigma,\sigma'} \quad \overset{\Omega\to\infty}{\to} \quad \frac{(2\pi\hbar)^3}{\Omega}\delta(\vec{p}-\vec{p'})\delta_{\sigma,\sigma'} \quad (1.38)$$

The completeness relation has the form

$$\hat{1} = \sum_{\{\vec{p}\},\sigma\in\{\uparrow,\downarrow\}} |\vec{p},\sigma\rangle\langle\vec{p},\sigma| \quad \overset{\Omega\to\infty}{\to} \quad \sum_{\sigma\in\{\uparrow,\downarrow\}} \Omega \int \frac{d^3p}{(2\pi\hbar)^3}\, |\vec{p},\sigma\rangle\langle\vec{p},\sigma| \quad (1.39)$$

[a] In the limit $\Omega\to\infty$, I use

$$1 = \sum_{\{\vec{p'}\}} \delta_{\vec{p},\vec{p'}} \overset{\Delta p = 2\pi\hbar/L}{=} \Omega \sum_{\{\vec{p'}\}} \frac{(\Delta p)^3}{(2\pi\hbar)^3}\delta_{\vec{p},\vec{p'}} \rightsquigarrow \Omega\int \frac{d^3p'}{(2\pi\hbar)^3}\, \frac{(2\pi\hbar)^3}{\Omega}\delta(\vec{p}-\vec{p'}) = 1\,. \quad (1.37)$$

The factors are verified by performing the sum, respectively, the integral, which, both, give 1 as result. I express this as $\delta_{p,p'} \rightsquigarrow \frac{(2\pi\hbar)^3}{\Omega}\delta(\vec{p}-\vec{p'})$.

1.1.7 Non-orthonormal and local orbitals

When studying atoms, it is often convenient to use local orbitals $|\chi_\alpha\rangle$. The local orbitals are reminiscent of **atomic orbitals**, because they usually have the same quantum numbers as the atomic wave functions. The quantum numbers of atomic orbitals are the **principal quantum number** n, the **angular-momentum quantum number** ℓ, the **magnetic quantum number** m, and **spin quantum number** σ. In addition, there is a site index R referring to a particular atom. Thus, the index $\alpha = (R, n, \ell, m, \sigma)$ is a composite index of all these quantum numbers.

The principal quantum number is often suppressed, because the main interest of many-particle problems is related to the valence states, to which only one main quantum number contributes for a given site R and angular momentum ℓ.

Often, but not always, we will assume that the local orbitals are orthonormal among each other, that is $\langle\chi_\alpha|\chi_\beta\rangle = \delta_{\alpha,\beta}$. This orthonormality is not compatible with true atomic orbitals, when orbitals from different sites are considered. However, in a solid, one can construct so-called **Wannier orbitals**[11], which are localized and at the same time orthonormal to each other.

In practice, however, also Wannier orbitals are often too extended to be of use. Furthermore the Wannier orbitals often have a complex shape. Therefore, it is often advantageous to work in a non-orthonormal basisset, which provides more flexibility. This is shown in the present section.

We consider a basisset of orbitals $|\chi_\alpha\rangle$, which has an overlap matrix

$$S_{\alpha,\beta} \overset{\text{def}}{=} \langle\chi_\alpha|\chi_\beta\rangle \quad (1.40)$$

The unit operator[6] expressed in the non-orthonormal basis has the form

$$\hat{1} = \sum_{\alpha,\beta} |\chi_\alpha\rangle \left(\boldsymbol{S}^{-1}\right)_{\alpha,\beta} \langle\chi_\beta| \quad (1.41)$$

We can define a **projector function** $\langle\pi_\alpha| = \sum_\beta \left(\boldsymbol{S}^{-1}\right)_{\alpha,\beta}\langle\chi_\beta|$, so that

$$\hat{1} = \sum_\alpha |\chi_\alpha\rangle\langle\pi_\alpha|\,. \quad (1.42)$$

[6] For a finite basisset, the unit operator below is defined as unity within this basisset. In the more extended Hilbert space of all square-integrable functions, the expression is a projection operator onto the basisset spanned by the local orbitals.

The projector function probes the state for a certain character. This character is quantified by the "weight" $\langle\pi_\alpha|\psi\rangle$ of a local orbital $|\chi_\alpha\rangle$ in the state $|\psi\rangle$. I consider the projector function as probe function.

In practical applications, the overlap matrix $\boldsymbol{S}$ is often singular[7], which implies that its inverse $\boldsymbol{S}^{-1}$ does not exist, respectively that it is not unique. This is the case whenever one works with finite, and therefore incomplete basissets. The ambiguity in the inverse reflects in a similar ambiguity for the projector functions. To make this ambiguity explicit, we use the projector functions as the fundamental quantity, as opposed to the $\boldsymbol{S}^{-1}$, and specify only the requirement for the projector function, namely the **bi-orthogonality condition**.

$$\langle\pi_\alpha|\chi_\beta\rangle = \delta_{\alpha,\beta} \tag{1.43}$$

The inverse of the overlap matrix becomes a quantity that is derived from the projector functions via

$$\langle\pi_\alpha|\pi_\beta\rangle = \langle\pi_\alpha|\hat{1}|\pi_\beta\rangle \overset{\text{Eq. 1.41}}{=} \sum_{\gamma,\delta}\langle\pi_\alpha|\chi_\gamma\rangle\left(\boldsymbol{S}^{-1}\right)_{\gamma,\delta}\langle\chi_\delta|\pi_\beta\rangle \overset{\text{Eq. 1.43}}{=} \left(\boldsymbol{S}^{-1}\right)_{\alpha,\beta} \tag{1.44}$$

NON-ORTHONORMAL ORBITALS

The wave function can be represented in terms of local orbitals $|\chi_\alpha\rangle$ as

$$|\psi(t)\rangle = \sum_\alpha |\chi_\alpha\rangle\langle\pi_\alpha|\psi(t)\rangle \tag{1.45}$$

where the state $|\pi_\alpha\rangle$ is the **projector function**[a], which extracts the contribution of a particular local orbital $|\chi_\alpha\rangle$ from the wave function $|\psi\rangle$.
The projector functions obey the bi-orthonormality condition

$$\langle\pi_\alpha|\chi_\beta\rangle \overset{\text{Eq. 1.43}}{=} \delta_{\alpha,\beta} \tag{1.46}$$

as well as

$$\begin{aligned}\langle\chi_\alpha|\chi_\beta\rangle &\overset{\text{Eq. 1.40}}{=} S_{\alpha,\beta}\\ \langle\pi_\alpha|\pi_\beta\rangle &\overset{\text{Eq. 1.44}}{=} \left(\boldsymbol{S}^{-1}\right)_{\alpha,\beta}\end{aligned} \tag{1.47}$$

Convention:

- observables $\hat{A}$ are written with the projector functions outward

$$\hat{A} = \sum_{\alpha,\beta} |\pi_\alpha\rangle \underbrace{\langle\chi_\alpha|\hat{A}|\chi_\beta\rangle}_{A_{\alpha,\beta}}\langle\pi_\beta| \tag{1.48}$$

- states $|\psi\rangle$, density matrices $\hat{\rho}$ and densities of states are written with the orbitals pointing outward

$$\hat{\rho} = \sum_{\alpha,\beta} |\chi_\alpha\rangle \underbrace{\langle\pi_\alpha|\hat{\rho}|\pi_\beta\rangle}_{\rho_{\alpha,\beta}}\langle\chi_\beta| \tag{1.49}$$

Non-orthonormal basissets are summarized in appendix B on p. 401.

[a] I introduced the terminology of a projector function in my paper on the projector augmented wave method[12].

[7] A matrix is singular, when it has a vanishing (left or right) eigenvalue.

One can easily verify that the projector functions extract the appropriate coefficients for any state $|\psi\rangle$ that is contained within the Hilbert space spanned by the local orbitals: Consider a wave function that can be represented by the local orbitals with some coefficients c_α

$$|\psi\rangle = \sum_\alpha |\chi_\alpha\rangle c_\alpha \tag{1.50}$$

A particular coefficient c_β can be obtained from the scalar product of the wave function $|\psi\rangle$ with the projector function

$$\langle\pi_\beta|\psi\rangle = \sum_\alpha \langle\pi_\beta|\chi_\alpha\rangle c_\alpha \overset{\text{Eq. 1.46}}{=} c_\beta \qquad q.e.d. \tag{1.51}$$

If the basis set is orthonormal, that is $\langle\chi_\alpha|\chi_\beta\rangle = \delta_{\alpha,\beta}$, the orbitals themselves can act as projector functions. This is what is done in nearly all text books. Distinguishing orbitals and projector functions, however, provides a lot of additional freedom.

The treatment of non-orthonormal orbitals is mathematically analogous to that of vectors using oblique coordinate systems. Distinguishing orbitals and projector functions is analogous to **covariant** and **contravariant** vectors in **skewed coordinate systems**. A comparison between bra-ket notation and the co- and contravariant notation is given in table 1.1.

Each one-particle orbital defines a coordinate axis $|\chi_\mu\rangle \hat{=} \vec{e}_\mu$ in the Hilbert space. The overlap matrix between the basis states plays the role of a metric tensor $S_{\mu,\nu} = \langle\chi_\mu|\chi_\nu\rangle \hat{=} g_{\mu,\nu} = \vec{e}_\mu\vec{e}_\nu$. On the one hand, co- and contra-variant indices distinguish between states and projector functions, a distinction which is not explicit in the bra-ket notation. On the other hand, the co- and contravariant notation does not distinguish between complex conjugate partners such as the distinction between bras and kets in the bra-ket notation: such a distinction is not required for real-valued vectors.

More detail can be found in section 5.4 of ΦSX:Classical Mechanics[13].

Table 1.1: Comparison of Dirac's bra-ket notation for quantum states and the co-and contravariant vector notation. I do not use Einstein notation, but use explicit sums.

Bra-Ket notation		co and contravariant notation	
Basis			
basis-state	$\|\chi_\mu\rangle$	$\vec{e}_\mu$	contravariant vector
projector-function	$\langle\pi_\alpha\|$	$\vec{e}^\mu$	co-variant vector
Scalar product and metric tensor $g_{\mu,\nu}$			
bi-orthogonality	$\langle\pi_\mu\|\chi_\nu\rangle = \delta_{\mu,\nu}$	$g^\mu{}_\nu = \vec{e}^\mu\vec{e}_\nu = \delta_{\mu,\nu}$	
overlap matrix	$S_{\mu,\nu} = \langle\chi_\mu\|\chi_\nu\rangle$	$g_{\mu,\nu} = \vec{e}_\mu\vec{e}_\nu$	contravariant metric tensor
inverse overlap	$\left(S^{-1}\right)_{\mu,\nu} = \langle\pi_\mu\|\pi_\nu\rangle$	$g^{\mu,\nu} = \vec{e}^\mu\vec{e}^\nu$	
scalar product	$\langle\psi\|\phi\rangle$	$\vec{r}\vec{s} = \sum_\mu u_\mu u^\mu$	
completeness	$\hat{1} = \sum_{\mu,\nu} \|\chi_\mu\rangle S^{-1}{}_{\mu,\nu}\langle\chi_\nu\|$	$\mathbf{1} = \sum_{\mu,\nu} g^{\mu,\nu}\vec{e}_\mu \otimes \vec{e}_\nu$	
States and projector-functions			
state	$\|\psi\rangle = \sum_\mu \|\chi_\mu\rangle c_\mu$	$\vec{r} = \sum_\mu \vec{e}_\mu u^\mu$	vector
coefficient	$c_\mu = \langle\pi_\mu\|\psi\rangle$	$u^\mu = \vec{e}^\mu\vec{r}$	co-variant coefficient
	$c_\mu = \sum_\nu S^{-1}_{\mu,\nu}\langle\chi_\nu\|\psi\rangle$	$u^\mu = \sum_\nu g^{\mu,\nu}u_\nu$	
	$\langle\chi_\mu\|\psi\rangle$	$u_\mu = \vec{e}_\mu\vec{r}$	

1.1.8 Bloch theorem

I provided derivations of **Bloch's theorem** earlier in ΦSX: Quantum Physics[14]. and in ΦSX: Introduction to Solid-State Theory[1]. This section is not meant as an independent derivation but as a brief reminder and the presentation of a "cooking recipe".

Let me first revisit some notions regarding symmetries in physical systems: Noether's theorem for classical particles or classical fields says that a conserved quantity emerges from of every continuous symmetry. In quantum mechanics, this translates into the notion that the Hamiltonian becomes block-diagonal when represented in terms of eigenstates of a commutating set of its symmetry operators. As a consequence, the matrix diagonalization of a big matrix is broken down in many diagonalization problems with smaller dimensions. Each block is characterized by the set eigenvalues from the commutating set of symmetry operators, i.e. the quantum numbers.

This concept is now applied to the lattice translation symmetry. **Bloch theorem** exploits the discrete lattice-translation symmetry of a lattice of atoms. Lattice-translation symmetry implies that the Hamiltonian is invariant under a lattice translation, i.e. $\langle \vec{r} - \vec{t}, \sigma | \hat{h} | \vec{r'} - \vec{t}, \sigma' \rangle = \langle \vec{r}, \sigma | \hat{h} | \vec{r'}, \sigma' \rangle$. The **lattice translation vectors** $\vec{t}$ are integer multiples of the **primitive lattice translation vectors** $\vec{T}_1, \vec{T}_2, \vec{T}_3$.

The conserved quantity resulting from the lattice-translation symmetry is the **crystal momentum** $\hbar\vec{k}$ or **Bloch vector** $\vec{k}$, simply called the k-point. The eigenstates of the lattice translation are **Bloch states**

$$\psi_{\vec{k}}(\vec{r}, \sigma) = u_{\vec{k}}(\vec{r}, \sigma) \mathrm{e}^{i\vec{k}\vec{r}} \tag{1.52}$$

where $u_{\vec{k}}(\vec{r})$ is periodic with the lattice. In words, *the wave functions are periodic functions* $u_{n,k}(\vec{r})$ *that are modulated by a plane wave* $\mathrm{e}^{i\vec{k}\vec{r}}$.

As a result of the lattice symmetry, the Hamilton operator does not mix wave functions with different Bloch vectors $\vec{k} \neq \vec{k'}$ in the same reciprocal unit cell, i.e. $\langle \psi_{\vec{k}} | \hat{h} | \psi_{\vec{k'}} \rangle = 0$.[8] As a consequence, the eigenstates of the Hamiltonian can be written as Bloch states.

A Bloch vector can be any vector in the reciprocal unit cell. In order to avoid the complications of an infinite space region and the corresponding continuous Bloch-vectors, one imposes periodic boundary conditions

$$\psi_{\vec{k}}(\vec{r} + \vec{T}_j^{\text{super}}) = \psi_{\vec{k}}(\vec{r}) \; . \tag{1.53}$$

on a large, but finite, supercell, with supercell lattice vectors $\vec{T}_1^{\text{super}} = \vec{T}_1 N_1$, $\vec{T}_2^{\text{super}} = \vec{T}_2 N_2$, $\vec{T}_3^{\text{super}} = \vec{T}_3 N_3$. N_1, N_2, N_3 are very large, but finite, integers. The limit $N_j \to \infty$ is taken typically towards the end of a calculation.

A discrete set of Bloch-vectors $\vec{k}$ is specified via the **quantization condition** imposed by periodic boundary conditions: The periodicity of the Bloch wave function Eq. 1.52 implies

$$\begin{aligned} & \mathrm{e}^{i\vec{k}\vec{T}_q^{\text{super}}} = 1 \qquad \text{for } q \in \{1,2,3\} \\ \Rightarrow \qquad & \vec{k}_{j_1 j_2 j_3} = \sum_{q=1}^{3} \vec{g}_q \frac{j_q}{N_q} \qquad \text{with } j_q \in \{0, 1, \ldots, N_q\} \end{aligned} \tag{1.54}$$

where the **primitive reciprocal lattice vectors** $\vec{g}_j$ are defined by

$$\vec{g}_i \vec{T}_j = 2\pi\delta_{i,j} \qquad \text{for } i,j \in \{1,2,3\} \tag{1.55}$$

The discrete k-point set are the reciprocal lattice points of the supercell.

[8] The eigenvalues and eigenstates are periodic with the reciprocal lattice. Therefore the Hamilton matrix elements do not necessarily vanish for two Bloch vectors related by a reciprocal-lattice translation vector.

Table 1.2: Symbols used for real and reciprocal lattice vectors

real space lattice	
$\vec{T}_1, \vec{T}_2, \vec{T}_3$	primitive lattice vectors
$\boldsymbol{T}$	matrix made from the three primitive lattice vectors
$\vec{t}$	general lattice vector
reciprocal space lattice	
$\vec{g}_1, \vec{g}_2, \vec{g}_3$	primitive lattice vectors
$\boldsymbol{g}$	matrix made from the three primitive lattice vectors
$\vec{G}$	general lattice vector
$\vec{g}_i \vec{T}_j = 2\pi\delta_{i,j}$ or $\boldsymbol{G}^\dagger \boldsymbol{T} = 2\pi \mathbf{1}$	

For atom-centered basissets $\{|\chi_{\alpha,\vec{t}}\rangle\}$, Bloch's theorem has an appearance that differs slightly from Eq. 1.52, namely

$$\begin{aligned} \psi_{\vec{k}}(\vec{r},\sigma) &\overset{\text{Eq. 1.52}}{=} \overbrace{\frac{1}{\sqrt{\sum_{\vec{t}}}} \sum_{\vec{t},\alpha} \chi_{\alpha,\vec{t}}(\vec{r},\sigma) \mathrm{e}^{-i\vec{k}(\vec{r}-\vec{t})} c_\alpha(\vec{k})}^{u_{n,k}(\vec{r})} \mathrm{e}^{i\vec{k}\vec{r}} \\ &= \frac{1}{\sqrt{\sum_{\vec{t}}}} \sum_{\vec{t},\alpha} \chi_{\alpha,\vec{t}}(\vec{r},\sigma) c_\alpha(\vec{k}) \mathrm{e}^{i\vec{k}\vec{t}} \end{aligned} \tag{1.56}$$

where $\vec{t}_{i_1,i_2,i_3} = \vec{T}_1 i_1 + \vec{T}_2 i_2 + \vec{T}_3 i_3$ is an arbitrary real-space lattice vector. The orbital $|\chi_{\alpha,\vec{t}}\rangle$ is centered at site $\vec{R}_\alpha + \vec{t}$, where R_α is the position of the equivalent atom in the first unit cell. The orbital index α identifies the orbitals of a specific site and may consist of the angular-momentum and spin quantum numbers (ℓ, m, σ). The complex-valued coefficients are denoted by $c_\alpha(\vec{k})$.

In the normalization factor, I use the symbol $\sum_{\vec{t}}$, meaning $\sum_{\vec{t}\in\mathbb{T}} 1 = N_1, N_2, N_3$, which counts the lattice translation vectors $\vec{t} \in \mathbb{T}$ in the supercell [9] used in Eq. 1.53. The set $\mathbb{T}$ is usually not made explicit.

Eq. 1.56 corresponds to constructing first a basisset of Bloch states $|\chi_{\alpha,\vec{k}}\rangle$ out of the individual local orbitals $|\chi_{\alpha,\vec{t}}\rangle$ and their corresponding projector functions $|\pi_{\alpha,\vec{k}}\rangle$.

$$\begin{aligned} |\chi_{\alpha,\vec{k}}\rangle &= \frac{1}{\sqrt{\sum_{\vec{t}}}} \sum_{\vec{t}} |\chi_{\alpha,\vec{t}}\rangle \mathrm{e}^{i\vec{k}\vec{t}} \\ |\pi_{\alpha,\vec{k}}\rangle &= \frac{1}{\sqrt{\sum_{\vec{t}}}} \sum_{\vec{t}} |\pi_{\alpha,\vec{t}}\rangle \mathrm{e}^{i\vec{k}\vec{t}} \end{aligned} \tag{1.57}$$

which satisfy the bi-orthogonality condition

$$\langle \pi_{\alpha,\vec{k}} | \chi_{\beta,\vec{k}'} \rangle = \delta_{\alpha,\beta} \delta_{\vec{k},\vec{k}'} \ . \tag{1.58}$$

Caution is required because the same symbol is used for the Bloch waves $|\chi_{\alpha,\vec{k}}\rangle$ and the site-centered orbitals $|\chi_{\alpha,\vec{t}}\rangle$. The two basissets are distinguished by the type of their indices, namely $\vec{t}$ versus $\vec{k}$. The Kronecker symbol $\delta_{\vec{k},\vec{k}'}$ refers to the discrete set of k-points, which result from the quantization condition, respectively, the periodic boundary conditions for a large but finite supercell.

[9] The set $\mathbb{T}$ is contains all lattice translation vectors $\vec{t}_{j_1,j_2,j_3} = \vec{T}_1 j_1 + \vec{T}_2 j_2 + \vec{T}_3 j_3$ with $j_1 \in \{0, 1, \ldots, N_1\}$, $j_2 \in \{0, 1, \ldots, N_2\}$, and $j_3 \in \{0, 1, \ldots, N_3\}$. where N_1, N_2, N_3 define, together with the primitive lattice translations, the supercell.

In the basis of Bloch orbitals, the Ansatz for the eigenstates of the Hamiltonian has the form

$$|\varphi_{n,\vec{k}}\rangle = \sum_{\alpha} |\chi_{\alpha,\vec{k}}\rangle c_{\alpha,n}(\vec{k}) \tag{1.59}$$

A k-dependent Hamiltonian in the discrete basis is obtained by transforming onto k-dependent orbitals given in Eq. 1.57.

Let me now rewrite the Schrödinger equation for a Bloch wave function $|\varphi_n(\vec{k})\rangle$. I represent Hamilton and overlap matrix elements in the form[10]

$$\begin{aligned}
\hat{h} &= \underbrace{\sum_{\alpha,\vec{t}} |\pi_{\alpha,\vec{t}}\rangle\langle\chi_{\alpha,\vec{t}}|}_{=\hat{1}}\, \hat{h} \underbrace{\sum_{\beta,\vec{t}'} |\chi_{\beta,\vec{t}'}\rangle\langle\pi_{\beta,\vec{t}'}|}_{=\hat{1}} = \sum_{\alpha,\beta}\sum_{\vec{t},\vec{t}'} |\pi_{\alpha,\vec{t}}\rangle \underbrace{\langle\chi_{\alpha,\vec{t}}|\hat{h}|\chi_{\beta,\vec{t}'}\rangle}_{h_{\alpha,\vec{t},\beta,\vec{t}'}} \langle\pi_{\beta,\vec{t}'}| \\
\hat{1} &= \underbrace{\sum_{\alpha,\vec{t}} |\pi_{\alpha,\vec{t}}\rangle\langle\chi_{\alpha,\vec{t}}|}_{=\hat{1}}\, \hat{1} \underbrace{\sum_{\beta,\vec{t}'} |\chi_{\beta,\vec{t}'}\rangle\langle\pi_{\beta,\vec{t}'}|}_{=\hat{1}} = \sum_{\alpha,\beta}\sum_{\vec{t},\vec{t}'} |\pi_{\alpha,\vec{t}}\rangle \underbrace{\langle\chi_{\alpha,\vec{t}}|\chi_{\beta,\vec{t}'}\rangle}_{S_{\alpha,\vec{t},\beta,\vec{t}'}} \langle\pi_{\beta,\vec{t}'}|
\end{aligned} \tag{1.60}$$

and I exploit lattice-translation symmetry of $\hat{h}$, namely $h_{\alpha,\vec{t},\beta,\vec{t}'} = h_{\alpha,\vec{0},\beta,\vec{t}'-\vec{t}}$.

Let me now set up the generalized eigenvalue for the periodic Hamiltonian:

$$\begin{aligned}
0 &= \left(\hat{h} - \epsilon_n(\vec{k})\hat{1}\right)|\varphi_n(\vec{k})\rangle \\
&\overset{\text{Eq. 1.56}}{=} \underbrace{\left(\sum_{\alpha,\beta}\sum_{\vec{t},\vec{t}'} |\pi_{\alpha,\vec{t}}\rangle h_{\alpha,\vec{t},\beta,\vec{t}'}\langle\pi_{\beta,\vec{t}'}|\right)}_{\hat{h}} - \epsilon_n(\vec{k}) \underbrace{\sum_{\alpha,\beta}\sum_{\vec{t},\vec{t}'} |\pi_{\alpha,\vec{t}}\rangle \overbrace{\langle\chi_{\alpha,\vec{t}}|\chi_{\beta,\vec{t}'}\rangle}^{S_{\alpha,\vec{t},\beta,\vec{t}'}} \langle\pi_{\beta,\vec{t}'}|}_{\hat{1}} \Big) \underbrace{\sum_{\gamma,\vec{t}''} |\chi_{\gamma,\vec{t}''}\rangle e^{i\vec{k}\vec{t}''} \frac{1}{\sqrt{\sum_{\vec{t}}}} c_{\gamma,n}(\vec{k})}_{|\varphi_n(\vec{k})\rangle} \\
&= \sum_{\alpha}\sum_{\vec{t}} |\pi_{\alpha,\vec{t}}\rangle \sum_{\beta,\gamma}\sum_{\vec{t}',\vec{t}''} \Big(h_{\alpha,\vec{t},\beta,\vec{t}'} - \epsilon_n(\vec{k}) S_{\alpha,\vec{t},\beta,\vec{t}'}\Big) \underbrace{\langle\pi_{\beta,\vec{t}'}|\chi_{\gamma,\vec{t}''}\rangle}_{\delta_{\beta,\gamma}\delta_{\vec{t}',\vec{t}''}} e^{i\vec{k}\vec{t}''} \frac{1}{\sqrt{\sum_{\vec{t}}}} c_{\gamma,n}(\vec{k}) \\
&= \sum_{\alpha,\vec{t}} |\pi_{\alpha,\vec{t}}\rangle e^{i\vec{k}\vec{t}} \frac{1}{\sqrt{\sum_{\vec{t}}}} \sum_{\beta} \left[\sum_{\vec{t}'} \Big(h_{\alpha,\vec{0},\beta,\vec{t}'-\vec{t}} - \epsilon_n(\vec{k}) S_{\alpha,\vec{0},\beta,\vec{t}'-\vec{t}}\Big) e^{i\vec{k}(\vec{t}'-\vec{t})}\right] c_{\beta,n}(\vec{k}) \\
&= \sum_{\alpha} \underbrace{\sum_{\vec{t}} |\pi_{\alpha,\vec{t}}\rangle e^{i\vec{k}\vec{t}} \frac{1}{\sqrt{\sum_{\vec{t}}}}}_{|\pi_{\alpha,\vec{k}}\rangle \text{ Eq. 1.57}} \sum_{\beta} \left[\underbrace{\sum_{\vec{t}''} h_{\alpha,\vec{0},\beta,\vec{t}''} e^{i\vec{k}\vec{t}''}}_{=:h_{\alpha,\beta}(\vec{k})} - \epsilon_n(\vec{k}) \underbrace{\sum_{\vec{t}''} S_{\alpha,\vec{0},\beta,\vec{t}''} e^{i\vec{k}\vec{t}''}}_{=:S_{\alpha,\beta}(\vec{k})}\right] c_{\beta,n}(\vec{k}) \\
&= \sum_{\alpha} |\pi_{\alpha,\vec{k}}\rangle \sum_{\beta} \Big[h_{\alpha,\beta}(\vec{k}) - \epsilon_n(\vec{k}) S_{\alpha,\beta}(\vec{k})\Big] c_{\beta,n}(\vec{k})
\end{aligned} \tag{1.61}$$

Given that the projector functions are linear independent, all coefficients must vanish so that we obtain the Schrödinger equation in matrix form

$$\sum_{\beta} \Big[h_{\alpha,\beta}(\vec{k}) - \epsilon_n(\vec{k}) S_{\alpha,\beta}(\vec{k})\Big] c_{\beta,n}(\vec{k}) = 0 \tag{1.62}$$

with

$$h_{\alpha,\beta}(\vec{k}) \overset{\text{def}}{=} \langle\chi_{\alpha,\vec{k}}|\hat{h}|\chi_{\beta,\vec{k}}\rangle \overset{\text{Eq. 1.57}}{=} \sum_{\vec{t}} h_{\alpha,\vec{0},\beta,\vec{t}} e^{i\vec{k}\vec{t}} \quad \text{and} \tag{1.63}$$

$$S_{\alpha,\beta}(\vec{k}) \overset{\text{def}}{=} \langle\chi_{\alpha,\vec{k}}|\chi_{\beta,\vec{k}}\rangle \overset{\text{Eq. 1.57}}{=} \sum_{\vec{t}} S_{\alpha,\vec{0},\beta,\vec{t}} e^{i\vec{k}\vec{t}}\,. \tag{1.64}$$

[10] It is often difficult to decide where the orbitals go and where the projector functions. The notation is completely symmetric with respect to an interchange between the two. As a rule of thumb, one uses orbitals to expand the wave functions, and since operators act on wave functions, operators are expanded in projector functions.

Notably, there is no coupling of states having a different Bloch vectors, which is the essence of Bloch's theorem.

We are almost done: Let us now impose the normalization on the eigenstates $\langle\varphi_m(\vec{k})|\varphi_n(\vec{k'})\rangle = \delta_{m,n}\delta_{\vec{k},\vec{k'}}$

$$\begin{aligned}
\langle\varphi_m(\vec{k})|\varphi_n(\vec{k'})\rangle &= \sum_{\alpha,\beta} c^*_{\alpha,m}(\vec{k})\langle\chi_\alpha(\vec{k})|\chi_\beta(\vec{k'})\rangle c_{\beta,n}(\vec{k'}) \\
&\overset{\text{Eq. 1.57}}{=} \sum_{\alpha,\beta} c^*_{\alpha,m}(\vec{k})\frac{1}{\sum_{\vec{t}}}\sum_{\vec{t},\vec{t'}} \mathrm{e}^{-i\vec{k}\vec{t}}\langle\chi_{\alpha,\vec{t}}|\chi_{\beta,\vec{t'}}\rangle \mathrm{e}^{i\vec{k'}\vec{t'}} c_{\beta,n}(\vec{k'}) \\
&= \sum_{\alpha,\beta} c^*_{\alpha,m}(\vec{k}) \underbrace{\frac{1}{\sum_{\vec{t}}}\sum_{\vec{t}} \mathrm{e}^{-i(\vec{k}-\vec{k'})\vec{t}}}_{\delta_{\vec{k},\vec{k'}}} \underbrace{\sum_{\vec{t'}}\langle\chi_{\alpha,\vec{t}}|\chi_{\beta,\vec{t'}}\rangle \mathrm{e}^{i\vec{k'}(\vec{t'}-\vec{t})}}_{S_{\alpha,\beta}(\vec{k'})} c_{\beta,n}(\vec{k'}) \\
&= \delta_{\vec{k},\vec{k'}} \sum_{\alpha,\beta} c^*_{\alpha,m}(\vec{k}) S_{\alpha,\beta}(\vec{k}) c_{\beta,n}(\vec{k}) \qquad (1.65)
\end{aligned}$$

The orthonormality between states having different Bloch-vector is inherent in the Ansatz of Bloch wave function.[11] The orthonormality of states with the same Bloch-vector needs to be enforced by setting

$$\sum_{\alpha,\beta} c^*_{\alpha,m}(\vec{k}) S_{\alpha,\beta}(\vec{k}) c_{\beta,n}(\vec{k}) = \delta_{m,n} \qquad (1.66)$$

[11] States with different Bloch vector have different eigenvalues of the symmetry operator and are therefore orthogonal.

COOKING RECIPE FOR NON-INTERACTING ELECTRONS ON A LATTICE

This implies the following recipe to construct the eigenvalues and eigenstates of the Hamiltonian of a lattice.

1. Extract the real-space Hamilton $h_{\alpha,\vec{0},\beta,\vec{t}'}$ and overlap $S_{\alpha,\vec{0},\beta,\vec{t}'}$ matrix elements connecting the orbitals in the first unit cell $\vec{t} = \vec{0}$ to those in a unit cell displaced by a real-space lattice translation vector $\vec{t}'$.

2. Determine the k-dependent Hamiltonian and overlap matrix from the matrix elements in real space

$$h_{\alpha,\beta}(\vec{k}) = \sum_{\vec{t}} h_{\alpha,\vec{0},\beta,\vec{t}} e^{i\vec{k}\vec{t}} \tag{1.67}$$

$$S_{\alpha,\beta}(\vec{k}) = \sum_{\vec{t}} S_{\alpha,\vec{0},\beta,\vec{t}} e^{i\vec{k}\vec{t}} \tag{1.68}$$

3. Solve the generalized eigenvalue problem and obtain k-dependent energies $\epsilon_n(\vec{k})$ and the eigenvectors $c_{\alpha,n}(\vec{k})$

$$0 = \sum_{\beta} \left[h_{\alpha,\beta}(\vec{k}) - \epsilon_n(\vec{k}) S_{\alpha,\beta}(\vec{k}) \right] c_{\beta,n}(\vec{k}) \tag{1.69}$$

with the normalization condition

$$\sum_{\alpha,\beta} c^*_{\alpha,m}(\vec{k}) S_{\alpha,\beta}(\vec{k}) c_{\beta,n}(\vec{k}) = \delta_{m,n} \tag{1.70}$$

4. Construct eigenstates of the Hamiltonian from the eigenvectors

$$|\varphi_n(\vec{k})\rangle = \sum_{\alpha} \underbrace{\sum_{\vec{t}} |\chi_{\alpha,\vec{t}}\rangle e^{i\vec{k}\vec{t}} \frac{1}{\sqrt{\sum_{\vec{t}'}}}}_{|\chi_{\alpha,\vec{k}}\rangle} c_{\alpha,n}(\vec{k}) \tag{1.71}$$

1.2 Functionals and their derivatives

In the lecture notes, I also use derivatives of a functional with respect to the bra or ket of a wave function. This is a straightforward, but uncommon generalization of functional derivatives. Let me motivate the notation here.

I found it convenient to write down the variation of functionals, which define functional derivatives, rather than using the usual rules for functional derivatives.

1. **normal derivative:** For a simple function $f(\vec{r})$ of a vector argument $\vec{r}$, the first variation is

$$\delta f(\vec{r}) = \sum_j \frac{\delta f}{\delta r_j} \delta r_j + O(\delta r^2) \tag{1.72}$$

The derivative is defined as the prefactor of the variation of the argument.

$$\frac{\partial f}{\partial r_j} \stackrel{\text{def}}{=} \frac{\delta f}{\delta r_j} \tag{1.73}$$

2. **functional derivative:** Making the index of the argument continuous, i.e. $j \rightsquigarrow s$, turns the vector $\vec{r}$ into a function $r(s)$ and the function $f(\vec{r})$ into a functional $F[r]$.

$$\delta F[r] = \int ds \underbrace{\frac{\delta F}{\delta r(s)}}_{=\partial F/\partial r(s)} \delta r(s) + O(\delta r^2) \tag{1.74}$$

which defines the functional derivative

$$\frac{\partial F}{\partial r(s)} \stackrel{\text{def}}{=} \frac{\delta F}{\delta r(s)} \tag{1.75}$$

It is common to differentiate a derivative from a functional derivative using the symbol ∂ for a partial derivative, δ for functional derivatives and d for total derivatives. Because, I consider these as variations of the same theme, I do not follow this distinction, at least not rigorously. Rather I use δ, when I have infinitesimal, but discrete displacements of a variable in mind, and ∂ for derivatives.

3. **Wirtinger derivative:** For complex-valued arguments, the concept of **Wirtinger derivatives** is useful. The concept is described in more detail in appendix A.3 on p. 386. It shows that the variation of a general function of a complex number, can be expressed by the variations with respect to those of the complex number and its complex conjugate. The complex number and its complex conjugate are treated as if they were independent. This is, however, only a formal "trick". It reflects that a complex number consists of two independent real numbers.

   In the following, I demonstrate the principle writing a function $f(c)$ once as function of complex-valued argument, and once as function with two real arguments, which represent real and imaginary part of c.

$$\begin{aligned}
f(\vec{c}) &= \bar{f}(\mathrm{Re}[c], \mathrm{Im}[c]) \\
\delta f(\vec{c}) &= \frac{\delta \bar{f}}{\delta \mathrm{Re}[c]} \delta \mathrm{Re}[c] + \frac{\delta \bar{f}}{\delta \mathrm{Im}[c]} \delta \mathrm{Im}[c] \\
&= \frac{\delta \bar{f}}{\delta \mathrm{Re}[c]} \frac{\delta c + \delta c^*}{2} + \frac{\delta \bar{f}}{\delta \mathrm{Im}[c]} \frac{\delta c - \delta c^*}{2i} \\
&= \underbrace{\frac{1}{2}\Big(\frac{\delta \bar{f}}{\delta \mathrm{Re}[c]} - i \frac{\delta \bar{f}}{\delta \mathrm{Im}[c]}\Big)}_{\frac{\delta f}{\delta c}} \delta c + \underbrace{\frac{1}{2}\Big(\frac{\delta \bar{f}}{\delta \mathrm{Re}[c]} + i \frac{\delta \bar{f}}{\delta \mathrm{Im}[c]}\Big)}_{\frac{\delta f}{\delta c^*}} \delta c^*
\end{aligned} \tag{1.76}$$

   This motivates the definition of the Wirtinger derivatives

$$\begin{aligned}
\frac{\partial f}{\partial c} &\stackrel{\text{def}}{=} \frac{1}{2}\Big(\frac{\delta \bar{f}}{\delta \mathrm{Re}[c]} - i \frac{\delta \bar{f}}{\delta \mathrm{Im}[c]}\Big) \\
\frac{\partial f}{\partial c^*} &\stackrel{\text{def}}{=} \frac{1}{2}\Big(\frac{\delta \bar{f}}{\delta \mathrm{Re}[c]} + i \frac{\delta \bar{f}}{\delta \mathrm{Im}[c]}\Big)
\end{aligned} \tag{1.77}$$

4. **Derivative with respect to a bra or ket:** Next we talk about functionals of complex functions such as quantum mechanical wave functions.

$$\begin{aligned}
\delta F[\phi(\vec{x}), \phi^*(\vec{x})] &= \int d^4x \underbrace{\frac{\delta F}{\delta \phi(\vec{x})}}_{\frac{\delta F}{\delta \langle \vec{x}|\phi\rangle}} \underbrace{\delta\phi(\vec{x})}_{\langle \vec{x}|\delta\phi\rangle} + \int d^4x \underbrace{\frac{\delta F}{\delta \phi^*(\vec{x})}}_{\frac{\delta F}{\delta \langle \phi|\vec{x}\rangle}} \underbrace{\delta\phi^*(\vec{x})}_{\langle \delta\phi|\vec{x}\rangle} + O(\delta\phi^2) \\
&= \int d^4x \left\langle \frac{\delta F}{\delta|\phi\rangle}\middle|\vec{x}\right\rangle \langle \vec{x}|\delta\phi\rangle + \int d^4x \langle \delta\phi|\vec{x}\rangle \left\langle \vec{x}\middle| \frac{\delta F}{\delta\langle\phi|}\right\rangle + O(\delta\phi^2) \\
&= \frac{\delta F}{\delta|\phi\rangle}|\delta\phi\rangle + \langle\delta\phi|\frac{\delta F}{\delta\langle\phi|} + O(\delta|\phi\rangle^2)
\end{aligned} \tag{1.78}$$

This motivates the following definition of the derivative with respect to a bra or a ket.

$$\begin{aligned}\frac{\delta F}{\delta|\phi\rangle} &\stackrel{\text{def}}{=} \int d^4x\ \frac{\delta F}{\delta\langle\vec{x}|\phi\rangle}\langle\vec{x}| = \int d^4x\ \frac{\delta F}{\delta\phi(\vec{x})}\langle\vec{x}| \\ \frac{\delta F}{\delta\langle\phi|} &\stackrel{\text{def}}{=} \int d^4x\ |\vec{x}\rangle\frac{\delta F}{\delta\langle\phi|\vec{x}\rangle} = \int d^4x\ |\vec{x}\rangle\frac{\delta F}{\delta\phi^*(\vec{x})}\end{aligned} \tag{1.79}$$

The same principles can be carried further to include derivatives with respect to operators or other objects.

1.3 N-particle wave functions

1.3.1 N-particle states

In order to describe N particles instead of only one, we need N position coordinates and N spin indices. Thus, the wave function of a N-particle state is

$$\psi(\vec{x}_1,\ldots,\vec{x}_N) = \langle\vec{x}_1,\ldots,\vec{x}_N|\psi\rangle \tag{1.80}$$

The absolute square of a two-particle wave function is the probability density for the first electron to be at $\vec{x}_1$ with position $\vec{r}_1$ with spin σ_1 and another one to be at $\vec{x}_2$ with position $\vec{r}_2$ with spin σ_2.

One basis set, which spans the N-particle Hilbert space, is $\{|\vec{x}_1,\ldots,\vec{x}_N\rangle\}$. The orthonormality has the form

$$\langle\vec{x}_1,\ldots,\vec{x}_N|\vec{x'}_1,\ldots,\vec{x'}_N\rangle = \delta(\vec{x}_1-\vec{x'}_1)\cdots\delta(\vec{x}_N-\vec{x'}_N) \tag{1.81}$$

and the completeness relation is

$$\hat{1} = \int d^4x_1\cdots\int d^4x_N\ |\vec{x}_1,\ldots,\vec{x}_N\rangle\langle\vec{x}_1\ldots,\vec{x}_N| \tag{1.82}$$

1.3.2 Product states

A **product state** of a set with N one-particle wave functions has the form

$$\Psi_{a,\ldots,z}(\vec{x}_1,\ldots,\vec{x}_N) = \langle\vec{x}_1,\ldots,\vec{x}_N|\Psi_{a,\ldots,z}\rangle = \varphi_a(\vec{x}_1)\cdots\varphi_z(\vec{x}_N) \tag{1.83}$$

Product states are useful, because they can be expressed simply by specifying N one-particle wave functions $|\varphi_j\rangle$.

Product states are often written in the form of a $\otimes$.

$$\begin{aligned}|\vec{x}_1,\vec{x}_2,\ldots,\vec{x}_N\rangle &= |\vec{x}_1\rangle\otimes|\vec{x}_2\rangle\otimes\cdots\otimes|\vec{x}_N\rangle \\ |\varphi_a,\varphi_b,\ldots,\varphi_z\rangle &= |\varphi_a\rangle\otimes|\varphi_b\rangle\otimes\cdots\otimes|\varphi_z\rangle\end{aligned} \tag{1.84}$$

I will not use the form on the right-hand side.

The set of all N-particle product states, that can be formed from a complete-and-orthonormal one-particle basisset, is again a complete-and-orthonormal basis set in the N-particle Hilbert space. Note, however, that the most general N-particle state is a superposition of all these product states.

An attempt to visualize the restrictions of product states is given in figure 1.1.

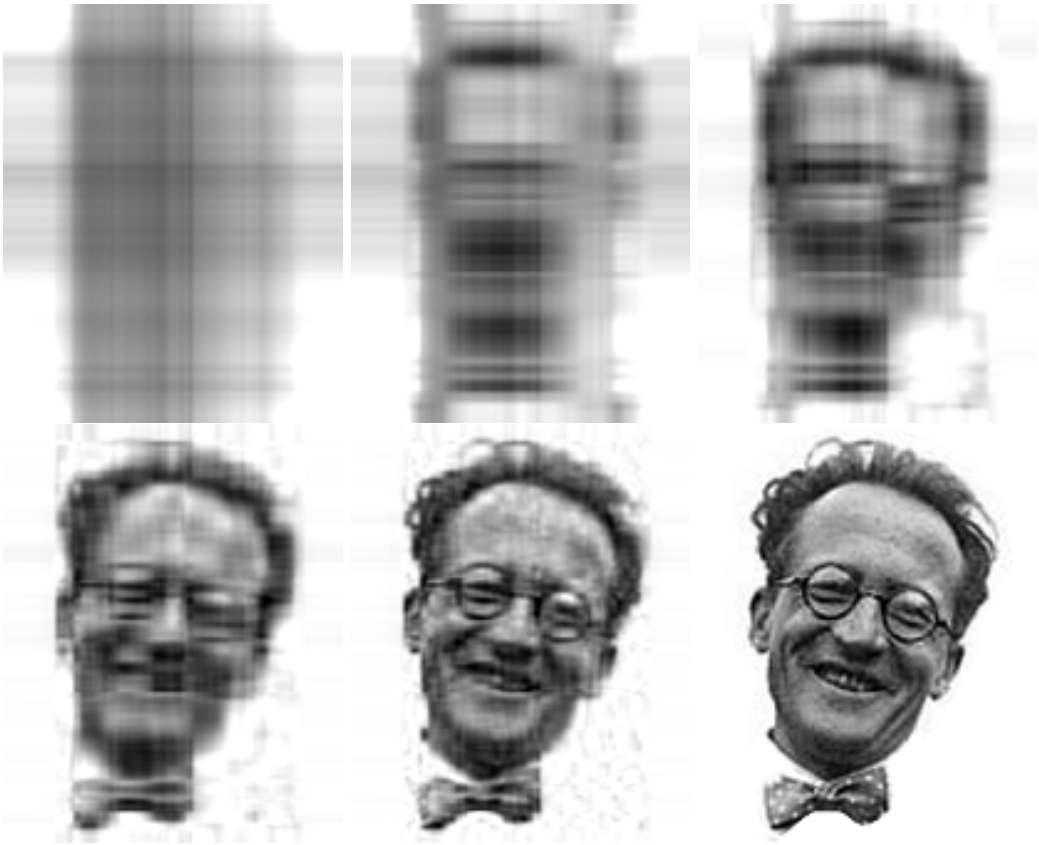

Fig. 1.1: Demonstration of product states and the superposition of product states. The grey-scale values $F(x, y)$ of the picture of Erwin Schrödinger is approximated by finite sums of product wave functions in the form $F(x, y) = \sum_{j=1}^{M} f_j(x) g_j(y)$ for $M = 1, 2, 4$ in the top row and for $M = 8, 16$ and the original figure in the bottom row. The functions $f_j(x)$ and $g_j(y)$ have been optimized individually to minimize the mean square deviation from the grey-scale values.

1.3.3 Slater determinants

The particles can be divided into classes of **identical particles**. Any physical Hamilton operator is symmetric under exchange of two identical particles. If that were not the case, it would be possible to distinguish the two particles which would make them non-identical.

Thus, the physical wave function is an eigenstate of the **permutation operator** between two identical particles. The permutation operator has the eigenvalues $+1$ and -1. Particles described by the permutation eigenvalue $+1$ are **bosons**, and those with permutation eigenvalue -1 are **fermions**. Fermionic wave functions are antisymmetric under exchange of two particles, while bosonic wave functions are symmetric under particle exchange.

Fermionic wave functions can be constructed from N one-particle wave functions $\varphi_i(\vec{x})$ with $i \in \{1, \ldots, N\}$ as antisymmetrized product state.

$$\underbrace{\Psi^F(\vec{x}_1, \ldots, \vec{x}_N)}_{\langle \vec{x}_1, \ldots, \vec{x}_N | \Psi^F \rangle} = \frac{1}{\sqrt{N!}} \sum_{i_1, \ldots, i_N = 1}^{N} \epsilon_{i_1, \ldots, i_N} \varphi_{i_1}(\vec{x}_1) \cdots \varphi_{i_N}(\vec{x}_N) \tag{1.85}$$

where $\epsilon_{i_1, \ldots, i_N}$ is the fully antisymmetric tensor.

The **fully antisymmetric tensor**, also called **Levi-Civita symbol**, is defined by

- It has the value 1 if the indices are in ascending order.

$$\epsilon_{1,2,\ldots,N} = 1 \tag{1.86}$$

- any permutation of two indices of the fully antisymmetric tensor changes its sign.
- the antisymmetric tensor is zero whenever two indices are equal.

Thus, every non-zero matrix element of the antisymmetric tensor corresponds to a permutation of the numbers $(1, 2, \ldots, N)$. Because there are $N!$ permutation of the indices $1, 2, \ldots, N$, the sum contributes $N!$ non-zero terms. Whenever the one-particle states $\varphi_j(\vec{x})$ are orthonormal, all terms in the sum Eq. 1.85 are orthonormal. Thus, the factor $1/\sqrt{N!}$ establishes the normalization of the final function. Non-orthonormal one-particle states can be used as well, but then the resulting many-particle wave function is not normalized.

The fully antisymmetric tensor can be used to evaluate the determinant of a matrix $\boldsymbol{A}$ via

$$\det|\boldsymbol{A}| = \sum_{i_1,\ldots,i_N=1}^{N} \epsilon_{i_1,\ldots,i_N} A_{i_1,1} A_{i_2,2} \cdots A_{i_N,N} \tag{1.87}$$

Thus, the antisymmetrized product wave function can also be expressed as a determinant of the matrix with elements $A_{i,j} = \varphi_i(\vec{x}_j)$.

$$\begin{aligned}\Psi^F(\vec{x}_1, \ldots, \vec{x}_N) &= \frac{1}{\sqrt{N!}} \sum_{i_1,\ldots,i_N} \epsilon_{i_1,\ldots,i_N} \varphi_{i_1}(\vec{x}_1) \cdots \varphi_{i_N}(\vec{x}_N) \\ &= \frac{1}{\sqrt{N!}} \det \begin{vmatrix} \varphi_1(\vec{x}_1) & \varphi_1(\vec{x}_2) & \ldots & \varphi_1(\vec{x}_N) \\ \varphi_2(\vec{x}_1) & \varphi_2(\vec{x}_2) & \ldots & \varphi_2(\vec{x}_N) \\ \vdots & \vdots & & \vdots \\ \varphi_N(\vec{x}_1) & \varphi_N(\vec{x}_2) & \ldots & \varphi_N(\vec{x}_N) \end{vmatrix}\end{aligned} \tag{1.88}$$

This is the reason for calling the antisymmetrized product wave functions **Slater determinants**.

The normalization factor $1/\sqrt{N!}$ makes sense[12] only for orthonormal one-particle wave functions $|\varphi_j\rangle$. While it is perfectly allowed to construct antisymmetrized wave functions from non-orthonormal one-particle wave functions, it is very inconvenient in practice. For example, the normalization of the resulting wave function is much more complicated.

For bosons, we need to symmetrize, rather than antisymmetrize, the product state under particle exchange, which can be accomplished by replacing the determinant by the **permanent** replacing the fully antisymmetric tensor by its absolute value.

$$\begin{aligned}\Psi^B(\vec{x}_1, \ldots, \vec{x}_N) &= \frac{1}{\sqrt{N! \prod_{k=1}^{N_d}(n_k!)}} \sum_{i_1,\ldots,i_N} \left|\epsilon_{i_1,\ldots,i_N}\right| \varphi_{i_1}(\vec{x}_1) \cdots \varphi_{i_N}(\vec{x}_N) \\ &= \frac{1}{\sqrt{N! \prod_{k=1}^{N_d}(n_k!)}} \mathrm{perm} \begin{vmatrix} \varphi_1(\vec{x}_1) & \varphi_1(\vec{x}_2) & \ldots & \varphi_1(\vec{x}_N) \\ \varphi_2(\vec{x}_1) & \varphi_2(\vec{x}_2) & \ldots & \varphi_2(\vec{x}_N) \\ \vdots & \vdots & & \vdots \\ \varphi_N(\vec{x}_1) & \varphi_N(\vec{x}_2) & \ldots & \varphi_N(\vec{x}_N) \end{vmatrix}\end{aligned} \tag{1.89}$$

The normalization of the permanent is non-trivial[13], because some of the orbitals may be identical to each other. Let me assume that the permanent is made out of N_d distinct orbitals. The multiplicity of the k-th set of distinct orbitals shall be n_k, saying that the k-th orbital is occupied by n_k particles. The total number of particles in the permanent is $\sum_{k=1}^{N_d} n_k = N$.

[12] For a non-orthonormal basisset, the resulting Slater determinant would not me normalized.
[13] No derivative of this factor is provided here.

The bosonic wave function is non-zero also if two orbitals are identical. For example, if $|\varphi_\alpha\rangle = |\varphi_\beta\rangle$, the permanent is

$$\langle \vec{x}_1, \vec{x}_2 | \psi^B_{\alpha,\beta} \rangle = \frac{1}{\sqrt{2}} [\varphi_\alpha(\vec{x}_1)\varphi_\beta(\vec{x}_2) + \varphi_\beta(\vec{x}_1)\varphi_\alpha(\vec{x}_2)] \quad \Rightarrow \quad \langle \vec{x}_1, \vec{x}_2 | \psi^B_{\alpha,\alpha} \rangle = \varphi_\alpha(\vec{x}_1)\varphi_\alpha(\vec{x}_2) \neq 0$$

For fermions, on the other hand, the Slater determinant of two identical one-particle orbitals is the zero state

$$\langle \vec{x}_1, \vec{x}_2 | \psi^F_{\alpha,\beta} \rangle = \frac{1}{\sqrt{2}} [\varphi_\alpha(\vec{x}_1)\varphi_\beta(\vec{x}_2) - \varphi_\beta(\vec{x}_1)\varphi_\alpha(\vec{x}_2)] \quad \Rightarrow \quad \langle \vec{x}_1, \vec{x}_2 | \psi^F_{\alpha,\alpha} \rangle = 0$$

1.4 Many-particle states and Fock space

Many-particle physics deals with situations where the particle number changes or where the wave function consists of contributions with different particle numbers. Therefore, we need to overcome the limitation of wave functions with fixed particle numbers. This extension will lead us to the concept of the Fock space.

Examples of problems which require states with different particle numbers are the following:

- A physical process may change the number of particles. An example would be an electron-positron collision, where two particles disappear while two photons are created.
- The number of particles in a so-called **open system** may change as particles migrate from the system under study and into the environment and vice versa.
- The number of particles may be variable, because the system is coupled to a thermodynamic particle reservoir. The situation is analogous to that of an open system, mentioned above. The main difference is that the coupling to the particle reservoir is considered infinitesimally small, so that the time scale of the particle exchange is considered infinite.

In order to describe systems with variable particle numbers, we need to generalize the concept of the N-particle Hilbert space to that of the **Fock space**. The Fock space is the union of all Hilbert spaces with N particles, where N can vary from zero to infinity. The zero-particle state is the so-called **vacuum state**. The vacuum state describes a system without particles, which is the true vacuum.[14]

The problem of the Fock space is that its states can no more be represented as wave functions in real space, because we cannot construct a function with a variable number of arguments. In order to describe a wave function in Fock space, we need to form the projection of the state onto each N-particle channel. For each N-particle channel we obtain a normalized N-particle wave function and a complex factor. The absolute square of this factor is the probability for the system to contain N particles. The phase factor describes the phase relations or the **entanglement**[15] between different N particle channels.

A basis for the Fock space is

$$\underbrace{|\mathcal{O}\rangle}_{\text{vacuum st.}} \cup \underbrace{\{|\vec{x}_1\rangle\}}_{\text{1p-Hilbert space}} \cup \underbrace{\{|\vec{x}_1, \vec{x}_2\rangle\}}_{\text{2p-Hilbert space}} \cup \underbrace{\{|\vec{x}_1, \vec{x}_2, \vec{x}_3\rangle\}}_{\text{3p-Hilbert space}} \cup \ldots \tag{1.91}$$

[14] The vacuum state is a normalized state and describes a physical situation, namely the vacuum, which does not have any particles in it. Thus, it is different from the zero state, which has a norm equal to 0, and which does not describe any physical situation.

[15] Two subsystems are called entangled, when the state of the combined system is a sum of the wave functions of the two parts $|\Psi\rangle = |\Psi_A\rangle + |\Psi_B\rangle e^{i\varphi}$ with a defined relative phase φ. The expectation values of an observable $\hat{O}$ depends on the relative phase

$$\langle \Psi | \hat{O} | \Psi \rangle = \langle \Psi_A | \hat{O} | \Psi_A \rangle + \langle \Psi_B | \hat{O} | \Psi_B \rangle + \mathrm{Re}\left[\langle \Psi_A | \hat{O} | \Psi_B \rangle e^{i\varphi} \right] \tag{1.90}$$

In an ensemble of wave functions, in which all relative phases contribute equally, the last term in the observable vanishes. This implies that the quantum mechanical coupling between the subsystems is absent and the two subsystems are not entangled. The phase relation is unimportant also, when the system is described by a product state $|\Psi\rangle = |\Psi_A, \Psi_B\rangle$.Editor: This is a first draft. Clean this up.

where the $\vec{x}_j = (\vec{r}_j, \sigma_j)$ denotes the combined position-and-spin argument. With $A \cup B$, I denote the union of the two sets A and B.

The basisset is orthonormal, that is, (1) two states with the same particle number N satisfy the same orthonormality conditions as those in the N-particle Hilbert space. (2) States with different particle numbers are orthonormal.

$$\langle \vec{x}_1, \ldots, \vec{x}_N | \vec{x'}_1, \ldots, \vec{x'}_{N'} \rangle = \begin{cases} 0 & \text{for } N \neq N' \\ \delta(\vec{x}_1 - \vec{x'}_1) \cdots \delta(\vec{x}_N - \vec{x'}_N) & \text{for } N = N' \end{cases} \tag{1.92}$$

One way to rationalize the orthonormality between states with differing particle number is that states with a given particle number are eigenstates of a particle-number operator. Eigenstates of a hermitian operator with different eigenvalues are orthonormal.[16]

The completeness relation in Fock space has the form

$$\hat{1} = \sum_{N=0}^{\infty} \int d^4x_1 \ldots \int d^4x_N \, |\vec{x}_1, \ldots, \vec{x}_N\rangle\langle \vec{x}_1, \ldots, \vec{x}_N| \tag{1.93}$$

1.4.1 Occupation-number representation

The Slater determinants formed from a given complete, ortho-normal one-particle basis set span the complete Fock space. The occupation-number representation is a convenient notation to describe this basis of many-particle states.

We start from an orthonormal set of one-particle basis functions $|\varphi_j\rangle$ which are arranged in a well-defined order, that is with indices increasing from left to right. Each subset of these functions specifies one Slater determinant. This subset is specified by a vector $\vec{\sigma}$ of occupation numbers $\sigma_1, \sigma_2, \ldots$. The index j of the occupation number σ_j refers to one of the one-particle wave functions $|\psi_j\rangle$. Each occupation number σ_j can be either zero or one. The one-particle states with occupation number equal to one are used to build the Slater determinant $|\vec{\sigma}\rangle$.

OCCUPATION NUMBERS AND SLATER DETERMINANTS

The occupation-number representation is defined such the one-particle orbitals in the Slater-determinant are arranged in the same order as the non-zero occupation numbers in the string $\vec{\sigma}$ of occupation numbers.

The Slater determinants formed in this way form a complete and orthonormal basis set of the Fock space, that is

$$\hat{1} = \sum_{\vec{\sigma}} |\vec{\sigma}\rangle\langle\vec{\sigma}| = \sum_{\sigma_1=0}^{1} \sum_{\sigma_2=0}^{1} \cdots |\sigma_1, \sigma_2, \ldots\rangle\langle\sigma_1, \sigma_2, \ldots| \tag{1.94}$$

The fact that Slater determinants form a complete basis in Fock space is the reason why Slater determinants are relevant even for interacting electron systems. Typically the eigenstates of the Hamiltonian for non-interacting electrons are Slater determinants. This is, however, not the case for interacting electrons.

A general many-particle state must be represented by a superposition of such Slater determinants. A general state in the Fock space has the form

$$|\Phi\rangle = \sum_{\vec{\sigma}} |\vec{\sigma}\rangle \underbrace{\langle\vec{\sigma}|\Phi\rangle}_{c_{\vec{\sigma}}} = \sum_{\vec{\sigma}} |\vec{\sigma}\rangle c_{\vec{\sigma}} \tag{1.95}$$

[16] This may not be a proof, because we probably need the orthonormality before we can define a hermitian particle-number operator.

1.4.2 Many-particle states of non-interacting electrons

If the one-particle basis used to define the Slater determinants are the eigenstates $|\varphi_j\rangle$ of the non-interacting Hamiltonian $\hat{h}$, the Slater determinants are eigenstates of that Hamiltonian and the particle-number operator[17] $\hat{N}$

$$\hat{h}|\vec{\sigma}\rangle = |\vec{\sigma}\rangle E_{\vec{\sigma}} \qquad \text{and} \qquad \hat{N}|\vec{\sigma}\rangle = |\vec{\sigma}\rangle N_{\vec{\sigma}} \tag{1.96}$$

with

$$E_{\vec{\sigma}} = \sum_j \epsilon_j \sigma_j \qquad \text{and} \qquad N_{\vec{\sigma}} = \sum_j \sigma_j \ . \tag{1.97}$$

The energy levels ϵ_j are the eigenvalues of the Hamiltonian $\hat{h}$ in the one-particle Hilbert space, i.e.

$$\hat{h}|\varphi_j\rangle = |\varphi_j\rangle \epsilon_j \ . \tag{1.98}$$

1.4.3 Size of Hilbert spaces

Consider a finite set of n one-particle states. The one-particle Hilbert space has n dimensions. The N-particle Hilbert space of distinguishable orbitals has N^n dimensions. The N-particle Hilbert space of fermionic wave functions has[18] $\frac{n(n-1)\ldots(n-N+1)}{1\cdot 2\cdots N} = \frac{n!}{(n-N)!(N!)} = \binom{n}{N}$ dimensions. The bosonic N-particle Hilbert space is larger and has $d = \frac{(N+n-1)!}{N!(n-N)!}$ dimensions.[19]

Table 1.3: Dimensions d of different spaces of quantum mechanical wave functions based on a n-dimensional one-particle Hilbert space. N is the number of particles in the N-particle wave function.

one-particle Hilbert space	$d = n$
N-particle Hilbert space, distinguishable particles	$d = n^N$
N-particle Hilbert space, fermions	$d = n!/[(n-N)!N!]$
N-particle Hilbert space, bosons	$d = (N+n-1)!/[N!(n-1)!]$
Fock space, fermions	$d = 2^n$

We see that the Fock space formed by a one-particle basisset of only 10 orbitals has dimension 1024. This is appropriate to describe the d-shell of a transition metal atom. The Hamiltonian for such a system has one million matrix elements, which can still be handled on a computer. If we consider 10 such atoms, i.e. 100 one-particle orbitals, the Fock space has dimension of order $d > 10^{30}$. This is beyond the capability of any computer. The rapid increase of the dimensionality of the problem has been coined as **dimensional bottleneck** of many-particle physics. It implies that, when dealing with many-particle physics, it is not sufficient to wait for larger computers: Each additional one-particle orbital doubles dimension of the problem and usually increases the computational by a factor four or eight.

[17] The eigenstates of the Hamiltonian can be represented as eigenstates of the particle-number operator, if the Hamiltonian commutates with the particle-number operator. In that case, the Hamilton operator conserves the particle number. Examples for a Hamilton operator, that does not conserve the particle number are the following: (1) A Hamiltonian that describes the annihilation of an electron-positron pair under creation of two photons. (2) A Hamiltonian describing a subsystem embedded into a bath, which can provide particles to the subsystem or accept particles leaving the subsystem.

[18] We can pick from n one-particle states as the first orbital. The second orbital can be picked from the $(n-1)$ remaining one-particle states, because each orbital may occur at most once in the Slater determinant. In the set of two-particle wave functions obtained in this way, each wave function is included twice. One of them has the orbitals in the reversed order. Therefore, I need to divide by two. In the end there are $n!/(n-N)!$ product states of N distinct orbitals irrespective of their order. This number is divided by the number $N!$ of permutations of the N orbitals, which yields the final dimension of the fermionic N-particle Hilbert space formed in a n-dimensional one-particle basisset.

[19] For bosons the dimension of a N-particle state is $d = \frac{(N+n-1)!}{N!(n-N)!}$. See `https://everettyou.github.io/teaching/PHYS212B/SecondQuantization.pdf`

1.5 Home study and practice: Simple one-particle problems

In order to explore the role of the formalism described in the book, we need a few simple systems with non-interacting particles as model systems.

The models are selected to be **minimal models**. A minimal model is the most simple model describing a certain effect. The idea is to capture the essence of an effect without obscuring it by the complexity of the calculations.

One of the most important models for the many-particle physics of extended systems is the so-called **Hubbard model**.[15, 16, 17] This model consists of a regular grid of hydrogen atoms, with electrons that strongly interact when they meet on the same hydrogen atom. While the purpose of the Hubbard model is to study interacting systems, in the models discussed here, we will discard the interaction. As we proceed towards interacting systems, we will study the role of interactions. Here, we will select two variants of the Hubbard model, namely the hydrogen molecule and the linear chain.

The **jellium model** is our model for a continuous system. In contrast to the Hubbard model, the atomic structure is absent in this model.

1.5.1 Hydrogen molecule

Introduction

The hydrogen molecule is the smallest non-trivial system for the study of electron correlation. Most calculations for this system can be done analytically, which makes it an ideal system to test the understanding and the workings of new concepts. It is also a cross link between the study of strong correlations in physics and chemistry. On the one-hand, the hydrogen dimer is the smallest Hubbard model.[15] As the interaction between the electrons is increased, one can study the mechanisms behind the so-called Mott-Hubbard insulator. On the other hand, when the hopping parameter is reduced in size, the hydrogen model describes the dissociation of a chemical bond. Because the ratio of interaction and hopping is large in this limit, one arrives at basically the same effects of strong correlations.

The first exercise is meant as an appetizer. We will frequently return to the hydrogen molecule during this lecture. Here, we study the hydrogen molecule without electron-electron interactions.

Problem

Consider a simplified hydrogen molecule. On each of the two sites, two orbitals are considered, one for spin up and the other for spin down.
The Hamiltonian has the form

$$\hat{h} = \underbrace{\sum_{\sigma\in\{\uparrow,\downarrow\}}\sum_{R=1}^{2} |\pi_{R,\sigma}\rangle\, \bar{\epsilon}\, \langle\pi_{R,\sigma}|}_{\text{atomic energies}} \underbrace{- \sum_{\sigma\in\{\uparrow,\downarrow\}} \Big(|\pi_{1,\sigma}\rangle\, \bar{t}\, \langle\pi_{2,\sigma}| + |\pi_{2,\sigma}\rangle\, \bar{t}\, \langle\pi_{1,\sigma}| \Big)}_{\text{hopping}} \tag{1.99}$$

where $\bar{\epsilon}$ is the so-called **atomic level** and $\bar{t}$ is the so-called **hopping parameter**[a] The orbital index $\alpha = (R, \sigma)$ selects a particular atom $R \in \{1, 2\}$ and a spin index $\sigma \in \{\uparrow, \downarrow\}$. The $|\pi_\alpha\rangle$ are the **projector functions**, which correspond to the local orbitals $|\chi_\alpha\rangle$, i.e. $\langle\pi_\alpha|\chi_\beta\rangle \overset{\text{Eq. 1.43}}{=} \delta_{\alpha,\beta}$. Despite the fact that we distinguish orbitals $|\chi_\alpha\rangle$ and projector functions $\langle\pi_\alpha|$, we consider orthonormal local orbitals $|\chi_\alpha\rangle$, that is $\langle\chi_\alpha|\chi_\beta\rangle = \delta_{\alpha,\beta}$.

1 Determine the eigenvalues and eigenstates of the Hamiltonian in the basis of local orbitals $|\chi_{R,\sigma}\rangle$, that is with the ansatz $|\psi_n\rangle = \sum_\alpha |\chi_\alpha\rangle c_{\alpha,n}$. The state index n is a composite index containing a spin quantum number and a non-spin index $j \in \{b, a\}$.

[a] I will use the sign convention that the hopping parameter has the same sign as the overlap matrix element of the orbitals. That is, the hopping parameter $\bar{t}$ between two s-orbitals is positive, while that between two p-orbitals pointing along the bond axis is negative. Editor: Caution: this adjustment may not be uniform in the lecture notes.

Solution

1 Determine the eigenvalues and eigenstates of the Hamiltonian in the basis of local orbitals $|\chi_{R,\sigma}\rangle$, that is with the ansatz $|\varphi_n\rangle = \sum_\alpha |\chi_\alpha\rangle c_{\alpha,n}$. The state index n is a composite index containing a spin quantum number and a non-spin index $j \in \{b, a\}$.

The result is as follows: The single-electron levels are

- the two lower, **b**onding states $|\varphi_{b,\sigma}\rangle$ for the two spin directions with energy $\epsilon_b = \bar{\epsilon} - |\bar{t}|$

$$|\varphi_{b,\sigma}\rangle = \frac{1}{\sqrt{2}}\Big(|\chi_{1,\sigma}\rangle + |\chi_{2,\sigma}\rangle \mathrm{sgn}(\bar{t}) \Big) \tag{1.100}$$

- and the two upper, **a**ntibonding states $|\varphi_{a,\sigma}\rangle$ with energy $\epsilon_a = \bar{\epsilon} + |\bar{t}|$.

$$|\varphi_{a,\sigma}\rangle = \frac{1}{\sqrt{2}}\Big(|\chi_{1,\sigma}\rangle - |\chi_{2,\sigma}\rangle \mathrm{sgn}(\bar{t})\Big) \tag{1.101}$$

For the hydrogen molecule, the orbitals are s orbitals, which have a positive overlap along the bond. Per our convention[20], the hopping parameter $\bar{t}$ has the same sign as the overlap matrix element. For the hydrogen molecule, the hopping parameter $\bar{t}$ is therefore positive.[21]

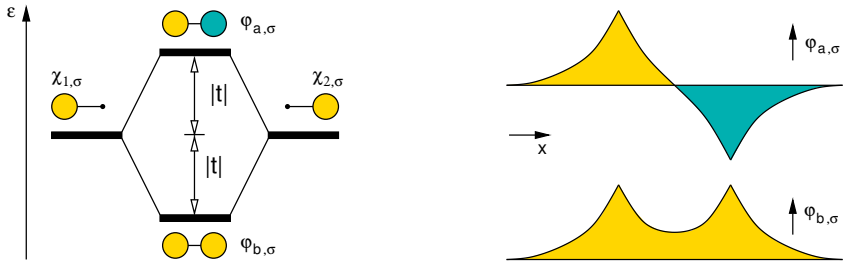

Fig. 1.2: Schematic representation of the energy level diagram (left) and the orbitals (left and right) of a hydrogen molecule. The atomic energy levels (outer bars) are split into a bonding (lower bar) and an antibonding (upper bar) state as the distance between the atoms approaches the bond distance. The orbital representation on the left is derived from an iso-contour plot of the wave function, with the color selecting the positive or negative contour value. Yellow and blue represent two signs of the wave function. On the right, the bonding state $|\varphi_{b,\sigma}\rangle$ and the antibonding state $|\varphi_{a,\sigma}\rangle$ are drawn along the bond axis.

[20] The convention that the sign of the hopping parameter $\bar{t}$ is equal to that of the overlap matrix element between the two orbitals, is not generally adapted.

[21] In contrast, the overlap between two p-orbitals, which are oriented along the bond, is negative. Consequently, also the hopping matrix element $\bar{t} < 0$ is negative. In this case, Eq. 1.100, would describe the upper, rather than the lower orbital, and it would be called the antibonding orbital. Analogously, Eq. 1.101 would be lower in energy and would be called the bonding orbital.

1.5.2 General diatomic molecule

Introduction

The general diatomic molecule is the model for a general 2-dimensional Hamiltonian. This problem is so important that its behavior should be known, even without doing the calculations. Whenever the coupling between two states stands out one can approximate the behavior by a 2-dimensional problem.

This problem will also make you familiar with a couple general rules, which do not require any calculation.

- Level repulsion: The presence of an off-diagonal matrix element between two states will lead to a repulsion of the energy levels. This repulsion will become weaker with the initial energy separation of the orbitals.
- Charge sum rule: The weight of an orbital summed over all eigenstates adds up to unity.
- Energy sum rule: the sum of all energy levels is equal to the sum of diagonal elements of the Hamiltonian.
- The character of an eigenstate is dominated by that basis-orbital, which is closest in energy.

These rules appear very simple, but later they will be key to understand the workings of Green's functions, which will be the topic of this course.

Problems with two orbitals will be important in these lecture notes, where we try to experience many-particle physics with minimal problems.

Problem

Exercise: Generalize the hydrogen molecule to a molecule with two distinct orbitals. That is, the "atomic energy levels" $\bar{\epsilon}_\alpha$ of both sites are distinct. Determine energy levels and eigenstates. Plot the energy levels as function of the hopping parameter. Identify the degenerate and the non-degenerate limit. What are the characteristic energy scales of the problem? Observe and describe the character of the wave functions in the limit of small and large hopping parameters, i.e. $\bar{t} \to 0$ and $\bar{t} \to \infty$.

Solution

The solution can also be found in section 2.3 of ΦSX:Quantum mechanics of the chemical bond[18].

In the following, I often suppress the spin index. Editor: Caution! The order of site and spin indices, respectively k- and spin indices is not consistent in the following. The spin index as quantum number is part of the orbital index, which should stand in front of the lattice translation.

The model Hamiltonian, we investigate, is

$$\boldsymbol{h} = \begin{pmatrix} \bar{\epsilon}_1 & -\bar{t} \\ -\bar{t} & \bar{\epsilon}_2 \end{pmatrix} \qquad \text{and} \qquad \boldsymbol{S} = \mathbf{1} = \begin{pmatrix} 1 & 0 \\ 0 & 1 \end{pmatrix} \tag{1.102}$$

Eigenvalues

We diagonalize the Hamiltonian by finding the zeros of the determinant of $\mathbf{H} - \epsilon\mathbf{1}$.[22]

[22] The condition that the determinant vanishes, that is $\det[\mathrm{H} - \epsilon\mathrm{O}] = 0$ determines the eigenvalues of the system. We need to determine the zeros of a polynomial of the energy. This polynomial is called the **characteristic polynomial**

The zero's of the characteristic polynomial

$$0 = (\bar{\epsilon}_1 - \epsilon)(\bar{\epsilon}_2 - \epsilon) - \bar{t}^2 \tag{1.103}$$

determine the eigenvalues ϵ_- and ϵ_+ of the two-center bond

$$\epsilon_\pm = \frac{\bar{\epsilon}_1 + \bar{\epsilon}_2}{2} \pm \sqrt{\left(\frac{\bar{\epsilon}_1 - \bar{\epsilon}_2}{2}\right)^2 + \bar{t}^2} \tag{1.104}$$

The eigenvalues are shown in fig. 1.3 for an **avoided crossing**: The hopping parameter $\bar{t}$ is fixed and the diagonal elements $\bar{\epsilon}_1(x)$ and $\bar{\epsilon}_2(x)$ depend on some unspecified variable x.

- To the left and to the right of the graph, the spacing $|\bar{\epsilon}_2(x) - \bar{\epsilon}_1(x)|$ is large compared to the hopping $\bar{t}$, which is the **non-degenerate limit**, $|\bar{\epsilon}_1 - \bar{\epsilon}_2| \gg \bar{t}$.
- In the center of the graph, the diagonal Hamilton elements cross as function of x. This is the **degenerate limit**, $|\bar{\epsilon}_1 - \bar{\epsilon}_2| \ll |\bar{t}|$.

The effect sees is, what I call **level repulsion**: Without hopping, the eigenvalues are equal to the diagonal elements. As the absolute value of the hopping is increased, the energy levels are displaced away from each other. The displacement is large when the energy levels are close, and it becomes negligible if the initial states are separated by a large amount.

- In the degenerate limit the spacing of the Hamilton eigenvalues are is twice the hopping parameter $\bar{t}$, i.e.

$$\epsilon_\pm \approx \bar{\epsilon}_{1/2} \pm |\bar{t}| \tag{1.105}$$

- In the non-degenerate limit the eigenvalues are shifted, in second-order perturbation theory of the Hopping parameter, by $\frac{|\bar{t}|^2}{|\bar{\epsilon}_2 - \bar{\epsilon}_1|}$ away from each other, i.e

$$\epsilon_\pm \approx \bar{\epsilon}_{1/2} \pm \frac{|\bar{t}|^2}{|\bar{\epsilon}_1 - \bar{\epsilon}_2|} \tag{1.106}$$

  where $\bar{\epsilon}_{1/2}$ is the lower atomic energy level for the bonding state with $\pm = -$ and the upper atomic energy level for the antibonding state with $\pm = +$. This equation is worth to remember for back-on-the-envelope considerations.

The mean value of the energy levels remains unchanged.[23]

If we start from one electron in each orbital, the energy gain consists of two parts. First we gain an amount $\bar{\epsilon}_2 - \bar{\epsilon}_1$ by transferring the electron from the upper orbital at $\bar{\epsilon}_2$ to the lower orbital at $\bar{\epsilon}_1$. This is the **ionic contribution**, because a cation and an anion are formed. Secondly, the lower orbital is lowered through **hybridization** with the higher orbital and we gain $\frac{2\bar{t}^2}{\bar{\epsilon}_2 - \bar{\epsilon}_1}$ for the electron pair. This covalent contribution becomes smaller the larger the initial energy separation. Thus, if the ionic contribution is large, the covalent contribution is usually small.

Eigenvectors

The eigenvectors are obtained from

$$\begin{pmatrix} \bar{\epsilon}_1 - \epsilon_\pm & -\bar{t} \\ -\bar{t} & \bar{\epsilon}_2 - \epsilon_\pm \end{pmatrix} \begin{pmatrix} c_{1,\pm} \\ c_{2,\pm} \end{pmatrix} = 0 \tag{1.107}$$

[23] This holds exactly, when the overlap matrix is the unity. It does not hold when the overlap matrix deviates from unity.

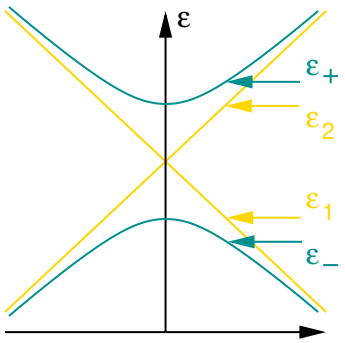

Fig. 1.3: Energy levels ϵ_-, ϵ_+ (green) as function of some parameter, which tunes the diagonal elements $\bar{\epsilon}_1$, $\bar{\epsilon}_1$ of the Hamiltonian at a fixed hopping parameter $\bar{t}$. Note the **level repulsion**, which is strongest, when the diagonal elements come close. The nature of the wave functions far from the avoided crossing, is as if the coupling of the states were absent.

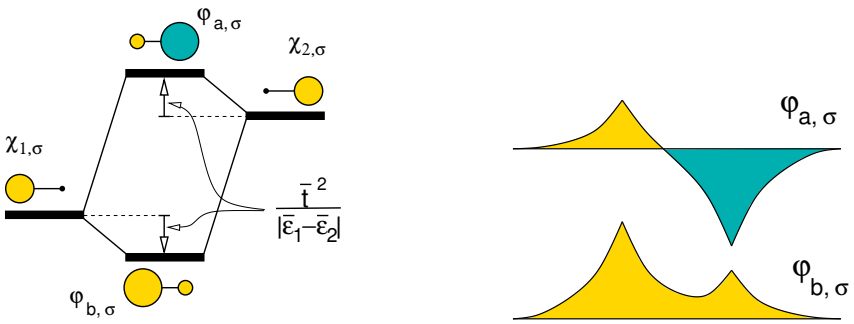

Fig. 1.4: Orbital diagram (left)and schematic cut through the bonding wave function and antibonding wave function for a non-degenerate bond. The level shifts $\frac{\bar{t}^2}{|\epsilon_1-\epsilon_2}$ are approximate, and become accurate in the non-degenerate limit.

where we insert the corresponding eigenvalues. For a two-dimensional Hamiltonian it is convenient to choose an ansatz that directly guarantees the orthonormality of the two eigenstates.

Namely, we exploit $\cos^2(x) + \sin^2(x) = 1$ $(x \in \mathbb{R})$

$$\begin{pmatrix} c_{1,-} \\ c_{2,-} \end{pmatrix} = \begin{pmatrix} \cos(\gamma \\ \sin(\gamma) \end{pmatrix} \quad \text{and} \quad \begin{pmatrix} c_{1,+} \\ c_{2,+} \end{pmatrix} = \begin{pmatrix} -\sin(\gamma \\ \cos(\gamma) \end{pmatrix} \tag{1.108}$$

Insertion of this Ansatz yields

$$\begin{aligned} 0 &\stackrel{!}{=} (\bar{\epsilon}_1 - \epsilon_-)\cos(\gamma) - \bar{t}\sin(\gamma) \\ \tan(\gamma) &= \frac{\bar{\epsilon}_1 - \epsilon_-}{\bar{t}} \\ &\stackrel{\text{Eq. 1.104}}{=} -\frac{1}{\bar{t}}\left(\frac{\bar{\epsilon}_1 + \bar{\epsilon}_2}{2} - \sqrt{\left(\frac{\bar{\epsilon}_1 - \bar{\epsilon}_2}{2}\right)^2 + \bar{t}^2} - \bar{\epsilon}_1\right) \\ &= -\left(\frac{\bar{\epsilon}_2 - \bar{\epsilon}_1}{2\bar{t}} - \sqrt{1 + \left(\frac{\bar{\epsilon}_2 - \bar{\epsilon}_1}{2\bar{t}}\right)^2}\right) \\ \gamma &= \operatorname{atan}\left\{-\left(\frac{\bar{\epsilon}_2 - \bar{\epsilon}_1}{2\bar{t}} - \sqrt{1 + \left(\frac{\bar{\epsilon}_2 - \bar{\epsilon}_1}{2\bar{t}}\right)^2}\right)\right\} \end{aligned} \tag{1.109}$$

Insertion of γ into the Ansatz leads to the desired result. This result appears cumbersome because of the trigonometric functions. However, the expression avoids divisions by zero, which otherwise tend to show up.

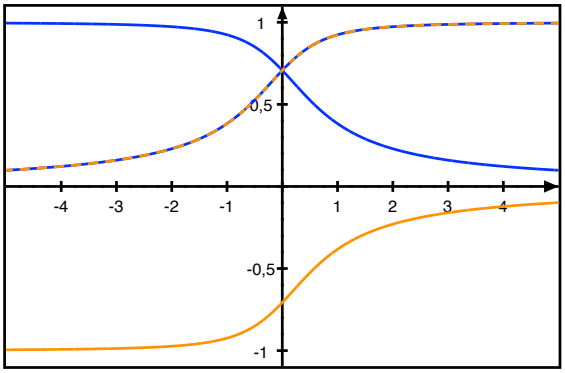

Fig. 1.5: Coefficients for the bonding (blue) and antibonding (orange) states of a two-center bond as function of $\frac{\bar{\epsilon}_2 - \bar{\epsilon}_1}{2\bar{t}}$. The blue-orange dashed line is $\cos(\gamma)$, the full blue line is $\sin(\gamma)$ and the full orange line is $\sin(\gamma)$. $\gamma\left(\frac{\bar{\epsilon}_2 - \bar{\epsilon}_1}{2\bar{t}}\right)$ is the mixing angle of the two orbitals. See text for discussion.

Let me summarize a few general observations, which are worth remembering. They will come up again later on. The reader may verify them for the example at hand. (The intention here is not to provide a derivation.)

- The eigenvectors are determined completely by the ratio $|\frac{\epsilon_1 - \epsilon_2}{2\bar{t}}|$. $|\epsilon_1 - \epsilon_2|$ is the relevant energy scale of the extreme non-degenerate limit, while $2|\bar{t}|$ is the energy-level spacing in the degenerate limit, the relevant energy scale in that limit.
- In the degenerate limit, the weight of the orbitals is equally distributed over both sides, i.e. $|c_{\alpha,\pm}| = \frac{1}{\sqrt{2}}$ for $\alpha \in \{1, 2\}$.
- In the lower (bonding) wave function, the two atomic orbitals add up in the bonding region between the two atoms, while the upper (antibonding) wave function has a node plane in the bonding region. The energy difference between the bonding and antibonding orbitals is due to the difference in kinetic energy, which is proportional to the squared gradient of the wave function: The kinetic energy of a wave function is $\int d^4x\, \psi^*(\vec{x}) \frac{-\hbar^2\vec{\nabla}^2}{2m_e}\psi(\vec{x}) = \frac{+\hbar^2}{2m_e}\int d^4x \left|\vec{\nabla}\psi(\vec{x})\right|^2$.

This shows up in our calculation as follows: For a positive hopping $\bar{t} = -h_{1,2} > 0$, the bonding orbital has coefficients with equal sign, while the coefficients of antibonding orbital have opposite sign. For negative hopping $\bar{t} = -h_{12} < 0$, the coefficients of the bonding orbital change sign and the antibonding orbitals have the same sign. The hopping is positive if the atomic orbitals point towards each other with the same sign as in the hydrogen molecule. When two orbitals point towards each other with the opposite sign, such as two p-orbitals pointing along the bond axis, the hopping parameter is negative.

- In a given wave function, the weight of that atomic orbital dominates, which has the closest atomic energy level. That is, for $\bar{\epsilon}_1 < \bar{\epsilon}_2$, the wave function of the bonding state (at ϵ_-) is concentrated on orbital 1, and the contribution of orbital 2 is smaller. The antibonding orbital (at ϵ_+) has its main contribution on atom 2.

- There are sum rules, namely that the sum $\epsilon_- + \epsilon_+$ of the energy eigenvalues is identical to the sum of the atomic levels $\bar{\epsilon}_1 + \bar{\epsilon}_2$. It can be shown that, for orthonormal atomic levels, the sum of eigenvalues is equal to the trace of the Hamiltonian matrix, i.e. $\sum_n \epsilon_n = \sum_n \bar{\epsilon}_n = \mathrm{Tr}[\boldsymbol{h}] = \mathrm{Tr}[\hat{h}]$ for arbitrary dimensions. This implies that the energy gain of the bonding orbital is compensated by the energy loss of the antibonding orbitals, when both are equally occupied.

- A second sum rule is that the total weight of each orbital, counting its contribution to all eigenstates, filled and empty, is the same before and after the bond formation. In our case, this implies $c_{\alpha,-}^2 + c_{\alpha,+}^2 = 1$ for both atomic orbitals $|\chi_\alpha\rangle$ with $\alpha \in \{1, 2\}$. Also this is a general result, which holds when the overlap matrix is unity.

What we observed are examples for two sum rules that are generally valid. They are presented here without proof.

NOTIONS ON DIAGONALIZATION

For an eigenvalue problem with a hermitian Hamiltonian $\boldsymbol{h}$

$$\Big(\boldsymbol{h} - \epsilon_n \mathbf{1})\vec{c}_n = 0 \tag{1.110}$$

with eigenvalues ϵ_n and eigenvectors $\vec{c}_n$, the following statements hold:

- **energy sum rule**:

$$\sum_n \epsilon_n = \mathrm{Tr}[\boldsymbol{h}] \tag{1.111}$$

- **charge sum rule**:

$$\sum_n |c_{j,n}|^2 = 1 \qquad \forall_j \tag{1.112}$$

Important note: This statements do not hold for a generalized eigenvalue problem, that is in the presence of an overlap matrix that differs from the unit matrix.

1.5.3 Linear chain of hydrogen atoms

The most simple model for an extended system is the linear chain. The linear chain describes hydrogen atoms placed on an equi-spaced one-dimensional grid with spacing a_{lat}. The spacing a_{lat} is the **lattice constant**.

We impose **periodic boundary conditions**. That is, we require the wave function to become identical after n beads. This describes either (1) a ring with N_s beads or (2) an infinite system with n k-points. Consider orthonormal local orbitals $|\chi_{j,\sigma}\rangle$ with $j = 1, \ldots N_s$, where N_s is the number of sites. Choose, whether the calculated eigenstates are normalized per one-atom unit cell of the linear chain or for the N_s-bead ring.

Problem

The linear chain has the Hamiltonian

$$\hat{h} = \underbrace{\sum_{\sigma\in\{\uparrow,\downarrow\}}\sum_{j=-\infty}^{\infty} |\pi_{\sigma,j}\rangle \bar{\epsilon} \langle\pi_{\sigma,j}|}_{\text{atomic energies}} - \underbrace{\sum_{\sigma\in\{\uparrow,\downarrow\}}\sum_{j=-\infty}^{\infty} \left(|\pi_{\sigma,j}\rangle \bar{t} \langle\pi_{\sigma,j+1}| + |\pi_{\sigma,j+1}\rangle \bar{t} \langle\pi_{\sigma,j}|\right)}_{\text{hopping}} \tag{1.113}$$

where j is the site index.

1. determine the eigenstates and eigenvalues of the linear chain with periodic boundary conditions with a repeat unit of N_s beads.

Solution

1. determine the eigenstates and eigenvalues of the linear chain with periodic boundary conditions with a repeat unit of N_s beads.

The linear chain is a worked example in section 6.7 of ΦSX:Quantum mechanics of the chemical bond.[18]. Here, I follow the recipe described in section 1.1.8 on p. 13.

In our problem, the primitive real-space lattice vector is $\vec{T} = a_{\text{lat}}\vec{e}_x$, where the lattice constant a_{lat} is the distance between the beads and $\vec{e}_x$ is a unit vector pointing along the chain (which is oriented in x-direction). The general lattice vectors are $\vec{t}_j = \vec{T} \cdot j = \vec{e}_x a_{\text{lat}} \cdot j$ with integer j.

In our problem, there are only two spin orbitals per unit cell. Therefore, the orbital index (α) is the same as the spin index σ. Bloch theorem already determines the wave functions, namely

$$|\varphi_{n,\vec{k}}\rangle = \sum_{\sigma\in\{\uparrow,\downarrow\}} \frac{1}{\sqrt{N_s}} \sum_{j=-\infty}^{\infty} |\chi_{\sigma,j}\rangle e^{i\vec{k}\vec{e}_x a_{\text{lat}} \cdot j} c_{\sigma,n}(\vec{k}) \tag{1.114}$$

N_s is the number of sites in the unit cell, which determines the set of k-points and the normalization of the wave functions.

In order to practice the recipe described in section 1.1.8 on p. 13, let me proceed in small steps. I leave out many explanations, because they are already given in section 1.1.8.

The recipe goes as follows:

1. *"Extract the real-space Hamilton $h_{\alpha,\vec{0},\beta,\vec{t}'}$ and overlap $S_{\alpha,\vec{0},\beta,\vec{t}'}$ matrix elements connecting the orbitals in the first unit cell $\vec{t} = \vec{0}$ to those in a unit cell displaced by a real-space lattice translation vector $\vec{t}'$."*

I obtain

$$\begin{aligned} h_{0,\sigma,0,\sigma'} &= \bar{\epsilon}\delta_{\sigma,\sigma'} \\ h_{0,\sigma,1,\sigma'} &= -\bar{t}\delta_{\sigma,\sigma'} \\ h_{0,\sigma,-1,\sigma'} &= -\bar{t}\delta_{\sigma,\sigma'} \end{aligned}$$

$$S_{0,\sigma,j,\sigma'} = \delta_{\sigma,\sigma'}\delta_{j,0} \tag{1.115}$$

2. *"Determine the k-dependent Hamiltonian and overlap matrix from the matrix elements in real space"*

$$\begin{aligned} h_{\sigma,\sigma'}(\vec{k}) &\overset{\text{Eq. 1.67}}{=} \sum_{j=-\infty}^{\infty} h_{\sigma,0,\sigma',j} e^{ik_x a_{\text{lat}} j} = \delta_{\sigma,\sigma'}\left(\bar{\epsilon} - 2\bar{t}\cos(k_x a_{\text{lat}})\right) \\ S_{\sigma,\sigma'}(\vec{k}) &\overset{\text{Eq. 1.68}}{=} \sum_{j=-\infty}^{\infty} S_{\sigma,0,\sigma',j} e^{ik_x a_{\text{lat}} j} = \delta_{\sigma,\sigma'} \end{aligned} \tag{1.116}$$

3. *"Solve the generalized eigenvalue problem and obtain k-dependent energies $\epsilon_n(\vec{k})$ and the eigenvectors $c_{\alpha,n}(\vec{k})$ satisfying the normalization condition"*

   The k-dependent energy levels are

$$\epsilon_n(\vec{k}) = \bar{\epsilon} - 2\bar{t}\cos(k_x a_{\text{lat}}) \tag{1.117}$$

   and the eigenvectors $\vec{c}_n(k_x) = (c_{\uparrow,n}(k_x), c_{\downarrow,n}(k_x))$ are $\vec{c}_1(k_x) = (1,0)$ and $\vec{c}_2(k_x) = (0,1)$. The first band (n=1) refers to the states with spin $\uparrow$ and the second band (n=2) has the spin $\downarrow$.

   The normalization condition

$$\sum_{\sigma,\sigma' \in \{\uparrow,\downarrow\}} c^*_{\sigma,m}(\vec{k}) S_{\sigma,\sigma'}(\vec{k}) c_{\sigma',n}(\vec{k}) = \delta_{m,n} \tag{1.118}$$

   is satisfied.

4. *"Construct eigenstates of the Hamiltonian from the eigenvectors"*

   The wave function is

$$|\varphi_n(\vec{k})\rangle \overset{\text{Eq. 1.71}}{=} \sum_{\sigma} \underbrace{\frac{1}{\sqrt{\sum_{\vec{t}'}}} \sum_{\vec{t}} |\chi_{\sigma,\vec{t}}\rangle e^{i\vec{k}\vec{t}}}_{|\chi_{\sigma,\vec{k}}\rangle} c_{\sigma,n}(\vec{k}) = \sum_j |\chi_{\sigma,j}\rangle \frac{1}{\sqrt{N_s}} e^{ik_x a_{\text{lat}} j} \tag{1.119}$$

   where N_s is the number of beads in the (super) unit cell, which defines the quantization condition for the k-points and the normalization of the eigenstates. The wave function extends over all space, but the wave function repeats every N_s sites.

The dispersion relation $\epsilon_n(k_x)$ of the linear chain and the resulting density of states is shown in figure 1.6. The shape of the density of states with the raised band edges is characteristic for quasi-one-dimensional structures in the material. This shape explains, why one-dimensional system tend to distort in order to open the band gap, such as in a **Peierls distortion**.

Editor: This concept needs to be explained. Consider the following line of thought: Consider the G vector connecting the two k-points for which the bands intersect the Fermi level. If a perturbation has a contribution with this G-vector, a band gap opens at the Fermi level. Out of the plane waves $e^{i\frac{G}{2}r}$ and $e^{-i\frac{G}{2}r}$, we can form a lower state of the form $\cos(\frac{G}{2}r)$ and an upper state $\sin(\frac{G}{2}r)$. The density of the lower state is proportional to $\cos(Gr)$, which is a charge density wave with a wave vector G. If

the electrons interact, this charge-density wave produces a perturbing potential with the same wave length, namely G, which was the perturbation causing the charge density wave in the first place. The band edges on both sides of the Fermi level have the spiked form of a one-dimensional density of states. This tells that the charge density wave is strong, stronger than in higher dimensions. This is the underlying reason for the observation that one-dimensional problems tend to undergo phase transitions.

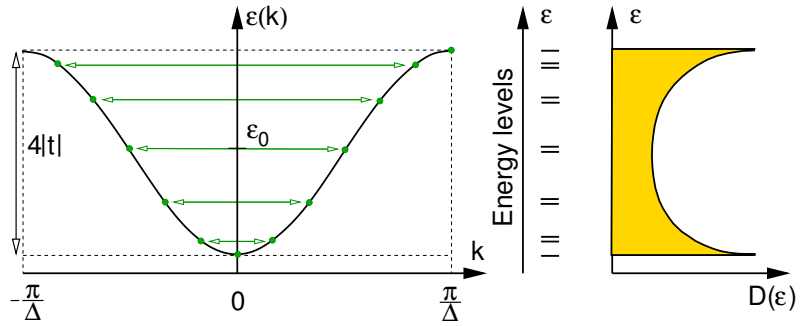

Fig. 1.6: Dispersion relation of linear chain of hydrogen atoms with periodic boundary conditions. The green points correspond to the energy levels of a ring with 14 atoms. In the middle figure we show the energy levels, and on the right the schematic density of states $D(\epsilon)$ for the infinite chain.

The boundary condition imposes

$$\langle \pi_{\sigma,N_s} | \varphi_n(k) \rangle = \langle \pi_{\sigma,0} | \varphi_n(k) \rangle \overset{\text{Eq. 1.114}}{\Rightarrow} e^{ik_x a_{\text{lat}} \cdot N_s} = 1 \quad \Rightarrow k_x a_{\text{lat}} \cdot N_s = 2\pi m$$
$$\Rightarrow \vec{k}_m = \vec{e}_x \frac{2\pi}{N_s a_{\text{lat}}} \cdot m \tag{1.120}$$

Only the k-points from the interval $-\frac{\pi}{a_{\text{lat}}} < k_m \leq \frac{\pi}{a_{\text{lat}}}$ are considered, because the wave functions of k_m and $k_m + N_s$ are identical.

1.5.4 Insulating linear chain

Introduction

While the linear chain is the minimal problem for a metallic system, we can also form the minimal model for an insulating system by doubling the periodicity of the half-filled linear chain.

In the most general form, this is the so-called **Rice-Mele model**[19], which is used to describe ferroelectric materials. When the atomic energy levels alternate, but the hopping parameters remain constant, the model describes an ionic insulator. If the hopping parameters vary, but the energy levels are constant, the model describes a covalent insulator. This latter special case, alternating hopping but constant energy levels, leads to the so-called **Su-Schrieffer-Heeger (SSH) model** [20], which is the minimal model system for a topological insulator.

One purpose of this exercise is to train Bloch-theorem for a case with more than one atom in the unit cell. Secondly, we become familiar with a frequently used toy model, for which we can investigate the role of interactions. Later, we will see that there are insulators, so-called Mott insulators, which turn insulating only due to interaction. The model described here allows to set the Mott insulator apart from the regular "band" insulators.

Problem

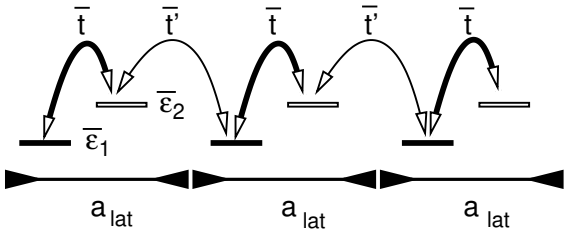

Fig. 1.7: Scheme to demonstrate the Hamiltonian of the alternating linear chain. It describes a chain with two atoms per unit cell with different ionicity, that is atomic energy levels $\bar{\epsilon}_1$ and $\bar{\epsilon}_2$. The atoms are connected by weak and strong bonds as characterized by the two hopping parameters $\bar{t}$ and $\bar{t}'$. With a_{lat} I denote the lattice constant.

1 Calculate the band structure of the linear chain with two distinct sites per unit cell. Both, the "atomic energies" $\bar{\epsilon}_1, \bar{\epsilon}_2$ and the hopping parameters $\bar{t}, \bar{t}'$ alternate. Alternating atomic levels describe a material with ionic character, while alternating hoppings describe materials with covalent bonds.

2 Determine the k-dependent wave functions.

Discussion

1 Calculate the band structure of the linear chain with two distinct sites per unit cell. Both, the "atomic energies" $\bar{\epsilon}_1, \bar{\epsilon}_2$ and the hopping parameters $\bar{t}, \bar{t}'$ alternate. Alternating atomic levels describe a material with ionic character, while alternating hoppings describe materials with covalent bonds.

The solution is a worked example in section 4.5 in ΦSX: Introduction to Solid State Theory[1], which has been included below. In contrast to the previous exercise for the linear chain, I do not express the Hamiltonian as abstract operator using the projector and orbital states, but I go directly to the matrix equation.

Let us consider the example of a linear chain made from atoms with one s-type orbital. There shall be two atoms per unit cell. The lattice constant shall be a_{lat}. The orbitals are denoted by (α, j), where $\alpha \in \{1, 2\}$ denote the two orbitals and j is the number of lattice displacements by a_{lat} from the origin to the current site.

The two atoms in the unit cell have orbital energies $\bar{\epsilon}_1$ and $\bar{\epsilon}_2$. We denote the hopping matrix element between orbitals $(1, j)$ and $(2, j)$ by $\bar{t}$ and the one between $(2, j)$ and $(1, j+1)$ by $\bar{t}'$. In the context of Slater-Koster matrix elements, both are matrix elements of the type $-h_{ss\sigma}$.

The difference of the atomic energy levels $\bar{\epsilon}_2 - \bar{\epsilon}_1$ describes relative **electronegativity** of the two atoms. The atom with the lower electron level is more electronegative than the one with the higher level. Without hopping, the electrons would accumulate at the more electronegative atom. This is analogous to rock salt (NaCl), where the sodium atom holds on only weakly to its valence electron, while the lowest unoccupied orbital of the chlorine atom is much stronger bound to the atom core. Therefore, sodium donates its electron to the chlorine atom, so that two ions Na^+ and Cl^- are formed.

The different hopping parameters describe that two of the atoms are pairwise closer together. That is, we describe a chain of molecules.

For the sake of simplicity, we only consider wave functions with one spin direction. The bands of the two spin direction are identical, because there is no magnetic field. When we consider one spin direction, the wave-function component of the other spin direction is zero.

The infinite Hamiltonian has the form

$$\mathbf{h} = \left(\begin{array}{c|cc|cc|cc|c} & \vdots & \vdots & \vdots & & & & \\ \hline \dots & \bar{\epsilon}_1 & -\bar{t} & 0 & 0 & \dots & & \\ \dots & -\bar{t} & \bar{\epsilon}_2 & -\bar{t}' & 0 & \dots & & \\ \hline \dots & 0 & -\bar{t} & \bar{\epsilon}_1 & -\bar{t} & 0 & 0 & \dots \\ \dots & 0 & 0 & -\bar{t} & \bar{\epsilon}_2 & -\bar{t}' & 0 & \dots \\ \hline & & \dots & 0 & -\bar{t}' & \bar{\epsilon}_1 & -\bar{t} & \dots \\ & & \dots & 0 & 0 & -\bar{t} & \bar{\epsilon}_2 & \dots \\ \hline & & & \vdots & \vdots & \vdots & \vdots & \end{array}\right) \tag{1.121}$$

The Hamilton matrix elements can also be written as

$$\boldsymbol{h}_{i,j} = \begin{pmatrix} \bar{\epsilon}_1 & -\bar{t} \\ -\bar{t} & \bar{\epsilon}_2 \end{pmatrix} \delta_{i,j} + \begin{pmatrix} 0 & 0 \\ -\bar{t}' & 0 \end{pmatrix} \delta_{i+1,j} + \begin{pmatrix} 0 & -\bar{t}' \\ 0 & 0 \end{pmatrix} \delta_{i-1,j} \tag{1.122}$$

where i and j are the indices of the lattice translations $\vec{t}_j = a_{\text{lat}} \cdot j$. The components of the 2×2 matrices $\boldsymbol{h}_{i,j}$ refer to the orbital indices in the primitive unit cell, while i, j identify a particular unit cell.

When we transform the Hamiltonian into the Bloch representation using Eq. 1.67, we obtain the k-dependent Hamiltonian with $\vec{t}_j = a_{\text{lat}} \cdot j$

$$\boldsymbol{h}(\vec{k}) \overset{\text{Eq. 1.67}}{=} \sum_j \boldsymbol{h}(0, j) \mathrm{e}^{ika_{\text{lat}}j} = \begin{pmatrix} \bar{\epsilon}_1 & -\bar{t} - \bar{t}'\mathrm{e}^{-ika_{\text{lat}}} \\ -\bar{t} - \bar{t}'\mathrm{e}^{ika_{\text{lat}}} & \bar{\epsilon}_2 \end{pmatrix} \tag{1.123}$$

The eigenvalues $\epsilon_n(k)$ and eigenvectors $c_\alpha(k)$ are obtained from the characteristic equation

$$\det|\boldsymbol{h}(k) - \epsilon\mathbf{1}| = 0.$$

$$\begin{aligned}
(\bar{\epsilon}_1 - \epsilon)(\bar{\epsilon}_2 - \epsilon) - \left(-\bar{t} - \bar{t}'\mathrm{e}^{-ika_{\mathrm{lat}}}\right)\left(-\bar{t} - \bar{t}'\mathrm{e}^{+ika_{\mathrm{lat}}}\right) &= 0 \\
\epsilon^2 - 2\frac{\bar{\epsilon}_1 + \bar{\epsilon}_2}{2}\epsilon + \left(\frac{\bar{\epsilon}_1 + \bar{\epsilon}_2}{2}\right)^2 - \left(\frac{\bar{\epsilon}_1 + \bar{\epsilon}_2}{2}\right)^2 + \bar{\epsilon}_1\bar{\epsilon}_2 &= \bar{t}^2 + \bar{t}'^2 + 2\bar{t}\bar{t}'\cos(ka_{\mathrm{lat}}) \\
\left(\epsilon - \frac{\bar{\epsilon}_1 + \bar{\epsilon}_2}{2}\right)^2 &= \left(\frac{\bar{\epsilon}_1 - \bar{\epsilon}_2}{2}\right)^2 + \bar{t}^2 + \bar{t}'^2 + 2\bar{t}\bar{t}'\cos(ka_{\mathrm{lat}}) \\
\epsilon_n(k) &= \frac{\bar{\epsilon}_1 + \bar{\epsilon}_2}{2} \pm \sqrt{\left(\frac{\bar{\epsilon}_1 - \bar{\epsilon}_2}{2}\right)^2 + \bar{t}^2 + \bar{t}'^2 + 2\bar{t}\bar{t}'\cos(ka_{\mathrm{lat}})}
\end{aligned} \tag{1.124}$$

The first band $n = 1$ is obtained with $\pm = -$ and the second band is obtained with $\pm = +$.

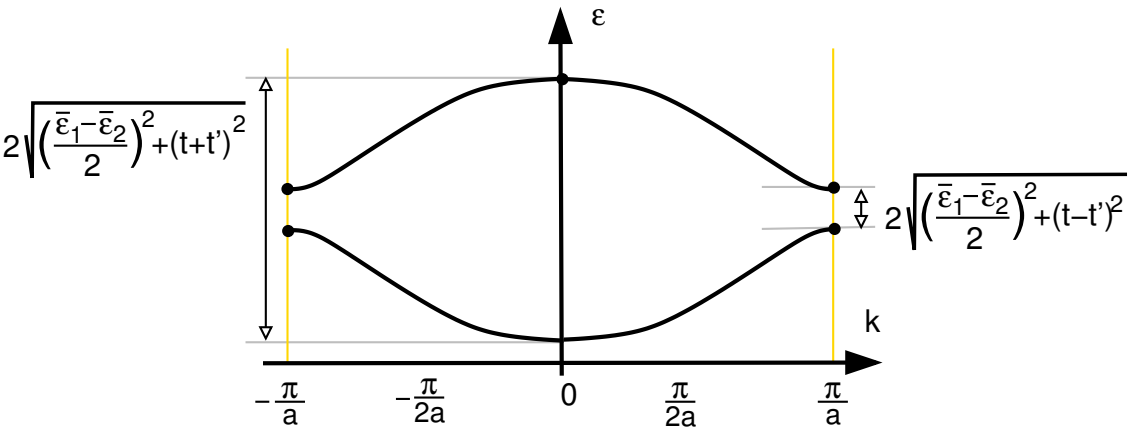

Fig. 1.8: Band structure of the alternating linear chain. See text for the definition of the symbols. The indices of the hopping parameters have been dropped. Editor: the hopping parameters in the figure need a bar

Let us investigate some special cases

- chain of decoupled molecules: We set one hopping parameter to zero, i.e. $\bar{t}' = 0$. The result are two k-independent bands for the molecular orbitals

$$\epsilon_n(k) = \frac{\bar{\epsilon}_1 + \bar{\epsilon}_2}{2} \pm \sqrt{\left(\frac{\bar{\epsilon}_1 - \bar{\epsilon}_2}{2}\right)^2 + \bar{t}^2} \tag{1.125}$$

- both atoms and hopping parameters are identical, i,e, $\bar{\epsilon}_1 = \bar{\epsilon}_2$ and $\bar{t} = \bar{t}'$.

$$\begin{aligned}
\epsilon_n(k) &= \bar{\epsilon}_1 \pm \sqrt{2\bar{t}^2 + 2\bar{t}^2\cos(ka_{\mathrm{lat}})} = \bar{\epsilon}_1 \pm |\bar{t}|\underbrace{\sqrt{2 + 2\cos(ka_{\mathrm{lat}})}}_{\sqrt{4\cos^2(ka_{\mathrm{lat}}/2)}} \\
&= \bar{\epsilon}_1 \pm \left|2\bar{t}\cos\left(\frac{1}{2}ka_{\mathrm{lat}}\right)\right|
\end{aligned} \tag{1.126}$$

This is the band structure of a mono-atomic chain

$$\epsilon(k) = \bar{\epsilon}_1 + 2\bar{t}\cos\left(\frac{ka_{\mathrm{lat}}}{2}\right)$$

folded back into the first Brillouin zone.

- for alternating orbital energies or alternating hopping matrix elements, The band gap at the zone boundary opens, so that an insulator is obtained if the orbitals are half filled.

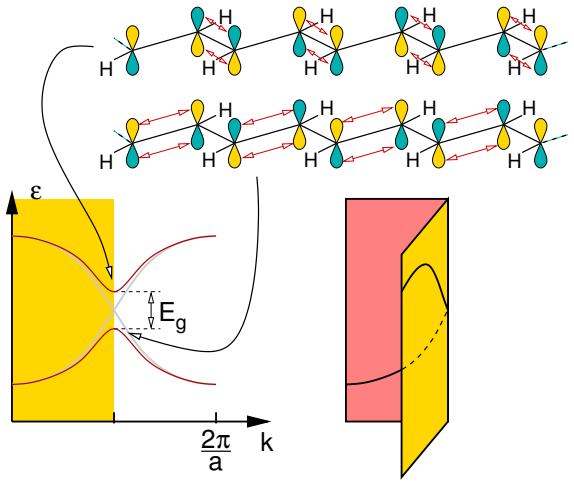

Fig. 1.9: Folding back of the band structure into the reciprocal cell of a doubled real-space unit cell. The example is shown for the one-dimensional molecule acetylene, which undergoes a Peierls distortion, which doubles the unit cell. Only the p-orbitals perpendicular to the molecular plane are considered. Editor: The commonly used picture of folding back is not exactly how the band structure is deformed. Rather it is a shift of the band structure by $\pi/2$. A new graph may be useful.

Note that $\bar{t}$ and $\bar{t}'$ are negative, because it is approximately equal to the overlap matrix element multiplied with the potential in the bond-center. The potential is negative.

2 Determine the k-dependent wave functions.

The eigenvectors $\vec{c}_\pm$ are obtained from

$$\Big[\boldsymbol{h}(k) - \epsilon_\pm(k)\mathbf{1}\Big]\vec{c}_\pm(\vec{k}) = 0 \tag{1.127}$$

where the k-dependent Hamiltonian is taken from Eq. 1.123. We parameterize the eigenstates in terms of a mixing angle $\gamma(\vec{k})$, i.e.

$$\begin{pmatrix} c_{1,-}(k) \\ c_{2,-}(k) \end{pmatrix} = \begin{pmatrix} \cos(\gamma(k)) \\ \sin(\gamma(k))\mathrm{e}^{i\phi(k)} \end{pmatrix} \quad \text{and} \quad \begin{pmatrix} c_{1,+}(k) \\ c_{2,+}(k) \end{pmatrix} = \begin{pmatrix} -\sin(\gamma(k))\mathrm{e}^{-i\phi(k)} \\ \cos(\gamma(k)) \end{pmatrix} \tag{1.128}$$

which ensures the normalization and the orthonormality of the two states

We use the k-dependent Hamiltonian Eq. 1.123 and the eigenvalue Eq. 1.124.

$$\begin{aligned} 0 &= \Big[h_{11}(k) - \epsilon_-(k)\Big]\cos(\gamma(k)) + h_{12}(k)\sin(\gamma(k))\mathrm{e}^{i\phi(k)} \\ &= \left(\frac{\bar{\epsilon}_1 - \bar{\epsilon}_2}{2} + \sqrt{\left(\frac{\bar{\epsilon}_1 - \bar{\epsilon}_2}{2}\right)^2 + \bar{t}^2 + \bar{t}'^2 + 2\bar{t}\bar{t}'\cos(k a_{\mathrm{lat}})}\right)\cos(\gamma(k)) + \left(-\bar{t} - \bar{t}'\mathrm{e}^{-ika_{\mathrm{lat}}}\right)\sin(\gamma(k))\mathrm{e}^{i\phi(k)} \end{aligned} \tag{1.129}$$

$$\begin{aligned} \mathrm{e}^{i\phi(k)} &= \left(\frac{\bar{t} + \bar{t}'\mathrm{e}^{-ika_{\mathrm{lat}}}}{|\bar{t} + \bar{t}'\mathrm{e}^{-ika_{\mathrm{lat}}}|}\right)^* \\ \phi(k) &= -\mathrm{atan}\left(\frac{\mathrm{Im}(\bar{t} + \bar{t}'\mathrm{e}^{-ika_{\mathrm{lat}}})}{\mathrm{Re}(\bar{t} + \bar{t}'\mathrm{e}^{-ika_{\mathrm{lat}}})}\right) = -\mathrm{atan}\left(\frac{\bar{t}'\sin(-ka_{\mathrm{lat}})}{\bar{t} + \bar{t}'\cos(-ka_{\mathrm{lat}})}\right) = \mathrm{atan}\left(\frac{\sin(ka_{\mathrm{lat}})}{\bar{t}/\bar{t}' + \cos(ka_{\mathrm{lat}})}\right) \end{aligned} \tag{1.130}$$

$$\left(\frac{\bar{\epsilon}_1-\bar{\epsilon}_2}{2}+\sqrt{\left(\frac{\bar{\epsilon}_1-\bar{\epsilon}_2}{2}\right)^2+\bar{t}^2+\bar{t}'^2+2\bar{t}\bar{t}'\cos(ka_{\text{lat}})}\right)\cos(\gamma(k))=\left|\bar{t}+\bar{t}'e^{-ika_{\text{lat}}}\right|\sin(\gamma(k)) \tag{1.131}$$

$$\begin{aligned}\gamma(k)&=\operatorname{atan}\left(\frac{\frac{\bar{\epsilon}_1-\bar{\epsilon}_2}{2}+\sqrt{\left(\frac{\bar{\epsilon}_1-\bar{\epsilon}_2}{2}\right)^2+\bar{t}^2+\bar{t}'^2+2\bar{t}\bar{t}'\cos(ka_{\text{lat}})}}{\left|\bar{t}+\bar{t}'e^{-ika_{\text{lat}}}\right|}\right)\\&=\operatorname{atan}\left(\frac{\bar{\epsilon}_1-\bar{\epsilon}_2}{2\sqrt{\bar{t}^2+\bar{t}'^2+2\bar{t}\bar{t}'\cos(ka_{\text{lat}})}}+\sqrt{1+\left(\frac{\bar{\epsilon}_1-\bar{\epsilon}_2}{2\sqrt{\bar{t}^2+\bar{t}'^2+2\bar{t}\bar{t}'\cos(ka_{\text{lat}})}}\right)^2}\right)\end{aligned} \tag{1.132}$$

Editor: finish it by inserting it into the expression for the eigenvectors
Editor: exploit

$$|\bar{t}\pm\bar{t}'e^{ika_{\text{lat}}}|^2=\bar{t}^2+\bar{t}'^2\pm2\bar{t}\bar{t}'\cos(ka_{\text{lat}}) \tag{1.133}$$

1.5.5 Free-electron gas or jellium model

Introduction

The **jellium model**, also called **free-electron gas**, describes a system of electrons with a homogeneous charge background ensuring overall charge neutrality.

In the jellium model, the atom-cores are smeared out into a neutralizing charge background, which effectively removes the effects of the atomic structure. We can still exploit the complete translational and rotational symmetry of free space. The Coulomb potential due to neutralizing charge background is captured by a constant potential V_0, which acts on the electrons. Usually, V_0 is set to zero, by using it as the zero of the energy scale. A global constant can be added to the potential because of the gauge symmetry of electric potential.[24] The gauge symmetry says that such a global potential shift has no effect on the observable properties of the system.

The Hamiltonian for the free-electron gas is

$$\hat{h} = \sum_{\sigma} \frac{\hat{\vec{p}}^2}{2m_e} + V_0 \tag{1.134}$$

where m_e is the electron mass.

When the Fermi level lies within the spectrum of the free-electron gas, i.e. $\mu > V_0$ (or better $\mu - V_0 \gg k_B T$), we call it a **degenerate electron gas**. The degenerate electron gas is a model for a metal.

The free-electron gas is not only useful to describe the behavior of metals, but it is also valuable to understand semi-conductors and insulators. In those cases, the free-electron gas is a model for electrons near the band edges, where the bands can be approximated by parabolic bands. These situations are described by a **dilute electron gas**, as opposed to the degenerate electron gas. A dilute electron gas is characterized by a Fermi level that lies below the bottom of the band, i.e. $\mu < V_0$ (or better $V_0 - \mu \gg k_B T$).

By changing the sign of the kinetic energy, for example by using a negative mass, the free-electron gas is a model for holes (missing electrons) in the valence band of a semiconductor.

Outloook on magnetism: This exercise contributes one ingredient to the understanding of magnetism:

- For the non-interacting electron gas, we find that the energy is lowest if the electron gas has no magnetic moment. We can evaluate the magnetic susceptibility of this non-interacting electron gas.
- The Pauli prinicple reduces the effective Coulomb repulsion of electrons with equal spin, because electrons with equal spin come close to each other only rarely. One consequence is **Hund's rule**, which says that electrons in a angular momentum shell of an atom tend to align with parallel spin. The same effect makes electrons with the same spin favorable also in an electron gas. The Coulomb interaction in combination with the Pauli principle favors a ferromagnetic alignment of the spins.

What keeps the electron gas to be magnetic is the kinetic energy of the electron gas that is calculated here. Hence, whether an electron gas is magnetic or not is decided by the balance between kinetic energy and the Coulomb interaction.

Problem

Let us describe the free-electron gas with **periodic boundary conditions** in a cubic box with side length L. The wave functions shall be normalized with in the box. As we approach the final result, we let L go to infinity.

[24] See gauge symmetry of the electromagnetic potentials in ΦSX: Elektrodynamik.[21].

1 Calculate the band structure of the free-electron gas

2 Calculate the density of states of the free-electron gas with a specified electron density.

3 Calculate the energy of the non-magnetic electron gas

4 Calculate the energy of the spin-polarized electron gas as function of the spin polarization n_s/n_t, where $n_s = n_\uparrow - n_\downarrow$ is the spin density and $n_t = n_\uparrow + n_\downarrow$ is the total electron density. Without restriction of generality (WroG), the magnetization is oriented along the z-direction.

Discussion

Band structure

1 Calculate the band structure of the free-electron gas

The wave functions are

$$|\psi_{\vec{k},\sigma}\rangle = \sum_{\sigma'} \int_V d^3r \; |\vec{r},\sigma'\rangle \frac{1}{\sqrt{L^3}} e^{i\vec{k}\vec{r}} \delta_{\sigma,\sigma'} \tag{1.135}$$

The integration region V is a three-dimensional cubic box of side-length L. The box is both, the normalization volume, and the supercell defining the periodic boundary conditions.

$$\psi(\vec{r} + \vec{e}_j L, \sigma) = \psi)\vec{r},\sigma) \tag{1.136}$$

where $\vec{e}_j$ is the unit vector pointing along the j-th cartesian coordinate.

The boundary conditions limit the wave vectors to a discrete set

$$\vec{k}_{i_1,i_2,i_3} = \frac{2\pi}{L} \begin{pmatrix} i_1 \\ i_2 \\ i_3 \end{pmatrix} \qquad \text{with integer } i_1, i_2, i_3 \in \mathbb{I} \tag{1.137}$$

The one-particle energies are

$$\epsilon_\sigma(\vec{k}) = \langle \psi_{\vec{k},\sigma} | \hat{h} | \psi_{\vec{k},\sigma} \rangle = V_0 + \frac{\hbar^2 \vec{k}^2}{2m_e} \tag{1.138}$$

This defines the dispersion relation, i.e. the band structure of the free-electron gas.

Density of states

2 Calculate the density of states of the free-electron gas

The **density of states** $D(\epsilon)$ is best evaluated[1] indirectly from the number-of-states function [25] $\mathcal{N}(\epsilon)$ as $D(\epsilon) = \partial_\epsilon \mathcal{N}(\epsilon)$.

The number of states of the free-electron gas is obtained from the the occupied region of k-space. In a free electron gas, the occupied states lie within a sphere with $\epsilon < (\hbar k)^2/2m_e$. The k-points

[25]

$$D(\epsilon) = \sum_n \delta(\epsilon - \epsilon_n) = \sum_n \partial_\epsilon \theta(\epsilon - \epsilon_n) = \partial_\epsilon \sum_n \theta(\epsilon - \epsilon_n) = \partial_\epsilon \mathcal{N}(\epsilon) \tag{1.139}$$

The number-of-states function $\mathcal{N}(\epsilon)$ is defined as the number of states with energy below ϵ. The particle number $N_{T,\mu}$ is only loosely related to the number of states function $\mathcal{N}(\epsilon)$. The relation is $N_{T=0,\mu} = \mathcal{N}(\mu)$.

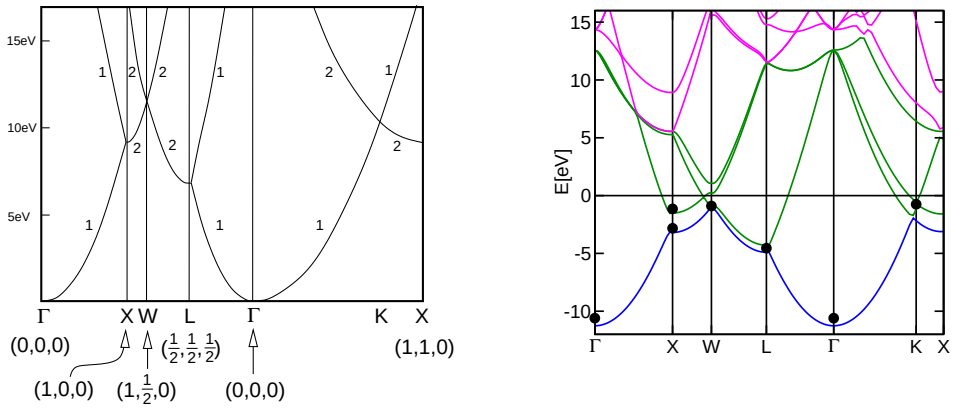

Fig. 1.10: Band structure of free, non-interacting electrons. The lattice is an fcc-cell with a lattice constant of 4.05 Å corresponding to aluminum. The high symmetry points are given in units of $\frac{2\pi}{a_{\text{lat}}}$. The numbers indicate the degeneracy beyond spin-degeneracy. On the right-hand side, the band structure of aluminum is shown in comparison.

are determined by the periodic boundary conditions. The reciprocal-space volume per k-point is $\Delta k^3 = (2\pi/L)^3$.

$$\begin{aligned}\mathcal{N}(\epsilon) &= \underbrace{\left(\sum_{\sigma\in\{\uparrow,\downarrow\}}\right)}_{2} \overbrace{\frac{4\pi}{3}\underbrace{\left(\frac{1}{\hbar}\sqrt{2m_e(\epsilon-V_0)}\right)}_{k(\epsilon)}{}^3}^{\text{occupied rec.space volume}} \underbrace{\left(\frac{2\pi}{L}\right)^{-3}}_{\Delta k^{-3}} \theta(\epsilon-V_0) \\ &= \underbrace{V}_{L^3}\underbrace{\left(\sum_{\sigma\in\{\uparrow,\downarrow\}}\right)}_{2}\left(\frac{\sqrt{2m_e}}{2\pi\hbar}\right)^3 \frac{4\pi}{3}(\epsilon-V_0)^{\frac{3}{2}}\theta(\epsilon-V_0) \end{aligned} \tag{1.140}$$

The Heaviside step function $\theta(\epsilon - V_0)$ has been included because the number of states is zero for energies below the parabola $\epsilon_\sigma(k)$ in Eq. 1.138, i.e. for $\epsilon \leq V_0$.

The density of states is thus

$$D(\epsilon) = \partial_\epsilon \mathcal{N}(\epsilon) = \underbrace{V}_{L^3}\underbrace{\left(\sum_{\sigma\in\{\uparrow,\downarrow\}}\right)}_{2}\left(\frac{\sqrt{2m_e}}{2\pi\hbar}\right)^3 2\pi\theta(\epsilon-V_0)\sqrt{\epsilon-V_0} \tag{1.141}$$

My convention to define the number of states and the density of states as extensive quantities is uncommon. Usually, the numbers are divided by volume or calculated for a specified unit cell of a crystal. I have chosen my convention to avoid ambiguity: Because of the volume occurring in the expression, it is apparent that it is an extensive quantity. By scaling the result, one obtains the other choices.

The square-root behavior of the density of states in Eq. 1.141 is characteristic for the density of states of parabolic bands in three dimensions. This behavior is regularly observed near band edges in three dimensions.[26]

Let us now turn to the thermodynamic properties.

[26] The dimensionality has a large impact in the shape of the density of states.

Energy of the non-magnetic electron gas

3 Calculate the energy of the non-magnetic electron gas with a specified electron density.

Editor:

$$E(N) = \operatorname*{stat}_{\mu} E(\mu) - \mu(\mathcal{N}(\mu) - N)$$
$$E(N_t, N_s) = \operatorname*{stat}_{B,V} E(\mu_\uparrow, \mu_\downarrow) - \mu_e B(N_\uparrow - N_\downarrow - N_s) + V(N_\uparrow + N_\downarrow - N_t) \tag{1.142}$$

The energy calculated from the density of states depends on the chemical potential μ. The particle number as function of chemical potential allows one to obtain the chemical potential.

Let me express particle number and the energy as an integral over the density of states, that has obtained earlier in Eq. 1.141. The chemical potential is the Fermi level.

$$\mathcal{N}(\mu) = \int_{-\infty}^{\mu} d\epsilon\, D(\epsilon) \quad \text{and} \quad E(\mu) = \int_{-\infty}^{\mu} d\epsilon\, D(\epsilon)\epsilon \tag{1.143}$$

The density of states of the free-electron gas in three dimensions, Eq. 1.141, can be written as

$$D(\epsilon) = C\theta(\epsilon - V_0)\sqrt{\epsilon - V_0} \qquad \text{with} \quad C = L^3 \underbrace{\left(\sum_{\sigma\in\{\uparrow,\downarrow\}}\right)}_{2} \left(\frac{\sqrt{2m_e}}{2\pi\hbar}\right)^3 2\pi \tag{1.144}$$

$$\mathcal{N}(\mu) \overset{\text{Eq. 1.143}}{=} C \underbrace{\frac{2}{3}(\mu - V_0)^{\frac{3}{2}}}_{\int_{V_0}^{\mu} d\epsilon\, \sqrt{\epsilon - V_0}} \qquad \Rightarrow \qquad \mu - V_0 = \left(\frac{3\mathcal{N}(\mu)}{2C}\right)^{\frac{2}{3}}$$

$$E(\mu) \overset{\text{Eq. 1.143}}{=} \underbrace{V_0\mathcal{N}(\mu) + \frac{2}{5}C(\mu - V_0)^{\frac{5}{2}}}_{C\int_{V_0}^{\mu} d\epsilon\, \epsilon\sqrt{\epsilon - V_0}}$$

$$= V_0\mathcal{N}(\mu) + \frac{2C}{5}\left(\frac{3\mathcal{N}(\mu)}{2C}\right)^{\frac{5}{3}} = V_0\mathcal{N}(\mu) + \frac{2}{5}C^{-\frac{2}{3}}\left(\frac{3\mathcal{N}(\mu)}{2}\right)^{\frac{5}{3}}$$

$$\overset{\text{Eq. 1.144}}{=} V_0\mathcal{N}(\mu) + \underbrace{\left[L^3\left(\sum_{\sigma\in\{\uparrow,\downarrow\}}\right)\left(\frac{\sqrt{2m_e}}{2\pi\hbar}\right)^3 2\pi\right]^{-\frac{2}{3}}}_{C} \frac{2}{5}\left(\frac{3}{2}\right)^{\frac{5}{3}} L^5\left(\frac{\mathcal{N}(\mu)}{L^3}\right)^{\frac{5}{3}}$$

$$= V_0\mathcal{N}(\mu) + L^3\left(\frac{1}{2}\sum_{\sigma\in\{\uparrow,\downarrow\}}\right)^{-\frac{2}{3}}\left[2\left(\frac{2}{4\pi^2}\right)^{\frac{3}{2}}2\pi\right]^{-\frac{2}{3}} \underbrace{\frac{3}{10}}_{\frac{2}{5}\cdot\frac{3}{2}} 2 \underbrace{\left(\frac{2}{3}\right)^{-\frac{2}{3}}}_{\frac{2}{3}\left(\frac{3}{2}\right)^{\frac{5}{3}}} \frac{\hbar^2}{m_e}\left(\frac{\mathcal{N}(\mu)}{L^3}\right)^{\frac{5}{3}}$$

$$= \underbrace{V_0\mathcal{N}(\mu)}_{E_{pot}} + \underbrace{L^3\frac{3}{10}\left(\frac{1}{2}\sum_{\sigma\in\{\uparrow,\downarrow\}}\right)^{-\frac{2}{3}}\left(3\pi^2\right)^{\frac{2}{3}}\frac{\hbar^2}{m_e}\left(\frac{\mathcal{N}(\mu)}{L^3}\right)^{\frac{5}{3}}}_{E_{kin}} \tag{1.145}$$

I use the factor $\frac{1}{2}\sum_{\sigma\in\{\uparrow,\downarrow\}}$ to make the spin-degeneracy explicit, while keeping the expression for a non-spin polarized electron gas simple, because this factor equals unity.

Thus, the potential energy per volume is

$$\frac{1}{L^3}E_{\text{pot}} = V_0 n_t \tag{1.146}$$

and the kinetic energy per volume is

$$\frac{1}{L^3}E_{\text{kin}}(n_t) = \frac{3}{10}\left(3\pi^2\right)^{\frac{2}{3}}\frac{\hbar^2}{m_e}n_t^{\frac{5}{3}} \tag{1.147}$$

where $n_t \stackrel{\text{def}}{=} \frac{1}{L^3}\mathcal{N}(\mu)$ is the total (both spin directions) electron density.

Energy functional for the spin-polarized electron gas

4 Calculate the energy of the spin-polarized electron gas as function of the spin polarization n_s/n_t, where $n_s = n_\uparrow - n_\downarrow$ is the spin density and $n_t = n_\uparrow + n_\downarrow$ is the total electron density. Without restriction of generality (WroG), the magnetization is oriented along the z-direction.

Next we can also determine the energy as function of the spin polarization. The spin polarization is the ratio between the spin density n_s and the total density n_t. The spin density for an electron gas polarized in z direction is $n_s = n_\uparrow - n_\downarrow$.

$$\frac{1}{L^3}\left(E_{\text{kin}}(n_\uparrow) + E_{\text{kin}}(n_\downarrow)\right) \stackrel{\text{Eq. 1.147}}{=} \frac{3}{10}\left(3\pi^2\right)^{\frac{2}{3}}\frac{\hbar^2}{m_e}\frac{1}{2}\left((2n_\uparrow)^{\frac{5}{3}} + (2n_\downarrow)^{\frac{5}{3}}\right) \tag{1.148}$$

With $n_\uparrow = \frac{1}{2}(n_t + n_S)$ and $n_\downarrow = \frac{1}{2}(n_t - n_S)$, we obtain

KINETIC ENERGY OF THE NON-INTERACTING FREE ELECTRON GAS

This is the Thomas-Fermi expression for the kinetic energy of a non-interacting homogeneous electron gas at zero Kelvin.

$$\frac{1}{L^3}E_{\text{kin}}(n_t, n_s) = \underbrace{\frac{3}{10}\left(3\pi^2\right)^{\frac{2}{3}}\frac{\hbar^2}{m_e}n_t^{\frac{5}{3}}}_{E(n_t,0)/L^3} \cdot \underbrace{\frac{1}{2}\left(\left(1+\frac{n_s}{n_t}\right)^{\frac{5}{3}} + \left(1-\frac{n_s}{n_t}\right)^{\frac{5}{3}}\right)}_{\approx 1+(2^{\frac{2}{3}}-1)\left(\frac{n_s}{n_t}\right)^2} \tag{1.149}$$

where $n_t \stackrel{\text{def}}{=} \frac{1}{L^3}\mathcal{N}(\mu) = n_\uparrow + n_\downarrow$ is the **total electron density** (both spin directions)and $n_s = n_\uparrow - n_\downarrow$ is the **spin density** .
The spin dependence of the kinetic energy is shown in Fig. 1.11. The dependence of the spin polarization can fairly well be approximated by a simple parabola.

This expression is significant to understand the interacting homogeneous electron gas. It is further used in the Thomas-Fermi approximation of electrons. The Thomas-Fermi approximation is a predecessor of the Density Functional Theory (DFT), for which its inventor Walter Kohn received the Nobel price in chemistry 1998.

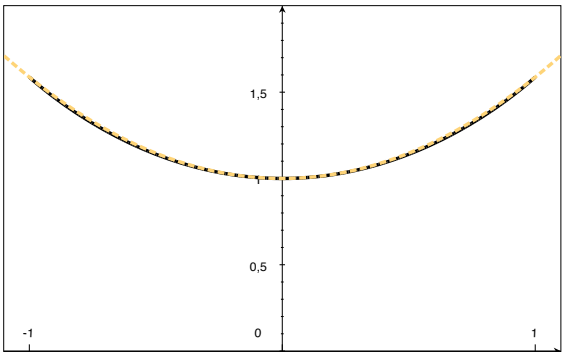

Fig. 1.11: Dependence of the kinetic energy of the free-electron gas on the spin polarization n_s/n_t. The dashed line is the approximation by a simple parabola, which is surprisingly accurate.

Chapter 2

Weakly interacting electrons

In order to explore the role of interactions, let us start with small interactions. The interaction energy can be obtained in first-order perturbation theory using the wave functions of the non-interacting system, namely Slater determinants. Slater determinants have a particularly simple structure, which allows one to express most quantities in terms of one-particle wave functions.

Because the Coulomb interaction between electrons is strong, one may question the reliability of such an approach. This concern is justified. However, in practice we do not start the perturbation theory from a truly non-interacting system: Rather, we choose an effective one-particle potential and a renormalized interaction. The effective potential considers also the electron-electron repulsion and the renormalized interaction takes into account that the interaction is screened by the electron gas between two charges. Both effects lead to substantially reduced effective interaction, which usually can be well described by perturbation theory.

One such description using one-particle wave functions is the self-consistent Hartree-Fock method. The **Hartree-Fock method** [22, 23, 24] is an electronic-structure method that is the work-horse of quantum chemistry. Today it plays an important role as a starting point of more accurate and involved methods.

"One may get the impression that modern many-body theory, of which one hears so much, goes far beyond Hartree-Fock, and that therefore we should not bother with such old-fashioned stuff. This is not at all true– in fact, modern many-body theory has mostly just served to show us how, where, and when to use Hartree-Fock theory and how flexible and useful a technique it can be." P.W. Anderson, 1963[25]

Another description using one-particle wave functions is **density-functional theory**(DFT). In contrast to the Hartree-Fock approximation, density functional theory is formally exact, albeit limited to ground states, respectively equilibrium ensembles. This method is the workhorse for first-principles calculations and widely used for quantitative calculations of materials and molecules considering the quantum nature of the electronic structure. Despite the different foundation of density functional theory and the Hartree-Fock method, they exhibit many similarities that provide a insights for first-principles calculations.

Let me return to the Hartree-Fock method discussed in this chapter: The basic idea of the Hartree-Fock method is to restrict the wave functions to Slater determinants[22]. The wave function is borrowed from a non-interacting system, but one chooses the very best non-interacting system for that purpose.

After having defined Slater determinants in the previous chapter, in this chapter we will gain some familiarity with them. We will see, how non-interacting many-particle systems can be described by a set of one-particle wave functions. Furthermore, we will become familiar with the most important contributions of the electron interaction, namely **Hartree energy** and **exchange energy**.

Then we will explore the energetics. I will directly step into the finite temperature formalism, in order to prepare the ground for the finite temperature Green's function formalism discussed later.

While being slighly more complex, the finite-temperature point of view avoids a number of difficulties inherent in the zero-temperature formalism. We will learn the implications of the mean-field approximation, which is inherent in Hartree-Fock approximation. While density functional theory does not make the mean-field approximation, the understanding of the Hartree-Fock approximation sheds light onto concepts of density-functional theory.

In this chapter, I will also introduce the concept **spectral function**, which can be probed experimentally. Besides determining the state the system is in, understanding the response of the system to an external perturbation is the second most important goal of theoretical solid state physics, if not of all physics.

- The state is often determined assuming thermal equilibrium.[1] Thermal equilibrium is based on the energy of the system.
- The response of the system requires the understanding of excited states. The latter are described by the spectral function.

2.1 Expectation values of Slater determinants

The development of a suitable notation had a large impact on many-partcle physics. We will later use the occupation-number representation and, creation and annihilation operators. Until then, we need to live with a conventional notation, which is a bit clumsy for many-particle physics. This means that it may not be worth trying to memorize formulas in this notation. Nevertheless, it will remain important to be able to translate the expressions from the elegant, but also abstract, notations into the conventional wave function notation.

2.1.1 One- and two-particle operators

The total energy[2] for an N-electron system has the form

$$E = E_{NN} + \langle\Psi|\hat{h} + \hat{W}|\Psi\rangle \tag{2.1}$$

where

$$E_{NN}(\vec{R}_1, \ldots, \vec{R}_M) \stackrel{\text{def}}{=} \frac{1}{2}\sum_{i\neq j}^{M} \frac{e^2 Z_i Z_j}{4\pi\epsilon_0|\vec{R}_i - \vec{R}_j|} \tag{2.2}$$

is the electrostatic repulsion between the nuclei. The operators acting on the electrons can be divided into a one-particle operator $\hat{h}$ and a two-particle operator $\hat{W}$.

The operator $\hat{h}$ in Eq. 2.1 describes the kinetic energy and the potential energy of the electrons in an external potential. The external potential describes the electrostatic attraction between electrons and nuclei with atomic number Z_j and position $\vec{R}_j$

$$v_{ext}(\vec{r}) = -\sum_{j=1}^{M} \frac{e^2 Z_j}{4\pi\epsilon_0|\vec{r} - \vec{R}_j|} \tag{2.3}$$

In the following, I will use the unit operator in Fock space

$$\hat{1} = \sum_{N=0}^{\infty} \int d^4x_1 \cdots \int d^4x_N \, |\vec{x}_1, \ldots, \vec{x}_N\rangle\langle\vec{x}_1, \ldots, \vec{x}_N| \tag{2.4}$$

[1] Non-equilibrium states are usually constructed by a controlled perturbation of thermal equilibrium state.

[2] We consider here the Born-Oppenheimer Hamiltonian $\hat{H}^{BO}(R)$ Eq. 2.4 of ΦSX: Introduction to Solid State Theory.

where $|\vec{x}_1, \ldots, \vec{x}_N\rangle = |\vec{x}_1\rangle \otimes \ldots \otimes |\vec{x}_N\rangle$ is a product state.[3] The term for $N = 0$ is the **vacuum state** $|\mathcal{O}\rangle$. The vacuum state cannot be described by a wave function, but only by a single complex number.

The Hamiltonian $\hat{h}$ is called a **one-particle operator**, because it acts on all particles, but only on one at a time. To make the distinction to an operator in one-particle Hilbert space explicit, I will call such operators also **one-particle-at-a-time operators** .

Let $\hat{h}_j$ be the Hamiltonian acting on the j-th electron of an N-particle state

$$\hat{h}_j = \int d^4x_1 \cdots \int d^4x_N \; |\vec{x}_1, \ldots, \vec{x}_N\rangle \left[\frac{-\hbar^2}{2m_e}\vec{\nabla}^2_{\vec{r}_j} + v_{ext}(\vec{r}_j)\right] \langle \vec{x}_1, \ldots, \vec{x}_N| \tag{2.5}$$

Each electron has the same kinetic energy and experiences the same external potential. The operator acting on all the electrons is the sum

$$\hat{h} = \sum_{N=0}^{\infty} \sum_{j=1}^{N} \hat{h}_j \tag{2.6}$$

The second operator in Eq. 2.1, $\hat{W}$, describes the Coulomb interaction between the electrons. The Coulomb interaction cannot be decomposed in a sum over all electrons. Rather, we need to consider electron pairs

$$\hat{W} = \sum_{N=0}^{\infty} \frac{1}{2} \sum_{i \neq j}^{N} \hat{W}_{i,j} \tag{2.7}$$

with

$$\hat{W}_{i,j} = \int d^4x_1 \cdots \int d^4x_N \; |\vec{x}_1, \ldots, \vec{x}_N\rangle \frac{e^2}{4\pi\epsilon_0 |\vec{r}_i - \vec{r}_j|} \langle \vec{x}_1, \ldots, \vec{x}_N| \tag{2.8}$$

As above, the indices i and j denote the two interacting electrons. Because two particles need to be considered at a time, the operator $\hat{W}$ is called a **two-particle operator**. The two-particle term is the cause for the dazzling complexity of many-particle physics.

To make the definition of one- and two-particle operators more concise, let me consider a general operator $\hat{A}$ in the Fock space space

$$\begin{aligned}
\hat{A} = & \underbrace{\sum_{N=0}^{\infty} \int d^4x_1 \cdots \int d^4x_N \; |\vec{x}_1, \ldots, \vec{x}_N\rangle\langle \vec{x}_1, \ldots, \vec{x}_N|}_{\hat{1}} \\
& \times \quad \hat{A} \quad \underbrace{\sum_{N'=0}^{\infty} \int d^4x'_1 \cdots \int d^4x'_{N'} \; |\vec{x'}_1, \ldots, \vec{x'}_{N'}\rangle\langle \vec{x'}_1, \ldots, \vec{x'}_{N'}|}_{\hat{1}} \\
= & \sum_{N,N'=0}^{\infty} \int d^4x_1 \cdots \int d^4x_N \int d^4x'_1 \cdots \int d^4x'_{N'} \\
& \times \quad |\vec{x}_1, \ldots, \vec{x}_N\rangle\langle \vec{x}_1, \ldots, \vec{x}_N|\hat{A}|\vec{x'}_1, \ldots, \vec{x'}_{N'}\rangle\langle \vec{x'}_1, \ldots, \vec{x'}_{N'}|
\end{aligned} \tag{2.9}$$

A matrix element $\langle \vec{x}_1, \ldots, \vec{x}_N|\hat{A}|\vec{x'}_1, \ldots, \vec{x'}_{N'}\rangle$ has therefore $N + N'$ arguments.

- If the matrix element of an operator has the special form

$$\langle \vec{x}_1, \ldots, \vec{x}_N|\hat{A}|\vec{x'}_1, \ldots, \vec{x'}_{N'}\rangle = \delta_{N,N'} \sum_{i=1}^{N} \underbrace{A(\vec{x}_i, \vec{x'}_i)}_{\langle \vec{x}_i|\hat{A}|\vec{x'}_i\rangle} \prod_{\substack{j=1 \\ j\neq i}}^{N} \delta(\vec{x}_j - \vec{x'}_j) \tag{2.10}$$

  we call the operator a **one-particle operator**.

[3] Some caution is required to distinguish product states from Slater determinants and permanents.

- If the matrix element of an operator has the special form

$$\langle \vec{x}_1, \ldots, \vec{x}_N | \hat{A} | \vec{x'}_1, \ldots, \vec{x'}_{N'} \rangle = \delta_{N,N'} \frac{1}{2} \sum_{i,j=1}^{N} \underbrace{A(\vec{x}_i, \vec{x}_j, \vec{x'}_i, \vec{x'}_j)}_{\langle \vec{x}_i, \vec{x}_j | \hat{A} | \vec{x'}_i, \vec{x'}_j \rangle} \prod_{\substack{k=1 \\ k \notin \{i,j\}}}^{N} \delta(\vec{x}_k - \vec{x'}_k) \tag{2.11}$$

  we call the operator a **two-particle operator**.

The term "one-particle operator" is ambiguous, which makes it confusing.

- On the one hand, it may be a **true one-particle operator** in the one-particle Hilbert space. It acts on states that describe exactly a single electron.

- On the other hand, it may be a **one-particle-at-a-time operator** in the N-particle Hilbert space or the Fock space. Such an operator acts on many-particle states, but it acts on one electron at a time. The result is a sum over the contributions from the individual particles.

Let us now work out the expectation values for the one-particle and two-particle operators for a Slater determinant.

2.1.2 Expectation value of a one-particle operator with a Slater determinant

Here, we will work out the expectation value of a one-particle-at-a-time operator for a Slater determinant. An example for such a one-particle operator is the non-interacting part of the Hamiltonian.

Explicit example for the two-particle wave function

The two-particle Slater determinant $|\Psi\rangle$ of two one-particle orbitals $|\varphi_a\rangle$ and $|\varphi_b\rangle$ has the form

$$\underbrace{\langle \vec{x}_1, \vec{x}_2 | \Psi \rangle}_{\Psi(\vec{x}_1, \vec{x}_2)} = \frac{1}{\sqrt{2}} \underbrace{\Big[\langle \vec{x}_1 | \varphi_a \rangle \langle \vec{x}_2 | \varphi_b \rangle - \langle \vec{x}_1 | \varphi_b \rangle \langle \vec{x}_2 | \varphi_a \rangle \Big]}_{\varphi_a(\vec{x}_1)\varphi_b(\vec{x}_2) - \varphi_b(\vec{x}_1)\varphi_a(\vec{x}_2)} \tag{2.12}$$

As a specific example for a one-particle operator, I choose the particle-density operator $\hat{n}(\vec{r})$ defined as

$$\hat{n}(\vec{r}) = \sum_{\sigma \in \{\uparrow, \downarrow\}} \int d^4x_1 \int d^4x_2 \, |\vec{x}_1, \vec{x}_2\rangle \Big[\delta(\underbrace{\vec{x}}_{(\vec{r},\sigma)} - \vec{x}_1) + \delta(\underbrace{\vec{x}}_{(\vec{r},\sigma)} - \vec{x}_2) \Big] \langle \vec{x}_1, \vec{x}_2 | \tag{2.13}$$

The electron density $n(\vec{r})$ at position $\vec{r}$ of a Slater determinant $|\Psi\rangle$ with two particles in the

one-particle orbitals $\varphi_a(\vec{x})$ and $\varphi_b(\vec{x})$ is

$$
\begin{aligned}
n(\vec{r}) &= \langle\Psi|\hat{n}(\vec{r})|\Psi\rangle \\
&\overset{\text{Eq. 2.13}}{=} \sum_{\sigma\in\{\uparrow,\downarrow\}} \int d^4x_1 \int d^4x_2\ \Psi^*(\vec{x}_1,\vec{x}_2)\Big[\delta(\vec{x}-\vec{x}_1)+\delta(\vec{x}-\vec{x}_2)\Big]\Psi(\vec{x}_1,\vec{x}_2) \\
&\overset{\Psi(\vec{x}_1,\vec{x}_2)=-\Psi(\vec{x}_2,\vec{x}_1)}{=} \sum_{\sigma\in\{\uparrow,\downarrow\}} \Bigg\{ \int d^4x_1 \int d^4x_2\ \Psi^*(\vec{x}_1,\vec{x}_2)\delta(\vec{x}-\vec{x}_1)\Psi(\vec{x}_1,\vec{x}_2) \\
&\qquad + \int d^4x_1 \int d^4x_2\ \Psi^*(\vec{x}_2,\vec{x}_1)\delta(\vec{x}-\vec{x}_2)\Psi(\vec{x}_2,\vec{x}_1)\Bigg\} \\
&\overset{\vec{x}_1\leftrightarrow\vec{x}_2}{=} \sum_{\sigma\in\{\uparrow,\downarrow\}} 2\int d^4x_1 \int d^4x_2\ \Psi^*(\vec{x}_1,\vec{x}_2)\delta(\vec{x}_1-\vec{x})\Psi(\vec{x}_1,\vec{x}_2) \\
&\overset{\text{Eq. 2.12}}{=} \sum_{\sigma\in\{\uparrow,\downarrow\}} \Bigg\{ 2\int d^4x_1 \int d^4x_2\ \frac{1}{\sqrt{2}}\Big[\varphi_a(\vec{x}_1)\varphi_b(\vec{x}_2)-\varphi_b(\vec{x}_1)\varphi_a(\vec{x}_2)\Big]^* \\
&\qquad \times \delta(\vec{x}-\vec{x}_1)\frac{1}{\sqrt{2}}\Big[\varphi_a(\vec{x}_1)\varphi_b(\vec{x}_2)-\varphi_b(\vec{x}_1)\varphi_a(\vec{x}_2)\Big]\Bigg\} \\
&= \sum_{\sigma\in\{\uparrow,\downarrow\}} \Bigg\{ \int d^4x_1 \int d^4x_2\ \varphi_a^*(\vec{x}_1)\varphi_b^*(\vec{x}_2)\delta(\vec{x}-\vec{x}_1)\varphi_a(\vec{x}_1)\varphi_b(\vec{x}_2) \\
&\qquad - \int d^4x_1 \int d^4x_2\ \varphi_a^*(\vec{x}_1)\varphi_b^*(\vec{x}_2)\delta(\vec{x}-\vec{x}_1)\varphi_b(\vec{x}_1)\varphi_a(\vec{x}_2) \\
&\qquad - \int d^4x_1 \int d^4x_2\ \varphi_b^*(\vec{x}_1)\varphi_a^*(\vec{x}_2)\delta(\vec{x}-\vec{x}_1)\varphi_a(\vec{x}_1)\varphi_b(\vec{x}_2) \\
&\qquad + \int d^4x_1 \int d^4x_2\ \varphi_b^*(\vec{x}_1)\varphi_a^*(\vec{x}_2)\delta(\vec{x}-\vec{x}_1)\varphi_b(\vec{x}_1)\varphi_a(\vec{x}_2)\Bigg\} \\
&= \sum_{\sigma\in\{\uparrow,\downarrow\}} \Bigg\{ \langle\varphi_a|\vec{x}\rangle\langle\vec{x}|\varphi_a\rangle \underbrace{\langle\varphi_b|\varphi_b\rangle}_{=1} - \langle\varphi_a|\vec{x}\rangle\langle\vec{x}|\varphi_b\rangle \underbrace{\langle\varphi_b|\varphi_a\rangle}_{=0} \\
&\qquad - \langle\varphi_b|\vec{x}\rangle\langle\vec{x}|\varphi_a\rangle \underbrace{\langle\varphi_a|\varphi_b\rangle}_{=0} + \langle\varphi_b|\vec{x}\rangle\langle\vec{x}|\varphi_b\rangle \underbrace{\langle\varphi_a|\varphi_a\rangle}_{=1}\Bigg\} \\
&= \sum_{\sigma\in\{\uparrow,\downarrow\}} \Big(\varphi_a^*(\vec{x})\varphi_a(\vec{x}) + \varphi_b^*(\vec{x})\varphi_b(\vec{x})\Big) \qquad (2.14)
\end{aligned}
$$

This result can be generalized to arbitrary one-particle operators. The derivation of the general result is provided in appendix H.2.1 on 543. It is summarized as follows:

EXPECTATION VALUE OF A ONE-PARTICLE OPERATOR WITH A SLATER DETERMINANT

The expectation value of a general one-particle operator $\hat{A} = \sum_{j=1}^{N} \hat{a}_j$ with a (N-particle) Slater determinant $|\vec{\sigma}\rangle$ built from orthonormal one-particle orbitals $|\varphi_j\rangle$ with occupation numbers σ_j is

$$\langle\vec{\sigma}|\sum_{j=1}^{N_{\vec{\sigma}}}\hat{a}_j|\vec{\sigma}\rangle \overset{\text{Eq. H.5}}{=} \sum_{j=1}^{N}\langle\varphi_j|\hat{a}|\varphi_j\rangle = \sum_{j=1}^{\infty}\sigma_j\langle\varphi_j|\hat{a}|\varphi_j\rangle\ , \qquad (2.15)$$

that is, a sum over the one-particle states in the Slater determinant, respectively, the sum over occupied one-particle states. Occupied are the one-particle orbitals with occupation numbers $\sigma_j = 1$.

Let me mention a few observations:

- The number of terms is drastically reduced just because we have used an orthonormal set of

one-particle wave functions. A Slater determinant for N electrons is a sum of $N!$ product states. An expectation value has $(N!)^2$ terms, not even considering the number (N) of terms in the operator itself. This is a daunting large number of terms. By exploiting the orthonormality of the one-particle orbitals, the number of terms for a N-particle system is reduced from $N(N!)^2$ to only N. For large systems, this is an enormous simplification. This simplification is the sole reason for (often) using orthonormal basissets in many-particle physics.

- The *sum over particles* is turned into a *sum over orbitals*. Eq. 2.15 is the reason that the sum of orbitals, is often considered as a sum over electrons. This statement is a misnomer, because we cannot attribute an electron to a specific one-particle orbital. Nevertheless, it offers a physical intuitive picture, which may be useful as long as one is aware of its limitations.

- The anti symmetry of the wave function ensures that the same expectation value is obtained, whether we work out a property of the first, the second, or any other electron.[4]

2.1.3 One-particle-reduced density matrix

The physics of non-interacting and weakly interacting particles can be described well by the **one-particle-reduced density matrix** $\hat{\rho}^{(1)}$. The superscript "(1)" distinguishes the one-particle-reduced density matrix from the von-Neumann density matrix $\hat{\rho}^{vN}$ introduced earlier in Eq. 2.54.

The **one-particle-reduced density matrix** of a general ensemble of many-particle wave functions $|\Phi_q\rangle$ with probabilities P_q is defined such that any expectation value $\langle A\rangle$ of a one-particle operator $\hat{A}$ is obtained as trace of the product of the operator and $\hat{\rho}^{(1)}$, i.e.

$$\langle A\rangle = \sum_q P_q \langle\Phi_q|\hat{A}|\Phi_q\rangle = \mathrm{Tr}\left[\hat{\rho}^{(1)}\hat{A}\right] . \tag{2.16}$$

Note, that the operator $\hat{A}$ on the left side (middle) is an operator in Fock space, which acts on each particle individually, while the one on the right side it is an operator in the one-particle Hilbert space. Unlike the similar Eq. 2.56 with the von-Neumann density matrix, the expression Eq. 2.16 above only holds for one-particle operators.

For the sake of completeness, let me include the expression for the one-particle-reduced density matrix of a many-particle wave function $|\Psi\rangle$

$$\hat{\rho}^{(1)} = \int d^4x \int d^4x' \left|\vec{x}\right\rangle \underbrace{\left\langle\Psi\middle|\left(\sum_{N=0}^{\infty} N \int d^4x_2 \cdots \int d^4x_N \left|\vec{x},\vec{x}_2,\ldots\vec{x}_N\right\rangle\left\langle\vec{x'},\vec{x}_2,\ldots,\vec{x}_N\right|\right)\middle|\Psi\right\rangle}_{\rho^{(1)}(\vec{x'},\vec{x})} \left\langle\vec{x'}\right| \tag{2.17}$$

which can be verified[5] with the help of Eq. 2.9 and Eq. 2.10. Notice, that the coordinates $\vec{x}$ and $\vec{x'}$ are seemingly interchanged. Notice also, that the $|\Psi\rangle$ is a state in Fock space, while $\hat{\rho}^{(1)}$ is a state in the one-particle Hilbert space.

The language of second quantization introduced later will offer a much more elegant and intuitive expression Eq. 3.57 for the one-particle-reduced density matrix.

[4] The wave function is, up to a sign, the same when the coordinates of the coordinates of the first and the second electron are interchanged. The sign drops out for expectation values, because the wave function enters twice. Example: Using the anti symmetry of the wave function $\psi(x,x') = -\psi(x',x)$ one can convert the density ρ_1 of the first particle $\rho_1(x) = \int dx'\ \psi^*(x,x')\psi(x,x') = (-1)^2 \int dx'\ \psi^*(x',x)\psi(x',x) = \rho_2(x)$ into the density $\rho_2(x)$ of the second.

[5] The sum $\sum_{N=0}^{\infty}$ sums over the different particle numbers beginning with the vacuum (zero-particle) state. The factor N is because the term spelled out considers only the density matrix of the first particle $\vec{x}_1 \to \vec{x},\vec{x'}$. The contribution of the other particle $\vec{x}_j \to \vec{x},\vec{x'}$ is not spelled out because the particles are indistinguishable and therefore produce the same result. The contribution of the other particles is taken into account by multiplying the result for the first particle with the number N of particles.

Natural orbitals and occupations: The one-particle-reduced density matrix is an operator in the one-particle Hilbert space. Because it is hermitian, it has real-valued eigenvalues and orthonormal eigenstates. The eigenstates $|\varphi_n\rangle$ of the one-particle-reduced density matrix are called **natural orbitals**[26] and the eigenvalues f_n are called **occupations**[26].

$$\hat{\rho}^{(1)}|\varphi_n\rangle = |\varphi_n\rangle f_n \tag{2.18}$$

ONE-PARTICLE-REDUCED DENSITY MATRIX

Expressed in terms of natural orbitals $|\varphi_n\rangle$ and occupations f_n, the one-particle-reduced density matrix of a general ensemble of many-particle wave functions can be written as

$$\hat{\rho}^{(1)} = \sum_n |\varphi_n\rangle f_n \langle\varphi_n| \ . \tag{2.19}$$

The **occupations** f_n are the eigenvalues and the **natural orbitals** $|\varphi_n\rangle$ are the eigenstates of the one-particle-reduced density matrix as defined in Eq. 2.18.

The expectation values of one particle operators are obtained by the well-known form

$$\left\langle A \right\rangle = \mathrm{Tr}\left[\hat{\rho}^{(1)}\hat{A}\right] = \sum_n f_n \langle\varphi_n|\hat{A}|\varphi_n\rangle \tag{2.20}$$

For a thermal ensemble of non-interacting electrons, the occupations are given by the **Fermi distribution**

$$f_{T,\mu}(\epsilon) \stackrel{\text{def}}{=} \left(1 + \mathrm{e}^{\beta(\epsilon-\mu)}\right)^{-1} \tag{2.21}$$

shown in figure 2.1.

For interacting electrons, the occupations differ from zero and one even at zero temperature.

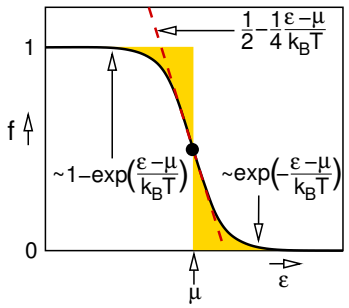

Fig. 2.1: Fermi distribution function Eq. 2.21 and common limits.

Slater determinants and idempotency of the one-particle-reduced density matrix: The comparison of Eq. 2.15 with Eq. 2.20 shows that the one-particle-reduced density matrix of a Slater determinant is

$$\hat{\rho}^{(1)} = \sum_{n=0}^{\infty} |\varphi_n\rangle \sigma_n \langle\varphi_n| \tag{2.22}$$

where σ_n is the occupation number of the n-th orbital from which the Slater determinant is built. The comparison shows also that these one-particle orbitals are also the natural orbitals. Furthermore, the

occupations f_n of a Slater determinant are the occupation numbers $\sigma_n \in \{0, 1\}$, which have integer values.

Because the occupations of a Slater determinant are either zero or one, the one-particle-reduced density matrix of a Slater determinant is **idempotent**[6], i.e.

$$\left(\hat{\rho}^{(1)}\right)^2 = \hat{\rho}^{(1)} \ . \tag{2.24}$$

The reverse is also true: An idempotent one-particle-reduced density matrix corresponds to a single Slater determinant.

Notice a possible confusion with the idempotency of the von-Neumann density matrix $\hat{\rho}^{vN} = \sum_q |\Phi_q\rangle P_q \langle\Phi_q|$. Idempotency of the von-Neumann density matrix implies that the system is in a **pure state** [7]. Idempotency of the one-particle-reduced density matrix is a stronger statement: It not only says that we deal with a single many-particle wave function, but also that this wave function can be expressed as a single Slater determinant.

The one-particle orbitals, from which the Slater determinant is built, are also its natural orbitals.[8]

N-representability: The occupations for a general fermionic many-particle wave function or any ensemble of them lies in the interval between zero and one[27]. That is,

$$0 \leq f_n \leq 1 \tag{2.25}$$

for any fermionic many-particle wave function or any ensemble of them. The converse statement is also true: any hermitian matrix with eigenvalues between zero and one can be represented as one-particle reduced density matrix of a fermionic wave function.[27] A matrix with this property is called *N*-**representable**.

Real-space-and-spin representation: Below, I will express the one-particle-reduced density matrix in terms of their real-space-and-spin components $\vec{x} = (\vec{r}, \sigma)$ respectively $\vec{x'} = (\vec{r'}, \sigma')$, with position $\vec{r}$ and spin index $\sigma \in \{\uparrow, \downarrow\}$

$$\rho^{(1)}(\vec{x}, \vec{x'}) = \langle \vec{x} | \hat{\rho}^{(1)} | \vec{x'} \rangle \tag{2.26}$$

Caution is required because the same symbol "σ" is used for the spin index and the occupation number of a Slater determinant.

The electron density can be obtained from the one-particle-reduced density matrix as

$$n(\vec{r}) = \sum_{\sigma \in \{\uparrow,\downarrow\}} \rho^{(1)}(\vec{x}, \vec{x}) \tag{2.27}$$

To become familiar with the expressions, let me write down the expectation values of a few common operators.

- electron density

$$n(\vec{r}) = \mathrm{Tr}\Big[\hat{\rho}^{(1)} \underbrace{\sum_{\sigma\in\{\uparrow,\downarrow\}} |\vec{r},\sigma\rangle\langle\vec{r},\sigma|}_{\hat{n}(\vec{r})}\Big] \overset{\text{Eq. 2.19}}{=} \sum_{\sigma\in\{\uparrow,\downarrow\}} \sum_n \langle\vec{r},\sigma|\varphi_n\rangle f_n \langle\varphi_n|\vec{r},\sigma\rangle$$

$$= \sum_{\sigma\in\{\uparrow,\downarrow\}} \sum_n f_n \varphi_n^*(\vec{r},\sigma)\varphi_n(\vec{r},\sigma) \tag{2.28}$$

[6]

$$\left(\hat{\rho}^{(1)}\right)^2 = \sum_{m,n} |\varphi_m\rangle \sigma_m \underbrace{\langle\varphi_m|\varphi_n\rangle}_{\delta_{m,n}} \sigma_n \langle\varphi_n| = \sum_n |\varphi_n\rangle \sigma_n^2 \langle\varphi_n| \overset{\sigma_n\in\{0,1\}}{=} \sum_n |\varphi_n\rangle\sigma_n\langle\varphi_n| = \hat{\rho}^{(1)} \ . \tag{2.23}$$

[7] A pure state is an ensemble with only a single many-particle wave function $|\Phi_q\rangle$

[8] Because the occupations are highly degenerate, there is a large flexibility of choosing the natural orbitals.

- kinetic energy

$$E_{\text{kin}} = \text{Tr}\left[\hat{\rho}^{(1)} \frac{\hat{\vec{p}}^2}{2m}\right] \overset{\text{Eq. 2.19}}{=} \sum_n f_n \left\langle \varphi_n \middle| \frac{\hat{\vec{p}}^2}{2m_e} \middle| \varphi_n \right\rangle \tag{2.29}$$

2.1.4 Expectation value of a two-particle operator with a Slater determinant

Let us now turn to the two-particle term. We introduce the symbol [9] $\hat{W}$ for the interaction operator. For the Coulomb interaction, the interaction acts pairwise on two particles at a time. The two-particle matrix elements $W(\vec{x}, \vec{x'})$ of the Coulomb interaction is

$$W(\vec{x}, \vec{x'}) = \frac{e^2}{4\pi\epsilon_0 |\vec{r} - \vec{r'}|} \tag{2.30}$$

where e is the elementary charge and ϵ_0 is the **electric constant** or **vacuum permittivity**. The Coulomb interaction is independent of the spin index. Furthermore it is local in the two coordinates.[10]

While a general derivation for the interaction energy of a Slater determinant is given in the appendix, let me work out here the interaction energy for a two-particle Slater determinant.

[9] The letter W stems for the German word *"Wechselwirkung"* for interaction.

[10] A general two-particle operator has the form

$$\begin{aligned}
\hat{W}_{1,2} &= \int dx_1 \cdots \int dx_N \int dx'_1 \cdots \int dx'_N |\vec{x}_1, \ldots, \vec{x}_N\rangle\langle\vec{x}_1, \ldots, \vec{x}_N| \hat{W}_{1,2} |\vec{x'}_1, \ldots, \vec{x'}_N\rangle\langle\vec{x'}_1, \ldots, \vec{x'}_N| \\
&= \int dx_1 \cdots \int dx_N \int dx'_1 \int dx'_2 |\vec{x}_1, \ldots, \vec{x}_N\rangle\langle\vec{x}_1, \ldots, \vec{x}_N| \hat{W}_{1,2} |\vec{x'}_1, \vec{x'}_2, \vec{x}_3, \ldots, \vec{x}_N\rangle\langle\vec{x'}_1, \vec{x'}_2, \vec{x}_3, \ldots, \vec{x}_N| \\
&= \int dx_1 \cdots \int dx_N \int dx'_1 \int dx'_2 |\vec{x}_1, \ldots, \vec{x}_N\rangle\langle\vec{x}_1, \vec{x}_2| \hat{W}_{1,2} |\vec{x'}_1, \vec{x'}_2\rangle\langle\vec{x'}_1, \vec{x'}_2, \vec{x}_3, \ldots, \vec{x}_N|
\end{aligned} \tag{2.31}$$

Thus, a general two-particle operator is nonlocal in the two particle coordinates and therefore its matrix elements depends on four arguments.

$$
\begin{aligned}
E_{int} &= \langle\Psi|\hat{W}|\Psi\rangle = \langle\Psi|\frac{1}{2}\sum_{\substack{i,j=1\\ i\neq j}}^{2}\hat{W}_{i,j}|\Psi\rangle \\
&= \int d^4x_1 \int d^4x_2\ \Psi^*(\vec{x}_1,\vec{x}_2)\frac{1}{2}\Big[W(\vec{x}_1,\vec{x}_2)+W(\vec{x}_2,\vec{x}_1)\Big]\Psi(\vec{x}_1,\vec{x}_2) \\
&\overset{\Psi(\vec{x}_1,\vec{x}_2)=-\Psi(\vec{x}_2,\vec{x}_1)}{=} \int d^4x_1 \int d^4x_2\ \Psi^*(\vec{x}_1,\vec{x}_2)W(\vec{x}_1,\vec{x}_2)\Psi(\vec{x}_1,\vec{x}_2) \\
&\overset{\text{Eq. 2.12}}{=} \int d^4x_1 \int d^4x_2\ \frac{1}{\sqrt{2}}\Big[\varphi_a(\vec{x}_1)\varphi_b(\vec{x}_2)-\varphi_a(\vec{x}_2)\varphi_b(\vec{x}_1)\Big]^* \\
&\qquad\qquad \cdot W(\vec{x}_1,\vec{x}_2)\frac{1}{\sqrt{2}}\Big[\varphi_a(\vec{x}_1)\varphi_b(\vec{x}_2)-\varphi_a(\vec{x}_2)\varphi_b(\vec{x}_1)\Big] \\
&= \frac{1}{2}\int d^4x_1 \int d^4x_2\ \varphi_a^*(\vec{x}_1)\varphi_b^*(\vec{x}_2)W(\vec{x}_1,\vec{x}_2)\varphi_a(\vec{x}_1)\varphi_b(\vec{x}_2) \\
&- \frac{1}{2}\int d^4x_1 \int d^4x_2\ \varphi_a^*(\vec{x}_1)\varphi_b^*(\vec{x}_2)W(\vec{x}_1,\vec{x}_2)\varphi_a(\vec{x}_2)\varphi_b(\vec{x}_1) \\
&- \frac{1}{2}\int d^4x_1 \int d^4x_2\ \varphi_a^*(\vec{x}_2)\varphi_b^*(\vec{x}_1)W(\vec{x}_1,\vec{x}_2)\varphi_a(\vec{x}_1)\varphi_b(\vec{x}_2) \\
&+ \frac{1}{2}\int d^4x_1 \int d^4x_2\ \varphi_a^*(\vec{x}_2)\varphi_b^*(\vec{x}_1)W(\vec{x}_1,\vec{x}_2)\varphi_a(\vec{x}_2)\varphi_b(\vec{x}_1) \\
&= \int d^4x_1 \int d^4x_2\ \varphi_a^*(\vec{x}_1)\varphi_b^*(\vec{x}_2)\frac{1}{2}\Big[W(\vec{x}_1,\vec{x}_2)+W(\vec{x}_2,\vec{x}_1)\Big]\varphi_a(\vec{x}_1)\varphi_b(\vec{x}_2) \\
&- \int d^4x_1 \int d^4x_2\ \varphi_a^*(\vec{x}_1)\varphi_b^*(\vec{x}_2)\frac{1}{2}\Big[W(\vec{x}_1,\vec{x}_2)+W(\vec{x}_2,\vec{x}_1)\Big]\varphi_a(\vec{x}_2)\varphi_b(\vec{x}_1) \\
&= \underbrace{\frac{1}{2}\sum_{i,j\in\{a,b\}}\int d^4x_1 \int d^4x_2\ \varphi_i^*(\vec{x}_1)\varphi_j^*(\vec{x}_2)\frac{1}{2}\Big[W(\vec{x}_1,\vec{x}_2)+W(\vec{x}_2,\vec{x}_1)\Big]\varphi_i(\vec{x}_1)\varphi_j(\vec{x}_2)}_{\text{Hartree}} \\
&- \underbrace{\frac{1}{2}\sum_{i,j\in\{a,b\}}\int d^4x_1 \int d^4x_2\ \varphi_i^*(\vec{x}_1)\varphi_j^*(\vec{x}_2)\frac{1}{2}\Big[W(\vec{x}_1,\vec{x}_2)+W(\vec{x}_2,\vec{x}_1)\Big]\varphi_j(\vec{x}_1)\varphi_i(\vec{x}_2)}_{\text{exchange}}
\end{aligned}
\tag{2.32}
$$

In the last step, I added terms with $i = j$ to the first term and subtracted them again from the second term. As shown in section 2.2.1 below, this has the advantage that the first term is simply the electrostatic selfenergy of the electron density.

Interesting is the term with the negative sign. It differs from the first term in that the arguments of the orbitals on the right-hand side are interchanged. This is why the term is called the **exchange term**. The exchange term is a direct consequence of the Pauli principle, that is, the antisymmetry of the wave function.

The general expectation value for a two-particle operator with a Slater determinant is worked out in appendix H.2.2 on p. 545. The result for the expectation value of the interaction energy is as follows.

EXPECTATION VALUE OF THE INTERACTION WITH A SLATER DETERMINANT

The expectation value of an interaction $\hat{W} = \frac{1}{2}\sum_{i\neq j}^{N} \hat{W}_{i,j}$ with a Slater determinant $|\vec{\sigma}\rangle$ built from orthonormal one-particle orbitals $|\varphi_j\rangle$ with occupation numbers σ_j is

$$\langle\vec{\sigma}|\hat{W}|\vec{\sigma}\rangle \overset{\text{Eq. } H.7}{=} \frac{1}{2}\sum_{i,j=1}^{\infty}\sigma_i\sigma_j\Big[\underbrace{\langle\varphi_i,\varphi_j|\hat{W}|\varphi_i,\varphi_j\rangle}_{\text{Hartree}} - \underbrace{\langle\varphi_i,\varphi_j|\hat{W}|\varphi_j,\varphi_i\rangle}_{\text{exchange}}\Big] \tag{2.33}$$

The terms $i = j$ have been included in the sum, because the two terms cancel each other.
The matrix elements used in the above equation Eq. 2.33 are matrix elements of two-particle product wave functions with the, e.g., Coulomb interaction

$$\langle\varphi_a,\varphi_b|\hat{W}|\varphi_c,\varphi_d\rangle \overset{\text{Eq. } H.8}{=} \sum_{\sigma,\sigma'\in\{\uparrow,\downarrow\}}\int d^3r\int d^3r'\,\varphi_a^*(\vec{r},\sigma)\varphi_b^*(\vec{r'},\sigma')\frac{e^2}{4\pi\epsilon_0|\vec{r}-\vec{r'}|}\varphi_c(\vec{r},\sigma)\varphi_d(\vec{r'},\sigma') \tag{2.34}$$

We can already look ahead and inspect the Feynman diagrams related to exchange and correlation. The diagrams related to the scattering processes are shown in fig. 2.2 on p. 57. The corresponding energy diagrams are shown in figure 11.1 on p. 332.

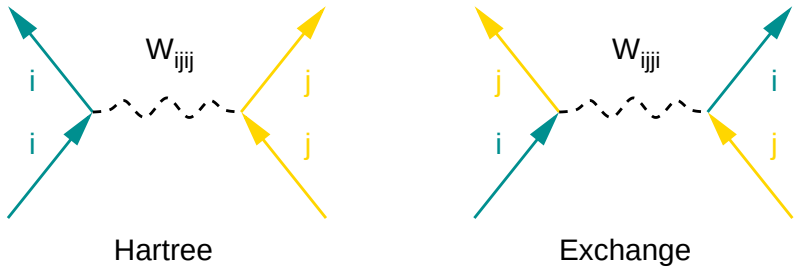

Fig. 2.2: The left diagram describes that two particles are scattered by the Coulomb interaction. The right diagram describes the same process, but the two electrons are exchanged. The second process is possible, because the two electrons are indistinguishable so that we cannot detect if the two electrons are still the same or not.

The equations that trace the matrix elements between Slater determinants to one particle orbitals, such as Eq. 2.15 and Eq. 2.34, are the so-called **Slater-Condon rules**. The expectation values shown here are due to Slater, while Condon generalized the expression to matrix elements between two different Slater determinants. They will be summarized in section 3.5 on p. 132 and they are derived in appendix H on p. 543.

2.2 Total energy of a Slater determinant

TOTAL ENERGY OF A SLATER DETERMINANT

The total energy of a Slater determinant $|\vec{\sigma}\rangle$ formed from orthonormal one-particle orbitals $|\varphi_j\rangle$ with occupation numbers σ_j is

$$\langle\vec{\sigma}|\hat{h}+\hat{W}|\vec{\sigma}\rangle = \underbrace{\sum_{j=1}^{\infty}\sigma_j\langle\varphi_j|\hat{h}|\varphi_j\rangle}_{\text{kinetic energy and external potential}} + \underbrace{\frac{1}{2}\sum_{i,j=1}^{\infty}\sigma_i\sigma_j\overbrace{\int d^4x\int d^4x'\,\frac{e^2\varphi_i^*(\vec{x})\varphi_j^*(\vec{x'})\varphi_i(\vec{x})\varphi_j(\vec{x'})}{4\pi\epsilon_0|\vec{r}-\vec{r'}|}}^{=\langle\varphi_i,\varphi_j|\hat{W}|\varphi_i,\varphi_j\rangle\quad\text{(Eq. 2.34)}}}_{\text{Hartree energy}}$$
$$\underbrace{-\frac{1}{2}\sum_{i,j=1}^{\infty}\sigma_i\sigma_j\overbrace{\int d^4x\int d^4x'\,\frac{e^2\varphi_i^*(\vec{x})\varphi_j^*(\vec{x'})\varphi_j(\vec{x})\varphi_i(\vec{x'})}{4\pi\epsilon_0|\vec{r}-\vec{r'}|}}^{=\langle\varphi_i,\varphi_j|\hat{W}|\varphi_j,\varphi_i\rangle\quad\text{(Eq. 2.34)}}}_{\text{exchange energy}} \tag{2.35}$$

$\hat{h}$ is the one-particle Hamiltonian, which describes the kinetic energy and the external potential imposed by the nuclei. $\hat{W}$ is the interaction term of the Hamiltonian.

The surprising fact of Eq. 2.33 is the appearance of two terms for the interaction. Therefore, let us try to give some physical meaning to the two contributions.

2.2.1 Hartree energy

The first interaction term in Eq. 2.33 is the so-called **Hartree energy**. The Hartree energy turns out to be the classical electrostatic interaction of the electron density.

$$\begin{aligned}E_H &= \frac{1}{2}\sum_{i,j=1}^{\infty}\sigma_i\sigma_j\int d^4x\int d^4x'\,\varphi_i^*(\vec{x})\varphi_j^*(\vec{x'})\frac{e^2}{4\pi\epsilon_0|\vec{r}-\vec{r'}|}\varphi_i(\vec{x})\varphi_j(\vec{x'})\\ &= \frac{1}{2}\int d^3r\int d^3r'\,\underbrace{\left[\sum_{i=1}^{\infty}\sigma_i\sum_{\sigma\in\{\uparrow,\downarrow\}}\varphi_i^*(\vec{x})\varphi_i(\vec{x})\right]}_{n(\vec{r})}\frac{e^2}{4\pi\epsilon_0|\vec{r}-\vec{r'}|}\underbrace{\left[\sum_{j=1}^{\infty}\sigma_j\sum_{\sigma'\in\{\uparrow,\downarrow\}}\varphi_j^*(\vec{x'})\varphi_j(\vec{x'})\right]}_{n(\vec{r'})}\end{aligned} \tag{2.36}$$

The sum over orbitals can be combined to the electron density Eq. 2.28. The occupations of a Slater determinant are either zero or one, so that the sum is limited to N-orbitals. Thus, w obtain the final expression for the Hartree energy expressed in terms of the electron density $\vec{n}(\vec{r})$

HARTREE ENERGY

$$E_H = \frac{1}{2}\int d^3r\int d^3r'\,\frac{e^2n(\vec{r})n(\vec{r'})}{4\pi\epsilon_0|\vec{r}-\vec{r'}|} \tag{2.37}$$

The Hartree energy corresponds to the electrostatic self energy[11] of a charge density $\rho(\vec{r}) = -en(\vec{r})$.

[11] The electrostatic expression is based on infinitesimal charges making up the charge density, so that the interaction of the charges with themselves can be ignored. The contribution due to the finite charge of an electron is considered in the exchange term discussed below.

The **Hartree potential** is defined as functional derivative of the Hartree energy with respect to the electron density $v_H(\vec{r}) = \delta E_H[n]/\delta n(\vec{r})$, which results in

$$v_H(\vec{r}) = \int d^3r' \, \frac{e^2 n(\vec{r'})}{4\pi\epsilon_0 |\vec{r} - \vec{r'}|} \qquad \text{or as operator} \qquad \hat{V}_H = \int d^4x \, |\vec{x}\rangle v_H(\vec{r}) \langle \vec{x}| \tag{2.38}$$

2.2.2 Exchange energy

The Hartree energy is clearly not the correct electrostatic energy of an N-electron system, because it describes the interaction of N electrons with N electrons. Instead, each electron can only interact with $N-1$ other electrons. Thus, the Hartree term also includes, incorrectly, the interaction of each electron with itself. This so-called **self interaction** is subtracted by the so-called **exchange energy**, the second interaction term in Eq. 2.33

$$\begin{aligned} E_X &= -\frac{1}{2} \sum_{i,j=1}^{\infty} \sigma_i \sigma_j \int d^4x \int d^4x' \, \varphi_i^*(\vec{x}) \varphi_j^*(\vec{x'}) \frac{e^2}{4\pi\epsilon_0 |\vec{r} - \vec{r'}|} \varphi_j(\vec{x}) \varphi_i(\vec{x'}) \\ &= -\frac{1}{2} \int d^4x \int d^4x' \, \underbrace{\left[\sum_{i=1}^{\infty} \sigma_i \varphi_i(\vec{x'}) \varphi_i^*(\vec{x}) \right]}_{\rho^{(1)}(\vec{x'}, \vec{x})} \frac{e^2}{4\pi\epsilon_0 |\vec{r} - \vec{r'}|} \underbrace{\left[\sum_{j=1}^{\infty} \sigma_j \varphi_j(\vec{x}) \varphi_j^*(\vec{x'}) \right]}_{\rho^{(1)}(\vec{x}, \vec{x'})} \end{aligned} \tag{2.39}$$

With the one-particle-reduced density matrix $\hat{\rho}^{(1)}$, Eq. 2.19 with integer occupations $f_n = \sigma_n$ for the Slater determinant, we arrive at the final expression for the exchange energy

EXCHANGE ENERGY

$$E_X = -\frac{1}{2} \int d^4x \int d^4x' \, \frac{e^2 \rho^{(1)}(\vec{x}, \vec{x'}) \rho^{(1)}(\vec{x'}, \vec{x})}{4\pi\epsilon_0 |\vec{r} - \vec{r'}|} \tag{2.40}$$

The **exchange potential** is defined as functional derivative of the exchange energy with respect to the one-particle-reduced density matrix $v_X(\vec{x}, \vec{x'}) = \delta E_X[\rho^{(1)}]/\delta\rho(\vec{x'}, \vec{x})$, which results in

$$v_X(\vec{x}, \vec{x'}) = -\frac{e^2 \rho^{(1)}(\vec{x}, \vec{x'})}{4\pi\epsilon_0 |\vec{r} - \vec{r'}|} \qquad \text{or as operator} \qquad \hat{V}_X = \int d^4x \int d^4x' \, |\vec{x}\rangle v_X(\vec{x}, \vec{x'}) \langle \vec{x'}| \tag{2.41}$$

Density matrix as projection: The one-particle-reduced density matrix of a Slater determinant is a projection operator[12] $\hat{P}_{occ}$ onto the occupied one-particle orbitals.

$$\hat{P}_{occ} = \sum_{j=1}^{\infty} |\varphi_j\rangle \sigma_j \langle \varphi_j| \overset{\text{Eq. 2.22}}{=} \hat{\rho}^{(1)}_{\vec{\sigma}} \tag{2.42}$$

If the interaction would be constant and repulsive, the exchange potential would simply shift the occupied states downward in energy. The spatial dependence of the interaction destroys this projection to a certain extent. Nevertheless, because the interaction is largest at short distances, electrons will favor *"similar orbitals"*.

As long as the one-particle orbitals making up the Slater determinant are either spin-up or spin-down orbitals, the exchange energy breaks up strictly in a sum of two terms, namely one for spin-up electrons and the other for spin-down electrons. While there are exchange-energy terms between

[12] A projection operator is **idempotent** , i.e. it obeys $\hat{P}^2 = \hat{P}$.

orbitals of like spin, there are none between orbitals of opposite spin. Thus, the exchange energy favors electrons which align ferromagnetically. **Hund's rule**, discussed below in section 2.8.5, is an expression of this effect.

Attraction vs. repulsion: It may be puzzling in the discussion of the exchange energy, that electrons tend arrange themselves preferably in "similar" orbitals despite the facts that (1) they stay away from each other due to the Pauli principle, and that (2) they repel each other via the Coulomb repulsion. The puzzle is resolved by noting that the repulsive features are captured by the Hartree energy, while the exchange energy compensates for the **self-interaction** of electrons that is included in the Hartree term. Because an electron does not interact with itself, this self interaction is removed again by the exchange energy. By considering changes that leave the Hartree term unaffected, we turn the focus on the attractive exchange term, which is responsible for the seemingly attractive behavior of electrons.

2.2.3 Non-interacting energy

The non-interacting energy in Eq. 2.35 describes the kinetic energy and the potential energy in an external potential. Because its Hamiltonian $\hat{h}$ is a one-particle operator, it is conveniently expressed in terms of the one-particle-reduced density matrix as

$$E_{1P} \overset{\text{Eq. 2.35}}{=} \sum_{j=1}^{\infty} \sigma_j \langle \varphi_j | \hat{h} | \varphi_j \rangle = \mathrm{Tr}[\hat{\rho}^{(1)} \hat{h}] \tag{2.43}$$

2.2.4 Total energy of a Slater determinant

The preceding sections show that the total energy of a Slater determinant can be expressed as **density-matrix functional**: the energy is a functional of the one-particle-reduced density matrix $\hat{\rho}^{(1)}$.

TOTAL ENERGY OF A SLATER DETERMINANT

The total energy of a Slater determinant $|\vec{\sigma}\rangle$ formed from orthonormal one-particle orbitals $|\varphi_j\rangle$ is

$$\langle\vec{\sigma}|\hat{h}+\hat{W}|\vec{\sigma}\rangle = \underbrace{\mathrm{Tr}\left[\hat{\rho}^{(1)}\hat{h}\right]}_{E_{1P}} + \underbrace{\frac{1}{2}\int d^3r \int d^3r' \, \frac{e^2 n(\vec{r})n(\vec{r'})}{4\pi\epsilon_0|\vec{r}-\vec{r'}|}}_{E_H} \underbrace{-\frac{1}{2}\int d^4x \int d^4x' \, \frac{e^2\rho^{(1)}(\vec{x},\vec{x'})\rho^{(1)}(\vec{x'},\vec{x})}{4\pi\epsilon_0|\vec{r}-\vec{r'}|}}_{E_X} \tag{2.44}$$

$\hat{h}$ is the one-particle Hamiltonian, which describes the kinetic energy and the external potential imposed by the nuclei.
The one-particle-reduced density matrix

$$\hat{\rho}^{(1)} \overset{\text{Eq. 2.19}}{=} \sum_{j=1}^{\infty} |\varphi_j\rangle f_j \langle\varphi_j| \tag{2.45}$$

can be expressed in terms of occupations f_j and natural orbitals $|\varphi_j\rangle$. For Slater determinants, the one-particle-reduced density matrix is idempotent, $\left(\hat{\rho}^{(1)}\right)^2 = \hat{\rho}^{(1)}$. In other words, the occupations for a Slater determinant are either zero or one, i.e. $f_j \in \{0,1\}$ and they are equal to the occupation numbers σ_j.
The density is obtained from the one-particle-reduced density matrix as $n(\vec{r}) = \sum_{\sigma\in\{\uparrow,\downarrow\}} \rho^{(1)}(\vec{x},\vec{x})$.

2.3 Exchange-correlation hole

2.3.1 Two-particle density and exchange-correlation hole

The first term of the interaction energy of a Slater determinant, the Hartree energy, is fairly easy to understand. The second term, the exchange energy, is, however, puzzling. Nevertheless, it can be expressed in intuitive manner in terms an **exchange hole**. Let me describe the underlying physics behind this term.

The notion of an exchange(-correlation) hole is not limited to the Hartree-Fock Theory. Let me therefore introduce this concept from a general point of view.

The **exchange** captures the effects described within Hartree-Fock theory, while the terms beyond Hartree Fock theory are called **correlation**. Both effects together are called exchange and correlation. Analogously, there is an exchange hole, a correlation hole[13] and the sum, the exchange correlation hole.

Consider the distribution of electrons when one of the electrons is at a specific location and has a specific spin. I call this electron the spectator electron and denote its coordinates with $\vec{r}_0$. If the system contains N electrons in total, there will only be $N-1$ other electrons. Thus, the electron with coordinates $\vec{r}_0$ will not see the total density, but only the density of the $N-1$ other electrons. The difference between the total density and that of the other $N-1$ electrons is the exchange-correlation hole.

The interaction energy of a system of interacting electrons can be expressed rigorously by the

[13] The correlation hole is not a hole in the literal sense, because it integrates to zero

two-particle density[14] $n^{(2)}(\vec{r},\vec{r'})$. Like the electron density $n^{(1)}(\vec{r})$ describes the density of electrons at a given point in space, the two-particle density describes the density of pairs of electrons[15], with one electron at $\vec{r}$ and the other one at $\vec{r'}$. The two-particle density is thus a density in six-dimensional space.

TWO-PARTICLE DENSITY

The two-particle density $n^{(2)}(\vec{r}_0,\vec{r'})$ is the electron density of the remaining $N-1$ electrons at position $\vec{r'}$, as "seen" by an spectator electron at site $\vec{r}_0$.

With the two-particle density $n^{(2)}(\vec{r},\vec{r'})$, the interaction energy can be written rigorously as

$$E_{int} \stackrel{\text{def}}{=} \langle\Phi|\hat{W}|\Phi\rangle = \frac{1}{2}\int d^3r \int d^3r' \, \frac{e^2 n^{(2)}(\vec{r},\vec{r'})}{4\pi\epsilon_0|\vec{r}-\vec{r'}|}$$

$$= E_H + \overbrace{\int d^3r \; n^{(1)}(\vec{r}) \, \frac{1}{2}\int d^3r' \; \frac{e^2}{4\pi\epsilon_0|\vec{r}-\vec{r'}|} \underbrace{\left(\frac{n^{(2)}(\vec{r},\vec{r'})}{n^{(1)}(\vec{r})} - n^{(1)}(\vec{r'})\right)}_{\text{hole density } h_{xc}(\vec{r},\vec{r'})}}^{=:U_{xc}} \quad (2.47)$$

while the Hartree energy can be expressed by the one-particle density $n^{(1)}(\vec{r})$ as

$$E_H = \frac{1}{2}\int d^3r \int d^3r' \, \frac{e^2 n^{(1)}(\vec{r}) n^{(1)}(\vec{r'})}{4\pi\epsilon_0|\vec{r}-\vec{r'}|} \quad (2.48)$$

The symbol U_{xc} has been used to discriminate the potential energy of exchange and correlation U_{xc} from the exchange and correlation energy E_{xc}. The exchange and correlation energy (of DFT) has an additional kinetic-energy contribution, that describes the loss of kinetic energy while adapting the exchange correlation hole for a finite interaction. This kinetic energy contribution is only present in the correlation, but not for exchange.

HOLE DENSITY

The hole density $h_{xc}(\vec{r}_0,\vec{r'})$ for the spectator electron at site $\vec{r}_0$ is

$$h_{xc}(\vec{r}_0,\vec{r'}) \stackrel{\text{def}}{=} \frac{n^{(2)}(\vec{r}_0,\vec{r'})}{n^{(1)}(\vec{r}_0)} - n^{(1)}(\vec{r'}) \quad (2.49)$$

[14] Two-particle density

$$n^{(2)}(\vec{r},\vec{r'}) = \int d^{4N}x \, |\Psi(\vec{x}_1,\ldots,\vec{x}_N)|^2 \sum_{\substack{i,j=1\\ i\neq j}}^{N} \delta(\vec{r}-\vec{r}_i)\delta(\vec{r'}-\vec{r}_j)$$

$$= N(N-1)\sum_{\sigma,\sigma'}\int d^4x_3\cdots d^4x_N \, |\Psi(\vec{x},\vec{x'},\vec{x}_3\ldots,\vec{x}_N)|^2 \quad (2.46)$$

[15] There are different definitions of the two-particle density, which differ by a factor 2. In our case, the two-particle density counts the pair $(1,2)$ and the pair $(2,1)$ as distinct. Thus, our two-particle density integrates up to twice the number of electron pairs. Other definitions normalize the two-particle density so that it integrates to the number of electron pairs, namely $N(N-1)/2$.

POTENTIAL ENERGY OF EXCHANGE AND CORRELATION

$$U_{xc} = \int d^3r\; n^{(1)}(\vec{r}) \underbrace{\frac{1}{2}\int d^3r'\; \frac{e^2 h_{xc}(\vec{r},\vec{r'})}{4\pi\epsilon_0|\vec{r}-\vec{r'}|}}_{\text{potential XC-energy per electron}} \tag{2.50}$$

It is as if each electron at $\vec{r}$ is surrounded by a positive charge density, namely $\frac{1}{2}eh(\vec{r},\vec{r'})$. This positive charge density counteracts the Coulomb repulsion described by the Hartree energy.

The exchange-correlation hole of a real material, namely silicon, is shown in fig. 2.3.

What has been gained? Once the exchange and correlation hole is known, the interaction energy can be evaluated without any approximations. In order to know the exchange-correlation hole, one needs to solve the complete many-particle problem. However, already rather simple models for its shape are quite successful to estimate the exchange-correlation energy.

The successes of **Density-Functional Theory**(DFT) [29, 30], one of the most successful theories for quantitative electronic-structure calculations of real materials from first principles, rests on the successful modeling of the exchange-correlation hole.

2.3.2 Properties of the exchange-correlation hole

The most important features of the exchange correlation hole are the following

- **charge sum rule**: The integrated exchange-correlation hole corresponds exactly to one hole.

$$\int d^3r\; h_{xc}(\vec{r},\vec{r'}) = -1 \tag{2.51}$$

- **negativity:** The exchange correlation hole must not exceed the electron density

$$-n(\vec{r}) \le h_{xc}(\vec{r},\vec{r'}) \le 0 \tag{2.52}$$

  The reason is that the density of the remaining $N-1$ electrons must not be negative.

- **near sightedness:** The exchange correlation hole vanishes at large distances of $|\vec{r}-\vec{r'}|$. There is no proof and violations are not excluded.

Size of the exchange-correlation hole

The size of the exchange-correlation hole in a material is typically that of a chemical bond, that is, of an atomic distance. The size can be seen in fig. 2.3, which shows the exchange hole in silicon. The size can be rationalized by the fact that a chemical bond typically has one electron per spin, which is the charge in the exchange-correlation hole according to the charge sum rule.

Far away from a material the electron density is small and therefore the exchange-correlation hole is very large. This is because the density of the $N-1$ other electrons can never be negative and thus, the hole density can never be larger in absolute value than the electron density, i.e. $n(\vec{r}) + h_{xc}(\vec{r},\vec{r}_0) \ge 0$.

If the material nearest to the reference electron is an atom or a molecule, the reference electron "sees" a positive ion. Thus, the exchange-correlation hole is the difference between the atom or molecule and its singly positive cation. A rough estimate for this density is the density of the highest occupied natural orbital of that atom or molecule.

If the reference electron is far away from a material and the next material is a surface, the exchange correlation hole is located at the surface.

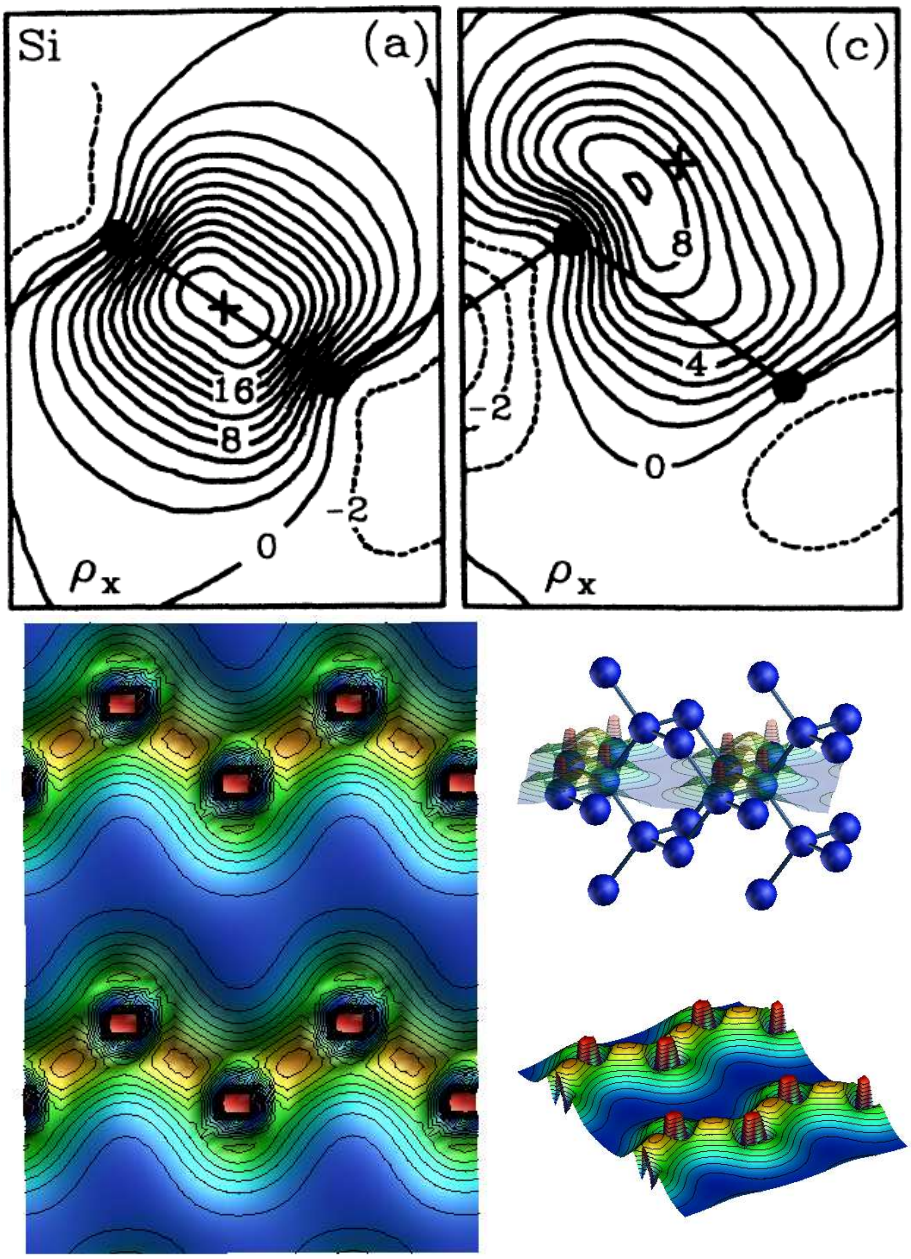

Fig. 2.3: Top: exchange hole in the 110 plane of silicon[28]. The cross indicates the position of the reference electron. In the bond, the exchange-correlation hole is centered on the reference electron, while in the tail region it is located off-center. Bottom: Valence charge density of silicon in the (110) plane. (With friendly permission by Mark Hybertsen)

These considerations provide an intuitive understanding of the exchange correlation hole, but they also indicate that the shape of the exchange correlation hole can depend in a complicated manner on the environment of the reference electron.

A lot more is understood about the exchange correlation hole. For further information on the properties of the exchange correlation hole see, for example Burke[31].

2.4 Energetics and thermodynamics in the Hartree-Fock approximation

In this section, we explore the energetics in the Hartree-Fock approximation. In the previous section, we have learned that the total energy of an interacting system can be expressed in terms of one-particle wave functions, if the wave function is a Slater determinant. Slater determinants are wave functions of non-interacting systems. The Hartree-Fock approximation attempts to describe an interacting system in terms of wave functions of non-interacting systems. The goal is to find that non-interacting system, which is suited best for that purpose.

Let me directly venture into the finite temperature formalism. This will prepare for the later chapters, which rest on the finite temperature description. The finite temperature formalism using ensembles avoids a number of nagging conceptional problems related to degenerate ground states and symmetry breaking.

Let me start this section with an introduction to thermodynamics of quantum systems. Some of it has been mentioned already in the first chapter. For this lecture, it will be important that we agree on some fundamental concepts from thermodynamics.

2.4.1 Ensembles of quantum states

ENSEMBLE

The fundamental entity of statistical mechanics is the **ensemble** $\{(|\Phi_q\rangle, P_q)\}$. An ensemble is a set of many-particle wave functions $|\Phi_q\rangle$ with their probabilities P_q. Each many-particle wave function describes a possible state of the system. Its probability P_q describes the likelihood that the system is in this specific state $|\Phi_q\rangle$.
The wave functions of the ensemble are normalized. The probabilities are positive and add up to one.

$$\langle\Phi_q|\Phi_q\rangle = 1 \quad \text{and} \quad P_q \geq 0 \quad \text{and} \quad \sum_q P_q = 1 \,. \tag{2.53}$$

The many-particle wave functions $|\Phi_q\rangle$ are called the **microstates**. The ensemble itself is called the **macrostate**. Note, that the terms "micro" and "macro" do **not** distinguish small and large systems in this context!

An ensemble is represented completely by its **von-Neumann density matrix** [32] (Eq. 6.1 of ΦSX: Statistical Physics[33]).

$$\hat{\rho}^{vN} = \sum_q |\Phi_q\rangle P_q \langle\Phi_q| \tag{2.54}$$

The von-Neumann density matrix is (1) hermitean, (2) positive definite, and (3) has a unit trace, i.e.

$$\hat{\rho}^{vN} = \left(\hat{\rho}^{vN}\right)^\dagger \qquad \text{and} \qquad \forall_{|\Psi\rangle}\ \langle\Psi|\hat{\rho}^{vN}|\Psi\rangle \geq 0 \qquad \text{and} \qquad \mathrm{Tr}\left[\hat{\rho}^{vN}\right] = 1 \,. \tag{2.55}$$

The von-Neumann density matrix contains the complete physical information on the system. The expectation value of any operator $\hat{A}$ is obtained from

$$\langle A\rangle = \sum_q P_q \langle\Phi_q|\hat{A}|\Phi_q\rangle = \mathrm{Tr}\left[\hat{\rho}^{vN}\hat{A}\right] \,. \tag{2.56}$$

Two ensembles $\{P_q, |\Phi_q\rangle\}$ with the same von-Neumann density matrix are equivalent, even though their microstates and probabilities may differ. They are equivalent, because there is no physical

observable that could differentiate between them.[16] This leaves some freedom in choosing the probabilities P_q and microstates $|\Phi_q\rangle$.

A particular choice for the microstates are the eigenstates of the von-Neumann density matrix. The resulting microstates are orthonormal. The corresponding probabilities, which are the eigenvalues of the von-Neumann density matrix, are also different. Each ensemble can therefore also be represented by a set of orthonormal microstates and their probabilities, that satisfy

$$\langle\Phi_q|\Phi_{q'}\rangle = \delta_{q,q'} \quad \text{and} \quad P_q \geq 0 \quad \text{and} \quad \sum_q P_q = 1 \; . \tag{2.57}$$

2.4.2 von-Neumann entropy

Thermodynamics in the sense of equilibrium statistical physics is rootet in the concept of **thermal equilibrium**. Thermal equilibrium lives from the basic assumption that all states are in principle accessible and equally likely. This means that a system, which is left alone for a sufficiently long time, will end up in a maximally unbiased ensemble. This connection between statistics and dynamics is the **ergodic theorem**.[34] (See also [35])

In order to discuss bias, we need to quantify the amount of uncertainty about the state of a system. This measure of uncertainty is the entropy. The entropy of a quantum system is the **von-Neumann entropy** S [32] (Eq. 6.8 of ΦSX: Statistical Physics[33]).

$$S\left(\hat{\rho}^{vN}\right) = -k_B \mathrm{Tr}\left[\hat{\rho}^{vN} \ln\left(\hat{\rho}^{vN}\right)\right] \tag{2.58}$$

If the microstates $|\Phi_q\rangle$ are chosen as the eigenstates of the von-Neumann density matrix, they are orthonormal, which allows to express the von-Neumann entropy in terms of the corresponding probabilities P_q as

$$S\Big(\sum_q |\Phi_q\rangle P_q \langle\Phi_q|\Big) \overset{\text{Eq. 2.58}}{=} -k_B \sum_q P_q \ln(P_q) \qquad \text{only, if } \langle\Phi_q|\Phi_{q'}\rangle = \delta_{q,q'} \tag{2.59}$$

This is, up to a factor, equivalent to Shannon's entropy[36] obtained from information theory.

2.4.3 Thermal ensembles and maximum-entropy principle

Finding the most unbiased ensemble is the essence of the **maximum-entropy principle**. [37, 38]. (See also Section 1.5 of ΦSX: Statistical Physics[33]). In order to determine the most unbiased ensemble, we maximize the **von-Neumann entropy** under constraints, that describe our state of knowledge on the system. The ensemble that maximimizes the entropy defines thermal equilibrium and is called a **thermal ensemble**. It is the most unbiased guess for an ensemble considering everything that we know about the system.[17]

Given that we know the thermal energy expectation value $\bar{E}$ and the thermal expectation value of the particle number $\bar{N}$, the maximum-entropy principle produces the **grand-canonical ensemble** with an appropriate temperature $T(\bar{E},\bar{N})$ and chemical potential $\mu(\bar{E},\bar{N})$.

The maximum entropy $S_{max}(\bar{E},\bar{N})$ for a system with a known thermal expectation value $\bar{E}$ for the energy and $\bar{N}$ for the particle number[18] , is obtained by a **constrained search** over all ensembles, respectively all allowed[19] von-Neumann density matrices, that are consistent with our knowledge of

[16] Two ensembles with the same von-Neumann density matrix yield the same expectation values for any observable,

[17] The reader may notice that I adhere to the subjective interpretation of probabilities: The probabilities describe the state of our mind, rather than a physical property of the system. A system does not care about what we know about it.

[18] The particle-number operator can be defined in terms of a complete set of Slater determinants $|\vec{\sigma}\rangle$ as $\hat{N} = \sum_{\vec{\sigma}} |\vec{\sigma}\rangle \left(\sum_{\vec{\sigma}} \sigma_n\right) \langle\vec{\sigma}|$

[19] A von-Neumann density matrix is hermitean, positive semi-definite and has a unit trace, as stated in Eq. 2.55.

$\bar{E}$ and $\bar{N}$.[20]

$$\begin{aligned} S_{max}(\bar{E},\bar{N}) &= \max_{\hat{\rho}^{vN}} \operatorname*{stat}_{T,\mu} \left\{ \overbrace{-k_B \mathrm{Tr}\left[\hat{\rho}^{vN} ln\left(\hat{\rho}^{vN}\right)\right]}^{S(\hat{\rho}^{vN})} - \frac{1}{T}\left(\overbrace{\mathrm{Tr}\left[\hat{\rho}^{vN}(\hat{h}+\hat{W})\right]}^{E(\hat{\rho}^{vN})} - \bar{E} \right) + \frac{\mu}{T}\left(\overbrace{\mathrm{Tr}\left[\hat{\rho}^{vN}\hat{N}\right]}^{N(\hat{\rho}^{vN})} - \bar{N} \right) \right\} \\ &\overset{\text{Eq. 2.61}}{=} \operatorname*{stat}_{T,\mu} \left[-\frac{1}{T}\left\{ \Omega_{T,\mu} - \bar{E} + \mu\bar{N} \right\} \right] \end{aligned} \tag{2.60}$$

where the grand potential $\Omega_{T,\mu}$ is defined below in Eq. 2.61. The constraints are enforced using the method of Lagrange multipliers. The Lagrange multipliers $\frac{1}{T}$ and $\frac{\mu}{T}$ are expressed by the temperature T and chemical potential μ.

The grand potential $\Omega_{T,\mu}$ in Eq. 2.60 is obtained as an ensemble minimum.

$$\Omega_{T,\mu} = \min_{\hat{\rho}^{vN}} \left\{ \overbrace{\mathrm{Tr}[\hat{\rho}^{vN}(\hat{h}+\hat{W})]}^{E(\hat{\rho}^{vN})} \overbrace{+k_B T\ \mathrm{Tr}\left[\hat{\rho}^{vN} ln\left(\hat{\rho}^{vN}\right)\right]}^{-TS(\hat{\rho}^{vN})} \overbrace{-\mu \mathrm{Tr}[\hat{\rho}^{vN}\hat{N}]}^{-\mu N(\hat{\rho}^{vN})} \right\} \tag{2.61}$$

The minimum condition for the grand potential $\Omega_{T,\mu}$ yields the density matrix for a system in thermal equilibrium with a **heat bath** and a **particle reservoir**.

$$\hat{\rho}^{vN}_{T,\mu} = \frac{\mathrm{e}^{-\frac{1}{k_B T}\left(\hat{h}+\hat{W}-\mu\hat{N}\right)}}{\mathrm{Tr}\left[\mathrm{e}^{-\frac{1}{k_B T}\left(\hat{h}+\hat{W}-\mu\hat{N}\right)}\right]} \tag{2.62}$$

In terms of (orthonormal) eigenstates of the Hamiltonian and particle number, the thermal von-Neumann density matrix Eq. 2.62 can be expressed in terms of Boltzmann factors.

$$\begin{aligned} \hat{\rho}^{vN}_{T,\mu} &\overset{\text{Eq. 2.62}}{=} \sum_q \left|\Phi_q\right\rangle \underbrace{\frac{\mathrm{e}^{-\frac{1}{k_B T}\left(E_q-\mu N_q\right)}}{\sum_{q'} \mathrm{e}^{-\frac{1}{k_B T}\left(E_{q'}-\mu N_{q'}\right)}}}_{P_q(T,\mu)} \left\langle\Phi_q\right| \\ &\text{with } (\hat{h}+\hat{W})|\Phi_q\rangle = |\Phi_q\rangle E_q \text{ and } \hat{N}|\Phi_q\rangle = |\Phi_q\rangle N_q \end{aligned} \tag{2.63}$$

So much to the reminder of the Statistical Mechanics of quantum systems.

2.4.4 Ensembles of Slater determinants

In a world, where we can only evaluate expectation values of single Slater determinants, the natural choice for an approximation is to limit the search for the maximum entropy to ensembles of Slater determinants. Let me investigate this approximation and, furthermore, let me only consider ensembles of Slater determinants that are constructed from one common one-particle basis.[21]

Let me work out the energy for this subclass of ensembles. The ensemble is characterized by Slater determinants $|\vec{\sigma}\rangle$ and their probabilities $P_{\vec{\sigma}}$. The Slater determinants are in a basis of an arbitrary orthonormal one-particle orbitals $|\varphi_n\rangle$. The energy of the ensemble is the weighted sum of

[20] With "stat", I denote the stationary condition, which is analogous to the maximum and minimum conditions, but also allows for saddle points.

[21] This additional limitation to Slater determinants from a common one-particle basis is taken for convenience. It might be interesting to explore the consequences of lifting this limitation.

the energies of the individual Slater determinants from Eq. 2.35.

$$
\begin{aligned}
E \quad &= \quad \sum_{\vec{\sigma}} P_{\vec{\sigma}} \langle \vec{\sigma} | \hat{h} + \hat{W} | \vec{\sigma} \rangle \\
&\overset{\text{Eq. 2.35}}{=} \underbrace{\sum_{n=1}^{\infty} \overbrace{\sum_{\vec{\sigma}} P_{\vec{\sigma}} \sigma_n}^{f_n} \langle \varphi_n | \hat{h} | \varphi_n \rangle}_{\text{kinetic energy and external potential}} + \underbrace{\frac{1}{2} \sum_{m,n=1}^{\infty} \overbrace{\sum_{\vec{\sigma}} P_{\vec{\sigma}} \sigma_m \sigma_n}^{\langle \sigma_m \sigma_n \rangle} \left(\overbrace{\langle \varphi_m \varphi_n | \hat{W} | \varphi_m \varphi_n \rangle}^{\rightsquigarrow \text{Hartree}} - \overbrace{\langle \varphi_m \varphi_n | \hat{W} | \varphi_n \varphi_m \rangle}^{\rightsquigarrow \text{exchange}} \right)}_{\text{interaction energy}} \\
&\overset{\text{Eq. 2.44}}{=} \underbrace{\underbrace{\overbrace{\mathrm{Tr}\left[\hat{\rho}^{(1)} \hat{h}\right]}^{\sum_{n=1}^{\infty} f_n \langle \varphi_n | \hat{h} | \varphi_n \rangle}}_{\text{one-particle energy}} + \underbrace{\overbrace{\frac{1}{2} \int d^3 r \int d^3 r' \, \frac{e^2 n(\vec{r}) n(\vec{r'})}{4\pi\epsilon_0 |\vec{r} - \vec{r'}|}}^{\frac{1}{2} \sum_{m,n=1}^{\infty} f_m f_n \left(\langle \varphi_m \varphi_n | \hat{W} | \varphi_m \varphi_n \rangle - \langle \varphi_m \varphi_n | \hat{W} | \varphi_n \varphi_m \rangle \right)}}_{\text{Hartree energy}} \underbrace{- \frac{1}{2} \int d^4 x \int d^4 x' \, \frac{e^2 \rho^{(1)}(\vec{x}, \vec{x'}) \rho^{(1)}(\vec{x'}, \vec{x})}{4\pi\epsilon_0 |\vec{r} - \vec{r'}|}}_{\text{exchange energy}}}_{\text{mean-field energy}} \\
&\quad + \underbrace{\frac{1}{2} \sum_{m,n=1; m \neq n}^{\infty} \Big(\langle \sigma_m \sigma_n \rangle - \langle \sigma_m \rangle \langle \sigma_n \rangle \Big) \Big(\langle \varphi_m \varphi_n | \hat{W} | \varphi_m \varphi_n \rangle - \langle \varphi_m \varphi_n | \hat{W} | \varphi_n \varphi_m \rangle \Big)}_{\text{energy due to correlated occupation-number fluctuations}}
\end{aligned}
\tag{2.64}
$$

I introduced the notation $\langle \sigma_m \sigma_n \rangle \overset{\text{def}}{=} \sum_{\vec{\sigma}} P_{\vec{\sigma}} \sigma_m \sigma_n$ and $\langle \sigma_n \rangle \overset{\text{def}}{=} \sum_{\vec{\sigma}} P_{\vec{\sigma}} \sigma_n = f_n$. The one-particle orbitals $|\varphi_n\rangle$ are the natural orbitals[22] of the ensemble. The electron density $n(\vec{r}) = \sum_n f_n \sum_{\sigma \in \{\uparrow,\downarrow\}} \varphi_n^*(\vec{x}) \varphi_n(\vec{x})$ and the one-particle reduced density matrix $\rho^{(1)}(\vec{x}, \vec{x'}) = \sum_n \langle \vec{x} | \varphi_n \rangle f_n \langle \varphi_n | \vec{x'} \rangle$ are those of the ensemble.

The first term, marked **mean-field energy**, has the same form as the total energy of a single Slater determinant given in Eq. 2.44 on p. 61. It differs only by the fact that the occupations f_n of the ensemble are fractional, while the occupations σ_n of a single Slater determinants are either zero or one.

The second term, which is due to **correlated occupation-number fluctuations**,

$$
\sum_{\vec{\sigma}} P_{\vec{\sigma}} \sigma_m \sigma_n - \Big(\sum_{\vec{\sigma}} P_{\vec{\sigma}} \sigma_m \Big) \Big(\sum_{\vec{\sigma}} P_{\vec{\sigma}} \sigma_n \Big) = \underbrace{\big\langle \sigma_m \sigma_n \big\rangle - \big\langle \sigma_m \big\rangle \big\langle \sigma_n \big\rangle}_{\big\langle \left(\sigma_m - f_m\right) \left(\sigma_n - f_n\right) \big\rangle}
\tag{2.65}
$$

is easily overlooked, because it magically drops out of many expressions. There is no such term in the energy Eq. 2.44 of a single Slater determinant: Slater determinants do not have fractional occupations and, therefore, they do do not exhibit occupation-number fluctuations.

2.4.5 Thermal ensembles of Slater determinants

For an ensemble of Slater determinants $|\vec{\sigma}\rangle$ with probabilities $P_{\vec{\sigma}}$, one can proceed along two distinct routes:

- In the so-called **Thermal Single-Determinant Approximation (TSDA)** [39], one proceeds as described above and arrives at Eq. 2.64: The search in the maximum-entropy principle is limited to ensembles of Slater determinants constructed from a common one-particle basisset. The energy is the ensemble average of the energies $\langle \vec{\sigma} | \hat{h} + \hat{W} | \vec{\sigma} \rangle$, Eq. 2.35 and Eq. 2.44, of the Slater determinants.

[22] The natural orbitals are the eigenstates of the one-particle-reduced density matrix of the ensemble.

Let me denote the one-particle-reduced density matrix of the Slater determinant $|\vec{\sigma}\rangle$ by $\hat{\rho}^{(1)}_{\vec{\sigma}}$. Eq. 2.64 can be written in the form

$$E = \sum_{\vec{\sigma}} P_{\vec{\sigma}} \underbrace{E^{HF}\left[\hat{\rho}^{(1)}_{\vec{\sigma}}\right]}_{\langle\vec{\sigma}|\hat{h}+\hat{W}|\vec{\sigma}\rangle} \tag{2.66}$$

where[23]

$$E^{HF}[\hat{\rho}^{(1)}] \stackrel{\text{def}}{=} \mathrm{Tr}\left[\hat{\rho}^{(1)}\hat{h}\right] + \frac{1}{2}\int d^3r \int d^3r' \, \frac{e^2 n(\vec{r}) n(\vec{r'})}{4\pi\epsilon_0|\vec{r}-\vec{r'}|} - \frac{1}{2}\int d^4x \int d^4x' \, \frac{e^2 \rho^{(1)}(\vec{x},\vec{x'})\rho^{(1)}(\vec{x'},\vec{x})}{4\pi\epsilon_0|\vec{r}-\vec{r'}|} \tag{2.67}$$

- Less accurate, but much easier is to handle is the **mean-field approximation** called the **Thermal Hartree-Fock Approximation (THFA)** [40]. Here, one restricts the search for the maximum-entropy state to ensembles of Slater determinants and, furthermore, to those without correlated occupation-number fluctuations, that is, with $\langle\sigma_m\sigma_n\rangle = \langle\sigma_m\rangle\langle\sigma_n\rangle$.[24]

  This energy amounts to

$$E = E^{HF}\Big[\underbrace{\sum_{\vec{\sigma}} P_{\vec{\sigma}}\hat{\rho}^{(1)}_{\vec{\sigma}}}_{\hat{\rho}^{(1)}}\Big] \tag{2.68}$$

  with E^{HF} from Eq. 2.67. Eq. 2.68 is a **mean-field approximation**. The averaged (mean) one-particle-reduced density matrix is simply that of the ensemble. The reader is encouraged to compare this expression Eq. 2.68 to the one Eq. 2.66 for the TSDA.

  The mean-field approximation exists in many different contexts. Therefore it is important to always specify the quantity that becomes the mean field. In this case, the mean field is the one-particle reduced density matrix averaged over the Slater determinants, respectively the averaged potential. In the Thermal Hartree-Fock Approximation (THF) all electrons experience the same mean potential, while in the Thermal Single-Determinant Approximation (TSDA), each Slater determinant experiences its own potential.

  The mean-field approximation can be described in two different ways:

  - ensembles with occupation-number fluctuations are excluded from the constrained search.
  - all Slater determinants in the ensemble experience the same effective potential.

  Both statements are equivalent. They are different points of view on the same procedure.

2.4.6 Boltzmann entropy

In the mean-field approximation Eq. 2.68, the energy depends only on the one-particle-reduced density matrix of the ensemble. Much of the information contained in the von-Neumann density matrix does not enter the mean-field energy.

However, the von-Neumann entropy Eq. 2.58 depends on the full von-Neumann density matrix, which is not available. How do we then arrive at the equilibrium ensemble?

The best we can do is to choose the most unbiased ensemble for a specific one-particle reduced density matrix $\hat{\rho}^{(1)}$. The resulting maximum entropy for a given one-particle reduced density matrix is what I call the **Boltzmann entropy**[25] $S^B[\hat{\rho}^{(1)}]$.

[23] The electron density is given by the one-particle-reduced density matrix as $n(\vec{r}) = \sum_{\sigma\in\{\uparrow,\downarrow\}} \rho^{(1)}(\vec{r},\sigma,\vec{r},\sigma)$.

[24] Editor: check this: This implies that the probabilities factorize into a product of probabilities for the individual one-particle orbitals, i.e. $P_{\vec{\sigma}} = \prod_{n=1}^{\infty} p_n(\sigma_n)$.

[25] The name "Boltzmann entropy" for this object is not common.

The Boltzmann entropy $S^B[\hat{\rho}^{(1)}]$ is the maximum von-Neumann entropy Eq. 2.58 for ensembles with a specified one-particle-reduced density matrix.[26]

$$S^B[\hat{\rho}^{(1)}] \stackrel{\text{def}}{=} \max_{\hat{\rho}^{vN}} \operatorname*{stat}_{\boldsymbol{B}} \left\{ -k_B \mathrm{Tr}\left[\hat{\rho}^{vN} \ln\left(\hat{\rho}^{vN}\right)\right] - \sum_{\alpha,\beta} k_B B_{\alpha,\beta} \left(\mathrm{Tr}\left[\hat{\rho}^{vN} \hat{c}_\alpha^\dagger \hat{c}_\beta\right] - \underbrace{\langle \pi_\beta | \hat{\rho}^{(1)} | \pi_\alpha \rangle}_{\rho^{(1)}_{\beta,\alpha}} \right) \right\} \tag{2.69}$$

The search for the maximum is performed over all allowed[27] von-Neumann density matrices $\hat{\rho}^{vN}$. The matrix $k_B\boldsymbol{B}$ is a Lagrange multiplier and $\mathrm{Tr}\left[\hat{\rho}^{vN} \hat{c}_\alpha^\dagger \hat{c}_\beta\right]$ is the expectation value for the one-particle-reduced density matrix element $\rho^{(1)}_{\beta,\alpha}$ of the corresponding ensemble. The expectation value is expressed in terms of creation and annihilation operators, that will be introduced only later. For the time being, it is sufficient to know that the one-particle-reduced density matrix can be obtained as expectation value of an operator in Fock space.

For fermions, the Boltzmann entropy[28] is

$$S^B\left[\hat{\rho}^{(1)}\right] = -k_B \mathrm{Tr}\left[\hat{\rho}^{(1)} \ln\left(\hat{\rho}^{(1)}\right) + \left(\hat{1} - \hat{\rho}^{(1)}\right) \ln\left(\hat{1} - \hat{\rho}^{(1)}\right)\right] \tag{2.70}$$

The fermionic Boltzmann entropy is known better in the form expressed in terms of occupations f_n.

$$S^B[\{f_n\}] = -k_B \sum_n \Big[f_n \ln(f_n) + (1 - f_n) \ln(1 - f_n) \Big] \tag{2.71}$$

Importantly, the maximum-entropy principle defining the Boltzmann entropy Eq. 2.69 establishes a unique mapping of the one-particle-reduced density matrix to the corresponding ensemble, respectively, to the von-Neumann density matrix

$$\hat{\rho}^{(1)} \qquad \stackrel{\text{Eq. 2.69}}{\longrightarrow} \qquad \hat{\rho}^{vN}\left[\hat{\rho}^{(1)}\right] = \sum_{\vec{\sigma}} |\vec{\sigma}\rangle \left[\prod_{n=1}^{\infty} f_n^{\sigma_n} (1 - f_n)^{1-\sigma_n} \right] \langle \vec{\sigma}| \tag{2.72}$$

where the occupations f_n are the eigenvalues of the one-particle-reduced density matrix and the Slater determinants $|\vec{\sigma}\rangle$ are constructed over the natural orbitals.

[26] See e.g. Eq. 8.39 of ΦSX:Introduction to Solid State Theory[1] or Eq. 8.26 of ΦSX: Statistical Physics.[33].

[27] Allowed, in this context, are operators in the fermionic Fock space, which are positive semi-definite and have unit trace.

[28] See e.g. Eq. 8.39 of ΦSX:Introduction to Solid State Theory[1] or Eq. 8.26 of ΦSX: Statistical Physics.[33].

The derivation of Eq. 2.72 may not be immediately obvious. It is an expression that one need not memorize, but one should know that it exists. Let me sketch the derivation here. I begin with the equilibrium condition in Eq. 2.69, which links the von-Neumann density matrix to the exponential of an one-particle-at-a-time operator expressed by the Lagrange multipliers $\boldsymbol{B}$. Remember that the trace-condition of the allowed von-Neumann density matrices must be taken into account by an additional constraint or a normalization factor.

$$\hat{\rho}^{vN}[\hat{\rho}^{(1)}] \overset{\text{Eq. 2.69}}{=} \frac{\mathrm{e}^{-\sum_{\alpha,\beta} B_{\alpha,\beta} \hat{c}^\dagger_\alpha \hat{c}_\beta}}{\mathrm{Tr}\left[\mathrm{e}^{-\sum_{\alpha',\beta'} B_{\alpha',\beta'} \hat{c}^\dagger_{\alpha'} \hat{c}_{\beta'}}\right]} \tag{2.73}$$

With the eigenstates and eigenvalues of $\boldsymbol{B}$

$$\sum_{\alpha,\beta} B_{\alpha,\beta} \hat{c}^\dagger_\alpha \hat{c}_\beta \big|\vec{\sigma}\big\rangle = \big|\vec{\sigma}\big\rangle \sum_n \sigma_n b_n \tag{2.74}$$

Eq. 2.73 has the form

$$\hat{\rho}^{vN}[\hat{\rho}^{(1)}] \overset{\text{Eq. 2.73}}{=} \sum_{\vec{\sigma}} |\vec{\sigma}\rangle \frac{\mathrm{e}^{-\sum_n b_n \sigma_n}}{\sum_{\vec{\sigma}} \mathrm{e}^{-\sum_j b_j \sigma_j}} \langle\vec{\sigma}| = \sum_{\vec{\sigma}} |\vec{\sigma}\rangle \underbrace{\left[\prod_n \frac{\mathrm{e}^{-b_n \sigma_n}}{1+\mathrm{e}^{-b_n}}\right]}_{P_{\vec{\sigma}}} \langle\vec{\sigma}| \tag{2.75}$$

The occupations are

$$\begin{aligned} f_n &= \sum_{\vec{\sigma}} P_{\vec{\sigma}} \sigma_n = \sum_{\vec{\sigma}} \left[\prod_j \frac{\mathrm{e}^{-b_j \sigma_j}}{1+\mathrm{e}^{-b_j}}\right] \sigma_n = \frac{\mathrm{e}^{-b_n}}{1+\mathrm{e}^{-b_n}} \quad \Rightarrow \quad \mathrm{e}^{-b_n} = \frac{f_n}{1-f_n} \\ \Rightarrow \quad \frac{\mathrm{e}^{-b_n \sigma_n}}{1+\mathrm{e}^{-b_n}} &= \left(\frac{f_n}{1-f_n}\right)^{\sigma_n} \frac{1}{1+\frac{f_n}{1-f_n}} = f_n^{\sigma_n} \big(1-f_n\big)^{-\sigma_n} \big(1-f_n\big) = f_n^{\sigma_n} (1-f_n)^{1-\sigma_n} \end{aligned} \tag{2.76}$$

Insertion into Eq. 2.75 yields the desired Eq. 2.69/

The fact that the probabilities $P_{\vec{\sigma}}$ are products of probabilities for each orbital shows already that the occupation-number fluctuations between different natural orbitals are uncorrelated.

The absence of correlated occupation-number fluctuations establishes that the equilibrium ensemble satisfies the conditions of the thermal Hartree-Fock approximation (THFA) despite using an extended search space.

2.4.7 Grand potential in the thermal Hartree-Fock approximation

The physical state (ensemble) and its grand potential is determined by a minimization Eq. 2.61. In the thermal Hartree-Fock approximation (THFA), this search is limited (1) to ensembles of Slater-determinants and, further, (2) to such ensembles without occupation-number fluctuations Eq. 2.65.

Energy and particle number are determined already by the one-particle-reduced density matrix. For each one-particle-reduced density matrix there are many ensembles in the search, which have different entropies. The minimum among those ensembles is determined by the largest entropy, which is the Boltzmann entropy $S^B[\hat{\rho}]$ for that one-particle-reduced density matrix. Thus, the grand potential can be obtained by a minimization over one-particle reduced density matrices. In other words, the grand potential of the thermal Hartree-Fock approximation is determined by a minimum principle of a **density-matrix functional**.

MEAN-FIELD APPROXIMATION OF THE HARTREE-FOCK GRAND POTENTIAL

In the mean-field approximation of Hartree-Fock, the grand potential $\Omega_{T,\mu}$ is the minimum of a functional of a one-particle-reduced density matrix $\hat{\rho}^{(1)}$, which defines $\rho^{(1)}(\vec{x},\vec{x'}) = \langle\vec{x}|\rho^{(1)}|\vec{x'}\rangle$ and the electron density $n(\vec{r}) = \sum_{\sigma\in\{\uparrow,\downarrow\}}\langle\vec{x}|\rho^{(1)}|\vec{x}\rangle$ The grand potential is

$$\begin{aligned}\Omega^{HF}_{T,\mu} = \min_{\hat{\rho}^{(1)}}\Bigg\{ & \underbrace{\mathrm{Tr}\Big[\hat{\rho}^{(1)}\hat{h}\Big]}_{E_{1P}} \\ & + \underbrace{\frac{1}{2}\int d^3r \int d^3r' \, \frac{e^2 n(\vec{r}) n(\vec{r'})}{4\pi\epsilon_0|\vec{r}-\vec{r'}|}}_{\text{Hartree energy } E_H} \underbrace{-\frac{1}{2}\int d^4x \int d^4x' \, \frac{e^2\rho^{(1)}(\vec{x},\vec{x'})\rho^{(1)}(\vec{x'},\vec{x})}{4\pi\epsilon_0|\vec{r}-\vec{r'}|}}_{\text{exchange energy } E_X} \\ & + \underbrace{k_B T\,\mathrm{Tr}\Big[\hat{\rho}^{(1)}\ln\Big(\hat{\rho}^{(1)}\Big) + \Big(\hat{1}-\hat{\rho}^{(1)}\Big)\ln\Big(\hat{1}-\hat{\rho}^{(1)}\Big)\Big]}_{-TS^B \quad \text{heat bath}} \underbrace{-\mu\mathrm{Tr}\big[\hat{\rho}^{(1)}\big]}_{\text{particle-reservoir}} \Bigg\}\end{aligned} \tag{2.77}$$

The minimum obeys the N-representability constraint $0 \le f_n \le 1$ because of the special choice of the entropy term. This will be confirmed with the final result.

The minimization of the grand potential Eq. 2.77 will provide us with the physical one-particle reduced density matrix but it does not provide the thermal ensemble, i.e. the von-Neumann density matrix. However, the definition of the Boltzmann entropy links the one-particle-reduced density matrix to the corresponding thermal ensemble, namely Eq. 2.72. Explicit expressions will be given in section 2.4.9 below.

With the ensemble in our hands, we can determine the expectation values of arbitrary observables, including the interaction energy. While these quantities are well defined in the thermal Hartree-Fock approximation, they are not necessarily exact.

2.4.8 Selfconsistency

Let me determine the minimum of the grand potential in Eq. 2.77. I will use the variational calculus, which I find convenient to determine the derivatives with respect to more complex objects such as functions and operators.[29] The equilibrium condition is the requirement that the first variation of the functional with respect to the one-particle reduced density matrix vanishes. It is equivalent to the requirement that the gradient vanishes at an extremum of a function.

For the following discussion, I need a name for the density-matrix functional inside the curly brackets of Eq. 2.77. Let me call it $\mathcal{F}_{T,\mu}[\hat{\rho}^{(1)}]$. Thus, Eq. 2.77 is written as $\Omega^{HF}_{T,\mu} = \min_{\hat{\rho}^{(1)}}\mathcal{F}_{T,\mu}[\hat{\rho}^{(1)}]$. The first variation $\delta\mathcal{F}_{T,\mu}$ of $\mathcal{F}_{T,\mu}$ with the one-particle reduced density matrix $\hat{\rho}^{(1)}$ is obtained via a Taylor expansion.

$$\mathcal{F}_{T,\mu}[\hat{\rho}^{(1)}+\delta\hat{\rho}^{(1)}] = \mathcal{F}_{T,\mu}[\hat{\rho}^{(1)}] + \underbrace{\sum_{\alpha,\beta}\delta\rho^{(1)}_{\alpha,\beta}\frac{\delta\mathcal{F}_{T,\mu}}{\delta\rho^{(1)}_{\alpha,\beta}}}_{\delta\mathcal{F}_{T,\mu}} + O\big([\delta\hat{\rho}^{(1)}]^2\big) \tag{2.78}$$

At the minimum of $\mathcal{F}_{T,\mu}$, the first variation $\delta\mathcal{F}_{T,\mu}$ vanishes. To minimize $\mathcal{F}_{T,\mu}[\hat{\rho}^{(1)}]$, let me therefore

[29] The first variation of a function $f(\vec{x})$ with respect to an argument $\vec{x}$ is the first order term of $f(\vec{x}+\delta\vec{x}) - f(x) = \delta f + O(\delta\vec{x}^2)$. It can be expressed in terms of the derivative $\delta f = \delta\vec{x}\vec{\nabla}f$

identify the zeros of the first variation.

$$
\begin{aligned}
0 \quad &\stackrel{!}{=} \quad \delta\mathcal{F}_{T,\mu} \\
&\stackrel{\text{Eq. 2.77}}{=} \delta\Bigg\{ \mathrm{Tr}\Big[\hat{\rho}^{(1)}\hat{h}\Big] + \frac{1}{2}\int d^4x \int d^4x' \, \frac{e^2\langle\vec{x}|\hat{\rho}^{(1)}|\vec{x}\rangle\langle\vec{x}'|\hat{\rho}^{(1)}|\vec{x}'\rangle}{4\pi\epsilon_0|\vec{r}-\vec{r}'|} - \frac{1}{2}\int d^4x \int d^4x' \, \frac{e^2\langle\vec{x}|\hat{\rho}^{(1)}|\vec{x}'\rangle\langle\vec{x}'|\hat{\rho}^{(1)}|\vec{x}\rangle}{4\pi\epsilon_0|\vec{r}-\vec{r}'|} \\
&\qquad\qquad + k_BT\,\mathrm{Tr}\Big[\hat{\rho}^{(1)}\ln\Big(\hat{\rho}^{(1)}\Big) + \Big(\hat{1}-\hat{\rho}^{(1)}\Big)\ln\Big(\hat{1}-\hat{\rho}^{(1)}\Big)\Big] - \mu\mathrm{Tr}\big[\hat{\rho}^{(1)}\big]\Bigg\} \\
&= \quad \mathrm{Tr}\Bigg\{\delta\hat{\rho}^{(1)}\Bigg[\hat{h} + \underbrace{\int d^4x|\vec{x}\rangle\Big(\int d^4x' \, \frac{e^2\langle\vec{x}'|\hat{\rho}^{(1)}|\vec{x}'\rangle}{4\pi\epsilon_0|\vec{r}-\vec{r}'|}\Big)\langle\vec{x}|}_{\hat{V}_H} - \underbrace{\int d^4x \int d^4x' \, |\vec{x}\rangle\Big(\frac{e^2\langle\vec{x}|\hat{\rho}^{(1)}|\vec{x}'\rangle}{4\pi\epsilon_0|\vec{r}-\vec{r}'|}\Big)\langle\vec{x}'|}_{\hat{V}_X} \\
&\qquad\qquad + k_BT\Big[\ln\Big(\hat{\rho}^{(1)}\Big) + \hat{1} - \ln\Big(\hat{1}-\hat{\rho}^{(1)}\Big) - \hat{1}\Big] - \mu\hat{1}\Bigg]\Bigg\} \\
&= \quad \mathrm{Tr}\Bigg\{\delta\hat{\rho}^{(1)}\Bigg[\underbrace{\hat{h}+\hat{V}_H+\hat{V}_X}_{\text{Fock operator }\hat{F}} + k_BT\ln\Big(\hat{\rho}^{(1)}\Big(\hat{1}-\hat{\rho}^{(1)}\Big)^{-1}\Big) - \mu\hat{1}\Bigg]\Bigg\}
\end{aligned}
\tag{2.79}
$$

The Hartree potential V_H and the exchange potential $\hat{V}_X$ have been defined in Eq. 2.38 and Eq. 2.41, respectively. The Fock operator $\hat{F}[\hat{\rho}^{(1)}] = \hat{h} + \hat{V}_H[\hat{\rho}^{(1)}] + \hat{V}_X[\hat{\rho}^{(1)}]$ is that obtained from the current one-particle-reduced density matrix and electron density. Remember, that the Fock operator, unlike "normal" operators, is itself a functional of the one-particle reduced density matrix.

FOCK OPERATOR

$$
\begin{aligned}
\hat{F} &\stackrel{\text{def}}{=} \hat{h} + \hat{V}_H + \hat{V}_X \\
&= \hat{h} + \overbrace{\int d^4x \, \Big|\vec{x}\Big\rangle \underbrace{\int d^3r' \, \frac{e^2 n(\vec{r}')}{4\pi\epsilon_0|\vec{r}-\vec{r}'|}}_{v_H(\vec{r})} \Big\langle\vec{x}\Big|}^{\hat{V}_H} - \overbrace{\int d^4x \int d^4x' \, \Big|\vec{x}\Big\rangle \underbrace{\frac{e^2\rho^{(1)}(\vec{x},\vec{x}')}{4\pi\epsilon_0|\vec{r}-\vec{r}'|}}_{-v_X(\vec{x},\vec{x}')} \Big\langle\vec{x}'\Big|}^{\hat{V}_X}
\end{aligned}
\tag{2.80}
$$

The Fock operator is a one-particle operator, which depends on density and one-particle-reduced density matrix.

The first variation of $\mathcal{F}_T$ vanishes only when the operator in brackets in Eq. 2.79 is the zero-operator. This yields the following operator identity, which can be resolved for the one-particle-reduced density matrix

$$
\begin{aligned}
\hat{0} &= \hat{h} + \hat{V}_H + \hat{V}_X + k_BT\ln\Big(\hat{\rho}^{(1)}\Big(\hat{1}-\hat{\rho}^{(1)}\Big)^{-1}\Big) - \mu\hat{1} \\
\Rightarrow \qquad \hat{\rho}^{(1)}_{T,\mu} &= \Big[\hat{1} + \mathrm{e}^{\frac{1}{k_BT}\left(\hat{h}+\hat{V}_H+\hat{V}_X-\mu\hat{1}\right)}\Big]^{-1}
\end{aligned}
\tag{2.81}
$$

This equation cannot be solved directly, because the Fock operator, respectively $\hat{V}_H+\hat{V}_X$, depends itself on the one-particle reduced density matrix.

SELF-CONSISTENT EQUATION FOR THERMAL HARTREE FOCK

Thus, the two equations

$$
\hat{\rho}^{(1)}_{T,\mu} \stackrel{\text{Eq. 2.81}}{=} \Big[\hat{1} + \mathrm{e}^{\frac{1}{k_BT}\left(\hat{F}-\mu\hat{1}\right)}\Big]^{-1} \qquad \text{and} \qquad \hat{F} = \hat{h} + \hat{V}_H[\hat{\rho}^{(1)}_{T,\mu}] + \hat{V}_X[\hat{\rho}^{(1)}_{T,\mu}] \tag{2.82}
$$

need to be solved simultaneously, i.e. self-consistently.

Using the eigenvalues ϵ_n and the eigenstates $|\varphi_n\rangle$ of the Fock operator

$$\left(\hat{h}+\hat{V}_H+\hat{V}_X\right)|\varphi_n\rangle = |\varphi_n\rangle\epsilon_n \tag{2.83}$$

the one-particle-reduced density matrix in THFA has the form

$$\hat{\rho}^{(1)}_{T,\mu} \overset{\text{Eq. 2.81}}{=} \sum_n |\varphi_n\rangle \underbrace{f_{T,\mu}(\epsilon_n)}_{\frac{1}{1+e^{\beta(\epsilon_n-\mu)}}}\langle\varphi_n| \tag{2.84}$$

where $f_{T,\mu}(\epsilon) = \left(1+\mathrm{e}^{\frac{1}{k_BT}(\epsilon-\mu)}\right)^{-1}$ is the Fermi function. This one-particle-reduced density matrix Eq. 2.81 is hermitian and N-representable, i.e. $0 \le f_n \le 1$.

2.4.9 Thermal ensemble in the THFA

The minimum principle in Eq. 2.77 specifies only the one-particle-reduced density matrix $\hat{\rho}^{(1)}_{T,\mu}$. To avoid the limitation to predictions for one-particl-at-a-time observables, we need to access to the corresponding ensemble, respectively its von-Neumann density matrix.

In the THFA, the von-Neumann density matrix is implicitly specified via the maximum-entropy principle used to obtain the Boltzmann entropy Eq. 2.70. The ensemble of many-particle states is that, which maximizes the entropy for the specified one-particle reduced density matrix is given in Eq. 2.72. The von Neumann density matrix of the THFA is thus obtained by inserting Eq. 2.84 into 2.72.

The thermal von-Neumann density matrix in the THFA is

$$\begin{aligned}
\hat{\rho}^{vN}_{T,\mu} &= \hat{\rho}^{vN}[\hat{\rho}^{(1)}_{T,\mu}] \\
&\overset{\text{Eq. 2.72}}{=} \sum_{\vec{\sigma}} |\vec{\sigma}\rangle \left[\prod_{n=1}^{\infty}\Big(f_{T,\mu}(\epsilon_n)\Big)^{\sigma_n}\Big(1-f_{T,\mu}(\epsilon_n)\Big)^{1-\sigma_n}\right]\langle\vec{\sigma}| \\
&= \frac{\sum_{\vec{\sigma}}|\vec{\sigma}\rangle \mathrm{e}^{-\frac{1}{k_BT}\sum_n \sigma_n(\epsilon_n-\mu)}\langle\vec{\sigma}|}{\sum_{\vec{\sigma}}\mathrm{e}^{-\frac{1}{k_BT}\sum_n\sigma_n(\epsilon_n-\mu)}} = \frac{\mathrm{e}^{-\beta(\hat{h}+\hat{V}_H+\hat{V}_X-\mu\hat{N})}}{\mathrm{Tr}\left[\mathrm{e}^{-\beta(\hat{h}+\hat{V}_H+\hat{V}_X-\mu\hat{N})}\right]}
\end{aligned} \tag{2.85}$$

The corresponding probabilities of the Slater determinants $|\vec{\sigma}\rangle$ are

$$P_{T,\mu,\vec{\sigma}} = \frac{1}{Z_{T,\mu}}\mathrm{e}^{-\beta\sum_n\sigma_n(\epsilon_n-\mu)} = \frac{1}{Z_{T,\mu}}\mathrm{e}^{-\beta\langle\vec{\sigma}|\hat{F}-\mu\hat{N}|\vec{\sigma}\rangle} \tag{2.86}$$

where $Z_{T,\mu}$ is the partition function, which normalizes the probability distribution, and ϵ_n are the eigenvalues of the self-consistent Fock operator $\hat{F} = \hat{h}+\hat{V}_X+\hat{V}_H$. It is understood, that the Slater determinants are formed from the eigenstates of the Fock operator.

As already mentioned while discussing the Boltzmann entropy in section 2.4.6 above, the occupation-number fluctuations in the resulting ensemble are uncorrelated, i.e. $\langle\sigma_m\sigma_n\rangle - \langle\sigma_m\rangle\langle\sigma_n\rangle = 0$ for $m \neq n$, so that the contribution of correlated occupation-number fluctuations to the energy of the ensemble vanishes. [30]

[30] Occupation-number fluctuations in the thermal ensemble of a non-interacting system are uncorrelated.

$$\begin{aligned}
\langle\sigma_m\sigma_n\rangle_{T,\mu} &= \sum_{\vec{\sigma}} \underbrace{\frac{\mathrm{e}^{-\beta\sum_j\sigma_j(\epsilon_j-\mu)}}{\sum_{\vec{\sigma}'}\mathrm{e}^{-\beta\sum_j\sigma'_j(\epsilon_j-\mu)}}}_{=P_{\vec{\sigma}}}\sigma_m\sigma_n = \frac{\sum_{\vec{\sigma}}\sigma_m\sigma_n\prod_j\mathrm{e}^{-\beta\sigma_j(\epsilon_j-\mu)}}{\sum_{\vec{\sigma}'}\prod_j\mathrm{e}^{-\beta\sigma'_j(\epsilon_j-\mu)}} \\
&\overset{m\neq n}{=} \frac{\sum_{\sigma_m}\sigma_m\mathrm{e}^{-\beta\sigma_m(\epsilon_m-\mu)}}{\sum_{\sigma_m}\mathrm{e}^{-\beta\sigma_m(\epsilon_j-\mu)}}\frac{\sum_{\sigma_n}\sigma_n\mathrm{e}^{-\beta\sigma_m(\epsilon_n-\mu)}}{\sum_{\sigma_n}\mathrm{e}^{-\beta\sigma_n(\epsilon_j-\mu)}} = \underbrace{\langle\sigma_m\rangle}_{f_m}\underbrace{\langle\sigma_n\rangle}_{f_n} \qquad \text{for } m\neq n
\end{aligned} \tag{2.87}$$

2.4.10 Possible misconceptions

There is some confusion between the interacting Hamiltonian

$$\hat{H} = \hat{h} + \hat{W} \,. \tag{2.88}$$

and the Fock-operator

$$\hat{F}[\hat{\rho}^{(1)}] = \frac{\delta E^{HF}}{\delta \hat{\rho}^{(1)}} = \hat{h} + \hat{V}_H + \hat{V}_X \tag{2.89}$$

Sometimes the Fock operator is also called the Hartree-Fock Hamiltonian, which I consider a misnomer. Let me *"vaccinate"* the reader with a few facts against these misunderstandings.

Energy: The energy E differs in a fundamental way from the expectation value of the Fock operator $\hat{F}$.

$$E = \mathrm{Tr}\Big[\hat{\rho}^{vN}\Big(\hat{h} + \hat{W}\Big)\Big] \neq \mathrm{Tr}\Big[\hat{\rho}^{vN} \underbrace{\Big(\hat{h} + \hat{V}_H[\hat{\rho}^{(1)}] + \hat{V}_X[\hat{\rho}^{(1)}]\Big)}_{\text{Fock operator}}\Big] \tag{2.90}$$

even if the Fock operator is obtained from the same ensemble $\hat{\rho}^{vN} \to \hat{\rho}^{(1)} \to \hat{V}_H + \hat{V}_X \to \hat{F}$. Instead, in the thermal Hartree-Fock approximation THFA, we can use a variant of the Galitski-Migdal-Koltun sum rule Eq. 8.36, which, however, introduces some factors one-half.

$$E \overset{\text{Eq. } 2.77}{=} \mathrm{Tr}\Big[\hat{\rho}^{vN}_{T,\mu}\Big(\hat{h} + \frac{1}{2}\hat{V}_H + \frac{1}{2}\hat{V}_X\Big)\Big] \tag{2.91}$$

This shows that the difference is not due to an approximation, but a misunderstanding.

Density matrix: On the other hand, the thermal von-Neumann density matrix Eq. 2.85 of the Thermal Hartree-Fock Approximation is given by the Fock operator, rather than the full Hamiltonian. Remember that the Fock operator is normally a one-particle operator in the one-particle Hilbert space, while it is used here as a one-particle-at-a-time operator in the Fock space.

$$\hat{\rho}^{vN,\mathrm{THFA}}_{T,\mu} \overset{\text{Eq. } 2.85}{=} \frac{\mathrm{e}^{-\beta(\hat{h}+\hat{V}_H+\hat{V}_X-\mu\hat{N})}}{\mathrm{Tr}\big[\mathrm{e}^{-\beta(\hat{h}+\hat{V}_H+\hat{V}_X-\mu\hat{N})}\big]} \neq \frac{\mathrm{e}^{-\beta(\hat{h}+\hat{W}-\mu\hat{N})}}{\mathrm{Tr}\big[\mathrm{e}^{-\beta(\hat{h}+\hat{W}-\mu\hat{N})}\big]} \overset{\text{Eq. } 2.62}{=} \hat{\rho}^{vN}_{T,\mu} \tag{2.92}$$

In this case, the left-hand side is an approximation of the right-hand side, namely the thermal Hartree Fock-approximation. Often it is a fairly good approximation. Why is the replacement in this case reasonable, but not for the energy? The maximum-entropy principle is sensitive to the derivatives of the energy, like the Fock operator, but not to the energy itself.

Expectation values: Often one uses the density matrix to extract expectation values

$$\langle A\rangle_{T,\mu} = \mathrm{Tr}\Big[\hat{\rho}^{vN}_{T,\mu}\hat{A}\Big] = \left.\frac{\mathrm{Tr}\Big[\hat{A}\mathrm{e}^{-\beta(\hat{H}+\gamma\hat{A})}\Big]}{\mathrm{Tr}\Big[\mathrm{e}^{-\beta(\hat{H}+\gamma\hat{A})}\Big]}\right|_{\gamma=0} \overset{\partial\hat{H}/\partial\gamma=0}{=} \left.\frac{d}{d\gamma}\right|_{\gamma=0} \underbrace{\Big[-k_BT\ln\mathrm{Tr}\Big[\mathrm{e}^{-\beta(\hat{H}+\gamma\hat{A})}\Big]\Big]}_{\Omega_{T,\mu}(\gamma)} \tag{2.93}$$

When one replaces the Hamiltonian by the Fock operator, this does not work any more: the identity on the right-hand side is no more valid because the γ-derivatives of the Fock operator do not vanish. [31]

[31] Unlike the Hamiltonian $\hat{H}$, the Fock operator depends itself on γ. Therefore, one does not obtain the expectation value as derivative of the thermodynamic potential.

$$\left.\frac{d}{d\gamma}\right|_{\gamma=0} \underbrace{\Big[-k_BT\ln\mathrm{Tr}\Big[\mathrm{e}^{-\beta(F(\hat{\gamma})+\gamma\hat{A})}\Big]\Big]}_{\Omega_{T,\mu}(\gamma)} = \left.\frac{\mathrm{Tr}\Big[\Big(\frac{d\hat{F}(\gamma)}{d\gamma}+\hat{A}\Big)\mathrm{e}^{-\beta(\hat{F}(\gamma)+\gamma\hat{A})}\Big]}{\mathrm{Tr}\Big[\mathrm{e}^{-\beta(\hat{F}(\gamma)+\gamma\hat{A})}\Big]}\right|_{\gamma=0} \neq \mathrm{Tr}\Big[\hat{\rho}^{vN,HF}_{T,\mu}\hat{A}\Big] \tag{2.94}$$

Energies of Slater determinants: The Galitski-Migdal-Koltun sum rule Eq. 8.36 allows one to express the energy with the help of the Fock operator. The Fock operator depends on the state, and it is essential to use the correct Fock operator for the problem at hand.

While it is a poor habit to describe the Hartree and exchange energies as expectation values such as $E_H = \frac{1}{2}\langle\vec{\sigma}|\hat{V}_H|\vec{\sigma}\rangle$, let me nevertheless do it in this section for the sake of the "vaccination".

We may calculate the energy expectation value for each Slater determinant using the Hartree and exchange energy from that Slater determinant, namely $\hat{V}_{H,\vec{\sigma}}$ and $\hat{V}_{X,\vec{\sigma}}$.

$$E_{\vec{\sigma}} = \big\langle\vec{\sigma}\big|\hat{h}+\hat{W}\big|\vec{\sigma}\big\rangle \overset{\text{Eq. 2.44}}{=} \big\langle\vec{\sigma}\big|\underbrace{\hat{h}+\frac{1}{2}\hat{V}_{H,\vec{\sigma}}+\frac{1}{2}\hat{V}_{X,\vec{\sigma}}}_{\frac{1}{2}\left(\hat{h}+\hat{F}\right)}\big|\vec{\sigma}\big\rangle \tag{2.95}$$

There is no contribution from correlated occupation-number fluctuations.

However, when the Hartree and exchange potentials of the ensemble are used, namely $\hat{V}_H^{\text{THFA}} = \sum_{\vec{\sigma}} P_{\vec{\sigma}}^{\text{THFA}}\hat{V}_{H,\vec{\sigma}}$ and $\hat{V}_X^{\text{THFA}} = \sum_{\vec{\sigma}} P_{\vec{\sigma}}^{\text{THFA}}\hat{V}_{X,\vec{\sigma}}$, the correlated occupation-number fluctuations are no more negligible, so that

$$E_{\vec{\sigma}} \neq \big\langle\vec{\sigma}\big|\hat{h}+\frac{1}{2}\hat{V}_H^{THFA}+\frac{1}{2}\hat{V}_X^{THFA}\big|\vec{\sigma}\big\rangle \tag{2.96}$$

What is missing can be expressed in terms of correlated occupation-number fluctuations as shown in Eq. 2.64.

When we add up the total energy of the thermal ensemble of the thermal Hartree-Fock approximation, the correlated occupation-number fluctuations miraculously drop out.

$$\sum_{\vec{\sigma}} P_{\vec{\sigma}}^{\text{THFA}}\langle\vec{\sigma}|\hat{h}+\hat{W}|\vec{\sigma}\rangle = \sum_{\vec{\sigma}} P_{\vec{\sigma}}^{\text{THFA}}\big\langle\vec{\sigma}\big|\hat{h}+\frac{1}{2}\hat{V}_H^{\text{THFA}}+\frac{1}{2}\hat{V}_X^{\text{THFA}}\big|\vec{\sigma}\big\rangle \tag{2.97}$$

The miracle is actually constructed, because we imposed the requirement on the THFA that the correlated occupation-number fluctuations vanish.

2.4.11 Beyond Slater determinants

The ground state of a general many-particle wave function is closely related to an ensemble of Slater determinants. Consider a general many-particle wave function

$$|\Phi\rangle = \sum_{\vec{\sigma}} |\vec{\sigma}\rangle c_{\vec{\sigma}}\,, \tag{2.98}$$

which is expanded in a complete set of Slater determinants $|\vec{\sigma}\rangle$. In this section, the Slater determinants are built from the natural orbitals[32] $|\varphi_n\rangle$ of the many-particle wave function.

The energy is

$$\begin{aligned} E &\overset{\text{def}}{=} \langle\Phi|\hat{h}+\hat{W}|\Phi\rangle \overset{\text{Eq. 2.98}}{=} \sum_{\vec{\sigma},\vec{\sigma}'} c_{\vec{\sigma}}^* c_{\vec{\sigma}'}\langle\sigma|\hat{h}+\hat{W}|\sigma'\rangle \\ &= \underbrace{\sum_{\vec{\sigma}} \overbrace{c_{\vec{\sigma}}^* c_{\vec{\sigma}}}^{P_{\vec{\sigma}}}\langle\sigma|\hat{h}+\hat{W}|\sigma\rangle}_{\text{ensemble of Slater determinants}} + \underbrace{\sum_{\vec{\sigma},\vec{\sigma}':\vec{\sigma}\neq\vec{\sigma}'} \overbrace{c_{\vec{\sigma}}^* c_{\vec{\sigma}'}}^{\sqrt{P_{\vec{\sigma}}P_{\vec{\sigma}'}}\,e^{i(\phi_{\vec{\sigma}'}-\phi_{\vec{\sigma}})}} \langle\sigma|\hat{h}+\hat{W}|\sigma'\rangle}_{\text{entanglement energy}} \end{aligned} \tag{2.99}$$

The absolute squares of the coefficients $c_{\vec{\sigma}}$ act like probabilities $P_{\vec{\sigma}}$ of the orthonormal set of Slater determinants: They are positive semi-definite and add they up to one. The coefficients $c_{\vec{\sigma}} = \sqrt{P_{\vec{\sigma}}}e^{i\phi_{\vec{\sigma}}}$ can be expressed by their absolute value $\sqrt{P_{\vec{\sigma}}}$ and a phase factor $e^{i\phi_{\vec{\sigma}}}$.

[32] The natural orbitals are the eigenstates of the one-particle-reduced density matrix.

The decomposition allows us to compare a **pure state** [33] $|\Phi\rangle$ with an ensemble $\{(P_{\vec{\sigma}}, |\vec{\sigma}\rangle)\}$ of Slater determinants. A pure state can be represented as **superposition** of Slater determinants. A superposition is very different from an ensemble, even if it consist of the same states: This is already evident from the entropy: A pure state has zero entropy, while an ensemble has a non-zero entropy, unless it is a pure state. The comparison between a pure state and an ensemble of Slater determinants is useful, (1) because the energy of an ensemble of Slater determinants more easy to evaluate than that of the superposition and (2) because the ensemble captures already the dominant energy contribution. The division of the energy in Eq. 2.99 above allows a systematic comparison between effective one-particle theories and many-particle quantum mechanics.

As shown above in Eq. 2.64, the energy of an ensemble of Slater determinants can further be divided into the mean-field energy and the energy of the correlated occupation-number fluctuations. Thus, the energy expectation value of an arbitrary many-particle wave functions can be decomposed into the following three contributions, namely the **mean-field energy** , the energy due to **correlated occupation-number fluctuations**, and the **entanglement energy**.

$$
\begin{aligned}
E &= \langle\Phi|\hat{h}+\hat{W}|\Phi\rangle \\
&= \underbrace{\overbrace{\sum_{n=1}^{\infty} f_n \langle\varphi_n|\hat{h}|\varphi_n\rangle}^{\text{one-particle energy}} + \overbrace{\frac{1}{2}\int d^3r \int d^3r' \, \frac{e^2 n(\vec{r}) n(\vec{r'})}{4\pi\epsilon_0|\vec{r}-\vec{r'}|}}^{\text{Hartree energy}} \overbrace{-\frac{1}{2}\int d^4x \int d^4x' \, \frac{e^2 \rho^{(1)}(\vec{x},\vec{x'})\rho^{(1)}(\vec{x'},\vec{x})}{4\pi\epsilon_0|\vec{r}-\vec{r'}|}}^{\text{exchange energy}}}_{\text{mean-field energy}} \\
&\quad + \underbrace{\frac{1}{2}\sum_{m,n=1;m\neq n}^{\infty} \Big(\langle\sigma_m\sigma_n\rangle - \langle\sigma_m\rangle\langle\sigma_n\rangle\Big)\Big(\langle\varphi_m\varphi_n|\hat{W}|\varphi_m\varphi_n\rangle - \langle\varphi_m\varphi_n|\hat{W}|\varphi_n\varphi_m\rangle\Big)}_{\text{energy due to correlated occupation-number fluctuations}} \\
&\quad + \underbrace{\sum_{\vec{\sigma},\vec{\sigma'}:\vec{\sigma}\neq\vec{\sigma'}} \sqrt{P_{\vec{\sigma}}P_{\vec{\sigma'}}}\, e^{i(\phi_{\vec{\sigma'}}-\phi_{\vec{\sigma}})} \underbrace{\langle\sigma|\hat{h}+\hat{W}|\sigma'\rangle}_{=\langle\sigma|\hat{W}-\hat{V}_H-\hat{V}_X|\sigma'\rangle}}_{\text{entanglement energy}}
\end{aligned}
\tag{2.100}
$$

1. The first line denoted as **mean-field energy** is the energy expression used in the Hartree-Fock approximation. However, the occupations and natural orbitals differ from those of thermal Hartree-Fock approximation (THFA). Rather than thermally excited electron-hole pairs present in the finite-temperature ensemble, the correlated many-particle wave function has quantum fluctuations. The quantum fluctuations may, for example, be electron-hole pairs formed to screen the Coulomb interaction between electrons.

2. The second term describes the contribution from **correlated occupation-number fluctuations**. They vanish for a single Slater determinant and, per construction, for the equilibrium ensemble of the thermal Hartree Fock approximation. However, they are present in (1) a general ensemble of Slater determinants and (2) in a general many-particle wave function or their ensembles.

   The factors $\langle\varphi_m,\varphi_n|\hat{W}|\varphi_m,\varphi_n\rangle - \langle\varphi_m,\varphi_n|\hat{W}|\varphi_n,\varphi_m\rangle$ are non-negative for all values (m,n)[34] and they vanish for $m=n$. They are large for electron pairs with opposite spin, because, for pairs with equal spin, the exchange term (2nd) counteracts the Hartree term (1st). For electrons pairs with opposite spin, the exchange term vanishes

   The correlated occupation-number fluctuations $\sum_{\vec{\sigma}} P_{\vec{\sigma}}(\sigma_m - f_m)(\sigma_n - f_n)$ are non-negative and vanish

   - for completely filled $f_n = 1$ and completely empty $f_n = 0$ orbitals, and

[33] A pure state corresponds to a single many-particle wave function as opposed to an ensemble, which contains many micro-states along with their probabilities. A pure state can also be described as an ensemble with probability one for a specific many-particle wave function.

[34] This follows from the fact that the electrostatic energy of any two-particle system is positive. This is also true if the two electrons are in a two-particle Slater determinant with the two orbitals $|\varphi_m\rangle$ and $|\varphi_n\rangle$. The factor mentioned is twice the Coulomb energy of this Slater determinant.

- statistically independent occupations, i.e. for

$$\left(\langle\sigma_m\sigma_n\rangle =\right) \sum_{\vec{\sigma}} P_{\vec{\sigma}}\sigma_m\sigma_n = \underbrace{\left(\sum_{\vec{\sigma}} P_{\vec{\sigma}}\sigma_m\right)}_{f_m}\underbrace{\left(\sum_{\vec{\sigma}} P_{\vec{\sigma}}\sigma_n\right)}_{f_n}\left(= \langle\sigma_m\rangle\langle\sigma_n\rangle\right) \qquad (2.101)$$

For a given set of occupations $f_n = \sum_{\vec{\sigma}} P_{\vec{\sigma}}\sigma_m$, a wave function with small **double occupancy**

$$d_{m,n} \stackrel{\text{def}}{=} \sum_{\vec{\sigma}} P_{\vec{\sigma}}\sigma_m\sigma_n \qquad (2.102)$$

will have a lower energy. That is, electrons with strong Coulomb repulsion try to get out of each other's way.

The optimum correlated occupation-number fluctuations $\langle\sigma_1\sigma_2\rangle - \langle\sigma_1\rangle\langle\sigma_2\rangle$ for two orbitals [35] is shown in figure 2.4.

3. The third term describes the **entanglement** of the Slater determinants. Let me call it **entanglement energy**. It describes the **hybridization**[36] of Slater determinants. This is the only term that depends on the relative phases of the coefficients of different Slater determinants.

   Imagine a special case with only two relevant Slater determinants $|\vec{\sigma}_1\rangle$ and $|\vec{\sigma}_2\rangle$, so that the many-particle wave functions have the form $|\Phi\rangle = |\vec{\sigma}_1\rangle c_1 + |\vec{\sigma}_2\rangle c_2$. Let us treat the two Slater determinants as basisset in Fock space and evaluate the matrix elements of the interacting 2×2 Hamiltonian. (assuming orthonormality)

$$H_{\alpha,\beta} = \langle\vec{\sigma}_\alpha|\hat{h} + \hat{W}|\vec{\sigma}_\beta\rangle \qquad \text{for } \alpha,\beta \in \{1,2\}. \qquad (2.104)$$

   We obtain a 2×2 Schrödinger equation.[37] We will obtain two eigenvectors $\vec{c}_\pm$ for two different energies $E_\pm$, where $\pm \in \{+,-\}$ identifies one or the other eigenstate. The complex coefficients of the eigenvectors $c_{\alpha,\pm} = \sqrt{P_\pm}e^{i\phi_{\alpha,\pm}}$ contain the phase relation $\phi_{2,\pm} - \phi_{1,\pm}$ between the two Slater determinants. When the two Slater determinants with different phases contribute with distinct weight, i.e. $P_{\vec{\sigma}_1} \neq P_{\vec{\sigma}_2}$, there will be a finite entanglement energy.

   The entanglement energy is the energy gain from optimizing the relative phases of the Slater determinants as compared to an averaged phases.

This shows that the energy of a general many-particle wave function can be mapped approximately onto the energy of an ensemble of Slater determinants. The approximation can be described by an average of the phases of the individual Slater determinants. Averaging over the phases will remove all off-diagonal elements in the Hamiltonian expressed in terms of Slater determinants, but it will leave the diagonal elements unchanged.

[35] Bounds for the correlated occupation-number fluctuations can be derived by considering each pair of states independently.

$$\max(0, f_m + f_n - 1) - f_m f_n \leq P_{\sigma_m,\sigma_n}(\sigma_m - f_m)(\sigma_n - f_n) \leq \min(1, f_m + f_n) - f_m f_n \qquad (2.103)$$

To avoid the double occupancy, one could estimate the occupation-number fluctuations from the lower of the two bounds, rather than ignoring the term as in the mean-field approximation. The result is shown in fig. 2.4 The independent-pair approximation relies on $P_{00} + P_{01} + P_{10} + P_{11} = 1$, $P_{10} + P_{11} = f_1$, $P_{01} + P_{11} = f_2$, $0 \leq P_{\sigma,\sigma'} \leq 1$.

[36] Hybridization is the formation of a superposition of orbitals to form a bond orbital or an antibonding orbital. The difference between a bond and an antibond can be attributed to a phase factor between the two orbitals forming the bonding and antibonding orbitals. The bond orbital of a hydrogen molecule is $(|\chi_1\rangle + \chi_2\rangle)/\sqrt{2}$ while that of an antibond is $(|\chi_1\rangle - \chi_2\rangle)/\sqrt{2}$. The plus and minus signs can be described by a relative phase factor $e^{i\varphi}$ with a real-valued phase of $\varphi = 0$ for the bond and $\varphi = \pi$ for the antibond. In the present case, it is Slater determinants rather than one-particle states that hybridize. The underlying concept is the matrix diagonalization, which is common to both cases.

[37] The problem of diagonalizing the 2×2 matrix is the same as that for the diatomic molecule. The difference to the diatomic molecule is that the Hamiltonian is formed from many-particle Slater determinants and the Hamiltonian contains also the interaction $\hat{W}$. As in the diatomic molecule, there will be **level repulsion** and superpositions of the two Slater determinants analogous to the bonding and the antibonding states of the diatomic molecule.

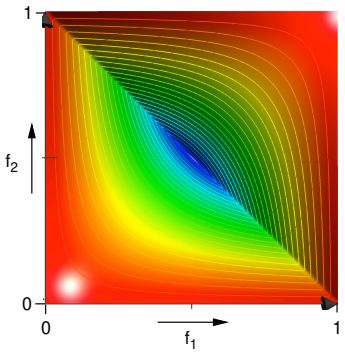

Fig. 2.4: Contour plot for the lower bound $\min_{\{P_{\sigma_1,\sigma_2}\}} \sum_{\sigma_1,\sigma_2} P_{\sigma_1,\sigma_2}(\sigma_1 - f_1)(\sigma_2 - f_2) = \min(0, f_1 + f_2 - 1) - f_1 f_2$ for the occupation-number fluctuations of two orbitals as a function of the occupations f_1 and f_2. The plot is drawn for $f_j \in [0, 1]$. The function values are zero at the boundaries of the area and the minimum, at $f_1 = f_2 = \frac{1}{2}$ has the value $-\frac{1}{4}$. (This graph is repeated in figure F.4 on p. 512)

2.5 Spectral properties

For non-interacting electrons, the one-particle energies determine both the thermodynamic properties of the system as well as its spectral properties such as optical absorption and emission. For interacting electrons this connection of spectral and thermodynamic properties is broken. Therefore, let me discuss in this section the role of interaction within the Hartree-Fock theory and show how one-particle energies are related to total energy differences.

2.5.1 Spectroscopies

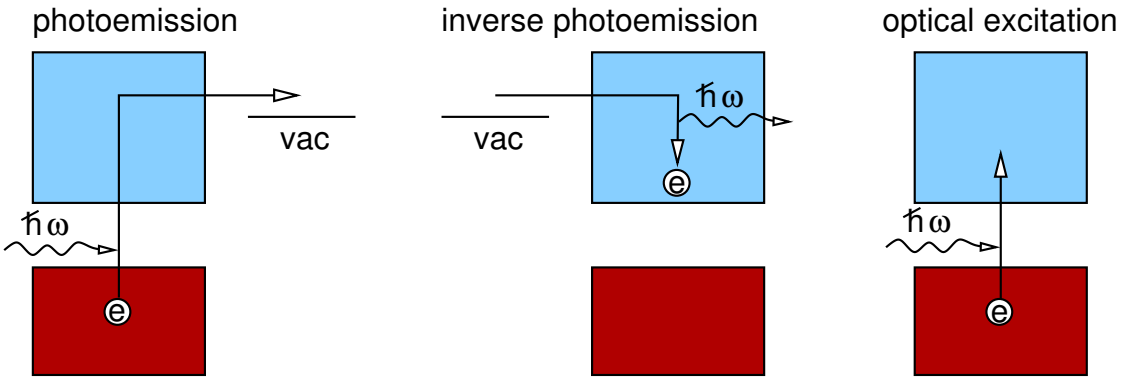

Fig. 2.5: Energy vs. position sketch of the photoemmission, inverse photoemission and optical excitation process. The red square represents the valence band, while the blue square represents the conduction band. The vacuum level is denoted by *"vac"*.

For sketches of the different spectroscopic techniques mentioned here, see figure 2.5.

- **photoemission**: a photon is absorbed, while an electron is emitted out of the system. The kinetic energy E_{kin} of the electron, which escapes from the system, is measured. The energy of the emitted electron is $E_{vac} + E_{\text{kin}}$, where the vacuum energy E_{vac} is the energy of an electron at rest in the vacuum. The energy difference of the emitted electron and the absorbed photon

$\hbar\omega$ is the energy of the electron before the photon absorption, because it is due to the removal (annihilation) of an electron from the valence band. The photoemission process thus detects the density of states of the occupied states.[38]

- **inverse photoemission**: The system captures an electron while emitting a photon. The electron injected drops from a high-lying energy level into a low-lying empty orbital. The energy difference of the emitted photon $\hbar\omega$ and the injected electron $E_{vac} + E_{\text{kin}}$ is due to the addition (creation) of an electron to the conduction band. The inverse photoemission process thus detects the density of states of the conduction band.

- **optical spectroscopy**: a photon is absorbed, while an electron-hole pair is created. That is, an electron is lifted into an empty orbital. It is described by a simultaneous removal (annihilation) of an electron from the valence bands and and the simultaneous addition (creation) of an electron in the conduction bands. While photo-emission and inverse photo-emmission are **one-particle excitations**, the optical absorption is an example for a **two-particle excitation**.

2.5.2 Excitations on the Hartree-Fock Level

Underlying the Hartree-Fock approximation is the assumption that the interaction is a small perturbation of the otherwise non-interacting electron gas. In first order, the wave functions are those of the unperturbed system, that is Slater determinants, which are the eigenstates of the non-interacting Hamiltonian.

In a second conceptual step, the non-interacting system is replaced by another non-interacting system, namely one with an effective potential. The effective potential is given by the Fock operator.

$$\hat{F} = \frac{\hat{\vec{p}}^2}{2m_e} + \underbrace{\hat{V}_{eff}}_{\hat{V}_{ext}+\hat{V}_H+\hat{V}_X} \tag{2.105}$$

In Hartree Fock, we take the many-particle states $|\vec{\sigma}\rangle$ from the effective non-interacting system, described by the Fock operator, but we use the energies obtained with full Hamiltonian.

$$\begin{aligned} \hat{F}|\vec{\sigma}\rangle &= |\vec{\sigma}\rangle\Lambda_{\vec{\sigma}} \\ E^{HF}_{\vec{\sigma}} &= \langle\vec{\sigma}|\hat{H}|\vec{\sigma}\rangle \overset{!!}{\neq} \langle\vec{\sigma}|\hat{F}|\vec{\sigma}\rangle \end{aligned} \tag{2.106}$$

A common mistake is to mix up the eigenvalues of the Fock operator with the approximate energy eigenvalues $E_{\vec{\sigma}}$ of the many-particle system.

Hartree-Fock Theory is one example, where a description based on non-interacting electrons, nevertheless accounts for the large contributions of the interaction.

An important consequence of the following sections is that the one-particle excitation energies can be described by the Fock operator, but not other excitations such as two-particle excitations. Note also, that excitations are energy differences and not many-particle energies themselves. The following will provide us with a physical interpretation of the Fock operator beyond the minimum condition for the energy of a Slater determinant.

Editor: Private remark:

$$\hat{H} \approx \sum_{\vec{\sigma}} |\vec{\sigma}\rangle E_{\vec{\sigma}} \langle\vec{\sigma}| = \sum_{\vec{\sigma}} |\vec{\sigma}\rangle\langle\vec{\sigma}|\hat{h} + \hat{W}|\vec{\sigma}\rangle\langle\vec{\sigma}| \tag{2.107}$$

where the Slater determinants are constructed from the natural orbitals of the grand ensemble. Thus, the approximated depends on the one-particle reduced density matrix of the system. This approximation allows one in turn to define an approximate grand potential as density matrix functional. $\Omega_{T,\mu} \approx -k_B T \ln\left[\sum_{\vec{\sigma}} \langle\vec{\sigma}|\hat{h} + \hat{W}|\vec{\sigma}\rangle - \mu N_\sigma\right]$

[38] Damascelli et al.[41] provide a insightful introduction to angular resolved photoemission spectroscopy (ARPES).

Editor: The following must be integrated into the text:

$$
\begin{aligned}
E_{\vec{\sigma}} - E^{HF} &= \underbrace{\sum_n \sigma_n \langle\varphi_n|\hat{h}|\varphi_n\rangle + \frac{1}{2}\sum_{m,n}\sigma_m\sigma_n\Big(\langle\varphi_n\varphi_m|\hat{W}|\varphi_n\varphi_m\rangle - \langle\varphi_n\varphi_m|\hat{W}|\varphi_m\varphi_n\rangle\Big)}_{E_{\vec{\sigma}} \quad \text{Eq. 2.35}} \\
&\quad - \underbrace{\Big\{\sum_n f_n\langle\varphi_n|\hat{h}|\varphi_n\rangle + \frac{1}{2}\sum_{m,n} f_n f_m\Big(\langle\varphi_n\varphi_m|\hat{W}|\varphi_n\varphi_m\rangle - \langle\varphi_n\varphi_m|\hat{W}|\varphi_m\varphi_n\rangle\Big)\Big\}}_{=E^{HF}=\Omega^{HF}+TS+\mu N \quad \text{Eq. 2.77}} \\
&= \underbrace{\sum_n(\sigma_n - f_n)\langle\varphi_n|\hat{h}|\varphi_n\rangle + \sum_n\Big(\sigma_n - f_n\Big)\underbrace{\sum_m f_m\Big(\langle\varphi_n\varphi_m|\hat{W}|\varphi_n\varphi_m\rangle - \langle\varphi_n\varphi_m|\hat{W}|\varphi_m\varphi_n\rangle\Big)}_{\langle\varphi_n|\hat{V}_H+\hat{V}_X|\varphi_n\rangle}}_{\sum_n(\sigma_n-f_n)\epsilon_n \qquad \text{with } \epsilon_n = \langle\varphi_n|\hat{h}+\hat{V}_H+\hat{V}_X|\varphi\rangle} \\
&\quad + \frac{1}{2}\sum_{m,n}\Big(\sigma_n - f_n\Big)\Big(\sigma_m - f_m\Big)\Big(\langle\varphi_n\varphi_m|\hat{W}|\varphi_n\varphi_m\rangle - \langle\varphi_n\varphi_m|\hat{W}|\varphi_m\varphi_n\rangle\Big) \\
&= \sum_n(\sigma_n - f_n)\epsilon_n + \frac{1}{2}\sum_{m,n}\Big(\sigma_n - f_n\Big)\Big(\sigma_m - f_m\Big)\Big(\langle\varphi_n\varphi_m|\hat{W}|\varphi_n\varphi_m\rangle - \langle\varphi_n\varphi_m|\hat{W}|\varphi_m\varphi_n\rangle\Big)
\end{aligned}
\tag{2.108}
$$

Here ϵ_n are the eigenvalues of the Fock operator of the equilibrium state. [a]
The picture for $|\vec{\sigma}\rangle$ emerges of an equilibrium state with additional quasi-particles, namely electrons and holes. Each quasi-particle has is own energy given by the eigenvalue of the Fock operator. In addition, the quasi-particle have an interaction between them, that is electrons repel electrons, holes repel holes and electrons attract holes. The Coulomb interaction is given in the mean-field spirit with fractional occupations $\sigma_n - f_n$. Note, that this does not introduce a mean-field like errors into E_σ. Rather, the mean-field like treatment of the interaction between the quasi-particles undoes the mean-field errors in the ground state energy E^{HF}.
It may be convenient to express the energy relative to the grand potential, rather than relative to the ensemble energy. This can be conveniently done by taking an entropy for the quasi-particles into account. Note however, that this entropy term does not reflect the entropy of the Slater determinant $|\vec{\sigma}\rangle$, but that of the ground state ensemble.

$$
\begin{aligned}
E_{\vec{\sigma}} - \Omega^{HF} &= \sum_n(\sigma_n - f_n)\epsilon_n + \frac{1}{2}\sum_{m,n}\Big(\sigma_n - f_n\Big)\Big(\sigma_m - f_m\Big)\Big(\langle\varphi_n\varphi_m|\hat{W}|\varphi_n\varphi_m\rangle - \langle\varphi_n\varphi_m|\hat{W}|\varphi_m\varphi_n\rangle\Big) \\
&\quad \underbrace{+ k_B T \sum_n \underbrace{|\sigma_n - f_n|\ln(|\sigma_n - f_n|) + (1 - |\sigma_n + f_n|)\ln(1 - |\sigma_n - f_n|)}_{=f_n\ln(f_n)+(1-f_n)\ln(1-f_n)}}_{\text{heat bath } -TS} - \underbrace{\mu\sum_n f_n}_{\text{particle reservoir}}
\end{aligned}
\tag{2.109}
$$

We can consider quasi-particle occupations $f_n^{QP} = |\sigma_n - f_n|$. The sign of $\sigma_n - f_n$ determines if this is an electron or a hole excitation.

[a] Note on a side: (Based on the creation and annihilation operators introduced only later.) The interacting Hamiltonian can be written in the form

$$
\hat{H} = E^{HF}\hat{1} + \sum_{\vec{\sigma}}|\vec{\sigma}\rangle(E_{\vec{\sigma}} - E^{HF})\langle\vec{\sigma}| + \sum_{\vec{\sigma}\neq\vec{\sigma'}}|\vec{\sigma}\rangle\langle\vec{\sigma}|\hat{H}|\vec{\sigma'}\rangle\langle\vec{\sigma'}| \qquad \text{where}
$$

$$
\sum_{\vec{\sigma}}|\vec{\sigma}\rangle E_{\vec{\sigma}}\langle\vec{\sigma}| = E^{HF}\hat{1} + \sum_n \epsilon_n\Big(\hat{a}_n^\dagger\hat{a}_n - \langle\hat{a}_n^\dagger\hat{a}_n\rangle\Big) + \frac{1}{2}\sum_{m,n}\Big(W_{m,n,m,n} - W_{m,n,n,m}\Big)\Big(\hat{a}_m^\dagger\hat{a}_m - \langle\hat{a}_m^\dagger\hat{a}_m\rangle\Big)\Big(\hat{a}_n^\dagger\hat{a}_n - \langle\hat{a}_n^\dagger\hat{a}_n\rangle\Big)
$$

with $f_n = \langle\hat{a}_m^\dagger\hat{a}_m\rangle = \langle\Phi^{HF}|\hat{a}_m^\dagger\hat{a}_m|\Phi^{HF}\rangle$, $W_{m,n,p,q} = \langle\varphi_m\varphi_n|\hat{W}|\varphi_p\varphi_q\rangle$, and $|\vec{\sigma}\rangle = \prod_{n=1}^\infty(\hat{a}_n^\dagger)^{\sigma_n}|\mathcal{O}\rangle$. The Hartree-Fock ground-state energy is

$$
E^{HF} = \sum_n \epsilon_n\langle\hat{a}_n^\dagger\hat{a}_n\rangle + \frac{1}{2}\sum_{m,n}\Big(W_{m,n,m,n} - W_{m,n,n,m}\Big)\langle\hat{a}_m^\dagger\hat{a}_m\rangle\langle\hat{a}_n^\dagger\hat{a}_n\rangle
$$

«««

Let me now consider the energy difference between two Slater determinants

$$\begin{aligned}
E_{\vec{\sigma}} - E_{\vec{\sigma'}} &= \sum_n (\sigma_n - \sigma'_n)\epsilon_n + \frac{1}{2}\sum_{m,n}\Big[\Big(\sigma_n - f_n\Big)\Big(\sigma_m - f_m\Big) - \Big(\sigma'_n - f_n\Big)\Big(\sigma'_m - f_m\Big)\Big] \\
&\quad \times\Big(\langle\varphi_n\varphi_m|\hat{W}|\varphi_n\varphi_m\rangle - \langle\varphi_n\varphi_m|\hat{W}|\varphi_m\varphi_n\rangle\Big) \\
&= \sum_n (\sigma_n - \sigma'_n)\epsilon_n + \sum_{,n}\Big(\sigma_n - \sigma'_n\Big)\Big[\sum_m\Big(\sigma'_m - f_m\Big)\Big(\langle\varphi_n\varphi_m|\hat{W}|\varphi_n\varphi_m\rangle - \langle\varphi_n\varphi_m|\hat{W}|\varphi_m\varphi_n\rangle\Big)\Big] \\
&\quad + \frac{1}{2}\sum_{m,n}\Big(\sigma_n - \sigma'_n\Big)\Big(\sigma_m - \sigma'_m\Big)\Big(\langle\varphi_n\varphi_m|\hat{W}|\varphi_n\varphi_m\rangle - \langle\varphi_n\varphi_m|\hat{W}|\varphi_m\varphi_n\rangle\Big)
\end{aligned} \tag{2.110}$$

»»»>

2.5.3 Photoemission

Let me consider the photoemission process, in which an electron is ejected by a photon from an occupied state. The energy loss, the photon energy minus the energy of the emitted electron can be calculated as energy difference of the initial and final Slater determinants.

Initially, there is a N-particle system at rest. Because we refer here to the Hartree-Fock approximation, we use the eigenstates of the Fock-operator as one-particle basisset. The corresponding many-particle states are Slater determinants $|\vec{\sigma}\rangle$ in this basisset, which I represent in the occupation-number representation. In this representation, the energy expectation value of a Slater determinant has the simple form

$$E_{\vec{\sigma}} \overset{\text{Eq. 2.35}}{=} \sum_{n=1}^{\infty}\sigma_n\langle\varphi_n|\hat{h}|\varphi_n\rangle + \frac{1}{2}\sum_{m,n=1}^{\infty}\sigma_m\sigma_n\Big(\langle\varphi_m,\varphi_n|\hat{W}|\varphi_m,\varphi_n\rangle - \langle\varphi_m,\varphi_n|\hat{W}|\varphi_n,\varphi_m\rangle\Big) \tag{2.111}$$

In the initial state, the first N one-electron states are occupied, while the others are empty. This state is also called the **Fermi sea**. It is denoted by $|\vec{\sigma}_0\rangle$ and has occupations $\sigma_j = 1$ for $j \leq N$ and $\sigma_j = 0$ otherwise.

In the photoemission process, an electron is ejected from an occupied state $|\varphi_n\rangle$ with $n \leq N$ and lifted into the vacuum. The energy of the emitted electron is the sum of vacuum level ϵ_{vac} and the kinetic energy E_{kin} of the emitted electron. The vacuum level ϵ_{vac} is the potential energy of an electron far above the surface of the material.

NOTATION

Let me denote the state of the system, after removing the electron from the orbital $|\varphi_n\rangle$ in $\vec{\sigma}_0$, by $|\vec{\sigma}_{-n}\rangle$, namely[a] *"the Slater determinant obtained from $|\vec{\sigma}_0\rangle$ after removing an electron from the one-particle orbital n"*. The energy of $|\vec{\sigma}_{-n}\rangle$ is $E(\vec{\sigma}_{-n})$.
Similarly, I will denote the Slater determinant obtained after adding an electron to the empty orbital $|\varphi_m\rangle$ of $\vec{\sigma}_0|$ by $|\vec{\sigma}_{+m}\rangle$.
A state obtained by removing an electron from the occupied orbital $|\varphi_m\rangle$ in $\vec{\sigma}_0$ and by placing it into the empty orbital $|\varphi_n\rangle$, is denoted by $|\vec{\sigma}_{-m/+n}\rangle$.

[a] The notation requires special attention: The state $|\vec{\sigma}_{-n}\rangle$ has the occupation number $\sigma_j - \delta_{j,n}$ for the j-th one-particle orbital, where σ_j is the occupation number of the j-th orbital of state $|\vec{\sigma}_0\rangle$.

The energy balance between the initial state, consisting of the incident photon with energy $\hbar\omega$ and the ground state $|\vec{\sigma}_0\rangle$ of the target, and the final state, consisting of the target after removal of

one electron from the n-th orbital and the emitted electron in the vacuum, is

$$\underbrace{\hbar\omega + E(\vec{\sigma}_0)}_{\text{initial state}} = \underbrace{E(\vec{\sigma}_{-n}) + \epsilon_{\text{vac}} + E_{\text{kin}}}_{\text{final state}} \tag{2.112}$$

The energy loss ΔE_{loss}, that is the energy absorbed by the material, is the energy cost for annihilating an electron in the material

$$\begin{aligned}
\Delta E_{\text{loss}} &= \hbar\omega - \left(\epsilon_{\text{vac}} + E_{\text{kin}}\right) \\
&\overset{\text{Eq. 2.112}}{=} E(\vec{\sigma}_{-n}) - E(\vec{\sigma}_0) \\
&\overset{\text{Eq. 2.111}}{=} -\langle\varphi_n|\hat{h}|\varphi_n\rangle - \frac{1}{2}\underbrace{\left(\langle\varphi_n\varphi_n|\hat{W}|\varphi_n\varphi_n\rangle - \langle\varphi_n\varphi_n|\hat{W}|\varphi_n\varphi_n\rangle\right)}_{=0\ \text{(A)}} \\
&\qquad - \sum_{m=1}^{N}\underbrace{\left(\langle\varphi_n\varphi_m|\hat{W}|\varphi_n\varphi_m\rangle - \langle\varphi_n\varphi_m|\hat{W}|\varphi_m\varphi_n\rangle\right)}_{\langle\varphi_n|\hat{V}_H+\hat{V}_X|\varphi_n\rangle\ \text{(B)}} \\
&\overset{Eqs.\ 2.38,2.41}{=} -\langle\varphi_n|\hat{h}+\hat{V}_H+\hat{V}_X|\varphi_n\rangle \overset{\text{Eq. } F.4}{=} -\underbrace{\langle\varphi_n|\hat{F}|\varphi_n\rangle}_{\epsilon_n} =: -\epsilon_n
\end{aligned} \tag{2.113}$$

The letters in parenthesis, (A) and (B), refer to figure 2.6.

Thus, the energy loss is–up to the sign–equal to an eigenvalue of the Fock operator. Therefore, we identify the eigenvalues of the Fock operator with the energy levels ϵ_n of the system. The Fock-operator is obtained from the ground-state Slater determinant rather than the one for the excited state. Thus, there is a single operator, the Fock operator of the ground state, which determines the spectrum of all one-particle addition and removal energies.

The picture, which emerges, is very similar to that of non-interacting particles. The main difference is that the energy levels are given by the Fock operator $\hat{F}$ and not the non-interacting Hamiltonian $\hat{h}$. The interaction shifts the energy levels relative to the non-interacting case. In contrast to the non-interacting electron gas, however, the total energy is not given by the expectation values of this operator.

2.5.4 Inverse photoemission

Let me now consider the inverse photoemission process, in which an electron is absorbed by the material and a photon is emitted, while the electron settles into a previously unoccupied orbital.

Let me denote the Slater determinant of the final state $|\vec{\sigma}_{+n}\rangle$. Compared to the initial state $|\vec{\sigma}_0\rangle$, it has an additional electron in state $|\varphi_n\rangle$ with $n > N$.

The energy conservation requires that the initial and finals energies are the same

$$\underbrace{E(\vec{\sigma}_0) + E_{\text{vac}} + E_{\text{kin}}}_{\text{initial state}} = \underbrace{E(\vec{\sigma}_{+n}) + \hbar\omega}_{\text{final state}} \tag{2.114}$$

The energy loss ΔE_{loss}, the energy $\epsilon_{\text{vac}} + E_{\text{kin}}$ of the injected electron minus the energy $\hbar\omega$ of the

emitted photon, can be calculated as energy difference of the initial and final Slater determinants.

$$\begin{aligned}
\Delta E_{\text{loss}} &= \epsilon_{\text{vac}} + E_{\text{kin}} - \hbar\omega \\
&\overset{\text{Eq. 2.114}}{=} E(\vec{\sigma}_{+n}) - E(\vec{\sigma}_0) \\
&\overset{\text{Eq. 2.111}}{=} \langle\varphi_n|\hat{h}|\varphi_n\rangle + \frac{1}{2}\underbrace{\Big(\langle\varphi_n\varphi_n|\hat{W}|\varphi_n\varphi_n\rangle - \langle\varphi_n\varphi_n|\hat{W}|\varphi_n\varphi_n\rangle\Big)}_{=0\ \text{(C)}} \\
&\qquad + \sum_{m=1}^{N}\underbrace{\Big(\langle\varphi_n\varphi_m|\hat{W}|\varphi_n\varphi_m\rangle - \langle\varphi_n\varphi_m|\hat{W}|\varphi_m\varphi_n\rangle\Big)}_{\langle\varphi_n|\hat{V}_H+\hat{V}_X|\varphi_n\rangle\ \text{(D)}} \\
&\overset{\text{Eqs. 2.38,2.41}}{=} \langle\varphi_n|\hat{h}+\hat{V}_H+\hat{V}_X|\varphi_n\rangle \overset{\text{Eq. F.4}}{=} \langle\varphi_n|\hat{F}|\varphi_n\rangle =: \epsilon_n
\end{aligned} \tag{2.115}$$

The letters in parenthesis, (C) and (D), refer to figure 2.6.

The electron-addition energies are the eigenvalues of the Fock operator.

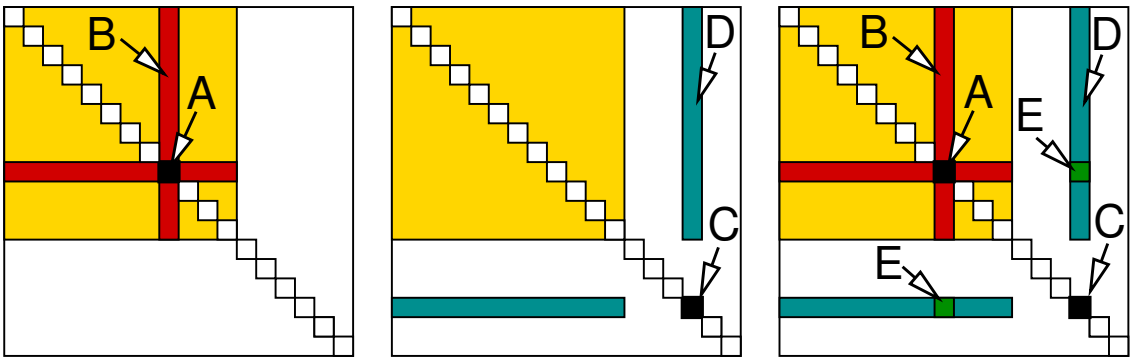

Fig. 2.6: Schematic representation of the matrix of interactions $\mathcal{W}_{m,n} = \frac{1}{2}\Big(\langle\varphi_m,\varphi_n|\hat{W}|\varphi_m,\varphi_n\rangle - \langle\varphi_m,\varphi_n|\hat{W}|\varphi_n,\varphi_m\rangle\Big)$ between one-particle orbitals of a Slater determinant. The graphs show the terms for electron removal in photo-emission (left), electron addition in inverse photoemission (middle) and the formation of an electron-hole pair (right). The yellow region denotes the occupied orbitals. The interaction matrix elements involving two identical orbitals vanish, which is indicated by the white, respectively black squares on the diagonal. The red bands (B) represents the interaction terms that are removed upon electron removal. The turquoise bands (D) represent the additional interactions upon electron addition. The graph on the right shows the interactions involved in the formation of an electron-hole pair. The interactions identified by the green squares need to be removed. This removal of the electron interaction describes the exciton binding energy.

Similarly, we can show that the occupied part of the spectrum of the Fock operator can be described as electron removal energies. Thus, the Fock operator provides us with the one-particle spectrum within the Hartree-Fock approximation.

2.5.5 Optical spectroscopy:

Let us now consider the energy required to lift an electron from an occupied state $|\varphi_m\rangle$ with $m \leq N$ into an empty orbital $|\varphi_n\rangle$ with $n > N$. Let me denote the state with the electron-hole pair as $|\vec{\sigma}_{-m/+n}\rangle$.

The energy loss in this case is simply the energy of the absorbed photon. The energy balance is

$$\underbrace{\hbar\omega + E(\vec{\sigma}_0)}_{\text{initial state}} = \underbrace{E(\vec{\sigma}_{-m/+n})}_{\text{final state}} \tag{2.116}$$

Thus, the energy loss upon removal of an electron in orbital $|\varphi_m\rangle$ and addition of one in orbital $|\varphi_n\rangle$ is

$$\begin{aligned}
\Delta E_{\text{loss}} &= E(\vec{\sigma}_{-m/+n}) - E(\vec{\sigma}_0) \\
&\overset{\text{Eq. 2.111}}{=} \langle\varphi_n|\hat{h}|\varphi_n\rangle + \frac{1}{2}\underbrace{\Big(\langle\varphi_n\varphi_n|\hat{W}|\varphi_n\varphi_n\rangle - \langle\varphi_n\varphi_n|\hat{W}|\varphi_n\varphi_n\rangle\Big)}_{=0\text{ (C)}} + \sum_{j=1}^{N}\underbrace{\Big(\langle\varphi_n\varphi_j|\hat{W}|\varphi_n\varphi_j\rangle - \langle\varphi_n\varphi_j|\hat{W}|\varphi_j\varphi_n\rangle\Big)}_{\langle\varphi_n|\hat{V}_H+\hat{V}_X|\varphi_n\rangle\text{ (D)}} \\
&- \langle\varphi_m|\hat{h}|\varphi_m\rangle - \frac{1}{2}\underbrace{\Big(\langle\varphi_m\varphi_m|\hat{W}|\varphi_m\varphi_m\rangle - \langle\varphi_m\varphi_m|\hat{W}|\varphi_m\varphi_m\rangle\Big)}_{=0\text{ (A)}} - \sum_{j=1}^{N}\underbrace{\Big(\langle\varphi_m\varphi_j|\hat{W}|\varphi_m\varphi_j\rangle - \langle\varphi_m\varphi_j|\hat{W}|\varphi_j\varphi_m\rangle\Big)}_{\langle\varphi_m|\hat{V}_H+\hat{V}_X|\varphi_m\rangle\text{ (B)}} \\
&- \Big(\langle\varphi_m\varphi_n|\hat{W}|\varphi_m\varphi_n\rangle - \langle\varphi_m\varphi_n|\hat{W}|\varphi_n\varphi_m\rangle\Big) \\
&= \epsilon_n - \epsilon_m - \underbrace{\Big(\langle\varphi_m\varphi_n|\hat{W}|\varphi_m\varphi_n\rangle - \langle\varphi_m\varphi_n|\hat{W}|\varphi_n\varphi_m\rangle\Big)}_{\text{exciton binding energy (E)}}
\end{aligned} \tag{2.117}$$

The letters in parenthesis, (A)-(E), refer to figure 2.6. The one-particle energies ϵ_n and ϵ_m are the eigenvalues of the Fock-operator, i.e.

$$\epsilon_n = \langle\varphi_n|\hat{h} + \hat{V}_H + \hat{V}_X|\varphi_n\rangle \tag{2.118}$$

The first two terms Eq. 2.117 are simply the electron-addition and removal energies, which are given by the one-particle spectrum. The last term is the electrostatic attraction of electron and hole. This is the so-called **exciton binding energy**. The second interaction term, the exchange term, counteracts the first, but it is only present when both orbitals have the same spin direction. Therefore, the Coulomb interaction between wave functions with opposite spin are much stronger than those with equal spin.

Nevertheless, the two-particle spectra $\mathcal{B}(\hbar\omega)$ are often closely related to a convolution of one-particle spectra as for non-interacting particles.

$$\mathcal{B}(\hbar\omega) = \int d\epsilon \int d\epsilon\, \mathcal{A}(\epsilon)\mathcal{A}(\epsilon')\delta(\hbar\omega - \epsilon - \epsilon') = \int d\epsilon; \mathcal{A}(\frac{1}{2}\hbar\omega + \epsilon)\mathcal{A}(\frac{1}{2}\hbar\omega - \epsilon) \tag{2.119}$$

If the kinetic energy of interacting quasi-particles is sufficiently large that no bound pairs can form, interaction effects become secondary and the two-particle spectrum will be similar to the non-interacting case.

2.5.6 Spectral function

For non-interacting electrons, the band structure $\epsilon_n(\vec{k})$ and the density of states are key quantities to understand both, the energy and the excitations of a system. As soon as an interaction is present, the situation becomes more complex.

The photo-emission and inverse photo-emission experiments probe one-particle excitations, that is electron addition and removal. These experiments extract the so-called **spectral function**, often written as total spectral function $\mathcal{A}(\epsilon)$ or as one-particle operator $\hat{\mathcal{A}}(\epsilon)$. For non-interacting systems, the spectral function is simply the density of states and it is obtained from the eigenvalues of the one-particle Hamilton operator as[39]

$$\hat{D}(\epsilon) = \sum_n |\varphi_n\rangle\delta(\epsilon - \epsilon_n)\langle\varphi_n| \tag{2.120}$$

[39] I consider the density of states as a one-particle operator, so that we can also determine projections onto certain orbitals and so-called Crystal Orbital Hamilton Populations (COHP)[42]. The latter provide insight into chemical binding.

For weak interactions, the one-particle excitations such as electron addition or removal can be described well by a spectral function, which is obtained analogously to Eq. 2.120, but with energies ϵ_n and one-particle wave functions $|\varphi_n\rangle$ obtained from the Fock operator rather than from the non-interacting Hamiltonian.

$$\underbrace{\left[\hat{h} + \hat{V}_H + \hat{V}_X\right]}_{\hat{F}} |\varphi_n\rangle = |\varphi_n\rangle \epsilon_n \tag{2.121}$$

This equation is closely related to the equation of motion Eq. 8.16 for the Green's function

$$\left[\epsilon - \hat{h} - \hat{\Sigma}(\epsilon)\right] \hat{G}(\epsilon) = \hat{1} \tag{2.122}$$

with the self-energy from Eq. 8.15. The equation of motion is general and not limited to weak interactions. We will come to Green's functions of many-particle systems later. At this point it is sufficient to remember that Hartree and exchange potential act as self energy in the Hartree-Fock description.

ELECTRON REMOVAL AND ADDITION ENERGIES

The one-particle spectrum probes the electron removal energies and electron addition energies. For weakly interacting systems they are determined by the eigenvalues of the Fock operator of the ground state. The resulting spectral function is

$$\hat{\mathcal{A}}(\epsilon) = \sum_n |\varphi_n\rangle \delta(\epsilon - \epsilon_n) \langle \varphi_n| \tag{2.123}$$

with one-particle energies ϵ_n and one-particle orbitals $|\varphi_n\rangle$ from the Fock-operator of the electronic ground state.

$$\underbrace{\left[\hat{h} + \hat{V}_H + \hat{V}_X\right]}_{\hat{F}} |\varphi_n\rangle = |\varphi_n\rangle \epsilon_n \tag{2.124}$$

Unlike non-interacting electrons, two-particle excitations of interacting particles can no more be obtained by from the one-particle spectral function alone. For excitations which create two or more particles, e.g. holes and electrons, the interaction between the excited quasi particles, i.e. electrons and holes, must be taken into account. For two-particle excitations, such as optical excitations, a different spectral function is required, which is specifically devised for, say, electron-hole excitations.

General interacting systems always have a well-defined one-particle spectral function $\hat{\mathcal{A}}(\epsilon)$, which generalizes the density of states of non-interacting electrons. The spectral function of interacting systems (beyond the Hartree-Fock method) is described later, in section 9.3 on p. 271.

2.5.7 Electron affinity and ionization potential

The spectral properties are connected to the electron addition and electron removal energies, respectively the formation energies of electron-hole pairs. The **ionization energy** I is the energy required to remove an electron from the system, i.e. to lift it up into the **vacuum level** E_{vac}. The **work function**[40] is the generalization of the ionization potential to solids. The **electron affinity** A is the energy gained by adding an electron to the system, while taking it from the vacuum level.

$$I \stackrel{\text{def}}{=} (E_{N-1} + E_{vac}) - E_N \tag{2.125}$$

$$A \stackrel{\text{def}}{=} (E_N + E_{vac}) - E_{N+1} \tag{2.126}$$

[40] German: Austrittsarbeit

The difference between ionization potential and electron affinity is the band gap of a material.

$$\epsilon_g \stackrel{\text{def}}{=} I - A = E_{N+1} - 2E_N + E_{N-1} \tag{2.127}$$

Similarly, the valence-band top ϵ_v and the bottom of the conduction-band ϵ_c are defined as

$$\begin{aligned} \epsilon_v &\stackrel{\text{def}}{=} E_N - E_{N-1} \\ \epsilon_c &\stackrel{\text{def}}{=} E_{N+1} - E_N \end{aligned} \tag{2.128}$$

These definitions are obvious in the context of non-interacting electrons. However, they are definitions, which also apply to many-particle systems in general, interacting or not.

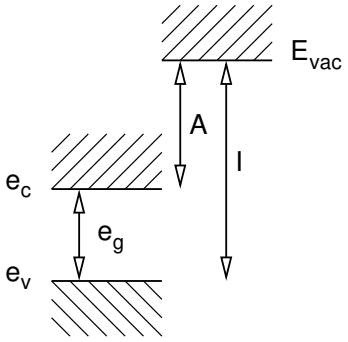

Fig. 2.7: Scheme to illustrate electron affinity A and ionization potential I in the context of a one-particle picture and non-interacting electrons. E_{vac} is the vacuum level, ϵ_c is the conduction band-minimum, ϵ_v is the valence-band maximum and ϵ_v is the band gap separating empty from filled one-particle states. The ground-state energy of a $N+1$ particle system is $E_{N+1} = E_N + \epsilon_c$, while that of an $N-1$ particle system is $E_{N-1} = E_N - \epsilon_v$. The energy of an N-particle system with one electron (hole) in the vacuum level is $E_N + E_{vac}$ ($E_N - E_{vac}$).

2.5.8 Spectral properties of the free-electron gas

Let me describe here the qualitative changes undergone by the band structure of the electron gas due to the interaction between electrons. I will summarize the main effects also beyond the Hartree-Fock limit. It shall provide an guiding overview of correlation effects related to a particularly simple system, the free electron gas.

Within the Hartree-Fock method, the free-electron gas can be treated analytically. This is shown in appendix E.3 on p. 449. The findings are not only relevant for the Hartree-Fock method but also beyond. Here, I will only discuss the main findings.

Editor: Include here a sequence pictures of band structures, i.e. k-resolved spectral functions, for the free-electron gas with different phenomena. 1. non-interacting free-electron gas. parabola 2) Hartree-Fock approximation: self-energy shift (large for filled states, small for empty states), zero density of states at the Fermi level. 3) screened Hartree Fock: smaller band width of the filled states, again finite density of states at the Fermi level. 4) RPA: Lifetime broadening of the spectral function, but infinite lifetime at the Fermi level. 5) Satellites, quasi-Particle weight. 6) Ferromagnetic phase transition. 7) Mott insulator?

1. **Non-interacting electrons:** the dispersion relation $\epsilon(\vec{k})$ of the non-interacting, free-electron gas is a simple parabola.

$$\epsilon(\vec{k}) = \frac{\hbar^2 \vec{k}^2}{2m_e} \tag{2.129}$$

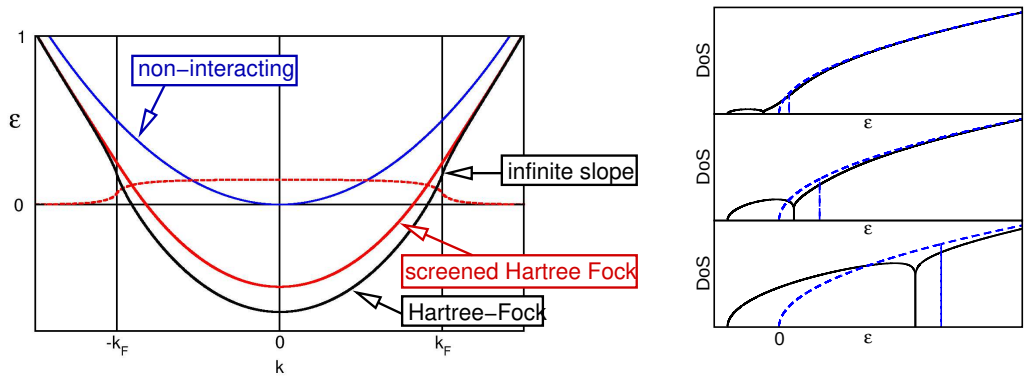

Fig. 2.8: Left: dispersion relation $\epsilon(k)$ of the free-electron gas as calculated without interactions (blue), with Hartree-Fock (black) and with screened Hartree-Fock (red). The Fermi momentum has been chosen as $k_F = 1/a_0$ and the screening length for the screened Hartree-Fock calculation has been 6 a_0, where a_0 is the Bohr radius. The red, dashed line is the quasi-particle shift due to screening. Only the bands of unscreened Hartree-Fock exhibit an infinite slope at the Fermi level. The Fermi level is at $\epsilon(k_F)$. Right: density of states of the free-electron gas without interactions (blue) and in the Hartree-Fock approximation. The straight line of the non-interacting electron gas is indicated by the straight line. The electron density increases from top to bottom. The density of states for the Hartree-Fock calculation drops to zero at the Fermi level. The energy of the bottom of the band is independent of the electron density and depends only on the strength of the interaction.

In a crystal lattice with primitive lattice vectors $\vec{T}_1, \vec{T}_2, \vec{T}_2$, a parabola is centered at each general reciprocal lattice vector $\vec{G}_n$, i.e.

$$\epsilon_n(\vec{k}) = \frac{\hbar^2}{2m_e}\left(\vec{k} - \vec{G}_n\right)^2 \tag{2.130}$$

The resulting dispersion relation has several bands and the band structure is periodic in the periodic lattice. The band structure of the free-electron gas in the **reduced zone scheme** is shown in figure 1.10 on p. 43.

2. **Hartree-Fock:** The exchange energy shifts the band structure down in energy. This is the so-called **quasi-particle shift**. The quasi-particle shift is large for the filled states, and vanishes for high kinetic energy $\epsilon(\vec{k})$. This can be attributed to the fact that the exchange term stabilizes states that are similar to filled states (Section 2.2.2). The empty states far above the Fermi level are little affected by the exchange hole. Loosely speaking, this is because the electrons are so fast that the exchange hole cannot properly form, respectively that the electron escapes the exchange hole.

   The Fermi-momentum $\hbar k_F$ is unchanged by a weak interaction. The Hartree-Fock approximation produces an **artifact at the Fermi surface**: as shown in figure 2.8, the slope of the dispersion relation becomes infinite and the spectral function drops to zero.

3. **Screened Hartree Fock:** The artifact at the Fermi surface (infinite slope and vanishing density of states) is due to long-ranged nature of the Coulomb interaction. In the presence of a Fermi-gas, the Coulomb interaction is screened: The electric field polarizes the electron density. This can be described by the formation of electron-hole pairs, forming electric dipoles, that oppose the electric field. This effect is described by a momentum- and frequency-dependent dielectric constant. The resulting screened Coulomb interaction is replaced by an approximate

Yukawa potential[41] with finite range. The picture just described is the essence of the so-called **random-wave approximation (RPA)** [43, 44, 45]. Screening removes the infinite slope of the energy bands at the Fermi level, which was an artifact of the Hartree-Fock approximation.

Furthermore, screening generally decreases the net quasiparticle shift compared to the Hartree-Fock description. Thus it affects the **band width** of metals, the energy distance from the bottom of the valence band to the Fermi level. For potassium, the band width of the free-electron gas is 2 eV, somewhat larger than the experimental result of 1.5-1.6 eV. The Hartree-Fock approximation yields a far too large value of 5.3 eV. (See lecture notes by Wolf-Dieter Schöne. 2001)

4. **Lifetime broadening:** An interacting electron travelling through an electron gas may collide with other electrons and thus transfer energy and momentum to electron-hole excitations in the surrounding electron gas. This energy dissipation acts like an effective friction which is responsible for the finite conductivity.

   The same effect results in a life-time broadening of the delta peaks $\delta(\epsilon - \epsilon(k))$ of the k-resolved spectral function. The electron level hybridizes with electron-hole excitations and mixes the electron-hole excitations into the electron spectral function.

   When one adds or removes an electron, one can also simultaneously create an electron-hole pair, which changes the addition- or removal energy. Thus, instead of a single energy level, there are many possible energy levels, which describe the addition or removal of an electron in combination with a formation or recombination of an electron-hole pair. In the spectral function one observes a broadening of the original delta-peak at $\epsilon(\vec{k})$.

   The total weight of the peak is conserved because of the **charge sum rule**[42]

5. **Satellites and plasmons:** Satellites are spectral features, which are separated from the main electron addition and removal energies as sketched in figure 2.9. They are due to the mixing of one-particle excitations with other particle-number conserving excitations. In the free-electron gas, an example for such a particle-number conserving excitation is a **plasmon**, a kind of collective charge fluctuation. If the electron removal leaves another excitation behind, the energy of the latter adds to the excitation energy. Therefore, additional spectral features are observed for the composite excitations at energies corresponding to the sum of the energies of its contributions.

   Due to the charge sum rule, the total weight of the spectrum of an orbital must sum up to one. The weight lost to the satellite is lost from the main peak. This leads to the so-called **quasi-particle weight** Z, which is less than one.

   A minimal model for a satellite is the topic of the exercise 9.6.1 on p. 279.

   A spectral function of the free-electron gas with the satellite due to plasmons is shown in Caruso et al.[46]. (`https://doi.org/10.48550/arXiv.1606.08573.pdf`) The satellite structure of silicon has been investigated, both experimentally and theoretically, by Lischner et al. [47].

   Editor: see `Figs/Fortran/Lundquist/src/code.f90`

6. **Phase transitions:** (Ferromagnet, Mott insulator?)

[41] A Yukawa potential has the form

$$v(\vec{r}) = \frac{C}{|\vec{r}|} e^{-\lambda|\vec{r}|} \tag{2.131}$$

where C is some prefactor and $1/lambda$ is the range of the interaction.

[42] As the weight of the original orbital is decreased by admixing the excitation, the electron-hole pair will also obtain a contribution from the electron removal or electron addition. The net weight of the electron removal or addition is conserved.

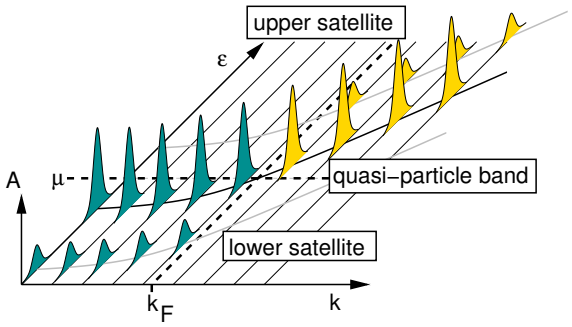

Fig. 2.9: Spectral function $A(\epsilon, k)$ of the free-electron gas with a single particle-conserving excitation with energy Δ and zero momentum producing satellite bands. The green shaded region denotes the occupied part of the spectral function, while the yellow shaded region denotes the unoccupied part. (This figure is repeated as figure 9.3.

2.5.9 Summary on spectral properties on the HF level

The following picture emerges:

- The electronic ground state forms the **Fermi sea** of electrons. The Fermi sea is treated like a vacuum state to which so-called **quasi particles**[43] can be added. We can not only add electrons, but also holes. Holes are electrons which are removed from the Fermi sea. The *"real particles"*, the electrons present in the ground state, are no more considered as individual particles but only as part of the Fermi sea.

- The **quasi-particle energies**, the energies ϵ_n of the quasi-particles, namely electrons and holes, are the eigenvalues of the Fock operator of the Slater determinant without excitations. The eigenvalues of the Fock operator define the **spectral function** $\mathcal{A}(\epsilon)$ in the Hartree-Fock method. The spectral function is the generalization of the **density of states** to interacting systems. The energy levels include a contribution from the electron interaction, the **quasi-particle shift** $\langle\varphi_n|\hat{V}_H + \hat{V}_X|\varphi_n\rangle$.

  Note, however, that the total energy is **not** the expectation value of the Fock operator, i.e. $E_{\text{tot}} \neq \langle\Phi|\hat{F}|\Phi\rangle$!

- The quasi-particles, electrons and holes, have their own charges and they interact with each other. In the case of electron-hole pairs, the Coulomb attraction can lead to the formation of bound states, which are called **excitons**.

  Excitons are often considered like quasi hydrogen atoms, where the proton is replaced by a hole. In a semi-conductor, one can estimate the exciton binding energy from this model using the effective masses of electrons and holes, as derived from the band structure, and the relative dielectric constant of the host material.

- Due to the interaction, the one-particle spectral function $\mathcal{A}(\epsilon)$ alone is not sufficient to describe two-particle excitations such as an electron-hole pair. This is a fundamental difference between interacting and non-interacting systems.

- Electrons and holes in a Fermi sea are analogous to electrons and its anti particles, the positrons, in a vacuum. The band gap of the vacuum is twice the rest energy $E_0 = m_0c^2$, where m_0 is the rest mass. Just like electrons and holes can recombine by emitting light, the electron-positron pair can annihilate by emitting two photons, each having the energy[44] $\hbar\omega = m_0c^2$.

[43] The meaning of term quasi-particle depends on the context.

[44] The wave length of these photons, which an energy equal to the rest mass of a particle, is the **Compton wavelength** $\ell = 2\pi/k \overset{\omega/k=c}{=} 2\pi c/\omega = 2\pi\hbar c/(\hbar\omega) = 2\pi\hbar c/(m_0c^2)$

2.5.10 Outlook: Electron correlation

The picture of excitation, which emerges from the Hartree-Fock description is that of addition and removal of electrons where the excitation energies are determined by the Fock operator of the ground state. Added electrons and holes experience each other via the Coulomb repulsion, but the Fermi gas is not affected at all by these excitations.

There is one effect missing in this picture: As an electron is added, it creates electric fields, which polarize the material. This **polarization** of the charge distribution can itself be described by the creation of electron-hole pairs. An excited electron is thus surrounded by a cloud of electron-hole pairs. This cloud is due to the correlated motion of many electrons. One speaks of **electron correlation**. This cloud reduces the electrostatic potential of the electron. On says that the induced electron-hole pairs **screen** the electric field produced by the excitation. The screening is governed by the dielectric constant $\epsilon_r(\vec{q},\omega)$ of the material.

The material polarizes, because it can lower its energy in the presence of an additional particle by rearranging its charge density. This indicates that the excitation energy is usually smaller than what the Fock operator predicts. This is what simulations show: the band gap obtained in the Hartree-Fock approximation is larger than what is measured.

The dielectric constant contains a frequency argument, which describes that it takes a certain time, until the polarization cloud is formed.

This modified picture sketched here motivated the **random-phase approximation (RPA)** [43, 44, 48]. In the random-phase approximation, the Fermi-sea is not considered as a rigid medium, but it can be polarized by the electric fields of the electrons and holes. The polarization of the Fermi sea can be described by a dielectric constant $\epsilon_r(q,\omega)$. The inclusion of the dielectric constant modifies the **bare Coulomb interaction** to a **screened Coulomb interaction**, which is short ranged and retarded.

This renormalization explains the success of the independent particle picture despite the strong Coulomb interaction.

2.6 Summary

- The eigenstates of non-interacting Hamiltonians $\hat{h}$ are Slater determinants

$$\begin{aligned}\hat{h}|\varphi_n\rangle &= |\varphi_n\rangle\epsilon_n \\ \hat{h}|\vec{\sigma}\rangle &= |\vec{\sigma}\rangle \underbrace{\sum_n \sigma_n\epsilon_n}_{E_{\vec{\sigma}}}\end{aligned} \tag{2.132}$$

- Expectation values of one-particle at a time operators are obtained as sum over occupied one-particle orbitals.

$$\langle A\rangle = \langle\vec{\sigma}|\hat{A}|\vec{\sigma}\rangle = \sum_n \sigma_n\langle\varphi_n|\hat{A}|\varphi_n\rangle = \mathrm{Tr}[\hat{\rho}^{(1)}\hat{A}] \tag{2.133}$$

- one-particle-reduced density matrix $\hat{\rho}^{(1)}$, occupations and natural orbitals.
- The expectation value of the interacting Hamiltonian with a Slater determinant. Hartree- and Exchange energy. Hartree and exchange potentials.
- Exchange-hole
- Hartree-Fock equations and Fock operator. Correlated occupation-number fluctuations.
- Spectroscopy: Photoemission, inverse photoemission, optical absorption

- One-particle excitations: Electron addition and removal. Two-particle excitations: e.g. formation of an electron-hole pair.
- One-particle spectral function: equivalent to density-of-states for non-interacting particles. Given by the eigenvalues of the Fock operator.
- Two-particle excitations have, in addition, a correction from the interaction of the two particles, such as the Coulomb attraction of electrons and holes.

In this section, we investigated the role of interaction for weakly interacting systems. The expansion in the interaction strength lead from the non-interacting electrons as zeroth-order term to the **Hartree-Fock approximation**, which includes the interaction to first order in the interaction strength. Higher-order terms in the interaction are counted to the so-called **correlation energy**.

In the Hartree-Fock approximation, the energy can be calculated for a wave function of a non-interacting electron gas, which is a Slater determinant. For Slater determinants the total energy can readily be expressed by sums or double sums over the one-particle orbitals in the Slater determinant. The interaction energy in Hartree-Fock can be divided into the Hartree energy and the exchange energy.

Besides the definition of the Hartree-Fock approximation as the first term in an expansion in the interaction strength, it can also be represented as the minimum of the total energy that can be obtained by Slater determinants.

In contrast to non-interacting electrons, total energy and excitations are no more described by a single Hamiltonian. The **Fock operator** describes the one-electron excitations of the system in the Hartree-Fock description. One-electron excitations are electrons and holes. The density-of-states of one-particle excitations is the **spectral function**. If two one-electron excitations are created simultaneously, they experience their Coulomb interaction. This can lead to the formation of bound states of electrons and holes, so-called **excitons**.

The Fock operator depends on the ground state wave function. It makes a difference between filled and empty states. Filled states are shifted downward relative to empty states. This leads to a splitting of the multiplet of partially occupied wave functions. Imagine a transition-metal oxide with a partially filled d-shell. The interaction has a large effect on opening a band gap. An example of this effect is the Mott-insulator, which is insulating only because of interaction effects.

To understand the interaction energy, the concept of the exchange hole is very useful. It allows to understand Hund's rule and magnetic transitions as described by Stoner's theory.

The Hartree-Fock approximation already describes a few correlation effects.

1. **Hund's rule**
2. **Magnetism**
3. Interaction-mediated splitting of empty and filled states. This is the first step to the so-called **Mott-Hubbard physics**.
4. others, like the left-right correlation in chemical bonds will be discussed later.

2.7 Further reading

Let me refer to the appendix F on p. 473, where I collected some material that I found interesting in this context.

2.8 Home study and Practice

2.8.1 Boltzmann entropy and Fermi distribution

Introduction

This exercise serves to strengthen the understanding of the origin of the Fermi distribution function and irs connection to the Boltzmann entropy. The second part shall refresh how to deal with functions of operators.

Problem

Derive the Fermi-distribution function as thermal occupation of non-interacting Fermions. The Hamiltonian of a non-interacting sustem can be represented in terms of its eigenstates and eigenvalues as $\hat{h} = \sum_n |\varphi_m\rangle \bar{\epsilon}_n \langle\varphi_n|$.

1 Minimize the grand canonical potential of a non-interacting system with the Boltzmann entropy

$$S^B[\{f_n\}] = -k_B \sum_n \Big[f_n \ln(f_n) + (1-f_n)\ln(1-f_n) \Big] \tag{2.134}$$

and show that the resulting thermal occupations are identical to the Fermi distribution.

2 Show, how the Boltzmann entropy expressed in terms of occupations is obtained from the more general expression using the one-particle reduced density matrix

$$S^B[\hat{\rho}^{(1)}] = -k_B \mathrm{Tr}\Big[\hat{\rho}^{(1)} \ln(\hat{\rho}^{(1)}) + (\hat{1} - \hat{\rho}^{(1)}) \ln(\hat{1} - \hat{\rho}^{(1)}) \Big] \tag{2.135}$$

Solution

1 Minimize the grand canonical potential of a non-interacting system with the Boltzmann entropy

$$S^B[\{f_n\}] = -k_B \Big[f_n \ln(f_n) + (1-f_n)\ln(1-f_n) \Big] \tag{2.136}$$

and show that the resulting thermal occupations are identical to the Fermi distribution.

$$\begin{aligned}
\Omega_{T,\mu} &= \min_{\{f_n\}} \sum_n f_n \bar{\epsilon}_n - T S^B[\{f_n\}] - \mu N[\{f_n\}] \\
&= \min_{\{f_n\}} \sum_n f_n \bar{\epsilon}_n + k_B T \sum_n \Big[f_n \ln(f_n) + (1-f_n)\ln(1-f_n) \Big] - \mu \sum_n f_n \\
\delta\Omega_{T,\mu} &= \sum_n \delta f_n \left\{ \bar{\epsilon}_n + k_B T \Big[\ln(f_n) + f_n \frac{1}{f_n} - \ln(1-f_n) - (1-f_n)\frac{1}{1-f_n} \Big] - \mu \right\} \stackrel{!}{=} 0 \\
0 &= \bar{\epsilon}_n + k_B T \ln\left[\frac{f_n}{1-f_n} \right] - \mu \\
\ln\Big[\frac{f_n}{1-f_n} \Big] &= -\frac{1}{k_B T}(\bar{\epsilon}_n - \mu) \\
f_n &= \mathrm{e}^{-\frac{1}{k_B T}(\bar{\epsilon}_n - \mu)} \Big(1 - f_n \Big) \\
f_n &= \frac{\mathrm{e}^{-\frac{1}{k_B T}(\bar{\epsilon}_n - \mu)}}{1 + \mathrm{e}^{-\frac{1}{k_B T}(\bar{\epsilon}_n - \mu)}} = \frac{1}{1 + \mathrm{e}^{+\frac{1}{k_B T}(\epsilon_n - \mu)}} = f_{T,\mu}(\bar{\epsilon})
\end{aligned} \tag{2.137}$$

This is the Fermi distribution function.

2 Show, how the Boltzmann entropy expressed in terms of occupations is obtained from the more general expression using the one-particle reduced density matrix

$$S^B[\hat{\rho}^{(1)}] = -k_B \sum_n \Big[\hat{\rho}^{(1)} \ln(\hat{\rho}^{(1)}) + (\hat{1} - \hat{\rho}^{(1)}) \ln(\hat{1} - \hat{\rho}^{(1)})\Big] \tag{2.138}$$

I represent the one-particle reduced density matrix in term of occupations and natural orbitals

$$\hat{\rho}^{(1)} = \sum_n |\varphi_n\rangle f_n \langle\varphi_n| \tag{2.139}$$

$$\begin{aligned} S^B[\hat{\rho}^{(1)}] &= -k_B \,\mathrm{Tr}\Big[\hat{\rho}^{(1)} \ln(\hat{\rho}^{(1)}) + (\hat{1} - \hat{\rho}^{(1)}) \ln(\hat{1} - \hat{\rho}^{(1)})\Big] \\ &= -k_B \mathrm{Tr}\Big[\Big(\sum_n |\varphi_n\rangle f_n \langle\varphi_n|\Big) \ln\Big(\sum_n |\varphi_n\rangle f_n \langle\varphi_n|\Big) \\ &\quad + \Big(\sum_n |\varphi_n\rangle (1-f_n) \langle\varphi_n|\Big) \ln\Big(\sum_n |\varphi_n\rangle (1-f_n) \langle\varphi_n|\Big)\Big] \end{aligned} \tag{2.140}$$

Now I exploit that a function $g(x)$ of an operator $\hat{x} = \sum_n |\varphi_n\rangle x_n \langle\varphi_n|$ in its diagonal form has the same eigenstates and its eigenvalues are the functions of the eigenvalues of the operator in the argument.

$$g\Big(\sum_n |\varphi_n\rangle x_n \langle\varphi_n|\Big) = \sum_n |\varphi_n\rangle g(x_n) \langle\varphi_n| \tag{2.141}$$

This statement follows from the similar relation for power-series expansions

$$g(x) = \sum_j a_j x^j \tag{2.142}$$

which can be proven recursively. The step from a power series expansion to general functions is done by using (local) Taylor expansions of the function g.

$$\begin{aligned} S^B[\hat{\rho}^{(1)}] &= -k_B \mathrm{Tr}\Big[\Big(\sum_n |\varphi_n\rangle f_n \langle\varphi_n|\Big)\Big(\sum_{n'} |\varphi_{n'}\rangle \ln(f_{n'}) \langle\varphi_{n'}|\Big) \\ &\quad + \Big(\sum_n |\varphi_n\rangle (1-f_n) \langle\varphi_n|\Big)\Big(\sum_{n'} |\varphi_{n'}\rangle \ln(1-f_{n'}) \langle\varphi_{n'}|\Big)\Big] \\ &= -k_B \mathrm{Tr}\Big[\sum_{n,n'}\Big(|\varphi_n\rangle f_n \underbrace{\langle\varphi_n|\varphi_{n'}\rangle}_{\delta_{n,n'}} \ln(f_{n'}) \langle\varphi_{n'}| + |\varphi_n\rangle (1-f_n) \underbrace{\langle\varphi_n|\varphi_{n'}\rangle}_{\delta_{n,n'}} \ln(1-f_{n'}) \langle\varphi_{n'}|\Big)\Big)\Big] \end{aligned} \tag{2.143}$$

Finally, I exploit the orthonormality of the natural orbitals and resolve the trace.

$$\begin{aligned} S^B[\hat{\rho}^{(1)}] &= -k_B \mathrm{Tr}\Big[\sum_n |\varphi_n\rangle \Big(f_n \ln(f_n) + (1-f_n)\ln(1-f_n)\Big)\Big] \langle\varphi_n|\Big) \\ &= -k_B \sum_n \Big(f_n \ln(f_n) + (1-f_n)\ln(1-f_n)\Big) \end{aligned} \tag{2.144}$$

2.8.2 The hydrogen atom in the Hartree-Fock approximation

Introduction

This is a little but extremely useful exercise, which clarifies some notions regarding many-particle physics and the Hartree-Fock approximation. It may be surprising that we study the hydrogen atom in a course on solid-state theory. However, many concepts from solid state theory are already there in the hydrogen atom and the hydrogen atom is the minimal problem for quite a few solid state effects.

Problem

Appendix hydrogen atom: section D.4

We will use here hydrogen 1s orbitals as one-particle basisset.

$$\chi_\sigma(\vec{r},\sigma') \overset{\text{Eq. } D.60}{=} \frac{1}{\pi a_0^3} \mathrm{e}^{-|\vec{r}|/a_0} \delta_{\sigma,\sigma'} \tag{2.145}$$

The two states are eigenstates of the non-interacting part $\hat{h}$ of the Hamiltonian

$$\hat{h}|\chi_\alpha\rangle = |\chi_\alpha\rangle\bar{\epsilon} \qquad \text{with } \bar{\epsilon} = -\frac{1}{2}H \tag{2.146}$$

The Bohr radius $a_0 = \frac{4\pi\epsilon_0\hbar^2}{e^2 m_e}$ and the Hartree $H = \frac{m_e e^4}{(4\pi\epsilon_0)^2\hbar^2}$ are the units for length and energy in the Hartree atomic unit system. The Hartree atomic units are defined by $\hbar = e = m_e = 4\pi\epsilon_0 = 1$.

The value $\bar{\epsilon}$ has been set equal to the ϵ_{1s} level of the hydrogen atom (See table D.8 on p. 434).

The interaction matrix element is defined as

$$W_{\alpha,\beta,\gamma,\delta} \overset{\text{Eq. } 2.34}{=} \int d^4x \int d^4x' \, \frac{e^2 \chi^*_\alpha(\vec{x}) \chi^*_\beta(\vec{x'}) \chi_\gamma(\vec{x}) \chi_\delta(\vec{x'})}{4\pi\epsilon_0 |\vec{r} - \vec{r'}|} \qquad \text{with } U \overset{\text{def}}{=} W_{\uparrow,\uparrow,\uparrow,\uparrow} = \frac{5}{8}H \tag{2.147}$$

1 Determine all 2^4 interaction matrix elements:

2 Specify the Hartree and exchange energy for the two-particle state.

3 Determine the total energy of the zero-particle state $|0\rangle$, the one-particle states $|\uparrow\rangle$ and $|\downarrow\rangle$, and two-particle state $|\uparrow\downarrow\rangle$ of the hydrogen atom using the one-particle Hilbert space described above.

4 Write down the Fock operator for the four many-particle eigenstates of the hydrogen atom.

5 Plot the density of states projected onto one of the one-particle orbitals for a one-particle system at low temperature.

6 Compare the density of states of an ensemble of eigenstates of the hydrogen atom with the mean-field Fock operator.

Discussion

1 Determine all 2^4 matrix interaction matrix elements:

$$\begin{aligned} W_{\alpha,\beta,\gamma,\delta} &= \begin{cases} U & \text{for } \sigma_\gamma = \sigma_\alpha \text{ and } \sigma_\delta = \sigma_\beta \\ 0 & \text{else} \end{cases} \\ &= U\delta_{\alpha,\gamma}\delta_{\beta,\delta} \end{aligned} \tag{2.148}$$

The U-parameter is one of the **Kanamori parameters**.[16] (See appendix F.2.3 on p. 480) Kanamori defined a set of parameters with which the interaction-tensor matrix elements of, for example, d-orbitals of a transition metal ion can be expressed. The interaction of the d-shell ($\ell = 2$) has $10^4 = 10000$ matrix elements. However, they can all be expressed by Editor: four? (check!) independent Kanamori parameters.

2 Specify the Hartree and exchange energy for the two-particle state.

The two orbitals of the hydrogen atom are characterized by their spin quantum number, i.e. $\alpha \in \{\uparrow, \downarrow\}$. In the two-particle state, both orbitals are occupied so that $f_\uparrow = f_\downarrow = 1$.

$$
\begin{aligned}
n(\vec{r}) &= \sum_{\sigma\in\{\uparrow,\downarrow\}} \sum_{\alpha\in\{\uparrow,\downarrow\}} f_\alpha |\chi_\alpha(\vec{r},\sigma)|^2 \\
E_H &\overset{\text{Eq. 2.37}}{=} \frac{1}{2}\int d^3r \int d^3r' \frac{e^2 n(\vec{r}) n(\vec{r'})}{4\pi\epsilon_0|\vec{r}-\vec{r'}|} = \frac{1}{2}\sum_{\alpha,\beta\in\{\uparrow,\downarrow\}} f_\alpha f_\beta \int d^4x \int d^4x' \frac{e^2 \chi_\alpha^*(\vec{x})\chi_\beta^*(\vec{x'})\chi_\alpha(\vec{x})\chi_\beta(\vec{x'})}{4\pi\epsilon_0|\vec{r}-\vec{r'}|} \\
&= \frac{1}{2}\sum_{\alpha,\beta\in\{\uparrow,\downarrow\}} \underbrace{W_{\alpha,\beta,\alpha,\beta}}_{} \overset{\text{Eq. 2.148}}{=} 2U \\
\rho^{(1)}(\vec{x},\vec{x'}) &= \sum_{\alpha\in\{\uparrow,\downarrow\}} f_\alpha \chi_\alpha(\vec{x})\chi_\alpha^*(\vec{x'}) \\
E_X &\overset{\text{Eq. 2.40}}{=} -\frac{1}{2}\int d^4x \int d^4x' \frac{e^2 \rho^{(1)}(\vec{x},\vec{x'})\rho^{(1)}(\vec{x'},\vec{x})}{4\pi\epsilon_0|\vec{r}-\vec{r'}|} \\
&= -\frac{1}{2}\sum_{\alpha,\beta\in\{\uparrow,\downarrow\}} f_\alpha f_\beta \int d^4x \int d^4x' \frac{e^2 \chi_\alpha^*(\vec{x})\chi_\beta^*(\vec{x'})\chi_\beta(\vec{x})\chi_\alpha(\vec{x'})}{4\pi\epsilon_0|\vec{r}-\vec{r'}|} \\
&= -\frac{1}{2}\sum_{\alpha,\beta\in\{\uparrow,\downarrow\}} \underbrace{W_{\alpha,\beta,\beta,\alpha}}_{U\delta_{\alpha,\beta}} \overset{\text{Eq. 2.148}}{=} -U
\end{aligned}
\tag{2.149}
$$

3 Determine the total energy of the zero-particle state $|0\rangle$, the one-particle states $|\uparrow\rangle$ and $|\downarrow\rangle$, and two-particle state $|\uparrow\downarrow\rangle$ of the hydrogen atom using the one-particle Hilbert space described above.

The total energy can be evaluated using Eq. 2.44.

$$
\begin{aligned}
E_{|0\rangle} &= \langle 0|\hat{H}|0\rangle = 0 \\
E_{|\uparrow\rangle} &= \langle\uparrow|\hat{H}|\uparrow\rangle = \bar{\epsilon} = -\frac{1}{2}H \\
E_{|\downarrow\rangle} &= \langle\downarrow|\hat{H}|\downarrow\rangle = \bar{\epsilon} = -\frac{1}{2}H \\
E_{|\uparrow\downarrow\rangle} &= \langle\uparrow\downarrow|\hat{H}|\uparrow\downarrow\rangle = 2\bar{\epsilon} + U = -\frac{3}{8}H
\end{aligned}
\tag{2.150}
$$

4 Write down the Fock operator for the four many-particle eigenstates of the hydrogen atom.

The density and one-particle-reduced density matrix is

$$
\begin{aligned}
n(\vec{r}) &= \sum_{\sigma\in\{\uparrow,\downarrow\}} \sum_{\alpha} f_\alpha \chi_\alpha^*(\vec{r},\sigma)\chi_\alpha(\vec{r},\sigma) \\
\rho^{(1)}(\vec{x},\vec{x'}) &= \sum_{\alpha} f_\alpha \chi_\alpha(\vec{x})\chi_\alpha^*(\vec{x'})
\end{aligned}
\tag{2.151}
$$

$$
\begin{aligned}
\hat{V}_H &\overset{\text{Eq. 2.38}}{=} \int d^4x\ |\vec{x}\rangle \left(\int d^3r'\ \frac{e^2 n(\vec{r'})}{4\pi\epsilon_0 |\vec{r} - \vec{r'}|} \right) \langle \vec{x}| \\
&= \underbrace{\sum_\beta |\pi_\beta\rangle\langle\chi_\beta|}_{\hat{1}} \int d^4x\ |\vec{x}\rangle \int d^4x'\ \frac{e^2 \sum_\alpha f_\alpha \chi^*_\alpha(\vec{x'})\chi_\alpha(\vec{x'})}{4\pi\epsilon_0|\vec{r} - \vec{r'}|} \langle\vec{x}| \underbrace{\sum_\gamma |\chi_\gamma\rangle\langle\pi_\gamma|}_{\hat{1}} \\
&= \sum_{\beta,\gamma} |\pi_\beta\rangle \sum_\alpha f_\alpha \int d^4x \int d^4x'\ \frac{e^2 \chi^*_\beta(\vec{x})\chi^*_\alpha(\vec{x'})\chi_\gamma(\vec{x})\chi_\alpha(\vec{x'})}{4\pi\epsilon_0|\vec{r} - \vec{r'}|} \langle\pi_\gamma| \\
&= \sum_{\alpha,\beta,\gamma} |\pi_\beta\rangle f_\alpha \underbrace{W_{\beta,\alpha,\gamma,\alpha}}_{U\delta_{\beta,\gamma}\delta_{\alpha,\alpha}} \langle\pi_\gamma| \\
&= \sum_\beta |\pi_\beta\rangle U \sum_\alpha f_\alpha \langle\pi_\beta| \qquad (2.152)
\end{aligned}
$$

$$
\begin{aligned}
\hat{V}_X &\overset{\text{Eq. 2.41}}{=} -\int d^4x \int d^4x'\ |\vec{x}\rangle \frac{e^2 \rho^{(1)}(\vec{x},\vec{x'})}{4\pi\epsilon_0|\vec{r} - \vec{r'}|} \langle\vec{x'}| \\
&= -\underbrace{\sum_\beta |\pi_\beta\rangle\langle\chi_\beta|}_{\hat{1}} \int d^4x\ |\vec{x}\rangle \int d^4x'\ \frac{e^2 \sum_\alpha \chi_\alpha(\vec{x}) f_\alpha \chi^*_\alpha(\vec{x'})}{4\pi\epsilon_0|\vec{r} - \vec{r'}|} \langle\vec{x'}| \underbrace{\sum_\gamma |\chi_\gamma\rangle\langle\pi_\gamma|}_{\hat{1}} \\
&= -\sum_{\beta,\gamma} |\pi_\beta\rangle \sum_\alpha f_\alpha \int d^4x \int d^4x'\ \frac{e^2 \chi^*_\beta(\vec{x})\chi^*_\alpha(\vec{x'})\chi_\alpha(\vec{x})\chi_\gamma(\vec{x'})}{4\pi\epsilon_0|\vec{r} - \vec{r'}|} \langle\pi_\gamma| \\
&= -\sum_{\alpha,\beta,\gamma} |\pi_\beta\rangle f_\alpha \underbrace{W_{\beta,\alpha,\alpha,\gamma}}_{U\delta_{\beta,\alpha}\delta_{\alpha,\gamma}} \langle\pi_\gamma| \\
&= -\sum_\alpha |\pi_\alpha\rangle f_\alpha U \langle\pi_\alpha| \qquad (2.153)
\end{aligned}
$$

The Fock operator $\hat{F}$ has the form

$$
\hat{F} = \hat{h} + \hat{V}_H + \hat{V}_X = \sum_{\alpha\in\{\uparrow,\downarrow\}} |\pi_\alpha\rangle \Big(\bar{\epsilon} + U\Big(\sum_{\gamma\in\{\uparrow,\downarrow\}} f_\gamma \Big) - U f_\alpha \Big) \langle\pi_\alpha| \qquad (2.154)
$$

For the individual states, the Fock operator is

- $|0\rangle$ $f_\uparrow = f_\downarrow = 0$

$$
\hat{F} = |\pi_\uparrow\rangle\bar{\epsilon}\langle\pi_\uparrow| + |\pi_\downarrow\rangle\bar{\epsilon}\langle\pi_\downarrow| \qquad (2.155)
$$

- $|\uparrow\rangle$ $f_\uparrow = 1, f_\downarrow = 0$

$$
\hat{F} = |\pi_\uparrow\rangle\bar{\epsilon}\langle\pi_\uparrow| + |\pi_\downarrow\rangle\Big(\bar{\epsilon} + U\Big)\langle\pi_\downarrow| \qquad (2.156)
$$

- $|\downarrow\rangle$ $f_\uparrow = 0, f_\downarrow = 1$

$$
\hat{F} = |\pi_\uparrow\rangle\Big(\bar{\epsilon} + U\Big)\langle\pi_\uparrow| + |\pi_\downarrow\rangle\bar{\epsilon}\langle\pi_\downarrow| \qquad (2.157)
$$

- $|\uparrow\downarrow\rangle$ $f_\uparrow = f_\downarrow = 1$

$$
\hat{F} = |\pi_\uparrow\rangle\Big(\bar{\epsilon} + U\Big)\langle\pi_\uparrow| + |\pi_\downarrow\rangle\Big(\bar{\epsilon} + U\Big)\langle\pi_\downarrow| \qquad (2.158)
$$

We recognize, that the one-particle systems have two different energy levels, which are separated by the Coulomb repulsion U. The lower level is the energy gained by removing an electron, while the upper level is the energy required to add an electron. When an electron is added, also the Coulomb repulsion with the electron, which already resides on the atom, has to be overcome. The electron addition energy is **electron affinity** and the electron removal energy is the **ionization potential**. The spectral function for general interacting electrons is discussed later in section 9.3.

5 Plot the density of states projected onto one of the one-particle orbitals for a one-particle system at low temperature.

The density-of-states of non-interacting electrons has been used previously in section 1.5.5. See *ΦSX: Introduction to Solid State Theory* for more information.[1].

The density-of-states for an ensemble of many-particle states is obtained as the ensemble average over the density-of-states functions calculated for the eigenstates of the many-particle Hamiltonian.

$$D(\epsilon) = \sum_q P_q D^{(q)}(\epsilon) \tag{2.159}$$

where $D^{(q)}$ is the density of states obtained for the particular many-particle wave function $|\Psi_q\rangle$.

For a non-interacting electron gas, the spectrum is the same for all many-particle states.

Therefore, the density of states is simply a sum of δ-functions on the eigenstates of the one-particle Hamiltonian. In the Hartree-Fock approximation, the density-of-states is given by the eigenvalues of the Fock operator. Because the Fock operator depends on the particular Slater-determinant chosen, the ensemble average needs to be performed.

The probability for the system to be in one of the many-particle states is

$$\begin{aligned}
P_{|\Phi\rangle} &= \frac{1}{Z} \mathrm{e}^{-\beta(E_{|\Phi\rangle} - \mu N_{|\Phi\rangle})} \\
&= \frac{1}{Z} \times \begin{cases} 1 & \text{for } |\Phi\rangle = |0\rangle \\ \mathrm{e}^{-\beta(\bar{\epsilon}-\mu)} & \text{for } |\Phi\rangle = |\uparrow\rangle \text{ or } |\Phi\rangle = |\downarrow\rangle \\ \mathrm{e}^{-\beta(2\bar{\epsilon}+U-2\mu)} & \text{for } |\Phi\rangle = |\uparrow\downarrow\rangle \end{cases} \\
Z &= \sum_{\Phi \in \{|0\rangle, |\uparrow\rangle, |\downarrow\rangle, |\uparrow,\downarrow\rangle\}} \mathrm{e}^{-\beta(E_{|\Phi\rangle} - \mu N_{|\Phi\rangle})} \\
&= \mathrm{e}^{-\beta(0-\mu 0)} + \mathrm{e}^{-\beta(\bar{\epsilon}-\mu)} + \mathrm{e}^{-\beta(\bar{\epsilon}-\mu)} + \mathrm{e}^{-\beta(2\bar{\epsilon}+U-2\mu)} \\
&= \left(1 + \mathrm{e}^{-\beta(\bar{\epsilon}-\mu)}\right)^2 + \mathrm{e}^{-\beta(2\bar{\epsilon}+U-2\mu)} - \mathrm{e}^{-\beta(2\bar{\epsilon}-2\mu)} \\
&= \left(1 + \mathrm{e}^{-\beta(\bar{\epsilon}-\mu)}\right)^2 + \mathrm{e}^{-\beta(2\bar{\epsilon}-2\mu)}\left(\mathrm{e}^{-\beta U} - 1\right)
\end{aligned} \tag{2.160}$$

The density of states is the weighted sum of the density of states obtained from the many-particle states in the ensemble.

$$\begin{aligned}
D_\uparrow(\epsilon) &= P_{|0\rangle}\delta(\epsilon - \bar{\epsilon}) + P_{|\uparrow\rangle}\delta(\epsilon - \bar{\epsilon}) + P_{|\downarrow\rangle}\delta(\epsilon - \bar{\epsilon} - U) + P_{|\uparrow\downarrow\rangle}\delta(\epsilon - \bar{\epsilon} - U) \\
&= \left(P_{|0\rangle} + P_{|\uparrow\rangle}\right)\delta(\epsilon - \bar{\epsilon}) + \left(P_{|\downarrow\rangle} + P_{|\uparrow\downarrow\rangle}\right)\delta(\epsilon - \bar{\epsilon} - U) \\
D_\downarrow(\epsilon) &= \left(P_{|0\rangle} + P_{|\downarrow\rangle}\right)\delta(\epsilon - \bar{\epsilon}) + \left(P_{|\uparrow\rangle} + P_{|\uparrow\downarrow\rangle}\right)\delta(\epsilon - \bar{\epsilon} - U)
\end{aligned} \tag{2.161}$$

See section **??** and in particular figure **??** on p. **??**.

6 Compare the density of states of an ensemble of eigenstates of the hydrogen atom with the mean-field Fock operator.

For an ensemble of eigenstates we superimpose the density of states of the individual many-particle

states weighted with their probabilities. The density of states consists of peaks at $\bar{\epsilon}$ and at $\bar{\epsilon} + U$. While the energy-level positions are unchanged, the weights of the peaks in the density of states depend on the specific ensemble.

For each orbital, there are contributions from both energies. These two energies can be interpreted as upper and lower **Hubbard band**. This is the underlying mechanism for the physics of **Mott insulators**.

In the mean-field solution, the position of the energy levels change with the ensemble

$$\hat{F}^{mf} \overset{\text{Eq. } 2.154}{=} \sum_{\alpha \in \{\uparrow,\downarrow\}} |\pi_\alpha\rangle \left(\bar{\epsilon} + U \sum_\gamma f_\gamma - U f_\alpha \right) \langle \pi_\alpha | \tag{2.162}$$

Thus, the density of states has peaks at $\bar{\epsilon} + UN_e - Uf_\alpha$, where N_e is the total number of electrons. If the occupations are equal, the two orbitals are degenerate. If the occupations are different the two energy levels are separated by $U|f_\uparrow - f_\downarrow|$. The mean value of the two energy levels shift upward with the particle number as UN_e. The weights of the peaks are always equal to one. I.e. there is one spin-up level and one spin-down level.

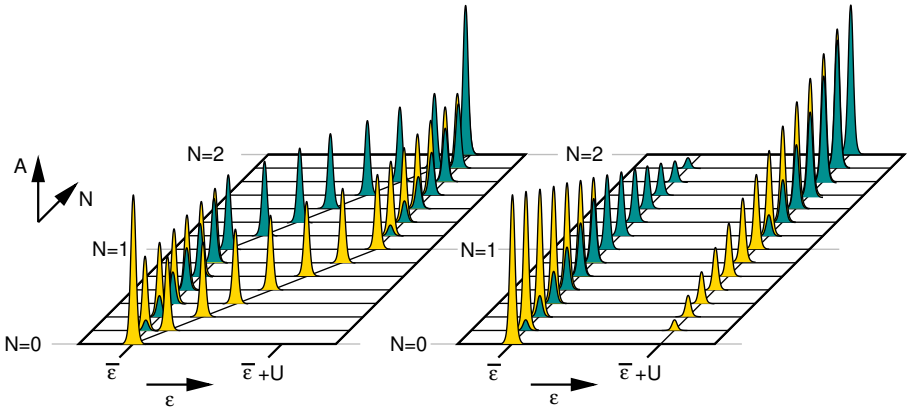

Fig. 2.10: Schematic figure of the spectral function $A_{tot}(\epsilon) = A_\uparrow(\epsilon) + A_\downarrow(\epsilon)$ of the Hubbard atom for several values of the particle number N. The occupied states are shown in green, while the unoccupied states are shown in yellow. On the left hand side, the spectral function from the mean-field Hartree-Fock approximation is shown. On the right-hand side the correct spectral function is shown. In the mean-field approximation the peaks have the same height, but their position adapts to the number of electrons. In the correct spectrum, the position of the peaks is independent of the number of electrons, but their weight adjusts.

2.8.3 Two one-dimensional particles in a box

Introduction

One example, which allows one to demonstrate many-particle effects in a most simple way, are two one-dimensional particles in a box. This system is mathematically identical to one two-dimensional particle in a box. This problem allows one to work out and visualize many-particle effects in a well known territory. The antisymmetry of the fermionic wave function is easily enforced and the interaction between two one-dimensional particles is analogous to an external one-particle potential for the two-dimensional particle. Then main interest is to work out the exchange hole, which will be central to the description of the interaction energy.

Problem

Let me introduce the notation I will use to describe spin-$\frac{1}{2}$ particles in one dimension. The position along the box will be denoted by the scalar r. The box ranges from $r = 0$ to $r = L$. The combined real-space-and-spin coordinate is $\vec{x} = (r, \sigma)$.

1. Calculate the electron density $n(r)$ of the two electrons as function of the position in the box of side length L. The exchange hole $h(r, \sigma, r', \sigma')$ is the difference between electron density of the other electron(s), given that one electron is at position r and has the spin $\sigma \in \{\uparrow, \downarrow\}$ and the total electron density. Consider first two electrons with the same spin. Then consider electrons with opposite spin and discuss changes.

   Plot the exchange hole,

   - for an electron close to the boundary of the box and in the center of the box
   - for two different sizes L of the box. (i.e. for different electron densities.
   - Consider the case of two electrons with opposite spin. What are the differences?

   Remark: I found it useful to work out the expressions for two abstract orbitals $\varphi_a(\vec{x})$ and $\varphi_b(\vec{x})$. Then, I calculated the one-particle orbitals in order to insert them into the expressions obtained previously. Finally, I used a plotting program.

2. Construct the two-particle wave function with lowest kinetic energy of two electrons with equal spin in a box of side-length L.

3. Construct the two-particle density for the wave function with lowest kinetic energy of two electrons with equal spin in a box of side-length L. Calculate the one-particle density. For example, from the two-particle density.

4. Construct the exchange hole for the wave function with lowest kinetic energy of two electrons with equal spin in a box of side-length L.

5. Calculate the density for the state with lowest energy for two electrons with opposite spin

6. Calculate the two-particle density for the state with lowest energy for two electrons with opposite spin

7. Calculate the exchange hole for the state with lowest energy for two electrons with opposite spin

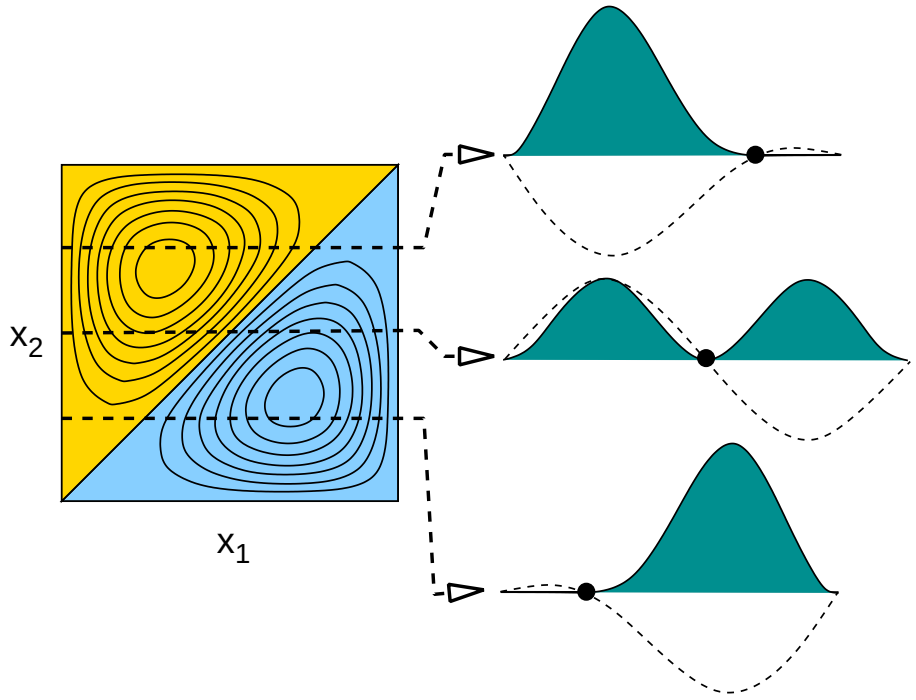

Fig. 2.11: Scheme to represent the many-particle wave function of two spin-less one-dimensional fermions in a box. Left: Many-particle wave function (Slater determinant) $\Phi(x_1, x_2)$. Right: wave function $\Phi(x_1, x_2)$ for a three different fixed position x_2 of the second particle (dashed). The filled function is density of the first particle, while the second particle is at a fixed position x_2. Notice, the exchange hole. Editor: include also the total density so that the exchange hole becomes evident.

Discussion

1. Calculate the electron density $n(r)$ of the two electrons as function of the position in the box of side length L. The exchange hole $h(r, \sigma, r', \sigma')$ is the difference between electron density of the other electron(s), given that one electron is at position r and has the spin $\sigma \in \{\uparrow, \downarrow\}$ and the total electron density. Consider first two electrons with the same spin. Then consider electrons with opposite spin and discuss changes.

   Plot the exchange hole,

   - for an electron close to the boundary of the box and in the center of the box
   - for two different sizes L of the box. (i.e. for different electron densities.
   - Consider the case of two electrons with opposite spin. What are the differences?

   Remark: I found it useful to work out the expressions for two abstract orbitals $\varphi_a(\vec{x})$ and $\varphi_b(\vec{x})$. Then, I calculated the one-particle orbitals in order to insert them into the expressions obtained previously. Finally, I used a plotting program.

2. Construct the two-particle wave function with lowest kinetic energy of two electrons with equal spin in a box of side-length L.

Let me first construct the one-particle orbitals relevant for this case. We use the two one-particle

orbitals with lowest kinetic energy, namely

$$\varphi_a(r,\sigma) = \sqrt{\frac{2}{L}}\sin(\pi r/L)\delta_{\sigma,\uparrow}$$
$$\varphi_b(r,\sigma) = \sqrt{\frac{2}{L}}\sin(2\pi r/L)\delta_{\sigma,\uparrow} \tag{2.163}$$

Notice that the spatial part of the two orbitals differs φ_a is node-less, while φ_b has one node in the spatial wave function.

The Slater determinant formed by these orbitals is

$$\begin{aligned}\Psi(\vec{x}_1,\vec{x}_2) &= \frac{1}{\sqrt{2}}\Big(\varphi_a(\vec{x}_1)\varphi_b(\vec{x}_2) - \varphi_b(\vec{x}_1)\varphi_a(\vec{x}_2)\Big)\\ &= \frac{1}{\sqrt{2}}\left(\sqrt{\frac{2}{L}}\sin(\pi r_1/L)\delta_{\sigma_1,\uparrow}\sqrt{\frac{2}{L}}\sin(2\pi r_2/L)\delta_{\sigma_2,\uparrow} - \sqrt{\frac{2}{L}}\sin(2\pi r_1/L)\delta_{\sigma_1,\uparrow}\sqrt{\frac{2}{L}}\sin(\pi r_2/L)\delta_{\sigma_2,\uparrow}\right)\end{aligned} \tag{2.164}$$

Side remark: Chemists like to take the spatial and spin parts apart. With the one-particle orbitals

$$\varphi_a(\vec{r},\sigma) = f(\vec{r})\delta_{\sigma\uparrow}$$
$$\varphi_b(\vec{r},\sigma) = g(\vec{r})\delta_{\sigma,\uparrow} \tag{2.165}$$

one constructs a two-particle Slater determinant

$$\begin{aligned}\Psi(\vec{x}_1,\vec{x}_2) &= \frac{1}{\sqrt{2}}\Big(\phi_a(\vec{x}_1)\phi_b(\vec{x}_2) - \phi_b(\vec{x}_1)\phi_1(\vec{x}_2)\Big)\Big)\\ &= \frac{1}{\sqrt{2}}\Big(f(\vec{r}_1)g(\vec{r}_2)\delta_{\sigma_1,\uparrow}\delta_{\sigma_2,\uparrow} - g(\vec{r}_1)f(\vec{r}_2)\delta_{\sigma_1,\uparrow}\delta_{\sigma_2,\uparrow}\Big)\\ &= \underbrace{\frac{1}{\sqrt{2}}\Big(f(\vec{r}_1)g(\vec{r}_2) - g(\vec{r}_1)f(\vec{r}_2)\Big)}_{\text{spatial part}}\underbrace{\Big(\delta_{\sigma_1,\uparrow}\delta_{\sigma_2,\uparrow}\Big)}_{\text{spin part}}\end{aligned} \tag{2.166}$$

One notices that the spin part by itself is symmetric under particle exchange and that the spatial part by itself is antisymmetric under particle exchange. For particle with opposite spin, the spatial part is symmetric and the spin-part is antisymmetric.

3. Construct the two-particle density for the wave function with lowest kinetic energy of two electrons with equal spin in a box of side-length L. Calculate the one-particle density. For example, from the two-particle density.

The two-particle density is obtained as the square of the wave function

$$\begin{aligned}n^{(2)}(\vec{r},\vec{r}') &\overset{\text{Eq. 2.46}}{=} \underbrace{2}_{N(N-1)}\langle\Psi|\left(\int d^4x_1\int d^4x_2\,\big|\vec{x}_1,\vec{x}_2\big\rangle\delta(\vec{r}-\vec{r}_1)\delta(\vec{r}'-\vec{r}_2)\big\langle\vec{x}_1,\vec{x}_2\big|\right)|\Psi\rangle\\ &= 2\int d^4x_1\int d^4x_2\,\delta(\vec{r}-\vec{r}_1)\delta(\vec{r}'-\vec{r}_2)\big\langle\Psi\big|\vec{x}_1,\vec{x}_2\big\rangle\big\langle\vec{x}_1,\vec{x}_2\big|\Psi\big\rangle\\ &= 2\sum_{\sigma_1,\sigma_2}\Big|\big\langle\vec{r},\sigma_1,\vec{r}',\sigma_2\big|\Psi\big\rangle\Big|^2\end{aligned} \tag{2.167}$$

This expression is valid for three dimensional position space. To go to the one-dimensional case, I use the scalar quantity r as the one-dimensional position and the two-dimensional $\vec{x} = (r,\sigma)$ as the composite real-space-and-spin coordinate.

$$
\begin{aligned}
n^{(2)}(r,r') &\overset{\text{Eq. 2.167}}{=} \underbrace{2}_{N(N-1)} \sum_{\sigma_1,\sigma_2} \left[\frac{1}{\sqrt{2}} \left(\frac{2}{L} \sin(\pi r/L) \sin(2\pi r'/L) - \frac{2}{L} \sin(2\pi r/L) \sin(\pi r'/L) \right) \delta_{\sigma_1,\uparrow} \delta_{\sigma_2,\uparrow} \right]^2 \\
&= \underbrace{2}_{N(N-1)} \left[\frac{1}{\sqrt{2}} \left(\frac{2}{L} \sin(\pi r/L) \sin(2\pi r'/L) - \frac{2}{L} \sin(2\pi r/L) \sin(\pi r'/L) \right) \right]^2 \underbrace{\sum_{\sigma_1,\sigma_2} \delta_{\sigma_1,\uparrow} \delta_{\sigma_2,\uparrow}}_{=1} \\
&= \frac{4}{L^2} \left(\sin(\pi r/L) \sin(2\pi r'/L) - \sin(2\pi r/L) \sin(\pi r'/L) \right)^2 \qquad (2.168)
\end{aligned}
$$

The density is obtained by integrating over all positions of the second particle.

$$
n(\vec{r}) = \int d^3r' \; n^{(2)}(\vec{r},\vec{r'}) = \frac{2}{L} \sin^2(\pi r/L) + \frac{2}{L} \sin^2(2\pi r/L) \qquad (2.169)
$$

I exploited the orthogonality of the spatial parts of the one-particle orbitals. The orthonormality can be seen from the symmetry properties. One orbital is symmetric under reflection at the box-center, while the other is antisymmetric.

4. Construct the exchange hole for the wave function with lowest kinetic energy of two electrons with equal spin in a box of side-length L.

$$
h(\vec{r},\vec{r'}) = \frac{1}{n^{(1)}(\vec{r})} \left(n^{(2)}(\vec{r},\vec{r'}) - n^{(1)}(\vec{r}) n^{(1)}(\vec{r'}) \right) \qquad (2.170)
$$

$n^{(2)}$:Eq. 2.168

$$
\begin{aligned}
h(r,r') = & \underbrace{\frac{1}{\frac{2}{L}\sin^2(\pi r/L) + \frac{2}{L}\sin^2(2\pi r/L)}}_{1/n(r)} \\
& \times \Bigg(\underbrace{\frac{4}{L^2} \left[\sin(\pi r/L) \sin(2\pi r'/L) - \sin(2\pi r/L) \sin(\pi r'/L) \right]^2}_{n^{(2)}(r,r')} \\
& - \underbrace{\left[\frac{2}{L}\sin^2(\pi r/L) + \frac{2}{L}\sin^2(2\pi r/L) \right]}_{n(r)} \underbrace{\left[\frac{2}{L}\sin^2(\pi r'/L) + \frac{2}{L}\sin^2(2\pi r'/L) \right]}_{n(r')} \Bigg) \\
= & \underbrace{\frac{1}{\frac{2}{L}\sin^2(\pi r/L) + \frac{2}{L}\sin^2(2\pi r/L)}}_{1/n(r)} \\
& \times \Bigg(\underbrace{\frac{4}{L^2} \left[\sin(\pi r/L) \sin(2\pi r'/L) - \sin(2\pi r/L) \sin(\pi r'/L) \right]^2}_{n^{(2)}(r,r')} \\
& - \underbrace{\left[\frac{2}{L}\sin^2(\pi r/L) + \frac{2}{L}\sin^2(2\pi r/L) \right]}_{n(r)} \underbrace{\left[\frac{2}{L}\sin^2(\pi r'/L) + \frac{2}{L}\sin^2(2\pi r'/L) \right]}_{n(r')} \Bigg) \qquad (2.171)
\end{aligned}
$$

The hole for different positions of the reference electron is shown in figure 2.12.

5. Calculate the density for the state with lowest energy for two electrons with opposite spin

For two electrons with opposite spin the two-particle wave function is

$$\begin{aligned}\Psi(x_1,\sigma_1,x_2,\sigma_2) &= \frac{1}{\sqrt{2}}\Big[\underbrace{\sqrt{\frac{2}{L}}\sin(\pi x_1/L)\delta_{\sigma_1,\uparrow}}_{\varphi_a(x_1,\sigma_1)}\underbrace{\sqrt{\frac{2}{L}}\sin(\pi x_2/L)\delta_{\sigma_2,\downarrow}}_{\varphi_b(x_2,\sigma_2)} - \underbrace{\sqrt{\frac{2}{L}}\sin(\pi x_1/L)\delta_{\sigma_1,\downarrow}}_{\varphi_b(x_1,\sigma_1)}\underbrace{\sqrt{\frac{2}{L}}\sin(\pi x_2/L)\delta_{\sigma_2,\uparrow}}_{\varphi_a(x_2,\sigma_2)}\Big] \\ &= \frac{2}{L}\sin(\pi x_1/L)\sin(\pi x_2/L)\frac{1}{\sqrt{2}}\Big(\delta_{\sigma_1,\uparrow}\delta_{\sigma_2,\downarrow} - \delta_{\sigma_1,\downarrow}\delta_{\sigma_2,\uparrow}\Big) \end{aligned} \tag{2.172}$$

The density can directly be evaluated using Eq. 2.15 by summing over the densities of the one-particle orbitals, because the precondition that the two one-particle orbitals are orthonormal is satisfied. The orthogonality is shown as follows:

$$\langle\varphi_a|\varphi_b\rangle = \sum_\sigma \int d^3r \left(\sqrt{\frac{2}{L}}\sin(\pi x/L)\delta_{\sigma,\uparrow}\right)\left(\sqrt{\frac{2}{L}}\sin(\pi x/L)\delta_{\sigma,\downarrow}\right) = 0 \tag{2.173}$$

because $\delta_{\sigma,\uparrow}\delta_{\sigma,\downarrow} = 0$ for all σ.

I now insert the orbitals into Eq. 2.15

$$n(\vec{r}) = \sum_{\alpha\in\{a,b\}}\sum_{\sigma\in\{\uparrow,\downarrow\}} |\varphi_\alpha(\vec{r},\sigma)|^2 \tag{2.174}$$

6. Calculate the two-particle density for the state with lowest energy for two electrons with opposite spin

The two-particle density is obtained as the square of the wave function

$$\begin{aligned} n^{(2)}(\vec{r},\vec{r}') &\overset{\text{Eq. 2.46}}{=} \underbrace{2}_{N(N-1)}\langle\Psi|\left(\int d^4x_1\int d^4x_2\,\big|\vec{x}_1,\vec{x}_2\big\rangle\delta(\vec{r}-\vec{r}_1)\delta(\vec{r}'-\vec{r}_2)\big\langle\vec{x}_1,\vec{x}_2\big|\right)|\Psi\rangle \\ &= 2\int d^4x_1\int d^4x_2\,\delta(\vec{r}-\vec{r}_1)\delta(\vec{r}'-\vec{r}_2)\big\langle\Psi\big|\vec{x}_1,\vec{x}_2\big\rangle\big\langle\vec{x}_1,\vec{x}_2\big|\Psi\big\rangle \\ &= 2\sum_{\sigma_1,\sigma_2}\Big|\big\langle\vec{r},\sigma_1,\vec{r}',\sigma_2\big|\Psi\big\rangle\Big|^2 \end{aligned} \tag{2.175}$$

This expression is valid for three dimensional position space. To go to the one-dimensional case, I use the scalar quantity r as the one-dimensional position and the two-dimensional $\vec{x} = (r,\sigma)$ as the composite real-space-and-spin coordinate.

$$\begin{aligned} n^{(2)}(r,r') &\overset{\text{Eq. 2.46}}{=} \underbrace{2}_{N(N-1)}\sum_{\sigma_1,\sigma_2}\left(\frac{2}{L}\sin(\pi r_1/L)\sin(\pi r_2/L)\frac{1}{\sqrt{2}}\Big(\delta_{\sigma_1,\uparrow}\delta_{\sigma_2,\downarrow} - \delta_{\sigma_1,\downarrow}\delta_{\sigma_2,\uparrow}\Big)\right)^2 \\ &= 2\frac{4}{L^2}\sin^2(\pi r_1/L)\sin^2(\pi r_2/L)\underbrace{\sum_{\sigma_1,\sigma_2}\frac{1}{2}\Big(\delta_{\sigma_1,\uparrow}\delta_{\sigma_2,\downarrow} - \delta_{\sigma_1,\downarrow}\delta_{\sigma_2,\uparrow}\Big)^2}_{=1} \\ &= 2\underbrace{\frac{2}{L}\sin^2(\pi r/L)}_{n_1(r)}\underbrace{\frac{2}{L}\sin^2(\pi r_2/L)}_{n_2(r)} \end{aligned} \tag{2.176}$$

The density is obtained by integrating over all positions of the second particle.

$$n(\vec{r}) = \int d^3r'\; n^{(2)}(\vec{r},\vec{r}') = 2\cdot\frac{2}{L}\sin^2(\pi r/L) \tag{2.177}$$

7. Calculate the exchange hole for the state with lowest energy for two electrons with opposite spin

The exchange-correlation hole is the difference of the total density $n(\vec{r}')$ and the density, in this case $n^{(2)}(\vec{r},\vec{r}')$ of the remaining particles, given that the first is at a specific position $\vec{r}$

$$h_{xc}(\vec{r},\vec{r}') \overset{\text{Eq. 2.49}}{=} \frac{1}{n(\vec{r})}\Big(n^{(2)}(\vec{r},\vec{r}') - n(\vec{r})n(\vec{r}')\Big) \tag{2.178}$$

$$\begin{aligned} h(r,r') &\overset{\text{Eq. 2.176}}{=} \frac{2}{L}\sin^2(\pi r'/L) - \underbrace{2\cdot\frac{2}{L}\sin^2(\pi r/L)}_{n(r')} \\ &= -\frac{2}{L}\sin^2(\pi r'/L) = -\frac{1}{2}n(r') \end{aligned} \tag{2.179}$$

Observations:

- Noticeable is the behavior of the hole for the opposite-spin wave function as the reference electron approaches one of the boundaries. The hole is not centered on the reference electron but displaced inside the box. This is because the density of the other electron must not be negative and thus the hole cannot exceed the density in absolute value. The hole must be, where the electrons are. The shape of the hole is governed by the electron density and thus remains unchanged until the reference electron moves sufficiently far into the box.
- The spin part of the wave function of the wave function for opposite spin electrons is that of a singlet term. One easily makes the mistake assuming that one has a singlet, whenever an $\uparrow$ orbital is combined with a $\downarrow$ orbital. This, however, only says that $S_z = 0$. It can still be a triplet $\frac{1}{\sqrt{2}}(\delta_{\sigma_1,\uparrow}\delta_{\sigma_2,\downarrow} + \delta_{\sigma_1,\downarrow}\delta_{\sigma_2,\uparrow})$ with $S^2 = \hbar^2 S(S+1) = 2\hbar^2$ and the spin perpendicular to the z axis. A simple product $\delta_{\sigma_1,\uparrow}\delta_{\sigma_2,\downarrow}$ is not a spin eigenstate, i.e. an eigenstate of $\hat{S}^2$, but a superposition of a singlet and a triplet state.
- The spatial wave function is symmetric under exchange of the two positions. If one forms a Slater determinant of two opposite-spin orbitals with different spatial parts, the result is not a spin eigenstate, but a superposition of a singlet and a triplet state. This is shown as follows.

$$\begin{aligned} \psi(x_1,\sigma_1,x_2,\sigma_2) &= \frac{1}{\sqrt{2}}\Big(f(x_1)\delta_{\sigma_1,\uparrow}g(x_2)\delta_{\sigma_2,\downarrow} - g(x_1)\delta_{\sigma_1,\downarrow}f(x_2)\delta_{\sigma_2,\uparrow}\Big) \\ &= \frac{1}{2}\Big\{\Big(f(x_1)g(x_2) + g(x_1)f(x_2)\Big)\frac{1}{\sqrt{2}}\Big(\delta_{\sigma_1,\uparrow}\delta_{\sigma_2,\downarrow} - \delta_{\sigma_1,\downarrow}\delta_{\sigma_2,\uparrow}\Big) \\ &+ \Big(f(x_1)g(x_2) - g(x_1)f(x_2)\Big)\frac{1}{\sqrt{2}}\Big(\delta_{\sigma_1,\uparrow}\delta_{\sigma_2,\downarrow} + \delta_{\sigma_1,\downarrow}\delta_{\sigma_2,\uparrow}\Big)\Big\} \end{aligned} \tag{2.180}$$

  A spatial part of a singlet wave function is always symmetric under particle exchange, while that of a triplet wave function is antisymmetric under particle exchange.
- Unlike two electrons with equal spin, electrons with opposite spin do not go out of each other's way. The exchange hole is equal in absolute value to the density of the corresponding one-particle orbital.

2.8.4 Two fermions in a 1d-box

Introduction and background

The goal of this exercise is to provide an understanding of many-particle wave functions and of identical particles. This exercise will also show the underlying reasons why non-interacting electrons are often a good model to describe interacting electrons despite their strong interaction and the breakdown of a perturbation theory.

Consider two non-interacting spin-less particles in a 1-dimensional box with side-length L. This problem is analogous to a single particle in a two-dimensional box, which can be solved analytically. The symmetry under permutation of particles, which defines fermions and bosons, is translated into a simple geometrical mirror symmetry.

To investigate the role of interactions, I introduce a hard-core repulsion of extent s

$$W(x,x') = \begin{cases} W_0 & \text{for } |x-x'| < s \\ 0 & \text{for } |x-x'| \geq s \end{cases} \tag{2.181}$$

in the limit $W_0 \to \infty$.

Tasks

1 Determine the wave functions and energy eigenvalues for a particle with mass m in a N-dimensional square box with side-length L.

2 Use the result from the previous question to determine the wave functions and the spectrum for N distinguishable particles in a one-dimensional box. Notice that the wave functions are single product wave functions formed from one-particle wave functions.

3 Discuss under the guidance of the tutor the following puzzles: (1) What is the wave function of a zero particle state? (2) What is the scalar product of two states with different particle numbers.

4 The real-space basis functions for two particles is $\{|x_1, x_2\rangle\}$, where x_1, x_2 denote the two coordinates of the particles.

$$\langle x_1, x_2 | x_1', x_2' \rangle = \delta(x_1 - x_1')\delta(x_2 - x_2')$$
$$\hat{1} = \int dx_1 \int dx_2 \, |x_1, x_2\rangle\langle x_1, x_2| \tag{2.182}$$

The particle-permutation operator for two one-dimensional particles is

$$\hat{P}_{1,2} = \int dx_1 \int dx_2 \, |x_2, x_1\rangle\langle x_1, x_2| \tag{2.183}$$

Show that the particle-permutation operator is unitary. Determine the eigenvalues and eigenstates of the particle-permutation operator.

5 Determine the wave functions and spectra for two fermions in a 1-d box and for two bosons. Show that bosonic and fermionic wave functions span the complete Hilbert space. (There are no other types of identical particles.) From the multiplicity of the states, respectively the spectra argue, why two identical fermions cannot be in one orbital (Pauli principle) and why bosons are preferably in the same orbital. That is, show that the probability to find two particles in the same orbital is higher for bosons than for distinguishable particles. (Bunching and anti-bunching.)

6 The wave functions for two particles with a hard-core interaction can be expressed in terms of the wave function of two non-interacting fermionic wave functions with side-length $L - s$, where s is the range of the interaction. In the case of an interaction the wave functions are zero in a strip of width s along the main diagonal $x_1 = x_2$. Such wave functions can be constructed by dividing the non-interacting wave function at the node-line, and by separating the two pieces out of the interaction region.

- Sketch the interaction in the two-dimensional box
- Use this principle to construct the exact fermionic and bosonic wave functions for the hard-core interaction.
- Determine the eigenvalue spectrum for fermions and for bosons.
- Estimate the eigenvalue spectrum using first-order perturbation theory in the interaction. (Use approximations)

Solution

1 Determine the wave functions and energy eigenvalues for a particle with mass m in a N-dimensional square box with side-length L.

1. **Particle in a one-dimensional box**

$$\varphi_n^{(1)}(x) = \sqrt{\frac{2}{L}} \sin\left(\frac{n\pi}{L}x\right)$$

The energy of this state is

$$\epsilon_n = \frac{\hbar^2\pi^2}{2m_e L^2} n^2$$

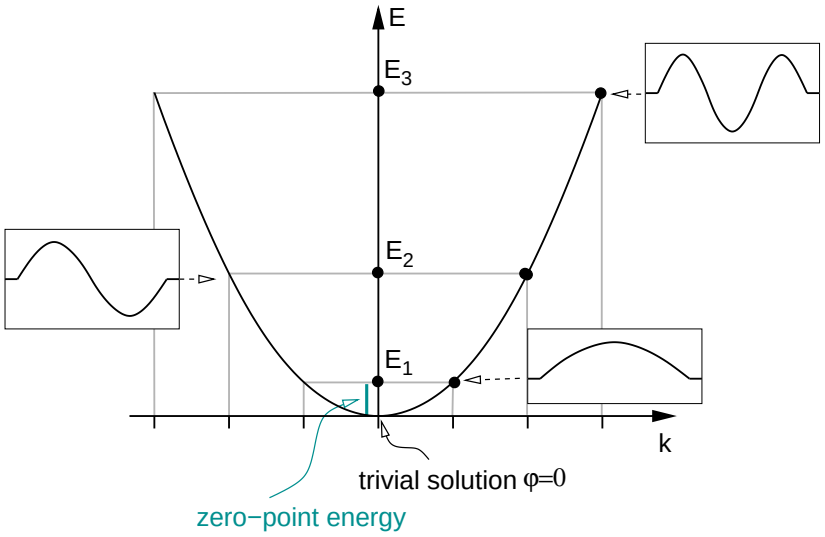

2. **Particle in a two-dimensional box** The two-dimensional box with side-length L covers the area $[0, L] \times [0, L]$.

The wave functions for a particle in a 2-dimensional box are of the form

$$\varphi_{n,m}(x, y) = \varphi_n(x)\varphi_m(y) = \frac{2}{L} \sin\left(\frac{n\pi}{L}x\right) \sin\left(\frac{m\pi}{L}y\right) \tag{2.184}$$

The energy of such a state is due to the kinetic energy. It is

$$E_{n,m} = \epsilon_n + \epsilon_m = \frac{\hbar^2\pi^2}{2m_e L^2}(n^2 + m^2) \tag{2.185}$$

3. **Particle in a N-dimensional box**

$$\varphi_{n_1,n_2,\ldots,n_N}(x_1, x_2, \ldots, x_N) = \prod_{j=1}^{N} \varphi_{n_j}(x_j) = \left(\frac{2}{L}\right)^{\frac{N}{2}} \prod_{j=1}^{N} \sin\left(\frac{n_j\pi}{L}x_j\right)$$

$$E_{n_1,n_2,\ldots,n_N} = \sum_{j=1}^{N} \epsilon_j = \frac{\hbar^2\pi^2}{2m_e L^2} \sum_{j=1}^{N} n_j^2$$

2 Use the result from the previous question to determine the wave functions and the spectrum for N distinguishable particles in a one-dimensional box. Notice that the wave functions are single product wave functions formed from one-particle wave functions.

The Schrödinger equation for a one-dimensional particle in a N-dimensional box is identical to that for N particles in a one-dimensional box. Thus, the wave functions and energy levels are equivalent.

$$\varphi_{n_1,n_2,\ldots,n_N}(x_1,x_2,\ldots,x_N) \overset{\text{Eq. 2.186}}{=} \prod_{j=1}^{N}\varphi_{n_j}(x_j) = \left(\frac{2}{L}\right)^{\frac{N}{2}}\prod_{j=1}^{N}\sin\left(\frac{n_j\pi}{L}x_j\right) \tag{2.186}$$

$$E_{n_1,n_2,\ldots,n_N} = \sum_{j=1}^{N}\epsilon_j \overset{\text{Eq. 2.186}}{=} \frac{\hbar^2\pi^2}{2m_eL^2}\sum_{j=1}^{N}n_j^2 \tag{2.187}$$

3 Discuss under the guidance of the tutor the following puzzles: (1) What is the wave function of a zero particle state? (2) What is the scalar product of two states with different particle numbers.

There is no zero-particle wave function, because it would not have any arguments. The zero-particle state, however, has a phase. Therefore, the zero particle state is a complex number.

A common mistake is to describe the zero particle state as a function of some particle coordinates, albeit with constant value. This mistake happens usually when trying to add a zero particle state and a one-particle state. The result cannot be simplified to a single function.

The scalar product of two states with different particle numbers can not be formed in real space, because the two functions have different numbers of arguments.

One can form the integral of two functions with different number of arguments such as $f(\vec{x}) = \int d^4x'\ \phi(\vec{x'})\psi(\vec{x},\vec{x'}$, which is a function of the additional argument. Such a construction will occur later in the context of quasi-particle wave functions. This is, however, not the scalar product. The scalar product $\langle\phi|\psi\rangle = 0$ of this example would be zero.

The scalar product can be given in the Fock space, because then the particle number is not a parameter but an observable represented by a hermitian operator. Since eigenstates of a hermitian operator to different eigenvalues are orthogonal, the scalar product of states with different particle numbers is zero.

4 The real-space basis functions for two particles is $\{|x_1,x_2\rangle\}$, where x_1, x_2 denote the two coordinates of the particles.

$$\langle x_1,x_2|x_1',x_2'\rangle = \delta(x_1-x_1')\delta(x_2-x_2')$$
$$\hat{1} = \int dx_1\int dx_2\ |x_1,x_2\rangle\langle x_1,x_2| \tag{2.188}$$

The particle-permutation operator for two one-dimensional particles is

$$\hat{P}_{1,2} = \int dx_1\int dx_2\ |x_2,x_1\rangle\langle x_1,x_2| \tag{2.189}$$

Show that the particle-permutation operator is unitary. Determine the eigenvalues and eigenstates of the particle-permutation operator.

1. **Show that the particle permutation operator is unitary:** The permutation operator is

$$\hat{P}_{12} = \int dx_1\int dx_2\ |x_2,x_1\rangle\langle x_1,x_2| \tag{2.190}$$

This implies for wave functions

$$\begin{aligned} |\Psi'\rangle &\stackrel{\text{def}}{=} \hat{P}_{12}|\Psi\rangle \\ \Psi'(x_1,x_2) &= \langle x_1,x_2|\hat{P}_{12}|\Psi\rangle = \langle x_2,x_1|\Psi\rangle = \Psi(x_2,x_1) \end{aligned} \tag{2.191}$$

An operator is unitary, if its adjoint is its inverse. That is, it is unitary if $\hat{P}\hat{P}^\dagger = \hat{1}$.

The adjoint can be obtained by exchanging bra's and kets.

$$\hat{P}_{12}^\dagger = \int dx_1 \int dx_2 \; |x_1,x_2\rangle\langle x_2,x_1| \tag{2.192}$$

The equation above also shows that the permutation operator is furthermore hermitian, i.e.

$$\hat{P}_{12}^\dagger = \hat{P}_{12} \tag{2.193}$$

Now we can show that particle permutation operator is unitary

$$\begin{aligned} \hat{P}_{12}\hat{P}_{12}^\dagger &\stackrel{?}{=} 1 \\ \hat{P}_{12}\hat{P}_{12}^\dagger &= \underbrace{\int dx_1 \int dx_2 \; |x_2,x_1\rangle\langle x_1,x_2|}_{\hat{P}_{12}} \underbrace{\int dx_1' \int dx_2' \; |x_1',x_2'\rangle\langle x_2',x_1'|}_{\hat{P}_{12}^\dagger} \\ &= \int dx_1 \int dx_2 \int dx_1' \int dx_2' \; |x_2,x_1\rangle \underbrace{\langle x_1,x_2|x_1',x_2'\rangle}_{\delta(x_1-x_1')\delta(x_2-x_2')} \langle x_2',x_1'| \\ &= \int dx_1 \int dx_2 \; |x_2,x_1\rangle\langle x_2,x_1| = \hat{1} \qquad \text{q.e.d} \end{aligned} \tag{2.194}$$

Thus, the permutation operator is unitary.

2. Eigenvalues of the permutation operator: As shown above, the permutation operator is unitary and hermitian. Hence, the permutation operator is cyclic $\hat{P}_{12}^2 = \hat{P}_{12}\hat{P}_{12}^\dagger = \hat{1}$.

   Because $\hat{P}_{12}^2 = 1$, the eigenvalues of $\hat{P}_{12}$ are $+1$ and -1.

3. Eigenstates of the permutation operator:

   - The eigenstates $|\Psi^B\rangle$ for eigenvalue $+1$ are bosonic states

   $$\begin{aligned} |\Psi^B\rangle &\stackrel{\text{Eq. 1.89}}{=} |\Psi^D\rangle + \hat{P}_{12}|\Psi^D\rangle \\ \Psi^B(x_1,x_2) &= \Psi^D(x_1,x_2) + \Psi^D(x_2,x_1) \end{aligned} \tag{2.195}$$

   where $\Psi^D(x_1,x_2)$ is an arbitrary wave function (for two distinguishable (D) particles). The resulting state is not normalized. It can occur that symmetrized wave function vanishes. (This occurs when Ψ is antisymmetric.)

   - The eigenstates Ψ^F for eigenvalue -1 are fermionic states

   $$\begin{aligned} |\Psi^F\rangle &= |\Psi^D\rangle - \hat{P}_{12}|\Psi^D\rangle \\ \Psi^F(x_1,x_2) &= \Psi^D(x_1,x_2) - \Psi^D(x_2,x_1) \end{aligned} \tag{2.196}$$

   where $\Psi^D(x_1,x_2)$ is an arbitrary wave function (for two distinguishable particles). The resulting state is not normalized. It can occur that antisymmetrized wave function vanishes. (This occurs when Ψ is symmetric.)

5 Determine the wave functions and spectra for two fermions in a 1-d box and for two bosons. Show that bosonic and fermionic wave functions span the complete Hilbert space. (There are no other types of identical particles.) From the multiplicity of the states, respectively the spectra argue, why two identical fermions cannot be in one orbital (Pauli principle) and why bosons are preferably in the same orbital. That is, show that the probability to find two particles in the same orbital is higher for bosons than for distinguishable particles. (Bunching and anti-bunching.)

1. **Construct the fermionic (anti symmetric) and bosonic (symmetric) eigenstates of the Hamiltonian**

Fermions:

$$|\Psi^F_{n,m}\rangle = \frac{1}{\sqrt{2}}\Big(|\Psi^D_{n,m}\rangle - \hat{P}_{12}|\Psi^D_{n,m}\rangle\Big)$$
$$\psi^F_{n,m}(x,y) = \frac{\sqrt{2}}{L}\left(\sin\left(\frac{n\pi}{L}x\right)\sin\left(\frac{m\pi}{L}y\right) - \sin\left(\frac{m\pi}{L}x\right)\sin\left(\frac{n\pi}{L}y\right)\right) \qquad \text{for } n > m \tag{2.197}$$

If a fermionic two-particle wave function $|\Psi_{nm}\rangle$ is constructed from two one-particle states $|\varphi_n\rangle$, $|\Psi_{n,m}\rangle$ is a Slater determinant.

$$\Psi^F_{n,m}(x,y) = \frac{\sqrt{2}}{L}\det\begin{vmatrix}\sin\left(\frac{n\pi}{L}x\right); \sin\left(\frac{m\pi}{L}x\right)\\ \sin\left(\frac{n\pi}{L}y\right); \sin\left(\frac{m\pi}{L}y\right)\end{vmatrix} \tag{2.198}$$

We find that the wave function with two electrons in the same orbital vanishes, $|\Psi^F_{n,n}\rangle = |\varnothing\rangle$, which says that there is no fermionic state with two identical fermions in the same one-particle state. This is one consequence of the Pauli principle.

We find $|\Psi^F_{n,m}\rangle = -|\Psi^F_{m,n}\rangle$. Interchanging the quantum numbers of a fermionic state does not produce a new state.

The energies are

$$E_{n,m} = \sum_{j=1}^{2}\epsilon_j = \frac{\hbar^2\pi^2}{2m_eL^2}(n^2+m^2) \qquad \text{for } n > m \tag{2.199}$$

Note that the states with $n < m$ are, up to a phase factor identical to the one with exchanged quantum numbers. States with two equal quantum numbers are zero states and therefore excluded from the sum. This indicates that fermions try to stay away from each other (anti bunching).

Bosons:

$$|\psi^B_{n,m}\rangle = \begin{cases}|\psi^D_{n,n}\rangle & \text{for } n = m\\ \frac{1}{\sqrt{2}}\big(|\Psi^D_{n,m}\rangle + \hat{P}_{12}|\Psi^D_{n,m}\rangle\big) & \text{for } m < n\end{cases}$$
$$\psi^B_{n,m}(x,y) = \begin{cases}\frac{2}{L}\sin\left(\frac{n\pi}{L}x\right)\sin\left(\frac{n\pi}{L}y\right) & \text{for } n = m\\ \frac{\sqrt{2}}{L}\left(\sin\left(\frac{n\pi}{L}x\right)\sin\left(\frac{m\pi}{L}y\right) + \sin\left(\frac{m\pi}{L}x\right)\sin\left(\frac{n\pi}{L}y\right)\right) & \text{for } m < n\end{cases} \tag{2.200}$$

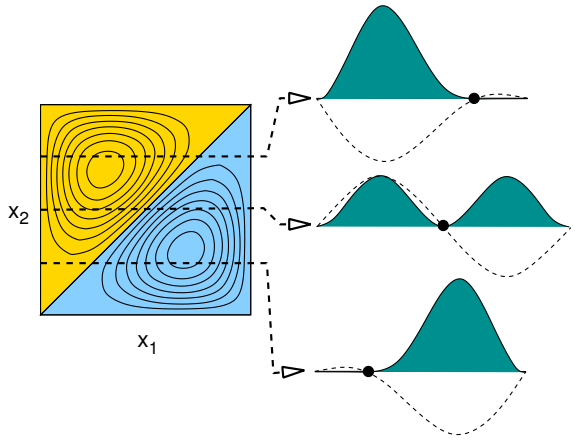

Fig. 2.12: Ground state wave function of two spin-less fermions in a 1d-box. The coordinates of the two electrons are x_1 and x_2. (Note, that x does not refer to the combined position-and-spin representation.) The colors indicate the sign of the wave function. On the right, the density (filled area) and wave function (dashed line) of the first electron is shown for specific frozen positions of the second electron.

The energies are

$$E_{n,m} = \sum_{j=1}^{2} \epsilon_j = \frac{\hbar^2 \pi^2}{2 m_e L^2} (n^2 + m^2) \qquad \text{for } m \leq n \tag{2.201}$$

Note here, that the states with equal quantum numbers are present. Per state with unequal quantum numbers, there are twice as many states with equal quantum numbers as in the case of distinguishable particles. This is an indication that bosons prefer to be next to each other (bunching).

2. **Show that, for two-particle systems, bosonic and fermionic wave functions span the complete Hilbert space for distinguishable particles.** Observe that the bosonic and fermionic wave basis functions taken together again span the complete two-particle Hilbert space. Compare the energy spectrum and degeneracies for fermionic and bosonic wave functions separately.

$$|\Psi^D_{n,m}\rangle = \begin{cases} \frac{1}{\sqrt{2}} \left(|\Psi^F_{n,m}\rangle + |\Psi^B_{n,m}\rangle \right) & \text{for } m \neq n \\ |\Psi^B_{n,m}\rangle & \text{for } m = n \end{cases} \tag{2.202}$$

Remark: bosonic and fermionic wave functions do however **not** span the complete space for distinguishable particles for three or more particles. Let me demonstrate that for three particles. The group of permutations can be generated from two permutations $P_{1,2}$ and $P_{2,3}$. The permutation $P_{1,3} = P_{1,2} P_{2,3} P_{1,2}$ can be expressed in terms of the other two permutations.
Editor: This needs to be expanded?

6 The wave functions for two particles with a hard-core interaction can be expressed in terms of the wave function of two non-interacting fermionic wave functions with side-length $L-s$, where s is the range of the interaction. In the case of an interaction the wave functions are zero in a strip of width s along the main diagonal $x_1 = x_2$. Such wave functions can be constructed by dividing the non-interacting wave function at the node-line, and by separating the two pieces out of the interaction region.

- Sketch the interaction in the two-dimensional box
- Use this principle to construct the exact fermionic and bosonic wave functions for the hard-core interaction.
- Determine the eigenvalue spectrum for fermions and for bosons.
- Estimate the eigenvalue spectrum using first-order perturbation theory in the interaction. (Use approximations)

Firstly, we introduce a mapping which cuts space in the main diagonal and shifts the two halfs apart by s.

Two particles at x_1 and x_2 interact if $|x_2 - x_1| < s$.

The wave function in the interaction region i.e. for $|x_2 - x_1|$ vanishes. At the boundary of the interaction region, the wave function vanishes just like the fermionic wave function vanishes at the node-line $x_1 = x_2$.

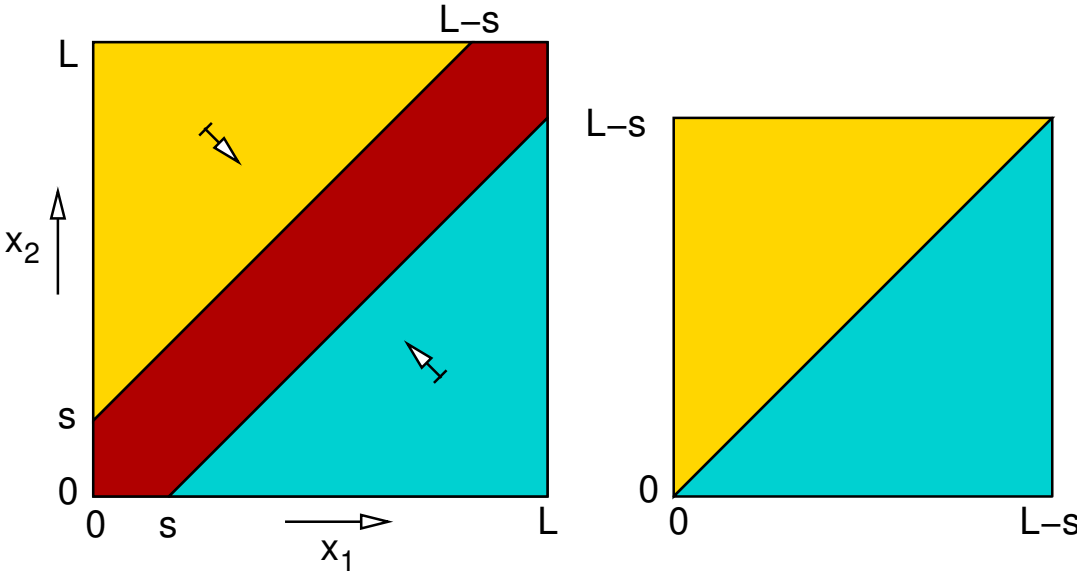

The wave function $|\Psi^{L,W}\rangle$ of the interacting system in a box of length L can be obtained from that $|\Psi^{L-s,0}\rangle$ of the non-interacting system with a smaller box-length $L-s$.

$$\Psi^{L,W}(x_1, x_2) = \Psi^{L-s,0}(x_1', x_2') \tag{2.203}$$

where the mapping from (x_1, x_2) to (x_1', x_2') is described below.

"Above" the interaction region, i.e. for $x_2 > x_1 + s$, I need to look up

$$\begin{pmatrix} x_1' \\ x_2' \end{pmatrix} = \begin{pmatrix} x_1 \\ x_2 \end{pmatrix} - s \begin{pmatrix} 0 \\ 1 \end{pmatrix} \tag{2.204}$$

and "below" the interaction region i.e. for $x_2 < x_1 - s$, I need to look up

$$\begin{pmatrix} x_1' \\ x_2' \end{pmatrix} = \begin{pmatrix} x_1 \\ x_2 \end{pmatrix} - s \begin{pmatrix} 1 \\ 0 \end{pmatrix} \tag{2.205}$$

This maps the points at the boundaries of the interaction region onto the node plane of the non-interacting system.

The non-interacting fermions in the box, which has been shrunk by the range of the interaction is

$$\Psi_{n,m}^{L-s,0}(x_1,x_2)=\frac{\sqrt{2}}{L-s}\left(\sin\left(\frac{n\pi}{L-s}x_1\right)\sin\left(\frac{m\pi}{L-s}x_2\right)-\sin\left(\frac{m\pi}{L-s}x_1\right)\sin\left(\frac{n\pi}{L-s}x_2\right)\right) \quad (2.206)$$

where $0 < x_{1/2} < L - s$.

The interacting fermionic wave function is

$$\Psi^W(x_1,x_2)=\begin{cases}\Psi^0(x_1,x_2-s) & \text{for } x_2 > x_1+s\\ 0 & \text{for } x_1-s < x_2 < x_1+s\\ \Psi^0(x_1-s,x_2) & \text{for } x_2 < x_1-s\end{cases} \quad (2.207)$$

with $m > n$ and the energies are

$$E_{m,n}^{L,W}=E_{m,n}^{L-s,0}=\frac{\hbar^2\pi^2}{2m_e(L-s)}(n^2+m^2) \quad (2.208)$$

We see that the energies of the interacting system are obtained from those of the non-interacting system by

$$\begin{aligned}E_{m,n}^{L,W}&=\frac{L}{L-s}E_{m,n}^{L,0}=\frac{1}{1-\frac{s}{L}}E_{m,n}^{L,0}\\ \Rightarrow\quad E_{m,n}^{L,W}-E_{m,n}^{L,0}&\approx\frac{s}{L}E_{m,n}^{L,0}\end{aligned} \quad (2.209)$$

This shows that the energy increases strongly with the density of the system. A very dilute system has a small collision probability and therefore the energy increase is negligible.

Interestingly there is a one-to-one correspondence between bosonic and fermionic eigenstates of the system in the limit of a hard-core repulsion. The energies are identical and the wave function is identical, except that there is no sign change under particle permutation of two bosons.

Gnuplot example

Fig. 2.12 has been drawn by graphical tool Gnuplot. Here, a small script is provided for gnuplot. Simply paste it into a file '`boxtwopartcle.gnu`' and run the command '`gnuplot boxtwopartcle.gnu`'

```
#Set terminal postscript
#set output "boxtwoparticle.eps"
set terminal png
set output "boxtwoparticle.png"
#set terminal latex
#set terminal fig
#set output "boxtwoparticle.fig"
#set size 1.0,1.0
set size ratio 1.0
set nokey
set contour
set view 30, 20
#set view 0, 0
set contour surface
set hidden3d
set isosamples 40, 40
set ticslevel -0.5
```

```
#unset surface
unset xtics
unset ytics
unset ztics
set cntrparam cubicspline
set cntrparam levels auto 20
splot[0:1][0:1](-sin(x*pi)*sin(2*y*pi)+sin(2*x*pi)*sin(y*pi))
```

2.8.5 Toy model for the exchange-correlation hole

Introduction

In this section, I will exploit only the two, probably most important properties of the exchange-correlation hole, to construct an extremely simple toy model for the exchange-correlation hole. Despite its simplicity, one can already rationalize a few physical effects. We will demonstrate, how solid-state magnetism can be understood in these terms.

The exchange-correlation hole of this model is a homogeneously charged sphere.

$$h_{xc}(\vec{r},\vec{r'}) = \overbrace{h_X(\vec{r},\vec{r})}^{\text{on-top value}}\ \theta\Big(R - |\vec{r'} - \vec{r}|\Big) \tag{2.210}$$

where $\theta(x)$ is the Heaviside function and R is the sphere radius. Consult the figure 2.13 on p. 116.

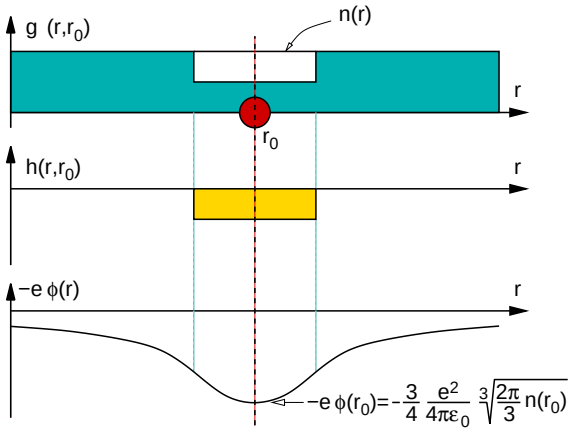

Fig. 2.13: Sketch of the construction of a simple model-density functional.

45

The charge on the sphere is determined from the **charge sum rule** Eq. 2.51. The size of the sphere is then obtained using the **on-top value**[46] of the exchange hole of the free-electron gas. **editor: The following sentence is not clear** This on-top value is obtained from the notion that the electrons with two spin directions behave like independent particles. The extension of the on-top value of the exchange hole to correlation can be found in the literature[31]

Working out the interaction energy then becomes a simple exercise of electrodynamics. This approximate interaction energy can then be combined with the kinetic energy of the free-electron gas, which we evaluated in a prior exercise, section 1.5.5 on p. 41. This will allow us to analyze, in this approximate model, how the electron gas will turn, at low density, into a ferromagnet.

Editor: Show the comparison of the exchange-correlation energy of the toy model with exact Hartree-Fock and quantum Monte Carlo calculations of the polarized and non-spinpolarized electron gas.

Editor: Compare the exact exchange hole of the free-electron gas as function of radius with the toy model. See figure E.2 on p.452.

[45] The first argument of $h_X(\vec{r},\vec{r'})$ is the position of the spectator electron, which experiences the Coulomb potential of the exchange hole. The second argument is value at which the hole-density is evaluated.

[46] The on-top value of the exchange hole is the value $h_X(\vec{r},\vec{r})$ of the exchange hole right at the position of the "spectator electron".

On-top value of the exchange hole

We will also need the **on-top value** $h_X(\vec{r},\vec{r})$ of the exchange hole. The on-top value is the value of the hole $h_x(\vec{r},\vec{r})$ right at the position of the spectator electron, i.e. for $\vec{r}=\vec{r'}$.

While the discussion of the exchange-correlation hole has been completely general so far, we can calculate the on-top value only for the exchange hole. The extension to correlation can be found in the literature[31]

The two-particle density $n^{(2)}$ of a Slater determinant is obtained analogously to the exchange energy E_X obtained in Eq. 2.40.

$$n^{(2)}(\vec{r},\vec{r'}) = n^{(1)}(\vec{r})n^{(1)}(\vec{r'}) - \sum_{\sigma,\sigma'} \rho^{(1)}(\vec{x},\vec{x'})\rho^{(1)}(\vec{x'},\vec{x}) \tag{2.211}$$

The corresponding hole density is

$$h_X(\vec{r},\vec{r'}) = -\frac{1}{n^{(1)}(\vec{r})} \sum_{\sigma,\sigma'\in\{\uparrow,\downarrow\}} \rho^{(1)}(\vec{x},\vec{x'})\rho^{(1)}(\vec{x'},\vec{x}) \tag{2.212}$$

The subscript X shall denote that this expression only considers the exchange contribution and ignores the correlation contribution.

The on-top value of the exchange hole is the hole for $\vec{r}=\vec{r'}$.

$$h_X(\vec{r},\vec{r}) = -\frac{1}{n^{(1)}(\vec{r})} \sum_{\sigma,\sigma'\in\{\uparrow,\downarrow\}} \rho^{(1)}(\vec{r},\sigma,\vec{r},\sigma')\rho^{(1)}(\vec{r},\sigma',\vec{r},\sigma) \tag{2.213}$$

The on-top value of the one-particle-reduced density matrix can be expressed in terms of total density n_t, i.e. $n^{(1)}$, and spin density $\vec{n}_S(\vec{r})$ and the Pauli matrices in the two-dimensional spin space as[47]

$$\begin{aligned}\rho^{(1)}(\vec{r},\sigma,\vec{r},\sigma') &\hat{=} \frac{1}{2}\left[n_t(\vec{r}) \underbrace{\begin{pmatrix}1&0\\0&1\end{pmatrix}}_{\mathbf{1}} + n_{S,x}(\vec{r}) \underbrace{\begin{pmatrix}0&1\\1&0\end{pmatrix}}_{\boldsymbol{\sigma}_x} + n_{S,y}(\vec{r}) \underbrace{\begin{pmatrix}0&-i\\i&0\end{pmatrix}}_{\boldsymbol{\sigma}_y} + n_{S,z}(\vec{r}) \underbrace{\begin{pmatrix}1&0\\0&-1\end{pmatrix}}_{\boldsymbol{\sigma}_z} \right] \\ &= \frac{1}{2}\begin{pmatrix} n_t + n_{S,z} & n_{S,x} - i n_{S,y} \\ n_{S,x} + i n_{S,y} & n_t - n_{S,z} \end{pmatrix} \end{aligned} \tag{2.215}$$

I will use the identity

$$\begin{aligned} \boldsymbol{A} &\overset{\text{def}}{=} a_0\mathbf{1} + \vec{a}\vec{\boldsymbol{\sigma}} \hat{=} \begin{pmatrix} a_0 + a_z & a_x - i a_y \\ a_x + i a_y & a_0 - a_z \end{pmatrix} \qquad \text{with } a_0 \in \mathbb{R}, \vec{a} \in \mathbb{R}^3 \\ &\Rightarrow \sum_{\sigma,\sigma'} A_{\sigma,\sigma'}A_{\sigma',\sigma} \overset{\boldsymbol{A}=\boldsymbol{A}^\dagger}{=} \sum_{\sigma,\sigma'} |A_{\sigma,\sigma'}|^2 = 2(a_0^2 + \vec{a}^2) \end{aligned} \tag{2.216}$$

and apply it to Eq. 2.213 with the one-particle-reduced density matrix $\rho^{(1)}$ from Eq. 2.215.

[47] In order to verify the factors, consider a spin density, which is fully polarized in z-direction. In that case $n_{S,z} = n_\uparrow - n_\downarrow = n_t$. The corresponding density matrix evaluated with Eq. 2.215 is

$$\rho^{(1)}(\vec{r},\sigma,\vec{r},\sigma') = \begin{pmatrix} n_t(\vec{r}) & 0 \\ 0 & 0 \end{pmatrix} \tag{2.214}$$

which is the anticipated result.

ON-TOP VALUE OF THE EXCHANGE HOLE

$$h_X(\vec{r},\vec{r}) = -\frac{1}{n_t(\vec{r})}\frac{1}{2}\left(\left(n_t(\vec{r})\right)^2 + \left(\vec{n}_s(\vec{r})\right)^2\right) = -n_t(\vec{r})\left[\frac{1}{2} + \frac{1}{2}\left(\frac{\vec{n}_S(\vec{r})}{n_t(\vec{r})}\right)^2\right] \qquad (2.217)$$

The on-top value of the exchange hole varies between half the density, for a non-spin polarized system, and once the density for a fully spin-polarized system.

The significance of this result is the dependence on the spin density. When, for a given total density, the spin density is increased, the hole becomes more compact. Because the hole is now closer to the reference electron, the energy is lowered. Hence, the exchange term favors spin polarization. This is the origin of magnetism in solid materials.

Problem:

1 Determine the size of the exchange correlation hole

2 Using the on-top value Eq. 2.217 to construct the exchange correlation hole as function of the electron density and the spin density.

3 Combine the approximate exchange energy with the kinetic energy to determine the total energy as function of electron density and spin density. Estimate the energy difference between an electron gas in the paramagnetic and the ferromagnetic state. Estimate the electron density where the transition occurs. Estimate the electron density for real materials considering only the valence electrons.

? Editor: Sketch only: Estimate the entropy of the electron gas to estimate the Curie temperature of a free-electron gas.

Solution

1 Determine the size of the exchange correlation hole

The density value is obtained from the on-top value Eq. 2.217 for a Slater determinant and the radius is obtained from the sum rule Eq. 2.51. This yields

$$\overbrace{-n_t(\vec{r})\left[\frac{1}{2} + \frac{1}{2}\left(\frac{\vec{n}_S(\vec{r})}{n_t(\vec{r})}\right)^2\right]}^{\text{on-top value Eq. 2.217}} \cdot \frac{4\pi}{3}R^3 = -1 \quad \Rightarrow \quad R = \sqrt[3]{\frac{3}{4\pi}}\left[\frac{1}{2} + \frac{1}{2}\left(\frac{\vec{n}_S(\vec{r})}{n_t(\vec{r})}\right)^2\right]^{-\frac{1}{3}} [n_t(\vec{r})]^{-\frac{1}{3}} \qquad (2.218)$$

2 Using the on-top value Eq. 2.217 to construct the exchange correlation hole as function of the electron density and the spin density.

Next, we evaluate the exchange energy

The interaction of an electron with its exchange correlation hole is the electrostatic potential of the hole multiplied with the charge of the electron.[48] Integration over all electrons, yields the exchange-

[48] The potential acting on electrons of a homogeneously charged sphere with charge $+e$ and radius R is

$$v(|\vec{r}|) = -\frac{e^2}{4\pi\epsilon_0 R}\begin{cases}\frac{3}{2} - \frac{1}{2}\left(\frac{r}{R}\right)^2 & \text{for } |\vec{r}| < R \\ \left(\frac{r}{R}\right)^{-1} & \text{for } |\vec{r}| > R\end{cases} \qquad (2.219)$$

correlation (here only the exchange energy) energy. In contrast to the exchange-correlation energy, the exchange energy does not have a kinetic energy contribution, so that the exchange energy E_X has only a potential energy contribution U_X.

$$\begin{aligned} E_X &\overset{\text{Eq. 2.50}}{=} \int d^3r\, n^{(1)}(\vec{r}) \frac{1}{2} \int d^3r' \, \frac{e^2 h_X(\vec{r},\vec{r'})}{4\pi\epsilon_0 |\vec{r}-\vec{r'}|} \\ &= \frac{1}{2}\frac{e^2}{4\pi\epsilon_0} \int d^3r\, n^{(1)}(\vec{r}) \frac{-3}{2R} \\ &\overset{\text{Eq. 2.218}}{=} -\frac{1}{2}\frac{e^2}{4\pi\epsilon_0}\frac{3}{2} \int d^3r\, n^{(1)}(\vec{r}) \left\{ \sqrt[3]{\frac{3}{4\pi}} \left[\frac{1}{2} + \frac{1}{2}\left(\frac{\vec{n}_S(\vec{r})}{n_t(\vec{r})} \right)^2 \right]^{-\frac{1}{3}} \left[n^{(1)}(\vec{r}) \right]^{-\frac{1}{3}} \right\}^{-1} \\ &= -\frac{1}{2}\frac{e^2}{4\pi\epsilon_0}\frac{3}{2}\sqrt[3]{\frac{4\pi}{3}} \int d^3r \, \left(n^{(1)}(\vec{r}) \right)^{\frac{4}{3}} \left[\frac{1}{2} + \frac{1}{2}\left(\frac{\vec{n}_S(\vec{r})}{n_t(\vec{r})} \right)^2 \right]^{+\frac{1}{3}} \end{aligned} \tag{2.220}$$

Despite its simplicity, the model captures many features of the real system. This is because it correctly captures the charge sum rule Eq. 2.51.

Because the system is charge neutral, the Hartree energy, the electrostatic self energy of the charge background and the interaction of electrons with the background cancel exactly. Hence only the kinetic energy and the exchange-correlation energy need to be considered.

> 3 Combine the approximate exchange energy with the kinetic energy to determine the total energy as function of electron density and spin density. Estimate the energy difference between an electron gas in the paramagnetic and the ferromagnetic state. Estimate the electron density where the transition occurs. Estimate the electron density for real materials considering only the valence electrons.

The total energy of the model is

$$\begin{aligned} E_{\text{tot}}(n_t, \vec{n}_S) = & \underbrace{\int d^3r \, \underbrace{\frac{3}{10}\left(3\pi^2\right)^{\frac{2}{3}} \frac{\hbar^2}{m_e} n_t^{\frac{5}{3}}}_{E(n_t,0)/L^3} \cdot \underbrace{\frac{1}{2}\left(\left(1+\frac{|\vec{n}_S|}{n_t}\right)^{\frac{5}{3}} + \left(1-\frac{|\vec{n}_S|}{n_t}\right)^{\frac{5}{3}} \right)}_{\approx 1+(2^{\frac{2}{3}}-1)\left(\frac{n_S}{n_t}\right)^2}}_{E_{kin} \quad \text{Eq. 1.149}} \\ & \underbrace{-\frac{1}{2}\frac{e^2}{4\pi\epsilon_0}\frac{3}{2}\sqrt[3]{\frac{4\pi}{3}} \int d^3r \, \left(n_t(\vec{r})\right)^{\frac{4}{3}} \left[\frac{1}{2} + \frac{1}{2}\left(\frac{\vec{n}_S(\vec{r})}{n_t(\vec{r})} \right)^2 \right]^{+\frac{1}{3}}}_{U_{xc} \quad \text{Eq. 2.220}} \end{aligned} \tag{2.221}$$

The resulting total energy

Editor: The model artificially stabilizes the ferromagnetic electron gas. This is probably due to the lack of correlation, the Coulomb hole. It may also be due to the kinetic energy. The kinetic energy correction can be estimated from excluded volume in a hard sphere model. The ferromagnetic electron gas becomes favorable only at very low densities with $r_s >>$ look up thesis of Graham George Spink 2017 in the group of Richard Needs. spink17_thesis.pdf

In the following, we will resort to the exchange-correlation hole to rationalize the findings related to the electron-electron interaction in real materials.

Hund's rule and Stoner parameter

The model provides the underlying reason for Hund's rule, which says that electrons will align their spin, unless the kinetic-energy cost is too large.

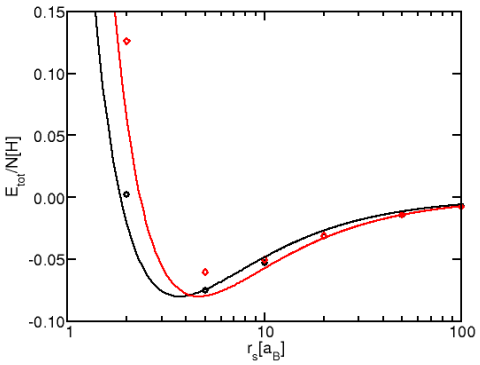

Fig. 2.14: Total energy per electron $(E_{kin} + U_{xc})/N$ of the paramagnetic free-electron gas (black) and of the ferromagnetic free-electron gas (red). The lines are obtained from Eq. 2.221. Circles and diamonds are from accurate quantum-Monte-Carlo calculations by Ceperley and Alder[49]. Compare also to [*"Energy, Specific Heat, and Magnetic Properties of the Low-Density Electron Gas"*, W. J. Carr, Jr., Phys. Rev. **122**, 1437 (1961), https://doi.org/10.1103/PhysRev.122.1437].

HUND'S RULE AND FERROMAGNETISM

Exchange acts only between electrons pairs with the same spin. Because exchange counteracts the Coulomb repulsion, it favors electrons with the same spin.

A result is **Hund's 1st rule**: *"For a given electron configuration, the term with maximum multiplicity has the lowest energy. The multiplicity is equal to $2S+1$, where S is the total spin angular momentum for all electrons. The term with lowest energy is also the term with maximum S."* [a] To be precise, the spin angular momentum is $\hbar S$.
Consider a set of degenerate one-particle states. Hund's rule says that the electrons will occupy this set so that the total spin is maximized. (The state with maximum spin has the largest multiplicity, namely $2S + 1$.) If many electrons have the same spin, the energy gain from the exchange term is large.

The same effect is responsible for the tendency of some solids to become **ferromagnetic**. Due to the finite band width of metals, spin-alignment leads to some loss of kinetic energy. The balance of kinetic energy and exchange determines whether ferromagnetism wins.

[a] Source `https://en.wikipedia.org/wiki/Hund%27s_rules`, retrieved Mar. 24, 2017.

Closely related to Hund's rule, which is useful for atoms, is Stoner's criterion for Ferromagnetism.

STONER CRITERION

If the density of states at the Fermi level of a non-magnetic metal obeys

$$D(\epsilon_F) I_{Stoner} > 1 \tag{2.222}$$

it exhibits an instability towards a ferromagnetism. I_{Stoner} is Stoner's exchange parameter.

While the concept underlying the tendency of electrons to arrange ferromagnetically is more general, studying this effect for our model as a specific example shall make the explanation more transparent. For this purpose, we can combine the exchange energy of the model-hole function Eq. 2.220 with the kinetic energy from Eq. 1.149 on p. 45.[49] This is a reasonably good model for

[49] The Hartree contribution of the electron interaction, the energy of the external potential (from the positive charge

a free-electron gas with interaction. It is able to describe, at least qualitatively, the transition to a ferromagnet with increasing interaction.

In the model, one can evaluate the energy as function of spin polarization $x = |\vec{n}_s|/n_t$ relative to the non-magnetic case. For the sake of simplicity, kinetic and exchange energies are scaled so that the kinetic energy is constant and the exchange energy can be scaled by the parameter a.

$$y(x) = \underbrace{\frac{1}{2}\left[(1+x)^{\frac{5}{3}} + (1-x)^{\frac{5}{3}}\right]}_{\sim \text{ kinetic energy Eq. 1.149}} \underbrace{-a(1+x^2)^{\frac{1}{3}}}_{\sim \text{exchange Eq. 2.220}} + a - 1 \tag{2.223}$$

The parameter a is a dimension-less ratio of the constants for the kinetic energy and exchange energy, which we will not work out in detail. The result Eq. 2.223 is shown figure 2.15. The model predicts a transition to a ferromagnet for $a = 5/3$.

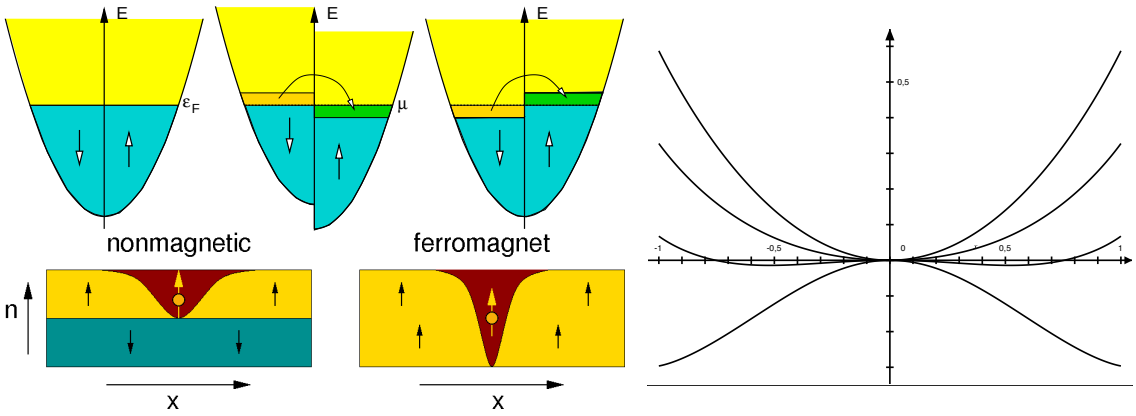

Fig. 2.15: Left, top: Scheme to explain the increasing kinetic energy with spin-polarization: density of states of a free-electron gas for spin-up and spin-down electrons. A magnetic moment can be induced, for example, by applying an external magnetic field, which makes the electrons of one spin direction more favorable than those with opposite spin. The kinetic energy increase is seen by removing the external field but maintaining the occupations of the spin-polarized system. Left,bottom: Scheme to explain the gain of interaction energy through spin polarization. The exchange hole of a ferromagnet has a higher density, namely $-n_t$ rather than $-n_t/2$. Considering the sum rule, the radius of the exchange hole is thus smaller. Thus, the interaction of electrons with the exchange hole is larger. Right: total energy Eq. 2.223 of the jellium model as function of the spin polarization $|\vec{n}_s|/n_t$ for different values of the interaction strength. The exchange energy is obtained with the model hole function of Eq. 2.220. The results are shown for $a = 0, 1, 2, 3$ from top to bottom. Without interaction, the Fermi gas is non-magnetic. For $a > 5/3$, however, the system becomes ferromagnetic.

The tendency towards ferromagnetism is a general feature of electrons, which is captured by the **Stoner criterion** for ferromagnetism:

When the kinetic energy dominates, the system strongly resists a spin polarization. We can say that the spin polarization requires electron-hole pairs, with the electron in the majority-spin channel and the hole in the minority-spin channel. When the density of states is small, as in a system in a large kinetic energy, a specific spin polarization requires electron-hole pairs with large energy. This energy cost must be overcome by the energy gain from the exchange energy. When the bands narrow, i.e. fairly flat, the density of states is high, and one can create many electron-hole pairs with small energy. In that case, ferromagnetism is favorable.

background) and the electrostatic self energy of the positive charge background cancel each other exactly and are therefore not accounted for. They cancel each other because they sum up to the total density of electrons and charge background. This total density vanishes per construction.

This is one explanation, why just the elemental 3-d transition-metals Fe, Co, Ni exhibit magnetism. Despite their energy position in the valence-band region, 3d-states have a radial extent similar to the 3s- and 3p-core states. Thus, they have a small hopping parameters and form fairly narrow bands with large density of states. For the heavier transition metals, of row 5 and 6 in the periodic table, the valence d-bands are wider. The larger radial extent of the 5d and 6d-states is due to the **Pauli repulsion**[50] with the lower 3d-states, which pushes the 4d and 5d states outward from the nucleus. The larger overlap with the neighboring atoms, which causes larger hopping parameters, and thus increases the band width.

[50] The Pauli repulsion describes an upward shift due to the orthogonality requirement with lower lying states.

Chapter 3

Second quantization

In this chapter, I will introduce the notion of creation and annihilation operators. This will lead to an elegant formulation of quantum mechanics in the Fock space.

I will place some emphasis on the definitions and the relations between different notations. The connection is easily lost. In particular, I consider the connection to wave functions (in real space) important for two reasons: Firstly, it connects to our knowledge base of one-particle quantum mechanics. Secondly, it allows one to connect to first-principles calculations with explicit wave functions.

3.1 Fock space

There are several ways towards second quantization. The most simple one is to define the Fock space. The **Fock space** is the combination of the Hilbert spaces for 0-particle states, 1-particle states, 2-particle states, etc. Let $\mathcal{H}_N$ be the Hilbert space of all N-particle states. The Fock space is the union[1] of all N-particle Hilbert spaces $\mathcal{H}^N$, that is

$$\mathcal{F} \stackrel{\text{def}}{=} \bigcup_{N=0}^{\infty} \mathcal{H}_N \tag{3.1}$$

The definition of the scalar product is that of the Hilbert spaces. What is missing is a definition of the scalar product between states with different particle numbers. We postulate that the scalar product of states with different particle numbers vanishes.[2]

As a curiosity, we introduced here also the 0-particle state, called **vacuum state**, that is not represented by a wave function at all.

Another way to define the Fock space[3] is the following.

1. Starting from a one-particle Hilbert space $\mathcal{H}$ one constructs the Hilbert space $\mathcal{H}^{\otimes N}$ of general N-particle states as tensor product of N one-particle states.
2. For identical particles these states are antisymmetrized (for fermions) or symmetrized (for bosons). The resulting space of fermionic N-particle wave functions is denoted by $\mathcal{H}^{-,\otimes N}$ –denoted above as $\mathcal{H}_N$ – and the one for bosonic N-particle wave functions is denoted by $\mathcal{H}^{+,\otimes N}$
3. The direct sum of all fermionic N-particle Hilbert spaces is the Fock space

$$\mathcal{F}^{(-)} = \bigoplus_{N=0}^{\infty} \mathcal{H}^{-,\otimes N} \,, \tag{3.2}$$

[1] germ.:union=Vereinigung

[2] This postulate is non-trivial and can be derived more naturally from the second quantization via introducing wave functions in the space of the fields describing the wave functions.

[3] Taken from `https://en.wikipedia.org/wiki/Fock_space`.

denoted above simply as $\mathcal{F}$. The definition for the bosonic Fock space is analogous.

$$\mathcal{F}^{(+)} = \bigoplus_{N=0}^{\infty} \mathcal{H}^{+,\otimes N} \tag{3.3}$$

3.2 Occupation-number representation

We are entering a new level of abstraction and it turned out to be useful to introduce a special notation for it. This will lead us to the occupation-number representation and to creation and annihilation operators.

In order to work within the Fock space, we need to select a suitable basis set. We have already learned that Slater determinants, which are constructed from a complete orthonormal one-particle basis, form a complete set of many-particle wave functions.

Each Slater determinant is uniquely defined, up to a sign, by the one-particle states used in its construction. Therefore, the Slater determinants can be written economically in the **occupation-number representation**. For a given, ordered, one-particle basisset, we form a vector, where each position corresponds to a particular one-particle orbital. Each entry can be zero or one, and describes if that particular orbital is present in the Slater determinant or not. If the occupation number is one, we say that the orbital is occupied, and if the occupation-number is zero, we say that it is unoccupied or empty. Thus, a Slater determinant can be expressed in a form like

$$|0,0,0,\underbrace{1}_{i_1},0,\underbrace{1}_{i_2},0,\ldots\rangle = |S_{i_1,i_2,\ldots}\rangle \qquad \text{with} \quad i_1 < i_2 < \ldots \tag{3.4}$$

where $S_{i_1,i_2,\ldots}$ is a Slater determinant made of the one-particle orbitals $|\varphi_{i_1}\rangle, |\varphi_{i_2}\rangle, \ldots$.

Because the Slater determinant changes its sign under permutation of two one-particle wave functions, we need to define the sign convention. The sign is fixed such that the one-particle orbitals must occur in the corresponding Slater determinant in the order of increasing index, that is $i_1 < i_2, \ldots$. Thus,

$$|1,1,0,0,\ldots\rangle = |S_{1,2}\rangle = -|S_{2,1}\rangle \tag{3.5}$$

$$\langle \vec{r}, \vec{r'}|1,1,0,0,\ldots\rangle = \frac{1}{\sqrt{2!}}\left[\varphi_1(\vec{r})\varphi_2(\vec{r'}) - \varphi_2(\vec{r})\varphi_1(\vec{r'})\right] \tag{3.6}$$

Note also, that there is an explicit **vacuum state**

$$|\mathcal{O}\rangle \stackrel{\text{def}}{=} |0,0,0,0,0,0,0,0,0,0,\ldots\rangle \tag{3.7}$$

The vacuum state describes a system without particles. Note that the vacuum state, which we denote by a calligraphic "O", $|\mathcal{O}\rangle$, is different from the zero state $|\varnothing\rangle$. The latter is obtained by multiplying an arbitrary state with zero.

The most general antisymmetric wave function has the form

$$|\Phi\rangle = \sum_{\vec{\sigma}} |\vec{\sigma}\rangle c_{\vec{\sigma}} = \sum_{\sigma_1,\sigma_2,\ldots=0}^{1} |\sigma_1,\sigma_2,\ldots\rangle c_{\sigma_1,\sigma_2,\ldots} \tag{3.8}$$

Example: hydrogen molecule

Let us consider a hydrogen molecule with only one s-orbital per site. The s-orbitals shall be combined into bonding and an antibonding orbitals. The ordered one-particle basis is $|b,\uparrow\rangle, |b,\downarrow\rangle, |a,\uparrow\rangle, |a,\downarrow\rangle$, where $|b,\sigma\rangle$ describes the bonding and $|a,\sigma\rangle$ describes the antibonding orbital.

Now, we can form the limited Fock space for this model. There are $2^4 = 16$ Slater determinants as shown in Fig. 3.1.

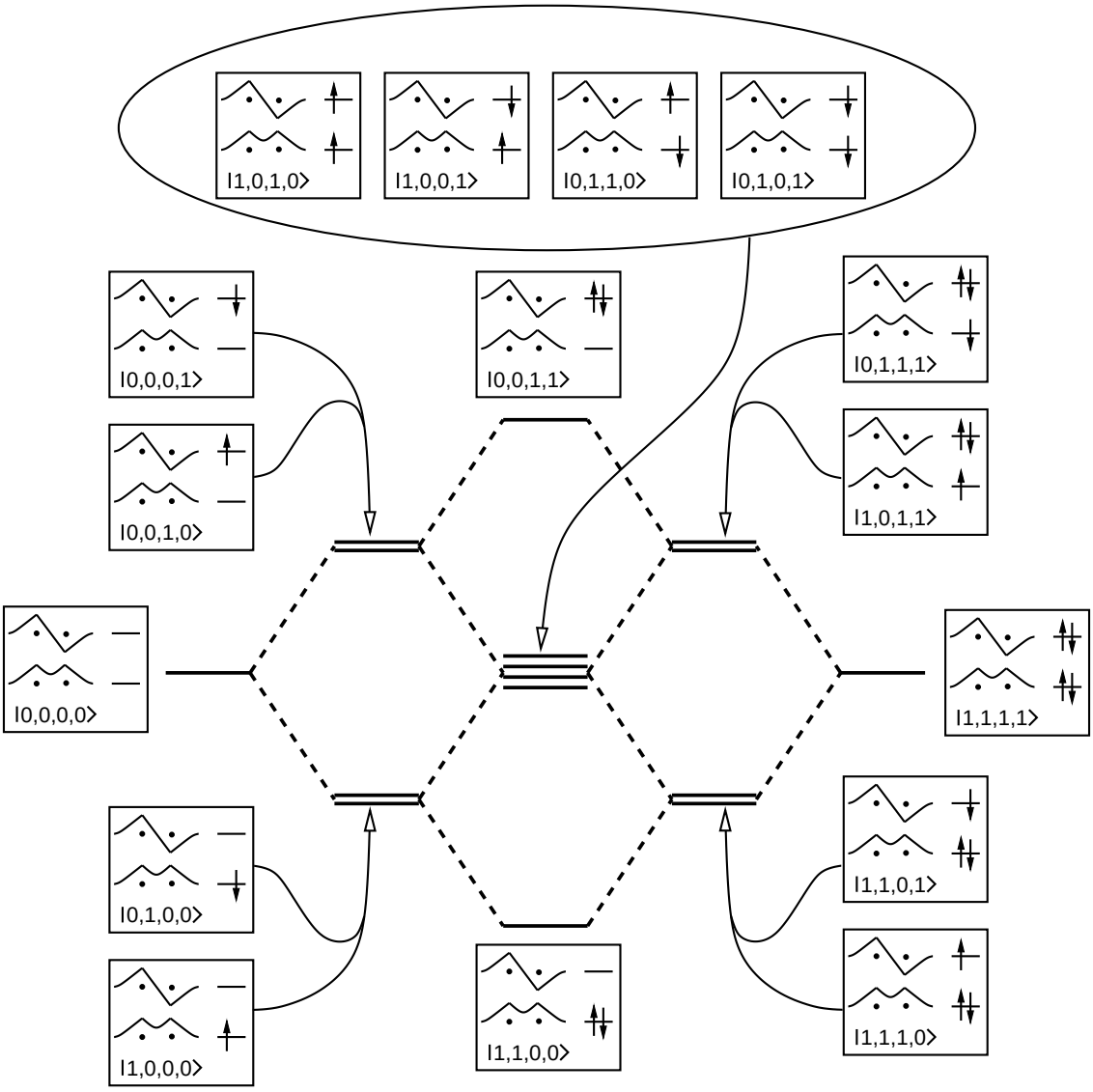

Fig. 3.1: Schematic representation of the Fock space build from the bonding and antibonding states of the hydrogen molecule. The middle diagram represents the many-particle energy levels assuming non-interacting electrons and with $\epsilon_a = -\epsilon_b$, where ϵ_a is the one-particle energy of the antibonding level and ϵ_b is the energy level of the bonding orbital. The insets correspond to the occupation-number representation and the corresponding one-electron energy level diagram. On the left it contains a schematic drawing of the one-particle wave functions.

- $|0000\rangle$ is the zero-particle state. It describes just the two protons without electrons.

- $|1000\rangle$, $|0100\rangle$, $|0010\rangle$ and $|0001\rangle$ are the one-particle states. Thus, they describe the H_2^+ ion. The states $|1000\rangle$ and $|0100\rangle$ correspond to the bound H_2^+ ion, while the remaining two states correspond to the electron in the antibonding state. The molecule in the latter configuration would be unstable.

- $|1100\rangle$ corresponds to the ground state of the H_2 molecule with two paired electrons in the bonding orbital. There are in total 6 two-electron Slater determinants of which 5 are excited states.

- There are four three-electron states, namely $|1110\rangle$ $|1101\rangle$, $|1011\rangle$,$|01111\rangle$. The three particle states describe the negative H_2^- ion.
- finally there is one four-electron state, $|1111\rangle$ which describes the H_2^{2-} ion.

Excursion: Integer representation representation of Slater determinants

Note that the sequence can be considered as a binary number with the digits. This allows one to identify each Slater determinant uniquely with one integer number.

The conversion of an integer into the number representation is to

$$\begin{aligned} 0 &\rightarrow |0,0,0,0,0,0,0,0,0,0,\ldots\rangle \\ 1 &\rightarrow |1,0,0,0,0,0,0,0,0,0,\ldots\rangle \\ 2 &\rightarrow |0,1,0,0,0,0,0,0,0,0,\ldots\rangle \\ 3 &\rightarrow |1,1,0,0,0,0,0,0,0,0,\ldots\rangle \\ 4 &\rightarrow |0,0,1,0,0,0,0,0,0,0,\ldots\rangle \\ \mathcal{I}(\vec{\sigma}) \stackrel{\text{def}}{=} \sum_j \sigma_j 2^{j-1} &\rightarrow |\sigma_1,\sigma_2,\ldots\rangle \end{aligned} \tag{3.9}$$

In FORTRAN, bits can be handled in a simple manner. If I is the integer representation of a Slater determinant and i is the position of a particular one-particle orbital, we obtain its occupation number by

$$\sigma_i = \texttt{BTEST}(\mathcal{I}-1, i-1) \tag{3.10}$$

The bits can be manipulated using the FORTRAN functions

$$\begin{aligned} \mathcal{I}' &= \texttt{IBCLR}(\mathcal{I}-1, i-1) \\ \mathcal{I}'' &= \texttt{IBSET}(\mathcal{I}-1, i-1) \end{aligned} \tag{3.11}$$

where $\mathcal{I}'$ is obtained from $\mathcal{I}(\vec{\sigma})$ by setting the occupation σ_i to zero, and $\mathcal{I}''$ is obtained by setting it to one.

In order to see the difficulty of many-particle physics let us count the number of states. If truncate the one-particle basisset to M orbitals, there are 2^M many-particle basisfunctions, because any one-particle state can be occupied or unoccupied. For $M = 10$ there are already $2^{10} = 1024$ states, which requires a kilobyte of memory to hold the coefficients. For $M = 20$ we already require a Megabyte and for 30 orbitals we need a Gigabyte.

3.3 Creation and annihilation operators

We define **creation operators** $\hat{a}_i^\dagger$ that increase the particle number in a given one-particle state. Using creation operators, we can create all many-particle states from the vacuum state.

From Slater determinants

DEFINITION OF A CREATION OPERATOR IN TERMS OF SLATER DETERMINANTS

We define the creation operator for a particular orbital as follows: When we apply a creation operator to a Slater determinant, it adds a row with the new orbital at the top of the corresponding matrix, and introduces a column with a new coordinate to the right.
This definition is the link between wave functions and the operator algebra used in the following.

It is important to watch the sign of the state. Let us consider an example where a third particle in state $|\varphi_2\rangle$ is created in a state that contains two particles, one in $|\varphi_1\rangle$ and one in $|\varphi_3\rangle$.

$$\hat{a}_2^\dagger \overbrace{\frac{1}{\sqrt{2!}}\det\begin{vmatrix}\varphi_1(\vec{x}_1) & \varphi_1(\vec{x}_2)\\ \varphi_3(\vec{x}_1) & \varphi_3(\vec{x}_2)\end{vmatrix}}^{|1,0,1,0,\ldots\rangle} = \overbrace{\frac{1}{\sqrt{3!}}\det\begin{vmatrix}\varphi_2(\vec{x}_1) & \varphi_2(\vec{x}_2) & \varphi_2(\vec{x}_3)\\ \varphi_1(\vec{x}_1) & \varphi_1(\vec{x}_2) & \varphi_1(\vec{x}_3)\\ \varphi_3(\vec{x}_1) & \varphi_3(\vec{x}_2) & \varphi_3(\vec{x}_3)\end{vmatrix}}^{\hat{a}_2^\dagger|1,0,1,0,\ldots\rangle}$$
$$= (-1)\cdot \underbrace{\frac{1}{\sqrt{3!}}\det\begin{vmatrix}\varphi_1(\vec{x}_1) & \varphi_1(\vec{x}_2) & \varphi_1(\vec{x}_3)\\ \varphi_2(\vec{x}_1) & \varphi_2(\vec{x}_2) & \varphi_2(\vec{x}_3)\\ \varphi_3(\vec{x}_1) & \varphi_3(\vec{x}_2) & \varphi_3(\vec{x}_3)\end{vmatrix}}_{|1,1,1,0,\ldots\rangle} \tag{3.12}$$

From the occupation-number representation

Each state $|\vec{\sigma}\rangle$ of the occupation-number representation can be translated uniquely into a Slater determinant. This translation rule requires the choice of an ordered, complete orthonormal set of one-particle wave functions $|\varphi_j\rangle$. Once we have this translation, we can translate the definition of creation operators into the occupation-number representation.

For the example Eq. 3.12 above, we obtain

$$\hat{a}_2^\dagger|1,0,1,0,0,\ldots\rangle = -|1,1,1,0,0,\ldots\rangle \tag{3.13}$$

The added one-particle state needs to be moved to the correct position in the Slater determinant. Each occupied orbital, one passes during that process, contributes a sign change. Thus, we need to count the number of occupied orbitals left of the final position. The net number of sign changes for adding an electron in orbital $|\varphi_i\rangle$ is thus $\sum_{j<i}\sigma_j$.

Generalizing this principle leads to

$$\hat{a}_i^\dagger|\sigma_1,\sigma_2,\ldots,\underbrace{0}_{\text{pos } i},\ldots\rangle = |\sigma_1,\sigma_2,\ldots,\underbrace{1}_{\text{pos } i},\ldots\rangle\ \left[(-1)^{\sum_{j<i}\sigma_j}\right]$$
$$\hat{a}_i^\dagger|\sigma_1,\sigma_2,\ldots,\underbrace{1}_{\text{pos } i},\ldots\rangle = |\varnothing\rangle \tag{3.14}$$

In short, we may write

$$\hat{a}_i^\dagger = \sum_{\vec{\sigma}}\Big|\sigma_1,\sigma_2,\ldots,\sigma_i+1,\ldots\Big\rangle\left(\left[(-1)^{\sum_{j<i}\sigma_j}\right]\sqrt{1-\sigma_i}\right)\Big\langle\sigma_1,\sigma_2,\ldots,\sigma_i,\ldots\Big| \tag{3.15}$$

The factor $\sqrt{1-\sigma_i}$ ensures that Eq. 3.15 does not produce states with occupations $\sigma_i \geq 2$. The square root has been chosen to be consistent with the case of bosons, discussed later: The factor for bosons is $\sqrt{1+\sigma}$. For fermions σ_j can only have values zero and one, for which $\delta_{\sigma,1} = \sigma = \sqrt{\sigma}$, so that the result is unchanged from $1-\sigma$ to $\sqrt{1-\sigma}$.

The hermitian conjugate of the creation operator is calculated from Eq. 3.15 using the general operator identity

$$\hat{A} = \sum_{m,n}|m\rangle A_{m,n}\langle n| \qquad \Leftrightarrow \qquad \hat{A}^\dagger = \sum_{m,n}|n\rangle A^*_{m,n}\langle m| = \sum_{m,n}|m\rangle A^*_{n,m}\langle n| \tag{3.16}$$

which yields for $\hat{a}_i = (\hat{a}_i^\dagger)^\dagger$

$$\hat{a}_i = \sum_{\vec{\sigma}}\Big|\sigma_1,\sigma_2,\ldots,\sigma_i,\ldots\Big\rangle\left(\left[(-1)^{\sum_{j<i}\sigma_j}\right]\sqrt{1-\sigma_i}\right)^*\Big\langle\sigma_1,\sigma_2,\ldots,\sigma_i+1,\ldots\Big|$$
$$= \sum_{\vec{\sigma}}\Big|\sigma_1,\sigma_2,\ldots,\sigma_i-1,\ldots\Big\rangle\left(\left[(-1)^{\sum_{j<i}\sigma_j}\right]\sqrt{\sigma_i}\right)\Big\langle\sigma_1,\sigma_2,\ldots,\sigma_i,\ldots\Big| \tag{3.17}$$

We see that $\hat{a}_i$ annihilates electrons and is thus named **annihilator**.

The last step in Eq. 3.17 is a little tricky. In first line of Eq. 3.17, the factor $\sqrt{1-\sigma}$ excludes the terms with $\sigma_i = 1$. In the second line, the factor $\sqrt{\sigma}$ excludes terms with $\sigma_i = 0$.

CREATION AND ANNIHILATION OPERATORS FOR FERMIONS

The definition of creation operators $\hat{a}_i^\dagger$ and annihilation operators $\hat{a}_i$ for fermions is

$$\hat{a}_i^\dagger \overset{\text{Eq. 3.15}}{=} \sum_{\vec{\sigma}} \Big|\sigma_1, \sigma_2, \ldots, \sigma_i + 1, \ldots\Big\rangle \left(\left[(-1)^{\sum_{j<i}\sigma_j}\right]\sqrt{1-\sigma_i}\right)\Big\langle\sigma_1, \sigma_2, \ldots, \sigma_i, \ldots\Big|$$

$$\hat{a}_i \overset{\text{Eq. 3.17}}{=} \sum_{\vec{\sigma}} \Big|\sigma_1, \sigma_2, \ldots, \sigma_i - 1 \ldots\Big\rangle \left(\left[(-1)^{\sum_{j<i}\sigma_j}\right]\sqrt{\sigma_i}\right)\Big\langle\sigma_1, \sigma_2, \ldots, \sigma_i, \ldots\Big| \tag{3.18}$$

The sum is performed over all vectors $|\vec{\sigma}\rangle$ with $\sigma_i \in \{0, 1\}$, where the indices j refer to a ordered, complete and orthonormal one-particle basisset.

It may disturb that states with forbidden occupations σ_i turn up with $\sigma_i < 0$ or $\sigma_i > 1$. This formal difficulty can be healed by simply defining those states as being the zero state $|\varnothing\rangle$. Thus,

$$|\sigma_1, \sigma_2, \ldots\rangle \overset{\text{def}}{=} |\varnothing\rangle \qquad \text{if there is an} \qquad \sigma_i \notin \{0, 1\} \tag{3.19}$$

Note, that the zero state $|\varnothing\rangle$ is different from the vacuum state $|\mathcal{O}\rangle$. The vacuum state describes a physical situation, namely one without particles. The zero state does not describe any physical situation. In a superposition of states, it can simply be left out.

Building up the Fock space from the vacuum state

The creation and annihilation operators lead us to one other representation of the basis states, which is distinct from the occupation-number representation and the Slater determinants. Each state can be identified with a product of creation operators.

We start out from the **vacuum state** defined in Eq. 3.7

$$|\mathcal{O}\rangle \overset{\text{def}}{=} |0, 0, 0, \ldots\rangle \tag{3.20}$$

The vacuum state is a zero-particle state. It represents the vacuum, which is a system without particles.[4]

Then, we fill electrons into the vacuum using the creation operators:

[4] Note, that the vacuum state differs from a zero state.

OCCUPATION-NUMBER REPRESENTATION AND CREATION OPERATORS

A state characterized in the occupation-number representation by a string $\vec{\sigma}$ of occupation numbers, i.e. a Slater determinant, can be constructed by successively applying creation operators to the vacuum state $|\mathcal{O}\rangle$ in the form

$$|\vec{\sigma}\rangle = \prod_{j=1}^{\infty} \left(\hat{a}_j^\dagger\right)^{\sigma_j} |\mathcal{O}\rangle$$
$$\langle\vec{\sigma}| = \langle\mathcal{O}| \underbrace{\prod_{j=1}^{\infty}}_{\text{Caution!}} (\hat{a}_j)^{\sigma_j} \tag{3.21}$$

For the ket, the indices in the product increase from the left to the right. This avoids sign changes as particles are created. A different order may induce sign changes. For the bra the order of the operator is opposite, i.e. from right to left. The reversed order of the product is indicated with an uncommon notation, namely by interchanging the lower and upper bound of the index in the product. As a special case, we obtain a representation of one-particle orbitals in terms of the vacuum state and the corresponding creation operator.

$$|\varphi_j\rangle = \hat{a}_j^\dagger |\mathcal{O}\rangle \tag{3.22}$$

A general quantum state $|\Psi\rangle$ is a superposition of Slater determinants $|\vec{\sigma}\rangle$. Also such a state can be built up from the vacuum state with the help of creation operators.

$$|\Psi\rangle = \sum_{\vec{\sigma}} |\vec{\sigma}\rangle c_{\vec{\sigma}} = \left(\sum_{\vec{\sigma}} c_{\vec{\sigma}} \prod_{j=1}^{\infty} \left(\hat{a}_j^\dagger\right)^{\sigma_j}\right)|\mathcal{O}\rangle \tag{3.23}$$

This is an important step: From this point on, not only the operators, but even the states, are represented by operators. Because there is only one vacuum state, the sequence of creation operators is sufficient to uniquely define a state. All expectation values are finally ones calculated with the vacuum state.

3.4 Anticommutator relations

Commutator relations play an important role in quantum mechanics. In the case of quantum field theory of fermions, it is the anticommutator relations between fermionic creation and annihilation operators.

We determine the anticommutator relation[5] between creation and annihilation operators in the following.

The origin of the anticommutator rules is Pauli's principle, i.e. the antisymmetry of the fermionic wave function.

- From the definition of the creation operators in terms of Slater determinants, i.e. Eq. 3.12, we know that an interchange of two particles changes the sign of the wave function, i.e.

$$\hat{a}_i^\dagger \hat{a}_j^\dagger |\Phi\rangle = -\hat{a}_j^\dagger \hat{a}_i^\dagger |\Phi\rangle \qquad \Rightarrow \qquad [\hat{a}_i^\dagger, \hat{a}_j^\dagger]_+ |\Phi\rangle = |\varnothing\rangle \tag{3.24}$$

  $|\varnothing\rangle$ is the null state. Because, the equation holds for any fermionic wave function $|\Phi\rangle$, it can

[5] The anticommutator of two operators $\hat{A}$ and $\hat{B}$ is denoted as $[\hat{A}, \hat{B}]_+ \stackrel{\text{def}}{=} \hat{A}\hat{B} + \hat{B}\hat{A}$.

simply be written as operator relation

$$\left[\hat{a}_i^\dagger, \hat{a}_j^\dagger\right]_+ = 0 \tag{3.25}$$

- The anticommutator for two annihilation operators is obtained as hermitian conjugate[6] of Eq. 3.25.

$$\left[\hat{a}_i, \hat{a}_j\right]_+ = 0 \tag{3.26}$$

- What happens if we interchange a creation and an annihilation operator?

  Let me start writing out the products using the definition Eq. 3.18. Below, we exploit that the first product gives the zero state, unless $\sigma'_n = 0$, and the second for $\sigma_n = 1$. Once σ_n is known, the values of other quantities can already be assigned. I indicate them with "$\rightsquigarrow$".

$$\begin{aligned}
\hat{a}_n^\dagger \hat{a}_n \overset{\text{Eq. 3.18}}{=} & \sum_{\vec{\sigma}'} \left|\sigma'_1, \sigma'_2, \ldots, \underbrace{\sigma'_n + 1}_{\rightsquigarrow 1}, \ldots\right\rangle \left(\underbrace{\left[(-1)^{\sum_{k<n}\sigma'_k}\right]\sqrt{1-\sigma'_n}}_{\delta_{\sigma'_n,0}}\right)\left\langle\sigma'_1, \sigma'_2, \ldots, \underbrace{\sigma'_n}_{\rightsquigarrow 0}, \ldots\right| \\
& \times \sum_{\vec{\sigma}} \left|\sigma_1, \sigma_2, \ldots, \underbrace{\sigma_n - 1}_{\rightsquigarrow 0} \ldots\right\rangle \left(\underbrace{\left[(-1)^{\sum_{k<n}\sigma_k}\right]\sqrt{\sigma_n}}_{\delta_{\sigma_n,1}}\right)\left\langle\sigma_1, \sigma_2, \ldots, \underbrace{\sigma_n}_{\rightsquigarrow 1}, \ldots\right| \\
= & \sum_{\vec{\sigma}} \left|\vec{\sigma}\right\rangle \left[(-1)^{\sum_{k<n}\sigma_k}\right]^2 \delta_{\sigma_n,1}\left\langle\vec{\sigma}\right| \\
= & \sum_{\vec{\sigma}} \left|\vec{\sigma}\right\rangle \delta_{\sigma_n,1}\left\langle\vec{\sigma}\right| \\
= & \sum_{\vec{\sigma}} \left|\vec{\sigma}\right\rangle \sigma_n \left\langle\vec{\sigma}\right|
\end{aligned} \tag{3.27}$$

  We proceed analogously with the product in reverse order. Then, a non-zero result requires $\sigma_n = 0$ and $\sigma'_n = 1$.

$$\begin{aligned}
\hat{a}_n \hat{a}_n^\dagger \overset{\text{Eq. 3.18}}{=} & \sum_{\vec{\sigma}'} \left|\sigma'_1, \sigma'_2, \ldots, \underbrace{\sigma'_n - 1}_{\rightsquigarrow 0}, \ldots\right\rangle \left(\underbrace{\left[(-1)^{\sum_{k<n}\sigma'_k}\right]\sqrt{\sigma'_n}}_{\delta_{\sigma'_n,1}}\right)\left\langle\sigma'_1, \sigma'_2, \ldots, \underbrace{\sigma'_n}_{\rightsquigarrow 1}, \ldots\right| \\
& \times \sum_{\vec{\sigma}} \left|\sigma_1, \sigma_2, \ldots, \underbrace{\sigma_n + 1}_{\rightsquigarrow 1} \ldots\right\rangle \left(\underbrace{\left[(-1)^{\sum_{k<n}\sigma_k}\right]\sqrt{1-\sigma_n}}_{\delta_{\sigma_n,0}}\right)\left\langle\sigma_1, \sigma_2, \ldots, \underbrace{\sigma_n}_{\rightsquigarrow 0}, \ldots\right| \\
= & \sum_{\vec{\sigma}} \left|\vec{\sigma}\right\rangle \left[(-1)^{\sum_{k<n}\sigma_k}\right]^2 \delta_{\sigma_n,0}\left\langle\vec{\sigma}\right| \\
= & \sum_{\vec{\sigma}} \left|\vec{\sigma}\right\rangle \delta_{\sigma_n,0}\left\langle\vec{\sigma}\right| \\
= & \sum_{\vec{\sigma}} \left|\vec{\sigma}\right\rangle (1-\sigma_n) \left\langle\vec{\sigma}\right|
\end{aligned} \tag{3.28}$$

  Thus, we obtain the anticommutator relation by adding Eqs. 3.27 and 3.28.

$$\left[\hat{a}_n^\dagger, \hat{a}_n\right]_+ \overset{\text{Eqs. 3.27,3.28}}{=} 1 \tag{3.29}$$

  On the way, we also obtained another useful operator, namely the one that provides the occupation of a specific orbital.

[6] Use $(\hat{A}\hat{B})^\dagger = \hat{B}^\dagger \hat{A}^\dagger$

OCCUPATION-NUMBER OPERATOR

.

$$\hat{n}_j \overset{\text{def}}{=} \hat{a}_j^\dagger \hat{a}_j \overset{\text{Eq. 3.27}}{=} \sum_{\vec{\sigma}} |\vec{\sigma}\rangle \sigma_j \langle \vec{\sigma}| \tag{3.30}$$

The expectation value of the occupation-number operator $\hat{n}_j$ is the mean number of particles in the j-th orbital.

Let me now turn to the products $\hat{a}_m^\dagger \hat{a}_n$ and $\hat{a}_n \hat{a}_m^\dagger$ with $m \neq n$. I use Eq. 3.18 to express the operators in the occupation-number representation.

In each of the two products below, only few terms are non-zero because of the factors $\sqrt{1-\sigma'_m}$ and $\sqrt{\sigma_n}$. I use the short-hand notation[7], that $\sum_{m\leq k<n}$ stands for $\sum_{\min(m,n)\leq k<\max(m,n)}$.

$$\begin{aligned}
\hat{a}_m^\dagger \hat{a}_n &\overset{\text{Eq. 3.18}}{=} \sum_{\vec{\sigma}'} \Big| \dots, \underbrace{\sigma'_m + 1}_{\rightsquigarrow \sigma_m + 1}, \dots, \underbrace{\sigma'_n}_{\rightsquigarrow \sigma_n - 1}, \dots \Big\rangle \Bigg(\underbrace{\Big[(-1)^{\sum_{k<m} \sigma'_k}\Big]}_{\rightsquigarrow \mathrm{sgn}(n-m)(-1)^{\sum_{k<m}\sigma_k}} \underbrace{\sqrt{1-\sigma'_m}}_{=\delta_{\sigma'_m,0} \rightsquigarrow \delta_{\sigma_m,0}} \Bigg) \Big\langle \dots, \underbrace{\sigma'_m}_{\rightsquigarrow \sigma_m}, \dots, \underbrace{\sigma'_n}_{\rightsquigarrow \sigma_n - 1}, \dots \Big| \\
&\times \sum_{\vec{\sigma}} \Big| \dots, \sigma_m, \dots, \sigma_n - 1, \dots \Big\rangle \Big(\Big[(-1)^{\sum_{k<n} \sigma_k}\Big] \underbrace{\sqrt{\sigma_n}}_{\delta_{\sigma_n,1}} \Big) \Big\langle \dots, \sigma_m, \dots, \sigma_n, \dots \Big| \\
&\overset{\text{Eq. 3.32}}{=} \sum_{\vec{\sigma}} \Big| \dots, \sigma_m + 1, \dots, \sigma_n - 1, \dots \Big\rangle \Big[\delta_{\sigma_m,0} \delta_{\sigma_n,1} \mathrm{sgn}(n-m) (-1)^{\sum_{m\leq k<n} \sigma_k} \Big] \Big\langle \vec{\sigma} \Big|
\end{aligned} \tag{3.33}$$

Now, I rewrite the product in reverse order analogously:

$$\begin{aligned}
\hat{a}_n \hat{a}_m^\dagger &\overset{\text{Eq. 3.18}}{=} \sum_{\vec{\sigma}'} \Big| \dots, \underbrace{\sigma'_m}_{\rightsquigarrow \sigma_m + 1}, \dots, \underbrace{\sigma'_n - 1}_{\rightsquigarrow \sigma_n - 1}, \dots \Big\rangle \Bigg(\underbrace{\Big[(-1)^{\sum_{k<n} \sigma'_k}\Big]}_{\rightsquigarrow \mathrm{sgn}(m-n)(-1)^{\sum_{k<n}\sigma_k}} \underbrace{\sqrt{\sigma'_n}}_{=\delta_{\sigma'_n,1} \rightsquigarrow \delta_{\sigma_n,1}} \Bigg) \Big\langle \dots, \underbrace{\sigma'_m}_{\rightsquigarrow \sigma_m + 1}, \dots, \underbrace{\sigma'_n}_{\rightsquigarrow \sigma_n}, \dots \Big| \\
&\times \sum_{\vec{\sigma}} \Big| \dots, \sigma_m + 1, \dots, \sigma_n, \dots \Big\rangle \Big(\Big[(-1)^{\sum_{k<m} \sigma_k}\Big] \underbrace{\sqrt{1-\sigma_m}}_{\delta_{\sigma_m,0}} \Big) \Big\langle \dots, \sigma_m, \dots, \sigma_n, \dots \Big| \\
&= \sum_{\vec{\sigma}} \Big| \dots, \sigma_m + 1, \dots, \sigma_n - 1, \dots \Big\rangle \Big[\delta_{\sigma_m,0} \delta_{\sigma_n,1} \underbrace{\mathrm{sgn}(m-n)}_{-\mathrm{sgn}(n-m)} (-1)^{\sum_{m\leq k<n} \sigma_k} \Big] \Big\langle \vec{\sigma} \Big|
\end{aligned} \tag{3.34}$$

Thus, the two operator products Eq. 3.33 and Eq. 3.34 are identical except for a sign change resulting from the different arguments of the sign function, so that

$$\left[\hat{a}_m^\dagger, \hat{a}_n\right]_+ = 0 \tag{3.35}$$

Eqs. 3.29 and 3.35 can be combined to

$$\left[\hat{a}_m^\dagger, \hat{a}_n\right]_+ = \delta_{m,n} \tag{3.36}$$

[7] Below, I exploit the orthonormality of the Slater determinants in the occupation-number representation, so that

$$\langle \dots, \sigma'_m, \dots \sigma'_n, \dots | \dots, \sigma_m, \dots, \sigma_n - 1, \dots \rangle = \delta_{\sigma'_m,\sigma_m} \delta_{\sigma'_n,1-\sigma_n} \prod_{k\notin\{m,n\}} \delta_{\sigma'_k,\sigma_k} = \delta_{\sigma'_n,1-\sigma_n} \prod_{k\notin\{n\}} \delta_{\sigma'_k,\sigma_k} \tag{3.31}$$

Thus, in the double sum over $\vec{\sigma}, \vec{\sigma}'$, all σ'_k can be replaced by σ_k, except for $k = n$.

$$\Big[(-1)^{\sum_{k<m} \sigma'_k}\Big] \Big\langle \dots, \sigma'_m, \dots \sigma'_n, \dots \Big| \dots, \sigma_m, \dots, \sigma_n - 1, \dots \Big\rangle = \mathrm{sgn}(n-m) \Big[(-1)^{\sum_{k<m} \sigma_k}\Big] \delta_{\sigma'_n,1-\sigma_n} \prod_{k\notin\{n\}} \delta_{\sigma'_k,\sigma_k} \tag{3.32}$$

The exchange of the primed σ'_n by the un-primed σ_n introduces a sign change, if $n < m$. The sign change is absent for $n > m$ because then it is not considered in the sign factor $(-1)^{\sum_{k<m} \sigma'_k}$. Thus, we can account the sign change when going from primed to un-primed numbers by an additional factor $\mathrm{sgn}(n-m)$.

The rules, we arrive at, are

ANTICOMMUTATION RULES FOR FERMIONIC CREATION AND ANNIHILATION OPERATORS

$$[\hat{a}_i^\dagger, \hat{a}_j^\dagger]_+ \overset{\text{Eq. 3.25}}{=} 0 \qquad \text{and} \qquad [\hat{a}_i, \hat{a}_j]_+ \overset{\text{Eq. 3.26}}{=} 0 \qquad \text{and} \qquad [\hat{a}_i^\dagger, \hat{a}_j]_+ \overset{\text{Eq. 3.36}}{=} \delta_{i,j} \tag{3.37}$$

The anticommutators Eq. 3.37 between creation and annihilation operators are numbers.[8] No such rule exists for the commutators of fermionic creation and annihilation operators: the commutators of fermion operators are still operators.

For bosons, similar relations exist, but for commutators, rather than for anticommutators.

Commutator relations in first quantization: The reader will remember that the commutator relations

$$\begin{aligned} [\hat{x}_i, \hat{x}_j]_- &= 0 \\ [\hat{p}_i, \hat{p}_j]_- &= 0 \\ [\hat{p}_i, \hat{x}_j]_- &= \frac{\hbar}{i}\delta_{i,j} \ , \end{aligned} \tag{3.38}$$

between positions and momenta have been central to formulation of quantum mechanics. In the second quantization of fermions, the anticommutator relations above play a similarly important role.

Commutator relations for the quantized harmonic oscillator: If we consider the harmonic oscillator, we found the commutator relations

$$\begin{aligned} [\hat{b}_i^\dagger, \hat{b}_j^\dagger]_- &= 0 \\ [\hat{b}_i, \hat{b}_j]_- &= 0 \\ [\hat{b}_i, \hat{b}_j^\dagger]_- &= \delta_{i,j} \end{aligned} \tag{3.39}$$

where the index refers to certain vibrational mode of a multidimensional harmonic oscillator. The resulting energy spectrum was equidistant and only bounded from below. In the second quantization of bosons, we say that the creation operator $b_i^\dagger$ creates a particle in a certain vibrational mode. We can construct any number of excitations, or particles, in a given vibration. The quantization of bosons follows naturally when one applies the **correspondence principle** to the wave function itself. Since the Lagrangian and the Hamiltonian of a one-particle system is quadratic in the wave function, it is natural that the quantization of a field leads to a harmonic oscillator. The difference between fermions and bosons is that the creation and annihilation operators obey an anticommutator relation in the fermionic case and a commutator relation in bosonic case.

3.5 Slater-Condon rules

The next step towards a description solely by creation and annihilation operators is to express one- and two-particle operators in terms of creation and annihilation operators.

For this purpose, we need to evaluate first the matrix elements $O_{\vec{\sigma},\vec{\sigma'}}$ of operators between Slater determinants $|\vec{\sigma}\rangle$.

$$\hat{O} = \sum_{\vec{\sigma},\vec{\sigma'}} |\vec{\sigma}\rangle O_{\vec{\sigma},\vec{\sigma'}} \langle\vec{\sigma'}| \tag{3.40}$$

[8] If an operator is an identity times a number, we call it a number.

In a next step, the matrix elements between Slater determinants can be expressed in terms of creation and annihilation operators. When we exploit that a set of all Slater determinants, which are formed from a complete orthonormal one-particle basisset, is a complete basis of Fock space, we can then represent a general one-particle or two-particle operator in terms of creation and annihilation operators.

While determining the matrix elements looks like a daunting task, it can be achieved in an elegant way as shown by Slater and Condon, when using an orthonormal set of one-particle orbitals. The resulting rules are the so-called **Slater-Condon rules**[22, 50]. A derivation of the Slater-Condon rules is given in appendix H on p. 543. I recommend, that the reader works through the derivation of at least one of the Slater-Condon rules.

The matrix elements can reasonably be worked out only using an orthonormal one-particle basisset. This is probably the sole reason, one almost exclusively works with orthonormal basissets in many-particle physics. Using orthonormal one-particle orbitals, is, however, by no means a requirement. Once the matrix elements are obtained in one basis, the results can be transformed into any other, even non-orthonormal basisset.

The Slater-Condon rules have been generalized to non-orthonormal basissets by Löwdin[26].

I only summarize the Slater-Condon rules here. The derivation is provided in appendix H on p. 543.

SLATER-CONDON RULES

The Slater-Condon rules provide the matrix elements of one-particle operators $\hat{A}$ and two-particle operators $\hat{W}$, between Slater determinants $|\Phi\rangle$ and $\Psi\rangle$. The Slater determinants must be expressed in an **orthonormal one-particle basisset** $\{|\varphi_j\rangle\}$ and they must be in **maximum coincidence**, which requires that any one-particle orbitals, which are present in both Slater determinants, must be in the same position in both Slater determinants (see also appendix H.1 on p. 543).

- Identical Slater determinants, i.e. $|\Psi\rangle = |\Phi\rangle$

$$\langle\Psi|\hat{A}|\Phi\rangle \overset{\text{Eq. } H.5}{=} \sum_{n=1}^{N}\langle\varphi_n|\hat{A}|\varphi_n\rangle$$

$$\langle\Psi|\hat{W}|\Phi\rangle \overset{\text{Eq. } H.7}{=} \frac{1}{2}\sum_{n,m}^{N}\Big(\underbrace{\langle\varphi_n\varphi_m|\hat{W}|\varphi_n\varphi_m\rangle}_{\rightsquigarrow\text{Hartree}} - \underbrace{\langle\varphi_n\varphi_m|\hat{W}|\varphi_m\varphi_n\rangle}_{\rightsquigarrow\text{exchange}}\Big) \tag{3.41}$$

  Notice, that the two terms in the sum for the two-particle term cancel each other for $n = m$.

  Eq. 3.41 are the so-called Slater rules[22]. They provide the expectation value with a Slater determinant. A general many-particle wave function is a superposition of many Slater determinants. To evaluate the expectation value with such a general, correlated, wave function also the off-diagonal matrix elements are required, which are obtained via the Condon rules[50] provided below.

- Slater determinants that differ by a single one-particle orbital φ_a and φ_b

$$\langle\Psi|\hat{A}|\Phi\rangle \overset{\text{Eq. } H.15}{=} \langle\varphi_a|\hat{A}|\varphi_b\rangle \tag{3.42}$$

$$\langle\Psi|\hat{W}|\Phi\rangle \overset{\text{Eq. } H.22}{=} \sum_{n=1;n\neq a,b}^{N-1}\Big(\langle\varphi_a\varphi_n|\hat{W}|\varphi_b\varphi_n\rangle - \langle\varphi_a\varphi_n|\hat{W}|\varphi_n\varphi_b\rangle\Big) \tag{3.43}$$

- Slater determinants that differ by two one-particle orbitals φ_a, φ_b and φ_c, φ_d

$$\langle\Psi|\hat{A}|\Phi\rangle \overset{\text{Eq. } H.23}{=} 0 \tag{3.44}$$

$$\langle\Psi|\hat{W}|\Phi\rangle \overset{\text{Eq. } H.25}{=} \langle\varphi_a\varphi_b|\hat{W}|\varphi_c\varphi_d\rangle - \langle\varphi_a\varphi_b|\hat{W}|\varphi_d\varphi_c\rangle \tag{3.45}$$

- Slater determinants that differ by more than two one-particle orbitals

$$\langle\Psi|\hat{A}|\Phi\rangle = 0 \tag{3.46}$$

$$\langle\Psi|\hat{W}|\Phi\rangle = 0 \tag{3.47}$$

The matrix elements of two-particle operators, such as an interaction $\hat{W}(\vec{x},\vec{x'})$, are defined as

$$\langle\varphi_a\varphi_b|\hat{W}|\varphi_c\varphi_d\rangle \overset{\text{def}}{=} \int d^4x \int d^4x'\ \varphi_a^*(\vec{x})\varphi_b^*(\vec{x'})W(\vec{x},\vec{x'})\varphi_c(\vec{x})\varphi_d(\vec{x'}) \tag{3.48}$$

3.6 Operators expressed by creation and annihilation operators

We have seen that all states of the Fock space can be expressed by creation operators and the vacuum state. Hence, the creation and annihilation operators also provide a means to transform the

states of the Fock space into each other, which is what a general operator does. This shows that each operator acting on the Fock space can be expressed by creation and annihilation operators.

In the previous section, we derived the Slater-Condon rules, which provide the matrix elements of one- and two-particle operators in terms of the Slater determinants that form the many-particle basisset. In appendix I on p. 551, we use the Slater-Condon rules to derive the explicit expressions for the one- and two-particle operators in this representation. Here, we just provide the results:

OPERATORS IN SECOND QUANTIZATION

A one-particle operator $\hat{A}$ has the form

$$\hat{A} = \sum_{i,j} A_{i,j} \hat{a}_i^\dagger \hat{a}_j \tag{3.49}$$

and a two-particle operator $\hat{W}$ has the form

$$\hat{W} = \frac{1}{2} \sum_{i,j,k,l} W_{i,j,k,l} \hat{a}_i^\dagger \hat{a}_j^\dagger \hat{a}_l \hat{a}_k \tag{3.50}$$

Note the reversed order of the annihilators relative to the indices.
The matrix elements are

$$\begin{aligned} A_{a,b} &\overset{\text{def}}{=} \langle \varphi_a | \hat{A} | \varphi_b \rangle \quad \overset{\text{def}}{=} \quad \int d^4x \; \varphi_a^*(\vec{x}) \hat{A} \varphi_b(\vec{x}) \\ W_{a,b,c,d} &\overset{\text{def}}{=} \langle \varphi_a \varphi_b | \hat{W} | \varphi_c \varphi_d \rangle \overset{\text{Eq. 3.48}}{=} \int d^4x \int d^4x' \; \varphi_a^*(\vec{x}) \varphi_b^*(\vec{x'}) W(\vec{x}, \vec{x'}) \varphi_c(\vec{x}) \varphi_d(\vec{x'}) \end{aligned} \tag{3.51}$$

Conventions: Often, the interaction matrix elements are defined differently from Eq. 3.51.They differ in the order of the indices in the tensor $\boldsymbol{W}$. Our choice is consistent with the "physicist notation" $< ab|cd >= W_{a,b,c,d}$ as used in the book of Szabo and Ostlund [51] (See their section 2.3.2 "Notations for One- and Two-Electron Integrals"). It is also consistent with the notation used in the lecture notes *Theoretische Festkörperphysik* (p.63, Eq. 15.47) by Franz Wegener. Szabo and Ostlund also refer to the "chemist notation" $[ij|kl]$ defined as $< ik|jl >= [ij|kl]$, which lists first both x coordinates and then both x' coordinates. This chemists notation is also used by Mahan's Book[52] (see Eq. 1.157).

$$\text{Physicist notation} \qquad < ab|cd > \overset{\text{def}}{=} W_{a,b,c,d} \tag{3.52}$$

$$\text{Chemist notation} \qquad [ac|bd] \overset{\text{def}}{=} W_{a,b,c,d} \tag{3.53}$$

3.6.1 One-particle-reduced density matrix in second quantization

The one-particle-reduced density matrix follows from Eq. 3.49. It has been defined so that a the expectation value of a general, one-particle operator $\hat{A}$ is obtained as

$$A = \mathrm{Tr}[\hat{\rho}^{(1)} \hat{A}] = \sum_{i,j} \rho_{i,j}^{(1)} A_{j,i} \tag{3.54}$$

From Eq. 3.49 the expectation value of a one-particle operator with general ensemble of many-particle states $|\Phi_q\rangle$ in Fock space and their probabilities P_q is

$$\langle A \rangle = \sum_q P_q \langle \Phi_q | \sum_{i,j} A_{i,j} \hat{a}_i^\dagger \hat{a}_j | \Phi_q \rangle = \sum_{i,j} A_{i,j} \underbrace{\sum_q P_q \langle \Phi_q | \hat{a}_i^\dagger \hat{a}_j | \Phi_q \rangle}_{\rho_{j,i}^{(1)}} \tag{3.55}$$

This provides us with the one-particle-reduced density matrix as

ONE-PARTICLE-REDUCED DENSITY MATRIX IN SECOND QUANTIZATION

$$\rho^{(1)}_{m,n} = \sum_q P_q \langle \Phi_q | \hat{a}^\dagger_n \hat{a}_m | \Phi_q \rangle \tag{3.56}$$

$$\hat{\rho}^{(1)} = \sum_{m,n} |\varphi_m\rangle \sum_q P_q \langle \Phi_q | \hat{a}^\dagger_n \hat{a}_m | \Phi_q \rangle \langle \varphi_n | \tag{3.57}$$

Note, that the indices m, n on the right side of the equation are in the opposite order than on the left side.

3.7 Real-space-and-spin representation of field operators

We obtained the basic elements of the theory, namely states, Eq. 3.21, and operators, Eq. 3.49 and Eq. 3.50. The formulation rests on the choice of a particular set of one-particle orbitals $|\varphi_i\rangle$. Here, we change the representation from this set of one-particle orbitals to the real-space-and-spin representation. The real-space-and-spin representation is then the reference, from which formulation can be transformed into any other basisset of one-particle orbitals.

Let me start with the representation of the orthonormal one-particle basis functions $|\varphi_j\rangle$ in terms of vacuum state and creation operator

$$\hat{a}^\dagger_j |\mathcal{O}\rangle \overset{\text{Eq. 3.22}}{=} |\varphi_j\rangle \tag{3.58}$$

Any one-particle state $|f\rangle$ can be expanded into the chosen one-particle basis $|\varphi_j\rangle$.

$$|f\rangle = \sum_j |\varphi_j\rangle\langle\varphi_j|f\rangle \overset{\text{Eq. 3.58}}{=} \sum_j \underbrace{\hat{a}^\dagger_j|\mathcal{O}\rangle}_{|\varphi_j\rangle}\langle\varphi_j|f\rangle = \Big(\sum_j \hat{a}^\dagger_j \langle\varphi_j|f\rangle\Big)|\mathcal{O}\rangle \tag{3.59}$$

Because the state $|f\rangle$ is arbitrary, we can insert a basisstate of the real-space-and-spin representation $|\vec{x}\rangle$, which yields

$$|\vec{x}\rangle = \underbrace{\Big(\sum_j \hat{a}^\dagger_j \langle\varphi_j|\vec{x}\rangle\Big)}_{=:\hat{\psi}^\dagger(\vec{x})} |\mathcal{O}\rangle \tag{3.60}$$

This defines the field operators

FIELD OPERATORS

$$\begin{aligned} \hat{\psi}^\dagger(\vec{x}) &\overset{\text{def}}{=} \sum_j \hat{a}^\dagger_j \langle\varphi_j|\vec{x}\rangle = \sum_j \varphi^*_j(\vec{x})\hat{a}^\dagger_j \\ \hat{\psi}(\vec{x}) &= \sum_j \langle\vec{x}|\varphi_j\rangle \hat{a}_j = \sum_i \varphi_j(\vec{x})\hat{a}_j \end{aligned} \tag{3.61}$$

An arbitrary one-particle state can then be written in the form

$$|f\rangle \overset{\text{Eq. 3.59}}{=} \Big(\sum_j \hat{a}_j^\dagger \langle\varphi_j|f\rangle\Big)|\mathcal{O}\rangle = \Big(\int d^4x \underbrace{\sum_j \hat{a}_j^\dagger \langle\varphi_j|\vec{x}\rangle}_{\hat{\psi}^\dagger(\vec{x})} \underbrace{\langle\vec{x}|f\rangle}_{f(\vec{x})}\Big)|\mathcal{O}\rangle$$
$$\overset{\text{Eq. 3.61}}{=} \Big(\int d^4x\, \hat{\psi}^\dagger(\vec{x}) f(\vec{x})\Big)|\mathcal{O}\rangle \tag{3.62}$$

Insertion of the basis function $|\varphi_j\rangle$ in place of the general state $|f\rangle$ yields the back transform.

$$\hat{a}_j^\dagger|\mathcal{O}\rangle \overset{\text{Eq. 3.58}}{=} |\varphi_j\rangle \overset{\text{Eq. 3.62}}{=} \Big(\int d^4x\, \hat{\psi}^\dagger(\vec{x})\varphi_j(\vec{x})\Big)|\mathcal{O}\rangle \tag{3.63}$$

ORBITAL CREATION AND ANNIHILATION OPERATORS FROM FIELD OPERATORS

$$\hat{a}_i^\dagger = \int d^4x\, \hat{\psi}^\dagger(\vec{x})\, \langle\vec{x}|\varphi_i\rangle = \int d^4x\, \hat{\psi}^\dagger(\vec{x})\varphi_i(\vec{x})$$
$$\hat{a}_i = \int d^4x\, \langle\varphi_i|\vec{x}\rangle\, \hat{\psi}(\vec{x}) = \int d^4x\, \varphi_i^*(\vec{x})\hat{\psi}(\vec{x}) \tag{3.64}$$

The symbol "psi" for the field operator $\hat{\psi}^\dagger(\vec{x})$ is not a space holder for a specific field. We would not write something like $\varphi^\dagger(\vec{x})$. This is different from the notation $\hat{a}_i^\dagger$ or $\hat{c}_j^\dagger$, for which the letters may indicate the choice of one or another basisset. For the field operators the basisset is already chosen: It is $\{|\vec{x}\rangle\}$.

3.7.1 Anticommutator relations in real space

The anti-commutator relations of the field operators in real space are obtained by insertion.

$$\begin{aligned}
\big[\hat{\psi}^\dagger(\vec{x}), \hat{\psi}(\vec{x'})\big]_+ &\overset{\text{Eq. 3.61}}{=} \big(\sum_j \hat{a}_j^\dagger \langle\varphi_j|\vec{x}\rangle\big)\big(\sum_k \langle\vec{x'}|\varphi_k\rangle \hat{a}_k\big) + \big(\sum_k \langle\vec{x'}|\varphi_k\rangle \hat{a}_k\big)\big(\sum_j \hat{a}_j^\dagger \langle\varphi_j|\vec{x}\rangle\big) \\
&= \sum_{j,k} \langle\vec{x'}|\varphi_k\rangle \underbrace{\big(\hat{a}_j^\dagger \hat{a}_k + \hat{a}_k \hat{a}_j^\dagger\big)}_{=[\hat{a}_j^\dagger, \hat{a}_k]_+ = \delta_{j,k}} \langle\varphi_j|\vec{x}\rangle\big) \\
&= \langle\vec{x'}| \underbrace{\Big(\sum_j \varphi_j\rangle\langle\varphi_j|\Big)}_{=\hat{1}} |\vec{x}\rangle \\
&= \underbrace{\delta(\vec{x} - \vec{x'})}_{\delta(\vec{r}-\vec{r'})\delta_{\sigma,\sigma'}}
\end{aligned} \tag{3.65}$$

For a continuous variable such as the position we need to remember that we have to use the delta-function instead of the Kronecker delta.

3.7.2 One-particle operators in real space

Let us now transform a general one-particle operator $\hat{A}$ into the real-space representation

$$\begin{aligned}
\hat{A} &\overset{\text{Eq. 3.49}}{=} \sum_{i,j} \langle \varphi_i | \hat{A} | \varphi_j \rangle \hat{a}_i^\dagger \hat{a}_j \\
&= \sum_{i,j} \langle \varphi_i | \underbrace{\int d^4x \, |\vec{x}\rangle\langle\vec{x}|}_{=1} \hat{A} \underbrace{\int d^4x' \, |\vec{x'}\rangle\langle\vec{x'}|}_{=1} |\varphi_j\rangle \hat{a}_i^\dagger \hat{a}_j \\
&= \int d^4x \int d^4x' \sum_{i,j} \underbrace{\langle \varphi_i | \vec{x} \rangle}_{\varphi_i^*(\vec{x})} \underbrace{\langle \vec{x} | \hat{A} | \vec{x'} \rangle}_{A(\vec{x},\vec{x'})} \underbrace{\langle \vec{x'} | \varphi_j \rangle}_{\varphi_j(\vec{x'})} \hat{a}_i^\dagger \hat{a}_j \\
&= \int d^4x \int d^4x' \, A(\vec{x},\vec{x'}) \underbrace{\sum_i \varphi_i^*(\vec{x}) \hat{a}_i^\dagger}_{\hat{\psi}^\dagger(\vec{x})} \underbrace{\sum_j \varphi_j(\vec{x'}) \hat{a}_j}_{\hat{\psi}(\vec{x'})} \\
&\overset{\text{Eq. 3.61}}{=} \int d^4x \int d^4x' \, A(\vec{x},\vec{x'}) \hat{\psi}^\dagger(\vec{x}) \hat{\psi}(\vec{x'})
\end{aligned} \tag{3.66}$$

Note that we deal here with two different types of operators: The creators and annihilators act on the Fock space. The operator $\hat{A}$ acts on a one-particle state if it is bracketed between two one-particle states.

Example: one-particle Hamiltonian

The one-particle part of the Hamiltonian has the form

$$\hat{h} = \int d^4x \int d^4x' \, |\vec{x}\rangle \underbrace{\delta(\vec{x}-\vec{x'}) \left(\frac{-\hbar^2}{2m_e} \vec{\nabla}'^2 + v_{ext}(\vec{x'}) \right)}_{h(\vec{x},\vec{x'}) = \langle \vec{x} | \hat{h} | \vec{x'} \rangle} \langle \vec{x'} | \tag{3.67}$$

with

$$h(\vec{x},\vec{x'}) = \delta(\vec{x}-\vec{x'}) \left(\frac{-\hbar^2}{2m_e} \vec{\nabla}'^2 + v_{ext}(\vec{x'}) \right) . \tag{3.68}$$

The corresponding one-particle-at-a-time Hamiltonian has the form[9]

$$\begin{aligned}
\hat{h} &\overset{\text{Eq. 3.66}}{=} \int d^4x \int d^4x' \, \delta(\vec{x}-\vec{x'}) \left(\frac{-\hbar^2}{2m_e} \vec{\nabla}'^2 + v_{ext}(\vec{x'}) \right) \hat{\psi}^\dagger(\vec{x}) \hat{\psi}(\vec{x'}) \\
&= \int d^4x \, \hat{\psi}^\dagger(\vec{x}) \left(\frac{-\hbar^2}{2m_e} \vec{\nabla}^2 + v_{ext}(\vec{x}) \right) \hat{\psi}(\vec{x})
\end{aligned} \tag{3.69}$$

The expression just looks like a normal expectation value of the one-particle Hamiltonian. However, since the wave functions are replaced by the creation and annihilation operators, the expression is an operator in Fock space.

[9] It may be puzzling to have a differential operator, the Laplacian, act on an operator. This object is to be interpreted as for normal functions as the differential quotient of the operator in the limit of small displacements.

3.7.3 Interaction operator in real space

Analogously, we can determine the interaction operator in real space as

$$\begin{aligned}
\hat{W} &\overset{\text{Eq. 3.50}}{=} \frac{1}{2}\sum_{i,j,k,l} W_{i,j,k,l}\hat{a}_i^\dagger \hat{a}_j^\dagger \hat{a}_l \hat{a}_k \\
&\overset{\text{Eq. 3.64}}{=} \frac{1}{2}\sum_{i,j,k,l} W_{i,j,k,l} \underbrace{\int d^4x_1\ \varphi_i(\vec{x_1})\hat{\psi}^\dagger(\vec{x}_1)}_{\hat{a}_i^\dagger} \underbrace{\int d^4x_2\ \varphi_j(\vec{x_2})\hat{\psi}^\dagger(\vec{x}_2)}_{\hat{a}_j^\dagger} \\
&\quad \underbrace{\int d^4x_4\ \varphi_l^*(\vec{x_4})\hat{\psi}(\vec{x}_4)}_{\hat{a}_l} \underbrace{\int d^4x_3\ \varphi_k^*(\vec{x_3})\hat{\psi}(\vec{x}_3)}_{\hat{a}_k} \\
&= \frac{1}{2}\int d^4x_1 \int d^4x_2 \int d^4x_3 \int d^4x_4 \underbrace{\sum_{i,j,k,l} W_{i,j,k,l}\varphi_i(\vec{x_1})\varphi_j(\vec{x_2})\varphi_k^*(\vec{x_3})\varphi_l^*(\vec{x_4})}_{W(\vec{x}_1,\vec{x}_2,\vec{x}_3,\vec{x}_4)} \\
&\quad \cdot\hat{\psi}^\dagger(\vec{x}_1)\hat{\psi}^\dagger(\vec{x}_2)\hat{\psi}(\vec{x}_4)\hat{\psi}(\vec{x}_3)
\end{aligned} \tag{3.70}$$

We use the expression for the matrix elements in the orbital basis

$$W_{i,j,k,l} \overset{\text{Eq. 3.51}}{=} \int d^4x \int d^4x'\ \varphi_i^*(\vec{x})\varphi_j^*(\vec{x'})v_{int}(\vec{x},\vec{x'})\varphi_k(\vec{x})\varphi_l(\vec{x'}) \tag{3.71}$$

to work out the real-space matrix elements of the interaction in Eq. 3.70. For our purposes the interaction potential is the Coulomb potential

$$v_{int}(\vec{x},\vec{x'}) = v_{int}(\vec{r},\sigma,\vec{r'},\sigma') = \frac{e^2}{4\pi\epsilon_0|\vec{r}-\vec{r'}|} \tag{3.72}$$

$$\begin{aligned}
W(\vec{x}_1,\vec{x}_2,\vec{x}_3,\vec{x}_4) &\overset{\text{def}}{=} \sum_{i,j,k,l} W_{i,j,k,l}\varphi_i(\vec{x_1})\varphi_j(\vec{x_2})\varphi_k^*(\vec{x_3})\varphi_l^*(\vec{x_4}) \\
&\overset{\text{Eq. 3.71}}{=} \sum_{i,j,k,l} \underbrace{\int d^4x \int d^4x' \left[\varphi_i^*(\vec{x})\varphi_j^*(\vec{x'})v_{int}(\vec{x},\vec{x'})\varphi_k(\vec{x})\varphi_l(\vec{x'})\right]}_{W_{i,j,k,l}} \left[\varphi_i(\vec{x_1})\varphi_j(\vec{x_2})\varphi_k^*(\vec{x_3})\varphi_l^*(\vec{x_4})\right] \\
&= \int d^4x \int d^4x' \underbrace{\sum_i \varphi_i^*(\vec{x})\varphi_i(\vec{x_1})}_{\delta(\vec{x}-\vec{x}_1)} \underbrace{\sum_j \varphi_j^*(\vec{x'})\varphi_j(\vec{x_2})}_{\delta(\vec{x'}-\vec{x}_2)} \\
&\qquad \times v_{int}(\vec{x},\vec{x'}) \underbrace{\sum_k \varphi_k(\vec{x})\varphi_k^*(\vec{x_3})}_{\delta(\vec{x}-\vec{x}_3)} \underbrace{\sum_l \varphi_l(\vec{x'})\varphi_l^*(\vec{x_4})}_{\delta(\vec{x'}-\vec{x}_4)} \\
&= v_{int}(\vec{x}_1,\vec{x}_2)\delta(\vec{x}_1-\vec{x}_3)\delta(\vec{x}_2-\vec{x}_4)
\end{aligned} \tag{3.73}$$

We insert this result into the above expression Eq. 3.70

$$\begin{aligned}
\hat{W} &\overset{Eqs.\ 3.70,3.73}{=} \frac{1}{2}\int d^4x_1 \int d^4x_2 \int d^4x_3 \int d^4x_4\ v_{int}(\vec{x}_1,\vec{x}_2)\delta(\vec{x}_1-\vec{x}_3)\delta(\vec{x}_2-\vec{x}_4) \\
&\quad \cdot\hat{\psi}^\dagger(\vec{x}_1)\hat{\psi}^\dagger(\vec{x}_2)\hat{\psi}(\vec{x}_4)\hat{\psi}(\vec{x}_3) \\
&= \frac{1}{2}\int d^4x_1 \int d^4x_2\ v_{int}(\vec{x}_1,\vec{x}_2)\hat{\psi}^\dagger(\vec{x}_1)\hat{\psi}^\dagger(\vec{x}_2)\hat{\psi}(\vec{x}_2)\hat{\psi}(\vec{x}_1) \\
&= \frac{1}{2}\int d^4x \int d^4x'\ \hat{\psi}^\dagger(\vec{x})\hat{\psi}^\dagger(\vec{x'})v_{int}(\vec{x},\vec{x'})\hat{\psi}(\vec{x'})\hat{\psi}(\vec{x})
\end{aligned} \tag{3.74}$$

3.7.4 Many-electron Hamiltonian in real space

The Hamiltonian has the form

MANY-PARTICLE HAMILTONIAN

$$\hat{H} = \int d^4x\, \hat{\psi}^\dagger(\vec{x}) \left(\frac{-\hbar^2}{2m_e} \vec{\nabla}^2 + v_{ext}(\vec{x}) \right) \hat{\psi}(\vec{x}) + \frac{1}{2} \int d^4x \int d^4x'\, \hat{\psi}^\dagger(\vec{x}) \hat{\psi}^\dagger(\vec{x'}) \underbrace{\frac{e^2}{4\pi\epsilon_0 |\vec{r} - \vec{r'}|}}_{v_{int}(\vec{x},\vec{x'})} \hat{\psi}(\vec{x'}) \hat{\psi}(\vec{x}) \tag{3.75}$$

Notice the order of the annihilation operators on the right-hand side of the interaction term!

3.8 Creation and annihilation operators in a non-orthonormal representation

The extension of creation and annihilation operators to non-orthonormal orbitals is possible. It is discussed in appendix B on p. 401.

3.9 From Hilbert space to Fock space and back

Often we encounter a problem expressed in one-particle wave functions and we want to express it in second quantization or vice versa. In this section, I am collecting examples and advice on how this can be done.

3.9.1 From Hilbert space to Fock space and back

I find it very useful to start with the representation of a one-particle state in the language of second quantization. I provide equations for orthonormal orbitals $|\varphi_n\rangle$, non-orthonormal states $|\chi_\alpha\rangle$ and the real-space-and-spin representation.

In a orthonormal basisset, each orbital $|\chi_\alpha\rangle$ is accompanied by a projector function $\langle\pi_\alpha|$. Projector functions and orbitals satisfy a bi-orthogonality condition $\langle\pi_\alpha|\chi_\beta\rangle = \delta_{\alpha,\beta}$ so that $|\psi\rangle = \sum_\alpha |\chi_\alpha\rangle\pi_\alpha|\psi\rangle$ if $|\psi\rangle$ lies in the Hilbert space spanned by the orbitals.

ONE-PARTICLE ORBITALS IN SECOND QUANTIZATION

$$|\varphi_n\rangle = \hat{a}_n^\dagger|\mathcal{O}\rangle \tag{3.76}$$

$$|\pi_\alpha\rangle \overset{\text{Eq. } B.5}{=} \hat{c}_\alpha^\dagger|\mathcal{O}\rangle \tag{3.77}$$

$$|\chi_\alpha\rangle = \sum_\beta \hat{c}_\beta^\dagger|\mathcal{O}\rangle\langle\chi_\beta|\chi_\alpha\rangle \tag{3.78}$$

$$|\vec{x}\rangle = \hat{\psi}^\dagger(\vec{x})|\mathcal{O}\rangle \tag{3.79}$$

Similarly, two-particle Slater determinants can be written in the form

$$|\varphi_\alpha\varphi_\beta\rangle = \hat{a}_\alpha^\dagger\hat{a}_\beta^\dagger|\mathcal{O}\rangle \tag{3.80}$$

respectively

$$|\vec{x},\vec{x'}\rangle = \hat{\psi}^\dagger(\vec{x})\hat{\psi}^\dagger(\vec{x'})|\mathcal{O}\rangle \tag{3.81}$$

A one-particle operator acting on the one-particle Hilbert space can be rewritten as follows:

$$\begin{aligned}\hat{A} &= \sum_{\alpha,\beta}|\pi_\alpha\rangle\underbrace{\langle\chi_\alpha|\hat{A}|\chi_\beta\rangle}_{A_{\alpha,\beta}}\langle\pi_\beta| = \sum_{\alpha,\beta}|\pi_\alpha\rangle A_{\alpha,\beta}\langle\pi_\beta| = \sum_{\alpha,\beta}\hat{c}_\alpha^\dagger|\mathcal{O}\rangle A_{\alpha,\beta}\langle\mathcal{O}|\hat{c}_\beta \\ &= \sum_{\alpha,\beta}A_{\alpha,\beta}\hat{c}_\alpha^\dagger\underbrace{|\mathcal{O}\rangle\langle\mathcal{O}|}_{\hat{P}_{|\mathcal{O}\rangle}}\hat{c}_\beta\end{aligned} \tag{3.82}$$

In the middle we have the projection operator $\hat{P}_{|\mathcal{O}\rangle}$ onto the zero-particle state, which limits the action of the operator to the one-particle channel. In order to generalize this result to the Fock space, we replace the projection operator by the unit operator in Fock space

$$\hat{A} = \sum_{\alpha,\beta}A_{\alpha,\beta}\hat{c}_\alpha^\dagger\underbrace{\sum_{\vec{\sigma}}|\vec{\sigma}\rangle\langle\vec{\sigma}|}_{\hat{1}}\hat{c}_\beta = \sum_{\alpha,\beta}A_{\alpha,\beta}\hat{c}_\alpha^\dagger\hat{c}_\beta \tag{3.83}$$

Despite the fact that we use the same symbols, the operators $\hat{A}$ Eq. 3.82 and Eq. 3.83 are in principle two different operators, because they act on different spaces.

Similarly, we can go backwards from Eq. 3.83 to Eq. 3.82, as long as the operator $\hat{A}$ is a one-particle operator, that is, it can be built up from products $\hat{a}_m^\dagger\hat{a}_n$.

3.10 Summary

In this chapter, we introduced creation and annihilation operators, and showed how many-particle wave functions and operators can be expressed by them. In addition to the creation and annihilation operators, only a single state, the vacuum state $|\mathcal{O}\rangle$ is required.

Field operators $\hat{\psi}^\dagger(\vec{x})$ and $\hat{\psi}(\vec{x})$ have been introduced by selecting the space-and-spin basiset. In this representation the Hamilton operator looks like the energy expectation value in one-particle quantum mechanics, with the difference that the wave function is replaced by the field operator. Special care is required, because of the anticommutator relation of the field operators, their order is not arbitrary.

The formulation given in this section can be extended to incomplete and non-orthonormal basis sets. This is shown in the appendix B on p. 401.

3.11 Home study and practice

3.11.1 Hydrogen molecule with interacting electrons

Introduction

Here we extend the earlier exercise on the hydrogen molecule in section 1.5.1 on p. 26 to interacting electrons. This example will give us a first glance on a number of electron-correlation effects. It may be helpful to inspect figure 3.1 on p. 125 which schematically shows the many-particle states of a hydrogen atom with non-interacting electrons.

Problem

1 Translate the non-interacting Hamiltonian for the hydrogen molecule from section 1.5.1 on p. 26 into second quantization using atomic hydrogen 1s orbitals.

2 Use a one-particle basisset of atomic hydrogen 1s orbitals. Ignore the non-orthonormality of the one-particle wave functions. List the two-particle Slater determinants of the hydrogen molecule and express them in terms of creation and annihilation operators and the vacuum state.

3 Consider the Hamiltonian

$$\hat{H} = \sum_{\alpha,\beta} h_{\alpha,\beta} \hat{c}_\alpha^\dagger \hat{c}_\beta + \frac{1}{2} \sum_{\alpha,\beta,\gamma,\delta} W_{\alpha,\beta,\gamma\delta} \hat{c}_\alpha^\dagger \hat{c}_\beta^\dagger \hat{c}_\delta \hat{c}_\gamma \tag{3.84}$$

with

$$h_{\alpha,\beta} = \bar{\epsilon}\delta_{\alpha,\beta} - t\delta_{\sigma_\alpha,\sigma_\beta}\left(1 - \delta_{R_\alpha,R_\beta}\right) \tag{3.85}$$

and

$$W_{\alpha,\beta,\gamma,\delta} = \delta_{\alpha,\gamma}\delta_{\beta,\delta}\Big[U\delta_{R_\alpha,R_\beta} + V(1 - \delta_{R_\alpha,R_\beta})\Big] \tag{3.86}$$

where the indices $\alpha, \beta, \ldots$ are combined indices $\alpha = (R, \sigma)$ holding a site index $R \in \{1, 2\}$ and a spin index $\sigma \in \{\uparrow, \downarrow\}$.

The on-site Coulomb parameter U describes the Coulomb repulsion of two electrons on the same site and the parameter V describes the Coulomb repulsion of two electrons on neighboring sites. We use the assumption $U > V$ which will be useful to avoid considering distinct cases.

Determine the Hamiltonian for the (4×4) subblock of two-particle states with $S_z = 0$. I recommend to first write out the Hamiltonian with the specific indices of the hydrogen molecule. Try to combine creation and annihilation operators to occupation-number operators $\hat{n}_j$. Then act with the Hamiltonian onto the four two-particle basis states and extract the matrix elements.

4 Exploit the reflection symmetry $\hat{P}$ of the hydrogen molecule to block-diagonalize the Hamiltonian in the two-particle channel. That is, construct the eigenstates of the parity operator under reflection symmetry of the molecule. These parity eigenstates are superpositions of the two-particle Slater determinants $|\Phi_i\rangle$ obtained previously. The Hamiltonian in terms of the symmetrized states[a] will "fall apart" into one 2×2 matrix and 1×1 blocks.

[a] With symmetrized states, I mean eigenstates of the symmetry operator. In the case of the parity operator these eigenstates may be symmetric or antisymmetric.

Discussion

1 Translate the non-interacting Hamiltonian for the hydrogen molecule from section 1.5.1 on p. 26 into second quantization using atomic hydrogen 1s orbitals.

The one-particle Hamilton operator in the one-particle Hilbert space given earlier has the form

$$\hat{h} = \underbrace{\sum_{\sigma\in\{\uparrow,\downarrow\}} \sum_{R=1}^{2} |\pi_{R,\sigma}\rangle\, \bar{\epsilon}\, \langle\pi_{R,\sigma}|}_{\text{atomic energies}} - \underbrace{\sum_{\sigma\in\{\uparrow,\downarrow\}} \Big(|\pi_{1,\sigma}\rangle\, t\, \langle\pi_{2,\sigma}| + |\pi_{2,\sigma}\rangle\, t\, \langle\pi_{1,\sigma}| \Big)}_{\text{hopping}} \tag{3.87}$$

For an operator in Fock space, the term one-particle means *"one particle at a time"*. The corresponding one-particle operator in Fock space is

$$\hat{h} = \underbrace{\sum_{\sigma\in\{\uparrow,\downarrow\}} \sum_{R=1}^{2} \bar{\epsilon} \hat{c}^{\dagger}_{R,\sigma} \hat{c}_{R,\sigma}}_{\text{atomic energies}} - \underbrace{\sum_{\sigma\in\{\uparrow,\downarrow\}} t\Big(\hat{c}^{\dagger}_{1,\sigma} \hat{c}_{2,\sigma} + \hat{c}^{\dagger}_{2,\sigma} \hat{c}_{1,\sigma} \Big)}_{\text{hopping}} \tag{3.88}$$

2 Use a one-particle basisset of atomic hydrogen 1s orbitals. Ignore the non-orthonormality of the one-particle wave functions. List the two-particle Slater determinants of the hydrogen molecule and express them in terms of creation and annihilation operators and the vacuum state.

Let me first set up the one-particle basisset and specify an order.

$$\begin{aligned} |\uparrow, 0\rangle &= |1000\rangle = \hat{c}^{\dagger}_{1,\uparrow} |\mathcal{O}\rangle \\ |\downarrow, 0\rangle &= |0100\rangle = \hat{c}^{\dagger}_{1,\downarrow} |\mathcal{O}\rangle \\ |0, \uparrow\rangle &= |0010\rangle = \hat{c}^{\dagger}_{2,\uparrow} |\mathcal{O}\rangle \\ |0, \downarrow\rangle &= |0001\rangle = \hat{c}^{\dagger}_{2,\downarrow} |\mathcal{O}\rangle \end{aligned} \tag{3.89}$$

The notation for the kets on the very left of the equation above follows a convention that has not been used or defined before. Here, the two entries refer to the two sites of the hydrogen molecule. The arrows indicate which orbitals on that molecule are occupied, namely none for 0, only the spin-up orbital for $\uparrow$, only the spin-down orbital for $\downarrow$, or both spin orbitals for $\uparrow\downarrow$. The notation is very intuitive for certain systems, but, in contrast to the occupation-number representation, it is not suitable in general.

The two-particle states are, with Eq. 3.21,

$$\begin{aligned} |\Phi_1\rangle &= |\uparrow\downarrow, 0\rangle = |1100\rangle = \hat{c}^{\dagger}_{1,\uparrow} \hat{c}^{\dagger}_{1,\downarrow} |\mathcal{O}\rangle \\ |\Phi_2\rangle &= |0, \uparrow\downarrow\rangle = |0011\rangle = \hat{c}^{\dagger}_{2,\uparrow} \hat{c}^{\dagger}_{2,\downarrow} |\mathcal{O}\rangle \\ |\Phi_3\rangle &= |\uparrow, \downarrow\rangle = |1001\rangle = \hat{c}^{\dagger}_{1,\uparrow} \hat{c}^{\dagger}_{2,\downarrow} |\mathcal{O}\rangle \\ |\Phi_4\rangle &= |\downarrow, \uparrow\rangle = |0110\rangle = \hat{c}^{\dagger}_{1,\downarrow} \hat{c}^{\dagger}_{2,\uparrow} |\mathcal{O}\rangle \\ |\Phi_5\rangle &= |\uparrow, \uparrow\rangle = |1010\rangle = \hat{c}^{\dagger}_{1,\uparrow} \hat{c}^{\dagger}_{2,\uparrow} |\mathcal{O}\rangle \\ |\Phi_6\rangle &= |\downarrow, \downarrow\rangle = |0101\rangle = \hat{c}^{\dagger}_{1,\downarrow} \hat{c}^{\dagger}_{2,\downarrow} |\mathcal{O}\rangle \end{aligned} \tag{3.90}$$

Please note the order of the operators, respectively the sign.

Let me check the number of two-particle states. With $n = 4$ one-particle orbitals, I can form $n(n-1)/2 = 6$ two-particle states.[10] Thus, the number of orbitals in our basisset is correct.

[10] There are four possibilities to select the first orbital. Because the second orbital must be different, there are only 3 possibilities to choose the second orbital. Now, however, each pair of orbitals has been selected twice, namely once for each order of the two orbitals. This is corrected by the division by two.

Discussion:

The first two two-particle states, $|\Phi_1\rangle$, $|\Phi_2\rangle$ have a doubly occupied hydrogen atom. They describe an ionic pair H^-H^+. The second pair of two-particle states $|\Phi_3\rangle$, $|\Phi_4\rangle$ describe antiferromagnetic electron distributions. The last two states $|\Phi_5\rangle$, $|\Phi_6\rangle$ are states with parallel spins along the z-axis.

The two antiferromagnetic states $|\Phi_3\rangle$, $|\Phi_4\rangle$ can be superimposed to give a **singlet state** or a **triplet state**. The singlet state has a total spin of zero, while the triplet state has a total spin S=1, while $S_z = 0\hbar$. This last state is called a *"triplet state"*, because there are three degenerate states with $S = 1$. The singlet state is called *"singlet"* because it has an energy different from the triplet state and it is non-degenerate.

3 Consider the Hamiltonian

$$\hat{H} = \sum_{\alpha,\beta} h_{\alpha,\beta}\hat{c}^\dagger_\alpha \hat{c}_\beta + \frac{1}{2}\sum_{\alpha,\beta,\gamma,\delta} W_{\alpha,\beta,\gamma\delta}\hat{c}^\dagger_\alpha \hat{c}^\dagger_\beta \hat{c}_\delta \hat{c}_\gamma \tag{3.91}$$

with

$$h_{\alpha,\beta} = \bar{\epsilon}\delta_{\alpha,\beta} - t\delta_{\sigma_\alpha,\sigma_\beta}\left(1 - \delta_{R_\alpha,R_\beta}\right) \tag{3.92}$$

and

$$W_{\alpha,\beta,\gamma,\delta} = \delta_{\alpha,\gamma}\delta_{\beta,\delta}\Big[U\delta_{R_\alpha,R_\beta} + V(1 - \delta_{R_\alpha,R_\beta})\Big] \tag{3.93}$$

The parameter U describes the Coulomb matrix elements of two electrons on the same site and the parameter V describes that of two electrons on different sites. We use the assumption $U > V$ which will be useful to avoid considering distinct cases.

Determine the Hamiltonian for the (4×4) subblock of two-particle states with $S_z = 0$. I recommend to first write out the Hamiltonian with the specific indices of the hydrogen molecule. Try to combine creation and annihilation operators to occupation-number operators $\hat{n}_j$. Then act with the Hamiltonian onto the four two-particle basis states and extract the matrix elements.

$$\begin{aligned}
\hat{h} &\overset{\text{Eq. 3.49}}{=} \sum_{\alpha,\beta} h_{\alpha,\beta}\hat{c}^\dagger_\alpha \hat{c}_\beta \\
&= \bar{\epsilon}\sum_{\sigma\in\{\uparrow,\downarrow\}}\sum_{R\in\{1,2\}} \underbrace{\hat{c}^\dagger_{R,\sigma}\hat{c}_{R,\sigma}}_{\hat{n}_{R,\sigma}} - t\sum_{\sigma\in\{\uparrow,\downarrow\}}\left(\hat{c}^\dagger_{1,\sigma}\hat{c}_{2,\sigma} + \hat{c}^\dagger_{2,\sigma}\hat{c}_{1,\sigma}\right) \\
\hat{W} &\overset{\text{Eq. 3.50}}{=} \frac{1}{2}\sum_{\alpha,\beta,\gamma,\delta} W_{\alpha,\beta,\gamma,\delta}\hat{c}^\dagger_\alpha \hat{c}^\dagger_\beta \hat{c}_\delta \hat{c}_\gamma \\
&= \frac{1}{2}U\sum_{R\in\{1,2\}}\sum_{\sigma,\sigma'\in\{\uparrow,\downarrow\}} \underbrace{\hat{c}^\dagger_{R,\sigma}\hat{c}^\dagger_{R,\sigma'}\hat{c}_{R,\sigma'}\hat{c}_{R,\sigma}}_{\text{see point A below}} + \frac{1}{2}V\sum_{R\neq R'\in\{1,2\}}\sum_{\sigma,\sigma'\in\{\uparrow,\downarrow\}} \hat{c}^\dagger_{R,\sigma}\hat{c}^\dagger_{R',\sigma'}\hat{c}_{R',\sigma'}\hat{c}_{R,\sigma} \qquad (3.94) \\
&= U\sum_{R\in\{1,2\}} \underbrace{\underbrace{\hat{c}^\dagger_{R,\uparrow}\hat{c}_{R,\uparrow}}_{\hat{n}_{R,\uparrow}}\underbrace{\hat{c}^\dagger_{R,\downarrow}\hat{c}_{R,\downarrow}}_{\hat{n}_{R,\downarrow}}}_{\text{double occupancy}} + V\sum_{\sigma,\sigma'\in\{\uparrow,\downarrow\}} \underbrace{\hat{c}^\dagger_{1,\sigma}\hat{c}^\dagger_{2,\sigma'}\hat{c}_{2,\sigma'}\hat{c}_{1,\sigma}}_{\hat{n}_{1,\sigma}\hat{n}_{2,\sigma'}} \qquad (3.95)
\end{aligned}$$

Thus, the Hamiltonian has the form

$$\begin{aligned}
\hat{H} \overset{\text{def}}{=} \hat{h} + \hat{W} = \bar{\epsilon}\sum_{R,\sigma}\hat{n}_{R,\sigma} + U\sum_R \hat{n}_{R,\uparrow}\hat{n}_{R,\downarrow} + V\Big(\sum_\sigma \hat{n}_{1,\sigma}\Big)\Big(\sum_{\sigma'}\hat{n}_{2,\sigma'}\Big) \\
-t\sum_\sigma\left(\hat{c}^\dagger_{1,\sigma}\hat{c}_{2,\sigma} + \hat{c}^\dagger_{2,\sigma}\hat{c}_{1,\sigma}\right)
\end{aligned} \tag{3.96}$$

Remarks:

- The occupation-number operators $\hat{n}_\alpha = \hat{c}_\alpha^\dagger \hat{c}_\alpha$ are convenient, because the Slater determinants in the same basisset are eigenstates of the occupation-number operator. Furthermore, the occupation-number operator commutates with the creation and annihilation operators in the same basisset.

- The factor $\frac{1}{2}$ in the interaction energy has been absorbed by making specific selections of spins, respectively sites.

- Point A in Eq. 3.95:

$$\begin{aligned}\hat{c}_{R,\sigma}^\dagger \hat{c}_{R,\sigma'}^\dagger \underbrace{\hat{c}_{R,\sigma'}\hat{c}_{R,\sigma}}_{-\hat{c}_{R,\sigma}\hat{c}_{R,\sigma'}} &= -\hat{c}_{R,\sigma}^\dagger \underbrace{\hat{c}_{R,\sigma'}^\dagger \hat{c}_{R,\sigma}}_{\delta_{\sigma,\sigma'}-\hat{c}_{R,\sigma}\hat{c}_{R,\sigma'}^\dagger} \hat{c}_{R,\sigma'} = \underbrace{-\delta_{\sigma,\sigma'}\hat{c}_{R,\sigma}^\dagger \hat{c}_{R,\sigma'}}_{\text{exchange}} + \underbrace{\hat{c}_{R,\sigma}^\dagger \hat{c}_{R,\sigma}\hat{c}_{R,\sigma'}^\dagger \hat{c}_{R,\sigma'}}_{\text{Hartree}} \\ &= \hat{n}_{R,\sigma}\hat{n}_{R,\sigma'} - \delta_{\sigma,\sigma'}\underbrace{\hat{n}_{R,\sigma}}_{=\hat{n}_{R,\sigma}^2} = \Big(1-\delta_{\sigma,\sigma'}\Big)\hat{n}_{R,\sigma}\hat{n}_{R,\sigma'}\end{aligned} \tag{3.97}$$

When the Hamiltonian acts onto the states with $S_z = 0$, namely $|\Phi_j\rangle$ with $j \in \{1,\dots,6\}$ from Eq. 3.90, one obtains

$$\begin{aligned}
\hat{H}\underbrace{\hat{c}_{1,\uparrow}^\dagger\hat{c}_{1,\downarrow}^\dagger|\mathcal{O}\rangle}_{|\Phi_1\rangle} &= \underbrace{\hat{c}_{1,\uparrow}^\dagger\hat{c}_{1,\downarrow}^\dagger|\mathcal{O}\rangle}_{|\Phi_1\rangle}\Big(2\bar{\epsilon}+U\Big) + \underbrace{\overbrace{\hat{c}_{2,\uparrow}^\dagger\hat{c}_{1,\downarrow}^\dagger}^{-\hat{c}_{1,\downarrow}^\dagger\hat{c}_{2,\uparrow}^\dagger}|\mathcal{O}\rangle}_{-|\Phi_4\rangle}\Big(-t\Big) + \underbrace{\hat{c}_{1,\uparrow}^\dagger\hat{c}_{2,\downarrow}^\dagger|\mathcal{O}\rangle}_{|\Phi_3\rangle}\Big(-t\Big) \\
\hat{H}\underbrace{\hat{c}_{2,\uparrow}^\dagger\hat{c}_{2,\downarrow}^\dagger|\mathcal{O}\rangle}_{|\Phi_2\rangle} &= \underbrace{\hat{c}_{2,\uparrow}^\dagger\hat{c}_{2,\downarrow}^\dagger|\mathcal{O}\rangle}_{|\Phi_2\rangle}\Big(2\bar{\epsilon}+U\Big) + \underbrace{\hat{c}_{1,\uparrow}^\dagger\hat{c}_{2,\downarrow}^\dagger|\mathcal{O}\rangle}_{|\Phi_3\rangle}\Big(-t\Big) + \underbrace{\overbrace{\hat{c}_{2,\uparrow}^\dagger\hat{c}_{1,\downarrow}^\dagger}^{-\hat{c}_{1,\downarrow}^\dagger\hat{c}_{2,\uparrow}^\dagger}|\mathcal{O}\rangle}_{-|\Phi_4\rangle}\Big(-t\Big) \\
\hat{H}\underbrace{\hat{c}_{1,\uparrow}^\dagger\hat{c}_{2,\downarrow}^\dagger|\mathcal{O}\rangle}_{|\Phi_3\rangle} &= \underbrace{\hat{c}_{1,\uparrow}^\dagger\hat{c}_{2,\downarrow}^\dagger|\mathcal{O}\rangle}_{|\Phi_3\rangle}\Big(2\bar{\epsilon}+V\Big) + \underbrace{\hat{c}_{2,\uparrow}^\dagger\hat{c}_{2,\downarrow}^\dagger|\mathcal{O}\rangle}_{|\Phi_2\rangle}\Big(-t\Big) + \underbrace{\hat{c}_{1,\uparrow}^\dagger\hat{c}_{1,\downarrow}^\dagger|\mathcal{O}\rangle}_{|\Phi_1\rangle}\Big(-t\Big) \\
\hat{H}\underbrace{\hat{c}_{1,\downarrow}^\dagger\hat{c}_{2,\uparrow}^\dagger|\mathcal{O}\rangle}_{|\Phi_4\rangle} &= \underbrace{\hat{c}_{1,\downarrow}^\dagger\hat{c}_{2,\uparrow}^\dagger|\mathcal{O}\rangle}_{|\Phi_4\rangle}\Big(2\bar{\epsilon}+V\Big) + \underbrace{\overbrace{\hat{c}_{2,\downarrow}^\dagger\hat{c}_{2,\uparrow}^\dagger}^{-\hat{c}_{2,\uparrow}^\dagger\hat{c}_{2,\downarrow}^\dagger}|\mathcal{O}\rangle}_{-|\Phi_2\rangle}\Big(-t\Big) + \underbrace{\overbrace{\hat{c}_{1,\downarrow}^\dagger\hat{c}_{1,\uparrow}^\dagger}^{-\hat{c}_{1,\uparrow}^\dagger\hat{c}_{1,\downarrow}^\dagger}|\mathcal{O}\rangle}_{-|\Phi_1\rangle}\Big(-t\Big) \\
\hat{H}\underbrace{\hat{c}_{1,\uparrow}^\dagger\hat{c}_{2,\uparrow}^\dagger|\mathcal{O}\rangle}_{|\Phi_5\rangle} &= \underbrace{\hat{c}_{1,\uparrow}^\dagger\hat{c}_{2,\uparrow}^\dagger|\mathcal{O}\rangle}_{|\Phi_5\rangle}\Big(2\bar{\epsilon}+V\Big) \\
\hat{H}\underbrace{\hat{c}_{1,\downarrow}^\dagger\hat{c}_{2,\downarrow}^\dagger|\mathcal{O}\rangle}_{|\Phi_6\rangle} &= \underbrace{\hat{c}_{1,\downarrow}^\dagger\hat{c}_{2,\downarrow}^\dagger|\mathcal{O}\rangle}_{|\Phi_6\rangle}\Big(2\bar{\epsilon}+V\Big)
\end{aligned} \tag{3.98}$$

Let $\hat{P}_2$ be the projector onto the two-particle Hilbert space. The results obtained above can be

condensed into the following equation for the Hamiltonian in the two-particle Hilbert space.

$$\begin{aligned}
\hat{P}_2\Big(\hat{h}+\hat{W}\Big)\hat{P}_2 &= \sum_{i,j=1}^{6} |\Phi_i\rangle\langle\Phi_i|\hat{h}+\hat{W}|\Phi_j\rangle\langle\Phi_j| \\
&= \begin{pmatrix} \hat{c}^\dagger_{1,\uparrow}\hat{c}^\dagger_{1,\downarrow}|\mathcal{O}\rangle \\ \hat{c}^\dagger_{2,\uparrow}\hat{c}^\dagger_{2,\downarrow}|\mathcal{O}\rangle \\ \hat{c}^\dagger_{1,\uparrow}\hat{c}^\dagger_{2,\downarrow}|\mathcal{O}\rangle \\ \hat{c}^\dagger_{1,\downarrow}\hat{c}^\dagger_{2,\uparrow}|\mathcal{O}\rangle \end{pmatrix} \begin{pmatrix} 2\bar{\epsilon}+U & 0 & -t & +t \\ 0 & 2\bar{\epsilon}+U & -t & +t \\ -t & -t & 2\bar{\epsilon}+V & 0 \\ +t & +t & 0 & 2\bar{\epsilon}+V \end{pmatrix} \begin{pmatrix} \langle\mathcal{O}|\hat{c}_{1,\downarrow}\hat{c}_{1,\uparrow} \\ \langle\mathcal{O}|\hat{c}_{2,\downarrow}\hat{c}_{2,\uparrow} \\ \langle\mathcal{O}|\hat{c}_{2,\downarrow}\hat{c}_{1,\uparrow} \\ \langle\mathcal{O}|\hat{c}_{2,\uparrow}\hat{c}_{1,\downarrow} \end{pmatrix} \\
&+ \begin{pmatrix} \hat{c}^\dagger_{1,\uparrow}\hat{c}^\dagger_{2,\uparrow}|\mathcal{O}\rangle \\ \hat{c}^\dagger_{1,\downarrow}\hat{c}^\dagger_{1,\downarrow}|\mathcal{O}\rangle \end{pmatrix} \begin{pmatrix} 2\bar{\epsilon}+V & 0 \\ 0 & 2\bar{\epsilon}+V \end{pmatrix} \begin{pmatrix} \langle\mathcal{O}|\hat{c}_{2,\uparrow}\hat{c}_{1,\uparrow} \\ \langle\mathcal{O}|\hat{c}_{2,\downarrow}\hat{c}_{1,\downarrow} \end{pmatrix} \\
&= \begin{pmatrix} |\Phi_1\rangle \\ |\Phi_2\rangle \\ |\Phi_3\rangle \\ |\Phi_4\rangle \\ |\Phi_5\rangle \\ |\Phi_6\rangle \end{pmatrix} \begin{pmatrix} 2\bar{\epsilon}+U & 0 & -t & +t & 0 & 0 \\ 0 & 2\bar{\epsilon}+U & -t & +t & 0 & 0 \\ -t & -t & 2\bar{\epsilon}+V & 0 & 0 & 0 \\ +t & +t & 0 & 2\bar{\epsilon}+V & 0 & 0 \\ 0 & 0 & 0 & 0 & 2\bar{\epsilon}+V & 0 \\ 0 & 0 & 0 & 0 & 0 & 2\bar{\epsilon}+V \end{pmatrix} \begin{pmatrix} \langle\Phi_1| \\ \langle\Phi_2| \\ \langle\Phi_3| \\ \langle\Phi_4| \\ \langle\Phi_5| \\ \langle\Phi_6| \end{pmatrix}
\end{aligned} \tag{3.99}$$

4 Exploit the reflection symmetry $\hat{P}$ of the hydrogen molecule to block-diagonalize the Hamiltonian in the two-particle channel. That is, construct the eigenstates of the parity operator under reflection symmetry of the molecule. These parity eigenstates are superpositions of the two-particle Slater determinants $|\Phi_i\rangle$ obtained previously. The Hamiltonian in terms of the symmetrized states[a] will "fall apart" into one 2×2 matrix and 1×1 blocks.

[a] With symmetrized states, I mean eigenstates of the symmetry operator. In the case of the parity operator these eigenstates may be symmetric or antisymmetric.

Determine parity eigenstates: Let $\hat{P}$ be the parity operator under space inversion.

$$\begin{aligned}
\hat{P}|\Phi_1\rangle &= \hat{P}\hat{c}^\dagger_{1\uparrow}\hat{c}^\dagger_{1\downarrow}|\mathcal{O}\rangle = \hat{c}^\dagger_{2\uparrow}\hat{c}^\dagger_{2\downarrow}|\mathcal{O}\rangle = |\Phi_2\rangle \\
\hat{P}|\Phi_2\rangle &= \hat{P}\hat{c}^\dagger_{2\uparrow}\hat{c}^\dagger_{2\downarrow}|\mathcal{O}\rangle = \hat{c}^\dagger_{1\uparrow}\hat{c}^\dagger_{1\downarrow}|\mathcal{O}\rangle = |\Phi_1\rangle \\
\hat{P}|\Phi_3\rangle &= \hat{P}\hat{c}^\dagger_{1\uparrow}\hat{c}^\dagger_{2\downarrow}|\mathcal{O}\rangle = \hat{c}^\dagger_{2\uparrow}\hat{c}^\dagger_{1\downarrow}|\mathcal{O}\rangle = -\hat{c}^\dagger_{1\downarrow}\hat{c}^\dagger_{2\uparrow}|\mathcal{O}\rangle = -|\Phi_4\rangle \\
\hat{P}|\Phi_4\rangle &= \hat{P}\hat{c}^\dagger_{1\downarrow}\hat{c}^\dagger_{2\uparrow}|\mathcal{O}\rangle = \hat{c}^\dagger_{2\downarrow}\hat{c}^\dagger_{1\uparrow}|\mathcal{O}\rangle = -\hat{c}^\dagger_{1\uparrow}\hat{c}^\dagger_{2\downarrow}|\mathcal{O}\rangle = -|\Phi_3\rangle \\
\hat{P}|\Phi_5\rangle &= \hat{P}\hat{c}^\dagger_{1\uparrow}\hat{c}^\dagger_{2\uparrow}|\mathcal{O}\rangle = \hat{c}^\dagger_{2\uparrow}\hat{c}^\dagger_{1\uparrow}|\mathcal{O}\rangle = -\hat{c}^\dagger_{1\uparrow}\hat{c}^\dagger_{2\uparrow}|\mathcal{O}\rangle = -|\Phi_5\rangle \\
\hat{P}|\Phi_6\rangle &= \hat{P}\hat{c}^\dagger_{1\downarrow}\hat{c}^\dagger_{2\downarrow}|\mathcal{O}\rangle = \hat{c}^\dagger_{2\downarrow}\hat{c}^\dagger_{1\downarrow}|\mathcal{O}\rangle = -\hat{c}^\dagger_{1\downarrow}\hat{c}^\dagger_{2\downarrow}|\mathcal{O}\rangle = -|\Phi_6\rangle
\end{aligned} \tag{3.100}$$

Just above, we worked out $\hat{P}|\Phi_j\rangle$ for $j = 1, 6$. Now we construct the parity eigenstates $|\Psi_j\rangle$ ($j \in \{a, b, c, d, e, f\}$).

The eigenstates $|\psi_j\rangle$ ($j \in \{a, b\}$) with parity eigenvalue $+1$ are

$$|\Psi_a\rangle \stackrel{\text{def}}{=} \frac{1}{\sqrt{2}}\Big(\hat{c}^\dagger_{1\uparrow}\hat{c}^\dagger_{1\downarrow} + \hat{c}^\dagger_{2\uparrow}\hat{c}^\dagger_{2\downarrow}\Big)|\mathcal{O}\rangle = \Big(|\Phi_1\rangle + |\Phi_2\rangle\Big)\frac{1}{\sqrt{2}} \tag{3.101}$$

$$|\Psi_b\rangle \stackrel{\text{def}}{=} \frac{1}{\sqrt{2}}\Big(\hat{c}^\dagger_{1\uparrow}\hat{c}^\dagger_{2\downarrow} - \hat{c}^\dagger_{1\downarrow}\hat{c}^\dagger_{2\uparrow}\Big)|\mathcal{O}\rangle = \Big(|\Phi_3\rangle - |\Phi_4\rangle\Big)\frac{1}{\sqrt{2}} \tag{3.102}$$

and the eigenstates $|\psi_j\rangle$ ($j \in \{c,d,e,f\}$) with parity eigenvalue -1 are

$$|\Psi_c\rangle \stackrel{\text{def}}{=} \frac{1}{\sqrt{2}}\Big(\hat{c}^\dagger_{1\uparrow}\hat{c}^\dagger_{1\downarrow} - \hat{c}^\dagger_{2\uparrow}\hat{c}^\dagger_{2\downarrow}\Big)|\mathcal{O}\rangle = \Big(|\Phi_1\rangle - |\Phi_2\rangle\Big)\frac{1}{\sqrt{2}} \tag{3.103}$$

$$|\Psi_d\rangle \stackrel{\text{def}}{=} \frac{1}{\sqrt{2}}\Big(\hat{c}^\dagger_{1\uparrow}\hat{c}^\dagger_{2\downarrow} + \hat{c}^\dagger_{1\downarrow}\hat{c}^\dagger_{2\uparrow}\Big)|\mathcal{O}\rangle = \Big(|\Phi_3\rangle + |\Phi_4\rangle\Big)\frac{1}{\sqrt{2}} \tag{3.104}$$

$$|\Psi_e\rangle \stackrel{\text{def}}{=} \hat{c}^\dagger_{1\uparrow}\hat{c}^\dagger_{2\uparrow}|\mathcal{O}\rangle = |\Phi_5\rangle \tag{3.105}$$

$$|\Psi_f\rangle \stackrel{\text{def}}{=} \hat{c}^\dagger_{1\downarrow}\hat{c}^\dagger_{2\downarrow}|\mathcal{O}\rangle = |\Phi_6\rangle \tag{3.106}$$

Determine Hamiltonian for parity eigenstates: Now, we start from the parity eigenstates and apply the Hamiltonian to them. As expected, the result does not contain a contribution of the opposite parity. This means that the Hamiltonian becomes block diagonal in the representation of parity eigenstates.

I use the matrix-vector notation in the basis of the two-particle states $|\Phi_j\rangle$ with $j \in \{1,\ldots,4\}$ defined in Eq. 3.90. The first term in Eq. 3.112 describes the Hamiltonian in the desired 4-dimensional subspace. To keep things simple, I exclude the states $|\Phi_e\rangle$ and $|\Phi_f\rangle$, because we know already, that they are eigenstates of the Hamiltonian.

I apply the Hamiltonian to the parity eigenstates $|\Psi_j\rangle$ with $j \in \{a,b,c,d\}$ one at a time. Choosing symmetry eigenstates, has the advantage that the result $(\hat{h}+\hat{W})|\Phi_j\rangle$ will be limited to few terms, namely the symmetry eigenstates with the same symmetry eigenvalues.

1. I begin with $|\Psi_a\rangle \stackrel{\text{Eq. 3.101}}{=} \Big(|\Phi_1\rangle + |\Phi_2\rangle\Big)/\sqrt{2}$

   The state $|\Psi_a\rangle$ is represented in the basis $|\Phi_j\rangle$ with $j \in \{1,\ldots,4\}$ by the vector $\vec{c}_a = (1,1,0,0)/\sqrt{2}$, i.e.

   $$|\Psi_a\rangle = \sum_{j=1}^{4} |\Phi_j\rangle c_{j,a} \tag{3.107}$$

   Let $\boldsymbol{H}$ be the matrix of the Hamiltonian $\hat{h}+\hat{W}$ our basiset

   $$\boldsymbol{H}\vec{c}_a = \begin{pmatrix} 2\bar{\epsilon}+U & 0 & -t & +t \\ 0 & 2\bar{\epsilon}+U & -t & +t \\ -t & -t & 2\bar{\epsilon}+V & 0 \\ +t & +t & 0 & 2\bar{\epsilon}+V \end{pmatrix} \begin{pmatrix} 1 \\ 1 \\ 0 \\ 0 \end{pmatrix} \frac{1}{\sqrt{2}} = \begin{pmatrix} 2\bar{\epsilon}+U \\ 2\bar{\epsilon}+U \\ -2t \\ +2t \end{pmatrix} \frac{1}{\sqrt{2}}$$

   $$= \begin{pmatrix} 1 \\ 1 \\ 0 \\ 0 \end{pmatrix} \frac{1}{\sqrt{2}}\Big(2\bar{\epsilon}+U\Big) + \begin{pmatrix} 0 \\ 0 \\ 1 \\ -1 \end{pmatrix} \frac{1}{\sqrt{2}}\Big(-2t\Big)$$

   $$\Rightarrow \quad (\hat{h}+\hat{W})|\Psi_a\rangle = |\Psi_a\rangle\Big(2\bar{\epsilon}+U\Big) + |\Psi_b\rangle\Big(-2t\Big) \tag{3.108}$$

2. $|\Psi_b\rangle \stackrel{\text{Eq. 3.102}}{=} \Big(|\Phi_3\rangle - |\Phi_4\rangle\Big)/\sqrt{2}$ with the vector representation $\vec{c}_b = (0,0,1,-1)/\sqrt{2}$ of $|\Psi_b\rangle$.

   $$\boldsymbol{H}\vec{c}_b = \begin{pmatrix} 2\bar{\epsilon}+U & 0 & -t & +t \\ 0 & 2\bar{\epsilon}+U & -t & +t \\ -t & -t & 2\bar{\epsilon}+V & 0 \\ +t & +t & 0 & 2\bar{\epsilon}+V \end{pmatrix} \begin{pmatrix} 0 \\ 0 \\ 1 \\ -1 \end{pmatrix} \frac{1}{\sqrt{2}} = \begin{pmatrix} -2t \\ -2t \\ 2\bar{\epsilon}+V \\ -(2\bar{\epsilon}+V) \end{pmatrix} \frac{1}{\sqrt{2}}$$

   $$\Rightarrow \quad (\hat{h}+\hat{W})|\Psi_b\rangle = |\Psi_a\rangle\Big(-2t\Big) + |\Psi_b\rangle\Big(2\bar{\epsilon}+V\Big) \tag{3.109}$$

3. $|\Psi_c\rangle \overset{\text{Eq. 3.103}}{=} \Big(|\Phi_1\rangle - |\Phi_2\rangle\Big)/\sqrt{2}$ with the vector representation $\vec{c}_c = (1,-1,0,0)/\sqrt{2}$ of $|\Psi_c\rangle$.

$$\boldsymbol{H}\vec{c}_c = \begin{pmatrix} 2\bar{\epsilon}+U & 0 & -t & +t \\ 0 & 2\bar{\epsilon}+U & -t & +t \\ -t & -t & 2\bar{\epsilon}+V & 0 \\ +t & +t & 0 & 2\bar{\epsilon}+V \end{pmatrix} \begin{pmatrix} 1 \\ -1 \\ 0 \\ 0 \end{pmatrix} \frac{1}{\sqrt{2}} = \begin{pmatrix} 2\bar{\epsilon}+U \\ -(2\bar{\epsilon}+U) \\ 0 \\ 0 \end{pmatrix} \frac{1}{\sqrt{2}}$$

$$\Rightarrow \quad (\hat{h}+\hat{W})|\Psi_c\rangle = |\Psi_c\rangle\Big(2\bar{\epsilon}+U\Big) \tag{3.110}$$

4. $|\Psi_d\rangle \overset{\text{Eq. ??}}{=} \Big(|\Phi_3\rangle + |\Phi_4\rangle\Big)/\sqrt{2}$ with the vector representation $\vec{c}_d = (0,0,1,1)/\sqrt{2}$ of $|\Psi_d\rangle$.

$$\boldsymbol{H}\vec{c}_d = \begin{pmatrix} 2\bar{\epsilon}+U & 0 & -t & +t \\ 0 & 2\bar{\epsilon}+U & -t & +t \\ -t & -t & 2\bar{\epsilon}+V & 0 \\ +t & +t & 0 & 2\bar{\epsilon}+V \end{pmatrix} \begin{pmatrix} 0 \\ 0 \\ 1 \\ 1 \end{pmatrix} \frac{1}{\sqrt{2}} = \begin{pmatrix} 0 \\ 0 \\ 2\bar{\epsilon}+V \\ 2\bar{\epsilon}+V \end{pmatrix} \frac{1}{\sqrt{2}}$$

$$\Rightarrow \quad (\hat{h}+\hat{W})|\Psi_d\rangle = |\Psi_d\rangle\Big(2\bar{\epsilon}+V\Big) \tag{3.111}$$

These expressions can be used to express the Hamiltonian Eq. 3.112 in terms of symmetry adapted orbitals $|\Psi_j\rangle$ with $j \in \{a,b,c,d,e,f\}$.

$$\hat{P}_2(\hat{h}+\hat{W})\hat{P}_2 = \begin{pmatrix} |\Phi_a\rangle \\ |\Phi_b\rangle \\ |\Phi_c\rangle \\ |\Phi_d\rangle \\ |\Phi_e\rangle \\ |\Phi_f\rangle \end{pmatrix} \begin{pmatrix} 2\bar{\epsilon}+U & -2t & 0 & 0 & 0 & 0 \\ -2t & 2\bar{\epsilon}+V & 0 & 0 & 0 & 0 \\ 0 & 0 & 2\bar{\epsilon}+U & 0 & 0 & 0 \\ 0 & 0 & 0 & 2\bar{\epsilon}+V & 0 & 0 \\ 0 & 0 & 0 & 0 & 2\bar{\epsilon}+V & 0 \\ 0 & 0 & 0 & 0 & 0 & 2\bar{\epsilon}+V \end{pmatrix} \begin{pmatrix} \langle\Phi_a| \\ \langle\Phi_b| \\ \langle\Phi_c| \\ \langle\Phi_d| \\ \langle\Phi_e| \\ \langle\Phi_f| \end{pmatrix} \tag{3.112}$$

All this effort has been done to obtain two block-diagonalize the Hamiltonian further. We obtained two additional eigenstates of the Hamiltonian, and one 2×2 block.

Diagonalize Hamiltonian in the basis of parity eigenstates: In the basis of eigenstates of the parity operator the Hamiltonian falls apart into two 1×1 blocks and one 2×2 block. The one-by-one blocks identify $|\Psi_c\rangle$ and $|\Psi_d\rangle$ as eigenstates. The eigenvalues are $E_c = 2\bar{\epsilon}+U$ and $E_d = 2\bar{\epsilon}+V$. The 2×2 block in the space spanned by $|\Psi_j\rangle$ with $j \in \{\Psi_a, \Psi_b\}$ has the form

$$\begin{pmatrix} 2\bar{\epsilon}+U & -2t \\ -2t & 2\bar{\epsilon}+V \end{pmatrix} \tag{3.113}$$

and has eigenvalues

$$E_\pm = 2\bar{\epsilon} + \frac{U+V}{2} \pm \sqrt{\left(\frac{U-V}{2}\right)^2 + 4t^2} \tag{3.114}$$

and eigenstates

$$|\Psi_\pm\rangle = |\Psi_a\rangle\cos(\gamma_\pm) + |\Psi_b\rangle\sin(\gamma_\pm) \tag{3.115}$$

Using cosine and sine takes care of the normalization, because $\cos^2(x)+\sin^2(x) = 1$.

The angle $\gamma_\pm$ is obtained from the eigenvector equation

$$\begin{pmatrix} 2\bar{\epsilon}+U-E_\pm & -2t \\ -2t & 2\bar{\epsilon}+V-E_\pm \end{pmatrix} \begin{pmatrix} \cos(\gamma_\pm) \\ \sin(\gamma_\pm) \end{pmatrix} = 0$$

$$\begin{aligned} \tan(\gamma_\pm) = \frac{\sin(\gamma_\pm)}{\cos(\gamma_\pm)} &= \frac{1}{2t}\Big(2\bar{\epsilon}+U-E_\pm\Big) \\ &= \frac{1}{2t}\left(2\bar{\epsilon}+U-2\bar{\epsilon}-\frac{U+V}{2} \mp \sqrt{\left(\frac{U-V}{2}\right)^2+4t^2}\right) \\ &= \frac{1}{2t}\left(\frac{U-V}{2} \mp \sqrt{\left(\frac{U-V}{2}\right)^2+4t^2}\right) \\ &= \frac{U-V}{4t} \mp \sqrt{1+\left(\frac{U-V}{4t}\right)^2} \\ &= q \mp \sqrt{1+q^2} \qquad \text{with} \qquad q=\frac{U-V}{4t} \\ \gamma_\pm &= \arctan\left(q \mp \sqrt{1+q^2}\right) \qquad \text{with} \qquad q=\frac{U-V}{4t} \end{aligned} \tag{3.116}$$

The parameter q is a measure for the importance of Coulomb interactions. For strong interaction, that is when hopping is small compared to the Coulomb terms, q is very large. On the other hand, the non-interacting limit is characterized by $q=0$.

The energy can be expressed in terms of the parameter q.

$$E_\pm = 2\bar{\epsilon}+\frac{U+V}{2} \underbrace{\pm\sqrt{\left(\frac{U-V}{2}\right)^2+4t^2}}_{-2t\tan(\gamma_\pm)+\frac{U-V}{2}} = 2\bar{\epsilon}+U-2t\underbrace{\left(q \mp \sqrt{1+q^2}\right)}_{\tan(\gamma_\pm)} \tag{3.117}$$

Thus, we obtained as eigenstates of the Hamiltonian in the two-particle channel

eigenstate	energy	parity	total spin	S_z	
$\|\Psi_-\rangle$	$2\bar{\epsilon}+U-2t(q+\sqrt{1+q^2})$	+1	0	$0\hbar$	antiferrom. singlet
$\|\Psi_+\rangle$	$2\bar{\epsilon}+U-2t(q-\sqrt{1+q^2})$	+1	0	$0\hbar$	antib. singlet
$\|\Psi_c\rangle$	$2\bar{\epsilon}+U$	-1	0	$0\hbar$	ionized (H^+H^-) state
$\|\Psi_d\rangle$	$2\bar{\epsilon}+V$	-1	1	$0\hbar$	triplet
$\|\Psi_e\rangle$	$2\bar{\epsilon}+V$	-1	1	$1\hbar$	triplet
$\|\Psi_f\rangle$	$2\bar{\epsilon}+V$	-1	1	$-1\hbar$	triplet

Discuss eigenstates Let me summarize the energy eigenstates and their energy levels. We make the plausible assumption that $U>V$.

1. The lowest state is

$$\begin{aligned} |\Psi_-\rangle &= |\Psi_a\rangle\cos(\gamma_-)+|\Psi_b\rangle\sin(\gamma_-) \\ &= \left[\frac{\cos\gamma_-}{\sqrt{2}}\Big(\hat{c}^\dagger_{1\uparrow}\hat{c}^\dagger_{1\downarrow}+\hat{c}^\dagger_{2\uparrow}\hat{c}^\dagger_{2\downarrow}\Big)+\frac{\sin(\gamma_-)}{\sqrt{2}}\Big(\hat{c}^\dagger_{1\uparrow}\hat{c}^\dagger_{2\downarrow}-\hat{c}^\dagger_{1\downarrow}\hat{c}^\dagger_{2\uparrow}\Big)\right]|\mathcal{O}\rangle \end{aligned} \tag{3.118}$$

with energy

$$\begin{aligned} E_- &= 2\bar{\epsilon}+\frac{U+V}{2}-\sqrt{\left(\frac{U-V}{2}\right)^2+4t^2} \\ &= 2\bar{\epsilon}+U-2t\tan(\gamma_-) \end{aligned} \tag{3.119}$$

This is corresponds to the bonding configuration of the hydrogen atom.

- In the non-interacting limit $q = (U - V)/(4t) = 0$, $\gamma = \pi/4$, the ground-state wave function is a superposition of four Slater determinants, which, however, can be written as a single Slater determinant of two bonding orbitals,.

$$|\Psi_-(q=0)\rangle = \frac{1}{\sqrt{2}}\left(\hat{c}^\dagger_{1,\uparrow} + \hat{c}^\dagger_{2,\uparrow}\right)\frac{1}{\sqrt{2}}\left(\hat{c}^\dagger_{1,\downarrow} + \hat{c}^\dagger_{2,\downarrow}\right)|\mathcal{O}\rangle \tag{3.120}$$

- In the limit with infinite interaction $q = (U-V)/(4t) = \infty$, $\gamma = \pi/2$, the contribution with double occupancy, namely $|\Psi_a\rangle$ is suppressed and the ground state is an **antiferromagnetic singlet**, namely $|\Psi_b\rangle$.

$$|\Psi_-(q=\infty)\rangle = |\Psi_b\rangle = \frac{1}{\sqrt{2}}\left(\hat{c}^\dagger_{1,\uparrow}\hat{c}^\dagger_{2,\downarrow} - \hat{c}^\dagger_{1,\downarrow}\hat{c}^\dagger_{2,\uparrow}\right)|\mathcal{O}\rangle \tag{3.121}$$

  An antiferromagnetic singlet describes a singlet state, which has no magnetization, but still an antiferromagnetic correlation between the spins on different sites.

- The mechanism that favors an antiferromagnetic alignment of spins over a ferromagnetic alignment is called **superexchange**. The usual explanation for this effect is as follows: When two electrons with equal spin are located on neighboring sites, the Pauli-principle prohibits any delocalization of electrons onto the neighboring site, because no two electrons with the same spin can occupy the same spatial orbital. If the electrons have opposite spin, each electron finds a vacant orbital with the same spin on the other site. The delocalization to the neighboring site requires to overcome the on-site Coulomb repulsion between the electrons, but it also lowers the kinetic energy. The lowering of the kinetic energy can be argued in terms of Heisenberg's uncertainty principle.
- This state expresses the **left-right correlation** of the electrons in a bond. If the spin-up electron is on the left side, the spin-down electron is on the right hand side and vice versa. That is, the electrons get out of each other's way to reduce their Coulomb repulsion. The price to pay, is that the electrons also loose their binding energy, because the electrons are confined to one of the two atoms. The energy in the strongly correlated limit is $E_-(q=\infty) = 2\bar{\epsilon} + V$.
- This left-right-correlated state is also the classical example for **entanglement**: The thought experiment goes as follows: Prepare hydrogen molecule in the left-right correlated state and separate the two hydrogen atoms. Two observers receive one hydrogen atom each. One observer measures the spin of his hydrogen atom. Due to the measurement, the wave function collapses "instantly" into either $\hat{c}_{1,\uparrow}\hat{c}_{2,\downarrow}|\mathcal{O}\rangle$ or $\hat{c}_{1,\downarrow}\hat{c}_{2,\uparrow}|\mathcal{O}\rangle$. This implies that by doing his measurement, he determines what the outcome of the measurement of the other observer will be. This gives the impression of an information transfer, which may even proceed faster than the speed of light, a seeming paradox.

2. The second-lowest state is

$$|\Psi_d\rangle \stackrel{\text{def}}{=} \frac{1}{\sqrt{2}}\left(\hat{c}^\dagger_{1\uparrow}\hat{c}^\dagger_{2\downarrow} + \hat{c}^\dagger_{1\downarrow}\hat{c}^\dagger_{2\uparrow}\right)|\mathcal{O}\rangle \tag{3.122}$$

with energy

$$E_d = 2\bar{\epsilon} + V \tag{3.123}$$

This is actually one of the three triplet states with parallel spins. $|\Psi_d\rangle$ has $S = 1$ and $S_z = 0\hbar$. The other two states of the triplet are

$$|\Psi_{S=1,S_z=+\hbar}\rangle = \hat{c}^\dagger_{1\uparrow}\hat{c}^\dagger_{2\uparrow}|\mathcal{O}\rangle \tag{3.124}$$

$$|\Psi_{S=1,S_z=-\hbar}\rangle = \hat{c}^\dagger_{1\downarrow}\hat{c}^\dagger_{2\downarrow}|\mathcal{O}\rangle \tag{3.125}$$

and have the same energy.

- The energy between the singlet ground state and the triplet is the so-called **singlet-triplet splitting**. It is the smallest excitation energy of a hydrogen molecule.

$$\Delta_{st} = E_d - E_- = \sqrt{\left(\frac{U-V}{2}\right)^2 + 4t^2} - \frac{U-V}{2} \approx \frac{(2t)^2}{U-V} \tag{3.126}$$

  This means that the excitation energy becomes smaller due to the Coulomb interaction.
- The singlet-triplet excitation is not a one-particle excitation and, therefore, it does not show up in the density of states or the spectral function. Rather, it is a two-particle excitation like an optical excitation.
- If we consider only the singlet ground state and the triplet as first excited state, we can describe the hydrogen molecule in the strongly interacting limit by a **Heisenberg model**, which is discussed in greater detail in section **??** on p. **??**. The Heisenberg model has the Hamiltonian

$$\hat{H}_H = -\sum_{R,R' \in n.n.} J_{R,R'} \hat{\vec{S}}_R \hat{\vec{S}}_{R'} \qquad \text{with}$$

$$J_{R,R'} \stackrel{\text{def}}{=} -\Delta_{st}/\hbar^{-2} \approx -\frac{(2t/\hbar)^2}{U-V} \text{ for } R, R' \text{ next neighbors} \tag{3.127}$$

  The indices R, R' refer to the individual hydrogen atoms. The double sum is executed over all nearest neighbors (n.n.). Each spin operator acts on a spin-one-half system, i.e. the electron on a specific hydrogen atom. The coupling J between two neighboring spins is called **exchange parameter**.[11] Because it is negative, it favors an antiferromagnetic coupling between the sites.

  The elementary excitations of the Heisenberg model are spin-waves, so-called **magnons**. A magnon is yet another elementary excitation of the solid state. Editor: I plan to describe magnons in more detail in appendix **??** on p. **??**.
- In the non-interacting case, the triplet states correspond to a state, where one electron is lifted from the bonding state into the antibonding state. The electron in the antibonding state prefers a parallel spin alignment because of Hund's rule. Therefore the excitation energy is reduced with increasing interaction and the lowest excitation goes from a singlet to a triplet state.

  Note, however, that the dominant optical excitation in the hydrogen molecule does not lead to the triplet states, but to the "ionized (H^+H^-) state" $|\Phi_c\rangle$ discussed below in Eq. 3.128. This is because the optic excitations, which dominate the absorption spectrum, conserve the spin. This is because the dominant excitations are due to the electric field and preserve the spin, while the excitations due to the magnetic field, which may induce spin flips, are much weaker.
- **Mott-Hubbard insulator**. In our example on the insulating linear chain in section 1.5.4, we learned how a band gap in a metal can be opened by breaking the translational symmetry. This is what is called a band insulator. Interaction does not play a role in the formation of an insulator.

  One important aspect of a non-magnetic band insulator is that it requires an even number of electrons in the unit cell. It was surprising to find that certain transition-metal oxides turned out to be insulating despite having an odd number of electrons. An example is the half-filled Hubbard model. A simple-minded picture is that, in a system with strong interactions, electrons occupy each site with one electron. An excitation must lift an electron from a singly occupied site to one that is already occupied. Therefore, the excitation energy is finite and of order U.

  Editor: This is not clear as such. Show that a band in the band structure must be broken up to create a gap with an odd number of electrons.

[11] The definition of exchange parameter J is not uniform.[53]

- The relevant Coulomb parameter for the excitation spectra is not the onsite Coulomb repulsion U, but the difference $U - V$ between onsite and offsite Coulomb parameters. Thus, the effective Coulomb parameter is smaller than anticipated. In the Hubbard model, the effect of the offsite Coulomb interaction is discarded from the beginning. In the so-called **extended Hubbard model** (see e.g.[54]), the off-site Coulomb interaction is taken into account. (In contrast to the simple Hubbard model with only onsite Coulomb terms, the extended Hubbard model can describe Plasmons [see Tosatti and Anderson, Japanese Journal of Applied Physics 13, 381 (1974)] and it can describe charge ordering.(see e.g.[55])

3. Above the triplet, we find the ionized (H^+H^-) state $|\Psi_c\rangle$

$$|\Psi_c\rangle \stackrel{\text{def}}{=} \frac{1}{\sqrt{2}}\left(\hat{c}^\dagger_{1\uparrow}\hat{c}^\dagger_{1\downarrow} - \hat{c}^\dagger_{2\uparrow}\hat{c}^\dagger_{2\downarrow}\right)|\mathcal{O}\rangle \tag{3.128}$$

with energy

$$E_c = 2\bar{\epsilon} + U \tag{3.129}$$

- this is a state with double occupancy. It is a superpositions of two Slater determinants, which describe ionic pairs, H^-H^+ and H^+H^-.

4. Finally, we find again a complicated singlet state

$$\begin{aligned}|\Psi_+\rangle &= |\Psi_a\rangle\cos(\gamma_+) + |\Psi_b\rangle\sin(\gamma_+)\\ &= \left[\frac{\cos\gamma_+}{\sqrt{2}}\left(\hat{c}^\dagger_{1\uparrow}\hat{c}^\dagger_{1\downarrow} + \hat{c}^\dagger_{2\uparrow}\hat{c}^\dagger_{2\downarrow}\right) + \frac{\sin(\gamma_+)}{\sqrt{2}}\left(\hat{c}^\dagger_{1\uparrow}\hat{c}^\dagger_{2\downarrow} - \hat{c}^\dagger_{1\downarrow}\hat{c}^\dagger_{2\uparrow}\right)\right]|\mathcal{O}\rangle\end{aligned} \tag{3.130}$$

with energy

$$E_+ = 2\bar{\epsilon} + \frac{U+V}{2} + \sqrt{\left(\frac{U-V}{2}\right)^2 + 4t^2} \approx 2\bar{\epsilon} + U + \frac{4t^2}{U-V} \tag{3.131}$$

- In the non-interacting system, this is a singlet state with both electrons in the antibonding orbitals.
- In the interacting system this state accumulates the contribution with double occupancy in order to compensate the suppression of the double occupancy in the singlet ground state. The total contribution of a given basisstate summed over all eigenstates of the system must be unity.

The many-particle energies are shown as function of the Coulomb interaction in figure 3.2
Let me combine the energy levels of the hydrogen molecule with interaction

$$E_- = \left(2\bar{\epsilon} + V\right) + 2t\left(\frac{U-V}{4t} - \sqrt{1 + \left(\frac{U-V}{4t}\right)^2}\right) \qquad \text{antiferromagnetic singlet} \tag{3.132}$$

$$E_d = \left(2\bar{\epsilon} + V\right) \qquad \text{(ferromagnetic) triplet} \tag{3.133}$$

$$E_c = \left(2\bar{\epsilon} + V\right) + 4t\frac{U-V}{4t} \qquad \text{ionized } (H^+H^-) \text{ state} \tag{3.134}$$

$$E_+ = \left(2\bar{\epsilon} + V\right) + 2t\left(\frac{U-V}{4t} + \sqrt{1 + \left(\frac{U-V}{4t}\right)^2}\right) \qquad \text{two antibonding electrons} \tag{3.135}$$

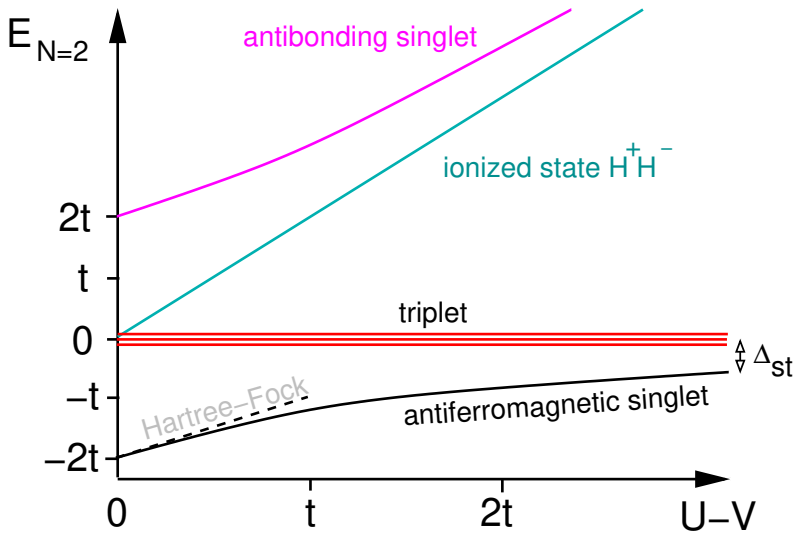

Fig. 3.2: Energies of the hydrogen molecule with two electrons are shown as function of $q = (U-V)/(4t)$ in units of the hopping t. The energies are shifted by $2t - 2\bar{\epsilon} - V$. The energy of the ground state E_-, the antiferromagnetic singlet is shown in blue. The energy triplet states $|\Psi_d\rangle$, $|\Psi_e\rangle$, and $|\Psi_f\rangle$, (artificially displaced) are shown in red. The energy of the double-occupancy state $|\Psi_c\rangle$ is shown in green and the state $|\Psi_+\rangle$ with two antibonding orbitals is shown in magenta. The black dashed line gives the spin-restricted Hartree-Fock energy with both electrons in the bonding orbital. Note that the Hartree-Fock ground state undergoes a transition to an antiferromagnetic broken-symmetry state for large q. Editor: A copy of this figure is fig. ?? on p. ?? Editor: Caution! for the figure $V = 0$ has been used.

3.11.2 Spin eigenstates

Purpose

The main purpose of this exercise is to practice the manipulation of creation and annihilation operators. The secondary purpose is to get used to one rather common two-particle operator, the squared spin. The result obtained here will be required later in section **??** and in appendix D.1.1.

Introduction

Consider a system with two orbital degrees of freedom and two spin degrees of freedom. The one-particle basis consists of four spin orbitals, namely $|1,\uparrow\rangle$, $|1,\downarrow\rangle$ $|2,\uparrow\rangle$, $|2,\downarrow\rangle$.

The orbital degrees of freedom $\{1,2\}$ are denoted by symbols f and c. The symbol f is derived from *"f-orbital"* ($\ell = 2$), which is a localized orbital with large Coulomb interaction, and the symbol c is derived from a delocalized *"conduction electron"*. The naming of the spatial orbitals is taken from the **Kondo model**, section **??**.

The corresponding creation operators are denoted as $\hat{c}^\dagger_{1,\uparrow} =: \hat{f}_\uparrow$, $\hat{c}_{1,\downarrow} =: \hat{f}_\downarrow$, $\hat{c}_{2,\uparrow} =: \hat{c}_\uparrow$, $\hat{c}_{2,\downarrow} =: \hat{c}_\downarrow$. That is, we use the letter to discriminate between the two sites of the dimer.[12]

Consider only the two-particle states spanned by the six Slater determinants given in table 3.1. The numbering is related to the integer representation described in section 3.2. **Note, that $\vec{\sigma}$ is the bit representation of $n-1$ rather than of the number n itself. Hence, the vacuum state has the number $n = 1$.**

[12] While this notation seems a bit clumsy, it is frequently used, which is why I want to expose the reader to it.

Table 3.1: Two-particle states of the asymmetric dimer with spin orbitals $|f,\uparrow\rangle$ and $|f,\downarrow\rangle$ on the "left" atom and $|c,\uparrow\rangle$ and $|c,\downarrow\rangle$ on the "right" atom.

$\|n\rangle$ with $n = 1 + \sum_{j=1}^{4} \sigma_j 2^{j-1}$	$\|\vec{\sigma}\rangle$	$\prod_{j=1}^{4} (\hat{c}_j^\dagger)^{\sigma_j} \|\mathcal{O}\rangle$
$\|4\rangle$	$\|1100\rangle$	$\hat{f}_\uparrow^\dagger \hat{f}_\downarrow^\dagger \|\mathcal{O}\rangle$
$\|6\rangle$	$\|1010\rangle$	$\hat{f}_\uparrow^\dagger \hat{c}_\uparrow^\dagger \|\mathcal{O}\rangle$
$\|7\rangle$	$\|0110\rangle$	$\hat{f}_\downarrow^\dagger \hat{c}_\uparrow^\dagger \|\mathcal{O}\rangle$
$\|10\rangle$	$\|1001\rangle$	$\hat{f}_\uparrow^\dagger \hat{c}_\downarrow^\dagger \|\mathcal{O}\rangle$
$\|11\rangle$	$\|0101\rangle$	$\hat{f}_\downarrow^\dagger \hat{c}_\downarrow^\dagger \|\mathcal{O}\rangle$
$13\rangle$	$\|0011\rangle$	$\hat{c}_\uparrow^\dagger \hat{c}_\downarrow^\dagger \|\mathcal{O}\rangle$

The main goal of this exercise is to determine matrix elements of $\hat{\vec{S}}^2$ and of $\hat{S}_z$ and their eigenstates. The individual questions shall give some guidance towards this goal.

Problem

1 Express $\hat{S}_x$, $\hat{S}_y$, and $\hat{S}_z$ in terms of creation operators and annihilation operators. Start from the Pauli matrices.

2 Express $\hat{\vec{S}}^2$ in terms of $\hat{S}_j$ with $j = 1, 2, 3$. Then, write it in terms of $\hat{S}_+ = \hat{S}_x + i\hat{S}_y$, $\hat{S}_- = \hat{S}_+^\dagger$ and S_z.

3 Determine the matrix elements of $\hat{S}_+$ and $\hat{S}_z$ with the two-particle states listed in table 3.1 on p.154 above.

4 Determine the matrix elements of $\hat{S}_-$ from those of $\hat{S}_+$ by spin reversal.

5 In the subspace of the two-particle states, express the spin operators $\hat{S}_+$, $\hat{S}_-$, and $\hat{S}_z$ as sum of dyadic products of the two-particle states given above. Use $\hat{P}_2$ as symbol for the projection operator onto the two-particle Hilbert space.

6 Determine the spin eigenstates in the two-particle Hilbert space

Discussion

1 Express $\hat{S}_x$, $\hat{S}_y$, and $\hat{S}_z$ in terms of creation operators and annihilation operators. Start from the Pauli matrices.

The spin operators are given by the Pauli matrices $\boldsymbol{\sigma}_x$, $\boldsymbol{\sigma}_y$ and $\boldsymbol{\sigma}_z$, defined in Eq. 1.22, as

$$\hat{S}_j \overset{\text{Eq. 3.49}}{=} \frac{\hbar}{2} \sum_{\sigma,\sigma' \in \{\uparrow,\downarrow\}} \sigma_{j,\sigma,\sigma'} \left(\hat{f}_\sigma^\dagger \hat{f}_{\sigma'} + \hat{c}_\sigma^\dagger \hat{c}_{\sigma'} \right) \tag{3.136}$$

The spin S_j is obtained by summing over both sites (orbitals).

Hence, the spin operators are

$$\begin{aligned}\hat{S}_z &= \frac{\hbar}{2}\left(\hat{f}_\uparrow^\dagger \hat{f}_\uparrow - \hat{f}_\downarrow^\dagger \hat{f}_\downarrow + \hat{c}_\uparrow^\dagger \hat{c}_\uparrow - \hat{c}_\downarrow^\dagger \hat{c}_\downarrow\right)\\ \hat{S}_x &= \frac{\hbar}{2}\left(\hat{f}_\uparrow^\dagger \hat{f}_\downarrow + \hat{f}_\downarrow^\dagger \hat{f}_\uparrow + \hat{c}_\uparrow^\dagger \hat{c}_\downarrow + \hat{c}_\downarrow^\dagger \hat{c}_\uparrow\right)\\ \hat{S}_y &= \frac{\hbar}{2}\left(-i\hat{f}_\uparrow^\dagger \hat{f}_\downarrow + i\hat{f}_\downarrow^\dagger \hat{f}_\uparrow - i\hat{c}_\uparrow^\dagger \hat{c}_\downarrow + i\hat{c}_\downarrow^\dagger \hat{c}_\uparrow\right)\end{aligned} \tag{3.137}$$

2 Express $\hat{\vec{S}}^2$ in terms of $\hat{S}_j$ with $j = 1, 2, 3$. Then, write it in terms of $\hat{S}_+ = \hat{S}_x + i\hat{S}_y$, $\hat{S}_- = \hat{S}_+^\dagger$ and S_z.

$$\hat{\vec{S}}^2 = \hat{S}_x^2 + \hat{S}_y^2 + \hat{S}_z^2 \tag{3.138}$$

While $\hat{S}_x$, $\hat{S}_y$ $\hat{S}_z$ are one-particle (one-particle-at-a-time) operators, $\hat{\vec{S}}^2$ is a two-particle operator.

It is convenient to introduce the operators

$$\begin{aligned}\hat{S}_+ &\stackrel{\text{def}}{=} \hat{\vec{S}}_x + i\hat{\vec{S}}_y = \left(\hat{f}_\uparrow^\dagger \hat{f}_\downarrow + \hat{c}_\uparrow^\dagger \hat{c}_\downarrow\right)\hbar\\ \hat{S}_- &\stackrel{\text{def}}{=} \hat{\vec{S}}_x - i\hat{\vec{S}}_y = \left(\hat{f}_\downarrow^\dagger \hat{f}_\uparrow + \hat{c}_\downarrow^\dagger \hat{c}_\uparrow\right)\hbar\end{aligned} \tag{3.139}$$

$\hat{S}_+$ raises S_z, while $\hat{S}_-$ lowers it. $\hat{S}_+$ annihilates a spin-down electron and, if possible, creates instead the corresponding spin-up electron.

For us, the advantage of the operators $\hat{S}_+$ and $\hat{S}_-$ is that $\hat{S}_+$ and $\hat{S}_-$ have less terms than $\hat{S}_x$ and $\hat{S}_y$, when expressed in terms of creation and annihilation operators.

In order to evaluate $\hat{\vec{S}}^2$, we first form the back transform from $(\hat{S}_x, \hat{S}_y)$ to $(\hat{S}_+, \hat{S}_-)$ before we insert it into the equation Eq. 3.138 above.

$$\begin{aligned}\hat{S}_x &= \frac{1}{2}\left(\hat{\vec{S}}_+ + \hat{\vec{S}}_-\right)\\ \hat{S}_y &= -i\frac{1}{2}\left(\hat{\vec{S}}_+ - \hat{\vec{S}}_-\right)\end{aligned} \tag{3.140}$$

This yields

$$\hat{\vec{S}}^2 \stackrel{\text{Eq. 3.138}}{=} \frac{1}{2}\left(\hat{S}_+\hat{S}_- + \hat{S}_-\hat{S}_+\right) + \hat{S}_z^2 \tag{3.141}$$

3 Determine the matrix elements of $\hat{S}_+$ and $\hat{S}_z$ with the two-particle states listed in table 3.1 on p.154 above.

We apply the operators $\hat{S}_+$ to the two-particle basis states. The idea is to permutate the annihilation operator towards the vacuum state. Each permutation produces a sign change. When the annihilation operator is interchanged with its corresponding creation operator, the anticommutator leaves a non-zero contribution. The annihilation operator acting on the vacuum state produces the zero

state.

$$\hat{\tilde{S}}_+|4\rangle = \hbar\Big(\hat{f}_\uparrow^\dagger\hat{f}_\downarrow + \hat{c}_\uparrow^\dagger\hat{c}_\downarrow\Big)\hat{f}_\uparrow^\dagger\hat{f}_\downarrow^\dagger|\mathcal{O}\rangle = \hat{f}_\uparrow^\dagger\hat{f}_\downarrow\hat{f}_\uparrow^\dagger\hat{f}_\downarrow^\dagger|\mathcal{O}\rangle\hbar = |\varnothing\rangle \tag{3.142}$$

$$\hat{\tilde{S}}_+|6\rangle = \hbar\Big(\hat{f}_\uparrow^\dagger\hat{f}_\downarrow + \hat{c}_\uparrow^\dagger\hat{c}_\downarrow\Big)\hat{f}_\uparrow^\dagger\hat{c}_\uparrow^\dagger|\mathcal{O}\rangle = |\varnothing\rangle \tag{3.143}$$

$$\hat{\tilde{S}}_+|7\rangle = \hbar\Big(\hat{f}_\uparrow^\dagger\hat{f}_\downarrow + \hat{c}_\uparrow^\dagger\hat{c}_\downarrow\Big)\hat{f}_\downarrow^\dagger\hat{c}_\uparrow^\dagger|\mathcal{O}\rangle = \hat{f}_\uparrow^\dagger\hat{f}_\downarrow\hat{f}_\downarrow^\dagger\hat{c}_\uparrow^\dagger|\mathcal{O}\rangle\hbar = \hat{f}_\uparrow^\dagger\hat{c}_\uparrow^\dagger|\mathcal{O}\rangle\hbar = |6\rangle\hbar \tag{3.144}$$

$$\hat{\tilde{S}}_+|10\rangle = \hbar\Big(\hat{f}_\uparrow^\dagger\hat{f}_\downarrow + \hat{c}_\uparrow^\dagger\hat{c}_\downarrow\Big)\hat{f}_\uparrow^\dagger\hat{c}_\downarrow^\dagger|\mathcal{O}\rangle = \hat{c}_\uparrow^\dagger\hat{c}_\downarrow\hat{f}_\uparrow^\dagger\hat{c}_\downarrow^\dagger|\mathcal{O}\rangle\hbar = -\hat{c}_\uparrow^\dagger\hat{f}_\uparrow^\dagger|\mathcal{O}\rangle\hbar = \hat{f}_\uparrow^\dagger\hat{c}_\uparrow^\dagger|\mathcal{O}\rangle\hbar = |6\rangle\hbar \tag{3.145}$$

$$\hat{\tilde{S}}_+|11\rangle = \hbar\Big(\hat{f}_\uparrow^\dagger\hat{f}_\downarrow + \hat{c}_\uparrow^\dagger\hat{c}_\downarrow\Big)\hat{f}_\downarrow^\dagger\hat{c}_\downarrow^\dagger|\mathcal{O}\rangle = \Big(\hat{f}_\uparrow^\dagger\hat{c}_\downarrow^\dagger - \hat{c}_\uparrow^\dagger\hat{f}_\downarrow^\dagger\Big)|\mathcal{O}\rangle\hbar = \Big(|10\rangle + |7\rangle\Big)\hbar \tag{3.146}$$

$$\hat{\tilde{S}}_+|13\rangle = \hbar\Big(\hat{f}_\uparrow^\dagger\hat{f}_\downarrow + \hat{c}_\uparrow^\dagger\hat{c}_\downarrow\Big)\hat{c}_\uparrow^\dagger\hat{c}_\downarrow^\dagger|\mathcal{O}\rangle = \hat{c}_\uparrow^\dagger\hat{c}_\downarrow\hat{c}_\uparrow^\dagger\hat{c}_\downarrow^\dagger|\mathcal{O}\rangle\hbar = -\hat{c}_\uparrow^\dagger\hat{c}_\uparrow^\dagger|\mathcal{O}\rangle\hbar = |\varnothing\rangle \tag{3.147}$$

$$\begin{aligned}
\hat{S}_z|4\rangle &= \frac{\hbar}{2}\Big(\hat{f}_\uparrow^\dagger\hat{f}_\uparrow - \hat{f}_\downarrow^\dagger\hat{f}_\downarrow + \hat{c}_\uparrow^\dagger\hat{c}_\uparrow - \hat{c}_\downarrow^\dagger\hat{c}_\downarrow\Big)\hat{f}_\uparrow^\dagger\hat{f}_\downarrow^\dagger|\mathcal{O}\rangle = |\varnothing\rangle \\
\hat{S}_z|6\rangle &= \hat{S}_z\hat{f}_\uparrow^\dagger\hat{c}_\uparrow^\dagger|\mathcal{O}\rangle = \hat{f}_\uparrow^\dagger\hat{c}_\uparrow^\dagger|\mathcal{O}\rangle\hbar = |6\rangle\hbar \\
\hat{S}_z|7\rangle &= |\varnothing\rangle \\
\hat{S}_z|10\rangle &= |\varnothing\rangle \\
\hat{S}_z|11\rangle &= |11\rangle(-\hbar) \\
\hat{S}_z|13\rangle &= |\varnothing\rangle
\end{aligned} \tag{3.148}$$

4 Determine the matrix elements of $\hat{S}_-$ from those of $\hat{S}_+$ by spin reversal.

Other matrix elements can be obtained by exchanging simultaneously

- $\uparrow$ and $\downarrow$ as well as
- $\hat{S}_+$ with $\hat{S}_-$ and
- $\hat{S}_z$ with $-\hat{S}_z$.

This yields

$$\begin{aligned}
-\hat{S}_-|4\rangle &\overset{\text{Eq. } 3.142}{=} |\varnothing\rangle \\
\hat{S}_-|11\rangle &\overset{\text{Eq. } 3.143}{=} |\varnothing\rangle \\
\hat{S}_-|10\rangle &\overset{\text{Eq. } 3.144}{=} |11\rangle\hbar \\
\hat{S}_-|7\rangle &\overset{\text{Eq. } 3.145}{=} |11\rangle\hbar \\
\hat{S}_-|6\rangle &\overset{\text{Eq. } 3.146}{=} \Big(|7\rangle + |10\rangle\Big)\hbar \\
-\hat{S}_-|13\rangle &\overset{\text{Eq. } 3.147}{=} |\varnothing\rangle
\end{aligned} \tag{3.149}$$

5 In the subspace of the two-particle states, express the spin operators $\hat{S}_+$, $\hat{S}_-$, and $\hat{S}_z$ as sum of dyadic products of the two-particle states given above. Use $\hat{P}_2$ as symbol for the projection operator onto the two-particle Hilbert space.

$$\begin{aligned}\hat{S}_+\hat{P}_2 = \hat{P}_2\hat{S}_+ &= \Big(|6\rangle\langle 10| + |6\rangle\langle 7| + |10\rangle\langle 11| + |7\rangle\langle 11|\Big)\hbar \\ \hat{P}_2\hat{S}_- = \hat{S}_-\hat{P}_2 &= \Big(|10\rangle\langle 6| + |7\rangle\langle 6| + |11\rangle\langle 10| + |11\rangle\langle 7|\Big)\hbar \\ \hat{P}_2\hat{S}_z = \hat{S}_z\hat{P}_2 &= \Big(|6\rangle\langle 6| - |11\rangle\langle 11|\Big)\hbar \end{aligned} \tag{3.150}$$

$$\begin{aligned}\hat{P}_2\hat{\vec{S}}^2\hat{P}_2 &= \frac{\hbar^2}{2}\Big(|6\rangle\langle 10| + |6\rangle\langle 7| + |10\rangle\langle 11| + |7\rangle\langle 11|\Big)\Big(|10\rangle\langle 6| + |7\rangle\langle 6| + |11\rangle\langle 10| + |11\rangle\langle 7|\Big) \\ &+ \frac{\hbar^2}{2}\Big(|10\rangle\langle 6| + |7\rangle\langle 6| + |11\rangle\langle 10| + |11\rangle\langle 7|\Big)\Big(|6\rangle\langle 10| + |6\rangle\langle 7| + |10\rangle\langle 11| + |7\rangle\langle 11|\Big) \\ &+ \hbar^2\Big(|6\rangle\langle 6| - |11\rangle\langle 11|\Big)^2 \\ &= \frac{\hbar^2}{2}\Big(|6\rangle\langle 6| + |6\rangle\langle 6| + |10\rangle\langle 10| + |10\rangle\langle 7| + |7\rangle\langle 10| + |7\rangle\langle 7|\Big) \\ &+ \frac{\hbar^2}{2}\Big(|10\rangle\langle 10| + |10\rangle\langle 7| + |7\rangle\langle 10| + |7\rangle\langle 7| + |11\rangle\langle 11| + |11\rangle\langle 11|\Big) \\ &+ \hbar^2\Big(|6\rangle\langle 6| + |11\rangle\langle 11|\Big) \\ &= 2\hbar^2\Big(|6\rangle\langle 6| + |11\rangle\langle 11|\Big) + \hbar^2\Big(|7\rangle\langle 7| + |7\rangle\langle 10| + |10\rangle\langle 7| + |10\rangle\langle 10|\Big)\end{aligned} \tag{3.151}$$

6 Determine the spin eigenstates in the two-particle Hilbert space

We recognize the eigenvalues having the form $\hbar^2 S(S+1)$ with the main spin angular-momentum quantum number S.

Thus, we obtain three states with spin quantum number $S = 1$, namely

$$\begin{aligned}|6\rangle &= \hat{f}_\uparrow^\dagger \hat{c}_\uparrow^\dagger |\mathcal{O}\rangle \\ |11\rangle &= \hat{f}_\downarrow^\dagger \hat{c}_\downarrow^\dagger |\mathcal{O}\rangle \\ \frac{1}{\sqrt{2}}\Big(|7\rangle + |10\rangle\Big) &= \frac{1}{\sqrt{2}}\Big(\hat{f}_\downarrow^\dagger \hat{c}_\uparrow^\dagger + \hat{f}_\uparrow^\dagger \hat{c}_\downarrow^\dagger\Big)|\mathcal{O}\rangle\end{aligned} \tag{3.152}$$

and three states with $S = 0$, namely

$$\begin{aligned}|4\rangle &= \hat{f}_\uparrow^\dagger \hat{f}_\downarrow^\dagger |\mathcal{O}\rangle \\ |13\rangle &= \hat{c}_\uparrow^\dagger \hat{c}_\downarrow^\dagger |\mathcal{O}\rangle \\ \frac{1}{\sqrt{2}}\Big(|7\rangle - |10\rangle\Big) &= \frac{1}{\sqrt{2}}\Big(\hat{f}_\downarrow^\dagger \hat{c}_\uparrow^\dagger - \hat{f}_\uparrow^\dagger \hat{c}_\downarrow^\dagger\Big)|\mathcal{O}\rangle\end{aligned} \tag{3.153}$$

The three states with $S = \hbar$ are degenerate in a system with spin rotation symmetry. Therefore, they are called **triplet states**. In contrast, the states with spin $S = 0$ are called **singlet states**.

3.11.3 Ground state of the linear chain in second quantization

Purpose

The purpose of this exercise is to, firstly, practice the translation between expressions in bra-ket notation of one-particle quantum mechanics and the notation of second quantization using creation and annihilation operators. Furthermore, it reminds of the transformation between one-particle basissets, in this case, local states versus Bloch states.

Introduction

In the first chapter we analyzed in section 1.5.3 on p. 33 the linear chain of hydrogen atoms.

Problem

We found that the eigenstates of the Hamiltonian for the linear chain

$$\hat{h} \overset{\text{Eq. } 1.113}{=} \underbrace{\sum_{\sigma\in\{\uparrow,\downarrow\}}\sum_{j=-\infty}^{\infty} |\pi_{j,\sigma}\rangle\epsilon_0\langle\pi_{j,\sigma}|}_{\text{atomic energies}} \underbrace{-\sum_{\sigma}\sum_{j=-\infty}^{\infty} |\pi_{j,\sigma}\rangle t\langle\pi_{j+1,\sigma}| - |\pi_{j,\sigma}\rangle t\langle\pi_{j-1,\sigma}|}_{\text{hopping}} \tag{3.154}$$

are

$$|\varphi_\sigma(k)\rangle \overset{\text{Eq. } 1.114}{=} \sum_j |\chi_{j,\sigma}\rangle \underbrace{\mathrm{e}^{ika_{\text{lat}}j}\frac{1}{\sqrt{n}}}_{\langle\pi_\sigma(k)|\varphi_\sigma(k)\rangle} \qquad \text{with } k_m = \frac{2\pi}{na_{\text{lat}}}m \tag{3.155}$$

where periodic boundary conditions after n beads are assumed.
The energies are

$$\epsilon_\sigma(k_m) \overset{\text{Eq. } 1.117}{=} \epsilon_0 - 2t\cos(k_m a_{\text{lat}}) \tag{3.156}$$

.
As in the first chapter, we assume that the basis functions are orthonormal.

1 Write the Hamiltonian in second quantization

2 Represent the ground state wave function of the half-filled linear chain in terms of creation and annihilation operators of local orbitals.

Discussion

1 Write the Hamiltonian in second quantization

In second quantization, the Hamiltonian is

$$\hat{h} = \sum_{j=1}^{n}\left\{\sum_{\sigma\in\{\uparrow,\downarrow\}}\epsilon_0\hat{c}^\dagger_{j,\sigma}\hat{c}_{j,\sigma} - t\sum_{\sigma\in\{\uparrow,\downarrow\}}\left(\hat{c}^\dagger_{j,\sigma}\hat{c}_{j+1,\sigma} + \hat{c}^\dagger_{j,\sigma}\hat{c}_{j-1,\sigma}\right)\right\} \tag{3.157}$$

2 Represent the ground state wave function of the half-filled linear chain in terms of creation and annihilation operators of local orbitals.

The wave function is a Slater determinant of all occupied eigenstates of the Hamiltonian. The creator for an eigenstate $|\varphi_m\rangle$ of the Hamiltonian is the superposition of the orbital creation operators multiplied with the coefficients of the eigenstate in the orbital representation.

$$|\varphi_\sigma(\vec{k})\rangle \overset{\text{Eq. } 1.119}{=} \sum_\alpha \underbrace{\sum_{\vec{t}} |\chi_{\alpha,\vec{t}}\rangle e^{i\vec{k}\vec{t}}}_{|\chi_{\alpha,\vec{k}}\rangle} c_{\alpha,n}(\vec{k}) = \sum_j |\chi_{\sigma j}\rangle e^{ik_x a_{\text{lat}} j} \frac{1}{\sqrt{n}} \tag{3.158}$$

$$\begin{aligned}
|\Phi\rangle &= \left\{ \prod_{m=1}^{n/2} \left(\hat{a}^\dagger_{m,\sigma} \right)^{\gamma_{j,\sigma}} \right\} |\mathcal{O}\rangle \\
&\overset{\text{Eq. } 3.64}{=} \left\{ \prod_{m=1}^{n/2} \left(\int d^4x \, \hat{\psi}^\dagger(\vec{x}) \langle \vec{x} | \varphi_{m,\sigma} \rangle \right)^{\gamma_{j,\sigma}} \right\} |\mathcal{O}\rangle \\
&\overset{\text{Eq. } B.17}{=} \left\{ \prod_{m=1}^{n/2} \left(\int d^4x \underbrace{\sum_{j,\sigma} \hat{c}^\dagger_{j,\sigma} \langle \chi_{j,\sigma} | \vec{x} \rangle}_{\hat{\psi}^\dagger(\vec{x})} \langle \vec{x} | \varphi_{m,\sigma} \rangle \right)^{\gamma_{j,\sigma}} \right\} |\mathcal{O}\rangle \\
&= \left\{ \prod_{m=1}^{n/2} \left(\sum_{j,\sigma} \hat{c}^\dagger_{j,\sigma} \langle \chi_{j,\sigma} | \varphi_{m,\sigma} \rangle \right)^{\gamma_{j,\sigma}} \right\} |\mathcal{O}\rangle \\
&\overset{\text{Eq. } 3.155}{=} \left\{ \prod_{m=1}^{n/2} \left(\sum_j \hat{c}^\dagger_{j,\sigma} \sum_{j'} \underbrace{\langle \chi_{j,\sigma} | \chi_{j',\sigma} \rangle}_{\delta_{j,j'}\delta_{\sigma,\sigma}} \underbrace{e^{ika_{\text{lat}}j'} \frac{1}{\sqrt{n}}}_{\langle \pi_{j',\sigma} | \varphi_{m,\sigma} \rangle} \right)^{\gamma_{j,\sigma}} \right\} |\mathcal{O}\rangle \\
&\overset{\text{Eq. } 3.155}{=} \left\{ \prod_{m=1}^{n/2} \left(\sum_j \hat{c}^\dagger_{j,\sigma} e^{ika_{\text{lat}}j} \frac{1}{\sqrt{n}} \right)^{\gamma_{j,\sigma}} \right\} |\mathcal{O}\rangle
\end{aligned} \tag{3.159}$$

$\gamma_{j,\sigma} \in \{0, 1\}$ are the occupation numbers of the Bloch states

$$\gamma_\sigma(k_m) = \theta(\mu - \epsilon_\sigma(k_m)) \tag{3.160}$$

where μ is the chemical potential. $\theta(x)$ is the Heaviside step function. $\gamma_\sigma(k_m)$ is unity, if the energy of the eigenstate is below the Fermi level, and zero, if it is above. In the limit $n \to \infty$ the chemical potential for a half filled linear chain lies at $\mu = \epsilon_0$.

Remark on a side: We have made the assumption that the orbitals $|\chi_{j,\sigma}\rangle$ are orthonormal. Without this assumption, the Bloch wave function would have a different form, when they are required to be orthonormal themselves. Specifically, they would carry the inverse square root of the overlap matrix as additional factor in Eq. 3.155. This factors would compensate the overlap matrix in the derivation above.

Chapter 4

Green's functions in one-particle quantum mechanics

Green's functions are a powerful tool of many-particle physics. However, they also play an important role in one-particle quantum mechanics. Even more, we use Green's functions in many contexts, often without realizing that we deal with them.

Because explaining Green's functions in the context of many-particle physics is a double difficulty, let us first become familiar with Green's function in the context of one-particle quantum mechanics.

4.1 Green's function as inverse of a differential operator

Let me first lay out the general concept of Green's functions:

In short, Green's functions are useful

- to solve inhomogeneous differential equations,
- to propagate solutions of in first-order differential equations in time,
- to map the effective influence of one subsystem onto another.

4.1.1 Definition

Consider a differential operator $D(\vec{x}, \vec{\nabla})$. The vector $\vec{x}$ shall be an n-dimensional vector, where n may also be one. The vector $\vec{x}$ may contain time coordinates, spatial coordinates, both, or any other set of variables.

GREEN'S FUNCTION AS INVERSE OF A DIFFERENTIAL OPERATOR

The Green's function $G(\vec{x}, \vec{x'})$ is defined as the inverse of the differential operator $D(\vec{x}\vec{\nabla})$

$$D(\vec{x}, \vec{\nabla})G(\vec{x}, \vec{x}_0) = \delta(\vec{x} - \vec{x}_0) \tag{4.1}$$

and a suitable set of boundary conditions.(see section 4.1.3 below!)

GREEN'S FUNCTION AND INHOMOGENEOUS DIFFERENTIAL EQUATIONS

An inhomogeneous differential equation can be solved with the help of the Green's function by

$$D(\vec{x},\vec{\nabla})f(\vec{x}) = I(\vec{x}) \quad \Leftrightarrow \quad f(\vec{x}) = \int d^n x'\, G(\vec{x},\vec{x'})I(\vec{x'}) \tag{4.2}$$

Hereby, $I(\vec{x})$ is the inhomogeneity.

The Green's function can be considered as an inverse of the differential operator. It behaves like that of an inverse matrix while solving a linear system of equations. Consider the solution of such a linear system of equations, expressed in terms of a matrix $\boldsymbol{A}$, an unknown vector $\vec{y}$ and a known vector $\vec{b}$.

$$\begin{aligned} \text{With} \qquad \boldsymbol{A}\boldsymbol{A}^{-1} &= \mathbf{1} \qquad \text{one obtains} \\ \boldsymbol{A}\vec{y} = \vec{b} \qquad &\Rightarrow \qquad \vec{y} = \boldsymbol{A}^{-1}\vec{b} \end{aligned} \tag{4.3}$$

On a more abstract level, the system of equations is identical to the differential equation Eq. 4.2: The matrix $\boldsymbol{A}$ replaces the differential operator $D(\vec{x},\vec{\nabla})$, the vector $\vec{y}$ replaces the function $f(\vec{x})$, the vector $\vec{b}$ the inhomogeneity $I(\vec{x})$ and the inverse $\boldsymbol{A}^{-1}$ replaces the Green's function $G(\vec{x},\vec{x'})$. The indices of matrix $\boldsymbol{A}$ and the vectors $\vec{y}$ and $\vec{b}$ in the system of equations replaces the continuous variable $\vec{x}$ in the differential equation.

4.1.2 Two simple examples:

Let me demonstrate the principle of the Green's function for a few well-known examples, the driven harmonic oscillator and the Poisson equation.

Driven harmonic oscillator

The Green's function can be used to solve the driven harmonic oscillator with damping

$$m\ddot{x} = -cx - \alpha\dot{x} + f(t) \tag{4.4}$$

Here, $x(t)$ is the particle position, m is the mass of the particle, c the force constant, α the friction coefficient and $f(t)$ is the driving force.

The differential operator of this problem is

$$D(t,\partial_t) = m\partial_t^2 + \alpha\partial_t + c \tag{4.5}$$

and the force $f(t)$ is the inhomogeneity.

According to the definition Eq. 4.1, the Green's function fulfills

$$\underbrace{\left(m\partial_t^2 + c + \alpha\partial_t\right)}_{D(t,\partial_t)} G(t,t_0) = \delta(t-t_0) \tag{4.6}$$

The boundary conditions are chosen so that value and derivative of the Green's function vanish at $t = -\infty$.

The Green's function is (see e.g. ΦSX: Klassische Mechanik[13])

$$\begin{aligned} G(t,t') &= \frac{-i}{m(\omega_1-\omega_2)}\left(\mathrm{e}^{i\omega_1(t-t')} - \mathrm{e}^{i\omega_2(t-t')}\right)\theta(t-t') \\ &= \frac{1}{m\sqrt{\frac{c}{m} - \left(\frac{\alpha}{2m}\right)^2}} \sin\left(\sqrt{\frac{c}{m} - \left(\frac{\alpha}{2m}\right)^2}\,(t-t')\right) \mathrm{e}^{-\frac{\alpha}{2m}(t-t')}\theta(t-t') \end{aligned} \tag{4.7}$$

where ω_1 and ω_2 are the complex eigenfrequencies of the damped harmonic oscillator.[1] The Green's function is shown in figure 4.1.

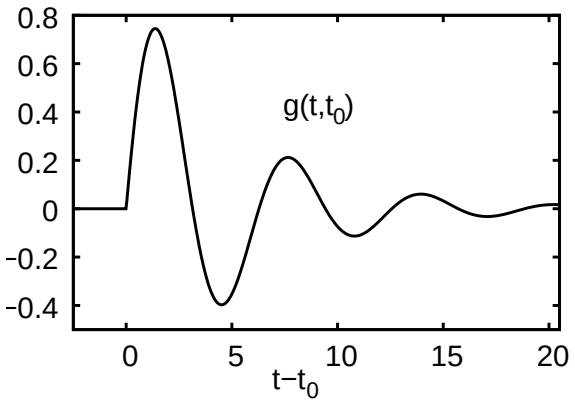

Fig. 4.1: Green's function for the driven harmonic oscillator with damping. Editor: Replace the symbol g by uppercase G.

Once the Green's function is known, we can immediately write down the solution for the driven harmonic oscillator, which fulfills the corresponding inhomogeneous equations of motion. The solution is

$$\begin{aligned} x(t) &= \int dt'\, G(t,t') f(t') \\ &\overset{\text{Eq. 4.7}}{=} \int_{-\infty}^{t} dt'\, \frac{\sin\left(\omega(t-t')\right) e^{-\frac{\alpha}{2m}(t-t')}}{m\omega} f(t') \qquad \text{with } \omega = \sqrt{\frac{c}{m} - \left(\frac{\alpha}{2m}\right)^2} \end{aligned} \tag{4.8}$$

In this case, the Green's function is the response to a Kraftstoß[2] The integral for the position in the presence of a driving force may still be difficult to evaluate, but an integration is usually much simpler than solving a differential equation.

Poisson equation

The Green's function has been used to solve the Poisson equation for the electrostatic potential $\Phi(\vec{r})$ in the presence of a charge density $\rho(\vec{r})$

$$\nabla^2 \Phi(\vec{r}) = -\frac{1}{\epsilon_0} \rho(\vec{r}) \tag{4.9}$$

The Green's function for this problem obeys

$$\nabla^2 G(\vec{r}, \vec{r'}) = \delta(\vec{r} - \vec{r'}) \tag{4.10}$$

which yields the Green's function

$$G(\vec{r}, \vec{r'}) = \frac{-1}{4\pi |\vec{r} - \vec{r'}|} \tag{4.11}$$

Natural boundary conditions have been used.

The solution of Poisson's equation is thus

$$\Phi(\vec{r}) = \int d^3 r'\, G(\vec{r}, \vec{r'}) \left(\frac{-\rho(\vec{r'})}{\epsilon_0} \right) = \int d^3 r'\, \frac{\rho(\vec{r'})}{4\pi\epsilon_0 |\vec{r} - \vec{r'}|} \tag{4.12}$$

[1] For the undamped harmonic oscillator the frequencies are $\omega_1 = \sqrt{\frac{c}{m}}$ and $\omega_2 = -\sqrt{\frac{c}{m}}$

[2] There does not seem to exist an English word for the German word "Kraftstoß". It describes a force peak in the form of a δ function, which transfers a finite momentum in an infinitesimal time interval.

4.1.3 Boundary conditions

An aspect which is often overlooked is that the definition of the Green's function is only complete when, besides the differential equation, also the boundary conditions are defined.

Let me go back to a differential equation. In order to determine a solution of a linear differential equation unambiguously, we need to define the boundary conditions. Given that one solution of the inhomogeneous differential equation has been found, one can immediately construct another one by adding an arbitrary solution of the homogeneous differential equation. A set of boundary conditions needs to be defined such that any such addition of a homogeneous differential equation would violate the boundary conditions. Only then the solution found is unique.

The same set of boundary conditions must be imposed on the Green's function in the defining equation Eq. 4.1 to make the Green's function unique and appropriate to the problem at hand.

4.2 Green's function of a time-independent Hamiltonian

4.2.1 In the time representation

Consider a time-independent Hamiltonian $\hat{h}$, which has eigenstates $|\varphi_n\rangle$ with eigenvalues ϵ_n. The differential operator[3] describing the Schrödinger equation has the form

$$\hat{D} = \left[i\hbar\partial_t - \hat{h}\right] = i\hbar\partial_t - \underbrace{\sum_n |\varphi_n\rangle\epsilon_n\langle\varphi_n|}_{\hat{h}} = \sum_n |\varphi_n\rangle \left(i\hbar\partial_t - \epsilon_n\right)\langle\varphi_n| \tag{4.13}$$

The Green's function is obtained from Eq. 4.1, which we adapt to the problem at hand.

EQUATION OF MOTION FOR THE GREEN'S FUNCTION OF A SINGLE PARTICLE

$$\left[\hat{1}i\hbar\partial_t - \hat{h}\right]\hat{G}(t,t') = \hat{1}\delta(t-t') \tag{4.14}$$

The boundary condition is $\hat{G}(-\infty, t') = 0$, which implies $\hat{G}(t,t') = 0$ for $t < t'$. This requirement is attributed to **causality**.

Let me work out the Green's function from Eq. 4.14 by introducing eigenstates of the Hamiltonian.

$$\overbrace{\sum_j |\varphi_j\rangle \left(i\hbar\partial_t - \epsilon_j\right)\langle\varphi_j|}^{=\hat{D}\quad\text{(See Eq. 4.13)}} \overbrace{\sum_{n,m} |\varphi_n\rangle G_{n,m}(t,t')\langle\varphi_m|}^{\hat{G}} = \overbrace{\sum_{n,m} |\varphi_n\rangle\delta_{n,m}\langle\varphi_m|}^{\hat{1}}\delta(t-t')$$

$$\sum_{j,n,m} |\varphi_j\rangle \left(i\hbar\partial_t - \epsilon_j\right)\underbrace{\langle\varphi_j|\varphi_n\rangle}_{\delta_{j,n}} G_{n,m}(t,t')\langle\varphi_m| = \sum_{n,m} |\varphi_n\rangle\delta_{n,m}\delta(t-t')\langle\varphi_m|$$

$$\Rightarrow \left(i\hbar\partial_t - \epsilon_n\right) G_{n,m}(t,t') = \delta_{n,m}\delta(t-t') \tag{4.15}$$

In the last step, I exploited that the eigenstates are linear independent, which implies that each operator cannot be represented by two different sets of matrix elements.

Thus, we arrived at an ordinary differential equation for the matrix elements, namely Eq. 4.15,

[3] Here, we use the bra-ket notation rather than the differential operator.

which has the solution[4]

$$G_{n,m}(t,t') = \frac{1}{i\hbar} e^{-\frac{i}{\hbar}\epsilon_n(t-t')}\theta(t-t')\delta_{n,m} \,. \tag{4.16}$$

With the matrix elements we can also express the Green's function in operator form

GREEN'S FUNCTION OF A SINGLE PARTICLE

$$\hat{G}(t,t') = \frac{1}{i\hbar}\theta(t-t')\sum_n |\varphi_n\rangle e^{-\frac{i}{\hbar}\epsilon_n(t-t')}\langle\varphi_n| = \frac{1}{i\hbar}\theta(t-t')e^{-\frac{i}{\hbar}\hat{h}(t-t')} \tag{4.17}$$

The wave functions $|\varphi_n\rangle$ are eigenstates of the Hamiltonian $\hat{h}$ with eigenvalues ϵ_n, i.e. $\hat{h}|\varphi_n\rangle = |\varphi_n\rangle\epsilon_n$. The states are chosen to be orthonormal,i.e. $\langle\varphi_m|\varphi_n\rangle = \delta_{m,n}$

The Green's function in real-space-and-spin representation is

$$\begin{aligned} G(\vec{x},t,\vec{x'},t') &\overset{\text{def}}{=} \langle\vec{x}|\hat{G}(t,t')|\vec{x'}\rangle = \sum_n \langle\vec{x}|\varphi_n\rangle \frac{1}{i\hbar}\theta(t-t_0)e^{-\frac{i}{\hbar}\epsilon_n(t-t')}\langle\varphi_n|\vec{x'}\rangle \\ &= \frac{1}{i\hbar}\sum_n \varphi_n(\vec{x})\varphi_n^*(\vec{x'})\theta(t-t_0)e^{-\frac{i}{\hbar}\epsilon_n(t-t')} \end{aligned} \tag{4.18}$$

4.2.2 In the energy representation

Because the Hamiltonian is time independent, the problem is time-translationally invariant and the Green's function depends only on the difference of its time arguments, i.e.

$$G(\vec{x},t,\vec{x'},t_0) = G(\vec{x},t-t_0,\vec{x'},0) \tag{4.19}$$

This allows one to Fourier transform the Green's function in the time-difference argument.

$$\begin{aligned} G(\vec{x},\vec{x'},\epsilon) &\overset{\text{def}}{=} \int_{-\infty}^{\infty} dt\; G(\vec{x},t,\vec{x'},0)\; e^{\frac{i}{\hbar}\epsilon t} \\ &\overset{\text{Eq. 4.17}}{=} \frac{1}{i\hbar}\sum_n \varphi_n(\vec{x})\varphi_n^*(\vec{x'}) \int_{-\infty}^{\infty} dt\; \theta(t) e^{-\frac{i}{\hbar}(\epsilon_n-\epsilon)t} \\ &= \frac{1}{i\hbar}\sum_n \varphi_n(\vec{x})\varphi_n^*(\vec{x'}) \int_0^{\infty} dt\; e^{-\frac{i}{\hbar}(\epsilon_n-\epsilon)t} \end{aligned} \tag{4.20}$$

The integral does not converge if we let the upper limit of the integral go to infinity, while ϵ is real. If we consider the energy argument of the Green's function to be a complex number, we see that the integral converges only, if the imaginary part of ϵ is positive. If it is real or if it has a negative

[4] Let us make the test (proof may continue on the next page):

$$\begin{aligned} &[i\hbar\partial_t - \epsilon_n]\frac{1}{i\hbar}e^{-\frac{i}{\hbar}\epsilon_n(t-t')}\theta(t-t')\delta_{n,m} \\ &= \left(\partial_t e^{-\frac{i}{\hbar}\epsilon_n(t-t')}\right)\theta(t-t')\delta_{n,m} + e^{-\frac{i}{\hbar}\epsilon_n(t-t')}\left(\partial_t\theta(t-t')\right)\delta_{n,m} - \frac{1}{i\hbar}\epsilon_n e^{-\frac{i}{\hbar}\epsilon_n(t-t')}\theta(t-t')\delta_{n,m} \\ &= \underbrace{\left(\frac{1}{i\hbar}\epsilon_n e^{-\frac{i}{\hbar}\epsilon_n(t-t')}\right)\theta(t-t')\delta_{n,m}}_{X} + \underbrace{e^{-\frac{i}{\hbar}\epsilon_n(t-t')}}_{=1 \text{ for } t=t'}\left(\delta(t-t')\right)\delta_{n,m} - \underbrace{\frac{1}{i\hbar}\epsilon_n e^{-\frac{i}{\hbar}\epsilon_n(t-t')}\theta(t-t')\delta_{n,m}}_{X} \\ &= \delta(t-t')\delta_{n,m} \end{aligned}$$

imaginary part, the result is undefined.

$$\begin{aligned} G(\vec{x},\vec{x'},\epsilon+i\eta) &\overset{\text{Eq. 4.20}}{=} \frac{1}{i\hbar}\sum_n \varphi_n(\vec{x})\varphi_n^*(\vec{x'})\int_0^\infty dt'\ \mathrm{e}^{-\frac{i}{\hbar}(\epsilon_n-\epsilon-i\eta)t'} \\ &= \frac{1}{i\hbar}\sum_n \varphi_n(\vec{x})\varphi_n^*(\vec{x'})\left[\frac{i\hbar}{\epsilon_n-\epsilon-i\eta}\mathrm{e}^{-\frac{i}{\hbar}(\epsilon_n-\epsilon-i\eta)t'}\right]_0^\infty \\ &\overset{\eta\geq 0}{=} \frac{1}{i\hbar}\sum_n \varphi_n(\vec{x})\varphi_n^*(\vec{x'})\frac{-i\hbar}{\epsilon_n-\epsilon-i\eta} \\ &= -\sum_n \frac{\varphi_n(\vec{x})\varphi_n^*(\vec{x'})}{\epsilon_n-\epsilon-i\eta} \\ &= \sum_n \frac{\varphi_n(\vec{x})\varphi_n^*(\vec{x'})}{\epsilon-\epsilon_n+i\eta} \qquad \text{for } \eta>0 \end{aligned} \tag{4.21}$$

Notice the restriction that the imaginary part of $\epsilon+i\eta$ must be positive. The Green's function is only defined in the upper half-plane of the complex plane. While we can evaluate the final expression also in the lower half plane, the Green's function is simply not defined there and the numbers are meaningless.[5]

Thus, we can express the Green's function as

GREEN'S FUNCTION IN THE ENERGY REPRESENTATION

$$\hat{G}(\epsilon+i\eta) \overset{\text{Eq. 4.21}}{=} \sum_n |\varphi_n\rangle\frac{1}{\epsilon-\epsilon_n+i\eta}\langle\varphi_n| = \left((\epsilon+i\eta)\hat{1}-\hat{h}\right)^{-1} \qquad \text{for} \quad \eta>0 \tag{4.22}$$

The imaginary part of the Green's function provides the density of states. A pole of the Green's function contributes a Lorentzian at the real axis, which turns into a delta-function, if the pole approaches the real-ϵ axis.

EQUATION OF MOTION FOR THE SINGLE-PARTICLE GREEN'S FUNCTION IN THE ENERGY REPRESENTATION

The Green's function as function of the energy obeys the equation

$$\left(\epsilon-\hat{h}\right)\hat{G}(\epsilon)=\hat{1} \qquad \text{with } \mathrm{Im}(\epsilon)>0. \tag{4.23}$$

where the energy ϵ is considered as complex variable

which can be verified by insertion

$$\left(\epsilon-\hat{h}\right)\hat{G}(\epsilon)=\left(\epsilon-\hat{h}\right)\sum_n |\varphi_n\rangle\frac{1}{\epsilon-\epsilon_n}\langle\varphi_n| = \sum_n |\varphi_n\rangle\frac{\epsilon-\epsilon_n}{\epsilon-\epsilon_n}\langle\varphi_n| = \sum_n |\varphi_n\rangle\langle\varphi_n| = \hat{1} \tag{4.24}$$

4.3 Green's function as propagator

There is a very close relationship between the Green's function and the propagator. With these relations we can proceed to Green's functions for time-dependent Hamilton operators.

[5] The part with $\eta<0$ describes an anti-causal Green's function.

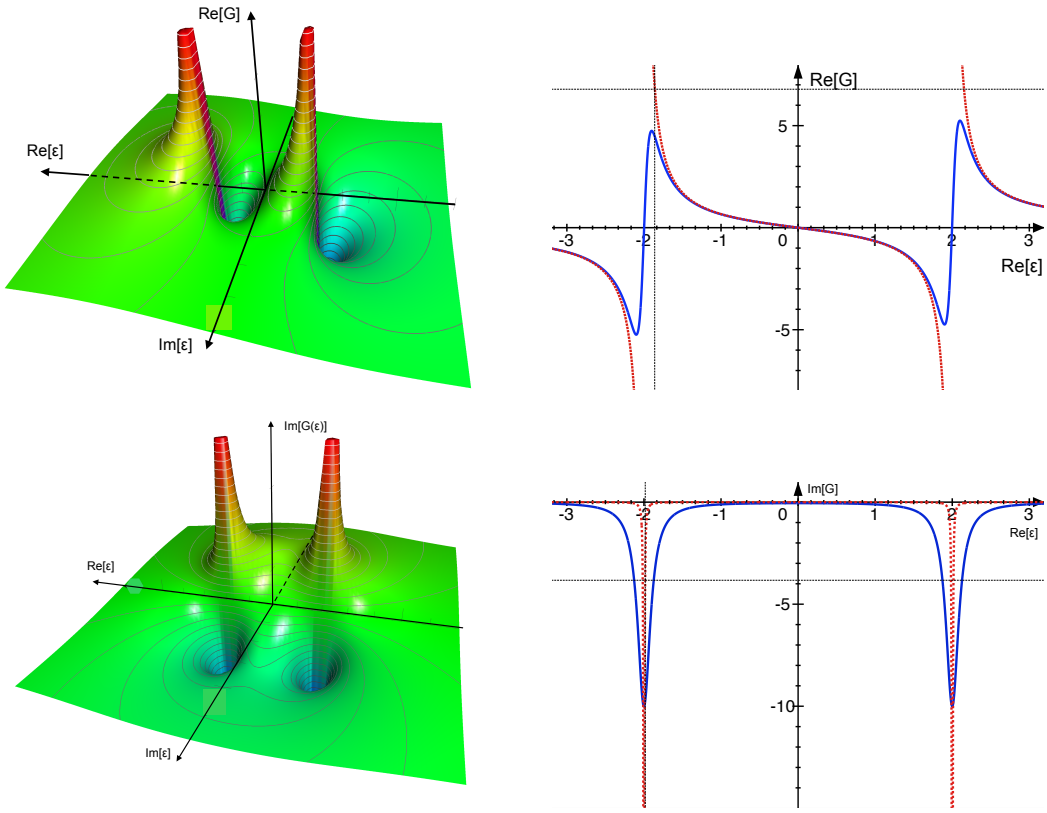

Fig. 4.2: Green's function for a system with two eigenvalues $\epsilon_{\pm} = \pm 2$ a.u. This example describes one spin component of a non-interacting hydrogen molecule and hopping $t = 2$. Left: Green's function $G(\epsilon)$ in the complex-ϵ plane. Caution: The Re[ϵ]-axis points towards the left and the Im(ϵ)-axis points forward. The energy-dependent Green's function is meaningful only in the half-plane with Im(ϵ) > 0. Right: Green's function $G(\epsilon + i\eta)$ as function of real ϵ with a small, positive η. The full, blue line is with $\eta = 0.1$ while the dashed,red line is for $\eta = 10^{-4}$. Top: real part of $G(\epsilon)$. Bottom: imaginary part.

4.3.1 Definition of the propagator

Let me define the **propagator** [6] $\hat{U}(t, t')$, which transforms an initial state at time t' into a final state at time t according to

$$|\psi(t)\rangle = \hat{U}(t, t')|\psi(t')\rangle \tag{4.25}$$

where $|\psi(t)\rangle$ obeys the time-dependent Schrödinger equation with the Hamiltonian $\hat{h}(t)$.

[6] in German: Zeitentwicklungsoperator

DEFINING EQUATIONS FOR THE PROPAGATOR

The propagator operator $\hat{U}(t,t')$ obeys the differential equation

$$\Big(i\hbar\partial_t - \hat{h}(t)\Big)\hat{U}(t,t') = \hat{0} \tag{4.26}$$

with the boundary condition

$$\hat{U}(t,t) = \hat{1}\ . \tag{4.27}$$

How can we construct the propagator $\hat{U}(t,t')$? We begin with solving the time-dependent Schrödinger equations for a number of different initial conditions. This yields a set of time-dependent wave functions $|\varphi_n(t)\rangle$ that satisfy the time-dependent Schrödinger equation

$$\Big(i\hbar\partial_t - \hat{h}(t)\Big)|\varphi_n(t)\rangle = 0\ . \tag{4.28}$$

These wave functions need not be eigenstates of the Hamiltonian $\hat{h}(t)$ at any time t.

Because the propagator for equal times $\hat{U}(t,t) = \hat{1}$, let me represent the identity in terms of these solutions of the Schrödinger equation.

$$\hat{1} = \sum_{m,n} |\varphi_m(t)\rangle O^{-1}_{m,n}(t)\langle\varphi_n(t)| \tag{4.29}$$

where $O_{m,n}(t') = \langle\varphi_m(t')|\varphi_n(t')\rangle$ is the time-dependent overlap matrix. I use the notation $O^{-1}_{m,n}(t) = \big(O^{-1}(t)\big)_{m,n}$.

The Schrödinger equation and the initial conditions can simultaneously be satisfied by

$$\hat{U}(t,t_0) = \sum_{m,n} |\varphi_m(t)\rangle O^{-1}_{m,n}(t_0)\langle\varphi_n(t_0)| \tag{4.30}$$

which can be verified by inserting $\hat{U}(t,t_0)|\psi(t_0)\rangle$ with a general wave function $|\psi(t_0)\rangle = \sum_n |\varphi_n(t_0)\rangle c_n$ into the Schrödinger equation and its initial conditions. Notice that the overlap operator is evaluated from the initial state. This apparent asymmetry between initial and final state is OK because the propagator must not be symmetric under interchange of initial and final time arguments.

PROPAGATOR

The propagator can be written in closed form as[a]

$$\hat{U}(t,t') = \sum_m \Big|\varphi_m(t)\Big\rangle \underbrace{\sum_n \Big(\boldsymbol{O}^{-1}(t')\Big)_{m,n}\Big\langle\varphi_n(t')\Big|}_{\langle\pi_m(t')|} \quad \text{with } O_{n,m}(t') = \Big\langle\varphi_n(t')\Big|\varphi_m(t')\Big\rangle \tag{4.31}$$

where each of the states $|\varphi_n(t)\rangle$ obeys the time-dependent Schrödinger equation and where the set $\{|\varphi_n(t')\rangle\}$ spans the complete, but not necessarily orthonormal, one-particle Hilbert space.

[a] It is not a mistake that the expression is not symmetric with respect to exchanging t and t'. For times t, t' on the real axis, the overlap operator is time independent.

From Eq. 4.31, we can immediately extract some properties of $\hat{U}_I(t)$

PROPERTIES OF THE PROPAGATOR

$$\hat{U}(t,t) \overset{\text{Eq. 4.31}}{=} \hat{1} \qquad \text{initial condition} \tag{4.32}$$

$$\hat{U}(t_2,t_3)\hat{U}(t_3,t_1) \overset{\text{Eq. 4.31}}{=} \hat{U}(t_2,t_1) \qquad \text{transitivity} \tag{4.33}$$

$$\hat{U}(t_1,t_2)\hat{U}(t_2,t_1) \overset{Eqs.\ 4.33,4.32}{=} \hat{1} \qquad \text{time inversion} \tag{4.34}$$

$$\hat{U}(t_2,t_1) \overset{\text{Eq. 4.34}}{=} \hat{U}^{-1}(t_1,t_2) \qquad \text{inverse} \tag{4.35}$$

Two other conditions hold only for real-valued time arguments. We will not make use of them, because, later, we will use complex-valued time arguments, where they are no more valid. Caution is required, because they are widely used and taken for granted.

$$\hat{U}(t_2,t_1) \overset{\text{Eq. 4.31}}{=} \hat{U}^\dagger(t_1,t_2) \qquad \text{for } t_1,t_2 \in \mathbb{R}\text{; hermitian conjugate} \tag{4.36}$$

$$\hat{U}^\dagger(t_2,t_1) \overset{Eqs.\ 4.35,4.36}{=} \hat{U}^{-1}(t_2,t_1) \qquad \text{for } t_1,t_2 \in \mathbb{R}\text{; unitarity} \tag{4.37}$$

4.3.2 Relation between Green's function and propagator

GREEN'S FUNCTION AND PROPAGATOR

The Green's function can be expressed by the propagator $\hat{U}$as

$$\hat{G}(t,t') = \frac{1}{i\hbar}\theta(t-t')\hat{U}(t,t') \tag{4.38}$$

where $\theta(x)$ is the Heaviside step function.

The relation is proven by inserting ansatz Eq. 4.38 into the equation of motion Eq. 4.14 of the Green's function. Note that the derivative of the Heaviside step function is the delta function.

$$\begin{aligned}\left(i\hbar\partial_t - \hat{h}(t)\right)\hat{G}(t,t') &\overset{\text{Eq. 4.38}}{=} \left(i\hbar\partial_t - \hat{h}(t)\right)\underbrace{\frac{1}{i\hbar}\theta(t-t')\hat{U}(t,t')}_{\hat{G}(t,t')} \\ &= \underbrace{\left(i\hbar\partial_t \frac{1}{i\hbar}\theta(t-t')\right)}_{\delta(t-t')}\hat{U}(t,t') + \frac{1}{i\hbar}\theta(t-t')\underbrace{\left(i\hbar\partial_t - \hat{h}(t)\right)\hat{U}(t,t')}_{=0 \quad \text{(Eq. 4.26)}} \\ &\overset{\text{Eq. 4.26}}{=} \underbrace{\hat{U}(t,t')}_{=\hat{1} \quad \text{for } t=t'}\delta(t-t') \overset{\text{Eq. 4.32}}{=} \hat{1}\delta(t-t')\end{aligned} \tag{4.39}$$

The comparison with the equation of motion Eq. 4.14 of the Green's function completes the proof of Eq. 4.38.

4.3.3 Propagator as time-ordered exponential

Evaluating the propagator using Eq. 4.31 requires the knowledge of the wave functions at all times. This is of little practical value. Here, I will derive an expression that refers to the Hamiltonian, namely

PROPAGATOR AS TIME-ORDERED EXPONENTIAL

$$\hat{U}(t_2, t_1) = \mathcal{T}_{\mathcal{D}} \exp\left(-\frac{i}{\hbar}\int_{t_1}^{t_2} dt'\ \hat{h}(t')\right) \tag{4.40}$$

where $\mathcal{T}_D$ is Dyson's time-ordering operator defined below. [a]

[a] Compare with Eq. 31 of[56]

Consider the propagation of a wave function with a time-dependent Hamiltonian.

$$\Big[i\hbar\partial_t \hat{1} - \hat{h}(t)\Big]|\psi(t)\rangle = 0 \tag{4.41}$$

Let me build up an iterative equation, by replacing the derivative by its differential quotient.

$$\begin{aligned}
\frac{|\psi(t+\Delta)\rangle - |\psi(t)\rangle}{\Delta} &= -\frac{i}{\hbar}\hat{h}(t)|\psi(t)\rangle + O(\Delta) \\
\Rightarrow \qquad |\psi(t+\Delta)\rangle &= |\psi(t)\rangle - \frac{i}{\hbar}\hat{h}(t)|\psi(t)\rangle\Delta + O(\Delta^2) \\
&= \Big(\hat{1} - \frac{i}{\hbar}\hat{h}(t)\Delta\Big)|\psi(t)\rangle + O(\Delta^2) \\
&= \exp\Big(-\frac{i}{\hbar}\hat{h}(t)\Delta\Big)|\psi(t)\rangle + O(\Delta^2) \\
\Rightarrow \qquad |\psi(t)\rangle &= \underbrace{\lim_{\Delta\to 0}\left[\prod_{N-1}^{j=0} \exp\Big(-\frac{i}{\hbar}\hat{h}(t_j)\Delta\Big)\right]}_{\hat{U}(t,0)}|\psi(0)\rangle
\end{aligned} \tag{4.42}$$

where $t_j = j\Delta$ and $\Delta = t/N$.

I have introduced the product sign with the reversed positions of initial and final value of the running index to indicate that the terms are arranged in the opposite order than normal, namely

$$\prod_{j=0}^{N} X_j \stackrel{\text{def}}{=} X_1 X_2 \cdots X_N \qquad \text{and} \qquad \prod_{N}^{j=0} X_j \stackrel{\text{def}}{=} X_N X_{N-1} \cdots X_1 \tag{4.43}$$

Now comes the difficult point: It is desirable to combine the exponentials of Eq. 4.42 in a single exponential of an integral. For this purpose, I need the rule $e^a e^b = e^{a+b}$. This rule is valid for numbers, but not for operators that do not commutate. The reason is that a and b occur in different orders for the left-hand and the right-hand side. For the left-hand side

$$e^a e^b = \left(\sum_{n=0}^{\infty}\frac{1}{n!}a^n\right)\left(\sum_{m=0}^{\infty}\frac{1}{m!}b^m\right) \tag{4.44}$$

the terms a are always left of the terms b. For the right-hand side

$$e^{a+b} = \sum_{n=0}^{\infty}\frac{1}{n!}(a+b)^n \tag{4.45}$$

the terms a and b are in a different order.

This problem that $e^{\hat{a}+\hat{b}}$ differs from $e^{\hat{a}}e^{\hat{b}}$ for non-commutating operators $\hat{a}$ and $\hat{b}$, is solved by a simple trick: We simply define a recipe $\mathcal{T}_{ab}$ that places the $\hat{a}$ terms in every product of the expansion of $e^{\hat{a}+\hat{b}}$ in front of the $\hat{b}$ terms. This leads to the identity

$$e^{\hat{a}}e^{\hat{b}} = \mathcal{T}_{ab}e^{\hat{a}+\hat{b}} \tag{4.46}$$

For the problem at hand we need a recipe that arranges the Hamiltonians $h(t_j)$ in ascending order from right to left. This recipe is Dyson's time-ordering operator.

DYSON'S TIME-ORDERING OPERATOR

Dyson's time-ordering operator rearranges the operators in a product $\prod_j \hat{A}_j(t_j)$ such that they appear in increasing order from right to left.
Dyson's time-ordering operator $\mathcal{T}_D$ (named P-product in Eq. 29 of [56]) is

$$\mathcal{T}_D \hat{A}(t)\hat{B}(t') = \begin{cases} \hat{A}(t)\hat{B}(t') & \text{for } t \geq t' \\ \hat{B}(t')\hat{A}(t) & \text{for } t < t' \end{cases} \tag{4.47}$$

The time-ordering operator is not an operator in the conventional sense: Namely, it does not act on states in the Hilbert or Fock space to map them onto other states. Rather, it is a prescription for manipulating a mathematical expression.

Later, we will learn about another time-ordering operator, namely **Wick's time-ordering operator**[57] . Wick's time-ordering operator is similar to Dyson's time-ordering operator, but it introduces a sign change for every interchange of fermionic operators.

With the time-ordering operator, the propagator can be expressed as

$$\begin{aligned} \hat{U}(t,0) &\overset{\text{Eq. 4.42}}{=} \lim_{\Delta\to 0}\left[\prod_{N-1}^{j=0} \exp\Big(-\frac{i}{\hbar}\hat{h}(t_j)\Delta\Big)\right] \\ &= \mathcal{T}_D \lim_{\Delta\to 0}\left[\prod_{N-1}^{j=0} \exp\Big(-\frac{i}{\hbar}\hat{h}(t_j)\Delta\Big)\right] \\ &= \mathcal{T}_D \lim_{\Delta\to 0}\left[\exp\Big(-\frac{i}{\hbar}\sum_{j=0}^{N}\hat{h}(t_j)\Delta\Big)\right] \\ &= \mathcal{T}_D \exp\left(-\frac{i}{\hbar}\int_0^t dt\ \hat{h}(t)\right) \end{aligned} \tag{4.48}$$

With this, we arrived at the desired form Eq. 4.40 for the propagator as a time-ordered exponential.

Finally, we can express the Green's function in terms of a time-ordered exponential

GREEN'S FUNCTION AND TIME-ORDERED EXPONENTIAL

$$\hat{G}(t_2,t_1) \overset{\text{Eq. 4.38}}{=} \frac{1}{i\hbar}\theta(t_2-t_1)\mathcal{T}_D \exp\left(-\frac{i}{\hbar}\int_{t_1}^{t_2} dt'\ \hat{h}(t')\right) \tag{4.49}$$

4.4 Projected Density of States

So far, the Green's function is still a fairly abstract object. Let us therefore show a few physical quantities that can be obtained from the Green's function. With the density of states $\hat{D}(\epsilon)$, we gain access to the excitation spectrum of the Hamiltonian.

On the one hand, the projected **density of states** is an extremely useful quantity which can be obtained from the Green's function. On the other hand, the Green's function can be obtained from a known density of states $D(\epsilon)$.

The density of states has been defined discussed extensively in ΦSX: Introduction to solid-state

theory.[1][7]. The role of the density of states will be taken over by the **spectral function**, when we deal with interacting electron systems.

4.4.1 Density of states from the Green's function

PROJECTED DENSITY OF STATES

For a system with time-translation symmetry, the Green's function provides us with the **density of states**

$$\hat{D}(\epsilon) = \underbrace{\sum_n |\varphi_n\rangle\delta(\epsilon-\epsilon_n)\langle\varphi_n|}_{\sum_{\alpha,\beta}|\chi_\alpha\rangle D_{\alpha,\beta}(\epsilon)\langle\chi_\beta|} = -\frac{1}{2\pi i}\lim_{\eta\to 0^+}\left(\hat{G}(\epsilon+i\eta)-\hat{G}^\dagger(\epsilon+i\eta)\right). \tag{4.50}$$

This result follows[a] from the better known equation for the density of states projected onto a state $|\psi\rangle$, namely

$$D_\psi(\epsilon) = \sum_n \langle\psi|\varphi_n\rangle\delta(\epsilon-\epsilon_n)\langle\varphi_n|\psi\rangle \overset{\text{Eq. 4.22}}{=} -\frac{1}{\pi}\lim_{\eta\to 0^+}\mathrm{Im}[\langle\psi|\hat{G}(\epsilon+i\eta)|\psi\rangle] \tag{4.51}$$

[a] Eq. 4.50 follows from Eq. 4.51, because two operators are identical, when all conceivable expectation values are identical.

Proof of Eq. 4.51 In appendix A.5 on p. 388, we show that the imaginary part of a pole in the complex plane is a Lorentzian[8] and that the Lorentzian turns into a delta function when the pole approaches the real axis, that is

$$\lim_{\eta\to 0^+}\mathrm{Im}\left(-\frac{1}{\pi}\frac{1}{x+i\eta}\right) = \delta(x)\,. \tag{4.53}$$

This will be required in the following.

Let me begin the proof with the right-hand side of Eq. 4.51.

$$\begin{aligned}
-\frac{1}{\pi}\lim_{\eta\to 0^+}\mathrm{Im}\left(\langle\psi|\hat{G}(\epsilon+i\eta)|\psi\rangle\right) &\overset{\text{Eq. 4.22}}{=} -\frac{1}{\pi}\lim_{\eta\to 0^+}\mathrm{Im}\left(\sum_n\langle\psi|\varphi_n\rangle\frac{1}{\epsilon-\epsilon_n+i\eta}\langle\varphi_n|\psi\rangle\right)\\
&\overset{\langle\psi|\varphi_n\rangle\langle\varphi_n|\psi\rangle\in\mathbb{R}}{=} \sum_n\langle\psi|\varphi_n\rangle\left\{-\frac{1}{\pi}\lim_{\eta\to 0^+}\mathrm{Im}\left(\frac{1}{\epsilon-\epsilon_n+i\eta}\right)\right\}\langle\varphi_n|\psi\rangle\\
&\overset{\text{Eq. 4.53}}{=} \sum_n\langle\psi|\varphi_n\rangle\delta(\epsilon-\epsilon_n)\langle\varphi_n|\psi\rangle = \langle\psi|\hat{D}(\epsilon)|\psi\rangle \qquad \text{q.e.d.}
\end{aligned} \tag{4.54}$$

Thus, we arrived at the expression for the density of states projected onto the orbital $|\psi\rangle$. This concludes the proof of Eq. 4.51.

[7] The density of states is defined in Eq. 5.16 of ΦSX: Introduction to solid state physics. The projected density of states is defined in Eq. 5.23 therein.

[8] A Lorentzian is a function of the form

$$L_{\bar{\epsilon},\Gamma}(\epsilon) = \frac{1}{\pi}\frac{\frac{1}{2}\Gamma}{(\epsilon-\bar{\epsilon})^2+(\frac{1}{2}\Gamma)^2} \tag{4.52}$$

The function is normalized and has a peak at position $\bar{\epsilon}$ of width Γ. It is the prototypical spectral line shape. Editor: The definition here is consistent with https://mathworld.wolfram.com/LorentzianFunction.html. It differs from the definition in Eq. A.22 on p. 388 by a factor 2 in the width parameter.

Proof of Eq. 4.50 From Eq. 4.51 proven just before, we obtain

$$\begin{aligned}\langle\psi|\hat{D}(\epsilon)|\psi\rangle &= \sum_n \langle\psi|\varphi_n\rangle\delta(\epsilon-\epsilon_n)\langle\varphi_n|\psi\rangle \overset{\text{Eq. 4.51}}{=} -\frac{1}{\pi}\lim_{\eta\to 0^+}\mathrm{Im}[\langle\psi|\hat{G}(\epsilon+i\eta)|\psi\rangle] \\ &= -\frac{1}{\pi}\lim_{\eta\to 0^+}\frac{\langle\psi|\hat{G}(\epsilon+i\eta)|\psi\rangle - \langle\psi|\hat{G}(\epsilon+i\eta)|\psi\rangle^*}{2i} \\ &= \left\langle\psi\middle|\left\{-\frac{1}{\pi}\lim_{\eta\to 0^+}\frac{\hat{G}(\epsilon+i\eta)-\hat{G}^\dagger(\epsilon+i\eta)}{2i}\right\}\middle|\psi\right\rangle \end{aligned} \tag{4.55}$$

The equation above holds for any state $|\psi\rangle$. Now, I exploit that if an identity holds for arbitrary expectation values, then also the underlying operator identity holds.

This

$$\hat{D}(\epsilon) = \sum_n |\varphi_n\rangle\delta(\epsilon-\epsilon_n)\langle\varphi_n| = -\frac{1}{2\pi i}\lim_{\eta\to 0^+}\left(\hat{G}(\epsilon+i\eta)-\hat{G}^\dagger(\epsilon+i\eta)\right). \tag{4.56}$$

which proves Eq. 4.50.

4.4.2 Total density of states

The total density of states[9] can be obtained

$$\begin{aligned} D_{\text{tot}}(\epsilon) &\overset{\text{def}}{=} \sum_n \delta(\epsilon-\epsilon_n) \\ &= \sum_n \int d^4x\ \langle\vec{x}|\varphi_n\rangle\delta(\epsilon-\epsilon_n)\langle\varphi_n|\vec{x}\rangle \\ &\overset{\text{Eq. 4.51}}{=} -\frac{1}{\pi}\mathrm{Im}\left[\int d^4x\ \langle\vec{x}|\hat{G}(\epsilon+i\eta)|\vec{x}\rangle\right] \\ &= -\frac{1}{\pi}\lim_{\eta\to 0^+}\mathrm{Im}\Big(\mathrm{Tr}[\hat{G}(\epsilon+i\eta)]\Big) \end{aligned} \tag{4.57}$$

4.4.3 Electron density

Integration over the occupied states provides us with the probability that an electron is in a given orbital. The orbital $|\psi\rangle$ could also be $|\vec{x}\rangle$, in which case we obtain the electron density.

$$\begin{aligned} n(\vec{r}) &= \sum_\sigma\sum_n \int^{\epsilon_F} d\epsilon\ \langle\vec{r},\sigma|\varphi_n\rangle\delta(\epsilon-\epsilon_n)\langle\varphi_n|\vec{r},\sigma\rangle \\ &= -\frac{1}{\pi}\sum_\sigma \int^{\epsilon_F} d\epsilon\ \mathrm{Im}\left(\langle\vec{r},\sigma|\hat{G}(\epsilon)|\vec{r},\sigma\rangle\right) \end{aligned} \tag{4.58}$$

4.5 Green's function from the density of states

The density of states can be defined as an energy-dependent operator

$$\hat{D}(\epsilon) = \sum_n |\varphi_n\rangle\delta(\epsilon-\epsilon_n)\langle\varphi_n| \tag{4.59}$$

where $|\varphi_n\rangle$ and ϵ_n are eigenstates and eigenvalues of the Hamiltonian.

[9] The total density of states is defined in Eq. 5.22 of ΦSX: Introduction to solid state physics[1]

Because the Green's function is itself a sum over the states of the system, we can represent the Green's function in terms of the density of states. This implies that we should be able to work with the density of states or the spectral function as the fundamental quantity, from which the Green's function is constructed in the desired form when it is required.

GREEN'S FUNCTION FROM THE DENSITY OF STATES

With the density of states Eq. 4.59 the one-particle Green's function is

$$\hat{G}(t,t') \overset{\text{Eq. 4.17}}{=} \frac{1}{i\hbar} \int d\epsilon \, \hat{D}(\epsilon) \, \theta(t-t') \mathrm{e}^{-\frac{i}{\hbar}\epsilon(t-t')}$$

$$\hat{G}(\epsilon + i\eta) \overset{\text{Eq. 4.22}}{=} \int d\epsilon' \, \frac{\hat{D}(\epsilon')}{\epsilon - \epsilon' + i\eta} \tag{4.60}$$

4.6 Home study and practice

4.6.1 Role of boundary conditions

Editor: This needs to be done: show in an exercise why and how boundary conditions for Green's functions are considered

4.6.2 Green's function for a Lorentzian-shaped density of states

Introduction

The band structure $\bar{\epsilon}_n(\vec{k})$ of a solid describes the position of the poles of the Green's function. For a non-interacting system, the poles of the Green's function lie on the real axis. For every k-point, the k-resolved density of states, respectively the spectral function $\mathcal{A}(\epsilon, \vec{k})$, is a sequence of delta-peaks at the corresponding one-particle energies $\bar{\epsilon}_n(\vec{k})$.

$$\mathcal{A}(\epsilon, \vec{k}) = \sum_n \Omega \int \frac{d^3k}{(2\pi)^3} \delta(\epsilon - \bar{\epsilon}_n(\vec{k})) \tag{4.61}$$

As the interaction between the electrons is switched on, the electrons scatter at other electrons. As a result neither the energy nor the crystal momentum of the electron is a conserved quantity any more. A scattering process is described by annihilating the electron and by creating it again with a new energy and momentum. This implies that the electrons obtain a finite life time. The finite lifetime $\tau = \hbar/\Gamma(\vec{k})$ results in a broadening of the band structure. The poles of the Green's function move away from the real energy axis into the complex plane and the delta-peaks of the spectral functions turn into Lorentzians.

$$\mathcal{A}(\epsilon, \vec{k}) = \sum_n \Omega \int \frac{d^3k}{(2\pi)^3} \frac{1}{\pi} \frac{\Gamma_n(\vec{k})}{(\epsilon - \bar{\epsilon}_n(\vec{k}))^2 + \Gamma_n^2(k)} \tag{4.62}$$

As a result, each band obtains a width inversely proportional to its life time. Note, that the description via single poles breaks down, when the interaction become sufficiently strong.

The occurrence of finite lifetimes and the corresponding broadening of spectral densities is a general feature of systems coupled to a continuous spectrum of states. In this exercise, we will explore a single state with finite lifetime.

Problem

Exercise: A very general observation is that a finite line width of an absorption or emission band is related to a finite lifetime of an excitation. The prototypical shape of a band with a finite line width is a Lorentzian. Here we determine the corresponding Green's function.
A Lorentzian shaped density of states has the form

$$\langle\pi|\hat{D}(\epsilon)|\pi\rangle = \frac{1}{\pi}\frac{\Gamma}{(\epsilon-\bar{\epsilon})^2+\Gamma^2} \tag{4.63}$$

The density of states is normalized so that its weight integrated to one. The peak is centered at energy $\bar{\epsilon}$, and it has a **full-width-at-half-maximum** (**FWHM**)[a] of 2Γ.
The Green's function for the Lorentzian-shaped density of states has a surprisingly simple form of a single damped oscillation.

$$\langle\pi|\hat{G}(t,t')|\pi\rangle = \frac{1}{i\hbar}\theta(t-t')\mathrm{e}^{-\frac{i}{\hbar}(\bar{\epsilon}-i\Gamma)(t-t')} \tag{4.64}$$

This result can be represented by a single pole in the complex plane at $\epsilon = \bar{\epsilon} - i\Gamma$.
Problem:

1. Derive Eq. 4.64 from Eq. 4.63. (Hint: I used residue theorem.)
2. determine the Green's function in energy representation.

[a] The german expression for FWHM is *"Halbwertsbreite"*.

Discussion

1. Derive Eq. 4.64 from Eq. 4.63. (Hint: I used residue theorem.)

$$\begin{aligned}\langle\pi|G(t,t')|\pi\rangle &\overset{\text{Eq. 4.60}}{=} \frac{1}{i\hbar}\int d\epsilon\ \langle\pi|\hat{D}(\epsilon)|\pi\rangle\ \theta(t-t')\mathrm{e}^{-\frac{i}{\hbar}\epsilon(t-t')}\\ &\overset{\text{Eq. 4.63}}{=} \frac{1}{i\hbar}\int_{-\infty}^{\infty} d\epsilon\ \frac{1}{\pi}\frac{\Gamma}{(\epsilon-\bar{\epsilon})^2+\Gamma^2}\theta(t-t')\mathrm{e}^{-\frac{i}{\hbar}\epsilon(t-t')}\\ &= \theta(t-t')\frac{\Gamma}{i\pi\hbar}\int_{-\infty}^{\infty} d\epsilon\ \frac{1}{(\epsilon-\bar{\epsilon}+i\Gamma)(\epsilon-\bar{\epsilon}-i\Gamma)}\mathrm{e}^{-\frac{i}{\hbar}\epsilon(t-t')}\end{aligned} \tag{4.65}$$

These integrals can be solved with the **residue theorem**:

RESIDUE THEOREM

When $f(z)$ is holomorphic in the region Ω of the complex plane, i.e. $\frac{\partial f}{\partial z^*} = 0$, with the exception of discrete points, the counterclockwise integral about the boundary $\partial\Omega$ of Ω can be mapped to the sum of the residues of the poles in Ω.

$$\oint_{\partial\Omega} f(z) = 2\pi i\sum_j \mathrm{Res}_{z_j}[f] \tag{4.66}$$

The residual for a simple pole is $\mathrm{Res}_{z_j}[f] = \lim_{z\to z_j}(z-z_j)f(z)$.

The function $f(\epsilon) = \frac{1}{(\epsilon-\bar{\epsilon}+i\Gamma)(\epsilon-\bar{\epsilon}-i\Gamma)} e^{-\frac{i}{\hbar}\epsilon(t-t')}$ has two poles at $\epsilon = \bar{\epsilon} \mp \Gamma$. The residuals are

$$\begin{aligned} \text{Res}_{\bar{\epsilon}+i\Gamma}[f] &= \frac{1}{2i\Gamma} e^{-\frac{i}{\hbar}(\bar{\epsilon}+i\Gamma)(t-t')} \\ \text{Res}_{\bar{\epsilon}-i\Gamma}[f] &= \frac{-1}{2i\Gamma} e^{-\frac{i}{\hbar}(\bar{\epsilon}-i\Gamma)(t-t')} \end{aligned} \tag{4.67}$$

The exponential function $e^{-\frac{i}{\hbar}\epsilon(t-t')}$ damps out the function for $\text{Im}(\epsilon) \to -\infty$. Therefore, we choose a contour for the residual theorem, that proceeds along the real axis from $+R+\bar{\epsilon}$ to $-R+\bar{\epsilon}$ and closes via a half-circle passing through $-iR+\bar{\epsilon}$.

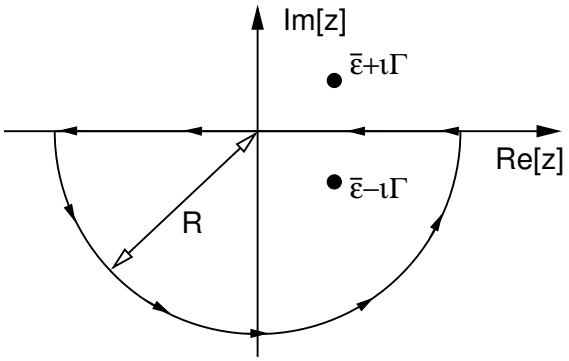

1. In the limit $R \to \infty$, the integral of the half circle goes to zero. This is because the function values fall off like $\frac{1}{R^2}$, while the length of the half-circle expands like πR. I describe the half-circle as $r(s) = \bar{\epsilon} + R\, e^{is} = \bar{\epsilon} + R\, \cos(s) + iR\, \sin(s)$

$$\left| \int_0^\pi ds\, \frac{dr}{ds} f(r(s)) \right| = \left| \int_0^\pi ds\, iR\, e^{is}\, \frac{1}{|r(s)-\bar{\epsilon}+i\Gamma|^2)} \underbrace{e^{-\frac{i}{\hbar}r(s)(t-t')}}_{\left|e^{-\frac{i}{\hbar}r(s)(t-t')}\right| \leq 1 \text{ for } \text{Im}(r(s))<0} \right| \tag{4.68}$$

$$\leq \left| \int_0^\pi ds\, iR\, e^{is}\, \frac{1}{R^2} \right| < \frac{\pi}{R} \to 0 \text{ for } R \to \infty \tag{4.69}$$

2. The integral along the closed contour is

$$\int_\gamma d\epsilon\, f(z) = 2\pi i \text{Res}_{\bar{\epsilon}-i\Gamma}[f] = \frac{-\pi}{\Gamma} e^{-\frac{i}{\hbar}(\bar{\epsilon}-i\Gamma)(t-t')} \tag{4.70}$$

3. Thus, the integral along the real axis in the positive direction is

$$\int_{-\infty}^{\infty} d\epsilon\, f(\epsilon) = \frac{\pi}{\Gamma} e^{-\frac{i}{\hbar}(\bar{\epsilon}-i\Gamma)(t-t')} \tag{4.71}$$

Combining this result with the prefactors, I obtain

$$\begin{aligned} \langle \pi | \hat{G}(t,t') | \pi \rangle &= \theta(t-t') \frac{\Gamma}{i\pi\hbar} \int_{-\infty}^{\infty} d\epsilon\, \frac{1}{(\epsilon-\bar{\epsilon}+i\Gamma)(\epsilon-\bar{\epsilon}-i\Gamma)} e^{-\frac{i}{\hbar}\epsilon(t-t')} \\ &= \theta(t-t') \frac{\Gamma}{i\pi\hbar} \frac{\pi}{\Gamma} e^{-\frac{i}{\hbar}(\bar{\epsilon}-i\Gamma)(t-t')} \\ &= \frac{1}{i\hbar} \theta(t-t') e^{-\frac{i}{\hbar}(\bar{\epsilon}-i\Gamma)(t-t')} \end{aligned} \tag{4.72}$$

2. determine the Green's function in energy representation.

The energy representation is obtained via Eq. 4.60. Simpler is however the direct back Fourier transform of the Green's function on the time domain.

$$\begin{aligned} G(\epsilon) &= \int dt\; G(t,0) e^{\frac{i}{\hbar}\epsilon t} \\ &= \int_{-\infty}^{\infty} dt \frac{1}{i\hbar}\theta(t) e^{-\frac{i}{\hbar}(\bar{\epsilon}-i\Gamma)t} e^{\frac{i}{\hbar}\epsilon t} \\ &= \int_{0}^{\infty} dt\; \frac{1}{i\hbar} e^{-\frac{i}{\hbar}(\bar{\epsilon}-\epsilon-i\Gamma)t} \\ &= \frac{1}{i\hbar}\; \frac{e^{-\frac{i}{\hbar}(\bar{\epsilon}-\epsilon-i\Gamma)t}}{-\frac{i}{\hbar}(\bar{\epsilon}-\epsilon-i\Gamma)}\Bigg|_0^{\infty} \\ &= \frac{1}{\epsilon-\bar{\epsilon}+i\Gamma} \end{aligned} \tag{4.73}$$

Thus, the Green's function has a single pole in the complex plane. The pole is displaced from the real energy axis by Γ.

Observations

1. Interesting is that such a complicated density of states such as a Lorentzian yields a simple result, namely a single harmonic contribution.
2. the Green's function falls off exponentially with time. It seems that a perturbation of the system dies out after a certain while, when it is characterized by Lorentzian peaks in the density of states.
3. The Lorentzian shaped density of states has infinite energy moments $\int d\epsilon\; D(\epsilon)(\epsilon-\bar{\epsilon})^n$ with $n \geq 2$. Editor: Discuss problems and how to cope with it.
4. Editor: Is the dynamics still unitary? This question requires the link to the propagator to be established.

Chapter 5

Composite and open systems: down-folding and retarded potentials

Deep down, the purpose of a Green's function is to describe the influence of one subsystem onto another or to describe the influence of an environment onto the system of interest. In many-particle physics, the environment is an electron gas, which affects the motion of electrons and holes in a solid. Let me therefore describe how the Green's function enters the description of open systems.

Consider a composite system consisting of two subsystems.

Examples:

- A molecule A adsorbed to a surface B. We can investigate the broadening of the molecular levels, and thus the spectroscopic properties of the adsorbed molecule.
- A material consisting of two spatially separated materials A and B with an interface in between.
- A traveling electron A that interacts with a phonon B. We may want to understand the transport properties of the electron in the presence of the phonon, which may act as an elastic or inelastic scattering center.
- A open system A in contact with an environment B, called a bath. This problem allows one to investigate questions such as decoherence, dephasing, loss of information.

The coupling may however be also more general: We may consider a finite set of one-particle orbitals to describe main features of a system. The subset of Fock space spanned by Slater determinants from these orbitals is system A. The one-particle orbitals orthogonal to those of subsystem A are used to define system B. The impact of the subsystem B can be incorporated into the description of system A just as an environment can be considered in a physical subsystem.

5.1 Systems in contact: down-folding

Let us consider a Hilbert space, which is divided into an important subspace $A = \{|\chi_\alpha^A\rangle\}$ and an unimportant subspace $B = \{|\chi_\alpha^B\rangle\}$. The subspace A may describe the system of interest, while the system B may describe the **environment**. The latter is often also called the **bath**.

We consider non-interacting electrons and a time-independent Hamiltonian. Furthermore, let me limit the discussion to orthonormal basissets $\{|\chi_\alpha\rangle\}$.

A one-particle wave function of the complete system is a superposition of the one-particle basis states of the system A of interest and the bath B.

$$|\psi\rangle = \sum_{\alpha\in A} |\chi^A_\alpha\rangle c^A_\alpha + \sum_{\beta\in B} |\chi^B_\beta\rangle c^B_\beta \tag{5.1}$$

The stationary Schrödinger equation has the form[1]

$$\begin{pmatrix} \boldsymbol{H}^{AA} - \epsilon \mathbf{1}^{AA} & \boldsymbol{V}^{AB} \\ \boldsymbol{V}^{BA} & \boldsymbol{H}^{BB} - \epsilon \mathbf{1}^{BB} \end{pmatrix} \begin{pmatrix} \vec{c}^A \\ \vec{c}^B \end{pmatrix} = 0 \tag{5.3}$$

with the norm

$$|\vec{c}^A|^2 + |\vec{c}^B|^2 = 1 \tag{5.4}$$

for an orthonormal basisset.

The Hamilton matrix elements are

$$\begin{aligned} H^{AA}_{\alpha,\beta} &= \langle \chi^A_\alpha | \hat{H} | \chi^A_\beta \rangle && \text{with } \alpha,\beta \in A \\ H^{BB}_{\alpha,\beta} &= \langle \chi^B_\alpha | \hat{H} | \chi^B_\beta \rangle && \text{with } \alpha,\beta \in B \\ V^{AB}_{\alpha,\beta} &= \langle \chi^A_\alpha | \hat{H} | \chi^B_\beta \rangle && \text{with } \alpha \in A,\ \beta \in B \\ V^{BA}_{\alpha,\beta} &= \langle \chi^B_\alpha | \hat{H} | \chi^A_\beta \rangle = \left(V^{A,B}_{\beta,\alpha}\right)^* && \text{with } \alpha \in B,\ \beta \in A \end{aligned} \tag{5.5}$$

The matrices $\mathbf{1}^{AA}$, $\mathbf{1}^{BB}$, $\mathbf{0}^{AB}$, and $\mathbf{0}^{BA}$ are the unit and zero-matrices in the respective subspaces.

Down-folding: From the second line of the Schrödinger equation Eq. 5.3, we obtain a relation that links $\vec{c}_B$ to $\vec{c}_A$.

$$\begin{aligned} & \boldsymbol{V}^{BA}\vec{c}^A + (\boldsymbol{H}^{BB} - \epsilon \mathbf{1}^{BB})\vec{c}^B = 0 \\ & \qquad \Rightarrow \qquad \vec{c}^B = (\epsilon \mathbf{1}^{BB} - \boldsymbol{H}^{BB})^{-1} \boldsymbol{V}^{BA}\vec{c}^A \overset{\text{Eq. 4.23}}{=} \bar{\boldsymbol{G}}^{BB}(\epsilon)\boldsymbol{V}^{BA}\vec{c}^A \end{aligned} \tag{5.6}$$

where

$$\bar{\boldsymbol{G}}^{BB}(\epsilon) \overset{\text{def}}{=} (\epsilon \mathbf{1}^{BB} - \boldsymbol{H}^{BB})^{-1} \tag{5.7}$$

is the Green's function of the isolated bath, i.e. of system B. The bar on-top of the symbol for the **bath Green's function** distinguishes it from the BB matrix elements of the Green's function for the entire system.

---

[1]

$$\left(\begin{array}{cccc|ccc} H^{AA}_{1,1}-\epsilon & H^{AA}_{1,2} & \dots & H^{AA}_{1,M} & V^{AB}_{1,1} & \dots & V^{AB}_{1,N} \\ H^{AA}_{2,1} & H^{AA}_{2,2}-\epsilon & \dots & H^{AA}_{2,M} & V^{AB}_{2,1} & \dots & V^{AB}_{2,N} \\ \vdots & \vdots & \ddots & \vdots & \vdots & \ddots & \vdots \\ H^{AA}_{M,1} & H^{AA}_{M,2} & \dots & H^{AA}_{M,M}-\epsilon & V^{AB}_{M,1} & \dots & V^{AB}_{M,N} \\ \hline V^{BA}_{1,1} & V^{BA}_{1,2} & \dots & V^{BA}_{1,M} & H^{BB}_{1,1}-\epsilon & \dots & H^{BB}_{1,N} \\ \vdots & \vdots & \ddots & \vdots & \vdots & \ddots & \vdots \\ V^{BA}_{N,1} & V^{BA}_{N,2} & \dots & V^{BA}_{N,M} & H^{BB}_{N,1} & \dots & H^{BB}_{N,N}-\epsilon \end{array}\right) \left(\begin{array}{c} c^A_1 \\ c^A_2 \\ \vdots \\ c^A_M \\ \hline c^B_1 \\ \vdots \\ c^N_M \end{array}\right) = 0 \tag{5.2}$$

The wave function $|\psi\rangle$ of the complete system can be represented by energy-dependent orbitals $|\tilde{\chi}^A_\alpha\rangle$ from system A

$$\begin{aligned}
|\psi\rangle &= \sum_{\alpha\in A}|\chi^A_\alpha\rangle c^A_\alpha + \sum_{\beta\in B}|\chi^B_\beta\rangle c^B_\beta \\
&\overset{\text{Eq. 5.6}}{=} \sum_{\alpha\in A}|\chi^A_\alpha\rangle c^A_\alpha + \sum_{\beta\in B}|\chi^B_\beta\rangle \underbrace{\sum_{\alpha\in A}\sum_{\gamma\in B}\bar{G}^{BB}_{\beta,\gamma}(\epsilon)V^{BA}_{\gamma,\alpha}c^A_\alpha}_{c^B_\beta} \\
&= \sum_{\alpha\in A}\underbrace{\left(|\chi^A_\alpha\rangle + \sum_{\beta\in B}|\chi^B_\beta\rangle\sum_{\gamma\in B}\bar{G}^{BB}_{\beta,\gamma}(\epsilon)V^{BA}_{\gamma,\alpha}\right)}_{|\tilde{\chi}^A_\alpha(\epsilon)\rangle}c^A_\alpha \\
&= \sum_{\alpha\in A}|\tilde{\chi}^A_\alpha(\epsilon)\rangle c^A_\alpha
\end{aligned} \tag{5.8}$$

The energy-dependent orbitals $|\tilde{\chi}^A_\alpha\rangle$ have the contribution of the environment glued on, that is they leak into the environment.

ORBITALS WITH DOWN-FOLDED ENVIRONMENT

$$\begin{aligned}
|\tilde{\chi}^A_\alpha(\epsilon)\rangle &\overset{\text{def}}{=} |\chi^A_\alpha\rangle + \sum_{\beta,\gamma\in B}|\chi^B_\beta\rangle\bar{G}^{BB}_{\beta,\gamma}(\epsilon)V^{BA}_{\gamma,\alpha} \qquad \text{for } \alpha\in A \\
&= \Big(\hat{1} + \sum_{\beta,\gamma\in B,\delta\in A}|\chi^B_\beta\rangle\bar{G}^{BB}_{\beta,\gamma}(\epsilon)V^{BA}_{\gamma,\delta}\langle\pi_\delta|\Big)|\chi^A_\alpha\rangle \qquad \text{for } \alpha\in A
\end{aligned} \tag{5.9}$$

where $\langle\pi_\delta|\chi_\alpha\rangle = \delta_{\delta,\alpha}$.

Equation for the coefficients in A: The result Eq. 5.6 for the wave-function coefficients $\vec{c}^B$ in subsystem B is inserted into back into the first line of the Schrödinger equation Eq. 5.3

$$\begin{aligned}
&(\boldsymbol{H}^{AA} - \epsilon\mathbf{1}^{AA})\vec{c}^A + \boldsymbol{V}^{AB}\vec{c}^B = 0 \\
\overset{\text{Eq. 5.6}}{\Rightarrow} \quad &\Big[\underbrace{\boldsymbol{H}^{AA} + \boldsymbol{V}^{AB}\bar{\boldsymbol{G}}^{BB}(\epsilon)\boldsymbol{V}^{BA}}_{\boldsymbol{M}(\epsilon)} - \epsilon\mathbf{1}^{AA}\Big]\vec{c}^A = 0 \\
\overset{\text{Eq. 5.12}}{\Rightarrow} \quad &\Big[\boldsymbol{M}(\epsilon) - \epsilon\mathbf{1}^{AA}\Big]\vec{c}^A = 0
\end{aligned} \tag{5.10}$$

DOWN-FOLDED WAVE-FUNCTION EQUATION

The energies ϵ and corresponding wave-function coefficients $\vec{c}^A$, in the energy-dependent basis set Eq. 5.9, are obtained from

$$\left[\boldsymbol{M}(\epsilon) - \epsilon \mathbf{1}^{AA}\right] \vec{c}^A = 0 \tag{5.11}$$

where

$$\boldsymbol{M}(\epsilon) \stackrel{\text{def}}{=} \boldsymbol{H}^{AA} + \underbrace{\boldsymbol{V}^{AB} \bar{\boldsymbol{G}}^{BB}(\epsilon) \boldsymbol{V}^{BA}}_{\boldsymbol{\Sigma}^{AA}(\epsilon)} \tag{5.12}$$

If Eq. 5.11 has a solution $\vec{c}^A$ for a given energy ϵ, the wave function

$$|\psi\rangle = \sum_{\alpha \in A} |\tilde{\chi}^A_\alpha(\epsilon)\rangle c^A_\alpha \tag{5.13}$$

solves the Schrödinger equation for the complete system with that energy. The orbitals $|\tilde{\chi}^A_\alpha(\epsilon)\rangle$ have contributions, both, in A and in B. For a normalized wave function $|\psi\rangle$, the norm $\sum_{\alpha \in A} |\vec{c}^A_\alpha|^2$ of vector $\vec{c}^A$ differs usually from 1.

In order to obtain a solution for Eq. 5.11, one needs to find those energies for which $\boldsymbol{M}(\epsilon) - \epsilon \mathbf{1}^{AA}$ has a zero eigenvalue. This is the case, when the determinant $\det[\boldsymbol{M}(\epsilon) - \epsilon \mathbf{1}^{AA}]$ vanishes. For an energy-independent matrix $\boldsymbol{M}$, this is equivalent to solving the characteristic equation for the energy levels. For an energy-dependent $\boldsymbol{M}(\epsilon)$, one needs to calculate the determinant as function of energy, and, when a zero is encountered, to determine the eigenvector of $\boldsymbol{M}(\epsilon) - \epsilon \mathbf{1}^{AA}$ with eigenvalue zero, respectively the eigenvector of $\boldsymbol{M}(\epsilon)$ with energy ϵ. This procedure quickly becomes a difficult task for larger systems.

Eq. 5.11 looks like a Schrödinger equation with an energy-dependent Hamiltonian $\boldsymbol{M}(\epsilon)$. On the positive side, the size of the matrix equation corresponds to only the subsystem A, which is usually much smaller than the complete system. On the negative side, the matrix equation has, unlike the Schrödinger equation, a non-linear energy dependence. As defined in Eq. 5.12, $\boldsymbol{M}(\epsilon)$ appears like a Hamiltonian with an energy-dependent potential. This potential is called the **self energy** $\boldsymbol{\Sigma}^{AA}(\epsilon)$.

SELF ENERGY DESCRIBING THE COUPLING TO A BATH

$$\boldsymbol{\Sigma}^{AA}(\epsilon) \stackrel{\text{def}}{=} \boldsymbol{V}^{AB} \bar{\boldsymbol{G}}^{BB}(\epsilon) \boldsymbol{V}^{BA} \tag{5.14}$$

$\bar{\boldsymbol{G}}^{BB}$ is the Green's function of the isolated subsystem B.

The self energy will play an important, and more general, role in the Green's functions world.

Role of the self energy

Editor: Relate the self energy to level repulsion and lifetime. Use a one-pole model $G(\hbar\omega) = 1/[\hbar\omega - \epsilon + i\Gamma]$. Real part produced energy level shift, Imaginary part produces broadening. This may not be the best place for this discussion.

5.1.1 Effective Schrödinger equation for an embedded system:

One should resist the impetus to simply drop the energy dependence of $\boldsymbol{M}(\epsilon)$ and interprete Eq. 5.11 as an approximate Schrödinger equation. With little extra effort, one can solve a linear-algebraic problem, which is substantially more accurate and that preserves a lot of the physical content of the

non-linear equation Eq. 5.11. In this section, I describe how we arrive at an Schrödinger equation of an open system. This Schrödinger equation is approximate, but in many cases already quite accurate. In this section, I will also show different ways to arrive at this very same Schrödinger equation. Each of these routes emphasizes a different physical aspect of the problem. In practice you will encounter these as seemingly distinct methodologies. It is useful to understand that and how they are related.

Editor: Is it simpler, to first linearize the equation and then show that Hamilton and overlap matrices coincide with the matrix elements with orbitals at fixed energies?

Approximation of an energy-independent basisset

Despite the similarity, Eq. 5.11 also has a fundamental difference to the Schrödinger equation, namely that the normalization of the vector $\vec{c}^A$ needs to consider the bath contribution. In this section, we will show the relation to the Schrödinger equation. Here the normalization is taken into account by an overlap matrix.

In order to make the connection of Eq. 5.12 with a Schrödinger equation evident, let us work out[2] the Hamiltonian and the overlap matrix for the energy-dependent basisset defined in Eq. 5.9.

$$
\begin{aligned}
\tilde{H}_{\alpha,\beta}(\epsilon) &\overset{\text{def}}{=} \langle\tilde{\chi}^A_\alpha|\hat{H}|\tilde{\chi}^A_\beta\rangle \\
&\overset{\text{Eq. 5.9}}{=} \left(\langle\chi^A_\alpha| + \sum_\gamma \left(\boldsymbol{V}^{AB}\bar{\boldsymbol{G}}^{BB}(\epsilon)\right)_{\alpha,\gamma}\langle\chi^B_\gamma|\right)\hat{H}\left(|\chi^A_\beta\rangle + \sum_\delta |\chi^B_\delta\rangle\left(\bar{\boldsymbol{G}}^{BB}(\epsilon)\boldsymbol{V}^{BA}\right)_{\delta,\beta}\right) \\
&\overset{\text{Eq. 5.5}}{=} \left(\boldsymbol{H}^{AA} + 2\boldsymbol{V}^{AB}\bar{\boldsymbol{G}}^{BB}(\epsilon)\boldsymbol{V}^{BA} + \boldsymbol{V}^{AB}\bar{\boldsymbol{G}}^{BB}(\epsilon)\underbrace{\boldsymbol{H}^{BB}}_{\epsilon\mathbf{1}-\underbrace{(\epsilon\mathbf{1}-\boldsymbol{H}^{BB})}_{(G^{BB})^{-1}}}\bar{\boldsymbol{G}}^{BB}(\epsilon)\boldsymbol{V}^{BA}\right)_{\alpha,\beta} \\
&\overset{\text{Eq. 5.7}}{=} \left(\boldsymbol{H}^{AA} + \boldsymbol{V}^{AB}\bar{\boldsymbol{G}}^{BB}(\epsilon)\boldsymbol{V}^{BA} + \epsilon\,\boldsymbol{V}^{AB}\left(\bar{\boldsymbol{G}}^{BB}(\epsilon)\right)^2\boldsymbol{V}^{BA}\right)_{\alpha,\beta} \qquad (5.15) \\
\tilde{O}_{\alpha,\beta}(\epsilon) &\overset{\text{def}}{=} \langle\tilde{\chi}^A_\alpha|\tilde{\chi}^A_\beta\rangle \\
&\overset{\text{Eq. 5.9}}{=} \left(\langle\chi^A_\alpha| + \sum_\gamma \left(\boldsymbol{V}^{AB}\bar{\boldsymbol{G}}^{BB}(\epsilon)\right)_{\alpha,\gamma}\langle\chi^B_\gamma|\right)\left(|\chi^A_\beta\rangle + \sum_\delta |\chi^B_\delta\rangle\left(\bar{\boldsymbol{G}}^{BB}(\epsilon)\boldsymbol{V}^{BA}\right)_{\delta,\beta}\right) \\
&\overset{\text{Eq. 5.5}}{=} \left(\mathbf{1}^{AA} + \boldsymbol{V}^{AB}\left(\bar{\boldsymbol{G}}^{BB}(\epsilon)\right)^2\boldsymbol{V}^{BA}\right)_{\alpha,\beta} \qquad (5.16)
\end{aligned}
$$

Now, we fix the energy defining the orbitals to a specific value ϵ_ν and write down the resulting Schrödinger equation.

$$
\left[\tilde{\boldsymbol{H}}(\epsilon_\nu) - \epsilon\,\tilde{\boldsymbol{O}}(\epsilon_\nu)\right]\vec{c}^A = 0 \qquad (5.17)
$$

This expression is approximate, because it ignores the energy dependence of the basis states $|\tilde{\chi}^A_\alpha(\epsilon)\rangle$ of Eq. 5.9. No other approximations are made.

Taylor expansion in the energy

Below, I will show that the very same Schrödinger equation as Eq. 5.17 can also be obtained from a Taylor expansion of $\boldsymbol{M}(\epsilon) - \epsilon\mathbf{1}^{AA}$ to first order in the energy.

[2] We use that the Green's function $\bar{\boldsymbol{G}}^{BB}(\epsilon)$ is hermitian, which follows from the defining equation.

EFFECTIVE SCHRÖDINGER EQUATION

Eq. 5.11 for the energies and wave functions can be linearized by discarding non-linear terms in $\epsilon-\epsilon_\nu$. An approximate Schrödinger equation is obtained

$$\Bigg[\underbrace{\Big(\boldsymbol{M}(\epsilon_\nu)-\epsilon_\nu \mathbf{1}^{AA}\Big)}_{\tilde{\boldsymbol{H}}(\epsilon_\nu)-\epsilon_\nu\tilde{\boldsymbol{O}}(\epsilon_\nu)\text{ (Eq. 5.23)}} +(\epsilon-\epsilon_\nu)\underbrace{\left.\frac{d(\boldsymbol{M}(\epsilon)-\epsilon\mathbf{1}^{AA})}{d\epsilon}\right|_{\epsilon_\nu}}_{-\tilde{\boldsymbol{O}}(\epsilon_\nu)\text{ (Eq. 5.25)}}\Bigg]\vec{c}^{A} \overset{\text{Eqs. 5.21,5.22}}{=} \Big[\tilde{\boldsymbol{H}}(\epsilon_\nu)-\epsilon\,\tilde{\boldsymbol{O}}(\epsilon_\nu)\Big]\vec{c}^{A} \underbrace{\approx 0}_{=O\left((\epsilon-\epsilon_\nu)^2\right)} \tag{5.18}$$

with the normalization

$$\vec{c}^{A,*}\tilde{\boldsymbol{O}}(\epsilon_\nu)\vec{c}^{A}=1 \tag{5.19}$$

The eigenvector $\vec{c}^{A}$ defines the wave function $|\psi\rangle$ via

$$|\psi\rangle=\sum_{\alpha\in A}|\tilde{\chi}^{A}_{\alpha}(\epsilon_\nu)\rangle c^{A}_{\alpha} \tag{5.20}$$

with orbitals defined by Eq. 5.9.

The (approximate) equation Eq. 5.18 is of fundamental importance. It describes the down-folding of the environment contribution into the description of an effective system, which is of the size of the system of interest. Down-folding leads at first to an equation (Eq. 5.11) that is non-linear in the energy. This nonlinear problem is mapped approximately onto an eigenvalue problem (Eq. 5.18), which can be solved with standard methods from linear algebra.

DOWN-FOLDED HAMILTON- AND OVERLAP MATRICES FROM SELF ENERGY

The energy-dependent matrix $\boldsymbol{M}(\epsilon) \overset{\text{Eq. 5.12}}{=} \boldsymbol{H}^{AA}+\boldsymbol{\Sigma}^{AA}(\epsilon)$ determines the downfolded Hamilton- and overlap matrices by

$$\tilde{H}_{\alpha,\beta}(\epsilon_\nu) \overset{\text{def}}{=} \big\langle\tilde{\chi}^{A}_{\alpha}(\epsilon_\nu)\big|\hat{H}\big|\tilde{\chi}^{A}_{\beta}(\epsilon_\nu)\big\rangle \overset{\text{Eq. 5.23}}{=} M_{\alpha,\beta}(\epsilon_\nu)-\epsilon_\nu\left.\frac{dM_{\alpha,\beta}}{d\epsilon}\right|_{\epsilon_\nu} \tag{5.21}$$

$$\tilde{O}_{\alpha,\beta}(\epsilon_\nu) \overset{\text{def}}{=} \big\langle\tilde{\chi}^{A}_{\alpha}(\epsilon_\nu)\big|\tilde{\chi}^{A}_{\beta}(\epsilon_\nu)\big\rangle \overset{\text{Eq. 5.25}}{=} \delta_{\alpha,\beta}-\left.\frac{dM_{\alpha,\beta}}{d\epsilon}\right|_{\epsilon_\nu} \tag{5.22}$$

The matrix elements include the environment (B) contribution.

The two identities needed to prove the identity Eq. 5.18, respectively Eqs. 5.21, 5.22, are derived below in Eq. 5.23 and Eq. 5.25.

1. Firstly, we show the identity for $\epsilon=\epsilon_\nu$. We use the definitions for Hamiltonian Eq. 5.15 and

overlap matrix Eq. 5.16.

$$\begin{aligned}\tilde{\boldsymbol{H}}(\epsilon)-\epsilon\tilde{\boldsymbol{O}}(\epsilon) &= \overbrace{\left(\boldsymbol{H}^{AA}+2\boldsymbol{V}^{AB}\bar{\boldsymbol{G}}^{BB}(\epsilon)\boldsymbol{V}^{BA}+\boldsymbol{V}^{AB}\bar{\boldsymbol{G}}^{BB}(\epsilon)\boldsymbol{H}^{BB}\bar{\boldsymbol{G}}^{BB}(\epsilon)\boldsymbol{V}^{BA}\right)}^{\tilde{\boldsymbol{H}}(\epsilon)\text{ (Eq. 5.15)}} \\ &\quad -\epsilon\underbrace{\left(\mathbf{1}^{AA}+\boldsymbol{V}^{AB}\left(\bar{\boldsymbol{G}}^{BB}(\epsilon)\right)^2\boldsymbol{V}^{BA}\right)}_{\tilde{\boldsymbol{O}}(\epsilon)\text{ (Eq. 5.16)}} \\ &= \left(\boldsymbol{H}^{AA}-\epsilon\mathbf{1}^{AA}\right)+2\boldsymbol{V}^{AB}\bar{\boldsymbol{G}}^{BB}(\epsilon)\boldsymbol{V}^{BA}+\boldsymbol{V}^{AB}\bar{\boldsymbol{G}}^{BB}(\epsilon)\underbrace{\underbrace{\left(\boldsymbol{H}^{BB}-\epsilon\mathbf{1}^{BB}\right)}_{-\bar{\boldsymbol{G}}^{-1}(\epsilon)}\bar{\boldsymbol{G}}^{BB}(\epsilon)}_{=-\mathbf{1}^{BB}}\boldsymbol{V}^{BA} \\ &= \left(\boldsymbol{H}^{AA}-\epsilon\mathbf{1}^{AA}\right)+\boldsymbol{V}^{AB}\bar{\boldsymbol{G}}^{BB}(\epsilon)\boldsymbol{V}^{BA}\overset{\text{Eq. 5.12}}{=}\boldsymbol{M}(\epsilon)-\epsilon\mathbf{1}^{AA}\end{aligned} \tag{5.23}$$

2. Now, we determine [3]the energy derivative of $\boldsymbol{M}(\epsilon)-\epsilon\mathbf{1}$

$$\begin{aligned}\frac{d(\boldsymbol{M}(\epsilon)-\epsilon\mathbf{1}^{AA})}{d\epsilon} &\overset{\text{Eq. 5.12}}{=} \boldsymbol{V}^{AB}\underbrace{\frac{d\left(\epsilon\mathbf{1}^{BB}-\boldsymbol{H}^{BB}\right)^{-1}}{d\epsilon}}_{d\bar{\boldsymbol{G}}^{BB}(\epsilon)/d\epsilon}\boldsymbol{V}^{BA}-\mathbf{1}^{AA} \\ &= -\mathbf{1}^{AA}+\boldsymbol{V}^{AB}\left[-\underbrace{\left(\epsilon\mathbf{1}^{BB}-\boldsymbol{H}^{BB}\right)^{-1}}_{\bar{\boldsymbol{G}}^{BB}(\epsilon)}\underbrace{\frac{d\left(\epsilon\mathbf{1}^{BB}-\boldsymbol{H}^{BB}\right)}{d\epsilon}}_{\mathbf{1}^{BB}}\underbrace{\left(\epsilon\mathbf{1}^{BB}-\boldsymbol{H}^{BB}\right)^{-1}}_{\bar{\boldsymbol{G}}^{BB}(\epsilon)}\right]\boldsymbol{V}^{BA} \\ &= -\left[\mathbf{1}^{AA}+\boldsymbol{V}^{AB}\left(\bar{\boldsymbol{G}}^{BB}(\epsilon)\right)^2\boldsymbol{V}^{BA}\right]\overset{\text{Eq. 5.16}}{=}-\tilde{\boldsymbol{O}}(\epsilon)\end{aligned} \tag{5.25}$$

This completes the proof of Eq. 5.18

Energies accurate to second order in $(\epsilon-\epsilon_\nu)$**:** In order to judge the accuracy of the Schrödinger equation, we need to investigate the error introduced by the first-order Taylor expansion in energy. We will see, that the error in the energy is of second order in $(\epsilon-\epsilon_\nu)$.

I start from the assumption that the error of the eigenvector $\vec{c}^A$ is of first order in $(\epsilon-\epsilon_\nu)$. This is a reasonable assumption because the result is correct for $\epsilon=\epsilon_\nu$.

The energy can be obtained from the Schrödinger equation as

$$\left[\tilde{\boldsymbol{H}}-\epsilon\tilde{\boldsymbol{O}}\right]\vec{c}^A=0 \quad\Rightarrow\quad \vec{c}^{A*}\left[\tilde{\boldsymbol{H}}-\epsilon\tilde{\boldsymbol{O}}\right]\vec{c}^A=0 \quad\Rightarrow\quad \epsilon=\frac{\vec{c}^{A*}\tilde{\boldsymbol{H}}\vec{c}^A}{\vec{c}^{A*}\tilde{\boldsymbol{O}}\vec{c}^A} \tag{5.26}$$

Next, we consider the energy as a functional of the vector $\vec{c}^A$. We will see that the energy depends only to second order on an error in the $\vec{c}^A$. Given that that $\vec{c}^A$ is accurate to first order in $\epsilon-\epsilon_\nu$,

[3]The derivative of an inverse matrix is

$$\frac{d\boldsymbol{A}^{-1}(x)}{dx}=-\boldsymbol{A}^{-1}(x)\frac{d\boldsymbol{A}(x)}{dx}\boldsymbol{A}^{-1}(x) \tag{5.24}$$

This relation is obtained by forming the derivative of $\boldsymbol{A}(x)\boldsymbol{A}^{-1}(x)=\mathbf{1}$.

this will show that the energy is only sensitive to second order in $\epsilon - \epsilon_\nu$.

$$\begin{aligned}
\delta\epsilon &= \epsilon + (\delta\vec{c}^A)^* \left[\frac{\tilde{\boldsymbol{H}}\vec{c}^A}{\vec{c}^{A*}\tilde{\boldsymbol{O}}\vec{c}^A} - \frac{\tilde{\boldsymbol{O}}\vec{c}^A \left(\vec{c}^{A*}\tilde{\boldsymbol{H}}\vec{c}^A \right)}{\left(\vec{c}^{A*}\tilde{\boldsymbol{O}}\vec{c}^A \right)^2} \right] + \left[\cdots \right] \delta\vec{c}^A + O((\delta\vec{c}^A)^2) \\
&= \epsilon + \delta\vec{c}^{A*} \left[\frac{\tilde{\boldsymbol{H}}\vec{c}^A}{\vec{c}^{A*}\tilde{\boldsymbol{O}}\vec{c}^A} - \frac{\tilde{\boldsymbol{O}}\vec{c}^A \left(\vec{c}^{A*}\tilde{\boldsymbol{O}}\vec{c}^A\, \epsilon \right)}{\left(\vec{c}^{A*}\tilde{\boldsymbol{O}}\vec{c}^A \right)^2} \right] + \left[\cdots \right] \delta\vec{c}^A + O((\delta\vec{c}^A)^2) \\
&= \epsilon + \frac{\delta\vec{c}^{A*} \overbrace{\left(\tilde{\boldsymbol{H}} - \epsilon\tilde{\boldsymbol{O}} \right)\vec{c}^A}^{=0}}{\vec{c}^{A*}\tilde{\boldsymbol{O}}\vec{c}^A} + \frac{\overbrace{\vec{c}^{A*}\left(\tilde{\boldsymbol{H}} - \epsilon\tilde{\boldsymbol{O}} \right)}^{=0}\delta\vec{c}^A}{\vec{c}^{A*}\tilde{\boldsymbol{O}}\vec{c}^A} + O((\delta\vec{c}^A)^2) \\
&= \epsilon + O((\delta\vec{c}^A)^2) = \epsilon + O((\epsilon - \epsilon_\nu)^2)
\end{aligned} \tag{5.27}$$

Limitations

While the non-linear equation Eq. 5.11 is exact, the Schrödinger equation Eq. 5.18 is only approximate. It is valid in an energy region around the expansion energy ϵ_ν.

Convergence radius: The Taylor expansion has one important caveat: Every Taylor expansion has a convergence radius beyond which the Taylor expansion does no more converge to the correct result. Usually, the convergence radius is given by the distance of the next pole or discontinuity from the expansion point. In the present case, the eigenstates of the isolated subsystem B introduce a singularity into the Green's function $\bar{\boldsymbol{G}}^{BB}$. Thus, the Taylor expansion will usually be reliable within a band gap of the bath B, but the validity will not reach beyond the band edges of its spectrum.

Contact with Green's functions

In this section on embedding, we encountered already a number of relations that are fundamental to the Green's-function formalism.

- One central quantity is the self energy defined in Eq. 5.14. On the one hand, the downfolding of a subsystem (B) introduces an additional energy-dependent potential acting on A. On the other hand, the coupling V^{AB}, V^{BA}, enters only as part of the self energy.
- Below, in Eq. 5.40, we will see that $\boldsymbol{M}(\epsilon)$ is directly related to the Green's function projected onto the system of interest, namely

$$\epsilon \mathbf{1}^{AA} - \boldsymbol{M}(\epsilon) \overset{\text{Eq. 5.40}}{=} \left(\boldsymbol{G}^{AA}(\epsilon) \right)^{-1} \tag{5.28}$$

- We can use the two relations Eq. 5.25 and Eq. 5.23 together with Eq. 5.28 to extract the effective Hamiltonian from the Green's function

$$\begin{aligned}
\tilde{\boldsymbol{H}}(\epsilon) &= \epsilon \frac{d\left(\boldsymbol{G}^{AA}(\epsilon) \right)^{-1}}{d\epsilon} - \left(\boldsymbol{G}^{AA}(\epsilon) \right)^{-1} \\
\tilde{\boldsymbol{O}}(\epsilon) &= \frac{d\left(\boldsymbol{G}^{AA}(\epsilon) \right)^{-1}}{d\epsilon}
\end{aligned} \tag{5.29}$$

5.2 Green's function of a system coupled to a bath

In the previous section, the embedding has been described based on wave functions. We have seen how the Green's function of the bath enters in the description. A quantity of central importance

has been the matrix $\boldsymbol{M}(\epsilon)$. We mentioned already that this matrix is closely related to $G^{AA}(\epsilon)$, the Green's function for the entire system projected on the system of interest. While the wave-function based description is more transparent, I want translate the same into the more abstract language of Green's functions.

One of the main advantages of the Green's-function formalism is that Green's functions are modular building blocks, that can be stacked together to construct the Green's function for more complex systems.

5.2.1 Coupling to a bath in the energy domain

Let me express the equation defining the Green's function for a composite system. We use the same notation as in the previous section.

$$\begin{pmatrix} \epsilon \mathbf{1}^{AA} - \boldsymbol{H}^{AA} & -\boldsymbol{V}^{AB} \\ -\boldsymbol{V}^{BA} & \epsilon \mathbf{1}^{BB} - \boldsymbol{H}^{BB} \end{pmatrix} \begin{pmatrix} \boldsymbol{G}^{AA}(\epsilon) & \boldsymbol{G}^{AB}(\epsilon) \\ \boldsymbol{G}^{BA}(\epsilon) & \boldsymbol{G}^{BB}(\epsilon) \end{pmatrix} \overset{\text{Eq. 4.23}}{=} \begin{pmatrix} \mathbf{1}^{AA} & \mathbf{0}^{AB} \\ \mathbf{0}^{BA} & \mathbf{1}^{BB} \end{pmatrix} \tag{5.30}$$

After performing the matrix multiplication, we select the two equations, which contain both, $\boldsymbol{G}^{AA}(\epsilon)$ and $\boldsymbol{G}^{BA}(\epsilon)$. One equation expresses $\boldsymbol{G}^{BA}(\epsilon)$ by $\boldsymbol{G}^{AA}(\epsilon)$

$$\begin{aligned} -\boldsymbol{V}^{BA}\boldsymbol{G}^{AA}(\epsilon) + \left(\epsilon \mathbf{1}^{BB} - \boldsymbol{H}^{BB}\right)\boldsymbol{G}^{BA}(\epsilon) &\overset{\text{Eq. 5.30}}{=} \mathbf{0}^{BA} \\ \Rightarrow \qquad \boldsymbol{G}^{BA}(\epsilon) &= \left(\epsilon \mathbf{1}^{BB} - \boldsymbol{H}^{BB}\right)^{-1} \boldsymbol{V}^{BA}\boldsymbol{G}^{AA}(\epsilon) \end{aligned} \tag{5.31}$$

The result is used to eliminate $\boldsymbol{G}^{BA}(\epsilon)$ from the other equation

$$\begin{aligned} \left(\epsilon \mathbf{1}^{AA} - \boldsymbol{H}^{AA}\right)\boldsymbol{G}^{AA}(\epsilon) - \boldsymbol{V}^{AB}\boldsymbol{G}^{BA}(\epsilon) &\overset{\text{Eq. 5.30}}{=} \mathbf{1}^{AA} \\ \Rightarrow \qquad \Big(\underbrace{\epsilon \mathbf{1}^{AA} - \boldsymbol{H}^{AA}}_{[\bar{\boldsymbol{G}}^{AA}(\epsilon)]^{-1}} - \underbrace{\boldsymbol{V}^{AB}\left(\epsilon \mathbf{1}^{BB} - \boldsymbol{H}^{BB}\right)^{-1}\boldsymbol{V}^{BA}}_{\boldsymbol{\Sigma}^{AA}(\epsilon)}\Big)\boldsymbol{G}^{AA}(\epsilon) &= \mathbf{1}^{AA} \end{aligned} \tag{5.32}$$

This yields an equation for $\boldsymbol{G}^{AA}(\epsilon)$, the Green's function projected onto the system of interest.

RETARDED POTENTIALS BY COUPLING TO A BATH

$$\left[\epsilon \mathbf{1}^{AA} - \boldsymbol{H}^{AA} - \boldsymbol{\Sigma}^{AA}(\epsilon)\right]\boldsymbol{G}^{AA}(\epsilon) = \mathbf{1}^{AA} \tag{5.33}$$

with the energy-dependent self energy defined in Eq. 5.14

$$\boldsymbol{\Sigma}^{AA}(\epsilon) \overset{\text{Eq. 5.14}}{=} \boldsymbol{V}^{AB}\bar{\boldsymbol{G}}^{BB}(\epsilon)\boldsymbol{V}^{BA} \tag{5.34}$$

$\bar{\boldsymbol{G}}^{BB}$ is the Green's function of the isolated subsystem B.

Isolated Green's function and coupling are sufficient: Eq. 5.33 shows that the Green's function $\boldsymbol{G}^{AA}(\epsilon)$ of the composite system can be constructed from the Green's functions of the isolated systems and the Hamilton matrix elements connecting the two systems. This is convenient because it shows how a complex system can be built up by stacking together the Green's function of its components.

With the Green's function of the isolated systems,

$$\bar{\boldsymbol{G}}^{AA}(\epsilon) \overset{\text{def}}{=} \left(\epsilon \mathbf{1}^{AA} - \boldsymbol{H}^{AA}\right)^{-1} \tag{5.35}$$

and $\bar{\boldsymbol{G}}^{BB}(\epsilon)$ defined in Eq. 5.7, we obtain

$$\boldsymbol{G}^{AA}(\epsilon) \overset{\text{Eq. 5.33}}{=} \left[\left(\bar{\boldsymbol{G}}^{AA}(\epsilon)\right)^{-1} - \boldsymbol{V}^{AB}\bar{\boldsymbol{G}}^{BB}(\epsilon)\boldsymbol{V}^{BA}\right]^{-1} \tag{5.36}$$

Eq. 5.36 is a variant of the so-called **Dyson equation**. It will show up repeatedly in equivalent forms such as

$$\boldsymbol{G}^{AA} \overset{\text{Eq. 5.36}}{=} \left[\left(\bar{\boldsymbol{G}}^{AA}\right)^{-1} - \boldsymbol{\Sigma}\right]^{-1} \tag{5.37}$$

$$\left(\boldsymbol{G}^{AA}\right)^{-1} \overset{\text{Eq. 5.36}}{=} \left(\bar{\boldsymbol{G}}^{AA}\right)^{-1} - \boldsymbol{\Sigma} \tag{5.38}$$

$$\begin{aligned}\boldsymbol{G}^{AA} &\overset{\text{Eq. 5.36}}{=} \bar{\boldsymbol{G}}^{AA} + \bar{\boldsymbol{G}}^{AA}\boldsymbol{\Sigma}\boldsymbol{G}^{AA} \\ &= \bar{\boldsymbol{G}}^{AA} + \bar{\boldsymbol{G}}^{AA}\boldsymbol{\Sigma}\bar{\boldsymbol{G}}^{AA} + \bar{\boldsymbol{G}}^{AA}\boldsymbol{\Sigma}\bar{\boldsymbol{G}}^{AA}\boldsymbol{\Sigma}\bar{\boldsymbol{G}}^{AA} + \bar{\boldsymbol{G}}^{AA}\boldsymbol{\Sigma}\bar{\boldsymbol{G}}^{AA}\boldsymbol{\Sigma}\bar{\boldsymbol{G}}^{AA}\boldsymbol{\Sigma}\bar{\boldsymbol{G}}^{AA} + \dots\end{aligned} \tag{5.39}$$

The last form shows the principles for the perturbation expansion of the Green's function.

Green's function and $M(\epsilon)$: In Eq. 5.12 of the previous section, we introduced the object $\boldsymbol{M}(\epsilon)$, which plays the central role for the description of an embedded system. It defines the wave functions and its energies of the composite system.

$\boldsymbol{M}(\epsilon)$ is directly related to $\boldsymbol{G}^{AA}(\epsilon)$ defined in Eq. 5.33.

$$\begin{aligned}\boldsymbol{M}(\epsilon) &\overset{\text{Eq. 5.12}}{=} \boldsymbol{H}^{AA} + \underbrace{\boldsymbol{V}^{AB}\bar{\boldsymbol{G}}^{BB}(\epsilon)\boldsymbol{V}^{BA}}_{\boldsymbol{\Sigma}^{AA}(\epsilon)} \overset{\text{Eq. 5.14}}{=} \epsilon\mathbf{1}^{AA} - \left(\epsilon\mathbf{1}^{AA} - \boldsymbol{H}^{AA} - \boldsymbol{\Sigma}^{AA}(\epsilon)\right) \\ &\overset{\text{Eq. 5.33}}{=} \epsilon\mathbf{1}^{AA} - \left(\boldsymbol{G}^{AA}(\epsilon)\right)^{-1}\end{aligned} \tag{5.40}$$

This equation is equivalent to Eq. 5.28 on p. 186, which had been introduced earlier without proof.

Eq. 5.11, which defines the energies and wave functions is equivalent to

$$\left(\boldsymbol{G}^{AA}(\epsilon)\right)^{-1}\vec{c}^{A} \overset{\text{Eq. 5.11}}{=} 0 \tag{5.41}$$

It thus specifies the poles of $\boldsymbol{G}^{AA}(\epsilon)$ as the energies of the composite system. The singular vectors are the corresponding eigenstates.

The normalization condition needed to define $\vec{c}^{A}$ is specified by the same Green's function $\boldsymbol{G}^{AA}(\epsilon)$:

$$\begin{aligned}1 &\overset{\text{Eq. 5.19}}{=} \vec{c}^{A,*}\tilde{\boldsymbol{O}}(\epsilon)\vec{c}^{A} \overset{\text{Eq. 5.25}}{=} \vec{c}^{A,*}\frac{d(\epsilon\mathbf{1}^{AA} - \boldsymbol{M}(\epsilon))}{d\epsilon}\vec{c}^{A} \overset{\text{Eq. 5.40}}{=} \vec{c}^{A,*}\frac{d\left(\boldsymbol{G}^{AA}(\epsilon)\right)^{-1}}{d\epsilon}\vec{c}^{A} \\ \Rightarrow \qquad & \vec{c}^{A,*}\frac{d\left(\boldsymbol{G}^{AA}(\epsilon)\right)^{-1}}{d\epsilon}\vec{c}_{A} = 1\end{aligned} \tag{5.42}$$

Where are all the bath states: It seems surprising that nearly all the information of a composite system can be mapped onto a small subsystem.

Indeed some information is lost: If the isolated bath has eigenstates that do not couple to the system of interest, so that $\boldsymbol{V}^{A,B}\vec{c}^{B} = 0$, they do not show up in the self energy. Thus, they do not have any effect on the system $\boldsymbol{G}^{AA}$.

Such states however are related to a pole of the bath Green's function. This pole leads to a singularity in the extended orbital defined in Eq. 5.9. If theses singularities are ignored, a large amount of the bath B is unaccounted. However, this is exactly what is desired when focusing on system A.

5.2.2 Coupling to a bath in the time domain

The energy representation is limited to systems with time translation symmetry. Furthermore it obscures the dynamical properties of the system, which is a source of misunderstandings. Therefore, I will repeat the same derivation in the time domain.

Let me consider the defining equation Eq. 4.14 of the Green's function for a composite system. While we do not make the time dependence of the Hamilton matrix elements explicit, the derivation also works for time-dependent problems.

$$\begin{pmatrix} \mathbf{1}^{AA} i\hbar\partial_t - \boldsymbol{H}^{AA} & -\boldsymbol{V}^{AB} \\ -\boldsymbol{V}^{BA} & \mathbf{1}^{BB} i\hbar\partial_t - \boldsymbol{H}^{BB} \end{pmatrix} \begin{pmatrix} \boldsymbol{G}^{AA}(t,t') & \boldsymbol{G}^{AB}(t,t') \\ \boldsymbol{G}^{BA}(t,t') & \boldsymbol{G}^{BB}(t,t') \end{pmatrix} = \begin{pmatrix} \mathbf{1}^{AA} & \mathbf{0}^{AB} \\ \mathbf{0}^{BA} & \mathbf{1}^{BB} \end{pmatrix} \delta(t-t') \quad (5.43)$$

The symbols are defined in Eq. 5.5.

As in the previous section, I select the two equations containing both, $\boldsymbol{G}^{AA}(t,t')$ and $\boldsymbol{G}^{BA}(t,t')$.

Let me collect the upper-left element of this equation Eq. 5.43

$$\left(\mathbf{1}^{AA} i\hbar\partial_t - \boldsymbol{H}^{AA}\right)\boldsymbol{G}^{AA}(t,t') - \boldsymbol{V}^{AB}\boldsymbol{G}^{BA}(t,t') = \mathbf{1}^{AA}\delta(t-t') \quad (5.44)$$

I eliminate $\boldsymbol{G}^{BA}$ in Eq. 5.44 by expressing it in terms of $\boldsymbol{G}^{AA}$. For that purpose, I take the lower-left element of Eq. 5.43, which is the second equation besides Eq. 5.44 containing both Green's functions.

$$\begin{aligned} -\boldsymbol{V}^{BA}\boldsymbol{G}^{AA}(t,t') + \left(\mathbf{1}^{BB} i\hbar\partial_t - \boldsymbol{H}^{BB}\right)\boldsymbol{G}^{BA}(t,t') &= \mathbf{0}^{BA} \\ \Rightarrow \qquad \left(\mathbf{1}^{BB} i\hbar\partial_t - \boldsymbol{H}^{BB}\right)\boldsymbol{G}^{BA}(t,t') &= \boldsymbol{V}^{BA}\boldsymbol{G}^{AA}(t,t') \end{aligned} \quad (5.45)$$

Let me now introduce the bath Green's function defined earlier in Eq. 5.7 in an energy representation. Here, we need a more general definition, which is also valid for time-dependent Hamiltonians.

$$\left(\mathbf{1}^{BB} i\hbar\partial_t - \boldsymbol{H}^{BB}(t)\right)\bar{\boldsymbol{G}}^{BB}(t,t') = \mathbf{1}^{BB}\delta(t-t') \quad (5.46)$$

Insertion of the bath Green's function $\bar{\boldsymbol{G}}^{BB}$ into Eq. 5.45 for $\boldsymbol{G}^{BA}$ yields

$$\begin{aligned} \left(\mathbf{1}^{BB} i\hbar\partial_t - \boldsymbol{H}^{BB}\right)\boldsymbol{G}^{BA}(t,t') &\overset{\text{Eq. 5.45}}{=} \int dt'' \overbrace{\left(\mathbf{1}^{BB} i\hbar\partial_t - \boldsymbol{H}^{BB}\right)\bar{\boldsymbol{G}}^{BB}(t,t'')}^{\mathbf{1}^{BB}\delta(t-t'')}\boldsymbol{V}^{BA}\boldsymbol{G}^{AA}(t'',t') \\ &\overset{\text{Eq. 5.46}}{=} \left(\mathbf{1}^{BB} i\hbar\partial_t - \boldsymbol{H}^{BB}\right)\left[\int dt''\, \bar{\boldsymbol{G}}^{BB}(t,t'')\boldsymbol{V}^{BA}\boldsymbol{G}^{AA}(t'',t')\right] \\ \Rightarrow \qquad \boldsymbol{G}^{BA}(t,t') &= \int dt''\, \bar{\boldsymbol{G}}^{BB}(t,t'')\boldsymbol{V}^{BA}\boldsymbol{G}^{AA}(t'',t') + \boldsymbol{C}^{BA}_{\text{hom}}(t,t') \end{aligned} \quad (5.47)$$

The object $C^{BA}_{\text{hom}}(t,t')$ is any object that obeys the Schrödinger equation for subsystem B. It describes contributions from system B, that are not induced by subsystem A.

The result for G^{BA} can now be inserted into Eq. 5.44 to obtain an equation for $\boldsymbol{G}^{AA}$

$$\left(\mathbf{1}^{AA} i\hbar\partial_t - \boldsymbol{H}^{AA}\right)\boldsymbol{G}^{AA}(t,t') - \boldsymbol{V}^{AB}\int dt''\, \bar{\boldsymbol{G}}^{BB}(t,t'')\boldsymbol{V}^{BA}\boldsymbol{G}^{AA}(t'',t') - \boldsymbol{V}^{AB}\boldsymbol{C}^{BA}_{\text{hom}}(t,t') = \mathbf{1}^{AA}\delta(t-t') \quad (5.48)$$

This equation can also be written in the form

$$\int dt'' \left[\left(\mathbf{1}^{AA} i\hbar\partial_t - \boldsymbol{H}^{AA}\right)\delta(t-t'') - \boldsymbol{V}^{AB}\bar{\boldsymbol{G}}^{BB}(t,t'')\boldsymbol{V}^{BA}\right]\boldsymbol{G}^{AA}(t'',t') = \mathbf{1}^{AA}\delta(t-t') + \boldsymbol{V}^{AB}\boldsymbol{C}^{BA}_{\text{hom}}(t,t') \quad (5.49)$$

What happens with $\boldsymbol{C}^{BA}_{hom}$? Together with the differential equation Eq. 4.14 defining the Green's function, also the boundary condition has been specified as $\hat{G}(-\infty, t') = \hat{0}$, which implies $\hat{G}(t, t') = \hat{0}$ for $t < t'$. This boundary condition is specific for the causal Green's function.[4]

A homogeneous solution of the Schrödinger equation $(\mathbf{1}^{BB} i\hbar\partial_t - \boldsymbol{H}^{BB})\vec{c} = 0$ is either zero or non-zero for all times.[5] Because also $\boldsymbol{G}^{AA}$ and $\bar{\boldsymbol{G}}^{BB}$ are causal, the block $\boldsymbol{G}^{BA}$ of the Green's function is only causal if $\boldsymbol{C}^{BA}$ vanishes.

RETARDED POTENTIALS BY COUPLING TO A BATH

$$\int dt'' \left[\Big(\mathbf{1}^{AA} i\hbar\partial_t - \boldsymbol{H}^{AA}(t)\Big)\delta(t-t'') - \boldsymbol{\Sigma}^{AA}(t,t'')\right]\boldsymbol{G}^{AA}(t'',t') = \mathbf{1}^{AA}\delta(t-t') \tag{5.50}$$

with the retarded potential

$$\boldsymbol{\Sigma}^{AA}(t,t') = \boldsymbol{V}^{AB}(t)\bar{\boldsymbol{G}}^{BB}(t,t')\boldsymbol{V}^{BA}(t') \tag{5.51}$$

$\bar{\boldsymbol{G}}^{BB}$ is the Green's function of the isolated subsystem B, which satisfies Eq. 5.46.

Instead of a differential equation for the Green's function, we obtain now an integro-differential equation.

5.3 Retarded and time-dependent potentials

In this section, I want to elaborate on the role of retarded and time-dependent potentials. Both refer to a time dependence of the self energy, which is why they are easily confused. I will show, how a retarded and an energy-dependent potential appears in the energy-based representation.

5.3.1 Time-independent Schrödinger equation with a retarded potential

Consider a Schrödinger equation that has a nonlocal potential in time. That is, it has a Hamiltonian $\hat{h} + \hat{\Sigma}(t,t')$ with a **retarded potential** $\hat{\Sigma}(t,t')$.

$$\left[i\hbar\partial_t - \hat{h}\right]|\psi(t)\rangle - \int dt'\, \hat{\Sigma}(t,t')|\psi(t')\rangle = 0 \tag{5.52}$$

I am using here the symbol $\hat{\Sigma}$, which is later used for the **self energy**, because the self energy has the form for a retarded potential. At this point, its meaning is more general.

In order to ensure **causality**, the retarded potential has to obey $\hat{\Sigma}(t,t') = 0$ for $t' > t$.

For a translation-invariant problem in time, for which the potential $\hat{\Sigma}(t,t')$ depends only on the relative time argument $t - t'$, we can go into the energy representation.[6]

$$\hat{\Sigma}(t,t') \overset{\text{Eq. A.4}}{=} \int \frac{d\epsilon}{2\pi\hbar}\, \hat{\Sigma}(\epsilon) \mathrm{e}^{-\frac{i}{\hbar}\epsilon(t-t')} \tag{5.53}$$

and use the following Ansatz for the wave function

$$|\psi(t)\rangle \overset{\text{Eq. A.4}}{=} \int \frac{d\epsilon}{2\pi\hbar}\, |\psi(\epsilon)\rangle \mathrm{e}^{-\frac{i}{\hbar}\epsilon t} \tag{5.54}$$

[4] Later, we will see that there are Green's function for which this requirement is modified.
[5] This is evident from the conservation of the norm of the wave function.
[6] A word regarding units. $\Sigma(t,t')$ has the unit energy divided by time. $\Sigma(\epsilon)$ has the unit energy.

I insert this potential $\hat{\Sigma}$ into the retarded Schrödinger equation Eq. 5.52

$$\begin{aligned}
\left[i\hbar\partial_t - \hat{h}\right]|\psi(t)\rangle - \int dt' \overbrace{\int \frac{d\epsilon}{2\pi\hbar}\,\hat{\Sigma}(\epsilon)\mathrm{e}^{-\frac{i}{\hbar}\epsilon(t-t')}}^{\hat{\Sigma}(t,t')}|\psi(t')\rangle &= 0 \\
\left[i\hbar\partial_t - \hat{h}\right]\underbrace{\int \frac{d\epsilon}{2\pi\hbar}\,|\psi(\epsilon)\rangle\mathrm{e}^{-\frac{i}{\hbar}\epsilon t}}_{|\psi(t)\rangle \quad \text{from Eq. 5.54}} - \int \frac{d\epsilon}{2\pi\hbar}\,\mathrm{e}^{-\frac{i}{\hbar}\epsilon t}\hat{\Sigma}(\epsilon)\underbrace{\int dt'\,\mathrm{e}^{\frac{i}{\hbar}\epsilon t'}|\psi(t')\rangle}_{|\psi(\epsilon)\rangle \quad \text{via Eq. A.3}} &= 0 \\
\Rightarrow \qquad \int \frac{d\epsilon}{2\pi\hbar}\,\mathrm{e}^{-\frac{i}{\hbar}\epsilon t}\Big(\epsilon - \hat{h} - \hat{\Sigma}(\epsilon)\Big)\big|\psi(\epsilon)\big\rangle &= 0
\end{aligned} \tag{5.55}$$

This equation is satisfied for all times only if all coefficients vanish individually, i.e.

$$\left[\epsilon\hat{1} - \hat{h} - \hat{\Sigma}(\epsilon)\right]|\psi(\epsilon)\rangle = 0\,. \tag{5.56}$$

In the energy representation, the retarded potential is thus turned into an energy-dependent potential. If the potential were local in time, its Fourier transform would be a constant in ϵ and the potential $\Sigma(\epsilon)$ would be energy independent.

In order to solve the above equation, we must satisfy

SCHRÖDINGER EQUATION WITH A RETARDED POTENTIAL

For a system with a retarded potential $\hat{\Sigma}$, which is invariant under time-translations, the Schrödinger equation has the form

$$\left[\epsilon\hat{1} - \hat{h} - \hat{\Sigma}(\epsilon)\right]|\psi(\epsilon)\rangle = 0 \tag{5.57}$$

with an energy-dependent Hamiltonian $\hat{h} + \hat{\Sigma}(\epsilon)$.
An approximate Schödinger equation with an energy-independent potential can be obtained from Eq. 5.57 by a first-order Taylor expansion in the deviation $\epsilon - \epsilon_\nu$ about some reference energy ϵ_ν. This will naturally include an overlap operator.

If we consider the case, where the self energy is due to coupling to another system, the wave function $|\psi(\epsilon)\rangle = \sum_{\alpha\in A}|\chi^A_\alpha\rangle c^A_\alpha$ is localized on the subsystem A. The wave function $|\tilde{\psi}(\epsilon)\rangle$, which also contains the contribution of system B, is recovered using Eq. 5.9.

$$|\tilde{\psi}(\epsilon)\rangle \overset{\text{Eq. 5.9}}{=} \left(\hat{1} + \sum_{\beta,\gamma\in B,\delta\in A}|\chi^B_\beta\rangle\bar{G}^{BB}_{\beta,\gamma}(\epsilon)V^{BA}_{\gamma,\delta}\langle\pi_\delta|\right)|\psi(\epsilon)\rangle \tag{5.58}$$

with $\langle\pi_\alpha|\chi_\beta\rangle = \delta_{\alpha,\beta}$.

Note however, that the energies obtained from this equation are, in general, complex and that the wave functions are not necessarily orthonormal. (I do not have a proof either way.)

5.3.2 Time-dependent potential in an energy representation

In order to make the contrast to the retarded potential clear, let me investigate a time-dependent potential in the same manner.

Let me consider a time-dependent Hamiltonian $\hat{h} + \hat{W}(t)$ with

$$\hat{W}(t) = \sum_n \hat{w}_n\mathrm{e}^{-i\omega_n t} \tag{5.59}$$

and represent the wave function in the form

$$|\psi(t)\rangle = \int \frac{d\epsilon}{2\pi\hbar}\,|\psi(\epsilon)\rangle\mathrm{e}^{-\frac{i}{\hbar}\epsilon t} \tag{5.60}$$

The Schrödinger equation with the time-dependent potential is

$$\begin{aligned} \Big[i\hbar\partial_t\hat{1} - \hat{h} - \hat{W}(t)\Big]|\psi(t)\rangle = 0 \\ \Rightarrow \quad \int \frac{d\epsilon}{2\pi\hbar}\, \mathrm{e}^{-\frac{i}{\hbar}\epsilon t}\Big[(\epsilon\hat{1} - \hat{h})|\psi(\epsilon)\rangle - \sum_n \hat{w}_n|\psi(\epsilon - \hbar\omega_n)\rangle\Big] = 0 \\ \Rightarrow \qquad (\epsilon\hat{1} - \hat{h})|\psi(\epsilon)\rangle - \sum_n \hat{w}_n|\psi(\epsilon - \hbar\omega_n)\rangle = 0 \end{aligned} \tag{5.61}$$

The energy components of the wave functions are no more independent of each other. Each Fourier component in the potential introduces a sequence of **overtones** in the wave function, that is, components with $\epsilon + \hbar\omega_n$. The overtones are responsible for a non-trivial dynamics of the wave function beyond a harmonic oscillation.

For further information on strong time-dependent potentials, I refer to Floquet theory. **Floquet theory** studies perturbations that are periodic in time. In this case it is possible to translate Bloch theorem, formulated for potentials that are periodic in space, to potentials that are periodic in time[7]

We can remember, that a wave function having contributions with distinct energies has a non-linear time evolution and is not the result of a Hamiltonian with time-translation symmetry.

5.3.3 Summary

In this section we learned that a part of a quantum system can be investigated, if the Green's function of the isolated remaining system, $\hat{\bar{G}}^{BB}$ is available. The remaining system acts on the system of interest with a retarded potential, which we call a self energy $\hat{\Sigma}(t, t')$. The retardation describes the time delay between action on the remaining system and its back-action, like in an echo. In an energy representation the self energy acts like an energy-dependent potential. If the back-action is instantaneous, the potential is local in time, that is non-retarded, and hence also energy-independent.

Schrödinger equations with an energy-dependent Hamiltonian can be solved by piece-wise linearization in the energy, which yields, for each piece, a generalized eigenvalue problem with an overlap matrix. The overlap matrix differs from unity, because the wave function has a "tail" extending into the remaining system.

The reader should be able to distinguish time-dependent from retarded potentials. The reader should be able to translate each between the time-representation and energy representation.

Editor: This is under construction. Drop this

1. general potential

$$V(\epsilon, \epsilon') = \int dt \int dt'\, V(t, t')\mathrm{e}^{\frac{i}{\hbar}(\epsilon t + \epsilon' t')} \tag{5.62}$$

2. local in time, but time dependent

3. retarded, but time independent

4. constant: time independent and local in time

$$\begin{aligned} \hat{V}(t, t') = \hat{F} \\ \hat{V}(\epsilon, \epsilon') = \hat{F}\delta(\epsilon)\delta(\epsilon') \end{aligned} \tag{5.63}$$

Further information about one-particle Green's functions can be found in the Book by Economou[58].

[7] Floquet theorem actually predates Bloch theorem. The latter is an application of the Floquet theorem, which is more general.

5.3.4 Other uses of retarded or energy-dependent potentials

- In the proximity of the nucleus the kinetic energy of the electrons becomes so large that they become relativistic. In order to describe relativistic effects, one often down-folds the two small components of the four-component spinor in the Dirac equation. The small components can be attributed to positrons, the antiparticles of electrons. As result one obtains an energy-dependent equation for a two-component spinor describing the spin-up and spin-down electrons.

5.4 Home study and practice

5.4.1 Minimal model for a quantum system coupled to a bath

Introduction

The following set of three problems shall demonstrate different aspects of dealing with composite systems using Green's functions. In problem 5.4.1, I start with two atoms forming a molecule, which has already discussed explicitly in 1.5.1 and 1.5.2. Then, in problem 5.4.2, I replace one of the atoms with one having a finite life time. In the third problem 5.4.3, the second atom is replaced by an explicit extended system.

In order to gain insight into the coupling between systems, let me investigate a minimal model. The model describes a spin-less Hubbard dimer without interaction: The two Hubbard atoms are denoted as A and B. The hopping parameter between the two subsystems is t and the energy of the orbital at A is at zero, i.e. $\bar{\epsilon}_A = 0$. The orbital of the bath site B is at energy $\bar{\epsilon}_B$. In order to practice, how to replace one part of a combined system by another one, we start with a symmetric dimer $\bar{\epsilon}_B = \bar{\epsilon}_A$. An asymmetric dimer is then constructed by replacing atom B by one with a different atomic level, i.e. $\bar{\epsilon}_B \neq \bar{\epsilon}_A$.

This technique is used, for example, to study point defects in crystals. One example is the **Anderson impurity model**[59], which describes a strongly correlated atom, the **Anderson impurity**, in an otherwise perfect crystal, the **bath**[8]. The Anderson model was introduced to explain that impurities in a free-electron-like metal can produce local magnetic moments observed experimentally. The Anderson model has also been used to explain the **Kondo effect**, an unsuspected increase of the electric resistance below the **Kondo temperature**. The Kondo effect is one of the famous quantum effects of interacting electrons. For more information, I refer to chapter **??** on p. **??**. The Hubbard dimer can be considered as a minimal Anderson impurity model. The subsystem A represents the Anderson impurity, while the subsystem B represents the bath. In the following problems, I exclude the electron interaction for the sake of simplicity. This turns the Anderson model into the simpler **Fano model**[60], which has been introduced almost simultaneously with the Anderson model. The Fano model has been introduced to study the asymmetric line-shape of absorption lines.

[8] The term *bath* is probably related to that of the *heat bath* of thermodynamics.

Problem

Consider the spin-less dimer with the Hamiltonian

$$\hat{h} = |\pi_A\rangle\bar{\epsilon}_A\langle\pi_A| + |\pi_B\rangle\bar{\epsilon}_B\langle\pi_B| - t\Big(|\pi_A\rangle\langle\pi_B| + |\pi_B\rangle\langle\pi_A|\Big) \tag{5.64}$$

Without restriction of generality we choose $\bar{\epsilon}_A = 0$.
I use the notation for non-orthonormal local orbitals with local orbitals $|\chi_\alpha\rangle$ and projector functions $|\pi_\alpha\rangle$, that obey the bi-orthogonality condition $\langle\chi_\alpha|\pi_\beta\rangle = \delta_{\alpha,\beta}$. Nevertheless, in this problem the orbitals are assumed to be orthonormal, that is $\langle\chi_\alpha|\chi_\beta\rangle = \delta_{\alpha,\beta}$.

1. Determine the Green's function $\hat{G}(\epsilon)$ for the dimer with a given value for $\bar{\epsilon}_B = 0$. Calculate $G^{AA}(\epsilon)$, $G^{BB}(\epsilon)$ and the Green's function $\bar{G}^{BB}(\epsilon)$ of the isolated atom B.
2. Calculate the retarded potential $\Delta\Sigma^{AA}(\epsilon)$, which acts on system A due to replacing atom B by one with the atomic level at $\bar{\epsilon}_B$.
3. Construct the Green's function for atom A in the asymmetric dimer (with $\bar{\epsilon}_B \neq 0$) from the Green's function of the symmetric dimer and the retarded potentials produced by site B.
4. Determine the density of states on site A
5. Editor: This problem shall describe how the charge oscillates in sites A, when it is in contact with B. The initial condition is that the particle is completely on site A. The charge oscillates on A as it oscillates back and forth between A and B with the excitation frequency. In the next problem we can discuss how a continuous spectrum in B leads to a decay of the occupation in A, as it leaks into an environment with an infinite number of states.

Discussion

1. Determine the Green's function $\hat{G}(\epsilon)$ for the dimer with a given value for $\bar{\epsilon}_B = 0$. Calculate $G^{AA}(\epsilon)$, $G^{BB}(\epsilon)$ and the Green's function $\bar{G}^{BB}(\epsilon)$ of the isolated atom B.

The Hamiltonian of the dimer with $\bar{\epsilon}_B = 0$ is

$$\boldsymbol{h} = \begin{pmatrix} 0 & -t \\ -t & 0 \end{pmatrix} \tag{5.65}$$

The Hamiltonian is at times represented as 2×2-matrix and sometimes as operator. The operator form has the vector of kets attached on the left side to the matrix and the vector of bras on the right side. The operator form has the advantage, that the basisset is made explicit when it is used. In the exercise at hand, we also deal with one-dimensional Hilbert spaces, namely for the isolated atom A and the isolated atom B. In that case, the matrix becomes a number.

One can evaluate the Green's function by inverting the matrix $\epsilon\mathbf{1} - \boldsymbol{h}$. This can be done either directly, or via eigenstates and eigenvalues. While both methods are demonstrated, only one is required.

- Green's function by inversion of $\epsilon\mathbf{1} - \boldsymbol{h}$

$$\boldsymbol{G}(\epsilon) \overset{\text{Eq. 4.23}}{=} \big(\epsilon\mathbf{1} - \boldsymbol{h}\big)^{-1} = \frac{1}{\epsilon^2 - t^2}\begin{pmatrix} \epsilon & -t \\ -t & \epsilon \end{pmatrix} \tag{5.66}$$

I have been using the simple formula for the inversion of a 2×2 matrix.[9]

- Green's function by diagonalization: This method is more involved than direct inversion, but it is instructive.

  The eigenstates of $\boldsymbol{h}$ are

$$\vec{c}_1 = \frac{1}{\sqrt{2}} \begin{pmatrix} 1 \\ 1 \end{pmatrix} \qquad \text{with energy } \epsilon_1 = -t \qquad \text{and} \tag{5.68}$$
$$\vec{c}_2 = \frac{1}{\sqrt{2}} \begin{pmatrix} 1 \\ -1 \end{pmatrix} \qquad \text{with energy } \epsilon_2 = +t$$

  The Green's function is (with the dyadic (outer) product $\otimes$)

$$\begin{aligned} \boldsymbol{G}(\epsilon) &= \sum_{n\in\{1,2\}} \frac{\vec{c}_n \otimes \vec{c}_n^*}{\epsilon - \epsilon_n} = \frac{1}{2} \begin{pmatrix} 1 & 1 \\ 1 & 1 \end{pmatrix} \frac{1}{\epsilon + t} + \frac{1}{2} \begin{pmatrix} 1 & -1 \\ -1 & 1 \end{pmatrix} \frac{1}{\epsilon - t} \\ &= \frac{1}{\epsilon^2 - t^2} \left[\frac{1}{2} \begin{pmatrix} 1 & 1 \\ 1 & 1 \end{pmatrix} (\epsilon - t) + \frac{1}{2} \begin{pmatrix} 1 & -1 \\ -1 & 1 \end{pmatrix} (\epsilon + t) \right] \\ &= \frac{1}{\epsilon^2 - t^2} \begin{pmatrix} \epsilon & -t \\ -t & \epsilon \end{pmatrix} \end{aligned} \tag{5.69}$$

From this result, I can directly look up the diagonal elements of the Green's function

$$G^{AA}(\epsilon) = \frac{\epsilon}{\epsilon^2 - t^2} \qquad \text{and} \qquad G^{BB}(\epsilon) = \frac{\epsilon}{\epsilon^2 - t^2} \tag{5.70}$$

respectively, as operators,

$$\hat{G}^{AA}(\epsilon) = |\chi_A\rangle \frac{\epsilon}{\epsilon^2 - t^2} \langle \chi_A| \qquad \text{and} \qquad \hat{G}^{BB}(\epsilon) = |\chi_B\rangle \frac{\epsilon}{\epsilon^2 - t^2} \langle \chi_B| \tag{5.71}$$

The Green's function $\bar{G}^{BB}$ for the isolated bath is obtained directly from the 1×1 Hamiltonian h^{BB} by inverting $\epsilon - h^{BB}$. In our special case, we have set $\bar{\epsilon}_B = \bar{\epsilon}_A = 0$.

$$\bar{G}^{BB}(\epsilon) = \frac{1}{\epsilon} \tag{5.72}$$

2. Calculate the retarded potential $\Delta\Sigma^{AA}(\epsilon)$, which acts on system A due to replacing atom B by one with the atomic level at $\bar{\epsilon}_B$.

The self energy of the bath site with a specified $\bar{\epsilon}_B$ is

$$\Sigma^{AA}(\epsilon) \overset{\text{Eq. } 5.34}{=} V^{AB} \bar{G}^{BB}(\epsilon) V^{BA} = \frac{t^2}{\epsilon - \bar{\epsilon}_B} \tag{5.73}$$

The site B is replaced by replacing the self energy with that of the new system. This implies that the replacement is represented by a self energy $\Delta\Sigma$, which is the difference of the one with $\bar{\epsilon}_B \neq 0$ and the one with $\bar{\epsilon}_B = 0$

$$\Delta\Sigma(\epsilon) = \frac{t^2}{\epsilon - \bar{\epsilon}_B} - \frac{t^2}{\epsilon} = \frac{\bar{\epsilon}_B t^2}{\epsilon(\epsilon - \bar{\epsilon}_B)} \tag{5.74}$$

[9]
$$\begin{pmatrix} a & b \\ c & d \end{pmatrix}^{-1} = \frac{1}{ad - bc} \begin{pmatrix} d & -b \\ -c & a \end{pmatrix} \tag{5.67}$$

3. Construct the Green's function for atom A in the asymmetric dimer $\bar{\epsilon}_B \neq 0$ from the Green's function of the symmetric dimer and the retarded potentials produced by site B.

In the following, I use two arguments for the Green's function: the second is the "normal" energy argument, while the first is the value of $\bar{\epsilon}_B$, which can be either $\bar{\epsilon}_B$ or zero.

The equation for the Green's function on site A is

$$\begin{aligned}
\hat{G}^{AA}(\bar{\epsilon}_B;\epsilon) &= \left[\epsilon\hat{1}^{AA} - \hat{h}^{AA} - \hat{V}^{AB}\hat{\bar{G}}^{BB}(\bar{\epsilon}_B;\epsilon)\hat{V}^{BA}\right]^{-1} \\
&= \Big[\underbrace{\epsilon\hat{1}^{AA} - \hat{h}^{AA} - \hat{V}^{AB}\hat{\bar{G}}^{BB}(0;\epsilon)\hat{V}^{BA}}_{\left(\hat{G}^{AA}(0;\epsilon)\right)^{-1}} - \underbrace{\hat{V}^{AB}\left(\hat{\bar{G}}^{BB}(\bar{\epsilon}_B;\epsilon) - \hat{\bar{G}}^{BB}(0;\epsilon)\right)\hat{V}^{BA}}_{\Delta\hat{\Sigma}^{AA}}\Big]^{-1} \\
&= \left[\left(\hat{G}^{AA}(0;\epsilon)\right)^{-1} - \Delta\hat{\Sigma}^{AA}(\epsilon)\right]^{-1}
\end{aligned} \tag{5.75}$$

Let me now insert the "numbers". $G^{AA}(\epsilon)$ is the sole matrix element of $\hat{G}^{AA}(\epsilon) = |\chi_A\rangle G^{AA}(\epsilon)\langle\chi_A|$.

$$\begin{aligned}
G^{AA}(\bar{\epsilon}_B;\epsilon) &\overset{\text{Eqs. 5.70, 5.74}}{=} \Big[\underbrace{\frac{\epsilon^2 - t^2}{\epsilon}}_{\left(G^{AA}(0;\epsilon)\right)^{-1}} - \underbrace{\frac{t^2\bar{\epsilon}_B}{\epsilon(\epsilon-\bar{\epsilon}_B)}}_{\Delta\Sigma^{AA}(\epsilon)}\Big]^{-1} \\
&= \frac{\epsilon(\epsilon-\bar{\epsilon}_B)}{(\epsilon^2-t^2)(\epsilon-\bar{\epsilon}_B) - t^2\bar{\epsilon}_B} \\
&= \frac{\epsilon(\epsilon-\bar{\epsilon}_B)}{\epsilon^3 - t^2\epsilon - \epsilon^2\bar{\epsilon}_B + t^2\bar{\epsilon}_B - t^2\bar{\epsilon}_B} \\
&= \frac{\epsilon-\bar{\epsilon}_B}{\epsilon^2 - t^2 - \epsilon\bar{\epsilon}_B} \\
&= \frac{\epsilon-\bar{\epsilon}_B}{\left(\epsilon - \frac{1}{2}\bar{\epsilon}_B - \sqrt{\left(\frac{1}{2}\bar{\epsilon}_B\right)^2 + t^2}\right)\left(\epsilon - \frac{1}{2}\bar{\epsilon}_B + \sqrt{\left(\frac{1}{2}\bar{\epsilon}_B\right)^2 + t^2}\right)}
\end{aligned} \tag{5.76}$$

With this result we could in principle stop. However, the expression is still fairly intransparent. Let us therefore divide the result into the sum of the two poles.

Let us perform a **partial-fraction decomposition**[10]

$$\frac{x-c}{(x-a)(x-b)} = \frac{\frac{c-b}{a-b}(x-a) - \frac{c-a}{a-b}(x-b)}{(x-a)(x-b)} = \frac{a-c}{a-b}\frac{1}{x-a} + \frac{c-b}{a-b}\frac{1}{x-b} \tag{5.77}$$

with

$$\begin{aligned}
c &= \bar{\epsilon}_B \\
a &= \frac{1}{2}\bar{\epsilon}_B + \sqrt{\left(\frac{1}{2}\bar{\epsilon}_B\right)^2 + t^2} \\
b &= \frac{1}{2}\bar{\epsilon}_B - \sqrt{\left(\frac{1}{2}\bar{\epsilon}_B\right)^2 + t^2} \\
\Rightarrow \frac{a-c}{a-b} &= \frac{-\bar{\epsilon}_B/2 + \sqrt{(\bar{\epsilon}_B/2)^2 + t^2}}{2\sqrt{(\bar{\epsilon}_B/2) + t^2}} = \frac{1}{2}\left(1 - \frac{\bar{\epsilon}_B/2}{\sqrt{(\bar{\epsilon}_B/2)^2 + t^2}}\right) \\
\frac{c-b}{a-b} &= \frac{\bar{\epsilon}_B/2 + \sqrt{(\bar{\epsilon}_B/2)^2 + t^2}}{2\sqrt{(\bar{\epsilon}_B/2) + t^2}} = \frac{1}{2}\left(1 + \frac{\bar{\epsilon}_B/2}{\sqrt{(\bar{\epsilon}_B/2)^2 + t^2}}\right)
\end{aligned} \tag{5.78}$$

[10] German(partial fraction decomposition)=Partialbruchzerlegung.

$$G^{AA}(\bar{\epsilon}_B;\epsilon) \overset{\text{Eq. 5.77}}{=} \frac{1}{2}\frac{1-\frac{\bar{\epsilon}_B/2}{\sqrt{(\bar{\epsilon}_B/2)^2+t^2}}}{\epsilon-\bar{\epsilon}_B/2-\sqrt{(\bar{\epsilon}_B/2)^2+t^2}} + \frac{1}{2}\frac{1+\frac{\bar{\epsilon}_B/2}{\sqrt{(\bar{\epsilon}_B/2)^2+t^2}}}{\epsilon-\bar{\epsilon}_B/2+\sqrt{(\bar{\epsilon}_B/2)^2+t^2}} \tag{5.79}$$

The first term is the pole with the upper energy and the second term is the pole with the lower energy.

- The poles of the Green's function lie exactly at the energy eigenvalues of the asymmetric dimer. This is a sanity check that the method works.
- For the symmetric dimer, i.e. for $\bar{\epsilon}_B = 0$, we obtain $G^{(0)}_{AA}(\epsilon)$ obtained previously.
- For $\bar{\epsilon}_B \to \infty$ we obtain the Green's function for the isolated atom A.
- The weights of the two poles add up to one. This demonstrates an important sum rule for the Green's function.

4. Determine the projected density of states on site A

The density of states on site A is obtained as

$$D_A(\epsilon) \overset{\text{Eq. 4.50}}{=} -\frac{1}{\pi}\lim_{\eta\to 0}\mathrm{Im}\left[\langle\pi_A|\hat{G}(\epsilon+i\eta)|\pi_A\rangle\right] \tag{5.80}$$

where the $|\pi_A\rangle$ are the projector functions for the orbitals $|\chi_\alpha\rangle$.

The density of states is a 2×2 matrix in a two-dimensional basisset $\hat{D}(\epsilon) = \sum_{\alpha,\beta\in\{A,B\}}|\chi_\alpha\rangle D_{\alpha,\beta}\langle\chi_\beta|$. The projected density of states for site A is the matrix element $D_{AA}(\epsilon)$ on the diagonal, which I abbreviate as $D_A(\epsilon)$.

In the following, I will use

$$\lim_{\eta\to 0^+}\mathrm{Im}\Big(-\frac{1}{\pi}\frac{1}{x+i\eta}\Big) \overset{\text{Eq. 4.53}}{=} \delta(x) \tag{5.81}$$

The projected density of states is

$$D_A(\epsilon) = -\frac{1}{\pi}\lim_{\eta\to 0^+}\mathrm{Im}\left[\langle\pi_A|\hat{G}(\epsilon+i\eta)|\pi_A\rangle\right] = -\frac{1}{\pi}\lim_{\eta\to 0}\mathrm{Im}\left[G^{AA}(\bar{\epsilon}_B;\epsilon+i\eta)\right] \tag{5.82}$$

We use the Green's function from Eq. 5.79

$$G^{AA}(\bar{\epsilon}_B;\epsilon+i0^+) \overset{\text{Eq. 5.79}}{=} \frac{1}{2}\frac{1-\frac{\bar{\epsilon}_B/2}{\sqrt{(\bar{\epsilon}_B/2)^2+t^2}}}{\epsilon-\bar{\epsilon}_B/2-\sqrt{(\bar{\epsilon}_B/2)^2+t^2}} + \frac{1}{2}\frac{1+\frac{\bar{\epsilon}_B/2}{\sqrt{(\bar{\epsilon}_B/2)^2+t^2}}}{\epsilon-\bar{\epsilon}_B/2+\sqrt{(\bar{\epsilon}_B/2)^2+t^2}} \tag{5.83}$$

to obtain the projected density of states.

$$\begin{aligned}\Rightarrow \quad D_A(\epsilon) = &\frac{1}{2}\left(1-\frac{\bar{\epsilon}_B/2}{\sqrt{(\bar{\epsilon}_B/2)^2+t^2}}\right)\underbrace{\delta\left(\epsilon-\bar{\epsilon}_B/2-\sqrt{(\bar{\epsilon}_B/2)^2+t^2}\right)}_{\text{upper peak}}\\ &+\frac{1}{2}\left(1+\frac{\bar{\epsilon}_B/2}{\sqrt{(\bar{\epsilon}_B/2)^2+t^2}}\right)\underbrace{\delta\left(\epsilon-\bar{\epsilon}_B/2+\sqrt{(\bar{\epsilon}_B/2)^2+t^2}\right)}_{\text{lower peak}}\end{aligned} \tag{5.84}$$

The result is shown in figure 5.1.

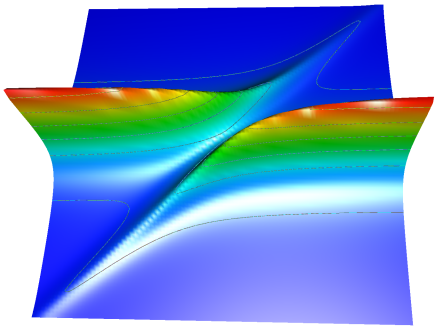

Fig. 5.1: Density of states projected onto orbital A, which is coupled to a second orbital B. The energy axis is the left edge of the graph and the projected density of states is the height. The orbital energy $\bar{\epsilon}_B$ changes from left $\bar{\epsilon}_B \ll \bar{\epsilon}_A$ to right $\bar{\epsilon}_B \gg \bar{\epsilon}_A$. As $\bar{\epsilon}_B$ crosses the energy $\bar{\epsilon}_A$, an avoided band crossing occurs. The positions of the maxima are the positions of the two energy levels. The height is the contribution of of that state at the first atom.

When we choose a $|\bar{\epsilon}_B| \gg t$, we recognize one peak of the density of states lies near zero, i.e. near $\bar{\epsilon}_A$, while the other lies near $\bar{\epsilon}_B$. The peak near $\bar{\epsilon}_B$ has the smaller weight compared to the one near zero. For $\bar{\epsilon}_B$ near zero, we can observe the **level repulsion**.

It shows that the spectral function at site A is only affected by site B if the two energies are close to each other.

One can verify that the peaks of the density of states obtained this way coincide precisely with the energies obtained for the asymmetric dimer in the exercise Eq. 1.5.2 on p. 28.

There is a sum rule, which says that the integral of the density of states Eq. 2.120 projected onto one orbital integrates to one, respectively to the norm of that orbital. [11]

$$\int d\epsilon \, \langle \chi | \hat{D}(\epsilon) | \chi \rangle = \langle \chi | \chi \rangle \tag{5.87}$$

Hence, the weight of a side-peak in the density of states is lost from main peak.

5. Editor: This problem shall describe how the charge oscillates in sites A, when it is in contact with B. The initial condition is that the particle is completely on site A. The charge oscillates on A as it oscillates back and forth between A and B with the excitation frequency. In the next problem we can discuss how a continuous spectrum in B leads to a decay of the occupation in A, as it leaks into an environment with an infinite number of states.

[11] One exploits that the density of states

$$\hat{D}(\epsilon) \overset{\text{Eq. 2.120}}{=} \sum_n |\varphi_n\rangle \delta(\epsilon - \epsilon_n) \langle \varphi_n | \tag{5.85}$$

integrates to the unit operator.

$$\int_{-\infty}^{\infty} d\epsilon \, \hat{D}(\epsilon) = \sum_n |\varphi_n\rangle \underbrace{\Big(\int_{-\infty}^{\infty} d\epsilon \, \delta(\epsilon - \epsilon_n) \Big)}_{=1} \langle \varphi | = \sum_n |\varphi_n\rangle \langle \varphi | = \hat{1} \tag{5.86}$$

Editor: The following is not finished yet!

$$
\begin{aligned}
\hat{G}(t,t') &\overset{\text{Eq. 4.60}}{=} \frac{1}{i\hbar}\theta(t-t')\int d\epsilon\ \hat{D}(\epsilon)\mathrm{e}^{-\frac{i}{\hbar}\epsilon(t-t')} \\
\hat{G}(t,t') &\overset{\text{Eq. 4.38}}{=} \frac{1}{i\hbar}\theta(t-t')\hat{U}(t,t') \\
|\psi(t)\rangle &= \hat{U}(t,t')|\psi(t')\rangle = i\hbar\hat{G}^{AA}(t,t')|\psi(t')\rangle \quad \text{for } t>t' \\
|\psi(t)\rangle &= i\hbar\left(\frac{1}{i\hbar}\int d\epsilon\ \hat{D}(\epsilon)\mathrm{e}^{-\frac{i}{\hbar}\epsilon(t-t')}\right)|\psi(t')\rangle \\
&= \int d\epsilon\ \hat{D}(\epsilon)\mathrm{e}^{-\frac{i}{\hbar}\epsilon(t-t')}|\psi(0)\rangle
\end{aligned}
\tag{5.88}
$$

$$
\langle\pi_A|\psi(t)\rangle = \langle\pi_A|\int d\epsilon\ \hat{D}(\epsilon)\mathrm{e}^{-\frac{i}{\hbar}\epsilon(t-t')}|\psi(0)\rangle \tag{5.89}
$$

5.4.2 System in contact with a bath having a finite lifetime

Introduction

Problem

Consider a two-state system, such as a spin-less Hubbard dimer with a ground state at energy 0 and one excited state at energy ϵ_A. This two-state system is coupled to a bath having a Lorentzian spectral function centered at $\bar{\epsilon}_B$ and having a life-time broadening Γ. The **full-width-at-half-maximum** (**FWHM**) is 2Γ.
The density of states (or spectral function) of a Lorentzian peak at energy $\bar{\epsilon}$ with lifetime $\hbar/\Gamma$ is (see also Eq. 4.63)

$$D(\epsilon) = \frac{1}{\pi}\frac{\Gamma}{(\epsilon-\bar{\epsilon})^2+\Gamma^2} \tag{5.90}$$

In Eq. 4.73, we obtained the Green's function for this system as

$$\bar{G}(\epsilon) = \frac{1}{\epsilon-\bar{\epsilon}+i\Gamma} \tag{5.91}$$

Consider the Hamiltonian from exercise 5.4.1 and replace the subsystem B by a system with Lorentzian density of states.

1. Determine the Green's function on subsystem A in the time and the energy representation. Plot the result.
2. Determine the energy in subsystem A, the expectation value of the Hamiltonian in the subspace A, as function of time. Discuss energy conservation.
3. Determine the wave function of subsystem A as function of time.

Discussion

1. Determine the Green's function on subsystem A in the time and the energy representation. Plot the result.

$$\begin{aligned}\Sigma^{AA}(\epsilon) &= V^{AB}\bar{G}^{BB}(\epsilon)V^{BA} = \frac{t^2}{\epsilon-\bar{\epsilon}_B+i\Gamma}\\ \Delta\Sigma^{AA}(\epsilon) &= \frac{t^2}{\epsilon-\bar{\epsilon}_B+i\Gamma}-\frac{t^2}{\epsilon} = \frac{t^2(\bar{\epsilon}_B-i\Gamma)}{\epsilon(\epsilon-\bar{\epsilon}_B+i\Gamma)}\end{aligned} \tag{5.92}$$

$$
\begin{aligned}
G^{AA}(\epsilon) &= \frac{\overbrace{\left(\bar{G}^{AA}\right)^{-1}}}{\left(\underbrace{\epsilon - h^{AA}}_{G^{AA}(0;\epsilon)} - \Sigma^{AA,(0)}(\epsilon)\right)^{-1}} - \Delta\Sigma^{AA}(\epsilon)\Bigg)^{-1} \\
&= \left(\frac{\epsilon^2 - t^2}{\epsilon} - \frac{t^2(\bar{\epsilon}_B - i\Gamma)}{\epsilon(\epsilon - \bar{\epsilon}_B + i\Gamma)}\right)^{-1} \\
&= \left(\frac{(\epsilon^2 - t^2)(\epsilon - \bar{\epsilon}_B + i\Gamma) - t^2(\bar{\epsilon}_B - i\Gamma)}{\epsilon(\epsilon - \bar{\epsilon}_B + i\Gamma)}\right)^{-1} \\
&= \left(\frac{\epsilon^3 - (\bar{\epsilon}_B - i\Gamma)\epsilon^2 - t^2\epsilon + (\bar{\epsilon}_B - i\Gamma)t^2 - t^2(\bar{\epsilon}_B - i\Gamma)}{\epsilon(\epsilon - \bar{\epsilon}_B + i\Gamma)}\right)^{-1} \\
&= \left(\frac{\epsilon^2 - (\bar{\epsilon}_B - i\Gamma)\epsilon - t^2}{\epsilon - \bar{\epsilon}_B + i\Gamma}\right)^{-1} \\
&= \frac{\epsilon - \bar{\epsilon}_B + i\Gamma}{\epsilon^2 - (\bar{\epsilon}_B - i\Gamma)\epsilon - t^2} \\
&= \frac{\epsilon - \bar{\epsilon}_B + i\Gamma}{\left[\epsilon - (\bar{\epsilon}_B - i\Gamma)/2 - \sqrt{\left(\frac{\bar{\epsilon}_B - i\Gamma}{2}\right)^2 + t^2}\right]\left[\epsilon - (\bar{\epsilon}_B - i\Gamma)/2 + \sqrt{\left(\frac{\bar{\epsilon}_B - i\Gamma}{2}\right)^2 + t^2}\right]}
\end{aligned}
\tag{5.93}
$$

Editor: This is sufficient for plotting. One should continue with the partial fraction decomposition. See Eq. 5.77 on p. 197

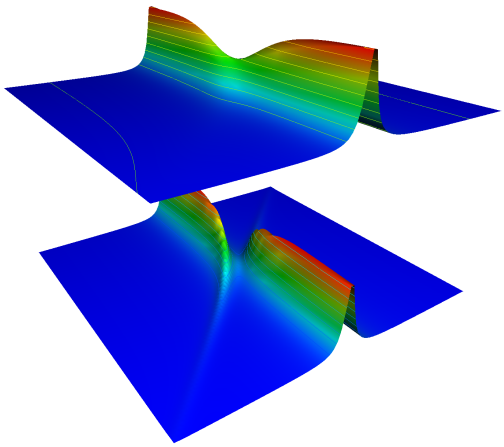

Fig. 5.2: Density of states (up) at an avoided band crossing, where the crossing band has a finite lifetime (top), compared to that for site B with infinite lifetime (bottom). Density of states as function of the energy (front-to-back) at the first orbital $|\chi_A\rangle$ in the dimer as function of the energy $\bar{\epsilon}_B$ (left-to-right) of the second orbital. The positions of the maxima are the positions of the two energy levels. The height is the contribution of of that state at the first atom.

Editor: This is nonsense!!!: Let me now transform the Green's function into the

time domain:

$$
\begin{aligned}
G^{AA}(\epsilon) &= \int_{-\infty}^{\infty} d\tau\, \mathrm{e}^{\frac{i}{\hbar}\epsilon\tau} G^{AA}(t+\tau,t) \\
G^{AA}(t+\tau,t) &= \int_{-\infty}^{\infty} d\epsilon\, \mathrm{e}^{-\frac{i}{\hbar}\epsilon\tau} G^{AA}(\epsilon) \\
&= \int_{-\infty}^{\infty} d\epsilon\, \mathrm{e}^{-\frac{i}{\hbar}\epsilon\tau} \frac{1}{\epsilon - \bar{\epsilon}_B + i\Gamma} \\
&= \mathrm{e}^{\frac{1}{\hbar}(i\bar{\epsilon}+\Gamma)\tau} \int_{-\infty}^{\infty} d\epsilon\, \mathrm{e}^{-\frac{i}{\hbar}(\epsilon-\bar{\epsilon}+i\Gamma)\tau} \frac{1}{\epsilon - \bar{\epsilon}_B + i\Gamma}
\end{aligned}
\tag{5.94}
$$

2. Determine the energy in subsystem A, the expectation value of the Hamiltonian in the subspace A, as function of time. Discuss energy conservation.

Editor: This problem is not yet done!

3. Determine the wave function of subsystem A as function of time.

Editor: This problem is not yet done!

5.4.3 Fano-Anderson model

Introduction

Editor: Check out

- Coherent Two-Dimensional Spectroscopy of a Fano Model'', by Daniel Finkelstein-Shapiro and Felipe Poulsen and Tõnu Pullerits and Thorsten Hansen, https://arxiv.org/pdf/1605.08572.pdf for introduction and references. See also ''Erratum: Coherent two-dimensional spectroscopy of a Fano model [Phys. Rev. B 94, 205137 (2016)]'' D Finkelstein-Shapiro, F Poulsen, T Pullerits, T Hansen Physical Review B 96 (23), 239906

- ''On the Ubiquity of Beutler-Fano Profiles: from Scattering to Dissipative Processes'' Daniel Finkelstein-Shapiro and Arne Keller, https://arxiv.org/pdf/1710.04800.pdf

- Non-linear Fano Interferences in Open Quantum Systems: an Exactly Solvable Model, https://arxiv.org/pdf/1509.04653.pdf

The Fano model[12][60] describes an atom which is adsorbed on a metal. It demonstrates the broadening of an energy level when it couples to a continuum.

[12] This exercise follows Stefanucci and van Leeuwen[2], section 2.3.2.

Problem

The Fano model describes a spinless electron with the Hamiltonian

$$\hat{h} = \underbrace{\epsilon_d \hat{d}^\dagger \hat{d}}_{\hat{H}^{AA}} + \underbrace{\sum_{\vec{k}} \epsilon_{\vec{k}} \hat{c}_{\vec{k}}^\dagger \hat{c}_{\vec{k}}}_{\hat{H}^{BB}} + \underbrace{\sum_{\vec{k}} \left(V_{\vec{k}} \hat{d}^\dagger \hat{c}_{\vec{k}} + V_{\vec{k}}^* \hat{c}_{\vec{k}}^\dagger \hat{d} \right)}_{\hat{H}^{AB} + \hat{H}^{BA}} \tag{5.95}$$

The creation operator $\hat{d}^\dagger$ creates a particle on the impurity A. The creation operators $\hat{c}_{\vec{k}}^\dagger$ create particles in the bath B. The index $\vec{k}$ reminds of a Bloch vector, albeit here it can be any label identifying the bath states.
The Hamiltonian corresponds to a non-interacting many-particle system. The one-particle Green's function is an operator in the one-particle Hilbert space, even for a many-particle system. [a]For a non-interacting system, the Green's function is identical to that of the one-particle system.

1. Calculate the Hamilton matrix with elements $h_{\alpha,\beta}$.
2. Determine the bath Green's function
3. Determine the self energy due to coupling to the bath. Work out real and imaginary part of the self energy at the real axis.
4. Determine the Green's function at the impurity, when it is coupled to the bath
5. Sketch the density of states at the impurity for two cases:
   - The impurity state lies within the spectrum of the bath
   - The impurity state lies outside the spectrum of the bath

   Consider a rectangular density of states of the bath with a width W and value $\frac{1}{W}$. Let the center of the density of states be $\bar{\epsilon}$. The hopping $V_{\vec{k}} = -t$ shall be constant.

[a]For a many-particle Hamiltonian $\hat{H}$ in Fock space, $(E\hat{1} - \hat{H})^{-1}$ is called **resolvent** rather than Green's function. The resolvent is an operator in Fock space.

Discussion

1. Calculate the Hamilton matrix with elements $h_{\alpha,\beta}$.

The Hamiltonian can be expressed as $\hat{h} = \sum_{\alpha,\beta} h_{\alpha,\beta} \hat{c}_\alpha^\dagger \hat{c}_\beta$ with

$$\boldsymbol{h} = \begin{pmatrix} \epsilon_d & \dots & V_{\vec{k}} & \dots \\ \vdots & \ddots & & 0 \\ V_{\vec{k}}^* & & \epsilon_{\vec{k}} & \\ \vdots & 0 & & \ddots \end{pmatrix} \tag{5.96}$$

The Hamilton operator in one-particle Hilbert space would be

$$\hat{h} = \sum_{\alpha,\beta} |\pi_\alpha\rangle h_{\alpha,\beta} \langle\pi_\beta| \tag{5.97}$$

where $\langle\pi_\alpha|$ are the projector functions for the set of orbitals $|\chi_\alpha\rangle$. In our case, the first orbital is

$|\chi_d\rangle$, while the remaining orbitals $|\chi_{\vec{k}}\rangle$ are Bloch waves in the bath, which are characterized by the Bloch-vector $\vec{k}$.

2. Determine the bath Green's function

The Green's function of the isolated bath is

$$\hat{\tilde{G}}^{BB}(\epsilon) \overset{\text{Eq. 5.7}}{=} \sum_{\vec{k}} |\chi_{\vec{k}}\rangle \frac{1}{\epsilon - \epsilon_{\vec{k}}} \langle \chi_{\vec{k}}| \tag{5.98}$$

3. Determine the self energy due to coupling to the bath. Work out real and imaginary part of the self energy at the real axis.

The self energy is

$$\hat{\Sigma}^{AA}(\epsilon) \overset{\text{Eq. 5.34}}{=} \hat{V}^{AB}\hat{\tilde{G}}^{BB}(\epsilon)\hat{V}^{BA} = |\pi_d\rangle \left(\sum_{\vec{k}} \frac{|V_{\vec{k}}|^2}{\epsilon - \epsilon_{\vec{k}}} \right) \langle \pi_d| \tag{5.99}$$

4. Determine the Green's function at the impurity, when it is coupled to the bath

In the complex plane, the Green's function is

$$\hat{G}^{AA}(\epsilon) \overset{\text{Eq. 5.33}}{=} \Big(\underbrace{|\pi_d\rangle(\epsilon - \epsilon_d)\langle \pi_d|}_{\hat{\tilde{G}}^{AA}(\epsilon)} - \hat{\Sigma}^{AA}(\epsilon) \Big)^{-1} \qquad \text{for } \mathrm{Im}(\epsilon) > 0 \tag{5.100}$$

The retarded Green's function is only defined in the half-plane with positive imaginary part of the energy.Editor: refer to where this has been discussed [13]

On the real energy axis,

$$\hat{G}^{AA}(\epsilon) \overset{\text{Eq. 5.33}}{=} \lim_{\eta \to 0^+} \Big(\underbrace{|\pi_d\rangle(\epsilon + i\eta - \epsilon_d)\langle \pi_d|}_{\hat{\tilde{G}}^{AA}(\epsilon + i\eta)} - \hat{\Sigma}^{AA}(\epsilon + i\eta) \Big)^{-1} \qquad \text{for } \epsilon \in \mathbb{R} \tag{5.101}$$

Let me divide the self energy into real and imaginary part

$$\hat{\Sigma}^{AA}(\epsilon) = |\pi_d\rangle \Big(\Lambda(\epsilon) + i\Gamma(\epsilon) \Big) \langle \pi_d| \qquad \text{for } \mathrm{Im}(\epsilon) > 0 \tag{5.102}$$

Right on the real axis, the self energy is real-valued, but also ill defined, because the imaginary part of the self energy is discontinuous as one crosses the real energy axis. Because we are interested in the retarded Green's function, we need to select a positive imaginary part of the energy, where the self energy is complex-valued.

[13] The retarded Green's function $G(t_2, t_1) = 0$ vanishes for $t_2 < t_1$. The energy-dependent Green's function is linked to the energy-dependent Green's function via Eq. 4.20 $\hat{G}(\epsilon, t_1) = \int_{-\infty}^{\infty} dt_2 \hat{G}(t_2, t_1) \mathrm{e}^{\frac{i}{\hbar}\epsilon(t_2 - t_1)}$.

The Green's function is[14]

$$\begin{aligned}\hat{G}^{AA}(\epsilon) &= \Big(|\pi_d\rangle\Big(\epsilon-\epsilon_d-\Lambda(\epsilon)-i\Gamma(\epsilon)\Big)\langle\pi_d|\Big)^{-1}\\ &= |\chi_d\rangle\Big(\epsilon-\epsilon_d-\Lambda(\epsilon)-i\Gamma(\epsilon)\Big)^{-1}\langle\chi_d|\\ &= |\chi_d\rangle\frac{\epsilon-\epsilon_d-\Lambda(\epsilon)+i\Gamma(\epsilon)}{\Big(\epsilon-\epsilon_d-\Lambda(\epsilon)\Big)^2+\Gamma^2(\epsilon)}\langle\chi_d| \end{aligned} \tag{5.105}$$

The imaginary part of the self energy is connected[15] to the density of states of the isolated system B weighted with the coupling parameters $|V_{\vec{k}}|^2$ to system A.

$$\lim_{\eta\to 0^+}\Gamma(\epsilon+i\eta)=\lim_{\eta\to 0^+}\mathrm{Im}\left(\sum_{\vec{k}}\frac{|V_{\vec{k}}|^2}{\epsilon+i\eta-\epsilon_{\vec{k}}}\right)=-\pi\sum_{\vec{k}}|V_{\vec{k}}|^2\delta(\epsilon-\epsilon_{\vec{k}}) \tag{5.106}$$

I used Eq. A.20 on p. 388, $\lim_{\eta\to 0^+}\mathrm{Im}(1/(x+i\eta))=-\pi\delta(x)$.

5. Sketch the density of states at the impurity for two cases:
   - The impurity state lies within the spectrum of the bath
   - The impurity state lies outside the spectrum of the bath

   Consider a rectangular density of states of the bath with a width W and value $\frac{1}{W}$. Let the center of the density of states be $\bar{\epsilon}$. The hopping $V_{\vec{k}}=-t$ shall be constant.

The density of states projected onto the atomic orbital of subsystem A is obtained via Eq. 4.51 from[16]

[14] The inverse of an operator $\hat{A}=\sum_{\alpha,\beta}|\pi_\alpha\rangle A_{\alpha,\beta}\langle\pi_\beta|$ is

$$\hat{A}^{-1}=\sum_{\gamma,\delta}|\chi_\gamma\rangle\left(A^{-1}\right)_{\gamma,\delta}\langle\chi_\delta| \tag{5.103}$$

Here the $\langle\pi_\alpha|$ are the projector functions for the orbitals $|\chi_\alpha\rangle$, which obey the bi-orthogonality condition $\langle\pi_\alpha|\chi_\beta\rangle=\delta_{\alpha,\beta}$. The projector functions can be written as $\langle\pi_\alpha|=\sum_\beta S^{-1}_{\alpha,\beta}\langle\chi_\beta|$, when both span the same Hilbert space. With these definitions, we can test the form of the inverse. We need to show $\hat{A}\hat{A}^{-1}=\hat{1}$.

$$\begin{aligned}\hat{1}&\stackrel{!}{=}\underbrace{\sum_{\alpha,\beta}|\pi_\alpha\rangle A_{\alpha,\beta}\langle\pi_\beta|}_{\hat{A}}\underbrace{\sum_{\gamma,\delta}|\chi_\gamma\rangle\left(A^{-1}\right)_{\gamma,\delta}\langle\chi_\delta|}_{\hat{A}^{-1}}=\sum_{\alpha,\beta}\sum_{\gamma,\delta}|\pi_\alpha\rangle A_{\alpha,\beta}\underbrace{\langle\pi_\beta|\chi_\gamma\rangle}_{\delta_{\beta,\gamma}}\left(A^{-1}\right)_{\gamma,\delta}\langle\chi_\delta|\\ &=\sum_{\alpha,\delta}|\pi_\alpha\rangle\underbrace{\sum_\beta A_{\alpha,\beta}\left(A^{-1}\right)_{\beta,\delta}}_{\delta_{\alpha,\delta}}\langle\chi_\delta|=\sum_\alpha|\pi_\alpha\rangle\langle\chi_\alpha|=\sum_{\alpha,\beta}|\chi_\beta\rangle S^{-1}_{\beta,\alpha}\langle\chi_\alpha|=\hat{1}\qquad q.e.d\end{aligned} \tag{5.104}$$

[15] The imaginary part of the Green's function of system B is related to its density of states and the self energy is the Green's function times the coupling of the subsystems.

[16] The matrix element is formed with the projector functions $|\pi_d\rangle$ rather than with the orbitals $|\chi_d\rangle$. For an orthonormal set like ours the two can be chosen identical. We have chosen the projector function, because this is the correct choice also for a non-orthonormal basisset. The convention is that matrix elements of observables a built with the orbitals $|\chi\rangle$ and act with the projector functions onto states. The density of states is, like the density matrix, not an observable but it describes a state. Therefore the matrix elements are build with the projector functions and they act with the orbitals onto observables.

p. 172.

$$\begin{aligned} D_d(\epsilon) &\overset{\text{Eq. 4.51}}{=} -\frac{1}{\pi}\lim_{\eta\to 0^+}\mathrm{Im}\big[\langle\pi_d|\hat{G}(\epsilon+i\eta)|\pi_d\rangle\big] \qquad \text{for } \epsilon\in\mathbb{R} \\ &\overset{\text{Eq. 5.102}}{=} -\frac{1}{\pi}\mathrm{Im}\left[\Big(\epsilon-\epsilon_d-\Lambda(\epsilon)-i\Gamma(\epsilon)\Big)^{-1}\right] \\ &= -\frac{1}{\pi}\left[\frac{\Gamma(\epsilon)}{\Big(\epsilon-\epsilon_d-\Lambda(\epsilon)\Big)^2+\Gamma^2(\epsilon)}\right] \\ &= \frac{1}{\pi}\frac{-\Gamma(\epsilon)}{\Big(\epsilon-\epsilon_d-\Lambda(\epsilon)\Big)^2+\Gamma^2(\epsilon)} \end{aligned} \tag{5.107}$$

Constant density of states in the bath: Let me start the discussion with the most simple case, namely that the self energy is a constant, i.e. energy-independent. Hence, also Λ and Γ are constants. The resulting density of states $D_d(\epsilon)$ of system A in contact with B is a Lorentzian centered at $\epsilon_d+\Lambda$ with a width proportional to $|\Gamma|$. This shows that an energy level broadens, when it is coupled to a continuum of states. The width of the resulting peak is the **life-time broadening**. Its inverse is related to the time, for which the particle remains in system A before it is scattered into the environment, namely system B. The position of the Lorentzian is shifted by the **quasi-particle shift** $\mathrm{Re}\Sigma=\Lambda$ away from the original position of the d-level.

Box-shaped bath density of states: Let me now investigate the next more realistic case: The bath shall have a box-shaped density of states with a finite with. The coupling $V_{\vec{k}}$ shall be, again, constant, i.e. $V_{\vec{k}}=-t$.

$$D^B(\epsilon)=\sum_{\vec{k}}\delta(\epsilon-\bar{\epsilon}_{\vec{k}})=\begin{cases}\frac{1}{W} & \text{for } \bar{\epsilon}-\frac{1}{2}W<\epsilon<\bar{\epsilon}+\frac{1}{2}W\\ 0 & \text{else}\end{cases} \tag{5.108}$$

The result for density of states projected onto the impurity is shown in the lower graph[17] of Fig. 5.3. In the following I will discuss this figure. Let me consider two limiting cases.

- If the coupling t is small compared to the band width W of system B, we can approximate the system by the limit of infinite band width of system B. In that case, the situation is close to the case of a constant self energy discussed before. The resulting density of states $D_d(\epsilon)$ on system A is a Lorentzian with a lifetime broadening that grows with the coupling t between the two systems.
- If the coupling t is large compared to the band width W of system B, the band width of system B can be neglected and system B can be approximated by a single energy level at the center of the band. The situation is close to the case of a dimer, where one atom is the system A and the other is system B. The density of states has one bonding level at low energies and an antibonding level at high energies. For the degenerate case $\bar{\epsilon}_d-\bar{\epsilon}\ll t$ the weight of the two peaks on system A will be similar. In the non-degenerate limit $\bar{\epsilon}_d-\bar{\epsilon}\gg t$, the weight of the state, which is closer to the d-level, will be dominant compared to the other, which is further away.

[17] The graph Fig. 5.3 shows the density of state D_d shifted by $15t$ for better visibility.

$$\begin{aligned} D_d(\epsilon) &= -\frac{1}{\pi}\mathrm{Im}\Big[\frac{1}{\epsilon-\epsilon_d+i\eta+\frac{t^2}{W}\ln\left(\frac{\epsilon-\frac{1}{2}W+i\eta}{\epsilon+\frac{1}{2}W+i\eta}\right)}\Big] \\ \epsilon_d &= \frac{1}{4}; \qquad W=1; \qquad \eta=0.01; \qquad t\in\{0,\frac{1}{10},\frac{2}{10},\frac{3}{10},\frac{4}{10},\frac{5}{10},\frac{6}{10},\frac{7}{10}\} \end{aligned} \tag{5.109}$$

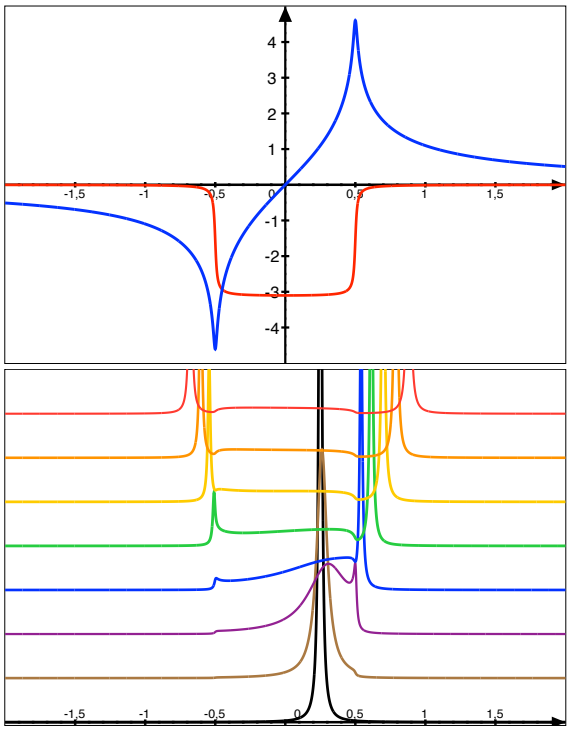

Fig. 5.3: Upper graph: Real part (blue) and imaginary part (red) of the bath Green's function $\bar{G}^{BB}(\epsilon) = -\frac{1}{W}\ln(\frac{\epsilon - W/2 + i\eta}{\epsilon + W/2 + i\eta})$ for $\eta = 0.01$ and $W = 1$ with a constant density of states $D(\epsilon) = 1$ in the energy window between $-\frac{1}{2} \leq \epsilon \leq \frac{1}{2}$. Lower graph: Density of states at atom A in contact with the bath B for $\epsilon_d = \frac{1}{4}$ and hopping parameters $t \in \{0, \frac{1}{10}, \ldots, \frac{7}{10}\}$.

Let me now walk you through the individual results in figure 5.3 step by step: For small hopping $t = 0.1$ the density of states of the d-level broadens due to the hybridization with the bath. As the coupling increases, the d-level broadens further. A peak emerges beyond the band of the bath, which inherits the life time from the original energy level. Also at the lower end of the bath spectrum a second peak emerges. The two peaks correspond to the bonding states and the antibonding states between the two systems. The weight that enters into the separated peaks i removed from the density of states in within the spectrum of the bath.

Analogy with the dimer: I find it useful to rationalize the findings considering one bath state at a time. A pair of states is analogous to the di-atomic molecule investigated in exercises 1.5.1 and 1.5.2. For the following discussion, I recommend to inspect figure 1.4 on p. 30, which I am repeating here for your convenience.

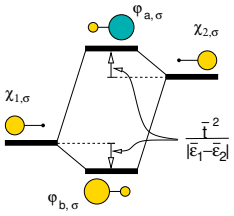

Let me identify the orbital $|\chi_1\rangle$ on the left atom with the impurity A, and the orbital $|\chi_2\rangle$ on the right with the bath B. Let me leave the obvious level repulsion aside and let us focus on the wave functions. As the two states $|\chi_1\rangle$ and $|\chi_2\rangle$ hybridize and form the bonding and antibonding states.

Some weight from site A is transferred from the bonding to the antibonding state. That is, also the antibonding state $|\varphi_a\rangle$ has a contribution from $|\chi_1\rangle$. The density of states projected onto the impurity has a large contribution at the energy of the impurity level and a smaller contribution at the energy of the bath level. The charge sum rule ensures that the total weight from the impurity is still equal to unity. When we take many bath states into account in a similar way, we will notice that the density of states projected onto the impurity is smeared out. Because the hybridization becomes smaller when the initial levels are more distant, the density of states is peaked close to the position of the original impurity level and it falls of further away. This effect is the **lifetime broadening**.

Editor: Why is it called lifetime broadening? Imagine a wave function which is completely localized on the impurity site A. If the impurity is coupled to the bath, the initial state is not an eigenstate of the combined system. The wave function is

$$|\psi(t)\rangle = \sum_{n\in\{a,b\}} |\varphi_n\rangle e^{-\frac{i}{\hbar}\epsilon_n t}\langle\varphi_n|\chi_1\rangle \tag{5.110}$$

The time-dependent probability on site A is thus... Editor: This argument needs to be completed

Editor: Are the limiting cases covered? (1) impurity level in the continuum of bath states. (2) impurity level separated far from the bath states. (3) strong coupling: impurity and surface site form a dimer, which is weakly coupled to the continuum.

Sanity check: Correspondence with Fano's paper

Editor: This section is not meant for the reader.

The exercise presented here is closely connected to the original paper by Fano[60]. As a sanity check of the derivations, am adding here a one-to-one correspondence of the most relevant equations from Fano's paper and the formulas above.

1. Fano-Eq.2 is Eq. 5.1

$$\begin{aligned} |\Psi_E\rangle &= |\varphi\rangle a + \int d\epsilon'\, |\psi_{E'}\rangle b(E') \qquad \text{Fano-Eq.2} \\ |\psi\rangle &= |\chi^A\rangle c^A + \sum_{\beta\in B} |\chi^B_\beta\rangle c^B_\beta \qquad \text{This text Eq. 5.1} \end{aligned} \tag{5.111}$$

2. Fano-Eq.3a,b is my Eq. 5.3. The definitions $E_\varphi = \langle\varphi|\hat{H}|\varphi\rangle$ and $V_E = \langle\varphi|\hat{H}|\psi(E)\rangle$ are used.

$$\begin{aligned} \langle\varphi|\Big(\hat{H} - E\hat{1}\Big)\Big(|\varphi\rangle a + \int dE'\, |\psi(E')\rangle b(E')\Big) &= 0 \\ \Rightarrow \qquad (E_\varphi - E)a + \int dE'\, V^*_{E'} b(E') &= 0 \qquad \text{Fano-Eq.3a} \\ \langle\psi_{E''}|\Big(\hat{H} - E\hat{1}\Big)\Big(|\varphi\rangle a + \int dE'\, |\psi(E')\rangle b(E')\Big) &= 0 \\ \Rightarrow \qquad V_{E''} a + \int dE'\, (E'' - E)\delta(E'' - E') b(E') &= 0 \\ \Rightarrow \qquad V_{E'} a + (E' - E) b(E') &= 0 \qquad \text{Fano-Eq.3b} \end{aligned} \tag{5.112}$$

3. Fano-Eq.4 is my Eq. 5.6.

$$\begin{aligned} b_{E'} &= \left[\frac{1}{E - E'} + z(E)\delta(E - E')\right] V_{E'} a \qquad \text{Fano-Eq.4} \\ \vec{c}^B &= (\epsilon \mathbf{1}^{BB} - \boldsymbol{H}^{BB})^{-1} \boldsymbol{V}^{BA} \vec{c}^A \qquad \text{This work Eq. 5.6} \end{aligned} \tag{5.113}$$

Fano introduces the quantity $z(E)$. Fano refers to the PhD thesis of van Kampen[61]. (Check chapter 6, p 50). We may add to $\vec{c}^B$ any state from the bath, for which $(\epsilon \mathbf{1}^{BB} - \boldsymbol{H}^{BB})\vec{c}^B = 0$. This solution of the homogeneous equation is described by Fano by adding $z(E)$

Fano obtains $z(E)$ by inserting his Eq.4 into his Eq.3a.

$$\begin{aligned} E_\varphi a + \int dE'\, V^*_{E'} \left[\frac{1}{E-E'} + z(E)\delta(E-E') \right] V_{E'} a = Ea \\ E_\varphi + \left(\int dE'\, \frac{|V_{E'}|^2}{E-E'} \right) + z(E)|V_E|^2 = E \\ z(E) = \frac{1}{|V_E|^2} \left(E - E_\varphi + \int dE'\, \frac{|V_{E'}|^2}{E-E'} \right) \qquad \text{Fano-Eq.9 with Fano-Eq.8} \end{aligned} \tag{5.114}$$

Let me repeat this in my notation

$$\begin{aligned} \Big(\boldsymbol{H}^{AA} - \epsilon \mathbf{1}^{AA} \Big) \vec{c}^A + V^{AB} \vec{c}^B = 0 \\ \Big(\boldsymbol{H}^{AA} - \epsilon \mathbf{1}^{AA} \Big) \vec{c}^A + V^{AB} \left[(\epsilon \mathbf{1}^{BB} - \boldsymbol{H}^{BB})^{-1} \boldsymbol{V}^{BA} \vec{c}^A + \vec{c}^{B,hom} \right] = 0 \\ \Big(\boldsymbol{H}^{AA} - \epsilon \mathbf{1}^{AA} + V^{AB} (\epsilon \mathbf{1}^{BB} - \boldsymbol{H}^{BB})^{-1} \boldsymbol{V}^{BA} \Big) \vec{c}^A + V^{AB} \vec{c}^{B,hom} = 0 \end{aligned} \tag{5.115}$$

Let me now write $\vec{c}^{B,hom} = \boldsymbol{V}^{AB} \boldsymbol{z}(E) \boldsymbol{V}^{\boldsymbol{BA}} \vec{c}^A$.

$$\begin{aligned} \Big(\boldsymbol{H}^{AA} - \epsilon \mathbf{1}^{AA} + \boldsymbol{V}^{AB} (\epsilon \mathbf{1}^{BB} - \boldsymbol{H}^{BB})^{-1} \boldsymbol{V}^{BA} \Big) \vec{c}^A + \boldsymbol{V}^{AB} \boldsymbol{z} \boldsymbol{V}^{BA} \vec{c}^A = 0 \\ \boldsymbol{V}^{AB} \boldsymbol{z} \boldsymbol{V}^{BA} = - \Big(\boldsymbol{H}^{AA} - \epsilon \mathbf{1}^{AA} + \boldsymbol{V}^{AB} (\epsilon \mathbf{1}^{BB} - \boldsymbol{H}^{BB})^{-1} \boldsymbol{V}^{BA} \Big) \end{aligned} \tag{5.116}$$

$$\begin{aligned} |\Psi_E\rangle &= |\varphi\rangle + \int dE'\, |\psi_{E'}\rangle \frac{|V_{E'}|^2}{E-E'} + \int dE'\, |\psi_{E'}\rangle V^*_{E'} z(E) \delta(E-E') V_{E'} \\ &= |\varphi\rangle + \int dE'\, |\psi_{E'}\rangle \frac{|V_{E'}|^2}{E-E'} + |\psi_E\rangle V^*_E z(E) V_E \\ &= |\varphi\rangle + \int dE'\, |\psi_{E'}\rangle \frac{|V_{E'}|^2}{E-E'} - |\psi_E\rangle \underbrace{\left(E - E_\varphi - \int dE'\, \frac{|V_{E'}|^2}{E-E'} \right)}_{|V_E|^2 z(E)} \end{aligned} \tag{5.117}$$

$$\begin{aligned} |\Psi(E)\rangle &= |\varphi\rangle + \int dk\, |\psi_k\rangle \frac{|V_k|^2}{E-E_k} + \int dk\, |\psi_k\rangle |V_k|^2 z(k) \delta(E-E_k) \\ &= |\varphi\rangle + \int dk\, |\psi_k\rangle \frac{|V_k|^2}{E-E_k} + |\psi_{k(E)}\rangle V^*_{k(E)} z(E) V_{k(E)} \\ &= |\varphi\rangle + \int dk\, |\psi_k\rangle \frac{|V_k|^2}{E-E_k} - |\psi_{k(E)}\rangle \underbrace{\left(E - E_\varphi - \int dk\, \frac{|V_k|^2}{E-E_k} \right)}_{|V_{k(E)}|^2 z(E(k))} \\ &= |\varphi\rangle + |\psi_{k(E)}\rangle \Big(E - E_\varphi \Big) + \int dk\, \Big(|\psi_k\rangle - |\psi_{k(E)}\rangle \Big) \frac{|V_k|^2}{E-E_k} \end{aligned} \tag{5.118}$$

Fano-Anderson model by direct diagonalization

Editor: This is not finished. It is not meant for the reader.

In this section, I perform a numerical calculation on the Fano model with a finite number of bath states. The goal is to explore in detail, how the surface states separate from the continuum.

Editor: Caution: Here I am using the symbol $\bar{\epsilon}_a$, rather than $\bar{\epsilon}_d$ used before.

I start from the Hamiltonian

$$\begin{aligned}\hat{h} &= |\pi_a\rangle\bar{\epsilon}_a\langle\pi_a| + \sum_k |\pi_k\rangle\bar{\epsilon}_k\langle\pi_k| + \sum_k \Big(|\pi_a\rangle V_k\langle\pi_k| + |\pi_k\rangle V_k^*\langle\pi_a|\Big)\\ \hat{h} &= \bar{\epsilon}_a\hat{c}_a^\dagger\hat{c}_a + \sum_k \bar{\epsilon}_k\hat{c}_k^\dagger\hat{c}_k + \sum_k \Big(V_k\hat{c}_a^\dagger\hat{c}_k + V_k^*\hat{c}_k^\dagger\hat{c}_a\Big)\\ &= \begin{pmatrix}\hat{c}_a^\dagger\\ \hat{c}_1^\dagger\\ \hat{c}_2^\dagger\\ \vdots\end{pmatrix}\begin{pmatrix}\bar{\epsilon}_a & V_1 & V_2 & \cdots\\ V_1^* & \bar{\epsilon}_1 & 0 & \cdots\\ V_2^* & 0 & \bar{\epsilon}_2 & \cdots\\ \vdots & \vdots & \vdots & \vdots\end{pmatrix}\begin{pmatrix}\hat{c}_a\\ \hat{c}_1\\ \hat{c}_2\\ \vdots\end{pmatrix}\end{aligned} \tag{5.119}$$

The first Hamiltonian in the equation above is a one-particle Hamiltonian, while the second, despite using the same symbol, is a one-particle-at-a-time Hamiltonian, which acts in Fock space.

Eigenvalues The characteristic equation is

$$\Big(\bar{\epsilon}_a - \epsilon - \sum_k \frac{|V_k|^2}{\bar{\epsilon}_k - \epsilon}\Big)\prod_k(\bar{\epsilon}_k - \epsilon) = 0 \Rightarrow \qquad \epsilon - \bar{\epsilon}_a - \overbrace{\sum_k \frac{|V_k|^2}{\epsilon - \bar{\epsilon}_k}}^{\Sigma(\epsilon)} = 0 \tag{5.120}$$

The zeros of the function determine the positions of the eigenstates.

It is convenient to take the arcus tangens of this function to avoid the infinities. We name the resulting function $y(\epsilon)$

$$y(\epsilon) \stackrel{\text{def}}{=} -\frac{1}{\pi}\arctan\left(\sum_k \frac{V_k^2}{\epsilon - \bar{\epsilon}_k} + \bar{\epsilon}_a - \epsilon\right) \tag{5.121}$$

This function is shown in figure 5.4 for the case at hand.

To be concrete, let me choose a specific coupling V_k between bath and impurity: The system B shall be a metallic system with band edges at A and B. The squared coupling parameters shall sum up to t, an effective hopping parameter. First an energy-dependent coupling parameter $V(\epsilon)$ is defined. It has the shape of an inverted parabola, with zeros at the band edges and with the desired norm $\int_A^B d\epsilon\, V^2(\epsilon) = t$. Then we choose a specific number M of bath sites and obtain the coupling parameters as $V_k^2 = \frac{1}{M}V(\epsilon_k)$

The bare energies $\bar{\epsilon}_k$ of the bath sites are placed on an equi-spaced grid with $M-1$ points with $A < \bar{\epsilon}_k < B$. (The value $\bar{\epsilon}_M = B$ does not contribute, because $V_M = 0$.)

$$\begin{aligned}\bar{\epsilon}_k &= A + (B-A)\frac{k}{M}\\ V_k &= t\sqrt{\frac{(\bar{\epsilon}_k - A)(B - \bar{\epsilon}_k) + 10^{-3}}{-AB(B-A) - \frac{1}{3}(B^3 - A^3) + \frac{1}{2}(B^2 - A^2)(A+B)}}\end{aligned} \tag{5.122}$$

A good guidance is obtained by an approximation of the real system, where the continuum of states is replaced by a single state at $\bar{\epsilon}_b$, the center of gravity of the spectrum of system B,

$$\bar{\epsilon}_b = \frac{\sum_k |V_k|^2\bar{\epsilon}_k}{\sum_k |V_k|^2}\,, \tag{5.123}$$

with a hopping term equal to $t = \frac{1}{M}\sum_{k=1}^M V_k^2$.

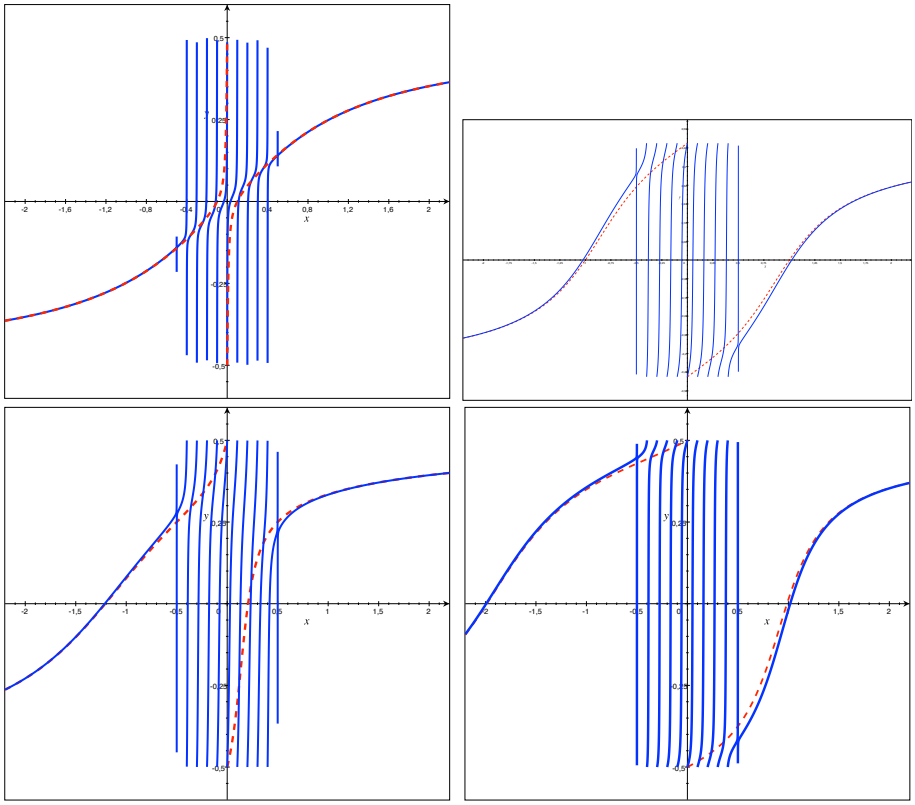

Fig. 5.4: $y(\epsilon) = -\frac{1}{\pi}\arctan\left(\frac{1}{M}\sum_{j=1}^{M}\frac{V^2(\epsilon_j)}{\epsilon-\bar{\epsilon}_k} + \bar{\epsilon}_a - \epsilon\right)$ as function of energy. The dashed line replaces the "continuum" by a single state in its center. (1) $\bar{\epsilon}_a = 0$, $t = 0.2$, $A = -0.5$, $B = 0.5$, $M = 10$ Bonding and antibonding states with the impurity inside the continuum. (2) $\bar{\epsilon}_a = 0$, $t = 1$, $A = -0.5$, $B = 0.5$, $M = 10$ Bonding and antibonding states with the impurity outside the continuum. (3) $\bar{\epsilon}_a = -1$, $t = 0.5$, $A = -0.5$, $B = 0.5$, $M = 10$ (3) $\bar{\epsilon}_a = -1$, $t = 0.5$, $A = -0.5$, $B = 0.5$, $M = 10$ (4) $\bar{\epsilon}_a = -1$, $t = 1.4$, $A = -0.5$, $B = 0.5$, $M = 10$

The eigenstates of the approximate system are determined by the zeros of the function $\bar{y}(\epsilon)$, which is shown as dashed red line

$$\bar{y}(\epsilon) = -\frac{1}{\pi}\arctan\left(\frac{t^2}{\epsilon - \frac{1}{2}(A+B)} + \bar{\epsilon}_a - \epsilon\right) \tag{5.124}$$

whose zeros describe the eigenstates of the approximate system shown in figure 5.4.

There are three possible cases

- Weak coupling: bonding and antibonding state of the two-state problem lie in the continuum. The impurity level is broadened into a resonance inside the continuum.
- one of the two states of the two-state problem lies inside the continuum and the other outside.
- Strong coupling: the bonding state of the two-state problem lies below the continuum and a the antibonding state lies outside. Two sharp states lie outside the continuum.

Level repulsion by the impurity level displaces the energy levels in the continuum, but the continuum levels cannot be displaced beyond the neighboring energy level. Thus, the displacement in the continuum is of order $\frac{1}{M}$. In the limit $M \to \infty$, the displacement approaches zero, but the overall

displacement of the weight $\sim M\frac{1}{M}$ remains finite. This is also important to satisfy the sumrule that the trace of the Hamiltonian is invariant under unitary transformation, which says that the sum of the energy levels is equal to the trace.

Eigenstates

$$|\psi\rangle = |\chi_a\rangle a + \sum_k |\chi_k\rangle b_k$$
$$(\hat{h}-\epsilon)|\psi\rangle = |\chi_a\rangle \underbrace{\Big((\bar{\epsilon}_a-\epsilon)a + \sum_k V_k b_k\Big)}_{(A)} + \sum_k |\varphi_k\rangle \underbrace{\Big(V_k a + (\bar{\epsilon}_k-\epsilon)b_k\Big)}_{(B)} \stackrel{!}{=} 0 \qquad (5.125)$$

This equation can only be satisfied at the zeros of the characteristic equation, respectively of $y(\epsilon)$, defined earlier.

Let me satisfy the equation above by finding the zeros of (B) and then of (A).

$$\underbrace{V_k a + (\bar{\epsilon}_k-\epsilon)b_k}_{(B)} = 0 \qquad \Rightarrow \qquad b_k = \frac{1}{\epsilon-\bar{\epsilon}_k} V_k a$$
$$|\psi\rangle = \Big[|\chi_a\rangle + \sum_k |\varphi_k\rangle \frac{1}{\epsilon-\bar{\epsilon}_k} V_k\Big] a = \frac{|\chi_a\rangle + \sum_k |\varphi_k\rangle \frac{1}{\epsilon-\bar{\epsilon}_k} V_k}{\sqrt{1+\sum_k \frac{|V_k|^2}{(\epsilon-\bar{\epsilon}_k)^2}}} \qquad (5.126)$$

The second equation,

$$0 = \underbrace{(\bar{\epsilon}_a-\epsilon)a + \sum_k V_k b_k}_{(A)} = \Big[(\bar{\epsilon}_a-\epsilon) + \underbrace{\sum_k V_k \frac{1}{\epsilon-\bar{\epsilon}_k} V_k}_{\Sigma(\epsilon)}\Big] a\,, \qquad (5.127)$$

is, in essence, identical to the characteristic equation and determines the positions of the energy levels of the combined system.

The energy of the impurity level in contact with system B is estimated by a Taylor expansion of (A) about the bare impurity level $\bar{\epsilon}_a$

$$0 = (\bar{\epsilon}_a-\epsilon) + \underbrace{\sum_k V_k \frac{1}{\bar{\epsilon}_a-\bar{\epsilon}_k} V_k}_{\Sigma(\bar{\epsilon}_a)} - \underbrace{\sum_k V_k \frac{1}{(\bar{\epsilon}_a-\bar{\epsilon}_k)^2} V_k}_{\partial_\epsilon \Sigma(\bar{\epsilon}_a)} (\epsilon-\bar{\epsilon}_a) + O(\epsilon-\bar{\epsilon}_a)^2$$
$$\epsilon = \bar{\epsilon}_a + \frac{\Sigma(\bar{\epsilon}_a)}{1+\partial_\epsilon|_{\bar{\epsilon}_a}\Sigma} \qquad \text{for small } |\epsilon-\bar{\epsilon}_a| \qquad (5.128)$$

This energy is the next zero of the characteristic polynomial, respectively of $y(\epsilon)$, which lies next to $\bar{\epsilon}_a$. In the continuum limit for the spectrum of subsystem B, the energy derivative of the self energy approaches infinity inside the spectrum of B. This result is not meaningful. Thus, the expression above provides an approximation for the shift of the impurity level, only if the bare level lies outside the spectrum of system B.

Editor: This is open ended...

5.4.4 Surface Green's function of a one-dimensional linear chain

Editor: For the Greens function of a few simple examples, see "The pedagogical introduction to equilibrium Green's function" by Odashima et al.[62].

Introduction

In the previous problem on the Fano model, we studied an adsorbed atom on a surface. For the surface, however, we simply assumed the shape of the density of states. The Green's function of the surface will be a useful model to study (1) adsorbed atoms, (2) two-dimensional band structures of three-dimensional systems and (3) interfaces obtained by gluing to surfaces together.

Problem

Consider a half-infinite one-dimensional chain of atoms with one orbital per site. To keep things simple, consider only a single spin direction. The orbital energy is $\bar{\epsilon}$ and the hopping parameter is t.

$$\hat{h} = \sum_{j=1}^{N} |\pi_j\rangle \bar{\epsilon} \langle \pi_j| - t \sum_{j=1}^{N} \Big(|\pi_j\rangle\langle \pi_{j+1}| + |\pi_{j+1}\rangle\langle \pi_j| \Big) \tag{5.129}$$

1. Construct eigenvalues and eigenstates of a finite chain of hydrogen atoms. Inspect the dispersion relation, the quantization of wave vectors, the energy levels, and the density of states in the limit of an infinitely long chain. Ensure that the eigenstates are normalized and describe how. Trick: Extend the chain by one bead in each direction to formulate the boundary conditions.
2. Form the Green's function of the finite chain.
3. Let one of the ends of the chain go to infinity and thus form the Green's function of the half-infinite chain.
4. Calculate the density of states on each atom of the half-infinite chain. Discuss the changes of the density of states as function of distance from the surface. Discuss, how the density of states of the infinite chain is obtained.
5. Calculate the Green's function of the terminal site as function of $\frac{\epsilon-\bar{\epsilon}}{2t}$.

During the calculation, I required the integral formula [Bronstein-Eq. 347 on p.55[63]] below:

$$\int dx \, \frac{1}{a+\cos(x)} = \begin{cases} \frac{2}{\sqrt{a^2-1}} \arctan \frac{(a-1)\tan(x/2)}{a^2-1} & \text{for } a^2 > 1 \\ \frac{1}{\sqrt{1-a^2}} \ln \frac{(1-a)\tan(x/2)+\sqrt{1-a^2}}{(1-a)\tan(x/2)-\sqrt{1-a^2}} & \text{for } a^2 < 1 \end{cases} \tag{5.130}$$

Discussion

1. Construct eigenvalues and eigenstates of a finite chain of hydrogen atoms. Inspect the dispersion relation, the quantization of wave vectors, the energy levels, and the density of states in the limit of an infinitely long chain. Ensure that the eigenstates are normalized and describe how.

   Trick: Extend the chain by one bead in each direction to formulate the boundary conditions.

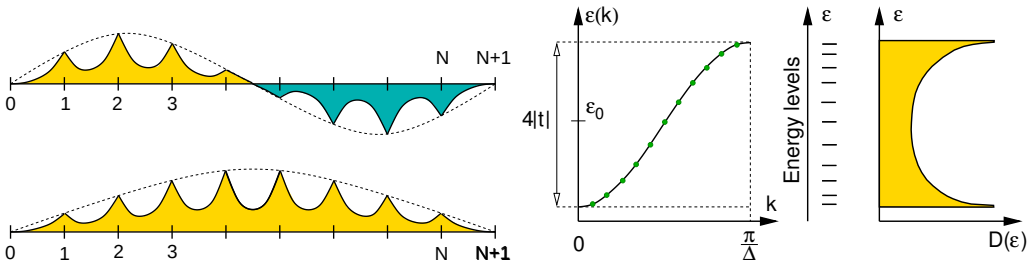

Consider a finite chain with N atoms. The distance between the atoms is the lattice constant a_{lat}.

The Hamiltonian is

$$\hat{h} = \sum_{j=1}^{N} |\pi_j\rangle \bar{\epsilon} \langle \pi_j| - t \sum_{j=1}^{N-1} \Big(|\pi_j\rangle\langle\pi_{j+1}| + |\pi_{j+1}\rangle\langle\pi_j| \Big) \tag{5.131}$$

The eigenstates can be built up from plane waves with the correct dispersion relation and boundary conditions. The dispersion relation follows from the Schrödinger equation.

$$\begin{aligned} \Big[\hat{h} - \epsilon \hat{1}\Big] \sum_{j=1}^{N} |\chi_j\rangle c_{j,n} &= 0 \\ \Rightarrow \quad -t c_{j+1} - t^* c_{j-1} + (\bar{\epsilon} - \epsilon) c_j &= 0 \end{aligned} \tag{5.132}$$

Except for the end-points the problem has translation invariance which suggests to use the eigenstates of the translation, namely plane waves $c_{j,n} = C \mathrm{e}^{i k_n a_{\text{lat}} j}$.

$$\begin{aligned} -t \mathrm{e}^{i k_n a_{\text{lat}}} - t^* \mathrm{e}^{-i k_n a_{\text{lat}}} + (\bar{\epsilon} - \epsilon_n) &= 0 \\ \epsilon_n = \bar{\epsilon} - 2\mathrm{Re}[t \mathrm{e}^{i k_n a_{\text{lat}}}] = \bar{\epsilon} - 2\mathrm{Re}[t] \cos(k_n a_{\text{lat}}) + 2\mathrm{Im}[t] \sin(k_n a_{\text{lat}}) & \end{aligned} \tag{5.133}$$

In the following, we consider the hopping parameter as real-valued quantity. Editor: Nevertheless let us discuss the role of the imaginary part of the Hopping parameter. (no time inversion symmetry, magnetic fields?....

The boundary conditions can be enforced as follows. Let us extend the chain by one bead in each direction, so that there is one atom at $j = 0$ and one with $j + 1$. This ensures that all atoms with $j \in \{1, \ldots, N\}$ do not experience the surface. Then I introduce the boundary condition that the coefficients $c_{0,n} = 0$ and $c_{N+1,n} = 0$. This ensures that the outermost true atoms obey the equation appropriate for the surface. (no contribution from $j = 0$ and $j = N + 1$.

With this argument the wave functions can be written down as

$$|\varphi(k_n)\rangle = \sum_{j=1}^{N} |\chi_j\rangle \sin(k_n a_{\text{lat}} j) \sqrt{\frac{2}{N+1}} \tag{5.134}$$

and

$$\epsilon(k_n) = \bar{\epsilon} - 2t \cos(k_n a_{\text{lat}}) \tag{5.135}$$

with

$$k_n = \frac{\pi}{a_{\text{lat}}(N+1)} n \quad \text{for } n = 1, \ldots, N \tag{5.136}$$

The quantization condition follows from $\sin(k_n a_{\text{lat}}(N+1)) = 0$, so that $k_n = \frac{\pi}{a_{\text{lat}}(N+1)} n$

The normalization comes from the fact that the $\frac{1}{\pi} \int_0^\pi dx \ \sin^2(x) = \frac{1}{2}$ Editor: This also holds for a discrete sum, which needs to be shown.

2. Form the Green's function of the finite chain.

The Green's function is

$$\begin{aligned}\hat{G}(\epsilon+i\eta) &= \sum_{n=1}^{N}|\varphi_n\rangle\frac{1}{\epsilon-\epsilon_n+i\eta}\langle\varphi_n| \\ &= \sum_{j,j'=1}^{N}\sum_{n=1}^{N}|\chi_j\rangle\langle\pi_j|\varphi_n\rangle\underbrace{\frac{\epsilon-\epsilon_n-i\eta}{(\epsilon-\epsilon_n)^2+\eta^2}}_{\frac{1}{\epsilon-\epsilon_n}-i\pi\delta(\epsilon-\epsilon_n)}\langle\varphi_n|\pi_{j'}\rangle\langle\chi_{j'}| \\ &= \sum_{j,j'=1}^{N}|\chi_j\rangle\Bigg\{\underbrace{\sum_{n=1}^{N}\frac{\langle\pi_j|\varphi_n\rangle\langle\varphi_n|\pi_{j'}\rangle}{\epsilon-\epsilon_n}}_{\text{hermitian}}\underbrace{-i\pi\sum_{n=1}^{N}\langle\pi_j|\varphi_n\rangle\langle\varphi_n|\pi_{j'}\rangle\delta(\epsilon-\epsilon_n)}_{\text{anti hermitian}}\Bigg\}\langle\chi_{j'}| \end{aligned} \tag{5.137}$$

This is a good point to learn about the **Kramers-Kronig relations**. The equation above shows that the Green's function can be obtained directly from the density of states.

1. Let me extract the density of states using Eq. 4.50.

$$\begin{aligned}\hat{D}(\epsilon) &\overset{\text{Eq. 4.50}}{=} -\frac{1}{2\pi i}\lim_{\eta\to 0^+}\left(\hat{G}(\epsilon+i\eta)-\hat{G}^\dagger(\epsilon+i\eta)\right). \\ &= \sum_{j,j'=1}^{N}|\chi_j\rangle\Bigg\{\sum_{n=1}^{N}\langle\pi_j|\varphi_n\rangle\langle\varphi_n|\pi_{j'}\rangle\delta(\epsilon-\epsilon_n)\Bigg\}\langle\chi_{j'}|\end{aligned} \tag{5.138}$$

2. Later, we can reconstruct the Green's function from the density of states as

$$\hat{G}(\epsilon+i0^+) = \int d\epsilon'\,\frac{\hat{D}(\epsilon')}{\epsilon-\epsilon'+i0^+} = \int d\epsilon'\,\frac{\hat{D}(\epsilon')}{\epsilon-\epsilon'} - i\pi\hat{D}(\epsilon) \tag{5.139}$$

The last equation uses the **Kramers-Kronig relation**, which allows to construct the real part from the imaginary part of a function that is analytic in the positive half plane.

Now, I work out the density of states. Even though only the Green's function, and thus the density of states has only been requested for the terminal site, I will show here the derivation for the full density-of-states matrix, because it will allow me to demonstrate some interesting physical effects.

$$\begin{aligned}\hat{D}(\epsilon) &= \sum_{j,j'=1}^{N}|\chi_j\rangle\Bigg\{\sum_{n=1}^{N}\langle\pi_j|\varphi_n\rangle\langle\varphi_n|\pi_{j'}\rangle\delta(\epsilon-\epsilon_n)\Bigg\}\langle\chi_{j'}| \\ &= \sum_{j,j'=1}^{N}|\chi_j\rangle\Bigg\{\sum_{n=1}^{N}\langle\pi_j|\varphi(k_n)\rangle\langle\varphi(k_n)|\pi_{j'}\rangle\delta(\epsilon-\epsilon(k_n))\Bigg\}\langle\chi_{j'}| \\ &= \sum_{j,j'=1}^{N}|\chi_j\rangle\Bigg\{\sum_{n=1}^{N}\frac{2}{N+1}\sin(k_n a_{\text{lat}}j)\sin(k_n a_{\text{lat}}j')\delta\Big(\epsilon-\bar{\epsilon}+2t\cos(k_n a_{\text{lat}})\Big)\Bigg\}\langle\chi_{j'}| \\ &= \sum_{j,j'=1}^{N}|\chi_j\rangle\Bigg\{\frac{2a_{\text{lat}}}{\pi}\underbrace{\sum_{n=1}^{N}\Delta k}_{\to\int_0^{\frac{\pi}{a_{\text{lat}}}}dk}\sin(k_n a_{\text{lat}}j)\sin(k_n a_{\text{lat}}j')\delta\Big(\epsilon-\bar{\epsilon}+2t\cos(k_n a_{\text{lat}})\Big)\Bigg\}\langle\chi_{j'}|\end{aligned} \tag{5.140}$$

where $k_n = \frac{n\pi}{a_{\text{lat}}(N+1)}$ for $n = 1,\ldots,N$ and $\Delta k = \frac{\pi}{a_{\text{lat}}(N+1)}$.

Let me do the continuum limit $N \to \infty$. I will use $k(\epsilon) = \frac{1}{a_{\rm lat}} \arccos\left(\frac{\epsilon-\bar{\epsilon}}{2t}\right)$. which is obtained from the dispersion relation Eq. 5.135.

$$\begin{aligned}
\hat{D}(\epsilon) &= \sum_{j,j'=1}^{N} |\chi_j\rangle \left\{ \frac{2a_{\rm lat}}{\pi} \int_0^{\frac{\pi}{a_{\rm lat}}} dk \ \sin(ka_{\rm lat}j)\sin(ka_{\rm lat}j')\delta\Big(\epsilon - \bar{\epsilon} + 2t\cos(ka_{\rm lat})\Big)\right\} \langle\chi_{j'}| \\
&= \sum_{j,j'=1}^{N} |\chi_j\rangle \left\{ \frac{2a_{\rm lat}}{\pi} \int_{\bar{\epsilon}-2t}^{\bar{\epsilon}+2t} d\epsilon \ \left(\frac{d\epsilon}{dk}\right)^{-1} \sin(k(\epsilon)a_{\rm lat}j)\sin(k(\epsilon)a_{\rm lat}j')\delta\Big(\epsilon - \bar{\epsilon} + 2t\cos(k(\epsilon)a_{\rm lat})\Big)\right\} \langle\chi_{j'}| \\
&= \sum_{j,j'=1}^{N} |\chi_j\rangle \left\{ \frac{2a_{\rm lat}}{\pi} \int_{\bar{\epsilon}-2t}^{\bar{\epsilon}+2t} d\epsilon \ \frac{\sin(k(\epsilon)a_{\rm lat}j)\sin(k(\epsilon)a_{\rm lat}j')}{2ta_{\rm lat}\sin(k(\epsilon)a_{\rm lat})}\delta\Big(\epsilon - \bar{\epsilon} + 2t\cos(k(\epsilon)a_{\rm lat})\Big)\right\} \langle\chi_{j'}| \\
&= \sum_{j,j'=1}^{N} |\chi_j\rangle \left\{ \frac{2}{2\pi t} \frac{\sin(k(\epsilon)a_{\rm lat}j)\sin(k(\epsilon)a_{\rm lat}j')}{\sin(k(\epsilon)a_{\rm lat})}\right\} \langle\chi_{j'}| \qquad (5.141)
\end{aligned}$$

I will come back to this result in Eq. 5.141 later. Let me now limit the derivation again to the terminal site and work out the Green's function.

$$\begin{aligned}
\langle\pi_1|\hat{D}(\epsilon)|\pi_1\rangle &\overset{\text{Eq. 5.141}}{=} \frac{2}{2\pi t}\sin\Big(k(\epsilon)a_{\rm lat}\Big) = \frac{2}{2\pi t}\sin\left(\arccos\left(\frac{\epsilon-\bar{\epsilon}}{2t}\right)\right) \\
&= \frac{1}{\pi t}\sqrt{1-\left(\frac{\epsilon-\bar{\epsilon}}{2t}\right)^2} \qquad (5.142)
\end{aligned}$$

The density of states at the terminal site has the form of a half circle $x^2 + y^2 = 1$ with $y(x) = \sqrt{1-x^2}$. This allows one to check whether the density of states integrates up to one.

$$\int_{\bar{\epsilon}-2t}^{\bar{\epsilon}+2t} d\epsilon \ \underbrace{\frac{1}{\pi t}\sqrt{1-\left(\frac{\epsilon-\bar{\epsilon}}{2t}\right)^2}}_{D_{1,1}(\epsilon)} = \underbrace{\frac{1}{2}\pi(2t)^2}_{\text{area of half circle}} \underbrace{\frac{1}{2\pi t^2}}_{\text{adjust height to } 1/(\pi t)} = 1 \qquad (5.143)$$

The Green's function is then reconstructed from the density of states

$$\begin{aligned}
\hat{G}(\epsilon + i0^+) &= \int d\epsilon' \ \frac{\hat{D}(\epsilon')}{\epsilon - \epsilon' + i0^+} = \int d\epsilon' \ \frac{\hat{D}(\epsilon')}{\epsilon - \epsilon'} - i\pi\hat{D}(\epsilon) \\
&= \int_{\bar{\epsilon}-2t}^{\bar{\epsilon}+2t} d\epsilon' \ \frac{1}{\epsilon - \epsilon'} \underbrace{\frac{2}{2\pi t}\sqrt{1-\left(\frac{\epsilon'-\bar{\epsilon}}{2t}\right)^2}}_{D_{1,1}(\epsilon')} - i\pi \underbrace{\frac{2}{2\pi t}\sqrt{1-\left(\frac{\epsilon-\bar{\epsilon}}{2t}\right)^2}}_{D_{1,1}(\epsilon)} \\
&\overset{x=\frac{\epsilon'-\bar{\epsilon}}{2t}}{=} \frac{2}{2\pi t}\int_{-1}^{1} dx \ \frac{\sqrt{1-x^2}}{\frac{\epsilon-\bar{\epsilon}}{2t} + x} - i\frac{1}{t}\sqrt{1-\left(\frac{\epsilon-\bar{\epsilon}}{2t}\right)^2} \qquad (5.144)
\end{aligned}$$

Let me resolve the integral for the real part of the Green's function I use $a \overset{\text{def}}{=} \frac{\epsilon-\bar{\epsilon}}{2t}$.

$$\begin{aligned}
&\int_{\bar{\epsilon}-2t}^{\bar{\epsilon}+2t} d\epsilon' \ \frac{\sqrt{1-\left(\frac{\epsilon'-\bar{\epsilon}}{2t}\right)^2}}{\epsilon - \epsilon'} = \int_{-1}^{1} dy \ \frac{\sqrt{1-y^2}}{a-y} \overset{y=-\cos(x)}{=} \int_0^{\pi} dx \ \sin(x)\frac{\sqrt{1-\cos^2(x)}}{a+\cos(x)} = \int_0^{\pi} dx \ \frac{1-\cos^2(x)}{a+\cos(x)} \\
&= \int_0^{\pi} dx \ \frac{1-a^2+a^2-\cos^2(x)}{a+\cos(x)} = (1-a^2)\left(\int_0^{\pi} dx \ \frac{1}{a+\cos(x)}\right) + \left(\int_0^{\pi} dx \ (a-\cos(x))\right) \\
&= (1-a^2)\left(\int_0^{\pi} dx \ \frac{1}{a+\cos(x)}\right) + \Big(ax - \sin(x)\Big)_0^{\pi} = a\pi + (1-a^2)\left(\int_0^{\pi} dx \ \frac{1}{a+\cos(x)}\right) \qquad (5.145)
\end{aligned}$$

The remaining integral is nontrivial. I use Bronstein-Eq. 347 on p.55[63].

$$\int dx\ \frac{1}{a+\cos(x)} \overset{\text{Eq. 5.130}}{=} \begin{cases} \frac{2}{\sqrt{a^2-1}} \arctan \frac{(a-1)\tan(x/2)}{a^2-1} & \text{for } a^2>1 \\ \frac{1}{\sqrt{1-a^2}} \ln \frac{(1-a)\tan(x/2)+\sqrt{1-a^2}}{(1-a)\tan(x/2)-\sqrt{1-a^2}} & \text{for } a^2<1 \end{cases} \tag{5.146}$$

Now, I insert the boundary values. For $a^2>0$, I use $\lim_{\delta\to 0^+} \arctan(c\tan(\frac{\pi}{2}-\delta)) = \frac{\pi}{2}\text{sgn}(x)$.

$$\begin{aligned} \int_0^\pi dx\ \frac{1}{a+\cos(x)} &= \begin{cases} \frac{2}{\sqrt{a^2-1}} \overbrace{\arctan \frac{\tan(\pi/2)}{a+1}}^{\frac{\pi}{2}\text{sgn}(a-1)} & \text{for } a^2>1 \\ \frac{1}{\sqrt{1-a^2}} \underbrace{\Big[\ln[1]-\ln[-1]\Big]}_{=0} & \text{for } a^2<1 \end{cases} \\ &= \theta(a^2-1)\frac{2}{\sqrt{a^2-1}}\frac{\pi}{2}\text{sgn}(a-1) \\ &= \frac{\pi}{\sqrt{a^2-1}}\text{sgn}(a-1)\theta(a^2-1) \end{aligned} \tag{5.147}$$

where $\theta(x)$ is the Heaviside step function.

$$\begin{aligned} \Rightarrow \quad \int_{\bar\epsilon-2t}^{\bar\epsilon+2t} d\epsilon'\ \frac{\sqrt{1-\left(\frac{\epsilon'-\bar\epsilon}{2t}\right)^2}}{\epsilon-\epsilon'} &= a\pi + \left(1-a^2\right)\int_0^\pi dx\ \frac{1}{a+\cos(x)} \\ &= a\pi + (1-a^2)\frac{\pi}{\sqrt{a^2-1}}\ \text{sgn}(a-1)\theta(a^2-1) \\ &= a\pi - \pi\sqrt{a^2-1}\text{sgn}(a-1)\theta(a^2-1) \\ &= \pi\left\{\frac{\epsilon-\bar\epsilon}{2t} - \sqrt{\left(\frac{\epsilon-\bar\epsilon}{2t}\right)^2-1}\ \text{sgn}\Big(\frac{\epsilon-\bar\epsilon}{2t}-1\Big)\theta\Big(\Big(\frac{\epsilon-\bar\epsilon}{2t}\Big)^2-1\Big)\right\} \\ &= \pi\left\{\frac{\epsilon-\bar\epsilon}{2t} - \sqrt{\left(\frac{\epsilon-\bar\epsilon}{2t}\right)^2-1}\ \text{sgn}(\epsilon-\bar\epsilon)\theta\Big(|\epsilon-\bar\epsilon|-2|t|\Big)\right\} \end{aligned} \tag{5.148}$$

The resulting Green's function at the terminal site is

$$\begin{aligned} \hat G(\epsilon+i0^+) &= \frac{2}{2\pi t}\overbrace{\pi\left\{\frac{\epsilon-\bar\epsilon}{2t} - \sqrt{\left(\frac{\epsilon-\bar\epsilon}{2t}\right)^2-1}\ \text{sgn}(\epsilon-\bar\epsilon)\theta\Big(|\epsilon-\bar\epsilon|-2|t|\Big)\right\}} - i\frac{1}{t}\sqrt{1-\left(\frac{\epsilon-\bar\epsilon}{2t}\right)^2} \\ &= \frac{1}{t}\left\{\frac{\epsilon-\bar\epsilon}{2t} - \sqrt{\left(\frac{\epsilon-\bar\epsilon}{2t}\right)^2-1}\ \text{sgn}(\epsilon-\bar\epsilon)\theta\Big(|\epsilon-\bar\epsilon|-2|t|\Big) - i\sqrt{1-\left(\frac{\epsilon-\bar\epsilon}{2t}\right)^2}\right\} \end{aligned} \tag{5.149}$$

The Green's function of the terminal site is shown in fig. 5.5.

- The imaginary part of the Green's function is, up to the prefactor, equal to the density of states on the terminal site. The states at the surface are concentrated closer to the center to the band as compared to the bulk, which can be attributed to the reduced number of nearest neighbors.
- The real part of the Green's function describes the "quasi-particle shift" of the energy levels of an adsorbate due to the coupling to the half infinite chain. This effect is the **level repulsion**, which we already encountered in the case of the molecular dimer.
  - An adsorbate with an energy level below the band of the half-infinite chain will form a bond and will be shifted to lower energies. The antibond will have its main weight in the spectrum of the half-infinite chain.

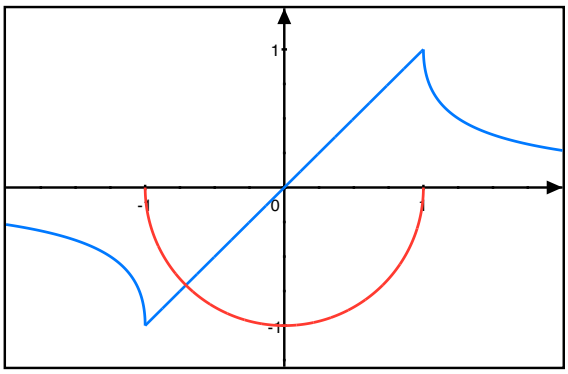

Fig. 5.5: Green's function $G_{11}(\epsilon)$ of the half-infinite chain of hydrogen atoms at the terminal site. The real part is shown in blue, and the imaginary part in red. The atomic energy level $\bar{\epsilon}$ is placed to zero and the hopping parameter has been chosen to $t = \frac{1}{2}$.

– An adsorbate with an energy level above the band of the half-infinite chain will form an anti-bond and will be shifted to higher energies. The bond will have its main weight in the spectrum of the half-infinite chain.

If one is familiar with the density of states of a linear chain in the bulk, the density of states on the surface is surprising. In the bulk, the density of states is strongly peaked at the band edges. Here, on the surface, the density of states has its maximum in the center and it falls of at the band edges. This has to do with the fact that the wave functions behave like at the edges like $\sin(kx)$, which has a small slope at the band edges, where ka_{lat} is close to zero or close to π. Because of this small slope, the probability can only rise slowly away from the surface.

Discussion

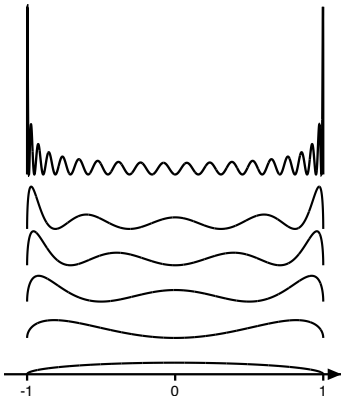

Fig. 5.6: Density of states at the surface of a linear chain of hydrogen atoms. Layers 1,2,3,4,5 and layer 20 are shown from bottom to top and displaced vertically for better visibility. The horizontal axis shows $\frac{\epsilon-\bar{\epsilon}}{2t}$. Editor: The density of states in the bulk exhibits rapid oscillations with energy. This may be an expression that no propagating solutions are allowed, because the system is fully coherent. Probably, this differs from a Green's function calculated with periodic boundary conditions.

++++++++++++++++++++++++++

This section will be removed

- Next, I decompose the product of the sine functions

$$\begin{aligned}\sin(ax)\sin(bx) &= \frac{e^{iax}-e^{-iax}}{2i}\frac{e^{ibx}-e^{-ibx}}{2i}\\ &= -\frac{1}{4}\Big(e^{i(a+b)x}-e^{i(a-b)x}-e^{-i(a-b)x}+e^{-i(a+b)x}\Big)\\ &= -\frac{1}{2}\Big[\cos\big((a+b)x\big)-\cos\big((a-b)x\big)\Big]\end{aligned} \tag{5.150}$$

-

$$\begin{aligned}\cos(nx) &= \frac{1}{2}\Big(e^{inx}+e^{-inx}\Big) = \frac{1}{2}\Big(\big(e^{ix}\big)^n+\big(e^{-ix}\big)^n\Big) = \mathrm{Re}\Big[\big(e^{ix}\big)^n\Big]\\ &= \mathrm{Re}\Big[\big(\cos(x)+i\sin(x)\big)^n\Big] = \mathrm{Re}\Big[\big(\cos(x)\pm i\sqrt{1-\cos^2(x)}\big)^n\Big]\end{aligned} \tag{5.151}$$

  The sign $\pm$ is undetermined, because $\sin^2(x)+\cos^2(x)=1$ determines only the absolute value of the sinus, not its sign. However, because only the real part of the expression is of interest, the result is independent of the sign chosen.

- Finally, I insert the dispersion relation $\cos\Big(k(\epsilon)\frac{1}{a_{\mathrm{lat}}}\Big) = \frac{\epsilon-\bar{\epsilon}}{2t}$.

- Here an attempt to obtain the complete Green's function. Skip this

The full Green's function is then obtained from the Kramers-Kronig relation

$$\hat{G}(\epsilon + i0^+) = \int d\epsilon \, \frac{\hat{D}(\epsilon')}{\epsilon - \epsilon'} - i\pi \hat{D}(\epsilon) \tag{5.152}$$

Within the band, the Green's function exhibits a branch cut at the real axis. Therefore, we do not expect to find a closed solution. However, there is a solution only outside the band, that is for $|\epsilon - \bar{\epsilon}| \geq 2t$.
We use the integral formula Bronstein: p68, Eq.25

$$\int_0^\pi dx \frac{\cos(nx)}{1 + b^2 - 2b\cos(x)} = \frac{\pi b^n}{1 - b^2} \quad \Leftrightarrow \quad \int_0^\pi dx \frac{\cos(nx)}{\frac{1+b^2}{2b} - \cos(x)} = \frac{2\pi b^{n+1}}{1 - b^2} \tag{5.153}$$

which yields

$$\frac{1 + b^2}{2b} = \frac{\epsilon - \bar{\epsilon}}{2t} \quad \Rightarrow \quad b^2 - 2\frac{\epsilon - \bar{\epsilon}}{2t} b + 1 = 0 \quad \Rightarrow \quad \left(b - \frac{\epsilon - \bar{\epsilon}}{2t}\right)^2 = \left(\frac{\epsilon - \bar{\epsilon}}{2t}\right)^2 - 1$$

$$b = \frac{\epsilon - \bar{\epsilon}}{2t} \pm \sqrt{\left(\frac{\epsilon - \bar{\epsilon}}{2t}\right)^2 - 1} \overset{|b|\leq 1}{=} \frac{\epsilon - \bar{\epsilon}}{2t}\left(1 - \sqrt{1 - \left(\frac{2t}{\epsilon - \bar{\epsilon}}\right)^2}\right) \tag{5.154}$$

For $|\epsilon - \bar{\epsilon}| \geq 2t$, this yields

$$\begin{aligned}
\hat{G}(\epsilon) &= -\frac{1}{\pi} \sum_{j,j'=1}^{\infty} |\chi_j\rangle \int_0^\pi dy \frac{\cos\left(y(j + j')\right) - \cos\left(y(j - j')\right)}{\epsilon - \bar{\epsilon} - 2t\cos(y)} \langle\chi_j| \\
&= -\frac{1}{2\pi t} \sum_{j,j'=1}^{\infty} |\chi_j\rangle \left(\frac{2\pi(b^{j+j'+1} - b^{j-j'+1})}{1 - b^2}\right) \langle\chi_j| \quad \text{with } b = \frac{\epsilon - \bar{\epsilon}}{2t}\left(1 - \sqrt{1 - \left(\frac{2t}{\epsilon - \bar{\epsilon}}\right)^2}\right) \\
&= -\frac{1}{t} \sum_{j,j'=1}^{\infty} |\chi_j\rangle \left(\frac{b^{j+j'+1} - b^{j-j'+1}}{1 - b^2}\right) \langle\chi_j| \quad \text{with } b = \frac{\epsilon - \bar{\epsilon}}{2t}\left(1 - \sqrt{1 - \left(\frac{2t}{\epsilon - \bar{\epsilon}}\right)^2}\right)
\end{aligned} \tag{5.155}$$

6. Determine the self energy describing the coupling to the half infinite chain

Editor: Remark: the self energy is not hermitian!! Check once again whether this assumption has been made somewhere in the text.

The self-energy at site 0 is

$$\hat{\Sigma}(\epsilon) = \hat{V}^{AB}\hat{\bar{G}}^{BB}\hat{V}^{BA} = |\pi_0\rangle t \langle\pi_1|\hat{G}(\epsilon)|\pi_1\rangle t \langle\pi_0| \tag{5.156}$$

where $\hat{G}(\epsilon)$ is given in Eq. 5.149.

The self energy is has different factors but otherwise it reflects the Green's function on the terminal site of the half-infinite chain shown in Fig. 5.5.

7. Construct the density of states of the adsorbate via the self energy

$$\begin{aligned}
\left(\hat{G}^{AA}(\epsilon)\right)^{-1} &= |\pi_0\rangle\left[\epsilon - \bar{\epsilon}^A - t_A^2\langle\pi_1|\hat{\bar{G}}^{BB}(\epsilon)|\pi_1\rangle\right]\langle\pi_0| \\
\hat{G}^{AA}(\epsilon+i\eta) &= |\chi_0\rangle\frac{1}{\epsilon - \bar{\epsilon}^A - t_A^2\mathrm{Re}\left[\langle\pi_1|\hat{\bar{G}}^{BB}(\epsilon)|\pi_1\rangle\right] - it_A^2\mathrm{Im}\left[\langle\pi_1|\hat{\bar{G}}^{BB}(\epsilon)|\pi_1\rangle\right] + i\eta}\langle\chi_0| \\
&= |\chi_0\rangle\frac{\epsilon - \bar{\epsilon}^A - t_A^2\mathrm{Re}\left[\langle\pi_1|\hat{\bar{G}}^{BB}(\epsilon)|\pi_1\rangle\right] + it_A^2\mathrm{Im}\left[\langle\pi_1|\hat{\bar{G}}^{BB}(\epsilon)|\pi_1\rangle\right] - i\eta}{\left(\epsilon - \bar{\epsilon}^A - t_A^2\mathrm{Re}\left[\langle\pi_1|\hat{\bar{G}}^{BB}(\epsilon)|\pi_1\rangle\right]\right)^2 + \left(t_A^2\mathrm{Im}\left[\langle\pi_1|\hat{\bar{G}}^{BB}(\epsilon)|\pi_1\rangle\right] + \eta\right)^2}\langle\chi_0|
\end{aligned} \tag{5.157}$$

The resulting density of states is obtained from the anti-hermitian part of the Green's function

$$\hat{D}^{AA}(\epsilon) \overset{\text{Eq. 4.50}}{=} -\frac{1}{\pi}\lim_{\eta\to 0}|\chi_0\rangle\frac{t_A^2\mathrm{Im}\left[\langle\pi_1|\hat{\bar{G}}^{BB}(\epsilon)|\pi_1\rangle\right] - \eta}{\left(\epsilon - \bar{\epsilon}^A - t_A^2\mathrm{Re}\left[\langle\pi_1|\hat{\bar{G}}^{BB}(\epsilon)|\pi_1\rangle\right]\right)^2 + \left(t_A^2\mathrm{Im}\left[\langle\pi_1|\hat{\bar{G}}^{BB}(\epsilon)|\pi_1\rangle\right] + \eta\right)^2}\langle\chi_0| \tag{5.158}$$

The small factor η is required to describe any states that result from the adsorbate and lie outside of the spectrum of the half-infinite chain.

The adsorbate contributes an energy level at

$$\epsilon = \bar{\epsilon}^A + t_A^2\mathrm{Re}\left[\langle\pi_1|\hat{\bar{G}}^{BB}(\epsilon)|\pi_1\rangle\right] \tag{5.159}$$

if this energy lies outside the spectrum of the half infinite chain. Then, the imaginary part of the Green's function vanishes at the position of the new energy level, and the width will be governed by the small parameter η. Such a state will contribute a delta function to the density of states.

Because the self energy is a nonlinear function, Eq. 5.159 can have several solutions. For example, when the coupling t^A to the bath is much larger than the band width of the bath, there will be a bonding energy level below the band of the half-infinite chain and one antibonding energy level above. These two states resemble the bonding and antibonding states of a general dimeric molecule, where the terminal site of the half-infinite chain plays the role of one of the atoms in the dimer.

When this energy level falls into the spectrum of the band of the bath, the broadening is due to the coupling to the bath.

8. Determine the wave functions of the adsorbate and chain Editor: This needs to go into the problem formulation.

Here we explore the tail of the wave function in the half-infinite chain, when an atom is absorbed at the surface.

$$\begin{aligned}
|\tilde{\chi}_\alpha^A(\epsilon)\rangle &\overset{\text{Eq. 5.9}}{=} |\chi_\alpha^A\rangle + \sum_{\beta,\gamma\in B}|\chi_\beta^B\rangle\bar{G}_{\beta,\gamma}^{BB}(\epsilon)V_{\gamma,\alpha}^{BA} \qquad \text{for } \alpha\in A \\
&= \left(\hat{1} + \sum_{\beta,\gamma\in B,\delta\in A}|\chi_\beta^B\rangle\bar{G}_{\beta,\gamma}^{BB}(\epsilon)V_{\gamma,\delta}^{BA}\langle\pi_\delta|\right)|\chi_\alpha^A\rangle \qquad \text{for } \alpha\in A
\end{aligned} \tag{5.160}$$

$$
\begin{aligned}
|\tilde{\chi}^A\rangle &\overset{\text{Eq. 5.9}}{=} \left(|\chi_0^A\rangle + \sum_{j=1}^{N} |\chi_j^B\rangle \bar{G}^{BB}_{j,1}(\epsilon) t^A\right) c^A \\
&= \left(|\chi_0\rangle + \sum_{j=1}^{N} |\chi_j^B\rangle \sum_n \langle \pi_j|\varphi_n\rangle \frac{1}{\epsilon - \epsilon(k_n) + i\eta} \langle \varphi_n|\pi_1\rangle t_A\right) c_A \\
&\overset{\text{Eqs. 5.134 ,5.135}}{=} \left(|\chi_0^A\rangle + \frac{2t_A}{N+1} \sum_{j=1}^{N} |\chi_j^B\rangle \sum_{n=1}^{N} \Delta k \underbrace{\frac{1}{\pi}(N+1)a_{\text{lat}}}_{1/\Delta k} \frac{\sin(k_n a_{\text{lat}} j)\sin(k_n a_{\text{lat}})}{\epsilon - \bar{\epsilon} + 2t\cos(k_n a_{\text{lat}}) + i0^+}\right) c_A \\
&= \left(|\chi_0^A\rangle + \frac{2a_{\text{lat}} t_A}{\pi} \sum_{j=1}^{\infty} |\chi_j^B\rangle \int_0^{\pi} dk \frac{\sin(k a_{\text{lat}} j)\sin(k a_{\text{lat}})}{\epsilon - \bar{\epsilon} + 2t\cos(k a_{\text{lat}}) + i0^+}\right) c_A
\end{aligned}
\tag{5.161}
$$

The coefficient c_A acts as a normalization constant. In order to know a true solution of the Schrödinger equation, we still need to determine the correct energy ϵ.

Let me do a variable transform

$$
y = -2t\cos(k a_{\text{lat}}) \quad \Rightarrow \quad \begin{cases} dy = 2t a_{\text{lat}} \sin(k a_{\text{lat}}) dk \\ k a_{\text{lat}} = \arccos\left(-\frac{y}{2t}\right) \end{cases} \tag{5.162}
$$

$$
|\tilde{\chi}^A_\alpha(\epsilon)\rangle = \left(|\chi_0\rangle + \frac{t_A}{\pi t} \sum_{j=1}^{N} |\chi_j^B\rangle \int_{-2t}^{+2t} dy \frac{\sin\left[j \arccos\left(-\frac{y}{2t}\right)\right]}{\epsilon - \bar{\epsilon} - y + i0^+}\right) c_A \tag{5.163}
$$

Editor: This result shall be analyzed numerically. The shape shall be shown.

- when the energy is far away from the band, the decay of the wave function is expected to be exponential and rapid.
- when the energy lies inside the band, the wave function has a real and an imaginary contribution. The imaginary contribution describes probably the continuum of the half-infinite chain.

Once we found the behavior of the wave function as function of energy, we need to determine the physical energies. For this purpose, we need to determine the poles of the Green's function.

For that purpose, I analyze the adsorbate Green's function $G^{AA}(\epsilon)$. The poles are defined by the equation

Editor: The following is guesswork!

$$
\begin{aligned}
\epsilon - \bar{\epsilon}^A - t_A^2 \langle \pi_1|\bar{G}^{BB}(\epsilon)|\pi_1\rangle &= 0 \\
\frac{\epsilon - \bar{\epsilon}}{2t} - \frac{\bar{\epsilon}^A - \bar{\epsilon}}{2t} + \frac{t_A^2}{t}\left(\frac{\epsilon - \bar{\epsilon}}{2t} - i\pi\sqrt{1 - \left(\frac{\epsilon - \bar{\epsilon}}{2t}\right)^2}\right) &= 0 \\
x - x_A + Bx - i\pi B\sqrt{(1-x^2)} &= 0 \\
(1+B)x - x_A &= i\pi B\sqrt{1-x^2}
\end{aligned}
\tag{5.164}
$$

$$
Re[x] = \frac{x_A}{1+B} \quad \text{and} \quad \text{Im}[x] = \pi\frac{B}{1+B}\sqrt{1 - \left(\frac{x_A}{1+B}\right)^2 - \text{Im}[x]^2} \tag{5.165}
$$

for $|\frac{\epsilon - \bar{\epsilon}}{2t}| < 1$

$$
\begin{aligned}
&|\pi_0\rangle t^2\left[\int d\epsilon'\ \frac{D_{11}(\epsilon')}{\epsilon-\epsilon'} - i\pi D_{11}(\epsilon)\right]\langle\pi_0| \\
&= -\frac{1}{\pi t}|\pi_0\rangle t^2\left[\int_{\bar\epsilon-2t}^{\bar\epsilon+2t} d\epsilon'\ \frac{\sqrt{1-\left(\frac{\epsilon'-\bar\epsilon}{2t}\right)^2}}{\epsilon-\epsilon'} - i\pi\sqrt{1-\left(\frac{\epsilon-\bar\epsilon}{2t}\right)^2}\right]\langle\pi_0| \\
&= -\frac{1}{\pi t}|\pi_0\rangle t^2\left[-\pi\frac{\epsilon-\bar\epsilon}{2t} - i\pi\sqrt{1-\left(\frac{\epsilon-\bar\epsilon}{2t}\right)^2}\right]\langle\pi_0| \\
&= |\pi_0\rangle t\left[\frac{\epsilon-\bar\epsilon}{2t} + i\sqrt{1-\left(\frac{\epsilon-\bar\epsilon}{2t}\right)^2}\right]\langle\pi_0| \\
&= |\pi_0\rangle t\exp\left(i\arccos\left(\frac{\epsilon-\bar\epsilon}{2t}\right)\right)\langle\pi_0| \quad \text{for } |\epsilon-\bar\epsilon|<|2t|
\end{aligned}
\tag{5.166}
$$

This result is apparently only valid for energies within the band.

Bronstein p.55, Eq. 347

$$
\begin{aligned}
\int dx\ \frac{1}{a-\cos(x)} &= \frac{1}{\sqrt{1-a^2}}\ln\left|\frac{(1+a)\tan(x/2)-\sqrt{1-a^2}}{(1+a)\tan(x/2)+\sqrt{1-a^2}}\right| \quad \text{for } a^2<1 \\
\int_0^\pi dx\ \frac{1}{a-\cos(x)} &= \frac{1}{\sqrt{1-a^2}}\Big[\ln|1|-\ln|-1|\Big] = 0
\end{aligned}
\tag{5.167}
$$

For the surface site, the Green's function for $\frac{\epsilon-\bar\epsilon}{2t}|>1$ is

$$
\begin{aligned}
\langle\pi_1|\hat G(\epsilon)|\pi_1\rangle &\overset{\text{Eq. 5.155}}{=} -\frac{1}{t}\left(\frac{b^3-b}{1-b^2}\right) = \frac{1}{t}b \\
&= \frac{1}{t}\frac{\epsilon-\bar\epsilon}{2t} \pm \sqrt{\left(\frac{\epsilon-\bar\epsilon}{2|t|}\right)^2-1} \quad \text{with } |\epsilon-\bar\epsilon|>|2t|
\end{aligned}
\tag{5.168}
$$

Now we combine the two regions of the self energy to

$$
\hat\Sigma(\epsilon) = |t|\begin{cases} |\pi_0\rangle\left[\frac{\epsilon-\bar\epsilon}{2t} + i\sqrt{1-\left(\frac{\epsilon-\bar\epsilon}{2t}\right)^2}\right]\langle\pi_0| & \text{for } |\epsilon-\bar\epsilon|<|2t| \\ |\pi_0\rangle\left[\frac{\epsilon-\bar\epsilon}{2|t|} \pm \sqrt{\left(\frac{\epsilon-\bar\epsilon}{2|t|}\right)^2-1}\right]\langle\pi_0| & \text{for } |\epsilon-\bar\epsilon|>|2t| \end{cases}
\tag{5.169}
$$

Editor: The sign of the hopping parameter is still inconsistent.

$$
\begin{aligned}
\left(G^{AA}(\epsilon)\right)^{-1} &= |\pi_0\rangle\left\{\epsilon-\bar\epsilon^A \pm t_A^2\bar G_{11}^{BB}\right\}\langle\pi_0|] \\
&= \begin{cases} |\pi_0\rangle\left[\epsilon-\bar\epsilon^A - t_A\left(\frac{\epsilon-\bar\epsilon}{2t} + i\sqrt{1-\left(\frac{\epsilon-\bar\epsilon}{2t}\right)^2}\right)\right]\langle\pi_0| & \text{for } |\epsilon-\bar\epsilon|<|2t| \\ |\pi_0\rangle\left[\epsilon-\bar\epsilon^A - t_A\left(\frac{\epsilon-\bar\epsilon}{2|t|} - \sqrt{\left(\frac{\epsilon-\bar\epsilon}{2|t|}\right)^2-1}\right)\right]\langle\pi_0| & \text{for } |\epsilon-\bar\epsilon|>|2t| \end{cases}
\end{aligned}
\tag{5.170}
$$

- For $|\epsilon-\bar\epsilon|<|2t|$ we obtain

$$
\hat G^{AA}(\epsilon) = |\chi_0\rangle\frac{1}{t_A}\left\{\frac{\frac{\epsilon-\bar\epsilon^A}{t_A} - \frac{\epsilon-\bar\epsilon}{2t} + i\sqrt{1-\left(\frac{\epsilon-\bar\epsilon}{2t}\right)^2}}{\left(\frac{\epsilon-\bar\epsilon^A}{t_A} - \frac{\epsilon-\bar\epsilon}{2t}\right)^2 + 1 - \left(\frac{\epsilon-\bar\epsilon}{2t}\right)^2}\right\}\langle\chi_0|
\tag{5.171}
$$

- For $|\epsilon - \bar{\epsilon}| > |2t|$ we obtain (This is still wrong!!!)

$$\hat{G}^{AA}(\epsilon) = |\chi_0\rangle \frac{1}{t_A} \left\{ \frac{1}{\frac{\epsilon-\bar{\epsilon}^A}{t_A} - \frac{\epsilon-\bar{\epsilon}}{2t} + \sqrt{\left(\frac{\epsilon-\bar{\epsilon}}{2t}\right)^2 - 1}} \right\} \langle\chi_0| \tag{5.172}$$

5.4.5 Downfold the positronic degrees of freedom in the Dirac equation

Editor: This is only a collection of stuff to formulate a problem later.

Electrons are described by the Dirac equation which describes an electron by a four-component spinor wave function.

$$\left(\gamma^\mu i\hbar\partial_\mu - mc\right)\psi(\vec{x}) = 0 \tag{5.173}$$

with

$$\gamma^0 = \begin{pmatrix} \mathbf{1} & \mathbf{0} \\ \mathbf{0} & -\mathbf{1} \end{pmatrix} \qquad \text{and} \qquad \gamma^j = \begin{pmatrix} \mathbf{0} & \boldsymbol{\sigma}_j \\ -\boldsymbol{\sigma}_j & \mathbf{0} \end{pmatrix} \tag{5.174}$$

Minimal coupling

$$E \to E - q\Phi \tag{5.175}$$
$$\vec{p} \to \vec{p} - q\vec{A} \tag{5.176}$$

$$\epsilon \stackrel{\text{def}}{=} E - m_0 c^2 \tag{5.177}$$
$$M \stackrel{\text{def}}{=} m_0 + \frac{\epsilon - q\Phi}{2c^2} \tag{5.178}$$

$$\begin{pmatrix} q\Phi - \epsilon & \sum_{j\in\{x,y,z\}} \sigma_j(p_i - qA_i)c \\ \sum_{j\in\{x,y,z\}} \sigma_j(p_i - qA_i)c & -2Mc^2 \end{pmatrix} \begin{pmatrix} |\phi\rangle \\ |\chi\rangle \end{pmatrix} = 0 \tag{5.179}$$

$$(\vec{\boldsymbol{\sigma}}\vec{A})(\vec{\boldsymbol{\sigma}}\vec{B}) = \mathbf{1}\vec{A}\vec{B} + i\vec{\boldsymbol{\sigma}}(\vec{A}\times\vec{B}) \tag{5.180}$$

5.4.6 Inelastic tunneling (Sketch only)

Editor: Skip this. It is only a sketch

M. Galperin and MarC Ratner and Nitxzan, Arxiv, *Inelastic electromn tunneling spectroscopy in molecular junctions: Peaks and dips*
S. Tikhodeev et al. Surf. Sci. 493,63 (2001)
T. Mii, S. Tikhodeev et al., Surf. Sci. 502-503, 26 (2002)
B.N.J. Persson and A. Baratovv, PRL 59,339 (1987)
B.N.J. Persson, Physica Scripta 38, 282 (1988)
A. Baratoff and Persson, J. Vacuum Science and Technology A 6, 331 (1988)

Consider an electron traveling along a Hubbard chain, which interacts on a single site with a two-state system. The two-site system could be any system that may accept from or donate energy to the traveling electron.

The Hamiltonian of the Hubbard chain is

$$H_{i,j}^{AA} = \begin{cases} t & \text{for } j = i \pm 1 \\ 0 & \text{else} \end{cases} \tag{5.181}$$

The two-state system has the Hamiltonian

$$\boldsymbol{H}^{BB} = \begin{pmatrix} 0 & 0 \\ 0 & \Delta \end{pmatrix} \tag{5.182}$$

The only non-zero element of the coupling is $V_{0,2}^{AB} = \lambda$.

Solution:

$$\boldsymbol{G}^{BB}(\epsilon) = \begin{pmatrix} \frac{1}{\epsilon} & 0 \\ 0 & \frac{1}{\epsilon - \Delta} \end{pmatrix} \tag{5.183}$$

The retarded potential has the form

$$\boldsymbol{\Sigma}_{0,0}^{AA} = \frac{\lambda^2}{\epsilon - \Delta} \tag{5.184}$$

Chapter 6

Dynamics in Fock space and complex time

In this chapter, we step again into many-particle physics. We prepare the ground the unified formulation of Green's functions in many-particle physics. The key to this generality is to use a time variable that evolves along a time contour in the complex plane. The various Green's function approaches can then be related to a particular choice of the time contour.

1. propagator in Fock space
2. ensembles
3. complex time contour
4. linear response
5. Heisenberg operators

6.1 Propagator in Fock space

In section 4.3.1, we introduced the propagator in the one-particle Hilbert space. As we proceed to many-particle systems, we need to generalize it to the complete Fock space. The definition is analogous: Instead of a complete basis of one-particle wave functions, we use now a complete basis in the Fock space.

In order to make the distinction between one-particle and many-particle quantities evident, I will use, as much as as possible, uppercase symbols for the many-particle properties and quantities that refer to interacting systems.

Consider the time evolution for any many-particle state $|\Psi(t)\rangle$ which is governed by the many-particle Schrödinger equation

$$\left[i\hbar\partial_t - \hat{H}(t)\right]|\Psi(t)\rangle = 0 \tag{6.1}$$

with the many-particle Hamiltonian $\hat{H} = \hat{h} + \hat{W}$.

The time evolution for any many-particle state $|\Psi(t)\rangle$ can be expressed by the propagator $\hat{\mathcal{U}}(t, t')$ in Fock space

$$|\Psi(t)\rangle = \hat{\mathcal{U}}(t, t')|\Psi(t')\rangle \tag{6.2}$$

The many-particle propagator $\hat{\mathcal{U}}$ differs from one-particle propagator $\hat{U}$, used earlier. $\hat{\mathcal{U}}$ acts in the Fock space, while $\hat{U}$ acts on the one-particle Hilbert space.

The many-particle propagator is defined by the differential equation

$$\Big[i\hbar\partial_t - \hat{H}(t)\Big]\,\hat{\mathcal{U}}(t,t') = 0 \tag{6.3}$$

and the boundary condition is (with the unit operator $\hat{1}$ in Fock space)

$$\hat{\mathcal{U}}(t,t) = \hat{1}\ . \tag{6.4}$$

Closed expression: The propagator has the form

$$\hat{\mathcal{U}}(t,t') = \sum_{m,n} \big|\Phi_m(t)\big\rangle \Big(\big\langle\Phi_m(t')\big|\Phi_n(t')\big\rangle\Big)^{-1}_{m,n} \big\langle\Phi_n(t')\big| \tag{6.5}$$

where the many-particle wave functions $|\Phi_n(t')\rangle$ form a complete basisset in Fock space. Each such state obeys the time-dependent Schrödinger equation

$$\Big[i\hbar\partial_t - \hat{H}(t)\Big]|\Phi_n(t)\rangle = 0 \tag{6.6}$$

The many-particle propagator obeys the same rules as those specified in section 4.3.1 on p. 169 for the propagator in the one-particle Hamiltonian.

Alternatively, we can also use the ordered exponential with Dyson's time-ordering operator $\mathcal{T}_D$.

$$\hat{\mathcal{U}}(t,t') = \mathcal{T}_D \exp\left(-\frac{i}{\hbar}\int_{t'}^{t} dt''\ \hat{H}(t'')\right) \tag{6.7}$$

Propagator for time-independent systems: For a stationary system, the propagator has the form

$$\hat{\mathcal{U}}(t,t') = \sum_n |\Phi_n\rangle \mathrm{e}^{-\frac{i}{\hbar}E_n(t-t')}\langle\Phi_n| \tag{6.8}$$

where the $|\Phi_n\rangle$ are the orthonormal eigenstates of the time-independent Schrödinger equation in Fock space.

$$\hat{H}|\Phi_n\rangle = |\Phi_n\rangle E_n \tag{6.9}$$

For a time-independent Hamiltonian $\hat{H}$, the propagator $\hat{\mathcal{U}}(t,t')$ from Eq. 6.8 can be expressed in the compact form

$$\hat{\mathcal{U}}(t,t') = \mathrm{e}^{-\frac{i}{\hbar}\hat{H}(t-t')} \tag{6.10}$$

which is verified by insertion into the Schrödinger equation:

$$i\hbar\partial_t \underbrace{\hat{\mathcal{U}}(t,t')|\psi(t')\rangle}_{|\psi(t)\rangle} = \hat{H}\,\underbrace{\hat{\mathcal{U}}(t,t')|\psi(t')\rangle}_{|\psi(t)\rangle} \tag{6.11}$$

Propagator for time-independent systems without interaction: For a non-interacting and time-independent Hamiltonian $\hat{H} = \hat{h}$, the propagator is, in occupation-number representation,

$$\hat{\mathcal{U}}(t,t') = \sum_{\vec{\sigma}} |\vec{\sigma}\rangle \mathrm{e}^{-\frac{i}{\hbar}(\sum_j \sigma_j\epsilon_j)(t-t')}\langle\vec{\sigma}| \tag{6.12}$$

Because the system is non-interacting, the eigenstates are Slater-determinants expressed in the one-particle basis with states $|\varphi_j\rangle$, that obey[1]

$$\hat{h}|\varphi_j\rangle = |\varphi_j\rangle\epsilon_j \tag{6.13}$$

[1]Using $\hat{h}$ both in the Fock space and the one-particle Hilbert space may be irritating. In this special case, it is allowed considering that the one-particle Hilbert space is a sub-space of the Fock space.

We use the occupation-number representation. (See also section 1.4.1 on p. 23)

The Hamilton eigenstates for this non-interacting Hamiltonian $\hat{H} = \hat{h}$ obey the eigenvalue equation

$$\hat{h}|\vec{\sigma}\rangle = |\vec{\sigma}\rangle E_{\vec{\sigma}} \tag{6.14}$$

with energies

$$E_{\vec{\sigma}} = \sum_{j=1}^{\infty} \sigma_j \epsilon_j \tag{6.15}$$

6.2 Time as complex variable

6.2.1 Motivation

By allowing arbitrary time contours in the complex plane, the Green's-function formalism can be introduced in a unified way[**?**] rather than considering several distinct theories for zero-temperature time-dependent problems, finite-temperature static problems and non-equilibrium problems.

This section, 6.2.1, aims at providing a motivation, before I describe what needs to be considered in connection with complex time contours.

Allowing the time to vary along a contour in the complex plane is related to a mathematical trick used in connection with finite temperature. The gist of this trick is that both propagator $\hat{\mathcal{U}}(t, t')$ and thermal state-operator $\hat{\rho}_{T,\mu}$ are both expressed in terms of exponentials of the Hamiltonian. By allowing complex time arguments, the state operator can be expressed, partly, by a propagator.

$$\hat{\rho}_{T,\mu} = \frac{\mathrm{e}^{-\beta(\hat{H}-\mu\hat{N})}}{\mathrm{Tr}[\mathrm{e}^{-\beta(\hat{H}-\mu\hat{N})}]} = \frac{\mathrm{e}^{\beta\mu\hat{N}}\hat{\mathcal{U}}(-i\hbar\beta, 0)}{\mathrm{Tr}[\mathrm{e}^{\beta\mu\hat{N}}\hat{\mathcal{U}}(-i\hbar\beta), 0]} \tag{6.16}$$

where I used the propagator (with frozen $\hat{H}$)

$$\hat{\mathcal{U}}(-i\hbar\beta, 0) = \exp\Big(-\frac{i}{\hbar}\hat{H}\cdot\underbrace{(-i\hbar\beta)}_{(t-0)}\Big) = \mathrm{e}^{-\beta\hat{H}} \tag{6.17}$$

A time-dependent expectation value is obtained by propagating the states of the ensemble to the desired time. This allows us to start with a specific ensemble at $t = 0$ and propagate with a time-dependent Hamiltonian to the desired time.

$$\big\langle A(t)\big\rangle_{T,\mu} = \frac{\mathrm{Tr}\left\{\mathrm{e}^{\beta\mu\hat{N}}\hat{\mathcal{U}}(-i\hbar\beta, 0)\hat{\mathcal{U}}(0, t)\hat{A}\hat{\mathcal{U}}(t, 0)\right\}}{\mathrm{Tr}\left\{\mathrm{e}^{\beta\mu\hat{N}}\hat{\mathcal{U}}(-i\hbar\beta, 0)\hat{\mathcal{U}}(0, t)\hat{\mathcal{U}}(t, 0)\right\}} = \frac{\mathrm{Tr}\left[\mathrm{e}^{\beta\mu\hat{N}}\mathcal{T}_{\mathcal{C}}\left\{\hat{A}_S(t)\mathrm{e}^{-\frac{i}{\hbar}\int_{\mathcal{C}} dt'\ \hat{H}(t')}\right\}\right]}{\mathrm{Tr}\left[\mathrm{e}^{\beta\mu\hat{N}}\mathcal{T}_{\mathcal{C}}\left\{\mathrm{e}^{-\frac{i}{\hbar}\int_{\mathcal{C}} dt'\ \hat{H}(t')}\right\}\right]} \tag{6.18}$$

The propagation proceeds along the contour $\mathcal{C}$ leading along $0 \to t \to 0 \to -i\hbar\beta$ in the complex-time plane. The time argument $\hat{A}_S(t) = \hat{A}$ is only present to guide the time-ordering operator $\mathcal{T}_{\mathcal{C}}$, which is redefined to order along the one-dimensional time contour in the complex plane. A proper definition of this time-ordering operator will follow in Eq. 6.36 on p. 235. The Schrödinger operator $\hat{A}_S(t)$ must not confused with a Heisenberg operator $\hat{A}_H(t)$.

This example shall demonstrate the general principle, rather than providing a working technique. The ensemble propagated here is, admittedly, weird. At this point this shall not disturb us. The complex time contour will later be put into more reasonable use. The goal is to make it plausible that thermal properties can be described with time arguments on the imaginary axis. For the time being, this shall suffice as motivation. Details will be made clear later.

While I will not exploit the complex time contour for quite some time, introducing it here allows me to define quantities already in its final generality.

6.2.2 Definitions and working rules

Complex time contour: Consider time to proceed along a one-dimensional contour $\mathcal{C}$ in the complex plane. Thus, time $t(s) \in \mathbb{C}$ is a complex-valued function of a one-dimensional real parameter $s \in \mathbb{R}$.

$$t(s) : \mathbb{R} \to \mathbb{C} \tag{6.19}$$

An example of such complex time contour is shown in the box containing Eq. 10.22 on p. 301.

Let me write down some definitions that are required to describe the dynamics along a complex contour.

- a **contour integral** of a function $f(t)$, along a contour $\mathcal{C}$ in the complex plane has the form

$$\int_{\mathcal{C};t_a\in\mathcal{C}}^{t_b\in\mathcal{C}} dt\; f(t) \stackrel{\text{def}}{=} \int_{s_a}^{s_b} ds\; \frac{dt(s)}{ds} f(t(s)) \tag{6.20}$$

  where $t_a = t(s_a)$ and $t_b = t(s_b)$.

- Similarly, the **contour derivative** is

$$\frac{df}{dt} \stackrel{\text{def}}{=} \frac{df(t(s))}{ds} \left(\frac{dt}{ds}\right)^{-1} = \lim_{\Delta\to 0} \frac{f(t(s+\Delta)) - f(t(s))}{t(s+\Delta) - t(s)} \tag{6.21}$$

  The contour derivative is not to be confused with the Wirtinger derivatives (see appendix A.3 on p. 386)

$$df = \frac{df}{dt} dt + \frac{df}{dt^*} dt^* \tag{6.22}$$

- The **contour step function** for time arguments on the contour will be generalized so that it refers to the parameter s.

$$\theta_{\mathcal{C}}(t_1 - t_2) \stackrel{\text{def}}{=} \theta(s_1 - s_2) \qquad \text{where } t_1 = t(s_1) \text{ and } t_2 = t(s_2) \tag{6.23}$$

- the **contour delta function** is defined as the derivative of the contour step function. Thus, we can use

$$\delta(s) = \frac{d\theta(s)}{ds} = \frac{d\theta(t)}{dt}\frac{dt}{ds} = \delta(t)\frac{dt}{ds} \tag{6.24}$$

  Thus,

$$\delta_{\mathcal{C}}(t - t') \stackrel{\text{def}}{=} \left(\frac{dt}{ds}\right)^{-1} \delta(s - s') \tag{6.25}$$

- The **contour Schrödinger equation** translates into

$$\left[i\hbar\partial_t - \hat{H}(t)\right]|\psi(t)\rangle = \left[i\hbar\left(\frac{dt}{ds}\right)^{-1}\partial_s - \hat{H}(s)\right]|\psi(s)\rangle = 0 \tag{6.26}$$

  This converts the Schrödinger equation into a differential equation with respect to the real one-dimensional parameter s.

- The propagator $\hat{U}(t, t')$ of the one-particle states has been introduced previously in section 4.3.1 on p. 167. The **contour propagator** has the same form, which also holds for complex-valued time arguments.

$$\hat{U}(t, t') = \sum_{m,n} |\varphi_m(t)\rangle O^{-1}_{m,n}(t')\langle\varphi_n(t')| \tag{6.27}$$

The time-dependent one-particle states $\{|\varphi_n(t)\rangle\}$ form a complete set of wave functions that satisfy the contour Schrödinger equation. With

$$O_{m,n}(t) = \langle\varphi_m(t)|\varphi_n(t)\rangle \,, \tag{6.28}$$

we denote the time-dependent overlap matrix. The orthonormality of wave functions is conserved along the real time axis, but not away from it. Notice that the time argument of the inverse overlap matrix is connected to the second time argument of the propagator, which makes the expression asymmetric.

As a side remark, let me alert the you to an aspect that may easily be overlooked: The propagator for a time-independent Hamiltonian has a surprisingly simple form, despite being valid in the complex-time plane. Let me consider the solutions $|\varphi_n(t)\rangle$ of the contour Schrödinger equation for a *time-independent* Hamiltonian. The states shall be orthonormal at $t = 0$ and eigenstates of the Hamiltonian with eigenvalues ϵ_n

$$\begin{aligned}
& |\varphi_n(t)\rangle = |\varphi_n(0)\rangle \mathrm{e}^{-\frac{i}{\hbar}\epsilon_n t} \\
\Rightarrow \quad & \langle\varphi_n(t)| = \mathrm{e}^{+\frac{i}{\hbar}\epsilon_n t^*} \langle\varphi_n(0)| \\
\Rightarrow \quad & O_{m,n}(t) = \langle\varphi_m(t)|\varphi_n(t)\rangle = \mathrm{e}^{+\frac{i}{\hbar}\epsilon_n t^*} \underbrace{\langle\varphi_m(0)|\varphi_n(0)\rangle}_{\delta_{m,n}} \mathrm{e}^{-\frac{i}{\hbar}\epsilon_n t} = \delta_{m,n} \mathrm{e}^{+\frac{i}{\hbar}\epsilon_n (t^*-t)}
\end{aligned}$$

$$\Rightarrow \quad \sum_n O^{-1}_{m,n}(t) \langle\varphi_n(t)| = \sum_n \underbrace{\delta_{m,n} \mathrm{e}^{-\frac{i}{\hbar}\epsilon_n (t^*-t)}}_{O^{-1}_{m,n}(t)} \underbrace{\mathrm{e}^{+\frac{i}{\hbar}\epsilon_n t^*} \langle\varphi_n(0)|}_{\langle\varphi_n(t)|} = \mathrm{e}^{+\frac{i}{\hbar}\epsilon_m t} \langle\varphi_m(0)| \tag{6.29}$$

The propagator for a time-independent Hamiltonian $\hat{h}$ is

$$\begin{aligned}
\hat{U}(t,t') &= \sum_{m,n} \underbrace{|\varphi_m(0)\rangle \mathrm{e}^{-\frac{i}{\hbar}\epsilon_m t}}_{|\varphi_m(t)\rangle} \underbrace{\delta_{m,n} \mathrm{e}^{-\frac{i}{\hbar}\epsilon_n ((t')^* - t')}}_{O^{-1}_{m,n}(t')} \underbrace{\mathrm{e}^{+\frac{i}{\hbar}\epsilon_n (t')^*} \langle\varphi_n(0)|}_{\langle\varphi_n(t')|} \\
&= \sum_n |\varphi_n(0)\rangle \mathrm{e}^{-\frac{i}{\hbar}\epsilon_n (t-t')} \langle\varphi_n(0)| = \mathrm{e}^{-\frac{i}{\hbar}\hat{h}(t-t')}
\end{aligned} \tag{6.30}$$

The result is simple in a non-trivial way. The complications related to the complex-conjugate time and the inverse overlap matrix disappear.

For later reference, table 6.1 summarizes the rules for symbols on a complex contour. The subscript $\mathcal{C}$ will not be carried through consistently.

∂_t	$\left(\frac{dt}{ds}\right)^{-1} \partial_s$	contour derivative
$\int_{t(s_a)}^{t(s_b)} dt$	$\int_{s_a}^{s_b} ds \frac{dt}{ds}$	contour integral
$\theta_{\mathcal{C}}(t-t')$	$\theta(s-s')$	step function
$\delta_{\mathcal{C}}(t-t')$	$\left(\frac{dt}{ds}\right)^{-1} \delta(s-s')$	delta function

Table 6.1: Translation rules of quantities defined on a complex-time contour $t(s)$ onto the real-valued contour parameter s.

6.2.3 Memory hook

In this section, I make an attempt to make the choices for the contour derivatives, contour integrations etc. plausible using a minimal problem, namely one with a one-dimensional Hilbert space. A one-dimensional Hilbert space is spanned by a single orbital.

Consider the propagator in this one-dimensional Hilbert space, which is a simple complex function in the complex time plane. To simplify the discussion, we only consider the relative time argument, rather than the arguments of initial and final time.

$$u(t) = \mathrm{e}^{-\frac{i}{\hbar}\epsilon t} \tag{6.31}$$

in the complex plane. This function is a cartoon of a propagator described below.

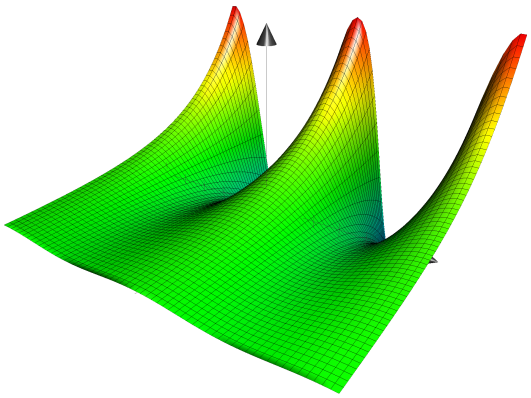

Fig. 6.1: Real part of the propagator $u(t)$ in a one-dimensional Hilbert space in the complex time plane. The propagator is a plane wave in the direction of the real time axis (towards right-front) and an exponential along the imaginary time axis. (towards right-back)

Contour derivative: $u(t) = \mathrm{e}^{-\frac{i}{\hbar}\epsilon t}$ obeys the differential equation

$$\Big(i\hbar\partial_t - \epsilon\Big)u(t) = 0 \tag{6.32}$$

when t proceeds along the real axis. This differential equation is analogous to the Schrödinger equation.

Consider now a path along the imaginary time axis,i.e. $t(s) = is$. The variable

$$\tau \stackrel{\text{def}}{=} -it \tag{6.33}$$

is called the **imaginary time**. Expressed in imaginary time, the propagator obeys the differential equation

$$\Big(\hbar\partial_\tau - \epsilon\Big)u(t(\tau)) = 0 \tag{6.34}$$

This is the Schrödinger equation in **imaginary time**. Its solution $u(t(\tau)) = \mathrm{e}^{\frac{1}{\hbar}\epsilon\tau}$ is an exponential, rather than a plane wave $u(t(\tau)) = \mathrm{e}^{-\frac{i}{\hbar}\epsilon\tau}$ obtained from the equation in real-valued time.

Both equations, Eq. 6.32 and Eq. 6.34, can be translated into each other using the replacement rule

$$\partial_t = \underbrace{\left(\frac{dt}{d\tau}\right)^{-1}}_{-i}\partial_\tau \tag{6.35}$$

Both differential equations, Eq. 6.32 and Eq. 6.34, can be considered as differential equations along one-dimensional contours $\mathcal{C}$ in the complex plane. In one case, the contour is defined by $t(s) = s$ and proceeds along the real time axis. In the other case, the contour is defined by $t(s) = is$ and proceeds along the imaginary-time axis.

6.2.4 Contour time-ordering operator

In section 4.3.3 on p. 169, the propagator has been represented as time-ordered exponential. In order to correct for the misordering of operators, Dyson's time-ordering operator Eq. 4.40 has been introduced.

In order to use this expression in connection with Heisenberg-type creation and annihilation operators, we need to introduce Wick's time-ordering operator. Wick's time-ordering operator introduces a sign change for every interchange of fermionic creation and annihilation operators.

Wick's time-ordering operator can be considered as a generalization of Dyson's time-ordering operator. Dyson's time-ordering operator has been introduced for observables, for which the fermionic operators occur in pairs. In this case, the sign changes introduced by Wick's time-ordering operator compensate.

Wick's time-ordering operator on the complex time contour is what we call the **contour time-ordering operator**.

CONTOUR TIME-ORDERING OPERATOR

The time-ordering operator acts on a product of operators $\hat{A}(t)$, which depend on the time-point $t(s)$ on a contour $\mathcal{C}$ in the complex plane. The time contour $\mathcal{C} : s \to t(s)$ is parameterized by a one-dimensional real-valued argument s.
The time-ordering operator rearranges the operators in the product such that the argument s increases from right to left. The time-ordering operators are no operators in the conventional sense: Namely, they do not act on states in the Hilbert or Fock space to map them onto other states. Rather, it is a prescription in which order the operators in a product shall be arranged.
Wick's time-ordering operator[57] or **contour time-ordering operator**. In his seminal paper[57] laying the foundation for the diagrammatic expansion of the Green's function, Wick introduced his time-ordering operator. This object is generalized to the contour time-ordering operator $\mathcal{T}_{\mathcal{C}}$.

$$\mathcal{T}_{\mathcal{C}}\hat{A}(t(s))\hat{B}(t(s')) = \begin{cases} \hat{A}(t(s))\hat{B}(t(s')) & \text{for } s \geq s' \\ \hat{B}(t(s'))\hat{A}(t(s)) & \text{for } s < s' \text{ and either } \hat{A} \text{ or } \hat{B} \text{ or both bosonic} \\ -\hat{B}(t(s'))\hat{A}(t(s)) & \text{for } s < s' \text{ and } \hat{A} \text{ and } \hat{B} \text{ fermionic} \end{cases} \tag{6.36}$$

Creation and annihilation operators of identical fermions are called fermionic operators. Odd-numbered products of such operators are themselves fermionic. Creation and annihilation operators of identical bosons are called bosonic operators. Even numbered products are of bosonic type. Thus, a Hamilton operator, which conserves the particle number is necessarily of bosonic type in the present context. This is confusing because this Hamiltonian still describes fermions).
The special rule for fermionic operators is due to Wick's theorem derived later. (In the expression for the time-ordered exponential, the special rule would actually be incorrect. We use the same object because Hamiltonians with fermionic operators are usually particle-number conserving, so that fermionic operators occur in pairs. Pairs of fermionic operators are again bosonic so that only the bosonic rule applies.) Editor: This should be explained better.

Time-ordered exponential on the contour

The propagator in Fock space with a time-dependent Hamiltonian $\hat{H}(t)$ has the form

$$\hat{\mathcal{U}}(t_2, t_1) = \mathcal{T}_{\mathcal{C}} e^{\frac{i}{\hbar}\int_{\mathcal{C},t_1}^{t_2} dt'\, \hat{H}(t)} \tag{6.37}$$

In the future, the contour will be implied in the time integral.

Expressed in the mapping $t(s)$ the time-ordered exponential is more explicitly given as.

$$\hat{\mathcal{U}}\big(t(s_2), t(s_1)\big) = \mathcal{T}_{\mathcal{C}} e^{\frac{i}{\hbar}\int_{\mathcal{C},s_1}^{s_2} ds\, \frac{dt(s)}{ds}\hat{H}\left(t(s)\right)} \tag{6.38}$$

It will be important that the propagator is not unitary for time arguments away from the real time axis. Transitivity still holds.

$$\begin{aligned} \hat{\mathcal{U}}(t_1,t_2)\,\hat{\mathcal{U}}(t_2,t_1) &= \hat{1} \\ \hat{\mathcal{U}}(t_1,t_2) &\neq \hat{\mathcal{U}}^\dagger(t_2,t_1) \end{aligned} \tag{6.39}$$

6.2.5 Heisenberg operators

Special care is required with the generalization of Heisenberg operators to the complex time contour, because the propagator is unitary only when the contour lies on the real axis. We define the Heisenberg operators as follows:

HEISENBERG OPERATORS

A Heisenberg operator $\hat{A}_H(t)$ is obtained from a Schrödinger operator $\hat{A}_S(t)$ with the propagator $\hat{\mathcal{U}}(t,t') = \mathcal{T}_D \mathrm{e}^{-\frac{i}{\hbar}\int_{\mathcal{C}} dt' \hat{H}(t')}$ as

$$\hat{A}_H(t) \stackrel{\text{def}}{=} \hat{\mathcal{U}}(0,t)\hat{A}_S(t)\hat{\mathcal{U}}(t,0) \tag{6.40}$$

In the Heisenberg picture, the creation and annihilation operators are no more complex conjugates of each other, unless the time lies on the real axis. Therefore, I introduce an alternate symbol $+$ to denote the creation operator in the Heisenberg picture, which is distinct from the one $\dagger$ used to denote the hermitian conjugate.

$$\begin{aligned} \hat{\psi}_H(\vec{x},t) &\stackrel{\text{def}}{=} \hat{\mathcal{U}}(0,t)\hat{\psi}_S(\vec{x})\hat{\mathcal{U}}(t,0) \\ \hat{\psi}^+_H(\vec{x},t) &\stackrel{\text{def}}{=} \hat{\mathcal{U}}(0,t)\hat{\psi}^\dagger_S(\vec{x})\hat{\mathcal{U}}(t,0) \end{aligned} \tag{6.41}$$

The creation and annihilation operators are not in general hermitian conjugates of each other.

$$\hat{\psi}^+_H(\vec{x},t) \neq \left(\hat{\psi}_H(\vec{x},t)\right)^\dagger \quad \text{unless for } t \in \mathbb{R} \tag{6.42}$$

The field operators in the Heisenberg picture obey the commutator relations known from the Schrödinger picture only for equal times.

$$\begin{aligned} \left[\psi^+_H(\vec{x},t),\psi_H(\vec{x'},t')\right]_+ &= \delta(\vec{x}-\vec{x'}) \qquad \text{only for } t=t' \\ \left[\psi^+_H(\vec{x},t),\psi^+_H(\vec{x'},t')\right]_+ &= 0 \qquad \text{only for } t=t' \\ \left[\psi_H(\vec{x},t),\psi_H(\vec{x'},t')\right]_+ &= 0 \qquad \text{only for } t=t' \end{aligned} \tag{6.43}$$

With this definition, the differential equation for the Heisenberg operators has the usual form[2]

$$\begin{aligned} i\hbar\partial_t A_H(t) &= \left(i\hbar\partial_t \hat{\mathcal{U}}(0,t)\right)\hat{A}_S(t)\hat{\mathcal{U}}(t,0) + \hat{\mathcal{U}}(0,t)\left(i\hbar\partial_t \hat{A}_S(t)\right)\hat{\mathcal{U}}(t,0) + \hat{\mathcal{U}}(0,t)\hat{A}_S(t)\left(i\hbar\partial_t \hat{\mathcal{U}}(t,0)\right) \\ &= \left[\hat{A}_H(t), \hat{H}_H(t)\right]_- + i\hbar\left(\frac{\partial \hat{A}}{\partial t}\right)_H \end{aligned} \tag{6.45}$$

However, the time-dependent expectation value is obtained only for times on the real axis.

$$\langle A(t)\rangle \overset{\text{def}}{=} \frac{\langle\psi_S(t)|\hat{A}_S|\psi_S(t)\rangle}{\langle\psi_S(t)|\psi_S(t)\rangle} \overset{t\in\mathbb{R}}{=} \frac{\langle\psi_H|\hat{A}_H(t)|\psi_H\rangle}{\langle\psi_H|\psi_H\rangle} \qquad \text{for } t \in \mathbb{R} \tag{6.46}$$

6.3 Home study and practice

[2]We use the differential equation $[i\hbar\partial_t - \hat{H}_S(t)]\hat{\mathcal{U}}(t,0) = 0$ and $\hat{\mathcal{U}}(0,t)\hat{\mathcal{U}}(t,0) = \hat{1}$. Specifically,

$$\begin{aligned} & \hat{\mathcal{U}}(0,t)\left[\left(i\hbar\partial_t \hat{\mathcal{U}}(t,0)\right) - \hat{H}_S\hat{\mathcal{U}}(t,0)\right]\hat{\mathcal{U}}(0,t) = 0 \\ \Rightarrow \quad & \hat{\mathcal{U}}(0,t)\underbrace{i\hbar\partial_t \hat{\mathcal{U}}(t,0)\hat{\mathcal{U}}(0,t)}_{=\hat{0}} - \underbrace{\hat{\mathcal{U}}(0,t)\hat{\mathcal{U}}(t,0)}_{\hat{1}} i\hbar\partial_t\hat{\mathcal{U}}(0,t) - \hat{\mathcal{U}}(0,t)\hat{H}_S\underbrace{\hat{\mathcal{U}}(t,0)\hat{\mathcal{U}}(0,t)}_{=\hat{1}} = 0 \end{aligned} \tag{6.44}$$

From the latter, we obtain $i\hbar\partial_t\hat{\mathcal{U}}(0,t) = -\hat{\mathcal{U}}(0,t)\hat{H}_S(t)$, respectively $i\hbar\partial_t\hat{\mathcal{U}}(0,t) = -\hat{H}_H\hat{\mathcal{U}}(0,t)$.

Chapter 7

Green's functions in many-particle physics

The transition of the Green's-function formalism from one-particle systems to a many-particle problems is conceptually non-trivial. There are a number of equations that remain the same, but the Green's function in many-particle physics is a generalization of the one-particle case, which has a different mathematical foundation. Often, I find that the Green's function is defined as mathematical expression, and the motivation becomes evident only a posteriori. In this chapter, I will try to motivate the choices that lead to the many-particle Green's function beforehand.

7.1 One-particle Green's functions in second quantization

The first step on the route from the Green's function for one-particle systems to that for many particles is to reformulate the one-particle Green's function in the language of second quantization.

The Green's function is obtained from the propagator $\hat{U}(t_2, t_1)$ via Eq. 4.38. In order to extend our definitions to the Fock space, I represent this propagator in terms of creation and annihilation operators. Note, however, that we still work with a one-particle problem. Let me choose a basisset of Hamilton eigenstates $|\varphi_m\rangle$ and the corresponding creation and annihilation operators $\hat{a}_m^\dagger$ and $\hat{a}_m$. The basis functions can be expressed by the vacuum state $|\mathcal{O}\rangle$ and the creation operator as

$$|\varphi_m\rangle \overset{\text{Eq. 3.22}}{=} \hat{a}_m^\dagger |\mathcal{O}\rangle \; . \tag{7.1}$$

Because the basis $\{|\varphi_m\rangle\}$ is orthonormal and complete, we obtain

$$\begin{aligned}
\hat{U}(t_2, t_1) &= \sum_{m,n} |\varphi_m\rangle\langle\varphi_m|\hat{U}(t_2, t_1)|\varphi_n\rangle\langle\varphi_n| \\
&\overset{\text{Eqs. 3.22, 6.2}}{=} \sum_{m,n} |\varphi_m\rangle\langle\mathcal{O}|\hat{a}_m\hat{\mathcal{U}}(t_2, t_1)\hat{a}_n^\dagger|\mathcal{O}\rangle\langle\varphi_n| \\
&\overset{\hat{\mathcal{U}}(t,0)|\mathcal{O}\rangle=|\mathcal{O}\rangle}{=} \sum_{m,n} |\varphi_m\rangle \underbrace{\langle\mathcal{O}|\hat{\mathcal{U}}(0, t_2)}_{\langle\mathcal{O}|}\hat{a}_m\hat{\mathcal{U}}(t_2, t_1)\hat{a}_n^\dagger \underbrace{\hat{\mathcal{U}}(t_1, 0)|\mathcal{O}\rangle}_{=|\mathcal{O}\rangle}\langle\varphi_n|
\end{aligned} \tag{7.2}$$

where I used the many-particle propagator $\hat{\mathcal{U}}(t, t')$ in Fock space.

The propagators from $t = 0$ to t_1 and from t_2 to $t = 0$ have been included to make the final result independent of a global shift of the energies. A global shift by Δ introduces a phase factor $e^{-\frac{i}{\hbar}\Delta(t_2-t_1)}$ into the propagator Eq. 6.7. The propagation back to the initial state ensures that a global shift, which is the energy of the vacuum state, does not affect the result. The invariance of observables with respect to a global energy shift is attributed to gauge invariance in electrodynamics.

The one-particle Green's function is therefore

$$\hat{G}(t_2,t_1) \stackrel{\text{Eq. 4.38}}{=} \frac{1}{i\hbar}\theta_{\mathcal{C}}(t_2-t_1)\sum_{m,n}|\varphi_m\rangle\langle\mathcal{O}|\hat{\mathcal{U}}(0,t_2)\hat{a}_m\hat{\mathcal{U}}(t_2,t_1)\hat{a}_n^\dagger\hat{\mathcal{U}}(t_1,0)|\mathcal{O}\rangle\langle\varphi_n| \tag{7.3}$$

Even though they describe only a single particle, the many-particle states in the matrix element live in Fock space and are propagated by the many-particle propagator $\hat{\mathcal{U}}(t,t')$ rather than the one-particle propagator $\hat{U}(t,t')$. The Green's function itself is still an operator in the one-particle Hilbert space.

Eq. 7.3 suggests an interpretation of the Green's function

$$\begin{aligned} G(\vec{x}_2,t_2,\vec{x}_1,t_1) &= \langle\vec{x}_2|\hat{G}(t_2,t_1)|\vec{x}_1\rangle \\ &= \frac{1}{i\hbar}\theta_{\mathcal{C}}(t_2-t_1)\langle\mathcal{O}|\hat{\mathcal{U}}(0,t_2)\hat{\psi}(\vec{x}_2)\hat{\mathcal{U}}(t_2,t_1)\hat{\psi}^\dagger(\vec{x}_1)\hat{\mathcal{U}}(t_1,0)|\mathcal{O}\rangle \end{aligned} \tag{7.4}$$

as probability amplitude for finding a particle at time t_2 in position $\vec{x}_2$, which has been added to the system at time t_1 in position $\vec{x}_1$. This will be a guiding principle in the definition of the Green's function for many-particle systems.

7.2 Propagate electrons in a non-interacting electron gas

While Eq. 7.3 describes an electron added to empty space, let us now study an electron added to a non-interacting many-electron system. To keep things simple, I limit the discussion to time-independent problems.

To generalize Eq. 7.3, I replace the vacuum state $|\mathcal{O}\rangle$ in Eq. 7.2 by an eigenstate $|\vec{\sigma}\rangle$ of a non-interacting Hamiltonian $\hat{h}$. I use the occupation-number representation for the eigenstates $|\vec{\sigma}\rangle$ of $\hat{h}$ with energies $E_{\vec{\sigma}} = \sum_{n=1}^{\infty}\sigma_n\epsilon_n$. In this way, Eq. 7.2 generalizes to

$$\begin{aligned} \hat{U}^{(e)}(t_2,t_1) &= \sum_{n,m}|\varphi_m\rangle\Bigg[\langle\vec{\sigma}|\underbrace{\hat{\mathcal{U}}(0,t_2)\,\hat{a}_m\underbrace{\hat{\mathcal{U}}(t_2,t_1)\underbrace{\hat{a}_n^\dagger\hat{\mathcal{U}}(t_1,0)|\vec{\sigma}\rangle}_{\hat{a}_n^\dagger|\vec{\sigma}\rangle e^{-\frac{i}{\hbar}E_{\vec{\sigma}}t_1}}}_{\hat{a}_m\hat{a}_n^\dagger|\vec{\sigma}\rangle e^{-\frac{i}{\hbar}(E_{\vec{\sigma}}+\epsilon_n)(t_2-t_1)}e^{-\frac{i}{\hbar}E_{\vec{\sigma}}t_1}}}_{\hat{a}_m\hat{a}_n^\dagger|\vec{\sigma}\rangle e^{-\frac{i}{\hbar}(E_{\vec{\sigma}}+\epsilon_n-\epsilon_m)(0-t_2)}e^{-\frac{i}{\hbar}(E_{\vec{\sigma}}+\epsilon_n)(t_2-t_1)}e^{-\frac{i}{\hbar}E_{\vec{\sigma}}t_1}}\Bigg]\langle\varphi_n| \\ &\stackrel{\text{Eq. 6.12}}{=} \sum_{n,m}|\varphi_m\rangle\Bigg[\underbrace{\delta_{m,n}(1-\sigma_n)}_{\langle\vec{\sigma}|\hat{a}_m\hat{a}_n^\dagger|\vec{\sigma}\rangle}e^{-\frac{i}{\hbar}\epsilon_n(t_2-t_1)}\Bigg]\langle\varphi_n| \\ &= \sum_n(1-\sigma_n)\,|\varphi_n\rangle e^{-\frac{i}{\hbar}\epsilon_n(t_2-t_1)}\langle\varphi_n| \end{aligned} \tag{7.5}$$

Except for the factor $(1-\sigma_n)$, this is identical to the propagator for a one-particle system Eq. 6.12. The factor $(1-\sigma_n)$ filters away all occupied states in the Slater determinant $|\vec{\sigma}\rangle$. This reflects that an electron can not be added to a filled orbital.

Let me construct a similar propagator for the occupied states. The occupied states are selected

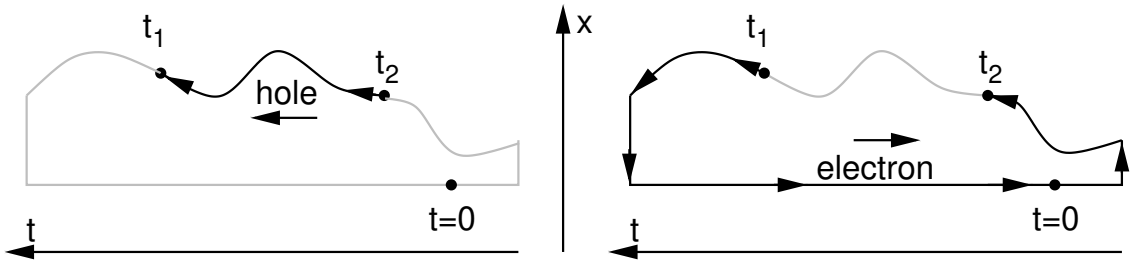

Fig. 7.1: Comparison of a hole propagation forward in time with that of an electron backward in time.

by first (at t_2) applying the annihilator and later (at t_1) the creator.

$$\begin{aligned}
\hat{U}^{(h)}(t_1,t_2) &= \sum_{n,m}|\varphi_m\rangle\Big[\langle\vec{\sigma}|\quad \hat{\mathcal{U}}(0,t_1)\,\hat{a}_n^\dagger\hat{\mathcal{U}}(t_1,t_2)\,\underbrace{\hat{a}_m\hat{\mathcal{U}}(t_2,0)|\vec{\sigma}\rangle}_{\hat{a}_m|\vec{\sigma}\rangle e^{-\frac{i}{\hbar}E_{\vec{\sigma}}t_2}}\quad\Big]\langle\varphi_n| \\
&\qquad \underbrace{\qquad\qquad}_{\hat{a}_n^\dagger\hat{a}_m|\vec{\sigma}\rangle e^{-\frac{i}{\hbar}(E_{\vec{\sigma}}-\epsilon_m)(t_1-t_2)}e^{-\frac{i}{\hbar}E_{\vec{\sigma}}t_2}} \\
&\qquad \underbrace{\qquad\qquad\qquad\qquad}_{\hat{a}_n^\dagger\hat{a}_m|\vec{\sigma}\rangle e^{-\frac{i}{\hbar}(E_{\vec{\sigma}}-\epsilon_m+\epsilon_n)(0-t_1)}e^{-\frac{i}{\hbar}(E_{\vec{\sigma}}-\epsilon_m)(t_1-t_2)}e^{-\frac{i}{\hbar}E_{\vec{\sigma}}t_2}} \\
&\overset{\text{Eq. 6.12}}{=} \sum_{n,m}|\varphi_m\rangle\Big[\underbrace{\delta_{m,n}\sigma_n}_{\langle\vec{\sigma}|\hat{a}_n^\dagger\hat{a}_m|\vec{\sigma}\rangle}\ e^{-\frac{i}{\hbar}(-\epsilon_m)(t_1-t_2)}\Big]\langle\varphi_n| \\
&= \sum_n \sigma_n\,|\varphi_n\rangle e^{+\frac{i}{\hbar}\epsilon_n(t_1-t_2)}\langle\varphi_n| \qquad (7.6)
\end{aligned}$$

The factor σ_n filters away the empty states, so that this term projects exactly onto the occupied states, that have been missing in the electron propagator. However, because we removed an electron, rather than adding one, the energy ϵ_n enters with a minus sign.

Combining the electron and hole propagators reproduces the one-particle propagator.

$$\begin{aligned}
\hat{U}(t_2,t_1) &= \sum_n |\varphi_n\rangle e^{-\frac{i}{\hbar}(t_2-t_1)}\langle\varphi_n| \\
&= \hat{U}^{(e)}(t_2,t_1)+\hat{U}^{(h)}(t_1,t_2) \\
&= \sum_{m,n}|\varphi_m\rangle\langle\vec{\sigma}|\Big(\hat{\mathcal{U}}(0,t_2)\hat{a}_{S,m}\hat{\mathcal{U}}(t_2,t_1)\hat{a}_{S,n}^+\hat{\mathcal{U}}(t_1,0)+\hat{\mathcal{U}}(0,t_1)\hat{a}_{S,n}^+\hat{\mathcal{U}}(t_1,t_2)\hat{a}_{S,m}\hat{\mathcal{U}}(t_2,0)\Big)|\vec{\sigma}\rangle\langle\varphi_n| \\
&= \sum_{m,n}|\varphi_m\rangle\langle\vec{\sigma}|\Big[\hat{a}_{H,m}(t_2),\hat{a}_{H,n}^+(t_1)\Big]_+|\vec{\sigma}\rangle\langle\varphi_n| \qquad (7.7)
\end{aligned}$$

The time arguments for the hole propagator enter in the reversed order. This can loosely be explained by considering a hole as an electron moving backwards in time: (see also Fig,7.1)

- A hole propagates from t_2 to t_1 with $t_1 > t_2$. At time t_2 a positive charge appears and, at time t_1 it disappears. Rather than letting the positive charge disappear at t_1 one could also have created a negative charge, which compensates the positive charge created earlier.
- An electron propagates from a later time t_1 to an earlier time t_2 with $t_1 > t_2$: At the later time t_1 an electron is added and propagates into the future, returns to time $t = 0$ and from there to t_2, where it is removed from the system.

In both cases, the system becomes more positive at t_2 and it becomes more negative at t_1, indicating that the process is the same, albeit expressed in different words.

7.3 From the propagator of non-interacting electrons to the Green's function

So far, we generalized the propagator of an isolated electron to a propagator Eq. 7.2 of an electron, respectively a hole that has been added to a non-interacting many-electron system.

In order to obtain the Green's function, let us inspect the relation Eq. 4.38 from one-particle quantum mechanics, which links the Green's function to the propagator.

$$\begin{aligned}\hat{G}(t_2,t_1) &= \frac{1}{i\hbar}\theta(t_2-t_1)\hat{U}(t_2,t_1) - \frac{C}{i\hbar}\hat{U}(t_2,t_1) \\ &= (1-C)\frac{1}{i\hbar}\theta(t_2-t_1)\hat{U}(t_2,t_1) - \frac{C}{i\hbar}\theta(t_1-t_2)\hat{U}(t_2,t_1)\end{aligned} \tag{7.8}$$

I extended Eq. 4.38 by adding the propagator scaled by a real-valued constant C. For the one-particle case, the additional term is, up to a constant, the propagator, which obeys the Schrödinger equation. Therefore, the Green's function $\hat{G}(t,t')$ satisfies the defining differential equation for the Green's function for any finite C. For $C \neq 0$, however, it violates the initial condition $\hat{G}(t,t') = \hat{0}$ for $t = -\infty$.

In the many-particle case, the propagator has two terms: one for electrons and one for holes. Each term solves the one-particle Schrödinger equation independently. I am free to convert the propagator into Green's functions for electrons and for holes independently.

I am using $C = 0$ for the electrons and $C = 1$ for the holes and I add the electron and hole contributions together. In this way, the contour-ordered Green's function is obtained.

$$\begin{aligned}\hat{G}^{\mathcal{C}}(t_2,t_1) &= \frac{1}{i\hbar}\theta_{\mathcal{C}}(t_2-t_1)\hat{U}^e(t_2,t_1) - \frac{1}{i\hbar}\theta_{\mathcal{C}}(t_1-t_2)\hat{U}^h(t_1,t_2) \\ &= \sum_{m,n}|\varphi_m\rangle\Bigg\{\frac{1}{i\hbar}\theta_{\mathcal{C}}(t_2-t_1)\underbrace{\langle\vec{\sigma}|\hat{\mathcal{U}}(0,t_2)\hat{a}_n\hat{\mathcal{U}}(t_2,t_1)\hat{a}_m^\dagger\hat{\mathcal{U}}(t_1,0)|\vec{\sigma}\rangle}_{\text{electrons from } (m,t_1) \text{ to } (n,t_2)} \\ &\qquad -\frac{1}{i\hbar}\theta_{\mathcal{C}}(t_1-t_2)\underbrace{\langle\vec{\sigma}|\hat{\mathcal{U}}(0,t_1)\hat{a}_m^\dagger\hat{\mathcal{U}}(t_1,t_2)\hat{a}_n\hat{\mathcal{U}}(t_2,0)|\vec{\sigma}\rangle}_{\text{holes from } (n,t_2) \text{ to } (m,t_1)}\Bigg\}\langle\varphi_n|\end{aligned} \tag{7.9}$$

The order of the time arguments of the Green's function does not specify, whether the system is propagated forward or backward in time, but whether electrons or holes are propagated. For $t_2 > t_1$, this Green's function describes the propagator for electrons (but not holes) from the earlier time t_1 to the later time t_2. For $t_1 > t_2$, the Green's function describes the propagator for holes (but not electrons) from the earlier time t_2 to the later time t_1.

Other choices for the Green's function are possible. For example, I could have used $C = 1$ for both, the electron and the hole channel, which would lead again to a Green's function, albeit another one. It would produce the one-particle propagator for a non-interacting system, and it would solve the differential for the Green's function. What would change, is the boundary condition at $t_2 = -\infty$. However, we make a different choice.

Why did we make this particular choice? From the background we have so far, we cannot motivate it. We will see later, that this choice is required for Wick's theorem, which again is the basis of the diagrammatic expansion of the Green's function. Other Green's function are typically obtained from the contour-ordered Green's function. The reason will become clear in the derivation of Wick's theorem in appendix K on p. 561, and it will be discussed on p. p. 582

Make things compact: The contour-ordered Green's function can be economically represented using operators in the Heisenberg picture Eq. 6.40. Furthermore, we can make use of the contour time-ordering operator $\mathcal{T}_{\mathcal{C}}$ from Eq. 6.36. (Remember that an interchange of two fermionic operators by $\mathcal{T}_{\mathcal{C}}$ produces a sign flip.) Combining the propagators with the creation and annihilation operators,

we obtain

$$\begin{aligned}\hat{G}^{\mathcal{C}}(t_2,t_1) &\overset{\text{Eq. 6.40}}{=} \sum_{m,n}|\varphi_m\rangle\Big\{\frac{1}{i\hbar}\theta_{\mathcal{C}}(t_2-t_1)\langle\vec{\sigma}|\hat{a}_{H,m}(t_2)\hat{a}^+_{H,n}(t_1)|\vec{\sigma}\rangle \\ &\qquad -\frac{1}{i\hbar}\theta_{\mathcal{C}}(t_1-t_2)\langle\vec{\sigma}|\hat{a}^+_{H,n}(t_1)\hat{a}_{H,m}(t_2)|\vec{\sigma}\rangle\Big\}\langle\varphi_n| \\ &\overset{\text{Eq. 6.36}}{=} \sum_{m,n}|\varphi_m\rangle\frac{1}{i\hbar}\langle\vec{\sigma}|\mathcal{T}_{\mathcal{C}}\hat{a}_{H,m}(t_2)\hat{a}^+_{H,n}(t_1)|\vec{\sigma}\rangle\langle\varphi_n| \end{aligned} \tag{7.10}$$

Some thought is required regarding the contour $\mathcal{C}$ chosen. Here the contour starts at zero, passes to $t=-\infty$, proceeds along the real axis to $t=+\infty$, before it returns back to $t=0$. The contour can be modified by clipping closed loops. One exploits $\hat{\mathcal{U}}(t_2,t_1)\hat{\mathcal{U}}(t_1,t_2)=\hat{1}$. Therefore, it is not necessary to move all the way to $-\infty$ or $+\infty$.

7.4 Propagate interacting electrons at finite temperature

From the choices done so far, the remaining steps are straightforward.

General (potentially interacting) electron systems: For the generalization from non-interacting electrons to a general interacting electron system, we choose firstly the appropriate many-particle propagator for interacting electrons. Secondly, we determine the expectation value with a specified many-particle state $|\Phi\rangle$, which is not necessarily a Slater determinant. If one is interested in zero-temperature results, one would choose the ground state of the interacting electron system.

$$\hat{G}^{\mathcal{C}}(t_2,t_1)=\sum_{m,n}|\varphi_m\rangle\frac{1}{i\hbar}\langle\Phi|\mathcal{T}_{\mathcal{C}}\hat{a}_{H,m}(t_2)\hat{a}^+_{H,n}(t_1)|\Phi\rangle\langle\varphi_n| \tag{7.11}$$

Finite temperature: In order to obtain results at finite temperature, we need to generalize the Green's function to general ensembles $\{|\Phi_q\rangle,P_q\}$, which can be described by the state operator $\hat{\rho}=\sum_q|\Phi_q\rangle P_q\langle\Phi_q|$.

$$\begin{aligned}\hat{G}^{\mathcal{C}}(t_2,t_1) &= \sum_{m,n}|\varphi_m\rangle\frac{1}{i\hbar}\sum_q P_q\langle\Phi_q|\mathcal{T}_{\mathcal{C}}\hat{a}_{H,m}(t_2)\hat{a}^+_{H,n}(t_1)|\Phi_q\rangle\langle\varphi_n| \\ &= \sum_{m,n}|\varphi_m\rangle\frac{1}{i\hbar}\mathrm{Tr}\Big\{\hat{\rho}\,\mathcal{T}_{\mathcal{C}}\hat{a}_{H,m}(t_2)\hat{a}^+_{H,n}(t_1)\Big\}\langle\varphi_n| \end{aligned} \tag{7.12}$$

This is the most general expression for the contour-ordered Green's function. It is convenient to specialize this expression somewhat. Namely, we introduce thermal ensembles instead of the most general ensemble. The limitation to thermal ensembles leads to considerable simplifications. Nevertheless, I will show in section 7.6 below, that this is not a restriction. Namely, for an arbitrary ensemble, one can construct a Hamiltonian that produces exactly that desired ensemble in thermal equilibrium.

For a grand-canonical ensemble, the (von-Neumann) density matrix is ($\beta=1/(k_BT)$)

$$\hat{\rho}_{T,\mu}\overset{\text{Eq. ??}}{=}\frac{1}{Z_{T,\mu}}\mathrm{e}^{-\beta(\hat{H}-\mu\hat{N})} \tag{7.13}$$

with the **partition function**

$$Z_{T,\mu}=\mathrm{Tr}\Big\{\mathrm{e}^{-\beta(\hat{H}-\mu\hat{N})}\Big\}\,. \tag{7.14}$$

With the thermal density matrix Eq. 7.13, we obtain the propagator in the form

$$\hat{G}^{\mathcal{C}}(t_2,t_1)=\sum_{m,n}|\varphi_m\rangle\frac{1}{i\hbar}\mathrm{Tr}\Big\{\hat{\rho}_{T,\mu}\,\mathcal{T}_{\mathcal{C}}\hat{a}_{H,m}(t_2)\hat{a}^{+}_{H,n}(t_1)\Big\}\langle\varphi_n| \tag{7.15}$$

This is now our final definition for the contour-ordered Green's function. Let us now switch to a representation of general orbitals $|\chi_\alpha\rangle$, for which the creation and annihilation operators are $\hat{c}^\dagger_\alpha$ and $\hat{c}_\alpha$ ($\hat{c}^\dagger_\alpha|\mathcal{O}\rangle \overset{\text{Eq. 3.77}}{=} |\pi_\alpha\rangle$ with $\langle\pi_\alpha|\chi_\beta\rangle=\delta_{\alpha,\beta}$).

CONTOUR-ORDERED GREEN'S FUNCTION FOR COMPLEX TIME ARGUMENTS

The contour-ordered Green's function in complex time and orbital basis has the form

$$G^{\mathcal{C}}_{\alpha,\beta}(t,t')=\frac{1}{i\hbar}\mathrm{Tr}\Big\{\hat{\rho}^{(W)}_{T,\mu}\mathcal{T}_{\mathcal{C}}\hat{c}_{H,\alpha}(t)\hat{c}^{+}_{H,\beta}(t')\Big\} \tag{7.16}$$

where $\hat{\rho}_{T,\mu}=\frac{1}{Z_{T,\mu}}\mathrm{e}^{-\beta(\hat{H}-\mu\hat{N})}$ is the many-particle density matrix and $\hat{H}$ is the Hamiltonian with interaction.[a] The operators

$$\begin{aligned}\hat{c}_{H,\alpha}(t)&=\hat{\mathcal{U}}(0,t)\hat{c}_{S,\alpha}\hat{\mathcal{U}}(t,0)\\ \hat{c}^{+}_{H,\alpha}(t)&=\hat{\mathcal{U}}(0,t)\hat{c}^\dagger_{S,\alpha}\hat{\mathcal{U}}(t,0)\end{aligned} \tag{7.17}$$

are Heisenberg operators defined with the many-particle propagator $\hat{\mathcal{U}}(t,t')$ along the complex time contour $\mathcal{C}$

Below, I will tend to omit the superscript $\mathcal{C}$ of the Green's function. The superscript will be made explicit, when is required to separate the contour-ordered Green's function from another type of Green's function. Editor: The reader should nevertheless be cautious, because the convention may not be carried through everywhere.

[a] I have attached the subscript (W) to the density operator to emphasize the difference to that for non-interacting electrons, which will be used later.

7.5 Contour-ordered Green's function of non-interacting particles

We will frequently use the Green's function for non-interacting particles: Firstly, the non-interacting system is the reference for a perturbation expansion in the interaction. Secondly, the non-interacting system is used to explore the underlying physics for a particularly simple system.

Let me consider a non-interacting, time-dependent Hamiltonian $\hat{h}(t)$. The time argument is considered as complex-valued, but the Hamiltonian $\hat{h}(t)$ depends only on the real-part of the time argument. We can use Eq. K.1 and Eq. K.2 from p. 562, which are derived in the appendix.

$$\hat{c}^{+}_{I,\alpha}(t)\overset{\text{Eq. K.1}}{=}\sum_\beta \hat{c}^\dagger_{S,\beta}\langle\chi_\beta|\hat{U}(0,t)|\pi_\alpha\rangle \tag{7.18}$$

$$\hat{c}_{I,\alpha}(t)\overset{\text{Eq. K.2}}{=}\sum_\beta \langle\pi_\alpha|\hat{U}(t,0)|\chi_\beta\rangle\hat{c}_{S,\beta} \tag{7.19}$$

The operators with subscript I are in the interaction picture, while the subscript S denotes the common Schrödinger operators. For a non-interacting Hamiltonian considered here, the interaction picture is identical to the Heisenberg picture. The propagator $\hat{U}(t,t')$, Eqs. 4.31, 6.27, is the propagator for the one-particle wave functions with the one-particle Hamiltonian $\hat{h}(t)$.

The creation and annihilation operators refer to a one-particle basisset $\{|\chi_\alpha\rangle\}$, which may be

non-orthonormal. Each orbital has a projector function $\langle\pi_\alpha| = \sum_\beta S^{-1}_{\alpha,\beta}\langle\chi_\beta|$.

$$
\begin{aligned}
G^{\mathcal{C},(0)}_{\alpha,\beta}(t,t') &\overset{\text{Eq. 7.16}}{=} \frac{1}{i\hbar}\mathrm{Tr}\Big\{\hat\rho^{(0)}_{T,\mu}\mathcal{T}_\mathcal{C}\hat c_{H,\alpha}(t)\hat c^+_{H,\beta}(t')\Big\} \\
&\overset{\text{Eqs. K.1, K.2}}{=} \frac{\theta_\mathcal{C}(t-t')}{i\hbar}\mathrm{Tr}\Big\{\hat\rho^{(0)}_{T,\mu}\overbrace{\sum_\gamma \langle\pi_\alpha|\hat U(t,0)|\chi_\gamma\rangle\hat c_{S,\gamma}}^{\hat c_{H,\alpha}(t)}\overbrace{\sum_\delta \hat c^\dagger_{S,\delta}\langle\chi_\delta|\hat U(0,t')|\pi_\beta\rangle}^{\hat c^+_{H,\beta}(t')}\Big\} \\
&\quad - \frac{\theta_\mathcal{C}(t'-t)}{i\hbar}\mathrm{Tr}\Big\{\hat\rho^{(0)}_{T,\mu}\overbrace{\sum_\delta \hat c^\dagger_{S,\delta}\langle\chi_\delta|\hat U(0,t')|\pi_\beta\rangle}^{\hat c^+_{H,\beta}(t')}\overbrace{\sum_\gamma \langle\pi_\alpha|\hat U(t,0)|\chi_\gamma\rangle\hat c_{S,\gamma}}^{\hat c_{H,\alpha}(t)}\Big\} \\
&= \frac{\theta_\mathcal{C}(t-t')}{i\hbar}\sum_{\gamma,\delta}\langle\pi_\alpha|\hat U(t,0)|\chi_\gamma\rangle\underbrace{\mathrm{Tr}\Big\{\hat\rho^{(0)}_{T,\mu}\hat c_{S,\gamma}\hat c^\dagger_{S,\delta}\Big\}}_{\delta_{\gamma,\delta}-\rho^{(1)(0)}_{\gamma,\delta}\quad\text{Eq. 3.56}}\langle\chi_\delta|\hat U(0,t')|\pi_\beta\rangle \\
&\quad - \frac{\theta_\mathcal{C}(t'-t)}{i\hbar}\sum_{j,k}\langle\pi_\alpha|\hat U(t,0)|\chi_\gamma\rangle\underbrace{\mathrm{Tr}\Big\{\hat\rho^{(0)}_{T,\mu}\hat c^\dagger_{S,\delta}\hat c_{S,\gamma}\Big\}}_{\rho^{(1)(0)}_{\gamma,\delta}\quad\text{Eq. 3.56}}\langle\chi_\delta|\hat U(0,t')|\pi_\beta\rangle \\
&= \frac{1}{i\hbar}\langle\pi_\alpha|\hat U(t,0)\Big(\underbrace{\theta_\mathcal{C}(t-t')\Big(\hat 1-\hat\rho^{(1),(0)}_{T,\mu}\Big)}_{\text{empty}} - \underbrace{\theta_\mathcal{C}(t'-t)\hat\rho^{(1),(0)}_{T,\mu}}_{\text{filled}}\Big)\hat U(0,t')|\pi_\beta\rangle
\end{aligned}
\tag{7.20}
$$

The Green's function is conveniently expressed as an operator in the one-particle Hilbert space as

$$
\begin{aligned}
\hat G^{\mathcal{C},(0)}(t,t') &= \sum_{\alpha,\beta}|\chi_\alpha\rangle G^{\mathcal{C},(0)}_{\alpha,\beta}(t,t')\langle\chi_\beta| \\
&= \frac{1}{i\hbar}\hat U(t,0)\Big(\underbrace{\theta_\mathcal{C}(t-t')\Big(\hat 1-\hat\rho^{(1),(0)}_{T,\mu}\Big)}_{\text{empty}} - \underbrace{\theta_\mathcal{C}(t'-t)\hat\rho^{(1),(0)}_{T,\mu}}_{\text{filled}}\Big)\hat U(0,t')
\end{aligned}
\tag{7.21}
$$

Unlike the von-Neumann density matrix $\hat\rho^{(0)}_{T,\mu}$, the one-particle-reduced density matrix $\hat\rho^{(1)(0)}_{T,\mu} = \sum_{\gamma,\delta}|\chi_\gamma\rangle\rho_{\gamma,\delta}\langle\chi_\delta|$ is an operator in the one-particle Hilbert space. The subscripts T,μ for temperature and chemical potential indicate that it is, like the von-Neumann density matrix $\hat\rho^{(0)}_{T,\mu}$, a thermal density matrix in the grand canonical ensemble.

For the non-interacting system, the one-particle reduced density matrix can be expressed in terms of the Fermi distribution $f_{T,\mu}(\epsilon) \overset{\text{def}}{=} (1+\mathrm{e}^{\beta(\epsilon-\mu)})^{-1}$ as

$$
\hat\rho^{(1),(0)}_{T,\mu} = \sum_n |\varphi_n\rangle f_{T,\mu}(\epsilon_n)\langle\varphi_n|
\tag{7.22}
$$

by the eigenvalues ϵ_n and eigenstates $|\varphi_n\rangle$ of the one-particle Hamiltonian $\hat h(0)$ at the time origin.

Let me consider now some common special cases

- If the creation and annihilation operators are formulated in terms of natural orbitals (the eigenstates of the $\hat\rho^{(1)}$), i.e. $\hat\rho^{(1)}|\varphi_n\rangle = |\varphi_n\rangle f_n$, the Green's function has the form

$$
\hat G^{\mathcal{C},(0)}(t,t') = \frac{1}{i\hbar}\sum_n \underbrace{\hat U(t,0)|\varphi_n\rangle}_{|\varphi_n(t)\rangle}\Big(\theta_\mathcal{C}(t-t')(1-f_n) - \theta_\mathcal{C}(t'-t)f_n\Big)\underbrace{\langle\varphi_n|\hat U(0,t')}_{\sum_j O^{-1}_{n,j}\langle\varphi_j(t')|}
\tag{7.23}
$$

  Here I also introduced the time-dependent orbitals $|\varphi_n(t)\rangle = \hat U(t,0)|\varphi_n\rangle$.

- For a time-independent Hamiltonian $\hat{h}$, the contour propagator for the one-particle states is given by Eq. 6.30

$$\hat{U}(t,t') = \mathrm{e}^{-\frac{i}{\hbar}\hat{h}(t-t')} \tag{7.24}$$

so that

$$\hat{G}^{\mathcal{C},(0)}_{m,n}(t,t') = \frac{1}{i\hbar}\sum_n |\varphi_n\rangle \Big(\theta_{\mathcal{C}}(t-t')(1-f_n) - \theta_{\mathcal{C}}(t'-t)f_n\Big)\mathrm{e}^{-\frac{i}{\hbar}\epsilon_n(t-t')}\langle\varphi_n| \tag{7.25}$$

where $\hat{h}|\varphi_n\rangle = |\varphi_n\rangle\epsilon_n$ and where the occupations are given by the Fermi-distribution $f_n = (1+\mathrm{e}^{-\beta(\epsilon_n-\mu)})^{-1}$.

- The bare contour Green's function for a time-independent and translation-invariant system, speak, of the **homogeneous electron gas** is the topic of the exercise 7.7.2 on p. 250. The result is provided in Eq. 7.53 below.

Green's function as function of energy

For a time-independent Hamiltonian, we can also evaluate the Fourier transform of the Green's function in terms of the time difference $t-t'$. Note that we consider here only the branch of the contour running along the real time axis in the positive direction.

$$\begin{aligned}
\hat{G}^{\mathcal{C},(0)}_{m,n}(\epsilon) &\stackrel{\text{def}}{=} \lim_{\eta\to 0^+}\int_{-\infty}^{\infty} d\tau\; \hat{G}^{\mathcal{C},(0)}_{m,n}(t+\tau,t)\mathrm{e}^{\frac{i}{\hbar}\epsilon\tau-\eta|\tau|} \\
&= \frac{1}{i\hbar}\sum_n |\varphi_n\rangle \int_{-\infty}^{\infty} d\tau\; \Big(\theta(\tau)(1-f_n) - \theta_{\mathcal{C}}(-\tau)f_n\Big)\mathrm{e}^{-\frac{1}{i\hbar}\left[(\epsilon-\epsilon_n)\tau+i\hbar\eta|\tau|\right]}\langle\varphi_n| \\
&= \frac{1}{i\hbar}\sum_n |\varphi_n\rangle \Big(\frac{1-f_n}{\frac{1}{i\hbar}(\epsilon-\epsilon_n+i\eta)} + \frac{f_n}{\frac{1}{i\hbar}(\epsilon-\epsilon_n-i\eta)}\Big)\langle\varphi_n| \\
&= \sum_n |\varphi_n\rangle \Big(\frac{1-f_n}{\epsilon-\epsilon_n+i\eta} + \frac{f_n}{\epsilon-\epsilon_n-i\eta}\Big)\langle\varphi_n|
\end{aligned} \tag{7.26}$$

The infinitesimal parameter η has been introduced to make the Fourier transform of the Green's function defined. This is a kind of **regularization**. The limes $\eta \to 0^+$ has been made explicit only in the first appearance, which is common practice. If η is sufficiently small, it does not affect the emerging physical picture. The parameter mimics a physical effect that is not part of the mathematical formulation, namely the environment: An environment introduces a finite coherence time and, consequently, a finite lifetime broadening of the spectral features. Introducing the small parameter η is analogous to my trick of considering a "finite Universe" to avoid continuous spectra by limiting the wave functions to a very large, albeit finite region.

The poles of the Green's function of the empty states lie in below the real energy axis, while the poles of the filled states lie in above the real energy axis. Editor: Interesting are partially filled states, for which there are two poles, one on each side of the real energy axis.

Let me summarize this result in an orbital representation:

NON-INTERACTING GREEN'S FUNCTIONS FOR COMPLEX TIME ARGUMENTS

The contour-ordered Green's function for a non-interacting many-particle system which initially, at time $t = 0$, is in thermal equilibrium with a heat bath and a particle reservoir is

$$\begin{aligned}\hat{G}^{\mathcal{C},(0)}(t,t') &= \frac{1}{i\hbar}\hat{U}(t,0)\Big\{\underbrace{\theta_{\mathcal{C}}(t-t')\big(\hat{1}-\hat{\rho}^{(1),(0)}_{T,\mu}\big)}_{\text{electrons}} - \underbrace{\theta_{\mathcal{C}}(t'-t)\hat{\rho}^{(1)}_{T,\mu}}_{\text{holes}}\Big\}\hat{U}(0,t') \\ &= \frac{1}{i\hbar}\sum_n \underbrace{\hat{U}(t,0)|\varphi_n\rangle}_{|\varphi_n(t)\rangle}\Big\{\underbrace{\theta_{\mathcal{C}}(t-t')(1-f_n)}_{\text{electrons}} - \underbrace{\theta_{\mathcal{C}}(t'-t)f_n}_{\text{holes}}\Big\}\underbrace{\langle\varphi_n|\hat{U}(0,t')}_{\sum_j O^{-1}_{n,j}(t')\langle\varphi_j(t')|}\end{aligned} \tag{7.27}$$

where $\hat{\rho}^{(1)}_{T,\mu}$ is the one-particle-reduced density matrix, which is in thermal equilibrium with the initial Hamiltonian $\hat{h}(0)$. $\hat{U}(t,t')$ is the propagator in the one-particle Hilbert space. The backward propagator $\hat{U}(0,t) = \hat{U}^{-1}(t,0)$ is the inverse of the forward propagator, but not necessarily its hermitian conjugate.[a]

$|\varphi_n\rangle$ are the natural orbitals and the $f_n = f_{T,\mu}(\epsilon_n)$ are the occupations of the initial state. The energies ϵ_n are the eigenvalues of the initial Hamiltonian $\hat{h}(0)$. $|\varphi_n(t)\rangle = \hat{U}(t,0)|\varphi_n\rangle$ are the natural orbitals propagated in time. $O_{m,n}(t) = \langle\varphi_m(t)|\varphi_n(t)\rangle$ are the overlap matrix elements of the time-dependent orbitals.

For a time-independent Hamiltonian with eigenstates $|\varphi_n\rangle$ and eigenvalues ϵ_n, the Green's function is

$$\hat{G}^{\mathcal{C},(0)}(t,t') \overset{\text{Eq. 7.27}}{=} \frac{1}{i\hbar}\sum_n |\varphi_n\rangle\Big\{\underbrace{\frac{\theta_{\mathcal{C}}(t-t')}{1+\mathrm{e}^{-\beta(\epsilon_n-\mu)}}}_{\text{empty, }\sim(1-f_n)} - \underbrace{\frac{\theta_{\mathcal{C}}(t'-t)}{1+\mathrm{e}^{+\beta(\epsilon_n-\mu)}}}_{\text{filled, }\sim f_n}\Big\}\,\mathrm{e}^{-\frac{i}{\hbar}\epsilon_n(t-t')}\langle\varphi_n| \tag{7.28}$$

The energy-dependent Green's function for a time-independent non-interacting Hamiltonian is obtained as Fourier transform of the retardation $t - t'$.

$$\begin{aligned}\hat{G}^{\mathcal{C},(0)}(\epsilon) &\overset{\text{def}}{=} \int_{-\infty}^{\infty} d\tau\; \hat{G}^{\mathcal{C},(0)}(t+\tau,t)\mathrm{e}^{\frac{i}{\hbar}\epsilon\tau-\eta|\tau|} \\ &= \sum_n |\varphi_n\rangle\Big(\frac{1-f_n}{\epsilon-\epsilon_n+i\eta} + \frac{f_n}{\epsilon-\epsilon_n-i\eta}\Big)\langle\varphi_n|\end{aligned} \tag{7.29}$$

For the position of the poles, see also figure 9.1 on p. 267. In that figure $\hbar\omega$ translates into ϵ.

The matrix elements of the Green's function for (potentially non-orthonormal) orbitals $|\chi_\alpha\rangle$ with projector functions $\langle\pi_\alpha|$, respectively the Green's for the real-space-and-spin basis are

$$\begin{aligned}G^{\mathcal{C},(0)}_{\alpha,\beta}(t,t') &= \langle\pi_\alpha|\hat{G}^{\mathcal{C},(0)}(t,t')|\pi_\beta\rangle \\ G^{\mathcal{C},(0)}(\vec{x},t,\vec{x'},t') &= \langle\vec{x}|\hat{G}^{\mathcal{C},(0)}(t,t')|\vec{x'}\rangle\end{aligned} \tag{7.30}$$

[a] The difference is because we allow for complex-valued time arguments, so that the propagator is no more strictly unitary.

$$\hat{U}(t,0) = \sum_{m,n}|\varphi_n(t)\rangle\underbrace{O^{-1}_{m,n}(0)}_{\delta_{m,n}}\langle\varphi_n(0)|$$

$$\hat{U}(0,t) = \hat{U}^{-1}(t,0) = \sum_{m,n}|\varphi_n(0)\rangle O^{-1}_{m,n}(t)\langle\varphi_n(t)| \qquad \text{while} \qquad \hat{U}^\dagger(t,0) = \sum_n |\varphi_n(0)\rangle\langle\varphi_n(t)|$$

If the reader gets confused by the complex time arguments, he may simply follow the arguments

in the first run having a time contour on the real axis in mind. In a second reading, she may verify that the arguments also hold for complex time arguments.

7.6 Generality of the problem

7.6.1 Initial state:

The Green's functions, and thus all quantities derived from it, are thermal expectation values in a grand canonical ensemble. Many of the relations derived in the following apply to thermal (equilibrium) ensembles rather than arbitrary ensembles specified by many-particle states and their probabilities. I was wondering, whether this is a severe restriction of the theory, and whether the theory can be generalized to arbitrary non-equilibrium ensembles. Here, I show, that the generalization should be possible, because for any ensemble, there is a specific Hamiltonian, for which this ensemble is a thermal ensemble. Unfortunately, this Hamiltonian is much more complicated that the physical Hamiltonians we are used to.

Here, I will show that the form of a grand canonical ensemble can be used to describe an arbitrary ensemble without any reference to thermal equilibrium.[64]

Let us start with an arbitrary ensemble, which is characterized by its many-particle density matrix $\hat{\rho}$. Our goal is to construct a many-particle Hamiltonian $\hat{H}^{ini}$ which produces this, specified, state operator $\hat{\rho}$ in thermal equilibrium.

$$\hat{\rho} \stackrel{!}{=} \frac{1}{Z^{ini}_{T,\mu}} \mathrm{e}^{-\beta(\hat{H}^{ini}-\mu\hat{N})} \qquad \text{with } Z^{ini}_{T,\mu} = \mathrm{Tr}\left[\mathrm{e}^{-\beta(\hat{H}^{ini}-\mu\hat{N})}\right] \tag{7.31}$$

Firstly, let us first determine the eigenvalues and eigenstates of the density operator.

$$\hat{\rho}|\Phi_q\rangle = |\Phi_q\rangle P_q \tag{7.32}$$

Because the density matrix $\hat{\rho}$ is hermitian, the eigenstates $|\Phi_q\rangle$ are orthonormal and the eigenvalues P_q are real. The condition $\mathrm{Tr}[\hat{\rho}] = 1$ reflects in $\sum_q P_q = 1$.

By taking the logarithm of Eq. 7.31

$$\begin{aligned} -k_B T \ln(\hat{\rho}) &= \hat{H}^{ini} - \mu\hat{N} + k_B T \ln(Z_{T,\mu}) \\ \Leftrightarrow \hat{H}^{ini} &= -k_B T \ln(\hat{\rho}) + \mu\hat{N} \underbrace{-k_B T \ln(Z_{T,\mu})}_{\Omega_{T,\mu}} \\ &= \mu\hat{N} + \sum_q |\Phi_q\rangle \Big(-k_B T \ln(P_q)\Big) \langle\Phi_q| + \Omega_{T,\mu}\hat{1} \end{aligned} \tag{7.33}$$

The last term, the grand potential, is a global energy shift, which does not have physical consequences: When the probabilities are calculated from the Boltzmann factors, they are normalized with the help of the partition function.

The density matrix, specified initially, can thus be written in the form of a grand canonical ensemble for a Hamiltonian

$$\underbrace{\hat{H}^{ini,\prime}}_{\hat{H}^{ini}-\Omega_{T,\mu}\hat{1}} = \mu\hat{N} + \sum_q |\Phi_q\rangle \Big(-k_B T \ln(P_q)\Big) \langle\Phi_q| \tag{7.34}$$

The Hamiltonian H^{ini} used here is not necessarily related to a physical Hamiltonian of the system. It merely describes the initial ensemble.

7.7 Home study and practice

7.7.1 Non-interacting contour Green's function for the non-interacting hydrogen molecule

Calculate the contour-ordered Green's function for the non-interacting hydrogen molecule.

We use the expression Eq. 7.27 for the Green's function of a non-interacting electron system.

$$G^{\mathcal{C},(0)}_{\alpha,\beta}(t,t') \overset{\text{Eq. 7.27}}{=} \frac{1}{i\hbar}\sum_n \langle\pi_\alpha|\psi_n\rangle\Big\{\underbrace{\theta_{\mathcal{C}}(t-t')(1-f_n)}_{\text{electrons}} - \underbrace{\theta_{\mathcal{C}}(t'-t)f_n}_{\text{holes}}\Big\}\, \mathrm{e}^{-\frac{i}{\hbar}\epsilon_n(t-t')}\langle\psi_n|\pi_\beta\rangle \tag{7.35}$$

First, we determine the eigenvalues and eigenstates of the one-particle Hamiltonian. The non-interacting Hamiltonian in second quantization is

$$\hat{h} = \sum_{j\in\{1,2\}}\sum_{\sigma\in\{\uparrow,\downarrow\}} \bar{\epsilon}\hat{c}^\dagger_{j,\sigma}\hat{c}_{j,\sigma} - \bar{t}\sum_{\sigma\in\{\uparrow,\downarrow\}}\Big(\hat{c}^\dagger_{1,\sigma}\hat{c}_{2,\sigma} + \hat{c}^\dagger_{2,\sigma}\hat{c}_{1,\sigma}\Big) \tag{7.36}$$

This Hamilton operator is translated in one-particle quantum mechanics Editor: Is it clear how this is done?

$$\hat{h} = \sum_{j\in\{1,2\}}\sum_{\sigma\in\{\uparrow,\downarrow\}} |\pi_{j,\sigma}\rangle\bar{\epsilon}\langle\pi_{j,\sigma}| - \sum_{\sigma\in\{\uparrow,\downarrow\}}\Big(|\pi_{1,\sigma}\rangle\bar{t}\langle\pi_{2,\sigma}| + |\pi_{2,\sigma}\rangle\bar{t}\langle\pi_{1,\sigma}|\Big) \tag{7.37}$$

The eigenstates are (see section 1.5.1 on p. 26)

$$|\varphi_{\pm,\sigma}\rangle = \frac{1}{\sqrt{2}}\Big(|\chi_{1,\sigma}\rangle \mp |\chi_{2,\sigma}\rangle\Big) \tag{7.38}$$

with energies

$$\epsilon_{\pm,\sigma} = \bar{\epsilon} \pm \bar{t} \tag{7.39}$$

We had made the assumption that the orbitals $|\chi_\alpha\rangle$ are orthonormal.

In insert the eigenstates and eigenvalues. I use $\langle\pi_\alpha|\chi_\beta\rangle = \delta_{\alpha,\beta}$.

$$\begin{aligned}
G^{\mathcal{C},(0)}_{j,\sigma;j',\sigma'}(t,t') &= \frac{1}{i\hbar}\sum_{n\in\{+,-\}}\sum_{\sigma''\in\{\uparrow,\downarrow\}} \underbrace{\langle\pi_{j,\sigma}|\varphi_{n,\sigma''}\rangle}_{=\delta_{\sigma,\sigma''}\frac{1}{\sqrt{2}}\left(\delta_{j,1}\mp\delta_{j,2}\right)\text{ for } n=\pm} \times \underbrace{\langle\varphi_{n,\sigma''}|\pi_{j',\sigma'}\rangle}_{=\delta_{\sigma'',\sigma'}\frac{1}{\sqrt{2}}\left(\delta_{j',1}\mp\delta_{j',2}\right)\text{ for } n=\pm} \\
&\quad\times\Big\{\theta_{\mathcal{C}}(t-t')\underbrace{\left(1-\frac{1}{1+\mathrm{e}^{\beta(\epsilon_{n,\sigma''}-\mu)}}\right)}_{\frac{1}{1+\mathrm{e}^{-\beta(\epsilon_{n,\sigma''}-\mu)}}} - \theta_{\mathcal{C}}(t'-t)\frac{1}{1+\mathrm{e}^{\beta(\epsilon_{n,\sigma''}-\mu)}}\Big\}\,\mathrm{e}^{-\frac{i}{\hbar}\epsilon_{n,\sigma}(t-t')} \\
&= \frac{1}{i\hbar}\delta_{\sigma,\sigma'}\Big\{\frac{1}{2}\Big(\delta_{j,1}+\delta_{j,2}\Big)\Big(\delta_{j',1}+\delta_{j',2}\Big)\left[\frac{\theta_{\mathcal{C}}(t-t')}{1+\mathrm{e}^{-\beta(\bar{\epsilon}-\bar{t}-\mu)}} - \frac{\theta_{\mathcal{C}}(t'-t)}{1+\mathrm{e}^{+\beta(\bar{\epsilon}-\bar{t}-\mu)}}\right]\mathrm{e}^{-\frac{i}{\hbar}(\bar{\epsilon}-\bar{t})(t-t')} \\
&\qquad+\frac{1}{2}\Big(\delta_{j,1}-\delta_{j,2}\Big)\Big(\delta_{j',1}-\delta_{j',2}\Big)\left[\frac{\theta_{\mathcal{C}}(t-t')}{1+\mathrm{e}^{-\beta(\bar{\epsilon}+\bar{t}-\mu)}} - \frac{\theta_{\mathcal{C}}(t'-t)}{1+\mathrm{e}^{+\beta(\bar{\epsilon}+\bar{t}-\mu)}}\right]\mathrm{e}^{-\frac{i}{\hbar}(\bar{\epsilon}+\bar{t})(t-t')}\Big\} \\
&= \frac{1}{i\hbar}\delta_{\sigma,\sigma'}\mathrm{e}^{-\frac{i}{\hbar}\bar{\epsilon}(t-t')} \\
&\qquad\times\Big\{\frac{1}{2}\Big(\delta_{j,1}+\delta_{j,2}\Big)\Big(\delta_{j',1}+\delta_{j',2}\Big)\left[\frac{\theta_{\mathcal{C}}(t-t')\mathrm{e}^{+\frac{i}{\hbar}\bar{t}(t-t')}}{1+\mathrm{e}^{-\beta(\bar{\epsilon}-\bar{t}-\mu)}} - \frac{\theta_{\mathcal{C}}(t'-t)\mathrm{e}^{+\frac{i}{\hbar}\bar{t}(t-t')}}{1+\mathrm{e}^{+\beta(\bar{\epsilon}-\bar{t}-\mu)}}\right] \\
&\qquad+\frac{1}{2}\Big(\delta_{j,1}-\delta_{j,2}\Big)\Big(\delta_{j',1}-\delta_{j',2}\Big)\left[\frac{\theta_{\mathcal{C}}(t-t')\mathrm{e}^{-\frac{i}{\hbar}\bar{t}(t-t')}}{1+\mathrm{e}^{-\beta(\bar{\epsilon}+\bar{t}-\mu)}} - \frac{\theta_{\mathcal{C}}(t'-t)\mathrm{e}^{-\frac{i}{\hbar}\bar{t}(t-t')}}{1+\mathrm{e}^{+\beta(\bar{\epsilon}+\bar{t}-\mu)}}\right]\Big\}
\end{aligned} \tag{7.40}$$

$$\begin{pmatrix} G^{\mathcal{C},(0)}_{1,\sigma;1,\sigma'} & G^{\mathcal{C},(0)}_{1,\sigma;2,\sigma'} \\ G^{\mathcal{C},(0)}_{2,\sigma;1,\sigma'} & G^{\mathcal{C},(0)}_{2,\sigma;2,\sigma'} \end{pmatrix} = \frac{1}{2i\hbar}\delta_{\sigma,\sigma'}\mathrm{e}^{-\frac{i}{\hbar}\bar{\epsilon}(t-t')} \times\Bigg\{ \begin{pmatrix} +1 & +1 \\ +1 & +1 \end{pmatrix} \left[\frac{\theta_{\mathcal{C}}(t-t')\mathrm{e}^{+\frac{i}{\hbar}\bar{t}(t-t')}}{1+\mathrm{e}^{-\beta(\bar{\epsilon}-\bar{t}-\mu)}} - \frac{\theta_{\mathcal{C}}(t'-t)\mathrm{e}^{+\frac{i}{\hbar}\bar{t}(t-t')}}{1+\mathrm{e}^{+\beta(\bar{\epsilon}-\bar{t}-\mu)}} \right] + \begin{pmatrix} +1 & -1 \\ -1 & +1 \end{pmatrix} \left[\frac{\theta_{\mathcal{C}}(t-t')\mathrm{e}^{-\frac{i}{\hbar}\bar{t}(t-t')}}{1+\mathrm{e}^{-\beta(\bar{\epsilon}+\bar{t}-\mu)}} - \frac{\theta_{\mathcal{C}}(t'-t)\mathrm{e}^{-\frac{i}{\hbar}\bar{t}(t-t')}}{1+\mathrm{e}^{+\beta(\bar{\epsilon}+\bar{t}-\mu)}} \right] \Bigg\} \quad (7.41)$$

This is the desired result.

Let me consider some limiting cases

- In the high-temperature limit $\beta \to 0$ the Fermi function contributes a factor $1/2$.

$$\begin{pmatrix} G^{\mathcal{C},(0)}_{1,\sigma;1,\sigma'} & G^{\mathcal{C},(0)}_{1,\sigma;2,\sigma'} \\ G^{\mathcal{C},(0)}_{2,\sigma;1,\sigma'} & G^{\mathcal{C},(0)}_{2,\sigma;2,\sigma'} \end{pmatrix} = \frac{1}{i\hbar}\delta_{\sigma,\sigma'}\mathrm{e}^{-\frac{i}{\hbar}\bar{\epsilon}(t-t')} \underbrace{\Big(\theta_{\mathcal{C}}(t-t')-\theta_{\mathcal{C}}(t'-t)\Big)}_{\mathrm{sgn}(t-t')} \times \begin{pmatrix} \cos\left(\frac{1}{\hbar}\bar{t}(t-t')\right) & i\sin\left(\frac{1}{\hbar}\bar{t}(t-t')\right) \\ i\sin\left(\frac{1}{\hbar}\bar{t}(t-t')\right) & \cos\left(\frac{1}{\hbar}\bar{t}(t-t')\right) \end{pmatrix} \quad (7.42)$$

  One sees that the Green's function is not hermitian.

- For $\mu = \bar{\epsilon}$, we obtain the system with two particles. In the low-temperature limit, $\beta \to \infty$ only the bonding states contribute for $t < t'$ and the antibonding states contribute for $t > t'$.

$$\begin{pmatrix} G^{\mathcal{C},(0)}_{1,\sigma;1,\sigma'} & G^{\mathcal{C},(0)}_{1,\sigma;2,\sigma'} \\ G^{\mathcal{C},(0)}_{2,\sigma;1,\sigma'} & G^{\mathcal{C},(0)}_{2,\sigma;2,\sigma'} \end{pmatrix} = \frac{1}{2i\hbar}\delta_{\sigma,\sigma'}\mathrm{e}^{-\frac{i}{\hbar}\bar{\epsilon}(t-t')} \times\Bigg\{ \begin{pmatrix} +1 & +1 \\ +1 & +1 \end{pmatrix} \left[-\theta_{\mathcal{C}}(t'-t)\mathrm{e}^{+\frac{i}{\hbar}\bar{t}(t-t')} \right] + \begin{pmatrix} +1 & -1 \\ -1 & +1 \end{pmatrix} \left[\theta_{\mathcal{C}}(t-t')\mathrm{e}^{-\frac{i}{\hbar}\bar{t}(t-t')} \right] \Bigg\} \quad (7.43)$$

7.7.2 Bare contour Green's function of the homogeneous electron gas

Introduction

The homogeneous electron gas is a common model system. Therefore, the it is corresponding Green's function will be handy in many occasions.

The current exercise is special because (1) it determines the contour Green's function for arbitrary complex-valued time arguments, (2) it allows for arbitrary dispersion relations $\epsilon_{\vec{k},\sigma}$, (3) it works with a one particle basisset with periodic boundary conditions in a finite unit cell.

The use of an arbitrary dispersion relation provides access also to band-structures which experience a self-energy shift from the interaction, such as the Hartree-Fock approximation or the screened Hartree-Fock approximation. Furthermore it is possible to introduce band gaps into the band structure and study insulators. This aspect may be of interest to investigate the implications of Fermi-liquid theory on insulators.

Problem

Consider a non-interacting system, which is translation invariant in space an time, with a Hamiltonian

$$\hat{h} = \sum_{\vec{k}} \sum_{\sigma \in \{\uparrow,\downarrow\}} |\vec{k},\sigma\rangle \epsilon_{\vec{k},\sigma} \langle \vec{k},\sigma| \tag{7.44}$$

The band structure $\epsilon_{\vec{k},\sigma}$ is not determined any further.

1 determine the bare Green's function for the above-mentioned system. Use Eq. 7.27.

Discussion

1 determine the bare Green's function for the above-mentioned system. Use Eq. 7.27.

We start out from the expression Eq. 7.27 from p. 247 for the non-interacting Greens' function.

$$\begin{aligned}\hat{G}^{\mathcal{C},(0)}(t,t') &= \frac{1}{i\hbar}\hat{U}(t,0)\Big\{\underbrace{\theta_{\mathcal{C}}(t-t')\big(\hat{1}-\hat{\rho}^{(1),(0)}_{T,\mu}\big)}_{\text{electrons}} - \underbrace{\theta_{\mathcal{C}}(t'-t)\hat{\rho}^{(1)}_{T,\mu}}_{\text{holes}}\Big\}\hat{U}(0,t') \\ &= \frac{1}{i\hbar}\sum_n \underbrace{\hat{U}(t,0)|\varphi_n\rangle}_{|\varphi_n(t)\rangle}\Big\{\underbrace{\theta_{\mathcal{C}}(t-t')(1-f_n)}_{\text{electrons}} - \underbrace{\theta_{\mathcal{C}}(t'-t)f_n}_{\text{holes}}\Big\}\underbrace{\langle\varphi_n|\hat{U}(0,t')}_{\sum_j O^{-1}_{n,j}(t')\langle\varphi_j(t')|}\end{aligned} \tag{7.45}$$

Let me use a plane wave basisset as the orbital set.

$$\langle \vec{r},\sigma'|\vec{k},\sigma\rangle = \delta_{\sigma,\sigma'}\frac{1}{\sqrt{L^3}}e^{i\vec{k}\vec{r}} \tag{7.46}$$

I use periodic boundary conditions in a cubic box of side-length L, which ultimately shall approach infinity.

$$\begin{aligned} k_j L &= 2\pi j \Rightarrow k_j = \frac{2\pi}{L}j \\ \underbrace{(\Delta k)^3}_{\Rightarrow d^3k} &= \frac{(2\pi)^3}{L^3}\end{aligned} \tag{7.47}$$

The orbitals are normalized within the corresponding box:

$$\int_{L^3} d^3r \sum_{\sigma''} \big|\langle \vec{k},\sigma|\vec{r},\sigma''\rangle\big|^2 = 1 \tag{7.48}$$

The wave functions $|\varphi_{\vec{k},\sigma}(t)\rangle$, which satisfy the time-dependent Schrödinger equation

$$\Big(i\hbar\partial_t - \sum_{\vec{k}',\sigma'}|\vec{k}',\sigma'\rangle\epsilon_{\vec{k}',\sigma'}\langle\vec{k}',\sigma'|\Big)|\varphi_{\vec{k},\sigma}(t)\rangle = 0 \tag{7.49}$$

along the time contour are

$$|\varphi_{\vec{k},\sigma}(t)\rangle = |\vec{k},\sigma\rangle e^{-\frac{i}{\hbar}\epsilon_{\vec{k},\sigma}t} \tag{7.50}$$

The wave functions are orthonormal on the real time axis, but not away from it in the complex time plane. The time-dependent overlap matrix is.

$$O_{\vec{k},\sigma,\vec{k}',\sigma'}(t) = \langle\varphi_{\vec{k},\sigma}(t)|\varphi_{\vec{k}',\sigma'}(t)\rangle = \delta_{\vec{k},\vec{k}'}\delta_{\sigma,\sigma'}e^{+\frac{i}{\hbar}\epsilon\left(t^*-t\right)} = \delta_{\vec{k},\vec{k}'}\delta_{\sigma,\sigma'}e^{+\frac{2}{\hbar}\epsilon_{\vec{k},\sigma}\mathrm{Im}[t]} \tag{7.51}$$

The Green's function in the complex-time plane is

$$
\begin{aligned}
G^{\mathcal{C},(0)}_{\vec{k},\sigma,\vec{k}',\sigma'}(t,t') &= \langle \vec{k},\sigma|\hat{G}^{\mathcal{C},(0)}(t,t')|\vec{k}',\sigma'\rangle \\
&= \frac{1}{i\hbar}\sum_{\vec{k}'',\sigma''} \underbrace{\langle \vec{k},\sigma|\varphi_{\vec{k}'',\sigma''}(t)\rangle}_{\delta_{\vec{k},\vec{k}''}\delta_{\sigma,\sigma''}\mathrm{e}^{-\frac{i}{\hbar}\epsilon_{\vec{k},\sigma}t}} \left\{ \frac{\theta_{\mathcal{C}}(t-t')}{1+\mathrm{e}^{-\beta(\epsilon_{\vec{k}'',\sigma''}-\mu)}} - \frac{\theta_{\mathcal{C}}(t'-t)}{1+\mathrm{e}^{+\beta(\epsilon_{\vec{k}'',\sigma''}-\mu)}} \right\} \\
&\qquad \times \underbrace{\mathrm{e}^{-\frac{2}{\hbar}\epsilon_{\vec{k}'',\sigma''}\mathrm{Im}[t']}}_{O^{-1}(t')\rightsquigarrow} \underbrace{\langle \varphi_{\vec{k}'',\sigma''}(t')|\vec{k}',\sigma'\rangle}_{\delta_{\vec{k}',\vec{k}''}\delta_{\sigma',\sigma''}\mathrm{e}^{+\frac{i}{\hbar}\epsilon_{\vec{k}',\sigma'}(t')^*}} \\
&= \frac{1}{i\hbar}\delta_{\vec{k},\vec{k}'}\delta_{\sigma,\sigma'}\mathrm{e}^{-\frac{i}{\hbar}\epsilon_{\vec{k},\sigma}t}\left\{ \frac{\theta_{\mathcal{C}}(t-t')}{1+\mathrm{e}^{-\beta(\epsilon_{\vec{k},\sigma}-\mu)}} - \frac{\theta_{\mathcal{C}}(t'-t)}{1+\mathrm{e}^{+\beta(\epsilon_{\vec{k},\sigma}-\mu)}} \right\} \underbrace{\mathrm{e}^{+\frac{i}{\hbar}\epsilon_{\vec{k},\sigma}(t'-(t')^*)}}_{O^{-1}(t')\rightsquigarrow} \mathrm{e}^{\frac{i}{\hbar}\epsilon_{\vec{k},\sigma}(t')^*} \\
&= \frac{1}{i\hbar}\delta_{\vec{k},\vec{k}'}\delta_{\sigma,\sigma'}\left\{ \frac{\theta_{\mathcal{C}}(t-t')}{1+\mathrm{e}^{-\beta(\epsilon_{\vec{k},\sigma}-\mu)}} - \frac{\theta_{\mathcal{C}}(t'-t)}{1+\mathrm{e}^{+\beta(\epsilon_{\vec{k},\sigma}-\mu)}} \right\}\mathrm{e}^{-\frac{i}{\hbar}\epsilon_{\vec{k},\sigma}(t-t')} \\
&= \frac{1}{i\hbar}\delta_{\vec{k},\vec{k}'}\delta_{\sigma,\sigma'}\left\{ \theta_{\mathcal{C}}(t-t')\Big(1-f_{T,\mu}(\epsilon_{\vec{k},\sigma})\Big) - \theta_{\mathcal{C}}(t'-t)f_{T,\mu}(\epsilon_{\vec{k},\sigma}) \right\}\mathrm{e}^{-\frac{1}{\hbar}\epsilon_{\vec{k},\sigma}(t-t')} \qquad (7.52)
\end{aligned}
$$

where $f_{T,\mu}(\epsilon)$ is the Fermi function.

BARE CONTOUR GREEN'S FUNCTION OF THE HOMOGENEOUS ELECTRON GAS

The bare contour Green's function of a homogeneous electron gas with a dispersion relation $\epsilon_{\vec{k},\sigma}$ is

$$
\begin{aligned}
\hat{G}^{\mathcal{C},(0)}(t,t') \overset{\text{Eq. 7.52}}{=} \frac{1}{i\hbar}\sum_{\vec{k}}\sum_{\sigma\in\{\uparrow,\downarrow\}} |\vec{k},\sigma\rangle &\left\{ \theta_{\mathcal{C}}(t-t')\Big(1-f_{T,\mu}(\epsilon_{\vec{k},\sigma})\Big) - \theta_{\mathcal{C}}(t'-t)f_{T,\mu}(\epsilon_{\vec{k},\sigma}) \right\} \\
&\times \mathrm{e}^{-\frac{i}{\hbar}\epsilon_{\vec{k},\sigma}(t-t')}\langle \vec{k},\sigma| \qquad (7.53)
\end{aligned}
$$

where $f_{T,\mu}(\epsilon) = \left(1+\mathrm{e}^{\beta(\epsilon-\mu)}\right)^{-1}$ is the Fermi function. The one-particle basis states are plane waves $\langle \vec{r},\sigma|\vec{k},\sigma'\rangle = \delta_{\sigma,\sigma'}\frac{1}{\sqrt{L^3}}\mathrm{e}^{i\vec{k}\vec{r}}$ with periodic boundary conditions in simple cubic unit cell with side length L, which also determines the normalization volume. That is $\vec{k}_{i,j,k} = \frac{2\pi}{L}(i,j,k)$ with integer i,j,k.

Chapter 8

Exact properties of the many-particle Green's function

The typical approach towards many-body Green's functions is many-body perturbation theory (MBPT), which expands the Green's function about that of a (quasi) non-interacting case. Many-body perturbation theory is widely known through its elegant formulation in terms of Feynman diagrams. However, MBPT is also plagued by the often limited convergence radius of the perturbation expansion. Therefore, I find it important to know the few exact statements about Green's functions of many-particle systems.

In this chapter, I will introduce the equation of motion for the Green's function and the self energy as the second most important quantity. The self energy acts like a potential acting on the electrons, which however is non-local in time. It is retarded like an echo, as the electron influences its surrounding electron gas and, at a later, this perturbation of the electron gas acts back on the dynamics of the traveling electron. Here the self energy will be expressed in terms of a well-defined expectation value of the many-electron wave functions.

The Green's function contains all information on the dynamics of single electrons in contact with an electron gas. Thus, it is no surprise that the Green's function provides the one-particle-reduced density matrix. As the only two-particle expectation value, the interaction energy can be extracted from the Green's function. Thus, we obtain access to the total energy of the system.

8.1 Equation of motion for the many-particle Green's function

The Green's function of a many-particle system is not a Green's function in the mathematical sense. In mathematics, a Green's function is the inverse of a differential operator. This applies only to the Green function of one-particle systems. In solid state physics, only the physical meaning of the Green's function has been kept, namely as probability amplitude between two events.

When we try to set up a differential equation analogous to the one-particle case, we are lead to higher Green's functions involving more and more particles. Nevertheless, we can define a retarded one-particle potential that replaces the action of the many-particle system. This potential is the **self energy**. If the self-energy is included, the Green's function obeys a differential equation as in the one-particle case.

In the following, I derive a differential equation for the interacting many-body Green's function.

The first step is to find a differential equation for a Heisenberg operator $\hat{c}_{H,\zeta}(t)$, because the time derivative will act on this operator within the expression for the Green's function

$$i\hbar\partial_t \hat{c}_{H,\zeta}(t) = \hat{\mathcal{U}}(0,t)\left[\hat{c}_{S,\zeta}, \hat{H}(t)\right]_- \hat{\mathcal{U}}(t,0) \tag{8.1}$$

In the remainder of the derivation, I will drop the time argument of the Hamiltonian, while I consider the Hamilton matrix elements to depend on the current time.

In order to continue, we need the commutator of the annihilation operator in the Schrödinger picture with the Hamiltonian. For the sake of simplicity, we drop the explicit subscript S denoting the Schrodinger picture. It is implicitly assumed.

$$\hat{H}(t) = \sum_{\alpha,\beta} h_{\alpha,\beta}(t)\hat{c}^\dagger_\alpha \hat{c}_\beta + \frac{1}{2}\sum_{\alpha,\beta,\gamma,\delta} W_{\alpha,\beta,\delta,\gamma}(t)\hat{c}^\dagger_\alpha \hat{c}^\dagger_\beta \hat{c}_\gamma \hat{c}_\delta \tag{8.2}$$

We begin with the one-particle operator

$$\left[\hat{c}_\zeta, \sum_{\alpha,\beta} h_{\alpha,\beta}\hat{c}^\dagger_\alpha \hat{c}_\beta\right]_- = \sum_{\alpha,\beta} h_{\alpha,\beta}\Bigg(\underbrace{\hat{c}_\zeta \hat{c}^\dagger_\alpha}_{\delta_{\zeta,\alpha}-\hat{c}^\dagger_\alpha\hat{c}_\zeta}\hat{c}_\beta - \hat{c}^\dagger_\alpha \underbrace{\hat{c}_\beta \hat{c}_\zeta}_{-\hat{c}_\zeta\hat{c}_\beta}\Bigg) = \sum_{\alpha,\beta} h_{\alpha,\beta}\delta_{\zeta,\alpha}\hat{c}_\beta = \sum_\beta h_{\zeta,\beta}\hat{c}_\beta \tag{8.3}$$

and continue with the interaction

$$\begin{aligned}
\left[\hat{c}_\zeta, \frac{1}{2}\sum_{\alpha,\beta,\gamma,\delta} W_{\alpha,\beta,\delta,\gamma}\hat{c}^\dagger_\alpha \hat{c}^\dagger_\beta \hat{c}_\gamma \hat{c}_\delta\right]_- &= \frac{1}{2}\sum_{\alpha,\beta,\gamma,\delta} W_{\alpha,\beta,\delta,\gamma}\Big(\hat{c}_\zeta \hat{c}^\dagger_\alpha \hat{c}^\dagger_\beta \hat{c}_\gamma \hat{c}_\delta - \hat{c}^\dagger_\alpha \hat{c}^\dagger_\beta \underbrace{\hat{c}_\gamma \hat{c}_\delta \hat{c}_\zeta}_{\hat{c}_\zeta\hat{c}_\gamma\hat{c}_\delta}\Big) \\
&= \frac{1}{2}\sum_{\alpha,\beta,\gamma,\delta} W_{\alpha,\beta,\delta,\gamma}\Bigg(\underbrace{\hat{c}_\zeta \hat{c}^\dagger_\alpha}_{\delta_{\zeta,\alpha}-\hat{c}^\dagger_\alpha\hat{c}_\zeta}\hat{c}^\dagger_\beta - \hat{c}^\dagger_\alpha \underbrace{\hat{c}^\dagger_\beta \hat{c}_\zeta}_{\delta_{\beta,\zeta}-\hat{c}_\zeta\hat{c}^\dagger_\beta}\Bigg)\hat{c}_\gamma \hat{c}_\delta \\
&= \frac{1}{2}\sum_{\alpha,\beta,\gamma,\delta} W_{\alpha,\beta,\delta,\gamma}\Big(\delta_{\zeta,\alpha}\hat{c}^\dagger_\beta - \hat{c}^\dagger_\alpha \delta_{\beta,\zeta}\Big)\hat{c}_\gamma \hat{c}_\delta \\
&= \frac{1}{2}\sum_{\beta,\gamma,\delta} W_{\zeta,\beta,\delta,\gamma}\hat{c}^\dagger_\beta \hat{c}_\gamma \hat{c}_\delta - \frac{1}{2}\sum_{\alpha,\gamma,\delta} \underbrace{W_{\alpha,\zeta,\delta,\gamma}}_{W_{\zeta,\alpha,\gamma,\delta}}\hat{c}^\dagger_\alpha \underbrace{\hat{c}_\gamma \hat{c}_\delta}_{-\hat{c}_\delta\hat{c}_\gamma} \\
&= \frac{1}{2}\sum_{\beta,\gamma,\delta} W_{\zeta,\beta,\delta,\gamma}\hat{c}^\dagger_\beta \hat{c}_\gamma \hat{c}_\delta + \frac{1}{2}\sum_{\beta,\gamma,\delta} W_{\zeta,\beta,\gamma,\delta}\hat{c}^\dagger_\beta \hat{c}_\delta \hat{c}_\gamma \\
&= \frac{1}{2}\sum_{\beta,\gamma,\delta} W_{\zeta,\beta,\delta,\gamma}\hat{c}^\dagger_\beta \hat{c}_\gamma \hat{c}_\delta + \overbrace{\frac{1}{2}\sum_{\beta,\gamma,\delta} W_{\zeta,\beta,\delta,\gamma}\hat{c}^\dagger_\beta \hat{c}_\gamma \hat{c}_\delta}^{\gamma\leftrightarrow\delta} \\
&= \sum_{\beta,\gamma,\delta} W_{\zeta,\beta,\delta,\gamma}\hat{c}^\dagger_\beta \hat{c}_\gamma \hat{c}_\delta
\end{aligned} \tag{8.4}$$

We exploited that a simultaneous interchange of the first two and, at the same time, the last two arguments leaves the value of the interaction matrix elements unchanged, i.e. $W_{\alpha,\beta,\gamma,\delta} = W_{\beta,\alpha,\delta,\gamma}$. This symmetry follows from the form of the interaction matrix elements defined in Eq. 3.51 on p. 135. Editor: This argument refers to the Coulomb interaction. What about the most general definition as $W(t) = \hat{H}(t) - \hat{h}$?

With the results Eqs. 8.3,8.4, we can return to Eq. 8.1 and evaluate the time derivative of the annihilator in the Heisenberg picture as

$$\begin{aligned}
i\hbar\partial_t \hat{c}_{H,\zeta}(t) &= \hat{\mathcal{U}}(0,t)\left[\hat{c}_{S,\zeta}, \hat{H}\right]_- \hat{\mathcal{U}}(t,0) \\
&\overset{Eqs.\ 8.3,8.4}{=} \hat{\mathcal{U}}(0,t)\left(\sum_\beta h_{\zeta,\beta}\hat{c}_{S,\beta} + \sum_{\gamma,\delta,\rho} W_{\zeta,\beta,\delta,\gamma}\hat{c}^\dagger_{S,\beta}\hat{c}_{S,\gamma}\hat{c}_{S,\delta}\right)\hat{\mathcal{U}}(t,0) \\
&= \sum_\beta h_{\zeta,\beta}\hat{c}_{H,\beta}(t) + \sum_{\beta,\gamma,\delta} W_{\zeta,\beta,\delta,\gamma}\hat{c}^+_{H,\beta}(t)\hat{c}_{H,\gamma}(t)\hat{c}_{H,\delta}(t)
\end{aligned} \tag{8.5}$$

Now, we can evaluate the time derivative of the Green's function Eq. 7.16. We use the short-hand notation $\left\langle \dots \right\rangle_{T,\mu} \overset{\text{def}}{=} \mathrm{Tr}\{\hat{\rho}^{(W)}_{T,\mu} \dots\}$. Note below that the time derivative acts only on t, but not on

the second time argument t'.

$$
\begin{aligned}
& i\hbar\partial_t G^{\mathcal{C}}_{\alpha,\beta}(t,t') \\
\overset{\text{Eq. 7.16}}{=}\ & i\hbar\partial_t\left[\frac{\theta(t-t')}{i\hbar}\left\langle \hat{c}_{H,\alpha}(t)\hat{c}^+_{H,\beta}(t')\right\rangle_{T,\mu} - \frac{\theta(t'-t)}{i\hbar}\left\langle \hat{c}^+_{H,\beta}(t')\hat{c}_{H,\alpha}(t)\right\rangle_{T,\mu}\right] \\
=\ & \delta(t-t')\left\langle \hat{c}_{H,\alpha}(t)\hat{c}^+_{H,\beta}(t')\right\rangle_{T,\mu} + \delta(t'-t)\left\langle \hat{c}^+_{H,\beta}(t')\hat{c}_{H,\alpha}(t)\right\rangle_{T,\mu} \\
+\ & \frac{\theta(t-t')}{i\hbar}\left\langle \left(i\hbar\partial_t\hat{c}_{H,\alpha}(t)\right)\hat{c}^+_{H,\beta}(t')\right\rangle_{T,\mu} - \frac{\theta(t'-t)}{i\hbar}\left\langle \hat{c}^+_{H,\beta}(t')\left(i\hbar\partial_t\hat{c}_{H,\alpha}(t)\right)\right\rangle_{T,\mu} \\
\overset{\text{Eq. 8.5}}{=}\ & \delta(t-t')\left\langle \left[\hat{c}_{H,\alpha}(t),\hat{c}^+_{H,\beta}(t')\right]_+\right\rangle_{T,\mu} \\
+\ & \frac{\theta(t-t')}{i\hbar}\left\langle \left(\sum_b h_{\alpha,b}\hat{c}_{H,b}(t) + \sum_{b,c,d} W_{\alpha,b,d,c}\hat{c}^+_{H,b}(t)\hat{c}_{H,c}(t)\hat{c}_{H,d}(t)\right)\hat{c}^+_{H,\beta}(t')\right\rangle_{T,\mu} \\
-\ & \frac{\theta(t'-t)}{i\hbar}\left\langle \hat{c}^+_{H,\beta}(t')\left(\sum_b h_{\alpha,b}\hat{c}_{H,b}(t) + \sum_{b,c,d} W_{\alpha,b,d,c}\hat{c}^+_{H,b}(t)\hat{c}_{H,c}(t)\hat{c}_{H,d}(t)\right)\right\rangle_{T,\mu} \\
=\ & \delta(t-t')\left\langle \left[\hat{c}_{H,\alpha}(t),\hat{c}^+_{H,\beta}(t')\right]_+\right\rangle_{T,\mu} \\
+\ & \sum_b h_{\alpha,b}\left(\frac{\theta(t-t')}{i\hbar}\left\langle \hat{c}_{H,b}(t)\hat{c}^+_{H,\beta}(t')\right\rangle_{T,\mu} - \frac{\theta(t'-t)}{i\hbar}\left\langle \hat{c}^+_{H,\beta}(t')\hat{c}_{H,b}(t)\right\rangle_{T,\mu}\right) \\
+\ & \sum_{b,c,d} W_{\alpha,b,d,c}\left(\frac{\theta(t-t')}{i\hbar}\left\langle \hat{c}^+_{H,b}(t)\hat{c}_{H,c}(t)\hat{c}_{H,d}(t)\hat{c}^+_{H,\beta}(t')\right\rangle_{T,\mu} - \frac{\theta(t'-t)}{i\hbar}\left\langle \hat{c}^+_{H,\beta}(t')\hat{c}^+_{H,b}(t)\hat{c}_{H,c}(t)\hat{c}_{H,d}(t)\right\rangle_{T,\mu}\right) \\
\overset{\text{Eq. 8.7}}{=}\ & \delta(t-t')\delta_{\alpha,\beta} + \sum_b h_{\alpha,b}G_{b,\beta}(t,t') \\
+\ & \sum_{b,c,d} W_{\alpha,b,d,c}\underbrace{\left(\frac{\theta(t-t')}{i\hbar}\left\langle \overbrace{\hat{c}^+_{H,b}(t)\hat{c}_{H,c}(t)\hat{c}_{H,d}(t)}^{A}\,\hat{c}^+_{H,\beta}(t')\right\rangle_{T,\mu} - \frac{\theta(t'-t)}{i\hbar}\left\langle \hat{c}^+_{H,\beta}(t')\,\overbrace{\hat{c}^+_{H,b}(t)\hat{c}_{H,c}(t)\hat{c}_{H,d}(t)}^{A}\right\rangle_{T,\mu}\right)}_{\frac{1}{i\hbar}\left\langle \mathcal{T}_{\mathcal{C}}\hat{c}^+_{H,b}(t)\hat{c}_{H,c}(t)\hat{c}_{H,d}(t)\hat{c}^+_{H,\beta}(t')\right\rangle_{T,\mu}}
\end{aligned}
\tag{8.6}
$$

The anticommutator relations for the Schrödinger operators do not hold for Heisenberg operators. Nevertheless, we have made use of the fact that the anticommutator is only required for equal times

$$
\left[\hat{c}^+_{H,\beta}(t),\hat{c}_{H,\alpha}(t)\right]_+ = \hat{\mathcal{U}}(0,t)\left[\hat{c}^\dagger_{S,\beta},\hat{c}_{S,\alpha}\right]_+\hat{\mathcal{U}}(t,0) = \hat{\mathcal{U}}(0,t)\delta_{\alpha,\beta}\hat{\mathcal{U}}(t,0) = \delta_{\alpha,\beta} \tag{8.7}
$$

Eq. 8.6 can be brought into a form similar to the defining equation Eq. 4.13 of the Green's function for non-interacting systems.

EQUATION OF MOTION FOR THE INTERACTING GREEN'S FUNCTION

$$\sum_\gamma \Big(\delta_{\alpha,\gamma} i\hbar\partial_t - h_{\alpha,\gamma}(t)\Big) G^{\mathcal{C}}_{\gamma,\beta}(t,t') =$$

$$= \delta_{\mathcal{C}}(t-t')\delta_{\alpha,\beta} + \sum_\gamma \sum_{b,c} W_{\alpha,b,\gamma,c}(t) \overbrace{\frac{1}{i\hbar}\mathrm{Tr}\Big\{\hat\rho^{(W)}_{T,\mu}\mathcal{T}_{\mathcal{C}}\underbrace{\hat c^+_{H,b}(t)\hat c_{H,c}(t)}_{\sim\text{density operator}}\hat c_{H,\gamma}(t)\hat c^+_{H,\beta}(t')\Big\}}^{G^{(2)}_{c,\gamma,b,\beta}(t,t,t^+,t')\quad\text{Eq. 8.14}} \quad (8.8)$$

$$= \delta_{\mathcal{C}}(t-t')\delta_{\alpha,\beta} + \sum_\gamma \frac{1}{i\hbar}\mathrm{Tr}\Big\{\hat\rho^{(W)}_{T,\mu}\mathcal{T}_{\mathcal{C}}\underbrace{\Big(\sum_{b,c} W_{\alpha,b,\gamma,c}(t)\underbrace{\hat c^+_{H,b}(t)\hat c_{H,c}(t)}_{\sim\text{density operator}}\Big)}_{\hat V_{ee}(t)}\hat c_{H,\gamma}(t)\hat c^+_{H,\beta}(t')\Big\} \quad (8.9)$$

$\hat V_{ee}$ is the operator describing the Coulomb potential from the (other) electrons . The two versions on the right-hand side are identical, but emphasize certain groupings of the terms.[a]

[a] Eq. 8.8 is analogous to Eq. 10.11 in the book of Abrikosov, Gorkov, Dzyaloshinski[65].

Physical meaning of the interaction term: To get closer to the physical meaning interaction term of Eq. 8.8, let me do a rather crude approximation, which is equivalent to the Hartree approximation.[1][2]

$$\begin{aligned}
&\frac{1}{i\hbar}\mathrm{Tr}\Big\{\hat\rho^{(W)}_{T,\mu}\mathcal{T}_{\mathcal{C}}\hat c^+_{H,b}(t)\hat c_{H,c}(t)\hat c_{H,\gamma}(t)\hat c^+_{H,\beta}(t')\Big\}\\
&\approx \underbrace{\mathrm{Tr}\Big\{\hat\rho^{(W)}_{T,\mu}\mathcal{T}_{\mathcal{C}}\hat c^+_{H,b}(t)\hat c_{H,c}(t)\Big\}}_{\rho^{(1)}_{c,b}(t)\quad\text{from Eq. 3.56}}\underbrace{\frac{1}{i\hbar}\mathrm{Tr}\Big\{\hat\rho^{(W)}_{T,\mu}\mathcal{T}_{\mathcal{C}}\hat c_{H,\gamma}(t)\hat c^+_{H,\beta}(t')\Big\}}_{G^{\mathcal{C}}_{\gamma,\beta}(t,t')\quad\text{from Eq. 7.16}}\\
&= \rho^{(1)}_{c,b}(t)G^{\mathcal{C}}_{\gamma,\beta}(t,t') \qquad (8.10)
\end{aligned}$$

In this approximation, the interaction simply replaces the interaction term in Eq. 8.8 by the Hartree potential

$$\Delta\hat h_{\alpha,\beta}(t) = \sum_{b,c} W_{\alpha,b,\beta,c}\rho^{(1)}_{c,b}(t) \qquad (8.11)$$

which is added to $\hat h$.

Interaction term and two-particle Green's function: Eq. 8.8 allows a recipe to determine the Green's function, however, only if the interaction term on the right-hand side is known. The evaluation of this term is even more complicated than the direct calculation of the Green's function. It requires the knowledge of the two-particle Green's function

$$G^{(2)}(\vec x_1,t_1,\vec x_2,t_2;\vec x'_1,t'_1,\vec x'_2,t'_2) \stackrel{\text{def}}{=} \frac{1}{i\hbar}\mathrm{Tr}\Big\{\hat\rho^{(W)}_{T,\mu}\mathcal{T}_{\mathcal{C}}\hat\psi_H(\vec x_1,t_1)\hat\psi_H(\vec x_2,t_2)\hat\psi^+_H(\vec x'_1,t'_1)\hat\psi^+_H(\vec x'_2,t'_2)\Big\} \qquad (8.12)$$

respectively, in an orbital representation,

$$G^{(2)}_{\alpha,\beta;\gamma,\delta}(t_1,,t_2;t'_1,t'_2) \stackrel{\text{def}}{=} \frac{1}{i\hbar}\mathrm{Tr}\Big\{\hat\rho^{(W)}_{T,\mu}\mathcal{T}_{\mathcal{C}}\hat c_{H,\alpha}(t_1)\hat c_{H,\beta}(t_2)\hat c^+_{H,\gamma}(t'_1)\hat c^+_{H,\delta}(t'_2)\Big\} \qquad (8.13)$$

[1] Note that $\mathrm{Tr}[\hat\rho_{T,\mu}\cdots] = \langle\ldots\rangle_{T,\mu}$ is the thermal expectation value.
[2] we replace the product of the two operators marked in blue by their thermal expectation value

The interaction term in the equation of motion, Eq. 8.8, can be expressed in terms of the two-particle Green's function as

$$\sum_{\gamma}\sum_{b,c} W_{\alpha,b,\gamma,c}\frac{1}{i\hbar}\mathrm{Tr}\left\{\hat{\rho}^{(W)}_{T,\mu}\mathcal{T}_{\mathcal{C}}\underbrace{\hat{c}^{+}_{H,b}(t^{+})\hat{c}_{H,c}(t)}_{\sim\text{density operator}}\hat{c}_{H,\gamma}(t)\hat{c}^{+}_{H,\beta}(t')\right\}$$
$$= \sum_{\gamma}\sum_{b,c} W_{\alpha,b,\gamma,c}G^{(2)}_{c,\gamma,b,\beta}(t,t,t^{+},t') \tag{8.14}$$

Thus, the equation of motion for the one-particle Green's function $G^{\mathcal{C}}$ has an additional inhomogeneity, which depends on the two-particle Green's function.

One could proceed to determine an equation of motion for the two-particle Green's function, which however would introduce a term containing a three particle Green's function. In order to determine the latter we obtain a differential equation, where even higher-order Green's functions enter. We end up with an infinite sequence of increasingly more complicated differential equations, the so-called **Martin-Schwinger hierarchy**[66](see also [67]). One can hope that the terms will become smaller with each step in the hierarchy, so that it can be truncated.

8.2 Self energy

Eq. 8.8 shows that the Green's function of an interacting systems does not obey the same differential equation as the Green's function of non-interacting electrons.

DEFINITION OF THE SELF ENERGY

In order to recover a form more closely related to the defining equation of a Green's function we define a **self energy** $\Sigma_{\alpha,\beta}(t,t')$ via

$$\sum_{\gamma}\int_{\mathcal{C}} dt''\,\Sigma_{\alpha,\gamma}(t,t'')G_{\gamma,\beta}(t'',t') = \sum_{b,c,d} W_{\alpha,b,d,c}\frac{1}{i\hbar}\mathrm{Tr}\left\{\hat{\rho}^{(W)}_{T,\mu}\mathcal{T}_{\mathcal{C}}\hat{c}^{+}_{H,b}(t)\hat{c}_{H,c}(t)\hat{c}_{H,d}(t)\hat{c}^{+}_{H,\beta}(t')\right\} \tag{8.15}$$

so that the equation of motion Eq. 8.8 assumes the form

$$\sum_{\gamma}\int dt''\left[\delta(t-t'')\Big(\delta_{\alpha,\gamma}i\hbar\partial_{t''}-h_{\alpha,\gamma}\Big)-\Sigma_{\alpha,\gamma}(t,t'')\right]G_{\gamma,\beta}(t'',t') = \delta(t-t')\delta_{\alpha,\beta} \tag{8.16}$$

The self energy captures the Coulomb potential of the other electrons in the form of a retarded potential. Eq. 8.16 is analogous to Eq. 5.50 on p. 190 for a Green's function, which describes a one-particle system that experiences a retarded potential due to coupling to a bath.

Editor: Shall I mention that the self energy is also non-local in space?

Eqs. 8.15 and 8.16 have exactly the same information content as Eq. 8.8. They merely introduce the self energy as a quantity with an accessible physical interpretation. Furthermore, they introduce an equation of motion for the many-particle Green's function that is analogous to that in one-particle quantum mechanics.

Relation to the Hartree-Fock method: The self energy of the Hartree-Fock approximation is the sum of Hartree and exchange potential

$$\Sigma_{\alpha,\beta}(t,t') = \langle\chi_{\alpha}|\hat{V}_H+\hat{V}_X|\chi_{\beta}\rangle\delta(t,t') \tag{8.17}$$

With this choice, the equation of motion turns into the Schrödinger equation with the Fock operator $\hat{h}+\hat{V}_H+\hat{V}_X$ (times $\delta(t-t')$) in place of $\hat{h}+\hat{\Sigma}$.

Dyson's equation: Editor: This is not suitable for the lecture. Introduce the concept of the inverse in the $\{\alpha, t\}$ space properly and make the section optional. Can Dyson's equation also be obtained conventionally?

Editor: Generalized multiplication and inverse

$$\langle(\boldsymbol{A}\circ\boldsymbol{B}\rangle)_{(\alpha,t),(\beta,t')} = \sum_{\gamma}\int dt'' A_{(\alpha,t),(\gamma,t'')}B_{(\gamma,t''),(\beta,t')}$$
$$\langle(\boldsymbol{A}^{\circ,-1}\circ\boldsymbol{A}\rangle)_{(\alpha,t),(\beta,t')} = \delta_{\alpha,\beta}\delta(t-t') \tag{8.18}$$

Eq. 8.16 is a **Dyson equation**, which has the form $(G_0^{-1}-\Sigma)G = 1$. In order to make the connection evident, let me introduce the non-interacting Green's function $G^{(0)}_{\gamma,\beta}(t,t')$, which obeys

$$\sum_{\gamma}\Big(\delta_{\alpha,\gamma}i\hbar\partial_t - h_{\alpha,\gamma}\Big)G^{(0)}_{\gamma,\beta}(t,t') = \delta_{\alpha,\beta}\delta(t-t') \tag{8.19}$$

We define a new inverse of the non-interacting Green's function with respect to matrix elements **and** time arguments as

$$\sum_{\gamma}\int dt''\; G^{(0),\circ,-1}_{\alpha,\gamma}(t,t'')G^{(0)}_{\gamma,\beta}(t'',t') = \delta(t-t')\delta_{\alpha,\beta} \tag{8.20}$$

Note, that this is not the simple matrix inversion. Rather it is a generalized matrix inversion that considers the time arguments on the same level as the orbital indices.

Comparison of Eq. 8.20 with Eq. 8.19, provides us with the identification

$$G^{(0),\circ,-1}_{\alpha,\beta}(t,t') = \delta(t-t')\Big(\delta_{\alpha,\gamma}i\hbar\partial_{t'} - h_{\alpha,\gamma}\Big) \tag{8.21}$$

With this definition, we can use Eq. 8.21 to rewrite Eq. 8.16 in the form of a Dyson's equation

$$\sum_{\gamma}\int dt''\;\Big[G^{(0)}_{\alpha,\gamma},\circ,-1(t,t'') - \Sigma_{\alpha,\gamma}(t,t'')\Big]G_{\gamma,\beta}(t'',t') = \delta(t-t')\delta_{\alpha,\beta} \tag{8.22}$$

or after multiplication of a non-interacting Green's function from the left and after moving the self-energy term to the right-hand side, we obtain the better known form of the Dyson's equation.

DYSON'S EQUATION

$$G_{\alpha,\beta}(t,t') = G^{(0)}_{\alpha,\beta}(t,t') + \sum_{\gamma,\delta}\int dt''\int dt'''\; G^{(0)}_{\alpha,\gamma}(t,t'')\Sigma_{\gamma,\delta}(t'',t''')G_{\delta,\beta}(t''',t')\;. \tag{8.23}$$

It can be represented by the following diagram

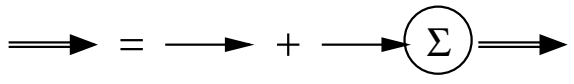

where a double arrow represents the full Green's function $\boldsymbol{G}$, a single arrow represents a non-interacting (bare) Green's function $\boldsymbol{G}^{(0)}$ and the circle represents the self energy $\boldsymbol{\Sigma}$.
Dyson's equation is the equation of motion Eq. 8.8 for the Green's function expressed in terms of the self energy Eq. 8.15.

Editor: Check the following and make it more precise! It is a bit puzzling that the inverse of a matrix function is a differential operator, but this is a consequence to using the generalized inversion which includes the time argument. Most of the time, one will work in an energy representation with respect to the relative argument $t-t'$ instead of a time representation. The time convolution will turn into a simple product in the energy representation. As a result this generalized inversion will turn into a simple matrix inversion.

8.3 Expectation value of one-particle operators

Consider a one-particle operator, which can always be expressed as

$$\hat{A}_S(t) = \sum_{\alpha,\beta} A_{\alpha,\beta}(t)\hat{c}^\dagger_{S,\alpha}\hat{c}_{S,\beta} = \int d^4x \int d^4x'\, A(\vec{x},\vec{x}',t)\hat{\psi}^\dagger_S(x)\hat{\psi}_S(\vec{x}') \tag{8.24}$$

To keep things general, I allow for a time dependence of the operator $\hat{A}_S(t)$.

For most practical purposes, one would like to obtain the stationary expectation value. We can, however, easily deal with a more complex problem. Consider a thermal ensemble of many-particle states at time[3] $t = 0$. The Hamiltonian may, however, be time dependent and the wave functions $|\Phi_n(t)\rangle$ will change in time. As a consequence one obtains a time-dependent expectation value $\langle A(t)\rangle_{T,\mu}$, even if the operator $\hat{A}_S$ itself does not depend on time.

The thermal expectation value at time t is obtained from the ensemble at time $t = 0$ and the propagator from $t = 0$ to the time of the "measurement".

$$\begin{aligned}
\Big\langle A(t)\Big\rangle_{T,\mu} &\overset{\text{def}}{=} \mathrm{Tr}\Big\{\hat{\rho}_{T,\mu}\hat{\mathcal{U}}(0,t)\hat{A}_S(t)\hat{\mathcal{U}}(t,0)\Big\} = \mathrm{Tr}\Big\{\hat{\rho}_{T,\mu}\hat{A}_H(t)\Big\} \\
&= \sum_{\alpha,\beta} A_{\alpha,\beta}(t)\mathrm{Tr}\Big\{\hat{\rho}_{T,\mu}\hat{\mathcal{U}}(0,t)\hat{c}^\dagger_{S,\alpha}\underbrace{\hat{\mathcal{U}}(t,0)\hat{\mathcal{U}}(0,t)}_{\hat{1}}\hat{c}_{S,\beta}\hat{\mathcal{U}}(t,0)\Big\} \\
&= \sum_{\alpha,\beta} A_{\alpha,\beta}(t)(-1)\lim_{t'\to t^+}\mathrm{Tr}\Big\{\hat{\rho}_{T,\mu}\mathcal{T}_\mathcal{C}\hat{c}_{H,\beta}(t)\hat{c}^+_{H,\alpha}(t')\Big\} \qquad (8.25) \\
&\overset{\text{Eq. 7.16}}{=} -i\hbar\lim_{t'\to t^+}\sum_{\alpha,\beta} A_{\alpha,\beta}(t)G_{\beta,\alpha}(t,t') \qquad (8.26)
\end{aligned}$$

EXPECTATION VALUES OF ONE-PARTICLE OPERATORS FROM GREEN'S FUNCTIONS

The thermal expectation value at time t of an operator $\hat{A}_S(t) = \sum_{\alpha,\beta} A_{\alpha,\beta}(t)\hat{c}^\dagger_\alpha\hat{c}_\beta$ is

$$\Big\langle A(t)\Big\rangle_{T,\mu} = -i\hbar\lim_{t'\to t^+}\sum_{\alpha,\beta} A_{\alpha,\beta}(t)G_{\beta,\alpha}(t,t') \tag{8.27}$$

One-particle expectation values can be expressed by the one-particle reduced density matrix $\boldsymbol{\rho}^{(1)}$ as $\mathrm{Tr}\{\boldsymbol{\rho}^{(1)}\boldsymbol{A}\}$. Thus, we indirectly obtain the **one-particle-reduced density matrix** of the many-particle system as

ONE-PARTICLE-REDUCED DENSITY MATRIX FROM GREEN'S FUNCTION

$$\rho^{(1)}_{\alpha,\beta}(t) = -i\hbar\lim_{t'\to t^+} G_{\alpha,\beta}(t,t') \tag{8.28}$$

8.4 Migdal-Galitskii-Koltun (MGK) sum rule and total energy

The equation of motion for the Green's function, Eq. 8.8, leads to the **Migdal-Galitskii-Koltun sum rule**[68], which gives the total energy in terms of the Green function.

[3] This is not a restriction because the zero of the time axis can be placed arbitrarily.

In the previous section, we learned how to evaluate the thermal expectation value of a one-particle operator. The expectation value of two-particle operators, however, cannot be extracted from a one-particle Green's function. There is one exception, namely the interaction energy. The reason is that the equation of motion links an expectation value of the two-particle Green's function to the one-particle Green's function.

The interaction energy is

$$\begin{aligned}\left\langle \hat{W}(t)\right\rangle_{T,\mu} &= \frac{1}{2}\sum_{\alpha,b,c,d} W_{\alpha,b,d,c}\left\langle \hat{\mathcal{U}}(0,t)\hat{c}^\dagger_{S,\alpha}\hat{c}^\dagger_{S,b}\hat{c}_{S,c}\hat{c}_{S,d}\hat{\mathcal{U}}(t,0)\right\rangle_{T,\mu} \\ &= \frac{1}{2}\sum_{\alpha,b,c,d} W_{\alpha,b,d,c}\left\langle \hat{c}^+_{H,\alpha}(t)\hat{c}^+_{H,b}(t)\hat{c}_{H,c}(t)\hat{c}_{H,d}(t)\right\rangle_{T,\mu} \end{aligned} \tag{8.29}$$

The time dependence is understood as in the previous section. The interaction operator is time independent. At time $t = 0$, the system is prepared in a thermal ensemble. The dynamics may however, drive the system away from equilibrium, resulting in a time-dependent expectation value of the interaction energy.

The right-hand side of the equation of motion Eq. 8.8 for the Green's function is

$$Y_{\alpha,\beta}(t,t') \stackrel{\text{def}}{=} \delta_{\alpha,\beta}\delta(t-t') + \sum_{b,c,d} W_{\alpha,b,d,c}\frac{1}{i\hbar}\left\langle \mathcal{T}_\mathcal{C}\hat{c}^+_{H,b}(t)\hat{c}_{H,c}(t)\hat{c}_{H,d}(t)\hat{c}^+_{H,\beta}(t')\right\rangle_{T,\mu} \tag{8.30}$$

In order to get the second creation operator to the front as in the interaction energy Eq. 8.29, we choose the time argument t' infinitesimally later than t. Then, the time-ordering operator places $\hat{c}^+_{H,\beta}(t')$ to the very left, while switching the sign for any permutation of two fermionic operators.

Shifting the time argument forward along the contour by an infinitesimal amount will be required frequently, so that a symbol[4] t^+ has been introduced. It denotes $t^+ \stackrel{\text{def}}{=} t(s+\delta)$, where δ is an infinitesimally small, positive number. $t(s)$ is the mapping onto the time contour. An example is

$$F(t,t^+) = \lim_{s'\to s^+} F(t,t(s')) = \lim_{\delta\to 0^+} F(t,t(s+\delta)) \tag{8.31}$$

Any time argument can be displaced in this manner. It would be OK to write "2^+ seconds". The notation t^+ under the limes has a similar but still different meaning than using t^+ as argument. It specifies that the limes is taken from the positive side. In contrast, using t^+ as argument implies implicitly that a limes is to be taken.

With this notation, we obtain

$$Y_{\alpha,\beta}(t,t^+) = -\sum_{b,c,d} W_{\alpha,b,d,c}\frac{1}{i\hbar}\left\langle \hat{c}^+_{H,\beta}(t^+)\hat{c}^+_{H,b}(t)\hat{c}_{H,c}(t)\hat{c}_{H,d}(t)\right\rangle_{T,\mu} \tag{8.32}$$

Comparison with Eq. 8.29 shows

$$\left\langle \hat{W}(t)\right\rangle_{T,\mu} = -\frac{i\hbar}{2}\sum_\alpha Y_{\alpha,\alpha}(t,t^+) \tag{8.33}$$

$Y(t,t')$ is the right-hand side of the equation of motion Eq. 8.8 for the Green's function, which can be replaced by the left-hand side of the equation of Eq. 8.8.

$$\begin{aligned}\left\langle \hat{W}(t)\right\rangle_{T,\mu} &\stackrel{\text{Eq. 8.8}}{=} -\frac{i\hbar}{2}\sum_\alpha \underbrace{\sum_\gamma\left(\delta_{\alpha,\gamma}i\hbar\partial_t - h_{\alpha,\gamma}\right)G_{\gamma,\alpha}(t,t^+)}_{Y_{\alpha,\alpha}(t,t^+)} \\ &= \frac{1}{2}\sum_{\alpha,\gamma}\left(\delta_{\alpha,\gamma}i\hbar\partial_t - h_{\alpha,\gamma}\right)\left(-i\hbar G_{\gamma,\alpha}(t,t^+)\right)\end{aligned} \tag{8.34}$$

[4] see e.g. Fetter and Walecka[3] p.66 Eq.7.8

Thus, we obtain an expression for the interaction energy. This is probably the only two-particle expectation value that can be obtained directly from the one-particle Green's function.

We may now add the expectation value of the non-interacting Hamiltonian to obtain the expectation value of the total energy.

$$\left\langle \hat{h}(t) \right\rangle_{T,\mu} \overset{\text{Eq. 8.27}}{=} -i\hbar \lim_{t' \to t^+} \sum_{\alpha,\beta} h_{\alpha,\beta}(t) G_{\beta,\alpha}(t,t') \tag{8.35}$$

Because of the factor one-half in Eq. 8.34, adding the non-interacting Hamiltonian only changes the sign of the corresponding term.

MIGDAL-GALITSKII-KOLTUN SUM RULE

The thermal expectation value of $\hat{h} + \hat{W}$, the total energy at time t is

$$\left\langle E_{\text{tot}}(t) \right\rangle_{T,\mu} = \frac{1}{2} \lim_{t' \to t^+} \sum_{\alpha,\beta} \left(\delta_{\alpha,\beta} i\hbar \partial_t \overset{!}{+} h_{\alpha,\beta}(t) \right) \left(-i\hbar G_{\beta,\alpha}(t,t') \right) \tag{8.36}$$

The positive sign in front of $h_{\alpha,\beta}$ is correct! (see above). The time derivative acts only on the first argument of the Green's function.

The equation Eq. 8.36 for the total energy differs only by the sign in front of the non-interacting Hamilton matrix elements $h_{\alpha,\gamma}$ from that of the interaction energy Eq. 8.34. Remember, that Migdal-Galtskii sum rule relies on that the interaction term is a two-particle interaction such as the Coulomb interaction. A generalization may be possible, but needs to be done.

Energy is not grand potential: The total energy given by Eq. 8.36 is the thermal expectation value of non-interacting Hamiltonian and the interaction energy. Except for zero temperature, the quantity obtained is not a thermodynamic potential, from which the complete thermodynamic information can be extracted. In order to obtain the grand potential, which is the thermodynamic potential for a system in contact with a heat bath and a particle reservoir, i.e. a (T,μ)-ensemble, we would need to add the entropy. The entropy, however, cannot be extracted from the Green's function alone. At zero temperature $T = 0$ the entropy vanishes, so that the expectation value of the total energy becomes identical with the internal energy.

A consequence of this is that there is no minimum principle for the total energy at finite temperature.

Use the self energy to obtain the total energy: The Migdal-Galitsky sum rule can be used to obtain the total energy, if the self energy is known. For this purpose, we use Dyson's equation Eq. 8.16 to replace the time derivative in Eq. 8.36. This yields

$$\begin{aligned} \left\langle E_{\text{tot}}(t) \right\rangle_{T,\mu} &\overset{\text{Eq. 8.36}}{=} \frac{1}{2} \lim_{t' \to t^+} \sum_{\alpha,\beta} \left(\delta_{\alpha,\beta} i\hbar \partial_t + h_{\alpha,\beta}(t) \right) \left(-i\hbar G_{\beta,\alpha}(t,t') \right) \\ &= -i\hbar \left\{ \sum_{\alpha,\beta} h_{\alpha,\beta} G_{\beta,\alpha}(t,t^+) + \frac{1}{2} \int dt'' \sum_{\alpha,\beta} \Sigma_{\alpha,\beta}(t,t'') G_{\beta,\alpha}(t'',t^+) \right\} \end{aligned} \tag{8.37}$$

In this expression the division into non-interacting Hamiltonian and interaction is again intact. The term containing the self energy is the expectation value of the interaction.

8.5 Home study and practice

8.5.1 Self-energy and contour Green's function of the Hubbard atom

Editor: needs to be done

Editor: See [69] on the Hubbard atom

The Hamiltonian for the Hubbard atom is

$$\begin{aligned}\hat{H} &= \underbrace{\sum_{\sigma\in\{\uparrow,\downarrow\}} \bar{\epsilon}\hat{c}^\dagger_{S,\sigma}\hat{c}_{S,\sigma}}_{\hat{h}} + \underbrace{\frac{1}{2}\sum_{\sigma,\sigma'\in\{\uparrow,\downarrow\}} U\hat{c}^\dagger_{S,\sigma}\hat{c}^\dagger_{S,\sigma'}\hat{c}_{S,\sigma'}\hat{c}_{S,\sigma}}_{\hat{W}} \\ &= \sum_{\sigma\in\{\uparrow,\downarrow\}} \bar{\epsilon}\hat{c}^\dagger_{S,\sigma}\hat{c}_{S,\sigma} + U\hat{c}^\dagger_{S,\uparrow}\hat{c}_{S,\uparrow}\hat{c}^\dagger_{S,\downarrow}\hat{c}_{S,\downarrow}\end{aligned} \tag{8.38}$$

The eigenstates of the many-particle Hamiltonian are

$$\begin{aligned}|\Phi_0\rangle &= |\mathcal{O}\rangle \\ |\Phi_\uparrow\rangle &= \hat{c}^\dagger_{S,\uparrow}|\mathcal{O}\rangle \\ |\Phi_\downarrow\rangle &= \hat{c}^\dagger_{S,\downarrow}|\mathcal{O}\rangle \\ |\Phi_{\uparrow,\downarrow}\rangle &= \hat{c}^\dagger_{S,\uparrow}\hat{c}^\dagger_{S,\downarrow}|\mathcal{O}\rangle\end{aligned} \tag{8.39}$$

and the corresponding energies are

$$\begin{aligned}E_0 &= 0 \\ E_\uparrow &= \bar{\epsilon} \\ E_\downarrow &= \bar{\epsilon} \\ E_{\uparrow,\downarrow} &= 2\bar{\epsilon} + U\end{aligned} \tag{8.40}$$

The contour Green's function is defined as

$$
\begin{aligned}
G^{\mathcal{C}}_{\sigma,\sigma'}(t,t') &\overset{\text{Eq. 7.16}}{=} \frac{1}{i\hbar}\frac{\mathrm{Tr}\left\{\mathrm{e}^{-\beta(\hat{H}-\mu\hat{N})}\mathcal{T}_{\mathcal{C}}\hat{c}_{H\sigma}(t)\hat{c}^{+}_{H\sigma}(t')\right\}}{\mathrm{Tr}\left\{\mathrm{e}^{-\beta(\hat{H}-\mu\hat{N})}\right\}} \\
&= \frac{1}{i\hbar}\underbrace{\frac{1}{1+2\mathrm{e}^{-\beta(\bar{\epsilon}-\mu)}+\mathrm{e}^{-\beta(2\bar{\epsilon}+U-2\mu)}}}_{1/Z_{T,\mu}}\Bigg\{1\langle\mathcal{O}|\theta(t-t')\hat{c}_{H\sigma}(t)\hat{c}^{+}_{H\sigma'}(t')|\mathcal{O}\rangle \\
&+ \sum_{\bar{\sigma}\in\{\uparrow,\downarrow\}}\mathrm{e}^{-\beta(\bar{\epsilon}-\mu)}\langle\mathcal{O}|\hat{c}_{S,\bar{\sigma}}\Big(\theta(t-t')\hat{c}_{H\sigma}(t)\hat{c}^{+}_{H\sigma'}(t')-\theta(t'-t)\hat{c}^{+}_{H\sigma'}(t')\hat{c}_{H\sigma}(t)\Big)\hat{c}_{S,\bar{\sigma}}|\mathcal{O}\rangle \\
&+ \mathrm{e}^{-\beta(2\bar{\epsilon}+U-2\mu)}\langle\mathcal{O}|\hat{c}_{S,\downarrow}\hat{c}_{S,\uparrow}\Big(-\theta(t'-t)\hat{c}^{+}_{H\sigma'}(t')\hat{c}_{H\sigma}(t)\Big)\hat{c}^{+}_{S,\uparrow}\hat{c}^{+}_{S,\downarrow}|\mathcal{O}\rangle\Bigg\} \\
&= \frac{1}{i\hbar}\frac{1}{1+2\mathrm{e}^{-\beta(\bar{\epsilon}-\mu}+\mathrm{e}^{-\beta(2(\bar{\epsilon}-\mu)+U)}}\Bigg\{\delta_{\sigma,\sigma'}\theta(t-t')\mathrm{e}^{-\frac{i}{\hbar}\bar{\epsilon}(t-t')} \\
&+ \sum_{\bar{\sigma}\in\{\uparrow,\downarrow\}}\delta_{\sigma,\sigma'}\mathrm{e}^{-\beta(\bar{\epsilon}-\mu)}\Big(\theta(t-t')\delta_{\bar{\sigma},-\sigma}\mathrm{e}^{-\frac{i}{\hbar}(\bar{\epsilon}+U)(t-t')}-\theta(t'-t)\delta_{\bar{\sigma},\sigma}\mathrm{e}^{-\frac{i}{\hbar}(-\bar{\epsilon})(t'-t)}\Big) \\
&+ \mathrm{e}^{-\beta(2\bar{\epsilon}+U-2\mu)}\delta_{\sigma,\sigma'}\Big(-\theta(t'-t)\mathrm{e}^{-\frac{i}{\hbar}(-\bar{\epsilon}-U+\mu)(t'-t)}\Big)\Bigg\} \\
&= \frac{1}{i\hbar}\frac{\delta_{\sigma,\sigma'}}{1+2\mathrm{e}^{-\beta(\bar{\epsilon}-\mu)}+\mathrm{e}^{-\beta(2(\bar{\epsilon}-\mu)+U)}}\Bigg\{\theta(t-t')\Big(\mathrm{e}^{-\frac{i}{\hbar}\bar{\epsilon}(t-t')}+\mathrm{e}^{-\beta(\bar{\epsilon}-\mu)}\mathrm{e}^{-\frac{i}{\hbar}(\bar{\epsilon}+U)(t-t')}\Big) \\
&- \theta(t'-t)\Big(\mathrm{e}^{-\beta(\bar{\epsilon}-\mu)}\mathrm{e}^{+\frac{i}{\hbar}\bar{\epsilon}(t'-t)}+\mathrm{e}^{-\beta(2\bar{\epsilon}+U-2\mu)}\mathrm{e}^{+\frac{i}{\hbar}(\bar{\epsilon}+U)(t'-t)}\Big)\Bigg\} \\
&= \frac{\delta_{\sigma,\sigma'}}{i\hbar}\Bigg\{\theta(t-t')\frac{\mathrm{e}^{-\frac{i}{\hbar}\bar{\epsilon}(t-t')}\Big(1+\mathrm{e}^{-\beta(\bar{\epsilon}-\mu)}\mathrm{e}^{-\frac{i}{\hbar}U(t-t')}\Big)}{1+2\mathrm{e}^{-\beta(\bar{\epsilon}-\mu)}+\mathrm{e}^{-\beta(2(\bar{\epsilon}-\mu)+U)}} \\
&\quad -\theta(t'-t)\frac{\mathrm{e}^{-\beta(\bar{\epsilon}-\mu)}\mathrm{e}^{+\frac{i}{\hbar}\bar{\epsilon}(t'-t)}\Big(1+\mathrm{e}^{-\beta(\bar{\epsilon}-\mu+U)}\mathrm{e}^{+\frac{i}{\hbar}U(t'-t)}\Big)}{1+2\mathrm{e}^{-\beta(\bar{\epsilon}-\mu)}+\mathrm{e}^{-\beta(2(\bar{\epsilon}-\mu)+U)}}\Bigg\}
\end{aligned}
\tag{8.41}
$$

Special cases:

- $\mu \ll \bar{\epsilon}$

$$G^{\mathcal{C}}_{\sigma,\sigma'}(t,t') = \frac{\delta_{\sigma,\sigma'}}{i\hbar}\theta(t-t')\mathrm{e}^{-\frac{i}{\hbar}\bar{\epsilon}(t-t')} \tag{8.42}$$

  This Green's function describes the propagation of a single electron in an empty Hubbard atom.

- $\mu \gg \bar{\epsilon}+U$

$$G^{\mathcal{C}}_{\sigma,\sigma'}(t,t') = -\frac{\delta_{\sigma,\sigma'}}{i\hbar}\theta(t'-t)\mathrm{e}^{+\frac{i}{\hbar}(\bar{\epsilon}+U)(t'-t)} \tag{8.43}$$

  This Green's function describes the propagation of a hole in a doubly occupied Hubbard atom.

- $\mu = \bar{\epsilon}+\frac{1}{2}U$

$$
\begin{aligned}
G^{\mathcal{C}}_{\sigma,\sigma'}(t,t') = \frac{\delta_{\sigma,\sigma'}}{i\hbar}\Bigg\{&\theta(t-t')\frac{\mathrm{e}^{-\frac{i}{\hbar}\bar{\epsilon}(t-t')}\Big(1+\mathrm{e}^{\frac{1}{2}\beta U}\mathrm{e}^{-\frac{i}{\hbar}U(t-t')}\Big)}{2+2\mathrm{e}^{\frac{1}{2}\beta U}} \\
&-\theta(t'-t)\frac{\mathrm{e}^{+\frac{i}{\hbar}\bar{\epsilon}(t'-t)}\Big(1+\mathrm{e}^{-\frac{1}{2}\beta U}\mathrm{e}^{+\frac{i}{\hbar}U(t'-t)}\Big)}{2+2\mathrm{e}^{-\frac{1}{2}\beta U}}\Bigg\}
\end{aligned}
\tag{8.44}
$$

– For the non-interacting limit, i.e. $\beta U = 0$, I obtain

$$G^{\mathcal{C}}_{\sigma,\sigma'}(t,t') = \frac{\delta_{\sigma,\sigma'}}{i\hbar}\frac{\theta(t-t')-\theta(t'-t)}{2}\mathrm{e}^{-\frac{i}{\hbar}\bar{\epsilon}(t-t')} \tag{8.45}$$

The non-interacting limit is identical to the high-temperature limit.

– for strongly interacting limit, i.e. $\beta U \gg 1$, I obtain

$$G^{\mathcal{C}}_{\sigma,\sigma'}(t,t') = \frac{\delta_{\sigma,\sigma'}}{i\hbar}\frac{\theta(t-t')-\theta(t'-t)}{2}\mathrm{e}^{-\frac{i}{\hbar}(\bar{\epsilon}+U)(t-t')} \tag{8.46}$$

The strongly interacting limit is identical to the low-temperature limit, unless U vanishes precisely.

– in the intermediate regime, I obtain a superposition of two oscillations, one with $\bar{\epsilon}$ and the other with $\bar{\epsilon}+U$.

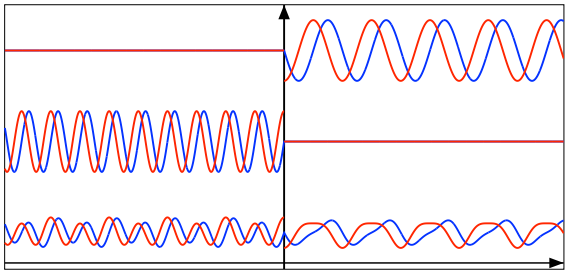

Fig. 8.1: Green's function $G(t,t')$ of the H^+ Hubbard ion, of the H^- Hubbard ion (middle), and of a half-filled Hubbard atom H^0 at finite temperature as function of the relative time argument $t-t'$. Real parts are shown in blue and imaginary parts are shown in red. Greens functions are displaced vertically for better visibility. The parameters are $\mathrm{e}^{\frac{1}{2}\beta U} = 1/4$ and $U = \bar{\epsilon}$.

Chapter 9

Spectral properties

The spectral function describes one-particle excitations such as electron addition or electron removal in a general many-particle system. Thus, it provides the link to measured spectra from photo-emission or inverse photo-emission experiments.

There is a one-to-one correspondence between the spectral function and the Green's function. On the one side, this is useful, because one can develop a physical understanding the spectral function, which is more difficult for the more abstract Green's function. On the other side, there is a more fundamental role in determining the regime of "physical" Green's functions: The regime of physical spectral functions is more easily specified. The regime of physical Green's functions follows from that of the physical spectral functions. The regime of the physical Green's function is relevant for Green's function functional theories, which may provide the Green's function via a variational principle.

Spectral functions have been discussed earlier in section 2.5 in the context of the Hartree-Fock approximation. The reader my revisit that chapter.

The following chapter is mostly limited to time-independent Hamiltonians.

9.1 Lehmann representation

Starting from the assumption of a time-independent Hamiltonian, I can use the eigenvalue equation for the many-particle eigenstates $|\Phi_n\rangle$ and many-particle eigenvalues E_n of the interacting Hamiltonian.

$$\hat{H}|\Phi_n\rangle = |\Phi_n\rangle E_n \qquad \text{and} \qquad \hat{N}|\Phi_n\rangle = |\Phi_n\rangle N_n \tag{9.1}$$

- In this representation, the state operator $\hat{\rho}^{(W)}_{T,\mu}$ has the form

$$\hat{\rho}^{(W)}_{T,\mu} = \sum_n |\Phi_n\rangle P_n \langle\Phi_n| \tag{9.2}$$

  where the probabilities $P_n = \frac{1}{Z^{(W)}_{T,\mu}} \mathrm{e}^{-\beta(E_n-\mu N_n)}$ are given by the Boltzmann factor and the partition function $Z^{(W)}_{T,\mu} = \sum_n \mathrm{e}^{-\beta(E_n-\mu N_n)}$.

- We resolve the Heisenberg operators using the eigenvalue equations and the corresponding Schrödinger operators. This step is responsible for the limitation to time-independent Hamiltonians.

$$\begin{aligned} \langle\Phi_m|\hat{c}_{H,\alpha}(t)|\Phi_n\rangle &= \langle\Phi_m|\hat{c}_{S,\alpha}|\Phi_n\rangle \mathrm{e}^{-\frac{i}{\hbar}(E_n-E_m)t} \\ \langle\Phi_m|\hat{c}^{+}_{H,\beta}(t')|\Phi_n\rangle &= \langle\Phi_m|\hat{c}^{\dagger}_{S,\beta}|\Phi_n\rangle \mathrm{e}^{-\frac{i}{\hbar}(E_n-E_m)t'} \end{aligned} \tag{9.3}$$

After rewriting the Green's function accordingly, a unit operator $\hat{1} = \sum_m |\Phi_m\rangle\langle\Phi_m|$ is inserted between the two field operators.

$$
\begin{aligned}
G^{\mathcal{C}}_{\alpha,\beta}(t,t') &\overset{\text{Eq. 7.16}}{=} \frac{1}{i\hbar}\mathrm{Tr}\Big\{\hat{\rho}^{(W)}_{T,\mu}\mathcal{T}_{\mathcal{C}}\hat{c}_{H,\alpha}(t)\hat{c}^{+}_{H,\beta}(t')\Big\} \\
&= \frac{1}{i\hbar}\mathrm{Tr}\Big\{\underbrace{\sum_n |\Phi_n\rangle P_n\langle\Phi_n|}_{\hat{\rho}_{T,\mu}}\Big(\theta(t-t')\hat{c}_{H,\alpha}(t)\hat{c}^{+}_{H,\beta}(t') - \theta(t'-t)\hat{c}^{+}_{H,\beta}(t')\hat{c}_{H,\alpha}(t)\Big)\Big\} \\
&\overset{cycl.perm.}{=} \frac{1}{i\hbar}\sum_n P_n\Big(\langle\Phi_n|\hat{c}_{H,\alpha}(t)\underbrace{\sum_m |\Phi_m\rangle\langle\Phi_m|}_{=\hat{1}}\hat{c}^{+}_{H,\beta}(t')|\Phi_n\rangle\theta(t-t') \\
&\qquad -\langle\Phi_n|\hat{c}^{+}_{H,\beta}(t')\underbrace{\sum_m |\Phi_m\rangle\langle\Phi_m|}_{=\hat{1}}\hat{c}_{H,\alpha}(t)|\Phi_n\rangle\theta(t'-t)\Big) \\
&= \frac{1}{i\hbar}\sum_{n,m} P_n\Big\{\langle\Phi_n|\hat{c}_{S,\alpha}|\Phi_m\rangle\langle\Phi_m|\hat{c}^{\dagger}_{S,\beta}|\Phi_n\rangle\theta(t-t')\mathrm{e}^{+\frac{i}{\hbar}(E_n-E_m)(t-t')} \\
&\qquad -\langle\Phi_n|\hat{c}^{\dagger}_{S,\beta}|\Phi_m\rangle\langle\Phi_m|\hat{c}_{S,\alpha}|\Phi_n\rangle\theta(t'-t)\mathrm{e}^{-\frac{i}{\hbar}(E_n-E_m)(t-t')}\Big\} \qquad (9.4)
\end{aligned}
$$

GREEN'S FUNCTION IN LEHMANN REPRESENTATION

The contour Green's function in Lehmann representation has the form

$$
\begin{aligned}
G^{\mathcal{C}}_{\alpha,\beta}(t,t') = \frac{1}{i\hbar}\sum_{n,m} P_n\Big\{&\underbrace{\langle\Phi_n|\hat{c}_{S,\alpha}|\Phi_m\rangle\langle\Phi_m|\hat{c}^{\dagger}_{S,\beta}|\Phi_n\rangle\theta(t-t')\mathrm{e}^{+\frac{i}{\hbar}(E_n-E_m)(t-t')}}_{\text{electrons added to empty states}} \\
&-\underbrace{\langle\Phi_n|\hat{c}^{\dagger}_{S,\beta}|\Phi_m\rangle\langle\Phi_m|\hat{c}_{S,\alpha}|\Phi_n\rangle\theta(t'-t)\mathrm{e}^{-\frac{i}{\hbar}(E_n-E_m)(t-t')}}_{\text{holes added to filled states}}\Big\} \qquad (9.5)
\end{aligned}
$$

The thermal probability is $P_n = \frac{1}{Z_{T,\mu}}\mathrm{e}^{-\beta(E_n-\mu N_n)}$.

The inner sum over many-particle states $|\Phi_m\rangle$ contributes nonzero contributions from only those wave functions that either have one particle more or one particle less than the state $|\Phi_n\rangle$.

Energy representation In order to transform this expression into the energy representation we use the relations Eq. A.10 derived in Appendix A.2.2 (p. 386)

$$
\int_{-\infty}^{\infty} dt\ \theta(t)\mathrm{e}^{\frac{i}{\hbar}(\epsilon+i\eta)t} = \frac{i\hbar}{\epsilon+i\eta} \qquad \text{and} \qquad \int_{-\infty}^{\infty} dt\ \theta(-t)\mathrm{e}^{\frac{i}{\hbar}(\epsilon-i\eta)t} = \frac{-i\hbar}{\epsilon-i\eta} \qquad (9.6)
$$

The time integration is a contour integration along the entire real time axis in the positive direction.

This yields the

LEHMANN REPRESENTATION OF THE GREEN'S FUNCTION

$$G_{\alpha,\beta}(\hbar\omega) \stackrel{\text{def}}{=} \int_{-\infty}^{\infty} dt\; e^{\frac{i}{\hbar}(\hbar\omega t + i\eta|t|)} G_{\alpha,\beta}(t,0) \tag{9.7}$$

$$= \sum_{n,m} P_n \left[\underbrace{\frac{\langle\Phi_n|\hat{c}_{S,\alpha}|\Phi_m\rangle\langle\Phi_m|\hat{c}^\dagger_{S,\beta}|\Phi_n\rangle}{\hbar\omega - (E_m - E_n) + i\eta}}_{\text{electron like}} + \underbrace{\frac{\langle\Phi_n|\hat{c}^\dagger_{S,\beta}|\Phi_m\rangle\langle\Phi_m|\hat{c}_{S,\alpha}|\Phi_n\rangle}{\hbar\omega + (E_m - E_n) - i\eta}}_{\text{hole like}} \right] \tag{9.8}$$

The time integration proceeds along the real-time axis in the positive direction. η is an infinitesimally small, positive number.

This expression makes the structure of the Green's function evident. It is shown in Fig.9.1 The Green's functions has poles at the one-particle excitation energies. For the electron excitations, i.e. above the Fermi level, the poles are infinitesimally below the real frequency axis and for hole excitation, i.e. below the Fermi level they lie above the real axis. For infinitely large systems, the excitations may form a continuous spectrum. As a result, the discrete poles usually merge into a **branch cut**.

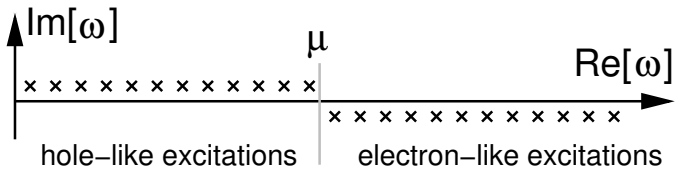

Fig. 9.1: Position of the poles of the Green's function for non-interacting electrons. The poles are located in the complex ω plane at the positions given by the excitation energy (real part) and $\pm\eta$ (imaginary part). For an interacting system the excitations may move a finite distance away from the real axis, which corresponds to a finite life time of the corresponding quasi particles.

9.2 Quasi-particle wave functions

The concept of **quasi-particle wave functions**[1] extends the concept of one-particle states from one-particle quantum mechanics, non-interacting electrons and Hartree-Fock Slater determinants.

The quasi-particle wave functions are also called **Lehmann amplitudes** or **Dyson orbitals**. [2] [3]

[1] Editor: Check the following reference, whether it refers to quasi-particle wave functions. I am not sure it is appropriate.*"A proper way of calculating quasiparticle energies is provided by the Green function theory.[70, 71]"* . Citation taken from Aryasetiawan[72] (p.2)in Anisimov's Book "Strong Coulomb correlations in electronic-structue calculations".

[2] For the definition of Dyson orbitals see e.g. the perspective article by Ortiz[73] or the Book of Fulde[5] (Fulde-Eq. 9.2.61 and 9.2.62)

[3] See *Introduction to many-body Green-function theory*, J. Toulouse, 2015 https://www.lct.jussieu.fr/pagesperso/toulouse/enseignement/introduction_green.pdf retrieved June 3, 2020. Editor: Here the Dyson orbitals are defined as eigenstates of the Dyson equation $[\hat{h} + \hat{\Sigma}(\epsilon) - \epsilon]|\psi\rangle = 0$ evaluated at the pole of the Green's function.

The quasi-particle wave functions $\psi^{(qp)}_{m,n}(\vec{x})$ are defined by [4] [5]

$$\psi^{(qp)}_{m,n}(\vec{x}) = \langle \Phi_m | \hat{\psi}_S(\vec{x}) | \Phi_n \rangle \qquad \text{and} \qquad \left(\psi^{(qp)}_{m,n}(\vec{x})\right)^* = \langle \Phi_n | \hat{\psi}^\dagger_S(\vec{x}) | \Phi_m \rangle \tag{9.11}$$

where $|\Phi_m\rangle$ are eigenstates of the many-electron Hamiltonian and $\hat{\psi}(\vec{x})$ is the field operator that annihilates an electron with coordinate $\vec{x}$. In other words, the quasi-particle wave functions are the matrix elements of the annihilation operator for two many-particle states. The quasi-particle wave functions are non-zero only, when they connect N-particle states $|\Phi_n\rangle$ with $(N-1)$-particle states $|\Phi_m\rangle$.

The energies of the quasi-particle wave functions[6] are

$$\epsilon_{n,m} = \frac{E_n - E_m}{N_n - N_m} \tag{9.12}$$

this energy can be attributed to the energy of an additional electron. Because the change in the particle number is ± 1, the denominator $N_n - N_m$ is usually suppressed.

In order to make contact with wave functions we can express the quasi-particle wave function in terms of N-electron wave functions.

$$\begin{aligned} \psi^{(qp)}_{m,n}(\vec{x}) &= \langle \Phi_m | \hat{\psi}(\vec{x}) | \Phi_n \rangle \\ &= \underbrace{\sqrt{N_n}}_{N_n/\sqrt{N_n}} \int d^4x_2 \cdots d^4x_N \; \underbrace{\Phi^{(N-1),*}_m(\vec{x}_2, \ldots, \vec{x}_{N_n})}_{N-1 \text{ particles}} \underbrace{\Phi^{(N)}(\vec{x}, \vec{x}_2, \ldots, \vec{x}_{N_n})}_{N \text{ particles}} \end{aligned} \tag{9.13}$$

Editor: check the factor $\sqrt{N}$.

$$f_j = \langle \Phi_n | \sum_j \hat{a}^\dagger_j \hat{a}_j | \Phi_n \rangle \tag{9.14}$$

Rather than in the real-space representation, the quasi-particle wave functions can also be represented in terms of any other basisset $\{|\chi_\alpha\rangle\}$ with annihilators $\hat{c}_\alpha$, be it orthonormal or not[7]. It rests on the identity $\hat{\psi}(\vec{x}) \overset{\text{Eq. 3.61}}{=} \sum_j \langle \vec{x} | \varphi_j \rangle \hat{a}_j \overset{\text{Eq. B.6}}{=} \sum_\alpha \langle \vec{x} | \chi_\alpha \rangle \hat{c}_\alpha$, where the orbitals $|\varphi_j\rangle$ are orthonormal, while the $|\chi_\alpha\rangle$ may be non-orthonormal.

$$\begin{aligned} \left|\psi^{(qp)}_{m,n}\right\rangle &= \int d^4x \; |\vec{x}\rangle \langle \Phi_m | \hat{\psi}(\vec{x}) | \Phi_n \rangle = \int d^4x \; |\vec{x}\rangle \langle \Phi_m | \underbrace{\sum_\alpha \chi_\alpha(\vec{x}) \hat{c}_\alpha}_{\hat{\psi}(\vec{x})} | \Phi_n \rangle \\ &\overset{\text{Eq. B.6}}{=} \sum_\alpha |\chi_\alpha\rangle \underbrace{\langle \Phi_m | \hat{c}_\alpha | \Phi_n \rangle}_{\langle \pi_\alpha | \psi^{(qp)}_{m,n} \rangle} \end{aligned} \tag{9.15}$$

[4] Compare Stefanucci and van Leeuwen[2] Stefanucci-Eq. 6.84.

[5] The definition to quasi-particle wave functions can easily be generalized to time-dependent problems by including the time dependence of the many-particle wave functions, which start as eigenstates of an initial Hamiltonian and which are propagated using the time-dependent Schrödinger equation.

$$\psi^{(qp,td)}_{m,n}(\vec{x}, t) \overset{\text{def}}{=} \langle \Phi_m(t) | \hat{\psi}_S(\vec{x}) | \Phi_n(t) \rangle \tag{9.9}$$

For time-independent Hamiltonians, the time dependence can be described by

$$\psi^{(qp,td)}_{m,n}(\vec{x}, t) = \langle \Phi_m | \hat{\psi}_S(\vec{x}) | \Phi_n \rangle e^{-\frac{i}{\hbar}(E_n - E_m)t} = \psi^{(qp)}_{m,n}(\vec{x}) e^{-\frac{i}{\hbar}\epsilon_{n,m}t} \tag{9.10}$$

with $\epsilon_{n,m} = E_n - E_m$.

[6] There is a close connection to the expression of the one-particle energy $\epsilon_j = \frac{\partial E}{\partial f_j}$ in a mean-field-like theory as derivative of the energy with respect to the occupation f_j . This relation is the essence of Janak's theorem.[74].

[7] For non-orthonormal one-particle orbitals, we refer to Eq. B.6. The analogous equation, restricted to orthonormal one-particle states, is provided in Eq. 3.61.

so that

$$\begin{aligned}
\overbrace{\langle\Phi_m|}^{N-1}\,\hat{c}_\alpha\,\overbrace{|\Phi_n\rangle}^{N} &= \langle\pi_\alpha|\psi^{(qp)}_{m,n}\rangle \\
\underbrace{\langle\Phi_m|}_{N}\,\hat{c}^\dagger_\alpha\,\underbrace{|\Phi_n\rangle}_{N-1} &= \langle\psi^{(qp)}_{n,m}|\pi_\alpha\rangle = \Big(\langle\pi_\alpha|\psi^{(qp)}_{n,m}\rangle\Big)^*
\end{aligned} \tag{9.16}$$

Notice the order of the indices of the many-particle states on the right-hand side. One way to memorize it is: *"Because the quasi-particle wave function is the matrix element of the annihilator, the particle number decreases from the wave function of the right index to that of the left index."*

To become familiar with the concept of the quasi-particle wave functions, let me consider two special cases

- In the special case that the many-particle wave function is itself a one-particle state, i.e. $|\Phi_n\rangle = |\varphi\rangle$, there is only one other state which produces a finite quasi-particle wave function, namely the vacuum state $|\Phi_m\rangle = |\mathcal{O}\rangle$. The corresponding quasi-particle wave function is the wave function itself.

$$\psi^{(qp)}_{m,n}(\vec{x}) = \varphi(\vec{x}) \tag{9.17}$$

- In the special case that $|\Phi_n\rangle = |\Phi_{\vec{\sigma}}\rangle$ and $|\Phi_m\rangle = |\Phi_{\vec{\sigma}'}\rangle$ are Slater determinants in a basis of the (ortho-normal) one-particle states $|\varphi_j\rangle$, the quasi-particle wave functions are the one-particle wave functions from which the Slater determinants are made. These one-particle states are retrieved by

$$\varphi_j(\vec{x}) = \begin{cases} \psi^{(qp)}_{\vec{\sigma}',\vec{\sigma}}(\vec{x}) & \text{if } \sigma'_j = \sigma_j - 1 \\ \Big(\psi^{(qp)}_{\vec{\sigma},\vec{\sigma}'}(\vec{x})\Big)^* & \text{if } \sigma'_j = \sigma_j + 1 \end{cases} \tag{9.18}$$

  while all other occupation numbers $\neq j$ are identical between $\vec{\sigma}$ and $\vec{\sigma}$.

Let me now turn towards the general case with an interacting many-electron Hamiltonian. Note that each many-particle Hamiltonian defines a set of quasi-particle wave functions and their energies. In contrast to nearly independent electrons, the quasi-particle wave functions are not orthonormal. The number of quasi-particle wave functions is substantially larger than the one-particle basisset. Consider a finite one-particle basis with M orbitals. The number of Slater determinants with this basis is 2^M because each one-particle orbital can be occupied or not. This is also the size of the corresponding Fock space. Each state in Fock space is, in principle, able to contribute a quasi-particle wave function. Even if we consider only the states with $N+1$ and $N-1$ electrons, we arrive at a huge number given that the number of N-particle Slater-determinants in a one-particle basis of M orbitals is $\frac{M!}{(M-N)!N!}$.[8] In a solid, the quasi-particle states may also form a continuum rather than a discrete set.

There is a sum-rule for the quasi-particle wave functions. The unit operator in the one-particle

[8] For a one-particle basisset with $M = 100$ one-particle states and $N = 10$ electrons there are more than 10^{14} states with $N+1$ and with $N-1$ electrons.

Hilbert space can be expressed in terms of quasi-particle wave functions.

$$\begin{aligned}
\hat{1} &= \int dx \int dx' \, |\vec{x}\rangle \delta(\vec{x}-\vec{x}') \langle \vec{x}'| = \int dx \int dx' \, |\vec{x}\rangle \big[\hat{\psi}^\dagger(\vec{x}), \hat{\psi}(\vec{x}')\big]_+ \langle \vec{x}'| \\
&= \int dx \int dx' \, |\vec{x}\rangle \sum_n P_n \langle \Phi_n | \big[\hat{\psi}^\dagger(\vec{x}), \hat{\psi}(\vec{x}')\big]_+ |\Phi_n\rangle \langle \vec{x}'| \\
&= \int dx \int dx' \, |\vec{x}\rangle \sum_n P_n \Big(\langle \Phi_n | \hat{\psi}^\dagger(\vec{x}) \underbrace{\sum_m |\Phi_m\rangle\langle\Phi_m|}_{=\hat{1}} \hat{\psi}(\vec{x}') |\Phi_n\rangle + \langle \Phi_n | \hat{\psi}(\vec{x}') \underbrace{\sum_m |\Phi_m\rangle\langle\Phi_m|}_{=\hat{1}} \hat{\psi}^\dagger(\vec{x}) |\Phi_n\rangle \Big) \langle \vec{x}'| \\
&= \int dx \int dx' \, |\vec{x}\rangle \sum_{n,m} P_n \Big(\langle \Phi_n | \hat{\psi}^\dagger(\vec{x}) |\Phi_m\rangle\langle\Phi_m| \hat{\psi}(\vec{x}') |\Phi_n\rangle + \langle \Phi_n | \hat{\psi}(\vec{x}') |\Phi_m\rangle\langle\Phi_m| \hat{\psi}^\dagger(\vec{x}) |\Phi_n\rangle \Big) \langle \vec{x}'| \\
&= \int dx \int dx' \, |\vec{x}\rangle \sum_{m,n} P_n \Big(\psi^{(qp)*}_{m,n}(\vec{x}) \psi^{(qp)}_{m,n}(\vec{x}') + \psi^{(qp)*}_{n,m}(\vec{x}) \psi^{(qp)}_{n,m}(\vec{x}') \Big) \langle \vec{x}'| \\
&= \sum_{m,n} P_n \Big(\underbrace{|\psi^{(qp)}_{m,n}\rangle\langle\psi^{(qp)}_{m,n}|}_{\text{filled}} + \underbrace{|\psi^{(qp)}_{n,m}\rangle\langle\psi^{(qp)}_{n,m}|}_{\text{empty}} \Big)
\end{aligned} \tag{9.19}$$

This identity is valid for any many-particle ensemble $\{P_n, |\Phi_n\rangle\}$.

The first term can be identified with the one-particle-reduced density matrix of state $|\Phi_n\rangle$, while the second term describes the unoccupied states.

$$\begin{aligned}
\sum_n P_n \sum_m \psi^{(qp),*}_{m,n}(\vec{x}) \psi^{(qp)}_{m,n}(\vec{x}') &= \sum_{n,m} P_n \langle \Phi_n | \hat{\psi}^\dagger(\vec{x}) |\Phi_m\rangle\langle\Phi_m| \hat{\psi}(\vec{x}') |\Phi_n\rangle \\
&= \sum_n P_n \langle \Phi_n | \hat{\psi}^\dagger(\vec{x}) \hat{\psi}(\vec{x}') |\Phi_n\rangle = \rho^{(1)}(\vec{x}, \vec{x}') \\
\Rightarrow \quad \hat{\rho}^{(1)} &= \sum_{m,n} P_n \big|\psi^{(qp)}_{m,n}\big\rangle\big\langle\psi^{(qp)}_{m,n}\big|
\end{aligned} \tag{9.20}$$

The density matrix is that of an ensemble of many-electron wave functions $|\Phi_n\rangle$ with probabilities P_n. The sum over m extends over a the complete set of eigenstates of the many-particle Hamiltonian, which span the complete Fock space. However, only those with ± 1 electrons contribute a non-zero quasi-particle wave function. Similarly we obtain

$$\begin{aligned}
\sum_{m,n} P_n \psi^{(qm),*}_{n,m}(\vec{x}) \psi^{(qp)}_{n,m}(\vec{x}) &= \sum_{m,n} P_n \langle \Phi_n | \hat{\psi}(\vec{x}') |\Phi_m\rangle\langle\Phi_m| \hat{\psi}^\dagger(\vec{x}) |\Phi_n\rangle \\
&= \sum_n P_n \langle \Phi_n | \hat{\psi}(\vec{x}') \hat{\psi}^\dagger(\vec{x}) |\Phi_n\rangle = \sum_n P_n \langle \Phi_n | \delta(\vec{x}-\vec{x}') - \hat{\psi}^\dagger(\vec{x}) \hat{\psi}(\vec{x}') |\Phi_n\rangle \\
&= \delta(\vec{x}-\vec{x}') - \hat{\rho}^{(1)}(\vec{x}, \vec{x}') \\
\Rightarrow \quad \hat{1} - \hat{\rho}^{(1)} &= \sum_{m,n} P_n \big|\psi^{(qp)}_{n,m}\big\rangle\big\langle\psi^{(qp)}_{n,m}\big|
\end{aligned} \tag{9.21}$$

The two equations allow a spectral decomposition of filled and empty states. Let me define the spectral function

$$\begin{aligned}
\hat{\mathcal{A}}(\epsilon) &\stackrel{\text{def}}{=} \sum_{m,n} P_n \Big(|\psi^{(qp)}_{m,n}\rangle \delta(\epsilon - (E_n - E_m)) \langle \psi^{(qp)}_{m,n}| + |\psi^{(qp)}_{n,m}\rangle \delta(\epsilon - (E_m - E_n)) \langle \psi^{(qp)}_{n,m}| \Big) \\
&= \sum_{m,n} \delta(\epsilon - \epsilon_{n,m}) P_n \Big(\underbrace{|\psi^{(qp)}_{m,n}\rangle\langle\psi^{(qp)}_{m,n}|}_{\text{filled}} + \underbrace{|\psi^{(qp)}_{n,m}\rangle\langle\psi^{(qp)}_{n,m}|}_{\text{empty}} \Big) \\
&= \sum_{m,n} \big|\psi^{(qp)}_{m,n}\big\rangle \delta(\epsilon - \epsilon_{n,m}) \big(P_n + P_m\big) \big\langle\psi^{(qp)}_{m,n}\big|
\end{aligned} \tag{9.22}$$

with the quasiparticle energies defined in Eq. 9.12.

With the quasi-particle amplitudes and energies, the Green's function from Eq. 9.5 has the form.

$$
\begin{aligned}
G^{\mathcal{C}}_{\alpha,\beta}(t,t') &\overset{\text{Eq. 9.5}}{=} \frac{1}{i\hbar}\sum_{n,m} P_n \Big\{ \overbrace{\langle \Phi_n|\hat{c}_{S,\alpha}|\Phi_m\rangle}^{\langle \pi_\alpha|\psi^{(qp)}_{n,m}\rangle} \langle \Phi_m|\hat{c}^\dagger_{S,\beta}|\Phi_n\rangle \theta(t-t') \mathrm{e}^{+\frac{i}{\hbar}(E_n-E_m)(t-t')} \\
&\qquad\qquad - \langle \Phi_n|\hat{c}^\dagger_{S,\beta}|\Phi_m\rangle \langle \Phi_m|\hat{c}_{S,\alpha}|\Phi_n\rangle \theta(t'-t) \mathrm{e}^{-\frac{i}{\hbar}(E_n-E_m)(t-t')} \Big\} \\
&\overset{\text{Eq. 9.16}}{=} \underbrace{\frac{1}{i\hbar}\sum_n P_n \sum_m \langle \pi_\alpha|\psi^{(qp)}_{n,m}\rangle \langle \psi^{(qp)}_{n,m}|\pi_\beta\rangle \theta(t-t') \mathrm{e}^{-\frac{i}{\hbar}(E_m-E_n)(t-t')}}_{\text{electrons added to empty orbitals}} \\
&\quad - \underbrace{\frac{1}{i\hbar}\sum_n P_n \sum_m \langle \pi_\alpha|\psi^{(qp)}_{m,n}\rangle \langle \psi^{(qp)}_{m,n}|\pi_\beta\rangle \theta(t'-t) \mathrm{e}^{-\frac{i}{\hbar}(E_n-E_m)(t-t')}}_{\text{hole added to filled orbitals}}
\end{aligned}
\tag{9.23}
$$

To make the expression more transparent, consider a system in a pure state, that is $P_n = \delta_{n,0}$, where $|\Phi_0\rangle$ is the electronic ground state. In this case, one obtains one quasi-particle amplitude for each one-particle excitation, that is the one-electron addition energy or the electron removal energy.

9.3 Spectral function

The spectral function is a central quantity in Green's-function formalism. Firstly, the spectral function forms the link between different types of Green's function and can be used for their conversion into each other. For time-independent Hamiltonians, it contains the complete physical information of the Green's function. Secondly, the spectral function is a quantity that is directly accessible by spectroscopy experiments as discussed in section 2.5.

In section F.7.2, we discussed the spectral function for an ensemble of Slater determinants. Here we extend this definition to ensembles of general many-particle states. An early review on the spectral function of interacting electrons can be found by Hedin et al.[75]

The total spectral function represents the electron addition and removal energies.

- The electron-addition energies are $\epsilon = E_{N+1} - E_N$ and electron-removal energies are $\epsilon = E_N - E_{N-1}$, so that we can interprete the energies as those of the electron that is added or removed.

- Of all eigenstates of the many-particle Hamiltonian considered, only the states are considered, that have either one electron more or one electron less than the initial state.

- We consider the spectrum of an ensemble of eigenstates of the Hamiltonian $\{|\Phi_n\rangle, P_n\}$, i.e. $[\hat{h} + \hat{W}]|\Phi_n\rangle = |\Phi_n\rangle E_n$

In order to arrive at a general definition of the spectral function, let me work out the following

decomposition of the one-particle reduced density matrix in terms of one-electron energies.

$$
\begin{aligned}
\hat{\rho}^{(1)} &\overset{\text{Eq. } 3.57}{=} \sum_{\alpha,\beta} |\chi_\alpha\rangle \left(\sum_n P_n \langle \Phi_n | \hat{c}^\dagger_{S,\beta} \hat{c}_{S,\alpha} | \Phi_n \rangle \right) \langle \chi_\beta | \\
&= \sum_{\alpha,\beta} |\chi_\alpha\rangle \sum_n P_n \langle \Phi_n | \hat{c}^\dagger_{S,\beta} \underbrace{\sum_m |\Phi_m\rangle \overbrace{\int_{-\infty}^{\infty} d\epsilon\, \delta\Big(\epsilon - (E_n - E_m)\Big)}^{=1} \langle \Phi_m|}_{=\hat{1}} \hat{c}_{S,\alpha} | \Phi_n \rangle \langle \chi_\beta | \\
&= \int_{-\infty}^{\infty} d\epsilon \sum_{\alpha,\beta} |\chi_\alpha\rangle \underbrace{\left\{ \sum_{n,m} P_n \underbrace{\langle \Phi_n | \hat{c}^\dagger_{S,\beta} | \Phi_m \rangle}_{=0 \text{ for } N_n \neq N_m + 1} \delta\Big(\epsilon - \underbrace{(E_n - E_m)}_{N_n = N_m + 1}\Big) \underbrace{\langle \Phi_m | \hat{c}_{S,\alpha} | \Phi_n \rangle}_{=0 \text{ for } N_m \neq N_n - 1} \right\}}_{\mathcal{A}^{(h)}_{\alpha,\beta}(\epsilon)} \langle \chi_\beta | \\
&= \int_{-\infty}^{\infty} d\epsilon \sum_{\alpha,\beta} |\chi_\alpha\rangle \mathcal{A}^{(h)}_{\alpha,\beta}(\epsilon) \langle \chi_\beta |
\end{aligned}
\tag{9.24}
$$

where

$$
\mathcal{A}^{(h)}_{\alpha,\beta}(\epsilon) \overset{\text{def}}{=} \sum_{m,n} P_n \langle \Phi_n | \hat{c}^\dagger_{S,\beta} | \Phi_m \rangle \langle \Phi_m | \hat{c}_{S,\alpha} | \Phi_n \rangle \delta\Big(\epsilon - (E_n - E_m)\Big) \tag{9.25}
$$

is the spectral function for **hole addition**. Editor: The naming is inconvenient, because one thinks of the electrons that are present, before it is removed. Therefore the name *"electron spectral function"* would be better that *"spectral function for hole addition"*. The naming *electron* or *hole* spectral function, is confusing, because the electron spectral function probes the empty states and the hole spectral function probes the filled states, i.e. the electrons. The names make sense because they reflect the quasi-particle, electron or hole, which is that is added to the system.

Only states $|\Phi_m\rangle$ contribute to the spectral function for hole addition Eq. 9.25, that have one electron less than the state $|\Phi_n\rangle$ in the ensemble, i.e. $N_m = N_n - 1$. The spectral function has peaks at the **energies of electrons that can be removed from the system**, that is at $\epsilon = E_n - E_m$ with $N_n = N_m + 1$. The removal of an electron can also be described as the addition of a hole, which explains the name *"hole-addition spectral function"*. The name is confusing because it also describes an electron, which is present in the system, before it is removed.

We arrived at a spectral decomposition of the one-particle-reduced density matrix. This gives us access only to the occupied part of the spectrum. Let us now consider the empty part of the spectrum by decomposing $\hat{1} - \hat{\rho}$. The derivation is analogous to the one for the filled states. I use the identity

$$
\begin{aligned}
\hat{1} &= \sum_{\alpha,\beta} |\chi_\alpha\rangle \langle \pi_\alpha | \pi_\beta \rangle \langle \chi_\beta | \overset{\text{Eq. } B.16}{=} \sum_{\alpha,\beta} |\chi_\alpha\rangle [\hat{c}^\dagger_\alpha, \hat{c}_\beta]_+ \langle \chi_\beta | \\
&= \sum_{\alpha,\beta} |\chi_\alpha\rangle \sum_n P_n \langle \Phi_n | [\hat{c}^\dagger_\alpha, \hat{c}_\beta]_+ | \Phi_n \rangle \langle \chi_\beta |
\end{aligned}
\tag{9.26}
$$

which is obvious for an orthonormal basisset. For a non-orthonormal basisset, the anticommutator is more complicated, and is given by the overlap of the projector function, $[\hat{c}^\dagger_\alpha, \hat{c}_\beta]_+ \overset{\text{Eq. } B.16}{=} \langle \pi_\alpha | \pi_\beta \rangle$, respectively in the inverse overlap of the orbitals $|\chi_\alpha\rangle$.

The one-particle-reduced density matrix of the empty states is

$$\begin{aligned}
\hat{1} - \hat{\rho}^{(1)} &\overset{\text{Eq. 3.57}}{=} \sum_{\alpha,\beta} |\chi_\alpha\rangle \left(\sum_n P_n \langle\Phi_n| \left([\hat{c}_{S,\alpha}, \hat{c}_{S,\beta}]_+ - \hat{c}^\dagger_{S,\beta} \hat{c}_{S,\alpha} \right) |\Phi_n\rangle \right) \langle\chi_\beta| \\
&= \sum_{\alpha,\beta} |\chi_\alpha\rangle \left(\sum_n P_n \langle\Phi_n| \hat{c}_{S,\alpha} \hat{c}^\dagger_{S,\beta} |\Phi_n\rangle \langle\chi_\beta| \right. \\
&= \sum_{\alpha,\beta} |\chi_\alpha\rangle \sum_n P_n \langle\Phi_n| \hat{c}_{S,\alpha} \underbrace{\sum_m |\Phi_m\rangle \overbrace{\int_{-\infty}^{\infty} d\epsilon\, \delta\Big(\epsilon - (E_m - E_n)\Big)}^{=1} \langle\Phi_m|}_{=\hat{1}} \hat{c}^\dagger_{S,\beta} |\Phi_n\rangle \langle\chi_\beta| \\
&= \int_{-\infty}^{\infty} d\epsilon \sum_{\alpha,\beta} |\chi_\alpha\rangle \underbrace{\left\{ \sum_{n,m} P_n \langle\Phi_n| \hat{c}_{S,\alpha} |\Phi_m\rangle \delta\Big(\epsilon - \underbrace{(E_m - E_n)}_{N_m = N_n + 1}\Big) \langle\Phi_m| \hat{c}^\dagger_{S,\beta} |\Phi_n\rangle \right\}}_{\mathcal{A}^{(e)}_{\alpha,\beta}(\epsilon)} \langle\chi_\beta| \\
&= \int_{-\infty}^{\infty} d\epsilon \sum_{\alpha,\beta} |\chi_\alpha\rangle \mathcal{A}^{(e)}_{\alpha,\beta}(\epsilon) \langle\chi_\beta| \qquad (9.27)
\end{aligned}$$

where

$$\mathcal{A}^{(e)}_{\alpha,\beta}(\epsilon) \overset{\text{def}}{=} \sum_{m,n} P_n \langle\Phi_n| \hat{c}_{S,\alpha} |\Phi_m\rangle \langle\Phi_m| \hat{c}^\dagger_{S,\beta} |\Phi_n\rangle \delta\Big(\epsilon - (E_m - E_n)\Big) \qquad (9.28)$$

is the **spectral functions for electron addition**. The energies were chosen such that they refer to energies of electrons.

After interchanging the indices m and n in the hole spectral function, the electron and hole spectral function can be combined into the **total spectral function**

$$\begin{aligned}
\mathcal{A}^{\text{tot}}_{\alpha,\beta}(\epsilon) &\overset{\text{def}}{=} \mathcal{A}^{(e)}_{\alpha,\beta}(\epsilon) + \mathcal{A}^{(h)}_{\alpha,\beta}(\epsilon) \\
&= \sum_{m,n} (P_n + P_m) \langle\Phi_n| \hat{c}_{S,\alpha} |\Phi_m\rangle \langle\Phi_m| \hat{c}^\dagger_{S,\beta} |\Phi_n\rangle \delta\Big(\epsilon - (E_m - E_n)\Big) \qquad (9.29)
\end{aligned}$$

Thermal ensembles: The expressions for the spectral function given above are very general and hold for arbitrary ensembles. For a thermal ensemble, such as the grand canonical ensemble, the relations can be simplified:

Electron and hole spectral functions can be recovered from the total spectral function with the help of the Fermi distribution function. The probabilities in the grand ensemble are

$$P_n = \mathrm{e}^{-\beta(E_n - \mu N_n - \Omega_{T,\mu})} \qquad (9.30)$$

where grand potential $\Omega_{T,\mu} = -k_B T \ln(Z_{T,\mu})$ accounts for the normalization of the probability distribution. The electron and hole spectral functions can be recovered from the total spectral function by including a factor of the following kind:

$$\frac{P_n}{P_n + P_m} = \frac{1}{1 + \mathrm{e}^{\beta(E_{n,m} - \mu N_{n,m})}} = f_{T,\mu}(E_{n,m}) \qquad (9.31)$$

where $E_{n,m} = E_n - E_m$ and $N_{n,m} = N_n - N_m$. Because this factor depends only on the excitation energies, it can be taken out of the sum over many-particle states in Eq. 9.29. This allows one to obtain the electron and hole spectral functions from the total spectral function by multiplication with the Fermi function $f_{T,\mu}(\epsilon)$ or $1 - f_{T,\mu}(\epsilon)$. It is surprising that the Fermi distribution function, which has been obtained as equilibrium occupation of the non-interacting electron gas, also selects the filled states out of a spectral function of an interacting system.

Thus, we obtain

SPECTRAL FUNCTIONS

The spectral function is

$$\mathcal{A}^{\text{tot}}_{\alpha,\beta}(\epsilon) \overset{\text{Eq. 9.29}}{=} \sum_{m,n}(P_n + P_m)\langle\Phi_n|\hat{c}_{S,\alpha}|\Phi_m\rangle\langle\Phi_m|\hat{c}^\dagger_{S,\beta}|\Phi_n\rangle\delta\Big(\epsilon - (E_m - E_n)\Big) \tag{9.32}$$

The terms proportional to P_n are the electron addition energies. while the terms proportional to P_m are the hole addition energies.
Specifically, for thermal ensembles (grand ensemble), the electron and hole contributions can be obtained with the help of the Fermi-distribution function.

$$\mathcal{A}^{(e)}_{\alpha,\beta}(\epsilon) = \mathcal{A}^{\text{tot}}_{\alpha,\beta}(\epsilon)\Big(1 - f_{T,\mu}(\epsilon)\Big) \tag{9.33}$$

$$\mathcal{A}^{(h)}_{\alpha,\beta}(\epsilon) = \mathcal{A}^{\text{tot}}_{\alpha,\beta}(\epsilon) f_{T,\mu}(\epsilon) \tag{9.34}$$

The hole contribution describes the filled states and the electron distribution describes the empty part of the spectrum.

Properties: Let me summarize some properties of the spectral functions.

- the spectral function $\hat{\mathcal{A}}(\epsilon)$ is an operator in the one-particle Hilbert space. One can also construct spectral functions for two-particle excitations, which would be operators in the two-particle Hilbert space. However, these spectral functions differ from the spectral functions for one-particle excitations discussed here.
- The spectral functions are hermitian, which is seen from the defining equations Eq. 9.28 and 9.25.
- The integral of the hole spectral function $\hat{A}^{(h)}$ is the one-particle-reduced density matrix.

$$\int d\epsilon\, f_{T,\mu}(\epsilon)\mathcal{A}^{(tot)}_{\alpha,\beta}(\epsilon) \overset{\text{Eq. 9.34}}{=} \int d\epsilon\, \mathcal{A}^{(h)}_{\alpha,\beta}(\epsilon) \overset{\text{Eq. 9.25}}{=} \sum_n P_n\langle\Phi_n|\hat{c}^\dagger_{S,\beta}\hat{c}_{S,\alpha}|\Phi_n\rangle \overset{\text{Eq. 3.56}}{=} \rho^{(1)}_{\alpha,\beta} \tag{9.35}$$

- The total spectral function $\hat{\mathcal{A}}^{(tot)}(\epsilon)$ obeys the sum rule

$$\int d\epsilon\, \mathcal{A}^{(tot)}_{\alpha,\beta}(\epsilon) = [\hat{c}^\dagger_{S,\beta}, \hat{c}_{S,\alpha}]_+ \tag{9.36}$$

  For an orthonormal one-particle basisset, the anticommutator has the usual form $[\hat{c}^\dagger_\alpha, \hat{c}_\beta]_+ = \delta_{\alpha,\beta}$. For a non-orthonormal basisset, the relation is more complex, i.e. $[\hat{c}^\dagger_{S,\beta}, \hat{c}_{S,\alpha}]_+ \overset{\text{Eq. B.16}}{=} \langle\pi_\beta|\pi_\alpha\rangle$.
- The peak positions of the spectral function are determined by the Hamiltonian $\hat{h} + \hat{W}$, respectively the differences $E_m - E_n$ of its eigenvalues. They do not depend on temperature or chemical potential. The quantities, that change with the thermodynamic state, are the intensities of the spectral peaks. The intensities are governed by the probabilities $\{P_n\}$.

  This is analogous to the spectrum in the average-phase approximation and it differs from the mean-field approximation on the Hartree-Fock level. As discussed in section F.7.2 on p. 515, the peak positions shift in the mean-field approximation, due to the change of the Fock operator, while the intensities of the bands remain unchanged. However, see also Fig. F.5 on p. 516, which shows how the true spectral function can produce an apparent behavior of the mean-field spectral function.

9.3.1 Green's function from spectral function

We have introduced the spectral function without any reference to the Green's functions. I will show in the following, how one can obtain the Green's function from the spectral function.

I start with the Green's function in the Lehmann representation Eq. 9.5

$$\begin{aligned} G^{\mathcal{C}}_{\alpha,\beta}(t,t') &\overset{\text{Eq. 9.5}}{=} \frac{1}{i\hbar}\sum_{n,m} P_n\Big\{\underbrace{\langle\Phi_n|\hat{c}_{S,\alpha}|\Phi_m\rangle\langle\Phi_m|\hat{c}^\dagger_{S,\beta}|\Phi_n\rangle\theta(t-t')\mathrm{e}^{+\frac{i}{\hbar}(E_n-E_m)(t-t')}}_{\text{electrons added to empty states}} \\ &\qquad - \underbrace{\langle\Phi_n|\hat{c}^\dagger_{S,\beta}|\Phi_m\rangle\langle\Phi_m|\hat{c}_{S,\alpha}|\Phi_n\rangle\theta(t'-t)\mathrm{e}^{-\frac{i}{\hbar}(E_n-E_m)(t-t')}}_{\text{holes added to filled states}}\Big\} \\ &= \frac{1}{i\hbar}\int d\epsilon \underbrace{\left[\sum_{n,m} P_n\Big\{\langle\Phi_n|\hat{c}_{S,\alpha}|\Phi_m\rangle\langle\Phi_m|\hat{c}^\dagger_{S,\beta}|\Phi_n\rangle\delta(\epsilon-(E_m-E_n))\right]}_{\mathcal{A}^{(e)}_{\alpha,\beta}(\epsilon)=\mathcal{A}^{(tot)}_{\alpha,\beta}(\epsilon)(1-f_{T,\mu}(\epsilon))} \theta(t-t')\mathrm{e}^{-\frac{i}{\hbar}\epsilon(t-t')} \\ &- \frac{1}{i\hbar}\int d\epsilon \underbrace{\left[\sum_{n,m} P_n\langle\Phi_n|\hat{c}^\dagger_{S,\beta}|\Phi_m\rangle\langle\Phi_m|\hat{c}_{S,\alpha}|\Phi_n\rangle\delta(\epsilon+(E_m-E_n))\right]}_{\mathcal{A}^{(h)}_{\alpha,\beta}(\epsilon)=\mathcal{A}^{(tot)}_{\alpha,\beta}(\epsilon)f_{T,\mu}(\epsilon)} \theta(t'-t)\mathrm{e}^{-\frac{i}{\hbar}\epsilon(t-t')}\Big\} \end{aligned} \tag{9.37}$$

which leads to the following expression for the Green's function

CONTOUR GREEN'S FUNCTION FROM SPECTRAL FUNCTION

The Green's function for a time-independent Hamiltonian can be expressed by the spectral function as

$$G^{\mathcal{C}}_{\alpha,\beta}(t,t') = \frac{1}{i\hbar}\int_{-\infty}^{\infty} d\epsilon\, \mathcal{A}^{(tot)}_{\alpha,\beta}(\epsilon)\Big([1-f_{T,\mu}(\epsilon)]\theta(t-t') - f_{T,\mu}(\epsilon)\theta(t'-t)\Big)\mathrm{e}^{-\frac{i}{\hbar}\epsilon(t-t')} \tag{9.38}$$

and in the energy representation

$$\begin{aligned} G^{\mathcal{C}}_{\alpha,\beta}(\hbar\omega) &\overset{\text{def}}{=} \lim_{\eta\to 0^+}\int_{-\infty}^{\infty} dt\, \mathrm{e}^{\frac{i}{\hbar}(\hbar\omega t + i\eta|t|)} G^{\mathcal{C}}_{\alpha,\beta}(t,0) \quad \text{for } \hbar\omega\in\mathbb{R} \\ &= \lim_{\eta\to 0^+}\int_{-\infty}^{\infty} d\epsilon\, \mathcal{A}^{(tot)}_{\alpha,\beta}(\epsilon)\left[\frac{1-f_{T,\mu}(\epsilon)}{\hbar\omega-\epsilon+i\eta} + \frac{f_{T,\mu}(\epsilon)}{\hbar\omega-\epsilon-i\eta}\right] \end{aligned} \tag{9.39}$$

The time integration proceeds along the real-time axis in the positive direction.

The expression above is valid for arbitrarily strong interaction. Nevertheless, it looks like the expression for the non-interacting Green's function. All the many-particle effects relevant for the Green's function are encapsulated in the spectral function.

The Green's function is a unique functional of the spectral function, which forms the basis of the spectral-density functional approach (SDFT)[76].

While the spectral functions have been motivated by a Fourier transform of the Green's function along the real axis only, the Green's function can be expressed by the spectral functions for the entire contour.

Electron spectral function from Green's function: Eqs. 9.39 allows us to extract the spectral function from the Green's function. Below, I will use that the spectral function is hermitian. Editor: Check, whether that is true for the entire contour or only along the real axis. In

contrast, the energy-dependent Green's function is not hermitian.

$$\begin{aligned}
G^{\mathcal{C}}_{\alpha,\beta}(\hbar\omega) - G^{\mathcal{C},*}_{\beta,\alpha}(\hbar\omega) &\overset{\text{Eq. 9.39}}{=} \lim_{\eta\to 0^+}\int_{-\infty}^{\infty} d\epsilon\ \underbrace{\mathcal{A}^{(tot)}_{\alpha,\beta}(\epsilon)}_{=\mathcal{A}^{(tot),*}_{\beta,\alpha}(\epsilon)} \\
&\quad\times\left[\frac{1-f_{T,\mu}(\epsilon)}{\hbar\omega-\epsilon+i\eta}+\frac{f_{T,\mu}(\epsilon)}{\hbar\omega-\epsilon-i\eta}-\frac{1-f_{T,\mu}(\epsilon)}{\hbar\omega-\epsilon-i\eta}-\frac{f_{T,\mu}(\epsilon)}{\hbar\omega-\epsilon+i\eta}\right] \\
&= \lim_{\eta\to 0^+}\int_{-\infty}^{\infty} d\epsilon\ \underbrace{\mathcal{A}^{(tot)}_{\alpha,\beta}(\epsilon)}_{=\mathcal{A}^{(tot),*}_{\beta,\alpha}(\epsilon)}\left[\frac{1-2f_{T,\mu}(\epsilon)}{\hbar\omega-\epsilon+i\eta}-\frac{1-2f_{T,\mu}(\epsilon)}{\hbar\omega-\epsilon-i\eta}\right] \\
&= \int_{-\infty}^{\infty} d\epsilon\ \mathcal{A}^{(tot)}_{\alpha,\beta}(\epsilon)\Big(1-2f_{T,\mu}(\epsilon)\Big)\underbrace{\lim_{\eta\to 0^+}\frac{-2i\eta}{(\hbar\omega-\epsilon)^2+\eta^2}}_{-2i\pi\delta(\hbar\omega-\epsilon)} \\
&= -2i\pi\Big(1-2f_{T,\mu}(\hbar\omega)\Big)\mathcal{A}^{(tot)}_{\alpha,\beta}(\hbar\omega) \\
\Rightarrow\quad \mathcal{A}^{(tot)}_{\alpha,\beta}(\hbar\omega) &= \frac{-1}{2\pi i}\frac{1}{1-2f_{T,\mu}(\hbar\omega)}\Big(G^{\mathcal{C}}_{\alpha,\beta}(\hbar\omega)-G^{\mathcal{C},*}_{\beta,\alpha}(\hbar\omega)\Big) \qquad (9.40)
\end{aligned}$$

We exploited

$$\lim_{\eta\to 0}\frac{1}{\pi}\frac{\eta}{x^2+\eta^2}=\delta(x) \qquad (9.41)$$

Thus, we obtain the following relation between Green's function and spectral function.

SPECTRAL FUNCTION AND CAUSAL GREEN'S FUNCTION

For a grand canonical ensemble of fermions, the total spectral function $\hat{A}^{(tot)}$ is obtained from

$$\hat{\mathcal{A}}^{(tot)}(\hbar\omega)=\frac{1}{1-2f_{T,\mu}(\hbar\omega)}\left(-\frac{1}{2\pi i}\left[\hat{G}^{\mathcal{C}}(\hbar\omega)-\hat{G}^{\mathcal{C},\dagger}(\hbar\omega)\right]\right) \qquad (9.42)$$

Spectral function for non-interacting electrons and holes: In order to develop some understanding for the spectral functions it is helpful to determine the spectral function for a non-interacting system. For a non-interacting system the eigenstates $|\vec{\sigma}\rangle$ of the Hamiltonian can be build up by the one-particle eigenstates $|\varphi_n\rangle$ of the Hamiltonian and the corresponding creation operators $\hat{a}^\dagger_{S,n}$.

$$\begin{aligned}
\mathcal{A}^{(tot)}_{\alpha,\beta}(\epsilon) &\overset{\text{Eq. 9.32}}{=} \sum_{m,n}\langle\pi_\alpha|\varphi_m\rangle\sum_{\vec{\sigma},\vec{\sigma'}}\Big(P_{\vec{\sigma}}+P_{\vec{\sigma'}}\Big)\langle\vec{\sigma}|\hat{a}_{S,m}|\vec{\sigma'}\rangle\langle\vec{\sigma'}|\hat{a}^\dagger_{S,n}|\vec{\sigma}\rangle \\
&\quad\times\delta\Big(\epsilon-(E_{\vec{\sigma'}}-E_{\vec{\sigma}})\Big)\langle\varphi_n|\pi_\beta\rangle \qquad (9.43)
\end{aligned}$$

For each state $|\vec{\sigma}\rangle$, only one state $|\sigma'\rangle$ contributes, namely $|\sigma'\rangle=\hat{a}^\dagger_n|\vec{\sigma}\rangle$. With this selection, the matrix elements are

$$\begin{aligned}
\langle\vec{\sigma'}|\hat{a}^\dagger_n|\vec{\sigma}\rangle &\overset{|\vec{\sigma'}\rangle=\hat{a}^\dagger_n|\vec{\sigma}\rangle}{=} (1-\sigma_n) \\
\langle\vec{\sigma}|\hat{a}_m|\vec{\sigma'}\rangle &\overset{|\vec{\sigma'}\rangle=\hat{a}^\dagger_n|\vec{\sigma}\rangle}{=} (1-\sigma_m)\delta_{m,n} \qquad (9.44)
\end{aligned}$$

The energy difference is

$$E_{\vec{\sigma'}}\overset{|\vec{\sigma'}\rangle=\hat{a}^\dagger_n|\vec{\sigma}\rangle}{=}E_{\vec{\sigma}}+\epsilon_n \qquad (9.45)$$

and the probability of this state is

$$P_{\vec{\sigma}'} \overset{|\vec{\sigma}'\rangle=\hat{a}_n^\dagger|\vec{\sigma}\rangle}{=} P_{\vec{\sigma}} e^{-\beta(\epsilon_n-\mu)} \tag{9.46}$$

This yields[9]

$$\begin{aligned}
\mathcal{A}^{(tot)}_{\alpha,\beta}(\epsilon) &\overset{\text{Eq. 9.32}}{=} \sum_{m,n}\langle\pi_\alpha|\varphi_m\rangle \sum_{\vec{\sigma}} P_{\vec{\sigma}}\Big(1+e^{-\beta(\epsilon_n-\mu)}\Big)(1-\sigma_m)\delta_{m,n}(1-\sigma_n) \\
&\quad \times\delta\Big(\epsilon-\epsilon_n\Big)\langle\varphi_n|\pi_\beta\rangle \\
&= \sum_n \langle\pi_\alpha|\varphi_n\rangle \underbrace{\Big(\sum_{\vec{\sigma}} P_{\vec{\sigma}}(1-\sigma_n)\Big)}_{1-f_{T,\mu}(\epsilon_n)} \underbrace{\Big(1+e^{-\beta(\epsilon_n-\mu)}\Big)}_{1/[1-f_{T,\mu}(\epsilon_n)]} \times\delta\Big(\epsilon-\epsilon_n\Big)\langle\varphi_n|\pi_\beta\rangle \\
&= \sum_n \langle\pi_\alpha|\varphi_n\rangle\delta\Big(\epsilon-\epsilon_n\Big)\langle\varphi_n|\pi_\beta\rangle \\
&= D_{\alpha,\beta}(\epsilon)
\end{aligned} \tag{9.48}$$

Thus, we obtain the one-particle density of states $D_{\alpha,\beta} = \sum_n \langle\pi_\alpha|\varphi_n\rangle\delta(\epsilon-\epsilon_n)\langle\varphi_n|\pi_\beta\rangle$.

SPECTRAL FUNCTION FOR NON-INTERACTING PARTICLES

For non-interacting electrons the spectral function is identical to the one-particle density of states.

$$\mathcal{A}^{\text{tot}}_{\alpha,\beta}(\epsilon) \overset{\text{Eq. 9.48}}{=} D_{\alpha,\beta}(\epsilon) \tag{9.49}$$

9.4 Physical content of the spectral function

Editor: Discuss here the spectral function. The relation to the band structure, such as self energy shift and life time broadening. The double (triple) peak structure (donor and acceptor energies). Discuss the spectral function for a system undergoing period doubling, such as antiferromagnetism.(Band structure in the original basis).

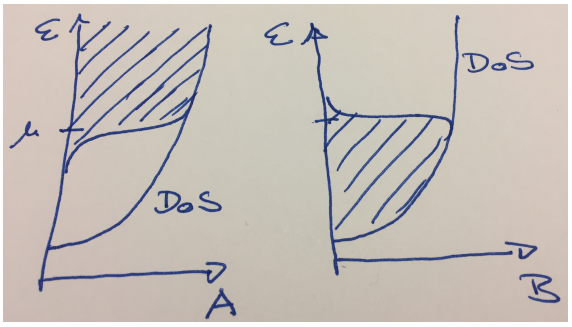

Sketch of the complete spectral function $\text{Tr}[A(\epsilon)]$ for electrons and $\text{Tr}[B(\epsilon)]$ for holes for a free-electron gas. The shaded regions show the spectral functions, which are equal to the density of states multiplied with $1-f_{T,\mu}(\epsilon)$ for the electron spectral function and with $f_{T,\mu}(\epsilon)$ for the hole spectral function.

[9]

$$1-f = 1-\frac{1}{1+e^{\beta(\epsilon-\mu)}} = \frac{e^{\beta(\epsilon-\mu)}}{1+e^{\beta(\epsilon-\mu)}} = \frac{1}{1+e^{-\beta(\epsilon-\mu)}} \Rightarrow 1+e^{-\beta(\epsilon-\mu)} = \frac{1}{1-f} \tag{9.47}$$

9.5 Attempt to generalize the spectral function to the time domain

Editor: This section is under construction and not meant for reading!

Consider an ensemble of time-dependent many-particle wave functions $|\Phi_n(t)\rangle$ and time-independent probabilities P_n. The many-particle wave functions satisfy the time-dependent Schrödinger equation and they are chosen wrog orthonormal at time $t = 0$ i.e. $\langle\Phi_m(0)|\Phi_n(0)\rangle = \delta_{m,n}$. Because the time evolution is unitary, the orthonormality is valid for all (real-valued) times.

With a subscript S, I indicate Schrödinger operators, while Heisenberg operators are indicated by a subscript H. The indices α, β refer to one-particle states.

Let me define the two-time spectral function

$$\begin{aligned}
\mathcal{A}^{tot}_{\alpha,\beta}(t,t') &\stackrel{?}{=} \sum_{m,n}(P_m + P_n)\langle\Phi_n(t)|\hat{c}_{S,\alpha}|\Phi_m(t)\rangle\langle\Phi_m(t')|\hat{c}^\dagger_{S,\beta}|\Phi_n(t')\rangle \\
&= \sum_m P_m\Big(\langle\Phi_n(t)|\hat{c}_{S,\alpha}|\Phi_m(t)\rangle\langle\Phi_m(t')|\hat{c}^\dagger_{S,\beta}|\Phi_n(t')\rangle + \langle\Phi_n(t')|\hat{c}^\dagger_{S,\beta}|\Phi_m(t')\rangle\langle\Phi_m(t)|\hat{c}_{S,\alpha}|\Phi_n(t)\rangle\Big) \\
&= \mathrm{Tr}\Big[\hat{\rho}^W\Big(\hat{c}_{H,\alpha}(t)\hat{c}^\dagger_{H,\beta}(t') + \hat{c}^\dagger_{H,\beta}(t')\hat{c}_{H,\alpha}(t)\Big)\Big] \\
&= \mathrm{Tr}\Big(\hat{\rho}^W\Big[\hat{c}_{H,\alpha}(t), \hat{c}^\dagger_{H,\beta}(t')\Big]_+\Big)
\end{aligned} \tag{9.50}$$

An ensemble $\{P_n, |\Phi_n(0)\rangle\}$ is defined at a specific time, which we choose at time zero. The von-Neumann density matrix is

$$\hat{\rho}^W = \sum_n |\Phi_n(0)\rangle P_n \langle\Phi_n(0)| \tag{9.51}$$

The time-dependent Schrödinger equation is used to determine the full time dependence of the many-particle wave functions $|\Phi_n(t)\rangle$.

The equation is (hopefully) valid for fermions. For bosons, the anti-commutator is replaced by the commutator.

The spectral function can be written as operator in the one-particle Hilbert space as

$$\hat{\mathcal{A}}(t,t') = \sum_{\alpha,\beta} |\chi_\alpha\rangle \mathcal{A}_{\alpha,\beta}(t,t')\langle\chi_\beta| \tag{9.52}$$

$$\begin{aligned}
G^{\mathcal{C}}_{\alpha,\beta}(t,t') &\stackrel{\text{Eq. 7.16}}{=} \frac{1}{i\hbar}\mathrm{Tr}\Big\{\hat{\rho}^{(W)}_{T,\mu}\mathcal{T}_{\mathcal{C}}\hat{c}_{H,\alpha}(t)\hat{c}^+_{H,\beta}(t')\Big\} \\
&= \frac{1}{i\hbar}\mathrm{Tr}\Big\{\hat{\rho}^{(W)}_{T,\mu}\Big(\theta(t-t')\hat{c}_{H,\alpha}(t)\hat{c}^+_{H,\beta}(t') - \underbrace{\theta(t'-t)}_{1-\theta(t-t')}\hat{c}^+_{H,\beta}(t')\hat{c}_{H,\alpha}(t)\Big)\Big\} \\
G^{\mathcal{C}}_{\beta,\alpha}(t',t) &= \frac{1}{i\hbar}\mathrm{Tr}\Big\{\hat{\rho}^{(W)}_{T,\mu}\Big(\theta(t'-t)\hat{c}_{H,\beta}(t')\hat{c}^+_{H,\alpha}(t) - \theta(t-t')\hat{c}^+_{H,\alpha}(t)\hat{c}_{H,\beta}(t')\Big)\Big\} \\
\big(G^{\mathcal{C}}_{\beta,\alpha}(t',t)\big)^* &\stackrel{t\in R}{=} \frac{-1}{i\hbar}\mathrm{Tr}\Big\{\hat{\rho}^{(W)}_{T,\mu}\Big(\theta(t'-t)\hat{c}_{H,\alpha}(t)\hat{c}^+_{H,\beta}(t') - \theta(t-t')\hat{c}^+_{H,\beta}(t')\hat{c}_{H,\alpha}(t)\Big)\Big\} \\
G^{\mathcal{C}}_{\alpha,\beta}(t,t') - \big(G^{\mathcal{C}}_{\beta,\alpha}(t',t)\big)^* &= \frac{1}{i\hbar}\mathrm{Tr}\Big\{\hat{\rho}^{(W)}_{T,\mu}\Big(\hat{c}_{H,\alpha}(t)\hat{c}^+_{H,\beta}(t') - \hat{c}^+_{H,\beta}(t')\hat{c}_{H,\alpha}(t)\Big)\Big\} \\
G^{\mathcal{C}}_{\alpha,\beta}(t,t') + \big(G^{\mathcal{C}}_{\beta,\alpha}(t',t)\big)^* &= \mathrm{sgn}(t-t')\frac{1}{i\hbar}\mathrm{Tr}\Big\{\hat{\rho}^{(W)}_{T,\mu}\Big(\hat{c}_{H,\alpha}(t)\hat{c}^+_{H,\beta}(t') + \hat{c}^+_{H,\beta}(t')\hat{c}_{H,\alpha}(t)\Big)\Big\}
\end{aligned} \tag{9.53}$$

$$\Big(G^{\mathcal{C}}_{\alpha,\beta}(t,t') + \big(G^{\mathcal{C}}_{\beta,\alpha}(t',t)\big)^*\Big)\mathrm{sgn}(t-t') = \frac{1}{i\hbar}\mathrm{Tr}\Big\{\hat{\rho}^{(W)}_{T,\mu}\Big[\hat{c}_{H,\alpha}(t),\hat{c}^+_{H,\beta}(t')\Big]_+\Big\}$$
$$+++ = -\frac{1}{i\hbar}\mathrm{Tr}\Big\{\hat{\rho}^{(W)}_{T,\mu}\hat{c}^+_{H,\beta}(t')\hat{c}_{H,\alpha}(t)\Big\} + \theta(t-t')\frac{1}{i\hbar}\mathrm{Tr}\Big\{\hat{\rho}^{(W)}_{T,\mu}\big[\hat{c}_{H,\alpha}(t),\hat{c}^+_{H,\beta}(t')\big]_+\Big\} \tag{9.54}$$

Identity with previous definitions for time-invariant problems

Firstly, I need to verify that for the time-translational invariant case, one obtains the definition of the energy-dependent spectral function. I use $|\Phi_n(t)\rangle = |\Phi_n(0)\rangle \mathrm{e}^{-\frac{i}{\hbar}E_n t}$.

$$\begin{aligned}
\mathcal{A}^{tot}_{\alpha,\beta}(\epsilon) &\stackrel{?}{=} \int_{-\infty}^{\infty}\frac{dt'}{2\pi\hbar}\,\mathcal{A}^{tot}_{\alpha,\beta}(t',t)\mathrm{e}^{\frac{i}{\hbar}\epsilon(t'-t)-\frac{\eta}{\hbar}|t'-t|}\\
&= \sum_{m,n}(P_m+P_n)\langle\Phi_n(0)|\hat{c}_{S,\alpha}|\Phi_m(0)\rangle\langle\Phi_m(0)|\hat{c}^\dagger_{S,\beta}|\Phi_n(0)\rangle\\
&\quad\times\underbrace{\int_{-\infty}^{\infty}\frac{dt'}{2\pi\hbar}\,\mathrm{e}^{-\frac{i}{\hbar}\Big[(E_m-E_n-\epsilon)(t'-t)-i\eta|t'-t|\Big]}}_{\frac{1}{\frac{i}{\hbar}\Big[E_m-E_n-\epsilon-i\eta\Big]}-\frac{1}{\frac{i}{\hbar}\Big[E_m-E_n-\epsilon+i\eta|}}\\
&= \sum_{m,n}(P_m+P_n)\langle\Phi_n(0)|\hat{c}_{S,\alpha}|\Phi_m(0)\rangle\langle\Phi_m(0)|\hat{c}^\dagger_{S,\beta}|\Phi_n(0)\rangle\\
&\quad\times\frac{1}{2\pi\hbar}\Big(-i\hbar\Big)\left(\frac{(E_m-E_n-\epsilon)+i\eta}{(E_m-E_n-\epsilon)^2+\eta^2}-\frac{E_m-E_n-\epsilon-i\eta}{(E_m-E_n-\epsilon)+\eta^2}\right)\\
&= \sum_{m,n}(P_m+P_n)\langle\Phi_n(0)|\hat{c}_{S,\alpha}|\Phi_m(0)\rangle\langle\Phi_m(0)|\hat{c}^\dagger_{S,\beta}|\Phi_n(0)\rangle\frac{1}{2\pi\hbar}\underbrace{\frac{2\hbar\eta}{(E_m-E_n-\epsilon)^2+\eta^2}}_{\to 2\pi\hbar\delta\left(\epsilon-(E_n-E_m)\right)}\\
&= \sum_{m,n}(P_m+P_n)\langle\Phi_n(0)|\hat{c}_{S,\alpha}|\Phi_m(0)\rangle\langle\Phi_m(0)|\hat{c}^\dagger_{S,\beta}|\Phi_n(0)\rangle\delta\big(\epsilon-(E_n-E_m)\big)
\end{aligned} \tag{9.55}$$

This expression is identical to Eq. 9.32 on p. 274, what had to be shown.

Spectral functions and Green's functions

The energy-dependent spectral function has the convenient property that all Green's functions can be expressed as convolutions of the spectral function. Is this true also for time-dependent Hamiltonians, and time-dependent spectral functions?

The contour ordered Green's function $G^{\mathcal{C}}_{\alpha,\beta}(t,t')$, Eq. 7.16, is obtained from the spectral function on the contour ...

9.6 Home-study and practice

9.6.1 Satellites in the spectral function

Introduction

In addition to the features in the spectral function that can be compared to the density of states of non-interacting electrons, one often observes so-called **satellites**, namely small peaks of the spectral function, which lie several eV below or above the main features. These satellites are due to the

combination of a one-particle excitation, such as electron addition or electron removal, with a particle-number-conserving excitation. Such a particle-number-conserving excitation could be the creation of an electron-hole pair, a plasmon, spin waves, phonons or something else.

Editor: Include a figure with an experimental spectrum exhibiting a satellite.

A theory such as the Hartree-Fock approximation, that describes the ground state by a single Slater determinant, can not describe satellites. When the ground state or the final state of the excitation is a superposition of several Slater determinants, the "transition" to or from these Slater determinants contributes additional features in the spectral function. The reason for the admixture is the interaction $\hat{W}$. The transition can take these Slater determinants to eigenstates of the Hamiltonian that have not been accessible before. These eigenstates can be described in terms of particle-conserving excitations of those eigenstates contributing in the absence of the admixture. This excitation adds to the energy of the original transition. If the excitation energies are small, they lead to the **life-time broadening** of the quasi-particle peaks. If they are large, they produce separate replica of the quasi-particle peaks, which are then called **satellites**.

In this exercise, we will study a minimal model for a one-particle level that couples to a particle-number-conserving excitation.

The model consists of a one-particle state $|a\rangle$, to which we will add and remove a particle, and an electron-hole excitation from state $|b\rangle$ to $|c\rangle$. The one particle level has energy $\bar{\epsilon}_a$. The excitation raises an electron from the energy level $\bar{\epsilon}_b$ to level $\bar{\epsilon}_c$. Let me consider the case $\bar{\epsilon}_b \ll \mu$ and $\mu \ll \bar{\epsilon}_c$.

The non-interacting Hamiltonian has the form

$$\hat{h} = \bar{\epsilon}_a \hat{a}^\dagger \hat{a} + \bar{\epsilon}_b \hat{b}^\dagger \hat{b} + \bar{\epsilon}_c \hat{c}^\dagger \hat{c} \tag{9.56}$$

where $\hat{a}, \hat{a}^\dagger$, $\hat{b}, \hat{b}^\dagger$, $\hat{c}, \hat{c}^\dagger$ are the annihilation and creation operators for the three one-particle orbitals.

The spectral function of this non-interacting model

$$\hat{\mathcal{A}}(\epsilon) = |a\rangle\delta\big(\epsilon - \bar{\epsilon}_a\big)\langle a| + |b\rangle\delta\big(\epsilon - \bar{\epsilon}_b\big)\langle b| + |c\rangle\delta\big(\epsilon - \bar{\epsilon}_c\big)\langle c| \tag{9.57}$$

has delta-peaks at the one-particle levels $\bar{\epsilon}_a$, $\bar{\epsilon}_b$, $\bar{\epsilon}_c$. The spectral function projected on orbital $|a\rangle$ has only one delta function at $\bar{\epsilon}_a$

Let me now add the interaction. I will consider specifically one contribution, that allows me to demonstrate satellites without adding other complications.

$$\hat{h} = \bar{\epsilon}_a \hat{a}^\dagger \hat{a} + \bar{\epsilon}_b \hat{b}^\dagger \hat{b} + \bar{\epsilon}_c \hat{c}^\dagger \hat{c} + V \hat{a}^\dagger \hat{a}\Big(\hat{b}^\dagger \hat{c} + \hat{c}^\dagger \hat{b}\Big) \tag{9.58}$$

The interaction term describes the Coulomb interaction of an electron in $|a\rangle$ with the charge density of the electron-hole pair. When the electron is present in a, the many-particle eigenstates have an admixture of the electron-hole pair. In other words the wave functions are superpositions of $|1,1,0\rangle$ and $|1,0,1\rangle$, so that both can be accessed by adding an electron to $|0,1,0\rangle$ in orbital $|a\rangle$.

Let me now simplify the Hamiltonian, while maintaining the features, which are required to describe the physical effect of interest, the satellites: I introduce the symbol $\Delta \stackrel{\text{def}}{=} \bar{\epsilon}_c - \bar{\epsilon}_b$ for the excitation energy of the electron-hole excitation. The Hamiltonian above preserves the number $n_b + n_v$ of electrons in the orbitals $|b\rangle$ and $|c\rangle$. For our purpose, only the case $n_B + n_C = 1$ with one electron in the orbitals $|b\rangle$ and $|c\rangle$ is of interest. The energy $n_b\bar{\epsilon}_b + n_c\bar{\epsilon}_c$ is a constant in the relevant subspace. Therefore, I simplify the Hamiltonian by setting $\bar{\epsilon}_B + \bar{\epsilon}_C = -\frac{\Delta}{2}$. Finally, I drop the subscript from $\bar{\epsilon}_a$.

The resulting, simplified model Hamiltonian is

$$\hat{H} = \bar{\epsilon}\hat{a}^\dagger \hat{a} + \Delta \hat{c}^\dagger \hat{c} + V \hat{a}^\dagger \hat{a}\Big(\hat{b}^\dagger \hat{c} + \hat{c}^\dagger \hat{b}\Big) \tag{9.59}$$

For our purposes we can exclude states with zero or two particles in $|b\rangle$ and $|c\rangle$. The relevant

Fock space is spanned by four Slater determinants

$$\begin{aligned} |0,\downarrow\rangle &\stackrel{\text{def}}{=} |0,1,0\rangle \\ |0,\uparrow\rangle &\stackrel{\text{def}}{=} |0,0,1\rangle \\ |1,\downarrow\rangle &\stackrel{\text{def}}{=} |1,1,0\rangle \\ |1,\uparrow\rangle &\stackrel{\text{def}}{=} |1,0,1\rangle \end{aligned} \tag{9.60}$$

I have introduced a notation which makes explicit that one two states are allowed for the excitation. Either the electron is in the lower level $\downarrow\rangle$ or it is in the upper level $|\uparrow\rangle$.

Problem

Consider the model with a Hamiltonian

$$\hat{H} = \bar{\epsilon}\hat{a}^\dagger\hat{a} + \Delta\hat{c}^\dagger\hat{c} + V\left(\hat{b}^\dagger\hat{a}^\dagger\hat{a}\hat{c} + \hat{c}^\dagger\hat{a}^\dagger\hat{a}\hat{b}\right) \tag{9.61}$$

with three one particle levels $|a\rangle$, $|b\rangle$ and $|c\rangle$. The model describes an electron acceptor $|a\rangle$, which is coupled to an excitation of an electron from state $|b\rangle$ to state $|c\rangle$.

1 Determine the many-particle eigenvalues and the eigenstates of the model with $n_b + n_c = 1$.

2 Construct the spectral function for the electron accepting orbital for particle numbers ranging from one to two.

Solution

1 Determine the many-particle eigenvalues and the eigenstates of the model with $n_b + n_c = 1$.

The Hamiltonian is

$$\hat{H} = \begin{pmatrix} |0,\downarrow\rangle \\ |0,\uparrow\rangle \\ |1,\downarrow\rangle \\ |1,\uparrow\rangle \end{pmatrix} \begin{pmatrix} 0 & 0 & 0 & 0 \\ 0 & \Delta & 0 & 0 \\ 0 & 0 & \bar{\epsilon} & V \\ 0 & 0 & V & \bar{\epsilon}+\Delta \end{pmatrix} \begin{pmatrix} \langle 0,\downarrow| \\ \langle 0,\uparrow| \\ \langle 1,\downarrow| \\ \langle 1,\uparrow| \end{pmatrix} \tag{9.62}$$

where the notation of Eq. 9.60 has been used for the basisstates. States with $n_b + n_c \neq 1$ have been excluded.

The energy eigenvalues are

$$\begin{aligned} E_{0,\downarrow} &= 0 \qquad \text{with } |\Psi_{0,\downarrow}\rangle = |0,\downarrow\rangle \\ E_{0,\uparrow} &= \Delta \qquad \text{with } |\Psi_{0,\uparrow}\rangle = |0,\uparrow\rangle \\ E_{1,\pm} &= \bar{\epsilon} + \frac{\Delta}{2} \pm \sqrt{\left(\frac{\Delta}{2}\right)^2 + V^2} = \bar{\epsilon} + \frac{\Delta}{2}\left[1 \pm \underbrace{\sqrt{1+\left(\frac{2V}{\Delta}\right)^2}}_{=:1+2q/\Delta}\right] \approx \begin{cases} \bar{\epsilon} - \frac{V^2}{\Delta} \\ \bar{\epsilon} + \Delta + \frac{V^2}{\Delta} \end{cases} \end{aligned} \tag{9.63}$$

The eigenstates are

$$\begin{aligned} |\Psi_{1,-}\rangle &= |1,\downarrow\rangle\cos(\gamma) + |1,\uparrow\rangle\sin(\gamma) \\ |\Psi_{1,+}\rangle &= |1,\uparrow\rangle\cos(\gamma) - |1,\downarrow\rangle\sin(\gamma) \end{aligned} \tag{9.64}$$

with the mixing angle γ defined by the eigenvalue equation of the Hamiltonian Eq. 9.62.

$$\left\{\bar{\epsilon}-\bar{\epsilon}-\frac{\Delta}{2}\left(1\pm\sqrt{1+\left(\frac{2V}{\Delta}\right)^2}\right)\right\}\cos(\gamma)+V\sin(\gamma)=0$$

$$\left\{1\pm\sqrt{1+\left(\frac{2V}{\Delta}\right)^2}\right\}\cos(\gamma)-\frac{2V}{\Delta}\sin(\gamma)=0$$

$$\tan(\gamma)=\frac{\Delta}{2V}\left[1\pm\sqrt{1+\left(\frac{2V}{\Delta}\right)^2}\right] \tag{9.65}$$

$$\begin{aligned}
\cos(\gamma) &\overset{x=\tan(\gamma)}{=} \cos(\arctan(x))=\frac{1}{\sqrt{1+x^2}}=\frac{1}{\sqrt{1+\tan^2(\gamma)}} \\
&= \left(1+\left[\frac{\Delta}{2V}\left(1\pm\sqrt{1+\left(\frac{2V}{\Delta}\right)^2}\right)\right]^2\right)^{-\frac{1}{2}} \\
&= \frac{2V}{\Delta}\left(\left(\frac{2V}{\Delta}\right)^2+\left[1\pm\sqrt{1+\left(\frac{2V}{\Delta}\right)^2}\right]^2\right)^{-\frac{1}{2}} \\
&= \frac{2V}{\Delta}\left(\left(\frac{2V}{\Delta}\right)^2+1\pm 2\sqrt{1+\left(\frac{2V}{\Delta}\right)^2}+1+\left(\frac{2V}{\Delta}\right)^2\right)^{-\frac{1}{2}} \\
&= \frac{2V}{\Delta}\frac{1}{\sqrt{2}}\left(1+\left(\frac{2V}{\Delta}\right)^2\pm\sqrt{1+\left(\frac{2V}{\Delta}\right)^2}\right)^{-\frac{1}{2}} \\
&\approx \begin{cases}
\frac{1}{2}\frac{2V}{\Delta} & \text{for } |V|\ll|\Delta| \text{ and } \pm=+ \\
\frac{1}{\sqrt{2}}\mathrm{sgn}\left(\frac{2V}{\Delta}\right) & \text{for } |V|\gg|\Delta| \text{ and } \pm=+ \\
\left[1-\frac{1}{2}\left(\frac{V}{\Delta}\right)^2\right]\mathrm{sgn}\left(\frac{2V}{\Delta}\right) & \text{for } |V|\ll|\Delta| \text{ and } \pm=- \\
\frac{1}{\sqrt{2}}\mathrm{sgn}\left(\frac{2V}{\Delta}\right) & \text{for } |V|\gg|\Delta| \text{ and } \pm=-
\end{cases}
\end{aligned} \tag{9.66}$$

The solution that is relevant for us is the one with $V\ll\Delta$ and $\pm=-$, because this connects $|1,-\rangle$ with $|1,\downarrow\rangle$ in the absence of V.

The many-particle states and their energies are

j	E_j	$\lvert\Psi_j\rangle$
1	0	$\lvert 0,\downarrow\rangle$
2	Δ	$\lvert 0,\uparrow\rangle$
3	$\bar{\epsilon}-q$	$\lvert 1,\downarrow\rangle\cos(\gamma)+\lvert 1,\uparrow\rangle\sin(\gamma)$
4	$\bar{\epsilon}+\Delta+q$	$\lvert 1,\uparrow\rangle\cos(\gamma)-\lvert 1,\downarrow\rangle\sin(\gamma)$

The parameter q has been defined in Eq. 9.63 as

$$q=\frac{\Delta}{2}\left(\sqrt{1+\left(\frac{2V}{\Delta}\right)^2}-1\right)\approx\frac{V^2}{\Delta}\quad\text{for } V\ll\Delta \tag{9.67}$$

2 Construct the spectral function projected on site a for T=0 of the system for particle numbers ranging from one to two.

Let me consider the spectral function of the accepting orbital as function of the number of electrons.

The electron acceptor can accept between zero and one electrons. This number is denoted by x. The probabilities for the states are $P_1 = 1 - x$ and $P_3 = x$, while $P_2 = P_4 = 0$ at zero temperature.

The spectral function is

$$\begin{aligned}
\mathcal{A}^{\text{tot}}_{\alpha,\beta}(\epsilon) &\overset{\text{Eq. 9.32}}{=} \sum_{m,n}(P_n + P_m)\langle\Phi_n|\hat{c}_{S,\alpha}|\Phi_m\rangle\langle\Phi_m|\hat{c}^\dagger_{S,\beta}|\Phi_n\rangle\delta\Big(\epsilon - (E_m - E_n)\Big) \\
\mathcal{A}^{\text{tot}}_{a,a}(\epsilon) &= \underbrace{|\langle\Phi_2|\hat{c}^\dagger_{S,a}|\Phi_1\rangle|^2}_{0}\,\delta\Big(\epsilon - \underbrace{(E_2 - E_1)}_{\Delta}\Big)\underbrace{(1-x)}_{P_1+P_2} \\
&+ \underbrace{|\langle\Phi_3|\hat{c}^\dagger_{S,a}|\Phi_1\rangle|^2}_{\cos^2(\gamma)}\,\delta\Big(\epsilon - \underbrace{(E_3 - E_1)}_{\bar{\epsilon}-q}\Big)\underbrace{1}_{P_1+P_3} \\
&+ \underbrace{|\langle\Phi_4|\hat{c}^\dagger_{S,a}|\Phi_1\rangle|^2}_{\sin^2(\gamma)}\,\delta\Big(\epsilon - \underbrace{(E_4 - E_1)}_{\bar{\epsilon}+\Delta+q}\Big)\underbrace{1-x}_{P_1+P_4} \\
&+ \underbrace{|\langle\Phi_3|\hat{c}^\dagger_{S,a}|\Phi_2\rangle|^2}_{\sin^2(\gamma)}\,\delta\Big(\epsilon - \underbrace{(E_3 - E_2)}_{\bar{\epsilon}-q-\Delta}\Big)\underbrace{x}_{P_2+P_3} \\
&= \underbrace{\overbrace{\cos^2(\gamma)}^{Z}\,\delta\Big(\epsilon - (\bar{\epsilon} - q)\Big)}_{\text{quasi-particle peak}} \\
&+ \underbrace{\overbrace{\sin^2(\gamma)}^{1-Z}\Big[(1-x)\delta\Big(\epsilon - (\bar{\epsilon} + \Delta + q)\Big) + x\delta\Big(\epsilon - (\bar{\epsilon} - \Delta - q)\Big)\Big]}_{\text{satellites}} \qquad (9.68)
\end{aligned}$$

The spectral function is sketched in figure 9.2.

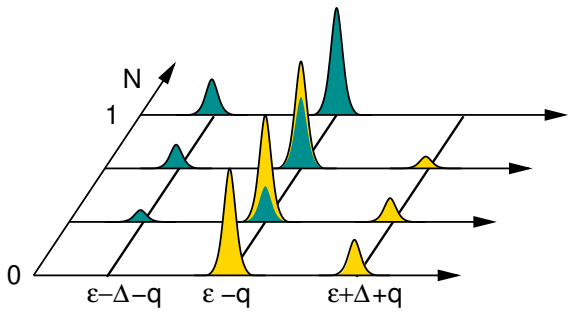

Fig. 9.2: Spectral function on the electron acceptor exhibiting satellites for different number of electrons. In contrast to a mean-field spectrum, the energies do not shift with changing number of electrons, but the intensity of the satellites changes. The green shaded region denotes the occupied part of the spectral function, while the yellow shaded region denotes the unoccupied part.

Discussion

For the non-interacting system with $V = 0$, the spectral function has one spectral peak with energy $\epsilon = \bar{\epsilon}$. This feature is independent of the particle number on the electron acceptor level a.

When the interaction is taken into account, the main peak at $\bar{\epsilon}$ loses weight, and this weight is transferred to two satellites, which occur in the spectrum. One satellite is located Δ below the main peak and the other is located Δ above the main peak. If the acceptor level is empty, the satellite occurs above the main peak. As the electron number is increased, the weight is transferred continuously from

the upper to the lower satellite. Editor: Note that the spectral function integrates to one, as required. Derive the charge sum rule for interacting many-particle systems. So-far we derived it for non-interacting systems as intrinsic property of a matrix diagonalization

The satellites describe that an excitation can occur in parallel with the electron addition or removal. The one-electron excitation is coupled to the particle-number-conserving excitation by the interaction.

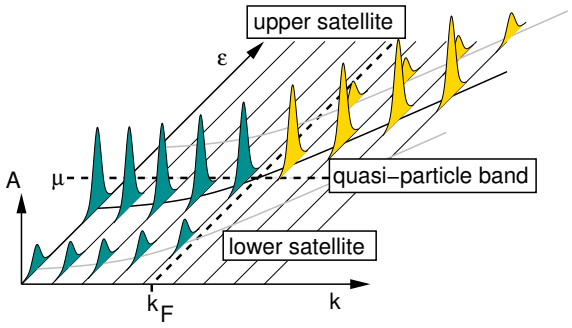

Fig. 9.3: Spectral function $A(\epsilon, k)$ of the free-electron gas with a single particle-conserving excitation with energy Δ and zero momentum producing satellite bands. The green shaded region denotes the occupied part of the spectral function, while the yellow shaded region denotes the unoccupied part.

The main peak at $\approx \bar{\epsilon}$ is the so-called **quasi-particle peak**. Its weight is the **quasi-particle weight** Z The quasi-particle weight is less than unity, because some of the weight is transferred to the satellites. The total weight on the orbital a is one.

In the mean-field approximation, the energy levels shift with increasing electron number, because the effective potential depends on the charge distribution. In the full calculation, the level positions are fixed, but the weights rearrange with the particle number.

The one-particle excitation is shifted from $\bar{\epsilon}$ in the non-interacting case to $\bar{\epsilon} - q$ in the presence of the interaction. The parameter q defined in Eq. 9.67 is the **quasi-particle shift**. The quasi-particle shift is due to **screening**. The Coulomb potential of the additional electron on the acceptor level induces a dipole on the bond. This dipole produces a favorable Coulomb potential stabilizing on the electron on the acceptor level. The formation of the induced electrostatic dipole is the origin of the **polarization** known from electrostatics.

The model is closely related to two famous approximations in many-particle physics, the random-phase approximation and, related, the GW method. In these methods the screening occurs through plasmons, which are cooperative charge oscillations the electron gas in a material. Satellites due to plasmon excitations have been calculated by Lundqvist[77**?** , 78] (see figure 2 of [78]). At that time one attributed the satellite peak to a quasi-particle called **plasmaron** made from and electron and a plasmon. The spectral function of the free-electron gas exhibiting the satellite structure has been calculated by Caruso and Giustino[46]. For the satellite structure in the spectral function of sodium, see [79].

9.6.2 Model for strongly retarded Green's function

Introduction

In an earlier exercise, section 4.6.2 on p. 175, we learned that a Lorentzian peak in the density of states, can be described by a Green's function having a pole in the complex plane. At that time we have still been studying one-particle systems.

The exercise at hand is related, but works the other way round. We show how a spectral function

is obtained from the contour ordered Green's function in real-valued time.

Problem

The non-interacting Green's function is changed upon a weak interaction by a shift of the poles of the Greens function into the complex plane. A minimal problem consists of only a single orbital with the Green's function having one orbital with a pole in the complex plane.

$$G(t_2,t_1) = \frac{1}{i\hbar}\left[(1-f_{T,\mu})\theta(t_2-t_1)\mathrm{e}^{-\frac{i}{\hbar}(\epsilon_0-i\Gamma)(t_2-t_1)} - f_{T,\mu}\theta(t_1-t_2)\mathrm{e}^{-\frac{i}{\hbar}(\epsilon_0+i\Gamma)(t_2-t_1)}\right] \quad (9.69)$$

1. Determine the spectral function $\mathcal{A}^{\mathrm{tot}}(\epsilon)$.
2. Determine the electron and hole Green's function separately.

Discussion

1. Determine the spectral function $\mathcal{A}^{\mathrm{tot}}(\epsilon)$.

The spectral function is obtained from Eq. 9.42. Because Γ is finite, the pole is already displaced away from the real axis. Thus, we need not include the infinitesimal displacement $\eta \to 0$ of the energy away from the real axis

We begin with Eq. 9.42. Because we consider only one orbital, we can treat the Green's function as a matrix element, which is a complex-valued number[10] rather than an operator. Therefore

$$\mathcal{A}(\epsilon) \overset{\text{Eq. 9.42}}{=} \frac{1}{1-2f_{T,\mu}(\epsilon)}\left(-\frac{1}{2\pi i}\left[G^{\mathcal{C}}(\epsilon) - G^{\mathcal{C},*}(\epsilon)\right]\right) = -\frac{1}{\pi}\frac{\mathrm{Im}[G^{\mathcal{C}}(\epsilon)]}{1-2f_{T,\mu}(\epsilon)} \quad (9.70)$$

We need to transform the Green's function into the energy representation, i.e. we need to Fourier transform it in the relative argument $t_2 - t_1$. In this case, the integration proceeds only along the real axis, not the contour $\mathcal{C}$.

$$\begin{aligned}
G^{\mathcal{C}}(\epsilon) &= \int_{-\infty}^{\infty} dt\; G^{\mathcal{C}}(t,0)\mathrm{e}^{\frac{i}{\hbar}\epsilon t} \\
&\overset{\text{Eq. 9.69}}{=} \frac{1-f}{i\hbar}\int_0^{\infty} dt\; \mathrm{e}^{\frac{i}{\hbar}(\epsilon-\epsilon_0+i\Gamma)t} - \frac{f}{i\hbar}\int_{-\infty}^{0} dt\; \mathrm{e}^{\frac{i}{\hbar}(\epsilon-\epsilon_0-i\Gamma)t} \\
&= \frac{1-f}{i\hbar}\left[\frac{\mathrm{e}^{\frac{i}{\hbar}(\epsilon-\epsilon_0+i\Gamma)t}}{\frac{i}{\hbar}(\epsilon-\epsilon_0+i\Gamma)}\right]_0^{\infty} - \frac{f}{i\hbar}\left[\frac{\mathrm{e}^{\frac{i}{\hbar}(\epsilon-\epsilon_0-i\Gamma)t}}{\frac{i}{\hbar}(\epsilon-\epsilon_0-i\Gamma)}\right]_{-\infty}^{0} \\
&= \frac{1-f}{i\hbar}\frac{-1}{\frac{i}{\hbar}(\epsilon-\epsilon_0+i\Gamma)} - \frac{f}{i\hbar}\frac{1}{\frac{i}{\hbar}(\epsilon-\epsilon_0-i\Gamma)} \\
&= \frac{(1-f)}{\epsilon-\epsilon_0+i\Gamma} + \frac{f}{\epsilon-\epsilon_0-i\Gamma} \\
&= \frac{(1-f)(\epsilon-\epsilon_0-i\Gamma)+f(\epsilon-\epsilon_0+i\Gamma)}{(\epsilon-\epsilon_0)^2+\Gamma^2} \\
&= \frac{\epsilon-\epsilon_0}{(\epsilon-\epsilon_0)^2+\Gamma^2} - i\frac{(1-2f)\Gamma}{(\epsilon-\epsilon_0)^2+\Gamma^2}
\end{aligned} \quad (9.71)$$

$$\mathcal{A}(\epsilon) = -\frac{1}{\pi}\frac{\mathrm{Im}[G^{\mathcal{C}}(\epsilon)]}{1-2f_{T,\mu}(\epsilon)} = -\frac{1}{\pi}\frac{-\Gamma}{(\epsilon-\epsilon_0)^2+\Gamma^2} = \frac{1}{\pi}\frac{\Gamma}{(\epsilon-\epsilon_0)^2+\Gamma^2} \quad (9.72)$$

[10] $z = \mathrm{Re}[z] + i\mathrm{Im}[z] \Rightarrow \mathrm{Im}[z] = \frac{z-z^*}{2i}$

Thus, we obtained a Lorentzian spectral function from this model Green's function, which is the desired result.

The model Green's function can be generalized to the form

$$G_{\alpha,\beta}(t_2,t_1) = \frac{1}{i\hbar}\sum_n \langle \pi_\alpha|\varphi_n\rangle \Big[(1-f_n)\theta(t_2-t_1)\mathrm{e}^{-\frac{i}{\hbar}(\epsilon_{0,n}-i\Gamma_n)(t_2-t_1)} - f_n\theta(t_1-t_2)\mathrm{e}^{-\frac{i}{\hbar}(\epsilon_{0,n}+i\Gamma_n)(t_2-t_1)}\Big]\langle\varphi_n|\pi_\beta\rangle \tag{9.73}$$

where the φ_n are a set of orthonormal one-particle functions. This model Green's function is defined by the parameters $\langle\pi_\alpha|\varphi_n\rangle, \epsilon_{0,n}, \Gamma_n$ and f_n.

The corresponding spectral function is

$$\mathcal{A}_{\alpha,\beta}(\epsilon) = \frac{1}{\pi}\sum_n \langle\pi_\alpha|\varphi_n\rangle \frac{\Gamma_n}{(\epsilon-\epsilon_{0,n})^2+\Gamma_n^2}\langle\varphi_n|\pi_\beta\rangle \tag{9.74}$$

The value of Γ indicates that this Green's function corresponds to a macroscopic system, which has a continuous spectrum. The delta-function peak of the spectral function in a non-interacting system is now smeared out into a Lorentzian peak. For a band structure, this implies that the bands are no more sharp but that they are a little smeared out, due to the lifetime of the quasi-particle described by $|\varphi_n\rangle$.

A strongly correlated system would differ in that the single peak would split into several distinct peaks or another a broad distribution. In that case the quasi-particles can no more considered as almost independent particles, albeit with a finite life-time, but the correlations are a fundamental property of the system.

1. Determine the electron and hole Green's function separately.

$$\begin{aligned}\mathcal{A}^e_{T,\mu}(\epsilon) &= \mathcal{A}^{\mathrm{tot}}(\epsilon)(1-f_{T,\mu}(\epsilon)) = \frac{1}{\pi}\frac{\Gamma_n}{(\epsilon-\epsilon_{0,n})^2+\Gamma_n^2}\frac{1}{1+\mathrm{e}^{-\beta(\epsilon-\mu)}}\\ \mathcal{A}^h_{T,\mu}(\epsilon) &= \mathcal{A}^{\mathrm{tot}}(\epsilon)f_{T,\mu}(\epsilon) = \frac{1}{\pi}\frac{\Gamma_n}{(\epsilon-\epsilon_{0,n})^2+\Gamma_n^2}\frac{1}{1+\mathrm{e}^{+\beta(\epsilon-\mu)}}\end{aligned} \tag{9.75}$$

In contrast to the total spectral function, the electron and hole contributions depend on temperature and chemical ensemble.

9.6.3 One-particle spectrum of the Hubbard dimer

Exercise: Let us evaluate the spectral function for an interacting electron system, the Hubbard dimer. The Hubbard dimer, respectively the Hydrogen atom has been investigated previously in section 1.5.1 and 3.11.1.
The Hamiltonian of the Hubbard dimer is

$$\hat{H} = \sum_{j=1}^{2} \sum_{\sigma\in\{\uparrow,\downarrow\}} \bar{\epsilon}\hat{c}^\dagger_{j,\sigma}\hat{c}_{j,\sigma} - |t| \sum_{\sigma\in\{\uparrow,\downarrow\}} \left(\hat{c}^\dagger_{1,\sigma}\hat{c}_{2,\sigma} + \hat{c}^\dagger_{2,\sigma}\hat{c}_{1,\sigma}\right) + U\sum_{j=1}^{2} \sum_{\sigma,\sigma'\in\{\uparrow,\downarrow\}} \hat{c}^\dagger_{l,\sigma}\hat{c}^\dagger_{j,\sigma'}\hat{c}_{j,\sigma'}\hat{c}_{j,\sigma} \quad (9.76)$$

1. Rewrite the Hamiltonian in terms of occupation-number operators as much as possible to simplify the Hamiltonian. As we start with a basisset of Slater determinants, which are eigenstates of the occupation-number operator, this makes the calculation efficient.
2. Set up a complete basis of Slater determinants for the Hubbard dimer
3. Construct the joint eigenstates of $\hat{N}, \hat{S}_z, \hat{S}^2$ and $\hat{P}$, where $\hat{P}$ is the point-inversion about the bond center.
4. determine the eigenstates of the Hamiltonian and their energies
5. determine the peak positions of the spectral function
6. determine the quasi-particle wave functions
7. construct the spectral function as energy-dependent matrix
8. extract the projected density of states

Solution

The solution is given in the appendix D on p. 411. Section D.1 on p. 411 covers the general aspects, while section D.2 covers the specifically the Hubbard dimer.

Hamiltonian in terms of occupation-number operators The Hamiltonian of the Hubbard dimer is provided in Eq. D.15.

Complete basis of Slater determinants The Slater determinants that serve as basisset for our limited Fock space is given in table D.1

Eigenstates of $\hat{N}, \hat{S}_z, \hat{S}^2$ and $\hat{P}$, where $\hat{P}$ is the point-inversion about the bond center: The symmetry-adapted states of the Hubbard dimer are given in table D.4.

Eigenstates and their energies Except for one 2×2-block, all symmetry adapted states are also eigenstates of the Hamiltonian. Their energy expectation values are are also their energy eigenvalues.

The 2×2-block can be diagonalized and yields the ground state Eq. D.22 with energy Eq. D.23.

peak positions of the spectral function The spectral function consists of delta functions centered at the energy differences of states, which differ by $\Delta N = \pm 1$.

$\bar{\epsilon} - \lvert t\rvert$	$\bar{\epsilon} + \lvert t\rvert$	(0/1),(1/2) lower Hubbard band
$\bar{\epsilon} + U - \lvert t\rvert$	$\bar{\epsilon} + U + \lvert t\rvert$	(1/2),(3/4) upper Hubbard band
$\bar{\epsilon} - \lvert t\rvert - \Delta_{st}$	$\bar{\epsilon} + \lvert t\rvert - \Delta_{st}$	(1/2)
$\bar{\epsilon} + U - \lvert t\rvert + \Delta_{st}$	$\bar{\epsilon} + U + \lvert t\rvert + \Delta_{st}$	(1/2)

quasi-particle wave functions

Spectral function

Projected density of states In Eq. 3.118, we obtained the ground state of the half-filled Hubbard dimer as

$$\begin{aligned} |\Psi_-\rangle &\overset{\text{Eq. } 3.118}{=} \\ &= \left[\frac{\cos\gamma_-}{\sqrt{2}}\left(\hat{c}^\dagger_{1\uparrow}\hat{c}^\dagger_{1\downarrow} + \hat{c}^\dagger_{2\uparrow}\hat{c}^\dagger_{2\downarrow}\right) + \frac{\sin(\gamma_-)}{\sqrt{2}}\left(\hat{c}^\dagger_{1\uparrow}\hat{c}^\dagger_{2\downarrow} - \hat{c}^\dagger_{1\downarrow}\hat{c}^\dagger_{2\uparrow}\right)\right]|\mathcal{O}\rangle \end{aligned} \tag{9.77}$$

with energy Eq. 3.119

$$\begin{aligned} E_- &\overset{\text{Eq. } 3.119}{=} 2\bar{\epsilon} + \frac{U+V}{2} - \sqrt{\left(\frac{U-V}{2}\right)^2 + 4|t|^2} \\ &= 2\bar{\epsilon} + U - 2|t|\tan(\gamma_-) \end{aligned} \tag{9.78}$$

γ_- changes from $\pi/8 = 45°$ for the non-interacting system to $\pi/4 = 90°$ in the strongly correlated limit.

Solution: At temperature much smaller than the singlet-triplet splitting, we only need to consider the singlet wave function.

We start from Eq. 9.42 for the spectral function

$$\mathcal{A}^{(tot)}_{\alpha,\beta}(\epsilon) \overset{\text{Eq. } 9.42}{=} -\frac{1}{\pi}\lim_{\zeta\to 0}\mathrm{Im}\left\{\int_{-\infty}^{\infty} dt\; G^{\mathcal{C}}_{\alpha,\beta}(t,0)\mathrm{sgn}(t)\mathrm{e}^{-\zeta|t|}\mathrm{e}^{\frac{i}{\hbar}\epsilon t}\right\} \tag{9.79}$$

At zero temperature and the appropriate chemical potential for half-filling, the probability for the state $|\Psi_-\rangle$ is one and the other probabilities vanish.

$$|\Psi\rangle \overset{\text{Eq. } 3.118}{=} \frac{1}{\sqrt{2}}\left(\hat{c}^\dagger_{1,\uparrow}\hat{c}^\dagger_{2,\downarrow} - \hat{c}^\dagger_{1,\downarrow}\hat{c}^\dagger_{2,\uparrow}\right)|\mathcal{O}\rangle \tag{9.80}$$

with energy

$$E \overset{\text{Eq. } 3.132}{=} 2\bar{\epsilon} + V + 2|t|\left(\frac{U-V}{4|t|} - \sqrt{1 + \left(\frac{U-V}{4|t|}\right)^2}\right) \tag{9.81}$$

The triplet states Eq. 3.122, 3.124, and 3.125 have the energy

$$E_d \overset{\text{Eq. } 3.133}{=} \left(2\bar{\epsilon} + V\right) \tag{9.82}$$

In order to obtain the spectral function with the Lehmann representation starting from the two-particle channel, we need to evaluate the many-particle states in the one-particle channel and the three-particle channel.

one-particle states: The one-particle states are obtained from section 1.5.1 by translating the bonding and antibonding orbitals into second quantization. We obtain four one-particle states

$$\begin{aligned}\Psi^{1p}_{b,\sigma} &= \frac{1}{\sqrt{2}}\left(\hat{c}^\dagger_{1,\sigma} + \hat{c}^\dagger_{1,\sigma}\right)|\mathcal{O}\rangle \\ \Psi^{1p}_{a,\sigma} &= \frac{1}{\sqrt{2}}\left(\hat{c}^\dagger_{1,\sigma} - \hat{c}^\dagger_{1,\sigma}\right)|\mathcal{O}\rangle\end{aligned} \tag{9.83}$$

with energies

$$\begin{aligned}E^{1p}_{b,\sigma} &= \bar{\epsilon} - 2|t| \\ E^{1p}_{a,\sigma} &= \bar{\epsilon} + 2|t|\end{aligned} \tag{9.84}$$

Obviously the interaction terms are not present in the case of a one-particle system.

three-particle states: The three-particle states can be obtained by exploiting **particle-hole symmetry**Editor: Demonstrate particle hole symmetry.

I construct the four-particle state and then create a hole. The bonding state has the hole in the antibonding state, and vice versa.

$$\begin{aligned}\Psi^{3p}_{b,\sigma} &= \frac{1}{\sqrt{2}}\left(\hat{c}_{1,\sigma} - \hat{c}_{1,\sigma}\right) \prod_{R\in\{1,2\},\sigma'\in\{\uparrow,\downarrow\}} \hat{c}^\dagger_{R,\sigma'}|\mathcal{O}\rangle \\ \Psi^{3p}_{a,\sigma} &= \frac{1}{\sqrt{2}}\left(\hat{c}_{1,\sigma} - \hat{c}_{1,\sigma}\right)|\mathcal{O}\rangle \prod_{R\in\{1,2\},\sigma'\in\{\uparrow,\downarrow\}} \hat{c}^\dagger_{R,\sigma'}\end{aligned} \tag{9.85}$$

The energies are Editor: Caution! this is guessed!

$$E^{3p}_{b,\sigma} = 3\bar{\epsilon} + 3V + U - 2|t| \tag{9.86}$$

Spectral function for one site and spin:

$$\mathcal{A}_{\alpha,\beta}(\epsilon) = \tag{9.87}$$

9.6.4 Anderson impurity model

Editor: To be done

The **Anderson impurity model** [59] is a standard model for strongly correlated systems. It models on impurity having a strongly correlated orbital in contact with a bath of non-interacting conduction electrons. The conduction electrons are modeled by a one-dimensional chain of hydrogen atoms, which is characterized by a vanishing orbital energy and a nearest-neighbor hopping parameter. This chain is described with periodic boundary conditions. The impurity is coupled to one of the atoms in the chain with a hopping parameter V. The spatial Coulomb integral on the impurity defines the U-parameter.

1. Set up the many-particle Hamiltonian for the isolated impurity and bring it into the form that it can be expressed by the occupation-number operators. Once the Hamiltonian is obtained in second quantization, express the many-particle Hamiltonian as matrix.

2. Evaluate the finite-temperature Green's function of the isolated impurity in contact with a particle reservoir.

3. Evaluate the Green's function of the conduction electrons at finite temperature in contact with a particle reservoir.

4. determine the Green's function of the Anderson impurity in contact with the conduction electrons.

5. plot the spectral function using the equation for the density of states, which has been derived for non-interacting electrons for different temperatures and chemical potentials.

6. calculate the particle number on the impurity as function of temperature and chemical potential.

7. Discuss the results in the light of the characteristic energy scales of the problem $k_B T$, the band width of the bath t, the position of the empty impurity orbital ϵ_A, the coupling between impurity and bath V, and the Coulomb interaction U. Discuss the isolated limit, the strongly correlated limit, the high-temperature limit.

8. Read the original paper of Anderson[59]

9.6.5 Spectral function and momentum density of a 1d chain

Editor: This exercise is not finished yet!

Introduction

One of the puzzling findings in the early days of studying the interacting free-electron gas was that the momentum density does not resemble a step function as in the non-interacting free-electron gas.[78] Rather, one finds tails that emerge from the step function, which are interpreted as electron-hole pairs that screen the interaction.

The **momentum density** $\rho(\vec{p})$ of electrons is (See for example [80])

$$\rho(\vec{p}) \stackrel{\text{def}}{=} \sum_n f_n |\langle p|\varphi_n\rangle|^2 = \langle \vec{p}|\hat{\rho}^{(1)}|\vec{p}\rangle \tag{9.88}$$

where $|\varphi_n\rangle$ are the natural orbitals and f_n are their occupations. $|\vec{p}\rangle$ are the momentum eigenstates. $\hat{\rho}^{(1)}$ is the one-particle-reduced density matrix. The momentum density is thus related to the Fourier transform of the natural orbitals.

The momentum distribution is easily mistaken by the Fermi distribution. This misunderstanding is resolved by carefully distinguishing the expectation values of the momentum $\langle \varphi_{n,\vec{k}}|\hat{p}|\varphi_{n,\vec{k}}\rangle$ from the crystal momentum $\hbar\vec{k}$.

Secondly, at the origin of the Fermi distribution are non-interacting electrons. However, it also occurs rigorously in the division of the spectral function of an interacting system into the occupied and the empty contribution. At first, this seems to contradict the result for the momentum distribution.

$$f_{T,\mu}(\epsilon_n(\vec{k})) \neq \sum_n \int d\epsilon \; f_{T,\mu}(\epsilon_n(\vec{k}))\langle \vec{p}|\hat{\mathcal{A}}(\epsilon)|\vec{p}\rangle \tag{9.89}$$

In this exercise, an analogous effect will be investigated, but instead of the interaction we use a lattice potential.

For the spectral function and the momentum distribution in the RPA, see Lundqvist[78] Editor: Lundqvists work contains the explicit expressions, which shall be used to construct the relevant graphs. For a measurement of the momentum density in Al see Metz et al.[80].

Editor: Add a remark regarding Compton profiles.

Problem

1 Calculate the one-particle eigenstates $|\varphi_n(k)\rangle$ and energies $\epsilon(k)$ for a one-dimensional linear chain.

2 Calculate momentum density of the one-dimensional linear chain.

3 Introduce a cos-like potential, which doubles the lattice constant. Calculate the new eigenstates and energies.

4 Calculate the momentum density of the perturbed system

Discussion

1 Calculate the one-particle eigenstates $|\varphi_n(k)\rangle$ and energies $\epsilon(k)$ for a one-dimensional linear chain.

The wave functions of the linear chain are

$$|\varphi_k^{(0)}\rangle = \sum_{j=1}^{N} |\chi_j\rangle \frac{1}{\sqrt{N}} e^{ika_{\text{lat}}j} \tag{9.90}$$

$$\epsilon^{(0)}(k) = \bar{\epsilon} - 2t\cos(ka_{\text{lat}}) \tag{9.91}$$

The variable N is the supercell for the periodic boundary conditions, which determines the normalization and the quantization of the wave vectors.

The quantization condition for the k-points is $k_n a_{\text{lat}} N = 2\pi n$, that is

$$k_n = \frac{2\pi}{Na_{\text{lat}}} n \quad \text{with } -\frac{N}{2} < n \leq \frac{N}{2} \text{ and } n \in \mathbb{I} \tag{9.92}$$

The orbitals $|\chi_j\rangle$ are related to each other by a translation

$$|\chi_j\rangle = \underbrace{\int d^3r' \, |\vec{r'} + \vec{R}_j\rangle\langle\vec{r'}|}_{\text{translation by } \vec{R}_j} |\chi_0\rangle \quad \Leftrightarrow \quad \langle\vec{r}|\chi_j\rangle = \langle\vec{r} - \vec{R}_j|\chi_0\rangle \tag{9.93}$$

2 Calculate momentum density of the one-dimensional linear chain.

Editor: The formulation of the integration region is probably not concise. Editor: I am using vectors $\vec{k}, \vec{p}$ and switch to scalars. This needs more attention.

$$\begin{aligned}
\langle\vec{p}|\varphi_{\vec{k}}^{(0)}\rangle &= \int_{0\leq x<Na_{\text{lat}}} d^3r \, e^{-\frac{i}{\hbar}\vec{p}\vec{r}} \langle\vec{r}|\varphi_k^{(0)}\rangle \quad \text{with } \vec{p} \in \left\{\frac{2\pi\hbar}{Na_{\text{lat}}} j; j \in \mathbb{I}\right\} \\
&\overset{\text{Eq. 9.90}}{=} \sum_{j=0}^{N-1} \int d^3r \, e^{-\frac{i}{\hbar}\vec{p}\vec{r}} \langle\vec{r}|\chi_j\rangle \frac{1}{\sqrt{N}} e^{ika_{\text{lat}}j} \\
&\overset{\text{Eq. 9.93}}{=} \sum_{j=0}^{N-1} \frac{1}{\sqrt{N}} e^{ika_{\text{lat}}j} \, e^{-\frac{i}{\hbar}\vec{p}\vec{R}_j} \underbrace{\int d^3r \, e^{-\frac{i}{\hbar}\vec{p}(\vec{r}-\vec{R}_j)} \langle\vec{r} - \vec{R}_j|\chi_0\rangle}_{\langle\vec{p}|\chi_0\rangle} \\
&\overset{\vec{R}_j = \vec{e}_x a_{\text{lat}} j}{=} \langle\vec{p}|\chi_0\rangle \frac{1}{\sqrt{N}} \underbrace{\sum_{j=0}^{N-1} e^{i(k-\frac{1}{\hbar}p)a_{\text{lat}}j}}_{=N\delta_{\hbar k,p}} = \langle\vec{p}|\chi_0\rangle \sqrt{N}\delta_{\hbar k,p}
\end{aligned} \tag{9.94}$$

I used that a the discrete average of a plane wave over an equi-spaced grid for a full period vanishes, except when it is a constant.[11] That is

$$\begin{aligned}\rho(p) &= \sum_k f_{T,\mu}(\epsilon_k) \left|\langle \vec{p}|\varphi_k^{(0)}\rangle\right|^2 \\ &= |\langle \vec{p}|\chi_0\rangle|^2 \sum_k f_{T,\mu}(\epsilon_k) N\delta_{p,\hbar k} \\ &= N\,|\langle \vec{p}|\chi_0\rangle|^2\, f_{T,\mu}\Big(\epsilon\left(\frac{1}{\hbar}p\right)\Big)\end{aligned} \tag{9.95}$$

I selected the momenta on the discrete grid of k-points $p = \frac{2\pi}{Na_{\text{lat}}} j$ with $j \in \mathbb{I}$.

We notice that the momentum density reproduces the Fermi distribution function, with an additional modulation from the shape of the local orbitals. This result holds for zero and for finite temperatures.

3 Introduce a cos-like potential, which doubles the lattice constant. Calculate the new eigenstates and energies.

- The potential, which doubles the unit cell is

$$\hat{V} = \sum_j |\pi_j\rangle \bar{V} \cos\Big(\underbrace{\frac{\pi}{a_{\text{lat}}}}_{q} \cdot \underbrace{a_{\text{lat}} j}_{R_j}\Big) \langle\pi_j| = \sum_j |\pi_j\rangle \bar{V}(-1)^j \langle\pi_j| \tag{9.96}$$

- For each k-point, the new wave functions are superpositions of the ones from k and $k+q$, where $q = \pi/a_{\text{lat}}$. The Brillouin zone of the perturbed system is half as large as that of the unperturbed one. The k-points for the perturbed system are from the interval

$$k_n \in]-\frac{\pi}{2a_{\text{lat}}}, \frac{\pi}{2a_{\text{lat}}}] \tag{9.97}$$

$$|\varphi_k^V\rangle = |\varphi_k^0\rangle c_{1,k} + |\varphi_{k+q}^0\rangle c_{2,k} \tag{9.98}$$

- The Hamiltonian for the perturbed Hamiltonian is

$$\begin{aligned}\hat{H} &= \sum_k \begin{pmatrix} |\varphi_k^{(0)}\rangle \\ |\varphi_{k+q}^{(0)}\rangle \end{pmatrix} \begin{pmatrix} \epsilon^{(0)}(k) & \bar{V} \\ \bar{V} & \epsilon^{(0)}(k+\frac{\pi}{a}) \end{pmatrix} \begin{pmatrix} \langle\varphi_k^{(0)}| \\ \langle\varphi_{k+q}^{(0)}| \end{pmatrix} \\ &= \sum_k \begin{pmatrix} |\varphi_k^{(0)}\rangle \\ |\varphi_{k+q}^{(0)}\rangle \end{pmatrix} \begin{pmatrix} \bar{\epsilon} - 2t\cos(ka) & \bar{V} \\ \bar{V} & \bar{\epsilon} + 2t\cos(ka) \end{pmatrix} \begin{pmatrix} \langle\varphi_k^{(0)}| \\ \langle\varphi_{k+q}^{(0)}| \end{pmatrix}\end{aligned} \tag{9.99}$$

- The eigenvalues are

$$\begin{aligned}\Big(\bar{\epsilon} - 2t\cos(ka) - \epsilon\Big)\Big(\bar{\epsilon} + 2t\cos(ka) - \epsilon\Big) - \bar{V}^2 &= 0 \\ \epsilon_\pm^V(k) = \bar{\epsilon} \pm \sqrt{V^2 + 4t^2\cos^2(ka)}\end{aligned} \tag{9.100}$$

- The eigenvectors obey $\vec{c}_\pm(k) = (\cos(\gamma_\pm(k), \sin(\gamma_\pm(k)))$ are

$$\begin{aligned}\Big(-2t\cos(ka) \mp \sqrt{V^2 + 4t^2\cos^2(ka)}\Big)\cos(\gamma_\pm(k)) + V\sin(\gamma_\pm(k)) &= 0 \\ \gamma_\pm(k) = \operatorname{atan}\left(\frac{1}{V}\Big(2t\cos(ka) \pm \sqrt{V^2 + 4t^2\cos^2(ka)}\Big)\right)\end{aligned} \tag{9.101}$$

[11] This can be worked out by considering the sum as finite geometric series.

The wave functions are

$$|\varphi^V_{\pm}(k)\rangle = |\varphi^{(0)}_k\rangle \cos(\gamma_{\pm}(k)) + |\varphi^{(0)}_{k+q}\rangle \sin_{\pm}(k) \tag{9.102}$$

The momentum matrix element is

$$\begin{aligned}\langle p|\varphi^V_{\pm,k}\rangle &= \langle p|\varphi^{(0)}_k\rangle \cos(\gamma_{\pm}(k)) + \langle p|\varphi^{(0)}_{k+q}\rangle \sin_{\pm}(k)\\ &= \langle \vec{p}|\chi_0\rangle\sqrt{N}\delta_{\hbar k,p}\cos(\gamma_{\pm}(k)) + \langle \vec{p}|\chi_0\rangle\sqrt{N}\delta_{\hbar k,p+\hbar q}\sin(\gamma_{\pm}(k))\\ &= \langle \vec{p}|\chi_0\rangle\sqrt{N}\Big(\delta_{\hbar k,p}\cos(\gamma_{\pm}(k)) + \delta_{\hbar k,p+\hbar q}\sin(\gamma_{\pm}(k))\Big)\end{aligned} \tag{9.103}$$

In the half-filled case, the states are filled for Bloch vectors $-\pi/(2a) < k < \pi/(2a)$ in the extended zone scheme. Each filled state contributes, two plane waves. A large contribution $\cos^2(\gamma_-(k))$ to the momentum density has a smaller momentum $|p| < \hbar\pi/(2a)$ while the second plane wave contributes with $\sin^2(\gamma_-(k))$ at a momentum $\hbar\pi/(2a) < |p|\hbar\pi/a$.

Editor: This is probably still incorrect!!!

4 Calculate the momentum density of the perturbed system

For zero temperature and a half-filled band, we obtain the momentum density

$$\begin{aligned}\rho(\vec{p}) &= \sum_{n\in\{+,-\}}\sum_{k\in\left]-\frac{\pi}{2a_{\text{lat}}},\frac{\pi}{2a_{\text{lat}}}\right]} f_{T,\mu}(\epsilon_{\pm,k})\left|\langle\vec{p}|\varphi^{(V)}_{n,k}\rangle\right|^2\\ &\overset{T=0,\mu=\bar{\epsilon}}{=} \sum_{k\in\left]-\frac{\pi}{2a_{\text{lat}}},\frac{\pi}{2a_{\text{lat}}}\right]}\left|\langle\vec{p}|\varphi^{(V)}_{-,k}\rangle\right|^2\\ &= \sum_{k\in\left]-\frac{\pi}{2a_{\text{lat}}},\frac{\pi}{2a_{\text{lat}}}\right]}\left|\langle\vec{p}|\chi_0\rangle\right|^2 N\Big(\delta_{\hbar k,p}\cos(\gamma_-(k)) + \delta_{\hbar k,p+\hbar q}\sin(\gamma_-(k))\Big)^2\\ &= \sum_{k\in\left]-\frac{\pi}{2a_{\text{lat}}},\frac{\pi}{2a_{\text{lat}}}\right]}\left|\langle\vec{p}|\chi_0\rangle\right|^2 N\Big(\delta_{\hbar k,p}\cos^2(\gamma_-(k)) + \delta_{\hbar(k-q),p}\sin^2(\gamma_-(k))\Big)\end{aligned} \tag{9.104}$$

Grapher-image: Draw fat bands with $100\Delta \in \{-5,-1,\ldots,5\}$, $V = 0.3$, $t = 1$ as function of $x = ka/\pi$.

$$\begin{aligned}y(x) &= \begin{cases}-\sqrt{V^2 + t^2\cos^2(x\pi)} + \Delta\cos^2(\gamma_-(x\pi))\\ +\sqrt{V^2 + t^2\cos^2(x\pi)} + \Delta\sin^2(\gamma_-(x\pi))\end{cases}\\ \gamma_-(ka) &= \operatorname{atan}\left(\frac{1}{V}\left(t\cos(ka) - \sqrt{V^2 + t^2\cos^2(ka)}\right)\right)\end{aligned} \tag{9.105}$$

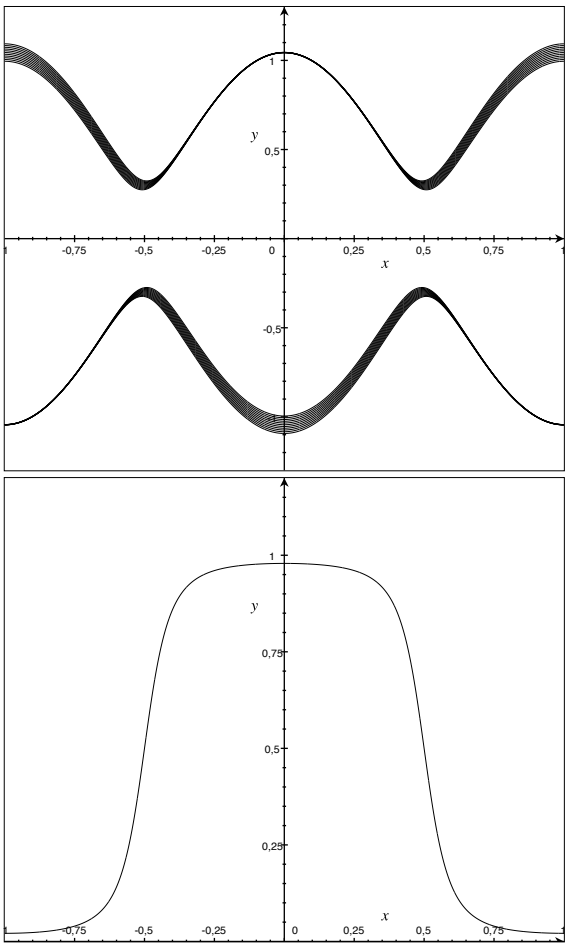

In the case of an external potential discussed here, we obtain a momentum distribution, which does not stop abruptly at the Fermi momentum as anticipated for a free-electron gas or the unperturbed linear chain. We can discuss this effect, in analogy with the RPA, as the formation of electron-hole pairs by the external potential. The electron-hole pairs mentioned here are those of the unperturbed system. Here, the electron-hole pairs are not created by the Coulomb interaction between the electrons but by an external potential. The momentum density has a smooth transition despite the presence of a band gap.

Editor: Idea: Plot the band structure in the extended zone scheme using

$$\pm = s(k) = \begin{cases} -1 & \text{for } |k| < \pi/(2a) \\ +1 & \text{for } \pi/(2a) < |ka| < \pi/a \end{cases} \tag{9.106}$$

Chapter 10

Diagrammatic expansion of the Green's function

So far, we defined the Green's function and we have shown what it is good for. Here, we explore one of the most common ways to evaluate the Green's functions, namely the perturbation expansion in orders of the interaction. This expansion rests on Wick's theorem.

Several ways for this diagrammatic expansions are around. (1) Feynman's zero-temperature formalism for time-dependent phenomena, (2) Matsubara's finite temperature formalism for equilibrium properties[81], (3) Keldysh's non-equilibrium formalism. As shown by Wagner in 1991[64], all these approaches can be merged in the (4) non-equilibrium formalism using contour integrations. The paper of Wagner is very recommendable and can be used alongside these lecture notes.

10.1 Interacting Green's function expressed by non-interacting ground states

Let me state the problem discussed in this chapter: the goal is to determine the Green's function

$$G^{\mathcal{C}}(x,t,x',t') \overset{\text{Eq. 7.16}}{=} \frac{1}{i\hbar}\mathrm{Tr}\left\{\hat{\rho}^{(W)}_{T,\mu}\mathcal{T}_{\mathcal{C}}\left(\hat{\psi}_H(\vec{x},t)\hat{\psi}^{+}_H(\vec{x'},t')\right)\right\}; \tag{10.1}$$

where the state operator $\hat{\rho}^{(W)}_{T,\mu}$ of the grand canonical ensemble with $\hat{H}^{(W)} = \hat{h} + \hat{W}$ is

$$\hat{\rho}^{(W)}_{T,\mu} \overset{\text{Eq. ??}}{=} \frac{1}{Z_{T,\mu}} \mathrm{e}^{-\beta(\hat{H}^{(W)}-\mu\hat{N})} \tag{10.2}$$

and the partition function is

$$Z_{T,\mu} \overset{\text{Eq. ??}}{=} \mathrm{Tr}\left\{\mathrm{e}^{-\beta(\hat{H}^{(W)}-\mu\hat{N})}\right\}. \tag{10.3}$$

10.1.1 From Heisenberg to interaction picture:

Due to the presence of the Heisenberg operators in Eq. 10.1 and because of the statistical operator, we need to deal with exponentials of the interacting Hamiltonian $\hat{H}^{(W)}$. For this problem, it is convenient to switch from the Heisenberg picture to the interaction picture.

The interaction picture, which will be introduced below, limits the time-evolution of operators to the non-interacting Hamiltonian $\hat{h}$. The interaction $\hat{W}$ is moved into the propagator for the states. The diagrammatic expansion of this propagator will then express it in terms of non-interacting Green's functions and the interaction matrix elements.

INTERACTION PICTURE

With the operators $\hat{A}_I$ and the states $|\psi_I\rangle$ in the interaction picture

$$\hat{A}_I(t) = \underbrace{\hat{\mathcal{U}}_S^{(0)}(0,t)}_{\mathcal{T}_C e^{-\frac{i}{\hbar}\int_t^0 dt'\ \hat{h}(t')}} \hat{A}_S(t) \underbrace{\hat{\mathcal{U}}_S^{(0)}(t,0)}_{\mathcal{T}_C e^{-\frac{i}{\hbar}\int_0^t dt'\ \hat{h}(t')}} \tag{10.4}$$

$$|\Psi_I(t)\rangle = \underbrace{\hat{\mathcal{U}}_S^{(0)}(0,t)}_{\mathcal{T}_C e^{-\frac{i}{\hbar}\int_0^t dt'\ \hat{h}(t')}} |\Psi_S(t)\rangle \tag{10.5}$$

the equations of motion are

$$\begin{aligned} i\hbar\partial_t \hat{A}_I(t) &= \left[\hat{A}_I(t), \hat{h}_I(t)\right]_- + i\hbar\left(\partial_t \hat{A}\right)_I \\ i\hbar\partial_t |\Psi_I(t)\rangle &= \hat{W}_I(t)|\Psi_I(t)\rangle \end{aligned} \tag{10.6}$$

$\hat{\mathcal{U}}_S^{(0)}(t',t)$ propagates the wave function under the action of the non-interacting Hamiltonian $\hat{h}(t)$, i.e. $|\Psi_S(t')\rangle = \hat{\mathcal{U}}_S^{(0)}(t',t)|\Psi_S(t)\rangle$, when $i\hbar\partial_t|\Psi_S(t)\rangle = \hat{h}(t)|\Psi_S(t)\rangle$.

The Heisenberg picture has been introduced earlier in Eq. 6.40 on p. 236. It is shown here for comparison

HEISENBERG PICTURE

With the operators $\hat{A}_H$ and the states $|\psi_H\rangle$ in the interaction picture

$$\hat{A}_H(t) = \underbrace{\hat{\mathcal{U}}_S^{(W)}(0,t)}_{\mathcal{T}_C e^{-\frac{i}{\hbar}\int_t^0 dt'\ \hat{H}(t')}} \hat{A}_S(t) \underbrace{\hat{\mathcal{U}}_S^{(W)}(t,0)}_{\mathcal{T}_C e^{-\frac{i}{\hbar}\int_0^t dt'\ \hat{H}(t')}} \tag{10.7}$$

$$|\Psi_H(t)\rangle = |\Psi_S(0)\rangle \tag{10.8}$$

the equations of motion are

$$\begin{aligned} i\hbar\partial_t \hat{A}_H(t) &= \left[\hat{A}_H(t), \hat{H}_S(t)\right]_- + i\hbar\left(\partial_t \hat{A}\right)_H \\ i\hbar\partial_t |\Psi_H(t)\rangle &= 0 \end{aligned} \tag{10.9}$$

$\hat{\mathcal{U}}_S^{(W)}(t',t)$ propagates the wave function under the action of the interacting Hamiltonian $\hat{H}(t) = \hat{h}(t) + \hat{W}(t)$, i.e. $|\Psi_S(t')\rangle = \hat{\mathcal{U}}_S^{(W)}(t',t)|\Psi_S(t)\rangle$, when $i\hbar\partial_t|\Psi_S(t)\rangle = \hat{H}(t)|\Psi_S(t)\rangle$.

Let me translate a general Heisenberg operator $\hat{A}_H(t)$ into the interaction picture, where $\hat{A}_S(t)$ is the corresponding operator in the Schrödinger picture and $\hat{A}_I(t)$ is the **operator in the interaction picture**.

$$\begin{aligned} \hat{A}_H(t) &= \hat{\mathcal{U}}_S^{(W)}(0,t)\hat{A}_S(t)\hat{\mathcal{U}}_S^{(W)}(t,0) \\ &= \overbrace{\hat{\mathcal{U}}_S^{(0)}(0,0)}^{\hat{1}}\, \underbrace{\hat{\mathcal{U}}_S^{(W)}(0,t)\hat{\mathcal{U}}_S^{(0)}(t,0)}_{\hat{\mathcal{U}}_I^{(W)}(0,t)}\, \underbrace{\hat{\mathcal{U}}_S^{(0)}(0,t)\hat{A}_S(t)\hat{\mathcal{U}}_S^{(0)}(t,0)}_{\hat{A}_I(t)}\, \underbrace{\hat{\mathcal{U}}_S^{(0)}(0,t)\hat{\mathcal{U}}_S^{(W)}(t,0)}_{\hat{\mathcal{U}}_I^{(W)}(t,0)}\, \overbrace{\hat{\mathcal{U}}_S^{(0)}(0,0)}^{\hat{1}} \\ &= \hat{\mathcal{U}}_I^{(W)}(0,t)\hat{A}_I(t)\hat{\mathcal{U}}_I^{(W)}(t,0) \end{aligned} \tag{10.10}$$

We have introduced the **propagator in the interaction picture** as

$$\hat{\mathcal{U}}_I^{(W)}(t,t') \stackrel{\text{def}}{=} \hat{\mathcal{U}}_S^{(0)}(0,t)\hat{\mathcal{U}}_S^{(W)}(t,t')\hat{\mathcal{U}}_S^{(0)}(t',0) \tag{10.11}$$

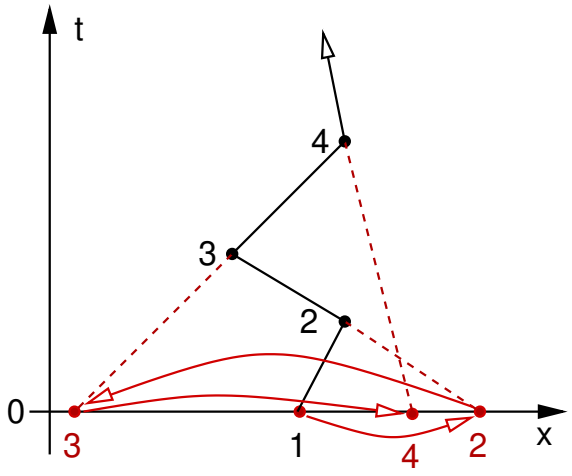

Fig. 10.1: Cartoon as memory hook for the interaction picture. A particle (here classical) propagates while repeatedly scattering at scattering centers, which may be due to the interaction with other particles. Each scattering event can be replaced by a change of the initial state by propagating the scattered trajectory backward in time without scattering. Thus, at each time, the state is replaced by the initial condition, which produces the same state without scattering.

10.1.2 S-matrix

Let me now rewrite the Green's function in terms of operators in the interaction picture.

$$\begin{aligned} G^{\mathcal{C}}(\vec{x},t,\vec{x'},t') &\overset{\text{Eq. 10.1}}{=} \frac{1}{i\hbar}\mathrm{Tr}\Big\{\hat{\rho}^{(W)}_{T,\mu}\mathcal{T}_{\mathcal{C}}\left(\hat{\psi}_H(\vec{x},t)\hat{\psi}^{+}_H(\vec{x'},t')\right)\Big\} \\ &\overset{\text{Eq. 10.10}}{=} \frac{1}{i\hbar}\mathrm{Tr}\Big\{\hat{\rho}^{(W)}_{T,\mu}\mathcal{T}_{\mathcal{C}}\hat{\mathcal{U}}^{(W)}_I(0,t)\hat{\psi}_I(\vec{x},t)\underbrace{\hat{\mathcal{U}}^{(W)}_I(t,t')}_{\hat{\mathcal{U}}^{(W)}_I(t,0)\hat{\mathcal{U}}^{(W)}_I(0,t')}\hat{\psi}^{+}_I(\vec{x'},t')\hat{\mathcal{U}}^{(W)}_I(t',0)\Big\} \\ &= \frac{1}{i\hbar}\mathrm{Tr}\Big\{\hat{\rho}^{(W)}_{T,\mu}\mathcal{T}_{\mathcal{C}}\hat{\mathcal{S}}_{I,\mathcal{C}}\hat{\psi}_I(\vec{x},t)\hat{\psi}^{+}_I(\vec{x'},t')\Big\} \end{aligned} \tag{10.12}$$

In the last step, I combined the propagators in a single operator, the S-matrix $\hat{\mathcal{S}}_{I,\mathcal{C}}$, which I will define below in more detail. The S-matrix[1] is the propagator in the interaction picture along the chosen contour $\mathcal{C}$. As a result of the particle-number conservation, the Hamiltonian contains only terms with an even number of fermionic operators. Therefore, sign-changes due to the interchanges of two Hamilton operators need not be considered.

S-matrix: The propagator in the interaction picture along the entire contour is the S-matrix $\hat{\mathcal{S}}_{I,\mathcal{C}}$. For a general time contour $\mathcal{C}$, the **S-matrix** is

$$\hat{\mathcal{S}}_{I,\mathcal{C}} \overset{\text{def}}{=} \lim_{N\to\infty}\prod_{j=1}^{N}\hat{\mathcal{U}}^{(W)}_I(t_j,t_{j-1}) \qquad \text{with } t_j = \tau\left(s_i + \frac{s_f - s_i}{N}\cdot j\right) \tag{10.13}$$

where s_i and s_f mark the initial and final values of the time contour and where $\tau(s)$ defines the time contour.

The S-matrix can alternatively be expressed as time-ordered exponential

$$\mathcal{S}_{I,\mathcal{C}} \overset{\text{def}}{=} \mathcal{T}_{\mathcal{C}}\exp\left(-\frac{i}{\hbar}\int_{\mathcal{C}} dt\,\hat{W}_I(t)\right) \tag{10.14}$$

[1] My notation differs somewhat from the common definitions. The S matrix is often used as propagator with explicit time arguments.

where the time integral proceeds along the time contour. This expression is analogous to Eq. 4.40 on p. 170.

With the help of the time-ordering operator, the exponential can be expanded as power-series expansion in the interaction

$$\begin{aligned}\mathcal{S}_{I,\mathcal{C}} &\overset{\text{Eq. 10.14}}{=} \mathcal{T}_{\mathcal{C}} \exp\left(-\frac{i}{\hbar}\int_{\mathcal{C}} dt\, \hat{W}_I(t)\right) \\ &= \mathcal{T}_{\mathcal{C}} \sum_{n=0}^{\infty} \frac{1}{n!}\left(-\frac{i}{\hbar}\int_{\mathcal{C}} dt\, \hat{W}_I(t)\right)^n \\ &= \sum_{n=0}^{\infty} \frac{1}{n!}\left(\frac{1}{i\hbar}\right)^n \int_{\mathcal{C}} dt_1 \cdots \int_{\mathcal{C}} dt_n\, \mathcal{T}_{\mathcal{C}} \hat{W}_I(t_1)\cdots\hat{W}_I(t_n) \end{aligned} \tag{10.15}$$

The S-matrix should be considered as a sum of product of many creation and annihilation operators, each having its own time argument. This is required so that the time-ordering operator can place every operator into the correct position along the contour. It is a bit misleading that these time arguments are implicit and do not show up in the expression of the S-matrix.

The S-matrix for the specific time contour $\mathcal{C}$ is

$$\hat{\mathcal{S}}_{I,\mathcal{C}} = \hat{\mathcal{U}}_I^{(W)}(0,\infty)\hat{\mathcal{U}}_I^{(W)}(\infty,-\infty)\hat{\mathcal{U}}_I^{(W)}(-\infty,0) \tag{10.16}$$

The observant reader will notice that this S-matrix is just the unit operator. The S-matrix becomes useful in the context of a time-ordered product with other operators. Then the S-matrix is split up into individual propagators in between the other operators. In case of doubt one should always refer to the definition Eq. 10.13, which divides the S-matrix into propagators along infinitesimally short time steps.[2]

With the help of the time contour and the S-matrix defined on it, the Green's function Eq. 10.12 obtains the simpler form of Eq. 10.17.

GREEN'S FUNCTION WITH TIME CONTOUR

$$G^{\mathcal{C}}(\vec{x},t,\vec{x}',t') \overset{\text{Eq. 10.12}}{=} \frac{1}{i\hbar}\mathrm{Tr}\left\{\hat{\rho}_{T,\mu}^{(W)}\mathcal{T}_{\mathcal{C}}\hat{S}_{I,\mathcal{C}}\hat{\psi}_I(\vec{x},t)\hat{\psi}_I^{+}(\vec{x}',t')\right\} \tag{10.17}$$

where the time contour $\mathcal{C}$ in the complex-time plane proceeds along the points

$$0 \to -\infty \to \min(t,t') \to \max(t,t') \to \infty \to 0 \tag{10.18}$$

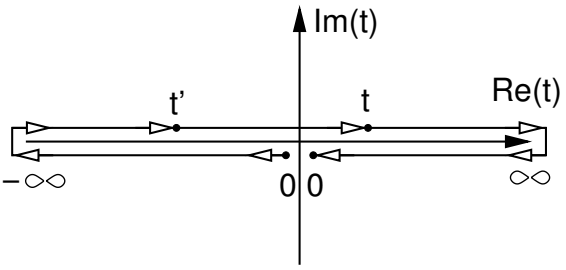

The drawing does not imply that the time is displaced from the real time axis into the complex plane.

[2] This is one of the origins of the path-integral formulation of quantum physics.

Uniqueness of initial time: The ensemble is defined such that it is in thermal equilibrium at time $t = 0$. The Hamiltonian usually drives the system out of thermal equilibrium as it propagates along the time contour. Choosing the time, at which the ensemble is in equilibrium, at time $t = 0$ is not a restriction, because a global time translation can shift it to any other time without changing the physical processes.

10.1.3 Interacting from non-interacting ensemble: complex-time contour

The Green's function in the form of Eq. 10.12 requires not only the propagator $\hat{S}_{I,\mathcal{C}}$ of the interacting system but also the state operator $\hat{\rho}^{(W)}_{T,\mu}$ for the interacting system. Below, I will show how the interaction contained in the state operator $\hat{\rho}^{(W)}_{T,\mu}$ can be incorporated into the S-matrix by adjusting the time contour. The resulting contour will leave the real-time axis and extend into the complex plane. This justifies, why I introduced the propagator for arbitrary contours in the complex-time plane.

I exploit [3] the similarity between the statistical operator $\hat{\rho}^{(W)}_{T,\mu} = \frac{1}{Z^{(W)}_{T,\mu}} \mathrm{e}^{-\beta(\hat{H}^{(W)} - \mu\hat{N})}$ in the grand ensemble with the propagator $\hat{\mathcal{U}}(t,t') = \mathrm{e}^{\frac{1}{i\hbar}\hat{H}^{(W)}(t-t')}$ for a time-independent Hamiltonian.

The von-Neumann density matrix $\hat{\rho}^{(W)}_{T,\mu}$ of the interacting system is related to the exponential of the Hamiltonian and the partition function $Z^{(W)}_{T,\mu} = \mathrm{Tr}\left(\exp[-\beta(\hat{H}^{(W)} - \mu\hat{N})]\right)$. With the help of the propagator in imaginary time, it can be related to the density matrix $\hat{\rho}^{(0)}_{T,\mu}$ of the non-interacting system and its partition function $Z^{(0)}_{T,\mu} = \mathrm{Tr}\left(\exp[-\beta(\hat{h} - \mu\hat{N})]\right)$. The following steps rely on particle-number conservation, i.e. that the particle-number operator commutates with the Hamiltonian independent of the interaction strength.

$$
\begin{aligned}
\hat{\rho}^{(W)}_{T,\mu} &= \frac{1}{Z^{(W)}_{T,\mu}} \mathrm{e}^{-\beta(\hat{H}^{(W)} - \mu\hat{N})} \\
&= \frac{1}{Z^{(W)}_{T,\mu}} \mathrm{e}^{\beta\mu\hat{N}}\, \mathrm{e}^{-\frac{i}{\hbar}\hat{H}^{(W)}(-i\hbar\beta - 0)} \\
&\overset{[\hat{H},\hat{N}]_-=0}{=} \frac{1}{Z^{(W)}_{T,\mu}} \underbrace{\frac{Z^{(0)}_{T,\mu}}{Z^{(0)}_{T,\mu}}}_{=1} \underbrace{\mathrm{e}^{-\beta(\hat{h}-\mu\hat{N})} \mathrm{e}^{\frac{i}{\hbar}\hat{h}(-i\hbar\beta)}}_{=\mathrm{e}^{\beta\mu\hat{N}}} \mathrm{e}^{-\frac{i}{\hbar}\hat{H}^{(W)}(-i\hbar\beta-0)} \underbrace{\mathrm{e}^{-\frac{i}{\hbar}\hat{h}(0)}}_{=\hat{1}} \\
&\overset{[\hat{h},\hat{N}]_-=0}{=} \frac{Z^{(0)}_{T,\mu}}{Z^{(W)}_{T,\mu}} \underbrace{\frac{1}{Z^{(0)}_{T,\mu}} \mathrm{e}^{-\beta(\hat{h}-\mu\hat{N})}}_{\hat{\rho}^{(0)}_{T,\mu}} \underbrace{\mathrm{e}^{\frac{i}{\hbar}\hat{h}(-i\hbar\beta)} \mathrm{e}^{-\frac{i}{\hbar}\hat{H}^{(W)}(-i\hbar\beta-0)} \mathrm{e}^{-\frac{i}{\hbar}\hat{h}(0)}}_{\hat{\mathcal{U}}^{(W)}_I(-i\hbar\beta,0) \quad \text{Eq. 10.11}} \\
&= \frac{Z^{(0)}_{T,\mu}}{Z^{(W)}_{T,\mu}} \hat{\rho}^{(0)}_{T,\mu} \hat{\mathcal{U}}^{(W)}_I(-i\hbar\beta, 0)
\end{aligned}
\tag{10.19}
$$

The interesting point is that the interaction can be absorbed in a propagator along the imaginary axis of the complex-time plane.

The factor $Z^{(0)}_{T,\mu}/Z^{(W)}_{T,\mu}$ can be rewritten using the normalization condition of the state operator

[3] Literature:

- Joseph Maciejko, *An introduction to Nonequilibrium Many-Body Theory*, Lecture notes (2007) (`http://www.physics.arizona.edu/~stafford/Courses/560A/nonequilibrium.pdf`, retrieved July 2, 2016)
- Robert van Leeuwen and Nils Erik Dahlen, *An Introduction to Nonequilibrium Green Functions* (2005) (`http://theochem.chem.rug.nl/research/vanleeuwen/literature/NGF.pdf` retrieved July,2 2016); Lecture Notes Collection FreeScience.info ID1576 (`https://archive.org/details/R_van_Leeuwen_and_N_E_Dahlen__An_Introduction_to_Nonequilibrium_Green_Functions`)

$\hat{\rho}^{(W)}_{T,\mu}$

$$1 = \mathrm{Tr}\left\{\hat{\rho}^{(W)}_{T,\mu}\right\} \overset{\text{Eq. 10.19}}{=} \frac{Z^{(0)}_{T,\mu}}{Z^{(W)}_{T,\mu}} \mathrm{Tr}\left\{\hat{\rho}^{(0)}_{T,\mu}\hat{\mathcal{U}}^{(W)}_{I}(-i\hbar\beta,0)\right\}$$

$$\Rightarrow \qquad \frac{Z^{(0)}_{T,\mu}}{Z^{(W)}_{T,\mu}} = \frac{1}{\mathrm{Tr}\left\{\hat{\rho}^{(0)}_{T,\mu}\hat{\mathcal{U}}^{(W)}_{I}(-i\hbar\beta,0)\right\}} = \frac{1}{\mathrm{Tr}\left\{\hat{\rho}^{(0)}_{T,\mu}\mathcal{T}_{\mathcal{C}}\hat{\mathcal{S}}_{I,\mathcal{C}}\right\}} \tag{10.20}$$

The contour is now the one from $t = 0$ along the imaginary time axis towards $-i\hbar\beta$. Furthermore, I extended the propagator by a closed contour around the real axis. This closed circle is a unit operator and thus does not change the result.

Remember, that the S-matrix should be considered as a product of short-time propagators between infinitesimally spaced points along the time contour, so that the time-ordering operator can divide it into the proper pieces and insert it between any other operators that occur in the time-ordered product.

Insertion of Eq. 10.20 into Eq. 10.19 for the density matrix of the interacting system yields

$$\hat{\rho}^{(W)}_{T,\mu} = \frac{\hat{\rho}^{(0)}_{T,\mu}\hat{\mathcal{U}}^{(W)}_{I}(-i\hbar\beta,0)}{\mathrm{Tr}\left\{\hat{\rho}^{(0)}_{T,\mu}\mathcal{T}_{\mathcal{C}}\hat{\mathcal{S}}_{I,\mathcal{C}}\right\}} \tag{10.21}$$

where the S-matrix is evaluated for the new contour $0 \to -\infty \to +\infty \to 0 \to -i\hbar\beta$.

Insertion of this density matrix for the grand potential into the Green's function Eq. 10.17 yields our result, which provides the Green's function as an expectation value of the density operator of the non-interacting system. The interaction appears only in one object, the S-matrix.

GREEN'S FUNCTION AS EXPECTATION VALUE OF THE NON-INTERACTING SYSTEM

$$G^{\mathcal{C}}(\vec{x},t,\vec{x'},t') \overset{\text{Eq. } 10.17}{=} \frac{1}{i\hbar}\frac{\mathrm{Tr}\left\{\hat{\rho}^{(0)}_{T,\mu}\mathcal{T}_{\mathcal{C}}\hat{S}_{I,\mathcal{C}}\hat{\psi}_I(\vec{x},t)\hat{\psi}^{+}_I(\vec{x'},t')\right\}}{\mathrm{Tr}\left\{\hat{\rho}^{(0)}_{T,\mu}\mathcal{T}_{\mathcal{C}}\hat{S}_{I,\mathcal{C}}\right\}}$$

$$\Leftrightarrow \quad G^{\mathcal{C}}_{\alpha,\beta}(t,t') \overset{\text{Eq. } 10.17}{=} \frac{1}{i\hbar}\frac{\mathrm{Tr}\left\{\hat{\rho}^{(0)}_{T,\mu}\mathcal{T}_{\mathcal{C}}\hat{S}_{I,\mathcal{C}}\hat{c}_{I,\alpha}(t)\hat{c}^{+}_{I,\beta}(t')\right\}}{\mathrm{Tr}\left\{\hat{\rho}^{(0)}_{T,\mu}\mathcal{T}_{\mathcal{C}}\hat{S}_{I,\mathcal{C}}\right\}} \tag{10.22}$$

where the time contour $\mathcal{C}$ in the complex-time plane proceeds along the points

$$0 \to -\infty \to \min(t,t') \to \max(t,t') \to \infty \to 0 \to -i\hbar\beta \tag{10.23}$$

and the S-matrix

$$\hat{S}_{I,\mathcal{C}} = \mathcal{T}_{\mathcal{C}} \exp\Big(-\frac{i}{\hbar}\int_{\mathcal{C}} dt\, \hat{W}_I(t)\Big) \tag{10.24}$$

is the propagator along the same contour in the interaction picture.

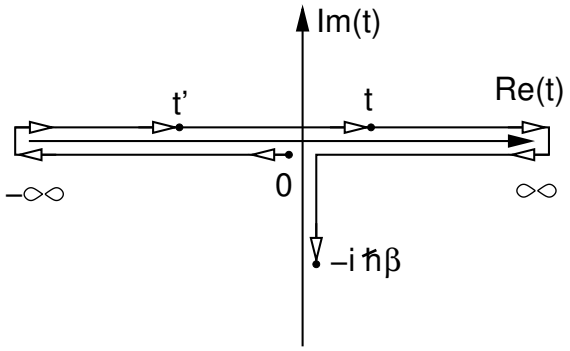

In practice, other contours are in use, which may be obtained by deforming the one given here.

The big advantage is that we work now with the density operator of the non-interacting system, which is converted into that of the interacting system by a propagation along the imaginary-time axis towards the real-time axis. Inspection of the expression for the Green's function shows that the interaction is now entirely contained in the propagator. Wick's theorem shows how the perturbation expansion in terms of interaction strength can be accomplished.

Grand potential: The partition function will establish an important link to the grand potential, namely

$$\Omega^{(W)}_{T,\mu} \overset{\text{Eq. ??}}{=} -k_B T \ln\left(Z^{(W)}_{T,\mu}\right) \overset{\text{Eq. } 10.20}{=} \underbrace{-k_B T \ln\left(Z^{(0)}_{T,\mu}\right)}_{\Omega^{(0)}_{T,\mu}} - k_B T \ln\left(\mathrm{Tr}\left\{\hat{\rho}^{(0)}_{T,\mu}\mathcal{T}_{\mathcal{C}}\hat{\mathcal{S}}_{I,\mathcal{C}}\right\}\right) \tag{10.25}$$

This equation of the grand potential, respectively its interaction part, will be converted below, Eq. 10.59 on p. 316, into a functional of the interaction matrix elements and the Green's function. In this form, the grand potential will become the key quantity for the diagrammatic expansion of the Green's function.

The grand potential of a non-interacting electron gas in a Hamiltonian $\hat{h}$ has been worked out

earlier, in Eq. **??**, as

$$\Omega^{(0)}_{T,\mu} = -k_B T \ln\left(Z^{(0)}_{T,\mu}\right) \overset{\text{Eq. ??}}{=} -k_B T \ \mathrm{Tr}\Big\{\ln\Big(\underbrace{1+\mathrm{e}^{-\beta(\hat{h}-\mu\hat{1})}}_{\left(\hat{1}-f_{T,\mu}(\hat{h})\right)^{-1}}\Big)\Big\} \tag{10.26}$$

which can be expressed[4] in terms of the equilibrium one-particle-reduced density matrix $\hat{\rho}^{(1),0} = \left[1+\mathrm{e}^{\beta(\hat{h}-\mu\hat{1})}\right]^{-1}$ of the non-interacting system, or in terms of the non-interacting Green's function as

$$\Omega^{(0)}_{T,\mu} = +k_B T \mathrm{Tr}\Big[\ln\left(\hat{1}-\hat{\rho}^{(1),0}\right)\Big] \overset{\text{Eq. 8.28}}{=} +k_B T \mathrm{Tr}\Big[\ln\left(\hat{1}+i\hbar\lim_{t'\to t^+}\hat{G}^{(0)}(t,t')\right)\Big] \tag{10.28}$$

Editor: See also section K.4.7 on p. 582 and Eq. 10.70 on p. 319. There is probably some material duplicated.

10.2 Wick's theorem

We can obtain the Green's function using Eq. 10.22 as the ratio of two expectation values in the ensemble of non-interacting states. The interaction is completely contained in the S-matrix. The interaction is a product of creation and annihilation operators in the interaction picture. Thus, a perturbation expansion of the S-matrix in terms of the interaction strength

$$\mathrm{Tr}\Big\{\hat{\rho}^{(0)}_{T,\mu}\mathcal{T}_{\mathcal{C}}\hat{S}_{I,\mathcal{C}}\hat{c}_{I,\alpha}(t)\hat{c}^{+}_{I,\beta}(t')\Big\} \overset{\text{Eq. 10.14}}{=} \sum_{n=0}^{\infty}\frac{1}{n!}\left(\frac{1}{i\hbar}\right)^n\int dt_1\cdots dt_n$$
$$\times\mathrm{Tr}\Big\{\hat{\rho}^{(0)}_{T,\mu}\mathcal{T}_{\mathcal{C}}\hat{W}_I(t_n)\hat{W}_I(t_{n-1})\cdots\hat{W}_I(t_1)\hat{c}_{I,\alpha}(t)\hat{c}^{+}_{I,\beta}(t')\Big\} \tag{10.29}$$

will decompose the numerator and the denominator separately into a sum of expectation values of products of creation and annihilation operators in the interaction picture.

Wick's theorem shows how this expectation value of time-ordered products of creation and annihilation operators can be expressed as sum over products of non-interacting Green's functions.

While the original version of Wick's theorem[57] has been developed in the 1950's, we present here what is also called the generalized Wick's theorem. The generalized Wick's theorem has been proved by Matsubara[81]. The central part of Wick's theorem for finite temperatures rests on the so-called[5] **trace theorem** proven by Gaudin[82].

The generalized Wick's theorem has also been presented in the book Fetter and Walecka (Section 24).[3]

Before we arrive at the central points of Wick's theorem, let me introduce a few notations, that will simplify the derivation.

10.2.1 Notation: Incoming and outgoing indices

In the following, I will try to adhere to the convention to label an annihilation operator with an index i, which stands for **"incoming"**. A creation operator will be labeled by o, which stands for **"outgoing"**. This is inspired by the Feynman diagrams, that will be introduced later: A Green's function $G_{i,o}(t_i, t_o)$ is represented by an arrow, which begins with an outgoing index and ends at an incoming index. When there are several incoming (or outgoing indices, I will attach another index as in $G_{i_1,o_1}(t_{i_1}, t_{o_1})$.

[4]
$$\hat{\rho}^{(1)} = \left[1+\mathrm{e}^{\beta(\hat{h}-\mu\hat{1})}\right]^{-1} \quad\Rightarrow\quad \frac{1-\hat{\rho}^{(1)}}{\hat{\rho}^{(1)}} = \mathrm{e}^{\beta(\hat{h}-\mu\hat{1})} \quad\Rightarrow\quad 1+\mathrm{e}^{-\beta(\hat{h}-\mu\hat{1})} = 1+\frac{\hat{\rho}^{(1)}}{1-\hat{\rho}^{(1)}} = \frac{1}{\hat{1}-\hat{\rho}^{(1)}} \tag{10.27}$$

[5] Naming and reference from "Wick's Theorem at Finite temperature", T.S. Evans and D.A. Steer, arxiv:hep-ph/9601268

10.2.2 Time order inside the interaction

Special care is required when translating the interaction into the interaction picture, because the interaction contains four operators with the same time argument. As a result, the time order of these operators is ambiguous. This problem was not present, when we introduced the time ordering in the context of one-particle quantum mechanics.

Each interaction operator is composed of creation and annihilation operators.

$$\hat{W} = \frac{1}{2} \sum_{i_1,o_1,i_2,o_2} W_{o_1,o_2,i_1,i_2} \hat{c}^\dagger_{S,o_1} \hat{c}^\dagger_{S,o_2} \hat{c}_{S,i_2} \hat{c}_{S,i_1} \tag{10.30}$$

which are transformed into the interaction picture

$$\begin{aligned}
\hat{W}_I(t) &= \hat{\mathcal{U}}^{(0)}(0,t)\hat{W}_S(t)\hat{\mathcal{U}}^{(0)}(t,0) \\
&= \frac{1}{2} \sum_{i_1,o_1,i_2,o_2} W_{o_1,o_2,i_1,i_2} \hat{\mathcal{U}}^{(0)}(0,t)\hat{c}^\dagger_{S,o_1}\hat{c}^\dagger_{S,o_2}\hat{c}_{S,i_2}\hat{c}_{S,i_1}\hat{\mathcal{U}}^{(0)}(t,0) \\
&= \frac{1}{2} \sum_{i_1,o_1,i_2,o_2} W_{o_1,o_2,i_1,i_2} \\
&\times \underbrace{\hat{\mathcal{U}}^{(0)}(0,t)\hat{c}^\dagger_{S,o_1}}_{\hat{c}^+_{I,o_1}(t^+)} \overbrace{\hat{\mathcal{U}}^{(0)}(t,0)\hat{\mathcal{U}}^{(0)}(0,t)}^{\hat{1}} \hat{c}^\dagger_{S,o_2} \overbrace{\hat{\mathcal{U}}^{(0)}(t,0)\hat{\mathcal{U}}^{(0)}(0,t)}^{\hat{1}} \hat{c}_{S,i_2} \overbrace{\hat{\mathcal{U}}^{(0)}(t,0)\hat{\mathcal{U}}^{(0)}(0,t)}^{\hat{1}} \hat{c}_{S,i_1}\hat{\mathcal{U}}^{(0)}(t,0) \\
&= \frac{1}{2} \sum_{i_1,o_1,i_2,o_2} W_{o_1,o_2,i_1,i_2} \mathcal{T}_\mathcal{C}\Big\{\hat{c}^+_{I,o_1}(t^+)\hat{c}^+_{I,o_2}(t^+)\hat{c}_{I,i_2}(t)\hat{c}_{I,i_1}(t)\Big\}
\end{aligned} \tag{10.31}$$

In the last step, I introduced the contour time-ordering operator $\mathcal{T}_\mathcal{C}$. The time argument for the creation operators has been shifted forward by an infinitesimal amount[6] δ to the new time $t^+ = t(s+\delta)$. This is required, because the time-ordered product would otherwise be undefined: If creation and annihilation operators have the same time argument, the time-ordered product can produce two different values, depending on which time argument is considered later than the other.

$$\begin{aligned}
\mathcal{T}_\mathcal{C}\hat{c}^+_\alpha(t^+)\hat{c}_\beta(t) &= \hat{c}^+_\alpha(t^+)\hat{c}_\beta(t) = [\hat{c}^+_\alpha(t^+),\hat{c}_\beta(t)]_+ - \hat{c}_\beta(t)\hat{c}^+_\alpha(t^+) \\
\mathcal{T}_\mathcal{C}\hat{c}^+_\alpha(t)\hat{c}_\beta(t^+) &= -\hat{c}_\beta(t^+)\hat{c}^+_\alpha(t)
\end{aligned} \tag{10.32}$$

The two results differ by an anticommutator. This ambiguity does not exist for the product of either two annihilation operators or of two creation operators, because their anticommutator vanishes. The ambiguity is lifted by ensuring that the time arguments of creation and annihilation operators are different, i.e. by distinguishing t and t^+. By increasing the time of the creation operators they are brought into the order they occur in the interaction.

This feature, namely the distinction of t and t^+, has important consequences for the evaluation of Feynman diagrams lateron.

10.2.3 Generalized Wick theorem

The perturbation expansion of the S-matrix used above in Eq. 10.29 shows that we need to work out the expectation value of time-ordered products of creation and annihilation operators in the interaction picture. For the denominator of the Green's function Eq. 10.22, the products result directly from the expansion of the S-matrix. The numerator of Eq. 10.22 has one additional pair of creation and annihilation operators connected to the arguments of the Green's function.

[6] For the notation see Eq. 8.31 on p. 260

All these expectation values have the form

$$Y \stackrel{\text{def}}{=} \mathrm{Tr}\Big\{\hat{\rho}^{(0)}_{T,\mu}\hat{A}_1(t_1)\cdots\hat{A}_M(t_M)\Big\} \qquad \text{with } t_1 \geq t_2 \geq \ldots \geq t_M \tag{10.33}$$

The operators $\hat{A}_j(t)$ are creation or annihilation operators in the interaction picture with a time-dependent, non-interacting Hamiltonian $\hat{h}(t)$. The initial ensemble is defined by thermal equilibrium with the initial, non-interacting Hamiltonian $\hat{h}(0)$. The corresponding von-Neumann density matrix is

$$\hat{\rho}^{(0)}_{T,\mu} = \frac{1}{Z^{(0)}_{T,\mu}}\mathrm{e}^{-\beta(\hat{h}(0)-\mu\hat{N})} \tag{10.34}$$

The gist of Wick's theorem is to map Y in Eq. 10.33, a complicated trace in Fock space, onto expectation values in the one-particle Hilbert space. The result will be a large sum of products of non-interacting Green's functions.

Rather than working out Wick's theorem with all detail in the main text, I shifted the proof into the appendix K on p. 561. Here, I will only sketch the main steps.

As shown by Eq. K.1 and Eq. K.2 on p. 562, the creation and annihilation operators in the interaction picture are equal to the ones in the Schrödinger picture multiplied with the one-particle propagator of the (non-interacting) electrons.

$$\hat{c}^\dagger_{I,\alpha}(t) \stackrel{\text{Eq. } K.1}{=} \sum_\beta \hat{c}^\dagger_{S,\beta}\ \langle\chi_\beta|\hat{U}(0,t)|\pi_\alpha\rangle \tag{10.35}$$

$$\hat{c}_{I,\alpha}(t) \stackrel{\text{Eq. } K.2}{=} \sum_\beta \langle\pi_\alpha|\hat{U}(t,0)|\chi_\beta\rangle\ \hat{c}_{S,\beta} \tag{10.36}$$

As a consequence, the anticommutators Eqs. K.51, K.52 and K.53 of creation and annihilation operators in the interaction picture are not operators in Fock space but numbers: namely the matrix elements of the one-particle propagator.

$$\left[\hat{c}_{I,\alpha}(t_2), \hat{c}^+_{I,\beta}(t_1)\right]_+ \stackrel{\text{Eq. } K.51}{=} \left\langle \pi_\alpha \middle| \hat{U}(t_2,t_1) \middle| \pi_\beta \right\rangle \hat{1} \tag{10.37}$$

The $\hat{1}$ on the right-hand side is the unit operator in Fock space. The anticommutators between two creation operators Eq. K.52, respectively between to annihilation operators K.53, vanish as in the Schrödinger picture.

Furthermore, as shown in Eq. K.56 and Eq. K.57, the product of a creation or annihilation operator with the density matrix can be interchanged while attaching an additional factor.

As shown in section K.4, each operator in Y can be permutated using the anticommutators in a cycle until it stands again in the same position of the product. While interchanging the operator with the density matrix, the one-particle reduced density matrix emerges. This term, together with the anticommutator combines in a non-trivial manner, to the Green's function of the non-interacting system. The result of is a sum of terms, each containing one Green's function and a trace of a time-ordered product with two operators less.

The same procedure can be applied recursively on the result, until a large sum with $M!$ terms emerges. Each term contains a product of M Green's function and a fully antisymmetric tensor, keeping track of the sign changes.

10.2.4 Generalized Wick's theorem at finite temperature

Thus, we obtain the central message of Wick's theorem

WICK'S THEOREM

Wick's theorem maps the thermal expectation value of a time-ordered product of creation and annihilation operators in the interaction picture $\hat{A}_j \in \{\hat{c}^+_{I,\alpha}(t), \hat{c}_{I,\alpha}(t)\}$, onto a sum of products of non-interacting contour-ordered Green's functions. The ensemble is determined by thermal equilibrium with the initial ($t = 0$), non-interacting Hamiltonian $\hat{h}(0)$. The corresponding von-Neumann density matrix is $\hat{\rho}^{vN,(0)}_{T,\mu} = \frac{1}{Z^{(0)}_{T,\mu}} \mathrm{e}^{-\beta(\hat{h}(0)-\mu\hat{N})}$. $\mathcal{T}_\mathcal{C}$ is the time-ordering operator along the contour $\mathcal{C}$ in the complex-time plane.

$$\mathrm{Tr}\Big\{\hat{\rho}^{vN,(0)}_{T,\mu}\mathcal{T}_\mathcal{C}\prod_{j=1}^{L}\hat{c}_{I,i_j}(t'_j)\hat{c}^+_{I,o_j}(t_j)\Big\} \overset{\text{Eq. } K.100}{=} \sum_{\vec{\mathcal{P}}}\epsilon_{\mathcal{P}_1,\ldots,\mathcal{P}_L}(i\hbar)^L\prod_{j=1}^{L}G^{\mathcal{C},(0)}_{i_{\mathcal{P}_j},o_j}(t'_{\mathcal{P}_j},t_j)\,. \tag{10.38}$$

$\epsilon_{\mathcal{P}_1,\ldots,\mathcal{P}_L}$ is the fully antisymmetric tensor and the sum includes all integer vectors with elements $\mathcal{P}_j \in \{1,\ldots,L\}$. The fully antisymmetric tensor $\epsilon_{\mathcal{P}_1,\mathcal{P}_2,\ldots,\mathcal{P}_M}$ selects the permutation vectors with $\mathcal{P}_j \neq \mathcal{P}_k$.
The one-particle basisset $\{|\chi_\alpha\rangle\}$ defining the creation and annihilation operators may be non-orthonormal. The overlap matrix is $S_{\alpha,\beta} = \langle\chi_\alpha|\chi_\beta\rangle$. Each orbital $|\chi_\alpha\rangle$ has a projector function $\langle\pi_\alpha| = \sum_\beta S^{-1}_{\alpha,\beta}\langle\chi_\beta|$. The anticommutator relation of annihilation and creation operators in the Schrödinger picture is $\left[\hat{c}_\alpha, \hat{c}^\dagger_\beta\right]_+ = \langle\pi_\alpha|\pi_\beta\rangle$.
The non-interacting contour-ordered Green's function $G^{\mathcal{C}(0)}_{i,o}(t',t)$ has been defined in Eq. 7.27 (p.247) as

$$G^{\mathcal{C},(0)}_{i,o}(t',t) \overset{\text{Eq. } 7.27}{=} \frac{1}{i\hbar}\Big\langle\pi_i\Big|\hat{U}(t',0)\Big\{\underbrace{\theta_\mathcal{C}(t-t')\big(\hat{1}-\hat{\rho}^{(1)(0)}_{T,\mu}\big)}_{\text{electrons}} - \underbrace{\theta_\mathcal{C}(t'-t)\hat{\rho}^{(1)(0)}_{T,\mu}}_{\text{holes}}\Big\}\hat{U}(0,t)\Big|\pi_o\Big\rangle$$

The time-ordering operator $\mathcal{T}_\mathcal{C}$ rearranges the product in increasing order along some directed contour in the complex plane. The step function $\theta_\mathcal{C}(t-t')$ refers to the time ordering along the time contour consistent with the definition of the time-ordering operator.
Wick's theorem can also be expressed by a determinant

$$\mathrm{Tr}\Big\{\hat{\rho}^{(0)}_{T,\mu}\mathcal{T}_\mathcal{C}\prod_{j=1}^{L}\hat{c}_{I,\alpha_j}(t_j)\hat{c}^+_{I,\beta_j}(t'_j)\Big\} = (i\hbar)^L\det\begin{vmatrix} G^{\mathcal{C},(0)}_{\alpha_1,\beta_1}(t_1,t'_1)\; G^{\mathcal{C},(0)}_{\alpha_1,\beta_2}(t_1,t'_2)\;\ldots \\ G^{\mathcal{C},(0)}_{\alpha_2,\beta_1}(t_2,t'_1)\; G^{\mathcal{C},(0)}_{\alpha_2,\beta_2}(t_2,t'_2)\;\ldots \\ \vdots \qquad\qquad \vdots \qquad\quad \ddots \end{vmatrix} \tag{10.39}$$

10.3 Perturbation expansion of the Green's function

Let us use Wick's theorem to evaluate the Green's function.

$$G_{\alpha,\beta}(t,t') \overset{\text{Eq. } 10.22}{=} \frac{1}{i\hbar} \frac{\mathrm{Tr}\left\{\hat{\rho}^{(0)}_{T,\mu}\mathcal{T}_{\mathcal{C}}\hat{S}_{I,\mathcal{C}}\hat{c}_{I,\alpha}(t)\hat{c}^{+}_{I,\beta}(t')\right\}}{\mathrm{Tr}\left\{\hat{\rho}^{(0)}\mathcal{T}_{\mathcal{C}}\hat{S}_{I,\mathcal{C}}\right\}} \tag{10.40}$$

10.3.1 Outline

In the following sections, we will go through several theorems to set up a diagrammatic expansion of the Green's function and to simplify this expansion.

The steps, we will go through are

1. Enumerate and evaluate diagrams in the denominator of Eq. 10.40: closed diagrams
2. Obtain diagrams of the numerator of Eq. 10.40 from those in the denominator.
3. Green's function from "grand potential functional"
4. sign theorem (section 11.3)
5. linked-cluster theorem (section 11.4)
6. topologically inequivalent diagrams and symmetry factors (section 11.5)

When we are done, we arrived at an expression for the diagrammatic expansion of a grand potential $\mathcal{Q}_{T,\mu}[\boldsymbol{G}^{(0)}]$, which is a functional of the non-interacting Green's function. Each diagram has a value, Eq. 11.36, respectively Eq. 11.50, which itself is a functional of the non-interacting Green's function.

The derivative of the grand potential with the Green's function provides the **reducible self energy**, from which the interacting Green's function is obtained via Dyson's equation Eq. 10.60. I will call the reducible self energy also the **total self energy**.

10.3.2 Interaction with two time arguments

Editor: Unfinished!!!!

It will be convenient to introduce the interaction with two time arguments rather than one. The reason is two-fold:

- it will simplify the expression for a Feynman diagram introduced later.
- Renormalization will later introduce a screened interaction, which will replace the bare Coulomb interaction in some of the expressions. The screened interaction is retarded and has naturally two time arguments.

Eq. K.95

$$\hat{W}_I(t) = \tag{10.41}$$

10.3.3 Expansion of the S-matrix

The S-matrix can be expanded into a Taylor expansion

$$
\begin{aligned}
\hat{S}_{I,\mathcal{C}} &\overset{\text{Eq. } 10.14}{=} \mathcal{T}_{\mathcal{C}} \exp\left(-\frac{i}{\hbar}\int_{\mathcal{C}} dt\, \hat{W}_I(t)\right) \\
&\overset{\text{Eq. } 10.15}{=} \sum_{n=0}^{\infty} \frac{1}{n!}\left(\frac{1}{i\hbar}\right)^n \int_{\mathcal{C}} dt_1 \cdots \int_{\mathcal{C}} dt_n\, \mathcal{T}_{\mathcal{C}} \hat{W}_I(t_1)\cdots\hat{W}_I(t_n) \\
&\overset{\text{Eq. } K.95}{=} \sum_{n=0}^{\infty} \frac{1}{n!}\left(\frac{1}{i\hbar}\right)^n \int_{\mathcal{C}} dt_1 \cdots \int_{\mathcal{C}} dt_n \sum_{o_1,i_1,\ldots,o_{2n},i_{2n}} \left[\frac{1}{2^n}\prod_{j=1}^{n} W_{o_{2j-1},o_{2j},i_{2j-1},i_{2j}}(t_j)\right] \\
&\quad \times \mathcal{T}_{\mathcal{C}}\Big[\underbrace{\hat{c}_{I,i_1}(t_1)\hat{c}^+_{I,o_1}(t_1^+)\hat{c}_{I,i_2}(t_1)\hat{c}^+_{I,o_2}(t_1^+)}_{\text{from } \hat{W}_I(t_1)} \cdots \underbrace{\hat{c}_{I,i_{2n-1}}(t_n)\hat{c}^+_{I,o_{2n-1}}(t_n^+)\hat{c}_{I,i_{2n}}(t_n)\hat{c}^+_{I,o_{2n}}(t_n^+)}_{\text{from } \hat{W}_I(t_n)}\Big]
\end{aligned}
\tag{10.42}
$$

The creation and annihilation operators have been brought into the desired order according to Eq. **??** on p. **??**, and the time argument of the creation operators in each interaction term has been shifted according to Eq. K.95 on p. 581. The time dependence in the interaction matrix elements is present for the adiabatic switching factor in the zero-temperature theory.

The matrix elements are

$$
W_{o_1,o_2,i_1,i_2} \overset{\text{Eq. } 3.51}{=} \int d^4x \int d^4x' \, \frac{e^2 \chi^*_{o_1}(\vec{x})\chi^*_{o_2}(\vec{x'})\chi_{i_1}(\vec{x})\chi_{i_2}(\vec{x'})}{4\pi\epsilon_0|\vec{r}-\vec{r'}|} \tag{10.43}
$$

It will be convenient to **double the number of time variables**.

$$
\begin{aligned}
\hat{S}_{I,\mathcal{C}} &\overset{\text{Eq. } 10.42}{=} \sum_{n=0}^{\infty} \frac{1}{n!}\left(\frac{1}{i\hbar}\right)^n \int_{\mathcal{C}} dt_1 \cdots \int_{\mathcal{C}} dt_{2n} \sum_{o_1,i_1,\ldots,o_{2n},i_{2n}} \left[\frac{1}{2^n}\prod_{j=1}^{n} W_{o_{2j-1},o_{2j},i_{2j-1},i_{2j}} \delta_{\mathcal{C}}(t_{2j-1}-t_{2j})\right] \\
&\quad \times \mathcal{T}_{\mathcal{C}}\Big[\underbrace{\hat{c}_{I,i_1}(t_1)\hat{c}^+_{I,o_1}(t_1^+)\hat{c}_{I,i_2}(t_2)\hat{c}^+_{I,o_2}(t_2^+)}_{\text{from } \hat{W}_I(t_1,\,t_2)} \cdots \underbrace{\hat{c}_{I,i_{2n-1}}(t_{2n-1})\hat{c}^+_{I,o_{2n-1}}(t_{2n-1}^+)\hat{c}_{I,i_{2n}}(t_{2n})\hat{c}^+_{I,o_{2n}}(t_{2n}^+)}_{\text{from } \hat{W}_I(t_{2n-1},\,t_{2n})}\Big]
\end{aligned}
\tag{10.44}
$$

While it appears at first as an unnecessary complication, this choice has a number of advantages

- it will simplify the expression for a Feynman diagram introduced later by treating time and orbital arguments in an analogous manner.
- Renormalization will later introduce a screened interaction, which will replace the bare Coulomb interaction in some of the expressions. The screened interaction is retarded and has naturally two time arguments.

10.3.4 Expansion of the denominator of the Green's function

The expansion Eq. 10.44 of the S-matrix is inserted into denominator and numerator of the Green's function Eq. 10.40.

Let me investigate the denominator first. Firstly, it is simpler. Secondly, the terms of the numerator can be derived from those of the denominator. This will be shown below.

In the denominator of the Green's function Eq. 10.40, we insert the expansion of the S-matrix Eq. 10.44, which turns it into a large sum of operator products. The contour time-ordered operator products in the sum are resolved via Wick's theorem Eq. 10.38 on p. 305. This turns the denominator

of the Green's function into a sum of products of the non-interacting Green's function.

$$\begin{aligned}
\mathrm{Tr}\Big\{\hat{\rho}^{(0)}_{T,\mu}\mathcal{T}_{\mathcal{C}}\hat{S}_{I,\mathcal{C}}\Big\} &\overset{\text{Eq. 10.44}}{=} \sum_{n=0}^{\infty}\frac{1}{n!}\left(\frac{1}{i\hbar}\right)^n\int_{\mathcal{C}}dt_1\cdots\int_{\mathcal{C}}dt_{2n}\sum_{o_1,i_1,\ldots,o_{2n},i_{2n}}\left[\frac{1}{2^n}\prod_{j=1}^{n}W_{o_{2j-1},o_{2j},i_{2j-1},i_{2j}}\delta_{\mathcal{C}}(t_{2j-1}-t_{2j})\right]\\
&\times\mathrm{Tr}\Big\{\hat{\rho}^{(0)}_{T,\mu}\mathcal{T}_{\mathcal{C}}\Big[\underbrace{\hat{c}_{I,i_1}(t_1)\hat{c}^{+}_{I,o_1}(t_1^{+})\hat{c}_{I,i_2}(t_2)\hat{c}^{+}_{I,o_2}(t_2^{+})}_{\text{from } W_I(t_1,t_2))}\cdots\underbrace{\hat{c}_{I,i_{2n-1}}(t_{2n-1})\hat{c}^{+}_{I,o_{2n-1}}(t_{2n-1}^{+})\hat{c}_{I,i_{2n}}(t_{2n})\hat{c}^{+}_{I,o_{2n}}(t_{2n}^{+})}_{\text{from } W(t_n)}\Big]\Big\}\\
&\overset{\text{Eq. 10.38}}{=} \sum_{n=0}^{\infty}\frac{1}{n!}\left(\frac{1}{i\hbar}\right)^n\int_{\mathcal{C}}dt_1\cdots\int_{\mathcal{C}}dt_{2n}\sum_{o_1,i_1,\ldots,o_{2n},i_{2n}}\left[\frac{1}{2^n}\prod_{j=1}^{n}W_{o_{2j-1},o_{2j},i_{2j-1},i_{2j}}\delta_{\mathcal{C}}(t_{2j-1}-t_{2j})\right]\\
&\times\ (i\hbar)^{2n}\sum_{\vec{\mathcal{P}}}\epsilon_{\mathcal{P}_1,\ldots,\mathcal{P}_{2n}}G^{(0)}_{i_{\mathcal{P}_1},o_1}\Big(t_{\mathcal{P}_1},t_1^{+}\Big)\cdots G^{(0)}_{i_{\mathcal{P}_{2n}},o_{2n}}\Big(t_{\mathcal{P}\mathcal{P}_{2n}},t_{2n}^{+}\Big) \qquad (10.45)\\
&= \quad\sum_{n=0}^{\infty}\frac{1}{n!2^n}\sum_{\vec{\mathcal{P}}\in\mathbb{A}_n}V(\vec{\mathcal{P}}) \qquad (10.46)
\end{aligned}$$

The sum over the permutation vectors $\vec{\mathcal{P}}\in\mathbb{A}_n$ includes all $2n$-dimensional vectors with values $\mathcal{P}_j\in\{1,2,\ldots,2n\}$. The nonzero terms are related to permutation vectors $\vec{\mathcal{P}}$ that are obtained as permutation of the components of the vector $(1,\ldots,2n)$. This selection is enforced by the fully antisymmetric tensor $\epsilon_{\mathcal{P}_1,\ldots,\mathcal{P}_{2n}}$, which also includes the proper sign.

The time argument t_j^{+} of the creation operators is infinitesimally displaced forward in time relative to t_j.

Instantaneous interaction: The reason for this complicated mapping of the time arguments is that the Coulomb interaction is treated as instantaneous. This is a consequence of the non-relativistic description employed here. In a relativistic formulation the Coulomb interaction $v(\vec{r},t,\vec{r'},t')$ would be retarded, so that each spatial coordinate of the interaction would also have in independent time argument. Consequently, there would be twice as many time integrations in Eq. 10.45. In the non-relativistic formulation the interaction is of the form $v(\vec{r},t,\vec{r'},t')=\frac{e^2}{4\pi\epsilon_0|\vec{r}-\vec{r'}|}\delta(t-t')$. The delta function and half of the integrations cancel each other leading to the form of Eq. 10.45 above.

10.3.5 Diagrams of the denominator

It will be useful to represent the terms in the denominator as follows

SUM AND VALUES OF CLOSED DIAGRAMS

$$\mathrm{Tr}\Big\{\hat{\rho}^{(0)}_{T,\mu}\mathcal{T}_{\mathcal{C}}\hat{S}_{I,\mathcal{C}}\Big\}\overset{\text{Eq. 10.45}}{=}\sum_{n=0}^{\infty}\sum_{\vec{\mathcal{P}}\in\mathbb{A}_n}\frac{V(\vec{\mathcal{P}})}{n!2^n} \qquad (10.47)$$

where

$$\begin{aligned}
V(\vec{\mathcal{P}}) = \epsilon_{\mathcal{P}_1,\ldots,\mathcal{P}_{2n}}(i\hbar)^n\int_{\mathcal{C}}dt_1\cdots\int_{\mathcal{C}}dt_{2n}\sum_{o_1,i_1,\ldots,o_{2n},i_{2n}}\left(\prod_{j=1}^{n}W_{o_{2j-1},o_{2j},i_{2j-1},i_{2j}}\delta_{\mathcal{C}}(t_{2j-1}-t_{2j})\right)\\
\times G^{\mathcal{C},(0)}_{i_{\mathcal{P}_1},o_1}(t_{\mathcal{P}_1},t_1^{+})\cdots G^{\mathcal{C},(0)}_{i_{\mathcal{P}_{2n}},o_{2n}}(t_{\mathcal{P}_{2n}},t_{2n}^{+}) \qquad (10.48)
\end{aligned}$$

The value of zeroth order diagrams is defined to be equal to 1. The reason is that $\mathrm{Tr}\left\{\hat{\rho}^{(0)}_{T,\mu}\right\}=1$, which is the normalization of the density operator.

When the interaction tensor W and the non-interacting Green's function are known, each term is

completely characterized by the permutation vector $\vec{\mathcal{P}}$. The dimension of $\vec{\mathcal{P}}$ determines the order n of the diagram. For example, the permutation vector $\vec{\mathcal{P}}$ in Eq. 10.48 has the dimension $2n$.

The value $V(\vec{\mathcal{P}})$ of each term is dimension-less.[7]

10.3.6 Feynman diagrams

Editor: include here two graphs: one of a single interaction line with two vertices and at each vertex one incoming and one outgoing stump. The second graph shall be a non-interacting Green's function line with one outgoing and one incoming index. Also show the vertex.

Fig. 10.2: Elementary ingredients of a Feynman diagram for electrons with a Coulomb interaction. An arrow (a), called particle line, represents a bare (non-interacting) Green's function. A wriggly line, called an interaction line represents an interaction matrix element. The point where particle and interaction lines meet, is called a vertex. The vertex connects an incoming and an outgoing particle line with one end of an interaction line.

Each term $V(\mathcal{P})$ can be represented by a graph, which is called a **diagram**. The basic elements of a diagram are **interaction lines**, represented by wriggly lines, and **particle lines**, represented by arrows. The particle lines correspond to non-interacting Green's functions, while the interaction lines correspond the interaction matrix elements. Interaction and particle lines are joined at so-called **vertices**. A vertex is the junction of an interaction line, an incoming particle line and an outgoing particle line. The outgoing particle line is connected to the vertex with the right index and the right time argument, while the incoming index, the arrow, is connected to the vertex with the left index and the left time argument.

The graphical representation of the diagram proceeds as follows:

- Draw n wriggly lines. Each wriggly line represents an interaction. The interaction has two ends, which are called **vertices**. Each vertex has an incoming index i and an outgoing index o.

  For the j-th interaction, one vertex has the outgoing index o_{2j-1} and the incoming index i_{2j-1}. the other vertex has the indices o_{2j} and i_{2j}

- Now draw $2n$ arrows representing Green's functions. The k-th Green's function ($k \in \{1, \ldots, 2n\}$) starts at the k-th vertex and is connected to the outgoing index o_k. It stops at vertex $\mathcal{P}_k$ and is connected to the incoming index $i_{\mathcal{P}_k}$.

Example: Let us draw the diagram for the specified permutation vector $\vec{\mathcal{P}} = (3, 4, 1, 6, 2, 5)$.

- We draw three wriggly lines and number the vertices. (Each interaction has one vertex with an odd number and one with the next higher even number.)

- We look up the permutation vector and form the ordered index pairs representing the Green's functions

$$(1 \to \underbrace{3}_{\mathcal{P}_1}); (2 \to \underbrace{4}_{\mathcal{P}_2}); (3 \to \underbrace{1}_{\mathcal{P}_3}); (4 \to \underbrace{6}_{\mathcal{P}_4}); (5 \to \underbrace{2}_{\mathcal{P}_5}); (6 \to \underbrace{5}_{\mathcal{P}_6}); \qquad (10.49)$$

[7] This is the reason for leaving the factor $(i\hbar)^n$ with the diagram.

Now we connect the vertices according to this mapping.

- finally we rearrange the graph so that all connections remain intact but such that it is not all mixed up.

The result is shown in Fig. 10.3.

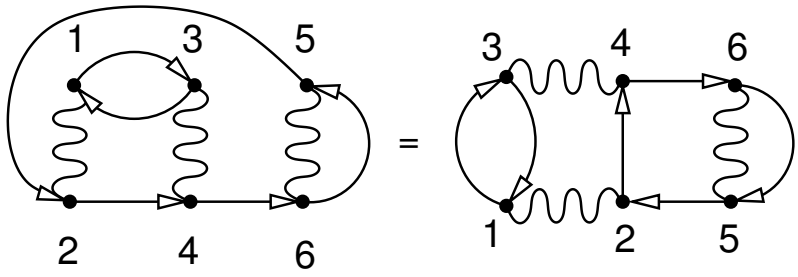

Fig. 10.3: Example for a Feynman diagram corresponding to the permutation vector $\vec{\mathcal{P}} = (3, 4, 1, 6, 2, 5)$. Normally the numbers are not drawn.

Example:

Let me work out the value of the diagram shown in Fig. 10.3 using Eq. 10.48.

Permutation vector: First we determine the permutation vector. For that purpose, we number the vertices such that vertices $(1, 2)$, $(3, 4)$, etc are related to one interaction. There are many ways of doing this, but each will give the same result. In the example shown in Fig. 10.3, the vertices are already numbered.

Now we can read off the end point of the Green's function starting at a given vertex. This gives the following mapping

outgoing vertex	1	2	3	4	5	6
incoming vertex	3	4	1	6	2	5

The array of incoming indices is the permutation vector $\vec{\mathcal{P}} = (3, 4, 1, 6, 2, 5)$.

Sign: The sign is obtained by enumerating the pair-wise permutations that bring the sequence P into increasing order. We start out with a given permutation vector $\vec{\mathcal{P}} = (3, 4, 1, 6, 2, 5)$ and interchange its elements step by step as follows:

341625	+
3**14**625	-
134625	+
134**26**5	-
13**24**65	+
1**23**465	-
1234**56**	+

Each permutation causes a sign change shown in the second column. Thus, $\epsilon_{3,4,1,6,2,5} = +1$.

In section 11.3 below, we will learn how the sign can be determined in a simple manner using the so-called sign theorem.

All together: Let us put the result for the value of the diagram together

$$V(\vec{\mathcal{P}}) \overset{\text{Eq. } 10.48}{=} \underbrace{+1}_{\text{sign}} (i\hbar)^3 \int_{\mathcal{C}} dt_1 \int_{\mathcal{C}} dt_2 \int_{\mathcal{C}} dt_3 \sum_{o_1,i_1,o_2,i_2\ldots,o_6,i_6} W_{o_1,o_2,i_1,i_2}(t_1) W_{o_3,o_4,i_3,i_4}(t_2) W_{o_5,o_6,i_5,i_6}(t_3) \times G^{(0)}_{i_3,o_1}(t_2,t_1^+) G^{(0)}_{i_4,o_2}(t_2,t_1^+) G^{(0)}_{i_1,o_3}(t_1,t_2^+) G^{(0)}_{i_6,o_4}(t_3,t_2^+) G^{(0)}_{i_2,o_5}(t_1,t_3^+) G^{(0)}_{i_5,o_6}(t_3,t_3^+) \quad (10.50)$$

10.4 Diagrams of the numerator of the Green's function

10.4.1 Numerator from Wick's theorem

The decomposition Eq. 10.47 of the denominator of the Green's function Eq. 10.40 into Feynman diagrams helps us to determine the diagrammatic expansion of the numerator

$$\mathrm{Tr}\Big\{\hat{\rho}^{(0)}_{T,\mu} \mathcal{T}_{\mathcal{C}} \hat{S}_{I,\mathcal{C}} \hat{c}_{I,\alpha}(t) \hat{c}^+_{I,\beta}(t')\Big\} \quad (10.51)$$

Using $2n+1$ dimensional permutation vector: Following the recipe developed for Wick's theorem, Eq. 10.38, the diagrams in the numerator of the Green's function Eq. 10.40 can be constructed using permutation vectors. Compared to the diagrams of order n in the denominator, there is one additional pair of operators in the numerator. The diagrams of order n can then be described by a $2n+1$ dimensional permutation vector. The additional creation operator $\hat{c}^+_{I,\beta}(t')$ is treated together with the outgoing indices, that is $(\beta, t') = o_{2n+1}$. The annihilation operator $\hat{c}_{I,\alpha}(t)$ with index α, is treated together with the incoming indices, that is (α, t).

The two operators $\hat{c}^+_{I,\beta}(t')$ and $\hat{c}_{I,\alpha}(t)$, , which are not connected to the interaction, are described as **external vertices**. Unlike the vertices connected to the interaction, only one Green's function is connected to an external vertex. We may describe the external indices of the Green's function also **half vertex** in the sense that each half of a vertex is connected to one end of a Green's function.

The table connecting outgoing and incoming indices is

o_j	1	2	...	$2n$	$2n+1$
i_j	$\mathcal{P}_1$	$\mathcal{P}_2$	...	$\mathcal{P}_{2n}$	$\mathcal{P}_{2n+1}$

Use the permutation vector of the denominator: Instead of constructing the $2n+1$ dimensional permutation vectors from scratch, they can be constructed from the $2n$ dimensional permutation vectors used for the denominator.

We pick one diagram from the expansion of the denominator as parent diagram for a subset of diagrams for the numerator. The parent diagram is identified by a $2n$-dimensional permutation vector $\vec{\mathcal{P}}_{\text{parent}}$. An example is given in figure 10.4.a for $\mathcal{P} = (1,4,2,3)$.

- We begin with one diagram for the numerator, which consists of the parent diagram and a non-interacting Green's function line pointing directly from $o_{2n+1} = (\beta, t')$ to $i_{2n+1} = (\alpha, t)$. It is described by

o_j	1	2	...	$2n$	$2n+1$
i_j	$\mathcal{P}_1$	$\mathcal{P}_2$	...	$\mathcal{P}_{2n}$	$2n+1$

  For our example with parent $\mathcal{P} = (1,4,2,3)$, this diagram is sketched in figure 10.4.b.

- The remaining $2n$ diagrams derived from the selected parent diagram are obtained by removing one Green's function line from the parent diagram, as shown in figure 10.4.d. This leaves one unconnected outgoing vertex o_j and one unconnected incoming index $i_{\mathcal{P}_j}$. Now, we attach one

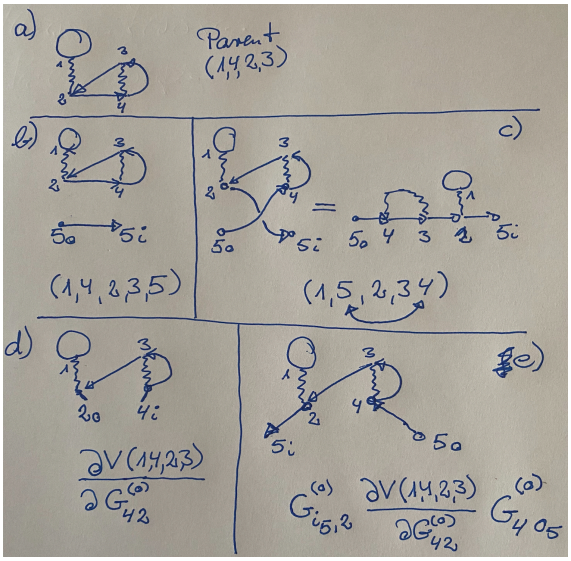

Fig. 10.4: Sketches to demonstrate the construction of diagrams in the numerator from those in the denominator.

Green's function line connecting the unconnected outgoing index o_j with to the external vertex $\alpha = i_{n+1}$. Then, the we attach a further Green's function line connecting the external index $\beta = o_{n+1}$ to the unconnected incoming index $i_{\mathcal{P}_j}$. This is sketched in figure 10.4.c and e.

Translated into the language of permutation vectors $\vec{\mathcal{P}}$, the last incoming index i_{2n+1} is exchanged with any of the other incoming indices. For each $j \in \{1, \ldots, 2n\}$, we obtain a permutation vector of the type

o_j	1	$\cdots$	j	$\cdots$	$2n$	$2n+1$
i_j	$\mathcal{P}_1$	$\cdots$	$2n+1$	$\cdots$	$\mathcal{P}_{2n}$	$\mathcal{P}_j$

This procedure produces $2n+1$ diagrams for the numerator out of each diagram in the denominator. This is exactly the number of terms we obtain by increasing the dimension of the permutation vector by 1, confirming that all diagrams are considered. For our example, the resulting diagrams are shown, together with the corresponding parent diagram, in figure 10.5.

We need to ensure that (1) this procedure constructs all $2n+1$ dimensional permutation vectors from the $2n$ dimensional permutation vectors and that (2) no diagram is constructed twice.

- The proof that no diagram is constructed twice needs to show that none of the $2n+1$ dimensional permutation vectors is obtained from two different $2n$ dimensional permutation vectors. This is shown by giving a recipe to reconstruct the corresponding parent permutation vector. The recipe is to exchange the component with the highest value $\mathcal{P}_j = 2n+1$ with the value $\mathcal{P}_{2n+1}$ in the last position. This unique procedure produces the parent permutation vector on the first $2n$ components.

- The permutation vectors resulting from one parent diagram are distinguishable by the position of the index j of the component with $\mathcal{P}_j = 2n+1$.

- given that no two diagrams are constructed twice, we can show that all diagrams are constructed by counting the number $(2n+1)$ of additional diagrams.

Example: Let me demonstrate the construction using one second-order diagram of the denominator as example.

The permutation vector is $\vec{\mathcal{P}} = (1, 4, 2, 3)$

o_j	1	2	3	4
i_j	1	4	2	3

The first diagram derived from the diagram above is characterized by the permutation vector $\vec{\mathcal{P}} = (1, 4, 2, 3, 5)$. As described above the last entry connects the two external vertices. Thus, this diagram simply adds a **bare Green's-function line** [8] connecting the two external indices to the diagram of the denominator.

The other $2n$ permutation vectors are obtained by exchanging any of the $2n$ outgoing indices with the last one. In total, we obtain the permutation vectors

$$\begin{aligned}
\vec{\mathcal{P}} &= (\mathbf{5}, 4, 2, 3, \mathbf{1}) \\
\vec{\mathcal{P}} &= (1, \mathbf{5}, 2, 3, \mathbf{4}) \\
\vec{\mathcal{P}} &= (1, 4, \mathbf{5}, 3, \mathbf{2}) \\
\vec{\mathcal{P}} &= (1, 4, 2, \mathbf{5}, \mathbf{3}) \\
\vec{\mathcal{P}} &= (1, 4, 2, 3, \mathbf{5})
\end{aligned} \tag{10.52}$$

The j-th permutation vector has the incoming vertex on the j-th position.

10.4.2 Numerator from functional derivative of denominator

Editor: Show first, how the procedure is related to the graphical construction. Then show how the graphical construction translates step by step into the expression below.

The procedure just outlined can be related to an equation using functional derivatives of the parent diagram.

- We begin from specific parent diagram from the denominator such as the one shown in the upper left of Fig. 10.5. The diagram is specified by the permutation vector $\vec{\mathcal{P}}_{\text{parent}}$. For our example, the permutation vector of the parent diagram is $\vec{\mathcal{P}}_{\text{parent}} = (1, 4, 2, 3)$. The diagram is considered as a functional of the bare (non-interacting) Green's function.

- one of the derived diagrams is the parent diagram combined with a bare Green's function connecting the external vertices. The value of this diagram Eq. 10.48[9] There is no sign change, because all permutation are those of the parent diagram, while the last Green's function is simply attached to the end of its permutation vector.

- the removal of bare Green's functions $G^{(0)}_{\alpha,\beta}(t, t')$ from the parent diagram can be expressed by a functional derivative of the value $V(\vec{\mathcal{P}})$ of the parent diagram

$$dV[\vec{\mathcal{P}}] = \sum_{\delta,\gamma} \int_{\mathcal{C}} dt' \int_{\mathcal{C}} dt'' \, \frac{\delta V(\vec{\mathcal{P}})}{\delta G^{(0)}_{\delta,\gamma}(t', t'')} dG^{(0)}_{\delta,\gamma}(t', t'') \tag{10.53}$$

  For each parent diagram of order n, this expression leads to a sum of $2n$ diagrams. Each is obtained by replacing one bare Green's functions at a time by its variation $dG^{(0)}$.

- Connecting the external indices (α, t) and (β, t') implies to replace

$$dG^{(0)}_{\delta,\gamma}(t', t'') \qquad \text{by} \qquad G^{(0)}_{\alpha,\gamma}(t_2, t'') G^{(0)}_{\delta,\beta}(t', t_1) \tag{10.54}$$

[8] A non-interacting Green's function is also called a bare Green's function.

[9] We use the same expression Eq. 10.48 for value of closed diagrams also for the **open diagrams**[10] This choice is consistent with Eq. 10.38.

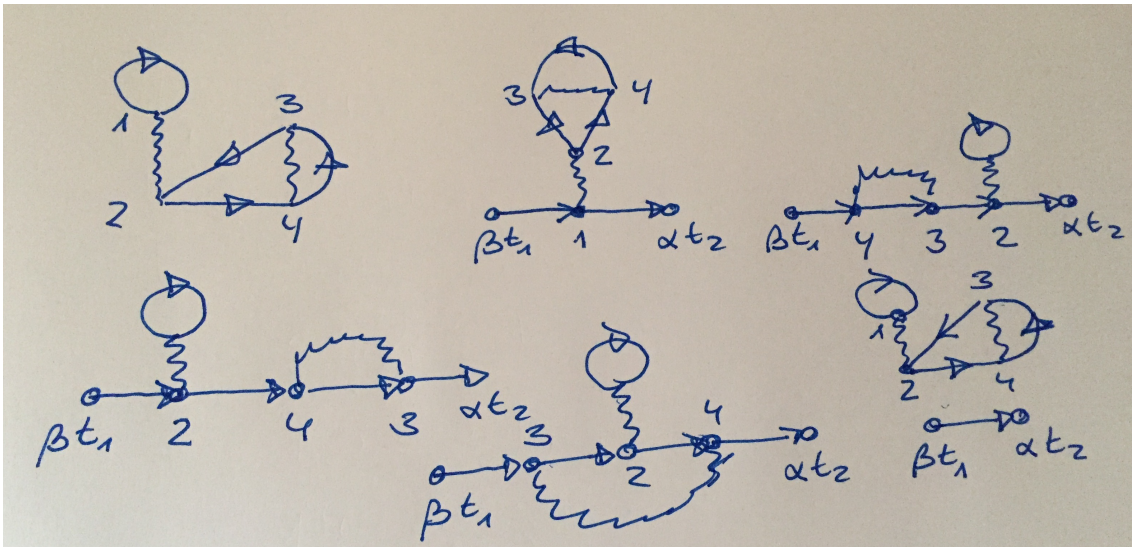

Fig. 10.5: Example for the construction of the diagrams in the numerator of the Green's function from those in the denominator. The diagram in the upper left shows a second-order diagram of the denominator, which is described by the permutation vector $\vec{\mathcal{P}} = (1, 4, 2, 3)$. The other diagrams are obtained by connecting one of the internal indices with the outgoing external index and by connecting the incoming external index to the no open vertex position. In the last diagram the two external vertices are directly connected.

- Combining all $2n + 1$ diagrams derived from the same parent diagram $V(\vec{\mathcal{P}})$ yields

$$\underbrace{V(\vec{\mathcal{P}})}_{\text{parent}} \rightsquigarrow \underbrace{i\hbar G^{(0)}_{\alpha,\beta}(t_2, t_1)V(\vec{\mathcal{P}})}_{\text{“first term”}} \underbrace{-i\hbar \sum_{\gamma,\delta} \int dt' \int dt''\, G^{(0)}_{\alpha,\gamma}(t_2, t'') \frac{\delta V(\vec{\mathcal{P}})}{\delta G^{(0)}_{\delta,\gamma}(t', t'')} G^{(0)}_{\delta,\beta}(t', t_1)}_{\text{“second term”}} \tag{10.55}$$

  The right-hand side is the sum of the values of all diagrams derived from the corresponding parent diagram on the left-hand side.

  The minus sign results from the fact that each diagram in the second term is obtained from the diagram in the first term by one permutation of two elements of the permutation vector. (see Eq. 10.38.)

This implies that the diagrams for the numerator are obtained as derivative of the diagrams in the denominator with respect to a non-interacting Green's function.

$$\mathrm{Tr}\left\{\hat{\rho}^{(0)}_{T,\mu}\mathcal{T}_{\mathcal{C}}\hat{S}_{I,\mathcal{C}}\right\} = \sum_{n=0}^{\infty} \sum_{\vec{\mathcal{P}}\in\mathbb{A}_n} \frac{1}{n!2^n} V(\vec{\mathcal{P}}) \tag{10.56}$$

$$
\begin{aligned}
&\rightsquigarrow \quad \mathrm{Tr}\Big\{\hat{\rho}^{(0)}_{T,\mu}\mathcal{T}_{\mathcal{C}}\hat{S}_{I,\mathcal{C}}\hat{c}_{I,\alpha}(t_2)\hat{c}^{+}_{I,\beta}(t_1)\Big\} \\
&\overset{\text{Eq. } 10.55}{=} \sum_{n=0}^{\infty}\sum_{\vec{\mathcal{P}}\in\mathbb{A}_n}\frac{1}{n!2^n}\, i\hbar\left[G^{(0)}_{\alpha,\beta}(t_2,t_1)V(\vec{\mathcal{P}}) - \sum_{\gamma,\delta}\int dt'\int dt''\, G^{(0)}_{\alpha,\gamma}(t_2,t'')\frac{\partial V(\vec{\mathcal{P}})}{\partial G^{(0)}_{\delta,\gamma}(t',t'')}G^{(0)}_{\delta,\beta}(t',t_1)\right] \\
&= \quad i\hbar\left[G^{(0)}_{\alpha,\beta}(t_2,t_1)\mathrm{Tr}\Big\{\hat{\rho}^{(0)}_{T,\mu}\mathcal{T}_{\mathcal{C}}\hat{S}_{I,\mathcal{C}}\Big\} - \sum_{\gamma,\delta}\int dt'\int dt''\, G^{(0)}_{\alpha,\gamma}(t_2,t'')\frac{\partial \mathrm{Tr}\Big\{\hat{\rho}^{(0)}_{T,\mu}\mathcal{T}_{\mathcal{C}}\hat{S}_{I,\mathcal{C}}\Big\}}{\partial G^{(0)}_{\delta,\gamma}(t',t'')}G^{(0)}_{\delta,\beta}(t',t_1)\right]
\end{aligned}
\tag{10.57}
$$

Insertion into the expression for the Green's function Eq. 10.40, yields[11]

$$
\begin{aligned}
G_{\alpha,\beta}(t,t') &\overset{\text{Eq. } 10.40}{=} \frac{1}{i\hbar}\frac{\mathrm{Tr}\Big\{\hat{\rho}^{(0)}_{T,\mu}\mathcal{T}_{\mathcal{C}}\hat{S}_{I,\mathcal{C}}\hat{c}_{I,\alpha}(t)\hat{c}^{+}_{I,\beta}(t')\Big\}}{\mathrm{Tr}\Big\{\hat{\rho}^{(0)}\mathcal{T}_{\mathcal{C}}\hat{S}_{I,\mathcal{C}}\Big\}} \\
&\overset{\text{Eq. } 10.57}{=} G^{(0)}_{\alpha,\beta}(t_2,t_1) + \sum_{\gamma,\delta}\int dt'\int dt''\, G^{(0)}_{\alpha,\gamma}(t_2,t'')\frac{\partial\left(-\ln \mathrm{Tr}\Big\{\hat{\rho}^{(0)}_{T,\mu}\mathcal{T}_{\mathcal{C}}\hat{S}_{I,\mathcal{C}}\Big\}\right)}{\partial G^{(0)}_{\delta,\gamma}(t',t'')}G^{(0)}_{\delta,\beta}(t',t_1)
\end{aligned}
\tag{10.58}
$$

Eq. 10.58 is an important result: There is one functional of the bare Green's function, namely $\mathcal{Q}_{T,\mu}$ which provides the interacting Green's function.

[11] $\frac{1}{x}\frac{dy}{dx} = \frac{d\ln(y(x))}{dx}$.

GREEN'S FUNCTION FROM A FUNCTIONAL

The one-particle Green's function is completely defined by a functional[a] $\mathcal{Q}$ of the non-interacting Green's function

$$\mathcal{Q}_{T,\mu}[\boldsymbol{G}^{(0)}] \stackrel{\text{def}}{=} -k_B T \ln \mathrm{Tr}\Big\{\hat{\rho}^{(0)}_{T,\mu}\mathcal{T}_{\mathcal{C}}\hat{S}_{I,\mathcal{C}}\Big\} \stackrel{\text{Eq. } 10.47}{=} -\frac{1}{\beta}\ln\left[\sum_{n=0}^{\infty}\frac{1}{n!}\sum_{\vec{\mathcal{P}}\in\mathbb{A}_n}\frac{1}{2^n}V(\vec{\mathcal{P}})\right] \tag{10.59}$$

where $\beta = 1/(k_B T)$. With $\vec{\mathcal{P}} \in \mathbb{A}_n$, I denote all permutation vectors of length $2n$, with components that are permutations of $(1, 2, \ldots, 2n)$.
The non-interacting Green's function is specified on a time-contour $\mathcal{C}$. The functional furthermore depends on the interaction matrix elements, which can be time dependent along the contour.
The functional derivative specifies the Green's function via Dyson's equation

$$\begin{aligned} G_{\alpha,\beta}(t_2,t_1) &= G^{(0)}_{\alpha,\beta}(t_2,t_1) + \sum_{\gamma,\delta}\int_{\mathcal{C}} dt_4 \int_{\mathcal{C}} dt_3\, G^{(0)}_{\alpha,\gamma}(t_2,t_4)\underbrace{\frac{1}{k_B T}\frac{\delta\mathcal{Q}_{T,\mu}[G^{(0)},W]}{\delta G^{(0)}_{\delta,\gamma}(t_3,t_4)}}_{=:\Sigma^{\text{red}}_{\gamma,\delta}(t_4,t_3)} G^{(0)}_{\delta,\beta}(t_3,t_1) \\ &= G^{(0)}_{\alpha,\beta}(t_2,t_1) + \sum_{\gamma,\delta}\int_{\mathcal{C}} dt_4 \int_{\mathcal{C}} dt_3\, G^{(0)}_{\alpha,\gamma}(t_2,t_4)\Sigma^{\text{red}}_{\gamma,\delta}(t_4,t_3)G^{(0)}_{\delta,\beta}(t_3,t_1) \end{aligned} \tag{10.60}$$

The self energy

$$\hat{\Sigma}^{red}(t,t') \stackrel{\text{def}}{=} \sum_{\alpha,\beta}|\pi_\alpha\rangle\frac{1}{k_B T}\frac{\delta\mathcal{Q}_{T,\mu}[G^{(0)},W]}{\delta G^{(0)}_{\beta,\alpha}(t',t)}\langle\pi_\beta| \tag{10.61}$$

is the so-called **reducible self energy** , which differs from the self energy used earlier.
With $\langle\pi_\alpha|$, I denote the projector function corresponding to the local basis function $\langle\chi_\alpha|$. The Green's function has the form $\hat{G}(t,t') = \sum_{\alpha,\beta}|\chi_\alpha\rangle G_{\alpha,\beta}(t,t')\langle\chi_\beta|$. The biorthogonality $\langle\pi_\alpha|\chi_\beta\rangle = \delta_{\alpha,\beta}$ holds.

[a] This functional is identical to $\Phi_r[G]$ Stefanucci and van Leeuwen[2]. See their Eqs. 11.12-11.13

Table 10.1: Terminology for Green's functions and self energies. *"Irreducible"* stands here for **one-particle irreducible (1PI)**, which means that the corresponding diagram does not fall apart by removing any single particle line (Green's function). The reducible self energy Σ^{red} contains also irreducible diagrams and should actually be named *"reducible and irreducible"*, which I have not heard so-far. However, I encountered the naming *"proper and improper diagrams"*.

Terminology	
$\hat{G}(t,t')$	**full** Green's function, **dressed** G.f., **interacting** G.f.
$\hat{G}^{(0)}(t,t')$	**bare** Green's function, **non-interacting** G.f.
$\hat{\Sigma}^{\text{red}}(t,t')$	**reducible** self energy, (proper and) **improper** s.e.
$\hat{\Sigma}(t,t')$	**proper** self energy, **irreducible** s.e., **1PI** s.e.

Reducible (improper) and irreducible (proper) self energy: The reducible self energy Eq. 10.61 differs from the self energy defined earlier in Eq. 8.15 on p. 257 (and in Eq. 5.34 on p. 187).

Eq. 10.60, which has the diagrammatic form

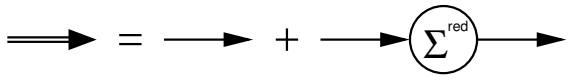

$$\hat{G}(t_2,t_1) = \hat{G}^{(0)}(t_2,t_1) + \int dt' \int dt''\, \hat{G}^{(0)}(t_2,t'')\hat{\Sigma}^{\text{red}}(t'',t')\hat{G}^{(0)}(t',t_1) \tag{10.62}$$

reminds of Dyson's equation Eq. 8.23 on p. 258.

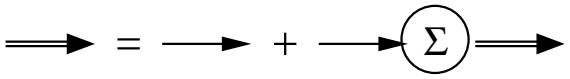

$$\hat{G}(t_2,t_1) \overset{\text{Eq. 8.23}}{=} \hat{G}^{(0)}(t_2,t_1) + \int dt' \int dt''\, \hat{G}^{(0)}(t_2,t'')\hat{\Sigma}(t'',t')\hat{G}(t',t_1) \tag{10.63}$$

When we iterate Dyson's equation by repeatedly inserting Dyson's equation for the full Green's function on the right hand side [12], it becomes identical to the equation above, when we identify the reducible self energy with

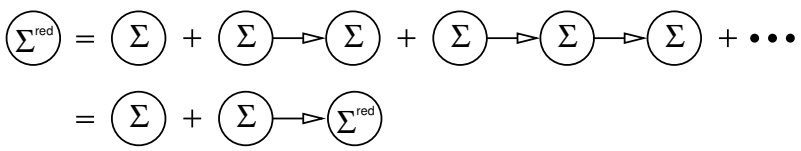

Expressed with explicit time arguments, the self energies obey

$$\hat{\Sigma}^{\text{red}}(t_2,t_1) = \hat{\Sigma}(t_2,t_1) + \int dt \int dt'\, \hat{\Sigma}(t_2,t)\hat{G}^{(0)}(t,t')\hat{\Sigma}^{red}(t',t_1) \tag{10.65}$$

Proper self energy from the generating functional It may be tempting to obtain the proper self energy by removing all one-particle reducible self-energy diagrams from the reducible self energy. This is a valid procedure for the exact generating functional, but it is not allowed for approximate ones. [13] This is unfortunate, because the generating functional is often used to arrive at consistent approximations.

[12] Let me work out the relation between proper and total self energy by comparing Dyson's equation with Eq. 10.60. I write the Green's function and self energies here as operators in one-particle Hilbert space and I suppress the time arguments. As shown below, each product also implies an integration of the common time argument.

$$\begin{aligned}
\boldsymbol{G} &\overset{\text{Eq. 8.23}}{=} \boldsymbol{G}^{(0)} + \boldsymbol{G}^{(0)}\boldsymbol{\Sigma}\boldsymbol{G} \\
&= \boldsymbol{G}^{(0)} + \boldsymbol{G}^{(0)}\boldsymbol{\Sigma}\underbrace{\left(\boldsymbol{G}^{(0)} + \boldsymbol{G}^{(0)}\boldsymbol{\Sigma}\boldsymbol{G}\right)}_{\boldsymbol{G}} \\
&= \boldsymbol{G}^{(0)} + \boldsymbol{G}^{(0)}\boldsymbol{\Sigma}\boldsymbol{G}^{(0)} + \boldsymbol{G}^{(0)}\boldsymbol{\Sigma}\boldsymbol{G}^{(0)}\boldsymbol{\Sigma}\underbrace{\left(\boldsymbol{G}^{(0)} + \boldsymbol{G}^{(0)}\boldsymbol{\Sigma}\boldsymbol{G}\right)}_{\boldsymbol{G}} \\
&= \boldsymbol{G}^{(0)} + \boldsymbol{G}^{(0)}\underbrace{\left(\boldsymbol{\Sigma} + \boldsymbol{\Sigma}\boldsymbol{G}^{(0)}\boldsymbol{\Sigma} + \boldsymbol{\Sigma}\boldsymbol{G}^{(0)}\boldsymbol{\Sigma}\boldsymbol{G}^{(0)}\boldsymbol{\Sigma} + \ldots\right)}_{\boldsymbol{\Sigma}^{\text{red}}}\boldsymbol{G}^{(0)} \\
&\overset{!}{=} \boldsymbol{G}^{(0)} + \boldsymbol{G}^{(0)}\boldsymbol{\Sigma}^{\text{red}}\boldsymbol{G}^{(0)} \qquad \text{compare with Eq. 10.60}
\end{aligned} \tag{10.64}$$

[13] First, we notice that, usually, the one-particle irreducible (1PI) self-energy insertions in the approximated reducible self energy are different from each other. Furthermore, inserting the 1PI self-energy diagram Σ obtained from an approximate generating functional into Dyson's equation

$$\Sigma^{red} = \Sigma + \Sigma G^{\mathcal{C},(0)}\Sigma^{red} \neq \beta\frac{\delta\mathcal{Q}_{T,\mu}}{\delta G^{\mathcal{C},(0)}} \tag{10.66}$$

generates an infinite number of terms, even if the approximate generating functional has only few terms.

The proper self energy must be obtained from the reducible self energy using Dyson's equation. In a short-hand notation this implies

$$\begin{aligned} \Sigma^{red} &= \Sigma + \Sigma G^{\mathcal{C},(0)} \Sigma^{red} = \Sigma \Big(1 + G^{\mathcal{C},(0)} \Sigma^{red} \Big) \\ \Rightarrow \qquad \Sigma &= \Sigma^{red} - \Sigma G^{\mathcal{C},(0)} \Sigma^{red} = \Sigma^{red} \sum_{n=0}^{\infty} \Big(-G^{\mathcal{C},(0)} \Sigma^{red} \Big)^n \end{aligned} \tag{10.67}$$

This is itself a Dyson's equation for the proper self energy Σ, which must be solved iteratively. It produces an infinite number of terms, even if the generating functional is approximated by a few terms. Truncating this Dyson's equation will lead to yet another approximation, which has a complicated generating functional, reducible self energy and Green's function.

The construction of a generating functional for the proper self energy rather than the reducible self energy is the topic of chapter 12 on the **Luttinger-Ward functional**.

Generating functional $\mathcal{Q}_{T,\mu}$ from the reducible self energy: We just learned that the reducible self energy can be obtained from the generating functional $\mathcal{Q}_{T,\mu}[G^{\mathcal{C},(0)}]$. The reverse is also true, however with a restriction: We need to know the self energy divided into individual orders of the interaction.

If we close a diagram of the reducible self energy with a non-interacting Green's function, we obtain a closed diagram, namely the parent diagram from which the specific self-energy diagram has been obtained. However, a diagram of the generating functional produces $2n$ self-energy diagrams, because the diagram is a product of $2n$ Green's functions. Thus, we overcount diagrams when we add up all self-energy diagrams after closing them.

Let me divide the self energy into powers of the interaction

$$\hat{\Sigma}^{red} = \sum_{n=1}^{\infty} \hat{\Sigma}^{red,(n)} \tag{10.68}$$

where $\hat{\Sigma}^{red,(n)}$ is the contribution of n-th order in the interaction.

With the reducible self energy available in individual orders of the interaction allows one to reconstruct the generating functional as

$$\mathcal{Q}_{T,\mu}[G^{\mathcal{C},(0)}] = \sum_{n=1}^{\infty} \frac{1}{2n} \int_{\mathcal{C}} dt \int_{\mathcal{C}} dt' \, \Sigma^{red,(n)}_{\alpha,\beta}(t,t') G^{\mathcal{C},(0)}_{\beta,\alpha}(t',t) \tag{10.69}$$

If the approximation is defined via a proper self energy, the corresponding reducible self energy need to be constructed first via Dyson's equation, before the generating functional $\mathcal{Q}[\boldsymbol{G}^{(0)}]$ can be obtained.

The reconstruction of the generating functional may be useful in order to arrive at a consistent theory from an approximate reducible self energy.

Relation to the grand potential: This functional $\mathcal{Q}[\boldsymbol{G}^{(0)}]$, is closely related to the **grand potential**. It is the interaction part of the grand potential, namely $\mathcal{Q}_{T,\mu} = \Omega^{(W)}_{T,\mu} - \Omega^{(0)}_{T,\mu}$. This makes contact with the thermodynamics of an interacting electron gas. The close relation of $\mathcal{Q}[\boldsymbol{G}^{(0)}]$ with the grand potential has been the reason for adding the factor $k_B T$ in the definition of the grand potential $\mathcal{Q}_{T,\mu}$.

The grand potential of the interacting system is given in Eq. 10.25 on p. 301. It depends on the

grand potential of the non-interacting system which is given in Eq. 10.28 from p. 302.

$$\begin{aligned}\Omega^{(W)}_{T,\mu} &\overset{\text{Eq. 10.25}}{=} \underbrace{+k_B T \mathrm{Tr}\left\{\ln\left[\hat{1} + i\hbar \lim_{t'\to t^+} \hat{G}^{(0)}(t,t')\right]\right\}}_{=-k_B T \ln(Z_{T,\mu})^{(0)} = \Omega^{(0)}_{T,\mu}[\boldsymbol{G}^{(0)}] \quad \text{Eq. 10.28}} \underbrace{-k_B T \ln\left(\mathrm{Tr}\left\{\hat{\rho}^{(0)}_{T,\mu}\mathcal{T}_{\mathcal{C}}\hat{\mathcal{S}}_{I,\mathcal{C}}\right\}\right)}_{\mathcal{Q}_{T,\mu} \quad \text{Eq. 10.59}} \\ &= \underbrace{+k_B T \mathrm{Tr}\left\{\ln\left[\hat{1} + i\hbar \lim_{t'\to t^+} \hat{G}^{(0)}(t,t')\right]\right\}}_{\Omega^{(0)}_{T,\mu}[\boldsymbol{G}^{(0)}]} + \underbrace{\mathcal{Q}_{T,\mu}[\boldsymbol{G}^{(0)}]}_{\Omega^{(W)}_{T,\mu}[\boldsymbol{G}^{(0)}] - \Omega^{(0)}_{T,\mu}[\boldsymbol{G}^{(0)}]} \end{aligned} \tag{10.70}$$

Editor: See also section K.4.7. and Eq. 10.28 on p. 10.28. There are probably some duplications.

In the remainder of this chapter, we will concentrate entirely on how to determine the functional $\mathcal{Q}(\boldsymbol{G}^{(0)})$.

Editor: In this section, we could also show that

$$G^W = \frac{\delta\Omega}{\delta(G^{(0)})^{-1}} \tag{10.71}$$

. However, this grand potential contains also the one without interaction.

10.5 Home study and practice

10.5.1 Green's function from generating functional

Introduction

Editor: The term generating functional needs to be properly explained. It must be clear that this generates the reducible self energy and not the correlation functions.

In this problem, we practice the calculation of the Green's function from the generating functional. To simplify matters, only a single diagram is considered in the generating functional. An expression for the generating functional used here, will emerge only in the following chapter through the linked-cluster theorem.

The linked-cluster theorem provides the generating functional in terms of linked diagrams $D \in \mathbb{L}$ as

$$\mathcal{Q}_{T,\mu}[G^{(0)}] \overset{\text{Eq. 11.17}}{=} -\frac{1}{\beta}\sum_{n=1}^{\infty}\sum_{D\in\mathbb{L}_n}\frac{V(D)}{n!2^n} \tag{10.72}$$

where the logarithm is absent.

Problem

Calculate the Green's function from a specific generating functional $\bar{\mathcal{Q}}_{T,\mu}[G^{(0)}]$, namely

$$\bar{\mathcal{Q}}_{T,\mu}[G^{\mathcal{C}(0)}] = -\frac{1}{\beta}\frac{V(D)}{n!2^n} \tag{10.73}$$

To simplify the task, only a single diagram D contributes to this generating functional, which is specified by the permutation vector $\vec{\mathcal{P}} = (1,4,2,3)$. I use the bar on-top of the symbol for the generating functional to distinguish it from the correct, general functional.
Caution: Using one diagram in the expression obtained so far, i.e. in Eq. 10.59, is much more difficult and it leads to a different result than using the form obtained after the linked-cluster theorem Eq. 11.17.

1 Write down the value of the diagram D with $\mathcal{P} = (1,4,2,3)$ as functional of the bare Green's function and the interaction tensor.

2 Use the result to write down $\bar{\mathcal{Q}}_{T,\mu}[G^{\mathcal{C},(0)}]$

3 extract the reducible self energy from $\bar{\mathcal{Q}}_{T,\mu}[G^{\mathcal{C},(0)}]$. It is advisable to identify the expressions for Hartree and exchange potential in order to make the expressions more compact.

4 construct the Green's function from $\bar{\mathcal{Q}}_{T,\mu}[G^{\mathcal{C},(0)}]$.

5 Draw the Feynman diagrams for

- the generating functional $\bar{\mathcal{Q}}_{T,\mu}[G^{\mathcal{C},(0)}]$
- the reducible self energy Σ^{red}
- the Green's function $G^{\mathcal{C}}$

Discussion

1 Write down the value of the diagram D with $\mathcal{P} = (1,4,2,3)$ as functional of the bare Green's function and the interaction tensor.

Let me work out the Green's function from a generating functional, which consists out of only a single Feynman diagram, namely the closed diagram in figure 10.5. The diagram belongs to the permutation vector $\mathcal{P} = (1,4,2,3)$.

First, we need to write out the value of the diagram itself

$$\begin{aligned}
V(\vec{\mathcal{P}}) &\overset{\text{Eq. 10.48}}{=} \epsilon_{\mathcal{P}_1,\ldots,\mathcal{P}_{2n}} (i\hbar)^n \int_{\mathcal{C}} dt_1 \cdots \int_{\mathcal{C}} dt_{2n} \sum_{o_1,i_1,\ldots,o_{2n},i_{2n}} \left(\prod_{j=1}^{n} W_{o_{2j-1},o_{2j},i_{2j-1},i_{2j}} \delta_{\mathcal{C}}(t_{2j-1} - t_{2j}) \right) \\
&\quad \times G^{\mathcal{C},(0)}_{i_{\mathcal{P}_1},o_1}(t_{\mathcal{P}_1}, t_1^+) \cdots G^{\mathcal{C},(0)}_{i_{\mathcal{P}_{2n}},o_{2n}}(t_{\mathcal{P}_{2n}}, t_{2n}^+) \\
&\overset{\vec{\mathcal{P}}=(1423)}{=} \underbrace{\epsilon_{1,4,2,3}}_{=+1} \underbrace{(i\hbar)^2}_{-\hbar^2} \int_{\mathcal{C}} dt_1 \cdots \int_{\mathcal{C}} dt_4 \sum_{o_1,i_1,\ldots,o_4,i_4} W_{o_1,o_2,i_1,i_2} \delta_{\mathcal{C}}(t_1 - t_2) W_{o_3,o_4,i_3,i_4} \delta_{\mathcal{C}}(t_3 - t_4) \\
&\quad \times G^{\mathcal{C},(0)}_{i_1,o_1}(t_1, t_1^+) G^{\mathcal{C},(0)}_{i_4,o_2}(t_4, t_2^+) G^{\mathcal{C},(0)}_{i_2,o_3}(t_2, t_3^+) G^{\mathcal{C},(0)}_{i_3,o_4}(t_3, t_4^+) \\
&= -\hbar^2 \sum_{o_1,i_1,\ldots,o_4,i_4} W_{o_1,o_2,i_1,i_2} W_{o_3,o_4,i_3,i_4} \\
&\quad \times \int_{\mathcal{C}} dt_1 \int_{\mathcal{C}} dt_3 \; G^{\mathcal{C},(0)}_{i_1,o_1}(t_1, t_1^+) G^{\mathcal{C},(0)}_{i_4,o_2}(t_3, t_1^+) G^{\mathcal{C},(0)}_{i_2,o_3}(t_1, t_3^+) G^{\mathcal{C},(0)}_{i_3,o_4}(t_3, t_3^+)
\end{aligned} \tag{10.74}$$

2 Use the result to write down $\bar{\mathcal{Q}}_{T,\mu}[G^{\mathcal{C},(0)}]$

For our specific example we use just one diagram so that

$$\begin{aligned}\bar{\mathcal{Q}}_{T,\mu}[G^{(0)}] &= -\frac{1}{\beta}\frac{V(\overbrace{\vec{\mathcal{P}}}^{(1,4,2,3)})}{8} \\ &\overset{\text{Eq. 10.74}}{=} \frac{\hbar^2}{8\beta}\sum_{o_1,i_1,\ldots,o_4,i_4} W_{o_1,o_2,i_1,i_2}W_{o_3,o_4,i_3,i_4} \\ &\quad\times\int_{\mathcal{C}} dt_1\int_{\mathcal{C}} dt_3\; G^{\mathcal{C},(0)}_{i_1,o_1}(t_1,t_1^+)G^{\mathcal{C},(0)}_{i_4,o_2}(t_3,t_1^+)G^{\mathcal{C},(0)}_{i_2,o_3}(t_1,t_3^+)G^{\mathcal{C},(0)}_{i_3,o_4}(t_3,t_3^+)\end{aligned} \tag{10.75}$$

3 extract the reducible self energy from $\bar{\mathcal{Q}}_{T,\mu}[G^{\mathcal{C},(0)}]$. It is advisable to identify the expressions for Hartree and exchange potential in order to make the expressions more compact.

Let me first work out the corresponding reducible self energy. I start with the first variation of the functional $\mathcal{Q}_{T,\mu}$ with respect to changes of the non-interacting Green's function.

$$\begin{aligned}d\bar{\mathcal{Q}}_{T,\mu} &= \frac{1}{8}k_BT\hbar^2\sum_{o_1,i_1,\ldots,o_4,i_4} W_{o_1,o_2,i_1,i_2}W_{o_3,o_4,i_3,i_4}\int_{\mathcal{C}} dt_1\int_{\mathcal{C}} dt_3 \\ &\quad\times\Big\{dG^{\mathcal{C},(0)}_{i_1,o_1}(t_1,t_1^+)G^{\mathcal{C},(0)}_{i_4,o_2}(t_3,t_1^+)G^{\mathcal{C},(0)}_{i_2,o_3}(t_1,t_3^+)G^{\mathcal{C},(0)}_{i_3,o_4}(t_3,t_3^+) \\ &\quad+G^{\mathcal{C},(0)}_{i_1,o_1}(t_1,t_1^+)dG^{\mathcal{C},(0)}_{i_4,o_2}(t_3,t_1^+)G^{\mathcal{C},(0)}_{i_2,o_3}(t_1,t_3^+)G^{\mathcal{C},(0)}_{i_3,o_4}(t_3,t_3^+) \\ &\quad+G^{\mathcal{C},(0)}_{i_1,o_1}(t_1,t_1^+)G^{\mathcal{C},(0)}_{i_4,o_2}(t_3,t_1^+)dG^{\mathcal{C},(0)}_{i_2,o_3}(t_1,t_3^+)G^{\mathcal{C},(0)}_{i_3,o_4}(t_3,t_3^+) \\ &\quad+G^{\mathcal{C},(0)}_{i_1,o_1}(t_1,t_1^+)G^{\mathcal{C},(0)}_{i_4,o_2}(t_3,t_1^+)G^{\mathcal{C},(0)}_{i_2,o_3}(t_1,t_3^+)dG^{\mathcal{C},(0)}_{i_3,o_4}(t_3,t_3^+)\Big\} \\ &= \frac{1}{8}k_BT\hbar^2\sum_{\delta,\gamma}\sum_{o_1,i_1,\ldots,o_4,i_4} W_{o_1,o_2,i_1,i_2}W_{o_3,o_4,i_3,i_4}\int_{\mathcal{C}} dt_1\int_{\mathcal{C}} dt_3 \\ &\quad\times\Big\{\delta_{i_1,\delta}\delta_{o_1,\gamma}\delta(t_1-t_a)\delta(t_1^+-t_b)G^{\mathcal{C},(0)}_{i_4,o_2}(t_3,t_1^+)G^{\mathcal{C},(0)}_{i_2,o_3}(t_1,t_3^+)G^{\mathcal{C},(0)}_{i_3,o_4}(t_3,t_3^+) \\ &\quad+G^{\mathcal{C},(0)}_{i_1,o_1}(t_1,t_1^+)\delta_{i_4,\delta}\delta_{o_2,\gamma}\delta(t_3-t_a)\delta(t_1^+-t_b)G^{\mathcal{C},(0)}_{i_2,o_3}(t_1,t_3^+)G^{\mathcal{C},(0)}_{i_3,o_4}(t_3,t_3^+) \\ &\quad+G^{\mathcal{C},(0)}_{i_1,o_1}(t_1,t_1^+)G^{\mathcal{C},(0)}_{i_4,o_2}(t_3,t_1^+)\delta_{i_2,\delta}\delta_{o_3,\gamma}\delta(t_1-t_a)\delta(t_3^+-t_b)G^{\mathcal{C},(0)}_{i_3,o_4}(t_3,t_3^+) \\ &\quad+G^{\mathcal{C},(0)}_{i_1,o_1}(t_1,t_1^+)G^{\mathcal{C},(0)}_{i_4,o_2}(t_3,t_1^+)G^{\mathcal{C},(0)}_{i_2,o_3}(t_1,t_3^+)\delta_{i_3,\delta}\delta_{o_4,\gamma}\delta(t_3-t_a)\delta(t_3^+-t_b)\Big\}dG^{\mathcal{C},(0)}_{\delta,\gamma}(t_a,t_b) \\ &\overset{!}{=} \int_{\mathcal{C}} dt_a\int_{\mathcal{C}} dt_b\sum_{\delta,\gamma}\underbrace{\frac{\delta\mathcal{Q}_{T,\mu}[G^{(0)},W]}{\delta G^{\mathcal{C},(0)}_{\delta,\gamma}(t_a,t_b)}}_{k_BT\Sigma^{\text{red}}_{\gamma,\delta}(t_b,t_a)}dG^{\mathcal{C},(0)}_{\delta,\gamma}(t_a,t_b)\end{aligned} \tag{10.76}$$

The reducible self energy Σ^{red} is

$$
\begin{aligned}
\Sigma^{\text{red}}_{\gamma,\delta}(t_b,t_a) &= \frac{1}{k_B T}\frac{\delta \mathcal{Q}_{T,\mu}[G^{(0)},W]}{\delta G^{\mathcal{C},(0)}_{\delta,\gamma}(t_a,t_b)} \\
&= \frac{\hbar^2}{8}\sum_{o_1,i_1,\ldots,o_4,i_4} W_{o_1,o_2,i_1,i_2}W_{o_3,o_4,i_3,i_4}\int_{\mathcal{C}} dt_1 \int_{\mathcal{C}} dt_3 \\
&\times \Big\{ \delta_{i_1,\delta}\delta_{o_1,\gamma}\delta(t_1-t_a)\delta(t_1^+-t_b)G^{\mathcal{C},(0)}_{i_4,o_2}(t_3,t_1^+)G^{\mathcal{C},(0)}_{i_2,o_3}(t_1,t_3^+)G^{\mathcal{C},(0)}_{i_3,o_4}(t_3,t_3^+) \\
&\quad + G^{\mathcal{C},(0)}_{i_1,o_1}(t_1,t_1^+)\delta_{i_4,\delta}\delta_{o_2,\gamma}\delta(t_3-t_a)\delta(t_1^+-t_b)G^{\mathcal{C},(0)}_{i_2,o_3}(t_1,t_3^+)G^{\mathcal{C},(0)}_{i_3,o_4}(t_3,t_3^+) \\
&\quad + G^{\mathcal{C},(0)}_{i_1,o_1}(t_1,t_1^+)G^{\mathcal{C},(0)}_{i_4,o_2}(t_3,t_1^+)\delta_{i_2,\delta}\delta_{o_3,\gamma}\delta(t_1-t_a)\delta(t_3^+-t_b)G^{\mathcal{C},(0)}_{i_3,o_4}(t_2,t_3^+) \\
&\quad + G^{\mathcal{C},(0)}_{i_1,o_1}(t_1,t_1^+)G^{\mathcal{C},(0)}_{i_4,o_2}(t_3,t_1^+)G^{\mathcal{C},(0)}_{i_2,o_3}(t_1,t_3^+)\delta_{i_3,\delta}\delta_{o_4,\gamma}\delta(t_3-t_a)\delta(t_3^+-t_b)\Big\} \\
&= \frac{\hbar^2}{8}\sum_{o_2,i_2,o_3,o_3,o_4,i_4} W_{\gamma,o_2,\delta,i_2}W_{o_3,o_4,i_3,i_4}\delta(t_a-t_b)\int_{\mathcal{C}} dt_3\; G^{\mathcal{C},(0)}_{i_4,o_2}(t_3,t_a^+)G^{\mathcal{C},(0)}_{i_2,o_3}(t_a,t_3^+)G^{\mathcal{C},(0)}_{i_3,o_4}(t_3,t_3^+) \\
&\quad + \frac{\hbar^2}{8}\sum_{o_1,i_1,i_2,o_3,i_3,o_4} W_{o_1,\gamma,i_1,i_2}W_{o_3,o_4,i_3,\delta}G^{\mathcal{C},(0)}_{i_1,o_1}(t_b,t_b^+)G^{\mathcal{C},(0)}_{i_2,o_3}(t_b,t_a^+)G^{\mathcal{C},(0)}_{i_3,o_4}(t_a,t_a^+) \\
&\quad + \frac{\hbar^2}{8}\sum_{o_1,i_1,o_2,i_3,o_4,i_4} W_{o_1,o_2,i_1,\delta}W_{\gamma,o_4,i_3,i_4}G^{\mathcal{C},(0)}_{i_1,o_1}(t_a,t_a^+)G^{\mathcal{C},(0)}_{i_4,o_2}(t_b,t_a^+)G^{\mathcal{C},(0)}_{i_3,o_4}(t_b,t_b^+) \\
&\quad + \frac{\hbar^2}{8}\sum_{o_1,i_1,o_2,i_2,o_3,o_4,i_4} W_{o_1,o_2,i_1,i_2}W_{o_3,\gamma,\delta,i_4}\delta(t_a-t_b)\int_{\mathcal{C}} dt_1\; G^{\mathcal{C},(0)}_{i_1,o_1}(t_1,t_1^+)G^{\mathcal{C},(0)}_{i_4,o_2}(t_a,t_1^+)G^{\mathcal{C},(0)}_{i_2,o_3}(t_1,t_a^+) \\
&= \frac{\hbar^2}{8}\delta(t_a-t_b)\sum_{o_2,i_2}W_{\gamma,o_2,\delta,i_2}\int_{\mathcal{C}} dt_3 \sum_{o_3,i_4} G^{\mathcal{C},(0)}_{i_2,o_3}(t_a,t_3^+)\underbrace{\Big(\sum_{i_3,o_4} W_{o_3,o_4,i_3,i_4}G^{\mathcal{C},(0)}_{i_3,o_4}(t_3,t_3^+)\Big)}_{\text{open oyster: } \frac{1}{i\hbar}v^{(0)}_{X,o_3,i_4}(t_3)} G^{\mathcal{C},(0)}_{i_4,o_2}(t_3,t_a^+) \\
&\quad + \frac{\hbar^2}{8}\sum_{i_2}\underbrace{\Big(\sum_{o_1,i_1} W_{o_1,\gamma,i_1,i_2}G^{\mathcal{C},(0)}_{i_1,o_1}(t_b,t_b^+)\Big)}_{\text{tadpole: } -\frac{1}{i\hbar}v^{(0)}_{H,\gamma,i_2}(t_b)}\sum_{o_3} G^{\mathcal{C},(0)}_{i_2,o_3}(t_b,t_a^+)\underbrace{\Big(\sum_{i_3,o_4} G^{\mathcal{C},(0)}_{i_3,o_4}(t_a,t_a^+)W_{o_3,o_4,i_3,\delta}\Big)}_{\text{open oyster: } \frac{1}{i\hbar}v^{(0)}_{X,o_3,\delta}(t_a)} \\
&\quad + \frac{\hbar^2}{8}\sum_{o_2,i_4}\underbrace{\Big(\sum_{i_3,o_4} W_{\gamma,o_4,i_3,i_4}G^{\mathcal{C},(0)}_{i_3,o_4}(t_b,t_b^+)\Big)}_{\text{open oyster: } \frac{1}{i\hbar}v^{(0)}_{X,\gamma,o4}(t_b)} G^{\mathcal{C},(0)}_{i_4,o_2}(t_b,t_a^+)\underbrace{\Big(\sum_{o_1,i_1} W_{o_1,o_2,i_1,\delta}G^{\mathcal{C},(0)}_{i_1,o_1}(t_a,t_a^+)\Big)}_{\text{tadpole: } -\frac{1}{i\hbar}v^{(0)}_{H,o_2,\delta}(t_a)} \\
&\quad + \frac{\hbar^2}{8}\delta(t_3-t_4)\sum_{o_2,i_2}\sum_{o_3,o_4,i_4} W_{o_3,\gamma,\delta,i_4}\int_{\mathcal{C}} dt_1\; G^{\mathcal{C},(0)}_{i_4,o_2}(t_a,t_1^+)\underbrace{\Big(\sum_{o_1,i_1} W_{o_1,o_2,i_1,i_2}G^{\mathcal{C},(0)}_{i_1,o_1}(t_1,t_1^+)\Big)}_{\text{tadpole: } -\frac{1}{i\hbar}v^{(0)}_{H,o_2,i_2}(t_1)} G^{\mathcal{C},(0)}_{i_2,o_3}(t_1,t_a^+)
\end{aligned}
\tag{10.77}
$$

In the last step, I grouped the terms in a sensible way. In that process I identified the Hartree potential

$$
v^{(0)}_{H,o,i}(t) = \sum_{o',i'} W_{o,o',i,i'}\underbrace{\Big(-i\hbar G^{\mathcal{C},(0)}_{i',o'}(t,t^+)\Big)}_{\rho^{(1),(0)}_{i',o'}(t)} \tag{10.78}
$$

and the exchange potential

$$
v^{(0)}_{X,o,i}(t) = -\sum_{o',i'} W_{o,o',i',i}\underbrace{\Big(-i\hbar G^{\mathcal{C},(0)}_{i',o'}(t)\Big)}_{\rho^{(1),(0)}_{i',o'}(t)} \tag{10.79}
$$

where $\rho^{(1),(0)}_{i,o}(t)$, is the one-particle-reduced density matrix Eq. 8.28 of the non-interacting electrons. The names *"tadpole"* and *"open oyster"* refer to the descriptive names of certain units of Feynman diagrams. (see p. 327 and p. 328.)

4 construct the Green's function from $\bar{\mathcal{Q}}_{T,\mu}[G^{\mathcal{C},(0)}]$.

Finally, we obtain the Greens function from

$$
\begin{aligned}
G^{\mathcal{C}}_{\alpha,\beta}(t_2,t_1) &\overset{\text{Eq. } 10.60}{=} G^{\mathcal{C},(0)}_{\alpha,\beta}(t_2,t_1) + \sum_{\gamma,\delta}\int_{\mathcal{C}} dt_4 \int_{\mathcal{C}} dt_3\; G^{\mathcal{C},(0)}_{\alpha,\gamma}(t_2,t_4) \underbrace{\frac{1}{k_B T}\frac{\delta \mathcal{Q}_{T,\mu}[G^{\mathcal{C},(0)},W]}{\delta G^{\mathcal{C},(0)}_{\delta,\gamma}(t_3,t_4)}}_{=:\Sigma^{\text{red}}_{\gamma,\delta}(t_4,t_3)} G^{\mathcal{C},(0)}_{\delta,\beta}(t_3,t_1) \\
&= G^{\mathcal{C},(0)}_{\alpha,\beta}(t_2,t_1) + \sum_{\gamma,\delta}\int_{\mathcal{C}} dt_4 \int_{\mathcal{C}} dt_3\; G^{\mathcal{C},(0)}_{\alpha,\gamma}(t_2,t_4) G^{\mathcal{C},(0)}_{\delta,\beta}(t_3,t_1) \\
\times\frac{\hbar^2}{8} &\Bigg\{ \delta(t_3-t_4)\sum_{o_2,i_2} W_{\gamma,o_2,\delta,i_2}(t_3)\int_{\mathcal{C}} dt_2 \sum_{o_3,i_4} G^{\mathcal{C},(0)}_{i_2,o_3}(t_3,t_2^+)\frac{-1}{i\hbar} v^{(0)}_{X,o_3,i_4}(t_2) G^{\mathcal{C},(0)}_{i_4,o_2}(t_2,t_3^+) \\
&+ \sum_{i_2,o_3}\frac{-v^{(0)}_{H,\gamma,i_2}(t_4)}{i\hbar} G^{\mathcal{C},(0)}_{i_2,o_3}(t_4,t_3^+)\frac{-v^{(0)}_{X,o_3,\delta}(t_3)}{i\hbar} \\
&+ \sum_{o_2,i_4}\frac{-1}{i\hbar} v^{(0)}_{X,\gamma,i_4} G^{\mathcal{C},(0)}_{i_4,o_2}(t_4,t_3^+)\frac{-v^{(0)}_{H,o_2,\delta}(t_3)}{i\hbar} \\
&+ \delta(t_3-t_4)\sum_{o_3,i_4} W_{o_3,\gamma,\delta,i_4}(t_3)\sum_{o_2,i_2}\int_{\mathcal{C}} dt_1 G^{\mathcal{C},(0)}_{i_4,o_2}(t_3,t_1^+)\frac{-v^{(1)}_{H,o_2,i_2}(t_1)}{i\hbar} G^{\mathcal{C},(0)}_{i_2,o_3}(t_1,t_3^+)\Bigg\}
\end{aligned}
\tag{10.80}
$$

5 Draw the Feynman diagrams for

- the generating functional $\bar{\mathcal{Q}}_{T,\mu}[G^{\mathcal{C},(0)}]$
- the reducible self energy Σ^{red}
- the Green's function $G^{\mathcal{C}}$

The graphical representation is provided in figure 10.6 below.

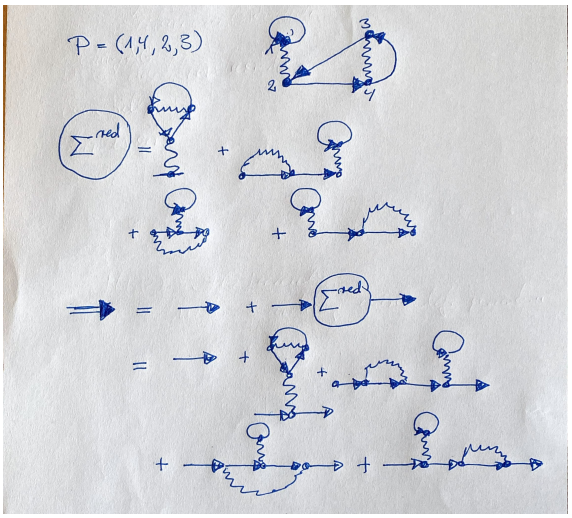

Fig. 10.6: Second part of the solution for the problem in section 10.5.1, demonstrating graphically the construction of the Green's function from a generating functional. Editor: The diagrams for the generating functional and the Green's function has been shown already in figure 10.5. The self energy graphs are not shown there.

Chapter 11

Diagrammatics of the generating functional

11.1 Classes of diagrams

In this section, I will present some terminology and names for diagrams, respectively for building blocks of them. By doing so, we will identify recurring patterns within the diagrams, that can be understood as one unit.

The elementary building blocks of a Feynman diagram are the particle line, the interaction line, and the vertex.

- The **particle line** represents a Green's function. The arrow with a single line represents a bare Green's function and the arrow with a double represents a full Green's function.

- The **interaction line** represents an interaction. It is represented by a wriggly line. When the wriggly line is drawn with a single line, the interaction line represents the bare Coulomb interaction. When it is drawn with a double line it represents the full or screened interaction.

- The point, which joins particle lines and interaction lines is the **vertex**. For the Coulomb interaction each vertex connects one incoming particle line, one outgoing particle line and one interaction line. The topology of the vertex was the reason for the naming incoming and outgoing indices of a particle line.

11.1.1 Green's function diagram

A general **Green's-function diagram** has two external *"half"*-vertices. One of the external half-vertices can accept an incoming particle line and an interaction line. The other can accept an outgoing particle line and an interaction line.

The most simple Green's function diagrams are the particle lines.

11.1.2 Interaction diagram

An **interaction diagram** has two external vertices, each of which can accept one incoming and one outgoing particle line.

11.1.3 Self-energy diagrams

A **self-energy diagram** has two external vertices. One of the external indices can accept an incoming particle line and the other can accept an outgoing particle line.

A self-energy diagram can be inserted into a self-energy diagram.

Examples are the tadpole on p. 327, the open-oyster diagram on p. 328 and the ring diagram on p. 329.

11.1.4 Polarization diagram

A **polarization diagram** has two external vertices, each of which can be connected to an interaction line.

A polarization diagram can be inserted into an interaction line.

A diagram with two external vertices, to which one can attach exactly one interaction lines each, is called a **polarization diagram** .

An example for a polarization diagram is the ring diagram on p. 329.

11.1.5 Vertex diagram

A diagram with three vertices, to which one can attach exactly one interaction line, one incoming and one outgoing Greens functions function line is called a **vertex diagram**.

11.1.6 Closed diagrams

The diagrams of the denominator of the Green's function are the so-called **closed diagrams**. They are called closed as opposed to the diagrams in the numerator of the Green's function, which have external indices. The closed diagrams with n interactions form the set of $\mathbb{A}_n$. This set of diagrams is easily constructed from all permutation vectors of dimension $2n$.

Editor: Note that the value of open diagrams has not been defined. Thus, their value should be taken with a grain of salt. I first have to supply a formula for the value.

A diagram that is not closed, is called **open diagram**. Open diagrams have an **external vertex**. An external vertex is one that is not fully connected by one interaction line, one incoming and one outgoing particle line.

11.1.7 Linked diagrams

A **linked diagram** or **linked cluster** is a diagram without disconnected parts, that are connected neither by a Green's function nor an interaction with the rest of the diagram.

The linked diagrams form a subset $\mathbb{L}_n$ of the set $\mathbb{A}_n$ of all closed, linked diagrams of order n.

From the second-order diagrams shown in figure 11.2, all diagrams but four are linked. The four exceptions are the two-by-two block in the upper-left corner. The unlinked diagrams consist of combinations of the closed diagrams of lower order.

11.1.8 One-particle irreducible (1PI) diagrams

A diagram is **one-particle irreducible (1PI)** if it does not fall apart when one Green's function is removed. Because Green's functions in closed diagrams form Fermi-loops, linked closed diagrams are one-particle irreducible.

11.1.9 Two-particle irreducible (2PI) diagrams

A diagram is **two-particle irreducible (2PI)** if it does not fall apart when two Green's function are removed. A diagram which is not two-particle irreducible, is called two-particle reducible. Closed, two-particle irreducible diagrams are also called **skeleton diagrams**. The set $\mathbb{S}_n$ of skeleton diagrams of order n is obtained from $\mathbb{L}_n$ by removing all two-particle reducible diagrams.

11.1.10 Named diagrams

There are patterns of diagrams that are easily recognized and interpreted. These structures shall be selected and discussed. In order to identify their values we refer to Eq. 10.48 on p. 308.

$$V(\vec{\mathcal{P}}) \overset{\text{Eq. } 10.48}{=} \epsilon_{\mathcal{P}_1,\ldots,\mathcal{P}_{2n}} (i\hbar)^n \int_{\mathcal{C}} dt_1 \cdots \int_{\mathcal{C}} dt_n \sum_{o_1,i_1,\ldots,o_{2n},i_{2n}} \prod_{j=1}^{n} W_{o_{2j-1},o_{2j},i_{2j-1},i_{2j}}(t_j) \times G^{(0)}_{i_{\mathcal{P}_1},o_1}\big(t(\mathcal{P}_1), t^+(1)\big) \cdots G^{(0)}_{i_{\mathcal{P}_{2n}},o_{2n}}\big(t(\mathcal{P}_{2n}), t^+(2n)\big) \tag{11.1}$$

Many diagram names are taken from Mattuck[4]. (bubble p.18, ladder p.18, oyster p18, ring p.18., open oyster p.66.). The tadpole diagram has been used by Abdus Salam[83].

- **bubble diagram**: density matrix

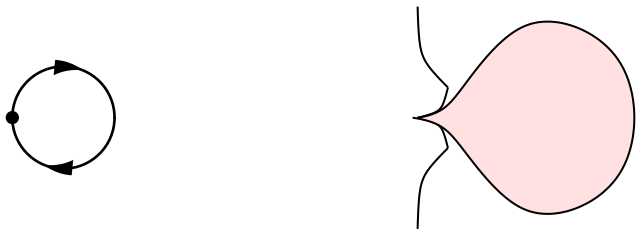

The bubble diagram can be identified with the density matrix of the non-interacting system at a given time.

$$-G^{(0)}_{i,o}(t, t^+) \overset{\text{Eq. } 8.28}{=} \frac{1}{i\hbar}\rho^{(1)(0)}_{i,o}(t) \tag{11.2}$$

In a real-space representation, the one-particle-reduced density matrix would reduce to the density at a given point in space and time. A bubble diagram with a double-lined arrow indicating a full Green's function would yield the one-particle-reduced density matrix of the interacting system.

- **tadpole diagram**: Hartree potential

The tadpole diagram can be attributed to the Hartree potential

$$-i\hbar \sum_{i_2,o_2} W_{o_1,o_2,i_1,i_2}(t) G^{(0)}_{i2,o2}(t, t^+) \overset{\text{Eq. } 8.28}{=} \sum_{i_2,o_2} W_{o_1,o_2,i_1,i_2}(t) \hat{\rho}^{(1)(0)}_{i2,o2}(t) \overset{\text{Eq. } 2.38}{=} v^{(0)}_{H,o_1,i_1}(t) \tag{11.3}$$

The tadpole diagram describes the Hartree potential of the non-interacting or the interacting density, depending on whether a non-interacting or an interacting Green's function is present.

The order (o, i) of the orbital indices of the potential is opposite to that (i, o) in the one-particle-reduced density matrix. One rationale is that the trace of potential and one-particle-reduced density matrix $2E_H = \sum_{i,o} \rho^{(1)}_{i,o} v_{H,o,i}$ is (twice) the Hartree energy. Editor: Think of something more convincing, e.g. working it out brute force.

- **eyeglass diagram** or **double-bubble diagram**: Hartree term

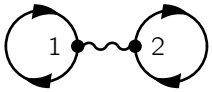

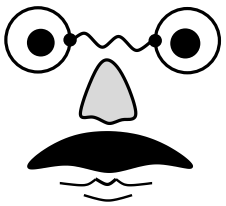

The eyeglass diagram can be attributed to the Hartree energy of the non-interacting electrons.

$$\begin{aligned} V(\text{eyeglass diagram}) &= i\hbar \int_{\mathcal{C}} dt \sum_{i_1,o_1 i_2,o_2} W_{o_1,o_2,i_1,i_2}(t) G^{(0)}_{i1,o1}(t,t^+) G^{(0)}_{i2,o2}(t,t^+) \\ &= \frac{1}{i\hbar} \int_{\mathcal{C}} dt \sum_{i_1,o_1 i_2,o_2} W_{o_1,o_2,i_1,i_2}(t) \rho^{(1)(0)}_{i1,o1}(t) \rho^{(1)(0)}_{i2,o2}(t) \end{aligned} \tag{11.4}$$

The Hartree energy of interacting electrons is obtained by replacing the bare Green's function by the full one.

- **oyster diagram**: exchange term

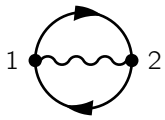

The oyster diagram can be attributed to the exchange energy

$$\begin{aligned} V(\text{oyster diagram}) &= i\hbar \int_{\mathcal{C}} dt \sum_{i_1,o_1,i_2,o_2} W_{o_1,o_2,i_1,i_2}(t) G^{(0)}_{i1,o2}(t,t^+) G^{(0)}_{i2,o1}(t,t^+) \\ &\overset{\text{Eq. 8.28}}{=} \frac{1}{i\hbar} \int_{\mathcal{C}} dt \sum_{i_1,o_1,i_2,o_2} W_{o_1,o_2,i_1,i_2}(t) \rho^{(1)(0)}_{i1,o2}(t) \rho^{(1)(0)}_{i2,o1}(t) \end{aligned} \tag{11.5}$$

- **open-oyster diagram** : exchange potential

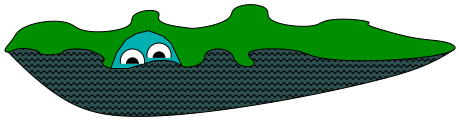

The open-oyster diagram can be attributed to the exchange potential

$$i\hbar \sum_{i_2,o_1} W_{o_1,o_2,i_1,i_2}(t) G^{(0)}_{i2,o1}(t,t^+) \overset{\text{Eq. 8.28}}{=} -\sum_{i_2,o_1} W_{o_1,o_2,i_1,i_2}(t) \rho^{(1)(0)}_{i2,o1}(t) \overset{\text{Eq. 2.41}}{=} v^{(0)}_{X,o_2,i_1}(t) \tag{11.6}$$

- **ring diagram**: virtual electron-hole pair. The electron-hole pair is induced by an electric field. I creates a dipole which screens the interaction. The screened interaction in a free-electron gas has an exponential tail, rather than the long-ranged $1/|\vec{r}|$ Coulomb tail.

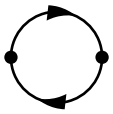

$$\Pi^{(ring)}_{i_1,o_1,i_2,o_2}(t,t') = -G^{(0)}_{i_2,o_1}(t',t)G^{(0)}_{i_1,o_2}(t,t') \tag{11.7}$$

Editor: Make the link to the bare polarization and electric susceptibility. Look up Mattuck-Eq.10.3.6. $\epsilon_{RPA}(\vec{q},\omega) = 1 + V_q\Pi(\vec{q},\omega)$.

- particle-hole ladder: Coulomb attraction between an electron and a hole. Responsible for exciton formation?

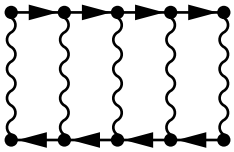

- particle-particle ladder: short-range Coulomb repulsion between two electrons or two holes.

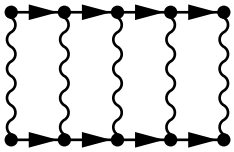

11.2 Systematic construction of closed diagrams

The diagrams can be constructed systematically by forming all permutation vectors of length n.

11.2.1 Construct all permutation vectors

The guiding principle is that we construct the permutation vectors $\vec{\mathcal{P}}$ in a specific order.

In order to keep track of this order, we construct for each vector $\vec{\mathcal{P}}$ of length $2n$ a unique integer number

$$Z(\vec{\mathcal{P}}) \stackrel{\text{def}}{=} \sum_{j=1}^{2n} \mathcal{P}_j \cdot (2n)^{2n-j} \tag{11.8}$$

The number has no physical meaning. Its only purpose is to place all permutation vectors into a well-defined order. By working through an ordered list, we ensure that none of the permutation vectors is missed or considered twice. Z gives a value to any sequence of $2n$ numbers in the given range $0 < \mathcal{P}_j < 2n$, not only true permutations: This is not problematic because the purpose is not to enumerate permutations, but arrange them in a unique order.

Next, we set up a construction scheme for the permutation vectors $\mathcal{P}$ such that $Z(\vec{\mathcal{P}})$ increases from step to step.

1. start with all $2n$ indices in ascending order, that is $\vec{\mathcal{P}} = (1, 2, \ldots, 2n)$.

2. for a given permutation vector $\vec{\mathcal{P}}$ find the longest rightmost subsequence in descending order. If the rightmost sequence is ascending, consider the last element as the descending sequence.

   Examples:

   - for the sequence $(2, 3, 4, 1)$, the rightmost descending sequence is $(4, 1)$
   - for the sequence $(1, 2, 3, 4)$, the rightmost descending sequence is (4)

3. If the sequence with descending indices starts at position m, i.e.

$$\mathcal{P}_{m-1} < \mathcal{P}_m > \mathcal{P}_{m+1} > \ldots > \mathcal{P}_{2n} \, ,$$

   the preceding number $\mathcal{P}_{m-1}$ needs to be increased by the smallest possible amount. We pick from the decreasing sequence $\{\mathcal{P}_m, \ldots, \mathcal{P}_{2n}\}$ the smallest number, which, however, still is larger than $\mathcal{P}_{m-1}$. This number, let us denote it as $\mathcal{P}_q$, is placed on position $m-1$, and the other numbers from $\{\mathcal{P}_{m-1}, \ldots, \mathcal{P}_{q-1}, \mathcal{P}_{q+1} \ldots, \mathcal{P}_{2n}\}$ are arranged in increasing order and placed into positions $m, \ldots, 2n$.

   The resulting permutation vector $\vec{\mathcal{P}}'$ is equal to the original vector $\vec{\mathcal{P}}$ for the first $m-1$ elements. On the position m, $\mathcal{P}'_m = \mathcal{P}_q$. The components of the new permutation vector $\mathcal{P}'_j$ with $j > m$ consists of the components of the old vector with $j > m-1$ with the exception of $\mathcal{P}_q$. These components are arranged in ascending order.

   Examples:

   - for the permutation vector $\vec{\mathcal{P}} = (2, 3, 4, 1)$, the rightmost descending sequence is $(4, 1)$. That is, $m = 3$. We need to increase the value of $\mathcal{P}_{m-1} = 3$. The next higher number in the descending sequence $(4, 1)$ is 4. That is, $q = 3$. We place $\mathcal{P}_q = 4$ into $\mathcal{P}'_{m-1} = 4$ and remove it from the sequence $(3, 4, 1)$. The remaining numbers $\{3, 1\}$ are arranged in ascending order $(1, 3)$ and placed behind $\mathcal{P}'_{m-1} = 4$. Thus, one obtains as next permutation $\vec{\mathcal{P}}' = (2, 4, 1, 3)$.
   - for the permutation vector $\vec{\mathcal{P}} = (1, 2, 3, 4)$, the rightmost descending sequence is (4). This is the fourth component so that $m = 4$. The preceding component $\mathcal{P}_{m-1} = 3$ needs to be increased in value by picking the next higher number in the decreasing sequence, namely $\mathcal{P}_q = 4$, where $q = 4$. The remaining number from the sequence $(3, 4)$, namely 3 is placed into the last position. Thus, one obtains as next permutation $\vec{\mathcal{P}}' = (1, 2, 4, 3)$.

4. this step is repeated until all indices are in decreasing order.

5. One should count the number of permutations constructed in this way to verify that all $(2n)!$ diagrams have been formed.

11.2.2 First-order diagrams

The order in the interaction is one. We start constructing the permutation vectors $2n = 2$ dimensions.

Nr	$\vec{\mathcal{P}}$	
1	1	2
2	2	1

Thus, we obtain two diagrams which can be expressed by the column-wise mappings of the vertices by Green's functions.

- The first diagram with $\vec{\mathcal{P}} = (1, 2)$ has the mapping

1	2	3	4	5	**6**
1	2	3	4	5	**6**
			4	**6**	**5**
			5	4	**6**
			5	**6**	**4**
			6	4	**5**
		3	**6**	**5**	**4**
		4	3	5	**6**
			3	**6**	**5**
			5	3	**6**
			5	**6**	**3**
			6	3	**5**
		4	**6**	**5**	**3**
		5	3	4	**6**
			3	**6**	**4**
			4	3	**6**
			4	**6**	**3**
			6	3	**4**
		5	**6**	**4**	**3**

1	2	5	**6**	**4**	**3**
		6	3	4	**5**
			3	**5**	**4**
			4	3	**5**
			4	**5**	**3**
			5	3	**4**
	2	**6**	**5**	**4**	**3**
	3	2	4	5	**6**
			4	**6**	**5**
			5	4	**6**
			5	**6**	**4**
			6	4	**5**
		2	**6**	**5**	**4**
		4	2	5	**6**
			2	**6**	**5**
			5	2	**6**
			5	**6**	**2**
			6	2	**5**
		4	**6**	**5**	**2**

1	3	4	**6**	**5**	**2**
		5	2	4	**6**
			2	**6**	**4**
			4	2	**6**
			4	**6**	**2**
			6	2	**4**
		5	**6**	**4**	**2**
		6	2	4	**5**
			2	**5**	**4**
			4	2	**5**
			4	5	**2**
			5	2	**4**
	3	**6**	**5**	**4**	**2**
	4	2	3	5	**6**
			3	**6**	**5**
			5	3	**6**
			5	**6**	**3**
			6	3	**5**
		2	**6**	**5**	**3**

Table 11.1: Example for building up permutation vectors of length 6 using the technique of section 11.2.1. Only the first 54 permutation vectors from 720 in total are shown. The trailing descending sequence is marked as bold faced. The preceding element, which is to be increased in value, is marked in red. Elements that do not change are omitted. The top line in each column is the reference for starting the sequence below. It is a repetition of the last entry of the previous column.

o	1	2
i	1	2

This will produce Hartree diagram, which is also called **eyeglass diagram**. It is shown on the left of figure 11.1.

- The second diagram with $\vec{\mathcal{P}} = (2, 1)$ has the mapping

o	1	2
i	2	1

This will produce exchange diagram, which is also called **oyster diagram**. It is shown on the right of figure 11.1.

11.2.3 Second-order diagrams

The order in the interaction is two. We start constructing the $(2n)! = 24$ permutation vectors $2n = 4$ dimensions.

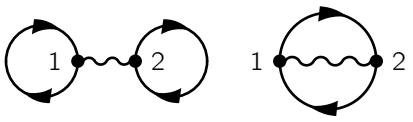

Fig. 11.1: First-order Feynman diagrams in the interaction. The left diagram is the Hartree diagram and the diagram to the right is the exchange diagram. The two diagrams describe the non-self-consistent Hartree-Fock approximation.

Nr	$\vec{\mathcal{P}}$			
1	1	2	3	4
2	1	2	4	3
3	1	3	2	4
4	1	3	4	2
5	1	4	2	3
6	1	4	3	2

Nr	$\vec{\mathcal{P}}$			
7	2	1	3	4
8	2	1	4	3
9	2	3	1	4
10	2	3	4	1
11	2	4	1	3
12	2	4	3	1

Nr	$\vec{\mathcal{P}}$			
13	3	1	2	4
14	3	1	4	2
15	3	2	1	4
16	3	2	4	1
17	3	4	1	2
18	3	4	2	1

Nr	$\vec{\mathcal{P}}$			
19	4	1	2	3
20	4	1	3	2
21	4	2	1	3
22	4	2	3	1
23	4	3	1	2
24	4	3	2	1

The diagrams are shown in figure 11.2. The diagrams are arranged line-by-line, as opposed to the column wise arrangement of the permutations given above.

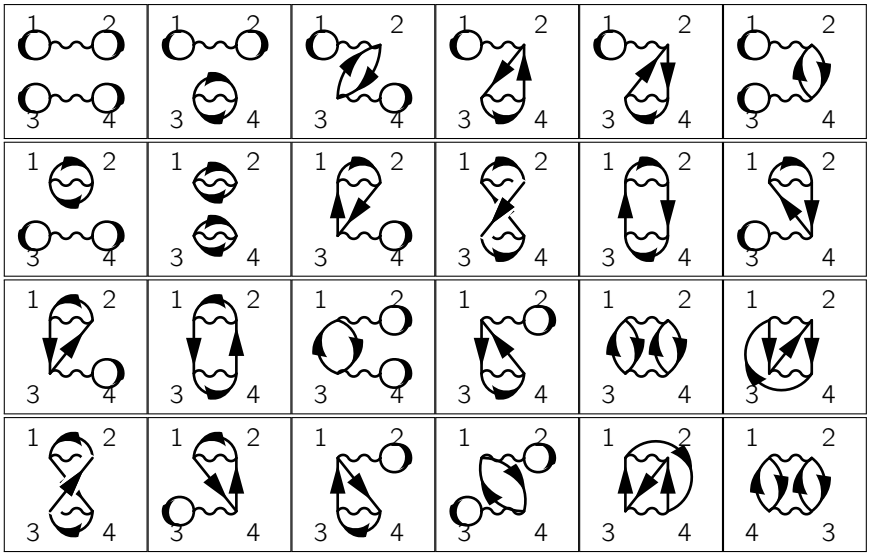

Fig. 11.2: Second-order Feynman diagrams in the interaction. Referring to the order of the pairings developed above the orderings run in rows rather than columns.

11.3 Sign theorem

The value $V(D)$ of a diagram D specified by a permutation vector $\vec{\mathcal{P}}$ is given by Eq. 10.48 on p. 308. It contains a **sign factor**, namely the fully antisymmetric tensor $\epsilon_{\mathcal{P}_1,\mathcal{P}_2,\ldots}$ of the permutation vector $\vec{\mathcal{P}}$ specifying the diagram. Evaluating the sign factor can be rather cumbersome. The **sign theorem** simplifies this task so that the sign can be trivially read off from a Feynman diagram.

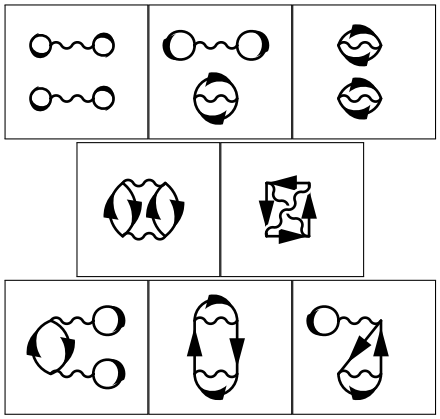

Fig. 11.3: Topologically distinct diagrams of second order grouped according to disconnected diagrams (top row), skeleton diagrams (middle row) and non-skeleton connected diagrams (bottom row). The number of Fermi loops L, the symmetry factor S, the multiplicities M and participating diagrams in parenthesis are: top-left: L=4, S=8, M=1, (1); top-middle: L=3,S=4, M=2, (2,7), top-right: L=2, S=8, M=1, (8), middle-left: L=2, S=4, M=2, (17,24), middle-right: L=1, S=4, M=2, (18,23); bottom-left: L=3, S=2, M=4, (3,6,22,15); bottom-middle: L=1, S=2, M=4, (10,11,14,19) bottom-right: L=2, S=1, M=8, (4,5,9,12,13,16,20,21). The graph numbers refer to the order in Fig. 11.2.

What is a Fermi loop?

Let me first introduce the concept of a **Fermi loop**: Consider any closed diagram: Let me pick out any Green's function in that diagram. The Green's function points to a vertex, which connects this Green's function to exactly one other (or the same) Green's function. When we proceed repeatedly from one Greens function to the next, we arrive at some point at the vertex where the first Green's function emerged from, because the diagram is closed. This ring of Green's function is called a Fermi loop. A closed diagram may have one or more such Fermi loops. A Fermi loop may only contain a single Green's function, which closes on itself, as in the tadpole diagram.

Identify Fermi-loops in a permutation vector $\vec{\mathcal{P}}$: Fermi loops can be identified from the permutation vector without drawing the diagram. The permutation vector is considered as a mapping between vertices, which allows to follow the Green's functions until they close a Fermi loop. Let me demonstrate the procedure at the following example:

$\vec{\mathcal{P}}_{tot} = \big($ 7, 1, 4, 3, 10, 5, 8, 2, 9 6 $\big)$

o	1	2	3	4	5	6	7	8	9	10
i	7	1	4	3	10	5	8	2	9	6

We start at the first outgoing vertex ($o = 1$) and follow the permutation vector to the corresponding incoming vertex $i = \mathcal{P}_1 = 7$. We denote this step by $(1 \to 7)$. Next, we choose the resulting vertex as outgoing vertex $o = 7$ and pass on to $i = \mathcal{P}_7 = 8$. We proceed until we arrive at the first vertex in the loop, namely 1, which implies that the first Fermi loop is closed. The Fermi loop consists of the hops

$$(1 \to 7), (7 \to 8), (8 \to 2), (2 \to 1) \tag{11.9}$$

and the vertices visited by the Fermi loop are

$$[1, 7, 8, 2] \tag{11.10}$$

The next Fermi loop starts at the first outgoing vertex that has not yet been visited, namely vertex 3. From here we identify the next Fermi loop.

$$(3 \to 4), (4 \to 3) \tag{11.11}$$

The vertices visited by the first two Fermi loops are

$$[1, 7, 8, 2][3, 4] \tag{11.12}$$

We proceed analogously to the third Fermi loop

$$(5 \to 10), (10 \to 6), (6 \to 5) \tag{11.13}$$

and the fourth Fermi loop

$$(9 \to 9)\ . \tag{11.14}$$

The grouping of the vertices into Fermi loops is therefore

$$\rightsquigarrow [1, 7, 8, 2][3, 4][5, 10, 6][9] \tag{11.15}$$

Now all vertices have been visited once. Thus, there are four Fermi loops in the corresponding diagram.

Sign theorem

With the concept of a Fermi loop, we can state the **sign theorem**:

SIGN THEOREM

The sign $\epsilon_{\vec{\mathcal{P}}}$ due to the permutations of field operators is obtained from the number L of Fermi loops in a diagram as $\epsilon_{\mathcal{P}_1,\mathcal{P}_2,\mathcal{P}_3,\ldots} = (-1)^L$.
A **Fermi loop** is a closed chain of Green's functions.
The sign theorem in the form presented here is applicable only to closed diagrams.

Proof of the sign theorem

Let me verify the sign theorem.

- Let me start with a diagram specified by the permutation vector $\vec{\mathcal{P}} = (1, 2, 3, \ldots)$. Because the elements of the permutation are in ascending order, the sign factor is $+1$. The corresponding diagram consists of a product of so-called **eyeglass diagrams**, one for each interaction. An eyeglass diagram has two Fermi loops. Hence, the number of Fermi loops is even, and the sign theorem predicts, correctly, a positive sign factor.
- A sign change due to $\epsilon_{\mathcal{P}_1,\mathcal{P}_2,\ldots}$ is related to a permutation of two components of the permutation vector. Each permutation changes the number of Fermi loops by ± 1.
  - Consider the interchange of two components of the permutation vector $\vec{\mathcal{P}}$, which refer to vertices of **distinct Fermi loops**. As shown below, this will merge the two Fermi loops into one big Fermi loop.

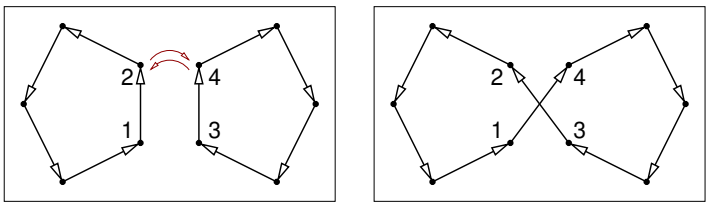

  - Consider the interchange of two components of the permutation vector, which refer to vertices in the **same Fermi loop**. Each of the two Greens function, which are reattached closes a Fermi loop, so that the Fermi loop is divided into two Fermi loops. Because this step is related to a permutation of two indices, it is related to a sign change.

This shows that an even number of Fermi loops is related to a positive sign and an odd number of Fermi loops is related to a negative sign. This proves the sign theorem.

Exercise: Verify the sign theorem by evaluating the sign for eye-glass and oyster diagram, once with the Levi-Civita symbol and using the sign theorem.

11.4 Linked-cluster theorem

The **linked-cluster theorem**[84] [1] allows one to get rid of the logarithm in the generating functional $\mathcal{Q}_{T,\mu}$ defined in Eq. 10.59.

$$\mathcal{Q}_{T,\mu} \overset{\text{Eq. 10.59}}{=} -k_B T \ln \mathrm{Tr}\Big\{\hat{\rho}^{(0)}_{T,\mu}\mathcal{T}_{\mathcal{C}}\hat{S}_{I,\mathcal{C}}\Big\} \overset{\text{Eq. 10.59}}{=} -\frac{1}{\beta}\ln\Big\{\sum_{n=0}^{\infty}\frac{1}{n!}\frac{1}{2^n}\sum_{D\in\mathbb{A}_n}V(D)\Big\} \tag{11.16}$$

Furthermore, the set $\mathbb{A}$ of general closed diagrams is reduced to a smaller set $\mathbb{L}$ of so-called linked diagrams.

[1] For the proof of the **linked-cluster theorem**, Luttinger points to Bloch and de Dominicis[85].

What is a linked diagram?

A **linked diagram** or **linked cluster** is a diagram without disconnected parts. Two parts of a diagram are disconnected, when they are neither connected by a Green's function nor by an interaction line.

Disconnected diagrams can easily be identified by inspection of the diagram. To identify disconnected diagrams on the computer or for formal derivations, a criterion based on the permutation vector $\vec{\mathcal{P}}$ is preferable. Let me develop such a criterion:

- The permutation vector maps a subset $\mathbb{B}$ of vertices onto another set $\mathbb{B}'$. When the permutation vector maps $\mathbb{B}$ onto itself, i.e. $\mathbb{B}' = \mathbb{B}$, this subset is not connected by Green's functions to the rest of the diagram. (It may still be connected by an interaction line.)

- Our rule to translate a permutation vector into a diagram enforces that an odd-numbered vertex j and the next higher even-numbered vertex $j+1$ are connected by an interaction line. This implies that all odd-even-numbered vertex pairs are connected by interaction lines.

This implies that a sub diagram is disconnected from the rest, if it consists of a subset $\mathbb{B}$ of vertices , which, firstly, consists of odd-even numbered vertex pairs, and which, secondly, is mapped onto itself by the permutation vector. A procedure to identify disconnected diagrams from a set of permutation vectors is described in the appendix L.1 on p. 585.

Linked-cluster theorem

Let me now state the linked-cluster theorem, which I will prove below.

LINKED-CLUSTER THEOREM

The linked-cluster theorem removes the logarithm and reduces the sums over closed diagrams to the sum over linked diagrams, i.e.

$$\mathcal{Q}_{T,\mu}[G^{(0)}] \overset{\text{Eq. } 10.59}{=} -\frac{1}{\beta}\ln\Big\{\sum_{n=0}^{\infty}\sum_{D\in\mathbb{A}_n}\frac{V(D)}{n!2^n}\Big\} = -\frac{1}{\beta}\sum_{n=1}^{\infty}\sum_{D\in\mathbb{L}_n}\frac{V(D)}{n!2^n} \tag{11.17}$$

where $\mathbb{L}_n$ is the subset of linked diagrams in $\mathbb{A}_n$, the set of all closed diagrams of order n.
Note, that the sum on the right-hand side starts with element $n=1$ and not with $n=0$ as on the left-hand side.

The linked-cluster theorem represents the generating functional $\mathcal{Q}_{T,\mu}$, and thus the Green's function, as a power-series expansion in the interaction. Without the linked-cluster theorem, the Green's function is a fraction of two terms, each of which is a power series expansion of the interaction. A single power-series expansion is important to preserve symmetries with their conservation laws and sum rules. Truncating a Taylor expansion at any given order preserves all sum rules that are valid independent of the interaction strength. Truncating the sum inside the logarithm would violate these sum rules.

Proof of the linked-cluster theorem

We start taking the exponential function of both sided of the linked-cluster theorem Eq. 11.17.

$$\begin{aligned}\sum_{n=0}^{\infty}\sum_{D\in\mathbb{A}_n}\frac{V(D)}{n!2^n} &\overset{\text{Eq. 11.17}}{=} \exp\left(\sum_{n=1}^{\infty}\sum_{D\in\mathbb{L}_n}\frac{V(D)}{2^n(n!)}\right)\\ &= \sum_{p=0}^{\infty}\frac{1}{p!}\left(\sum_{n=1}^{\infty}\sum_{D\in\mathbb{L}_n}\frac{V(D)}{2^n(n!)}\right)^p\\ &= 1+\underbrace{\frac{1}{1!}\left(\sum_{n=1}^{\infty}\sum_{D\in\mathbb{L}_n}\frac{V(D)}{2^n(n!)}\right)^1}_{\text{linked clusters}}+\underbrace{\frac{1}{2!}\left(\sum_{n=1}^{\infty}\sum_{D\in\mathbb{L}_n}\frac{V(D)}{2^n(n!)}\right)^2}_{\text{singly disconnected}}+\ldots \qquad (11.18)\end{aligned}$$

The second term on the right-hand side ($p=1$) contains all linked diagrams. The third term ($p=2$) contains all diagrams that consist of two disconnected parts. The next one ($p=3$) contains diagrams with three disconnected parts, etc.

The proof of the linked-cluster theorem Eq. 11.17 needs to verify Eq. 11.18. Our task is to establish a one-to-one map of arbitrary closed diagrams $D\in\mathbb{A}$ on the left side of Eq. 11.18 and the terms on the right-hand side of Eq. 11.18.

Let me consider a permutation vector $\vec{\mathcal{P}}_{tot}$ defining the diagram $D_{tot}\in\mathbb{A}$ on the left side of Eq. 11.18. Let me assume that it consists of p disconnected parts $D_1,\ldots,D_p$, which themselves are linked clusters.

The permutation vector $\vec{\mathcal{P}}_j$ of the sub-diagram D_j is obtained from the permutation vector $\vec{\mathcal{P}}_{tot}$ by relabeling the vertices of diagram D_j and by remapping $\vec{\mathcal{P}}_j$ accordingly. The order of the vertices within diagram D_j has to remain intact and the vertices have numbers from one to $2n_j$, where n is the order of the diagram D_j.

Example An example for a disconnected diagram in $\mathbb{A}$ is

$\vec{\mathcal{P}}_{tot} = \big($ 7, 1, 4, 3, 10, 5, 8, 2, 9, 6 $\big)$									
o	1	2	3	4	5	6	7	8	9	10
i	7	1	4	3	10	5	8	2	9	6

I have colored the sections of the permutation vector $\vec{\mathcal{P}}_{tot}$ belonging to disconnected sub-clusters. The table specifies the pairs of vertex labels corresponding to the outgoing (right) (o) and incoming (left) (i) indices of a Green's function.
The diagram above consists of the following three subdiagrams, which are linked clusters and disconnected from each other. The arrows indicate the remapping of the vertex labels from the combined diagram $\mathcal{P}_{tot}$ to that of an isolated linked cluster $\vec{\mathcal{P}}_j$.

$\vec{\mathcal{P}}_1 = \big($ 3, 1, 4, 2 $\big)$									
o	1	2	-	-	-	-	$7 \to 3$	$8 \to 4$	-	-
i	$7 \to 3$	1	-	-	-	-	$8 \to 4$	2	-	-

$\vec{\mathcal{P}}_2 = \big($ 2, 1 $\big)$									
o	-	-	$3 \to 1$	$4 \to 2$	-	-	-	-	-	-
i	-	-	$4 \to 2$	$3 \to 1$	-	-	-	-	-	-

$\vec{\mathcal{P}}_3 = \big($ 4, 1, 3, 2 $\big)$									
o	-	-	-	-	$5 \to 1$	$6 \to 2$	-	-	$9 \to 3$	$10 \to 4$
i	-	-	-	-	$10 \to 4$	$5 \to 1$	-	-	$9 \to 3$	$6 \to 2$

This last diagram $\mathcal{P}_3$ consists of two Fermi loops with vertices $[1, 4, 2]$ and $[3]$, which are connected by an interaction between vertices 3 and 2.

There is more than one diagram in $\mathbb{A}$ that falls apart into the same set of sub-diagrams. The number of such diagrams is obtained by counting the number of ways the interaction lines of the subdiagrams can be assigned to those of the combined diagram.

1. There are
$$\frac{n_{tot}(n_{tot}-1)\dots(n_{tot}-n_1+1)}{n_1!} = \frac{n_{tot}!}{n_1!(n_{tot}-n_1)!} \tag{11.19}$$
possibilities to assign the n_1 interaction lines of D_1 to the n_{tot} interaction lines of the combined diagram, while maintaining the internal order of the vertices in D_1. The count for preserving the internal order of the vertices is obtained by dividing by the number $n_1!$ of permutations of the interactions in D_1.

2. There are
$$\frac{(n_{tot}-n_1)(n_{tot}-n_1-1)\dots(n_{tot}-n_1+1)}{n_2!} = \frac{(n_{tot}-n_1)!}{n_2!(n_{tot}-n_1-n_2)!} \tag{11.20}$$
possibilities to assign the n_2 interactions of D_2 to those of the combined diagram, while maintaining the internal order of the vertices in D_2. The number of ways to distribute the interaction of D_1 and D_2 is
$$\frac{n_{tot}!}{n_1!n_2!(n_{tot}-n_1-n_2)!} \tag{11.21}$$

3. Let me proceed to the last diagram: There are
$$\frac{n_{tot}!}{\prod_{k=1}^{p} n_k!} \tag{11.22}$$

possibilities to assign the interactions of all sub-diagrams $D_1, \ldots, D_p$ to those of the combined diagram.

The set of diagrams D on the left-hand side of Eq. 11.18, which dissociate into the same specific set $\{D_1, \ldots, D_p\}$ of linked sub diagrams, contribute

$$\underbrace{\frac{n_{tot}!}{\prod_{k=1}^{p} n_k!}}_{\text{Eq. 11.22}} \frac{V(D)}{n_{tot}! 2^{n_{tot}}} = \prod_{k=1}^{p} \frac{V(D_k)}{n_k! 2^{n_k}} \tag{11.23}$$

which is the weight of the same set of diagrams $\{D_1, \ldots, D_p\}$ on the right-hand side of Eq. 11.18, if the diagrams in the set are all distinct. On the right-hand side the set occurs $p!$ times in the sum, which is compensated by a factor $\frac{1}{p!}$ in Eq. 11.18.

Let me now remove the restriction that the diagrams in the set $\{D_1, \ldots, D_p\}$ are distinct from each other:

When two sub diagrams are equal, an interchange of these diagrams does not produce a new composite diagram with another permutation vector. Therefore, the weight of this diagram in Eq. 11.23 must be divided by the number of interchanges of equivalent diagrams.

If there are q distinct sub diagrams in the set $\{D_1, \ldots, D_p\}$ with multiplicities $m_1, m_2, \ldots, m_q$ (with $m_1 + m_2 + \ldots + m_q = p$), an additional factor $\frac{1}{m_1! \cdots m_q!}$ needs to be considered.

With this correction, the weight of the diagrams on the left-hand side of Eq. 11.18 consisting of $D_1, \ldots, D_p$ is

$$\frac{1}{m_1! \cdots m_q!} \prod_{k=1}^{p} \frac{V(D_k)}{n_k! 2^{n_k}} \tag{11.24}$$

Let me now turn to the right-hand side of Eq. 11.18:

If the diagram D_{tot} consists of p linked sub-diagrams, its weight is contained in the term with power p in the Taylor expansion of the exponential function. The diagrams $D_1, \ldots, D_p$ occur $\frac{p!}{m_1! \cdots m_q!}$ times in the sum, if distinct diagrams have multiplicities $m_1, \ldots, m_q$. The factor $p!$ is due to the different orders of the diagrams in the sum.

The total weight of the diagrams consisting of the subdiagrams $D_1, \ldots, D_p$ on the right-hand side of Eq. 11.18 is

$$\frac{1}{p!} \frac{p!}{m_1! \cdots m_q!} \prod_{k=1}^{p} \frac{V(D_k)}{n_k! 2^{n_k}} \tag{11.25}$$

which is equivalent to the weight Eq. 11.24 obtained on the left-hand side of Eq. 11.18. Thus, for each diagram D occuring on the left-hand side Eq. 11.18, the weight is equal to that of the set of subdiagrams on the right-hand side of Eq. 11.18. This completes the proof of the linked-cluster theorem.

11.5 Topologically-equivalent diagrams and symmetry factors

In this section, I will show that the set $\mathbb{L}$ of linked diagrams of the generating functional can be reduced to a much smaller set $\mathbb{T}$ of so-called **topologically distinct**, linked diagrams. The vertex labels, used so far, become irrelevant for this new set. The reduction in the number of terms is compensated with the help of a so-called **symmetry factor** $S(D)$.

The result of this section can be summarized in the following box:

SUM OVER TOPOLOGICALLY DISTINCT DIAGRAMS

The generating functional $\mathcal{Q}_{T,\mu}\left[G^{(0)}\right]$ of Eq. 11.16 can be expressed in terms of topologically distinct diagrams and their symmetry factor $S(D)$ as

$$\mathcal{Q}_{T,\mu}\left[G^{(0)}\right] \overset{\text{Eq. 11.32}}{=} -\frac{1}{\beta}\sum_{n=1}^{\infty}\sum_{D\in\mathbb{T}_n}\frac{V(D)}{S(D)} \tag{11.26}$$

$\mathbb{T}_n$ is the set of all topologically distinct, linked, closed diagrams of order n. The value $V(D)$ of the diagram is defined in Eq. 10.48. $S(D)$ is the symmetry factor of the diagram, which is obtained as the number of mere deformations constructed by topology preserving transformations among vertex labels.

What are topologically equivalent diagrams?

The topology of a diagram refers to its network of particle lines and interaction lines.

Many diagrams of the generating functional $\mathcal{Q}_{T,\mu}$ Eq. 11.17, have the same value $V(D)$. Their values are equivalent, because the integrals in the expressions for $V(D)$, Eq. 10.48, are related by a mere renaming of integration variables. In the diagram, a renaming of the integration variables is equivalent to changing the vertex labels, while preserving the connectivity, the topology, of the diagram.

Relabeling vertices: Up to now, we have used so-called **labeled diagrams**, meaning that every vertex has a specific label (number). The labels allowed us to represent diagrams in terms of permutation vectors $\vec{\mathcal{P}}$.

Renaming (relabeling) the vertices can be done by a vector $\vec{M}$, which maps every vertex label j uniquely onto a new vertex label M_j. Mapping vectors $\vec{M}$ have much in common with permutation vectors $\vec{\mathcal{P}}$, because both are a unique mappings of the vertices in a diagram onto each other.

A Green's function that points from vertex j to vertex $\mathcal{P}_j$ turns, after remapping, into a Greens-function from vertex M_j to vertex $M_{\mathcal{P}_j}$. The new permutation vector satisfies therefore

$$\mathcal{P}'_{M_j} = M_{\mathcal{P}_j} \tag{11.27}$$

Considering both vectors as transformation operators acting on the vertex labels, this can also be written in the form[2]

$$\mathcal{P}' = M \circ \mathcal{P} \circ M^{-1} \tag{11.28}$$

[2]The inverse of the mapping M is obtained by, first, interchanging the sequences of outgoing and incoming vertices, and secondly reordering the (o, i) vertex pairs so that the new outgoing vertices are in ascending order.

o	1	2	3	4
i	2	1	3	4

$\overset{i\leftrightarrow o}{\rightarrow}$

o	2	1	3	4
i	1	2	3	4

$\overset{\text{order}}{\rightarrow}$

o	1	2	3	4
i	2	1	3	4

The inverse mapping $\vec{M}^{-1} = (2, 1, 3, 4)$ is, in this case, identical to the forward mapping $\vec{M} = (2, 1, 3, 4)$.

Example for relabeling a diagram:

o	1	2	3	4
i	$\mathcal{P}_1$	$\mathcal{P}_2$	$\mathcal{P}_3$	$\mathcal{P}_4$

$\xrightarrow{\text{remap}}$

o	M_1	M_2	M_3	M_4
i	$M_{\mathcal{P}_1}$	$M_{\mathcal{P}_2}$	$M_{\mathcal{P}_3}$	$M_{\mathcal{P}_4}$

$\xrightarrow{\text{order}}$

o	1	2	3	4
i	$\mathcal{P}'_1$	$\mathcal{P}'_2$	$\mathcal{P}'_3$	$\mathcal{P}'_4$

In the first step "remap", all vertex labels, incoming and outgoing, are relabeled so that the vertex with label j receives the new label M_j. In the second step "order", the columns (outgoing-incoming pairs) are rearranged such that the outgoing vertex labels are in ascending order. The resulting sequence of incoming vertex labels form the new permutation vector $\vec{\mathcal{P}}'$.
Let me consider a specific example with $\vec{\mathcal{P}} = (3, 1, 4, 2)$ and $\vec{M} = (2, 1, 3, 4)$, which yields the new permutation vector $\vec{\mathcal{P}}' = (2, 3, 4, 1)$.

o	1	2	3	4
i	3	1	4	2

$\xrightarrow{\text{remap}}$

o	2	1	3	4
i	3	2	4	1

$\xrightarrow{\text{order}}$

o	1	2	3	4
i	2	3	4	1

Topology-preserving transformations: Relabeling vertices in an arbitrary manner [3] preserves the network of Green's functions, but it could change the network of interactions lines. In order to also preserve the network of interaction lines, the following transformations are allowed:

- $n!$ interchanges of vertex-label pairs between interactions, while maintaining the internal odd-even-order of the vertex labels on each interaction.

- 2^n interchanges of the vertex labels within interactions.

These $n!2^n$ operations form a group G_n of transformations of vertex labels, which maintain the same network of particle lines and interaction lines and therefore leave the value of the diagram unchanged.[4] The mapping vectors $\vec{M}$ for the second-order terms in the interaction , i.e. $n = 2$, are given as an example in table 11.2.

Table 11.2: The $2^n n!$ mappings of the vertices for order $n = 2$ in the interaction, which leave the topology of a diagram unchanged. Required is that all interactions connect an odd numbered vertex with the next higher even-numbered vertex. There are $n!2^n = 8$ such mappings.

V_i	1	2	3	4	
$M_1 = I$	1	2	3	4	identity
M_2	2	1	3	4	flips vertices of 1st interaction
$M_3 = M_5 \circ M_2 \circ M_5$	1	2	4	3	flips vertices of 2st interaction
$M_4 = (M_2 \circ M_5)^2$	2	1	4	3	flips vertices of each interaction
M_5	3	4	1	2	interchanges two interactions
$M_6 = M_5 \circ M_2$	3	4	2	1	inverts 1st interaction and interchanges interactions
$M_7 = M_2 \circ M_5$	4	3	1	2	inverts 2st interaction and interchanges interactions
$M_8 = M_2 \circ M_5 \circ M_2$	4	3	2	1	inverts both interactions and interchanges interactions

[3] Also an arbitrary mapping vector must be unique mapping of the vertex labels onto each other.

[4] The generators of the group are (1) the interchange of the vertex labels on the first interaction and (2) the interchange of the vertex labels of every interaction, except the first, with the first. In total, the symmetry group for a diagram of order n has n generators. All other transformation of the symmetry group are obtained as products of these generators.

Mere deformations: Some of the topology-preserving transformations turn a diagram into itself, rather than into a different diagram with the same topology. More precisely, the resulting permutation vector is identical to the original one, i.e. $\vec{\mathcal{P}}' = \vec{\mathcal{P}}$. Such a transformation is called a **mere deformation**. Whether a transformation is a mere deformation depends on the diagram at hand. Following Eq. 11.27, a mere deformation satisfies

$$\mathcal{P}_{M_j} = M_{\mathcal{P}_j} \ . \tag{11.29}$$

When we consider permutation vector and mapping vector as transformations, Eq. 11.29 implies that these two transformations commutate.

Example for a mere deformation: Let us pick the same permutation vector $\vec{\mathcal{P}} = (3, 1, 4, 2)$ as in the example above, but transform it with another re-mapping, namely $\vec{M} = (4, 3, 2, 1)$. In that case we obtain

o	1	2	3	4
i	3	1	4	2

$\xrightarrow{\text{remap}}$

o	4	3	2	1
i	2	4	1	3

$\xrightarrow{\text{order}}$

o	1	2	3	4
i	3	1	4	2

This remapping produces the same permutation vector $\vec{\mathcal{P}}' = \vec{\mathcal{P}}$ as the original one. Thus, we have not produced a new diagram, but a mere deformation of the original diagram.
Let me now implement the criterion Eq. 11.29 for a mere deformation given above

$$\begin{aligned}
\left(1 \overset{\mathcal{P}}{\to} 3 \overset{M}{\to} 2\right) &= \left(1 \overset{M}{\to} 4 \overset{\mathcal{P}}{\to} 2\right) \\
\left(2 \overset{\mathcal{P}}{\to} 1 \overset{M}{\to} 4\right) &= \left(2 \overset{M}{\to} 3 \overset{\mathcal{P}}{\to} 4\right) \\
\left(3 \overset{\mathcal{P}}{\to} 4 \overset{M}{\to} 1\right) &= \left(3 \overset{M}{\to} 2 \overset{\mathcal{P}}{\to} 1\right) \\
\left(4 \overset{\mathcal{P}}{\to} 2 \overset{M}{\to} 3\right) &= \left(4 \overset{M}{\to} 1 \overset{\mathcal{P}}{\to} 3\right)
\end{aligned}$$

We observe, that the mapping commutates with the permutation, which identifies this mapping as a mere deformation of the diagram specified by the permutation.

Set $\mathbb{T}$ of the topologically inequivalent (linked) diagrams: The goal is to pick only one diagram out of a set of topologically equivalent diagrams. This can be done, diagram by diagram: First, the set of all diagrams $\{\vec{\mathcal{P}}'\}$ that are topologically equivalent to $\vec{\mathcal{P}}$ is constructed by applying all topology-preserving transformations to a specific diagram $\vec{\mathcal{P}}$. Then, we define a criterion to select exactly one specific diagram from this set. If the current diagram satisfies the criterion, it is kept. Otherwise the diagram is discarded.

The criterion is that the number[5] $Z(\vec{\mathcal{P}})$ assigned to its permutation vector

$$Z(\vec{\mathcal{P}}) \overset{\text{def}}{=} \sum_{j=1}^{2n} \mathcal{P}_j \cdot (2n)^{2n-j} \tag{11.30}$$

is the smallest in the set of topologically equivalent diagrams. The comparison of $Z(\vec{\mathcal{P}})$ of two diagrams $\vec{\mathcal{P}}$ and $\vec{\mathcal{P}}'$ is straightforward: We only need to compare the first distinct component of the permutation vectors from the left: If that component of $\vec{\mathcal{P}}$ is smaller than that of $\vec{\mathcal{P}}'$, this also holds for Z, i.e. $Z(\vec{\mathcal{P}}) < Z(\vec{\mathcal{P}}')$. That is

$$\mathcal{P}_j < \mathcal{P}'_j \quad \text{and} \quad \mathcal{P}_k = \mathcal{P}'_k \quad \text{for } k < j \qquad \Rightarrow Z(\vec{\mathcal{P}}) < Z(\vec{\mathcal{P}}') \tag{11.31}$$

Once the topologically equivalent diagrams have been removed from the set $\mathbb{L}$, the vertex labels are redundant. Any labeling of vertices that satisfies the odd-even rule[6] is as good as any other one.

[5] Eq. 11.30, has been introduced in order to systematically construct all permutation vectors in section 11.2.1.

[6] With odd-even rule I mean that an interaction always contains a vertex with an odd-numbered vertex and the vertex with the next higher even number.

Thus, we switch from a set $\mathbb{L}$ of linked **labeled diagrams** to the much smaller set $\mathbb{T}$ of **unlabeled** linked **diagrams**.

As shown in appendix L, there are 592 closed, linked diagrams of third order, while there are only 20 such topologically distinct diagrams (about 3 %). In the fourth order, the number of topologically distinct diagrams (107) is about 3 permille of the number of linked diagrams (33888).

Counting diagrams and symmetry factor: The weight of each diagram in the set $\mathbb{T}$ must account for topologically equivalent diagrams, that have been omitted.

The value $V(D)$ of a diagram has been defined so that each diagram in $\mathbb{L}$ (or $\mathbb{A}$) contributes with a weight $\frac{1}{n!2^n}$ to the generating functional $\mathcal{Q}_{T,\mu}$ as given in Eq. 11.17. There are exactly $n!2^n$ transformations of vertex labels that lead to either distinct, topologically equivalent diagrams or mere deformations. If there were no mere deformations, each diagram in $\mathbb{T}$ would contribute with its value $V(D)$: in this special case, there are $n!2^n$ topologically equivalent diagrams which would cancel the prefactor $\frac{1}{n!2^n}$. If the relabeling produces also mere deformations, the number of distinct, topologically equivalent diagrams is smaller than $n!2^n$ by a factor $S(D)$, which is called the **symmetry factor**.

Below, I will show that the symmetry factor is given as follows:

SYMMETRY FACTOR

The symmetry factor $S(D)$ is the number of mere deformations among the results of the topology-preserving transformations (including the identity) acted on the (labeled) diagram D.

Let me follow in spirit the argument given in section 2.3 of the textbook of Negele and Orland[6]: The topology-preserving transformations form a group G_n. [7] The transformations that produces mere deformations of a given diagram D form a subgroup F_D of the topology-preserving diagrams.

The sub-group F_D of transformations that produce mere deformations of a diagram D is constructed by applying all topology-preserving transformations of G_n to one diagram. If the permutation vector of a resulting diagram is identical to that of the original diagram, this specific transformation produces mere deformations. If a transformation produces a mere deformation for one diagram D it does so also for all other topologically equivalent diagrams. As an alternative to producing all topologically equivalent diagrams, one can use the test Eq. 11.29 to identify transformations in F_D. The number of elements of F_D will later be the symmetry factor.

The number of elements in the subgroup F_D must be a divisor of $n!2^n$: For any two distinct, but topologically equivalent diagrams, the transformations of the subgroup F_D produce two non-overlapping sets of mere deformations. Thus, the set of diagrams produced by the topology preserving transformations G_n falls apart into an integer number of non-overlapping subsets, each of which holds only mere deformations of each other. The diagrams of two different subsets are distinct. If F_D has $S(D)$ elements, the number of subsets of diagrams is therefore $n!2^n/S(D)$. In other words there are $n!2^n/S(D)$ distinct topologically equivalent diagrams in $\mathbb{L}$, which are combined into one diagram in the set $\mathbb{T}$ of topologically distinct diagrams.

$$\mathcal{Q}_{T,\mu} \overset{\text{Eq. 11.16}}{=} -\frac{1}{\beta}\sum_{n=1}^{\infty}\sum_{D\in\mathbb{L}_n}\frac{V(D)}{n!2^n} = -\frac{1}{\beta}\sum_{n=1}^{\infty}\sum_{D\in\mathbb{T}_n}\frac{n!2^n}{S(D)}\frac{V(D)}{n!2^n} = -\frac{1}{\beta}\sum_{n=1}^{\infty}\sum_{D\in\mathbb{T}_n}\frac{V(D)}{S(D)} \quad (11.32)$$

Exercise 11.10.3 on p. 357 is strongly recommended to understand how to determine symmetry factors in practice.

Graphical approach to determine the symmetry factor

As an alternative, one can relabel the vertices in the graphical diagram according to the topology-preserving transformations. Each relabeled diagram is then deformed so that the vertex labels fall

[7] A group is a set of elements with a binary operation $\circ$, which is (1) associative $A\circ(B\circ C) = (A\circ B)\circ C$, has (2) an identity $A\circ 1 = A$ and an (3) inverse of each element $A^{-1}\circ A = 1$.

on-top of those of the original diagram. The remapped diagram is a **deformation** of the original one, if the Green's function lines, *including their orientation*, can be superimposed to those of the original diagram, while they remain attached to the vertices of the transformed diagram. A mere deformation is simply the same diagram as the original one.

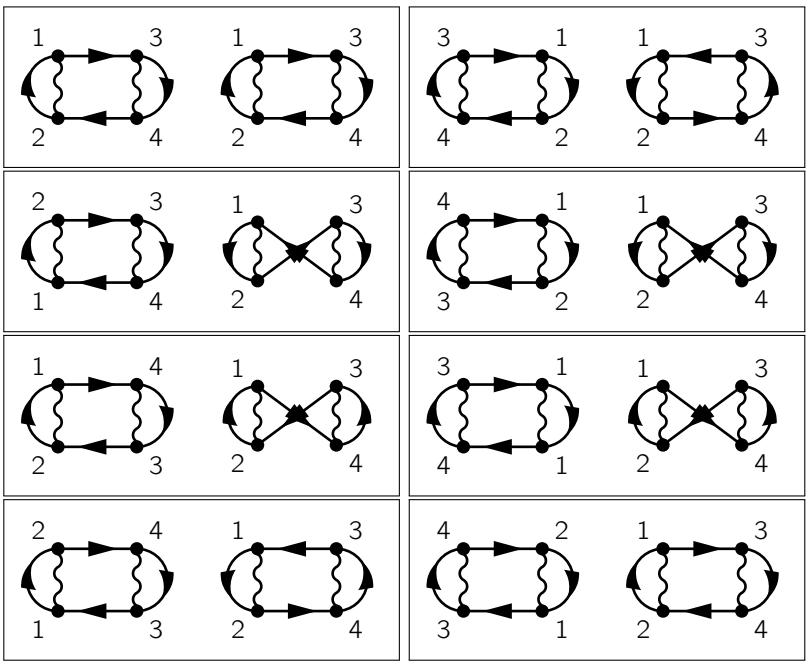

Fig. 11.4: Example for the graphical determination of the symmetry factor. Each box corresponds to one of the $n!2^n$ diagrams obtained by appropriate relabeling of the indices. In each box, the left diagram shows the same diagram after relabeling the indices. The right diagram in each box is obtained by deforming the diagram so that the vertices fall Ont of the original ones. If the diagrams on the right of two boxes look equivalent, considering also the directions of the Green's functions, the two boxes describe mere deformations of each other. The top-left and the bottom-right diagrams are mere deformations of the original diagram. Hence, the symmetry factor is $S(D) = 2$.

The example for the diagram Eq. 11.74 is given in Fig. 11.4. There are two mere deformations, (upper left and lower right) which are mere deformations of the original diagram. This the symmetry factor is $S(D) = 2$. Because the identity is always included, the symmetry factor is never zero.

Note, that the upper right diagram changes the orientation of the Green's functions, which makes it a distinct diagram.

The set of topologically equivalent diagrams in Fig. 11.4 is divided into four subsets, each of which contains two diagrams, which are mere deformations of each other.

11.5.1 Hand's-on for the evaluation of symmetry factors

In this section, the sum over all closed, linked diagrams for a given order $\mathbb{L}_n$ has been replaced by a sum over only the topologically inequivalent, closed, linked diagrams $\mathbb{T}_n$. This reduction in the number of diagrams has to be accounted for by a symmetry factor $S(D)$.

What does this mean? Let us consider the contribution from the second-order diagrams

$$\sum_{D\in\mathbb{L}_2} \frac{V(D)}{2!2^2} = \sum_{D\in\mathbb{L}_2} \frac{V(D)}{8} \tag{11.33}$$

where all diagrams $D \in \mathbb{A}_2$ are listed in Fig. 11.2 on p. 332.

Before we start, we need to exclude the four diagrams from Fig. 11.2, which are not linked. Unlinked diagrams are part of $\mathbb{A}_2$ but not part of $\mathbb{L}_2$. They have been excluded by the linked-cluster theorem, which removed the logarithm in front of the sum over diagrams and the unlinked diagrams.

Many of the remaining 20 diagrams are topologically equivalent, that is, they correspond to the same integral, only with some integration variables renamed. In other words, they differ only by the vertex labels and irrelevant deformations, that do not affect the connectivity of the vertices.

In figure 11.5, the diagrams are grouped into sets of topologically equivalent diagrams. Each set contributes one diagram to the set of topologically distinct diagrams. This diagram receives the entire weight of the set.

$$\sum_{D\in L_2} \frac{V(D)}{8}$$

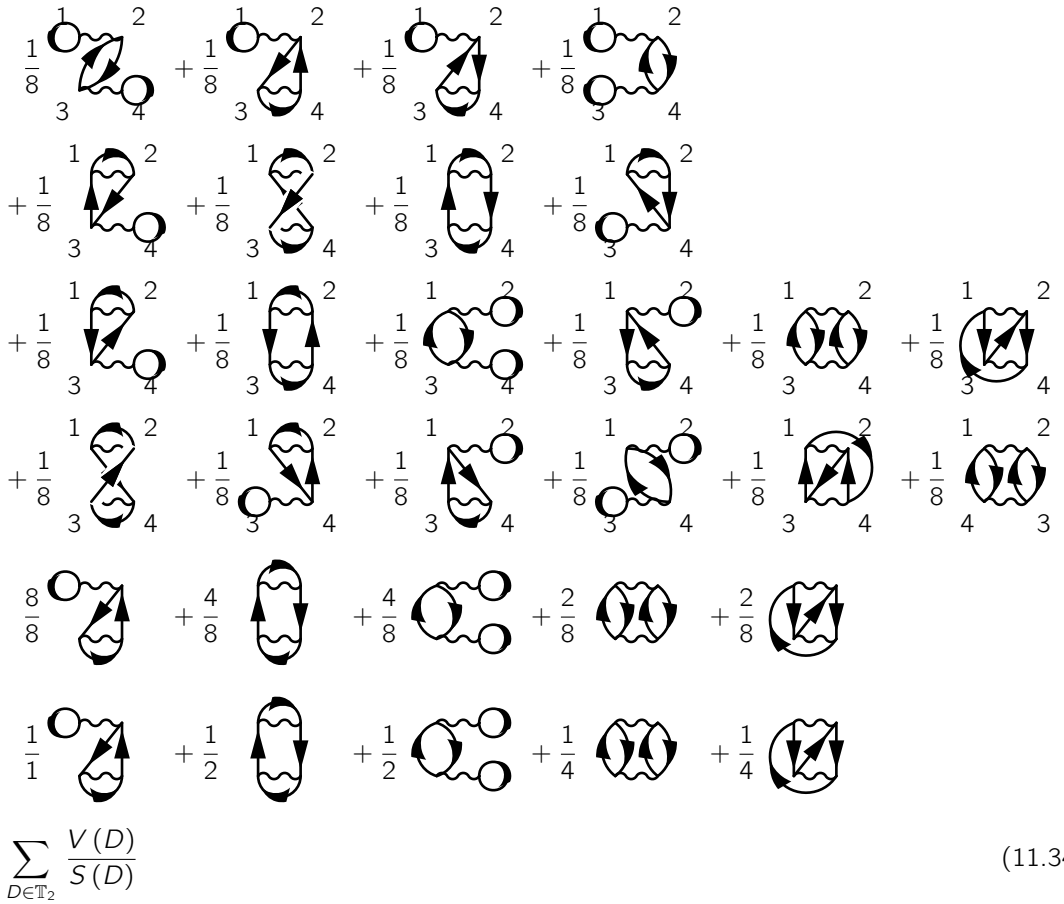

$$= \sum_{D\in \mathbb{T}_2} \frac{V(D)}{S(D)} \tag{11.34}$$

Fig. 11.5: Distribution of the second-order diagrams into sets of topologically equivalent diagrams, one for each topologically distinct diagram in $\mathbb{T}$. The weights are collected. The resulting prefactor $1/S(D)$ provides the symmetry factor S(D).

Confirm the result of figure 11.5 by yourself! The same scheme applies to all the other orders n in $\mathcal{Q}_{T,\mu}$. Therefore you should be able to check this for $n = 1$. And if you really want to have fun, you might also like to check it for $n = 3$, by taking all 720 diagrams for $n = 3$, rejecting all unlinked diagrams and identifying all topologically equivalent ones.

11.6 Systematic rule to construct all topologically distinct, linked, closed diagrams

Determine all closed diagrams of order n as follows:

1. construct all permutation vectors of length $2n$. as described in section 11.2.1 on p. 329.

2. remove all permutation vectors that produce disconnected (un-linked) diagrams. This can be done by inspection after drawing the diagram, or by a procedure on the elements of the permutation vector as described in section 11.4 on p. 335.

3. For each diagram construct the topologically equivalent diagrams using the topology-preserving transformations. These transformations are the (1) vertex exchanges on one interaction and the interchange of vertex pairs between interactions.

   Discard the current diagram if there is a topologically equivalent diagram with a value $Z(\vec{\mathcal{P}}')$ defined in Eq. 11.30 smaller than that of the current diagram.

   Determine the symmetry factor for the current diagram as the number of mere deformations as described in section 11.5 on p. 339.

11.7 Systematic rule to evaluate Feynman diagrams

11.7.1 Contour time and orbital basisset

GENERATING FUNCTIONAL

$$\mathcal{Q}_{T,\mu}[G^{(0)}] \overset{\text{Eq. } 10.59}{=} -\frac{1}{\beta}\mathrm{Tr}\left\{\hat{\rho}^{(0)}_{T,\mu}\mathcal{T}_{\mathcal{C}}\hat{S}_{I,\mathcal{C}}\right\} \overset{\text{Eq. } 11.17}{=} -\frac{1}{\beta}\sum_{n=1}^{\infty}\sum_{D\in\mathbb{L}_n}\frac{V(D)}{n!2^n} \overset{\text{Eq. } 11.26}{=} -\frac{1}{\beta}\sum_{n=1}^{\infty}\sum_{D\in\mathbb{T}_n}\frac{V(D)}{S(D)} \tag{11.35}$$

$\mathbb{L}_n$ is set of all linked, closed diagrams of order n in the interaction. $\mathbb{T}_n$ is set of all topologically distinct, linked, closed diagrams of order n in the interaction. $S(D)$ is the symmetry factor of the diagram D.
$V(D)$ is the value of the diagram given below. Each diagram of order n can be represented by a $2n$ dimensional permutation vector $\vec{\mathcal{P}}$

$$V(D) \overset{\text{Eq. } 10.48}{=} \epsilon_{\mathcal{P}_1,\ldots,\mathcal{P}_{2n}}(i\hbar)^n\int_{\mathcal{C}}dt_1\cdots\int_{\mathcal{C}}dt_{2n}\sum_{o_1,i_1,\ldots,o_{2n},i_{2n}}\left(\prod_{j=1}^{n}W_{o_{2j-1},o_{2j},i_{2j-1},i_{2j}}\delta_{\mathcal{C}}\left(t_{2j-1}-t_{2j}\right)\right)$$
$$\times G^{\mathcal{C},(0)}_{i_{\mathcal{P}_1},o_1}\left(t_{\mathcal{P}_1},t_1^+\right)\cdots G^{\mathcal{C},(0)}_{i_{\mathcal{P}_{2n}},o_{2n}}\left(t_{\mathcal{P}_{2n}},t_{2n}^+\right) \tag{11.36}$$

The interaction matrix elements are

$$W_{o_1,o_2,i_1,i_2} \overset{\text{Eq. } 3.48}{=} \int d^4x\int d^4x'\,\frac{e^2\chi^*_{o_1}(\vec{x})\chi^*_{o_2}(\vec{x'})\chi_{i_1}(\vec{x})\chi_{i_2}(\vec{x'})}{4\pi\epsilon_0|\vec{r}-\vec{r'}|} \tag{11.37}$$

and the non-interacting Green's function is

$$G^{\mathcal{C},(0)}_{i,o}(t,t') \overset{\text{Eq. } 7.27}{=} \frac{1}{i\hbar}\langle\pi_i|\hat{U}(t,0)\Big\{\underbrace{\theta_{\mathcal{C}}(t-t')\big(\hat{1}-\hat{\rho}^{(1),(0)}_{T,\mu}\big)}_{\text{electrons}}-\underbrace{\theta_{\mathcal{C}}(t'-t)\hat{\rho}^{(1)}_{T,\mu}}_{\text{holes}}\Big\}\hat{U}(0,t')|\pi_o\rangle \tag{11.38}$$

The full Green's function is obtained from the generating functional with Eq. 10.60 on p. 316 and the irreducible self energy is obtained by Eq. 10.61.

Draw a diagram from a permutation vector:

Determine the value of a drawn diagram

1. **Labels:** Label the vertices with numbers from 1 to $2n$ such that an odd-numbered vertex and the following even-numbered vertex on the same interaction line.

2. **Permutation vector:** The Green's function starting at vertex j points to vertex $\mathcal{P}_j$. While passing through the vertices in ascending order, note down the sequence of target vertices.

3. **Vertices:** For each vertex j include a time integral and a sum over all orbital indices for incoming and outgoing Green's functions.

$$\sum_{o_j,i_j}\int_{\mathcal{C}}dt_j \tag{11.39}$$

4. **Interaction lines:** For the interaction line with number j introduce a factor
$$i\hbar W_{o_{2j-1},o_{2j},i_{2j-1},i_{2j}}\delta_{\mathcal{C}}(t_{2j-1}-t_{2j}) \tag{11.40}$$

5. **Particle lines:**
   - For each particle line[8] introduce a factor
   $$G^{\mathcal{C},(0)}_{i_{\mathcal{P}_j},o_j}(t_{\mathcal{P}_j},t_j^+) \tag{11.41}$$
   j is the label of the vertex from which the Green's function emerges and $\mathcal{P}_j$ is the label of the vertex, where the Green's function arrives.
   The infinitesimal displacement Δ of the second time argument t_o of a Green's function to $t_o^+ = t_o + \Delta$ is only relevant for **non-propagating particle lines** , which otherwise have equal time arguments $t_i = t_o$. A **non-propagating Green's function**
   $$G^{\mathcal{C},(0)}_{i,o}(t,t^+) \overset{\text{Eq. 8.28}}{=} \frac{1}{i\hbar}\hat{\rho}^{(1),(0)}_{i,o}(t) \tag{11.42}$$
   starts and ends at the same interaction line. Non-propagating Green's function lines are present only in bubbles, oysters and open-oysters. This infinitesimal shift has been introduced in section 10.2.2 to ensure the proper order of creation and annihilation operators of one interaction.
   For **propagating** Green's function lines the infinitesimal shift is without consequence and can be disregarded.

6. **Sign factor**: count the number of Fermi loops, including all bubbles (tadpoles), and introduce a sign change for each.

7. **Symmetry factor:**
   - When only topologically distinct diagrams are considered, introduce a factor $\frac{1}{S(D)}$ where $S(D)$ is the symmetry factor of the diagram.
   - when all linked diagrams are considered, irrespective of whether they are topologically equivalent or not, introduce a factor $\frac{1}{n!2^n}$

Comparison with Stefanucci-vanLeeuwen

As a sanity check, let me compare our result with that of Stefanucci and van Leeuwen[2].

The generating functional Eq. 11.35 is identical to $-k_BT\ln\frac{Z}{Z_0} = \mathcal{Q}_{T,\mu}(G^{(0)},W)$ of Stefanucci-vanLeeuwen-Eq. 11.3.[9] [10]

Each diagram D of order n is represented by a permutation vector $\mathcal{P}$ of length $2n$. The sum over permutation vectors can be cast in the expression of a determinant, e.g.

$$\begin{aligned}&\sum_{\vec{\mathcal{P}}}\epsilon_{\mathcal{P}_1,\ldots,\mathcal{P}_{2n}}G^{(0)}_{o_1,i_{\mathcal{P}_1}}(t_{i_{\mathcal{P}_1}},t_{o_1}^+)G^{(0)}_{o_2,i_{\mathcal{P}_2}}(t_{i_{\mathcal{P}_2}},t_{o_2}^+)G^{(0)}_{o_3,i_{\mathcal{P}_3}}(t_{i_{\mathcal{P}_3}},t_{o_3}^+)\ldots G^{(0)}_{o_{2n},i_{\mathcal{P}_{2n}}}(t_{\mathcal{P}_{2n}},t_{o_{2n}}^+)\\ &= \det\begin{vmatrix} G^{(0)}_{o_1,i_1}(t_{i_1},t_{o_1}^+) & G^{(0)}_{o_1,i_2}(t_{i_2},t_{o_1}^+) & G^{(0)}_{o_1,i_3}(t_{i_3},t_{o_1}^+) & \ldots & G^{(0)}_{o_1,i_{2n}}(t_{i_{2n}},t_{o_1}^+)\\ G^{(0)}_{o_2,i_1}(t_{i_1},t_{o_2}^+) & G^{(0)}_{o_2,i_2}(t_{i_2},t_{o_2}^+) & G^{(0)}_{o_2,i_3}(t_{i_3},t_{o_2}^+) & \ldots & G^{(0)}_{o_2,i_{2n}}(t_{i_{2n}},t_{o_2}^+)\\ \vdots & \vdots & \vdots & & \vdots\\ G^{(0)}_{o_{2n},i_1}(t_{i_1},t_{o_{2n}}^+) & G^{(0)}_{o_{2n},i_2}(t_{i_2},t_{o_{2n}}^+) & G^{(0)}_{o_{2n},i_3}(t_{i_3},t_{o_{2n}}^+) & \ldots & G^{(0)}_{o_{2n},i_{2n}}(t_{i_{2n}},t_{o_{2n}}^+)\end{vmatrix}\end{aligned} \tag{11.43}$$

[8] In this context, one does not discriminate between particle lines and hole lines.

[9] Stefanucci-vanLeeuwen include the zero'th order term, which is absent in my equation. I consider that a omission on their side, because there is no zero-order term except $ln(Z_0)$ in Stefanucci-vanLeeuwenFig. 11.1.

[10] Stefanucci-vanLeeuwen do not explicitly write "det" and they set $\hbar = 1$

The determinant of Stefanucci-vanLeeuwen is limited to the terms representing connected (=linked) diagrams, just as the sum over linked diagrams $D \in \mathbb{L}_n$ in Eq. 11.35

The diagram Eq. 10.48 translates into $D_{c,i} \stackrel{\text{def}}{=} \frac{1}{n!2^n} V(\vec{\mathcal{P}})$ of Stefanucci-vanLeeuwen-Eq. 11.3.

In Stefanucci-vanLeeuwen-Eq. 11.12 the functional $\Phi_r[G^{(0)}, W]$ is introduced as

$$\Omega_{T,\mu} = -k_B T \ln[Z_{T,\mu}] = -k_B T \ln[Z^{(0)}_{T,\mu}] + k_B T \Phi_r[G^{(0)}, W] \tag{11.44}$$

In Stefanucci-vanLeeuwen-Eq. 11.13 it is shown how the reducible (improper) self energy is obtained as functional derivative of $\Phi_r[G^{(0)}, W]$ with respect to the bare Green's function $\hat{G}^{(0)}$.

11.7.2 Contour time and real-space-and-spin representation

In order to change the representation one usually simply reinterprets the orbital indices in another basisset. For the real-space and spin representation, there is a more simple procedure.

In the first step, I express the Green's function with orbital indices by the one with real-space-and-spin coordinates.

$$\begin{aligned}
G^{\mathcal{C},(0)}_{i,o}(t_i, t_o) &\stackrel{\text{Eq. 7.27}}{=} \frac{1}{i\hbar} \sum_n \langle \pi_i | \varphi_n \rangle \left\{ \underbrace{\theta_{\mathcal{C}}(t_i - t_o)(1 - f_n)}_{\text{electrons}} - \underbrace{\theta_{\mathcal{C}}(t_o - t_i) f_n}_{\text{holes}} \right\} \mathrm{e}^{-\frac{i}{\hbar}\epsilon_n (t_i - t_o)} \langle \varphi_n | \pi_o \rangle \\
&= \frac{1}{i\hbar} \sum_n \langle \pi_i | \underbrace{\int d^4 x_i \, |\vec{x}_i\rangle\langle\vec{x}_i|}_{=\hat{1}} | \varphi_n \rangle \left\{ \underbrace{\theta_{\mathcal{C}}(t_i - t_o)(1 - f_n)}_{\text{electrons}} - \underbrace{\theta_{\mathcal{C}}(t_o - t_i) f_n}_{\text{holes}} \right\} \\
&\quad \times \mathrm{e}^{-\frac{i}{\hbar}\epsilon_n (t_i - t_o)} \langle \varphi_n | \underbrace{\int d^4 x_o \, |\vec{x}_o\rangle\langle\vec{x}_o|}_{=\hat{1}} \pi_\beta \rangle \\
&= \int d^4 x_i \int d^4 x_o \, \langle \pi_i | \vec{x}_i \rangle \langle \vec{x}_o | \pi_o \rangle \\
&\quad \underbrace{\times \frac{1}{i\hbar} \sum_n \langle \vec{x}_i | \varphi_n \rangle \left\{ \underbrace{\theta_{\mathcal{C}}(t_i - t_o)(1 - f_n)}_{\text{electrons}} - \underbrace{\theta_{\mathcal{C}}(t_o - t_i) f_n}_{\text{holes}} \right\} \mathrm{e}^{-\frac{i}{\hbar}\epsilon_n (t_i - t_o)} \langle \varphi_n | \vec{x}_o \rangle}_{G^{\mathcal{C},(0)}(\vec{x}_i, t_i, \vec{x}_o, t_o)} \\
&= \int d^4 x_i \int d^4 x_o \, \langle \pi_i | \vec{x}_i \rangle \langle \vec{x}_o | \pi_o \rangle G^{\mathcal{C},(0)}(\vec{x}_i, t_i, \vec{x}_o, t_o)
\end{aligned} \tag{11.45}$$

For each argument of the Green's function, I obtain one space-spin "integration" and one projector function $\langle \pi | \vec{x} \rangle$.

In the second step, the projector functions from Eq. 11.45 $\langle \pi_\alpha | \vec{x} \rangle$ are combined with the corresponding orbitals $\langle \vec{x} | \chi_\beta \rangle$ from the interaction matrix elements

$$W_{o_1,o_2,i_1,i_2} \stackrel{\text{Eq. 3.48}}{=} \int d^4 x \int d^4 x' \, \frac{e^2 \chi^*_{o_1}(\vec{x}) \chi^*_{o_2}(\vec{x'}) \chi_{i_1}(\vec{x}) \chi_{i_2}(\vec{x'})}{4\pi\epsilon_0 |\vec{r} - \vec{r'}|} \, , \tag{11.46}$$

Then, one can exploit the completeness of the local orbitals

$$\sum_\alpha \langle \vec{x} | \chi_\alpha \rangle \langle \pi_\alpha | \vec{x'} \rangle = \langle \vec{x} | \vec{x'} \rangle = \delta(\vec{x} - \vec{x'}) \tag{11.47}$$

to remove the orbital summations.

The Coulomb interaction

$$v(\vec{x}, \vec{x'}) = \frac{e^2}{4\pi\epsilon_0 |\vec{r} - \vec{r'}|} \tag{11.48}$$

can be replaced by any other pair-wise interaction.

I combine, firstly, the interaction matrix elements with the corresponding orbital summations and, secondly, the integrations and projector functions resulting from the Green's function. Rather than the product of Green's function I use some arbitrary function $Y(\vec{x}_{i_1},\vec{x}_{i_2},\vec{x}_{o_1},\vec{x}_{o_2})$ of the coordinates, so that I can limit the discussion to only four arguments.

$$\begin{aligned}
&\sum_{i_1,o_1,i_2,o_2}\int d^4x_{o_1}\int d^4x_{i_1}\int d^4x_{o_2}\int d^4x_{i_2}\langle\pi_{i_1}|\vec{x}_{i_1}\rangle\langle\vec{x}_{o_1}|\pi_{o_1}\rangle\langle\pi_{i_2}|\vec{x}_{i_2}\rangle\langle\vec{x}_{o_2}|\pi_{o_2}\rangle\\
&\times W_{o_1,o_2,i_1,i_2}Y(\vec{x}_{i_1},\vec{x}_{i_2},\vec{x}_{o_1},\vec{x}_{o_2})\\
\overset{\text{Eq. 3.48}}{=}&\int d^4x\int d^4x'\int d^4x_{o_1}\int d^4x_{i_1}\int d^4x_{o_2}\int d^4x_{i_2}\frac{e^2}{4\pi\epsilon_0|\vec{r}-\vec{r}'|}Y(\vec{x}_{i_1},\vec{x}_{i_2},\vec{x}_{o_1},\vec{x}_{o_2})\\
&\times\underbrace{\sum_{i_1}\langle\vec{x}|\chi_{i_1}\rangle\langle\pi_{i_1}|\vec{x}_{i_1}\rangle}_{\delta(\vec{x}-\vec{x}_{i_1})}\underbrace{\sum_{o_1}\langle\vec{x}_{o_1}|\pi_{o_1}\rangle\langle\chi_{o_1}|\vec{x}\rangle}_{\delta(\vec{x}-\vec{x}_{o_1})}\underbrace{\sum_{i_2}\langle\vec{x}'|\chi_{i_2}\rangle\langle\pi_{i_2}|\vec{x}_{i_2}\rangle}_{\delta(\vec{x}'-\vec{x}_{i_2})}\underbrace{\sum_{o_2}\langle\vec{x}_{o_2}|\pi_{o_2}\rangle\langle\chi_{o_2}|\vec{x}'\rangle}_{\delta(\vec{x}'-\vec{x}_{o_2})}\\
=&\int d^4x\int d^4x'\,\frac{e^2}{4\pi\epsilon_0|\vec{r}-\vec{r}'|}Y(\vec{x},\vec{x}',\vec{x},\vec{x}')
\end{aligned}\tag{11.49}$$

By combining the terms from all interaction lines, and by replacing Y by the corresponding product of Green's functions I obtain the rule for the functional $\mathcal{Q}_{T,\mu}$.

SUM AND VALUES OF LINKED DIAGRAMS

$$\mathcal{Q}_{T,\mu}[G^{(0)}]=-\frac{1}{\beta}\mathrm{Tr}\left\{\hat{\rho}^{(0)}_{T,\mu}\mathcal{T}_{\mathcal{C}}\hat{S}_{I,\mathcal{C}}\right\}=-\frac{1}{\beta}\sum_{n=1}^{\infty}\sum_{D\in\mathbb{T}_n}\frac{V(D)}{S(D)}\tag{11.50}$$

$\mathbb{T}_n$ is set of all topologically distinct, linked, closed diagrams of order n in the interaction. $S(D)$ is the symmetry factor of the diagram D and $V(D)$ is the value of the diagram given below. Each diagram of order n can be represented by a $2n$ dimensional permutation vector $\vec{\mathcal{P}}$

$$\begin{aligned}
V(D)\overset{\text{Eq. 10.48}}{=}&\epsilon_{\mathcal{P}_1,\ldots,\mathcal{P}_{2n}}(i\hbar)^n\int_{\mathcal{C}}dt_1\cdots\int_{\mathcal{C}}dt_n\int d^4x_1\ldots\int d^4x_{2n}\left(\prod_{j=1}^{n}v(\vec{x}_{2j-1},\vec{x}'_{2j},t_j)\right)\\
&\times G^{\mathcal{C},(0)}\left(\vec{x}_{\mathcal{P}_1},t(\mathcal{P}_1),\vec{x}_1,t^+(1)\right)\cdots G^{\mathcal{C},(0)}\left(\vec{x}_{\mathcal{P}_{2n}},t(\mathcal{P}_{2n}),\vec{x}_{2n},t^+(2n)\right)
\end{aligned}\tag{11.51}$$

[a]

[a] I added a time dependence to the interaction matrix elements to allow for adiabatic switching on.

11.8 Exploit the symmetry of the problem

11.8.1 Exploit time-translation symmetry

Editor: to be done: (Energy representation $t\rightsquigarrow\epsilon$. Try to do the energy representation first without time translation symmetry to include inelastic scattering terms.

Time-translation symmetry is the condition for energy conservation. For the diagrammatic expansion of the generating functional it implies that the interaction matrix elements does not have an explicit time dependence. Furthermore, the Green's function depends only on the relative time

argument.[11]

$$G^{\mathcal{C}(0)}_{i,o}(t,t') = \sum_m G^{\mathcal{C}(0)}_{i,o}(\epsilon_m) \mathrm{e}^{-\frac{i}{\hbar}\epsilon_m(t-t') - \frac{1}{\hbar}\eta|t-t'|} \tag{11.52}$$

$$\begin{aligned}
V(D) &\overset{\text{Eq. 11.36}}{=} \epsilon_{\mathcal{P}_1,\dots,\mathcal{P}_{2n}} (i\hbar)^n \int_{\mathcal{C}} dt_1 \cdots \int_{\mathcal{C}} dt_n \sum_{o_1,i_1,\dots,o_{2n},i_{2n}} \left(\prod_{j=1}^{n} W_{o_{2j-1},o_{2j},i_{2j-1},i_{2j}}(t_j) \right) \\
&\quad \times G^{\mathcal{C},(0)}_{i_{\mathcal{P}_1},o_1}\Big(t(\mathcal{P}_1), t^+(1)\Big) \cdots G^{\mathcal{C},(0)}_{i_{\mathcal{P}_{2n}},o_{2n}}\Big(t(\mathcal{P}_{2n}), t^+(2n)\Big) \\
&\overset{\text{Eq. 7.27}}{=} \epsilon_{\mathcal{P}_1,\dots,\mathcal{P}_{2n}} (i\hbar)^n \sum_{o_1,i_1,\dots,o_{2n},i_{2n}} \left(\prod_{j=1}^{n} W_{o_{2j-1},o_{2j},i_{2j-1},i_{2j}}(0) \right) \int_{\mathcal{C}} dt_1 \cdots \int_{\mathcal{C}} dt_n \\
&\quad \times \underbrace{\sum_{m_1} G^{\mathcal{C}(0)}_{i_{\mathcal{P}_1},o_1}(\epsilon_{m_1}) \mathrm{e}^{-\frac{i}{\hbar}\epsilon_{m_1}\left(t(\mathcal{P}_1) - t^+(1)\right) - \frac{1}{\hbar}\eta\left|t(\mathcal{P}_1) - t^+(1)\right|} \dots}_{G^{\mathcal{C},(0)}_{i_{\mathcal{P}_1},o_1}\left(t(\mathcal{P}_1), t^+(1)\right)} \\
&\quad \times \underbrace{\sum_{m_1} G^{\mathcal{C}(0)}_{i_{\mathcal{P}_{2n}},o_{2n}}(\epsilon_{m_{2n}}) \mathrm{e}^{-\frac{i}{\hbar}\epsilon_{m_{2n}}\left(t(\mathcal{P}_{2n}) - t^+(2n)\right) - \frac{1}{\hbar}\eta\left|t(\mathcal{P}_{2n}) - t^+(2n)\right|}}_{G^{\mathcal{C},(0)}_{i_{\mathcal{P}_{2n}},o_{2n}}\left(t(\mathcal{P}_{2n}), t^+(2n)\right)} \\
&=
\end{aligned} \tag{11.53}$$

Note here that the generating functional is a functional of the non-interacting Green's function. Therefore it is not sensible to resolve the non-interacting Green's function Eq. 7.27 by the eigenvalues and eigenstates of the non-interacting system.

11.8.2 Exploit spatial translation symmetry

Editor: to be done: momentum representation (plane waves) $\vec{x} \rightsquigarrow (\vec{p}, \sigma)$.

11.8.3 Exploit spin-inversion symmetry

So-far we worked with general two-component spinor functions. However, often it is convenient to specialize the expressions to a basis set of $\hat{S}_z$ eigenstates.

In that case, the index of an creation or annihilation operator must be considered as a combined index $o = (\alpha(o), \sigma(o))$ describing the orbital index $\alpha(o)$ and the spin quantum number $\sigma(o)$ of the orbital.

$$W_{o_1,o_2,i_1,i_2} = W_{(\alpha_{o_1},\sigma_{o_1}),(\alpha_{o_2},\sigma_{o_2}),(\alpha_{i_1},\sigma_{i_1}),(\alpha_{i_2},\sigma_{i_2})} \delta_{\sigma_{o_1},\sigma_{i_1}} \delta_{\sigma_{o_2},\sigma_{i_2}} \tag{11.54}$$

Thus, the integration over all indices can be mapped onto an integration over all spatial indices, while the sum over spins is attributed to each vertex. The delta functions adds a sum rule, saying that the spin of the incoming Green's function is equal to that of the outgoing Green's function.

[11] The non-interacting Hamiltonian is time independent, as precondition for Wick's theorem. Therefore the non-interacting Green's function should automatically only depend on the relative time argument. However, later we will use the generating functional also with the full Green's function as arguments. Time translation symmetry implies that we may restrict the domain for the functional to Green's functions that only depend on the relative time argument.

11.8.4 Exploit Bloch theorem

If the one-particle Hamiltonian is periodic, we may choose a basisset of Bloch states. In that case the orbital index is a combined index referring to a Bloch-vector $\vec{k}$, a band index n and a spin index σ.

We can make use that the Green's function of the non-interacting system is block diagonal in a basis of the Bloch states, i.e.

$$G^{(0)}_{i,o}(t,t') = \delta\Big(\vec{k}_i - \vec{k}_o\Big) G^{(0)}_{(\vec{k}_i,n_i,\sigma_i),(\vec{k}_o,n_o,\sigma_o)}(t,t') \tag{11.55}$$

Because the Coulomb interaction is isotropic and translation invariant under a shift of both spatial coordinates of the Green's function, the interaction conserves the momentum and thus has the form

$$W_{o_1,o_2,i_1,i_2} = \delta\Big((\vec{k}_{o_1} - \vec{k}_{i_1}) - (\vec{k}_{o_2} - \vec{k}_{i_2})\Big) W_{(\vec{k}_{o_1},n_{o_1},\sigma_{o_1}),(\vec{k}_{o_2},n_{o_2},\sigma_{o_2}),(\vec{k}_{i_1},n_{i_1},\sigma_{i_1}),(\vec{k}_{i_2},n_{i_2},\sigma_{i_2})} \tag{11.56}$$

This results in the rule that we can attribute the interaction matrix elements to a momentum $\vec{q}$, that is transferred from one vertex of the interaction to the other. Thus, we have momentum conservation at each vertex between the incoming and outgoing Green's function and the interaction.

11.9 Zoo of diagrams

Editor: This section is in preparation

In this section, I will discuss common diagrams. The diagrams up to second order in the interaction and their self-energy diagrams are shown in figure 11.6 on p. 352

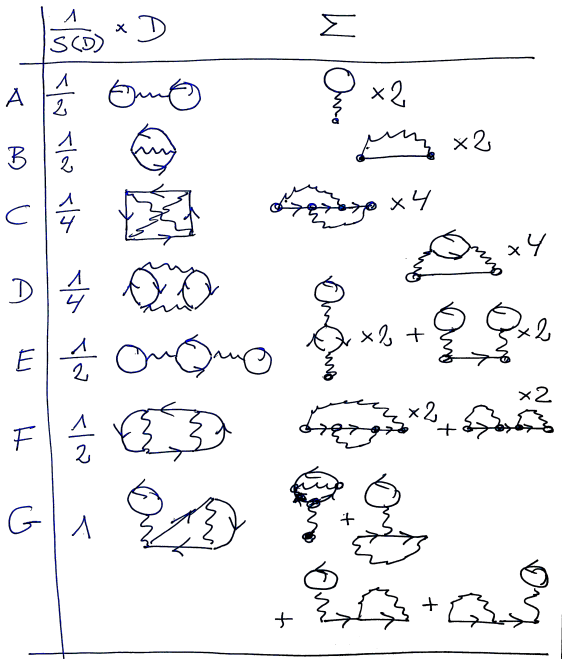

Fig. 11.6: Diagrams in $\mathbb{T}$ and their self-energy contributions up to second order in the interaction. The closed diagrams, which are part of the generating functional $\mathcal{Q}_{T,\mu}$ also carry the prefactor $1/S(D)$, where $S(D)$ is the symmetry factor. On the right, the self-energy diagrams resulting from the closed diagram on the left are shown including their multiplicity. See text for explanation.

Editor: Interestingly the prefactor given by the symmetry factor is exactly canceled by the multiplicity of the self-energy diagrams.

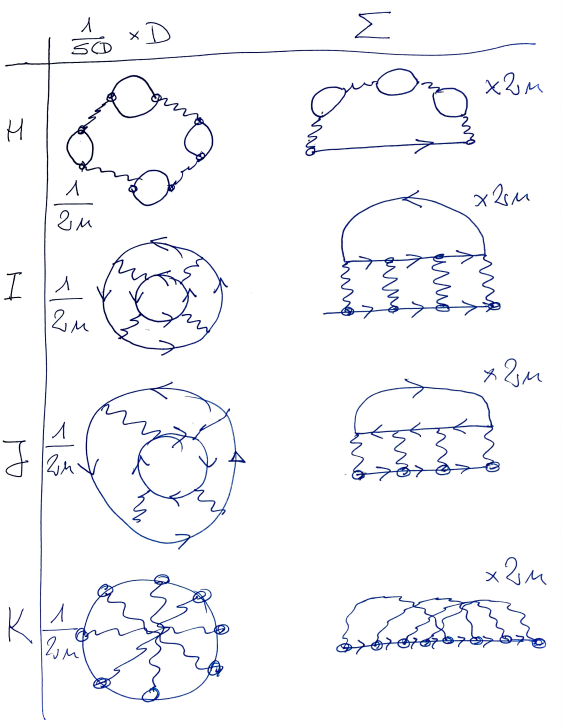

Fig. 11.7: Diagrams in $\mathbb{T}$ and their self-energy contributions in the interaction. The closed diagrams, which are part of the generating functional $\mathcal{Q}_{T,\mu}$ also carry the prefactor $1/S(D)$, where $S(D)$ is the symmetry factor. On the right, the self-energy diagrams resulting from the closed diagram on the left are shown including their multiplicity. See text for explanation.

11.9.1 First-order Hartree Fock

The diagrams A and B in figure 11.6 on p. 352, are the Hartree diagram (eyeglass) and exchange diagram (oyster).

The term Hartree-Fock approximation is used in many sometimes different context. Here we refer to the first order expansion in the interaction. The self-consistent Hartree-Fock approximation includes also higher order diagrams.

11.10 Home study and practice

11.10.1 Enumerate permutations

Introduction

In section 11.2.1, a method has been presented to enumerate all permutations of a sequence of numbers. This is a useful method not only in the context of Feynman diagrams. It can be used to calculate a determinant of a matrix, even though I do not claim that it is the most efficient method.

The method can also be coded up easily as shown in appendix L. Therefore, it is useful to get familiar with it.

Problem

- Enumerate all permutations of the sequence numbers (1,2,3,4). Check that there are 4! = 24 such permutations.
- assign the sign to each diagram in this sequence (Use the sign theorem.)

Discussion

- Enumerate all permutations of the sequence numbers (1,2,3,4). Check that there are 4! = 24 such permutations.
- assign the sign to each diagram in this sequence (Use the sign theorem.)

The permutation vectors are listed in section 11.2.3 on p. 331. The diagrams are shown in figure 11.2 arranged row-wise. Using sign-theorem described in section 11.3, the signs are obtained by counting Fermi loops.

Nr	$\vec{\mathcal{P}}$	sign	Nr	$\vec{\mathcal{P}}$	sign
1	(1,2,3,4)	+	13	(3,1,2,4)	+
2	(1,2,4,3)	-	14	(3,1,4,2)	-
3	(1,3,2,4)	-	15	(3,2,1,4)	-
4	(1,3,4,2)	+	16	(3,2,4,1)	+
5	(1,4,2,3)	+	17	(3,4,1,2)	+
6	(1,4,3,2)	-	18	(3,4,2,1)	-
7	(2,1,3,4)	-	19	(4,1,2,3)	-
8	(2,1,4,3)	+	20	(4,1,3,2)	+
9	(2,3,1,4)	+	21	(4,2,1,3)	+
10	(2,3,4,1)	-	22	(4,2,3,1)	-
11	(2,4,1,3)	-	23	(4,3,1,2)	-
12	(2,4,3,1)	+	24	(4,3,2,1)	+

One sanity check is to ensure that half of the diagrams have positive and the other half have negative sign.

The number of diagrams if 4! = 24.

11.10.2 Feynman diagrams from permutation vectors

The recipe to construct Feynman diagrams depends on the strict enforcement of a consistent set of rules. (There are different sets of rules in the literature.) Therefore, this exercise is to practice the set of rules provided in this text.

Problem

1 Draw the Feynman diagrams related to the permutation vectors

$$\vec{\mathcal{P}} = (1, 3, 5, 6, 2, 4) \tag{11.57}$$
$$\vec{\mathcal{P}} = (1, 3, 5, 6, 4, 2) \tag{11.58}$$
$$\vec{\mathcal{P}} = (2, 3, 1, 5, 6, 4) \tag{11.59}$$
$$\vec{\mathcal{P}} = (2, 3, 4, 5, 6, 1) \tag{11.60}$$
$$\vec{\mathcal{P}} = (2, 3, 5, 1, 6, 4) \tag{11.61}$$
$$\vec{\mathcal{P}} = (2, 3, 5, 6, 1, 4) \tag{11.62}$$

and

- count the number of Fermi loops,
- determine the sign of the diagrams,
- identify the 2-particle reducible diagrams,
- identify the 1-particle reducible diagrams,

2 determine the diagrams for the Green's function resulting from the closed diagram $\vec{\mathcal{P}} = (2, 3, 4, 5, 6, 1)$.

Discussion

1 Draw the Feynman diagrams related to the permutation vectors

$$\vec{\mathcal{P}} = (1, 3, 5, 6, 2, 4) \tag{11.63}$$
$$\vec{\mathcal{P}} = (1, 3, 5, 6, 4, 2) \tag{11.64}$$
$$\vec{\mathcal{P}} = (2, 3, 1, 5, 6, 4) \tag{11.65}$$
$$\vec{\mathcal{P}} = (2, 3, 4, 5, 6, 1) \tag{11.66}$$
$$\vec{\mathcal{P}} = (2, 3, 5, 1, 6, 4) \tag{11.67}$$
$$\vec{\mathcal{P}} = (2, 3, 5, 6, 1, 4) \tag{11.68}$$

and

- count the number of Fermi loops,
- determine the sign of the diagrams,
- identify the 2-particle reducible diagrams,
- identify the 1-particle reducible diagrams,

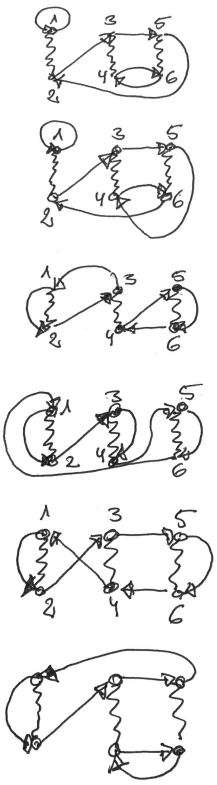

1. $\vec{\mathcal{P}} = (1, 3, 5, 6, 2, 4)$; 3 Fermi loops, sign= $-$, 2-particle reducible, 1-particle irreducible

2. $\vec{\mathcal{P}} = (1, 3, 5, 6, 4, 2)$ 2 Fermi loops, sign= $+$, 2-particle reducible, 1-particle irreducible

3. $\vec{\mathcal{P}} = (2, 3, 1, 5, 6, 4)$ 2 Fermi loops, sign= $+$, 2-particle reducible, 1-particle irreducible

4. $\vec{\mathcal{P}} = (2, 3, 4, 5, 6, 1)$ 1 Fermi loops, sign= $-$, 2-particle reducible, 1-particle irreducible

5. $\vec{\mathcal{P}} = (2, 3, 5, 1, 6, 4)$ 1 Fermi loops, sign= $-$, 2-particle reducible, 1-particle irreducible

6. $\vec{\mathcal{P}} = (2, 3, 5, 6, 1, 4)$ 2 Fermi loops, sign= $+$, 2-particle reducible, 1-particle irreducible

2 determine the diagrams for the Green's function resulting from the closed diagram $\vec{\mathcal{P}} = (2, 3, 4, 5, 6, 1)$.

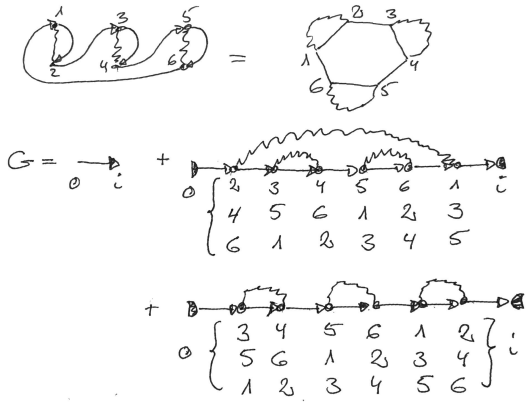

11.10.3 Evaluate symmetry factors

Introduction

The reduction to topologically inequivalent diagrams results in a tremendous saving in the number of terms to be evaluated. Nevertheless it requires to evaluate the symmetry factor. While the operations are not very complicated, one needs to practice them to learn the technique properly.

In this exercise we exercise the technique for two examples, namely one that has been used as example in the main text, and another one which is new.

Problem

1 Determine the topology-preserving transformations of diagrams for the second order of the interaction. Describe them in words and provide the mapping vectors.

2 Construct the permutation vectors of all diagrams which are topologically equivalent (distinct or mere deformation) to the diagram.

$$\vec{\mathcal{P}} = (3, 1, 4, 2) \tag{11.69}$$

3 Use the criterion that permutation and relabeling commutate to determine the symmetry factor for the same diagram.

$$\vec{\mathcal{P}} = (3, 1, 4, 2) \tag{11.70}$$

4 Construct graphically the diagrams which are topologically equivalent to

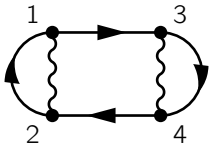

(11.71)

determine mere deformations and the symmetry factor.

5 Work out the symmetry factor for the following second-order diagrams

$$\vec{\mathcal{P}} = (1, 3, 2, 4) \tag{11.72}$$

using the method of your choice.

Do not use the trivial approach of constructing all linked diagrams of a given order and search for topologically equivalent ones. This would not be feasible for diagrams of higher order.

Solution

The final solution can be read off from Fig. 11.5 on p. 345, which keeps all second-order diagrams and their symmetry factor.

1 Determine the topology-preserving transformations of diagrams for the second order of the interaction. Describe them in words and provide the mapping vectors.

The topologically equivalent diagrams are obtained by

- 2^n interchanges of the two vertices of the same interaction line, and
- $n!$ permutations of the interaction lines, that is of their indices, while preserving the *"orientation"* of the interaction, that is odd indices are mapped again onto odd indices and the even indices are mapped onto even indices.

These vertex-mappings are given in table 11.2 on p. 341. The mappings for the second-order diagrams are

$\vec{M}_1 = (1234)$	$\vec{M}_5 = (3412)$
$\vec{M}_2 = (2134)$	$\vec{M}_6 = (4312)$
$\vec{M}_3 = (1243)$	$\vec{M}_7 = (3421)$
$\vec{M}_4 = (2143)$	$\vec{M}_8 = (4321)$

2 Construct the permutation vectors of all diagrams which are topologically equivalent (distinct or mere deformation) to the diagram.

$$\vec{\mathcal{P}} = (3,1,4,2) \tag{11.73}$$

The diagram represented by the permutation vector $\vec{\mathcal{P}} = (3,1,4,2)$ has the following appearance

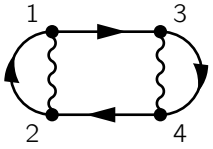

(11.74)

This diagram can be represented by the mapping from the indices o to the indices i.

o	1	2	3	4
i	3	1	4	2

(11.75)

The permutation vector defining this diagram is given by the second line, i.e. $\vec{\mathcal{P}} = (3,1,2,4)$. The Green's functions can be described as mappings between vertices, $G^{(0)}_{i_3,o_1} \hat{=} (1 \to 3)$, $G^{(0)}_{i_1,o_2} \hat{=} (2 \to 1)$, $G^{(0)}_{i_4,o_3} \hat{=} (3 \to 4)$, and $G^{(0)}_{i_2,o_4} \hat{=} (4 \to 2)$.

Let me now construct all topologically equivalent diagrams using the mappings

1. $\vec{M}_1 = (1234)$, $\vec{\mathcal{P}}' = (1234)$

o	1	2	3	4	remap $\to$	o	1	2	3	4	order $\to$	o	1	2	3	4
i	3	1	4	2		i	3	1	4	2		i	3	1	4	2

2. $\vec{M}_2 = (2134)$, $\vec{\mathcal{P}}' = (2341)$

o	1	2	3	4	remap $\to$	o	2	1	3	4	order $\to$	o	1	2	3	4
i	3	1	4	2		i	3	2	4	1		i	2	3	4	1

3. $\vec{M}_3 = (1243)$, $\vec{\mathcal{P}}' = (4123)$

o	1	2	3	4	remap $\to$	o	1	2	4	3	order $\to$	o	1	2	3	4
i	3	1	4	2		i	4	1	3	2		i	4	1	2	3

4. $\vec{M}_4 = (2143)$, $\vec{\mathcal{P}}' = (2413)$

o	1	2	3	4	remap $\to$	o	2	1	4	3	order $\to$	o	1	2	3	4
i	3	1	4	2		i	4	2	3	1		i	2	4	1	3

5. $\vec{M}_5 = (3412)$, $\vec{\mathcal{P}}' = (2413)$

o	1	2	3	4	remap $\to$	o	3	4	1	2	order $\to$	o	1	2	3	4
i	3	1	4	2		i	1	3	2	4		i	2	4	1	3

At this point we already encounter two diagrams that are mere deformation of each other, namely the last two above. Thus, we can identify one operation that produces mere deformations of this diagram. It is the inverse of the fourth mapping leading $\vec{M}_4 = (2143)$ followed by the fifth mapping $\vec{M}_5 = (3412)$. The fourth mapping interchanges the vertices of the first interaction and of the second interaction. Its inverse does the same. $\vec{M}_5 = (3412)$ interchanges the two interactions. The combined operation is $M_5 \circ M_4^{-1} = (4321) = M_8$. This transformation produces a mere deformation rather than a topologically equivalent but distinct diagram.

We can actually stop here, because the same operation will produce a mere deformation of any diagram of the four distinct diagrams obtained $\vec{M}_1$ to $\vec{M}_4$. Thus, there are four mere deformations and four distinct diagrams. We obtain $r_D = \frac{4}{8} = \frac{1}{2}$ and $S(D) = \frac{1}{1-r_D} = 2$.

For the sake of completeness let me work through the remaining three mappings.

6 $\vec{M}_6 = (4312)$, $\vec{\mathcal{P}}' = (2341)$

o	1	2	3	4	remap $\to$	o	4	3	1	2	order $\to$	o	1	2	3	4
i	3	1	4	2		i	1	4	2	3		i	2	3	4	1

7 $\vec{M}_7 = (3421)$
$\vec{\mathcal{P}}' = (4123)$

o	1	2	3	4
i	3	1	4	2

remap →

o	3	4	2	1
i	2	3	1	4

order →

o	1	2	3	4
i	4	1	2	3

8 $\vec{M}_8 = (4321)$
$\vec{\mathcal{P}}' = (1234)$

o	1	2	3	4
i	3	1	4	2

remap →

o	4	3	2	1
i	2	4	1	3

order →

o	1	2	3	4
i	3	1	4	2

3 Use the criterion that permutation and relabeling commutate to determine the symmetry factor for the same diagram

$$\vec{\mathcal{P}} = (3, 1, 4, 2) \tag{11.76}$$

used in the previous problem

$M_1 \circ \mathcal{P}$	3142	M_1	1234	$\mathcal{P} \circ M_1$	3142
$M_2 \circ \mathcal{P}$	3241	M_2	2134	$\mathcal{P} \circ M_2$	1342
$M_3 \circ \mathcal{P}$	4132	M_3	1243	$\mathcal{P} \circ M_3$	3124
$M_4 \circ \mathcal{P}$	4231	M_4	2143	$\mathcal{P} \circ M_4$	1324
$M_5 \circ \mathcal{P}$	1324	M_5	3412	$\mathcal{P} \circ M_5$	3412
$M_6 \circ \mathcal{P}$	1423	M_6	4312	$\mathcal{P} \circ M_6$	2431
$M_7 \circ \mathcal{P}$	2314	M_7	3421	$\mathcal{P} \circ M_7$	4213
$M_8 \circ \mathcal{P}$	2413	M_8	4321	$\mathcal{P} \circ M_8$	2413

To set up the table above, I proceeded as follows

- I fill the first column with the permutation vector $\vec{\mathcal{P}}$, the second one with 1234 and the third column again with $\vec{\mathcal{P}}$
- now I perform, line-by-line, the transformations on the sequences of the second and the third column. This will construct the vectors $\vec{M}$ in the second column and $\mathcal{P} \circ M$ in the third.
- Finally I transform the sequences of the first column, which currently holds $\vec{\mathcal{P}}$ in each line, by the corresponding transformation M from the middle column. Starting with the first component, I look up $\mathcal{P}_j$, which tells me at which position of $\vec{M}$ I find the new value $M_{\mathcal{P}_j}$ for the j-th component of the vector in the first column. For each component j, this step is efficiently on all lines simultaneously.

From the table above, we find that mere deformations are the identity M_1 and M_8. The identity is trivial and is discarded. Thus, there is one mere deformation, except for the identity M_1, among the eight transformations in the group.

4 Construct graphically the diagrams which are topologically equivalent to

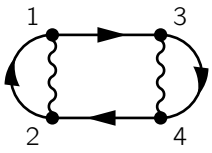

(11.77)

determine mere deformations and the symmetry factor.

The solution is given in figure 11.4 on p. 344.

5 Work out the symmetry factor for the following second-order diagram

$$\vec{\mathcal{P}} = (1, 3, 2, 4) \tag{11.78}$$

using the method of your choice.

This diagram is a ring diagram with a tadpole attached to either side.

$M_1 \circ \mathcal{P}$	1324	M_1	1234	$\mathcal{P} \circ M_1$	1324
$M_2 \circ \mathcal{P}$	2314	M_2	2134	$\mathcal{P} \circ M_2$	3124
$M_3 \circ \mathcal{P}$	1423	M_3	1243	$\mathcal{P} \circ M_3$	1342
$M_4 \circ \mathcal{P}$	2413	M_4	2143	$\mathcal{P} \circ M_4$	3142
$M_5 \circ \mathcal{P}$	3142	M_5	3412	$\mathcal{P} \circ M_5$	2413
$M_6 \circ \mathcal{P}$	4132	M_6	4312	$\mathcal{P} \circ M_6$	4213
$M_7 \circ \mathcal{P}$	3241	M_7	3421	$\mathcal{P} \circ M_7$	2431
$M_8 \circ \mathcal{P}$	4231	M_8	4321	$\mathcal{P} \circ M_8$	4231

There are two transformations including the identity that produce mere deformations of the given diagram, namely M_1 and M_8. Thus, the symmetry factor is $S(D) = 2$.

11.10.4 Value of a given Feynman diagrams

Editor: This exercise needs to be completed.

For the shown $\vec{\mathcal{P}} = (1, 4, 3, 2)$. Show the

$$P = (1432)$$

$$V(1,4,3,2) = \epsilon_{1,4,3,2}(i\hbar)^2 \sum_{i_1,o_1,i_2,o_2,i_3,o_3,i_4,o_4} \int_{\mathcal{C}} dt_1 \int_{\mathcal{C}} dt_2$$

$$\times W_{o_1,o_2,i_1,i_2}(t) W_{o_3,o_4,i_3,i_4}(t') \tag{11.79}$$

$$G_{i_1,o_1}(t_1, t_1^+) G_{i_4,o_2}(t_2, t_1) G_{i_3,o_3}(t_2, t_2^+) G_{i_2,o_4}(t_1, t_2) \tag{11.80}$$

Feynman diagram

- extract a permutation vector
- work out value of the Feynman diagram in terms of non-interacting Green's function and the interaction matrix

Solution: place numbers onto the vertices. Read of vertex the green's function points to.

11.10.5 Example: Evaluate the Green's function for a specific example

Editor: This exercise needs to be completed.

So-far we manipulated expressions given in terms of Green's functions and interaction matrix elements. We did not practice to work out the Green's function for a specific system. In this section, we will work out the Green's function for the Hartree-Fock approximation for the Hubbard dimer.

11.11 Summary

A sequence of theorems have been required to set up the diagrammatic expansion of the Green's function

1. interaction picture and introduction of the S-matrix
2. replacement of the interacting state operator by that of the non-interacting system. Description of the conversion by propagation along the imaginary time axis.
3. Wick's theorem
4. linked-cluster theorem
5. sign theorem
6. symmetry factors
7. conversion of $\mathcal{Q}_{T,\mu}$ into Green's functions

We learned how to enumerate all diagrams using permutation vectors.

Permutation vectors, Feynman diagrams and the expression for the value $V(D)$ of a diagram can be translated into each other.

Chapter 12

Luttinger-Ward functional

Truncating the diagrammatic expansion can lead to Green's functions that violate conservation laws such as particle-number conservation, energy conservation, momentum conservation, angular momentum conservation.

Kadanoff and Baym[86, 87] have shown that these conservation laws can be enforced when the equations for the Green's function are derived from the so-called Luttinger-Ward functional[88].

In this section, I am using a compact notation, in which a product involves a matrix product and the corresponding time integrations. Similarly the Trace includes also all time integrations.

12.1 Compact notations

12.1.1 Combined vertex indices

Often a short-hand notation is used:

- rather than listing orbital indices o_j, i_j, and time arguments t_j connected to a vertex with label j, only a number is used.
  - $G^{(0)}(1,2)$ expands into $G^{\mathcal{C},(0)}_{o_1,i_2}(t_1, t_2^+)$
  - $G(1,2)$ expands into $G^{\mathcal{C}}_{o_1,i_2}(t_1, t_2^+)$
  - $W(1,2)$ expands into $i\hbar W_{o_1,o_2,i_1,i_2}\delta_{\mathcal{C}}(t_1 - t_2)$
  - $\int d1$ expands into $\sum_{o_1,i_1}\int_{\mathcal{C}} dt_1$
- Einstein notation is used. That is, if a vertex label occurs twice in a product, a sum over orbital indices and a time integration, i.e. $\int d1$ is implicitly assumed.

As an example, Dyson's equation has the form

$$G(1,2) \overset{\text{Eq. } 8.23}{=} G^{(0)}(1,2) + G^{(0)}(1,3)\Sigma(3,4)G(4,2) \tag{12.1}$$

The value of a closed diagram Eq. 10.48 in a short-hand notation reads as follows

$$V(\vec{\mathcal{P}}) = \epsilon_{\mathcal{P}_1,\ldots,\mathcal{P}_{2n}}(i\hbar)^n \int d1 \cdots \int d2n \left(\prod_{j=1}^{n} W(2j-1, 2j)\right)\left(\prod_{k=1}^{2n} G^{\mathcal{C},(0)}(\mathcal{P}_k, k)\right) \tag{12.2}$$

From generating functional $\mathcal{Q}[\boldsymbol{G}^{(0)}, \boldsymbol{W}]$, we obtain the Green's function via

$$G(2,1) \overset{\text{Eq. } 10.60}{=} G^{(0)}(2,1) + \int_{3,4} G^{(0)}(2,4)\Sigma^{red}(4,3)G^{(0)}(3,1) \tag{12.3}$$

which is a short-hand notation for

$$G_{i_2,o_1}(t_2,t_1) = G^{(0)}_{i_2,o_1}(t_2,t_1) + \int_{\mathcal{C}} dt_1 \int_{\mathcal{C}} dt_2 \sum_{i_3,o_4} G^{(0)}_{i_2,o_4}(t_2,t_4)\Sigma^{red}_{o_4,i_3}(t_4,t_3)G^{(0)}_{i_3,o_1}(t_3,t_1) \quad (12.4)$$

where the reducible self energy Σ^{red} is the functional derivative of the generating functional.

$$\Sigma^{red}_{o_2,i_1}(t_1,t_2) \overset{\text{Eq. } 10.61}{=} \beta \frac{\partial \mathcal{Q}[G^{(0)}]}{\partial G^{(0)}_{i_1,o_2}(t_2,t_1)} \quad (12.5)$$

or, in the short-hand notation,

$$\Sigma^{red}(2,1) \overset{\text{Eq. } 10.61}{=} \beta \frac{\partial \mathcal{Q}[G^{(0)}]}{\partial G^{(0)}(1,2)} \quad (12.6)$$

How is the reducible self energy Σ^{red} related to the proper self energy Σ, introduced earlier? The proper self energy is defined in Eq. 8.15 on 257, which converts the equation of motion Eq. 8.8 for the Green's function into Dyson's equation Eq. 8.23.

$$G(2,1) \overset{\text{Eq. } 8.23}{=} G^{(0)}(2,1) + \int_{3,4} G^{(0)}(2,4)\Sigma(4,3)G(3,1) \quad (12.7)$$

The full Green's function is given by the equation of motion.

12.1.2 Generalized matrix algebra

In the following, I introduce another compact notation: We treat time argument and orbital index as one combined matrix index.

$$A_{\alpha,\beta}(t,t') \rightsquigarrow A_{(\alpha,t);(\beta,t')} \quad (12.8)$$

The time argument shall be considered discretized. The product is

$$C = AB \qquad \Leftrightarrow \qquad C_{\alpha,\beta}(t,t') = \sum_{\gamma} \int dt''\, A_{\alpha,\gamma}(t,t'')B_{\gamma,\beta}(t'',t') \quad (12.9)$$

This implies that another scalar product has been defined that involves also a time integration.

12.2 From the generating functional $\mathcal{Q}_{T,\mu}[G^{(0)}]$ of the bare Green's function to the Luttinger-Ward functional

From the reducible to the proper self energy

Let me rearrange Dyson's equation Eq. 12.7 to allow the comparison with Eq. 12.3

$$\begin{aligned} G &\overset{\text{Eq. } 12.7}{=} G^{(0)} + G^{(0)}\Sigma G^{(0)} + G^{(0)}\Sigma G^{(0)}\Sigma G^{(0)} + \dots \\ &= G^{(0)} + G^{(0)} \underbrace{\left(\Sigma + \Sigma G^{(0)}\Sigma + \dots\right)}_{\Sigma^{red}} G^{(0)} \end{aligned} \quad (12.10)$$

By comparing with Eq. 12.3, we obtain the reducible self energy in the form

$$\begin{aligned}
\Sigma^{red} &= \Sigma + \Sigma G^{(0)}\Sigma + \Sigma G^{(0)}\Sigma G^{(0)}\Sigma + \dots \\
&= \sum_{n=0}^{\infty} \left(\Sigma G^{(0)}\right)^n \Sigma \\
&= \sum_{n=0}^{\infty} \frac{1}{n+1} \frac{\partial}{\partial G^{(0)}}\Big|_{\Sigma} \mathrm{Tr}\left[\left(\Sigma G^{(0)}\right)^{n+1}\right] \\
&\overset{n+1\to n}{=} \frac{\partial}{\partial G^{(0)}}\Big|_{\Sigma} \sum_{n=1}^{\infty} \frac{1}{n} \mathrm{Tr}\left[\left(\Sigma G^{(0)}\right)^{n}\right] \\
&\overset{\ln(1-x)=-\sum_{n=1}^{\infty}\frac{1}{n}x^n}{=} -\frac{\partial}{\partial G^{0}}\Big|_{\Sigma} \mathrm{Tr}\left[\ln\left(1-\Sigma G^{(0)}\right)\right]
\end{aligned} \tag{12.11}$$

The logarithm and the inverse shall be understood as their Taylor expansions $(1-x)^{-1} = \sum_{n=0}^{\infty} x^n$ for $|x| < 1$ and $\ln(1-x) = -\sum_{n=1}^{\infty} \frac{1}{n} x^n$ for $|x| < 1$. The limited convergence radius implies that the expression is not defined when $\Sigma G^{(0)}$ has any eigenvalue with an absolute value equal or larger than 1.

This allows one to rewrite the identity

$$\beta \frac{\partial \mathcal{Q}}{\partial G^{(0)}} \overset{\text{Eq. } 12.5}{=} \Sigma^{red} \overset{\text{Eq. } 12.11}{=} -\frac{\partial}{\partial G^{0}}\Big|_{\Sigma} \mathrm{Tr}\left[\ln\left(1-\Sigma G^{(0)}\right)\right] \tag{12.12}$$

in the form of a stationary condition for a function that depends on the bare Green's function and the proper self energy.

$$0 = \frac{\partial}{\partial G^{(0)}}\Big|_{\Sigma} \left\{ \mathcal{Q}\left[G^{(0)}\right] + k_B T \, \mathrm{Tr}\left[\ln\left(1-\Sigma G^{(0)}\right)\right] \right\} \tag{12.13}$$

This suggests to define a functional of the proper self energy Σ. Remember that the products and derivatives use a compact notation. A product involves a summation over orbitals and a contour integral over the complex time contour. The logarithm is to be replaced by its power-series expansion.

A functional of the proper self energy

Let me define a **self-energy functional** [89, 90] [1] [2] $F(\Sigma)$ by a generalized Legendre transform[3].

$$F[\Sigma] \overset{\text{def}}{=} \underset{G^{(0)}}{\mathrm{stat}} \left\{ \mathcal{Q}[G^{(0)}] + k_B T \, \mathrm{Tr} \ln\left(1-\Sigma G^{(0)}\right) \right\} \tag{12.14}$$

What we just did is a generalized Legendre transform, which does not work with straight lines like a normal Legendre transform but with another family of functions. To explain, what I mean with generalized Legendre transform let me quickly review the ordinary Legendre transform in the following box.

[1] Hofmann et al. [90] show the generalization of the self-energy functional to non-equilibrium Green's functions.

[2] Editor: The bare Green's function can be parameterized by an effective potential, which may be useful.

[3] In order to brush up on Legendre transforms you may consult section 3.2 of ΦSX:Statistical Physics[33].

Legendre transform in thermodynamics: Let me consider a normal Legendre transform in thermodynamics. Start from an internal energy $U(S)$ as function of the entropy S. The derivative of the internal energy defines a physical quantity, namely the temperature T:

$$T = \frac{dU}{dS} \tag{12.15}$$

Let me consider the problem of finding the entropy for a given temperature: I define a Legendre transform of the internal energy, namely the free energy[a] $F(T)$ by

$$F(T) = \operatorname*{stat}_S \Big\{ U(S) - TS \Big\} \tag{12.16}$$

The stationary condition[b] encapsulates the definition Eq. 12.15 of the temperature. The derivative of the free energy, in turn, is the (negative) entropy

$$\frac{dF}{dT} = \underbrace{\frac{\partial (U(S) - TS)}{\partial S}}_{=0} \frac{\partial S}{\partial T} + \underbrace{\frac{\partial (U(S) - TS)}{\partial T}}_{=-S} = -S \tag{12.17}$$

This is the desired result, namely the entropy as function of the temperature. The Legendre transform describes a function $U(S)$ not by values $U(S)$ for a given argument S, but by values $F(T)$ for given slope T of the original function $U(S)$. $F(T)$ describes the vertical (along the U-axis) displacement of a tangent $y_T(S) = F(T) + TS$. to the function $U(S)$.
Some caution is necessary, because a Legendre transform does not guarantee that the back transform is identical to the original function. The Legendre transform is bijective only, if the original function is purely convex or purely concave. Otherwise, several tangents with the same slope may exist, so that the Legendre transformed function $F(T)$ would be double valued. If the other branches of the Legendre transform are omitted, one obtains the outer envelope of the original function. This route is taken in the Legendre-Fenchel transform.
The arguments, given here for one-dimensional functions are not meant to be exhaustive, but they should raise the attention to problems that have been an issue[91] related to the existence of the Luttinger-Ward functional.

[a] The free energy has nothing to do with our self-energy functional, despite using the same symbol.

[b] I invented the symbol stat as generalization of min and max to any point with vanishing gradient. That is, saddle points are explicitly considered as well.

Let us now turn from the reminder of the regular Legendre-Fenchel transform to the generalized Legendre transform at hand. Rather than describing a function $U(S)$ by a family of tangential straight lines $y_T(S) = U(S) - TS$, we can also use other functions, in this case $y_\Sigma(G^{(0)}) = -k_B T \ \ln(1 - \Sigma G^{(0)})$. The parameter Σ is determined such that the slope of the original function $\mathcal{Q}(G^{(0)})$ is identical to that of $y_\Sigma(G^{(0)})$ at the point, where the two functions touch.

The stationary condition of the self-energy functional Eq. 12.14 with respect to the bare Green's function encapsulates the expression Eq. 12.13 for the proper self energy via the reducible self energy expressed as functional derivative of the generating functional $\mathcal{Q}[G^{(0)}]$.

The functional derivative of the self-energy functional is, up to the sign, the full Green's function

$$\beta \frac{\partial F[\Sigma]}{\partial \Sigma} \overset{\text{Eq. } 12.14}{=} -G^{(0)} \Big(1 - \Sigma G^{(0)} \Big)^{-1} \overset{\text{Eq. } 12.7}{=} -G \tag{12.18}$$

Thus, the self-energy functional $F(\Sigma)$ is a generating functional of the full Green's function.

The expression Eq. 12.18 for the functional derivative can be rewritten as a stationary condition.

$$0 = \frac{\partial}{\partial \Sigma}\bigg|_G \Big\{ F[\Sigma] + k_B T \ \mathrm{Tr}\big[G\Sigma\big] \Big\} \tag{12.19}$$

Luttinger-Ward functional

Let me now define a new functional $\Phi_T^{LW}[G]$, the so-called **Luttinger-Ward functional** [4][88]. of the full Green's function by a second Legendre transform

$$\begin{aligned}\Phi_T^{LW}(G) &\overset{\text{def}}{=} \operatorname*{stat}_{\Sigma}\left\{F[\Sigma] + \frac{1}{\beta}\mathrm{Tr}\left[\Sigma G\right]\right\} \\ &\overset{\text{Eq. 12.14}}{=} \operatorname*{stat}_{\Sigma, G^{(0)}}\left\{\mathcal{Q}[G^{(0)}] + \frac{1}{\beta}\,\mathrm{Tr}\left[\ln\left(1-\Sigma G^{(0)}\right) + \Sigma G\right]\right\}\end{aligned} \tag{12.20}$$

The stationary conditions of the functional in curly brackets in Eq. 12.20 are,

- for the derivative with respect to the bare Green's function $G^{(0)}$,

$$0 \overset{!}{=} \underbrace{\frac{\delta\mathcal{Q}[G^{(0)}]}{\delta G^{(0)}}}_{=\frac{1}{\beta}\Sigma^{red}\ \text{(Eq. 10.61)}} + \frac{1}{\beta}\left[-\left(1-\Sigma G^{(0)}\right)^{-1}\Sigma\right] \quad \rightsquigarrow \quad \Sigma(G^{(0)}) \tag{12.21}$$

- and for the derivative with respect to the self energy Σ,

$$0 \overset{!}{=} \frac{1}{\beta}\left[-G^{(0)}\left(1-\Sigma G^{(0)}\right)^{-1} + G\right] \quad \rightsquigarrow \quad G(\Sigma, G^{(0)}) \tag{12.22}$$

Using the first stationary condition, we obtain the proper self energy $\Sigma = \Sigma^{red}(1 + G^{(0)}\Sigma^{red})^{-1}$ as function of the bare Green's function. The reducible self energy $\Sigma^{red} = \beta\delta\mathcal{Q}/\delta G^{(0)}$ is given by the derivative of the functional $\mathcal{Q}$, which itself is a functional of the bare Green's function. The second stationary condition is Dyson's equation, which provides the full Green's function in terms of the proper self energy Σ and the bare Green's function $G^{(0)}$. With these two equations, we can evaluate the Luttinger-Ward functional for a specified bare Green's function, and we can evaluate the full Green's function from the bare Green's function. That is, we can construct the pair of the functional Φ_T^{LW} and its argument G for a given bare Greens function $G^{(0)}$, but we cannot construct the functional $\Phi_T^{LW}(G)$ directly from the full Green's function.

Unfortunately, we do not know the mapping $G \rightsquigarrow G^{(0)}$, which would allow a direct evaluation of the Luttinger-Ward functional. While the mapping $G^{(0)} \rightsquigarrow G$ is unique, the inverse mapping $G \rightsquigarrow G^{(0)}$ may be multi-valued. Thus, it may contain physical and nonphysical branches.Editor: Provide citations

When we exploit the stationary conditions, the functional derivative of the Luttinger-Ward functional is readily obtained as proper self energy

$$\beta\frac{\delta\Phi_T^{LW}(G)}{\delta G} \overset{\text{Eq. 12.20}}{=} \Sigma \tag{12.23}$$

[4] You will find different expressions for the Luttinger-Ward functional. Using Dyson's equation $G = G^{(0)} + G^{(0)}\Sigma G = G^{(0)} + G\Sigma G^{(0)}$, we obtain $G(1-\Sigma G^{(0)}) = G^{(0)}$ and thus $(1-\Sigma G^{(0)}) = G^{(0)}G^{-1}$.

DEFINING PROPERTIES OF THE LUTTINGER-WARD FUNCTIONAL

The Luttinger-Ward function has the following properties:[92]

- The derivative

$$\frac{\beta\delta\Phi_T^{LW}[\boldsymbol{G},\hat{W}]}{\delta G_{b,a}(t',t)} = \Sigma_{a,b}(t,t')\,. \tag{12.24}$$

  of the Luttinger-Ward functional evaluated at a physical Green's function defined by Eq. **??** yields a self energy that obeys Eq. **??**.

- It is universal, that is it depends only on the interaction, the chemical potential and the temperature, but not on the non-interacting Hamiltonian $\hat{h}$.

- It vanishes in the non-interacting case.

The Luttinger-Ward functional $\Phi_T^{LW}(G)$ has substantially fewer Feynman diagrams than $\mathcal{Q}(G_{T,\mu}^{(0)}$, because several geometric series expansions are already considered by using the full Green's function rather than the bare Green's function. This will be discussed in the next section.

The stationary principles encapsulate a set of equations, which need to be solved self-consistently. As a result of the self-consistent equations, on obtains the quantities of interest, namely the proper self energy and the full Green's function.

Approximations which are done to the Luttinger-Ward functional are **conserving approximations**. [86, 87] This means that conservation laws are obeyed and the resulting theory is **thermodynamically consistent**.

Kadanoff-Baym functional

Performing the Legendre transformations backwards will express our generating functional in terms of the Luttinger-Ward functional.

$$\mathcal{Q}[G^0] \overset{\text{Eq. } 12.20}{=} \operatorname*{stat}_{\Sigma,G}\left\{\Phi_T^{LW}(G) - \frac{1}{\beta}\mathrm{Tr}\left[\ln\left(1-\Sigma G^{(0)}\right)+\Sigma G\right]\right\} \tag{12.25}$$

This expression

1. provides the grand potential $\Omega_{T,\mu}^W$ by adding the grand potential $\Omega_{T,\mu}^0$ of the non-interacting system and
2. it allows to construct an approximate generating functional $\mathcal{Q}_{T,\mu}(G^{(0)})$ from an approximation of the Luttinger-Ward functional $\Phi_T^{LW}(G)$.

The so-called[5] Kadanoff-Baym functional $\Psi_{T,\mu}^{KB}$ provides the grand potential

$$\Omega_{T,\mu}(\hat{h}+\hat{W}) = \operatorname*{stat}_{G,\Sigma}\Psi_{T,\mu}^{KB}[\boldsymbol{G},\boldsymbol{\Sigma},\boldsymbol{h},\hat{W}]\,, \tag{12.26}$$

where

$$\Psi_{T,\mu}^{KB}[\boldsymbol{G},\boldsymbol{\Sigma},\boldsymbol{h},\hat{W}] = \underbrace{\Omega_{T,\mu}^{(0)}[\boldsymbol{h}]}_{-\frac{1}{\beta}\mathrm{Tr}\ln(-i\hbar G^{(0)})} + \Phi_T^{LW}[\boldsymbol{G},\hat{W}] - \frac{1}{\beta}\mathrm{Tr}\left\{\ln\Big[\underbrace{\left(\mathbf{1}-\boldsymbol{G}^{(0)}\boldsymbol{\Sigma}\right)}_{[-i\hbar G]^{-1}[-i\hbar G^{(0)}]}\Big] + \boldsymbol{\Sigma}\boldsymbol{G}\right\}\,. \tag{12.27}$$

The terms shown below the underbraces are often found in the literature, and the bare Green's functions in the two logarithm terms are often canceled against each other. Some caution is required

[5] We adopt this naming of Luttinger-Ward and Kadanoff-Baym functional from Chitra and Kotliar [93].

because the expressions I found in the literature are expressed in the Matsubara formalism.Editor: Check whether this replacement is permitted. I am concerned because the Green's function may have units attached and must not stand alone in a logarithm. Secondly, $\mathrm{Tr}[AB] \neq Tr[A]Tr[B]$

Existence of the Luttinger-Ward functional

See `https://www.pnas.org/content/pnas/115/10/2282.full.pdf` for a recent paper summarizing the state about the existence or non-existence of the Luttinger-Ward functions. Tarantino et al.[69] explore the problem using the Hubbard atom as example.

Sanity check

The reader may skip this section. As a sanity check, let me compare Eq. 12.27 with the literature.

A few precautions are necessary: While my lecture notes works with a complex time contour, the results are often compared with the Matsubara formalism.

- Caution is required because many expressions are given in the Matsubara formalism. The Matsubara Green's function $\mathcal{G}(\tau_2, \tau_1) = -iG^{\mathcal{C}}(-i\tau_2, -i\tau_1)e^{\mu(\tau_2-\tau_1)/\hbar}$, Eq. **??** is defined different from the Matsubara part of the non-equilibrium Green's function used here.
- Secondly, the stationary condition for the self energy is usually resolved, so that $\Sigma = G^{(0),-1} - G^{-1}$ is eliminated. I do not do this step, because it is not yet clear to me, whether the required expressions are permitted on the complete complex-time contour.
- The non-interacting grand potential is often expressed as $\Omega^{(0)}_{T,\mu} = -\frac{1}{\beta}\mathrm{Tr}[\ln(-i\hbar G^{(0)})]$.Editor: caution check whether this holds on a general complex time contour. Once written in this form, it is canceled against another similar term in the other logarithm $\ln(1-\Sigma G^{(0)}) = \ln[G^{(0)}G^{-1}] = \ln(-i\hbar G^{(0)}) - \ln(-i\hbar G)$

with these remarks we can now compare to individual authors:

- Potthoff's equation[89]:

$$\Omega_{T,\mu}[G] = \Phi^{LW}_T[G] + \mathrm{Tr}\ln[-i\hbar G] - \mathrm{Tr}\Big[\underbrace{\big(G^{(0),-1} - G^{-1}\big)}_{\Sigma[G]} G\Big] \tag{12.28}$$

  can be compared with our Eq. 12.27. I have included a factor $i\hbar$, which is not present in Potthoff's expression.

- Luttinger and Ward [88] provide the connection between the grand potential (Y) and the Luttinger-Ward functional (Y') in their Eq. 47,

$$\Omega_{T,\mu} = -\frac{1}{\beta}\mathrm{Tr}\big[\ln(-G^{-1}) + G\Sigma\big] + \Phi^{LW}_T(G) \tag{12.29}$$

  Luttinger and Ward use the symbol G_r for the proper self energy, S_r for the full Green's function, while the bare Green's function is $1/(\zeta_l - \epsilon_r)$. As in the comparison with Pothoff given above, there is an additional factor $i\hbar$ in the comparison of Green's functions.

12.3 Skeleton diagrams

The Luttinger-Ward functional has a diagrammatic expansion very similar to that of our generating functional $\mathcal{Q}_{T,\mu}$. The diagrammatic expansion of the Luttinger-Ward functional is obtained by removing all two-particle reducible from the diagrammatic expansion of $\mathcal{Q}$. Secondly, the bare Green's function are replaced by the full Green's function.[88, 65] This shall be shown in the following.

Let me start with our generating functional $\mathcal{Q}_{T,\mu}$ and extract the reducible self energy.

$$\Sigma^{red}[G^{(0)}] \overset{\text{Eq. } 10.61}{=} \beta \frac{\delta \mathcal{Q}_{T,\mu}}{\delta G^{(0)}} \overset{\text{Eq. } 11.26}{=} \beta \frac{\partial}{\delta G^{(0)}} \underbrace{\left[-\frac{1}{\beta} \sum_{D \in \mathbb{T}} \frac{V(D)}{S(D)} \right]}_{\mathcal{Q}_{T,\mu}(G^{(0)})} \tag{12.30}$$

The diagrammatic expansion of $\mathcal{Q}_{T,\mu}$ contains all linked, closed, and topologically distinct diagrams D. $V(D)$ is the value of the diagram and $S(D)$ is the symmetry factor.

The reducible self energy is made from all open necklaces of proper self energies interconnected with bare Green's functions, Eq. 10.65.

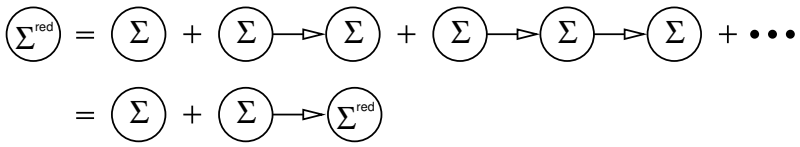

Therefore, one obtains the proper self energy by removing all self-energy diagrams, which are one-particle-reducible. That are all diagrams, which can be divided into two pieces by cutting through one bare Green's function.

The improper self energy Σ^{red} has been obtained by removing one bare Green's line from the Feynman-diagrams in $\mathcal{Q}_{T,\mu}(G^{(0)})$, which results in the self-energy diagrams given above. Removing all one-particle-reducible self-energy diagrams, leaves the proper self energy Σ.

The same result for the proper self energy is obtained, when we first remove all two-particle reducible diagrams from the functional $\mathcal{Q}_{T,\mu}(G^{(0)})$, and only then form the derivative with respect to the bare Green's function by removing a particle line. What is left, are the so-called two-particle irreducible (2PI) diagrams, also called **skeleton diagrams**. Hence

$$\Sigma[G^{(0)}] = \beta \frac{\partial}{\delta G^{(0)}} \Bigg[\underbrace{-\frac{1}{\beta} \sum_{\text{Skeleton-}D \in \mathbb{T}} \frac{V(D)}{S(D)}}_{\text{expressed in terms of bare Green's functions } G^{(0)}} \Bigg] \tag{12.31}$$

A skeleton diagram is a closed diagram, which cannot be divided into two distinct pieces by removing two particle lines.

Note that the diagrams D are still expressed in terms of bare Green's functions. However, because we are discussing functionals rather than values, one can name the argument as one wants and therefore one can replace the bare Green's function in $V(D)$ by the full Green's function.

$$\beta \frac{\delta \Phi_{T,\mu}[G]}{\delta G} = \Sigma[G] = \beta \frac{\partial}{\delta G} \Bigg[\underbrace{-\frac{1}{\beta} \sum_{\text{Skeleton-}D \in \mathbb{T}} \frac{V(D)}{S(D)}}_{\text{expressed in terms of full Green's functions } G} \Bigg] \tag{12.32}$$

This equation shows that the diagrammatic expansion on the right-hand side has the same functional derivatives as the Luttinger-Ward functional, namely the proper self energy. Hence the Skeleton expansion is equal to the Luttinger-Ward functional up to a constant. The identity of the skeleton expansion with the Luttinger-Ward functional can thus be established by showing that they agree for only one Green's function–which is not done here–. Hence,

$$\Phi_T^{LW}[G] = \Bigg[\underbrace{-\frac{1}{\beta} \sum_{\text{Skeleton-}D \in \mathbb{T}} \frac{V(D)}{S(D)}}_{\text{expressed in terms of full Green's functions } G} \Bigg] \tag{12.33}$$

which is identical to Eq. 12.23. With this, we have already obtained the most important property of the Luttinger-Ward functional.

So-far we have shown that the functional derivatives of the skeleton expansion and the Luttinger-Ward functionals are identical. We need to show, that they do not differ by a constant. Editor: This needs to be done.

Editor: Read the remark following Eq. 11.18 in the Book by Stefanucci and van Leeuwen[2]

12.4 Renormalized interaction

Editor: This is under construction! Do not read

Similar to the Green's function also the interaction can be renormalized. This results in an expansion in terms of a screened interaction, which lacks the long-ranged tail of the Coulomb interaction.

$$W^{scr} = W^{bare} + W^{bare}\Pi W^{scr} \tag{12.34}$$

Consider again the derivative of the generating functional $\mathcal{Q}$ with respect to an interaction line.

$$\frac{\partial \mathcal{Q}}{\partial W^{bare}} = \frac{1}{2}\chi \tag{12.35}$$

where χ is the reducible polarizibility (or susceptibility).

A polarization diagram is one with two outer vertices to which interactions can be attached. A polarization diagram can be reducible, if it falls into two disconnected pieces by removing one bare interaction line. If it cannot be divided in this way, it is called an irreducible polarization diagram.

The reducible polarization χ can be expressed by the irreducible polarizibility Π

$$\begin{aligned}
W^{scr} &= W^{bare} + W^{bare}\Pi W^{bare} + W^{bare}\Pi W^{bare}\Pi W^{bare} + \dots \\
&= \sum_{n=0}^{\infty} (W^{bare}\Pi)^n W^{bare} \\
&= \sum_{n=0}^{\infty} \frac{1}{n+1} \frac{\partial}{\partial W^{bare}}\bigg|_{G^{(0)}} \mathrm{Tr}\Big[(W^{bare}\Pi)^{n+1}\Big] \\
&\overset{n+1\to n}{=} \frac{\partial}{\partial W^{bare}}\bigg|_{G^{(0)}} \sum_{n=1}^{\infty} \frac{1}{n} \mathrm{Tr}\Big[(W^{bare}\Pi)^{n}\Big] \\
&= -\frac{\partial}{\partial W^{bare}}\bigg|_{G^{(0)}} \mathrm{Tr}\Big(\ln\Big(1 - W^{bare}\Pi\Big)\Big]
\end{aligned} \tag{12.36}$$

This defines a stationary principle

$$0 = \frac{\partial}{\partial W^{bare}}\bigg|_{G^{(0)}} \Big\{ \mathcal{Q}[G^{(0)}, W^{bare}] + k_B T \ \mathrm{Tr}\Big(\ln\Big(1 - W^{bare}\Pi\Big)\Big]\Big\} \tag{12.37}$$

Polarization functional

Thus, I can define a functional of the polarization

$$F(\Pi, G^{(0)}) = \underset{W^{bare}}{\mathrm{stat}} \Big\{ \mathcal{Q}[G^{(0)}, W^{bare}] + k_B T \ \mathrm{Tr}\Big[\ln\Big(1 - W^{bare}\Pi\Big)\Big]\Big\} \tag{12.38}$$

$$\frac{1}{k_B T}\frac{\partial F}{\partial \Pi} = -W^{bare}\Big(1 - W^{bare}\Pi\Big)^{-1} = -W^{scr} \tag{12.39}$$

Let me now define a new functional of the bare Green's function and the screened interaction.

$$\Psi[G, W^{scr}] = \tag{12.40}$$

Continue along section 11.8 of Setfanucci and van Leeuwen.

12.5 Conserving approximations

1. Hartree-Fock approximation
2. second-order Born approximation
3. Random-phase approximation
4. T-matrix approximation

Two additional classes of diagrams, which form geometric series, are described below, namely the particle-particle ladders and the wheel. I need to confirm, whether they also lead to conserving approximations. (They should.)

12.5.1 Hartree-Fock approximation

Fig. 12.1: The two diagrams in the Luttinger-Ward functional of the self-consistent Hartree-Fock approximation. The first is the Hartree diagram, while the second describes exchange.

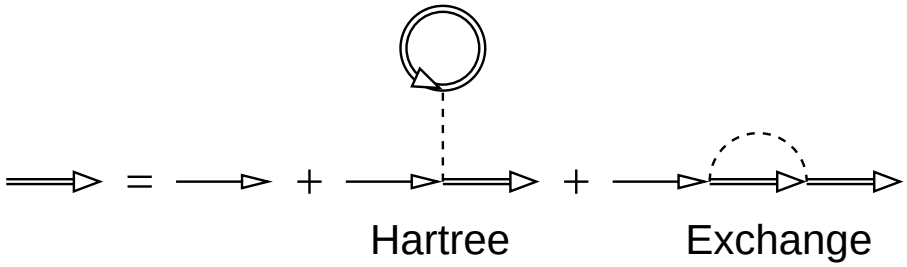

12.5.2 Second-order Born approximation

The Luttinger-Ward functional of the second-order Born approximation includes all skeleton diagrams of first and second order. The first-order diagrams, which are also part of the second-order Born approximation, are the ones from the Hartree-Fock approximation. In addition, two skeleton diagrams, shown in fig. 12.2, contribute to the second order in the interaction.

The second-order skeleton diagrams can be collected from all second-order diagrams shown in fig. 11.2 on p.332 by removing all non-skeleton diagrams. The various topologically distinct diagrams, un-closed, skeleton and closed non-skeleton, are shown in fig. 11.3.

12.5.3 Diagrammatic sequences that can be summed up analytically

There are sequences of Feynman diagrams that form a geometric series and can be summed up to infinite order. The **random-phase approximation** [43, 44, 45]. is one of them.

While there are many of such sequences, we concentrate on those that have four vertices of which two have an empty incoming and two have an empty outgoing index.

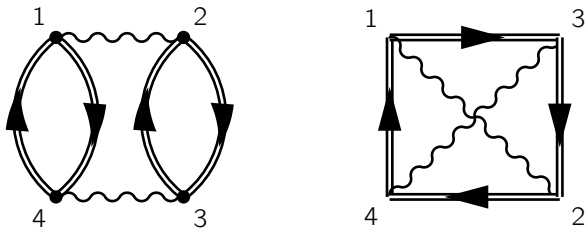

Fig. 12.2: The double-ring diagram and the double-exchange diagram are the only two second order contributions to the Luttinger-Ward functional. They are added to the first order terms.

- **ring necklace** (RPA, GW)

position	1	2	3	4	5	...	2n-1	2n
$\vec{\mathcal{P}}$	2n	3	2	5	4	...	2n-2	1

  Any even-numbered vertex is mapped onto the next higher index, while ever odd-numbered index is mapped to the next lower one. The diagram of lowest order is the oyster diagram of Hartree-Fock. The second-order ring-necklace is the double-ring diagram. To avoid double counting, it is important that these two diagrams are removed, before the geometric series of ring-necklaces is added.

  By inspection of the diagrams in section L.6 I obtain a symmetry factor $2n$ for a n-th order ring necklace and a sign of $(-1)^n$.

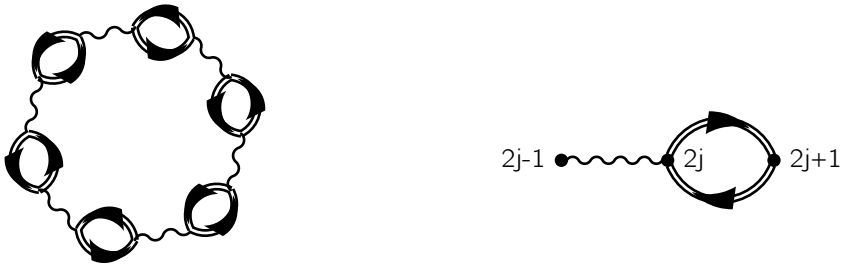

Fig. 12.3: The ring necklace and its elemental diagram.

- The **particle-hole ladder** (T-matrix approximation)

position	1	2	3	4	5	...	2n-1	2n
$\vec{\mathcal{P}}$	3	2n+1	5	2	7	...	1	2

  Any odd numbered vertex is mapped to the next-higher odd-numbered index. Any even-numbered vertex is mapped to the next lower even-numbered index. The diagram of lowest order is the eyeglass diagram of the Hartree approximation. The second-order diagram is the double-ring necklace.

  By inspection of the diagrams in section L.6, I obtain a symmetry factor $2n$ for a n-th order particle-hole ladders and a sign of $+1$.

- The **particle-particle ladders** are given by the permutation vectors.

position	1	2	3	4	5	...	2n-1	2n
$\vec{\mathcal{P}}$	3	4	5	6	7	...	1	2

  All vertices are mapped to the next-higher index, i.e. $\mathcal{P}_j = j + 2$ with cyclic permutation. The diagram of lowest order is the eyeglass diagram of the Hartree approximation. The second diagram is the double-ring diagram of the second-order approximation.

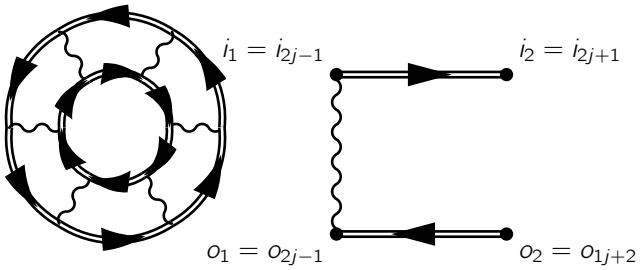

Fig. 12.4: Particle-hole ladder in the Luttinger-Ward functional. Ladders can also inserted into each ring diagram of the ring series.

By inspection of the diagrams in section L.6, I obtain a symmetry factor $2n$ for a n-th order particle-particle ladders and a sign of $+1$.

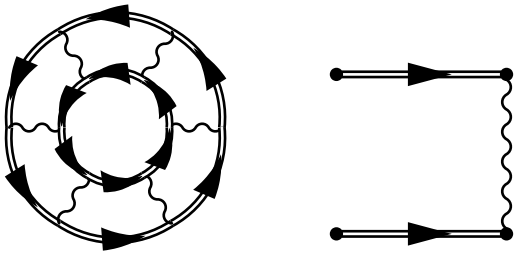

Fig. 12.5: The particle-particle ladder and its elemental diagram

- The **wheel** is given by the permutation vectors.

position	1	2	3	4	5	...	2n-1	2n
$\vec{\mathcal{P}}$	3	4	5	6	7	...	2	1

Any vertex, except the two last ones, is mapped to the second-next higher one. The last odd-numbered index, V_{2n-1} is mapped onto the first even-numbered vertex, V_2, and the last even-numbered vertex V_{2n} is mapped onto the first odd numbered index, V_1.

The diagram of lowest order is the oyster diagram of the Hartree-Fock approximation. The second-order wheel is second order exchange diagram of the second-order approximation.

By inspection of the diagrams in section L.6, I obtain a symmetry factor $2n$ for a n-th order wheel and a sign of -1.

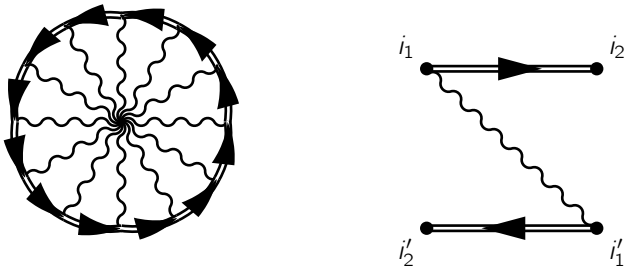

Fig. 12.6: The wheel and its elemental diagram

The wheel is obtained by introducing one exchange into particle-particle ladder as shown in figure 12.7.

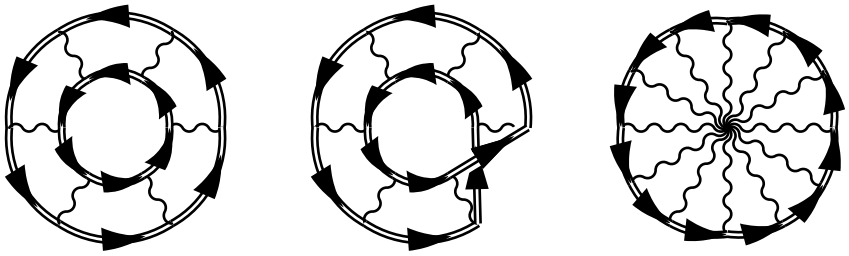

Fig. 12.7: The wheel diagram results from including exchanges into the particle-particle ladder. The diagram on the left is the particle-particle ladder. The diagram in the middle and on the right are equivalent: They contain one Fermi loop with $2n$ Green's functions, for which each interaction joins the Fermi loop after n Green's function again.

12.6 Symmetries and conservation laws

Editor: Include here the conservation laws starting with particle conservation.

Chapter 13

Organization and examination

13.1 Teaching goals

- Fock space, Slater determinants, occupation-number representation, Mazny-particle wave functions, ensembles.
- Hartree- and exchange energy, exchange-correlation hole. Hund's rule.
- mean-field approximation (Hartree Fock) and self-consistent equations, Fock operator
- creation and annihilation operators. Relation to Slater determinants. Calculations.
- Spectral function as electron addition and removal energies. quasi-particles and their interaction.
- downfolding, self energy, retarded potentials.
- one-particle Green's function of a many-particle system.
- many-body perturbation theory (MBPT). (limited to fermions interacting via the Coulomb interaction.)
  - Wick's theorem
  - enumerate diagrams
  - sign theorem
  - linked-cluster theorem
  - topologically inequivalent diagrams
  - symmetry factors
  - self energy (proper vs reducible)
- full Green's function from generating functional
- convert Feynman diagrams into formulas and vice versa

13.2 Examination

Here, I am collecting some material that could be relevant for the examination. When it is complete it should cover the main points conveyed in the lecture. `Editor: It is still far from complete!` The student can orient himself on this list while preparing for the lecture. I do not recommend, however, to use this as the sole approach to prepare because this will accumulate ill-connected

knowledge, which is of little practical value and which is thus easily forgotten. Rather the student is encouraged to consult this list during learning the material to remind himself and to gain confidence.

- know the Hartree and exchange energy. Derive the Fock operator.
- know the difference of the one-particle-reduced density matrix and the von-Neumann density matrix. Obtain the former from the latter.
- properties of the exchange hole. Relation of the exchange hole to the two-particle density.
- provide creation and annihilation operators in terms of Slater determinants, once as real-space- and spin wave functions, as well as using Slater determinants in occupation-number representation.
- explain the physical significance of the spectral function. (relation to photoemission, inverse photoemission and optical excitation) Why is the one-particle spectral function insufficient to describe optical spectra? What is missing?
- know the definition of natural orbitals and occupations.
- Convert a one-particle Hamiltonian in Dirac notation into a one-particle-at-a-time operator with creation and annihilation operators.
- Slater-Condon rules and maximum coincidence.
- down-folding: example is the non-interacting Hubbard dimer
- conversion between: (1) Slater determinant (2) occupation-number representation (3) creation and annihilation operators applied to vacuum state
- transformation of one-particle basis set between: (1) orbital representation (2) eigenstates of the non-interacting Hamiltonian (3) real-space (4) reciprocal space
- translate a general operator into its representation with creation and annihilation operators.
- manipulate expressions with creation and annihilation operators
- Schrödinger-, Heisenberg- and interaction picture
- construct the Green's function from the vacuum (closed) diagrams. (For example considering only a single diagram.)
- understand and work with retarded potentials
- derive the spectral function from a non-interacting Green's function
- express the propagator in Fock space once using energy dependent wave functions and once as time-ordered exponential.
- Lehmann's representation of the Green function
- spectral function in terms of quasiparticle amplitudes.
- spectral function of the interacting Hubbard atom
- express the Green's function using the spectral function. (for a time-independent Hamiltonian.)
- know the definition of a quasi-particle.
- properties of the propagator (in complex time)
- time-ordered exponential

- Green's function
  - construct the bare (non-interacting) Green's function with a given Hamiltonian
  - contour-ordered GF in the Heisenberg picture
  - contour-ordered GF in the interaction picture using the trace with the non-interacting ensemble.
  - Explain contours: What is the Matsubara branch good for?
  - extract the full Green's function from a given generating functional of the bare Green's function.
- know the main formulas: eg. one-particle-reduced density matrix, many-particle Green's function, self energy, equation of motion of the many-particle Green's function, Dyson's equation, Lehmann representation, spectral density, Wick's theorem.
- understand the difference between contours in the interaction and the Heisenberg picture. Why are the contours different?
- diagrams:
  - conversion between: (1) Feynman diagram (2) permutation vector (3) formula
  - sign factor using sign theorem
  - symmetry factors
  - Define the meaning of "sum over all diagrams" in the generating functional. Each labeled diagram of order n corresponds to an $2n$-dimensional permutation vector. Unlinked diagrams need to be excluded. Eeach labeled diagram carries a factor $1/(n!2^n)$ and each unlabeled diagram has a factor $1/S(D)$ where S is the symmetry factor of diagram D.
- perform functional derivatives
- transform Green's function from time arguments into energy arguments.
- be able to determine the time-dependent wave function in the presence of an energy dependent self energy.

13.3 Todo

This section collects suggestions from the students for improvements.

- make symbols uniform
- prepare a time plan for the material
- select one exercise per week. (The exercises are relatively extensive.) Also include smaller exercises in the spirit of examination questions as opposed to the "mini-projects".
- explain teaching goals for the exercises in their introduction and connect them with the material in the lecture.
- Specific: Introduce an exercise on functional derivatives before the derivation of the Fock operator.
- In the exercises add tasks such as "discuss the physics of the result just obtained"

13.4 Distribution of the teaching load

Editor: Do not read this. It is in preparation.

The teaching period of semester has 14 weeks. The lecture aims at four academic hours of teaching and two academic hours of exercise classes. An academic hour consists of 45 min teaching.

Type refers to lecture "L" and exercises "E". Sections refer to the section number in these lecture notes. Note, however that the numbers may become asynchronous with the lecture notes and need to be updated.

Week	type	sections	topics
1	L	1.1-1.2	**One-particle QM and N-particle QM**
			Bra-ket notation, spin orbitals, extended states, non-orthonormal orbitals
			Slater determinants
1	L	1.3-1.4	**Many-particle states and thermodynamics**
			Fock space, occupation-number representation
			ensembles, entropy, grand potential, Fermi distribution
1	E	1.5	**Non-interacting electrons**
			hydrogen molecule, linear chain, free-electron gas, 2 1-d particles in a box
2	L	2.1-2.4	**Hartree-Fock total energy and selfconsistency**
			one and two-particle operators, Slater rules, HF total energy
			Hartree and exchange energy, 1-p reduced density matrix, Fock operator
2	L	2.5-2.9	**Spectral properties and exchange hole**
			Experiments, addition and removal energies, spectral function
			exciton binding energy
			exchange hole, Hund's rule, HF of the free-electron gas
2	E		
3	L	3.1-3.5	**Creation and annihilation operators**
3	L	2.5-2.9	**Field operators, change of representation**
3	E		**Conversion to and from field operators**
4	L	4	**Green's functions in one-particle QM**
4	L	5	**Open systems and down folding**
4	E		**Simple Green's function problems**
5	L	6	**Propagator, time-ordering operator**
5	L	7.1-7.7	**Green's function concept in many-particle physics**
5	E		
5	L		
5	L		
5	E		
6	L		
6	L		
6	E		
7	L		
7	L		
7	E		

Week	type	sections	topics
8	L		
8	L		
8	E		
9	L		
9	L		
9	E		
10	L		
10	L		
10	E		
11	L		
11	L		
11	E		
12	L		
12	L		
12	E		
13	L		
13	L		
13	E		
14	L		
14	L		
14	E		

13.5 List of exercises

1. Chapter 1: Non-interacting electrons
   (a) 1.6.1 Hydrogen molecule
   (b) 1.6.2 General diatomic molecule
   (c) 1.6.3 Linear chain of hydrogen atoms
   (d) 1.6.4 Insulating linear chain
   (e) 1.6.5 Free-electron gas or jellium model
   (f) ~~1.6.6 Thermodynamics of the hydrogen molecule~~
2. Chapter 2: Weakly interacting electrons
   (a) 2.9.1 The hydrogen atom in the Hartree-Fock approximation
   (b) 2.9.2 Two one-dimensional particles in a box
   (c) 2.9.3 Two fermions in a 1d-box
   (d) 2.9.4 Self-made density functional
3. Chapter 3: Second Quantization
   (a) ~~3.11.1 Hartree Fock at finite temperature~~
   (b) 3.11.2 Hydrogen molecule with interacting electrons !
   (c) 3.11.3 Spin eigenstates !
   (d) 3.11.4 Ground state of the linear chain in second quantization

4. Chapter 4: Green's functions in one-particle quantum mechanics
   (a) 4.6.1 ~~Role of boundary conditions~~
   (b) 4.6.2 Green's function for a Lorentzian-shaped density of states
5. Chapter 5: Composite and open systems: down-folding and retarded potentials
   (a) 5.4.1 Minimal model for a quantum system coupled to a bath
   (b) 5.4.2 System in contact with a bath having a finite lifetime
   (c) 5.4.3 Fano-Anderson model
   (d) 5.4.5 Surface Green's function of a one-dimensional linear chain
   (e) 5.4.6 ~~Interfaces and metal-induced gap states (sketch only)~~
   (f) 5.4.7 ~~Inelastic tunneling (Sketch only)~~
6. Chapter 6: Dynamics in Fock space and complex time
   No exercises yet
7. Chapter 7: Green's functions in many-particle physics
   (a) 7.6.1 Non-interacting contour Green's function for the non-interacting hy- drogen molecule
8. Chapter 8: Exact properties of the many-particle Green's function
   (a) 8.5.1 Self-energy and contour Green's function of the Hubbard atom
9. Chapter 9: Spectral properties
   (a) 9.6.1 Model for strongly retarded Green's function
   (b) ~~9.6.3 Exercise: Anderson impurity model~~
   (c) ~~9.6.4 Home study and practice: spectral function and momentum density of a 1d chain~~
10. Chapter 10: Diagrammatic expansion of the Green's function
    (a) 10.5.1 Green's function from generating functional
11. Chapter 11: Diagrammatics of the generating functional
    (a) 11.9.1 Enumerate permutations !
    (b) 11.9.2 Feynman diagrams from permutation vectors !
    (c) 11.9.3 Value of a Feynman diagrams ! `Editor: complete`
    (d) 11.9.4 Evaluate the symmetry factor ! `Editor: complete`
    (e) ~~11.9.5 Example: Evaluate the Green's function for a specific example~~

Part II

Appendices

Appendix A

Mathematical expressions

A.1 Laplace expansion theorem (not needed)

Let D be the determinant of an $N \times N$ matrix $\boldsymbol{A}$, and let $D^{i,j}_{N-1}$ be the determinant of the matrix obtained from $\boldsymbol{A}$ by deleting the i-th line and the j-th column. Then

$$D = \sum_{i=1}^{N} (-1)^{i+j} A_{i,j} D^{i,j}_{N-1}$$

The Laplace expansion theorem can be applied twice, leading to

$$D = \sum_{i=1}^{N} \sum_{k=1}^{N} (-1)^{i+j+k+l} A_{i,j} A_{k,l} D^{ik,jl}_{N-2}$$

where $D^{ik,jl}$ is the determinant of the matrix $\boldsymbol{A}$ with the i-th and k-th line, and the j-th and l-th column deleted.

A.2 Fourier transforms

Here, I summarize only the main formulas used in this lecture. More on the Fourier transform can be found in ΦSX:Quantum physics[14].

A.2.1 Choices

Fourier transforms in time

$$F(\omega) = \int dt\ f(t) \mathrm{e}^{i\omega t} \tag{A.1}$$

$$f(t) = \int \frac{d\omega}{2\pi}\ F(\omega) \mathrm{e}^{-i\omega t} \tag{A.2}$$

$$F(\epsilon) = \int dt\ f(t) \mathrm{e}^{\frac{i}{\hbar}\epsilon t} \tag{A.3}$$

$$f(t) = \int \frac{d\epsilon}{2\pi\hbar}\ F(\omega) \mathrm{e}^{-\frac{i}{\hbar}\epsilon t} \tag{A.4}$$

$f(t)$	$F(\omega)$
$\delta(t)$	1
1	$2\pi\delta(\omega)$

Fourier transforms in space

$$F(\vec{k}) = \int d^3r\ f(\vec{r})\mathrm{e}^{-i\vec{k}\vec{r}} \tag{A.5}$$

$$f(\vec{r}) = \int \frac{d^3k}{(2\pi)^3} F(\vec{k})\mathrm{e}^{i\vec{k}\vec{r}} \tag{A.6}$$

$$F(\vec{p}) = \int d^3r\ f(\vec{r})\mathrm{e}^{-\frac{i}{\hbar}\vec{p}\vec{r}} \tag{A.7}$$

$$f(\vec{p}) = \int \frac{d^3p}{(2\pi\hbar)^3} F(\vec{k})\mathrm{e}^{i\vec{k}\vec{r}} \tag{A.8}$$

A.2.2 Fourier transform of the step function

Here, we derive the relation

$$\int_{-\infty}^{\infty} dt\ \theta(t)\mathrm{e}^{\frac{i}{\hbar}(\epsilon+i\eta)t} = \frac{i\hbar}{\epsilon+i\eta} \tag{A.9}$$

$$\int_{-\infty}^{\infty} dt\ \theta(-t)\mathrm{e}^{\frac{i}{\hbar}(\epsilon-i\eta)t} = \frac{-i\hbar}{\epsilon-i\eta} \tag{A.10}$$

where $\eta > 0$.

Derivation:

$$\int_{-\infty}^{\infty} dt\ \theta(t)\mathrm{e}^{\frac{i}{\hbar}(\epsilon+i\eta)t} = \int_{0}^{\infty} dt\ \mathrm{e}^{\frac{i}{\hbar}(\epsilon+i\eta)t} = \frac{1}{\frac{i}{\hbar}(\epsilon+i\eta)}\mathrm{e}^{\frac{i}{\hbar}(\epsilon+i\eta)t}\Big|_0^{\infty}$$
$$\overset{\eta\geq 0}{=} \frac{-1}{\frac{i}{\hbar}(\epsilon+i\eta)} = \frac{i\hbar}{\epsilon+i\eta}$$

$$\int_{-\infty}^{0} dt\ \theta(-t)\mathrm{e}^{\frac{i}{\hbar}(\epsilon-i\eta)t} = \int_{-\infty}^{0} dt\ \mathrm{e}^{\frac{i}{\hbar}(\epsilon-i\eta)t} = \frac{1}{\frac{i}{\hbar}(\epsilon-i\eta)}\mathrm{e}^{\frac{i}{\hbar}(\epsilon-i\eta)t}\Big|_{-\infty}^{0}$$
$$\overset{\eta\geq 0}{=} \frac{1}{\frac{i}{\hbar}(\epsilon-i\eta)} = \frac{-i\hbar}{\epsilon-i\eta}$$

The function is a simple pole at $\epsilon = -i\eta$ or $\epsilon = +i\eta$ respectively.

A.3 Wirtinger derivatives

In order to form the derivatives with respect to complex numbers, it is advantageous to be familiar with the **Wirtinger derivatives**, which are described briefly in ΦSX: Klassische Mechanik.

Wirtinger derivatives The essence of Wirtinger derivatives is that we can write the identity

$$\begin{aligned} df &= \frac{\partial f}{\partial \mathrm{Re}[z]} d\mathrm{Re}[z] + \frac{\partial f}{\partial \mathrm{Im}[z]} d\mathrm{Im}[z] \\ &= \underbrace{\frac{1}{2}\Big(\frac{\partial f}{\partial \mathrm{Re}[z]} - i\frac{\partial f}{\partial \mathrm{Im}[z]}\Big)}_{df/dz} \underbrace{\Big(d\mathrm{Re}[z] + i d\mathrm{Im}[z]\Big)}_{dz} + \underbrace{\frac{1}{2}\Big(\frac{\partial f}{\partial \mathrm{Re}[z]} + i\frac{\partial f}{\partial \mathrm{Im}[z]}\Big)}_{df/dz^*} \underbrace{\Big(d\mathrm{Re}[z] - i d\mathrm{Im}[z]\Big)}_{dz^*} \\ &= \frac{df}{dz} dz + \frac{df}{dz^*} dz^* \end{aligned} \tag{A.11}$$

for the first variation of f. Thus, we can form the variations of a function of complex arguments, as if the variable and its complex conjugate were completely independent variables.
The Wirtinger derivatives are defined as

$$\begin{aligned} \frac{\partial f}{\partial z} &= \frac{1}{2}\Big(\frac{\partial f}{\partial \mathrm{Re}[z]} - i\frac{\partial f}{\partial \mathrm{Im}[z]}\Big) \\ \frac{\partial f}{\partial z^*} &= \frac{1}{2}\Big(\frac{\partial f}{\partial \mathrm{Re}[z]} + i\frac{\partial f}{\partial \mathrm{Im}[z]}\Big). \end{aligned} \tag{A.12}$$

The Wirtinger derivatives obey the following rules:

- linearity

$$\begin{aligned} \frac{\partial\Big(af(z,z^*) + bg(z,z^*)\Big)}{\partial z} &= a\frac{\partial f(z,z^*)}{\partial z} + b\frac{\partial g(z,z^*)}{\partial z} \\ \frac{\partial\Big(af(z,z^*) + bg(z,z^*)\Big)}{\partial z^*} &= a\frac{\partial f(z,z^*)}{\partial z^*} + b\frac{\partial g(z,z^*)}{\partial z^*} \end{aligned} \tag{A.13}$$

- product rule

$$\begin{aligned} \frac{\partial\Big(f(z,z^*)g(z,z^*)\Big)}{\partial z} &= \frac{\partial f(z,z^*)}{\partial z} g(z,z^*) + f(z,z^*)\frac{\partial g(z,z^*)}{\partial z} \\ \frac{\partial\Big(f(z,z^*)g(z,z^*)\Big)}{\partial z^*} &= \frac{\partial f(z,z^*)}{\partial z^*} g(z,z^*) + f(z,z^*)\frac{\partial g(z,z^*)}{\partial z^*} \end{aligned} \tag{A.14}$$

- complex conjugation

$$\begin{aligned} \frac{\partial\,[f(z,z^*)]^*}{\partial z} &= \left(\frac{\partial f(z,z^*)}{\partial z^*}\right)^* \\ \frac{\partial\,[f(z,z^*)]^*}{\partial z^*} &= \left(\frac{\partial f(z,z^*)}{\partial z}\right)^* \end{aligned} \tag{A.15}$$

- chain rule

$$\begin{aligned} \frac{\partial\Big[f\left(g(z,z^*), g^*(z,z^*)\right)\Big]}{\partial z} &= \frac{\partial f(g,g^*)}{\partial g}\frac{\partial g(z,z^*)}{\partial z} + \frac{\partial f(g,g^*)}{\partial g^*}\left(\frac{\partial g^*(z,z^*)}{\partial z}\right) \\ \frac{\partial\Big[f\left(g(z,z^*), g^*(z,z^*)\right)\Big]}{\partial z^*} &= \frac{\partial f(g,g^*)}{\partial g}\frac{\partial g(z,z^*)}{\partial z^*} + \frac{\partial f(g,g^*)}{\partial g^*}\left(\frac{\partial g(z,z^*)}{\partial z}\right)^* \end{aligned} \tag{A.16}$$

A complex function is analytic, if $\frac{\partial f}{\partial z^*} = 0$.
My personal recommendation is to produce the rules from the first variation of the complex function in terms of dz and dz', rather than to memorize these equations.

For the derivatives, we use

$$\frac{d\Psi_n^*(\vec{r},\sigma)}{d\Psi_k^*(\vec{r}_0,\sigma_0)} = \delta(\vec{r}-\vec{r}_0)\delta_{\sigma,\sigma_0}\delta_{n,k} \qquad \text{and} \qquad \frac{d\Psi_n(\vec{r},\sigma)}{d\Psi_k^*(\vec{r}_0,\sigma_0)} = 0 \tag{A.17}$$

A.4 Cauchy relation

Editor: It is not clear whether it should be kept.

(Cauchy relation Eq.2.23 of Stefanucci.)

$$\lim_{\eta\to 0^+} \frac{1}{\epsilon-\epsilon_0 \pm i\eta} = P\frac{1}{\epsilon-\epsilon_0} \mp i\pi\delta(\epsilon-\epsilon_0) \tag{A.18}$$

where P denotes the principal part.

Cauchy principal value is[Bronstein and Semendyayev 1997, p. 283]

$$P\int_a^b dx\, f(x) = \lim_{\epsilon\to 0^+}\left[\int_a^{c-\epsilon} dx\, f(x) + \int_{c+\epsilon}^b dx\, f(x)\right] \tag{A.19}$$

A.5 Imaginary part of a pole and spectral density

In Eq. 4.51 on p. 4.51, we used the identity

IMAGINARY PART OF A POLE AND THE DELTA FUNCTION

$$-\frac{1}{\pi}\lim_{\eta\to 0}\mathrm{Im}\left(\frac{1}{x+i\eta}\right) = \delta(x) \tag{A.20}$$

It is used to extract the density of states respectively the spectral function from a Green's function.

First, we determine the imaginary part

$$\frac{1}{x+i\eta} = \frac{x-i\eta}{x^2+\eta^2} \qquad \Rightarrow \qquad \mathrm{Im}\left(\frac{1}{x+i\eta}\right) = \frac{-\eta}{x^2+\eta^2} \tag{A.21}$$

The imaginary part of an inverse pole in the complex plane is closely related to a **Lorentzian** $L_\eta(x)$.

LORENTZIAN

$$L_\eta(x) \stackrel{\text{def}}{=} \frac{1}{\pi}\frac{\eta}{x^2+\eta^2} = -\frac{1}{\pi}\mathrm{Im}\left(\frac{1}{x+i\eta}\right) \tag{A.22}$$

The Lorentzian is fairly pathological function because of its long ranged tails. While the integral is defined, its first and higher moments $M_n = \int_{-\infty}^{\infty} dx\, x^n L(x)$ with $n \geq 1$ are ill-defined.

Let me demonstrate that the Lorentzian integrates to one. [1]

$$\int_{-\infty}^{\infty} dx\ \frac{\eta}{x^2+\eta^2} = \int_{-\infty}^{\infty} \frac{dx}{\eta}\ \frac{1}{\left(1+\frac{x}{\eta}\right)^2} \overset{z\overset{\text{def}}{=}\frac{x}{\eta}}{=} \int_{-\infty}^{\infty} dz\ \frac{1}{1+z^2} \overset{z(q)=\tan(q)}{=} \int_{-\infty}^{\infty} dz\ \frac{dq}{dz} = \int_{-\frac{\pi}{2}}^{\frac{\pi}{2}} dq = \pi$$

$$\Rightarrow \qquad \int_{-\infty}^{\infty} dx\ L_\eta(x) = 1 \tag{A.25}$$

Next I will demonstrate, that the Lorentzians approach the delta function for $\eta \to 0$.

$$\lim_{\eta\to 0} L_\eta(x) = \lim_{\eta\to 0} \mathrm{Im}\Big[-\frac{1}{\pi}\frac{\eta}{x^2+\eta^2}\Big] = \delta(x) \tag{A.26}$$

In other words, when the position $x + i\eta$ of the pole approaches the real axis, its imaginary part approaches, up to a constant, a delta function.

A complete proof for the identity of $L_0(x)$ with the delta function would need to establish

$$\int dx\ L_0(x) g(x) = g(0) \tag{A.27}$$

for any function that is differentiable to arbitrary high order.

Here. we we will show that it is a series of functions, that (1) integrate to one, that (2) are positive and that (3) approach zero except for the origin.

- We have already shown above that the integral of the Lorentzian equals unity.
- From the defining equation Eq. A.22, it is easily seen that a Lorentzian is positive everywhere.
- In the limit $\eta \to 0$, the Lorentzian vanishes except at the origin.

$$\lim_{\eta\to 0} \frac{\eta}{x^2+\eta^2} \overset{x\neq 0}{=} \lim_{\eta\to 0} \frac{\eta}{x^2} = 0 \qquad \text{for} \qquad x \neq 0 \tag{A.28}$$

Thus, we have shown that Eq. A.20 is valid.

A.6 Padé approximation

Editor: In progress:

The Padé approximation[2] is used to perform an analytic continuation of the Matsubara Green's function or the self energy from the imaginary frequency axis to the real frequency axis. Its values on the real frequency axis is the spectral function.

In this section, I am following the article of Schött et al. [doi:10.1103/PhysRevB.93.075104].

The Padé approximation is an interpolation of a complex function by a rational polynomial.

$$P_{k,r}(z) = \frac{\sum_{i=1}^{k+1} a_i z^{i-1}}{\left[\sum_{i=1}^{r} b_i z^{i-1}\right] + z^r} \tag{A.29}$$

[1] In the derivation, we use the variable transform

$$q(z) \overset{\text{def}}{=} \mathrm{atan}(z) \qquad \Rightarrow \qquad q(z=\pm\infty) = \pm\frac{\pi}{2} \tag{A.23}$$

$$z(q) = \tan(q) \qquad \Rightarrow \qquad \frac{dz}{dq} = \frac{\sin^2(q)+\cos^2(q)}{\cos^2(q)} = \frac{\sin^2(q)}{\cos^2(q)} + 1 = 1 + \tan^2(q) = 1 + z^2 \tag{A.24}$$

[2] Named after the French Mathematician Henri Padé. Earlier work has been published by Georg Frobenius. (Source: Wikipeida: Padé approximation)

This polynomial has poles at the zeros of the denominator, while the numerator controls the weights of the poles.

For large $|z|$ the function approaches

$$P_{k,r}(z) \to a_{k+1}z^{k-r} + \Big(a_k - a_{k+1}b_r\Big)z^{k-r-1} + \dots \tag{A.30}$$

For Greens function which fall off as $\frac{1}{z}$ the case $k = r - 1$ is relevant. The self energy behaves similarly, once the static contribution is subtracted. Therefore, we will be concerned with

$$P_r(z) = \frac{\sum_{i=1}^{r} a_i z^{i-1}}{\left[\sum_{i=1}^{r} b_i z^{i-1}\right] + z^r} \tag{A.31}$$

A.6.1 Problems

It is often said that the analytic continuation using the Padé approximation is unreliable when using noisy data as those obtained from a Quantum Monte Carlo calculation.

I myself made a few observations:

1. The spectral function is obtained from the imaginary part of the Green's function on the real frequency axis. If the poles are still close to the real frequency axis, small numerical errors can create results that vary strongly.

   The reason is that the imaginary part of a complex function varies extremely rapidly along the imaginary direction.

   $$-\frac{1}{\pi}\mathrm{Im}\left(\frac{1}{x+iy}\right) = -\frac{1}{\pi}\frac{y}{x^2+y^2} \overset{x\to 0}{\to} -\frac{1}{\pi}\frac{1}{y} \tag{A.32}$$

   Thus, a small shift, which displaces the pole across the real axis, can even change the sign of the density of states. A negative spectral function is furthermore nonphysical and renders the description useless.

   A possible remedy of this problem is to determine the spectral function for several lines, which are displaced along the imaginary component. This allows to identify the position of the pole and to correct it such that is falls on the correct side of the real frequency axis.

2. Matsubara Green's function spreads the information unevenly along the imaginary frequency axis. The Laurent expansion coefficients of the Green's function contain the energy moments of the spectral function, while the behavior close to the origin determines the structure of the spectral function near the Fermi level. The details of the spectral function are probably exponentially damped out beyond a few times $k_B T$ away from the Fermi level

   Therefore, I suggest to take one point for the interpolation at $i\omega_x$, which is the outermost point on the grid. The next few points are chosen at $\omega_j = i\omega_x 2^{-j}$. This captures the first few moments of the density of states. For the remaining points one could take the Matsubara frequencies next to the origin. The attempt to improve the result by increasing the points to be interpolated may worsen the results because it may give too much weight to region, where the Matsubara Green's function does not carry significant information.

A.6.2 Least-square Padé

From the requirement that the function $f(z)$ to be interpolated is represented at a given point z by the rational polynomial, we obtain the conditions

$$f(z) = P_r(z) \overset{\text{Eq. A.31}}{=} \frac{\sum_{i=1}^{r} a_i z^{i-1}}{\left[\sum_{i=1}^{r} b_i z^{i-1}\right] + z^r} \tag{A.33}$$

we obtain

$$\sum_{i=1}^{r} \left(z^{i-1}\right) a_i + \sum_{i=1}^{r} \left(-f(z)z^{i-1}\right) b_i = f(z)z^r \tag{A.34}$$

Let us now require the identity $f(z) = P_r(z)$ for a set of M points z_j with $j = 1, \ldots, M$. We obtain an equation system with M equations and $2r$ unknowns, the coefficients a_i and b_i.

$$\sum_{i=1}^{r} \left(z_j^{i-1}\right) a_i + \sum_{i=1}^{r} \left(-f(z_j)z_j^{i-1}\right) b_i = f(z_j)z_j^r \quad \text{for } j = 1, M \tag{A.35}$$

This system of equations is overdetermined with $M > 2r$. Therefore, we solve it with singular-value decomposition, which amounts to a least-square fit. The singular-value decomposition is a standard linear algebra operation, which is for example implemented in the numerical library LAPACK.

The singular value decomposition rewrites a $M \times 2r$ matrix $\boldsymbol{A}$ as

$$\boldsymbol{A} = \boldsymbol{U}\boldsymbol{\Sigma}\boldsymbol{V}^\dagger \tag{A.36}$$

where $\boldsymbol{U}$ is a unitary $M \times M$ matrix, $\boldsymbol{\Sigma}$ is a diagonal $M \times 2r$ matrix holding the real-values singular values on the diagonal. $\boldsymbol{V}$ is a unitary $2r \times 2r$ matrix.

The equation system $\boldsymbol{A}\vec{x} = \vec{b}$ can be solves approximately by

$$\boldsymbol{A}\vec{x} = \boldsymbol{U}\boldsymbol{\Sigma}\boldsymbol{V}^\dagger\vec{x} = \vec{b} \quad \Rightarrow \quad \vec{x} = \boldsymbol{V}\Sigma^{-1}\boldsymbol{U}^\dagger\vec{b} \tag{A.37}$$

The inversion of the singular values is done such that the inverse of a zero singular value is set to zero. This implies that the corresponding contribution is projected out.

The resulting vector x contains the coefficients a_i and b_i. This defines the interpolating rational polynomial, which can be evaluated for the desired values.

Sum of poles: The rational polynomial can be transformed into a sum of poles

$$P_r(z) \overset{\text{Eq. A.31}}{=} \frac{\sum_{i=1}^{r} a_i z^{i-1}}{\left[\sum_{i=1}^{r} b_i z^{i-1}\right] + z^r} = \sum_{k=1}^{r} \frac{A_k}{z - \bar{z}_k} \tag{A.38}$$

The coefficients are obtained as follows. First, we determine the poles $\bar{z}_k$ of the rational polynomial. The pole positions are the zeros of the polynomial in the denominator of the rational polynomial. The zero's can be obtained using the method of Vieta.

$$\begin{aligned}
P_r(z) = \frac{\sum_{i=1}^{r} a_i z^{i-1}}{\prod_{j=1}^{r}(z - \bar{z}_j)} &= \sum_{k=1}^{r} \frac{A_k}{z - z_k} \\
\Leftrightarrow \quad \sum_{i=1}^{r} a_i z^{i-1} &= \sum_{k=1}^{r} A_k \prod_{j=1; j\neq k}^{r} (z - \bar{z}_j) \\
\Rightarrow \quad \sum_{i=1}^{r} a_i \bar{z}_\ell^{i-1} &= \sum_{k=1}^{r} A_k \prod_{j=1; j\neq k}^{r} (\bar{z}_\ell - \bar{z}_j) = A_\ell \prod_{j=1; j\neq \ell}^{r} (\bar{z}_\ell - \bar{z}_j) \\
\Rightarrow \quad A_\ell &= \frac{\sum_{i=1}^{r} a_i \bar{z}_\ell^{i-1}}{\prod_{j=1; j\neq \ell}^{r}(\bar{z}_\ell - \bar{z}_j)}
\end{aligned} \tag{A.39}$$

Thus, we obtain as interpolation

$$P(z) = \sum_{k=1}^{r} \frac{1}{z - \bar{z}_k} \frac{\sum_{i=1}^{r} a_i \bar{z}_k^{i-1}}{\prod_{j=1; j\neq k}^{r}(\bar{z}_k - \bar{z}_j)} \tag{A.40}$$

Sum of poles: If the poles are on the wrong side of the real frequency axis, it will contribute with the wrong sign to the spectral function. Therefore, we shift all poles with the wrong imaginary part onto the real frequency axis.

In order to smoothen the spectral function I evaluate the spectral function on the imaginary axis.

A.7 Baker-Hausdorff Theorem

The Baker-Hausdorff theorem [3][94, 95, 96, 97, 98, 99] provides a method to evaluate the product of two exponentials of non-commutating operators[100]. Specifically we look for the resulting operator $\hat{C}$ of

$$e^{\hat{A}}e^{\hat{B}} = e^{\hat{C}}$$

for two given operators A, B.

Here, we will only investigate a few special cases.

A.7.1 Baker-Hausdorff Theorem

Here I show a specialization of the Baker-Haussdorf theorem, which applies if certain commutator relations hold.

BAKER-HAUSDORFF THEOREM

$$e^{\hat{A}+\hat{B}} = e^{\hat{A}}e^{\hat{B}}e^{-\frac{1}{2}[\hat{A},\hat{B}]_-} \tag{A.41}$$

if both operators commutate with their commutator, i.e.

$$[\hat{A},[\hat{A},\hat{B}]_-]_- = [\hat{B},[\hat{A},\hat{B}]_-]_- = 0 \tag{A.42}$$

Proof:[4]

$$\begin{aligned} F(\alpha) &\stackrel{\text{def}}{=} e^{\alpha\hat{A}+\beta\hat{B}} \\ \frac{dF}{d\alpha} &= \frac{d}{d\alpha}\sum_{n=0}^{\infty}\frac{1}{n!}(\alpha\hat{A}+\beta\hat{B})^n \\ &= \sum_{n=0}^{\infty}\frac{1}{n!}\sum_{j=0}^{n-1}(\alpha\hat{A}+\beta\hat{B})^j\hat{A}(\alpha\hat{A}+\beta\hat{B})^{n-j-1} \end{aligned}$$

Let us now analyze the individual terms:

$$\begin{aligned} (\alpha\hat{A}+\beta\hat{B})\hat{A} &= \hat{A}(\alpha\hat{A}+\beta\hat{B}) + \beta[\hat{B},\hat{A}]_- \\ (\alpha\hat{A}+\beta\hat{B})^k\hat{A} &= (\alpha\hat{A}+\beta\hat{B})^{k-1}\hat{A}(\alpha\hat{A}+\beta\hat{B}) + (\alpha\hat{A}+\beta\hat{B})^{k-1}\beta[\hat{B},\hat{A}]_- \\ &\stackrel{\text{Eq. A.42}}{=} (\alpha\hat{A}+\beta\hat{B})^{k-1}\hat{A}(\alpha\hat{A}+\beta\hat{B}) + \beta[\hat{B},\hat{A}]_-(\alpha\hat{A}+\beta\hat{B})^{k-1} \\ &= \hat{A}(\alpha\hat{A}+\beta\hat{B})^k + k\beta[\hat{B},\hat{A}]_-(\alpha\hat{A}+\beta\hat{B})^{k-1} \end{aligned}$$

[3] Felix Hausdorff, 1868-1942 German mathematician. Professor in Leipzig, Bonn, Greifswald, Bonn. Is considered as co-founder of the modern topology. He invented the Hausdorff dimension, which is used to characterize fractals. The corresponding work is the most cited original paper in mathematics between 1910 and 1920. The Jewish Hausdorff, his wife and her sister committed suicide as they about to be deported into a concentration camp under the NS Dictatorship.

[4] from *Cavity Quantum Electrodynamics: The Strange Theory of Light in a Box*, S.M. Dutra, (John Wiley, 2005)

$$\begin{aligned}
\frac{dF}{d\alpha} &= \sum_{n=0}^{\infty}\frac{1}{n!}\sum_{j=0}^{n-1}(\alpha\hat{A}+\beta\hat{B})^j\hat{A}(\alpha\hat{A}+\beta\hat{B})^{n-j-1} \\
&= \sum_{n=0}^{\infty}\frac{1}{n!}\sum_{j=0}^{n-1}\left(\hat{A}(\alpha\hat{A}+\beta\hat{B})^{n-1}+j\beta[\hat{B},\hat{A}]_-(\alpha\hat{A}+\beta\hat{B})^{n-2}\right) \\
&= \sum_{n=0}^{\infty}\frac{1}{n!}\left(n\hat{A}(\alpha\hat{A}+\beta\hat{B})^{n-1}+\frac{n(n-1)}{2}\beta[\hat{B},\hat{A}]_-(\alpha\hat{A}+\beta\hat{B})^{n-2}\right) \\
&= \hat{A}\sum_{n=1}^{\infty}\frac{1}{(n-1)!}(\alpha\hat{A}+\beta\hat{B})^{n-1}+\frac{1}{2}\beta[\hat{B},\hat{A}]_-\sum_{n=2}^{\infty}\frac{1}{(n-2)!}(\alpha\hat{A}+\beta\hat{B})^{n-2} \\
&= \left(\hat{A}+\frac{1}{2}\beta[\hat{B},\hat{A}]_-\right)F(\alpha)
\end{aligned}$$

This is a differential equation for $F(\alpha)$, which can be solved as if the operator were a number because only one operator, namely $\hat{A}+\frac{1}{2}\beta[\hat{B},\hat{A}]_-$ is involved.

We obtain

$$\begin{aligned}
F(\alpha) = F(0)\mathrm{e}^{\alpha\left(\hat{A}+\frac{1}{2}\beta[\hat{B},\hat{A}]_-\right)} &= \mathrm{e}^{\beta\hat{B}}\left(\mathrm{e}^{\alpha\hat{A}}\mathrm{e}^{\frac{1}{2}\alpha\beta[\hat{B},\hat{A}]_-}\right) \\
\Rightarrow \qquad \mathrm{e}^{\alpha\hat{A}+\beta\hat{B}} = \mathrm{e}^{\beta\hat{B}}\mathrm{e}^{\alpha\hat{A}}\mathrm{e}^{\frac{1}{2}\alpha\beta[\hat{B},\hat{A}]_-} &= \mathrm{e}^{\beta\hat{B}}\mathrm{e}^{\alpha\hat{A}}\mathrm{e}^{-\frac{1}{2}\alpha\beta[\hat{A},\hat{B}]_-} \qquad \text{q.e.d.}
\end{aligned}$$

In the last step, we exploited that $\hat{A}$ commutates with the commutator $[\hat{A},\hat{B}]_-$, so that we can disentangle the exponential as if the operators were numbers.

A.7.2 Hadamard Lemma

The Hadamard Lemma is a specialization of Zassenhaus formula[100], which again is a variant of the Baker-Campbell-Hausdorff theorem. It is useful to work out simple operators in the interaction picture.

HADAMARD' S LEMMA

$$\begin{aligned}
\mathrm{e}^{\lambda\hat{A}}\hat{B}\mathrm{e}^{-\lambda\hat{A}} &\overset{\text{Eq. A.47}}{=} \sum_{n=0}^{\infty}\hat{X}_n\lambda^n \\
\text{with} \qquad \hat{X}_{n+1} &= \frac{1}{n+1}[\hat{A},\hat{X}_n]_- \qquad \text{and} \qquad \hat{X}_0 = \hat{B}
\end{aligned} \tag{A.43}$$

$$\mathrm{e}^{\lambda\hat{A}}\hat{B}\mathrm{e}^{-\lambda\hat{A}} = \left(\sum_{i=0}^{\infty}\frac{1}{i!}(\lambda\hat{A})^i\right)\hat{B}\left(\sum_{j=0}^{\infty}\frac{1}{j!}(-\lambda\hat{A})^j\right) \tag{A.44}$$

$$= \sum_{n=0}^{\infty}\lambda^n\underbrace{\left(\sum_{j=0}^{n}\frac{(-1)^j}{(n-j)!j!}\hat{A}^{n-j}\hat{B}\hat{A}^j\right)}_{\hat{X}_n} \tag{A.45}$$

Let us now work out the expression denoted $\hat{X}_n$ in Eq. A.45. $\hat{X}_0 = \hat{B}$ can be determined directly. The higher $\hat{X}_n$ are obtained by recursion.

$$\begin{aligned}
[\hat{A}, \hat{X}_n]_- &= \sum_{j=0}^{n} \frac{(-1)^j}{(n-j)!j!} \hat{A}^{n+1-j} \hat{B} \hat{A}^j - \sum_{j=0}^{n} \frac{(-1)^j}{(n-j)!j!} \hat{A}^{n-j} \hat{B} \hat{A}^{j+1} \\
&= \sum_{j=0}^{n} \frac{(n+1-j)(-1)^j}{(n+1-j)!j!} \hat{A}^{n+1-j} \hat{B} \hat{A}^j + \sum_{j=0}^{n} \frac{(j+1)(-1)^{j+1}}{(n+1-(j+1))!(j+1)!} \hat{A}^{n+1-(j+1))} \hat{B} \hat{A}^{j+1} \\
&\overset{j+1 \to j}{=} \sum_{j=0}^{n} \frac{(n+1-j)(-1)^j}{(n+1-j)!j!} \hat{A}^{n+1-j} \hat{B} \hat{A}^j + \sum_{k=1}^{n+1} \frac{j(-1)^j}{(n+1-j)!j!} \hat{A}^{n+1-j))} \hat{B} \hat{A}^j \\
&= (n+1) \sum_{j=0}^{n+1} \left(\frac{(-1)^j}{(n+1-j)!j!} \hat{A}^{n+1-j} \hat{B} \hat{A}^j \right. \\
&= (n+1) \hat{X}_{n+1}
\end{aligned} \tag{A.46}$$

Thus, we obtain the Baker-Campbell-Hausdorff theorem saying

$$\begin{aligned}
e^{\lambda \hat{A}} \hat{B} e^{-\lambda \hat{A}} &\overset{\text{Eq. A.45}}{=} \sum_{n=0}^{\infty} \hat{X}_n \lambda^n \\
\text{with} \qquad \hat{X}_{n+1} &\overset{\text{Eq. A.46}}{=} \frac{1}{n+1} [\hat{A}, \hat{X}_n]_- \qquad \text{and} \qquad \hat{X}_0 = \hat{B}
\end{aligned} \tag{A.47}$$

A.8 Sum rules related to the f-sum rule

Source: W. Thomas, "Über die Zahl der Dispersionselectronen, die einem stationären Zustande zugeordnet sind. Vorläufige Mitteilung", Naturwiss. 13, 627 (1925); W. Kuhn, "Über die Gesamtstärke der von einem Zustande ausgehenden Absorptionslinien", Z. Phys. 33, 408-412 (1925); F. Reiche and W. Thomas, "Über die Zahl der Dispersionselektronen, die einem stationären Zustand zugeordnet sind", ibid. 34, 510-525 (1925)

A.8.1 General derivation by Wang

I follow here the very general derivation given by Wang[101], from which a number of other sum rules can be derived in a straightforward manner.

For a general operator $\hat{A}$ we obtain

$$\begin{aligned}
\sum_n (E_n - E_0) \left| \langle 0|\hat{A}|n\rangle \right|^2 &= \sum_n (E_n - E_0) \langle 0|\hat{A}|n\rangle \langle n|\hat{A}^\dagger|0\rangle \\
&= \sum_n \Big(-\langle 0|\hat{H}\hat{A}|n\rangle + \langle 0|\hat{A}\hat{H}|n\rangle \Big) \langle n|\hat{A}^\dagger|0\rangle \\
&= \sum_n \langle 0|[\hat{A}, \hat{H}]_-|n\rangle \langle n|\hat{A}^\dagger|0\rangle \\
&= \langle 0|[\hat{A}, \hat{H}]_- \hat{A}^\dagger|0\rangle
\end{aligned} \tag{A.48}$$

We proceed completely analogously but for the commutator with the second matrix element

$$\begin{aligned}\sum_n (E_n - E_0)\left|\langle 0|\hat{A}^\dagger|n\rangle\right|^2 &= \sum_n (E_n - E_0)\langle 0|\hat{A}^\dagger|n\rangle\langle n|\hat{A}|0\rangle \\ &= \sum_n \langle 0|\hat{A}^\dagger|n\rangle\Big(\langle n|\hat{H}\hat{A}|0\rangle - \langle n|\hat{A}\hat{H}|0\rangle\Big) \\ &= -\sum_n \langle 0|\hat{A}^\dagger|n\rangle\langle n|[\hat{A},\hat{H}]|0\rangle \\ &= -\langle 0|\hat{A}^\dagger[\hat{A},\hat{H}]|0\rangle \end{aligned} \tag{A.49}$$

Adding the two results, Eq. A.48 and Eq. A.49, yields

WANG'S SUM RULE

$$\sum_n (E_n - E_0)\left(\left|\langle 0|\hat{A}|n\rangle\right|^2 + \left|\langle 0|\hat{A}^\dagger|n\rangle\right|^2\right) = \langle 0|\left[\hat{A}^\dagger,\left[\hat{A},\hat{H}\right]_-\right]_-|0\rangle \tag{A.50}$$

This is a rather general result, from which the f-sum rule can be obtained by choosing $\hat{A} = \hat{x}$ and the one-dimensional Hamilton operator of the form $\hat{H} = \frac{\hat{p}^2}{2m} + V(\hat{x})$.

A.8.2 f-sum rule or Thomas-Reiche-Kuhn sum rule

The **f-sum rule** or **Thomas-Reiche-Kuhn sum rule** can be obtained from Eq. A.50 with $\hat{A} = \hat{\vec{r}}$ and the one-dimensional Hamilton operator of the form $\hat{H} = \frac{\hat{\vec{p}}^2}{2m} + V(\hat{\vec{r}})$. Here we first calculate the one-dimensional case from which the three-dimensional can be obtained immediately.

Hence, we insert $\hat{A} = \hat{x}$ and the one-dimensional Hamilton operator of the form $\hat{H} = \frac{\hat{p}^2}{2m} + V(\hat{x})$ into Wang's sum rule Eq. A.50. We begin with the right-hand side of Eq. A.50.

$$\begin{aligned}\left[\hat{H},\hat{x}\right]_- &= \left[\frac{\hat{p}^2}{2m} + V(\hat{x}),\hat{x}\right]_- = \frac{1}{2m}\Big(\hat{p}^2\hat{x} \underbrace{-\hat{p}\hat{x}\hat{p} + \hat{p}\hat{x}\hat{p}}_{=0} - \hat{x}\hat{p}^2\Big) \\ &= \frac{1}{2m}\Big(\hat{p}\left[\hat{p},\hat{x}\right]_- + \left[\hat{p},\hat{x}\right]_-\hat{p}\Big) = \frac{1}{2m}\frac{\hbar}{i}\Big(\hat{p}+\hat{p}\Big) = \frac{-i\hbar}{m}\hat{p}\end{aligned} \tag{A.51}$$

$$\left[\hat{x}^\dagger,\left[\hat{H},\hat{x}\right]_-\right]_- \overset{\text{Eq. A.51}}{=} \left[\hat{x}^\dagger,\frac{-i\hbar}{m}\hat{p}\right]_- = \frac{-i\hbar}{m}\left[\hat{x}^\dagger,\hat{p}\right]_- = \frac{\hbar^2}{m} \tag{A.52}$$

Thus, we obtain with Eq. A.50

$$\sum_n (E_n - E_0)\left|\langle 0|\hat{x}|n\rangle\right|^2 = \frac{\hbar^2}{2m} \tag{A.53}$$

which is the one-dimensional version of the f-sum rule.

Now, we sum over the three coordinates and obtain the f- or Thomas-Reiche sum rule.

F-SUM RULE OR THOMAS-REICHE-KUHN SUM RULE

$$\sum_n (E_n - E_0)\left|\langle 0|\hat{\vec{r}}|n\rangle\right|^2 = \frac{3\hbar^2}{2m} \tag{A.54}$$

A.8.3 Bethe sum rule

The **Bethe sum rule** can be obtained from Eq. A.50 with $\hat{A} = e^{i\vec{q}\hat{r}}$ and the Hamiltonian $\hat{H} = \frac{\hat{\vec{p}}^2}{2m} + V(\hat{r})$.

$$\begin{aligned}\left[\hat{H}, e^{i\vec{q}\hat{r}}\right]_- &= \left[\frac{\hat{\vec{p}}^2}{2m} + V(\hat{r}), e^{i\vec{q}\hat{r}}\right]_- = \frac{1}{2m}\Big(\hat{\vec{p}}^2 e^{i\vec{q}\hat{r}} \underbrace{-\hat{\vec{p}} e^{i\vec{q}\hat{r}}\hat{\vec{p}} + \hat{\vec{p}} e^{i\vec{q}\hat{r}}\hat{\vec{p}}}_{=0} - e^{i\vec{q}\hat{r}}\hat{\vec{p}}^2\Big) \\ &= \frac{1}{2m}\Big(\hat{\vec{p}}\left[\hat{\vec{p}}, e^{i\vec{q}\hat{r}}\right]_- + \left[\hat{\vec{p}}, e^{i\vec{q}\hat{r}}\right]_-\hat{\vec{p}}\Big) = \frac{1}{2m}\Big(\hat{\vec{p}}\hbar\vec{q}e^{i\vec{q}\hat{r}} + \hbar\vec{q}e^{i\vec{q}\hat{r}}\hat{\vec{p}}\Big) \\ &= \frac{\hbar\vec{q}}{2m}\Big(\hat{\vec{p}}e^{i\vec{q}\hat{r}} + e^{i\vec{q}\hat{r}}\hat{\vec{p}}\Big) \end{aligned} \tag{A.55}$$

$$\begin{aligned}\left[\left(e^{i\vec{q}\hat{r}}\right)^\dagger, \left[\hat{H}, e^{i\vec{q}\hat{r}}\right]_-\right]_- &\overset{\text{Eq. A.55}}{=} \left[e^{-i\vec{q}\hat{r}}, \frac{\hbar\vec{q}}{2m}\Big(\hat{\vec{p}}e^{i\vec{q}\hat{r}} + e^{i\vec{q}\hat{r}}\hat{\vec{p}}\Big)\right]_- \\ &= \frac{\hbar\vec{q}}{2m}\Big(e^{-i\vec{q}\hat{r}}\underbrace{\hat{\vec{p}}e^{i\vec{q}\hat{r}}}_{\hbar\vec{q}e^{i\vec{q}\hat{r}}+e^{i\vec{q}\hat{r}}\hat{\vec{p}}} \underbrace{+\hat{\vec{p}} - \hat{\vec{p}}}_{=0} - e^{i\vec{q}\hat{r}}\underbrace{\hat{\vec{p}}e^{-i\vec{q}\hat{r}}}_{-\hbar\vec{q}e^{-i\vec{q}\hat{r}}+e^{-i\vec{q}\hat{r}}\hat{\vec{p}}}\Big) \\ &= \frac{\hbar\vec{q}}{2m}\Big((\hbar\vec{q} + \hat{\vec{p}}) - (-\hbar\vec{q} + \hat{\vec{p}})\Big) = \frac{(\hbar\vec{q})^2}{m} \end{aligned} \tag{A.56}$$

Insertion into Wang's sum rule Eq. A.50 results in **Bethe's sum rule**.

BETHE SUM RULE

$$\sum_n (E_n - E_0)\left|\langle 0|e^{i\vec{q}\hat{r}}|n\rangle\right|^2 = \frac{(\hbar\vec{q})^2}{2m} \tag{A.57}$$

A.9 Friedel sum rule

Editor: This section on the Friedel sum rule is preliminary. It is geared strongly towards the Anderson impurity model

Editor: For the Friedel sum rule, see also Jones and March *"Theoretical Solid State Physics"* Vol. 2 section 10.3.3, p.993.

Editor: I am following Antoine Georges[102], *" The beauty of impurities: Two revivals of Friedel's virtual bound-state concept"* C. R. Physique 17 (2016) 430-446. (C.R.Physique=Comptes Rendus Physique) http://dx.doi.org/10.1016/j.crhy.2015.12.005

Consider an impurity in an otherwise homogeneous material

$$\hat{H} = \sum_\sigma \epsilon_d \hat{d}^\dagger_\sigma \hat{d}_\sigma + \sum_k \sum_{\sigma\in\{\uparrow,\downarrow\}} \epsilon_{\vec{k}} \hat{c}^\dagger_{\vec{k},\sigma}\hat{c}_{\vec{k},\sigma} + \sum_{\sigma\in\{\uparrow,\downarrow\}}\sum_k V_{\vec{k},\sigma}\left(\hat{d}^\dagger_\sigma \hat{c}_{\vec{k},\sigma} + \hat{c}^\dagger_{\vec{k},\sigma}\hat{d}_\sigma\right) \tag{A.58}$$

For the sake of simplicity, I drop the spin index.

$$\hat{H} = \epsilon_d \hat{d}^\dagger \hat{d} + \sum_k \epsilon_{\vec{k}}\hat{c}^\dagger_{\vec{k}}\hat{c}_{\vec{k}} + \sum_k V_{\vec{k}}\left(\hat{d}^\dagger\hat{c}_{\vec{k}} + \hat{c}^\dagger_{\vec{k}}\hat{d}\right) \tag{A.59}$$

The resulting Hamiltonian describes **spin-less fermions**. The physics, however, is that of paired electrons, where the spin-up electrons behave exactly like the spin-down electrons. Other names would be that of a **spin-restricted** or **non-spin-polarized** calculation.

The bare Green's functions for the isolated impurity of the decoupled bath are

$$\begin{aligned}\bar{G}_d(\epsilon) &= \frac{1}{\epsilon - \bar{\epsilon}_d + i0^+} \\ \bar{G}^{(c)}_{\vec{k},\vec{k'}}(\epsilon) &= \delta_{\vec{k},\vec{k'}} \frac{1}{\epsilon - \bar{\epsilon}(\vec{k}) + i0^+}\end{aligned} \tag{A.60}$$

The full Green's function are then

$$\begin{aligned}G^{(d)}(\epsilon) &= \left(\left(\bar{G}^{(d)}(\epsilon) \right)^{-1} - \underbrace{\vec{V} \boldsymbol{\bar{G}}^{(c)}(\epsilon) \vec{V}}_{\Sigma^{(d)}(\epsilon)} \right)^{-1} = \left(\epsilon - \bar{\epsilon}_d - \Sigma^{(d)}(\epsilon) \right)^{-1} \\ G^{(d)}(\epsilon) &= \left(\epsilon - \bar{\epsilon}_d - \sum_{\vec{k},\vec{k'}} V_{\vec{k}} \bar{G}^{(c)}_{\vec{k},\vec{k'}}(\epsilon) V_{\vec{k'}} \right)^{-1} \\ \boldsymbol{G}^{(c)}(\epsilon) &= \left(\left(\bar{\boldsymbol{G}}^{(c)}(\epsilon) \right)^{-1} - \underbrace{\vec{V} \otimes \bar{G}^{(d)}(\epsilon) \otimes \vec{V}}_{\boldsymbol{\Sigma}^{(c)}(\epsilon)} \right)^{-1} \\ &= \sum_{n=0}^{\infty} \left(\bar{\boldsymbol{G}}^{(c)} \boldsymbol{\Sigma}^{(c)} \right)^n \bar{\boldsymbol{G}}^{(c)} \\ &= \bar{\boldsymbol{G}}^{(c)} + \bar{\boldsymbol{G}}^{(c)} \underbrace{\left[\sum_{n=0} \left(\boldsymbol{\Sigma}^{(c)} \bar{\boldsymbol{G}}^{(c)} \right)^n \boldsymbol{\Sigma}^{(c)} \right]}_{= \boldsymbol{T} \text{ reducible self energy}} \bar{\boldsymbol{G}}^{(c)} \\ &= \bar{\boldsymbol{G}}^{(c)}(\epsilon) + \bar{\boldsymbol{G}}^{(c)}(\epsilon) \boldsymbol{T}^{(c)} \bar{\boldsymbol{G}}^{(c)}(\epsilon) \\ G^{(c)}_{\vec{k},\vec{k'}}(\epsilon) &= \bar{G}^{(c)}_{\vec{k}}(\epsilon) \delta_{\vec{k},\vec{k'}} + \bar{G}^{(c)}_{\vec{k}}(\epsilon) T_{\vec{k},\vec{k'}}(\epsilon) G^{(c)}_{\vec{k'}}(\epsilon)\end{aligned} \tag{A.61}$$

where $\boldsymbol{T}$ is the **scattering T-matrix**. The T-matrix is the reducible self energy for the conduction electrons.

$$\boldsymbol{T} = \boldsymbol{\Sigma} + \boldsymbol{\Sigma} \bar{\boldsymbol{G}}^{(c)} \boldsymbol{\Sigma} + \ldots = \boldsymbol{\Sigma} + \boldsymbol{\Sigma} \bar{\boldsymbol{G}}^{(c)} \boldsymbol{T} \tag{A.62}$$

In the present case this yields

$$\begin{aligned}\boldsymbol{T} &= \boldsymbol{\Sigma} + \boldsymbol{\Sigma} \bar{\boldsymbol{G}}^{(c)} \boldsymbol{\Sigma} + \ldots \\ &= \underbrace{\vec{V} \left\{ \bar{G}^{(d)} + \bar{G}^{(d)} \underbrace{\vec{V} \bar{\boldsymbol{G}}^{(c)} \vec{V}}_{\Sigma^{(d)}} \bar{G}^{(d)} + \bar{G}^{(d)} \underbrace{\vec{V} \bar{\boldsymbol{G}}^{(c)} \vec{V}}_{\Sigma^{(d)}} \bar{G}^{(d)} \underbrace{\vec{V} \bar{\boldsymbol{G}}^{(c)} \vec{V}}_{\Sigma^{(d)}} \bar{G}^{(d)} + \ldots \right\} \vec{V}}_{G^{(d)}(\epsilon)} \\ &= \vec{V} G^{(d)}(\epsilon) \vec{V}\end{aligned} \tag{A.63}$$

I used the impurity Green's function

$$\begin{aligned}G^{(d)}(\epsilon) &= \frac{1}{\epsilon - \epsilon_d - \Sigma^d(\epsilon) + i\Gamma} = \frac{1}{\epsilon - \epsilon_d - \mathrm{Re}\left[\Sigma^d(\epsilon)\right] - i\left(\mathrm{Im}\left[\Sigma^d(\epsilon)\right] - \Gamma\right)} \\ &= \frac{\left(\epsilon - \epsilon_d - \mathrm{Re}[\Sigma^d]\right) + i\left(\mathrm{Im}[\Sigma^d] - \Gamma\right)}{\left(\epsilon - \epsilon_d - \mathrm{Re}[\Sigma^d]\right)^2 + \left(\mathrm{Im}[\Sigma^d] - \Gamma\right)^2}\end{aligned} \tag{A.64}$$

Scattering phase shift: The **scattering phase shift** $\delta(\omega)$ is defined by

$$T_{\vec{k},\vec{k'}}(\epsilon) = -|T_{\vec{k},\vec{k'}}(\epsilon)| e^{i\varphi_{\vec{k},\vec{k'}}(\epsilon)} \tag{A.65}$$

Under the simplification, that the coupling parameters $V_{\vec{k}}$ are all real-valued, the phase shifts $\varphi_{\vec{k},\vec{k}'}(\epsilon)$ are equal to that of the bare impurity Green's function, and thus they are equal for all scattering processes. Editor: Is this a harmless restriction, or is it central to the proof?

$$G^{(d)}(\epsilon) = -|G^{(d)}(\epsilon)|e^{i\varphi(\epsilon)} \tag{A.66}$$

Hence

$$\begin{aligned}\varphi(\epsilon) &= \arg(-G^{(d)}(\epsilon)) = \frac{\pi}{2} + n\pi - \arctan\left[\frac{\mathrm{Re}[G^{(d)}(\epsilon)]}{\mathrm{Im}[G^{(d)}(\epsilon)]}\right] \\ \tan\left(\varphi(\epsilon)\right) &= \frac{\mathrm{Im}[G^{(d)}(\epsilon)]}{\mathrm{Re}[G^{(d)}(\epsilon)]} = \frac{\mathrm{Im}\left[\Sigma^{d}(\epsilon)\right] - \Gamma}{\epsilon - \epsilon_d - \mathrm{Re}[\Sigma^{d}]}\end{aligned} \tag{A.67}$$

The factor $n\pi$ has been added, because n counts the number of states below the chosen energy. (Number of nodes)

Spectral function: The spectral function on the impurity is

$$\begin{aligned}\mathcal{A}^{(d)}(\epsilon) &= \frac{1}{\pi}\mathrm{Im}[G^{(d)}(\epsilon)] = \frac{1}{\pi}\frac{\left(\mathrm{Im}\left[\Sigma^{d}(\epsilon)\right] - \Gamma\right)}{\left(\epsilon - \epsilon_d - \mathrm{Re}\left[\Sigma^{d}(\epsilon)\right]\right)^2 + \left(\mathrm{Im}\left[\Sigma^{d}(\epsilon)\right] - \Gamma\right)^2} \\ &\overset{\text{Eq. A.67}}{=} \frac{1}{\pi}\frac{\left(\mathrm{Im}[\Sigma^{d}] - \Gamma\right)}{\left(\tan^{-2}\left(\varphi(\epsilon)\right) + 1\right)\left(\mathrm{Im}\left[\Sigma^{d}(\epsilon)\right] - \Gamma\right)^2} = \frac{1}{\pi\left(\mathrm{Im}\left[\Sigma^{d}(\epsilon)\right] - \Gamma\right)}\frac{1}{1 + \tan^{-2}\left(\varphi(\epsilon)\right)} \\ &= \frac{\sin^2(\varphi(\epsilon))}{\pi\left(\mathrm{Im}\left[\Sigma^{d}(\epsilon)\right] - \Gamma\right)}\end{aligned} \tag{A.68}$$

Occupation on the impurity: Let me integrate the bare Green's function of the impurity to obtain the number of d-electrons. **The bare Green's function is used as opposed to the full d-Green's function for the sake of simplicity.**

$$\begin{aligned}n_d &\approx \int_{-\infty}^{\mu} d\epsilon\, \bar{\mathcal{A}}_d(\epsilon) \\ &= \int_{-\infty}^{\mu} d\epsilon \left(-\frac{1}{\pi}\mathrm{Im}[\bar{G}_d(\epsilon)]\right) \\ &= \int_{-\infty}^{\mu} d\epsilon\, \frac{1}{\pi}\frac{\Gamma}{(\epsilon - \epsilon_d)^2 + \Gamma^2} \\ &= \frac{1}{\pi}\int_{-\infty}^{\mu} \frac{d\epsilon}{\Gamma}\, \frac{1}{1 + \left(\frac{\epsilon - \epsilon_d}{\Gamma}\right)^2} \\ &= \frac{1}{\pi}\int_{-\infty}^{(\mu-\epsilon_d)/\Gamma} dx\, \underbrace{\frac{1}{1+x^2}}_{\partial_x \arctan(x)} \\ &= \frac{1}{\pi}\arctan(\frac{\mu - \epsilon_d}{\Gamma}) + 1/2\end{aligned} \tag{A.69}$$

Attention! This result is for a spin-less model. In the spin-dependent model we need a factor two for the spin degeneracy.

Thus, we obtain including the spin degeneracy

$$n_d = 1 + \frac{2}{\pi}\arctan\left(\frac{\mu - \epsilon_d}{\Gamma}\right) \tag{A.70}$$

Friedel sum rule At the Fermi level we exploit the quasi-particle lifetime in a Fermi-liquid becomes infinite at the Fermi level. Hence also

$$\begin{aligned} & \Sigma^{(d)}(\epsilon) = \vec{V}\bar{\boldsymbol{G}}^{(c)}(\epsilon)\vec{V} \\ \Rightarrow \quad & \mathrm{Im}[\Sigma^{(d)}(\mu)] = \vec{V}\underbrace{\mathrm{Im}\left[\bar{\boldsymbol{G}}^{(c)}(\mu)\right]}_{=0}\vec{V} = 0 \end{aligned} \tag{A.71}$$

Thus,

$$\tan\left(\varphi(\mu)\right) \overset{\text{Eq. A.67}}{=} \frac{\mathrm{Im}\left[\Sigma^{d}(\mu)\right] - \Gamma}{\mu - \epsilon_d - \mathrm{Re}[\Sigma^{d}]} \overset{\mathrm{Im}[G^{(c)}(\mu)]=0}{=} \frac{\Gamma}{\epsilon_d + \mathrm{Re}[\Sigma^{d}(\mu)] - \mu} \tag{A.72}$$

$$n_d = 1 + \frac{2}{\pi}\arctan\left(\frac{\mu - \epsilon_d}{\Gamma}\right) = \frac{2}{\pi}\arctan\left(\frac{\Gamma}{\epsilon_d - \mu}\right) \approx \frac{2}{\pi}\varphi(\mu) \tag{A.73}$$

FRIEDEL SUM RULE

The occupation of an orbital is given by the scattering phase shift $\varphi(\epsilon)$ at the Fermi level.

$$n_d \approx \frac{2}{\pi}\varphi(\mu) \tag{A.74}$$

Caveat: The derivation is approximate, while Friedel sum rule is probably strictly valid.

Density of states at the Fermi level: Friedel's sum rule links the scattering phase shift firstly to the occupation of the orbital and secondly to the density of states

$$\mathcal{A}^{d}(\mu) \overset{\text{Eq. A.68}}{=} \frac{\sin^2\left(\varphi(\mu)\right)}{-\pi\Gamma} \overset{\text{Eq. A.74}}{=} -\frac{1}{\pi\Gamma}\sin^2\left(\frac{\pi}{2}n_d\right) \tag{A.75}$$

This result is of interest for the Kondo or **Abrikosov-Suhl resonance** [103, 104]. It shows that the density of states right at the Fermi level is linked to total d-occupation of the impurity. As the interaction is increased, which shift weight from the central quasi-particle peak to the Hubbard bands, the width of the Abrikosov-Suhl resonance shrinks, while the maximum value of the Dos at the Fermi level remains constant.

Appendix B

Non-orthonormal basissets

Quantum field theory is usually formulated in an orthonormal one-particle basisset. This is because of the enormous simplification of matrix elements in the form of the Slater-Condon rules. On the other hand, the interaction is most important at short distances and strongest between localized orbitals such as d- and f-orbitals. This suggests to use an atom-centered basisset.

Both properties, orthonormality and locality, can be satisfied by so-called **Wannier orbitals**.

However, in practical calculations, Wannier orbitals are still rather extended. In order to construct even more localized orbitals, we need to give up the orthonormality condition. It turns out that many-particle physics, at least on the basis of many-particle Green's functions, can be formulated in non-orthonormal basissets in a rather straight-forward way, without the exponential complexity of matrix elements between many-particle states.

In this appendix, I summarize the notation of non-orthonormal basissets using projector functions. Non-orthonormal basissets have been introduced in the main text in section 1.1.7 on p. 10.

B.1 Creation and annihilation operators for non-orthonormal orbitals

While it has been important to consider orthonormal orbitals for the evaluation of the Slater-Condon rules, the operators can easily be transformed into any non-orthonormal one-particle basis set.

Non-orthonormal basissets have been described in the introduction, namely in section 1.1.7 on p. 10.

Let us consider any non-orthonormal basisset of orbitals $|\chi_\alpha\rangle$ with the overlap matrix $S_{\alpha,\beta} = \langle\chi_\alpha|\chi_\beta\rangle$. For the basis functions, we define furthermore projector functions $|\pi_\alpha\rangle$, which obey the bi-orthogonality condition

$$\langle\pi_\alpha|\chi_\beta\rangle \overset{\text{Eq. 1.46}}{=} \delta_{\alpha,\beta} \tag{B.1}$$

If the orbitals $|\chi_\alpha\rangle$ and the projector functions $|\pi_\alpha\rangle$ are both complete, the unity can be expressed as

$$\hat{1} = \sum_\alpha |\chi_\alpha\rangle\langle\pi_\alpha| \tag{B.2}$$

or as

$$\hat{1} = \sum_\alpha |\pi_\alpha\rangle\langle\chi_\alpha| \ . \tag{B.3}$$

Let us now introduce creation and annihilation operators, analogously to Eq. 3.64, with the difference that the orbitals are no more orthonormal

$$\begin{aligned}\hat{c}_\alpha^\dagger &= \int d^4x\, \hat{\psi}^\dagger(\vec{x})\langle\vec{x}|\pi_\alpha\rangle \\ \hat{c}_\alpha &= \int d^4x\, \langle\pi_\alpha|\vec{x}\rangle\hat{\psi}(\vec{x})\end{aligned} \tag{B.4}$$

With this definition the creation operator produces the projector function.

$$|\pi_\alpha\rangle = \hat{c}_\alpha^\dagger|\mathcal{O}\rangle \tag{B.5}$$

There is some arbitrariness regarding the choice of using the projector functions in Eq. B.4 rather than the orbitals.[1] This is analogous to co- and contra-variant vectors in geometry. Our choice gives up the relation $|\chi_\alpha\rangle = \hat{c}_\alpha^\dagger|\mathcal{O}\rangle$ in favor of the form of matrix elements of operators defined later in Eq. B.9 and Eq. B.10.

Back transform to real-space field operators: Let us work out the back transform as

$$\hat{\psi}^\dagger(\vec{x}) = \int d^4x'\, \hat{\psi}^\dagger(\vec{x'})\, \underbrace{\langle\vec{x'}|\underbrace{\sum_\alpha |\pi_\alpha\rangle\langle\chi_\alpha|}_{\hat{1}}\vec{x}\rangle}_{\delta(\vec{x'}-\vec{x})} = \sum_\alpha \underbrace{\int d^4x'\, \hat{\psi}^\dagger(\vec{x'})\langle\vec{x'}|\pi_\alpha\rangle}_{\hat{c}_\alpha^\dagger}\langle\chi_\alpha|\vec{x}\rangle = \sum_\alpha \hat{c}_\alpha^\dagger\langle\chi_\alpha|\vec{x}\rangle$$

The back transform is

$$\begin{aligned}\hat{\psi}^\dagger(\vec{x}) &= \sum_\alpha \hat{c}_\alpha^\dagger\langle\chi_\alpha|\vec{x}\rangle \\ \hat{\psi}(\vec{x}) &= \sum_\alpha \langle\vec{x}|\chi_\alpha\rangle\hat{c}_\alpha\end{aligned} \tag{B.6}$$

Anticommutator relations with non-orthonormal orbitals

Special care is required with the anticommutator relations which are non-trivial.

$$\left[\hat{c}_\alpha, \hat{c}_\beta^\dagger\right]_+ \overset{\text{Eq. B.4}}{=} \int d^4x \int d^4x'\, \langle\pi_\alpha|\vec{x}\rangle \underbrace{\left[\hat{\psi}(\vec{x}), \hat{\psi}^\dagger(\vec{x'})\right]_+}_{\delta(\vec{x}-\vec{x'})}\langle\vec{x'}|\pi_\beta\rangle = \int d^4x \langle\pi_\alpha|\vec{x}\rangle\langle\vec{x}|\pi_\beta\rangle = \langle\pi_\alpha|\pi_\beta\rangle \tag{B.7}$$

Thus, we obtain the anticommutator relations for non-orthonormal orbitals as

$$\begin{aligned}\left[\hat{c}_\alpha, \hat{c}_\beta^\dagger\right]_+ &= \langle\pi_\alpha|\pi_\beta\rangle = S^{-1}_{\alpha,\beta} \\ \left[\hat{c}_\alpha^\dagger, \hat{c}_\beta^\dagger\right]_+ &= 0 \\ \left[\hat{c}_\alpha, \hat{c}_\beta\right]_+ &= 0\end{aligned} \tag{B.8}$$

[1] Exchanging projector functions and orbitals leads again to a mathematically consistent formalism. As a result it is not always obvious how to choose the correct one.

B.1.1 Operators and matrix elements

In order to represent the operators by creation and annihilation operators in the non-orthonormal basisset, we need to work out their matrix elements.

The derivation of the Slater-Condon rules in a non-orthonormal basisset is awfully cumbersome, because each matrix element of a N-particle Slater determinant produces in general $(N!)^2$ matrix elements of product states. Therefore, it is more economical to take the matrix elements in a orthonormal basisset, which has been obtained with the help of the Slater-Condon rules and transform the result into a general basisset. We even have a later starting point, because we can start from the real-space representation.

For a one-particle operator $\hat{A}$ we obtain

$$\begin{aligned}
\hat{A} &\overset{\text{Eq. 3.66}}{=} \int d^4x \int d^4x' \; A(\vec{x},\vec{x'})\hat{\psi}^\dagger(\vec{x})\hat{\psi}(\vec{x'}) \\
&\overset{\text{Eq. B.6}}{=} \sum_{\alpha,\beta}\Big(\int d^4x \int d^4x' \; \langle\chi_\alpha|\vec{x}\rangle A(\vec{x},\vec{x'})\langle\vec{x'}|\chi_\beta\rangle\Big)\hat{c}_\alpha^\dagger\hat{c}_\beta \\
&= \sum_{\alpha,\beta} A_{\alpha,\beta}\hat{c}_\alpha^\dagger\hat{c}_\beta
\end{aligned} \tag{B.9}$$

with

$$A_{\alpha,\beta} = \int d^4x \int d^4x' \; \langle\chi_\alpha|\vec{x}\rangle A(\vec{x},\vec{x'})\langle\vec{x'}|\chi_\beta\rangle = \langle\chi_\alpha|\hat{A}|\chi_\beta\rangle \tag{B.10}$$

The derivation for the matrix elements of an interaction operator $\hat{W}$ is obtained analogously. Take note of the order of the two annihilators in the following expressions!

$$\begin{aligned}
\hat{W} &\overset{\text{Eq. 3.75}}{=} \frac{1}{2}\int d^4x \int d^4x' \; \hat{\psi}^\dagger(\vec{x})\hat{\psi}^\dagger(\vec{x'})\frac{e^2}{4\pi\epsilon_0|\vec{r}-\vec{r'}|}\hat{\psi}(\vec{x'})\hat{\psi}(\vec{x}) \\
&\overset{\text{Eq. B.6}}{=} \frac{1}{2}\int d^4x \int d^4x' \; \frac{e^2}{4\pi\epsilon_0|\vec{r}-\vec{r'}|}\underbrace{\Big(\sum_\alpha \hat{c}_\alpha^\dagger\langle\chi_\alpha|\vec{x}\rangle\Big)}_{\hat{\psi}^\dagger(\vec{x})}\underbrace{\Big(\sum_\beta \hat{c}_\beta^\dagger\langle\chi_\beta|\vec{x'}\rangle\Big)}_{\hat{\psi}^\dagger(\vec{x'})}\underbrace{\Big(\sum_\gamma \langle\vec{x'}|\chi_\gamma\rangle\hat{c}_\gamma\Big)}_{\hat{\psi}(\vec{x'})}\underbrace{\Big(\sum_\delta \langle\vec{x}|\chi_\delta\rangle\hat{c}_\delta\Big)}_{\hat{\psi}(\vec{x})} \\
&= \frac{1}{2}\sum_{\alpha,\beta,\gamma,\delta}\left(\int d^4x \int d^4x' \; \frac{e^2\chi_\alpha^*(\vec{x})\chi_\beta^*(\vec{x'})\chi_\delta(\vec{x})\chi_\gamma(\vec{x'})}{4\pi\epsilon_0|\vec{r}-\vec{r'}|}\right)\hat{c}_\alpha^\dagger\hat{c}_\beta^\dagger\hat{c}_\gamma\hat{c}_\delta \\
&= \frac{1}{2}\sum_{\alpha,\beta,\gamma,\delta} W_{\alpha,\beta,\delta,\gamma}\hat{c}_\alpha^\dagger\hat{c}_\beta^\dagger\hat{c}_\gamma\hat{c}_\delta
\end{aligned} \tag{B.11}$$

with[2]

$$W_{\alpha,\beta,\gamma,\delta} = \int d^4x \int d^4x' \; \frac{e^2\chi_\alpha^*(\vec{x})\chi_\beta^*(\vec{x'})\chi_\gamma(\vec{x})\chi_\delta(\vec{x'})}{4\pi\epsilon_0|\vec{r}-\vec{r'}|} \tag{B.12}$$

The expression for the matrix elements maintain their simple form also in a non-orthonormal basisset. The complication shows up again when evaluating matrix elements of operators expressed in creation and annihilation operators, because every permutation of creation and annihilation operators introduces an inverse overlap matrix instead of a unit matrix. A usual technique to evaluate matrix elements is to permute the annihilators to the very right or the very left, which then blows up the number of terms in an non-orthonormal basisset tremendously. This problem is usually avoided by an intermediate basis transformation to an orthonormal basisset.

[2]Note the interchange of γ and δ!

Summary

Let me summarize here the equations for non-orthonormal orbitals for future reference. Memorizing these equations may be advantageous over memorizing the ones for orthonormal orbitals, because the latter are readily derived from the more general equations.

CREATION AND ANNIHILATION OPERATORS IN NON-ORTHONORMAL ORBITALS

Consider a set of non-orthonormal orbitals $|\chi_\alpha\rangle$ having the overlap matrix

$$S_{\alpha,\beta} \stackrel{\text{def}}{=} \langle\chi_\alpha|\chi_\beta\rangle \tag{B.13}$$

A set of projector functions $\langle\pi_\alpha|$ is defined which obeys the bi-orthogonality condition

$$\langle\pi_\alpha|\chi_\beta\rangle = \delta_{\alpha,\beta} \tag{B.14}$$

Thus,

$$\langle\pi_\alpha|\pi_\beta\rangle = \Big(\boldsymbol{S}\Big)^{-1}_{\alpha,\beta} \tag{B.15}$$

The creation and annihilation operators $\hat{c}^\dagger_\alpha$ and $\hat{c}^\dagger$ and obey the anticommutator relations

$$\begin{aligned}
\Big[\hat{c}^\dagger_\alpha, \hat{c}^\dagger_\beta\Big]_+ &\stackrel{\text{Eq. ??}}{=} 0 \\
\Big[\hat{c}_\alpha, \hat{c}_\beta\Big]_+ &\stackrel{\text{Eq. ??}}{=} 0 \\
\Big[\hat{c}^\dagger_\alpha, \hat{c}_\beta\Big]_+ &\stackrel{\text{Eq. ??}}{=} \langle\pi_\alpha|\pi_\beta\rangle
\end{aligned} \tag{B.16}$$

The creation and annihilation operators $\hat{c}^\dagger_\alpha$ and $\hat{c}^\dagger$ are related to the real-space field operators by

$$\begin{aligned}
\hat{\psi}^\dagger(\vec{x}) &\stackrel{\text{Eq. B.6}}{=} \sum_\alpha \hat{c}^\dagger_\alpha \langle\chi_\alpha|\vec{x}\rangle \\
\hat{\psi}(\vec{x}) &\stackrel{\text{Eq. B.6}}{=} \sum_\alpha \langle\vec{x}|\chi_\alpha\rangle \hat{c}_\alpha
\end{aligned} \tag{B.17}$$

and

$$\begin{aligned}
\hat{c}^\dagger_\alpha &\stackrel{\text{Eq. B.4}}{=} \int d^4x\, \hat{\psi}^\dagger(\vec{x}) \langle\vec{x}|\pi_\alpha\rangle \\
\hat{c}_\alpha &\stackrel{\text{Eq. B.4}}{=} \int d^4x\, \langle\pi_\alpha|\vec{x}\rangle \hat{\psi}(\vec{x})
\end{aligned} \tag{B.18}$$

A creation operator creates the projector function $|\pi_\alpha\rangle$, rather than the local orbital.

$$|\pi_\alpha\rangle \stackrel{\text{Eq. B.5}}{=} \hat{c}^\dagger_\alpha |\mathcal{O}\rangle \tag{B.19}$$

The Hamiltonian has the form

$$\hat{H} = \sum_{\alpha,\beta} h_{\alpha,\beta} \hat{c}^\dagger_\alpha \hat{c}_\beta + \frac{1}{2} \sum_{\alpha,\beta,\gamma,\delta} W_{\alpha,\beta,\delta,\gamma} \hat{c}^\dagger_\alpha \hat{c}^\dagger_\beta \hat{c}_\delta \hat{c}_\gamma \tag{B.20}$$

with matrix elements

$$h_{\alpha,\beta} = \langle\chi_\alpha|\hat{H}_0|\chi_\beta\rangle \tag{B.21}$$

and

$$W_{\alpha,\beta,\gamma,\delta} = \langle\chi_\alpha\chi_\beta|\hat{W}|\chi_\gamma\chi_\delta\rangle = \int d^4x \int d^4x' \, \frac{e^2 \chi^*_\alpha(\vec{x}) \chi^*_\beta(\vec{x'}) \chi_\gamma(\vec{x}) \chi_\delta(\vec{x'})}{4\pi\epsilon_0 |\vec{r} - \vec{r'}|} \tag{B.22}$$

Appendix C

Fermions and bosons

Editor: This is under construction and needs to be verified

The focus of these lecture notes are fermions. In this chapter, I will present the relevant expressions for fermions and bosons side-by-side. The expressions for fermions and bosons differ by the position of a sign-factor *"eta"* η_{FB}.

$$\begin{aligned} \eta_{FB} &= +1 \qquad \text{for bosons} \\ \eta_{FB} &= -1 \qquad \text{for fermions} \end{aligned} \tag{C.1}$$

The subscript "FB" indicates that the sign distingishes fermions and bosons.

Particle permutations

$$\langle \vec{x}_1, \vec{x}_2 | \Psi \rangle = \eta_{FB} \langle \vec{x}_2, \vec{x}_1 | \Psi \rangle \tag{C.2}$$

Fermionic wave functions are antisymmetric under exchange of two particles, while bosons are symmetric under particle exchange.

Slater determinants and permanents

The antisymmetrized product states relevant for fermions are Slater determinants Eq. 1.88. The symmetrized product states relevant for bosons are permanents Eq. 1.89.

- Fermions: The occupation numbers of fermions are $\sigma_n \in \{0, 1\}$. That is, for a specified, ordered set of one-particle states, a Slater determinant can be specified by $|\vec{\sigma}\rangle$, where $\vec{\sigma}$ is a string of zeros and ones.

- bosons: The occupation numbers of bosons are non-negative integers $\sigma_n \in \{0, 1, 2, \ldots\}$. That is, for a specified, ordered set of one-particle states, a permanent can be specified by $|\vec{\sigma}\rangle$, where $\vec{\sigma}$ is a string of non-negative integers.

Grand potential of non-interacting particles

The grand potential of non-interacting particles for fermions is given in Eq. **??**.

$$\Omega^{(0)}_{T,\mu} \overset{\text{Eq. ??}}{=} \eta_{FB} k_B T \ \mathrm{Tr}\left\{ \ln\left(1 - \eta_{FB} \mathrm{e}^{-\beta(\epsilon - \mu \hat{1})} \right) \right\} \tag{C.3}$$

Thermal occupations

The thermal occupations of non-interacting electrons are the Fermi- and Bose-distributions

$$f_{T,\mu}(\epsilon) = \frac{1}{\mathrm{e}^{+\beta(\epsilon-\mu)} - \eta_{FB}} \tag{C.4}$$

one-particle-reduced density matrix

$$\hat{\rho}^{(1)} = \sum_n |\varphi_n\rangle f_n \langle\varphi_n| \tag{C.5}$$

The occupations of fermions are $f_n \in [0, 1]$. The occupations of bosons are non negative, real-valued numbers.

Two-particle interaction

Interaction

$$\langle\Phi|\hat{W}|\Phi\rangle = \frac{1}{2}\sum_{m,n} f_m f_n \left[\langle\varphi_m, \varphi_n|\hat{W}|\varphi_m, \varphi_n\rangle + \eta_{FB}\langle\varphi_m, \varphi_n|\hat{W}|\varphi_n, \varphi_m\rangle\right] \tag{C.6}$$

The Coulomb interaction is usually not relevant for bosons. Exchange enhances the interaction matrix elements for bosons, in contrast to fermions.

Creation and annihilation operators

The creation and annihilation operators for fermions have been defined in Eqs. 3.15, 3.17 on p. 127.

$$\begin{aligned}
\hat{a}_i^\dagger &= \sum_{\vec{\sigma}} \Big|\sigma_1, \sigma_2, \ldots, \sigma_i + 1, \ldots\Big\rangle \left(\left[\eta_{FB}{}^{\sum_{j<i}\sigma_j}\right]\sqrt{1+\eta_{FB}\sigma_i}\right)\Big\langle\sigma_1, \sigma_2, \ldots, \sigma_i, \ldots\Big| \\
\hat{a}_i &= \sum_{\vec{\sigma}} \Big|\sigma_1, \sigma_2, \ldots, \sigma_i - 1, \ldots\Big\rangle \left(\left[\eta_{FB}{}^{\sum_{j<i}\sigma_j}\right]\sqrt{\sigma_i}\right)\Big\langle\sigma_1, \sigma_2, \ldots, \sigma_i, \ldots\Big|
\end{aligned} \tag{C.7}$$

This yields $\hat{n}_i = \hat{a}_i^\dagger \hat{a}_i = \sum_\sigma |\vec{\sigma}\rangle\sigma_i\langle\vec{\sigma}|$

Commutator- and anti-commutator rules

For creation and annihilation operators for an orthonormal one-particle basisset, the commutator, respectively anticommutator rules are

$$\begin{aligned}
\left[\hat{a}_m, \hat{a}_n^\dagger\right]_{-\eta_{FB}} &= \delta_{m,n} \\
\left[\hat{a}_m^\dagger, \hat{a}_n^\dagger\right]_{-\eta_{FB}} &= 0 \\
\left[\hat{a}_m, \hat{a}_n\right]_{-\eta_{FB}} &= 0
\end{aligned} \tag{C.8}$$

For non-orthonormal basissets $\{|\chi_\alpha\rangle\}$ with projector functions $\{|\pi_\alpha\rangle\}$, the inverse overlap operator replaces the unit matrix

$$\left[\hat{c}_\alpha, \hat{c}_\beta^\dagger\right]_{-\eta_{FB}} = \langle\pi_\alpha|\pi_\beta\rangle \tag{C.9}$$

where $S_{\alpha,\beta} = \langle\chi_\alpha|\chi_\beta\rangle$ is the overlap matrix of the orbitals and where the overlap of the projector functions $\langle\pi_\alpha|\pi_\beta\rangle = S^{-1}_{\alpha,\beta}$ is the inverse overlap of the orbitals

Spectral function

$$\begin{aligned}\mathcal{A}^{tot}_{\alpha,\beta}(\epsilon) &= \sum_n P_n \langle \Phi_n | \left[\hat{c}_{S,\alpha}, \hat{c}^\dagger_{S,\beta}\right]_{-\eta_{FB}} | \Phi_n \rangle \delta\Big(\epsilon - (E_m - E_n)\Big) \\ &= \sum_{m,n} \Big(P_n - \eta_{FB} P_m\Big) \langle \Phi_n | \hat{c}_{S,\alpha} | \Phi_m \rangle \langle \Phi_m | \hat{c}^\dagger_{S,\beta} | \Phi_n \rangle \delta\Big(\epsilon - (E_m - E_n)\Big) \end{aligned} \tag{C.10}$$

Appendix D

Hubbard dimer and hydrogen molecule

In these lecture notes, I am relying on dimer molecules with 1s orbitals to demonstrate many of the concepts introduced. The dimer serves as minimal model for a wealth of many-particle effects. Despite its simplicity, some of the calculations are quite involved and this distracts from the physical effects. Therefore, I introduce here the derivations of expressions, which I will refer to in the text. Note, that there are some repetitions in the text: In this appendix, I am using also advanced concepts that are only introduced later in the text than its first reference.

In this chapter, I am describing first the asymmetric dimer having a basis of 1s orbitals. Later, I will work out the matrix elements for the hydrogen molecule using atomic orbitals.[1]

Editor: see also Giesbertz[105] on reduced density matrix functional theory from many-particle perturbation theory and their calculations on the hubbard dimer.

D.1 Asymmetric two-site model

The asymmetric dimer consists of two distinct sites. It prepares the ground, both, for the Hubbard-dimer with two identical sites, and the Anderson dimer[106, 107] which describes one strongly interacting site coupled to a non-interacting environment.

The naming of the two sites relates to the Anderson impurity model, where one site contains d- or f-electrons described by the creation and annihilation operators $\hat{f}_\sigma^\dagger$ and $\hat{f}_\sigma$, while the other site has electrons described by $\hat{c}_\sigma^\dagger \hat{c}_\sigma$.

The Hamiltonian for the asymmetric dimer is

$$\hat{H} = \underbrace{\sum_\sigma \bar{\epsilon}_f \hat{f}_\sigma^\dagger \hat{f}_\sigma + \frac{1}{2} U_f \sum_{\sigma,\sigma'} \hat{f}_\sigma^\dagger \hat{f}_{\sigma'}^\dagger \hat{f}_{\sigma'} \hat{f}_\sigma}_{\text{atom F}} + \underbrace{\sum_\sigma \bar{\epsilon}_c \hat{c}_\sigma^\dagger \hat{c}_\sigma + \frac{1}{2} U_c \sum_{\sigma,\sigma'} \hat{c}_\sigma^\dagger \hat{c}_{\sigma'}^\dagger \hat{c}_{\sigma'} \hat{c}_\sigma}_{\text{atom C}} \underbrace{-t \sum_\sigma \left(\hat{f}_\sigma^\dagger \hat{c}_\sigma + \hat{c}_\sigma^\dagger \hat{f}_\sigma \right)}_{\text{hopping}} \tag{D.1}$$

For the calculations, it is convenient to combine the operators, wherever possible, to particle-

[1] A similar derivation has been done by Pavarini in the appendix of chapter 11 *"Dynamical Mean-Field Theory for Materials"* in *Many-Body Methods for Real materials* Schriftenreihe de Forschungszentrums Jülich, Reihe Modeling and Simulation, Vol. 9 (2019), https://www.cond-mat.de/events/correl19/manuscripts/correl19.pdf

number operators $\hat{n}_{f,\sigma} = \hat{f}_\sigma^\dagger \hat{f}_\sigma$ and $\hat{n}_{c,\sigma} = \hat{c}_\sigma^\dagger \hat{c}_\sigma$. [2]

$$\hat{H} = \overbrace{\sum_{\sigma\in\{\uparrow,\downarrow\}} \bar{\epsilon}_f \hat{n}_{f,\sigma} + U_f \hat{n}_{f,\uparrow}\hat{n}_{f,\downarrow} + \frac{1}{2}U_f \sum_{\sigma\in\{\uparrow,\downarrow\}} \underbrace{\hat{n}_{f,\sigma}\big(\hat{n}_{f,\sigma}-1\big)}_{=\hat{0}}}^{\text{atom F}}$$
$$+ \overbrace{\sum_{\sigma\in\{\uparrow,\downarrow\}} \bar{\epsilon}_c \hat{n}_{c,\sigma} + U_c \hat{n}_{c,\uparrow}\hat{n}_{c,\downarrow} + \frac{1}{2}U_c \sum_{\sigma\in\{\uparrow,\downarrow\}} \underbrace{\hat{n}_{c,\sigma}\big(\hat{n}_{c,\sigma}-1\big)}_{=\hat{0}}}^{\text{atom C}}$$
$$\underbrace{-t \sum_{\sigma\in\{\uparrow,\downarrow\}} \left(\hat{f}_\sigma^\dagger \hat{c}_\sigma + \hat{c}_\sigma^\dagger \hat{f}_\sigma\right)}_{\text{hopping}} \tag{D.3}$$

Each atom has two onsite Coulomb terms. The second shows up in the mean-field approximation, while it is exactly zero in the full description.[3]

D.1.1 Symmetry-adapted many-particle states

Before we determine the eigenstates for the Hamiltonian of the asymmetric dimer, I first construct symmetry eigenstates in order to block diagonalize the Hamiltonian.

I start with setting up the basis set of Slater determinants in the local basis. These states are given in table D.1.

[2]

$$\frac{1}{2}\sum_{\sigma,\sigma'\in\{\uparrow,\downarrow\}} \hat{f}_\sigma^\dagger \hat{f}_{\sigma'}^\dagger \hat{f}_{\sigma'}\hat{f}_\sigma = -\frac{1}{2}\sum_{\sigma,\sigma'} \hat{f}_\sigma^\dagger \hat{f}_{\sigma'}^\dagger \hat{f}_\sigma \hat{f}_{\sigma'} = -\frac{1}{2}\sum_{\sigma,\sigma'}\Big(\delta_{\sigma,\sigma'}\hat{f}_\sigma^\dagger \hat{f}_{\sigma'} - \hat{f}_\sigma^\dagger \hat{f}_\sigma \hat{f}_{\sigma'}^\dagger \hat{f}_{\sigma'}\Big) = \frac{1}{2}\sum_{\sigma,\sigma'} \hat{f}_\sigma^\dagger \hat{f}_\sigma \hat{f}_{\sigma'}^\dagger \hat{f}_{\sigma'} - \frac{1}{2}\sum_\sigma \hat{f}_\sigma^\dagger \hat{f}_\sigma$$
$$= \hat{n}_{f,\uparrow}\hat{n}_{f,\downarrow} + \frac{1}{2}\sum_\sigma \underbrace{\left(\hat{n}_{f,\sigma}^2 - \hat{n}_{f,\sigma}\right)}_{=0} \tag{D.2}$$

[3] $\hat{n}_{f,\sigma}(\hat{n}_{f,\sigma}-1)$ vanishes, because the occupation-number operator for fermions has eigenvalues zero and one, so that the eigenvalues of $\hat{n}_{f,\sigma}(\hat{n}_{f,\sigma}-1)$ vanish. Hence, is the zero operator $\hat{n}_{f,\sigma}(\hat{n}_{f,\sigma}-1)$.

Table D.1: Slater determinants, which form a basis set of many-particle wave functions for the asymmetric dimer.

Nr.	$\lvert f_\uparrow, f_\downarrow, c_\uparrow, c_\downarrow\rangle$	Basisstate	N	$S_z/\hbar$
1	$\lvert 0,0,0,0\rangle$	$\lvert\mathcal{O}\rangle$	$N=0$	$S_z=0$
2	$\lvert 1,0,0,0\rangle$	$f_\uparrow^\dagger\lvert\mathcal{O}\rangle$	$N=1$	$S_z=+\frac{1}{2}$
3	$\lvert 0,1,0,0\rangle$	$f_\downarrow^\dagger\lvert\mathcal{O}\rangle$	$N=1$	$S_z=-\frac{1}{2}$
4	$\lvert 1,1,0,0\rangle$	$f_\uparrow^\dagger f_\downarrow^\dagger\lvert\mathcal{O}\rangle$	$N=2$	$S_z=0$
5	$\lvert 0,0,1,0\rangle$	$c_\uparrow^\dagger\lvert\mathcal{O}\rangle$	$N=1$	$S_z=\frac{1}{2}$
6	$\lvert 1,0,1,0\rangle$	$f_\uparrow^\dagger c_\uparrow^\dagger\lvert\mathcal{O}\rangle$	$N=2$	$S_z=+1$
7	$\lvert 0,1,1,0\rangle$	$f_\downarrow^\dagger c_\uparrow^\dagger\lvert\mathcal{O}\rangle$	$N=2$	$S_z=0$
8	$\lvert 1,1,1,0\rangle$	$f_\uparrow^\dagger f_\downarrow^\dagger c_\uparrow^\dagger\lvert\mathcal{O}\rangle$	$N=3$	$S_z=+\frac{1}{2}$
9	$\lvert 0,0,0,1\rangle$	$c_\downarrow^\dagger\lvert\mathcal{O}\rangle$	$N=1$	$S_z=-\frac{1}{2}$
10	$\lvert 1,0,0,1\rangle$	$f_\uparrow^\dagger c_\downarrow^\dagger\lvert\mathcal{O}\rangle$	$N=2$	$S_z=0$
11	$\lvert 0,1,0,1\rangle$	$f_\downarrow^\dagger c_\downarrow^\dagger\lvert\mathcal{O}\rangle$	$N=2$	$S_z=-1$
12	$\lvert 1,1,0,1\rangle$	$f_\uparrow^\dagger f_\downarrow^\dagger c_\downarrow^\dagger\lvert\mathcal{O}\rangle$	$N=3$	$S_z=-\frac{1}{2}$
13	$\lvert 0,0,1,1\rangle$	$c_\uparrow^\dagger c_\downarrow^\dagger\lvert\mathcal{O}\rangle$	$N=2$	$S_z=0$
14	$\lvert 1,0,1,1\rangle$	$f_\uparrow^\dagger c_\uparrow^\dagger c_\downarrow^\dagger\lvert\mathcal{O}\rangle$	$N=3$	$S_z=+\frac{1}{2}$
15	$\lvert 0,1,1,1\rangle$	$f_\downarrow^\dagger c_\uparrow^\dagger c_\downarrow^\dagger\lvert\mathcal{O}\rangle$	$N=3$	$S_z=-\frac{1}{2}$
16	$\lvert 1,1,1,1\rangle$	$f_\uparrow^\dagger f_\downarrow^\dagger c_\uparrow^\dagger c_\downarrow^\dagger\lvert\mathcal{O}\rangle$	$N=4$	$S_z=0$

Before diagonalizing the Hamiltonian, I select common eigenstates of a set of symmetry operators of the Hamiltonian. In the basis of symmetry eigenstates, the Hamiltonian will become block diagonal, which simplifies the diagonalization. Alongside with the symmetry operators, I include also the particle number into the set of operators that commutate with the Hamiltonian and the other symmetry operators.

First, I classify the states in table D.1 according to their particle number and $\hat{S}_Z$ eigenvalues. Then, I will break up the blocks according to the $\vec{S}^2$ eigenvalues. The states in the individual blocks are given in table D.2.

One-particle channel

The Hamiltonian projected onto the one-particle sector ($N=1$) and the eigenstates with $S_z=\frac{\hbar}{2}\sigma$ is

$$\hat{P}_{1,\sigma}\hat{H}\hat{P}_{1,\sigma}=\begin{pmatrix}\hat{f}_\sigma^\dagger|\mathcal{O}\rangle\\ \hat{c}_\sigma^\dagger|\mathcal{O}\rangle\end{pmatrix}\begin{pmatrix}\bar{\epsilon}_f & -|t|\\ -|t| & \bar{\epsilon}_c\end{pmatrix}\begin{pmatrix}\langle\mathcal{O}|\hat{f}_\sigma\\ \langle\mathcal{O}|\hat{c}_\sigma\end{pmatrix} \tag{D.4}$$

where $\hat{P}_{1,\sigma}$ is the corresponding projection operator onto states with $N=1$ and $S_z=\frac{\hbar}{2}\sigma$.

The eigenvalues are

$$\epsilon_\pm=\frac{\bar{\epsilon}_f+\bar{\epsilon}_c}{2}\pm\sqrt{\left(\frac{\bar{\epsilon}_f-\bar{\epsilon}_c}{2}\right)^2+|t|^2} \tag{D.5}$$

Table D.2: Symmetry eigenstates states constructed from the Slater determinants in table D.1. The Slater determinants can be grouped according to their eigenvalues with respect to particle number N and S_z. Using the total spin, i.e. $\hat{\vec{S}}^2$, the block with $N = 2$ and $S_z = 0$ can be divided further into one triplet state with $S = 1$ and a block with three states with $S = 0$ as decribed in section D.1.1

N	$S_z/\hbar$	S		
0	0	0	$\|1\rangle$	$\|\mathcal{O}\rangle$
1	$-\frac{1}{2}$	$\frac{1}{2}$	$\|3\rangle, \|9\rangle$	$\hat{f}_\downarrow^\dagger\|\mathcal{O}\rangle$, $\hat{c}_\downarrow^\dagger\|\mathcal{O}\rangle$
1	$+\frac{1}{2}$	$\frac{1}{2}$	$\|2\rangle, \|5\rangle$	$\hat{f}_\uparrow^\dagger\|\mathcal{O}\rangle$, $\hat{c}_\uparrow^\dagger\|\mathcal{O}\rangle$
2	-1	1	$\|11\rangle$	$\hat{f}_\downarrow^\dagger\hat{c}_\downarrow^\dagger\|\mathcal{O}\rangle$
2	0	1	$\frac{1}{\sqrt{2}}\big(\|7\rangle + \|10\rangle\big)$	$\frac{1}{\sqrt{2}}\big(\hat{f}_\downarrow^\dagger\hat{c}_\uparrow^\dagger + \hat{f}_\uparrow^\dagger\hat{c}_\downarrow^\dagger\big)\|\mathcal{O}\rangle$
2	0	0	$\|4\rangle$,$\|13\rangle$, $\frac{1}{\sqrt{2}}\Big(\|7\rangle - \|10\rangle\Big)$	$\hat{f}_\uparrow^\dagger\hat{f}_\downarrow^\dagger\|\mathcal{O}\rangle$, $\hat{c}_\uparrow^\dagger\hat{c}_\downarrow^\dagger\|\mathcal{O}\rangle$, $\frac{1}{\sqrt{2}}\big(\hat{f}_\downarrow^\dagger\hat{c}_\uparrow^\dagger - \hat{f}_\uparrow^\dagger\hat{c}_\downarrow^\dagger\big)\|\mathcal{O}\rangle$
2	$+1$	1	$\|6\rangle$	$\hat{f}_\uparrow^\dagger\hat{c}_\uparrow^\dagger$
3	$-\frac{1}{2}$	$\frac{1}{2}$	$\|12\rangle, \|15\rangle$	$\hat{f}_\uparrow^\dagger\hat{f}_\downarrow^\dagger\hat{c}_\downarrow^\dagger\|\mathcal{O}\rangle$, $\hat{f}_\downarrow^\dagger\hat{c}_\uparrow^\dagger\hat{c}_\downarrow^\dagger\|\mathcal{O}\rangle$
3	$+\frac{1}{2}$	$\frac{1}{2}$	$\|8\rangle, \|14\rangle$	$\hat{f}_\uparrow^\dagger\hat{f}_\downarrow^\dagger\hat{c}_\uparrow^\dagger\|\mathcal{O}\rangle$, $\hat{f}_\uparrow^\dagger\hat{c}_\uparrow^\dagger\hat{c}_\downarrow^\dagger\|\mathcal{O}\rangle$
4	0	0	$\|16\rangle$	$\hat{f}_\uparrow^\dagger\hat{f}_\downarrow^\dagger\hat{c}_\uparrow^\dagger\hat{c}_\downarrow^\dagger\|\mathcal{O}\rangle$

The eigenstates $\psi_\pm$ are

$$\begin{aligned}|\psi_-\rangle &= \Big(\hat{f}_\sigma^\dagger\cos(\alpha_1) + \hat{c}_\sigma^\dagger\sin(\alpha_1)\Big)|\mathcal{O}\rangle \\ |\psi_+\rangle &= \Big(\hat{f}_\sigma^\dagger\sin(\alpha_1) - \hat{c}_\sigma^\dagger\cos(\alpha_1)\Big)|\mathcal{O}\rangle\end{aligned} \tag{D.6}$$

This Ansatz guarantees that the states are orthonormal.

The angle α_1 is obtained by inserting the Ansatz Eq. D.6 of $|\psi_-\rangle$ into the eigenvector equation with Eq. D.4

$$\begin{aligned}&(\bar{\epsilon}_f - \epsilon_-)\cos(\alpha_1) - |t|\sin(\alpha_1) = 0 \\ \Rightarrow \tan(\alpha_1) &= \frac{1}{|t|}\Big(\bar{\epsilon}_f - \epsilon_-\Big) \\ &= \frac{1}{|t|}\left(\frac{\bar{\epsilon}_f - \bar{\epsilon}_c}{2} + \sqrt{\left(\frac{\bar{\epsilon}_f - \bar{\epsilon}_c}{2}\right)^2 + |t|^2}\right) \\ &= \frac{\bar{\epsilon}_f - \bar{\epsilon}_c}{2|t|} + \sqrt{1 + \left(\frac{\bar{\epsilon}_f - \bar{\epsilon}_c}{2|t|}\right)^2} \\ \alpha_1 &= \operatorname{atan}\Big(q + \sqrt{1+q}\Big) \qquad \text{with } q = \frac{\bar{\epsilon}_f - \bar{\epsilon}_c}{2|t|}\end{aligned} \tag{D.7}$$

- For the symmetric case, $\bar{\epsilon}_f = \bar{\epsilon}_c$ we obtain $\tan(\alpha_1) = 1$ and $\alpha_1 = 45° = \pi/4$. This describes the bonding and antibonding orbitals.
- For the asymmetric limit $|\bar{\epsilon}_f - \bar{\epsilon}_c| \gg |t|$, I obtain $\tan(\alpha_1) = \infty$ or $\alpha_1 = 90° = \pi/2$. In this case each wave function is localized either on one or the other site.

Three-particle channel

The three-particle channel can be worked out analogous to the one-particle channel.

The Hamiltonian projected onto the three-particle sector and the eigenstates with $S_z = \frac{\hbar}{2}\sigma$ is

$$\hat{P}_{3,\sigma}\hat{H}\hat{P}_{3,\sigma} = \begin{pmatrix} \hat{f}_{\bar{\sigma}}^\dagger \hat{f}_\sigma^\dagger \hat{c}_\sigma^\dagger |\mathcal{O}\rangle \\ \hat{c}_{\bar{\sigma}}^\dagger \hat{f}_\sigma^\dagger \hat{c}_\sigma^\dagger |\mathcal{O}\rangle \end{pmatrix} \begin{pmatrix} 2\bar{\epsilon}_f + U_f + \bar{\epsilon}_c & -|t| \\ -|t| & \bar{\epsilon}_f + 2\bar{\epsilon}_c + U_c \end{pmatrix} \begin{pmatrix} \langle\mathcal{O}|\hat{c}_\sigma \hat{f}_\sigma \hat{f}_{\bar{\sigma}} \\ \langle\mathcal{O}|\hat{c}_\sigma \hat{f}_\sigma \hat{c}_{\bar{\sigma}} \end{pmatrix} \tag{D.8}$$

where $\hat{P}_{3,\sigma}$ is the projection operator on the three-particle states with $S_z = \frac{\hbar}{2}\sigma$. **With $\bar{\sigma}$, I denote the spin direction opposite to σ, i.e. $\bar{\sigma} = \downarrow$ for $\sigma = \uparrow$ and vice versa.**

The Slater determinants used here differ from the ones used initially by the order of the operators. Note, that $\hat{c}_{\bar{\sigma}}\hat{f}_\sigma\hat{c}_\sigma = +\hat{f}_\sigma\hat{c}_\sigma\hat{c}_{\bar{\sigma}}$. The order of the spin indices on the doubly occupied orbital is reversed in both orbitals. This changes the sign of one orbital with respect to the other.

The eigenvalues are

$$\epsilon_\pm = \frac{3\bar{\epsilon}_f + U_f + 3\bar{\epsilon}_c + U_c}{2} \pm \sqrt{\left(\frac{\bar{\epsilon}_f + U_f - \bar{\epsilon}_c - U_c}{2}\right)^2 + |t|^2} \tag{D.9}$$

The eigenstates $\psi_\pm$ are

$$\begin{aligned} |\psi_-\rangle &= \left(\hat{f}_{\bar{\sigma}}^\dagger \cos(\alpha_2) + \hat{f}_{\bar{\sigma}}^\dagger \sin(\alpha_2)\right) \hat{f}_\sigma^\dagger \hat{c}_\sigma^\dagger |\mathcal{O}\rangle \\ |\psi_+\rangle &= \left(\hat{f}_{\bar{\sigma}}^\dagger \sin(\alpha_2) - \hat{f}_{\bar{\sigma}}^\dagger \cos(\alpha_2)\right) \hat{f}_\sigma^\dagger \hat{c}_\sigma^\dagger |\mathcal{O}\rangle \end{aligned} \tag{D.10}$$

This Ansatz guarantees that the states are orthonormal.

The angle α_1 is obtained by inserting the Ansatz of $|\psi_-\rangle$ into the eigenvector equation

$$\begin{aligned} & (2\bar{\epsilon}_f + U_f + \bar{\epsilon}_c - \epsilon_-)\cos(\alpha_2) - |t|\sin(\alpha_2) = 0 \\ \Rightarrow \tan(\alpha_2) &= \frac{1}{|t|}\left(2\bar{\epsilon}_f + U_f + \bar{\epsilon}_c - \epsilon_-\right) \\ &= \frac{1}{|t|}\left(\frac{\bar{\epsilon}_f + U_f - \bar{\epsilon}_c - U_c}{2} + \sqrt{\left(\frac{\bar{\epsilon}_f + U_f - \bar{\epsilon}_c - U_c}{2}\right)^2 + |t|^2}\right) \\ &= \frac{\bar{\epsilon}_f + U_f - \bar{\epsilon}_c - U_c}{2|t|} + \sqrt{1 + \left(\frac{\bar{\epsilon}_f + U_f - \bar{\epsilon}_c - U_c}{2|t|}\right)^2} \\ \alpha_2 &= \operatorname{atan}\left(q + \sqrt{1+q}\right) \qquad \text{with } q = \frac{\bar{\epsilon}_f + U_f - \bar{\epsilon}_c - U_c}{2|t|} \end{aligned} \tag{D.11}$$

- For the symmetric case, $\bar{\epsilon}_f + U_f = \bar{\epsilon}_c + U_c$, I obtain $\tan(\alpha_2) = 1$ and $\alpha_2 = 45° = \pi/4$. This describes the bonding and antibonding orbitals for the minority-spin direction and a completely filled majority-spin direction.
- For the asymmetric limit $|\bar{\epsilon}_f + U_f - \bar{\epsilon}_c - U_c| \gg |t|$, I obtain $\tan(\alpha_2) = \infty$ or $\alpha_2 = 90° = \pi/2$. In this case one site has two electrons, while other has an occupied orbital in the majority-spin direction.
- The three-particle case is very similar to the one-particle sector, when the atomic orbital levels of the one-particle case are shifted up by the corresponding U-term.

Two-particle channel

In the basisset given in table D.1, the largest block of the Hamiltonian is the one with $N = 2$ and $S_z = 0$, which contains four states. In order to break down this block further, let us exploit the symmetry under spin rotation. $\hat{\vec{S}}^2$ commutates with the Hamiltonian and with the particle number and S_z. Thus, we can break down the blocks of the Hamiltonian into subblocks which are eigenstates of N, S_z and S^2.

This calculation is done in exercise 3.11.2 on p. 153. The eigenstates of $\hat{\vec{S}}^2$ in the two-particle channel are given in Eq. 3.153 and Eq. 3.152: We obtained three states with spin quantum number $S = 1$, namely

$$\begin{aligned} |6\rangle &\overset{\text{Eq. 3.152}}{=} \hat{f}_\uparrow^\dagger \hat{c}_\uparrow^\dagger |\mathcal{O}\rangle \qquad S_z = +1 \\ |11\rangle &\overset{\text{Eq. 3.152}}{=} \hat{f}_\downarrow^\dagger \hat{c}_\downarrow^\dagger |\mathcal{O}\rangle \\ \frac{1}{\sqrt{2}}\Big(|7\rangle + |10\rangle\Big) &\overset{\text{Eq. 3.152}}{=} \frac{1}{\sqrt{2}}\Big(\hat{f}_\downarrow^\dagger \hat{c}_\uparrow^\dagger + \hat{f}_\uparrow^\dagger \hat{c}_\downarrow^\dagger\Big)|\mathcal{O}\rangle \end{aligned} \tag{D.12}$$

and three states with $S = 0$, namely

$$\begin{aligned} |4\rangle &\overset{\text{Eq. 3.153}}{=} \hat{f}_\uparrow^\dagger \hat{f}_\downarrow^\dagger |\mathcal{O}\rangle \\ |13\rangle &\overset{\text{Eq. 3.153}}{=} \hat{c}_\uparrow^\dagger \hat{c}_\downarrow^\dagger |\mathcal{O}\rangle \\ \frac{1}{\sqrt{2}}\Big(|7\rangle - |10\rangle\Big) &\overset{\text{Eq. 3.153}}{=} \frac{1}{\sqrt{2}}\Big(\hat{f}_\downarrow^\dagger \hat{c}_\uparrow^\dagger - \hat{f}_\uparrow^\dagger \hat{c}_\downarrow^\dagger\Big)|\mathcal{O}\rangle \end{aligned} \tag{D.13}$$

This splits the subblock of the Hamiltonian with the four Slater determinants $\{|4\rangle, |7\rangle, |10\rangle, |13\rangle\}$ with $N = 2$ and $S_z = 0$ into one state with $S = 1$ and a block of three singlet states with $S = 0$. (The eigenvalues of $\hat{S}^2$ are $\hbar^2 S(S+1)$.)

The Hamiltonian projected onto the two-particle sector and the eigenstates with $S = 0$ is

$$\hat{P}_{2,0}\hat{H}\hat{P}_{2,0} = \begin{pmatrix} \hat{f}_\uparrow^\dagger \hat{f}_\downarrow^\dagger |\mathcal{O}\rangle \\ \hat{c}_\uparrow^\dagger \hat{c}_\downarrow^\dagger |\mathcal{O}\rangle \\ \frac{1}{\sqrt{2}}\big(\hat{f}_\uparrow^\dagger \hat{c}_\downarrow^\dagger - \hat{f}_\downarrow^\dagger \hat{c}_\uparrow^\dagger\big)|\mathcal{O}\rangle \end{pmatrix} \begin{pmatrix} 2\bar{\epsilon}_f + U_f & 0 & -\sqrt{2}|t| \\ 0 & 2\bar{\epsilon}_c + U_c & -\sqrt{2}|t| \\ -\sqrt{2}|t| & -\sqrt{2}|t| & \bar{\epsilon}_c + \bar{\epsilon}_f \end{pmatrix} \begin{pmatrix} \langle\mathcal{O}|\hat{f}_\downarrow \hat{f}_\uparrow \\ \langle\mathcal{O}|\hat{c}_\downarrow \hat{c}_\uparrow \\ \langle\mathcal{O}|\frac{1}{\sqrt{2}}\big(\hat{c}_\downarrow \hat{f}_\uparrow - \hat{c}_\uparrow \hat{f}_\downarrow\big) \end{pmatrix} \tag{D.14}$$

where $\hat{P}_{2,0}$ is the projection operator onto the two-particle states ($N = 2$) with $S_z = 0\hbar$.

Table D.3: Hamilton eigenstates of the asymmetric dimer.

N	S	$S_z/\hbar$	$\lvert\Phi\rangle$	$\langle\Phi\lvert\hat{H}\rvert\Phi\rangle$
$N=0$	$S=0$	$S_z=0$	$\lvert\mathcal{O}\rangle$	$E=0$
$N=1$	$S=\frac{1}{2}$	$S_z=+\frac{1}{2}$	$\Big(\hat{f}_\uparrow^\dagger\cos(\alpha_1)+\hat{c}_\uparrow^\dagger\sin(\alpha_1)\Big)\lvert\mathcal{O}\rangle$	$\frac{\bar{\epsilon}_c+\bar{\epsilon}_f}{2}-\sqrt{\big(\frac{\bar{\epsilon}_c-\bar{\epsilon}_f}{2}\big)^2+t^2}$
$N=1$	$S=\frac{1}{2}$	$S_z=+\frac{1}{2}$	$\Big(\hat{f}_\uparrow^\dagger\sin(\alpha_1)-\hat{c}_\uparrow^\dagger\cos(\alpha_1)\Big)\lvert\mathcal{O}\rangle$	$\frac{\bar{\epsilon}_c+\bar{\epsilon}_f}{2}+\sqrt{\big(\frac{\bar{\epsilon}_c-\bar{\epsilon}_f}{2}\big)^2+t^2}$
$N=1$	$S=\frac{1}{2}$	$S_z=-\frac{1}{2}$	$\Big(\hat{f}_\downarrow^\dagger\cos(\alpha_1)+\hat{c}_\downarrow^\dagger\sin(\alpha_1)\Big)\lvert\mathcal{O}\rangle$	$\frac{\bar{\epsilon}_c+\bar{\epsilon}_f}{2}-\sqrt{\big(\frac{\bar{\epsilon}_c-\bar{\epsilon}_f}{2}\big)^2+t^2}$
$N=1$	$S=\frac{1}{2}$	$S_z=-\frac{1}{2}$	$\Big(\hat{f}_\downarrow^\dagger\sin(\alpha_1)+\hat{c}_\downarrow^\dagger\cos(\alpha_1)\Big)\lvert\mathcal{O}\rangle$	$\frac{\bar{\epsilon}_c+\bar{\epsilon}_f}{2}+\sqrt{\big(\frac{\bar{\epsilon}_c-\bar{\epsilon}_f}{2}\big)^2+t^2}$
$N=2$	$S=0$	$S_z=0$	$\approx\hat{f}_\uparrow^\dagger\hat{f}_\downarrow^\dagger\lvert\mathcal{O}\rangle$	$\approx 2\bar{\epsilon}_f+U_f+O(t,1/U)$
$N=2$	$S=0$	$S_z=0$	$\approx\hat{c}_\uparrow^\dagger\hat{c}_\downarrow^\dagger\lvert\mathcal{O}\rangle$	$\approx 2\bar{\epsilon}_c+U_c+O(t,1/U)$
$N=2$	$S=0$	$S_z=0$	$\approx\frac{1}{\sqrt{2}}\big(\hat{f}_\uparrow^\dagger\hat{c}_\downarrow^\dagger-\hat{f}_\downarrow^\dagger\hat{c}_\uparrow^\dagger\big)\lvert\mathcal{O}\rangle$	$\approx\bar{\epsilon}_f+\bar{\epsilon}_c+O(t,1/U)$
$N=2$	$S=1$	$S_z=1$	$\hat{f}_\uparrow^\dagger\hat{c}_\uparrow^\dagger\lvert\mathcal{O}\rangle$	$E=\bar{\epsilon}_f+\bar{\epsilon}_c$
$N=2$	$S=1$	$S_z=0$	$\frac{1}{\sqrt{2}}\big(\hat{f}_\uparrow^\dagger\hat{c}_\downarrow^\dagger+\hat{f}_\downarrow^\dagger\hat{c}_\uparrow^\dagger\big)\lvert\mathcal{O}\rangle$	$E=\bar{\epsilon}_f+\bar{\epsilon}_c$
$N=2$	$S=1$	$S_z=-1$	$\hat{f}_\downarrow^\dagger\hat{c}_\downarrow^\dagger\lvert\mathcal{O}\rangle$	$E=\bar{\epsilon}_f+\bar{\epsilon}_c$
$N=3$	$S=\frac{1}{2}$	$S_z=+\frac{1}{2}$	$\hat{f}_\uparrow^\dagger\hat{c}_\uparrow^\dagger\Big(\hat{f}_\downarrow^\dagger\cos(\alpha_2)+\hat{c}_\downarrow^\dagger\sin(\alpha_2)\Big)\lvert\mathcal{O}\rangle$	$\frac{3\bar{\epsilon}_c+U_c+3\bar{\epsilon}_f+U_f}{2}-\sqrt{\big(\frac{\bar{\epsilon}_f+U_f-\bar{\epsilon}_c-U_c}{2}\big)^2+t^2}$
$N=3$	$S=\frac{1}{2}$	$S_z=+\frac{1}{2}$	$\hat{f}_\uparrow^\dagger\hat{c}_\uparrow^\dagger\Big(\hat{f}_\downarrow^\dagger\sin(\alpha_2)-\hat{c}_\downarrow^\dagger\cos(\alpha_2)\Big)\lvert\mathcal{O}\rangle$	$\frac{3\bar{\epsilon}_c+U_c+3\bar{\epsilon}_f+U_f}{2}+\sqrt{\big(\frac{\bar{\epsilon}_f+U-\bar{\epsilon}_c-U_c}{2}\big)^2+t^2}$
$N=3$	$S=\frac{1}{2}$	$S_z=-\frac{1}{2}$	$\hat{f}_\downarrow^\dagger\hat{c}_\downarrow^\dagger\Big(\hat{f}_\uparrow^\dagger\cos(\alpha_2)+\hat{c}_\uparrow^\dagger\sin(\alpha_2)\Big)\lvert\mathcal{O}\rangle$	$\frac{3\bar{\epsilon}_c+U_c+3\bar{\epsilon}_f+U_f}{2}-\sqrt{\big(\frac{\bar{\epsilon}_f+U_f-\bar{\epsilon}_c-U_c}{2}\big)^2+t^2}$
$N=3$	$S=\frac{1}{2}$	$S_z=-\frac{1}{2}$	$\hat{f}_\downarrow^\dagger\hat{c}_\downarrow^\dagger\Big(\hat{f}_\uparrow^\dagger\sin(\alpha_2)-\hat{c}_\uparrow^\dagger\cos(\alpha_2)\Big)\lvert\mathcal{O}\rangle$	$\frac{3\bar{\epsilon}_c+U_c+3\bar{\epsilon}_f+U_f}{2}+\sqrt{\big(\frac{\bar{\epsilon}_f+U_f-\bar{\epsilon}_c-U_c}{2}\big)^2+t^2}$
$N=4$	$S=0$	$S_z=0$	$\hat{f}_\uparrow^\dagger\hat{f}_\downarrow^\dagger\hat{c}_\uparrow^\dagger\hat{c}_\downarrow^\dagger\lvert\mathcal{O}\rangle$	$E=2\bar{\epsilon}_c+2\bar{\epsilon}_f+U_f+U_c$

D.2 Hubbard dimer

Let me now study the Hubbard dimer, which is the symmetric case of the asymmetric dimer studied in the previous section D.1.

The physics of the Hubbard dimer is described in section **??** on p. **??**.

The difference to the asymmetric dimer is that the atomic orbital energies, named $\bar{\epsilon}$, are equal, i.e. $\bar{\epsilon}_c = \bar{\epsilon}_f = \bar{\epsilon}$, and that the Coulomb repulsion parameters, named U, are equal too, i.e. $U_c = U_f$. We adhere to the notation naming the atoms F and C and their creators $\hat{f}_\sigma^\dagger$ and $\hat{c}_\sigma^\dagger$. The letters simply stand for left and right atom.

$$\begin{aligned}\hat{H} &= \underbrace{\sum_\sigma \bar{\epsilon}\hat{f}_\sigma^\dagger \hat{f}_\sigma + \frac{1}{2}U\sum_{\sigma,\sigma'}\hat{f}_\sigma^\dagger \hat{f}_{\sigma'}^\dagger \hat{f}_{\sigma'}\hat{f}_\sigma}_{\text{atom F}} + \underbrace{\sum_\sigma \bar{\epsilon}\hat{c}_\sigma^\dagger \hat{c}_\sigma + \frac{1}{2}U\sum_{\sigma,\sigma'}\hat{c}_\sigma^\dagger \hat{c}_{\sigma'}^\dagger \hat{c}_{\sigma'}\hat{c}_\sigma}_{\text{atom C}} \underbrace{-|t|\sum_\sigma\left(\hat{f}_\sigma^\dagger \hat{c}_\sigma + \hat{c}_\sigma^\dagger \hat{f}_\sigma\right)}_{\text{hopping}} \\ &= \overbrace{\sum_\sigma \bar{\epsilon}\hat{n}_{f,\sigma} + U\hat{n}_{f,\uparrow}\hat{n}_{f,\downarrow} + \underbrace{U\sum_\sigma \hat{n}_{f,\sigma}\left(\hat{n}_{f,\sigma}-1\right)}_{=0}}^{\text{atom F}} + \overbrace{\sum_\sigma \bar{\epsilon}\hat{n}_{c,\sigma} + U\hat{n}_{c,\uparrow}\hat{n}_{c,\downarrow} + \underbrace{U\sum_\sigma \hat{n}_{c,\sigma}\left(\hat{n}_{c,\sigma}-1\right)}_{=0}}^{\text{atom C}} \\ &\quad \underbrace{-|t|\sum_\sigma\left(\hat{f}_\sigma^\dagger \hat{c}_\sigma + \hat{c}_\sigma^\dagger \hat{f}_\sigma\right)}_{\text{hopping}}\end{aligned} \tag{D.15}$$

Table D.4: Symmetry adapted orbitals for the Hubbard dimer. The states are classified according to particle number, spin quantum numbers S and S_z and spatial inversion with eigenvalue $P = \pm 1$. The total spin eigenvalues are $\hbar^2 s(s+1)$. The spin in z-direction is $\hbar s_z$. The energies are the **energy expectation values** of the symmetry adapted states rather than the eigenvalues of the Hamiltonian. For the 2×2 block with $N = 2$, $S = 0$ and $P = +1$, they are not eigenstates of the Hamiltonian.

N	S	S_z	P	$\|\Phi\rangle$	$\langle\Phi\|\hat{H}\|\Phi\rangle$
$N=0$	$S=0$	$S_z=0$	$P=1$	$\|\mathcal{O}\rangle$	0
$N=1$	$S=\frac{1}{2}$	$S_z=+\frac{1}{2}$	$P=+1$	$\frac{1}{\sqrt{2}}\left(\hat{f}_\uparrow^\dagger + \hat{c}_\uparrow^\dagger\right)\|\mathcal{O}\rangle$	$\bar{\epsilon} - \|t\|$
$N=1$	$S=\frac{1}{2}$	$S_z=+\frac{1}{2}$	$P=-1$	$\frac{1}{\sqrt{2}}\left(\hat{f}_\uparrow^\dagger - \hat{c}_\uparrow^\dagger\right)\|\mathcal{O}\rangle$	$\bar{\epsilon} + \|t\|$
$N=1$	$S=\frac{1}{2}$	$S_z=-\frac{1}{2}$	$P=+1$	$\frac{1}{\sqrt{2}}\left(\hat{f}_\downarrow^\dagger + \hat{c}_\downarrow^\dagger\right)\|\mathcal{O}\rangle$	$\bar{\epsilon} - \|t\|$
$N=1$	$S=\frac{1}{2}$	$S_z=-\frac{1}{2}$	$P=-1$	$\frac{1}{\sqrt{2}}\left(\hat{f}_\downarrow^\dagger - \hat{c}_\downarrow^\dagger\right)\|\mathcal{O}\rangle$	$\bar{\epsilon} + \|t\|$
$N=2$	$S=0$	$S_z=0$	$P=-1$	$\frac{1}{\sqrt{2}}\left(\hat{f}_\uparrow^\dagger \hat{f}_\downarrow^\dagger - \hat{c}_\uparrow^\dagger \hat{c}_\downarrow^\dagger\right)\|\mathcal{O}\rangle$	$2\bar{\epsilon} + U$
$N=2$	$S=0$	$S_z=0$	$P=+1$	$\frac{1}{\sqrt{2}}\left(\hat{f}_\uparrow^\dagger \hat{f}_\downarrow^\dagger + \hat{c}_\uparrow^\dagger \hat{c}_\downarrow^\dagger\right)\|\mathcal{O}\rangle$	$2\bar{\epsilon} + U$
$N=2$	$S=0$	$S_z=0$	$P=+1$	$\frac{1}{\sqrt{2}}\left(\hat{f}_\uparrow^\dagger \hat{c}_\downarrow^\dagger - \hat{f}_\downarrow^\dagger \hat{c}_\uparrow^\dagger\right)\|\mathcal{O}\rangle$	$2\bar{\epsilon}$
$N=2$	$S=1$	$S_z=1$	$P=-1$	$\hat{f}_\uparrow^\dagger \hat{c}_\uparrow^\dagger\|\mathcal{O}\rangle$	$2\bar{\epsilon}$
$N=2$	$S=1$	$S_z=0$	$P=-1$	$\frac{1}{\sqrt{2}}\left(\hat{f}_\uparrow^\dagger \hat{c}_\downarrow^\dagger + \hat{f}_\downarrow^\dagger \hat{c}_\uparrow^\dagger\right)\|\mathcal{O}\rangle$	$2\bar{\epsilon}$
$N=2$	$S=1$	$S_z=-1$	$P=-1$	$\hat{f}_\downarrow^\dagger \hat{c}_\downarrow^\dagger\|\mathcal{O}\rangle$	$2\bar{\epsilon}$
$N=3$	$S=\frac{1}{2}$	$S_z=+\frac{1}{2}$	$P=-1$	$\hat{f}_\uparrow^\dagger \hat{c}_\uparrow^\dagger \frac{1}{\sqrt{2}}\left(\hat{f}_\downarrow^\dagger + \hat{c}_\downarrow^\dagger\right)\|\mathcal{O}\rangle$	$3\bar{\epsilon} + U - \|t\|$
$N=3$	$S=\frac{1}{2}$	$S_z=+\frac{1}{2}$	$P=+1$	$\hat{f}_\uparrow^\dagger \hat{c}_\uparrow^\dagger \frac{1}{\sqrt{2}}\left(\hat{f}_\downarrow^\dagger - \hat{c}_\downarrow^\dagger\right)\|\mathcal{O}\rangle$	$3\bar{\epsilon} + U + \|t\|$
$N=3$	$S=\frac{1}{2}$	$S_z=-\frac{1}{2}$	$P=-1$	$\hat{f}_\downarrow^\dagger \hat{c}_\downarrow^\dagger \frac{1}{\sqrt{2}}\left(\hat{f}_\uparrow^\dagger + \hat{c}_\uparrow^\dagger\right)\|\mathcal{O}\rangle$	$3\bar{\epsilon} + U - \|t\|$
$N=3$	$S=\frac{1}{2}$	$S_z=-\frac{1}{2}$	$P=+1$	$\hat{f}_\downarrow^\dagger \hat{c}_\downarrow^\dagger \frac{1}{\sqrt{2}}\left(\hat{f}_\uparrow^\dagger - \hat{c}_\uparrow^\dagger\right)\|\mathcal{O}\rangle$	$3\bar{\epsilon} + U + \|t\|$
$N=4$	$S=0$	$S_z=0$	$P=+1$	$\hat{f}_\uparrow^\dagger \hat{f}_\downarrow^\dagger \hat{c}_\uparrow^\dagger \hat{c}_\downarrow^\dagger\|\mathcal{O}\rangle$	$4\bar{\epsilon} + 2U$

D.2.1 Symmetry-adapted many-particle states

We start from the symmetry adapted states of the asymmetric dimer and include the spatial inversion with eigenvalue $P \in \{+, -\}$ as additional symmetry.

The symmetry-adapted many-particle states are given in table D.4. All states are eigenstates except for the 2×2 block in the 2-particle channel.

For a non-interacting system, the two states combine into a Slater determinant formed by two bonding orbitals or one with two antibonding orbitals.

$$\begin{aligned}
\frac{1}{\sqrt{2}}\left[\frac{1}{\sqrt{2}}\left(\hat{f}_\uparrow^\dagger \hat{f}_\downarrow^\dagger + \hat{c}_\uparrow^\dagger \hat{c}_\downarrow^\dagger\right) + \frac{1}{\sqrt{2}}\left(\hat{f}_\uparrow^\dagger \hat{c}_\downarrow^\dagger - \hat{f}_\downarrow^\dagger \hat{c}_\uparrow^\dagger\right)\right]|\mathcal{O}\rangle &= \frac{1}{2}\left(\hat{f}_\uparrow^\dagger + \hat{c}_\uparrow^\dagger\right)\left(\hat{f}_\downarrow^\dagger + \hat{c}_\downarrow^\dagger\right)|\mathcal{O}\rangle \\
\frac{1}{\sqrt{2}}\left[\frac{1}{\sqrt{2}}\left(\hat{f}_\uparrow^\dagger \hat{f}_\downarrow^\dagger + \hat{c}_\uparrow^\dagger \hat{c}_\downarrow^\dagger\right) - \frac{1}{\sqrt{2}}\left(\hat{f}_\uparrow^\dagger \hat{c}_\downarrow^\dagger - \hat{f}_\downarrow^\dagger \hat{c}_\uparrow^\dagger\right)\right]|\mathcal{O}\rangle &= \frac{1}{2}\left(\hat{f}_\uparrow^\dagger - \hat{c}_\uparrow^\dagger\right)\left(\hat{f}_\downarrow^\dagger - \hat{c}_\downarrow^\dagger\right)|\mathcal{O}\rangle
\end{aligned} \qquad \text{(D.16)}$$

2-particle channel

The Hamiltonian in the 2×2 sub-block with $N = 2$, $S = 0$, $P = 1$ is

$$\hat{P}_{N=2,S=0,P=1}\hat{H}\hat{P}_{N=2,S=0,P=1} = \begin{pmatrix} \frac{1}{\sqrt{2}}(\hat{f}_\uparrow^\dagger \hat{f}_\downarrow^\dagger + \hat{c}_\uparrow^\dagger \hat{c}_\downarrow^\dagger)|\mathcal{O}\rangle \\ \frac{1}{\sqrt{2}}(\hat{f}_\uparrow^\dagger \hat{c}_\downarrow^\dagger - \hat{f}_\downarrow^\dagger \hat{c}_\uparrow^\dagger)|\mathcal{O}\rangle \end{pmatrix} \begin{pmatrix} 2\bar{\epsilon} + U & -2|t| \\ -2|t| & 2\bar{\epsilon} \end{pmatrix} \begin{pmatrix} \langle\mathcal{O}|\frac{1}{\sqrt{2}}(\hat{f}_\downarrow \hat{f}_\uparrow + \hat{c}_\downarrow \hat{c}_\uparrow) \\ \langle\mathcal{O}|\frac{1}{\sqrt{2}}(\hat{c}_\downarrow \hat{f}_\uparrow - \hat{c}_\uparrow \hat{f}_\downarrow) \end{pmatrix} \tag{D.17}$$

The energy eigenvalues are

$$\begin{aligned} E_\pm &= 2\bar{\epsilon} + \frac{1}{2}U \pm \sqrt{\left(\frac{1}{2}U\right)^2 + 4t^2} \\ &= 2\bar{\epsilon} + 2|t|\left(\frac{U}{4|t|} \pm \sqrt{1 + \left(\frac{U}{4|t|}\right)^2}\right) \\ &= \begin{cases} 2\bar{\epsilon} - \Delta_{st} & \text{for } \pm = - \\ 2\bar{\epsilon} + U + \Delta_{st} & \text{for } \pm = + \end{cases} \end{aligned} \tag{D.18}$$

with the singlet-triplet splitting

$$\Delta_{st} = 2|t|\left(\sqrt{1+q^2} - q\right) \qquad \text{with } q = \frac{U}{4|t|} \tag{D.19}$$

The eigenstates are

$$\begin{aligned} |\Psi_-\rangle &= \frac{\cos(\gamma)}{\sqrt{2}} \underbrace{(\hat{f}_\uparrow^\dagger \hat{f}_\downarrow^\dagger + \hat{c}_\uparrow^\dagger \hat{c}_\downarrow^\dagger)|\mathcal{O}\rangle}_{\text{double occupancy}} + \frac{\sin(\gamma)}{\sqrt{2}} \underbrace{(\hat{f}_\uparrow^\dagger \hat{c}_\downarrow^\dagger - \hat{f}_\downarrow^\dagger \hat{c}_\uparrow^\dagger)|\mathcal{O}\rangle}_{\text{left-right correlated}} \\ |\Psi_+\rangle &= \frac{\sin(\gamma)}{\sqrt{2}}(\hat{f}_\uparrow^\dagger \hat{f}_\downarrow^\dagger + \hat{c}_\uparrow^\dagger \hat{c}_\downarrow^\dagger)|\mathcal{O}\rangle - \frac{\cos(\gamma)}{\sqrt{2}}(\hat{f}_\uparrow^\dagger \hat{c}_\downarrow^\dagger - \hat{f}_\downarrow^\dagger \hat{c}_\uparrow^\dagger)|\mathcal{O}\rangle \end{aligned} \tag{D.20}$$

The ansatz with cosine and sine of an angle for the eigenstates guarantee that the two states are orthonormal.

The angle is obtained by inserting the Ansatz for $|\Psi_-\rangle$ into the Schrödinger equation.

$$\begin{aligned} 0 &= (2\bar{\epsilon} + U - E_-)\cos(\gamma) - 2|t|\sin(\gamma) \\ \Rightarrow \qquad \tan(\gamma) &= \frac{1}{2|t|}(2\bar{\epsilon} + U - E_-) \\ &= \frac{1}{2|t|}\left(2\bar{\epsilon} + U - 2\bar{\epsilon} - \frac{1}{2}U + \sqrt{(\frac{1}{2}U)^2 + 4t^2}\right) \\ &= \frac{1}{2|t|}\left(\frac{1}{2}U + \sqrt{U^2 + 4t^2}\right) \\ &= \frac{U}{4|t|} + \sqrt{1 + \left(\frac{U}{4|t|}\right)^2} \\ \gamma &= \operatorname{atan}\left(q + \sqrt{1+q^2}\right) \qquad \text{with } q = \frac{U}{4|t|} \end{aligned} \tag{D.21}$$

2-PARTICLE GROUND STATE OF THE HUBBARD DIMER

The ground state energy of the Hubbard dimer in the two-particle sector

$$|\Psi_-\rangle = \frac{\cos(\gamma)}{\sqrt{2}} \underbrace{(\hat{f}_\uparrow^\dagger \hat{f}_\downarrow^\dagger + \hat{c}_\uparrow^\dagger \hat{c}_\downarrow^\dagger)|\mathcal{O}\rangle}_{\text{double occupancy}} + \frac{\sin(\gamma)}{\sqrt{2}} \underbrace{(\hat{f}_\uparrow^\dagger \hat{c}_\downarrow^\dagger - \hat{f}_\downarrow^\dagger \hat{c}_\uparrow^\dagger)|\mathcal{O}\rangle}_{\text{left-right correlated}} \tag{D.22}$$

and has the energy

$$E_- = 2\bar{\epsilon} - \underbrace{2|t|\left(\sqrt{1+q^2} - q\right)}_{=:\Delta_{st}} = 2\bar{\epsilon} - \Delta_{st} \tag{D.23}$$

with

$$\gamma = \text{atan}\left(q + \sqrt{1+q^2}\right) \qquad \text{and } q \stackrel{\text{def}}{=} \frac{U}{4|t|} \tag{D.24}$$

- In the non-interacting limit, $q = 0$, we obtain $\gamma = \pi/4 = 45°$, for which $\cos(\gamma) = \sin(\gamma) = \frac{1}{\sqrt{2}}$. The single-triplet splitting is $\Delta_{st} = 2|t|$, which corresponds to the energy to transfer one-electron from the bonding to the antibonding orbital. In order to flip the spin of one of the two electrons, it must be lifted into the antibonding state.

- In the strongly interacting limit, $q \to \infty$, we can approximate $\gamma \approx \text{atan}(2q) \to \pi/2 = 90°$. In this limit, we obtain a lower, exactly left-right-correlated state $|\Psi_-\rangle$ with energy $E_- = 2\bar{\epsilon} - \Delta_{st}$ and an upper state $|\Psi_+\rangle$ with double occupancy with energy $E_+ = 2\bar{\epsilon} + U + \Delta_{st}$. The singlet-triplet splitting is

$$\begin{aligned}\Delta_{st} &= 2|t|\Big(\sqrt{1+q^2} - q\Big) = 2|t|q\Big(\sqrt{1+(1/q)^2} - 1\Big) = 2|t|q\Big(1 + \frac{1}{2q^2} + O(q^{-4}) - 1\Big) \\ &= \frac{|t|}{q} + |t|O(q^{-4}\Big) = \frac{4|t|^2}{U} + |t|O\left(\left(\frac{4|t|}{U}\right)^4\right)\end{aligned} \tag{D.25}$$

Table D.5: One-particle excitations of the Hubbard dimer between 0-particle, 1-particle and 2-particle states. Note that the symbol $\hat{c}$ is overloaded and used once as a generic field operator $\hat{c}_\alpha \in \{\hat{c}_\uparrow, \hat{c}_\downarrow, \hat{f}_\uparrow, \hat{f}_\downarrow\}$ and once as the field operator at one of the sites $\hat{c}_\sigma$. The quasi-particle wave function is $|\psi^{\text{Dyson}}_{f,i}\rangle = \sum_\alpha \hat{c}^\dagger_\alpha q_\alpha |\mathcal{O}\rangle$ with $q_\alpha = \langle \Psi_i | \hat{c}_\alpha | \Psi_f \rangle$.

$\|\Psi_i\rangle$	$\|\Psi_f\rangle$	$\hat{c}^\dagger_\alpha$	$\langle \Psi_i \|\hat{c}_\alpha\| \Psi_f\rangle$	$\Delta E - \bar{\epsilon}$
$0 \to 1$ with final $S_z = -\hbar/2$				
$\|\mathcal{O}\rangle$	$\frac{1}{\sqrt{2}}\left(\hat{f}^\dagger_\downarrow + \hat{c}^\dagger_\downarrow\right)\|\mathcal{O}\rangle$	$\hat{f}^\dagger_\downarrow$	$\frac{1}{\sqrt{2}}$	$-\|t\|$
$\|\mathcal{O}\rangle$	$\frac{1}{\sqrt{2}}\left(\hat{f}^\dagger_\downarrow + \hat{c}^\dagger_\downarrow\right)\|\mathcal{O}\rangle$	$\hat{c}^\dagger_\downarrow$	$\frac{1}{\sqrt{2}}$	$-\|t\|$
$\|\mathcal{O}\rangle$	$\frac{1}{\sqrt{2}}\left(\hat{f}^\dagger_\downarrow - \hat{c}^\dagger_\downarrow\right)\|\mathcal{O}\rangle$	$\hat{f}^\dagger_\downarrow$	$\frac{1}{\sqrt{2}}$	$+\|t\|$
$\|\mathcal{O}\rangle$	$\frac{1}{\sqrt{2}}\left(\hat{f}^\dagger_\downarrow - \hat{c}^\dagger_\downarrow\right)\|\mathcal{O}\rangle$	$\hat{c}^\dagger_\downarrow$	$-\frac{1}{\sqrt{2}}$	$+\|t\|$
$1 \to 2$ with initial $S_z = -\hbar/2$				
$\frac{1}{\sqrt{2}}\left(\hat{f}^\dagger_\downarrow + \hat{c}^\dagger_\downarrow\right)\|\mathcal{O}\rangle$	$\hat{f}^\dagger_\downarrow \hat{c}^\dagger_\downarrow \|\mathcal{O}\rangle$	$\hat{f}^\dagger_\downarrow$	$\frac{1}{\sqrt{2}}$	$+\|t\|$
$\frac{1}{\sqrt{2}}\left(\hat{f}^\dagger_\downarrow + \hat{c}^\dagger_\downarrow\right)\|\mathcal{O}\rangle$	$\hat{f}^\dagger_\downarrow \hat{c}^\dagger_\downarrow \|\mathcal{O}\rangle$	$\hat{c}^\dagger_\downarrow$	$-\frac{1}{\sqrt{2}}$	$+\|t\|$
$\frac{1}{\sqrt{2}}\left(\hat{f}^\dagger_\downarrow + \hat{c}^\dagger_\downarrow\right)\|\mathcal{O}\rangle$	$\frac{1}{\sqrt{2}}\left(\hat{f}^\dagger_\uparrow \hat{f}^\dagger_\downarrow - \hat{c}^\dagger_\uparrow \hat{c}^\dagger_\downarrow\right)\|\mathcal{O}\rangle$	$\hat{f}^\dagger_\uparrow$	$\frac{1}{2}$	$+\|t\| + U$
$\frac{1}{\sqrt{2}}\left(\hat{f}^\dagger_\downarrow + \hat{c}^\dagger_\downarrow\right)\|\mathcal{O}\rangle$	$\frac{1}{\sqrt{2}}\left(\hat{f}^\dagger_\uparrow \hat{f}^\dagger_\downarrow - \hat{c}^\dagger_\uparrow \hat{c}^\dagger_\downarrow\right)\|\mathcal{O}\rangle$	$\hat{c}^\dagger_\uparrow$	$-\frac{1}{2}$	$+\|t\| + U$
$\frac{1}{\sqrt{2}}\left(\hat{f}^\dagger_\downarrow + \hat{c}^\dagger_\downarrow\right)\|\mathcal{O}\rangle$	$\frac{\cos(\gamma)}{\sqrt{2}}\left(\hat{f}^\dagger_\uparrow \hat{f}^\dagger_\downarrow + \hat{c}^\dagger_\uparrow \hat{c}^\dagger_\downarrow\right) + \frac{\sin(\gamma)}{\sqrt{2}}\left(\hat{f}^\dagger_\uparrow \hat{c}^\dagger_\downarrow - \hat{f}^\dagger_\downarrow \hat{c}^\dagger_\uparrow\right)\|\mathcal{O}\rangle$	$\hat{f}^\dagger_\uparrow$	$\frac{\cos(\gamma)+\sin(\gamma)}{2}$	$+\|t\| - \Delta_{st}$
$\frac{1}{\sqrt{2}}\left(\hat{f}^\dagger_\downarrow + \hat{c}^\dagger_\downarrow\right)\|\mathcal{O}\rangle$	$\frac{\cos(\gamma)}{\sqrt{2}}\left(\hat{f}^\dagger_\uparrow \hat{f}^\dagger_\downarrow + \hat{c}^\dagger_\uparrow \hat{c}^\dagger_\downarrow\right) + \frac{\sin(\gamma)}{\sqrt{2}}\left(\hat{f}^\dagger_\uparrow \hat{c}^\dagger_\downarrow - \hat{f}^\dagger_\downarrow \hat{c}^\dagger_\uparrow\right)\|\mathcal{O}\rangle$	$\hat{c}^\dagger_\uparrow$	$\frac{\sin(\gamma)+\cos(\gamma)}{2}$	$+\|t\| - \Delta_{st}$
$\frac{1}{\sqrt{2}}\left(\hat{f}^\dagger_\downarrow + \hat{c}^\dagger_\downarrow\right)\|\mathcal{O}\rangle$	$\frac{\sin(\gamma)}{\sqrt{2}}\left(\hat{f}^\dagger_\uparrow \hat{f}^\dagger_\downarrow + \hat{c}^\dagger_\uparrow \hat{c}^\dagger_\downarrow\right) - \frac{\cos(\gamma)}{\sqrt{2}}\left(\hat{f}^\dagger_\uparrow \hat{c}^\dagger_\downarrow - \hat{f}^\dagger_\downarrow \hat{c}^\dagger_\uparrow\right)\|\mathcal{O}\rangle$	$\hat{f}^\dagger_\uparrow$	$\frac{\sin(\gamma)-\cos(\gamma)}{2}$	$+\|t\| + U + \Delta_{st}$
$\frac{1}{\sqrt{2}}\left(\hat{f}^\dagger_\downarrow + \hat{c}^\dagger_\downarrow\right)\|\mathcal{O}\rangle$	$\frac{\sin(\gamma)}{\sqrt{2}}\left(\hat{f}^\dagger_\uparrow \hat{f}^\dagger_\downarrow + \hat{c}^\dagger_\uparrow \hat{c}^\dagger_\downarrow\right) - \frac{\cos(\gamma)}{\sqrt{2}}\left(\hat{f}^\dagger_\uparrow \hat{c}^\dagger_\downarrow - \hat{f}^\dagger_\downarrow \hat{c}^\dagger_\uparrow\right)\|\mathcal{O}\rangle$	$\hat{c}^\dagger_\uparrow$	$\frac{\sin(\gamma)-\cos(\gamma)}{2}$	$+\|t\| + U + \Delta_{st}$
$\frac{1}{\sqrt{2}}\left(\hat{f}^\dagger_\downarrow - \hat{c}^\dagger_\downarrow\right)\|\mathcal{O}\rangle$	$\hat{f}^\dagger_\downarrow \hat{c}^\dagger_\downarrow \|\mathcal{O}\rangle$	$\hat{f}^\dagger_\downarrow$	$-\frac{1}{\sqrt{2}}$	$-\|t\|$
$\frac{1}{\sqrt{2}}\left(\hat{f}^\dagger_\downarrow - \hat{c}^\dagger_\downarrow\right)\|\mathcal{O}\rangle$	$\hat{f}^\dagger_\downarrow \hat{c}^\dagger_\downarrow \|\mathcal{O}\rangle$	$\hat{c}^\dagger_\downarrow$	$-\frac{1}{\sqrt{2}}$	$-\|t\|$
$\frac{1}{\sqrt{2}}\left(\hat{f}^\dagger_\downarrow - \hat{c}^\dagger_\downarrow\right)\|\mathcal{O}\rangle$	$\frac{1}{\sqrt{2}}\left(\hat{f}^\dagger_\uparrow \hat{f}^\dagger_\downarrow - \hat{c}^\dagger_\uparrow \hat{c}^\dagger_\downarrow\right)\|\mathcal{O}\rangle$	$\hat{f}^\dagger_\uparrow$	$\frac{1}{2}$	$-\|t\| + U$
$\frac{1}{\sqrt{2}}\left(\hat{f}^\dagger_\downarrow - \hat{c}^\dagger_\downarrow\right)\|\mathcal{O}\rangle$	$\frac{1}{\sqrt{2}}\left(\hat{f}^\dagger_\uparrow \hat{f}^\dagger_\downarrow - \hat{c}^\dagger_\uparrow \hat{c}^\dagger_\downarrow\right)\|\mathcal{O}\rangle$	$\hat{c}^\dagger_\uparrow$	$\frac{1}{2}$	$-\|t\| + U$
$\frac{1}{\sqrt{2}}\left(\hat{f}^\dagger_\downarrow - \hat{c}^\dagger_\downarrow\right)\|\mathcal{O}\rangle$	$\frac{\cos(\gamma)}{\sqrt{2}}\left(\hat{f}^\dagger_\uparrow \hat{f}^\dagger_\downarrow + \hat{c}^\dagger_\uparrow \hat{c}^\dagger_\downarrow\right) + \frac{\sin(\gamma)}{\sqrt{2}}\left(\hat{f}^\dagger_\uparrow \hat{c}^\dagger_\downarrow - \hat{f}^\dagger_\downarrow \hat{c}^\dagger_\uparrow\right)\|\mathcal{O}\rangle$	$\hat{f}^\dagger_\uparrow$	$\frac{\cos(\gamma)-\sin(\gamma)}{2}$	$-\|t\| - \Delta_{st}$
$\frac{1}{\sqrt{2}}\left(\hat{f}^\dagger_\downarrow - \hat{c}^\dagger_\downarrow\right)\|\mathcal{O}\rangle$	$\frac{\cos(\gamma)}{\sqrt{2}}\left(\hat{f}^\dagger_\uparrow \hat{f}^\dagger_\downarrow + \hat{c}^\dagger_\uparrow \hat{c}^\dagger_\downarrow\right) + \frac{\sin(\gamma)}{\sqrt{2}}\left(\hat{f}^\dagger_\uparrow \hat{c}^\dagger_\downarrow - \hat{f}^\dagger_\downarrow \hat{c}^\dagger_\uparrow\right)\|\mathcal{O}\rangle$	$\hat{c}^\dagger_\uparrow$	$\frac{\sin(\gamma)-\cos(\gamma)}{2}$	$-\|t\| - \Delta_{st}$
$\frac{1}{\sqrt{2}}\left(\hat{f}^\dagger_\downarrow - \hat{c}^\dagger_\downarrow\right)\|\mathcal{O}\rangle$	$\frac{\sin(\gamma)}{\sqrt{2}}\left(\hat{f}^\dagger_\uparrow \hat{f}^\dagger_\downarrow + \hat{c}^\dagger_\uparrow \hat{c}^\dagger_\downarrow\right) - \frac{\cos(\gamma)}{\sqrt{2}}\left(\hat{f}^\dagger_\uparrow \hat{c}^\dagger_\downarrow - \hat{f}^\dagger_\downarrow \hat{c}^\dagger_\uparrow\right)\|\mathcal{O}\rangle$	$\hat{f}^\dagger_\uparrow$	$\frac{\sin(\gamma)+\cos(\gamma)}{2}$	$-\|t\| + U + \Delta_{st}$
$\frac{1}{\sqrt{2}}\left(\hat{f}^\dagger_\downarrow - \hat{c}^\dagger_\downarrow\right)\|\mathcal{O}\rangle$	$\frac{\sin(\gamma)}{\sqrt{2}}\left(\hat{f}^\dagger_\uparrow \hat{f}^\dagger_\downarrow + \hat{c}^\dagger_\uparrow \hat{c}^\dagger_\downarrow\right) - \frac{\cos(\gamma)}{\sqrt{2}}\left(\hat{f}^\dagger_\uparrow \hat{c}^\dagger_\downarrow - \hat{f}^\dagger_\downarrow \hat{c}^\dagger_\uparrow\right)\|\mathcal{O}\rangle$	$\hat{c}^\dagger_\uparrow$	$\frac{\sin(\gamma)+\cos(\gamma)}{2}$	$-\|t\| + U + \Delta_{st}$

D.2.2 Spectral function of the Hubbard dimer

The quasi-particle states and energies are obtained within the Lehman representation.

We use the many-particle energies and states from table D.4 and Eq. D.20 Eq. D.18

The one-particle excitations of the Hubbard dimer are listed in table D.5 and table D.6

Table D.6: One-particle excitations of the Hubbard dimer between 2-particle, 3-particle and 4-particle states. For additional details see caption of table D.5

$\|\Psi_i\rangle$	$\|\Psi_f\rangle$	$\hat{c}_\alpha^\dagger$	$\langle\Psi_i\|\hat{c}_\alpha\|\Psi_f\rangle$	$\Delta E - \bar{\epsilon}$
$2 \to 3$ with final $S_z = \hbar/2$				
$\hat{f}_\uparrow^\dagger \hat{c}_\uparrow^\dagger \|\mathcal{O}\rangle$	$\hat{f}_\uparrow^\dagger \hat{c}_\uparrow^\dagger \frac{1}{\sqrt{2}}\left(\hat{f}_\downarrow^\dagger + \hat{c}_\downarrow^\dagger\right)\|\mathcal{O}\rangle$	$\hat{f}_\uparrow^\dagger$	$\frac{1}{\sqrt{2}}$	$U - \|t\|$
$\hat{f}_\uparrow^\dagger \hat{c}_\uparrow^\dagger \|\mathcal{O}\rangle$	$\hat{f}_\uparrow^\dagger \hat{c}_\uparrow^\dagger \frac{1}{\sqrt{2}}\left(\hat{f}_\downarrow^\dagger + \hat{c}_\downarrow^\dagger\right)\|\mathcal{O}\rangle$	$\hat{c}_\uparrow^\dagger$	$\frac{1}{\sqrt{2}}$	$U - \|t\|$
$\hat{f}_\uparrow^\dagger \hat{c}_\uparrow^\dagger \|\mathcal{O}\rangle$	$\hat{f}_\uparrow^\dagger \hat{c}_\uparrow^\dagger \frac{1}{\sqrt{2}}\left(\hat{f}_\downarrow^\dagger - \hat{c}_\downarrow^\dagger\right)\|\mathcal{O}\rangle$	$\hat{f}_\uparrow^\dagger$	$\frac{1}{\sqrt{2}}$	$U + \|t\|$
$\hat{f}_\uparrow^\dagger \hat{c}_\uparrow^\dagger \|\mathcal{O}\rangle$	$\hat{f}_\uparrow^\dagger \hat{c}_\uparrow^\dagger \frac{1}{\sqrt{2}}\left(\hat{f}_\downarrow^\dagger - \hat{c}_\downarrow^\dagger\right)\|\mathcal{O}\rangle$	$\hat{c}_\uparrow^\dagger$	$-\frac{1}{\sqrt{2}}$	$U + \|t\|$
$\frac{\cos(\gamma)}{\sqrt{2}}\left(\hat{f}_\uparrow^\dagger \hat{f}_\downarrow^\dagger + \hat{c}_\uparrow^\dagger \hat{c}_\downarrow^\dagger\right) + \frac{\sin(\gamma)}{\sqrt{2}}\left(\hat{f}_\uparrow^\dagger \hat{c}_\downarrow^\dagger - \hat{f}_\downarrow^\dagger \hat{c}_\uparrow^\dagger\right)\|\mathcal{O}\rangle$	$\hat{f}_\uparrow^\dagger \hat{c}_\uparrow^\dagger \frac{1}{\sqrt{2}}\left(\hat{f}_\downarrow^\dagger + \hat{c}_\downarrow^\dagger\right)\|\mathcal{O}\rangle$	$\hat{f}_\uparrow^\dagger$	$\frac{\cos(\gamma)+\sin(\gamma)}{2}$	$U - \|t\| + \Delta_{st}$
$\frac{\cos(\gamma)}{\sqrt{2}}\left(\hat{f}_\uparrow^\dagger \hat{f}_\downarrow^\dagger + \hat{c}_\uparrow^\dagger \hat{c}_\downarrow^\dagger\right) + \frac{\sin(\gamma)}{\sqrt{2}}\left(\hat{f}_\uparrow^\dagger \hat{c}_\downarrow^\dagger - \hat{f}_\downarrow^\dagger \hat{c}_\uparrow^\dagger\right)\|\mathcal{O}\rangle$	$\hat{f}_\uparrow^\dagger \hat{c}_\uparrow^\dagger \frac{1}{\sqrt{2}}\left(\hat{f}_\downarrow^\dagger + \hat{c}_\downarrow^\dagger\right)\|\mathcal{O}\rangle$	$\hat{c}_\uparrow^\dagger$	$\frac{-\cos(\gamma)+\sin(\gamma)}{2}$	$U - \|t\| + \Delta_{st}$
$\frac{\cos(\gamma)}{\sqrt{2}}\left(\hat{f}_\uparrow^\dagger \hat{f}_\downarrow^\dagger + \hat{c}_\uparrow^\dagger \hat{c}_\downarrow^\dagger\right) + \frac{\sin(\gamma)}{\sqrt{2}}\left(\hat{f}_\uparrow^\dagger \hat{c}_\downarrow^\dagger - \hat{f}_\downarrow^\dagger \hat{c}_\uparrow^\dagger\right)\|\mathcal{O}\rangle$	$\hat{f}_\uparrow^\dagger \hat{c}_\uparrow^\dagger \frac{1}{\sqrt{2}}\left(\hat{f}_\downarrow^\dagger - \hat{c}_\downarrow^\dagger\right)\|\mathcal{O}\rangle$	$\hat{f}_\uparrow^\dagger$	$\frac{\cos(\gamma)+\sin(\gamma)}{2}$	$U + \|t\| + \Delta_{st}$
$\frac{\cos(\gamma)}{\sqrt{2}}\left(\hat{f}_\uparrow^\dagger \hat{f}_\downarrow^\dagger + \hat{c}_\uparrow^\dagger \hat{c}_\downarrow^\dagger\right) + \frac{\sin(\gamma)}{\sqrt{2}}\left(\hat{f}_\uparrow^\dagger \hat{c}_\downarrow^\dagger - \hat{f}_\downarrow^\dagger \hat{c}_\uparrow^\dagger\right)\|\mathcal{O}\rangle$	$\hat{f}_\uparrow^\dagger \hat{c}_\uparrow^\dagger \frac{1}{\sqrt{2}}\left(\hat{f}_\downarrow^\dagger - \hat{c}_\downarrow^\dagger\right)\|\mathcal{O}\rangle$	$\hat{c}_\uparrow^\dagger$	$\frac{-\cos(\gamma)+\sin(\gamma)}{2}$	$U + \|t\| + \Delta_{st}$
$3 \to 4$ with initial $S_z = \hbar/2$				
$\hat{f}_\uparrow^\dagger \hat{c}_\uparrow^\dagger \frac{1}{\sqrt{2}}\left(\hat{f}_\downarrow^\dagger + \hat{c}_\downarrow^\dagger\right)\|\mathcal{O}\rangle$	$\hat{f}_\uparrow^\dagger \hat{f}_\downarrow^\dagger \hat{c}_\uparrow^\dagger \hat{c}_\downarrow^\dagger \|\mathcal{O}\rangle$	$\hat{f}_\downarrow^\dagger$	$-\frac{1}{\sqrt{2}}$	$U + \|t\|$
$\hat{f}_\uparrow^\dagger \hat{c}_\uparrow^\dagger \frac{1}{\sqrt{2}}\left(\hat{f}_\downarrow^\dagger + \hat{c}_\downarrow^\dagger\right)\|\mathcal{O}\rangle$	$\hat{f}_\uparrow^\dagger \hat{f}_\downarrow^\dagger \hat{c}_\uparrow^\dagger \hat{c}_\downarrow^\dagger \|\mathcal{O}\rangle$	$\hat{c}_\downarrow^\dagger$	$\frac{1}{\sqrt{2}}$	$U + \|t\|$
$\hat{f}_\uparrow^\dagger \hat{c}_\uparrow^\dagger \frac{1}{\sqrt{2}}\left(\hat{f}_\downarrow^\dagger - \hat{c}_\downarrow^\dagger\right)\|\mathcal{O}\rangle$	$\hat{f}_\uparrow^\dagger \hat{f}_\downarrow^\dagger \hat{c}_\uparrow^\dagger \hat{c}_\downarrow^\dagger \|\mathcal{O}\rangle$	$\hat{f}_\downarrow^\dagger$	$\frac{1}{\sqrt{2}}$	$U - \|t\|$
$\hat{f}_\uparrow^\dagger \hat{c}_\uparrow^\dagger \frac{1}{\sqrt{2}}\left(\hat{f}_\downarrow^\dagger - \hat{c}_\downarrow^\dagger\right)\|\mathcal{O}\rangle$	$\hat{f}_\uparrow^\dagger \hat{f}_\downarrow^\dagger \hat{c}_\uparrow^\dagger \hat{c}_\downarrow^\dagger \|\mathcal{O}\rangle$	$\hat{c}_\downarrow^\dagger$	$\frac{1}{\sqrt{2}}$	$U - \|t\|$

D.3 Anderson dimer

The Anderson dimer is the dimer version for the Anderson model. The Anderson model describes a single site with strong interaction in contact with a metal. In the Anderson dimer the metal environment is replaced by a single site. Thus, there are two distinct atoms, of which only one has an Coulomb repulsion.

The Andersen dimer has been studied previously by Fulde et al.[106, 107].

The physics of the Anderson model is discussed in section **??** on p. **??**. This chapter describes the analytical calculations of the Anderson dimer.

This is not finished. It only contains notes after a talk.

This section is inspired by section 12.1 of Fulde's book *"Electron Correlation in Molecules and Solids"*, Springer 1995.

Editor: Check Figs/Codes/src

The model for the Kondo effect is a two-site model, where one represents an impurity orbital with strong Coulomb interaction and the second orbital represents the bath.

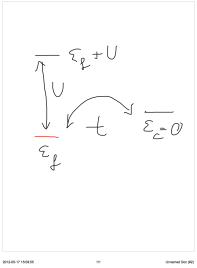

The Hamiltonian is [4]

$$\begin{aligned}\hat{H} &= \underbrace{\sum_\sigma \epsilon_f \hat{f}_\sigma^\dagger \hat{f}_\sigma + \frac{1}{2}U\sum_{\sigma,\sigma'} \hat{f}_\sigma^\dagger \hat{f}_{\sigma'}^\dagger \hat{f}_{\sigma'}\hat{f}_\sigma}_{\text{Anderson impurity}} + \underbrace{\sum_\sigma \epsilon_c \hat{c}_\sigma^\dagger \hat{c}_\sigma}_{\text{bath}} \underbrace{-|t|\sum_\sigma \left(\hat{f}_\sigma^\dagger \hat{c}_\sigma + \hat{c}_\sigma^\dagger \hat{f}_\sigma\right)}_{\text{hopping}} \\ &= \sum_\sigma \epsilon_f \hat{f}_\sigma^\dagger \hat{f}_\sigma + U\hat{f}_\uparrow^\dagger \hat{f}_\uparrow \hat{f}_\downarrow^\dagger \hat{f}_\downarrow + \underbrace{\frac{1}{2}U\sum_\sigma \hat{f}_\sigma^\dagger \hat{f}_\sigma\left(\hat{f}_\sigma^\dagger \hat{f}_\sigma - 1\right)}_{\text{self-interaction}} + \sum_\sigma \epsilon_c \hat{c}_\sigma^\dagger \hat{c}_\sigma - t\sum_\sigma \left(\hat{f}_\sigma^\dagger \hat{c}_\sigma + \hat{c}_\sigma^\dagger \hat{f}_\sigma\right) \\ &= \sum_\sigma \epsilon_f \hat{n}_{f,\sigma} + U\hat{n}_{f,\uparrow}\hat{n}_{f,\downarrow} + \underbrace{\frac{1}{2}U\sum_\sigma \hat{n}_{f,\sigma}\left(\hat{n}_{f,\sigma} - 1\right)}_{\text{self-interaction}} + \sum_\sigma \epsilon_c \hat{n}_{c,\sigma} - t\sum_\sigma \left(\hat{f}_\sigma^\dagger \hat{c}_\sigma + \hat{c}_\sigma^\dagger \hat{f}_\sigma\right) \quad \text{(D.27)}\end{aligned}$$

The self-interaction term is often ignored, because it contributes nothing when applied to a Slater determinant. Therefore it is also no more mentioned in the following discussion. Nevertheless, it gives a non-vanishing contribution in the mean-field approximation.

The interesting case is $\epsilon_f < \epsilon_c$ and $\epsilon_f + U > \epsilon_c$ with $N = 2$ particles. We consider all states because the states $N = 1$ and $N = 3$ will be required to evaluate the spectral properties.

---

[4]

$$\begin{aligned}\frac{1}{2}\sum_{\sigma,\sigma'} \hat{f}_\sigma^\dagger \hat{f}_{\sigma'}^\dagger \hat{f}_{\sigma'}\hat{f}_\sigma &= -\frac{1}{2}\sum_{\sigma,\sigma'} \hat{f}_\sigma^\dagger \hat{f}_{\sigma'}^\dagger \hat{f}_\sigma \hat{f}_{\sigma'} = -\frac{1}{2}\sum_{\sigma,\sigma'}\left(\delta_{\sigma,\sigma'}\hat{f}_\sigma^\dagger \hat{f}_{\sigma'} - \hat{f}_\sigma^\dagger \hat{f}_\sigma \hat{f}_{\sigma'}^\dagger \hat{f}_{\sigma'}\right) = \frac{1}{2}\sum_{\sigma,\sigma'} \hat{f}_\sigma^\dagger \hat{f}_\sigma \hat{f}_{\sigma'}^\dagger \hat{f}_{\sigma'} - \frac{1}{2}\sum_\sigma \hat{f}_\sigma^\dagger \hat{f}_\sigma \\ &= \hat{n}_\uparrow \hat{n}_\downarrow + \sum_\sigma\left(\hat{n}_\sigma^2 - \hat{n}_\sigma\right) \quad \text{(D.26)}\end{aligned}$$

D.3.1 Many-particle eigenstates

The symmetry adapted many-particle states, which I will use as a basisset are provided in table D.1 on p. 413. From the symmetry-adapted wave functions, the eigenstates of the Hamiltonian are constructed. They are listed in table D.3.

Table D.7: Energy eigenstates of the Andersen dimer.

N	S	S_z	eigenstate	energy
$N=0$	$S=0$	$S_z=0$	$\|\mathcal{O}\rangle$	$E=0$
$N=1$	$S=\frac{1}{2}$	$S_z=+\frac{1}{2}$	$\left(\hat{f}_\uparrow^\dagger\cos(\alpha_1)+\hat{c}_\uparrow^\dagger\sin(\alpha_1)\right)\|\mathcal{O}\rangle$	$\frac{\epsilon_c+\epsilon_f}{2}-\sqrt{\left(\frac{\epsilon_c-\epsilon_f}{2}\right)^2+t^2}$
$N=1$	$S=\frac{1}{2}$	$S_z=+\frac{1}{2}$	$\left(\hat{f}_\uparrow^\dagger\sin(\alpha_1)-\hat{c}_\uparrow^\dagger\cos(\alpha_1)\right)\|\mathcal{O}\rangle$	$\frac{\epsilon_c+\epsilon_f}{2}+\sqrt{\left(\frac{\epsilon_c-\epsilon_f}{2}\right)^2+t^2}$
$N=1$	$S=\frac{1}{2}$	$S_z=-\frac{1}{2}$	$\left(\hat{f}_\downarrow^\dagger\cos(\alpha_1)+\hat{c}_\downarrow^\dagger\sin(\alpha_1)\right)\|\mathcal{O}\rangle$	$\frac{\epsilon_c+\epsilon_f}{2}-\sqrt{\left(\frac{\epsilon_c-\epsilon_f}{2}\right)^2+t^2}$
$N=1$	$S=\frac{1}{2}$	$S_z=-\frac{1}{2}$	$\left(\hat{f}_\downarrow^\dagger\sin(\alpha_1)+\hat{c}_\downarrow^\dagger\cos(\alpha_1)\right)\|\mathcal{O}\rangle$	$\frac{\epsilon_c+\epsilon_f}{2}+\sqrt{\left(\frac{\epsilon_c-\epsilon_f}{2}\right)^2+t^2}$
$N=2$	$S=0$	$S_z=0$	$\approx\hat{f}_\uparrow^\dagger\hat{f}_\downarrow^\dagger\|\mathcal{O}\rangle$	$\approx 2\epsilon_f+U+O(t,1/U)$
$N=2$	$S=0$	$S_z=0$	$\approx\hat{c}_\uparrow^\dagger\hat{c}_\downarrow^\dagger\|\mathcal{O}\rangle$	$\approx 2\epsilon_c+O(t,1/U)$
$N=2$	$S=0$	$S_z=0$	$\approx\frac{1}{\sqrt{2}}(\hat{f}_\uparrow^\dagger\hat{c}_\downarrow^\dagger-\hat{f}_\downarrow^\dagger\hat{c}_\uparrow^\dagger)\|\mathcal{O}\rangle$	$\approx\epsilon_f+\epsilon_c+O(t,1/U)$
$N=2$	$S=1$	$S_z=1$	$\hat{f}_\uparrow^\dagger\hat{c}_\uparrow^\dagger\|\mathcal{O}\rangle$	$E=\epsilon_f+\epsilon_c$
$N=2$	$S=1$	$S_z=0$	$\frac{1}{\sqrt{2}}(\hat{f}_\uparrow^\dagger\hat{c}_\downarrow^\dagger+\hat{f}_\downarrow^\dagger\hat{c}_\uparrow^\dagger)\|\mathcal{O}\rangle$	$E=\epsilon_f+\epsilon_c$
$N=2$	$S=1$	$S_z=-1$	$\hat{f}_\downarrow^\dagger\hat{c}_\downarrow^\dagger\|\mathcal{O}\rangle$	$E=\epsilon_f+\epsilon_c$
$N=3$	$S=\frac{1}{2}$	$S_z=+\frac{1}{2}$	$\hat{f}_\uparrow^\dagger\hat{c}_\uparrow^\dagger\left(\hat{f}_\downarrow^\dagger\cos(\alpha_2)+\hat{c}_\downarrow^\dagger\sin(\alpha_2)\right)\|\mathcal{O}\rangle$	$\frac{3\epsilon_c+3\epsilon_f+U}{2}-\sqrt{\left(\frac{\epsilon_f+U-\epsilon_c}{2}\right)^2+t^2}$
$N=3$	$S=\frac{1}{2}$	$S_z=+\frac{1}{2}$	$\hat{f}_\uparrow^\dagger\hat{c}_\uparrow^\dagger\left(\hat{f}_\downarrow^\dagger\sin(\alpha_2)-\hat{c}_\downarrow^\dagger\cos(\alpha_2)\right)\|\mathcal{O}\rangle$	$\frac{3\epsilon_c+3\epsilon_f+U}{2}+\sqrt{\left(\frac{\epsilon_f+U-\epsilon_c}{2}\right)^2+t^2}$
$N=3$	$S=\frac{1}{2}$	$S_z=-\frac{1}{2}$	$\hat{f}_\downarrow^\dagger\hat{c}_\downarrow^\dagger\left(\hat{f}_\uparrow^\dagger\cos(\alpha_2)+\hat{c}_\uparrow^\dagger\sin(\alpha_2)\right)\|\mathcal{O}\rangle$	$\frac{3\epsilon_c+3\epsilon_f+U}{2}-\sqrt{\left(\frac{\epsilon_f+U-\epsilon_c}{2}\right)^2+t^2}$
$N=3$	$S=\frac{1}{2}$	$S_z=-\frac{1}{2}$	$\hat{f}_\downarrow^\dagger\hat{c}_\downarrow^\dagger\left(\hat{f}_\uparrow^\dagger\sin(\alpha_2)-\hat{c}_\uparrow^\dagger\cos(\alpha_2)\right)\|\mathcal{O}\rangle$	$\frac{3\epsilon_c+3\epsilon_f+U}{2}+\sqrt{\left(\frac{\epsilon_f+U-\epsilon_c}{2}\right)^2+t^2}$
$N=4$	$S=0$	$S_z=0$	$\hat{f}_\uparrow^\dagger\hat{f}_\downarrow^\dagger\hat{c}_\uparrow^\dagger\hat{c}_\downarrow^\dagger\|\mathcal{O}\rangle$	$E=2\epsilon_c+2\epsilon_f+U$

The singlet states in the two-particle sector require special attention. From Eq. D.14 on p. 416, we obtain

$$\hat{P}_{2,0}\hat{H}\hat{P}_{2,0}=\begin{pmatrix}\hat{f}_\uparrow^\dagger\hat{f}_\downarrow^\dagger|\mathcal{O}\rangle\\ \hat{c}_\uparrow^\dagger\hat{c}_\downarrow^\dagger|\mathcal{O}\rangle\\ \frac{1}{\sqrt{2}}(\hat{f}_\uparrow^\dagger\hat{c}_\downarrow^\dagger-\hat{f}_\downarrow^\dagger\hat{c}_\uparrow^\dagger)|\mathcal{O}\rangle\end{pmatrix}\begin{pmatrix}2\epsilon_f+U_f & 0 & -\sqrt{2}|t|\\ 0 & 2\epsilon_c & -\sqrt{2}|t|\\ -\sqrt{2}|t| & -\sqrt{2}|t| & \epsilon_c+\epsilon_f\end{pmatrix}\begin{pmatrix}\langle\mathcal{O}|\hat{f}_\downarrow\hat{f}_\uparrow\\ \langle\mathcal{O}|\hat{c}_\downarrow\hat{c}_\uparrow\\ \langle\mathcal{O}|\frac{1}{\sqrt{2}}(\hat{c}_\downarrow\hat{f}_\uparrow-\hat{c}_\uparrow\hat{f}_\downarrow)\end{pmatrix} \tag{D.28}$$

Of interest is the case where $\epsilon_f<\epsilon_c<\epsilon_f+U$, which is the case with one electron on the impurity. In that case the ground state has one electron in the impurity and a spin-paired state in the bath-site. The spin coupling is determined by the singlet-triplet splitting. The singlet-triplet splitting defines the **Kondo temperature**.

In the limit of large U and small t, the Hamiltonian is diagonal and we obtain (1) a state with two electrons in the bath site, and another one (2), with energy $\epsilon_c+\epsilon_f$, which is equally distributed

over the bath and the impurity. The third state lies at high energies and has two electrons on the impurity.

We can diagonalize the Hamiltonian approximately using **down-folding** as described in chapter 5 and specifically in Eq. 5.18 on p. 184.

In order to obtain an accurate description in the limit of large interaction, we down-fold the wave function with a doubly occupied impurity. The self energy due to the down-folded orbital is[5]

$$\mathbf{\Sigma}(E) \overset{\text{Eq. 5.14}}{=} \frac{2|t|^2}{E-2\epsilon_f-U_f}\begin{pmatrix}0&0\\0&1\end{pmatrix} \tag{D.29}$$

The self energy is added to the subblock of the two other orbitals

$$\begin{aligned}
\boldsymbol{M}(E) &= \begin{pmatrix} 2\epsilon_c - E & -t\sqrt{2} \\ -t\sqrt{2} & \epsilon_c+\epsilon_f+\frac{2|t|^2}{E-2\epsilon_f-U} - E \end{pmatrix} \\
&= \begin{pmatrix} 2\epsilon_c - E_\nu & -t\sqrt{2} \\ -t\sqrt{2} & \epsilon_c+\epsilon_f-\frac{2t^2}{2\epsilon_f+U-E_\nu} - E_\nu \end{pmatrix} - \begin{pmatrix} 1 & 0 \\ 0 & 1+\frac{2t^2}{(2\epsilon_f+U-E_\nu)^2} \end{pmatrix}(E-E_\nu) + O\left((E-E_\nu)^2\right) \\
&= \underbrace{\begin{pmatrix} 2\epsilon_c & -t\sqrt{2} \\ -t\sqrt{2} & \epsilon_c+\epsilon_f-\frac{2t^2}{2\epsilon_f+U-E_\nu}+\frac{2t^2E_\nu}{(2\epsilon_f+U-E_\nu)^2} \end{pmatrix}}_{\tilde{H}(E_\nu)} - \underbrace{\begin{pmatrix} 1 & 0 \\ 0 & 1+\frac{2t^2}{(2\epsilon_f+U-E_\nu)^2} \end{pmatrix}}_{\tilde{O}(E_\nu)} E + O\left((E-E_\nu)^2\right)
\end{aligned} \tag{D.30}$$

We can orthonormalize the states and obtain a new Hamiltonian

$$\begin{aligned}
\tilde{\boldsymbol{O}}^{-\frac{1}{2}}\tilde{\boldsymbol{H}}\tilde{\boldsymbol{O}}^{-\frac{1}{2}} &= \begin{pmatrix} 2\epsilon_c & -t\sqrt{2} \\ -t\sqrt{2} & \bar{E} \end{pmatrix} \\
\text{with}\quad \bar{E} &= \left(\epsilon_c+\epsilon_f-\frac{2t^2}{2\epsilon_f+U-E_\nu}+\frac{2t^2E_\nu}{(2\epsilon_f+U-E_\nu)^2}\right)\left(1+\frac{2t^2}{(2\epsilon_f+U-E_\nu)^2}\right)^{-1}
\end{aligned} \tag{D.31}$$

This yields the energies

$$E_\pm = \frac{2\epsilon_c+\bar{E}}{2} \pm \sqrt{\left(\frac{2\epsilon_c-\bar{E}}{2}\right)^2+2t^2} \tag{D.32}$$

For the state near $\epsilon_f+\epsilon_c$, one chooses $E_\nu = \epsilon_f+\epsilon_c$.

$$\begin{aligned}
\bar{E} &= \left(\epsilon_c+\epsilon_f-\frac{2t^2}{\epsilon_f+U-\epsilon_c}+\frac{2t^2(\epsilon_c+\epsilon_f)}{(\epsilon_f+U-\epsilon_c)^2}\right)\left(1+\frac{2t^2}{(\epsilon_f+U-\epsilon_c)^2}\right)^{-1} \\
&= \left(\epsilon_c+\epsilon_f-\frac{2t^2}{\epsilon_f+U-\epsilon_c}+\frac{4t^4}{(\epsilon_f+U-\epsilon_c)^3}\right)+O\left(\left(\frac{2t^2}{(\epsilon_f+U-\epsilon_c)^2}\right)^2\right)
\end{aligned} \tag{D.33}$$

In the limit of large U, we obtain a bonding and an antibonding state. For the bonding state the energy is below $\epsilon_c+\min(\epsilon_f,\epsilon_c)$ for the antibonding state it is at $\epsilon_c+\max(\epsilon_f,\epsilon_c)$

For large U, there lowest state with $N=2$ is a singlet state, for which one electron is in the non-interacting orbital, and the other is delocalized over both sites. This state is lower than the triplet state, irrespective of $\epsilon_f-\epsilon_c$.

We see that the singlet two-particle state lies below the triplet state, because only the singlet state can hybridize with higher lying states, when t is switched on. A simplification the infinite-U limit, in which case we may exclude any states with two electrons on the impurity. The stabilization is mainly due to the delocalization of the electron in one spin direction between impurity and bath. The Coulomb repulsion is a secondary effect.

[5]We use the symbol E for the many-particle energies, rather than the symbol ϵ which is used for one-particle energies.

D.3.2 Spectrum

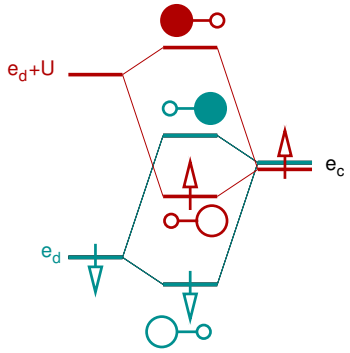

Fig. D.1: Schematic diagrams of the spectral function of the Kondo dimer. Scheme of the one-particle orbitals of the Kondo singlet. It represents only one of the two Slater determinants contributing to the two-particle ground state.

When we investigate the spectra for adding and removing electrons, we can use Lehman representation. Let me use the ground singlet ground state

$$|\Phi_s\rangle = \left[\hat{f}^\dagger_\uparrow \hat{f}^\dagger_\downarrow A + \hat{c}^\dagger_\uparrow \hat{c}^\dagger_\downarrow B + \frac{1}{\sqrt{2}}\left(\hat{f}^\dagger_\uparrow \hat{c}^\dagger_\downarrow - \hat{f}^\dagger_\downarrow \hat{c}^\dagger_\uparrow\right) C\right]|\mathcal{O}\rangle \tag{D.34}$$

with energy E_s.

For $\epsilon_c = 0$, $\epsilon_f = -1$, $U = 2$, $t = \frac{1}{2}$, I obtain (without full diagonalization of the $N = 2, S = 0$ channel)

ϵ	ψ_{qp}	
-1.048	$\|f,\sigma\rangle 0.68 + \|c,\sigma\rangle 0.06$	$f^1 \to f^0$
-0.029	$\|f,\sigma\rangle 0.20 + \|c,\sigma\rangle 0.70$	$f^1 \to f^0$
+0.029	$\|f,\sigma\rangle 0.20 - \|c,\sigma\rangle 0.70$	$f^0 \to f^1$
+1.048	$\|f,\sigma\rangle 0.68 - \|c,\sigma\rangle 0.06$	$f^0 \to f^1$

$$\begin{aligned}
\hat{f}^\dagger_\uparrow|\Psi_s\rangle &= \left[\hat{f}^\dagger_\uparrow \hat{c}^\dagger_\uparrow \hat{c}^\dagger_\downarrow b - \frac{1}{\sqrt{2}}\hat{f}^\dagger_\uparrow \hat{f}^\dagger_\downarrow \hat{c}^\dagger_\uparrow c\right]|\mathcal{O}\rangle \\
\hat{f}^\dagger_\downarrow|\Psi_s\rangle &= \left[\hat{f}^\dagger_\downarrow \hat{c}^\dagger_\uparrow \hat{c}^\dagger_\downarrow b - \frac{1}{\sqrt{2}}\hat{f}^\dagger_\uparrow \hat{f}^\dagger_\downarrow \hat{c}^\dagger_\downarrow c\right]|\mathcal{O}\rangle \\
\hat{c}^\dagger_\uparrow|\Phi_s\rangle &= \left[\hat{f}^\dagger_\uparrow \hat{f}^\dagger_\downarrow \hat{c}^\dagger_\uparrow a - \hat{f}^\dagger_\uparrow \hat{c}^\dagger_\uparrow \hat{c}^\dagger_\downarrow \frac{c}{\sqrt{2}}\right]|\mathcal{O}\rangle \\
\hat{c}^\dagger_\downarrow|\Psi_s\rangle &= \left[\hat{f}^\dagger_\uparrow \hat{f}^\dagger_\downarrow \hat{c}^\dagger_\uparrow a - \hat{f}^\dagger_\downarrow \hat{c}^\dagger_\uparrow \hat{c}^\dagger_\uparrow \frac{c}{\sqrt{2}}\right]|\mathcal{O}\rangle
\end{aligned} \tag{D.35}$$

Increasing the temperature reduces the singlet occupation which results in larger resistance.

Kondo Resonance=Abrikosov-Suhl resonance.

D.3.3 Andersen dimer and the Hartree-Fock method

In this section I want to explore how well the broken symmetry states obtained with a single Slater determinant are able to capture the Kondo physics. This is of relevance to understand the limitations

of conventional density-functional calculations. The Anderson dimer is a system where exact and Hartree-Fock calculations should be, firstly, feasible and, secondly, intelligible.

The following is an attempt to describe the two-particle state in terms of two Slater determinants. The singlet state is $|\Psi_s\rangle$ and the triplet state is $|\Psi_t\rangle$. In the singlet state, we can use the bonding state with the filled majority-spin f-orbital and the bonding state with the empty minority-spin f orbital. In contrast, the triplet state has to use bonding and antibonding states with the majority spin orbital. This is the origin of the singlet-triplet splitting.

$$\begin{aligned}
|\Psi_s\rangle &= \frac{1}{2}\Big[\Big(\hat{f}^\dagger_\uparrow\cos(\alpha)+\hat{c}^\dagger_\uparrow\sin(\alpha)\Big)\Big(\hat{f}^\dagger_\downarrow\sin(\beta)+\hat{c}^\dagger_\downarrow\cos(\beta)\Big)+\Big(\hat{f}^\dagger_\uparrow\sin(\beta)+\hat{c}^\dagger_\uparrow\cos(\beta)\Big)\Big(\hat{f}^\dagger_\downarrow\cos(\alpha)+\hat{c}^\dagger_\downarrow\sin(\alpha)\Big)\Big]|\mathcal{O}\rangle \\
&= \Big[\hat{f}^\dagger_\uparrow\hat{f}^\dagger_\downarrow\cos(\alpha)\sin(\beta)+\hat{c}^\dagger_\uparrow\hat{c}^\dagger_\downarrow\sin(\alpha)\cos(\beta) \\
&\quad +\hat{f}^\dagger_\uparrow\hat{c}^\dagger_\downarrow\frac{\cos(\alpha)\cos(\beta)+\sin(\alpha)\sin(\beta)}{2}+\hat{c}^\dagger_\uparrow\hat{f}^\dagger_\downarrow\frac{\sin(\alpha)\sin(\beta)+\cos(\alpha)\cos(\beta)}{2}\Big]|\mathcal{O}\rangle \\
&= \Big[\hat{f}^\dagger_\uparrow\hat{f}^\dagger_\downarrow\cos(\alpha)\sin(\beta)+\hat{c}^\dagger_\uparrow\hat{c}^\dagger_\downarrow\sin(\alpha)\cos(\beta)+\Big(\hat{f}^\dagger_\uparrow\hat{c}^\dagger_\downarrow-\hat{f}^\dagger_\downarrow\hat{c}^\dagger_\uparrow\Big)\frac{\cos(\alpha)\cos(\beta)+\sin(\alpha)\sin(\beta)}{2}\Big]|\mathcal{O}\rangle \\
|\Psi_t\rangle &= \Big(\hat{f}^\dagger_\uparrow\cos(\alpha)+\hat{c}^\dagger_\uparrow\sin(\alpha)\Big)\Big(\hat{f}^\dagger_\uparrow\sin(\alpha)-\hat{c}^\dagger_\uparrow\cos(\alpha)\Big)|\mathcal{O}\rangle \\
&= \Big[-\hat{f}^\dagger_\uparrow\hat{c}^\dagger_\uparrow\cos^2(\alpha)+\hat{c}^\dagger_\uparrow\hat{f}^\dagger_\uparrow\sin^2(\alpha)\Big]|\mathcal{O}\rangle \\
&= -\hat{f}^\dagger_\uparrow\hat{c}^\dagger_\uparrow|\mathcal{O}\rangle
\end{aligned} \tag{D.36}$$

Without coupling to the environment, one obtains the solution with $\alpha=\beta=0$. We find, that all the three Slater determinants contributing to the $S=0, N=2$ ground state contribute with independent parameters. (The three coefficients are constrained by the norm to two parameters, which can be expressed in terms of α and β.) This tells us that the Ansatz given above is able to capture the ground state wave function.

Broken-symmetry Slater determinants

Here, I want to explore the limits of the Hartree-Fock method.[6] I consider two broken-symmetry Slater-determinants, which are related by a global spin inversion. The two Slater determinants have $S_z=0$, so that we may recover singlet and triplet state, when both Slater determinants are superimposed. We use two one-particle orbitals that are polarized individually along the dimer axis.

$$\begin{aligned}
|\Phi_1\rangle &= \Big(\hat{f}^\dagger_\uparrow\cos(\alpha)+\hat{c}^\dagger_\uparrow\sin(\alpha)\Big)\Big(\hat{f}^\dagger_\downarrow\sin(\beta)+\hat{c}^\dagger_\downarrow\cos(\beta)\Big)|\mathcal{O}\rangle \\
|\Phi_2\rangle &= \Big(\hat{f}^\dagger_\uparrow\sin(\beta)+\hat{c}^\dagger_\uparrow\cos(\beta)\Big)\Big(\hat{f}^\dagger_\downarrow\cos(\alpha)+\hat{c}^\dagger_\downarrow\sin(\alpha)\Big)|\mathcal{O}\rangle
\end{aligned} \tag{D.37}$$

Now we work out Hamilton and overlap matrices in this two-dimensional sub-space $\{|\Phi_1(\alpha,\beta)\rangle, |\Phi_2(\alpha,\beta)\rangle\}$ of the Fock space. The one-particle orbitals of the two states can be varied in a two-dimensional space.

Overlap matrix elements of the broken-symmetry Slater determinants: The wave functions $|\Phi_1\rangle$, $|\Phi_2\rangle$ are, per construction, normalized, i.e.

$$\langle\Phi_j|\Phi_j\rangle = 1 \qquad \text{for } j\in\{1,2\} \tag{D.38}$$

The overlap is obtained as follows

$$\begin{aligned}
\langle\Phi_1|\Phi_2\rangle &= \cos^2(\alpha)\sin^2(\beta)+2\cos(\alpha)\sin(\alpha)\cos(\beta)\sin(\beta)+\sin^2(\alpha)\cos^2(\beta) \\
&= \Big(\cos(\alpha)\sin(\beta)+\sin(\alpha)\cos(\beta)\Big)^2 \\
&= \sin^2(\alpha+\beta)
\end{aligned} \tag{D.39}$$

[6] A similar analysis has been performed by Kamil et al.[108] for the symmetric dimer.

Note, that orthonormality between the two Slater determinants is not required.

Hamilton matrix elements of the Slater determinants:

$$
\begin{aligned}
\hat{H}|\Phi_1\rangle &= \hat{H}\Big[\hat{f}_\uparrow^\dagger \hat{f}_\downarrow^\dagger \cos(\alpha)\sin(\beta) + \hat{f}_\uparrow^\dagger \hat{c}_\downarrow^\dagger \cos(\alpha)\cos(\beta) + \hat{c}_\uparrow^\dagger \hat{f}_\downarrow^\dagger \sin(\alpha)\sin(\beta) + \hat{c}_\uparrow^\dagger \hat{c}_\downarrow^\dagger \sin(\alpha)\cos(\beta)\Big]\mathcal{O}\rangle \\
&= \Bigg[\Big((2\epsilon_f + U)\hat{f}_\uparrow^\dagger \hat{f}_\downarrow^\dagger - 2t\Big(\hat{c}_\uparrow^\dagger \hat{f}_\downarrow^\dagger + \hat{f}_\uparrow^\dagger \hat{c}_\downarrow^\dagger\Big)\Big)\cos(\alpha)\sin(\beta) \\
&\quad + \Big((\epsilon_f + \epsilon_c)\hat{f}_\uparrow^\dagger \hat{c}_\downarrow^\dagger - 2t\Big(\hat{f}_\uparrow^\dagger \hat{f}_\downarrow^\dagger + \hat{c}_\uparrow^\dagger \hat{c}_\downarrow^\dagger\Big)\Big)\cos(\alpha)\cos(\beta) \\
&\quad + \Big((\epsilon_f + \epsilon_c)\hat{c}_\uparrow^\dagger \hat{f}_\downarrow^\dagger - 2t\Big(\hat{f}_\uparrow^\dagger \hat{f}_\downarrow^\dagger + \hat{c}_\uparrow^\dagger \hat{c}_\downarrow^\dagger\Big)\Big)\sin(\alpha)\sin(\beta) \\
&\quad + \Big(2\epsilon_c \hat{c}_\uparrow^\dagger \hat{c}_\downarrow^\dagger - 2t\Big(\hat{f}_\uparrow^\dagger \hat{c}_\downarrow^\dagger + \hat{c}_\uparrow^\dagger \hat{f}_\downarrow^\dagger\Big)\Big)\sin(\alpha)\cos(\beta)\Bigg]|\mathcal{O}\rangle \\
&= \Bigg[\hat{f}_\uparrow^\dagger \hat{f}_\downarrow^\dagger \Big((2\epsilon_f + U)\cos(\alpha)\sin(\beta) - 2t\Big(\cos(\alpha)\cos(\beta) + \sin(\alpha)\sin(\beta)\Big)\Big) \\
&\quad + \hat{f}_\uparrow^\dagger \hat{c}_\downarrow^\dagger \Big((\epsilon_f + \epsilon_c)\cos(\alpha)\cos(\beta) - 2t\Big(\cos(\alpha)\sin(\beta) + \sin(\alpha)\cos(\beta)\Big)\Big) \\
&\quad + \hat{c}_\uparrow^\dagger \hat{f}_\downarrow^\dagger \Big((\epsilon_f + \epsilon_c)\sin(\alpha)\sin(\beta) - 2t\Big(\cos(\alpha)\sin(\beta) + \sin(\alpha)\cos(\beta)\Big)\Big) \\
&\quad + \hat{c}_\uparrow^\dagger \hat{c}_\downarrow^\dagger \Big(2\epsilon_c \sin(\alpha)\cos(\beta) - 2t\Big(\cos(\alpha)\cos(\beta) + \sin(\alpha)\sin(\beta)\Big)\Big)\Bigg]|\mathcal{O}\rangle
\end{aligned}
\tag{D.40}
$$

$$
\begin{aligned}
\langle\Phi_1|\hat{H}|\Phi_1\rangle = &\Big[\cos(\alpha)\sin(\beta)\Big((2\epsilon_f+U)\cos(\alpha)\sin(\beta)-2t\Big(\cos(\alpha)\cos(\beta)+\sin(\alpha)\sin(\beta)\Big)\Big)\\
&+\cos(\alpha)\cos(\beta)\Big((\epsilon_f+\epsilon_c)\cos(\alpha)\cos(\beta)-2t\Big(\cos(\alpha)\sin(\beta)+\sin(\alpha)\cos(\beta)\Big)\Big)\\
&+\sin(\alpha)\sin)\beta)\Big((\epsilon_f+\epsilon_c)\sin(\alpha)\sin(\beta)-2t\Big(\cos(\alpha)\sin(\beta)+\sin(\alpha)\cos(\beta)\Big)\Big)\\
&+\sin(\alpha)\cos(\beta)\Big(2\epsilon_c\sin(\alpha)\cos(\beta)-2t\Big(\cos(\alpha)\cos(\beta)+\sin(\alpha)\sin(\beta)\Big)\Big)\Big]\\
=&\cos^2(\alpha)\sin^2(\beta)\Big(2\epsilon_f+U\Big)+\sin^2(\alpha)\cos^2(\beta)2\epsilon_c\\
&+(\epsilon_f+\epsilon_c)\Big(\cos^2(\alpha)\sin^2(\beta)+\sin^2(\alpha)\cos^2(\beta)\Big)\\
&-2t\underbrace{\Big(2\cos(\beta)\sin(\beta)+2\cos(\alpha)\sin(\alpha)\Big)}_{2\cos^2(\alpha)\cos(\beta)\sin(\beta)+2\cos(\alpha)\sin(\alpha)\sin^2(\beta)+2\cos(\alpha)\sin(\alpha)\cos^2(\beta)+2\sin^2(\alpha)\cos(\beta)\sin(\beta)}\\
=&\cos^2(\alpha)\sin^2(\beta)\Big(\epsilon_f+U-\epsilon_c\Big)+\sin^2(\alpha)\cos^2(\beta)\Big(\epsilon_c-\epsilon_f\Big)\\
&+(\epsilon_f+\epsilon_c)\underbrace{\Big((\cos^2(\alpha)+\sin^2(\alpha))(\cos^2(\beta)+\sin^2(\beta))\Big)}_{=1}\\
&-2t\Big(2\cos(\beta)\sin(\beta)+2\cos(\alpha)\sin(\alpha)\Big)\\
=&(\epsilon_f+\epsilon_c)+\overbrace{\frac{1}{2}\Big(\cos(2\beta)-\cos(2\alpha)\Big)}^{\sin^2(\alpha)\cos^2(\beta)-\cos^2(\alpha)\sin^2(\beta)}\Big(\epsilon_c-\epsilon_f\Big)+\cos^2(\alpha)\sin^2(\beta)U\\
&-2t\Big(\sin(2\alpha)+\sin(2\beta)\Big)
\end{aligned}
\tag{D.41}
$$

$$
\begin{aligned}
\cos^2(x)\sin^2(y)+\sin^2(x)\cos^2(y)&=\frac{1}{4}\Big(2-\cos(2(x+y))-2\cos(2(x-y))\Big)\\
2\sin(x)\cos(x)&=\sin(2x)
\end{aligned}
\tag{D.42}
$$

$$
\begin{aligned}
\langle\Phi_2|\hat{H}|\Phi_1\rangle = \Bigg[&\cos(\alpha)\sin(\beta)\Big((2\epsilon_f+U)\cos(\alpha)\sin(\beta)-2t\Big(\cos(\alpha)\cos(\beta)+\sin(\alpha)\sin(\beta)\Big)\Big)\\
&+\sin(\alpha)\sin(\beta)\Big((\epsilon_f+\epsilon_c)\cos(\alpha)\cos(\beta)-2t\Big(\cos(\alpha)\sin(\beta)+\sin(\alpha)\cos(\beta)\Big)\Big)\\
&+\cos(\alpha)\cos(\beta)\Big((\epsilon_f+\epsilon_c)\sin(\alpha)\sin(\beta)-2t\Big(\cos(\alpha)\sin(\beta)+\sin(\alpha)\cos(\beta)\Big)\Big)\\
&+\sin(\alpha)\cos(\beta)\Big(2\epsilon_c\sin(\alpha)\cos(\beta)-2t\Big(\cos(\alpha)\cos(\beta)+\sin(\alpha)\sin(\beta)\Big)\Big)\Bigg]\\
=\Big((&2\epsilon_f+U)\cos^2(\alpha)\sin^2(\beta)+2(\epsilon_f+\epsilon_c)\cos(\alpha)\sin(\alpha)\cos(\beta)\sin(\beta)\\
&+2\epsilon_c\sin^2(\alpha)\cos^2(\beta)\\
&-2t\Big(\sin(2\beta)+\sin(2\alpha)\Big)
\end{aligned}
\tag{D.43}
$$

Minimum for the broken-symmetry Slater determinants

$$
\begin{aligned}
\langle\Phi_j|\hat{H}|\Phi_j\rangle &= (\epsilon_f+\epsilon_c)+\frac{1}{2}\Big(\cos(2\beta)-\cos(2\alpha)\Big)\Big(\epsilon_c-\epsilon_f\Big)+\cos^2(\alpha)\sin^2(\beta)U\\
&\quad -2t\Big(\sin(2\alpha)+\sin(2\beta)\Big)\\
\frac{\partial\langle\Phi_j|\hat{H}|\Phi_j\rangle}{\partial\alpha} &= +\sin(2\alpha)\Big(\epsilon_c-\epsilon_f\Big)-\overbrace{\sin(2\alpha)}^{2\cos(\alpha)\sin(\alpha)}\overbrace{\Big(\frac{1}{2}-\frac{1}{2}\cos(2\beta)\Big)}^{\sin^2(\beta)}U-4t\cos(2\alpha)\\
&= +\sin(2\alpha)\Big(\epsilon_c-\epsilon_f-\Big[\frac{1}{2}-\frac{1}{2}\cos(2\beta)\Big]U\Big)-4t\cos(2\alpha)\stackrel{!}{=}0\\
4t\cot(2\alpha) &= \Big(\epsilon_c-\epsilon_f-\Big[\frac{1}{2}-\frac{1}{2}\cos(2\beta)\Big]U\Big)\\
\frac{\partial\langle\Phi_j|\hat{H}|\Phi_j\rangle}{\partial\beta} &= -\sin(2\beta)\Big(\epsilon_c-\epsilon_f\Big)+\overbrace{\Big(\frac{1}{2}+\frac{1}{2}\cos(2\alpha)\Big)}^{\cos^2(\alpha)}\overbrace{\sin(2\beta)}^{2\sin(\beta)\cos(\beta)}U-4t\cos(2\beta)\\
&= -\sin(2\beta)\Big(\epsilon_c-\epsilon_f-\Big[\frac{1}{2}+\frac{1}{2}\cos(2\alpha)\Big]U\Big)-4t\cos(2\beta)\stackrel{!}{=}0\\
4t\cot(2\beta) &= -\Big(\epsilon_c-\epsilon_f-\Big[\frac{1}{2}+\frac{1}{2}\cos(2\alpha)\Big]U\Big)
\end{aligned}
\tag{D.44}
$$

Δ/t	U/t	α/π	β/π
0	0	1/4	1/4
0	∞	$\frac{1}{4}$	0
0	∞	$\frac{1}{2}$	0
0	∞	$\frac{1}{2}$	$\frac{1}{4}$
0	0	$\frac{1}{2}-\frac{1}{4}$	$\frac{1}{4}$
4	0	$\frac{1}{2}-\frac{1}{8}$	$\frac{1}{8}$
9	0	$\frac{1}{2}-\frac{1}{15}$	$\frac{1}{15}$
25	0	$\frac{1}{2}-\frac{1}{40}$	$\frac{1}{40}$
100	0	$(8/100)^2$	$\frac{1}{2}-\left(\frac{8}{100}\right)^2$
∞	0	$\frac{1}{2}$	0
10	100	$\frac{1}{2}-\frac{1}{20}$	$\frac{1}{20}$

Symmetric solution: There is one series of solutions with $\alpha+\beta=\frac{\pi}{2}$. With $\beta=\frac{\pi}{2}-\alpha$ the two Slater determinants $|\Phi_1\rangle$ and $|\Phi_2\rangle$ are identical and equal to

$$|\Phi_1\rangle = |\Phi_2\rangle = \Big(\hat{f}_\uparrow^\dagger \cos(\alpha) + \hat{c}_\uparrow^\dagger \sin(\alpha)\Big)\Big(\hat{f}_\downarrow^\dagger \cos(\alpha) + \hat{c}_\downarrow^\dagger \sin(\alpha)\Big)|\mathcal{O}\rangle \tag{D.45}$$

For this series of solutions both one-particle orbitals polarize in one direction to account for the asymmetry of the two sites. The strength of the polarization is described by $\gamma = \alpha - \frac{\pi}{4}$

$$\begin{aligned}
4t\cot(2\alpha) &= \left(\epsilon_c - \epsilon_f - \left[\frac{1}{2} - \frac{1}{2}\cos(\pi - 2\alpha)\right] U\right) \\
&= \left(\epsilon_c - \epsilon_f - \left[\frac{1}{2} + \frac{1}{2}\cos(2\alpha)\right] U\right) \\
4t\frac{\cos(\frac{\pi}{2} + 2\gamma)}{\sin(\frac{\pi}{2} - 2\gamma)} &= -\left(\epsilon_c - \epsilon_f - \left[\frac{1}{2} + \frac{1}{2}\cos(\frac{\pi}{2} + 2\gamma)\right] U\right) \\
-4t\frac{\sin(2\gamma)}{\cos(2\gamma)} &= -\left(\epsilon_c - \epsilon_f - \left[\frac{1}{2} - \frac{1}{2}\sin(2\gamma)\right] U\right) \\
4\sin(2\gamma) &= -\left(\frac{\epsilon_f - \epsilon_c}{t} + \frac{U}{2t}\right)\cos(2\gamma) + \sin(2\gamma)\cos(2\gamma)\frac{U}{2t} \\
\left(4 - \cos(2\gamma)\frac{U}{2t}\right)\sin(2\gamma) &= -\left(\frac{\epsilon_f - \epsilon_c}{t} + \frac{U}{2t}\right)\cos(2\gamma) \\
4\sin(2\gamma) &= -\left(\frac{\epsilon_f - \epsilon_c}{t} + \frac{U}{2t}\right)\cos(2\gamma) + \sin(2\gamma)\cos(2\gamma)\frac{U}{2t} \\
\overbrace{1 - \cos^2(2\gamma)}^{\sin^2(2\gamma)} &= \left(\frac{-\left(\frac{\epsilon_f - \epsilon_c}{t} + \frac{U}{2t}\right)\cos(2\gamma)}{4 - \cos(2\gamma)\frac{U}{2t}}\right)^2 \\
\overset{x=\cos(2\gamma)}{\Rightarrow} 1 - x^2 &= \left(\frac{-\left(\frac{\epsilon_f - \epsilon_c}{t} + \frac{U}{2t}\right)x}{4 - x\frac{U}{2t}}\right)^2 \\
0 &= 4 - 8x\frac{U}{2t} + x^2\left(\frac{U}{2t}\right)^2 - 4x^2 + 8x^3\frac{U}{2t} - x^4\left(\frac{U}{2t}\right)^2 - \left(\frac{\epsilon_f - \epsilon_c}{t} + \frac{U}{2t}\right)^2 x^2 \\
&= 4 - 8\frac{U}{2t}x + \left[\left(\frac{U}{2t}\right)^2 - 4 - \left(\frac{\epsilon_f - \epsilon_c}{t} + \frac{U}{2t}\right)^2\right] x^2 + 8x^3\frac{U}{2t} - x^4\left(\frac{U}{2t}\right)^2 \\
&= 4 - 8\frac{U}{2t}x - \left[4 + \left(\frac{\epsilon_f - \epsilon_c}{t}\right)^2 + 2\left(\frac{\epsilon_f - \epsilon_c}{t}\right)\frac{U}{2t}\right] x^2 + 8x^3\frac{U}{2t} - x^4\left(\frac{U}{2t}\right)^2 \\
&= 4 - 8\frac{U}{2t}(1 - x^2)x - \left[4 + \left(\frac{\epsilon_f - \epsilon_c}{t}\right)^2 + 2\left(\frac{\epsilon_f - \epsilon_c}{t}\right)\frac{U}{2t}\right] x^2 - x^4\left(\frac{U}{2t}\right)^2
\end{aligned} \tag{D.46}$$

This is a polynomial of fourth order.

Broken symmetry states: When the interaction is increased, this solution splits into three. For the symmetric case this is probably the transition into the antiferromagnetic broken-symmetry state. The solution with $\alpha + \beta = \frac{\pi}{2}$ becomes the unstable solution, while the two other states are stable solutions. For the symmetric solution we obtain

D.4 Hydrogen atom

This appendix shall provide the matrix elements for the hydrogen molecule using atomic orbitals as basis set. Many matrix elements can be evaluated analytically, which makes this a convenient system for

benchmarks.Editor: This is taken from the paw_lmto report of the PAW code on May 11, 2020. The text is thus duplicated. The PAW data have been removed in this version.

The Hartree-Fock energy of the hydrogen atom is

$$E_{\text{tot}} = \underbrace{\langle\psi|\frac{\hat{\vec{p}}^2}{2m_e}|\psi\rangle}_{E_{\text{kin}}} \underbrace{- \int d^3r \frac{e^2 n(\vec{r})}{4\pi\epsilon_0|\vec{r}-\vec{R}|}}_{E_{ne}} + \underbrace{\frac{1}{2}\int d^3r \int d^3r' \frac{e^2 n(\vec{r})n(\vec{r'})}{4\pi\epsilon_0|\vec{r}-\vec{r'}|}}_{E_H} \underbrace{-\frac{1}{2}\int d^4x \int d^4x' \frac{e^2\rho^{(1)}(\vec{x},\vec{x'})\rho^{(1)}(\vec{x'},\vec{x})}{4\pi\epsilon_0|\vec{r}-\vec{r'}|}}_{E_X} \tag{D.47}$$

The expression serves to define the energy terms evaluated below.

The exact energies of the hydrogen atom derived below are listed in table D.8.

Table D.8: Exact energies of the hydrogen atom. E_{self} is the electrostatic self energy of the electron density. $E_{\text{self}}+E_{\text{pot}}$ is the Hartree energy including electron-electron and electron-proton interactions. The energies in eV are approximate.

E_{tot}	E_{kin}	E_{pot}	ϵ_{1s}
$-\frac{1}{2}$ H	$\frac{1}{2}$ H	-1 H	$-\frac{1}{2}$ H
-13.606 eV	13.606 eV	-27.211 eV	-13.606 eV
$\epsilon_{2s}-\epsilon_{1s}$	$E_{\text{self}}+E_{\text{pot}}$	E_{self}	E_X
$\frac{3}{8}$ H	-11/16 H=-0.6875 H	5/16 H=+0.3125 H	-5/16 H=-0.3125 H
10.204 eV	-18.707 eV	8.503 eV	-8.503 eV

Wave function and density of the H-atom

The wave functions $\psi(\vec{r})$ of the hydrogen atom and its electron density $n(\vec{r})$ are[7]

$$\psi(\vec{r}) = \frac{1}{\sqrt{\pi a_0^3}} e^{-|\vec{r}|/a_0} \tag{D.50}$$

$$n(\vec{r}) = \frac{1}{\pi a_0^3} e^{-2|\vec{r}|/a_0} \tag{D.51}$$

[7]The wave functions of the hydrogen atom are taken from ΦSX: Quantum Physics. The Coulomb potential of the charge density is obtained with the help of Eq. 5.42 of PhiSX:Elektrodynamik. Furthermore, the following equations from Bronstein are used:

$$\int_0^x dx\, x e^{ax} = e^{ax}\left(\frac{x}{a}-\frac{1}{a^2}\right) \qquad \text{Bronstein p.61 Sec. 1.1.3.3 Eq.448}$$

$$\int_0^x dx\, x^2 e^{ax} = e^{ax}\left(\frac{x^2}{a}-\frac{2x}{a^2}+\frac{2}{a^3}\right) \qquad \text{Bronstein p.61 Sec. 1.1.3.3 Eq.449} \tag{D.48}$$

$$\int_0^\infty dx x^n e^{-ax} = \frac{n!}{a^{n+1}} \qquad \text{Bronstein p65 Sec. 1.1.3.4 Eq.1} \tag{D.49}$$

Kinetic energy of the H-atom

$$\begin{aligned}
E_{\text{kin}} &= \int d^3r\ \psi^*(\vec{r})\frac{-\hbar^2\vec{\nabla}^2}{2m_e}\psi(\vec{r}) \\
&= \frac{-\hbar^2}{2m_e}4\pi\int dr\ r^2\ \underbrace{\frac{1}{\sqrt{\pi a_0^3}}\mathrm{e}^{-|\vec{r}|/a_0}}_{=\psi^*(r)}\ \frac{1}{r}\partial_r^2 r\ \underbrace{\frac{1}{\sqrt{\pi a_0^3}}\mathrm{e}^{-|\vec{r}|/a_0}}_{=\psi(r)} \\
&= \frac{-\hbar^2}{2m_e}\frac{1}{\pi a_0^3}4\pi\int dr\ r^2\mathrm{e}^{-r/a_0}\quad \underbrace{\frac{1}{r}\partial_r^2 r\mathrm{e}^{-|\vec{r}|/a_0}}_{\underbrace{\frac{1}{r}\partial_r\left(\mathrm{e}^{-r/a_0}-\frac{r}{a_0}\mathrm{e}^{-r/a_0}\right)}_{-\frac{2}{ra_0}\mathrm{e}^{-r/a_0}+\frac{1}{a_0^2}\mathrm{e}^{-r/a_0}}} \\
&= \frac{-\hbar^2}{2m_e}\frac{1}{\pi a_0^3}\frac{2}{a_0^2}4\pi\int dr\ r^2\mathrm{e}^{-2r/a_0}\left(-\frac{a_0}{r}+\frac{1}{2}\right) \\
&= \frac{-\hbar^2}{2m_e}\frac{2}{a_0^2}\left(\frac{a_0 4\pi\epsilon_0}{e^2}\underbrace{\int d^3r\ \frac{1}{\pi a_0^3}\mathrm{e}^{-2r/a_0}\frac{-e^2}{4\pi\epsilon_0 r}}_{E_{ne}=-1\ H}+\frac{1}{2}\underbrace{\int d^3r\ \frac{1}{\pi a_0^3}\mathrm{e}^{-2r/a_0}}_{=1}\right) \\
&= +\frac{1}{2}\ H
\end{aligned} \tag{D.52}$$

Coulomb potential of the electrons of the H-atom

The Coulomb potential $v_e(\vec{r})$ of the electronic charge density $n(\vec{r})$ Eq. D.51 of the H-atom can be evaluated using the radial Green's function of the Poisson equation. (see ΦSX: Elektrodynamik.)

$$\begin{aligned}
v_e(\vec{r}) &= \int d^3r'\ \frac{e^2 n(\vec{r'})}{4\pi\epsilon|\vec{r}-\vec{r'}|} \\
&= \frac{e^2}{4\pi\epsilon_0}4\pi\left[\frac{1}{|\vec{r}|}\int_0^{|\vec{r}|}dr'\ (r')^2 n(r')+\int_{|\vec{r}|}^{\infty}dr'\ r' n(r')\right] \\
&= \frac{e^2}{4\pi\epsilon_0}4\pi\frac{1}{\pi a_0^3}\left[\frac{1}{|\vec{r}|}\int_0^{|\vec{r}|}dr'\ (r')^2\mathrm{e}^{-2r'/a_0}+\int_{|\vec{r}|}^{\infty}dr'\ r'\mathrm{e}^{-2r'/a_0}\right] \\
&= \frac{e^2}{4\pi\epsilon_0}4\pi\frac{1}{\pi a_0^3}\left\{\frac{1}{|\vec{r}|}\frac{a_0^3}{4}\left[1-\left(2\left(\frac{r}{a_0}\right)^2+2\left(\frac{r}{a_0}\right)+1\right)\mathrm{e}^{-2r/a_0}\right]+\frac{a_0^3}{4}\frac{1}{a_0}\left(2\frac{r}{a_0}+1\right)\mathrm{e}^{-2r/a_0}\right\} \\
&= \frac{e^2}{4\pi\epsilon_0}\left\{\frac{1}{|\vec{r}|}\left[1-\left(2\left(\frac{r}{a_0}\right)^2+2\left(\frac{r}{a_0}\right)+1\right)\mathrm{e}^{-2r/a_0}\right]+\frac{1}{r}\left(2\left(\frac{r}{a_0}\right)^2+\left(\frac{r}{a_0}\right)\right)\mathrm{e}^{-2r/a_0}\right\} \\
&= \frac{e^2}{4\pi\epsilon_0|\vec{r}|}\left\{\left[1-\left(\left(\frac{r}{a_0}\right)+1\right)\mathrm{e}^{-2r/a_0}\right]\right\}
\end{aligned} \tag{D.53}$$

Electron-proton interaction energy

The Coulomb interaction E_{ne} between the electron and the proton is evaluated using the Coulomb potential v_e of the electronic density

$$E_{ne} = \int d^3r\frac{-e^2 n(\vec{r})}{4\pi\epsilon_0|\vec{r}-\vec{R}|} = -v_e(\vec{R}) \overset{\text{Eq. D.53}}{=} -\frac{e^2}{4\pi\epsilon_0 a_0} = -1\ \mathrm{H} \tag{D.54}$$

Electronic Hartree energy

The electronic Hartree energy is the Coulomb self energy of the electronic charge density.

$$E_{\text{self}} = \frac{1}{2}\int d^3r \int d^3r' \frac{e^2 n(\vec{r}) n(\vec{r'})}{4\pi\epsilon_0 |\vec{r}-\vec{r'}|} \tag{D.55}$$

The self energy is the Coulomb interaction energy of the electron density with itself. This energy is canceled by the exchange energy. Thus, the self energy can be used to obtain, independently, the Hartree energy and the exchange energy.

$$\begin{aligned}
E_{\text{self}} &= \frac{1}{2}\int d^3r\; n(\vec{r}) v(\vec{r}) \\
&= \frac{1}{2}\left(\frac{1}{\pi a_0^3}\right)\left(\frac{e^2}{4\pi\epsilon_0}\right) 4\pi \int_0^\infty dr\; r^2 \mathrm{e}^{-2r/a_0} \frac{1}{r}\left[1-\left(\left(\frac{r}{a_0}\right)+1\right)\mathrm{e}^{-2r/a_0}\right] \\
&= \frac{1}{2}\left(\frac{1}{\pi a_0^3}\right)\left(\frac{e^2}{4\pi\epsilon_0}\right) 4\pi a_0^2 \int_0^\infty dx\; x\mathrm{e}^{-2x}\left[1-(x+1)\,\mathrm{e}^{-2x}\right] \\
&= \frac{1}{2}\frac{1}{\pi a_0^3}\frac{e^2}{4\pi\epsilon_0 a_0} 4\pi a_0^3 \int_0^\infty dx\; \left[x\mathrm{e}^{-2x} - x^2\mathrm{e}^{-4x} - x\mathrm{e}^{-4x}\right] \\
&= 2\underbrace{\frac{e^2}{4\pi\epsilon_0 a_0}}_{1H} \underbrace{\left[\frac{1!}{2^2}-\frac{2!}{4^3}-\frac{1!}{4^2}\right]}_{1/4-1/32-1/16=(8-1-2)/32=5/32} \\
&= \frac{5}{16}\frac{e^2}{4\pi\epsilon_0 a_0} = 0.3125\; H \qquad \textit{(exact)}
\end{aligned} \tag{D.56}$$

Exchange energy of the H-atom

The exchange energy of a one-electron system cancels the electronic Hartree energy precisely. Thus, the exchange energy is

$$E_X = -E_H = -\frac{5}{16}\frac{e^2}{4\pi\epsilon_0 a_0} = -0.3125\; H \qquad \textit{(exact)} \tag{D.57}$$

U-tensor of the H-atom

The U-tensor is twice the self energy, Eq. D.56, i.e.

$$U = 2E_{\text{self}} = 2E_X = \frac{5}{8}\frac{e^2}{4\pi\epsilon_0 a_0} \tag{D.58}$$

The energy E_{e-nuc} is the complete electrostatic energy including Hartree energy $E_{\text{pot}} + E_{\text{self}}$ and exchange energy E_X. This tells us that $E_X = -E_{\text{self}}$ This result for the exchange energy $E_X = -0.3125$ is also given in [P.M.W. Gill and J.A. Pople, Phys Rev. A 47, 2383 (1993)][109].

D.5 Hydrogen molecule

$$\begin{aligned}
E_{\text{tot}} = &\underbrace{\sum_{\sigma\in\{\uparrow,\downarrow\}} f_{b,\sigma}\langle\psi_{b,\sigma}|\frac{\hat{\vec{p}}^2}{2m_e}|\psi_{b,\sigma}\rangle}_{E_{\text{kin}}} \underbrace{- \sum_{R\in\{R_1,R_2\}}\int d^3r \frac{e^2\Big(n(\vec{r})+Z(\vec{r})\Big)\Big(n(\vec{r'})+Z(\vec{r'})\Big)}{4\pi\epsilon_0|\vec{r}-\vec{R}|}}_{E_H+E_{ne}+E_{nn}} \\
&\underbrace{-\frac{1}{2}\int d^4x \int d^4x'\; \frac{e^2\rho^{(1)}(\vec{x},\vec{x'})\rho^{(1)}(\vec{x'},\vec{x})}{4\pi\epsilon_0|\vec{r}-\vec{r'}|}}_{E_X}
\end{aligned} \tag{D.59}$$

All matrix elements are evaluated using atomic orbitals

$$\langle \vec{r}, \sigma | \chi_{j,\sigma'} \rangle = \frac{1}{\sqrt{\pi a_0^3}} \mathrm{e}^{-|\vec{r}-\vec{R}_j|/a_0} \delta_{\sigma,\sigma'} \tag{D.60}$$

The bound state wave function $|\psi_{b,\sigma}\rangle$ expressed in normalized atomic orbitals $|\chi_{j,\sigma}\rangle$ is

$$|\psi_{b,\sigma}\rangle = \Big(|\chi_{1,\sigma}\rangle + |\chi_{2,\sigma}\rangle \Big) \frac{1}{\sqrt{2(1+S)}} \tag{D.61}$$

with the off-site overlap matrix elements

$$S = \langle \chi_{1,\sigma} | \chi_{2,\sigma} \rangle \tag{D.62}$$

which are obtained below in Eq. D.68.

Editor: continue here!

The matrix elements of the hydrogen atom have been worked out by van Leeuwen[105].

D.5.1 Two-center integral of spherical functions

The integrations of interest are of the form of a two-center integral of two spherical functions with centers that are separated by the distance d.

$$\begin{aligned}
\langle f | g \rangle &= \int d^3r \; f(|\vec{r}|) g(|\vec{e}_z d - \vec{r}|) \\
&= \int_0^\infty dr \; r^2 \int_0^{2\pi} d\phi \int_0^\pi d\theta \sin(\theta) f(r) g(\sqrt{(d - r\cos(\theta))^2 + (r\sin(\theta))^2}) \\
&= 2\pi \int_0^\infty dr \; r^2 f(r) \int_0^\pi d\theta \sin(\theta) g(\sqrt{d^2 - 2dr\cos(\theta)) + r^2}) \\
&= 2\pi \int_0^\infty dr \; r^2 f(r) \frac{1}{dr} \int_{|d-r|}^{|d+r|} dy \; y g(y) \\
&= \frac{2\pi}{d} \int_0^\infty dr \; r f(r) \int_{|d-r|}^{|d+r|} dy \; y g(y) \\
&= \frac{2\pi}{d} \left[\int_0^d dr \; r f(r) \int_{d-r}^{r+d} dy \; y g(y) + \int_d^\infty dr \; r f(r) \int_{r-d}^{r+d} dy \; y g(y) \right]
\end{aligned} \tag{D.63}$$

We used

$$\begin{aligned}
y(\theta) = \sqrt{d^2 - 2dr\cos(\theta) + r^2} \qquad &\Rightarrow \qquad dy = \frac{1}{2y} 2dr \sin(\theta) d\theta \\
y(\theta = 0) = |d - r| \qquad &\text{and} \qquad y(\theta = \pi) = d + r
\end{aligned} \tag{D.64}$$

D.5.2 Overlap

Let me evaluate the overlap of two hydrogen orbitals $S(d)$ at centers separated by the distance d.

$$S(d) = \frac{1}{\pi a_0^3} \int d^3r \; \mathrm{e}^{-|\vec{r}|/a_0} \mathrm{e}^{-|\vec{r}-\vec{e}_z d|/a_0} \tag{D.65}$$

In the following, I will use the undetermined integrals from Bronstein,

$$\begin{aligned}
\int dx\, \mathrm{e}^{-ax} &= -\frac{1}{a}\mathrm{e}^{-ax} \\
\int dx\, x\mathrm{e}^{-ax} &= -\frac{ax+1}{a^2}\mathrm{e}^{-ax} \\
\int dx\, x^2\mathrm{e}^{-ax} &= -\frac{(ax)^2+2ax+2}{a^3}\mathrm{e}^{-ax} \\
\int dx\, x^n\mathrm{e}^{-ax} &= \frac{-n!}{a^{n+1}}\mathrm{e}^{-ax}\sum_{j=0}^{n}\frac{1}{j!}(ax)^j
\end{aligned} \tag{D.66}$$

The parameter a is unrelated to the Bohr radius a_0.

Let be introduce a dimensionless parameter $\vec{x} = \frac{\vec{r}}{a_0}$ and $z = \frac{d}{a_0}$. With $\vec{e}_z$, I denote the unit vector pointing along the z-axis. Caution: Here, the symbol $\vec{x}$ is unrelated to the combined position-and-spin variable $\vec{x} = (\vec{r}, \sigma)$.

$$\begin{aligned}
S(d = za_0) &= \frac{1}{\pi}\int d^3x\, \mathrm{e}^{-|\vec{x}|}\mathrm{e}^{-|\vec{x}-z\vec{e}_z|} \\
&\overset{\text{Eq. } D.63}{=} \frac{2}{z}\left[\int_0^z dx\, x\mathrm{e}^{-x}\int_{z-x}^{x+z} dy\, y\mathrm{e}^{-y} + \int_z^\infty dx\, x\mathrm{e}^{-x}\int_{x-z}^{x+z} dy\, y\mathrm{e}^{-y}\right] \\
&= \frac{2}{z}\left\{\int_0^z dx\, x\mathrm{e}^{-x}\Big[-(1+y)\mathrm{e}^{-y}\Big]_{z-x}^{x+z} + \int_z^\infty dx\, x\mathrm{e}^{-x}\Big[-(1+y)\mathrm{e}^{-y}\Big]_{x-z}^{x+z}\right\} \\
&= \frac{2}{z}\left\{\int_0^z dx\, x\mathrm{e}^{-x}\Big[-(1+x+z)\,\mathrm{e}^{-(x+z)} + (1+z-x)\,\mathrm{e}^{-(z-x)}\Big]\right. \\
&\quad \left. + \int_z^\infty dx\, x\mathrm{e}^{-x}\Big[-(1+x+z)\,\mathrm{e}^{-(x+z)} + (1+x-z)\,\mathrm{e}^{-(x-z)}\Big]\right\} \\
&= \frac{2}{z}\left\{\mathrm{e}^{-z}\int_0^z dx\, \Big[-(1+z)\,x\mathrm{e}^{-2x} - x^2\mathrm{e}^{-2x} + (1-z)\,x + x^2\Big]\right. \\
&\quad \left. + \int_z^\infty dx\, \Big[\Big(\mathrm{e}^{+z}(1-z) - \mathrm{e}^{-z}(1+z)\Big)x\mathrm{e}^{-2x} + \Big(\mathrm{e}^{+z} - \mathrm{e}^{-z}\Big)x^2\mathrm{e}^{-2x}\Big]\right\} \\
&= \frac{2}{z}\left\{\mathrm{e}^{-z}\left[-(1+z)\,\frac{-2x-1}{4}\mathrm{e}^{-2x} - \frac{(-2x)^2-2(-2x)+2}{-8}\mathrm{e}^{-2x} + \frac{1+z}{2}x^2 - \frac{1}{3}x^3\right]_0^z\right. \\
&\quad \left. + \left[\Big(\mathrm{e}^{+z}(1-z) - \mathrm{e}^{-z}(1+z)\Big)\frac{-2x-1}{4}\mathrm{e}^{-2x} + \Big(\mathrm{e}^{+z} - \mathrm{e}^{-z}\Big)\frac{(-2x)^2-2(-2x)+2}{-8}\mathrm{e}^{-2x}\right]_z^\infty\right\} \\
&= \frac{2}{z}\left\{\mathrm{e}^{-z}\left[(1+z)\,\frac{2z+1}{4}\mathrm{e}^{-2z} - \frac{2z^2+2z+1}{4}\mathrm{e}^{-2z} + \frac{1+z}{2}z^2 - \frac{1}{3}z^3 + (1+z)\,\frac{-1}{4} - \frac{1}{4}\right]\right. \\
&\quad \left. - \left[\Big(\mathrm{e}^{+z}(1-z) - \mathrm{e}^{-z}(1+z)\Big)\frac{-2z-1}{4}\mathrm{e}^{-2z} + \Big(\mathrm{e}^{+z} - \mathrm{e}^{-z}\Big)\frac{2z^2+2z+1}{-4}\mathrm{e}^{-2z}\right]\right\} \\
&= \Big(\frac{1}{3}z^2 + z + 1\Big)\mathrm{e}^{-z}
\end{aligned} \tag{D.67}$$

Thus, the overlap matrix element of two hydrogen 1s-orbitals is

OVERLAP OF TWO HYDROGEN 1S ORBITALS

$$S(d) = \left[\frac{1}{3}\left(\frac{d}{a_0}\right)^2 + \left(\frac{d}{a_0}\right) + 1\right]\mathrm{e}^{-\frac{d}{a_0}} \tag{D.68}$$

D.5.3 Coulomb repulsion between the protons

$$E_{nn}(d) = \frac{e^2}{4\pi\epsilon_0 d} \tag{D.69}$$

D.5.4 Electron-proton interaction matrix elements

The electrostatic energy between electron density on one site with a proton on the other side is obtained from the electrostatic potential $v_w(\vec{r})$ of the atomic density at the distance of the nucleus

$$\begin{aligned} E_{xx} &= -\int d^3r \frac{e^2 n_1(\vec{r})}{4\pi\epsilon_0|\vec{r}-\vec{R}_2|} = -v_e(d\vec{e}_z) \\ &\overset{\text{Eq. } D.53}{=} -\frac{e^2}{4\pi\epsilon_0 a_0}\left\{\left(\frac{d}{a_0}\right)^{-1}\left[1-\left(\left(\frac{d}{a_0}\right)+1\right)\mathrm{e}^{-2d/a_0}\right]\right\} \end{aligned} \tag{D.70}$$

D.5.5 Electron-nucleus Coulomb matrix elements

The matrix elements from this subsection are copied from the internet and they are not verified. `http://www.pci.tu-bs.de/aggericke/PC4e/Kap_II/H2-Ion.htm`

The **Coulomb integral** J is the Coulomb interaction of one atom with the nucleus of the other atom.

$$J = \frac{e^2}{4\pi\epsilon_0 d} - \int d^3r\, \psi_{1s}(\vec{r})\psi_{1s}(\vec{r})\frac{e^2}{4\pi\epsilon_0|\vec{r}-\vec{e}_z d|} = \left(1+\frac{1}{d}\right)\mathrm{e}^{-2d/a_0} \tag{D.71}$$

The **resonance integral** K describes the overlap density of two orbitals on different sites with the nucleus of one site

$$K = \frac{e^2 S(d)}{4\pi\epsilon_0 d} - \int d^3r\, \frac{e^2\psi_{1s}(\vec{r}-\vec{e}_z d)\psi_{1s}(\vec{r})}{4\pi\epsilon_0|\vec{r}-\vec{e}_z d|} = \frac{e^2}{4\pi\epsilon_0}\left(\frac{a_0}{d}-\frac{2}{3}\frac{d}{a_0}\right)\mathrm{e}^{-d/a_0} \tag{D.72}$$

D.5.6 U-tensor

The 31 matrix elements are those with three orbitals on one site and one on the other. The 22 matrix elements are those with one density on one site and another density on the other.

The U-tensor can be constructed from the following basic matrix elements. For the sake of simplicity we refer here only to the spatial part of the wave functions and ignore the spin part. The matrix elements $W_{\alpha,\beta,\gamma,\delta}$, which also account of the spin indices, can be calculated from these matrix elements U. The indices refer to the two sites of the H_2-molecule.

$$\begin{aligned} U_{1111} &= \int d^3r \int d^3r' \frac{e^2\chi_1^*(\vec{r})\chi_1^*(\vec{r'})\chi_1(\vec{r})\chi_1(\vec{r'})}{4\pi\epsilon_0|\vec{r}-\vec{r'}|} \\ U_{1112} &= \int d^3r \int d^3r' \frac{e^2\chi_1^*(\vec{r})\chi_1^*(\vec{r'})\chi_1(\vec{r})\chi_2(\vec{r'})}{4\pi\epsilon_0|\vec{r}-\vec{r'}|} = \int d^3r \left(v_e(\vec{r})\chi(\vec{r})\right)\chi(\vec{r}-\vec{e}_z d) \\ U_{1212} &= \int d^3r \int d^3r' \frac{e^2\chi_1^*(\vec{r})\chi_2^*(\vec{r'})\chi_1(\vec{r})\chi_2(\vec{r'})}{4\pi\epsilon_0|\vec{r}-\vec{r'}|} = \int d^3r \left(v_e(\vec{r})\right)\chi^2(\vec{r}-\vec{e}_z d) \\ U_{1221} &= \int d^3r \int d^3r' \frac{e^2\chi_1^*(\vec{r})\chi_2^*(\vec{r'})\chi_2(\vec{r})\chi_1(\vec{r'})}{4\pi\epsilon_0|\vec{r}-\vec{r'}|} \end{aligned} \tag{D.73}$$

The Coulomb potential v_e from the electrons of one hydrogen atom is Eq. D.53

$$v_e(\vec{r}) = \frac{e^2}{4\pi\epsilon_0|\vec{r}|}\left[1-\left(1+\frac{r}{a_0}\right)\mathrm{e}^{-2r/a_0}\right] \tag{D.74}$$

1. The element U_{1111} has four orbitals on one site, and can be identified with the U-parameter Eq. D.58 of the hydrogen atom.

2. The element U_{1112} describes the interaction of the electrons on one site with a bond charge density, i.e. the density from the overlap of orbitals from both sites.

3. The matrix element U_{1212} is the Coulomb interaction of the electronic charge density from one atom with that of the other.

4. The matrix element U_{1221} is the Coulomb interaction of the bond charge density with itself.Editor: I do not have an analytical expression for this matrix element yet.

Editor: Caution! The following derivation is not carried through to the end and need to be tested. At the end a Maple result is introduced! See Appendix A of [105].

The integrations for two matrix elements are of a similar form, namely $U_{1112} = I(3,1)$ and $U_{1212} = I(2,2)$ with

$$\begin{aligned}\frac{e^2}{4\pi\epsilon_0 a_0} I_{2+m,n}(d = z a_0) &\stackrel{\text{def}}{=} \int d^3r\; v_e(\vec{r})\psi_{1s}^n(\vec{r})\psi_{1s}^m(\vec{r} - \vec{e}_z d) \\ &= \frac{e^2}{4\pi\epsilon_0 a_0}\frac{1}{\pi a_0^3}\int d^3r\; \frac{a_0}{|\vec{r}|}\left[1 - \left(1 + \frac{|\vec{r}|}{a_0}\right)\mathrm{e}^{-2\frac{|\vec{r}|}{a_0}}\right]\mathrm{e}^{-m\frac{|\vec{r}|}{a_0}}\mathrm{e}^{-n\frac{|\vec{r}-\vec{e}_z d|}{a_0}} \\ &= \frac{e^2}{4\pi\epsilon_0 a_0}\frac{1}{\pi}\int d^3r\; \frac{1}{|\vec{x}|}\left[1 - (1 + |\vec{x}|)\,\mathrm{e}^{-2|\vec{x}|}\right]\mathrm{e}^{-m|\vec{r}|}\mathrm{e}^{-n|\vec{x}-\vec{e}_z z|} \qquad \text{(D.75)}\end{aligned}$$

with $z = d/a_0$.

$$
\begin{aligned}
I_{4-n,n}(z) &= \frac{1}{\pi}\int d^3r\,\frac{1}{|\vec{X}|}\left[1-(1+|\vec{X}|)\,\mathrm{e}^{-2|\vec{X}|}\right]\mathrm{e}^{-(2-n)|\vec{r}|}\mathrm{e}^{-n|\vec{X}-\vec{e}_z z|}\\
&= \frac{1}{\pi}\frac{2\pi}{z}\left\{\int_0^z dx\,x\underbrace{\frac{1}{x}\left[1-(1+x)\,\mathrm{e}^{-2x}\right]\mathrm{e}^{-(2-n)x}}_{f(x)}\int_{z-x}^{x+z} dy\,y\underbrace{\mathrm{e}^{-ny}}_{g(y)}\right.\\
&\quad\left.+\int_z^\infty dx\,x\underbrace{\frac{1}{x}\left[1-(1+x)\,\mathrm{e}^{-2x}\right]\mathrm{e}^{-(2-n)x}}_{f(x)}\int_{x-z}^{x+z} dy\,y\underbrace{\mathrm{e}^{-ny}}_{g(y)}\right\}\\
&= \frac{2}{z}\left\{\int_0^z dx\;\left[1-(1+x)\,\mathrm{e}^{-2x}\right]\mathrm{e}^{-(2-n)x}\left[\frac{-ny-1}{n^2}\mathrm{e}^{-ny}\right]_{z-x}^{x+z}\right.\\
&\quad\left.+\int_z^\infty dx\;\left[1-(1+x)\,\mathrm{e}^{-2x}\right]\mathrm{e}^{-(2-n)x}\left[\frac{-ny-1}{n^2}\mathrm{e}^{-ny}\right]_{x-z}^{x+z}\right\}\\
&= \frac{-2}{n^2 z}\left\{\int_0^z dx\;\left[1-(1+x)\,\mathrm{e}^{-2x}\right]\mathrm{e}^{-(2-n)x}\right.\\
&\qquad\qquad\times\left[(1+n(z+x))\mathrm{e}^{-nz}\mathrm{e}^{-nx}-(1+nz-nx)\mathrm{e}^{-nz}\mathrm{e}^{+nx}\right]\\
&\quad+\int_z^\infty dx\;\left[1-(1+x)\,\mathrm{e}^{-2x}\right]\mathrm{e}^{-(2-n)x}\\
&\qquad\qquad\left.\times\left[(1+nz+nx)\mathrm{e}^{-nz}-(1-nz+nx)\mathrm{e}^{+nz}\right]\mathrm{e}^{-nx}\right\}\\
&= \frac{-2}{n^2 z}\left\{\int_0^z dx\;\left[1-(1+x)\,\mathrm{e}^{-2x}\right]\right.\\
&\qquad\qquad\times\mathrm{e}^{-nz}\left[(1+nz+nx)\mathrm{e}^{-2x}-(1+nz-nx)\mathrm{e}^{-(2-2n)x}\right]\\
&\quad+\int_z^\infty dx\;\left[1-(1+x)\,\mathrm{e}^{-2x}\right]\\
&\qquad\qquad\left.\times\left[\Big((1+nz+nx)\mathrm{e}^{-nz}-(1-nz+nx)\mathrm{e}^{+nz}\Big)\right]\mathrm{e}^{-2x}\right\}
\end{aligned}
\tag{D.76}
$$

$$
\begin{aligned}
I_{22} = \frac{-2}{4z}\Bigg\{ & \int_0^z dx\ \left[1-(1+x)\,\mathrm{e}^{-2x}\right] \\
& \qquad \times \mathrm{e}^{-2z}\Big[(1+2z+2x)\mathrm{e}^{-2x}-(1+2z-2x)\mathrm{e}^{+2x}\Big] \\
& + \int_z^\infty dx\ \left[1-(1+x)\,\mathrm{e}^{-2x}\right] \\
& \qquad \times \Big[\Big((1+2z+2x)\mathrm{e}^{-2z}-(1-2z+2x)\mathrm{e}^{+2z}\Big)\Big]\mathrm{e}^{-2x}\Bigg\} \\
= \frac{-1}{2z}\Bigg\{ & \int_0^z dx\ \mathrm{e}^{-2z}\Big[(1+2z+2x)\mathrm{e}^{-2x}-(1+2z-2x)\mathrm{e}^{+2x}\Big] \\
& + \int_z^\infty dx\ \Big[\Big((1+2z+2x)\mathrm{e}^{-2z}-(1-2z+2x)\mathrm{e}^{+2z}\Big)\Big]\mathrm{e}^{-2x} \\
& - \int_0^z dx\ \mathrm{e}^{-2z}\Big[(1+2z+2x)\mathrm{e}^{-4x}-(1+2z-2x)\Big] \\
& - \int_z^\infty dx\ \Big[\Big((1+2z+2x)\mathrm{e}^{-2z}-(1-2z+2x)\mathrm{e}^{+2z}\Big)\Big]\mathrm{e}^{-4x} \\
& - \int_0^z dx\ \mathrm{e}^{-2z}\Big[(1+2z+2x)\mathrm{e}^{-4x}-(1+2z-2x)\Big]x \\
& - \int_z^\infty dx\ \Big[\Big((1+2z+2x)\mathrm{e}^{-2z}-(1-2z+2x)\mathrm{e}^{+2z}\Big)\Big]x\mathrm{e}^{-4x}\Bigg\} \\
= \frac{-1}{2z}\Bigg\{ & \left[\left(\frac{1+2z}{-2}-2\frac{1+2x}{4}\right)\mathrm{e}^{-2(x+z)}-\left(\frac{1+2z}{+2}+2\frac{1-2x}{4}\right)\mathrm{e}^{+2(x-z)}\right]_0^z \\
& + \left[\left(\frac{1+2z}{-2}-2\frac{2x+1}{4}\right)\mathrm{e}^{-2(x+z)}-\left(\frac{1-2z}{2}+2\frac{1-2x}{4}\right)\mathrm{e}^{+2(z-x)}\right)\Bigg]_z^\infty \\
& - \left[\left(\frac{1+2z}{-4}-2\frac{1+4x}{16}\right)\mathrm{e}^{-4x-2z}-\left(x+2xz-x^2\right)\mathrm{e}^{-2z}\right]_0^z \\
& - \left[\left(\frac{1+2z}{-4}-2\frac{1+4x}{16}\right)\mathrm{e}^{-2z-4x}-\left(\frac{1-2z}{-4}-2\frac{1+4x}{16}\right)\mathrm{e}^{+2z-4x}\right]_z^\infty \\
& - \left[\left(\frac{(1+2z)(1+4z)}{16}+2\frac{16x^2+8x+2}{(-4)^3}\right)\mathrm{e}^{-4x-2z}-\left(\frac{1+2z}{2}x^2-\frac{2}{3}x^3\right)\mathrm{e}^{-2z}\right]_0^z \\
& - \Bigg[\left(-\frac{(1+2z)(1+4x)}{16}+2\frac{16x^2+8x+2}{-4^3}\right)\mathrm{e}^{-2z-4x} \\
& \qquad -\left(-\frac{(1-2z)(1+4x)}{16}+2\frac{16x^2+8x+2}{-4^3}\right)\mathrm{e}^{+2z-4x}\Bigg]_z^\infty\Bigg\}
\end{aligned}
\tag{D.77}
$$

This calculation is not finished. I am continuing with the Result from Maple.

Maple:

$$
\begin{aligned}
I_{31}(z) &= \left(z^2+\frac{1}{8}z+\frac{5}{16}\right)\frac{1}{z}\mathrm{e}^{-z}-\left(\frac{1}{8}z+\frac{5}{16}\right)\frac{1}{z}\mathrm{e}^{-3z} \\
&= z\mathrm{e}^{-z}+\left(\frac{1}{8}z+\frac{5}{16}\right)\frac{1}{z}\left(\mathrm{e}^{-z}-\mathrm{e}^{-3z}\right) \\
I_{22} &= \frac{1}{z}-\left(\frac{1}{6}z^3+\frac{3}{4}z^2+\frac{11}{8}z+1\right)\frac{1}{z}\mathrm{e}^{-2z}
\end{aligned}
\tag{D.78}
$$

OFFSITE U-TENSOR MATRIX ELEMENTS

The offsite U-tensor matrix elements $U_{31} = W_{1,1,1,2}$ and $U_{22} = W_{1,2,1,2}$ are

$$U_{31}(d = za_0) = \frac{e^2}{4\pi\epsilon_0 a_0} I_{31} = \frac{e^2}{4\pi\epsilon_0 a_0}\left[z\mathrm{e}^{-z} + \left(\frac{1}{8}z + \frac{5}{16}\right)\frac{1}{z}\left(\mathrm{e}^{-z} - \mathrm{e}^{-3z}\right)\right]$$
$$U_{22}(d = za_0) = \frac{e^2}{4\pi\epsilon_0 a_0} I_{22} = \frac{e^2}{4\pi\epsilon_0 a_0}\left[\frac{1}{z} - \left(\frac{1}{6}z^3 + \frac{3}{4}z^2 + \frac{11}{8}z + 1\right)\frac{1}{z}\mathrm{e}^{-2z}\right] \quad \text{(D.79)}$$

- Both terms approach at short distances

$$I_{33}(z) = \frac{5}{8} + O(x^2)$$
$$I_{22}(z) = \frac{5}{8} + O(x^2) \quad \text{(D.80)}$$

  The limit $x \to 0$ is equal to the onsite U-tensor, because in this limit, all four orbitals are centered on a single site. The electrostatic self energy E_{self} of the hydrogen atom calculated above is 5/16, which is $\frac{1}{2}U$.

- at long distances the integrals approach

$$I_{22}(z) \overset{z\to\infty}{\to} \frac{1}{z}$$
$$I_{33}(z) \overset{z\to\infty}{\to} ze^{-z} \quad \text{(D.81)}$$

In order to remove the long-ranged part, I subtracted the multipole expansion of the 22 term. This, however, introduces singularities of the remaining term at the origin. A better strategy would be to replace 1/r by

$$\frac{1}{z} \to \frac{1}{z} - \left(1 - \frac{1}{2}(\lambda z)^2\right)\frac{\mathrm{e}^{-\lambda z}}{z} \cdot$$
$$\frac{1}{z^2} \to \frac{1}{z^2} - \left(1 + (\lambda z) - \frac{1}{3}(\lambda z)^3\right)\frac{\mathrm{e}^{-\lambda z}}{z^2}$$
$$\frac{1}{z^3} \to \frac{1}{z^3} - \left(1 + (\lambda z) + \frac{1}{2}(\lambda z)^2 - \frac{1}{8}(\lambda z)^4\right)\frac{\mathrm{e}^{-\lambda z}}{z^3}$$
$$\mathrm{e}^{-\lambda z} \to (1 + \lambda z)\mathrm{e}^{-\lambda z} \quad \text{(D.82)}$$

For a finite screening we need to multiply the right hand side with $(1+\gamma z)\mathrm{e}^{-\gamma z}$, so that the slope at the origin remains zero.

$$\frac{1}{z}\mathrm{e}^{-\gamma z} \to \left(\frac{1}{z} - \left(1 - \frac{1}{2}((\lambda + \gamma)z)^2\right)\frac{\mathrm{e}^{-\lambda z}}{z}\cdot\right)\mathrm{e}^{-\gamma z}$$
$$\frac{1}{z^2} \to \frac{1}{z^2} - \left(1 + (\lambda z) - \frac{1}{3}\lambda^2\right)\frac{\mathrm{e}^{-\lambda z}}{z^2}$$
$$\frac{1}{z^3} \to \frac{1}{z^3} - \left(1 + (\lambda z) + \frac{1}{2}\lambda^2 - \frac{1}{8}(\lambda x)^4\right)\frac{\mathrm{e}^{-\lambda z}}{z^3}$$
$$\mathrm{e}^{-\lambda z} \to (1 + \lambda z)\mathrm{e}^{-\lambda z} \quad \text{(D.83)}$$

D.6 Dihydrogen cation

The H_2^+ ion is another one-electron system. It will not be treated exactly, but rather in the basisset of the wave functions of atomic hydrogen. The goal of this is to benchmark the matrix elements for the off-site exchange.

With the knowledge of the matrix elements the individual contributions of the dihydrogen cation can be calculated in the basis of atomic orbitals.

Data are in `Testsimplelmto/Calc/H2cation`

The wave function is

$$|\psi\rangle = |\chi_1\rangle c_1 + |\chi_1\rangle c_2 = (|\chi_1\rangle + |\chi_1\rangle)\,\frac{1}{\sqrt{2+2S}} \tag{D.84}$$

where $S = \langle\chi_1|\chi_2\rangle$ is the offsite overlap matrix element.

Thus, the density matrix elements all have the same value

$$\rho_{\alpha,\beta} = c_\alpha c_\beta = \frac{1}{2+2S} \tag{D.85}$$

The number of electrons on a single site $N_{on,i}$ and that N_{off} in the off-site terms is thus

$$\begin{aligned} N_{on,i} &= c_\alpha^2 = \frac{1}{2+2S} \\ N_{off} &= c_1 S c_2 S + c_2 S c_1 = \frac{2S}{2+2S} \\ 1 &= N_{on,1} + N_{on,1} + N_{off} \end{aligned} \tag{D.86}$$

The onsite Hartree and the onsite exchange energy is

$$\begin{aligned} E_{H,on,i} &= \frac{1}{2} U_{1111}\rho_{11}\rho_{11} \overset{\text{Eq. } D.58}{=} \frac{1}{2}\frac{5}{8}\frac{1}{(2+2S)^2} = \frac{5}{16}\frac{1}{(2+2S)^2} \\ E_{X,on,i} &= -E_{H,on,i} \end{aligned} \tag{D.87}$$

The energy related to the offsite exchange terms are

$$\begin{aligned} E_{X,22} &= -\frac{1}{2}\sum_{R\neq R'}\sum_{\alpha,\gamma\in R}\sum_{\beta,\delta\in R} W_{\alpha,\beta,\gamma,\delta}\rho_{\delta,\alpha}\rho_{\gamma,\beta} \\ &= -\frac{1}{2}\Big(W_{1,2,1,2}\rho_{2,1}\rho_{1,2} + W_{2,1,2,1}\rho_{2,1}\rho_{1,2}\Big) = -\frac{U_{22}}{(2+2S)^2} \\ E_{X,31} &= -\frac{1}{2}\sum_{R\neq R'} 4 \sum_{\alpha,\beta,\gamma\in R}\sum_{\delta\in R'} W_{\alpha,\beta,\gamma,\delta}\rho_{\delta,\alpha}\rho_{\gamma,\beta} \\ &= -\frac{1}{2}4\Big(W_{1,1,1,2}\rho_{2,1}\rho_{1,1} + W_{2,2,2,1}\rho_{1,2}\rho_{2,2}\Big) = -\frac{4U_{31}}{(2+2S)^2} \end{aligned} \tag{D.88}$$

Appendix E

Homogeneous electron gas

In this chapter, I am including material on the homogeneous electron gas, which does not fit into the main text.

E.1 Energy contributions of the homogeneous electron gas

In figure E.1, the individual energy contributions per electron are shown as function of the density.

One observes that the Coulomb energy dominates in the low-density region. This is the region where one can expect the electron interaction to be dominant. In the ultra-low density region, the electrons even undergo a phase transition to a Wigner crystal.

In the low-density region, the simple box model provides a fairly good description of the exchange-correlation energy. This is anticipated because the exchange hole with a box-like shape minimizes the Coulomb repulsion between the electrons. Thus, it is best suited in strongly-interacting limit.

In the high-density region, the kinetic energy dominates over the Coulomb energy. As a consequence, the exchange-correlation hole is similar to that of a non-interacting electron gas, which is obtained in the Hartree-Fock approximation.

Both models, the Hartree-Fock approximation of the homogeneous electron gas and the box model, use a fixed shape of the exchange-correlation hole. The hole for different densities is only scaled in value and distance. As a result, the corresponding exchange-correlation energy per electron scales like $n^{\frac{1}{3}}$. The corresponding prefactor of the exchange-correlation energy of is determined by the different shapes. The exchange-correlation hole of interacting electron gas changes from the compact hole in the low-density region to a more dilute hole in the high-density region.

E.2 Non-interacting homogeneous electron gas

On p. 45, we calculated the kinetic energy of a non-interacting homogeneous electron gas with a specified total density and spin density. The result is

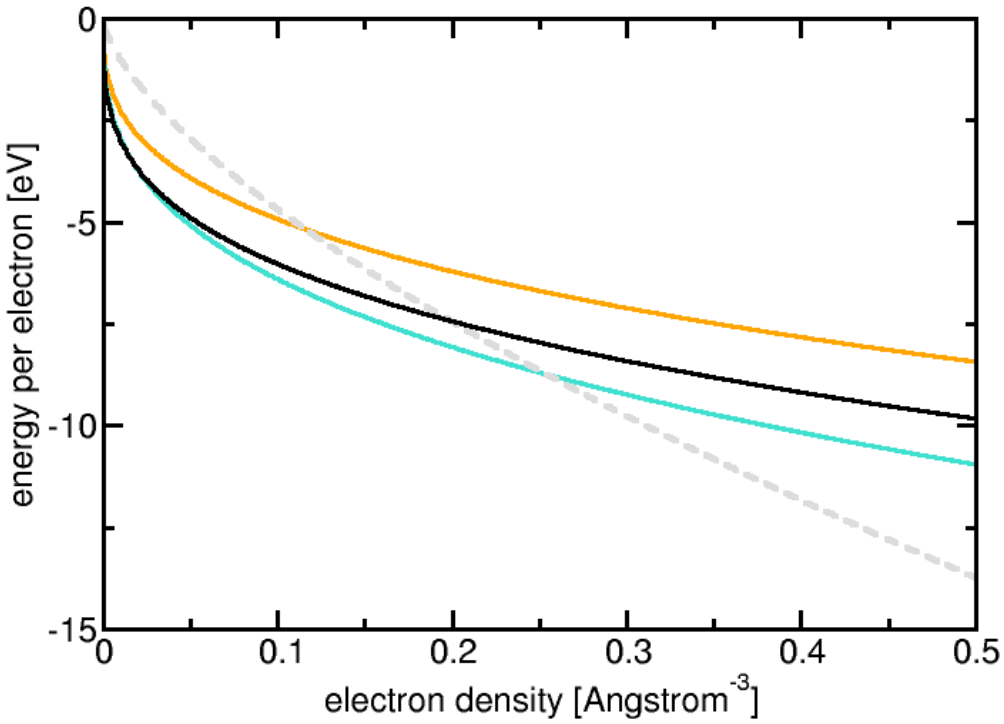

Fig. E.1: Energies of the free electron gas as function of the density. The grey dashed line is, up to a sign change, the kinetic energy per electron. The black line is the exchange-correlation energy per electron of the interacting electron gas, the orange line is from the Hartree Fock approximation and the green line is from the box model discussed in section 2.8.5 on p. 116. The box model replaces the exchange-correlation hole for each spin direction by a homogeneously charged sphere. The valence-electron density of bulk aluminium is 0.18 Å^{-3}.

KINETIC ENERGY OF THE NON-INTERACTING FREE ELECTRON GAS

This is the Thomas-Fermi expression for the kinetic energy of a non-interacting homogeneous electron gas at zero Kelvin.

$$\frac{1}{L^3}E_{\text{kin}}(n_t, n_s) \overset{\text{Eq. 1.149}}{=} \underbrace{\frac{3}{10}\left(3\pi^2\right)^{\frac{2}{3}}\frac{\hbar^2}{m_e}n_t^{\frac{5}{3}}}_{E(n_t,0)/L^3} \cdot \underbrace{\frac{1}{2}\left[\left(1+\frac{n_s}{n_t}\right)^{\frac{5}{3}}+\left(1-\frac{n_s}{n_t}\right)^{\frac{5}{3}}\right]}_{\approx 1+(2^{\frac{2}{3}}-1)\left(\frac{n_s}{n_t}\right)^2} \tag{E.1}$$

where $n_t \overset{\text{def}}{=} \frac{1}{L^3}\mathcal{N}(\mu) = n_\uparrow + n_\downarrow$ is the **total electron density** (both spin directions)and $n_s = n_\uparrow - n_\downarrow$ is the **spin density** .
The spin dependence of the kinetic energy is shown in Fig. 1.11. The dependence of the spin polarization can fairly well be approximated by a simple parabola.

E.2.1 Gradient correction of the kinetic energy

Von Weizsäcker[110] contributed a gradient correction to the kinetic energy [1]

GRADIENT CORRECTION FOR THE KINETIC ENERGY

The kinetic energy of a homogeneous electron gas can be be improved further by a gradient correction developed by von Weizsäcker.[110]

$$\frac{1}{\Omega}T_W \overset{\text{Eq. } E.16}{=} \frac{\hbar^2}{m}\frac{1}{8}\frac{|\vec{\nabla} n_t|^2}{n_t} \tag{E.3}$$

where Ω is the probe volume and n_t is the total electron density.
As shown below in Eq. E.16, the gradient correction is independent of the spin polarization factor $\zeta = \frac{n_s}{n_t}$, if ζ is a constant. (Siehe auch: `https://en.wikipedia.org/wiki/Thomas-Fermi_model`)

The von Weizsäcker formula for the kinetic energy is important for **orbital-free density-functional theory** . Historically it also played a role to improve on the Thomas-Fermi approximation, which is a predecessor of Density functional theory.

Derivation of v. Weizsäcker

In the following, I reproduce the derivation of Weizsäcker in order generalize the result to spin-polarized electron densities. While I follow the original proof closely in spirit, I hope that I could streamline it a bit.

I start with the density, the density gradient and the kinetic energy density e_{kin}. I only consider a specific spin direction $\sigma \in \{\uparrow, \downarrow\}$. The spin index is omitted until the results for the two spin directions are combined.

$$\begin{aligned}
n(\vec{r}) &= \sum_n f_n \psi_n^*(\vec{r})\psi_n(\vec{r}) \\
\vec{\nabla} n(\vec{r}) &= \sum_n f_n 2\mathrm{Re}\Big(\psi_n^*(\vec{r})\vec{\nabla}\psi_n(\vec{r})\Big) = \sum_n f_n \psi_n^*(\vec{r})\psi_n(\vec{r}) \cdot 2\mathrm{Re}\Big(\frac{\vec{\nabla}\psi_n(\vec{r})}{\psi_n(\vec{r})}\Big) \\
E_{kin} &= \int d^3r\; e_{kin} \quad \text{with} \qquad e_{kin} = \sum_n f_n \frac{\hbar^2}{2m}\left|\vec{\nabla}\psi_n(\vec{r})\right|^2
\end{aligned} \tag{E.4}$$

Note that we used the kinetic energy expression using the product of wave function gradients rather than the expression with the Laplacian. The form used here produces the kinetic energy density locally, while the other form requires the Gauss theorem, which relies on a global property, the boundary conditions.

v. Weizsäcker introduces an amplitute variation[2] in the wave functions of the free electron gas,

[1] Siehe Weizsäcker[110]-Gl.9 für die Energie pro Volumeneinheit (die Weizsäcker mit E_{kin} bezeichnet, wir jedoch mit $\frac{1}{\Omega}E_{kin}$.)

$$\frac{1}{\Omega}E_{kin} = \frac{4\pi(\overbrace{2\pi\hbar}^{h})^2}{5m}\left(\frac{3\rho}{8\pi}\right)^{\frac{5}{3}} + \frac{(\overbrace{2\pi\hbar}^{h})^2}{32\pi^2 m}\frac{|\vec{\nabla}\rho|^2}{\rho} = \frac{\hbar^2}{m}\frac{3}{10}\left(3\pi^2\right)^{\frac{2}{3}}\rho^{\frac{5}{3}} + \underbrace{\frac{\hbar^2}{m}\frac{1}{8}\frac{|\vec{\nabla}\rho|^2}{\rho}}_{\frac{1}{\Omega}T_W} \tag{E.2}$$

[2] The form used by v. Weizsäcker differs slightly from the one used here, namely

$$\psi_n(\vec{r}) = \frac{1}{\sqrt{\Omega}}\Big(1 + \vec{a}_n\vec{r}\Big)\mathrm{e}^{i\vec{k}_n\vec{r}} \tag{E.5}$$

which is governed by a state dependent, real-valued vector $\vec{a}_n$.

$$\psi_n(\vec{r}) = \frac{1}{\sqrt{\Omega}} \mathrm{e}^{(\vec{a}_n + i\vec{k}_n)\vec{r}} \tag{E.6}$$

so that

$$\vec{\nabla}\psi_n(\vec{r}) = (\vec{a}_n + i\vec{k}_n)\psi_n(\vec{r}) \tag{E.7}$$

These wave functions correspond to damped plane waves that fall off exponentially. Note, that these functions are not normalized nor normalizable. For $\vec{a}_n = \vec{0}$, the wave functions of the homogeneous electron gas are recovered.

The kinetic energy density is

$$\begin{aligned} e_{kin} &= \sum_n f_n \frac{\hbar^2}{2m} \left|\vec{\nabla}\psi_n(\vec{r})\right|^2 \overset{\text{Eq. } E.6}{=} \sum_n f_n \frac{\hbar^2}{2m} \psi_n^*(\vec{r})\psi_n(\vec{r}) \left(\vec{a}_n^2 + \vec{k}_n^2\right) \\ &= \underbrace{\sum_n f_n \frac{\hbar^2 \vec{k}_n^2}{2m} \psi_n^*(\vec{r})\psi_n(\vec{r})}_{E_{kin}/\Omega \text{ of the homogenous electron gas}} + \underbrace{\frac{\hbar^2}{2m} \sum_n f_n \psi_n^*(\vec{r})\psi_n(\vec{r}) \cdot \vec{a}_n^2}_{\rightsquigarrow T_W/\Omega} \end{aligned} \tag{E.8}$$

which produces two terms. One term is the the kinetic energy density for $\vec{a} = \vec{0}$, which is the kinetic energy for a homogeneous electron gas. The other will result in the correction T_W of v. Weizsäcker.

The density gradient is related to the vectors $\vec{a}_n$

$$\vec{\nabla} n \overset{\text{Eq. } E.6}{=} \sum_n f_n \psi_n^*(\vec{r})\psi_n(\vec{r}) 2\vec{a}_n \tag{E.9}$$

Now comes an ingenious[3] trick: v. Weizsäcker imposes Eq. E.9 for a specified density gradient as constraint on the values for $\vec{a}_n$. Then he minimizes the kinetic energy under that constraint.

$$\begin{aligned} e_{kin} = \sum_n f_n \frac{\hbar^2 \vec{k}_n^2}{2m} \psi_n^*(\vec{r})\psi_n(\vec{r}) + \min_{\vec{a}_n} \operatorname{stat}_{\lambda} \Bigg\{ & \frac{\hbar^2}{2m} \sum_n f_n \psi_n^*(\vec{r})\psi_n(\vec{r}) \cdot \vec{a}_n^2 \\ & - \frac{\hbar^2}{2m} \vec{\lambda} \Big(\sum_n f_n \psi_n^*(\vec{r})\psi_n(\vec{r}) 2\vec{a}_n - \vec{\nabla} n(\vec{r}) \Big) \Bigg\} \end{aligned} \tag{E.10}$$

The minimum condition for the variation of $\vec{a}_n$ yields

$$\vec{a}_n = \vec{\lambda} \tag{E.11}$$

which implies that the optimum set of vectors a_n is state independent.

The value of λ is determined so that the constraint is satisfied.

$$\vec{\nabla} n \overset{\vec{a}_n = \vec{\lambda}}{=} \underbrace{\sum_n f_n \psi_n^*(\vec{r})\psi_n(\vec{r})}_{n} 2\vec{\lambda} \qquad \Rightarrow \qquad \lambda = \vec{a}_n = \frac{\vec{\nabla} n}{2n} \tag{E.12}$$

Finally, we insert this expression for $\vec{a}_n$ into the expression for the kinetic energy Eq. E.8 obtained

[3] I am not yet sure, whether this is physics or number-magic. Given the local ansatz for the wave function, I have some doubts whether such a variational principle for the local density is justified. It serves the purpose to remove the freedom of choice of the Ansatz.

earlier

$$e_{kin} \overset{\text{Eq. } E.8}{=} \underbrace{\sum_n f_n \frac{\hbar^2 \vec{k}_n^2}{2m} \psi_n^*(\vec{r})\psi_n(\vec{r})}_{E_{kin}/\Omega \text{ of the homogenous electron gas}} + \frac{\hbar^2}{2m} \underbrace{\sum_n f_n \psi_n^*(\vec{r})\psi_n(\vec{r})}_{n} \cdot \underbrace{\left(\frac{\vec{\nabla} n}{2n}\right)^2}_{\vec{a}_n^2}$$

$$= \underbrace{\sum_n f_n \frac{\hbar^2 \vec{k}^2}{2m} \psi_n^*(\vec{r})\psi_n(\vec{r})}_{E_{kin}/\Omega \text{ of the homogenous electron gas}} + \underbrace{\frac{\hbar^2}{8m} \frac{\left(\vec{\nabla} n\right)^2}{n}}_{T_W/\Omega} \tag{E.13}$$

When we include both spin contributions, we obtain for the gradient correction of Weizsäcker

$$T_W = \frac{\hbar^2}{8m} \sum_{\sigma \in \{\uparrow,\downarrow\}} \frac{\left(\vec{\nabla} n_\sigma\right)^2}{n_\sigma} \tag{E.14}$$

For electrons with a fixed spin-polarization factor ζ

$$\zeta \overset{\text{def}}{=} \frac{n_s}{n_t} \qquad \Rightarrow \qquad n_\uparrow = \frac{1+\zeta}{2} n_t \qquad \text{and} \qquad n_\downarrow = \frac{1-\zeta}{2} n_t \tag{E.15}$$

the result depends only on the total density and not on the spin-polarization factor ζ.

$$T_W = \frac{\hbar^2}{8m} \sum_{\sigma \in \{\uparrow,\downarrow\}} \frac{\left(\vec{\nabla} n_\sigma\right)^2}{n_\sigma} = \frac{\hbar^2}{8m} \frac{\left(\vec{\nabla} n_t\right)^2}{n_t} \left(\frac{\left(\frac{1+\zeta}{2}\right)^2}{\frac{1+\zeta}{2}} + \frac{\left(\frac{1-\zeta}{2}\right)^2}{\frac{1-\zeta}{2}} \right) = \frac{\hbar^2}{8m} \frac{\left(\vec{\nabla} n_t\right)^2}{n_t} \tag{E.16}$$

This confirms the gradient correction Eq. E.3 for the kinetic energy.

E.3 Hartree-Fock description of the free-electron gas

Here, we derive the changes in the dispersion relation $\epsilon(\vec{k})$ of the free-electron gas due to the exchange potential discussed in section 2.5.8 on p. 87.

Because of the translation symmetry, we can assume that the charge density is spatially constant.[4] Since the problem is translation invariant, we can furthermore deduce that the eigenstates are plane waves.

E.3.1 Exchange potential as non-local potential

Let us evaluate the non-local exchange potential Eq. 2.41 using plane waves

$$\varphi_{\vec{k},\sigma}(\vec{r},\sigma') = \langle \vec{r},\sigma' | \varphi_{\vec{k},\sigma} \rangle = \frac{1}{\sqrt{\Omega}} \mathrm{e}^{i\vec{k}\vec{r}} \delta_{\sigma,\sigma'} \tag{E.17}$$

as defined in Eq. 1.36 as basis functions.

The exchange potential $\hat{V}_X$ has been expressed in terms of the one-particle-reduced density matrix $\hat{\rho}^{(1)}$ as

$$V_X(\vec{x},\vec{x'}) \overset{\text{Eq. } 2.41}{=} -\sum_{j=1}^{N} \frac{e^2 \rho^{(1)}(\vec{x},\vec{x'})}{4\pi\epsilon_0 |\vec{r} - \vec{r'}|} \tag{E.18}$$

[4] We assume that there is no symmetry breaking.

with the one-particle-reduced density matrix Eq. 2.19

$$\begin{aligned}\rho^{(1)}(\vec{x},\vec{x'}) &\overset{\text{Eq. 2.19}}{=} \sum_{n=1}^{\infty}\langle\vec{x}|\varphi_n\rangle f_n\langle\varphi_n|\vec{x'}\rangle \\ &\overset{\text{Eq. 1.36}}{=} \sum_{\vec{k}}\theta(k_F-|\vec{k}|)\underbrace{\frac{\overbrace{(2\pi)^3}^{1}}{\Omega}}_{\to d^3k}\frac{\Omega}{(2\pi)^3}\frac{\delta_{\sigma,\sigma'}}{\Omega}e^{i\vec{k}(\vec{r'}-\vec{r})} \\ &= \frac{\delta_{\sigma,\sigma'}}{(2\pi)^3}\int d^3k\;\theta(k_F-|\vec{k}|)e^{i\vec{k}(\vec{r'}-\vec{r})} \end{aligned} \tag{E.19}$$

where $\theta(x)$ is the Heaviside step function and k_F is the Fermi momentum. The **Fermi momentum** is defined for a free-electron gas and specifies the maximum wave vector of all occupied states. In other words, it is the radius of the so-called Fermi sphere. The electron density n is obtained as

$$\begin{aligned} n(\vec{r}) = \sum_{\sigma}\rho^{(1)}(\vec{r},\sigma,\vec{r},\sigma) &\overset{\text{Eq. E.19}}{=} \frac{2}{(2\pi)^3}\frac{4\pi}{3}k_F^3 \\ k_F &= 2\pi\sqrt[3]{\frac{1}{2}\frac{3n}{4\pi}} \end{aligned} \tag{E.20}$$

This relation[5] is used to obtain the Fermi momentum from a given electron density.

The integral in Eq. E.19 is isotropic in $\vec{r'}-\vec{r}$. Thus, we can assume, without loss of generality, that the distance vector $\vec{r'}-\vec{r}$ points in z-direction, that is $\vec{r'}-\vec{r}=\vec{e}_z s$ with $s=|\vec{r'}-\vec{r}|$. $\vec{e}_z$ is the unit vector pointing in z-direction.

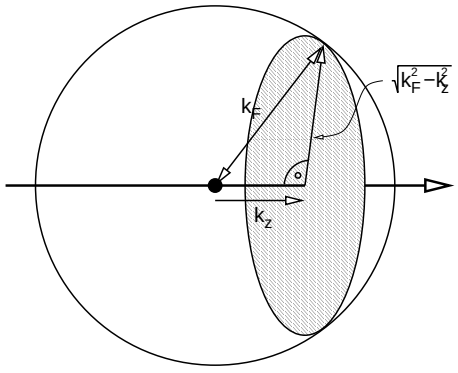

[5] The factor 1/2 stems from the spin degeneracy for a paramagnetic free-electron gas.

Let us resolve the integral without the factors.

$$\begin{aligned}
\int d^3k\ \theta(k_F - |\vec{k}|)\mathrm{e}^{i\vec{k}\vec{e}_z s} &= \int_{\vec{k}\leq k_F} d^3k\ \mathrm{e}^{ik_z s} = \int_{-k_F}^{k_F} dk_z\ \mathrm{e}^{ik_z s} \underbrace{\int_{k_x^2+k_y^2<k_F^2-k_z^2} dk_x dk_y}_{\pi(k_F^2-k_z^2)} \\
&= \int_{-k_F}^{k_F} dk_z\ \pi(k_F^2 - k_z^2)\mathrm{e}^{ik_z s} \\
&= \pi k_F^2 \int_{-k_F}^{k_F} dk_z\ \mathrm{e}^{ik_z s} - \pi \int_{-k_F}^{k_F} dk_z\ k_z^2 \mathrm{e}^{ik_z s} \\
&= \pi k_F^2 \int_{-k_F}^{k_F} dk_z\ \mathrm{e}^{ik_z s} + \pi \frac{d^2}{ds^2} \int_{-k_F}^{k_F} dk_z\ \mathrm{e}^{ik_z s} \\
&= \pi \left[k_F^2 + \frac{d^2}{ds^2}\right] \left[\frac{1}{is}\mathrm{e}^{ik_z s}\right]_{-k_F}^{k_F} \\
&= \pi \left[k_F^2 + \frac{d^2}{ds^2}\right] \frac{\mathrm{e}^{ik_F s} - \mathrm{e}^{-ik_F s}}{is} \\
&= 2\pi k_F^3 \left[1 + \frac{d^2}{d(k_F s)^2}\right] \frac{\sin(k_F s)}{k_F s} \\
&= 2\pi k_F^3 \left[\left(1 + \frac{d^2}{dx^2}\right) \frac{\sin(x)}{x}\right]_{x=k_F s} \\
&= 2\pi k_F^3 \left[\frac{\sin(x)}{x} - \frac{\sin(x)}{x} - \frac{2\cos(x)}{x^2} + \frac{2\sin(x)}{x^3}\right]_{x=k_F s} \\
&= \frac{4\pi}{3} k_F^3 \left[-3\frac{\cos(k_F s)}{(k_F s)^2} + 3\frac{\sin(k_F s)}{(k_F s)^3}\right]
\end{aligned} \tag{E.21}$$

Now we insert the integral Eq. E.21 into the one-particle-reduced density matrix Eq. E.19

$$\begin{aligned}
\rho^{(1)}(\vec{x},\vec{x'}) &\overset{\text{Eq. E.19}}{=} \frac{\delta_{\sigma,\sigma'}}{(2\pi)^3} \int d^3k\ \theta(k_F - |\vec{k}|)\mathrm{e}^{i\vec{k}(\vec{r'}-\vec{r})} \\
&\overset{\text{Eq. E.21}}{=} \frac{\delta_{\sigma,\sigma'}}{(2\pi)^3} \frac{4\pi}{3} k_F^3 \left[-3\frac{\cos(k_F|\vec{r}-\vec{r'}|)}{(k_F|\vec{r}-\vec{r'}|)^2} + 3\frac{\sin(k_F|\vec{r}-\vec{r'}|)}{(k_F|\vec{r}-\vec{r'}|)^3}\right]
\end{aligned} \tag{E.22}$$

Finally, I insert the one-particle-reduced density matrix Eq. E.22 into the expression for the non-local potential. With $s \overset{\text{def}}{=} |\vec{r}-\vec{r'}|$, we obtain

$$\begin{aligned}
V_X(\vec{x},\vec{x'}) &\overset{Eqs.\ E.18, E.22}{=} \frac{-e^2\delta_{\sigma,\sigma'}}{4\pi\epsilon_0|\vec{r}-\vec{r'}|} \frac{1}{(2\pi)^3} \underbrace{4\pi k_F^3 \left[-\frac{\cos(k_F s)}{(k_F s)^2} + \frac{\sin(k_F s)}{(k_F s)^3}\right]}_{\int d^3k\ \theta(k_F-|\vec{k}|)\mathrm{e}^{i\vec{k}(\vec{r'}-\vec{r})}} \\
&= \frac{e^2\delta_{\sigma,\sigma'}}{4\pi\epsilon_0 s} \frac{1}{(2\pi)^3} \frac{4\pi}{3} k_F^3 \left[3\frac{(k_F s)\cos(k_F s) - \sin(k_F s)}{(k_F s)^3}\right]
\end{aligned} \tag{E.23}$$

The exchange potential acts only between electrons of the same spin. It is important to realize that this non-local potential is not an interaction potential between two electrons, but it is a one-particle potential acting on each electron individually.

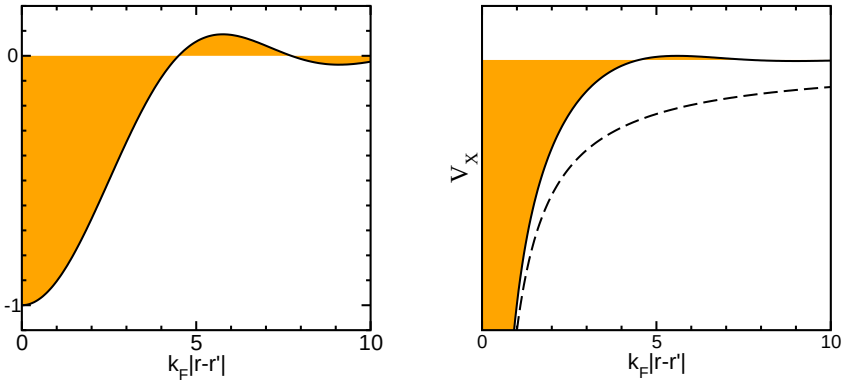

Fig. E.2: Non-local exchange potential $V_X(\vec{r},\sigma,\vec{r'},\sigma)$ Eq. E.23 as function of distance (right) for a free-electron gas as calculated in the Hartree-Fock method. The horizontal axis is $k_F|\vec{r}-\vec{r'}|$. The dashed line corresponds to a Coulomb interaction. On the left-hand side, the function $3\frac{x\cos(x)-\sin(x)}{x^3}$ is shown.

E.3.2 Exchange energy of the homogeneous electron gas

The exchange energy of the nonmagnetic homogeneous electron gas is obtained as

$$
\begin{aligned}
E_X^P &= -\frac{1}{2}\int d^4x \int d^4x' \, \frac{e^2\rho(\vec{x},\vec{x'})\rho(\vec{x'},\vec{x})}{4\pi\epsilon_0|\vec{r}-\vec{r'}|} \\
&\overset{\text{Eq. E.22}}{=} -\frac{1}{2}\int d^4x \int d^4x' \, \frac{e^2}{4\pi\epsilon_0|\vec{r}-\vec{r'}|}\left\{\frac{\delta_{\sigma,\sigma'}}{(2\pi)^3}\frac{4\pi}{3}k_F^3\left[-3\frac{\cos(k_F|\vec{r}-\vec{r'}|)}{(k_F|\vec{r}-\vec{r'}|)^2}+3\frac{\sin(k_F|\vec{r}-\vec{r'}|)}{(k_F|\vec{r}-\vec{r'}|)^3}\right]\right\}^2 \\
&= -\frac{1}{2}\int d^3r \sum_\sigma 4\pi\int_0^\infty ds\, s^2 \frac{e^2}{4\pi\epsilon_0 s}\left\{\frac{1}{(2\pi)^3}\frac{4\pi}{3}k_F^3\left[-3\frac{\cos(k_Fs)}{(k_Fs)^2}+3\frac{\sin(k_Fs)}{(k_Fs)^3}\right]\right\}^2 \\
&= -\frac{1}{2}\int d^3r \sum_\sigma \frac{e^2}{4\pi\epsilon_0}\frac{4\pi}{k_F^2}\left\{\frac{1}{(2\pi)^3}\frac{4\pi}{3}k_F^3\right\}^2\int_0^\infty d(k_Fs)\,(k_Fs)^2\frac{1}{k_Fs}\left\{\left[-3\frac{\cos(k_Fs)}{(k_Fs)^2}+3\frac{\sin(k_Fs)}{(k_Fs)^3}\right]\right\}^2 \\
&= -\frac{1}{2}\int d^3r \sum_\sigma \frac{e^2}{4\pi\epsilon_0}\underbrace{\frac{9\cdot 4\pi}{k_F^2}}_{\frac{9\cdot4\pi}{(3\pi^2 n_t)^{\frac{2}{3}}}}\underbrace{\left\{\frac{1}{(2\pi)^3}\frac{4\pi}{3}k_F^3\right\}^2}_{(\frac{1}{2}n_t)^2\quad\text{Eq. E.20}}\underbrace{\int_0^\infty dx\,\frac{\left(\sin(x)-x\cos(x)\right)^2}{x^5}}_{\frac{1}{4}} \\
&= -\left(\frac{1}{2}\sum_{\sigma\in\{\uparrow,\downarrow\}}\right)\frac{e^2}{4\pi\epsilon_0}\frac{9\cdot4\pi\frac{1}{4}\frac{1}{4}}{(3\pi^2)^{\frac{2}{3}}}\int d^3r\, n_t^{\frac{4}{3}} = -\left(\frac{1}{2}\sum_{\sigma\in\{\uparrow,\downarrow\}}\right)\frac{e^2}{4\pi\epsilon_0}\frac{3}{4}\left(\frac{3^3\pi^3}{3^2\pi^4}\right)^{\frac{1}{3}}\int d^3r\, n_t^{\frac{4}{3}} \\
&= -\underbrace{\left(\frac{1}{2}\sum_{\sigma\in\{\uparrow,\downarrow\}}\right)}_{=1}\underbrace{\frac{e^2}{4\pi\epsilon_0}}_{1H}\frac{3}{4}\left(\frac{3}{\pi}\right)^{\frac{1}{3}}\int d^3r\, n_t^{\frac{4}{3}} \qquad \text{(E.24)}
\end{aligned}
$$

The integral over $x = k_F s$ is solved in the footnote.[6]

The spin polarization dependence can be included when we exploit that the exchange consists of two independent spin contributions.

$$\begin{aligned} E_X(n_\uparrow, n_\downarrow) &= \frac{1}{2} \sum_{\sigma \in \{\uparrow,\downarrow\}} E_X^P(2n_\sigma) \\ &= -\frac{3}{4}\left(\frac{3}{\pi}\right)^{\frac{1}{3}} \underbrace{\frac{e^2}{4\pi\epsilon_0}}_{1H} \int d^3r \, \frac{(2n_\uparrow)^{\frac{4}{3}} + (2n_\downarrow)^{\frac{4}{3}}}{2} \\ &= -\frac{3}{4}\left(\frac{3}{\pi}\right)^{\frac{1}{3}} \underbrace{\frac{e^2}{4\pi\epsilon_0}}_{1H} \int d^3r \, n_t^{\frac{4}{3}} \frac{(1+\zeta)^{\frac{4}{3}} + (1-\zeta)^{\frac{4}{3}}}{2} \qquad \text{with } n_t = n_\uparrow + n_\downarrow \text{ and } \zeta = \frac{n_\uparrow - n_\downarrow}{n_t} \end{aligned} \tag{E.27}$$

E.3.3 Energy-level shifts by the exchange potential

In order to obtain the change of the band structure by the interaction, we need to evaluate the expectation values of this potential.

$$\begin{aligned} d\epsilon_n &= \langle \varphi_n | \hat{V}_X | \varphi \rangle = \int d^4x \int d^4x' \, \varphi_n^*(\vec{x}) V_X(\vec{x}, \vec{x'}) \varphi(\vec{x'}) \\ d\epsilon_{\vec{k},\sigma} &\overset{\text{Eq. E.17}}{=} \frac{1}{\Omega} \int d^3r \int d^3r' \, V_X(\vec{r}, \sigma, \vec{r'}, \sigma) e^{i\vec{k}(\vec{r}-\vec{r'})} \\ &= \int d^3s \, V_X(s) e^{i\vec{k}\vec{s}} \end{aligned} \tag{E.28}$$

whee I introduced the short-hand notation $V_X(s)$ for Eq. E.23, which makes evident that the exchange potential of the free-electron gas depends only on the distance between the two electron coordinates (and the relative spin orientation).

Now, we decompose the plane wave into spherical harmonics(see appendix "Distributionen, d-

[6] Solve the integral

$$\begin{aligned} \int_a^b dx \, \frac{[\sin(x) - x\cos(x)]^2}{x^5} &= \int_a^b dx \left(\frac{\sin^2(x)}{x^5} - 2\frac{\sin(x)\cos(x)}{x^4} + \frac{\cos^2(x)}{x^3} \right) \\ &= \frac{1}{2} \int_a^b d(2x) \left(2^5 \frac{\frac{1}{2}(1-\cos^2(2x))}{(2x)^5} - 2^5 \frac{\frac{1}{2}\sin(2x)}{(2x)^4} + 2^3 \frac{\frac{1}{2}(1+\cos(2x))}{(2x)^3} \right) \\ &= 2 \int_{2a}^{2b} dy \left(4\frac{1-\cos(y)}{y^5} - 4\frac{\sin(y)}{y^4} + \frac{1+\cos(y)}{y^3} \right) \\ &= 2 \left[-\frac{1}{x^4} - \frac{1}{2x^2} + \frac{\cos(x)}{x^4} + \frac{\sin(x)}{x^3} \right]_{2a}^{2b} \\ \int_0^\infty dx \, \frac{[\sin(x) - x\cos(x)]^2}{x^5} &= \frac{1}{4} \end{aligned} \tag{E.25}$$

Let me now use

$$\begin{aligned} \partial_x x^{-4}\cos(x) &= -4x^{-5}\cos(x) - x^{-4}\sin(x) \\ \partial_x x^{-3}\sin(x) &= -3x^{-4}\sin(x) + x^{-3}\cos(x) \\ \partial_x \left(-\frac{\cos(x)}{x^4} - \frac{\sin(x)}{x^3} \right) &= 4\frac{\cos(x)}{x^5} + \frac{\sin(x)}{x^4} + 3\frac{\sin(x)}{x^4} - \frac{\cos(x)}{x^4} \\ \left. \frac{\cos(x)}{x^4} + \frac{\sin(x)}{x^3} \right|_{2a}^{2b} &= \int_{2a}^{2b} dx \left(-4\frac{\cos(x)}{x^5} - 4\frac{\sin(x)}{x^4} + \frac{\cos(x)}{x^4} \right) \end{aligned} \tag{E.26}$$

Funktionen und Fourier transformationen in the text book of Messiah[111])

$$e^{i\vec{k}\vec{r}} = 4\pi \sum_{\ell=1}^{\infty} \sum_{m=-\ell}^{\ell} i^{\ell} j_{\ell}(|\vec{k}||\vec{r}|) Y^*_{\ell,m}(\vec{k}) Y^*_{\ell,m}(\vec{r}) \tag{E.29}$$

Insertion yields

$$\begin{aligned} d\epsilon_{\vec{k},\sigma} &= \int d^3s\, V_x(s) 4\pi \sum_{\ell=1}^{\infty} \sum_{m=-\ell}^{\ell} i^{\ell} j_{\ell}(|\vec{k}||\vec{s}|) Y^*_{\ell,m}(\vec{k}) Y^*_{\ell,m}(\vec{s}) \\ &= 4\pi \sum_{\ell=1}^{\infty} \sum_{m=-\ell}^{\ell} i^{\ell} Y^*_{\ell,m}(\vec{k}) \int d^3s\, V_x(s) j_{\ell}(|\vec{k}||\vec{s}|) Y^*_{\ell,m}(\vec{s}) \end{aligned} \tag{E.30}$$

Because the non-local potential is isotropic, only the term with $\ell = 0$ contributes.

$$\begin{aligned} d\epsilon_{\vec{k},\sigma} &= 4\pi \underbrace{Y^*_{0,0}(\vec{k})}_{\frac{1}{\sqrt{4\pi}}} \int d^3s\, V_x(s) \underbrace{j_0(|\vec{k}||\vec{s}|)}_{j_0(x)=\frac{\sin(x)}{x}} \underbrace{Y^*_{0,0}(\vec{s})}_{\frac{1}{\sqrt{4\pi}}} \\ &= \int d^3s\, V_x(s) \frac{\sin(|\vec{k}||\vec{s}|)}{|\vec{k}||\vec{s}|} \\ &\overset{s \overset{\text{def}}{=} |\vec{s}|}{=} 4\pi \int_0^{\infty} ds\, s^2 V_x(s) \frac{\sin(|\vec{k}|s)}{|\vec{k}|s} \\ &= \frac{4\pi}{|\vec{k}|} \int_0^{\infty} ds\, V_X(s) s \sin(|\vec{k}|s) \\ &\overset{\text{Eq. } E.23}{=} \frac{4\pi}{|\vec{k}|} \int_0^{\infty} ds\, \frac{e^2}{4\pi\epsilon_0 s} \frac{1}{(2\pi)^3} \frac{4\pi}{3} k_F^3 \left[3\frac{k_F s \cos(k_F s) - \sin(k_F s)}{(k_F s)^3} \right] s\, \sin(|\vec{k}|s) \\ &= \frac{4\pi}{|\vec{k}|} \frac{e^2}{4\pi\epsilon_0} \frac{1}{(2\pi)^3} \frac{4\pi}{3} k_F^3 \int_0^{\infty} ds\, \left[3\frac{k_F s \cos(k_F s) - \sin(k_F s)}{(k_F s)^3} \right] \sin(|\vec{k}|s) \\ &\overset{x \overset{\text{def}}{=} k_F s}{=} \frac{4\pi}{k_F |\vec{k}|} \frac{e^2}{4\pi\epsilon_0} \frac{1}{(2\pi)^3} \frac{4\pi}{3} k_F^3 \int_0^{\infty} dx\, \left[3\frac{x\cos(x) - \sin(x)}{x^3} \right] \sin\left(\frac{|\vec{k}|}{k_F} x \right) \end{aligned} \tag{E.31}$$

Now we need to solve the integral

$$I = \int_0^{\infty} dx\, \left[3\frac{x\cos(x) - \sin(x)}{x^3} \right] \sin(ax) \tag{E.32}$$

where $a = |\vec{k}|/k_F$. The difficulty with this integral is that we cannot take the two terms apart, because the individual parts of the integrand diverge at the origin. Thus, during the derivation, we have to deal with divergent expressions.

$$\partial_x \frac{\sin(x)}{x^{n-1}} = -(n-1)\frac{\sin(x)}{x^n} + \frac{\cos(x)}{x^{n-1}}$$
$$\Rightarrow \frac{\sin(x)}{x^n} = \frac{1}{(n-1)}\left[\frac{\cos(x)}{x^{n-1}} - \partial_x \frac{\sin(x)}{x^{n-1}}\right] \tag{E.33}$$

$$\overset{\text{Eq. } E.33}{\Rightarrow} \int_0^\infty dx \frac{\sin(x)}{x^3}\sin(ax) = \frac{1}{2}\int_0^\infty dx\ \frac{\cos(x)}{x^2}\sin(ax) - \frac{1}{2}\int_0^\infty dx\ \sin(ax)\partial_x\frac{\sin(x)}{x^2}$$
$$= \frac{1}{2}\int_0^\infty dx \frac{\cos(x)}{x^2}\sin(ax)$$
$$-\frac{1}{2}\left[\sin(ax)\frac{\sin(x)}{x^2}\right]_0^\infty + \frac{a}{2}\int_0^\infty dx\ \frac{\sin(x)}{x^2}\cos(ax)$$
$$= \frac{a}{2} + \frac{1}{2}\int_0^\infty dx \frac{\cos(x)\sin(ax) + a\sin(x)\cos(ax)}{x^2} \tag{E.34}$$

$$\overset{\text{Eq. } E.33}{\Rightarrow} \int_0^\infty dx \frac{\sin(x)}{x^2}\cos(ax) = \int_0^\infty dx\ \frac{\cos(x)}{x}\cos(ax) - \int_0^\infty dx\ \cos(ax)\partial_x\frac{\sin(x)}{x}$$
$$= \int_0^\infty dx \frac{\cos(x)}{x}\cos(ax)$$
$$-\left[\cos(ax)\frac{\sin(x)}{x}\right]_0^\infty - a\int_0^\infty dx\ \frac{\sin(x)}{x}\sin(ax)$$
$$= 1 + \int_0^\infty dx \frac{\cos(x)\cos(ax) - a\sin(x)\sin(ax)}{x} \tag{E.35}$$

Thus, we obtain

$$\begin{aligned}
I &= 3\int_0^\infty dx\ \frac{x\cos(x) - \sin(x)}{x^3}\sin(ax) \\
&= 3\int_0^\infty dx\ \frac{\cos(x)\sin(ax)}{x^2} - 3\int_0^\infty dx\ \frac{\sin(x)\sin(ax)}{x^3} \\
&\overset{\text{Eq. } E.34}{=} 3\int_0^\infty dx\ \frac{\cos(x)\sin(ax)}{x^2} - \frac{3a}{2} - \frac{3}{2}\int_0^\infty dx\ \frac{\cos(x)\sin(ax) + a\sin(x)\cos(ax)}{x^2} \\
&= -\frac{3a}{2} + \frac{3}{2}\int_0^\infty dx\ \frac{\cos(x)\sin(ax)}{x^2} - \frac{3a}{2}\int_0^\infty dx\ \frac{\sin(x)\cos(ax)}{x^2} \\
&= -\frac{3a}{2} + \frac{3a}{2}\int_0^\infty dy\ \frac{\cos(\frac{1}{a}y)\sin(y)}{y^2} - \frac{3a}{2}\int_0^\infty dx\ \frac{\sin(x)\cos(ax)}{x^2} \\
&\overset{\text{Eq. } E.35}{=} -\frac{3a}{2} + \frac{3a}{2}\left[1 + \int_0^\infty dy\ \frac{\cos(\frac{1}{a}y)\cos(y) - \frac{1}{a}\sin(\frac{1}{a}y)\sin(y)}{y}\right] \\
&\quad -\frac{3a}{2}\left[1 + \int_0^\infty dx\ \frac{\cos(ax)\cos(x) - a\sin(ax)\sin(x)}{x}\right] \\
&= -\frac{3a}{2} + \frac{3a}{2}\left[\int_0^\infty dx\ \frac{\cos(x)\cos(ax) - \frac{1}{a}\sin(x)\sin(ax)}{x}\right] \\
&\quad -\frac{3a}{2}\left[\int_0^\infty dx\ \frac{\cos(ax)\cos(x) - a\sin(ax)\sin(x)}{x}\right] \\
&= -\frac{3a}{2} + \frac{3a}{2}(-\frac{1}{a} + a)\left[\int_0^\infty dx\ \frac{\sin(x)\sin(ax)}{x}\right] \\
&= -\frac{3a}{2} + \frac{3}{2}(a^2 - 1)\left[\int_0^\infty dx\ \frac{\sin(x)\sin(ax)}{x}\right]
\end{aligned}$$

We recognize that the integral is the Fourier transform of $\frac{\sin(x)}{x}$. From the Fourier transform tables

of Bronstein[63] we take

$$\sqrt{\frac{2}{\pi}}\int_0^\infty dx\ \sin(xy)\frac{\sin(ax)}{x} \overset{Bronstein}{=} \frac{1}{\sqrt{2\pi}}\ln\left|\frac{y+a}{y-a}\right|$$
$$\overset{a\to 1; y\to a}{\Rightarrow} \int_0^\infty dx\ \sin(ax)\frac{\sin(x)}{x} = \frac{1}{2}\ln\left|\frac{a+1}{a-1}\right| = \frac{1}{2}\ln\left|\frac{1+a}{1-a}\right|$$

Thus, we obtain

$$I = -\frac{3a}{2} + \frac{3}{4}(a^2-1)\ln\left|\frac{1+a}{1-a}\right|$$

with $a = |\vec{k}|/k_F$ as defined below Eq. E.32. We are done with the Integral.

We insert the result into the correction for the energy eigenvalues Eq. E.31

$$\begin{aligned} d\epsilon_{\vec{k},\sigma} &\overset{\text{Eq. } E.31}{=} \frac{4\pi}{k_F|\vec{k}|}\frac{e^2}{4\pi\epsilon_0}\frac{1}{(2\pi)^3}\frac{4\pi}{3}k_F^3\left[-\frac{3a}{2}+\frac{3(a^2-1)}{4}\ln\left|\frac{a+1}{a-1}\right|\right] \\ &= \frac{4\pi}{k_F^2}\frac{e^2}{4\pi\epsilon_0}\frac{1}{(2\pi)^3}\frac{4\pi}{3}k_F^3\left[-\frac{3}{2}+\frac{3(a^2-1)}{4a}\ln\left|\frac{a+1}{a-1}\right|\right] \\ &= -\frac{e^2}{4\pi\epsilon_0}\frac{2k_F}{\pi}\left[\frac{1}{2}+\frac{1-a^2}{4a}\ln\left|\frac{1+a}{1-a}\right|\right] \end{aligned} \tag{E.36}$$

The function in parenthesis is shown in Fig. E.3 and the resulting dispersion relation is discussed in section 2.5.8 on p. 87.

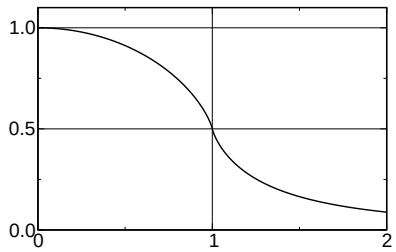

Fig. E.3: Lindhard function $f(a) = \left(\frac{1}{2} + \frac{1-a^2}{4a}\ln\left|\frac{1+a}{1-a}\right|\right)$ as function of $a = k/k_F$. The slope for $k = k_F$ is infinite. For $k \gg k_F$ the function approaches zero.

E.3.4 Density of states of the free-electron gas

The one-particle density of states of a non-interacting electrons has several physical meanings, which need to be differentiated when dealing with interacting electrons.

- The density of states is closely related to the thermodynamic properties of the system. Thus, the density of states can be obtained as the derivative of the number of electrons with respect to the Fermi level at zero temperature.

$$D(\epsilon) = \left.\frac{dN}{d\mu}\right|_{\mu=\epsilon} \tag{E.37}$$

- The density of states summarizes the optical excitation spectrum. (It does not reflect matrix elements, though.) Thus, it reflects the **spectral function**.

The two definitions are different and need not produce the same result. Thus, we need to be careful when discussing the spectrum of the Hartree-Fock method or interacting systems in general.

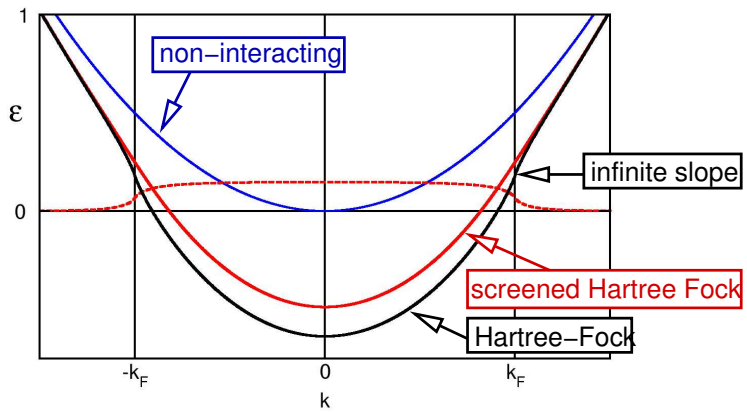

Fig. E.4: Dispersion relation $\epsilon(k)$ of the free-electron gas as calculated with Hartree-Fock (black), screened Hartree-Fock (red) and and without interactions (blue). The Fermi momentum has been chosen as $k_F = 1/a_0$ and the screening length for the screened Hartree-Fock calculation has been 6 a_0, where a_0 is the Bohr radius. The red, dashed line is the difference between the bands obtained with screened and unscreened Hartree-Fock. Only the bands of unscreened Hartree-Fock exhibit an infinite slope at the Fermi level. The Fermi level is at $\epsilon(k_F)$.

Density of states of the free-electron gas from the energy levels of the Hartree-Fock approximation

In this section, I describe how the density of states for the Hartree-Fock spectrum in Fig. E.5 on p. 458 has been evaluated.

Let me extract the density of states from the dispersion relation obtained from the Hartree-Fock approximation.

$$\epsilon_{\vec{k},\sigma} \overset{\text{Eq. ??}}{=} \frac{\hbar^2\vec{k}^2}{2m_e} - \frac{e^2}{4\pi\epsilon_0}\frac{2k_F}{\pi}\left[\frac{1}{2} + \frac{1-a^2}{4a}\ln\left|\frac{1+a}{1-a}\right|\right] \tag{E.38}$$

with $a = |\vec{k}|/k_F$ as defined below Eq. E.32

The number of states in a volume Ω for a given Fermi level μ at zero temperature is

$$N(\mu) = \Omega\int\frac{d^3k}{(2\pi)^3}\theta\big(\mu - \epsilon(\vec{k})\big) \tag{E.39}$$

The density of states is its derivative with respect to the Fermi level.

$$D(\epsilon) = \frac{dN(\epsilon)}{d\epsilon} \tag{E.40}$$

For the dispersion relation of the free-electron gas in the Hartree-Fock approximation, we obtain

$$N(\epsilon(k_F)) = \sum_{\sigma\in\uparrow,\downarrow}\frac{\frac{4\pi}{3}k_F^3}{(\frac{2\pi}{L})^3} = \Omega\sum_{\sigma\in\uparrow,\downarrow}\frac{k_F^3}{6\pi^2} \tag{E.41}$$

When doing the derivative we need to distinguish $k \overset{\text{def}}{=} |\vec{k}|$ and k_F. The band structure $\epsilon(k)$ depends on the Fermi momentum k_F. This is considered as a fixed parameter. The derivative is

taken not with respect to k_F but with respect to k, which plays the role of the Fermi wave vector albeit in a rigid band structure.

Thus,

$$\begin{aligned} D(\epsilon(k)) &= \Omega \sum_{\sigma\in\uparrow,\downarrow} \frac{k^2}{2\pi^2} \left(\frac{d\epsilon}{dk}\right)^{-1} \\ &= \Omega \sum_{\sigma\in\uparrow,\downarrow} \frac{k^2}{2\pi^2} \left(\frac{\hbar^2\vec{k}}{m_e} - \frac{e^2}{4\pi\epsilon_0}\frac{2k_F}{\pi}\Big[\frac{-2a}{4a}\ln\left|\frac{1+a}{1-a}\right| - \frac{1-a^2}{4a^2}\ln\left|\frac{1+a}{1-a}\right| \right. \\ &\quad \left. + \frac{1-a^2}{4a}\left(\frac{1+a}{1-a}\right)^{-1}\Big(\frac{1}{1-a} + \frac{1+a}{(1-a)^2}\Big)\Big]\frac{1}{k_F}\right)^{-1} \\ &= \Omega \sum_{\sigma\in\uparrow,\downarrow} \frac{k^2}{2\pi^2} \left(\frac{\hbar^2\vec{k}}{m_e} - \frac{e^2}{4\pi\epsilon_0}\frac{2}{\pi}\Big[-\frac{1+a^2}{4a^2}\ln\left|\frac{1+a}{1-a}\right| + \frac{1}{2a}\Big]\right)^{-1} \end{aligned} \tag{E.42}$$

The density of states here is given as function of the wave vector. By plotting the energy as function of wave vector versus the density of state as function of wave vector, the density of states as function of energy is obtained.

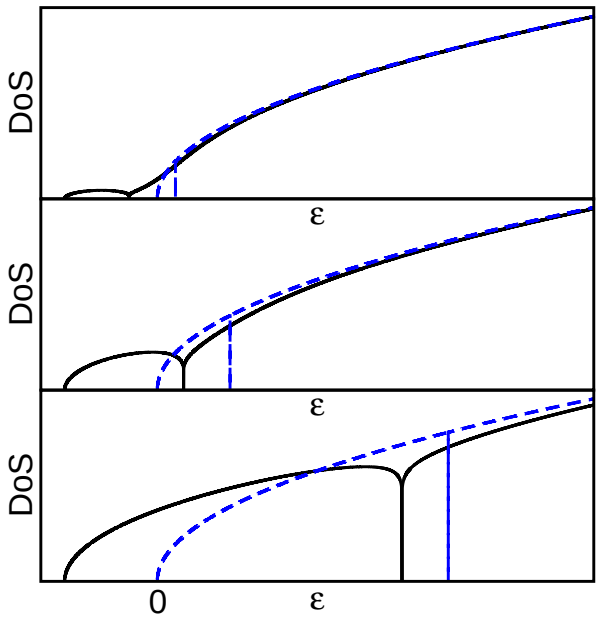

Fig. E.5: Density of states in the Hartree-Fock approximation (solid black) as compared to the free-electron gas (dashed blue) for different electron densities. The density of states is obtained from the energy dispersion of the Fock operator, and not from the thermodynamic properties, i.e. the total energies. The electron density increases from top to bottom. The density of states for the Hartree-Fock calculation drops to zero at the Fermi level. The energy of the bottom of the band is independent of the electron density and depends only on the strength of the interaction.

We observe that the density of states of the free-electron gas vanishes at the Fermi level, i.e.

for $a = 1$ due to the singularity of the logarithm. This behavior is nonphysical and it is healed by including electron correlation.

E.3.5 Exchange hole of the free-electron gas

The exchange hole can be expressed by the one-particle-reduced density matrix. The two-particle density can be extracted from the expression for the interaction energy of a Slater determinant.

$$n^{(2)}(\vec{r},\vec{r}') = n(\vec{r})n(\vec{r}') - \sum_{\sigma,\sigma'} \rho^{(1)}(\vec{x},\vec{x}')\rho^{(1)}(\vec{x}',\vec{x}) \tag{E.43}$$

$$\begin{aligned} h(\vec{r},\vec{r}') &= \frac{n^{(2)}(\vec{r},\vec{r}') - n^{(1)}(\vec{r})n^{(1)}(\vec{r}')}{n^{(1)}(\vec{r})} \\ &= -\frac{\sum_{\sigma,\sigma'} \left|\rho^{(1)}(\vec{r},\sigma,\vec{r}',\sigma')\right|^2}{\sum_{\sigma''} \rho^{(1)}(\vec{r},\sigma,\vec{r},\sigma'')} \\ &= \frac{1}{(2\pi)^3}\frac{4\pi}{3}k_F^3 \left(-3\frac{\cos(k_F|\vec{r}-\vec{r}'|)}{(k_F|\vec{r}-\vec{r}'|)^2} + 3\frac{\sin(k_F|\vec{r}-\vec{r}'|)}{(k_F|\vec{r}-\vec{r}'|)^3}\right)^2 \end{aligned} \tag{E.44}$$

Because of the Coulomb singularity, the behavior of the exchange hole at the origin is important. To explore the behavior at the origin, I use the Taylor expansion

$$\begin{aligned} -3\frac{\cos(x)}{x^2} + 3\frac{\sin(x)}{x^3} &= -6\sum_{k=1}^{\infty}\frac{(-1)^k\cdot k}{(2k+1)!}x^{2k-2} \\ &= 1 - \frac{1}{10}x^2 + \frac{1}{280}x^4 + O(x^6) \end{aligned} \tag{E.45}$$

To approximate exchange-correlation hole, one could consider a Gaussian

$$h(\vec{r},\vec{r}') \approx \frac{1}{(2\pi)^3}\frac{4\pi}{3}k_F^3 \exp\left(-\frac{1}{5}\left(k_F|\vec{r}-\vec{r}'|\right)^2\right) \tag{E.46}$$

The approximate form reproduces the Taylor expansion near $\vec{r} = \vec{r}'$ up to third order in the distance, and it has a reasonable overall agreement.

As expected, the on-top value of the exchange hole is exactly one-half the electron density. The radius of the exchange hole is proportional to k_F, respectively $n^{\frac{1}{3}}$.

E.4 Polarization insertion

Editor: This section is under construction. Do not read!

In this section, I am evaluating the polarization insertion of the homogeneous electron gas in lowest order. A **polarization insertion** is a diagram with two external vertices that can be inserted into an interaction line. Specifically, I am limiting myself the most simple and therefore prototypical polarization integral, the **ring diagram**.

The polarization is at the origin of **screening** and of **life-time broadening**. It will provide an approximate expression for the momentum and frequency dependent dielectric constant. Furthermore, it underpins **Fermi-liquid theory** by demonstrating that the lifetime broadening near the Fermi level is smaller than the quasi-particle energy $\epsilon - \mu$. Furthermore the polarization insertion is the starting point for **plasmons**.

A derivation of the polarization insertion can be found in the textbook of Fetter and Walecka on p. 158, "Evaluation of Π^0".Editor: See also Caruso et al.[46].

I redid the derivation myself in a slightly different manner and with a lot of detail in order to make the underlying principles evident and to understand, if and how the result can be carried beyond the free electron gas. Most importantly, I had to ensure that the result is compatible with a contour in the complex-time plane of the non-equilibrium Greens function. I will start from the fairly general expressions and I will become increasingly more specific as seems reasonable to keep the calculation managable. The reason is twofold. Once, the implications of the individual approximations shall become clear. Secondly, the more general equations may provide a suitable starting point for the implementation as computer code to obtain results for real materials.

The lowest order of the polarization insertion is the ring diagram, which is a product of two non-interacting Green's functions.

$$\Pi^{(0)}(\vec{r}_1,t_1,\vec{r}_2,t_2) \stackrel{\text{def}}{=} i\hbar \underbrace{(-1)}_{\text{Fermi loop}} \sum_{\sigma_1,\sigma_2\in\{\uparrow,\downarrow\}} G^{\mathcal{C},(0)}(\vec{x}_1,t_1,\vec{x}_2,t_2)G^{\mathcal{C},(0)}(\vec{x}_2,t_2,\vec{x}_1,t_1) \tag{E.47}$$

After considering the different normalization definitions.[7], this equation is equivalent to Eq.12.27 of Fetter-Walecka, The reason to connect the polarization insertion to two positions, rather than four orbitals, is that the interaction connects two, rather than four positions. Because the interaction is spin-independent, we perform the sum over the sum over spin degrees of freedom already inside the polarization insertion.

E.4.1 Polarisation insertion for homogeneous systems

The derivation is limited to the homogeneous systems with plane waves as Hamilton eigenstates

$$\langle \vec{r},\sigma'|\vec{k},\sigma\rangle = \frac{1}{\sqrt{L^3}} e^{i\vec{k}\vec{r}}\delta_{\sigma,\sigma'} \tag{E.48}$$

I am considering a normalization volume L^3 and periodic boundary conditions for a cubic box with side-length L. This results in a discrete grid of k-points with spacing $\frac{2\pi}{L}$.

Initially, I do not limit the band structure $\epsilon_{\vec{k},\sigma}$ to the free-electron parabola.

The derivation is based on the contour Green's function for a time-independent Hamiltonian. The zeroth-order polarization diagram, requires only the non-interacting Green's function as input. The bare contour Green's function is given in Eq. 7.53 on p. 252, respectively from Eq. 7.28 on p. 247.

$$\hat{G}^{\mathcal{C},(0)}(t,t') \stackrel{\text{Eq. 7.53}}{=} \frac{1}{i\hbar}\sum_{\vec{k}}\sum_{\sigma\in\{\uparrow,\downarrow\}} |\vec{k},\sigma\rangle\Big\{\theta_{\mathcal{C}}(t-t')\Big(1-f_{T,\mu}(\epsilon_{\vec{k},\sigma})\Big)-\theta_{\mathcal{C}}(t'-t)f_{T,\mu}(\epsilon_{\vec{k},\sigma})\Big\} \times e^{-\frac{i}{\hbar}\epsilon_{\vec{k},\sigma}(t-t')}\langle\vec{k},\sigma| \tag{E.49}$$

In position-and-spin representation this is

$$\stackrel{\text{Eq. E.48}}{\Rightarrow} G^{\mathcal{C},(0)}(\vec{x}_1,t_1,\vec{x}_2,t_2) = \frac{1}{i\hbar L^3}\sum_{\vec{k}}\sum_{\sigma\in\{\uparrow,\downarrow\}} \delta_{\sigma_1,\sigma}\delta_{\sigma_2,\sigma} e^{i\vec{k}(\vec{r}_1-\vec{r}_2)} e^{-\frac{i}{\hbar}\epsilon_{\vec{k},\sigma}(t_1-t_2)} \times\Big\{\theta_{\mathcal{C}}(t_1-t_2)\Big(1-f_{T,\mu}(\epsilon_{\vec{k},\sigma_1})\Big)-\theta_{\mathcal{C}}(t_2-t_1)f_{T,\mu}(\epsilon_{\vec{k},\sigma})\Big\} \tag{E.50}$$

[7] The polarization insertion has been defined in FW-Eq.-9.39, where FW stands for the textbook of Fetter and Walecka.[3]. Eq. E.47 compares to FW-Eq. 12.27.[3]. The convention for the Green's function is obtained by the comparison in FW-Eq. 7.1, i.e. $G^{\Phi SX} = \frac{1}{\hbar}G^{FW}$. The factor 2 in the FW-Eq. 12.27 is absorbed in the sum over spin orbitals of our Eq. E.47

The corresponding zeroth order polarization insertion Eq. E.47 is

$$
\begin{aligned}
\Pi^{(0)}(\vec{r}_1,t_1,\vec{r}_2,t_2) &\overset{\text{Eq. E.47}}{=} i\hbar \underbrace{(-1)}_{\text{Fermi loop}} \sum_{\sigma_1,\sigma_2\in\{\uparrow,\downarrow\}} G^{\mathcal{C},(0)}(\vec{x}_1,t_1,\vec{x}_2,t_2)G^{\mathcal{C},(0)}(\vec{x}_2,t_2,\vec{x}_1,t_1) \\
&\overset{\text{Eq. E.50}}{=} i\hbar \underbrace{(-1)}_{\text{Fermi loop}} \sum_{\sigma_1,\sigma_2\in\{\uparrow,\downarrow\}} \\
&\times \underbrace{\frac{1}{i\hbar L^3}\sum_{\vec{k}}\sum_{\sigma\in\{\uparrow,\downarrow\}} \delta_{\sigma_1,\sigma}\delta_{\sigma_2,\sigma} e^{i\vec{k}(\vec{r}_1-\vec{r}_2)} e^{-\frac{i}{\hbar}\epsilon_{\vec{k},\sigma}(t_1-t_2)} \Big\{\theta_{\mathcal{C}}(t_1-t_2)\Big(1-f_{T,\mu}(\epsilon_{\vec{k},\sigma})\Big) - \theta_{\mathcal{C}}(t_2-t_1) f_{T,\mu}(\epsilon_{\vec{k},\sigma})\Big\}}_{G^{\mathcal{C},(0)}(\vec{x}_1,t_1,\vec{x}_2,t_2)} \\
&\times \underbrace{\frac{1}{i\hbar L^3}\sum_{\vec{k}'}\sum_{\sigma'\in\{\uparrow,\downarrow\}} \delta_{\sigma_1,\sigma'}\delta_{\sigma_2,\sigma'} e^{i\vec{k}'(\vec{r}_2-\vec{r}_1)} e^{-\frac{i}{\hbar}\epsilon_{\vec{k}',\sigma'}(t_2-t_1)} \Big\{\theta_{\mathcal{C}}(t_2-t_1)\Big(1-f_{T,\mu}(\epsilon_{\vec{k}',\sigma'})\Big) - \theta_{\mathcal{C}}(t_1-t_2) f_{T,\mu}(\epsilon_{\vec{k}',\sigma'})\Big\}}_{G^{\mathcal{C},(0)}(\vec{x}_2,t_2,\vec{x}_1,t_1)} \\
&= \frac{1}{i\hbar}\underbrace{(-1)}_{\text{Fermi loop}} \sum_{\sigma\in\{\uparrow,\downarrow\}} \overbrace{\frac{1}{L^6}\sum_{\vec{k},\vec{k}'}}^{\sim\int\frac{d^3k}{(2\pi)^3}\int\frac{d^3k'}{(2\pi)^3}} e^{i(\vec{k}-\vec{k}')(\vec{r}_1-\vec{r}_2)} e^{-\frac{i}{\hbar}\left(\epsilon_{\vec{k},\sigma}-\epsilon_{\vec{k}',\sigma}\right)(t_1-t_2)} \\
&\times \Big\{\theta_{\mathcal{C}}(t_1-t_2)\Big(1-f_{T,\mu}(\epsilon_{\vec{k},\sigma})\Big) - \theta_{\mathcal{C}}(t_2-t_1) f_{T,\mu}(\epsilon_{\vec{k},\sigma})\Big\} \\
&\times \Big\{\theta_{\mathcal{C}}(t_2-t_1)\Big(1-f_{T,\mu}(\epsilon_{\vec{k}',\sigma})\Big) - \theta_{\mathcal{C}}(t_1-t_2) f_{T,\mu}(\epsilon_{\vec{k}',\sigma})\Big\} \\
&= \frac{1}{i\hbar}\underbrace{(-1)}_{\text{Fermi loop}} \sum_{\sigma\in\{\uparrow,\downarrow\}} \frac{1}{L^6}\sum_{\vec{k},\vec{k}'} e^{i(\vec{k}-\vec{k}')(\vec{r}_1-\vec{r}_2)} e^{-\frac{i}{\hbar}\left(\epsilon_{\vec{k},\sigma}-\epsilon_{\vec{k}',\sigma}\right)(t_1-t_2)} \\
&\times \Big\{-\theta_{\mathcal{C}}(t_1-t_2)\Big(1-f_{T,\mu}(\epsilon_{\vec{k},\sigma})\Big) f_{T,\mu}(\epsilon_{\vec{k}',\sigma}) - \theta_{\mathcal{C}}(t_2-t_1) f_{T,\mu}(\epsilon_{\vec{k},\sigma})\Big(1-f_{T,\mu}(\epsilon_{\vec{k}',\sigma})\Big)\Big\} \\
&= A(\vec{r}_1,t_1,\vec{r}_2,t_2) + A(\vec{r}_2,t_2,\vec{r}_1,t_1)
\end{aligned}
\tag{E.51}
$$

with

$$
\begin{aligned}
A(\vec{r}_1,t_1,\vec{r}_2,t_2) &\overset{\text{def}}{=} \overbrace{\frac{i}{\hbar}\theta_{\mathcal{C}}(t_2-t_1)}^{-\theta_{\mathcal{C}}(t_2-t_1)\frac{1}{i\hbar}} \underbrace{(-1)}_{\text{Fermi loop}} \sum_{\sigma\in\{\uparrow,\downarrow\}} \overbrace{\frac{1}{L^6}\sum_{\vec{k},\vec{k}'}}^{\sim\int\frac{d^3k}{(2\pi)^3}\frac{d^3k'}{(2\pi)^3}} e^{i(\vec{k}-\vec{k}')(\vec{r}_1-\vec{r}_2)} e^{-\frac{i}{\hbar}\left(\epsilon_{\vec{k},\sigma}-\epsilon_{\vec{k}',\sigma}\right)(t_1-t_2)} \\
&\times f_{T,\mu}(\epsilon_{\vec{k},\sigma})\Big(1-f_{T,\mu}(\epsilon_{\vec{k}',\sigma})\Big)
\end{aligned}
\tag{E.52}
$$

The function $A(x_1,t_1,x_2,t_2)$ contains the complete information of the polarization insertion. It is valid on the entire complex-valued-time contour.

Let me now work on $A(\vec{r}_1,t_1,\vec{r}_2,t_2)$: I introduce new variables $\vec{q}=\vec{k}'-\vec{k}$ and $\hbar\omega=\epsilon_{\vec{k}',\sigma}-\epsilon_{\vec{k},\sigma}=$

$\epsilon_{\vec{k}+\vec{q},\sigma} - \epsilon_{\vec{k},\sigma}$.

$$
\begin{aligned}
A(\vec{r}_1,t_1,\vec{r}_2,t_2) &= \theta_{\mathcal{C}}(t_2-t_1)\frac{i}{\hbar}\overbrace{(-1)}^{\text{Fermi loop}}\sum_{\sigma\in\{\uparrow,\downarrow\}}\overbrace{\frac{1}{L^3}\sum_{\vec{q}}}^{\sim\int\frac{d^3q}{(2\pi)^3}}\mathrm{e}^{-i\vec{q}(\vec{r}_1-\vec{r}_2)}\overbrace{\frac{1}{L^3}\sum_{\vec{k}}}^{\sim\int\frac{d^3k}{(2\pi)^3}}f_{T,\mu}(\epsilon_{\vec{k},\sigma})\Big(1-f_{T,\mu}(\epsilon_{\vec{k}+\vec{q},\sigma}\Big)\\
&\quad\times\underbrace{\int d\epsilon\;\delta(\epsilon-\epsilon_{\vec{k},\sigma})}_{=1}\underbrace{\int d\epsilon'\;\delta(\epsilon'-\epsilon_{\vec{k}+\vec{q},\sigma})}_{=1}\underbrace{\int d(\hbar\omega)\;\delta(\epsilon_{\vec{k}+\vec{q},\sigma}-\epsilon_{\vec{k},\sigma}-\hbar\omega)\mathrm{e}^{i\omega(t_1-t_2)}}_{=\mathrm{e}^{-\frac{i}{\hbar}(\epsilon_{\vec{k},\sigma}-\epsilon_{\vec{k}+\vec{q},\sigma})(t_1-t_2)}}\\
&= \theta_{\mathcal{C}}(t_2-t_1)\frac{i}{\hbar}\int d(\hbar\omega)\;\overbrace{\frac{1}{L^3}\sum_{\vec{q}}}^{\sim\int\frac{d^3q}{(2\pi)^3}}\mathrm{e}^{-i[\vec{q}(\vec{r}_1-\vec{r}_2)-\omega(t_1-t_2)]}\\
&\quad\times\underbrace{\overbrace{(-1)}^{\text{Fermi loop}}\sum_{\sigma\in\{\uparrow,\downarrow\}}\int d\epsilon\int d\epsilon'\;\delta(\epsilon'-\epsilon-\hbar\omega)f_{T,\mu}(\epsilon)\Big(1-f_{T,\mu}(\epsilon')\Big)\overbrace{\frac{1}{L^3}\sum_{\vec{k}}\;\delta(\epsilon-\epsilon_{\vec{k},\sigma})\;\delta(\epsilon'-\epsilon_{\vec{k}+\vec{q},\sigma})}^{K_{\vec{q}(\epsilon,\epsilon')}}}_{\bar{F}_{\vec{q}}(\hbar\omega)}\\
&= \theta_{\mathcal{C}}(t_2-t_1)\frac{i}{\hbar}\int d(\hbar\omega)\;\overbrace{\frac{1}{L^3}\sum_{\vec{q}}}^{\sim\int\frac{d^3q}{(2\pi)^3}}\mathrm{e}^{-i[\vec{q}(\vec{r}_1-\vec{r}_2)-\omega(t_1-t_2)]}\bar{F}_{\vec{q}}(\hbar\omega) \qquad \text{(E.53)}
\end{aligned}
$$

with

$$
\begin{aligned}
\bar{F}_{\vec{q}}(\hbar\omega) &\stackrel{\text{def}}{=} \underbrace{(-1)}_{\text{Fermi loop}}\sum_{\sigma\in\{\uparrow,\downarrow\}}\int d\epsilon\int d\epsilon'\;\delta(\epsilon'-\epsilon-\hbar\omega)K_{\vec{q}}(\epsilon,\epsilon')f_{T,\mu}(\epsilon)\Big(1-f_{T,\mu}(\epsilon')\Big)\\
&= \underbrace{(-1)}_{\text{Fermi loop}}\sum_{\sigma\in\{\uparrow,\downarrow\}}\int d\epsilon\;f_{T,\mu}(\epsilon)K_{\vec{q},\sigma}(\epsilon,\epsilon+\hbar\omega)\Big(1-f_{T,\mu}(\epsilon+\hbar\omega)\Big) \qquad \text{(E.54)}
\end{aligned}
$$

and

$$
K_{\vec{q},\sigma}(\epsilon,\epsilon') \stackrel{\text{def}}{=} \frac{1}{L^3}\sum_{\vec{k}}\delta(\epsilon-\epsilon_{\vec{k},\sigma})\delta(\epsilon'-\epsilon_{\vec{k}+\vec{q},\sigma}) \qquad \text{(E.55)}
$$

- Eq. E.51 for the polarization insertion is valid for complex-valued time arguments. It is limited to non-interacting systems that are translationally invariant in space and time. This enforces that the one-particle energies are time-independent and that the one-particle states are plane waves in real space. The dispersion relation $\epsilon_{\vec{k},\sigma}$, is given in the extended zone scheme but otherwiese not restricted.
- The function $\bar{F}_{\vec{q}}(\hbar\omega)$ is a real-valued quantity.
- For zero-temperature, the $\bar{F}_{\vec{q}}(\hbar\omega)$ vanishes for negative $\hbar\omega$.
- We can use the symmetry $F_{\vec{q}}(\hbar\omega) = F_{-\vec{q}}(-\hbar\omega)$. It uses the symmetry $K_{\vec{q}}(\epsilon,\epsilon') = K_{-\vec{q}}(\epsilon',\epsilon)$.
- $K_{\vec{q},\sigma}(\epsilon,\epsilon')$ is the one-dimensional intersection of two energy iso-surfaces of the band structure $\epsilon_{\vec{k},\sigma}$. One of the iso-surfaces is displaced in k-space by $\vec{q}$.
- It must not be forgotten that $\bar{F}_{\vec{q}}(\hbar\omega)$ is not a Fourier transform of $A(\vec{r},t,\vec{r}',t')$, because we work on a complex time contour. Therefore, it cannot directly be compared to similar expressions in the literature. Thus, the Fourier transform must be recovered from "our" $\bar{F}(\vec{q},\hbar\omega')$ by a complicated frequency integration.

- In the expression above, the wave vectors are taken from a discrete grid. The discrete sum over k-points can be turned into into an integral using $\sum_{\vec{k}} \to L^3 \int \frac{d^3k}{(2\pi)^3}$. I exploit that the reciprocal-space volume per k-point is $(2\pi/L)^3$.

  The infinities resulting from the factor L^3 are balanced by the norm of the basisfunctions, which are themselfes normalized on a volume of size L^3.

  With the transition to continuous momenta, the Kronecker for the momentum transfer $\vec{q}$ must be converted into a delta-function $\delta_{\vec{q},\vec{q}'} = (2\pi/L)^3 \delta(\vec{q}-\vec{q}') = d^3q\ \delta(\vec{q}-\vec{q}')$. The volume element d^3q is used later to convert the integral for the discrete mesh of momentum transfers into a density of continous values.

E.4.2 Material-specific term $K_{\vec{q}}(\epsilon, \epsilon')$

The term $K_{\vec{q}}(\epsilon, \epsilon')$ defined in Eq. E.54 contains all material-specific information. It is the intersection of the iso-energy surfaces at ϵ, ϵ', which are displaced in k-space by the vector $\vec{q}$.

The expression for $K_{\vec{q}}(\epsilon, \epsilon')$ can be expressed in terms of derivatives of a volume integral by exploiting $\delta(x) = \partial_x \theta(x) = -\partial_x \theta(-x)$.

$$\begin{aligned} K_{\vec{q},\sigma}(\epsilon,\epsilon') &\overset{\text{Eq. } E.55}{=} \frac{1}{L^3} \sum_{\vec{k}} \delta(\epsilon - \epsilon_{\vec{k},\sigma}) \delta(\epsilon' - \epsilon_{\vec{k}+\vec{q},\sigma}) \\ &= \frac{d}{d\epsilon}\frac{d}{d\epsilon'} \Bigg\{ \underbrace{\frac{1}{L^3} \sum_{\vec{k}}}_{\sim \int \frac{d^3k}{(2\pi)^3}} \theta(\epsilon_{\vec{k},\sigma} - \epsilon)\theta(\epsilon_{\vec{k}+\vec{q},\sigma} - \epsilon') \Bigg\} \end{aligned} \tag{E.56}$$

Isotropic systems: I introduce the **assumption** that the system is isotropic. Isotropy implies that the energy levels $\epsilon_{\vec{k},\sigma}$ depend only on the length of the reciprocal lattice vector $|\vec{k}|$ but not on its direction. With this assumption the calculation of $K_{\vec{q},\sigma}(\epsilon, \epsilon')$ can be reduced to a geometric problem, namely to evaluate the common volume of two spheres, each with its own radius, which are displaced by a vector $\vec{q}$.

The factor K is obtained via the lens-shaped intersection of two spheres.

$$K_{\vec{q},\sigma}(\epsilon,\epsilon') = \frac{d}{d\epsilon}\frac{d}{d\epsilon'} \Bigg\{ \underbrace{\frac{1}{L^3} \sum_{\vec{k}}}_{\sim \int \frac{d^3k}{(2\pi)^3}} \theta(\epsilon_{\vec{k},\sigma} - \epsilon)\theta(\epsilon_{\vec{k}+\vec{q},\sigma} - \epsilon') \Bigg\} \tag{E.57}$$

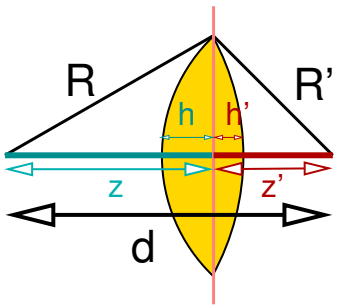

Volume of a spherical segment: Consider a spherical segment, i.e. the part of a sphere, which is cut off from the sphere by a plane. The radius of the sphere shall be r. The plane cuts through the sphere at distance z from the sphere center. The width of the spherical segment is $h = r - z$,

$h \in [0, 2r]$.

$$\begin{aligned} V &= \underbrace{\frac{1}{2}\frac{4\pi r^3}{3}}_{\text{half sphere}} - \int_0^{r-h} dz\ \underbrace{\pi(r^2 - z^2)}_{\text{circle area}} \\ &= \frac{2\pi r^3}{3} - \pi\left[r^2 z - \frac{1}{3}z^3\right]_0^{r-h} \\ &= \frac{2\pi r^3}{3} - \pi\left(r^2(r-h) - \frac{1}{3}(r-h)^3\right) \\ &= \frac{2\pi r^3}{3} - \frac{\pi}{3}\left(3r^3 - 3r^2 h - r^3 + 3r^2 h - 3rh^2 + h^3\right) \\ &= \frac{2\pi r^3}{3} - \frac{\pi}{3}\left(2r^3 - 3rh^2 + h^3\right) \\ &= \frac{\pi}{3}\left(3rh^2 - h^3\right) \qquad \text{for } h \in [0, 2r] \end{aligned} \tag{E.58}$$

For $h > 2r$, the formula above is meaningless and the volume is instead that of the sphere, namely $V = 4\pi r^3/3$. The radius must be positive.

Sphere overlap: For the lens-shaped object made from the two spherical segments, we obtain

$$\begin{aligned} & z^2 + a^2 = R^2 \qquad \text{and} \qquad (d-z)^2 + a^2 = (R')^2 \\ \Rightarrow \quad & (d-z)^2 - z^2 = (R')^2 - R^2 \\ \Rightarrow \quad & d^2 - 2dz = (R')^2 - R^2 \\ \Rightarrow \quad & z = \frac{d}{2} - \frac{(R')^2 - R^2}{2d} \\ & h(R, R', d) \stackrel{\text{def}}{=} R' - (d - z) = R' - \frac{1}{2}d - \frac{(R')^2 - R^2}{2d} = -\frac{(R'-d)^2 - R^2}{2d} \\ & h'(R, R', d) \stackrel{\text{def}}{=} R - z = R - \frac{d}{2} + \frac{(R')^2 - R^2}{2d} = \frac{(R')^2 - (R-d)^2}{2d} \end{aligned} \tag{E.59}$$

The overlapping volume of the two spheres is therefore

$$V + V' \stackrel{\text{Eq. } E.58}{=} \frac{\pi}{3}\left(h^2(3R' - h) + (h')^2(3R - h')\right) \qquad \text{for } R + R' > d \text{ and } |R - R'| < d \tag{E.60}$$

with $h(R, R', d)$ and $h'(R, R', d)$ from Eq. E.59. The requirement is that $R, R', d > 0$.

Intersection of sphere surfaces: Let me now do the second derivative with respect to the radii R and R'

$$\frac{d^2(V + V')}{dR\,dR'} \stackrel{\text{Eq. } E.60}{=} \frac{d}{dR'}\frac{d}{dR}\frac{\pi}{3}\left(3R'h^2 - h^3 + 3R(h')^2 - (h')^3\right) \tag{E.61}$$

where h and h' are themselfes functions of R, R', d given in Eq. E.59.

$$\begin{aligned}
\frac{d^2(V+V')}{dRdR'} &= \frac{d}{dR'}\frac{d}{dR}\frac{\pi}{3}\Big(3R'h^2 - h^3 + 3R(h')^2 - (h')^3\Big) \\
&= \frac{d}{dR'}\frac{\pi}{3}\left[\Big(6R'h - 3h^2\Big)\frac{\partial h}{\partial R} + 3(h')^2 + \Big(6Rh' - 3(h')^2\Big)\frac{\partial h'}{\partial R}\right] \\
&= \frac{\pi}{3}\Bigg[6h\underbrace{\frac{\partial h}{\partial R}}_{R/d} + \Big(6R' - 6h\Big)\underbrace{\frac{\partial h}{\partial R'}}_{(d-R')/d}\underbrace{\frac{\partial h}{\partial R}}_{R/d} + \Big(6R'h - 3h^2\Big)\underbrace{\frac{\partial^2 h}{\partial R\partial R'}}_{=0} \\
&\quad + 6h'\underbrace{\frac{\partial h'}{\partial R'}}_{R'/d} + \Big(6R - 6h'\Big)\underbrace{\frac{\partial h'}{\partial R'}}_{R'/d}\underbrace{\frac{\partial h'}{\partial R}}_{(d-R)/d} + \Big(6Rh' - 3(h')^2\Big)\underbrace{\frac{\partial^2 h'}{\partial R'\partial R}}_{=0}\Bigg] \\
&= 2\pi\left[h\frac{R}{d} + \Big(R' - h\Big)\frac{(d-R')R}{d^2} + h'\frac{R'}{d} + \Big(R - h'\Big)\frac{R'(d-R)}{d^2}\right] \\
&= \frac{2\pi}{d^2}\Bigg[\underbrace{hRd + RR'd - R(R')^2 - hRd + hRR'}_{(d-R'+h)RR'} + \underbrace{h'R'd + R'Rd - R^2R' - h'R'd + h'RR'}_{(d-R+h')RR'}\Bigg] \\
&= \frac{2\pi RR'}{d^2}\Big(2d - (R+R') + (h+h')\Big) \\
&= \frac{2\pi RR'}{d^2}\Big(2d - (R+R') + (R+R') - d\Big) \\
&= \frac{2\pi RR'}{d}\theta(R' - |d-R|)\theta(d+R-R')
\end{aligned} \tag{E.62}$$

Back to the polarization integral

$$\begin{aligned}
K_{\vec{q},\sigma}(\epsilon,\epsilon') &\overset{\text{Eq. } E.56}{=} \underbrace{\frac{d}{d\epsilon}}_{\left(\frac{d\epsilon}{dk}\right)^{-1}\frac{d}{dk}}\underbrace{\frac{d}{d\epsilon'}}_{\left(\frac{d\epsilon'}{dk'}\right)^{-1}\frac{d}{dk'}}\Bigg\{\underbrace{\frac{1}{L^3}\sum_{\vec{k}}}_{\sim\int\frac{d^3k}{(2\pi)^3}}\theta(\epsilon_{\vec{k},\sigma}-\epsilon)\theta(\epsilon_{\vec{k}+\vec{q},\sigma}-\epsilon')\Bigg\} \\
&\overset{\text{Eq. } E.62}{=} \left(\left.\frac{d\epsilon}{dk}\right|_{k_\sigma(\epsilon)}\right)^{-1}\left(\left.\frac{d\epsilon}{dk}\right|_{k_\sigma(\epsilon')}\right)^{-1}\frac{1}{(2\pi)^3}\frac{2\pi k_\sigma(\epsilon)k_\sigma(\epsilon')}{|\vec{q}|} \\
&\quad\times\theta\Big(k_\sigma(\epsilon') - \big|k_\sigma(\epsilon) - |\vec{q}|\big|\Big)\,\theta\Big(|\vec{q}| + k_\sigma(\epsilon) - k_\sigma(\epsilon')\Big)
\end{aligned} \tag{E.63}$$

where $k_\sigma(\epsilon)$ is the radius of the iso-energy surface with energy ϵ.

The two step functions limit the result to regions with intersection spheres, i.e. with

$$|k_\sigma(\epsilon) - |\vec{q}|| < k_\sigma(\epsilon') < k_\sigma(\epsilon) + |\vec{q}| \tag{E.64}$$

E.4.3 $\bar{F}_{\vec{q}}(\hbar\omega)$

The bounds for the k-integration region are determined in wave vectors, while the integrand is given by the energies. However for a (monotonic) isotropic system the integration can be mapped onto a two-dimensional integral in k-space.

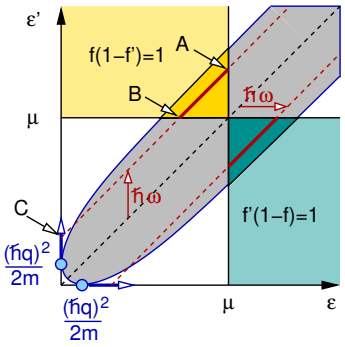

Fig. E.6: Integration region for the double energy integral in the ϵ, ϵ'-plane. The yellow and green regions select the electron-hole-pair excitations and are given by the occupations $f = f_{T,\mu}(\epsilon)$ and $f' = f_{T,\mu}(\epsilon')$. The straight red line implements the energy conservation $\hbar\omega = |\epsilon' - \epsilon|$. The grey region indicates the values for two quasi-particle energies, where the iso-energy surfaces intersect. Outside the grey region the contribution to the integral vanishes. In this graph the shape of grey region is taken from a free-electron-gas. It touches the axis at a point related to the momentum transfer. With increasing momentum transfer, the parabola grows wider, and its bottom shift upward along the main diagonal.

$$
\begin{aligned}
\bar{F}_{\vec{q}}(\hbar\omega) &\overset{\text{Eq. } E.54}{=} \underbrace{(-1)}_{\text{F.L.}} \sum_{\sigma\in\{\uparrow,\downarrow\}} \int d\epsilon \int d\epsilon'\, \delta(\epsilon' - \epsilon - \hbar\omega) f_{T,\mu}(\epsilon) K_{\vec{q},\sigma}(\epsilon,\epsilon') \Big(1 - f_{T,\mu}(\epsilon')\Big) \\
&\overset{\text{Eq. } E.63}{=} \underbrace{(-1)}_{\text{F.L.}} \sum_{\sigma\in\{\uparrow,\downarrow\}} \frac{1}{(2\pi)^3} \frac{2\pi}{|\vec{q}|} \int d\epsilon \int d\epsilon'\, \delta(\epsilon' - \epsilon - \hbar\omega) f_{T,\mu}(\epsilon) \Big(1 - f_{T,\mu}(\epsilon')\Big) \\
&\quad \times \underbrace{\left(\left.\frac{d\epsilon}{dk}\right|_{k_\sigma(\epsilon)}\right)^{-1} \left(\left.\frac{d\epsilon}{dk}\right|_{k_\sigma(\epsilon')}\right)^{-1} k_\sigma(\epsilon) k_\sigma(\epsilon')}_{\text{free-electron gas: } \left(\frac{m}{\hbar^2}\right)^2} \\
&\quad \times \underbrace{\theta\Big(k_\sigma(\epsilon') - \big|k_\sigma(\epsilon) - |\vec{q}|\big|\Big)}_{\text{free-electron gas: } \theta\left(\epsilon' - (\sqrt{\epsilon} - \frac{\hbar|\vec{q}|}{\sqrt{2m}})^2\right)} \underbrace{\theta\Big(|\vec{q}| + k_\sigma(\epsilon) - k_\sigma(\epsilon')\Big)}_{\text{free-electron gas: } \theta\left((\sqrt{\epsilon} + \frac{\hbar|\vec{q}|}{\sqrt{2m}})^2 - \epsilon'\right)}
\end{aligned}
\tag{E.65}
$$

E.4.4 free-electron gas at zero temperature

The result Eq. E.65 obtained so far has been valid for any isotropic dispersion relation. Now we become more specific: Le me drop temperature effects and let me choose the free-electron parabola as dispersion relation.

Let me now do the step to the **homogeneous electron gas at zero temperature**. This implies

$$
\epsilon(\vec{k},\sigma) = \frac{\hbar^2 k^2}{2m} \qquad \text{and} \qquad \frac{1}{k}\frac{d\epsilon}{dk} = \frac{\hbar^2}{m} \qquad \text{and} \qquad k(\epsilon,\sigma) = \frac{1}{\hbar}\sqrt{2m\epsilon}\,. \tag{E.66}
$$

I obtain for $T = 0$

$$\begin{aligned}
\bar{F}_{\vec{q}}(\hbar\omega) &\overset{\text{Eq. E.65}}{=} \underbrace{(-1)}_{\text{F.L.}} \sum_{\sigma\in\{\uparrow,\downarrow\}} \left(\frac{m}{2\pi\hbar^2}\right)^2 \frac{1}{|\vec{q}|} \int d\epsilon \int d\epsilon'\, \delta(\epsilon' - \epsilon - \hbar\omega) \\
&\times \quad \underbrace{\theta(\mu-\epsilon)}_{f_{T,\mu}(\epsilon)} \underbrace{\theta(\epsilon'-\mu)}_{1-f_{T,\mu}(\epsilon')} \theta\left(\epsilon' - \left(\sqrt{\epsilon} - \frac{\hbar|\vec{q}|}{\sqrt{2m}}\right)^2\right) \theta\left(\left(\sqrt{\epsilon} + \frac{\hbar|\vec{q}|}{\sqrt{2m}}\right)^2 - \epsilon'\right) \\
&= \quad \underbrace{(-1)}_{\text{F.L.}} \sum_{\sigma\in\{\uparrow,\downarrow\}} \left(\frac{m}{2\pi\hbar^2}\right)^2 \frac{1}{|\vec{q}|} \\
&\times \quad \int_{\mu-\hbar\omega}^{\mu} d\epsilon\, \theta\left(\epsilon + \hbar\omega - \left(\sqrt{\epsilon} - \frac{\hbar|\vec{q}|}{\sqrt{2m}}\right)^2\right) \theta\left(\left(\sqrt{\epsilon} + \frac{\hbar|\vec{q}|}{\sqrt{2m}}\right)^2 - \epsilon - \hbar\omega\right) \qquad \text{(E.67)}
\end{aligned}$$

Domains The step functions in Eq. E.67 limit the range of the remaining ϵ-integration to

$$\begin{aligned}
&\left(\sqrt{\epsilon} + \frac{\hbar|\vec{q}|}{\sqrt{2m}}\right)^2 - \epsilon - \hbar\omega > 0 \qquad \text{and} \qquad \epsilon + \hbar\omega - \left(\sqrt{\epsilon} - \frac{\hbar|\vec{q}|}{\sqrt{2m}}\right)^2 > 0 \\
&\Rightarrow \quad \left(\sqrt{\epsilon} + \frac{\hbar|\vec{q}|}{\sqrt{2m}}\right)^2 > \quad \epsilon + \hbar\omega \quad > \left(\sqrt{\epsilon} - \frac{\hbar|\vec{q}|}{\sqrt{2m}}\right)^2 \\
\Rightarrow \quad &\epsilon + 2\sqrt{\epsilon}\frac{\hbar|\vec{q}|}{\sqrt{2m}} + \left(\frac{\hbar|\vec{q}|}{\sqrt{2m}}\right)^2 > \quad \epsilon + \hbar\omega \quad > \epsilon - 2\sqrt{\epsilon}\frac{\hbar|\vec{q}|}{\sqrt{2m}} + \left(\frac{\hbar|\vec{q}|}{\sqrt{2m}}\right)^2 \\
&\Rightarrow \quad 2\sqrt{\epsilon}\frac{\hbar|\vec{q}|}{\sqrt{2m}} > \quad \hbar\omega - \tfrac{\hbar^2\vec{q}^2}{2m} \quad > -2\sqrt{\epsilon}\frac{\hbar|\vec{q}|}{\sqrt{2m}} \\
&\Rightarrow \quad \sqrt{\epsilon} > \tfrac{1}{2}\left(\tfrac{\sqrt{2m}}{\hbar|\vec{q}|}\right)\left(\hbar\omega - \tfrac{\hbar^2\vec{q}^2}{2m}\right) > -\sqrt{\epsilon} \\
&\Rightarrow \quad \epsilon > \tfrac{1}{4}\tfrac{2m}{\hbar^2\vec{q}^2}\left(\hbar\omega - \tfrac{\hbar^2\vec{q}^2}{2m}\right)^2 \qquad \text{(E.68)}
\end{aligned}$$

Thus, the ϵ-integration is limited to

$$\mu - \hbar\omega < \epsilon < \mu \qquad \text{and} \qquad \epsilon > \frac{1}{4}\frac{2m}{\hbar^2\vec{q}^2}\left(\hbar\omega - \frac{\hbar^2\vec{q}^2}{2m}\right)^2 \qquad \text{(E.69)}$$

This results in different regions in the q, ω plane that are treated differently. In the following, Let me determine the lines where the boundary of the gray region in figure E.6 touches the points A, B, C indicated in the same figure.

$$\begin{aligned}
\mathrm{A} &= (\epsilon, \epsilon') = (\mu, \mu + \hbar\omega) \\
\mathrm{B} &= (\epsilon, \epsilon') = (\mu - \hbar\omega, \mu) \\
\mathrm{C} &= (\epsilon, \epsilon') = (0, \hbar\omega) \qquad \text{(E.70)}
\end{aligned}$$

A:

$$\underbrace{\mu + \hbar\omega}_{\epsilon'} = \left(\underbrace{\sqrt{\mu}}_{\sqrt{\epsilon}} \pm \frac{\hbar|\vec{q}|}{\sqrt{2m}}\right)^2 \qquad \Rightarrow \qquad \hbar|\vec{q}| = \mp\sqrt{2m\mu} + \sqrt{2m(\mu+\hbar\omega)} \qquad \text{(E.71)}$$

Only the solution with the positive square root $\sqrt{2m(\mu+\hbar\omega)}$ is related to positive $\hbar q$ and positive $\hbar\omega$. Therefore the branch with the negative square root is excluded. The two branches bounded by the point A denote the region of momenta and frequency with a non-vanishing contribution to the polarization diagram.

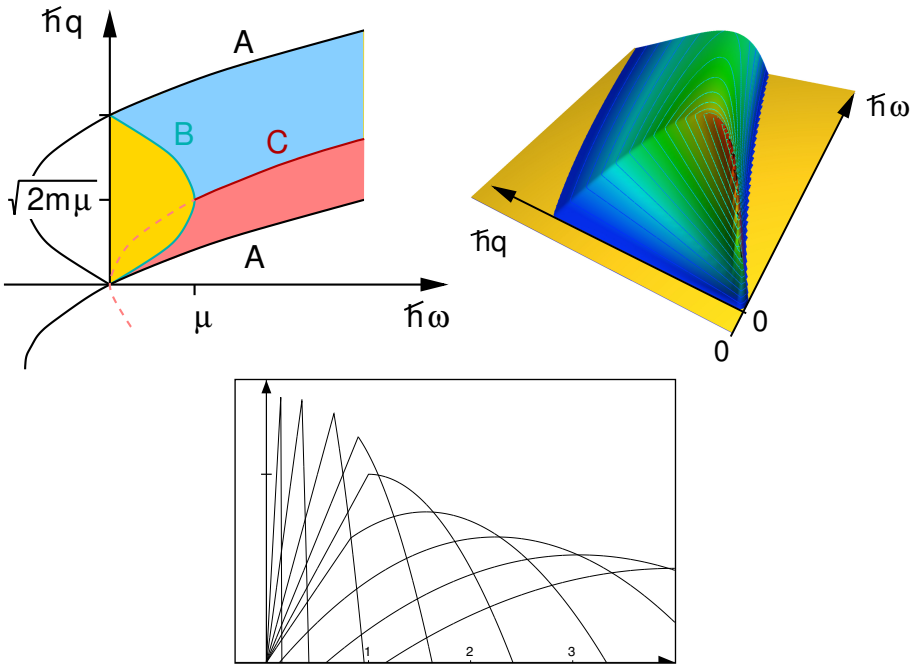

Fig. E.7: Region with finite polarization insertion **for non-interacting electrons** as function of momentum transfer $\hbar|\vec{q}|$ and energy transfer $\hbar\omega$. The contribution vanishes outside the colored regions. The lines denoted A, B, C indicate values where the boundary of the gray region in figure E.6 touches the points A, B, C. The bottom image shows $\bar{F}_{\vec{q}}(\hbar\omega)$ as function of the energy transfer $\hbar\omega$ for several values of $\hbar|\vec{q}|$

B:

$$\underbrace{\mu}_{\epsilon'} = \Big(\underbrace{\sqrt{\mu - \hbar\omega}}_{\sqrt{\epsilon}} \pm \frac{\hbar|\vec{q}|}{\sqrt{2m}}\Big)^2 \qquad \Rightarrow \qquad \hbar|\vec{q}| = \mp\sqrt{2m(\mu - \hbar\omega)} + \sqrt{2m\mu} \tag{E.72}$$

The region enclosed by the line B is the region where the line segment from A to B is not constrained by the theta functions.

C:

$$\underbrace{\hbar\omega}_{\epsilon'} = \Big(\underbrace{0}_{\sqrt{\epsilon}} \pm \frac{\hbar|\vec{q}|}{\sqrt{2m}}\Big)^2 \qquad \Rightarrow \qquad \hbar|\vec{q}| = \mp\sqrt{2m(\mu - \hbar\omega)} + \sqrt{2m\mu} \tag{E.73}$$

Back to the $\bar{F}$: Thus, I obtain

$$\begin{aligned}\bar{F}_{\vec{q}}(\hbar\omega) &\overset{\text{Eq. } E.67}{=} \underbrace{(-1)}_{\text{F.L.}} \sum_{\sigma\in\{\uparrow,\downarrow\}} \left(\frac{m}{2\pi\hbar^2}\right)^2 \frac{1}{|\vec{q}|} \\ &\quad \times\left\{\int_{\mu-\hbar\omega}^{\mu} d\epsilon\, \theta\Big(\underbrace{\epsilon+\hbar\omega}_{\epsilon'} - (\sqrt{\epsilon} - \frac{\hbar|\vec{q}|}{\sqrt{2m}})^2\Big)\theta\Big((\sqrt{\epsilon}+\frac{\hbar|\vec{q}|}{\sqrt{2m}})^2 - \underbrace{\epsilon-\hbar\omega}_{\epsilon'}\Big)\right. \\ &= \underbrace{(-1)}_{\text{F.L.}} \sum_{\sigma\in\{\uparrow,\downarrow\}} \left(\frac{m}{2\pi\hbar^2}\right)^2 \frac{1}{|\vec{q}|} \max\Bigg[0, \underbrace{\min\left(\hbar\omega, \mu - \frac{1}{4}\frac{2m}{\hbar^2\vec{q}^2}\left(\hbar\omega - \frac{\hbar^2\vec{q}^2}{2m}\right)^2\right)}_{\left\{\mu - \max\left(\mu-\hbar\omega, \frac{1}{4}\frac{2m}{\hbar^2\vec{q}^2}\left(\hbar\omega-\frac{\hbar^2\vec{q}^2}{2m}\right)^2\right)\right\}}\Bigg]\end{aligned} \tag{E.74}$$

I chose the maximum of zero and the calculated value to make the result defined, albeit zero, in the regions where the contribution vanishes.

The resulting function is shown in figure E.7.

It is evident that the dominant contribution comes from a ridge at small values of q and ω. This feature is specific to the lowest order polarization insertion. Editor: Caution! This need to be checked! It reminds of bosonic dispersion relation for a mass-less particle. Upon renormalization (necklace of ring diagrams), this feature disappears and a plasmon dispersion relation appears, which has a minimum frequency, the plasmon frequency. It seems that the mass-less polarin acquired mass upon renormalization.

From $\bar{F}$ to the polarization insertion: Note that $\bar{F}$ is not the polarization insertion itself.

The polarization insertion is

$$\Pi^{(0)}(\vec{r}_1, t_1, \vec{r}_2, t_2) \overset{\text{Eq. } E.51}{=} A(\vec{r}_1, t_1, \vec{r}_2, t_2) + A(\vec{r}_2, t_2, \vec{r}_1, t_1) \tag{E.75}$$

where

$$A(\vec{r}_1, t_1, \vec{r}_2, t_2) \overset{\text{Eq. } E.53}{=} \theta_{\mathcal{C}}(t_2 - t_1)\frac{i}{\hbar}\int d(\hbar\omega)\, \overbrace{\frac{1}{L^3}\sum_{\vec{q}}}^{\sim\int\frac{d^3q}{(2\pi)^3}} e^{-i[\vec{q}(\vec{r}_1-\vec{r}_2)-\omega(t_1-t_2)]}\bar{F}_{\vec{q}}(\hbar\omega) \tag{E.76}$$

Thus

$$\begin{aligned}\Pi^{(0)}(\vec{r}_1, t_1, \vec{r}_2, t_2) = \int d(\hbar\omega)\, &\overbrace{\frac{1}{L^3}\sum_{\vec{q}}}^{\sim\int\frac{d^3q}{(2\pi)^3}} \bar{F}_{\vec{q}}(\hbar\omega) \\ &\times\frac{i}{\hbar}\Big\{\theta_{\mathcal{C}}(t_2-t_1)e^{-i[\vec{q}(\vec{r}_1-\vec{r}_2)-\omega(t_1-t_2)]} + \theta_{\mathcal{C}}(t_1-t_2)e^{+i[\vec{q}(\vec{r}_1-\vec{r}_2)-\omega(t_1-t_2)]}\Big\}\end{aligned} \tag{E.77}$$

Editor: check here the symmetries of $\bar{F}$

Discussion of the lowest-order polarization insertion Editor: The following is a set of personal notes for the author. They have not been verified!

The polarization insertion in lowest order is shown in figure E.7. If the polarization insertion is renormalized by considering all chains of ring diagrams connected by interactions, a **plasmon branch** splits off from the continuum.

In lowest order we find a pronounced ridge for small energy- and momentum-transfer. It reminds of the dispersion relation of a boson with velocity equal to the Fermi velocity. Editor: Will this feature turn into the plasmon band, when interaction is switched on? When this feature is considered as a spectral function of bosons, they move marginally slower (line B in figure E.7) than the electrons (line A). (check this!) Hence an interacting system will transfer kinetic energy to this boson. This may be one possible explanation for the finite lifetime of the electrons.

At $\hbar\omega = \mu$, this ridge disappears in the continuum of electron-hole excitations. Editor: What is special at the Fermi energy? Is it that the excitation energy can reach the (flat) bottom of the free-electron band?

E.4.5 Screened interaction and dielectric constant

Editor: Sketch: do not read!!!

$$\begin{aligned}\Pi^{RPA} &= \Pi^{(0)} + \Pi^{(0)} V \Pi^{(0)} + \Pi^{(0)} V \Pi^{(0)} V \Pi^{(0)} + \dots \\ &= \Pi^{(0)} + \Pi^{(0)} V \Pi^{RPA} \\ \Pi^{RPA} &= \left(1 - \Pi^{(0)} V\right)^{-1} \Pi^{(0)}\end{aligned} \tag{E.78}$$

$$\begin{aligned}V^{scr,RPA} &= V^{(0)} + V^{(0)} \Pi^{(0)} V^{(0)} + V^{(0)} \Pi^{(0)} V^{(0)} \Pi^{(0)} V^{(0)} + \dots \\ &= V^{(0)} + V^{(0)} \Pi^{(0)} V^{(scr,RPA)} \\ &= \underbrace{\left(1 - V^{(0)} \Pi^{(0)}\right)^{-1}}_{\frac{1}{\epsilon_r^{RPA}}} V^{(0)}\end{aligned} \tag{E.79}$$

$$\epsilon_r^{RPA} = 1 - V^{(0)} \Pi^{(0)} \tag{E.80}$$

Of particular interest are the zeros of the dielectric constant. For those momenta $\hbar\vec{q}$ and energies $\hbar\omega$, the screened potential does not become smaller than the bare potential, but it becomes infinite. A charge fluctuation with these momenta and frequencies can occur spontaneously. It can be considered a quasi-particle, which is called a **plasmon**.

Four-center integrals in a plane-wave basis:

When the interaction matrix elements for the interaction are expressed in terms of plane waves, there are selection rules which require certain matric elements to be zero. Let me therefore analyze these four center integrals.

For our basisset the four-center integrals are

$$\begin{aligned}W_{\vec{k}_1,\sigma_1,\vec{k}_2,\sigma_2,\vec{k}_3,\sigma_3,\vec{k}_4,\sigma_4} &= \frac{e^2}{4\pi\epsilon_0} \delta_{\sigma_1,\sigma_3} \delta_{\sigma_2,\sigma_4} \int d^3r \int d^3r' \, \frac{1}{L^6} \frac{e^{i(\vec{k}_3-\vec{k}_1)\vec{r}} e^{i(\vec{k}_4-\vec{k}_2)\vec{r}'}}{|\vec{r}-\vec{r}'|} \\ &= \frac{e^2}{4\pi\epsilon_0} \delta_{\sigma_1,\sigma_3} \delta_{\sigma_2,\sigma_4} \underbrace{\int d^3r \, \frac{1}{L^3} e^{i(\vec{k}_3-\vec{k}_1+\vec{k}_4-\vec{k}_2)\vec{r}}}_{\delta_{\vec{k}_3-\vec{k}_1+\vec{k}_4-\vec{k}_2,0}} \frac{1}{L^3} \int d^3r' \, \frac{e^{i(\vec{k}_4-\vec{k}_2)\left(\vec{r}'-\vec{r}\right)}}{|\vec{r}-\vec{r}'|} \\ &= \frac{e^2}{4\pi\epsilon_0} \delta_{\sigma_1,\sigma_3} \delta_{\sigma_2,\sigma_4} \delta_{\vec{k}_3-\vec{k}_1+\vec{k}_4-\vec{k}_2,\vec{0}} \frac{4\pi}{|\vec{k}_4-\vec{k}_2|^2}\end{aligned} \tag{E.81}$$

I introduce $\vec{q} \stackrel{\text{def}}{=} \vec{k}_4 - \vec{k}_2$ and $\vec{q}' \stackrel{\text{def}}{=} \vec{k}_1 - \vec{k}_3$. The four-center matrix elements are

$$W_{\vec{k}_1,\sigma_1,\vec{k}_2,\sigma_2,\vec{k}_1-\vec{q}',\sigma_3,\vec{k}_2+\vec{q},\sigma_4} = \frac{4\pi e^2}{4\pi\epsilon_0|\vec{q}|^2}\delta_{\sigma_1,\sigma_3}\delta_{\sigma_2,\sigma_4}\delta_{\vec{q},\vec{q}'} \tag{E.82}$$

The four-center matrix elements do not depend on $\vec{k}_1$ nor on $\vec{k}_2$. More importantly it only depends on the difference of the two wave vectors and spins on each of the two vertices.

Appendix F

Hartree-Fock approximation

F.1 Hartree-Fock equations in the zero-temperature case

F.1.1 Prologue to this section

This section contains a chapter on the Hartree-Fock equations, which I lifted from the main course before I decided to get into finite temperature description right away. It may be used by the novice to get a direct entry to the Hartree-Fock method without the obstructions of the finite temperature formalism. It has the advantage that the formulation is closer to the wave function notation used in first-principles electronic structure methods. The zero-temperature formalism suffers from conceptual problems related to degenerate ground states and symmetry breaking.

F.1.2 Hartree-Fock equations

To first-order perturbation theory in the interaction $\hat{W}$, we can use the many-particle eigenstates of the non-interacting Hamiltonian $\hat{h}$ to estimate the energies of the interacting system. The wave functions of a non-interacting Hamiltonian are Slater determinants. Slater determinants are much simpler to handle than general many-particle wave functions. However, the eigenstates of the non-interacting Hamiltonian $\hat{h}$ may not be the best choice. Instead, one could also search for the "best possible" non-interacting system.

What is the best non-interacting system? Because the ground state of the system is the minimum of the energy $\langle\Phi|\hat{h}+\hat{W}|\Phi\rangle$ for all fermionic many-particle wave functions, any restriction of the wave function to Slater determinants leads to an upper bound of the ground-state energy. We consider the Slater determinant with the lowest energy as the best approximation of the ground state wave function by a Slater determinant.

To obtain this "best" Slater determinant, we start with the total energy Eq. 2.44 and determine its minimum with respect to the permitted variations of the one-particle reduced density matrix. The one-particle-reduced density matrix is expressed by its natural orbitals $|\varphi_n\rangle$ and occupations f_n. Therefore, we need to minimize the total energy with respect to the one-particle orbitals $|\varphi_n\rangle$ and the occupations f_n. The orbitals must be kept orthonormal and this constraint is enforced using the method of **Lagrange multipliers**. The occupations are kept in the allowed range by expressing it as the $f_n = \sin^2(\gamma_n)$, where γ_n can have any real value. [1]

[1] The careful reader may notice that for the problem at hand, we may set the occupations to either zero or one and keep them frozen. This implies a restriction of the search to Slater determinants. This is no problem, because we are only looking for solutions that are Slater determinants. Keeping general occupations, the results are readily generalized to finite temperatures and the search can be extended to arbitrary many-particle wave functions or their ensembles.

HARTREE-FOCK ENERGY FUNCTIONAL

In the Hartree-Fock approximation, the ground-state total energy for a given particle number N is the minimum of a functional of one-particle wave functions $|\varphi_n\rangle$ and occupations $f_n \in [0,1]$, which encode the one-particle-reduced density matrix

$$\hat{\rho}^{(1)} \overset{\text{Eq. 2.19}}{=} \sum_{n=0}^{\infty} |\varphi_n\rangle f_n \langle\varphi_n| \tag{F.1}$$

and the electron density $n(\vec{r}) = \sum_{\sigma\in\{\uparrow,\downarrow\}} \rho^{(1)}(\vec{x},\vec{x})$.

$$\begin{aligned} E_N^{GS-HF} \overset{\text{Eq. 2.44}}{=} \min_{\{|\varphi_n\rangle, f_n\in[0,1]\}} \operatorname*{stat}_{\mathbf{\Lambda},\mu} \Bigg\{ & \underbrace{\mathrm{Tr}\left[\hat{\rho}^{(1)}\hat{h}\right]}_{E_{1P}} \\ & + \underbrace{\frac{1}{2}\int d^3r \int d^3r' \, \frac{e^2 n(\vec{r}) n(\vec{r'})}{4\pi\epsilon_0 |\vec{r}-\vec{r'}|}}_{\text{Hartree energy } E_H} \underbrace{-\frac{1}{2}\int d^4x \int d^4x' \, \frac{e^2 \rho^{(1)}(\vec{x},\vec{x'})\rho^{(1)}(\vec{x'},\vec{x})}{4\pi\epsilon_0|\vec{r}-\vec{r'}|}}_{\text{exchange energy } E_X} \\ & - \sum_{i,j} \Lambda_{j,i} \underbrace{\left(\langle\varphi_i|\varphi_j\rangle - \delta_{i,j}\right)}_{\text{orthogonality constraint}} - \mu \underbrace{\left(\mathrm{Tr}\left[\hat{\rho}^{(1)}\right] - N\right)}_{\text{particle-number constraint}} \Bigg\} \end{aligned} \tag{F.2}$$

The N-representability constraint $0 \le f_n \le 1$ can, for example, be enforced by representing the occupation by $f_n = \sin^2(\gamma_n)$. Then the unrestricted variables γ_n are varied to scan the occupations in the permitted range.
Because the energy expression is valid only for single Slater determinants, the final occupations must be either zero or one. This implies, that the variation of the occupations should be suppressed. Allowing fractional occupations $f_n \notin \{0,1\}$ implies to impose an additional approximation, the mean-field approximation. This is a subtle point, that is discussed in section 2.4 below.

The matrix $\mathbf{\Lambda}$ are the Lagrange multipliers for the orthogonality constraint of the natural orbitals. We will see later that the eigenvalues of $\mathbf{\Lambda}$ are related to the one-particle energies.

The chemical potential μ is the Lagrange multiplier for the particle-number constraint. Note that $\mathrm{Tr}[\hat{\rho}^{(1)}] = \sum_n f_n$.

Minimum condition: Let me denote the term in the curly brackets of Eq. F.2 as $\mathcal{E}_N^{HF}[\{|\varphi_j\rangle, f_j\}]$. As elaborated below, the minimum condition of $\mathcal{E}_N^{HF}$. with respect to a variation of the one-particle orbitals $|\varphi_n\rangle$ is

$$0 \overset{!}{=} \frac{1}{f_n}\frac{\partial \mathcal{E}^{HF}}{\partial\langle\varphi_n|} = \underbrace{\left[\hat{h} + \hat{V}_H + \hat{V}_X\right]}_{\text{Fock operator } \hat{F}} |\varphi_n\rangle - |\varphi_n\rangle\mu - \sum_m |\varphi_m\rangle \Lambda_{m,n}\frac{1}{f_n} \tag{F.3}$$

where $\hat{F}$ is the **Fock operator**.

FOCK OPERATOR

$$\hat{F} \overset{\text{def}}{=} \hat{h} + \hat{V}_H + \hat{V}_X$$
$$= \hat{h} + \overbrace{\int d^4x \left|\vec{x}\right\rangle \underbrace{\int d^3r' \frac{e^2 n(\vec{r'})}{4\pi\epsilon_0|\vec{r}-\vec{r'}|}}_{v_H(\vec{r})} \left\langle\vec{x}\right|}^{\hat{V}_H} - \overbrace{\int d^4x \int d^4x' \left|\vec{x}\right\rangle \underbrace{\frac{e^2\rho^{(1)}(\vec{x},\vec{x'})}{4\pi\epsilon_0|\vec{r}-\vec{r'}|}}_{-v_X(\vec{x},\vec{x'})} \left\langle\vec{x'}\right|}^{\hat{V}_X} \quad \text{(F.4)}$$

The Fock operator is a one-particle operator, which depends on density and one-particle-reduced density matrix.

The Fock operator defines an **effective potential** $\hat{V}_{eff}$

$$\hat{F} = \hat{T} + \hat{V}_{ext} + \hat{V}_H + \hat{V}_X = \hat{T} + \hat{V}_{eff} \quad \text{(F.5)}$$

I used the symbol $\hat{T}$ to denote the kinetic-energy operator and $\hat{V}_{ext}$ to denote the external-potential operator, which typically is the Coulomb potential of the nuclei. Because of the exchange term, the effective potential is a non-local potential $\hat{V}_{eff} = \int d^4x \int d^4x' \, |\vec{x}\rangle v_{eff}(\vec{x},\vec{x'})\langle\vec{x}|$.

In order to arrive at Eq. F.3, let me work out the derivatives of the individual terms of the total energy functional Eq. F.2:

- The derivative of the energy E_{1P} from the non-interacting Hamiltonian $\hat{h}$ is[2]Eqs. 2.38,2.41

$$\frac{1}{f_n}\frac{\partial E_{1P}}{\partial\langle\varphi_n|} = \text{Tr}\left[\underbrace{\frac{\partial E_{1P}}{\partial\hat{\rho}^{(1)}}}_{\hat{h}} \frac{1}{f_n}\frac{\partial\hat{\rho}^{(1)}}{\partial\langle\varphi_n|}\right] = \text{Tr}\left[\hat{h}\,\frac{1}{f_n}\underbrace{\frac{\partial}{\partial\langle\varphi_n|}\overbrace{\sum_j |\varphi_j\rangle f_j\langle\varphi_j|}^{\hat{\rho}^{(1)}}}_{|\varphi_n\rangle f_n}\right] = \hat{h}|\varphi_n\rangle \quad \text{(F.8)}$$

- The derivative of the Hartree energy E_H is

$$\frac{1}{f_n}\frac{\partial E_H}{\partial\langle\varphi_n|} = \int d^3r \underbrace{\frac{dE_H}{dn(\vec{r})}}_{v_H(\vec{r})} \frac{1}{f_n}\frac{\partial n(\vec{r})}{\partial\langle\varphi_n|} \overset{\text{Eq. 2.38}}{=} \int d^3r \, v_H(\vec{r}) \frac{1}{f_n}\underbrace{\frac{\partial}{\partial\langle\varphi_n|}\overbrace{\sum_\sigma\sum_j \langle\vec{x}|\varphi_j\rangle f_j\langle\varphi_j|\vec{x}\rangle}^{n(\vec{r})}}_{\sum_\sigma |\vec{x}\rangle\langle\vec{x}|\varphi_n\rangle f_n}$$
$$= \underbrace{\sum_\sigma \int d^3r \, |\vec{x}\rangle v_H(\vec{r})\langle\vec{x}|\,\varphi_n\rangle}_{\hat{V}_H} = \hat{V}_H|\varphi_n\rangle \quad \text{(F.9)}$$

[2]The derivative with respect to a matrix is defined as follows:

$$dE = \sum_{i,j}\frac{\partial E(\boldsymbol{a})}{\partial a_{i,j}} da_{i,j} = \text{Tr}\left[\frac{\partial E(\boldsymbol{a})}{\partial \boldsymbol{a}} d\boldsymbol{a}\right] \Rightarrow \left(\frac{\partial E}{\partial \boldsymbol{a}}\right)_{i,j} \overset{\text{def}}{=} \frac{\partial E}{\partial \boldsymbol{a}_{j,i}} \quad \text{(F.6)}$$

Notice that the order of the indices in the definition is swapped. This corresponds to the so-called "numerator-layout notation".(see `https://en.wikipedia.org/wiki/Matrix_calculus`) There is also another notation called "denominator-layout notation", which will not be used here.

The derivative with respect to an operator is defined analogously to the matrix case, so that

$$dE = \text{Tr}\left[\frac{\partial E(\hat{a})}{\partial \hat{a}} d\hat{a}\right] \quad \text{(F.7)}$$

- The derivative of the exchange energy E_X is

$$\begin{aligned}\frac{1}{f_n}\frac{\partial E_X}{\partial\langle\varphi_n|} &= \int d^4x \int d^4x' \underbrace{\frac{dE_X}{d\rho^{(1)}(\vec{x},\vec{x'})}}_{v_X(\vec{x'},\vec{x})} \frac{1}{f_n}\frac{\partial\rho^{(1)}(\vec{x},\vec{x'})}{\partial\langle\varphi_n|} \\ &\overset{\text{Eq. 2.41}}{=} \int d^4x \int d^4x' \; v_X(\vec{x'},\vec{x})\frac{1}{f_n}\underbrace{\frac{\partial}{\partial\langle\varphi_n|}\sum_j \langle\vec{x}|\varphi_j\rangle f_j\langle\varphi_j|\vec{x'}\rangle}_{\sum_\sigma |\vec{x'}\rangle\langle\vec{x}|\varphi_n\rangle f_n} \\ &= \underbrace{\int d^4x \int d^4x' \; |\vec{x'}\rangle v_X(\vec{x'},\vec{x})\langle\vec{x}\,|}_{\hat{V}_X}|\varphi_n\rangle = \hat{V}_X|\varphi_n\rangle \end{aligned} \tag{F.10}$$

  I recommend to carefully inspect the order of the indices in the derivative of the exchange energy with the density matrix $\rho^{(1)}(\vec{x},\vec{x'})$ and those in $v_X(\vec{x'},\vec{x})$.

- Derivative of the orthonormality constraint:

$$\frac{1}{f_n}\frac{\partial}{\partial\langle\varphi_n|}\Big(-\sum_{i,j}\Lambda_{j,i}\left[\langle\varphi_i|\varphi_j\rangle-\delta_{i,j}\right]\Big) = -\sum_j |\varphi_j\rangle\Lambda_{j,n}\frac{1}{f_n} \tag{F.11}$$

- Derivative of the particle-number constraint:

$$\frac{1}{f_n}\frac{\partial}{\partial\langle\varphi_n|}\Big[-\mu\Big(\mathrm{Tr}\big[\hat{\rho}^{(1)}\big]-N\Big)\Big] = \frac{1}{f_n}\frac{\partial}{\partial\langle\varphi_n|}\Big[-\mu\Big(\sum_j f_j\langle\varphi_j|\varphi_j\rangle-N\Big)\Big] = -|\varphi_n\rangle\mu \tag{F.12}$$

These five derivatives are then combined to yield Eq. F.3, which, in turn, determines the Fock operator $\hat{F}$ in Eq. F.4.

The derivatives with respect to the occupation variables γ_n are determined analogously.

Self-consistency: For a given Fock operator, the system of equations can be solved by matrix diagonalization

$$\hat{F}|\varphi_n\rangle = |\varphi_n\rangle\epsilon_n \tag{F.13}$$

which yields the eigenstates $|\varphi_n\rangle$ and the one-particle energies ϵ_n. The matrix of Lagrange multipliers has the simple form $\Lambda_{m,n}\frac{1}{f_n} = \epsilon_n\delta_{m,n}$.

The Fock operator changes with changing density and one-particle reduced density matrix and, thus, with the orbitals.

This implies that one needs to solve the following system of equations

- The eigenvalue equation Eq. **??** with the Fock operator Eq. F.4 expressed in terms of Hartree and exchange potentials $\hat{V}_H$ and $\hat{V}_X$,

- Eq. F.1, which provides the density matrix $\rho^{(1)}$ and the density n from the orbitals $|\varphi_n\rangle$ and their occupations.

- Eq. 2.38 and Eq. 2.41, which provide the Hartree potential $\hat{V}_H$ and the exchange potential $\hat{V}_X$ from the density n and the density matrix $\rho^{(1)}$.

Fock operator and total energy: As we will see below, the Fock operator describes the spectral properties, but it does not provide directly the total energy as its expectation value.

$$E_{\text{tot}} \neq \langle\Phi|\hat{F}|\Phi\rangle \tag{F.14}$$

However, comparing the expectation value of the Fock operator with the total energy expression Eq. 2.35 or Eq. F.130, we find

$$E_{\text{tot}} = \langle\Phi|\frac{1}{2}\Big(\hat{h}+\hat{F}\Big)|\Phi\rangle = \sum_n f_n\langle\varphi_n|\frac{1}{2}\Big(\hat{h}+\hat{F}\Big)|\varphi_n\rangle \tag{F.15}$$

A similar expression, the **Migdal-Galitskii-Koltun sum rule** Eq. 8.36, is also valid for interactions of arbitrary strength. The Migdal-Galitskii-Koltun sum rule can be rewritten in the form Eq. 8.37, which is closer to the expression given above.

F.2 Contributions to exchange

While the Hartree energy has a very transparent physical interpretation, the exchange term is less accessible. The exchange is not only important in the Hartree-Fock approximation. Also in an approximation of many-particle theory, the random-phase approximation, the potential acting on the electrons can be represented by an exchange term, albeit with a screened interaction instead of the bare Coulomb potential. Another use is in a class of density functionals, the hybrid functionals which represent part of the exchange-correlation energy by a Fock term.

F.2.1 Decompose the exchange term into local orbitals

Let me express the exchange term in local orbitals $|\chi_\alpha\rangle$. The occupied one-particle wave function are expanded in these local orbitals

$$|\varphi_n\rangle = \sum_\alpha |\chi_\alpha\rangle c_{\alpha,n} \tag{F.16}$$

and the one-particle-reduced density matrix has the form

$$\hat{\rho}^{(1)} = \sum_n |\varphi_n\rangle f_n\langle\varphi_n| = \sum_{\alpha,\beta} |\chi_\alpha\rangle\rho^{(1)}_{\alpha,\beta}\langle\chi_\beta| \tag{F.17}$$

The exchange energy can be expressed by the matrix elements of the density matrix and the Coulomb matrix elements in local orbitals, called the four-center integrals.

$$\begin{aligned}
E_X &\overset{\text{Eq. 2.40}}{=} -\frac{1}{2}\sum_{m,n} f_m f_n \int d^4x \int d^4x' \, \frac{e^2\varphi^*_m(\vec{x})\varphi^*_n(\vec{x'})\varphi_n(\vec{x})\varphi_m(\vec{x'})}{4\pi\epsilon_0|\vec{r}-\vec{r'}|} \\
&= -\frac{1}{2}\sum_{\alpha,\beta,\gamma,\delta} \rho^{(1)}_{\alpha,\beta}\rho^{(1)}_{\gamma,\delta} \int d^4x \int d^4x' \, \frac{e^2\chi^*_\beta(\vec{x})\chi^*_\delta(\vec{x'})\chi_\gamma(\vec{x})\chi_\alpha(\vec{x'})}{4\pi\epsilon_0|\vec{r}-\vec{r'}|} \\
&= -\frac{1}{2}\sum_{\alpha,\beta,\gamma,\delta} \rho^{(1)}_{\alpha,\beta}\rho^{(1)}_{\gamma,\delta} W_{\beta,\delta,\gamma,\alpha} \\
\text{with} \qquad W_{\beta,\delta,\gamma,\alpha} &= \int d^4x \int d^4x' \, \frac{e^2\chi^*_\beta(\vec{x})\chi^*_\delta(\vec{x'})\chi_\gamma(\vec{x})\chi_\alpha(\vec{x'})}{4\pi\epsilon_0|\vec{r}-\vec{r'}|}
\end{aligned} \tag{F.18}$$

Compare the definition of the Coulomb matrix element given here with Eq. 3.51.

Two contributions will be of interest: The contribution E_X to the energy, and secondly to the one-particle spectrum of the electrons. The shift $\Delta\epsilon_n$ of the one-particle level ϵ_n due to exchange can be written as

$$\Delta\epsilon_n = \frac{\partial E_X}{\partial f_n} = -\sum_{\alpha,\beta}\langle\psi_n|\pi_\beta\rangle\Big(\sum_{\gamma,\delta} W_{\beta,\delta,\gamma,\alpha}\rho^{(1)}_{\gamma,\delta}\Big)\langle\pi_\alpha|\psi_n\rangle \tag{F.19}$$

where $|\pi_\alpha\rangle$ is the projector function for the local orbitl $|\chi_\alpha\rangle$.

F.2.2 Long-range exchange

Let me consider large distances, that is distances $|\vec{r}-\vec{r'}|$ so large hat the orbitals connected to different coordinates do not overlap.

For each orbital $|\chi_\alpha\rangle$, I define the position of the atom, on which it is centered as $\vec{R}_\alpha$. In order to approximate the position of the density of a product of two orbitals, let me furthermore define

$$\vec{R}_{\alpha,\beta} = \frac{1}{2}\Big(\vec{R}_\alpha + \vec{R}_\beta\Big) \tag{F.20}$$

$$\begin{aligned} E_X &\approx -\frac{1}{2}\sum_{\alpha,\beta,\gamma,\delta}\rho^{(1)}_{\alpha,\beta}\rho^{(1)}_{\gamma,\delta}\frac{e^2}{4\pi\epsilon_0|\vec{R}_{\beta,\gamma}-\vec{R}_{\alpha,\delta}|}\underbrace{\Big(\int d^4x\;\chi^*_\beta(\vec{x})\chi_\gamma(\vec{x})\Big)}_{O_{\beta,\gamma}}\underbrace{\Big(\int d^4x'\;\chi^*_\delta(\vec{x'})\chi_\alpha(\vec{x'})\Big)}_{O_{\delta,\alpha}} \\ &= -\frac{1}{2}\sum_{\alpha,\beta,\gamma,\delta}\rho^{(1)}_{\alpha,\beta}O_{\beta,\gamma}\rho^{(1)}_{\gamma,\delta}O_{\delta,\alpha}\frac{e^2}{4\pi\epsilon_0|\vec{R}_{\beta,\gamma}-\vec{R}_{\alpha,\delta}|} \end{aligned} \tag{F.21}$$

For an orthonormal basisset ($O_{\alpha,\beta}=\delta_{\alpha,\beta}$) this expression becomes even simpler, namely

$$E_X = -\frac{1}{2}\sum_{\alpha,\gamma}\frac{e^2\rho^{(1)}_{\alpha,\gamma}\rho^{(1)}_{\gamma,\alpha}}{4\pi\epsilon_0|\vec{R}_{\gamma,\gamma}-\vec{R}_{\alpha,\alpha}|} \qquad \text{for } O_{\alpha,\beta}=\delta_{\alpha,\beta} \tag{F.22}$$

Apparently the range of the exchange term is linked to the range of the density matrix. This range is itself connected to the **coherence length**.

In order to understand the concept of coherence length let me consider again the free-electron gas. The one-particle-reduced density matrix of a free-electron gas is Editor: up to some factors

$$\rho^{(1)}(\vec{r},\vec{r'}) = C\int d^3k\;\theta(k_F-|\vec{k}|)e^{i\vec{k}(\vec{r}-\vec{r'})} \overset{\text{Eq. } E.21}{=} C\cdot\frac{4\pi}{3}k_F^3\left[-3\frac{\cos(k_Fs)}{(k_Fs)^2}+3\frac{\sin(k_Fs)}{(k_Fs)^3}\right] \tag{F.23}$$

where $s=|\vec{r}-\vec{r'}|$. The expression shows that the exchange term falls off with order $|\vec{R}-\vec{R}|^{-5}$. The number of terms increases proportional to $|\vec{R}-\vec{R}|^2$, so that the contribution from a given radius falls of like $|\vec{R}-\vec{R}|^{-3}$.

This implies that the decay of the exchange contributions is algebraic rather than exponential. This changes as soon as temperature is switched on. Let me do a dimensional argument: at finite temperature the temperature broadening is proportional to k_BT. This leads to a momentum broadening of $\Delta\epsilon = \frac{\partial\epsilon}{\partial|\vec{k}|}\Delta k_F = v_F\Delta k_F$, where v_F is the Fermi velocity. Let me estimate the coherence length ℓ_c as that distance where the thermally excited electrons and holes are out of phase, i.e. $(k_F+\frac{1}{2}\Delta k_F)\ell_c = (k_F-\frac{1}{2}\Delta k_F)\ell_c+\pi$. We obtain the estimate

$$\ell_c = \frac{\pi}{\Delta k_F} = \frac{v_F\pi}{k_BT} \tag{F.24}$$

Editor: work out values.

Not only temperature reduces the coherence length. While temperature creates electron-hole pairs, which destroy the coherence, also the interaction can induce electron-hole pairs which essentially have the same effect. However, here the term is described as screening the potential. Electron-hole pairs are formed which act against the interaction, so that the Coulomb potential in the exchange term is replaced by a Yukawa potential having an exponential decay.

For insulators the decay of the density matrix is more rapid. Editor: I need to find an intuitive argument.

F.2.3 On-site exchange

Evaluation of onsite Coulomb parameters

For pure angular momentum eigenstates the Coulomb matrix elements can be traced back to simple radial integrations.

We make the assumption that the orbitals are eigenstates of angular momentum and spin, i.e. they can be expressed in terms of radial functions $\mathcal{R}_\alpha(r)$, spherical harmonics $Y_{\ell,m}(\vec{r})$ and eigenstates of $\hat{S}_z$ as

$$\chi_\alpha(\vec{r},\sigma) = \delta_{\sigma,\sigma_\alpha}\mathcal{R}_\alpha(|\vec{r}|)Y_{\ell_\alpha,m_\alpha}(\vec{r}) \tag{F.25}$$

The angular momentum eigenstates are combined into one, i.e. $L = (\ell, m)$. The spherical harmonics are defined such that

$$\frac{1}{r^2}\int d^3r\ \delta(|\vec{r}|-r)Y_L^*(\vec{r})Y_{L'}(\vec{r}) = \delta_{L,L'} \tag{F.26}$$

We make use of the Gaunt coefficients $C_{L,L',L''}$ defined via

$$Y_L(\vec{r}) = \sum_{L',L''} C_{L,L',L''}Y_{L'}(\vec{r})Y_{L''}(\vec{r}) \tag{F.27}$$

Furthermore we use

$$Y_{-L}(\vec{r}) = Y_L^*(\vec{r}) \tag{F.28}$$

where $-L$ is a short hand for $\ell, -m$. Note that this relation differs for real spherical harmonics!

For a density in an angular momentum decomposition

$$\rho(\vec{r}) = \sum_{\ell,m}\rho_{\ell,m}(|\vec{r}|)Y_{\ell,m}(\vec{r}) \tag{F.29}$$

the electrostatic potential is(see Eq. 5.42 in ΦSX: Elektrodynamik[21])

$$\begin{aligned}\Phi(\vec{r} &= \int d^3r' \frac{\rho(\vec{r'})}{4\pi\epsilon_0|\vec{r}-\vec{r'}|} \\ &= \frac{1}{4\pi\epsilon_0}\sum_{\ell,m}\frac{4\pi}{2\ell+1}Y_{\ell,m}(\vec{r})\left\{r^\ell\int_r^\infty dr_0\ r_0^2 r_0^{-\ell-1}\rho_{\ell,m}(r_0) + r^{-\ell-1}\int_0^r dr_0\ r_0^2 r_0^\ell\rho_{\ell,m}(r_0)\right\}\end{aligned} \tag{F.30}$$

Now we can evaluate the Coulomb matrix element

$$\begin{aligned}U_{L,L',L'',L'''} &= \int d^3r\int d^3r'\ \frac{e^2\left(\mathcal{R}_\ell^*(r)Y_L^*(\vec{r})\right)\left(\mathcal{R}_{\ell'}^*(r')Y_{L'}^*(\vec{r'})\right)\left(\mathcal{R}_{\ell''}(r)Y_{L''}(\vec{r})\right)\left(\mathcal{R}_{\ell'''}(r')Y_{L'''}(\vec{r'})\right)}{4\pi\epsilon_0|\vec{r}-\vec{r'}|} \\ &= \sum_{\bar{L},\bar{L}'}C_{\bar{L},-L,L''}C_{\bar{L}',-L',L'''}\int d^3r\int d^3r'\ \frac{e^2\left(\mathcal{R}_\ell^*(r)\mathcal{R}_{\ell''}(r)Y_{\bar{L}}(\vec{r})\right)\left(\mathcal{R}_{\ell'}^*(r')\mathcal{R}_{\ell'''}(r')Y_{\bar{L}'}(\vec{r'})\right)}{4\pi\epsilon_0|\vec{r}-\vec{r'}|} \\ &= \sum_{\bar{L}}\frac{4\pi}{2\bar{\ell}+1}C_{\bar{L},L,L''}C_{\bar{L},L',L'''}F^L_{\ell,\ell',\ell'',l'''}\end{aligned} \tag{F.31}$$

with the so-called **Slater integrals** [3]

$$F^L_{\ell,\ell',\ell'',l'''} \stackrel{\text{def}}{=} \frac{e^2}{4\pi\epsilon_0}\int dr\; r^2 \int dr'\; r'^2\; \mathcal{R}^*_\ell(r)\mathcal{R}_{\ell''}(r)\frac{[\min(r,r')]^\ell}{[\max(r,r')]^{\ell+1}}\mathcal{R}^*_{\ell'}(r')\mathcal{R}_{\ell'''}(r') \tag{F.32}$$

Kanamori parameters

Let me now consider the opposite limit, namely that all four orbitals contributing to a given exchange term are located on the same atom.

Kanamori parameters[16]

$$\begin{aligned}
U &= \int d^4x \int d^4x' \; \frac{e^2\chi^*_m(\vec{x})\chi^*_m(\vec{x'})\chi^*_m(\vec{x})\chi^*_m(\vec{x'})}{4\pi\epsilon_0|\vec{r}-\vec{r'}|}\\
U' &= \int d^4x \int d^4x' \; \frac{e^2\chi^*_m(\vec{x})\chi^*_{m'}(\vec{x'})\chi^*_m(\vec{x})\chi^*_{m'}(\vec{x'})}{4\pi\epsilon_0|\vec{r}-\vec{r'}|}\\
J &= \int d^4x \int d^4x' \; \frac{e^2\chi^*_m(\vec{x})\chi^*_{m'}(\vec{x'})\chi^*_{m'}(\vec{x})\chi^*_m(\vec{x'})}{4\pi\epsilon_0|\vec{r}-\vec{r'}|}\\
J' &= \int d^4x \int d^4x' \; \frac{e^2\chi^*_m(\vec{x})\chi^*_m(\vec{x'})\chi^*_{m'}(\vec{x})\chi^*_{m'}(\vec{x'})}{4\pi\epsilon_0|\vec{r}-\vec{r'}|}
\end{aligned} \tag{F.33}$$

- Terms that describe the interaction of spherical densities
  - the largest term is the one with all four indices equal. This term favors that the electrons accumulate in few spatial and spin orbitals. It disfavors that the electrons distribute over many orbitals. If the electrons are in one spatial orbital, this term favors that the electrons have the same spin. This term is identified with the *intraband Coulomb parameter* U.
  - The second largest term is $L_\alpha = -L_\delta$ and $L_\beta = -L_\delta$, but $L_\alpha \neq L_\beta$, because each pair produces a spherical contribution to the density. There is only a contribution if $\sigma_\alpha = \sigma_\delta$ and $\sigma_\beta = \sigma_\gamma$. This term is identified with the *interband Coulomb parameter* U'.

Model for an atom

Let me make a model (See Eq. 9 of [113]) of the interaction energy of an atom, which has the form

$$\begin{aligned}
\hat{H} &= \frac{1}{2}\sum_{m,m',\sigma} U\hat{n}_{m,\sigma}\hat{n}_{m',-\sigma} + \frac{1}{2}\sum_{m,m',\sigma;m\neq m'}(U-J)\hat{n}_{m,\sigma}\hat{n}_{m',\sigma}\\
&= \underbrace{\frac{1}{2}\sum_{m,m',\sigma,\sigma'} U\hat{n}_{m,\sigma}\hat{n}_{m',\sigma'}}_{\text{Hartree energy}} \underbrace{-\frac{1}{2}\sum_{m,\sigma}U\hat{n}^2_{m,\sigma} - \frac{1}{2}\sum_\sigma\sum_{m,m'}J\hat{n}_{m,\sigma}\hat{n}_{m',\sigma} + \frac{1}{2}\sum_{m,\sigma}J\hat{n}^2_{m,\sigma}}_{\text{exchange energy}}\\
&= \frac{1}{2}U\Big(\sum_{m,\sigma}\hat{n}_{m,\sigma}\Big)^2 - \frac{1}{2}J\underbrace{\sum_\sigma\Big(\sum_m\hat{n}_{m,\sigma}\Big)^2}_{\frac{1}{2}(\hat{n}_\uparrow+\hat{n}_\downarrow)^2+\frac{1}{2}(\hat{n}_\uparrow-\hat{n}_\downarrow)^2}\underbrace{-\frac{1}{2}(U-J)\sum_{m,\sigma}\hat{n}^2_{m,\sigma}}_{\text{self-energy correction}}\\
&= \frac{1}{2}(U-\frac{1}{2}J)\hat{n}^2_t - \frac{1}{4}J\hat{n}^2_s \underbrace{-\frac{1}{2}(U-J)\sum_{m,\sigma}\hat{n}^2_{m,\sigma}}_{\text{self-energy correction}}
\end{aligned} \tag{F.34}$$

[3] Compare the notation with Tran et al.[112]

where

$$\begin{aligned}\hat{n}_t &= \sum_{m,\sigma} \hat{n}_{m,\sigma} \\ \hat{n}_\sigma &= \sum_{m} \hat{n}_{m,\sigma} \\ \hat{n}_s &= \hat{n}_\uparrow - \hat{n}_\downarrow \end{aligned} \tag{F.35}$$

In order to arrive at the mean-field approximation, I express each operator by its expectation value and the fluctuation operator about the expectation value.

$$\begin{aligned}\hat{H} = &\frac{1}{2}\Big(U - \frac{1}{2}J\Big)\Big(\hat{n}_t - \langle n_t\rangle\Big)^2 - \frac{1}{4}J\Big(\hat{n}_s - \langle n_s\rangle\Big)^2 - \frac{1}{2}(U-J)\sum_{m,\sigma}\Big(\hat{n}_{m,\sigma} - \langle n_{m,\sigma}\rangle\Big)^2 \\ &+ \Big[\frac{1}{2}(U - \frac{1}{2}J)\langle n_t\rangle\Big]\Big(\hat{n}_t - \langle n_t\rangle\Big) - \Big[\frac{1}{2}J\langle n_s\rangle\Big]\Big(\hat{n}_s - \langle n_s\rangle\Big) - \sum_{m,\sigma}\Big[(U-J)\langle n_{m,\sigma}\rangle\Big]\Big(\hat{n}_{m,\sigma} - \langle n_{m,\sigma}\rangle\Big) \\ &+ \frac{1}{2}(U - \frac{1}{2}J)\langle n_t\rangle^2 - \frac{1}{4}J\langle n_s\rangle^2 - \frac{1}{2}(U-J)\sum_{m,\sigma}\langle n_{m,\sigma}\rangle^2 \end{aligned} \tag{F.36}$$

The Hartree-Fock approximation amounts to ignoring the quadratic terms in the fluctuations. The terms linear in the fluctuation define the band structure, but do not affect the total energy, because the expectation value of the fluctuations vanish, i.e.

$$\Big\langle \hat{n} - \langle n\rangle \Big\rangle = 0\ . \tag{F.37}$$

Thus, the total energy of the Hartree-Fock term is the last line

$$E^{HF} = \frac{1}{2}\Big(U - \frac{1}{2}J\Big)\langle n_t\rangle^2 - \frac{1}{4}J\langle n_s\rangle^2 - \frac{1}{2}\Big(U - J\Big)\sum_{m,\sigma}\langle n_{m,\sigma}\rangle^2 \tag{F.38}$$

and the energy levels are obtained from the second line, the mean-field Hamiltonian

$$\begin{aligned}\hat{H}_{MF} &= \Big[(U - \frac{1}{2}J)\langle n_t\rangle\Big]\hat{n}_t - \Big[\frac{1}{2}J\langle n_s\rangle\Big]\hat{n}_s - \sum_{m,\sigma}\Big[(U-J)\langle n_{m,\sigma}\rangle\Big]\hat{n}_{m,\sigma} \\ &= \sum_{m,\sigma}\Big(U\langle n_t\rangle - J\langle n_\sigma\rangle - (U-J)\langle n_{m,\sigma}\rangle\Big)\hat{n}_{m,\sigma} \\ \epsilon_{m,\sigma} &= \Big(U\langle n_t\rangle - J\langle n_\sigma\rangle - (U-J)\langle n_{m,\sigma}\rangle\Big) \\ &= \sum_{m'(\neq m)}(U-J)\langle n_{m',\sigma}\rangle + \sum_{m'} U\langle n_{m',-\sigma}\rangle \end{aligned} \tag{F.39}$$

It can be shown that Janak's Theorem[74] holds, that is the one-particle energies are obtained as derivatives

$$\epsilon^{HF}_{m,\sigma} = \frac{\partial E^{HF}}{\partial n_{m,\sigma}} \tag{F.40}$$

of the mean-field total energy with respect to the corresponding average occupation.

The first term of $\epsilon_{m,\sigma}$, $U\langle n_t\rangle$, expresses that the one-particle energy levels shift as result of the Coulomb repulsion. The second term, $-J\langle n_\sigma\rangle$, describes Hund's rule, i.e. electrons are stabilized by other electrons with the same spin, because they avoid each other better than electrons with equal spin. The last term, $-(U-J)\langle n_{m,\sigma}\rangle$, describes that filled orbitals are stabilized with respect to unoccupied orbitals by $U-J$.

The last term, the self-interaction correction is the most important term of Hartree-Fock compared to the Kohn-Sham bandstructure of DFT. This term is responsible for ensuring Koopmanns'

theorem[114, 115], which says that the energy difference can be calculated from energy levels. In other words it says that

$$\frac{\partial \epsilon^{HF}_{m,\sigma}}{\partial n_{m_\sigma}} = 0 \qquad \text{for } 0 < n_{m,\sigma} < 1 \tag{F.41}$$

Note, however, that this equation is only valid for the derivatives with respect to the occupation on the *same* orbital!

This property follows from the fact that for isolated systems a state with fractional occupation is a classical mixture of two states (ensembles) with different particle numbers.

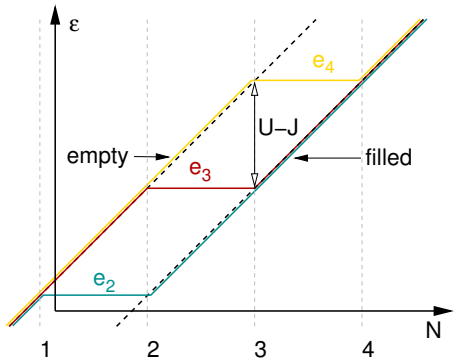

Fig. F.1: Energy level diagram of an atom with several degenerate atomic levels, that change only due to the Coulomb interaction. Occupied and unoccupied orbitals must be different, if the energy level, that receives an electron must not shift upon charging. The fact that the energy level remains constant upon charging reflects the fact that the energy is a sequence of piece-wise linear segments describing the coexistence of two ensembles with different particle numbers.

The self energy correction term makes sure that energy differences for different occupations can be estimated from the energy level differences as seen in Figure F.2.

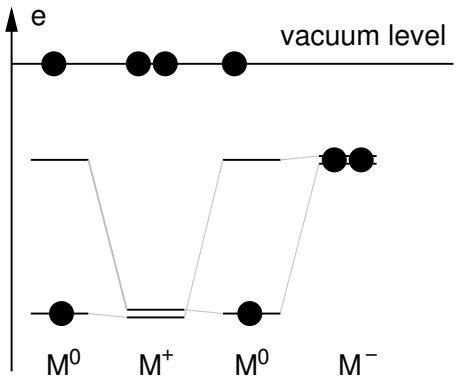

Fig. F.2: Schematic energy level of an atom in the Hartree-Fock approximation with two degenerate energy levels, that become different only via occupation. Note that the energy level, that changes its occupation remains fixed, while the other orbitals shift due to the coulomb interaction with the electron that is shifted around.

F.2.4 Bond-exchange

Let me consider a two-center bond. That is, the bonding orbital is polarized in one or the other bonding partner. The asymmetry is governed by the angle α. The bonding orbital $|\varphi_b\rangle$ and the antibonding orbital $|\varphi_a\rangle$ are

$$\begin{aligned} |\psi_b\rangle &= +|\chi_{1,\sigma}\rangle\cos(\alpha) + |\chi_{2,\sigma}\rangle\sin(\alpha) \quad \text{with occupation } f_b \\ |\psi_a\rangle &= -|\chi_{1,\sigma}\rangle\sin(\alpha) + |\chi_{2,\sigma}\rangle\cos(\alpha) \quad \text{with occupation } f_a \end{aligned} \tag{F.42}$$

$|\chi_1\rangle$ on the orbital on the left atom R_1 and $|\chi_2\rangle$ is the one on the right atom R_2.

A value of $\alpha = \pi/4 = 45°$ describes the symmetric case. In a half-filled system, i.e. $f_b = 1$ and $f_a = 0$,

- $\alpha = 0°$: the electron is localized on the left atom R_1
- $\alpha = 45°$: the electron is delocalized over both orbitals
- $\alpha = 90°$: the electron is localized on the right atom R_2.

The corresponding density matrix is

$$\begin{aligned} \boldsymbol{\rho} = \begin{pmatrix} \rho_{11} & \rho_{12} \\ \rho_{21} & \rho_{22} \end{pmatrix} &= \begin{pmatrix} f_b\cos^2(\alpha) + f_a\sin^2(\alpha) & (f_b - f_a)\cos(\alpha)\sin(\alpha) \\ (f_b - f_a)\cos(\alpha)\sin(\alpha) & f_b\sin^2(\alpha) + f_a\cos^2(\alpha) \end{pmatrix} \\ &= \frac{f_a + f_b}{2}\begin{pmatrix} 1 & 0 \\ 0 & 1 \end{pmatrix} + \frac{f_b - f_a}{2}\begin{pmatrix} \cos(2\alpha) & \sin(2\alpha) \\ \sin(2\alpha) & -\cos(2\alpha) \end{pmatrix} \end{aligned} \tag{F.43}$$

The exchange energy is

$$\begin{aligned} E_X &= -\frac{1}{2}\sum_{\alpha,\beta,\gamma,\delta} \rho^{(1)}_{\alpha,\beta}\rho^{(1)}_{\gamma,\delta} \int d^4x \int d^4x' \, \frac{e^2\chi^*_\beta(\vec{x})\chi^*_\delta(\vec{x'})\chi_\gamma(\vec{x})\chi_\alpha(\vec{x'})}{4\pi\epsilon_0|\vec{r} - \vec{r'}|} \\ &= -\frac{1}{2}\sum_{\alpha,\beta,\gamma,\delta} \rho^{(1)}_{\alpha,\beta}\rho^{(1)}_{\gamma,\delta} W_{\alpha,\beta,\gamma,\delta} \\ &= -\frac{1}{2}\sum_{\alpha=1}^{2} \underbrace{\rho^{(1)}_{\alpha,\alpha}\rho^{(1)}_{\alpha,\alpha} W_{\alpha,\alpha,\alpha,\alpha}}_{\text{onsite}} \\ &\quad -\frac{1}{2}\sum_{\alpha\neq\beta=1}^{2} \Big\{ \underbrace{\rho^{(1)}_{\alpha,\beta}\rho^{(1)}_{\beta,\alpha} W_{\beta,\alpha,\beta,\alpha}}_{\text{NDDO}} + \underbrace{\rho^{(1)}_{\alpha,\beta}\rho^{(1)}_{\alpha,\beta} W_{\beta,\beta,\alpha,\alpha} + \rho^{(1)}_{\alpha,\alpha}\rho^{(1)}_{\beta,\beta} W_{\alpha,\beta,\beta,\alpha}}_{\text{bondx}} \\ &\quad + \underbrace{\rho^{(1)}_{\alpha,\beta}\rho^{(1)}_{\beta,\beta} W_{\beta,\beta,\beta,\alpha} + \rho^{(1)}_{\beta,\alpha}\rho^{(1)}_{\beta,\beta} W_{\alpha,\beta,\beta,\beta} + \rho^{(1)}_{\beta,\beta}\rho^{(1)}_{\alpha,\beta} W_{\beta,\beta,\alpha,\beta} + \rho^{(1)}_{\beta,\beta}\rho^{(1)}_{\beta,\alpha} W_{\beta,\alpha,\beta,\beta}}_{\text{31 terms}} \Big\} \end{aligned} \tag{F.44}$$

Let me exploit the symmetry of the four-center integrals $W_{\alpha,\beta,\gamma,\delta}$:

$$W_{\alpha,\beta,\gamma,\delta} = W_{\beta,\alpha,\delta,\gamma} = W^*_{\gamma,\delta,\alpha,\beta} = W^*_{\delta,\gamma,\beta,\alpha} \tag{F.45}$$

For real-valued orbitals, where $\chi^*_\alpha(\vec{r})\chi_\beta(\vec{r}) = \chi^*_\beta(\vec{r})\chi_\alpha(\vec{r})$, we can furthermore exploit

$$\begin{aligned} W_{\alpha,\beta,\gamma,\delta} &= W_{\gamma,\beta,\alpha,\delta} = W_{\alpha,\delta,\gamma,\beta} \\ &= W_{\delta,\alpha,\beta,\gamma} = W_{\beta,\gamma,\delta,\delta} \\ &= W^*_{\alpha,\delta,\gamma,\beta} = W^*_{\gamma,\beta,\alpha,\delta} \\ &= W^*_{\beta,\gamma,\delta,\alpha} = W^*_{\delta,\alpha,\beta,\gamma} \end{aligned} \tag{F.46}$$

With these simplifications, we arrive at

$$E_X = \underbrace{-\frac{1}{2}\rho^{(1)}_{1,1}\rho^{(1)}_{1,1}W_{1,1,1,1} - \frac{1}{2}\rho^{(1)}_{2,2}\rho^{(1)}_{2,2}W_{2,2,2,2}}_{\text{onsite}}$$
$$\underbrace{-\rho^{(1)}_{1,2}\rho^{(1)}_{2,1}W_{1,2,1,2}}_{\text{NDDO}} \underbrace{-2\rho^{(1)}_{1,2}\rho^{(1)}_{1,2}W_{1,1,2,2}}_{\text{bondx}} \underbrace{-2\rho^{(1)}_{1,2}\rho^{(1)}_{2,2}W_{1,2,2,2} - 2\rho^{(1)}_{1,2}\rho^{(1)}_{1,1}W_{2,1,1,1}}_{\text{31-terms}} \tag{F.47}$$

Let me now insert the density matrix Eq. F.43

$$E_X = \underbrace{-\frac{1}{8}\Big((f_b+f_a)+(f_b-f_a)\cos(2\alpha)\Big)^2 W_{1,1,1,1} - \frac{1}{8}\Big((f_b+f_a)-(f_b-f_a)\cos(2\alpha)\Big)^2 W_{2,2,2,2}}_{\text{onsite}}$$
$$\underbrace{-\frac{1}{4}(f_b-f_a)^2\sin^2(2\alpha)\Big(W_{1,2,1,2}+2W_{1,1,2,2}\Big)}_{\text{NDDO}\quad\text{bondx}}$$
$$\underbrace{-\frac{1}{2}(f_b-f_a)\sin(2\alpha)\Big[\Big((f_b+f_a)-(f_b-f_a)\cos(2\alpha)\Big)W_{1,2,2,2}+\Big((f_b+f_a)+(f_b-f_a)\cos(2\alpha)\Big)W_{2,1,1,1}\Big)}_{\text{31-terms}} \tag{F.48}$$

Let me now calculate the shift of the band edges due to the exchange term for $f_b = 1$ and $f_a = 0$

$$\Delta\epsilon_a = \underbrace{-\frac{1}{4}\overbrace{\Big(1-\cos^2(2\alpha)\Big)}^{\sin^2(2\alpha)}W_{1,1,1,1} - \frac{1}{4}\overbrace{\Big(1-\cos^2(2\alpha)\Big)}^{\sin^2(2\alpha)}W_{2,2,2,2}}_{\text{onsite}}$$
$$+\frac{1}{2}\sin^2(2\alpha)\Big(\underbrace{W_{1,2,1,2}}_{\text{NDDO}}+\underbrace{2W_{1,1,2,2}}_{\text{bondx}}\Big)\underbrace{-\sin(2\alpha)\cos(2\alpha)\Big(W_{1,2,2,2}-W_{2,1,1,1}\Big)}_{\text{31-terms}} \tag{F.49}$$
$$\Delta\epsilon_b = \underbrace{-\frac{1}{8}\Big(1+\cos(2\alpha)\Big)^2 W_{1,1,1,1} - \frac{1}{8}\Big(1-\cos(2\alpha)\Big)^2 W_{2,2,2,2}}_{\text{onsite}}$$
$$-\frac{1}{2}\sin^2(2\alpha)\Big(\underbrace{W_{1,2,1,2}}_{\text{NDDO}}+\underbrace{2W_{1,1,2,2}}_{\text{bondx}}\Big)$$
$$\underbrace{-\sin(2\alpha)\Big(W_{1,2,2,2}+W_{1,2,2,2}\Big)+\sin(2\alpha)\cos(2\alpha)\Big(W_{1,2,2,2}-W_{1,2,2,2}\Big)}_{\text{31-terms}} \tag{F.50}$$

- Left-right correlation: Left-right correlation describes the tendency of electrons to localize on opposite sides of a bond, in order to reduce the energy cost of their Coulomb repulsion. Considering a symmetric bond, the onsite terms have the form

$$E_X = -\frac{W_{1111}}{4}\Big((f_a+f_b)^2+(f_b-f_a)^2\cos^2(2\alpha)\Big) \tag{F.51}$$

  This term favors the polarization of the bond to one or the other side.

  There is, however, a competition between the kinetic energy and this exchange term. The bond polarization destroys the delocalization of the electron over both bond partners and thus the chemical bond. A hydrogen molecule, the Hubbard dimer, undergoes a phase transition to an antiferromagnetic structure beyond a certain strength of the interaction. In the antiferromagnetic configuration, the spin-up electron is one atom and the spin-down electron is on the other atom. A weak delocalization to the other atom is still present. The spin-up electron can polarize in one or the other direction. Each of these two configurations can be described by a Slater determinant. The fully correlated state is a superposition of these two Slater determinants, resulting in a spin-singlet state with antiferromagnetic correlations.

- The term denoted NDDO describes the exchange term due to the intersite Coulomb interaction. The term favors $\alpha = 45°$, that is, it it favors a symmetric bond with delocalized electrons. This term is closely related to the kinetic energy $E_{\text{kin}} = -t(f_b - f_a)\sin(2\alpha)$. The terms (NDDO+BONDX) can be expressed as $E_X^{NDDO+BONDX} = -\frac{W_{1212}+2W_{1,1,22}}{4t^2} E_{\text{kin}}^2$.

  The term is sensitive to the phase shift of bonding and antibonding orbitals, and it tends to open up the band gaps which are due to covalent bond formation.

- The terms denoted *31-terms* open up the band gap for ionic bonds. The 31-terms do not shift the empty orbital in a symmetric bond. The empty orbital is shifted up when the bond is strongly polarized, while the effect vanishes for a completely polarized ?????.

  In a simple approximation (the density of the orbitals form a homogeneously charged sphere) the matrix elements can be related to the radius of the orbitals. $W_{1222} = \frac{Q_{12}}{r_2}$ $W_{2111} = \frac{Q_{12}}{r_1}$. Therefore, the level shift due to the 31 term is $\frac{1}{2}\sin(4\alpha)Q_{12}\left(\frac{1}{r_2} - \frac{1}{r_1}\right)$. Thus, the conduction band is shifted up if the bond is polarized towards the more extended orbital, which it is shifted down, if the orbital is polarized towards the more localized orbital.

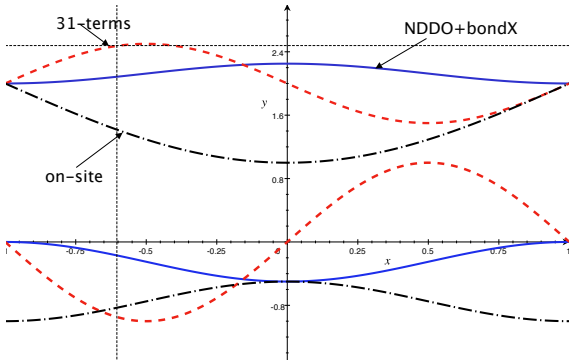

Fig. F.3: Shift of the band edges due to different exchange terms. full line in blue: NDDO+BONDX Red dash-dotted line: 31-terms and black dashed lines: symmetric onsite term. Empty states are shifted up for better visibility. Each term must be scaled by the respective matrix elements.

F.3 Double occupancy

In Eq. F.137 on p. 510 I investigated the terms of the interaction that are ignored in the mean-field approximation. The second term in this expression described an effect of occupation-number fluctuations. Here I want to consider a pair of these terms and investigate its role when a double occupancy is specified. The underlying idea is that this second term, which is absent in the mean-field expression, describes important correlation effects. These can be described by the repulsion of electrons in strongly interacting orbitals.

Consider two natural orbitals and probabilities P_{σ_a,σ_b}. Let me define the **double occupation** $d_{ab} \stackrel{\text{def}}{=} P_{\bar{\sigma}\sigma_a\sigma_b}$ which, in our case, equals $d = P_{11}$. For a given set of occupations (f_a, f_b) and a specified double occupation we obtain the probabilities as

$$\begin{aligned} P_{00} + P_{10} + P_{01} + P_{11} &= 1 \\ P_{10} + P_{11} &= f_a \\ P_{01} + P_{11} &= f_b \\ P_{11} &= d \end{aligned} \tag{F.52}$$

so that

$$P_{00} = 1 + d - f_1 - f_2; \qquad P_{10} = f_1 - d; \qquad P_{01} = f_2 - d \qquad \text{and} \qquad P_{11} = d \tag{F.53}$$

The double occupations cannot be chosen arbitrary. The requirement that all probabilities must be positive, leads to the following conditions

$$\begin{aligned} \max(0, f_1 + f_2 - 1) \leq d \leq \min(f_1, f_2) \\ -\min\Big(f_1 f_2, (1-f_1)(1-f_2)\Big) \leq d - f_1 f_2 \leq \min\Big(f_1(1-f_2), (1-f_1) f_2\Big) \end{aligned} \tag{F.54}$$

$$\begin{aligned} &\frac{1}{2}\sum_{m,n=1}^{\infty} \underbrace{\left(\sum_{\vec{\sigma}} P_{\vec{\sigma}}(\sigma_m - f_m)(\sigma_n - f_n)\right)}_{\left(\sum_{\vec{\sigma}} P_{\vec{\sigma}}\sigma_m\sigma_n\right) - f_m f_n} \Big(\langle\varphi_m,\varphi_n|\hat{W}|\varphi_m,\varphi_n\rangle - \langle\varphi_m,\varphi_n|\hat{W}|\varphi_n,\varphi_m\rangle\Big) \\ &\geq -\frac{1}{2}\sum_{m\neq n} \min\left\{f_m f_n, (1-f_m)(1-f_m)\right\} \Big(\langle\varphi_m,\varphi_n|\hat{W}|\varphi_m,\varphi_n\rangle - \langle\varphi_m,\varphi_n|\hat{W}|\varphi_n,\varphi_m\rangle\Big) \end{aligned} \tag{F.55}$$

F.4 Exact properties of the exchange-correlation hole

F.4.1 Bounds for the exchange-correlation hole

The lower bound of the exchange-correlation hole is

$$\begin{aligned} & & 0 \leq n^{(2)}(\vec{r},\vec{r}') &= n^{(1)}(\vec{r})\Big[n^{(1)}(\vec{r}') + h_{xc}(\vec{r},\vec{r}')\Big] \\ & \overset{n^{(1)}\geq 0}{\Rightarrow} & 0 \leq & \quad n^{(1)}(\vec{r}') + h_{xc}(\vec{r},\vec{r}') \\ \Rightarrow & & -n^{(1)}(\vec{r}') \leq & \quad h_{xc}(\vec{r},\vec{r}') \end{aligned} \tag{F.56}$$

Editor: Is there an upper bound $h_{xc}(\vec{r},\vec{r}') \leq 0$? It could be derived analogously from $n^{(2)}(\vec{r},\vec{r}') \leq n^{(1)}(\vec{r})n^{(1)}(\vec{r}')$, if the latter were a true statement.

F.5 Self-consistent Hartree-Fock code for finite temperatures

Below, I discuss how a Hartree-Fock code can be built for a finite system with known matrix elements for the non-interacting Hamiltonian and known interaction matrix elements. The code is built for demonstration purposes. It is simple, but neither efficient nor robust.

The code works at finite temperatures.

F.5.1 Theoretical background

At finite temperature T, the grand potential is, expressed as functional of the one-particle-reduced density matrix $\boldsymbol{\rho}^{(1)}$,

$$\begin{aligned} \Omega^{HF}_{T,\mu}[\boldsymbol{\rho}^{(1)}] = &\underbrace{\sum_{\alpha,\beta} h^{(0)}_{\alpha,\beta}\rho^{(1)}_{\beta,\alpha} + \frac{1}{2}\sum_{\alpha,\beta,\gamma,\delta}\Big(W_{\alpha,\beta,\gamma,\delta} - W_{\alpha,\beta,\delta,\gamma}\Big)\rho^{(1)}_{\gamma,\alpha}\rho^{(1)}_{\delta,\beta}}_{E_{\text{tot}}} \\ &+ \underbrace{k_B T\ \mathrm{Tr}\left[\boldsymbol{\rho}^{(1)}\ln(\boldsymbol{\rho}^{(1)}) + (\mathbf{1}-\boldsymbol{\rho}^{(1)})\ln(\mathbf{1}-\boldsymbol{\rho}^{(1)})\right]}_{-TS} \underbrace{-\mu\mathrm{Tr}[\boldsymbol{\rho}^{(1)}]}_{-\mu N} \end{aligned} \tag{F.57}$$

1. The first term describes the kinetic energy and the potential energy contribution from the interaction with the atom cores. The non-interacting Hamiltonian $\boldsymbol{h}^{(0)}$ contains the orbital energies on the diagonal and the hopping matrix elements on the off-diagonal elements.
2. The second term describes the electron-electron interaction with the interaction tensor is $\boldsymbol{W}$. It is divided into the Hartree energy (first) and the exchange energy (second).
3. The third term describes the heat bath, which exchanges heat with the electrons. For a single Slater determinant, this term would vanish, because the occupations are all either zero or one. We use the entropy expression of non-interacting electrons. This heat bath extends Hartree-Fock theory to finite temperatures.[4]
4. The fourth and last term is the particle reservoir.

The domain[5] of this free-energy functional are all hermitian matrices $\boldsymbol{\rho}$ in the one-particle Hilbert space with eigenvalues between zero and one.[27].

The derivative of the grand potential is

$$\frac{\partial \Omega_{T,\mu}[\boldsymbol{\rho}^{(1)}]}{\partial \rho^{(1)}_{u,v}} = \underbrace{h^{(0)}_{v,u} + \sum_{\alpha,\gamma}\Big(W_{\alpha,v,\gamma,u} - W_{\alpha,v,u,\gamma}\Big)\rho^{(1)}_{\gamma,\alpha}}_{h^{out}} + k_B T\left\{\ln\Big[\boldsymbol{\rho}^{(1)}(\mathbf{1}-\boldsymbol{\rho}^{(1)})^{-1}\Big]\right\}_{v,u} - \mu\delta_{u,v} \tag{F.58}$$

$$\frac{\partial \Omega_{T,\mu}[\boldsymbol{\rho}^{(1)}]}{\partial \mu} = \underbrace{-\mathrm{Tr}[\boldsymbol{\rho}^{(1)}]}_{-N}\,. \tag{F.59}$$

$$\frac{\partial \Omega_{T,\mu}[\boldsymbol{\rho}^{(1)}]}{\partial T} = \underbrace{k_B \mathrm{Tr}\left[\boldsymbol{\rho}^{(1)}\ln(\boldsymbol{\rho}^{(1)}) + (\mathbf{1}-\boldsymbol{\rho}^{(1)})\ln(\mathbf{1}-\boldsymbol{\rho}^{(1)})\right]}_{-S} \tag{F.60}$$

A new one-particle Hamiltonian $\boldsymbol{h}^{out}$ has been introduced, which we call output Hamiltonian and which is defined by the density matrix via

$$h^{out}_{\alpha,\beta} \overset{\text{def}}{=} h^{(0)}_{\alpha,\beta} + \sum_{\gamma,\delta}\Big(W_{\delta,\alpha,\gamma,\beta} - W_{\delta,\alpha,\beta,\gamma}\Big)\rho^{(1)}_{\gamma,\delta}\,. \tag{F.61}$$

Effective Hamiltonian

Next, we express the density matrix as functional of an effective Hamiltonian $\boldsymbol{h}^{eff}$

$$\boldsymbol{\rho}^{(1)}[\boldsymbol{h}^{eff},\mu] \overset{\text{def}}{=} \left[1 + \mathrm{e}^{\beta(\boldsymbol{h}^{eff}-\mu\mathbf{1})}\right]^{-1}$$

$$\Leftrightarrow \quad \rho^{(1)}_{\alpha,\beta}[\boldsymbol{h}^{eff},\mu] = \sum_n \psi_{\alpha,n}\frac{1}{1+\mathrm{e}^{\beta(\epsilon_n-\mu)}}\psi^*_{\beta,n} \tag{F.62}$$

where the ϵ_n are the eigenvalues of the effective Hamiltonian $\boldsymbol{h}^{eff}$ and $\vec{\psi}_n$ are its eigenvectors.

This representation simplifies the derivatives of the reservoirs $-TS-\mu N$ considerably, because we can use

$$\boldsymbol{h}^{eff} \overset{\text{Eq. } F.62}{=} \mu\mathbf{1} - k_B T \ln\Big[\boldsymbol{\rho}^{(1)}(\mathbf{1}-\boldsymbol{\rho}^{(1)})^{-1}\Big] \tag{F.63}$$

which leads to

$$\frac{d\Omega_{T,\mu}[\boldsymbol{\rho}^{(1)}]}{d\rho^{(1)}_{u,v}} \overset{\text{Eq. } F.58}{=} \underbrace{h^{(0)}_{v,u} + \sum_{\alpha,\gamma}\Big(W_{\alpha,v,\gamma,u} - W_{\alpha,v,u,\gamma}\Big)\rho^{(1)}_{\gamma,\alpha}}_{h^{out}} - h^{eff}_{v,u} = h^{out}_{v,u} - h^{eff}_{v,u} \tag{F.64}$$

[4] The extension to an ensemble of a Slater determinant is questionable, because the electron-electron interaction is no more consistent with a model of an ensemble of Slater determinants.

[5] The domain of a functional is the set of arguments for which the functional is defined.

The condition, that this derivative vanishes, determines the minimum of the grand potential. Thus, for the physical density matrix, the output Hamiltonian is identical to the effective Hamiltonian. This is the so-called self-consistency condition of the Hartree-Fock method.

Derivative of the density matrix with respect to the effective Hamiltonian

Let me work out the derivative of the one-particle-reduced density matrix with respect to the effective Hamiltonian. We need to consider that the variation $d\boldsymbol{h}$ of the Hamiltonian does not commutate with the Hamiltonian $\boldsymbol{h}$. Therefore, let me calculate the changes $d\epsilon_n$ of eigenvalues and those, $d\vec{\psi}_n$, of the eigenvectors by perturbation theory.

Let me consider a Hamiltonian $\hat{h}$, which has eigenvalues ϵ_n and eigenstates $|\psi_n\rangle$. The response of the density matrix with respect to a change of the Hamiltonian is obtained as follows.

$$\begin{aligned}
\delta\epsilon_n &= \langle\psi_n|\delta\hat{h}|\psi_n\rangle \\
\delta|\psi_n\rangle &= \sum_{m,m\neq n}|\psi_m\rangle\frac{\langle\psi_m|\delta\hat{h}|\psi_n\rangle}{\epsilon_n-\epsilon_m} \qquad \text{(F.65)}\\
\delta\hat{\rho}^{(1)} &= \sum_n|\delta\psi_n\rangle f_n\langle\psi_n| + \sum_n|\psi_n\rangle f_n\langle\delta\psi_n| + \sum_n|\psi_n\rangle\delta f_n\langle\psi_n| \\
&\overset{\text{Eq. F.65}}{=} \sum_{n,m;m\neq n}|\psi_m\rangle\frac{\langle\psi_m|\delta\hat{h}|\psi_n\rangle}{\epsilon_n-\epsilon_m}f_n\langle\psi_n| + \sum_{n,m;m\neq n}|\psi_n\rangle f_n\frac{\langle\psi_m|\delta\hat{h}|\psi_n\rangle^*}{\epsilon_n-\epsilon_m}\langle\psi_m| \\
&\quad + \sum_n|\psi_n\rangle\underbrace{\left(-\left[\frac{1}{1+\mathrm{e}^{\beta(\epsilon_n-\mu)}}\right]^{-2}\beta(\delta\epsilon_n-\delta\mu)\mathrm{e}^{\beta(\epsilon_n-\mu)}\right)}_{=\delta f_n=\delta\left[1+\mathrm{e}^{\beta(\epsilon_n-\mu)}\right]^{-1}=-\beta f_n(1-f_n)(\delta\epsilon_n-\delta\mu)}\langle\psi_n| \\
&= \sum_{n,m;m\neq n}|\psi_m\rangle\frac{\langle\psi_m|\delta\hat{h}|\psi_n\rangle}{\epsilon_n-\epsilon_m}f_n\langle\psi_n| + \sum_{n,m;m\neq n}|\psi_n\rangle\frac{\langle\psi_n|\delta\hat{h}|\psi_m\rangle}{\epsilon_n-\epsilon_m}f_n\langle\psi_m| \\
&\quad -\beta\sum_n|\psi_n\rangle f_n(1-f_n)\Big(\langle\psi_n|\delta\hat{h}|\psi_n\rangle-\delta\mu\Big)\langle\psi_n| \\
&= \sum_{n,m;m\neq n}|\psi_n\rangle\langle\psi_n|\delta\hat{h}|\psi_m\rangle\frac{f_n-f_m}{\epsilon_n-\epsilon_m}\langle\psi_m| - \beta\sum_n|\psi_n\rangle\langle\psi_n|\delta\hat{h}|\psi_n\rangle f_n(1-f_n)\langle\psi_n| \\
&\quad +\delta\mu\,\beta\sum_n|\psi_n\rangle f_n(1-f_n)\langle\psi_n| \\
\frac{\partial\rho^{(1)}_{\alpha,\beta}[\boldsymbol{h}^{eff},\mu]}{\partial h^{eff}_{\gamma,\delta}} &= \sum_{m,n}\psi_{\alpha,n}\psi^*_{\beta,m}\psi^*_{\gamma,n}\psi_{\delta,m}\begin{cases}(f_n-f_m)/(\epsilon_n-\epsilon_m) & \text{for } \epsilon_n\neq\epsilon_m\\ -\beta f_n(1-f_n) & \text{for } \epsilon_n=\epsilon_m\end{cases} \qquad \text{(F.66)}\\
\frac{\partial\rho^{(1)}_{\alpha,\beta}[\boldsymbol{h}^{eff},\mu]}{\partial\mu} &= \beta\sum_n\psi_{\alpha,n}f_n(1-f_n)\psi^*_{\beta,n} = \beta\Big(\boldsymbol{\rho}^{(1)}(\mathbf{1}-\boldsymbol{\rho}^{(1)}\Big)_{\alpha,\beta} \qquad \text{(F.67)}
\end{aligned}$$

For equal orbital indices, the quantity used, $-\beta f_n(1-f_n)$, is the limes of $(f_n-f_m)/(\epsilon_n-\epsilon_m)$ for $\epsilon_m-\epsilon_n\to 0$. Therefore, we use the same expression for equal diagonal terms also for any pair of degenerate eigenvalues.

The derivative has a symmetry, which we will exploit lateron.

$$\frac{\partial\rho^{(1)}_{\alpha,\beta}[\boldsymbol{h}^{eff},\mu]}{\partial h^{eff}_{\gamma,\delta}} \overset{\text{Eq. F.66}}{=} \frac{\partial\rho^{(1)}_{\delta,\gamma}[\boldsymbol{h}^{eff},\mu]}{\partial h^{eff}_{\beta,\alpha}} \qquad \text{(F.68)}$$

Thus, we may replace the upper and lower index pairs, if we also revert the order in each index pair.

Let me derive the inverse of $d\boldsymbol{\rho}^{(1)}[h_{eff},\mu]/d\boldsymbol{h}^{eff}$, because it will be used later. The inverse is

defined via

$$\sum_{\gamma,\delta} K_{\alpha',\beta',\gamma,\delta} \frac{\partial \rho^{(1)}_{\beta,\alpha}[\boldsymbol{h}^{eff},\mu]}{\partial h^{eff}_{\gamma,\delta}} = \delta_{\alpha,\alpha'}\delta_{\beta,\beta'} \tag{F.69}$$

The expression for the inverse,

$$K_{\alpha,\beta,\gamma,\delta} = \sum_{m,n} \psi^*_{\alpha,n}\psi_{\beta,m}\psi_{\gamma,n}\psi^*_{\delta,m} \begin{cases} (\epsilon_n - \epsilon_m)/(f_n - f_m) & \text{for } \epsilon_n \neq \epsilon_m \\ -[\beta f_n(1-f_n)]^{-1} & \text{for } \epsilon_n = \epsilon_m \end{cases} \tag{F.70}$$

can be verified by insertion of Eq. F.66 into the defining equation for the inverse Eq. F.70.

Derivative of the grand potential

Finally, we obtain the derivative of the energy with respect to the effective Hamiltonian in the form

$$\begin{aligned}
\delta\Omega_{T,\mu}\Big[\boldsymbol{\rho}^{(1)}[\boldsymbol{h}^{eff},\mu]\Big] &= \sum_{u,v} \frac{\partial \Omega_{T,\mu}[\boldsymbol{\rho}^{(1)}]}{\partial \rho^{(1)}_{u,v}} \delta\rho_{u,v} + \frac{\partial \Omega_{T,\mu}[\boldsymbol{\rho}^{(1)}]}{\partial \mu}\delta\mu \\
&= \sum_{u,v} \frac{\partial \Omega_{T,\mu}[\boldsymbol{\rho}^{(1)}]}{\partial \rho^{(1)}_{u,v}} \left(\sum_{x,y} \frac{\partial \rho^{(1)}_{u,v}[\boldsymbol{h}^{eff},\mu]}{\partial h^{eff}_{x,y}} \delta h^{eff}_{x,y} + \frac{\partial \rho^{(1)}_{u,v}[\boldsymbol{h}^{eff},\mu]}{\partial \mu}\delta\mu \right) + \frac{\partial \Omega_{T,\mu}[\boldsymbol{\rho}^{(1)}]}{\partial \mu}\delta\mu \\
&= \sum_{u,v} \frac{\partial \Omega_{T,\mu}[\boldsymbol{\rho}^{(1)}]}{\partial \rho^{(1)}_{u,v}} \sum_{x,y} \frac{\partial \rho^{(1)}_{u,v}[\boldsymbol{h}^{eff},\mu]}{\partial h^{eff}_{x,y}} \delta h^{eff}_{x,y} \\
&+ \left(\sum_{u,v} \frac{\partial \Omega_{T,\mu}[\boldsymbol{\rho}^{(1)}]}{\partial \rho^{(1)}_{u,v}} \frac{\partial \rho_{u,v}[\boldsymbol{h}^{eff},\mu]}{\partial \mu} + \frac{\partial \Omega_{T,\mu}[\boldsymbol{\rho}^{(1)}]}{\partial \mu} \right) \delta\mu \\
&= \sum_{u,v} \left(h^{out}_{v,u} - h^{eff}_{v,u} \right) \sum_{x,y} \frac{\partial \rho^{(1)}_{u,v}[\boldsymbol{h}^{eff},\mu]}{\partial h^{eff}_{x,y}} dh^{eff}_{x,y} \\
&+ \left(\sum_{u,v} \left(h^{out}_{v,u} - h^{eff}_{v,u} \right) \beta \Big(\boldsymbol{\rho}^{(1)}(\mathbf{1} - \boldsymbol{\rho}^{(1)}) \Big)_{u,v} - \mathrm{Tr}[\boldsymbol{\rho}^{(1)}] \right) d\mu
\end{aligned} \tag{F.71}$$

- For a variation at fixed chemical potential, we set $d\mu = 0$, which leaves us with the partial derivative with respect to the effective Hamiltonian.
- For a variation of the grand potential at fixed particle number we set

$$d\mu = \frac{\partial \mu[h^{eff}, N]}{\partial h^{eff}_{x,y}} dh^{eff}_{x,y} \tag{F.72}$$

At this point, I switch from the grand potential to the Helmholtz potential, the thermodynamic potential for an ensemble with fixed temperature and particle number.

$$A_{T,N}[\boldsymbol{h}^{eff}] = \Omega_{T,\mu(N)} + \mu(N) \cdot N \tag{F.73}$$

$$\begin{aligned}
\frac{dA_{T,N}[\boldsymbol{h}^{eff}]}{dh^{eff}_{x,y}} &= \frac{\partial \Omega_{T,\mu}[h^{eff}]}{\partial h^{eff}_{x,y}} + \left(\frac{\partial \Omega_{T,\mu}[h^{eff}]}{\partial \mu} + N \right) \frac{d\mu[h^{eff},N]}{dh^{eff}_{x,y}} \\
&= \sum_{u,v} \left(h^{out}_{v,u} - h^{eff}_{v,u} \right) \sum_{x,y} \left. \frac{d\rho^{(1)}_{u,v}[\boldsymbol{h}^{eff},\mu]}{\partial h^{eff}_{x,y}} \right|_{\mu[\boldsymbol{h}^{eff},N]} \\
&+ \left(\mathrm{Tr}\Big[\Big(\boldsymbol{h}^{out} - \boldsymbol{h}^{eff} \Big) \beta \boldsymbol{\rho}^{(1)}(\mathbf{1} - \boldsymbol{\rho}^{(1)}) \Big] \underbrace{-\mathrm{Tr}[\boldsymbol{\rho}^{(1)}] + N}_{=0} \right) \frac{d\mu[h^{eff},N]}{dh^{eff}_{x,y}}
\end{aligned} \tag{F.74}$$

The variation of the chemical potential at constant particle number is obtained from the constraint equation

$$\begin{aligned} \mathrm{Tr}[\boldsymbol{\rho}^{(1)}[h^{eff},\mu] = N \\ \Rightarrow \mathrm{Tr}\left[\frac{\partial \boldsymbol{\rho}}{\partial h^{eff}_{x,y}} dh^{eff}_{x,y} + \frac{\partial \boldsymbol{\rho}^{(1)}}{\partial \mu} d\mu\right] = 0 \\ \Rightarrow d\mu = -\left(\mathrm{Tr}\left[\frac{\partial \boldsymbol{\rho}^{(1)}}{\partial \mu}\right]\right)^{-1} \sum_{x,y} \frac{\partial \mathrm{Tr}[\boldsymbol{\rho}^{(1)}]}{\partial h^{eff}_{x,y}} dh^{eff}_{x,y} = \sum_{u,v} \frac{-\delta_{u,v}}{\mathrm{Tr}\left[\beta\boldsymbol{\rho}^{(1)}(\mathbf{1}-\boldsymbol{\rho}^{(1)})\right]} \frac{d\rho_{u,v}}{dh^{eff}_{x,y}} dh^{eff}_{x,y} \end{aligned} \tag{F.75}$$

This provides us with the derivative of the grand potential at constant particle number

$$\begin{aligned} \frac{dA_{T,N}[h^{eff}]}{dh^{eff}_{x,y}} &= \sum_{u,v}\left(h^{out}_{v,u} - h^{eff}_{v,u}\right) \sum_{x,y} \frac{d\rho^{(1)}_{u,v}[\boldsymbol{h}^{eff},\mu]}{\partial h^{eff}_{x,y}} \\ &\quad + \mathrm{Tr}\Big[\Big(\boldsymbol{h}^{out} - \boldsymbol{h}^{eff}\Big)\beta\boldsymbol{\rho}^{(1)}\big(\mathbf{1}-\boldsymbol{\rho}^{(1)}\big)\Big] \underbrace{\sum_{u,v} \frac{-\delta_{u,v}}{\mathrm{Tr}\left[\beta\boldsymbol{\rho}^{(1)}(\mathbf{1}-\boldsymbol{\rho}^{(1)})\right]} \frac{d\rho^{(1)}_{u,v}}{dh^{eff}_{x,y}}}_{d\mu/dh^{eff}} \\ &= \sum_{\alpha,\beta}\Bigg[\left(h^{out}_{\beta,\alpha} - h^{eff}_{\beta,\alpha}\right) - \underbrace{\frac{\mathrm{Tr}\Big[\big(\boldsymbol{h}^{out} - \boldsymbol{h}^{eff}\big)\beta\boldsymbol{\rho}^{(1)}\big(\mathbf{1}-\boldsymbol{\rho}^{(1)}\big)\Big]}{\mathrm{Tr}\left[\beta\boldsymbol{\rho}^{(1)}(\mathbf{1}-\boldsymbol{\rho}^{(1)})\right]}\delta_{\beta,\alpha}}_{\text{constraint}}\Bigg] \\ &\quad \times \underbrace{\sum_{m,n} \psi_{\alpha,n}\psi^*_{x,n}\psi_{y,m}\psi^*_{\beta,m} \begin{cases} (f_n - f_m)/(\epsilon_n - \epsilon_m) & \text{for } \epsilon_n \neq \epsilon_m \\ -\beta f_n(1-f_n) & \text{for } \epsilon_n = \epsilon_m \end{cases}}_{d\rho_{\alpha,\beta}/\partial h^{eff}_{x,y}} \end{aligned} \tag{F.76}$$

The term denoted *"constraint"* ensures that the gradient $dA_{T,N}/d\boldsymbol{h}$ is trace-less. This is due to a fact that a shift of the effective Hamiltonian by a constant energy does not affect the density matrix, because the chemical potential shifts along, if the particle-number constraint is enforced. This term could as well be implemented by simply removing the trace of the final expression for $dA_{T,N}/d\boldsymbol{h}^{eff}$.

The contribution of $d\rho_{\alpha,\beta}/\partial h^{eff}_{x,y}$ related to the terms diagonal in the band indices m, n describe the response of the Helmholtz potential to the eigenvalues of $\boldsymbol{h}^{eff}$. This means that only these diagonal terms are present if $\boldsymbol{h}^{out}$ is diagonal in the eigenstates of $\boldsymbol{h}^{eff}$.

Self-consistent cycle

1. The derivative of the free energy with respect to the effective Hamiltonian can used to set up a gradient-following scheme, which improves the effective Hamiltonian iteratively.

$$\boldsymbol{h}_{n+1} = \boldsymbol{h}_n - \alpha_f \left.\frac{dA_{T,N}}{d\boldsymbol{h}^{eff}}\right|_{\boldsymbol{h}_n} \tag{F.77}$$

   α_f is a suitably chosen mixing factor α.

2. The simple mixing is not efficient. A better choice is a two-parameter mixing

$$\boldsymbol{h}_{n+1} = \frac{2}{1+a_f}\boldsymbol{h}_n - \frac{1-a_f}{1+a_f}\boldsymbol{h}_{n-1} - \left.\frac{dA_{T,N}}{d\boldsymbol{h}^{eff}}\right|_{\boldsymbol{h}_n} \frac{\Delta^2}{1+a_f} \tag{F.78}$$

   The values of the two parameters can be chosen in the range $0 < a_f < 1$ and $0 < \Delta$. We call a_f **friction parameter** and Δ the **time step**.

   This scheme is inspired by the **Car-Parrinello method** .[116]. Here, we start from a Lagrangian

$$\mathcal{L}[\boldsymbol{h},\boldsymbol{v}] = \frac{1}{2}Tr\left[\boldsymbol{v}\boldsymbol{v}^\dagger\right] - A_{T,N}[\boldsymbol{h}] \tag{F.79}$$

together with the action

$$\mathcal{S}[\boldsymbol{h}(t)] = \int dt\, \mathcal{L}[\boldsymbol{h}, \dot{\boldsymbol{h}}] \tag{F.80}$$

The stationary principle of the action yields the Euler-Lagrange equation to which I added a friction term.

$$\ddot{\boldsymbol{h}}(t) = -\left.\frac{dA_{T,N}}{d\boldsymbol{h}^{eff}}\right|_{\boldsymbol{h}(t)} \underbrace{-\alpha_f \dot{\boldsymbol{h}}(t)}_{\text{friction}} \tag{F.81}$$

The differential equation is discretized using the Verlet algorithm. In the **Verlet algorithm**[117], the time derivatives are replaced by the differential quotients

$$\begin{aligned}\dot{\boldsymbol{h}}(t) &\to \frac{1}{2\Delta}\Big(\boldsymbol{h}(t+\Delta) - \boldsymbol{h}(t-\Delta)\Big)\\ \ddot{\boldsymbol{h}}(t) &\to \frac{1}{\Delta^2}\Big(\boldsymbol{h}(t+\Delta) - 2\boldsymbol{h}(t) + \boldsymbol{h}(t-\Delta)\Big)\end{aligned} \tag{F.82}$$

This turns the differential equation into an equation for the effective Hamiltonian at discrete times $t_n = \Delta \cdot n$. For a given time t_n it connects three successive Hamiltonians, $\boldsymbol{h}(t_n + \Delta)$, $\boldsymbol{h}(t_n)$ and $\boldsymbol{h}(t_n - \Delta)$. Resolving for $\boldsymbol{h}(t_n + \Delta)$ and identifying $\boldsymbol{h}_n^{eff} = \boldsymbol{h}(t_n)$ yields the iterative procedure suggested above. The parameter a_f in Eq. F.78 is related to α_f by $a_f = \alpha_f \Delta/2$.

3. Only those parts of the effective Hamiltonian, which affect the density matrix, experiences forces. Eigenstates of the effective Hamiltonian, which are sufficiently far from the Fermi level, will not be updated.

   One solution is to discard the term $d\boldsymbol{\rho}/d\boldsymbol{h}^{eff}$ and simply proceed to a mixing scheme of Hamiltonians.

$$\boldsymbol{h}^{eff,n+1} = \boldsymbol{h}^{eff,n} + \alpha\Big(\boldsymbol{h}^{out} - \boldsymbol{h}^{eff} - \mathbf{1}\frac{\mathrm{Tr}\left[\boldsymbol{h}^{out} - \boldsymbol{h}^{eff}\right]}{\mathrm{Tr}[\mathbf{1}]}\Big) \tag{F.83}$$

4. The price to be paid is that we arrive again at a fairly inefficient iteration scheme. Therefore, we return to the fictitious Lagrangian method of Car and Parrinello, but we change the kinetic energy. The new Lagrangian

$$\mathcal{L}[\boldsymbol{h}, \boldsymbol{v}] = -\frac{1}{2}\underbrace{\Big[\sum_{\alpha,\beta,\gamma,\delta} v_{\beta,\alpha}\left.\frac{d\rho^{(1)}_{\alpha,\beta}}{dh^{eff}_{\gamma,\delta}}\right|_{\boldsymbol{h}} v_{\gamma,\delta}\Big]}_{\mathrm{Tr}\left[\dot{\boldsymbol{h}}\dot{\boldsymbol{\rho}}^{(1)}\right]} - A_{T,N}[\boldsymbol{h}] \tag{F.84}$$

has the Euler-Lagrange equation

$$\begin{aligned}-\left.\frac{d\rho^{(1)}_{\beta,\alpha}}{dh^{eff}_{\gamma,\delta}}\right|_{\boldsymbol{h}} \ddot{h}_{\alpha,\beta} - \left.\frac{d^2\rho^{(1)}_{\beta,\alpha}}{dh^{eff}_{\gamma,\delta}\, dh^{eff}_{\zeta,\eta}}\right|_{\boldsymbol{h}} \dot{h}_{\zeta,\eta}\dot{h}_{\alpha,\beta} &= -\left.\frac{\partial A_{T,N}}{\partial h^{eff}_{\gamma,\delta}}\right|_{\boldsymbol{h}} = -\left.\frac{\partial A_{T,N}}{\partial \rho^{(1)}_{\beta,\alpha}}\right|_{\boldsymbol{\rho}[\boldsymbol{h},\mu[N]]}\left.\frac{\partial \rho^{(1)}_{\beta,\alpha}}{\partial h^{eff}_{\gamma,\delta}}\right|_{\boldsymbol{h}}\\ \Rightarrow \ddot{h}_{\alpha,\beta} &= +\left.\frac{\partial A_{T,N}}{\partial \rho^{(1)}_{\beta,\alpha}}\right|_{\boldsymbol{\rho}[\boldsymbol{h},\mu[N]]} + \sum_{\gamma,\delta,\alpha',\beta'} K_{\alpha,\beta;\gamma,\delta}\left.\frac{d^2\rho^{(1)}_{\beta',\alpha'}}{dh^{eff}_{\gamma,\delta}\, dh^{eff}_{\zeta,\eta}}\right|_{\boldsymbol{h}} \dot{h}_{\zeta,\eta}\dot{h}_{\alpha',\beta'}\end{aligned} \tag{F.85}$$

with $K_{\alpha',\beta';\gamma,\delta}$ defined by

$$\sum_{\gamma,\delta} K_{\alpha',\beta';\gamma,\delta}\left.\frac{d\rho^{(1)}_{\beta,\alpha}}{dh^{eff}_{\gamma,\delta}}\right|_{\boldsymbol{h}} = \delta_{\alpha,\alpha'}\delta_{\beta,\beta'} \tag{F.86}$$

The explicit form of $K_{\alpha',\beta';\gamma,\delta}$ is given in Eq. F.70.

We managed to get rid of $d\boldsymbol{\rho}^{(1)}/d\boldsymbol{h}^{eff}$ in the main terms, but we are left with a complicated velocity-dependent term. The latter term applies an effective friction if an eigenstate of the effective Hamiltonian approaches the chemical potential, and thus starts to contribute to the kinetic energy. Because this would break the energy conservation, the velocity is reduced to compensate its effect.

The remedy is to remove the velocity dependent term from the equation of motion, but to monitor the resulting energy change. When we add in addition a friction term we obtain

$$\ddot{h}_{\alpha,\beta} = \left.\frac{\partial A_{T,N}}{\partial \rho_{\beta,\alpha}}\right|_{\boldsymbol{\rho}^{(1)}[\boldsymbol{h},\mu[N]]} - \mathcal{C}\dot{h}_{\alpha,\delta} \tag{F.87}$$

This yields our equation of motion

$$\ddot{h}_{\alpha,\beta} = \left[\left(h^{out}_{\alpha,\beta} - h^{eff}_{\alpha,\beta}\right) - \underbrace{\frac{\mathrm{Tr}\left[(\boldsymbol{h}^{out} - \boldsymbol{h}^{eff})\beta\boldsymbol{\rho}^{(1)}(\mathbf{1}-\boldsymbol{\rho}^{(1)})\right]}{\mathrm{Tr}\left[\beta\boldsymbol{\rho}^{(1)}(\mathbf{1}-\boldsymbol{\rho}^{(1)})\right]}\delta_{\alpha,\beta}}_{\text{constraint}}\right] - \mathcal{C}\dot{h}_{\alpha,\delta} \tag{F.88}$$

The result appears trivial because it integrates the product of equation of motion and $\dot{\boldsymbol{\rho}}^{(1)}$.

Monitor energy conservation

$$\begin{aligned}
E &= \sum_i \frac{\partial \mathcal{L}}{\partial v_i} v_i - \mathcal{L}(\vec{x},\vec{v},t) \\
\dot{E} &= \left(\frac{d}{dt}\frac{\partial \mathcal{L}}{\partial v_i}\right) v_i + \underbrace{\frac{\partial \mathcal{L}}{\partial v_i}\dot{v}_i - \frac{\partial \mathcal{L}}{\partial v_i}\dot{v}_i}_{=0} - \frac{\partial \mathcal{L}}{\partial x_i}\dot{x}_i - \frac{\partial \mathcal{L}}{\partial t} \\
&\overset{v_i=\dot{x}_i}{=} \sum_i v_i\left(\frac{d}{dt}\frac{\partial \mathcal{L}}{\partial v_i} - \frac{\partial \mathcal{L}}{\partial x_i}\right) - \frac{\partial \mathcal{L}}{\partial t}
\end{aligned} \tag{F.89}$$

Es expected, we obtain the energy conservation law. The energy is conserved if (1) the Euler Lagrange equations are satisfied, and (2) the Lagrangian is not explicitly time dependent.

Let me now specialize the Lagrangian to be closed to our problem at hand

$$\mathcal{L}(\vec{x},\vec{v},t) = \frac{1}{2}\sum_{i,j} v_i M_{i,j}(\vec{x}) v_j - A(\vec{x}) \tag{F.90}$$

$$\dot{E} = \sum_i \dot{x}_i \Bigg(\underbrace{\sum_{j,k}\frac{dM_{i,j}(\vec{x})}{dx_k}\dot{x}_k\dot{x}_j + \sum_j M_{i,j}(\vec{x})\ddot{x}_j}_{d/dt\;\partial\mathcal{L}/\partial v_i} \underbrace{-\frac{1}{2}\sum_{j,k}\frac{dM_{j,k}}{dx_i}\dot{x}_j\dot{x}_k + \frac{A(\vec{x})}{\partial x_i}}_{-\partial\mathcal{L}/\partial x_i}\Bigg) \tag{F.91}$$

Instead of the Euler-Lagrange equations, which would lead to a conserved energy, I use another equation of motion, which is analogous to

$$\sum_j M_{i,j}(\vec{x})\ddot{x}_j + \frac{A(\vec{x})}{\partial x_i} + C\sum_i M_{i,j}(\vec{x})\dot{x}_j = 0 \tag{F.92}$$

With this equation of motion, I obtain

$$\begin{aligned}\dot{E} &= \sum_i \dot{x}_i \left(\sum_{j,k} \frac{dM_{i,j}(\vec{x})}{dx_k} \dot{x}_k \dot{x}_j - \frac{1}{2} \sum_{j,k} \frac{dM_{j,k}}{dx_i} \dot{x}_j \dot{x}_k - C \sum_j M_{i,j}(\vec{x}) \dot{x}_j \right) \\ &= \frac{1}{2} \sum_{i,j,k} \frac{dM_{i,j}(\vec{x})}{dx_k} \dot{x}_k \dot{x}_i \dot{x}_j - C \sum_{i,j} \dot{x}_i M_{i,j}(\vec{x}) \dot{x}_j \\ &= \frac{1}{2} \sum_{i,j} \dot{x}_i \dot{M}_{i,j} \dot{x}_j - C \sum_i \dot{x}_i M_{i,j} \dot{x}_j \\ &= \frac{d}{dt} \left(\frac{1}{2} \sum_{i,j} \dot{x}_i M_{i,j} \dot{x}_j \right) - \sum_{i,j} \dot{x}_i M_{i,j} \ddot{x}_j - C \sum_i \dot{x}_i M_{i,j} \dot{x}_j \end{aligned} \tag{F.93}$$

In order to obtain a conserved energy, we need to compensate for this energy change

$$\begin{aligned}\mathcal{E}_{cons} = \mathcal{L}(\vec{x}, \vec{v}, t) &= \sum_{i,j} \frac{1}{2} v_i M_{i,j}(\vec{x}) v_j + A(\vec{x}) - \dot{E} \\ &= \sum_{i,j} \frac{1}{2} v_i M_{i,j}(\vec{x}) v_j + A(\vec{x}) - \int dt \left(\frac{d}{dt} \left(\frac{1}{2} \sum_{i,j} \dot{x}_i M_{i,j} \dot{x}_j \right) - \sum_{i,j} \dot{x}_i M_{i,j} \ddot{x}_j - C \sum_i \dot{x}_i M_{i,j} \dot{x}_j \right) \\ &= A(\vec{x}) + \int dt \left(\sum_{i,j} \dot{x}_i M_{i,j} \ddot{x}_j + C \sum_i \dot{x}_i M_{i,j} \dot{x}_j \right) \end{aligned} \tag{F.94}$$

Translating this into our equation, using $\boldsymbol{M} = -d\boldsymbol{\rho}^{(1)}/d\boldsymbol{h}$, we obtain an energy

$$\begin{aligned}\mathcal{E}(t) &= A_{T,N}[\boldsymbol{h}] - \int dt \left\{ \sum_{\alpha,\beta,\gamma,\delta} \ddot{h}_{\alpha,\beta} \frac{\partial \rho^{(1)}_{\beta,\alpha}}{\partial h^{eff}_{\gamma,\delta}} \dot{h}_{\gamma,\delta} - C \sum_{\alpha,\beta,\gamma,\delta} \dot{h}_{\alpha,\beta} \frac{\partial \rho^{(1)}_{\beta,\alpha}}{\partial h^{eff}_{\gamma,\delta}} \dot{h}_{\gamma,\delta} \right\} \\ &= A_{T,N}[\boldsymbol{h}] - \int dt \left\{ \sum_{\alpha,\beta} \ddot{h}_{\alpha,\beta} \dot{\rho}^{(1)}_{\beta,\alpha} - C \sum_{\alpha,\beta} \dot{h}_{\alpha,\beta} \dot{\rho}^{(1)}_{\beta,\alpha} \right\} \\ &= A_{T,N}[\boldsymbol{h}] - \int dt \ \mathrm{Tr} \left[\ddot{\boldsymbol{h}} \dot{\boldsymbol{\rho}}^{(1)} + C \dot{\boldsymbol{h}} \dot{\boldsymbol{\rho}}^{(1)} \right] \end{aligned} \tag{F.95}$$

F.5.2 Calculating one step of the HF loop

We start the iteration with the non-interacting Hamiltonian $\boldsymbol{h}^{eff,n} = \boldsymbol{h}^{(0)}$ and $\boldsymbol{h}^{eff,n-1} = \boldsymbol{h}^{(0)}$. The superscript n of the effective Hamiltonian identifies a particular iteration in the sequence leading to the converged result.

1. The effective Hamiltonian $\boldsymbol{h}^{eff}$ is diagonalized

$$\sum_\gamma \hat{h}^{eff}_{\alpha,\beta} \psi_{\beta,n} = \psi_{\alpha,n} \epsilon_n \tag{F.96}$$

2. The occupations f_n are obtained as Fermi function.

$$f_n = \left(1 + \mathrm{e}^{\beta(\epsilon_n - \mu)} \right)^{-1} \qquad \text{with} \qquad \sum_n f_n = N \, . \tag{F.97}$$

   An internal loop adjusts the chemical potential consistent with the selected particle number N.

3. The one-particle-reduced density matrix is obtained as

$$\rho^{(1)}_{\alpha,\beta} = \sum_n \psi_{\alpha,n} f_n \psi^*_{\beta,n} \tag{F.98}$$

4. The Helmholtz potential is evaluated as

$$A_{T,N}[\boldsymbol{\rho}] = \underbrace{\sum_{\alpha,\beta} h^{(0)}_{\alpha,\beta}\rho^{(1)}_{\beta,\alpha} + \frac{1}{2}\sum_{\alpha,\beta,\gamma,\delta}\Big(W_{\alpha,\beta,\gamma,\delta} - W_{\alpha,\beta,\delta,\gamma}\Big)\rho^{(1)}_{\gamma,\alpha}\rho^{(1)}_{\delta,\beta}}_{E_{\text{tot}}} + \underbrace{k_B T\ \text{Tr}\left[\boldsymbol{\rho}^{(1)}\ln(\boldsymbol{\rho}^{(1)}) + (\mathbf{1}-\boldsymbol{\rho}^{(1)})\ln(\mathbf{1}-\boldsymbol{\rho}^{(1)})\right]}_{-TS} \tag{F.99}$$

5. The output potential is determined as

$$h^{out}_{\nu,u} = h^{(0)}_{\nu,u} + \sum_{\alpha,\gamma}\Big(W_{\alpha,\nu,\gamma,u} - W_{\alpha,\nu,u,\gamma}\Big)\rho^{(1)}_{\gamma,\alpha} \tag{F.100}$$

6. The derivative of the Helmholtz potential is

$$\frac{dA_{T,N}}{dh_{x,y}} = \sum_{\alpha,\beta}\left[\Big(h^{out}_{\beta,\alpha} - h^{eff}_{\beta,\alpha}\Big) - \frac{\text{Tr}\Big[(\boldsymbol{h}^{out}-\boldsymbol{h}^{eff})\beta\boldsymbol{\rho}^{(1)}(\mathbf{1}-\boldsymbol{\rho}^{(1)})\Big]}{\text{Tr}\left[\beta\boldsymbol{\rho}^{(1)}(\mathbf{1}-\boldsymbol{\rho}^{(1)})\right]}\delta_{\beta,\alpha}\right] \times \sum_{m,n}\psi_{\alpha,n}\psi^*_{x,n}\psi_{y,m}\psi^*_{\beta,m}\begin{cases}(f_n-f_m)/(\epsilon_n-\epsilon_m) & \text{for } \epsilon_n \neq \epsilon_m\\ -\beta f_n(1-f_n) & \text{for } \epsilon_n = \epsilon_m\end{cases} \tag{F.101}$$

7. The effective Hamiltonian is updated using the force and the effective Hamiltonians of the two previous iterations

$$\boldsymbol{h}^{eff,n+1} = \frac{1}{1+a}\boldsymbol{h}^{eff,n} - \frac{1-a}{1+a}\boldsymbol{h}^{eff,n-1} - \left.\frac{dA_{T,N}}{d\boldsymbol{h}^{eff}}\right|_{\boldsymbol{h}^{eff,n}}\frac{\Delta^2}{1+a} \tag{F.102}$$

8. In order to only store at most three effective Hamiltonians, the arrays are mapped $\boldsymbol{h}^{eff,n} \to \boldsymbol{h}^{eff,n-1}$ and then $\boldsymbol{h}^{eff,n+1} \to \boldsymbol{h}^{eff,n}$.

The sequence is repeated until the free energy $A(T,N)$ remains constant.

F.5.3 Source code

The source code uses the LAPACK library for the matrix diagonalization.

On my MacBook, I compile and run the code below with

```
gfortran -framework accellerate -o code.x code.f90
code.x
```

The input parameters are specified in the parameter section of the main code.

The code `hfscf.f90` can be downloaded from the ΦSX Website `phisx.org`. For the sake of completeness it is included below.

```
!
!     ...1.........2.........3.........4.........5.........6.........7.........8
      program main
!     ************************************************************************
!     ** hartree fock code for the hydrogen dimer.                           **
!     ** uses diagonalization of the effective hamiltonian and follows the   **
!     ** energy gradient                                                     **
!     **                                                                     **
```

```
!     ** caution: demonstration code:  simple rather than efficient          **
!     ** caution: do not choose the temperature too low                       **
!     **                                                                      **
!     ** for demonstration purposes only. use at own risk                    **
!     ****************************************Peter Bloechl, Goslar 2018*******
      implicit none
      integer(4),parameter :: norb=4        ! #(spin orbitals)
      real(8)   ,parameter :: kbt=1.d-3     ! k_B*T: T=temperature
      real(8)   ,parameter :: thop=1.d0     ! hopping parameter
      real(8)   ,parameter :: u=3.d0        ! interaction parameter
      real(8)   ,parameter :: nel=2.1d0     ! #(electrons)
      real(8)   ,parameter :: dt=5.d-2      ! time step (5.d-1 is still ok)
      real(8)   ,parameter :: anne=1.d-4    ! friction parameter
      logical(4),parameter :: tstopandgo=.false. ! accelerates optimization
      real(8)   ,parameter :: tol=1.d-6          ! scf convergence criterion
      real(8)   ,parameter :: ampran=1.d-1     ! size for initial randomization
      integer(4),parameter :: niter=10000      ! x#(iterations)
      integer(4),parameter :: nfilo=6
      integer(4),parameter :: nfiltra=1001
      complex(8),parameter :: cone=(1.d0,0.d0)  ! complex 1
      complex(8)           :: hni(norb,norb)    ! non-interacting hamiltonian
      complex(8)           :: w(norb,norb,norb,norb) !interaction tensor
      complex(8)           :: heff(norb,norb)   ! effective hamiltonian
      complex(8)           :: hm(norb,norb)
      complex(8)           :: hp(norb,norb)
      complex(8)           :: rhom(norb,norb)
      complex(8)           :: rhop(norb,norb)
      real(8)              :: etot
      real(8)              :: ekin
      real(8)              :: energyreservoir
      real(8)              :: efric
      real(8)              :: firstetot
      real(8)              :: etotlast
      real(8)              :: eig(norb)
      complex(8)           :: dedrho(norb,norb)
      complex(8)           :: psi(norb,norb)
      integer(4)           :: i,j,iter
      logical(4)           :: convg
!     ************************************************************************
      open(nfiltra,form='formatted',file='tra.dat')
      rewind nfiltra
!
!     ========================================================================
!     == set up hamiltonian
!     == (left,up)(left,dn),(right,up),(right,dn)
!     ========================================================================
      hni=(0.d0,0.d0)
      hni(1,3)=-cone*thop
      hni(2,4)=-cone*thop
      do i=1,norb
        do j=i+1,norb
          hni(j,i)=conjg(hni(i,j))
        enddo
      enddo
```

```
!
      w=(0.d0,0.d0)
      do i=1,2
        do j=1,2
          w(i,j,i,j)=cone*u
          w(i+2,j+2,i+2,j+2)=cone*u
        enddo
      enddo
!
!     ========================================================================
!     == scf loop
!     ========================================================================
!
!     == initial conditions ==================================================
      call randomham(norb,ampran,heff)
      heff=heff+hni
      hm=heff

      etotlast=huge(etotlast)
      energyreservoir=0.d0
      do iter=1,niter
!       == total energy and forces
        call hfetot(norb,kbt,nel,hni,w,heff,etot,dedrho)
!
!       == repeat previous step with zero velocity if energy goes up ===========
        if(tstopandgo.and.etot.gt.etotlast) then
          heff=hm
          efric=efric+energyreservoir
          energyreservoir=0.d0
          cycle
        end if
        etotlast=etot
!
!       == propagate ===========================================================
        hp=(heff*2.d0-hm*(1.d0-anne)+dedrho*dt**2)/(1.d0+anne)
!
!       == report ==============================================================
        call rhoofh(norb,kbt,nel,hm,rhom)
        call rhoofh(norb,kbt,nel,hp,rhop)

        ekin=-0.5d0*real(sum((hp-hm)*conjg(rhop-rhom)))/(2.d0*dt)**2
        energyreservoir=energyreservoir &
     &        -real(sum((hp-2.d0*heff+hm)*conjg(rhop-rhom)))/(2.d0*dt**2)
        efric=efric+4.d0*anne*ekin   ! dissipated energy
        write(*,fmt='(i10," ekin,etot,econs=",10f20.5)') &
      &                                iter,ekin,etot,etot+energyreservoir
        if(iter.eq.1)firstetot=etot
        write(nfiltra,fmt='(i10,10f20.5)')iter,ekin,etot-firstetot &
     &                                   ,ekin+etot-firstetot &
     &                                   ,etot-firstetot+energyreservoir
!
!       == check convergence and terminate loop ================================
        convg=maxval(abs(dedrho)).lt.tol
        if(convg) exit
```

```
!
!       == switch ==========================================================
        hm=heff
        heff=hp
      enddo
      if(convg) then
        write(*,fmt='("scf convergence ok")')
      else
        write(*,fmt='("scf loop not converged")')
      end if
!
!     ========================================================================
!     == write eigenvalues and eigenstates ===================================
!     ========================================================================
      write(*,*)
      call mydiag(norb,heff,eig,psi)
      do i=1,norb
        write(*,fmt='("ib=",i3," e=",f10.5," psi=",10(2f7.3,";  "))') &
     &               i,eig(i),psi(:,i)
      enddo
      stop
      end
!
!     ...1.........2.........3.........4.........5.........6.........7.........8
      subroutine randomham(norb,ampran,ranh)
!     ************************************************************************
!     ** produces a random hermitean matrix                                  **
!     ** the matrix elements are equally distributed in [-ampran,ampran]     **
!     ****************************************Peter Bloechl, Goslar 2018*******
      implicit none
      integer(4),intent(in) :: norb
      real(8)   ,intent(in) :: ampran            !
      complex(8),intent(out):: ranh(norb,norb)   !random matrix
      integer(4)            :: i,j
      real(8)               :: ran1,ran2
!     ************************************************************************
      do i=1,norb
        do j=1,norb
          call random_number(ran1)
          call random_number(ran2)
          ran1=(2.d0*ran1-1.d0)*ampran
          ran2=(2.d0*ran2-1.d0)*ampran
          ranh(i,j)=cmplx(ran1,ran2,kind=8)
          ranh(j,i)=cmplx(ran1,-ran2,kind=8)
        enddo
         ranh(i,i)=real(ranh(i,i),kind=8)
      enddo
      return
      end
!
!     ...1.........2.........3.........4.........5.........6.........7.........8
      subroutine hfetot(norb,kbt,nel,hni,w,heff,etot,dedrho)
!     ************************************************************************
!     ****************************************Peter Bloechl, Goslar 2018*******
```

```
      implicit none
      integer(4),intent(in) :: norb
      real(8)   ,intent(in) :: kbt
      real(8)   ,intent(in) :: nel
      complex(8),intent(in) :: hni(norb,norb)
      complex(8),intent(in) :: w(norb,norb,norb,norb)
      complex(8),intent(in) :: heff(norb,norb)
      real(8)   ,intent(out):: etot
      complex(8),intent(out):: dedrho(norb,norb)
      logical(4),parameter  :: tpr=.false.
      logical(4),parameter  :: ttest=.true.
      logical(4),parameter  :: tgrandpot=.false.
      complex(8),parameter  :: cnull=(0.d0,0.d0)
      complex(8),parameter  :: cone=(1.d0,0.d0)
      real(8)               :: eig(norb)
      complex(8)            :: psi(norb,norb)
      real(8)               :: occ(norb)
      complex(8)            :: rho(norb,norb)
      complex(8)            :: mat(norb,norb)
      real(8)               :: mu
      real(8)               :: nofmu
      real(8)               :: etot1
      real(8)               :: svar
      integer(4)            :: i,j,k
      real(8)               :: trdrhodmu,trdedrhodrhodmu
!     ************************************************************************
!
!     ========================================================================
!     ==  diagonalize heff using lapack routine
!     ========================================================================
      call mydiag(norb,heff,eig,psi)
!
!     ========================================================================
!     ==  determine chemical potential and occupations
!     ========================================================================
      call muofn(kbt,nel,norb,eig,mu,occ)
      nofmu=sum(occ)
!
!     ========================================================================
!     ==  determine density matrix
!     ========================================================================
      rho=cnull
      do i=1,norb
        do j=1,norb
          do k=1,norb
            rho(i,j)=rho(i,j)+psi(i,k)*occ(k)*conjg(psi(j,k))
          enddo
        enddo
      enddo
!
!     ========================================================================
!     ==  grand potential and derivative
!     ========================================================================
      call eofrho(norb,hni,w,rho,etot,dedrho)
```

```
      dedrho=dedrho-heff
!
!     == electron entropy ====================================================
      etot1=0.d0
      do k=1,norb
        if(occ(k).ne.0.d0.and.occ(k).ne.1.d0) then
          etot1=etot1+kbt*(occ(k)*log(occ(k))+(1.d0-occ(k))*log(1.d0-occ(k)))
        end if
      enddo
      etot=etot+etot1
!
!     ========================================================================
!     ==  constraint
!     ========================================================================
      mat=cnull
      do i=1,norb
        mat(i,i)=cone
      enddo
      mat=matmul(rho,mat-rho)/kbt   !drhodmu
!
      trdrhodmu=0.d0
      trdedrhodrhodmu=0.d0
      do i=1,norb
        trdrhodmu=trdrhodmu+real(mat(i,i),kind=8)
        do j=1,norb
          trdedrhodrhodmu=trdedrhodrhodmu+real(dedrho(i,j)*mat(j,i),kind=8)
        enddo
      enddo
!
!     == dedrho=dedrho-(domega/dmu*dmu+mu*N)/drho ============================
      svar=-trdedrhodrhodmu/trdrhodmu
      do i=1,norb
        dedrho(i,i)=dedrho(i,i)+svar
      enddo
      return
      end
!
!     ...1.........2.........3.........4.........5.........6.........7.........8
      subroutine eofrho(norb,hni,w,rho,etot,detot)
!     **************************************************************************
!     ****************************************Peter Bloechl, Goslar 2018*******
      implicit none
      integer(4),intent(in) :: norb
      complex(8),intent(in) :: hni(norb,norb)
      complex(8),intent(in) :: w(norb,norb,norb,norb)
      complex(8),intent(in) :: rho(norb,norb)
      real(8)   ,intent(out):: etot
      complex(8),intent(out):: detot(norb,norb)
      complex(8),parameter  :: cnull=(0.d0,0.d0)
      integer(4)            :: i,j,k,l
!     **************************************************************************
!     ****************************************Peter Bloechl, Goslar 2018*******
!
!     ========================================================================
!     ==  total energy and output hamiltonian
```

```
!     ========================================================================
      etot=0.d0
      detot(:,:)=cnull
!
      do i=1,norb
        do j=1,norb
          etot=etot+real(hni(i,j)*rho(j,i),kind=8)
          detot(i,j)=detot(i,j)+hni(i,j)
        enddo
      enddo
!
      do i=1,norb
        do j=1,norb
          do k=1,norb
            do l=1,norb
              etot=etot &
     &            +0.5d0*real((w(l,i,k,j)-w(l,i,j,k))*rho(k,l)*rho(j,i),kind=8)
              detot(i,j)=detot(i,j)+0.5d0*(w(l,i,k,j)-w(l,i,j,k))*rho(k,l)
              detot(l,k)=detot(l,k)+0.5d0*(w(l,i,k,j)-w(l,i,j,k))*rho(j,i)
            enddo
          enddo
        enddo
      enddo
!
      return
      end
!
!     ...1.........2.........3.........4.........5.........6.........7.........8
      subroutine rhoofh(norb,kbt,nel,heff,rho)
!     ************************************************************************
!     ****************************************Peter Bloechl, Goslar 2018*******
      implicit none
      integer(4),intent(in) :: norb
      real(8)   ,intent(in) :: kbt
      real(8)   ,intent(in) :: nel
      complex(8),intent(in) :: heff(norb,norb)
      complex(8),intent(out):: rho(norb,norb)
      complex(8),parameter  :: cnull=(0.d0,0.d0)
      real(8)               :: eig(norb)
      complex(8)            :: psi(norb,norb)
      real(8)               :: mu
      real(8)               :: occ(norb)
      integer(4)            :: i,j,k
!     ************************************************************************
!
!     ========================================================================
!     ==  diagonalize heff using lapack routine
!     ========================================================================
      call mydiag(norb,heff,eig,psi)
!
!     ========================================================================
!     ==  determine chemical potential and occupations
!     ========================================================================
      call muofn(kbt,nel,norb,eig,mu,occ)
```

```
!
!     ================================================================================
!     ==  determine density matrix
!     ================================================================================
      rho=cnull
      do i=1,norb
        do j=1,norb
          do k=1,norb
            rho(i,j)=rho(i,j)+psi(i,k)*occ(k)*conjg(psi(j,k))
          enddo
        enddo
      enddo
     return
     end
!
!     ...1.........2.........3.........4.........5.........6.........7.........8
      subroutine muofn(kbt,nel,norb,eig,mu,occ)
!     ********************************************************************************
!     ****************************************Peter Bloechl, Goslar 2018*******
      implicit none
      real(8)   ,intent(in) :: kbt
      real(8)   ,intent(in) :: nel
      integer(4),intent(in) :: norb
      real(8)   ,intent(in) :: eig(norb)
      real(8)   ,intent(out):: mu
      real(8)   ,intent(out):: occ(norb)
      logical(4),parameter  :: ttest=.true.
      logical(4),parameter  :: tpr=.false.
      real(8)   ,parameter  :: neltol=1.d-12
      real(8)   ,parameter  :: mutol=1.d-12
      real(8)               :: mulo,muhi
      real(8)               :: nlo,nhi,nofmu
      integer(4)            :: i
!     ********************************************************************************
      mulo=eig(1)   -30.d0*kbt
      muhi=eig(norb)+30.d0*kbt
      call occofmu(kbt,mulo,norb,eig,occ)
      nlo=sum(occ)
      call occofmu(kbt,muhi,norb,eig,occ)
      nhi=sum(occ)
      if((nlo-nel)*(nhi-nel).gt.0) then
        print*,'nlo,nhi=',nlo,nhi,' mulo,muhi=',mulo,muhi
        stop 'bisection error'
      end if
      do i=1,10000
        mu=0.5d0*(mulo+muhi)
        call occofmu(kbt,mu,norb,eig,occ)
        nofmu=sum(occ)
        if(abs(nofmu-nel).lt.neltol.and.(abs(muhi-mulo).lt.mutol)) then
          if(tpr) print*,'converged: iter=',i,' nofmu-n=',nofmu-nel &
     &                 ,'mulo muhi=',mulo,muhi
          exit
        end if
        if(nofmu.gt.nel) then
```

```
          muhi=mu
        else
          mulo=mu
        end if
      enddo

      if(ttest) then
        if(abs(nel-nofmu).gt.neltol) then
          print*,'abs(nel-nofmu) ',abs(nel-nofmu)
          stop 'test2 failed'
        end if
        if(abs(muhi-mulo).gt.mutol) then
          print*,'muhi-mulo ',muhi-mulo
          stop 'test3 failed'
        end if
      end if
      return
      end
!
!     ...1.........2.........3.........4.........5.........6.........7.........8
      subroutine occofmu(kbt,mu,norb,eig,occ)
!     ******************************************************************************
!     ****************************************Peter Bloechl, Goslar 2018*******
      implicit none
      real(8)   ,intent(in) :: kbt
      real(8)   ,intent(in) :: mu
      integer(4),intent(in) :: norb
      real(8)   ,intent(in) :: eig(norb)
      real(8)   ,intent(out):: occ(norb)
      real(8)   ,parameter  :: xexparg=700.d0
      integer(4)            :: i
      real(8)               :: svar
!     ******************************************************************************
      do i=1,norb
        svar=(eig(i)-mu)/kbt
        if(abs(svar).lt.xexparg) then
          occ(i)=1.d0/(1.d0+exp(svar))
        else
          occ(i)=0.d0
          if(svar.lt.0) occ(i)=1.d0
        end if
      enddo
      return
      end
!
!     ...1.........2.........3.........4.........5.........6.........7.........8
      subroutine mydiag(n,h,e,u)
!     ******************************************************************************
!     ****************************************Peter Bloechl, Goslar 2018*******
      implicit none
      integer(4),intent(in) :: n
      complex(8),intent(in) :: h(n,n)
      real(8)   ,intent(out):: e(n)
      complex(8),intent(out):: u(n,n)
```

```
      logical(4),parameter  :: ttest=.true.
      real(8)               :: rwork(3*n)
      integer(4),parameter  :: lwork=100
      complex(8)            :: cwork(lwork)
      complex(8)            :: hout(n,n)
      integer(4)            :: info
      integer(4)            :: i,j
!     ************************************************************************
      u=h
      call zheev('v','u',n,u,n,e,cwork,lwork,rwork,info)
      if(info.lt.0) then
        write(*,fmt='("the ",i3,"-th argument had an illegal value")')-info
        stop 'error stop in mydiag'
      else if(info.gt.0) then
        write(*,fmt='("the algorithm failed to converge")')
        write(*,fmt='(i3," off-diagonal elements of an intermediate")')info
        write(*,fmt='("tridiagonal form did not converge to zero")')
        stop 'error stop in mydiag'
      end if

      if(ttest) then
        hout=-h
        do i=1,n
          do j=1,n
            hout(i,j)=hout(i,j)+sum(u(i,:)*e(:)*conjg(u(j,:)))
          enddo
        enddo
        if(maxval(abs(hout)).gt.1.d-6) then
          print*,'deviation ',maxval(abs(hout))
          stop 'test1 failed'
        end if
      end if

      return
      end
```

F.5.4 Generalization to periodic systems

Editor: This section is under construction!

The discussion of the previous sections did not consider the translation symmetry of a crystal. The generalization to a system with translation symmetry is, however, quite straightforward.

The key element is to replace indices as followsEditor: Is the $\vec{t}$ correct? Time is not a vector...

$$\begin{aligned} \alpha &\to \alpha, \vec{t} \\ n &\to n, \vec{k} \end{aligned} \tag{F.103}$$

We consider a supercell with $\mathcal{N}$ primitive unit cells. In this supercell, we consider the wave functions to be strictly periodic. This requirement determines a discrete grid of $\mathcal{N}$ k-points in the reciprocal unit cell.

The goal is to generalize the Helmholtz potential of Eq. F.57 to periodic systems. Because the energy of an infinite system is infinite, we determine the Helmholtz potential per unit cell.

We start with the energy from Eq. F.57. We skip the entropy contribution later for the time

being and return to it later.

$$E = \frac{1}{\mathcal{N}}\Bigg\{ \sum_{\alpha,\vec{t},\beta,\vec{t'}} h_{(\alpha,\vec{t}),(\beta,\vec{t'})}\rho_{(\beta,\vec{t'}),(\alpha,\vec{t})} + \frac{1}{2}\sum_{\alpha,\vec{t},\beta,\vec{t'},\gamma,\vec{t''},\delta,\vec{t'''}} W_{(\alpha,\vec{t}),(\beta,\vec{t'}),(\gamma,\vec{t''}),(\delta,\vec{t'''})} \times\Big(\rho_{(\gamma,\vec{t''}),(\alpha,\vec{t})}\rho_{(\delta,\vec{t'''}),(\beta,\vec{t'})} - \rho_{(\delta,\vec{t'''}),(\alpha,\vec{t})}\rho_{(\gamma,\vec{t''}),(\beta,\vec{t'})}\Big)\Bigg\} \tag{F.104}$$

Now we use Bloch theorem to block-diagonalize the density matrix. The natural orbitals, i.e. the eigenstates of the density matrix, are expressed as Bloch states.

$$\psi_{(\alpha,\vec{t}),(n,\vec{k})} = \psi_{(\alpha,\vec{0}),(n,\vec{k})}\mathrm{e}^{i\vec{k}\vec{t}} \tag{F.105}$$

We normalize the wave function such that their contribution in one unit cell equals one.

$$\sum_{\alpha}\psi_{(\alpha,\vec{0}),(n,\vec{k})}\psi_{(\alpha,\vec{0}),(m,\vec{k})} = \delta_{n,m} \tag{F.106}$$

This differs from the discussion without lattice translation, where the norm is evaluated as a sum over the entire system.

Thus, the density matrix has the form

$$\begin{aligned}\rho_{(\alpha,\vec{t}),(\beta,\vec{t'})} &= \frac{1}{\mathcal{N}}\sum_{n,\vec{k}}\psi_{(\alpha,\vec{t}),(n,\vec{k})}f_{(n,\vec{k})}\psi^*_{(\beta,\vec{t'}),(n,\vec{k})}\\ &= \frac{1}{\mathcal{N}}\sum_{n,\vec{k}}\psi_{(\alpha,\vec{0}),(n,\vec{k})}f_{(n,\vec{k})}\psi^*_{(\beta,\vec{0}),(n,\vec{k})}\mathrm{e}^{i\vec{k}(t-t')}\\ &= \frac{1}{\mathcal{N}}\sum_{\vec{k}}\rho_{\alpha,\beta}(\vec{k})\mathrm{e}^{i\vec{k}(t-t')}\end{aligned} \tag{F.107}$$

with the k-dependent density matrix

$$\rho_{\alpha,\beta}(\vec{k}) \stackrel{\text{def}}{=} \sum_{n}\psi_{(\alpha,\vec{0}),(n,\vec{k})}f_{(n,\vec{k})}\psi^*_{(\beta,\vec{0}),(n,\vec{k})} \tag{F.108}$$

The potential acting on the electrons due to the interaction can be calculated as

$$\begin{aligned}v_{(\alpha,\vec{t}),(\beta,\vec{t'})} &\stackrel{\text{def}}{=} \frac{1}{\mathcal{N}}\frac{\partial E_{int}}{\partial\rho_{(\beta,\vec{t'}),(\alpha,\vec{t})}}\\ &= \frac{1}{\mathcal{N}}\sum_{(\gamma,\vec{t''}),(\delta,\vec{t'''})}\Big(W_{(\alpha,\vec{t}),(\delta,\vec{t'''}),(\beta,\vec{t'}),(\gamma,\vec{t''})} - W_{(\alpha,\vec{t}),(\delta,\vec{t'''}),(\gamma,\vec{t''}),(\beta,\vec{t'})}\Big)\rho_{(\gamma,\vec{t''}),(\delta,\vec{t'''})}\\ &= \frac{1}{\mathcal{N}}\sum_{\vec{k}}\sum_{\gamma,\delta}\Bigg\{\frac{1}{\mathcal{N}}\sum_{\vec{t''},\vec{t'''}}\Big(W_{(\alpha,\vec{t}),(\delta,\vec{t'''}),(\beta,\vec{t'}),(\gamma,\vec{t''})} - W_{(\alpha,\vec{t}),(\delta,\vec{t'''}),(\gamma,\vec{t''}),(\beta,\vec{t'})}\Big)\mathrm{e}^{i\vec{k}(\vec{t''}-\vec{t'''})}\Bigg\}\rho_{\gamma,\delta}(\vec{k})\end{aligned} \tag{F.109}$$

Now we insert the density matrix, expressed in terms of the k-dependent density matrix into the energy expression. Before doing so, however, we eliminate one sum over unit cells by exploiting the periodicity of the material.

$$\begin{aligned}h_{(\alpha,\vec{t}),(\beta,\vec{t'})} &= h_{(\alpha,\vec{0}),(\beta,\vec{t'}-\vec{t})}\\ W_{(\alpha,\vec{t}),(\beta,\vec{t'}),(\gamma,\vec{t''}),(\delta,\vec{t'''})} &= W_{(\alpha,\vec{0}),(\beta,\vec{t'}-\vec{t}),(\gamma,\vec{t''}-\vec{t}),(\delta,\vec{t'''}-\vec{t})}\end{aligned} \tag{F.110}$$

$$
\begin{aligned}
E = \frac{1}{\mathcal{N}}\Bigg\{ & \sum_{\alpha,\beta}\sum_{\vec{t},\vec{t}'} h_{(\alpha,\vec{t}),(\beta,\vec{t}')} \underbrace{\frac{1}{\mathcal{N}}\sum_{\vec{k}} \rho_{\beta,\alpha}(\vec{k}) \mathrm{e}^{i\vec{k}(\vec{t}'-\vec{t})}}_{\rho_{(\beta,\vec{t}'),(\alpha,\vec{t})}} \\
& + \frac{1}{2}\sum_{\alpha,\beta,\gamma,\delta}\sum_{\vec{t},\vec{t}',\vec{t}'',\vec{t}'''} W_{(\alpha,\vec{t}),(\beta,\vec{t}'),(\gamma,\vec{t}''),(\delta,\vec{t}''')} \\
& \times \Big(\underbrace{\frac{1}{\mathcal{N}}\sum_{\vec{k}} \rho_{\gamma,\alpha}(\vec{k}) \mathrm{e}^{i\vec{k}(\vec{t}''-\vec{t})}}_{\rho_{(\gamma,\vec{t}''),(\alpha,\vec{t})}} \underbrace{\frac{1}{\mathcal{N}}\sum_{\vec{k}'} \rho_{\delta,\beta}(\vec{k}') \mathrm{e}^{i\vec{k}'(\vec{t}'''-\vec{t}')}}_{\rho_{(\delta,\vec{t}'''),(\beta,\vec{t}')}} - \underbrace{\frac{1}{\mathcal{N}}\sum_{\vec{k}} \rho_{\delta,\alpha}(\vec{k}) \mathrm{e}^{i\vec{k}(\vec{t}'''-\vec{t})}}_{\rho_{(\delta,\vec{t}''),(\alpha,\vec{t})}} \underbrace{\frac{1}{\mathcal{N}}\sum_{\vec{k}'} \rho_{\gamma,\beta}(\vec{k}') \mathrm{e}^{i\vec{k}'(\vec{t}''-\vec{t}')}}_{\rho_{(\gamma,\vec{t}''),(\beta,\vec{t}')}} \Big\} \\
= & \frac{1}{\mathcal{N}}\sum_{\vec{k}}\sum_{\alpha,\beta} \underbrace{\left(\frac{1}{\mathcal{N}}\sum_{\vec{t}\vec{t}'} h_{(\alpha,\vec{t}),(\beta,\vec{t}')} \mathrm{e}^{i\vec{k}(\vec{t}'-\vec{t})}\right)}_{h_{\alpha,\beta}(\vec{k})} \rho_{\beta,\alpha}(\vec{k}) \\
& + \frac{1}{2}\frac{1}{\mathcal{N}^2}\sum_{\vec{k},\vec{k}'}\sum_{\alpha,\beta,\gamma,\delta} \Bigg\{ \underbrace{\left(\frac{1}{\mathcal{N}}\sum_{\vec{t},\vec{t}',\vec{t}'',\vec{t}'''} W_{(\alpha,\vec{t}),(\beta,\vec{t}'),(\gamma,\vec{t}''),(\delta,\vec{t}''')} \mathrm{e}^{i\vec{k}(\vec{t}''-\vec{t})} \mathrm{e}^{i\vec{k}'(\vec{t}'''-\vec{t}')}\right)}_{W_{\alpha,\beta,\gamma,\delta}(\vec{k},\vec{k}';\vec{k},\vec{k}')} \rho_{\gamma,\alpha}(\vec{k}) \rho_{\delta,\beta}(\vec{k}') \\
& \qquad - \underbrace{\left(\frac{1}{\mathcal{N}}\sum_{\vec{t},\vec{t}',\vec{t}'',\vec{t}'''} W_{(\alpha,\vec{t}),(\beta,\vec{t}'),(\gamma,\vec{t}''),(\delta,\vec{t}''')} \mathrm{e}^{i\vec{k}(\vec{t}'''-\vec{t})} \mathrm{e}^{i\vec{k}'(\vec{t}''-\vec{t}')}\right)}_{W_{\alpha,\beta,\gamma,\delta}(\vec{k},\vec{k}';\vec{k}',\vec{k})} \rho_{\delta,\alpha}(\vec{k}) \rho_{\gamma,\beta}(\vec{k}') \Bigg\} \\
= & \frac{1}{\mathcal{N}}\sum_{\vec{k}}\sum_{\alpha,\beta} h_{\alpha,\beta}(\vec{k}) \rho_{\beta,\alpha}(\vec{k}) \\
& + \frac{1}{2}\frac{1}{\mathcal{N}^2}\sum_{\vec{k},\vec{k}'}\sum_{\alpha,\beta,\gamma,\delta} \Big(W_{\alpha,\beta,\gamma,\delta}(\vec{k},\vec{k}',\vec{k},\vec{k}') - W_{\alpha,\beta,\delta,\gamma}(\vec{k},\vec{k}',\vec{k}',\vec{k}) \Big) \rho_{\gamma,\alpha}(\vec{k}) \rho_{\delta,\beta}(\vec{k}')
\end{aligned}
\tag{F.111}
$$

with

$$
\begin{aligned}
h_{\alpha,\beta}(\vec{k}) &\stackrel{\text{def}}{=} \sum_{\vec{t}} h_{(\alpha,\vec{0}),(\beta,\vec{t})} \mathrm{e}^{i\vec{k}\vec{t}} \\
W_{\alpha,\beta,\gamma,\delta}(\vec{k},\vec{k}';\vec{k}'',\vec{k}''') &= \frac{1}{\mathcal{N}}\sum_{\vec{t},\vec{t}',\vec{t}'',\vec{t}'''} W_{(\alpha,\vec{t}),(\beta,\vec{t}'),(\gamma,\vec{t}''),(\delta,\vec{t}''')} \mathrm{e}^{-i\vec{k}\vec{t}} \mathrm{e}^{-i\vec{k}\vec{t}'} \mathrm{e}^{i\vec{k}'\vec{t}''} \mathrm{e}^{i\vec{k}''\vec{t}'''} \\
&= \sum_{\vec{t}',\vec{t}'',\vec{t}'''} W_{(\alpha,\vec{0}),(\beta,\vec{t}'),(\gamma,\vec{t}''),(\delta,\vec{t}''')} \mathrm{e}^{-i\vec{k}\vec{t}'} \mathrm{e}^{i\vec{k}'\vec{t}''} \mathrm{e}^{i\vec{k}''\vec{t}'''}
\end{aligned}
\tag{F.112}
$$

Because of translation symmetry, many interaction matrix elements vanish

$$
W_{\alpha,\beta,\gamma,\delta}(\vec{k},\vec{k}';\vec{k}'',\vec{k}''') = 0 \qquad \text{for } \vec{k}+\vec{k}' \neq \vec{k}''+\vec{k}''' \tag{F.113}
$$

which is equivalent to momentum conservation during scattering.

Entropy contribution

We need to determine the entropy for the electrons in Eq. F.57. As for the energy, the entropy is calculated per unit cell.

$$
S[\boldsymbol{\rho}] = \frac{1}{\mathcal{N}}\left\{ -k_B \,\mathrm{Tr}\left[\boldsymbol{\rho}\ln(\boldsymbol{\rho}) + (\mathbf{1}-\boldsymbol{\rho})\ln(\mathbf{1}-\boldsymbol{\rho})\right]\right\} \tag{F.114}
$$

The density matrix of the entire system is already decomposed in eigenstates and eigenvalues of the density matrix.

$$\rho_{(\alpha,\vec{t}),(\beta,\vec{t}')} = \sum_{n,\vec{k}} \frac{1}{\sqrt{\mathcal{N}}} \psi_{(\alpha,\vec{t}),(n,\vec{k})} f_{(n,\vec{k})} \frac{1}{\sqrt{\mathcal{N}}} \psi^*_{(\beta,\vec{t}'),(n,\vec{k})} \tag{F.115}$$

The entropy can be written as

$$\begin{aligned} S[\boldsymbol{\rho}] &= -k_B \frac{1}{\mathcal{N}} \sum_{\vec{k}} \sum_{n} \left[f_{n,k} \ln(f_{n,k}) + (1 - f_{n,k}) \ln(1 - f_{n,k}) \right] \\ &= -k_B \frac{1}{\mathcal{N}} \sum_{\vec{k}} \mathrm{Tr} \left[\boldsymbol{\rho}(\vec{k}) \ln(\boldsymbol{\rho}(\vec{k})) + (\mathbf{1} - \boldsymbol{\rho}(\vec{k})) \ln(\mathbf{1} - \boldsymbol{\rho}(\vec{k})) \right] \end{aligned} \tag{F.116}$$

Helmholtz potential

Adding the energy Eq. F.111 and the entropy Eq. F.116, we arrive at the Helmholtz potential

$$\begin{aligned} A_{T,N}[\{\boldsymbol{\rho}(\vec{k})\}] = & \frac{1}{\mathcal{N}} \sum_{\vec{k}} \sum_{\alpha,\beta} h_{\alpha,\beta}(\vec{k}) \rho_{\beta,\alpha}(\vec{k}) \\ & + \frac{1}{2} \frac{1}{\mathcal{N}^2} \sum_{\vec{k},\vec{k}'} \sum_{\alpha,\beta,\gamma,\delta} \Big(W_{\alpha,\beta,\gamma,\delta}(\vec{k},\vec{k}',\vec{k},\vec{k}') - W_{\alpha,\beta,\delta,\gamma}(\vec{k},\vec{k}',\vec{k}',\vec{k}) \Big) \rho_{\gamma,\alpha}(\vec{k}) \rho_{\delta,\beta}(\vec{k}') \\ & + k_B T \frac{1}{\mathcal{N}} \sum_{\vec{k}} \mathrm{Tr} \left[\boldsymbol{\rho}(\vec{k}) \ln(\boldsymbol{\rho}(\vec{k})) + (\mathbf{1} - \boldsymbol{\rho}(\vec{k})) \ln(\mathbf{1} - \boldsymbol{\rho}(\vec{k})) \right] \end{aligned} \tag{F.117}$$

Effective one-particle Hamiltonian as independent variable

We introduce an effective Hamiltonian $h^{eff}_{\alpha,\beta}(\vec{k})$, which parameterizes the one-particle-reduced density matrix.

$$\boldsymbol{\rho}(\vec{k}) = \left[\mathbf{1} + \exp\Big(\beta(\hat{h}^{eff}(\vec{k}) - \mu \mathbf{1}) \Big) \right]^{-1} \tag{F.118}$$

The density matrix is evaluated by diagonalizing the effective potential

$$h^{eff}_{\alpha,\beta}(\vec{k}) \psi_{\alpha,0,n,\vec{k}} = \psi_{\alpha,0,n,\vec{k}} \epsilon_n(\vec{k}) \qquad \text{with} \qquad \sum_{\alpha} \psi_{\alpha,0,n,\vec{k}} \psi^*_{\alpha,0,m,\vec{k}} = \delta_{n,m} \tag{F.119}$$

which yields the density matrix as

$$\rho_{\alpha,\beta}(\vec{k}) = \sum_{n} \psi_{\alpha,0,n,\vec{k}} f_{n,\vec{k}} \psi^*_{\beta,0,n,\vec{k}} \tag{F.120}$$

with the occupations

$$f_{n,\vec{k}} = \frac{1}{1 + \exp\Big(\beta(\epsilon_n(\vec{k}) - \mu) \Big)} \tag{F.121}$$

The chemical potential is determined so that the particle number per unit cell is correct

$$N = \frac{1}{\mathcal{N}} \sum_{n,\vec{k}} f_{n,\vec{k}} \tag{F.122}$$

Thus, we obtain the k-dependent reduced density matrix as function of a k-dependent effective Hamiltonian. This in turn allows one to express the Helmholtz potential as functional of this Hamiltonian.

$$A_T[\{\boldsymbol{h}^{eff}(\vec{k})\}] = A_T \left[\left\{ \boldsymbol{\rho} \left(\vec{k}, \left\{ \boldsymbol{h}^{eff}(\vec{k}) \right\} \right) \right\} \right] \tag{F.123}$$

With braces we denote that the contributions from all k-points contribute.

Minimum condition

At self consistency the effective Hamiltonian has the form

$$\mathcal{N}\frac{\partial\Omega_{T,\mu}}{\partial\rho_{\beta,\alpha}(\vec{k})} = h_{\alpha,\beta}(\vec{k}) + \frac{1}{\mathcal{N}}\sum_{\vec{k}'}\sum_{\alpha,\beta,\gamma,\delta}\Big(W_{\alpha,\gamma,\beta,\delta}(\vec{k},\vec{k}',\vec{k},\vec{k}') - W_{\alpha,\gamma,\delta,\beta}(\vec{k},\vec{k}',\vec{k}',\vec{k})\Big)\rho_{\delta,\gamma}(\vec{k}') - h^{eff}_{\alpha,\beta}(\vec{k}) \stackrel{!}{=} 0 \tag{F.124}$$

This yields an expression for the effective Hamiltonian

$$h^{eff}_{\alpha,\beta}(\vec{k}) = h_{\alpha,\beta}(\vec{k}) + \frac{1}{\mathcal{N}}\sum_{\vec{k}'}\sum_{\alpha,\beta,\gamma,\delta}\Big(W_{\alpha,\gamma,\beta,\delta}(\vec{k},\vec{k}',\vec{k},\vec{k}') - W_{\alpha,\gamma,\delta,\beta}(\vec{k},\vec{k}',\vec{k}',\vec{k})\Big)\rho_{\delta,\gamma}(\vec{k}') \tag{F.125}$$

The derivative with respect to the Hamiltonian introduces a further term

$$\mathcal{N}\frac{\partial\Omega_{T,\mu}}{\partial h_{\alpha,\beta}(\vec{k})} = \mathcal{N}\sum_{\vec{k}}\sum_{\gamma,\delta}\frac{\partial\Omega_{T,\mu}}{\partial\rho_{\delta,\gamma}(\vec{k}')}\frac{\partial\rho_{\delta,\gamma}(\vec{k}')}{\partial h^{eff}_{\alpha,\beta}(\vec{k})} \tag{F.126}$$

where

$$\frac{\partial\rho_{\delta,\gamma}(\vec{k}')}{\partial(h^{eff}_{\alpha,\beta}(\vec{k}) - \mu\delta_{\alpha,\beta})} \stackrel{\text{Eq. F.66}}{=} \delta_{\vec{k},\vec{k}'}\sum_{m,n}\psi_{\delta,\vec{0},m,\vec{k}}\psi^*_{\alpha,\vec{0},m,\vec{k}}\psi_{\beta,\vec{0},n,\vec{k}}\psi^*_{\gamma,\vec{0},n,\vec{k}} \times \begin{cases} (f_{n,\vec{k}} - f_{m,\vec{k}})/(\epsilon_{n,\vec{k}} - \epsilon_{m,\vec{k}}) & \text{for } \epsilon_{n,\vec{k}} \neq \epsilon_{m,\vec{k}} \\ -\frac{1}{k_B T} f_{n,\vec{k}}(1 - f_{n,\vec{k}}) & \text{for } \epsilon_{n,\vec{k}} = \epsilon_{m,\vec{k}} \end{cases} \tag{F.127}$$

We obtain at fixed chemical potential

$$\frac{\partial\rho_{\delta,\gamma}(\vec{k}')}{\partial h^{eff}_{\alpha,\beta}(\vec{k})} = \sum_{u,v}\frac{\partial\rho_{\delta,\gamma}(\vec{k}')}{\partial(h^{eff}_{u,v}(\vec{k}) - \mu\delta_{u,v})}\frac{\partial h^{eff}_{u,v}(\vec{k})}{\partial h^{eff}_{\alpha,\beta}(\vec{k})} = \frac{\partial\rho_{\delta,\gamma}(\vec{k}')}{\partial(h^{eff}_{\alpha,\beta}(\vec{k}) - \mu\delta_{\alpha,\beta})} \tag{F.128}$$

Thus, we obtain

$$\begin{aligned}\frac{\partial\Omega_{T,\mu}}{\partial h_{\alpha,\beta}(\vec{k})} &= \sum_{\vec{k}}\sum_{\gamma,\delta}\frac{\partial\Omega_{T,\mu}}{\partial\rho_{\delta,\gamma}(\vec{k}')}\frac{\partial\rho_{\delta,\gamma}(\vec{k}')}{\partial h^{eff}_{\alpha,\beta}(\vec{k})} \\ &= \frac{1}{\mathcal{N}}\sum_{\vec{k}}\sum_{m,n}\psi_{\beta,\vec{0},n,\vec{k}}\Big(\sum_{\gamma,\delta}\psi^*_{\gamma,\vec{0},n,\vec{k}}\Big(h^{out}_{\gamma,\delta}(\vec{k}) - h^{eff}_{\gamma,\delta}(\vec{k})\Big)\psi_{\delta,\vec{0},m,\vec{k}}\Big)\psi^*_{\alpha,\vec{0},m,\vec{k}} \\ &\quad\times\begin{cases}(f_{n,\vec{k}} - f_{m,\vec{k}})/(\epsilon_{n,\vec{k}} - \epsilon_{m,\vec{k}}) & \text{for } \epsilon_{n,\vec{k}} \neq \epsilon_{m,\vec{k}} \\ -\frac{1}{k_B T} f_{n,\vec{k}}(1 - f_{n,\vec{k}}) & \text{for } \epsilon_{n,\vec{k}} = \epsilon_{m,\vec{k}}\end{cases}\end{aligned} \tag{F.129}$$

This term determines the forces acting on the effective Hamiltonian, which are required t=o steer the system towards self-consistency.

F.6 Mean-field approximation and beyond

Editor: This material has been been moved from the chapter on weak interaction. The most relevant material has been lifted. This implies that some material in the following section is duplicated.

So far, we investigated a world in which all wave functions are Slater determinants. With this limitation, the expectation values, including the total energy, have a simple form of Eq. 2.44 and can be written down without further approximations.

Here, we go beyond the restriction to single Slater determinants. However, in order to arrive at a theory with comparable complexity, we make a common approximation, the **mean-field approximation**.

For Slater determinants, the total energy can be expressed by Eq. 2.44 in terms of its one-particle-reduced density matrix. Consider now an ensemble of several Slater determinants: Shall we calculate the one-particle-reduced density matrix by averaging over the ensemble and insert the result into the total energy expression Eq. 2.44 as $E[\sum_{\vec{\sigma}} P_{\vec{\sigma}} \hat{\rho}^{(1)}_{\vec{\sigma}}]$? Or shall we instead average the total energies obtained from the Slater determinants individually as $\sum_{\vec{\sigma}} P_{\vec{\sigma}} E[\hat{\rho}^{(1)}_{\vec{\sigma}}]$? The two choices lead to different results.

In the mean-field approximation one works with the averaged one-particle-reduced density matrix. This is very efficient and intuitive and, therefore, the mean-field approximation is widely used. However, while it is usually accurate, it can also produce qualitatively incorrect results. In order to know, when it can be considered reliable, and when does it break down, it is important to understand this approximation.

F.6.1 Mean-field approximation

The Hartree-Fock approximation uses the total-energy expression for Slater determinants. However, then it makes an approximation, which is called **mean-field approximation** or *"self-consistent field" (SCF) approximation*.

We can generalize the total-energy expression for a Slater determinant Eq. 2.44 blindly to arbitrary many-particle states. We arrive at an **approximate** expression for the total energy of a many-particle wave function.

$$E^{mf}[\hat{\rho}^{(1)}] \stackrel{\text{def}}{=} \underbrace{\mathrm{Tr}\left[\hat{\rho}^{(1)}\hat{h}\right]}_{E_{1P}} + \underbrace{\frac{1}{2}\int d^3r \int d^3r' \, \frac{e^2 n(\vec{r}) n(\vec{r'})}{4\pi\epsilon_0 |\vec{r} - \vec{r'}|}}_{E_H} \underbrace{-\frac{1}{2}\int d^4x \int d^4x' \, \frac{e^2 \rho^{(1)}(\vec{x}, \vec{x'}) \rho^{(1)}(\vec{x'}, \vec{x})}{4\pi\epsilon_0 |\vec{r} - \vec{r'}|}}_{E_X} \tag{F.130}$$

with the general one-particle-reduced density matrix $\hat{\rho}^{(1)}$ Eq. 2.19 of a fermionic wave function and the density $n(\vec{r}) = \sum_\sigma \rho^{(1)}(\vec{r}, \sigma; \vec{r}, \sigma)$. In contrast to the energy Eq. 2.44 of a Slater determinant, the mean-field expression is defined also for non-integer occupations.

This mean-field energy E^{mf} differs from the energy expectation value of a many-particle state, unless the many-particle state is a Slater determinant. In other words: when the occupations defined in Eq. 2.18 are integer, the wave function is a Slater determinant, and the mean-field total energy Eq. F.130 is, according to Eq. 2.44, identical to the expectation value of the Hamiltonian. For fractional occupations, Eq. F.130 is approximate.

The mean-field theory is an approximation for the energy expectation value of a many-particle state, which is equally well or equally poorly justified for the ground and for excited states.[6]

[6] Density-functional theory on the other hand, which has some similarities with mean-field theory, is not approximate, but limited to the electronic ground state.

F.6.2 Beyond the mean-field approximation

In order to explore the errors introduced by the mean-field approximation, let me write down the total energy $\langle\Psi|\hat{h}+\hat{W}|\Psi\rangle$ for a general many-particle wave function $|\Psi\rangle$,

$$|\Psi\rangle \overset{\text{Eq. 1.95}}{=} \sum_{\vec{\sigma}} |\vec{\sigma}\rangle c_{\vec{\sigma}} \tag{F.131}$$

represented as superposition of Slater determinants $|\vec{\sigma}\rangle$ in a basis of natural orbitals $|\varphi_n\rangle$.

In this section, I will assume that the natural orbitals and the coefficients $c_{\vec{\sigma}}$ of the Slater determinants are known. This implies that the problem is already solved. Thus, the following considerations are not helpful to solve the many-electron problem, but they are invaluable for the understanding of the underlying energy contributions. They provide a suitable framework to rationalize many effects, which we will encounter lateron.

Let us divide the energy, into a sum over the diagonal terms $\vec{\sigma}=\vec{\sigma'}$ and the rest, the sum over the off-diagonal elements $\vec{\sigma}\neq\vec{\sigma'}$.

$$\begin{aligned}\langle\Psi|\hat{h}+\hat{W}|\Psi\rangle &\overset{\text{Eq. F.131}}{=} \sum_{\vec{\sigma},\vec{\sigma'}} c^*_{\vec{\sigma}} c_{\vec{\sigma'}} \langle\vec{\sigma}|\hat{h}+\hat{W}|\vec{\sigma'}\rangle \\ &= \underbrace{\sum_{\vec{\sigma}} \underbrace{c^*_{\vec{\sigma}} c_{\vec{\sigma}}}_{=:P_{\vec{\sigma}}} \langle\vec{\sigma}|\hat{h}+\hat{W}|\vec{\sigma}\rangle}_{\text{diagonal terms}} + \underbrace{\sum_{\vec{\sigma}\neq\vec{\sigma'}} c^*_{\vec{\sigma}} c_{\vec{\sigma'}} \langle\vec{\sigma}|\hat{h}+\hat{W}|\vec{\sigma'}\rangle}_{\text{off-diagonal terms}}\end{aligned} \tag{F.132}$$

The diagonal terms ($\vec{\sigma}=\vec{\sigma'}$) in Eq. F.132 require the expectation values of the interaction for Slater determinants, which can be determined *"easily"* using Eq. 2.44 in terms of the one-particle-reduced density matrices $\hat{\rho}^{(1)}_{\vec{\sigma}}$ of the individual Slater determinants $|\vec{\sigma}\rangle$.

The pre-factors

$$P_{\vec{\sigma}} \overset{\text{def}}{=} c^*_{\vec{\sigma}} c_{\vec{\sigma}} \tag{F.133}$$

of the diagonal matrix elements behave like probabilities: they are positive $P_{\vec{\sigma}} \geq 0$ and they are normalized $\sum_{\vec{\sigma}} P_{\vec{\sigma}} = 1$. Therefore, the sum over diagonal elements can be considered as an ensemble expectation value (Section **??**) with probabilities $P_{\vec{\sigma}}$.

The occupations are the averaged occupation numbers (without proof, yet.)Editor: This needs a proof!!

$$f_n = \sum_{\vec{\sigma}} P_{\vec{\sigma}} \sigma_n \tag{F.134}$$

Non-interacting Hamiltonian

The expectation value of the non-interacting Hamiltonian $\hat{h}$ can be obtained with the help of the one-particle-reduced density matrix $\hat{\rho}^{(1)}$. We exploit the definition Eq. 2.16 of the one-particle-reduced density matrix, which yields the expectation value of a one-particle operator as

$$\langle\Psi|\hat{h}|\Psi\rangle \overset{\text{Eq. 2.16}}{=} \mathrm{Tr}[\hat{\rho}^{(1)}\hat{h}] \tag{F.135}$$

Using Eq. F.134 and the representation of the one-particle-reduced density matrix in terms of natural orbitals and occupations, we can show that $\langle\Psi|\hat{h}|\Psi\rangle$ can be expressed as an ensemble average

with Slater determinants

$$\langle\Psi|\hat{h}|\Psi\rangle \overset{\text{Eq. } 2.16}{=} \mathrm{Tr}[\hat{\rho}^{(1)}\hat{h}] \overset{\text{Eq. } 2.18}{=} \sum_n f_n\langle\varphi_n|\hat{h}|\varphi_n\rangle \overset{\text{Eq. } F.134}{=} \sum_n \underbrace{\sum_{\vec{\sigma}} P_{\vec{\sigma}}\sigma_n}_{f_n}\langle\varphi_n|\hat{h}|\varphi_n\rangle$$

$$= \sum_{\vec{\sigma}} P_{\vec{\sigma}} \underbrace{\sum_n \sigma_n\langle\varphi_n|\hat{h}|\varphi_n\rangle}_{=\mathrm{Tr}[\hat{\rho}^{(1)}_{\vec{\sigma}}\hat{h}]=\langle\vec{\sigma}|\hat{h}|\vec{\sigma}\rangle} \overset{\text{Eq. } 2.22}{=} \sum_{\vec{\sigma}} P_{\vec{\sigma}}\langle\vec{\sigma}|\hat{h}|\vec{\sigma}\rangle \tag{F.136}$$

Note that there are no off-diagonal matrix elements, which connect different Slater determinants.

Interaction part of the Hamiltonian

Let me return to the interaction energy: As mentioned above, the interaction energy can be divided into one term diagonal in the Slater determinants, which corresponds to an ensemble of Slater determinants, and the off-diagonal terms, which reflect the entanglement between Slater determinants.

$$\langle\Psi|\hat{W}|\Psi\rangle \overset{\text{Eq. } F.131}{=} \overbrace{\sum_{\vec{\sigma}} \underbrace{c^*_{\vec{\sigma}}c_{\vec{\sigma}}}_{P_{\vec{\sigma}}}\langle\vec{\sigma}|\hat{W}|\vec{\sigma}\rangle}^{\sim\text{ensemble}} + \overbrace{\sum_{\vec{\sigma}\neq\vec{\sigma}'} c^*_{\vec{\sigma}}c_{\vec{\sigma}'}\langle\vec{\sigma}|\hat{W}|\vec{\sigma}'\rangle}^{\text{entanglement}}$$

$$\overset{\text{Eq. } 2.33}{=} \overbrace{\sum_{\vec{\sigma}} P_{\vec{\sigma}} \underbrace{\sum_{m,n}\sigma_m\sigma_n\Big(\langle\varphi_m,\varphi_n|\hat{W}|\varphi_m,\varphi_n\rangle - \langle\varphi_m,\varphi_n|\hat{W}|\varphi_n,\varphi_m\rangle\Big)}_{\langle\vec{\sigma}|\hat{W}|\vec{\sigma}\rangle}}^{\sim\text{ensemble}} + \overbrace{\sum_{\vec{\sigma}\neq\vec{\sigma}'} c^*_{\vec{\sigma}}c_{\vec{\sigma}'}\langle\vec{\sigma}|\hat{W}|\vec{\sigma}'\rangle}^{\text{entanglement}}$$

$$= \frac{1}{2}\sum_{m,n=1}^{\infty}\Bigg[\overbrace{f_mf_n}^{\rightsquigarrow\text{mean field}} + \overbrace{\underbrace{\Big(\sum_{\vec{\sigma}} P_{\vec{\sigma}}\sigma_m\sigma_n\Big) - f_mf_n}_{\frac{\left(\sum_{\vec{\sigma}} P_{\vec{\sigma}}\sigma_m\sigma_n\right)-f_m\left(\sum_{\vec{\sigma}} P_{\vec{\sigma}}\sigma_n\right)-\left(\sum_{\vec{\sigma}} P_{\vec{\sigma}}\sigma_m\right)f_n+f_mf_n}{\left(\sum_{\vec{\sigma}} P_{\vec{\sigma}}(\sigma_m-f_m)(\sigma_n-f_n)\right)}}}^{\rightsquigarrow\text{occupation-number fluctuations}}\Bigg]$$

$$\times\Big(\langle\varphi_m,\varphi_n|\hat{W}|\varphi_m,\varphi_n\rangle - \langle\varphi_m,\varphi_n|\hat{W}|\varphi_n,\varphi_m\rangle\Big) + \overbrace{\sum_{\vec{\sigma}\neq\vec{\sigma}'} c^*_{\vec{\sigma}}c_{\vec{\sigma}'}\langle\vec{\sigma}|\hat{W}|\vec{\sigma}'\rangle}^{\text{entanglement}}$$

$$\overset{\text{Eq. } 2.44}{=} \overbrace{\underbrace{\frac{1}{2}\int d^3r\int d^3r'\,\frac{e^2n(\vec{r})n(\vec{r'})}{4\pi\epsilon_0|\vec{r}-\vec{r'}|}}_{\text{Hartree energy } E_H} \underbrace{-\frac{1}{2}\int d^4x\int d^4x'\,\frac{e^2\rho^{(1)}(\vec{x},\vec{x'})\rho^{(1)}(\vec{x'},\vec{x})}{4\pi\epsilon_0|\vec{r}-\vec{r'}|}}_{\text{exchange energy } E_X}}^{\text{mean-field}}$$

$$+ \overbrace{\frac{1}{2}\sum_{m,n=1}^{\infty}\underbrace{\Big(\sum_{\vec{\sigma}} P_{\vec{\sigma}}(\sigma_m-f_m)(\sigma_n-f_n)\Big)}_{=\left(\sum_{\vec{\sigma}} P_{\vec{\sigma}}\sigma_m\sigma_n\right)-f_mf_n}\Big(\underbrace{\langle\varphi_m,\varphi_n|\hat{W}|\varphi_m,\varphi_n\rangle}_{\rightsquigarrow\text{Hartree}} - \underbrace{\langle\varphi_m,\varphi_n|\hat{W}|\varphi_n,\varphi_m\rangle}_{\rightsquigarrow\text{exchange}}\Big)}^{\text{occupation-number fluctuations}}$$

$$\underbrace{\qquad\qquad}_{>0\text{ for }m\neq n\text{ and }=0\text{ for }m=n}$$

$$+ \overbrace{\sum_{\vec{\sigma}\neq\vec{\sigma}'} c^*_{\vec{\sigma}}c_{\vec{\sigma}'}\langle\vec{\sigma}|\hat{W}|\vec{\sigma}'\rangle}^{\text{entanglement}} \tag{F.137}$$

1. The first line denoted as *"mean field"* is the interaction energy of the Hartree-Fock approximation: All terms can be expressed by one-particle expectation values. Combined with the

non-interacting energy, this is the energy Eq. F.130 in the **mean-field approximation**. The name *"self-consistent field" (SCF)* originates in this background.

2. The second term describes the effect of **correlated occupation-number fluctuations**. It vanishes for a single Slater determinant, but it is present in (1) an ensemble of Slater determinants and (2) in a many-particle wave function or an ensemble of them.

   The factors $\langle\varphi_m,\varphi_n|\hat{W}|\varphi_m,\varphi_n\rangle - \langle\varphi_m,\varphi_n|\hat{W}|\varphi_n,\varphi_m\rangle$ are non-negative for all values (m,n)[7] and they vanish for $m=n$. They are large for electron pairs with opposite spin, because for pairs with equal spin the exchange term (2nd) counteracts the Hartree term (1st). The exchange term vanishes for electrons pairs with opposite spin.

   The correlated occupation-number fluctuations $\sum_{\vec{\sigma}} P_{\vec{\sigma}}(\sigma_m - f_m)(\sigma_n - f_n)$ vanish

   - for completely filled $f_n = 1$ and completely empty $f_n = 0$ orbitals, and
   - statistically independent occupations, i.e. for

   $$\langle\sigma_m\sigma_n\rangle = \sum_{\vec{\sigma}} P_{\vec{\sigma}}\sigma_m\sigma_n = \underbrace{\Big(\sum_{\vec{\sigma}} P_{\vec{\sigma}}\sigma_m\Big)}_{f_m}\underbrace{\Big(\sum_{\vec{\sigma}} P_{\vec{\sigma}}\sigma_n\Big)}_{f_n} = \langle\sigma_m\rangle\langle\sigma_n\rangle \qquad \text{(F.138)}$$

   For a given set of occupations $f_n = \sum_{\vec{\sigma}} P_{\vec{\sigma}}\sigma_m$, a wave function with small **double occupancy**

   $$d_{m,n} \stackrel{\text{def}}{=} \sum_{\vec{\sigma}} P_{\vec{\sigma}}\sigma_m\sigma_n \qquad \text{(F.139)}$$

   will have a lower energy. That is, electrons with strong Coulomb repulsion try to get out of each other's way.[8]

3. The third term describes the **entanglement** of the Slater determinants. Let me call it **entanglement energy**. It describes the **hybridization**[9] of Slater determinants. This is the only term that depends on the relative phases of the coefficients of different Slater determinants.

   Imagine a special case with only two relevant Slater determinants $|\vec{\sigma}_1\rangle$ and $|\vec{\sigma}_2\rangle$, so that the many-particle wave functions have the form $|\Psi\rangle = |\vec{\sigma}_1\rangle c_1 + |\vec{\sigma}_2\rangle c_2$. Let us treat the two Slater determinants as basisset in Fock space and evaluate the matrix elements of the interacting 2×2 Hamiltonian. (assuming orthonormality)

   $$H_{\alpha,\beta} = \langle\vec{\sigma}_\alpha|\hat{h}+\hat{W}|\vec{\sigma}_\beta\rangle \qquad \text{for } \alpha,\beta\in\{1,2\}. \qquad \text{(F.141)}$$

   We obtain a 2×2 Schrödinger equation.[10] We will obtain two eigenvectors $\vec{c}_\pm$ for two different energies $E_\pm$, where $\pm\in\{+,-\}$ identifies one or the other eigenstate. The complex coefficients

[7] This follows from the fact that the electrostatic energy of any two-particle system is positive. This is also true if the two electrons are in a two-particle Slater determinant with the two orbitals $|\varphi_m\rangle$ and $|\varphi_n\rangle$. The factor mentioned is twice the Coulomb energy of this Slater determinant.

[8] This is a private note of the editor: Editor: Bounds for the correlated occupation-number fluctuations can be derived by considering each pair of states independently.

$$\max(0, f_m+f_n-1) - f_m f_n \le P_{\sigma_m,\sigma_n}(\sigma_m-f_m)(\sigma_n-f_n) \le \min(1, f_m+f_n) - f_m f_n \qquad \text{(F.140)}$$

To avoid the double occupancy, one could estimate the occupation-number fluctuations from the lower of the two bounds, rather than ignoring the term as in the mean-field approximation. The result is shown in fig. 2.4 The independent-pair approximation relies on $P_{00}+P_{01}+P_{10}+P_{11}=1$, $P_{10}+P_{11}=f_1$, $P_{01}+P_{11}=f_2$, $0\le P_{\sigma,\sigma'}\le 1$.

[9] Hybridization is the formation of a superposition of orbitals to form a bond orbital or an antibond orbital. The difference between a bond and an antibond can be attributed to a phase factor between the two orbitals forming the bonding and antibonding orbitals. The bond orbital of a hydrogen molecule is $(|\chi_1\rangle+\chi_2\rangle)/\sqrt{2}$ while that of an antibond is $(|\chi_1\rangle-\chi_2\rangle)/\sqrt{2}$. The plus and minus signs can be described by a relative phase factor $e^{i\varphi}$ with a real-valued phase of $\varphi=0$ for the bond and $\varphi=\pi$ for the antibond. In the present case, it is Slater determinants rather than one-particle states that hybridize. The underlying concept is the matrix diagonalization, which is common to both cases.

[10] The problem of diagonalizing the 2×2 matrix is the same as that for the diatomic molecule. The difference to the diatomic molecule is that the Hamiltonian is formed from many-particle Slater determinants and the Hamiltonian contains also the interaction $\hat{W}$. As in the diatomic molecule, there will be **level-repulsion** and superpositions of the two Slater determinants analogous to the bonding and the antibonding states of the diatomic molecule.

of the eigenvectors $c_{\alpha,\pm} = \sqrt{P_\pm} e^{i\phi_{\alpha,\pm}}$ contain the phase relation $\phi_{2,\pm} - \phi_{1,\pm}$ between the two Slater determinants. When the two Slater determinants with different phases contribute with distinct weight, i.e. $P_{\vec{\sigma}_1} \neq P_{\vec{\sigma}_2}$, there will be a finite entanglement energy.

The entanglement energy is the energy gain from optimizing the relative phases of the Slater determinants as compared to an averaged phases.

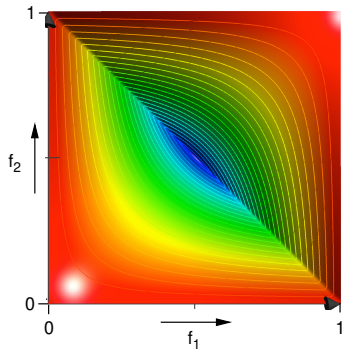

Fig. F.4: Contour plot for the lower bound $\min(0, f_1 + f_2 - 1) - f_1 f_2$ for the occupation-number fluctuations $\sum_{\sigma_1,\sigma_2} P_{\sigma_1,\sigma_2}(\sigma_1 - f_1)(\sigma_2 - f_2)$ of two orbitals as a function of the occupations f_1 and f_2. The plot is drawn for $f_j \in [0, 1]$. The function values are zero at the boundaries of the area and the minimum, at $f_1 = f_2 = \frac{1}{2}$ has the value $-\frac{1}{4}$. (This graph is repeated from figure 2.4 on p. 79)

The term "mean field"

Let us consider the first two terms of the interaction Eq. F.137, the mean-field term and the occupation-number fluctuations. These two terms correspond to the interaction energy of an ensemble of Slater determinants with probabilities $P_{\vec{\sigma}} = \hat{c}^*_{\vec{\sigma}} \hat{c}_{\vec{\sigma}}$ (see Eq. F.131).

The interaction energy of this ensemble is the weighted sum of the interaction energies of the Slater determinants.

$$E^{APA}_{int} = \sum_{\vec{\sigma}} P_{\vec{\sigma}} \langle \vec{\sigma} | \hat{W} | \vec{\sigma} \rangle = \frac{1}{2} \sum_{\vec{\sigma}} P_{\vec{\sigma}} \mathrm{Tr} \left[\hat{\rho}^{(1)}_{\vec{\sigma}} \left(\hat{V}_{H,\vec{\sigma}} + \hat{V}_{X,\vec{\sigma}} \right) \right] \tag{F.142}$$

With $\hat{\rho}^{(1)}_{\vec{\sigma}}$, I denote the one-particle reduced density matrix of the Slater determinant $\vec{\sigma}$ and with $\hat{V}_{H,\vec{\sigma}}$ and $\hat{V}_{X,\vec{\sigma}}$ I denote the Hartree potential Eq. 2.38 and exchange potentials Eq. 2.41 of that same Slater determinant.

We notice, that each Slater determinant experiences its own potential.

In the mean-field approximation, the individual potentials are replaced by the mean-field, i.e. the Hartree and exchange potentials averaged over the Slater determinants $|\vec{\sigma}\rangle$ with their respective weights $P_{\vec{\sigma}}$,

$$\hat{V}_{H,mf} + \hat{V}_{X,mf} \overset{\text{def}}{=} \sum_{\vec{\sigma}} P_{\vec{\sigma}} \left(\hat{V}_{H,\vec{\sigma}} + \hat{V}_{X,\vec{\sigma}} \right) \tag{F.143}$$

When the individual potentials are replaced by the mean-field potentials, the mean-field energy (first term in Eq. F.137) is obtained.

$$E^{mf}_{int} = \frac{1}{2} \sum_{\vec{\sigma}} P_{\vec{\sigma}} \mathrm{Tr} \Big[\hat{\rho}^{(1)}_{\vec{\sigma}} \underbrace{\Big[\sum_{\vec{\sigma}'} P_{\vec{\sigma}'} \left(\hat{V}_{H,\vec{\sigma}'} + \hat{V}_{X,\vec{\sigma}'} \right) \Big]}_{\hat{V}_{H,mf} + \hat{V}_{X,mf}} \Big] = \frac{1}{2} \mathrm{Tr} \left[\hat{\rho}^{(1)} \left(\hat{V}_{H,mf} + \hat{V}_{X,mf} \right) \right] \tag{F.144}$$

Notice the prefactor $\frac{1}{2}$ in Eq. F.144 which makes mean-field energy different from the expectation value of the mean-field potential.

The comparison with Eq. F.137 shows that the difference between the mean-field energy E_{int}^{mf} in Eq. F.144 and that of the averaged phase approximation E_{int}^{APA} in Eq. F.142 is due to the occupation-number fluctuations.

Random(average)-phase approximation

The first and second lines of Eq. F.137 together describe the interaction energy for an ensemble of Slater determinants $|\vec{\sigma}\rangle$ with probabilities $P_{\vec{\sigma}}$.

$$W = \sum_{\vec{\sigma}} P_{\vec{\sigma}} \langle \vec{\sigma} | \hat{W} | \vec{\sigma} \rangle \tag{F.145}$$

The neglect of the entanglement energy (third term of Eq. F.137) can be described as random(average)-phase approximation.[11]

Let me now work out the random(average)-phase approximation of the interaction energy. First, the interaction energy $\langle \Psi | \hat{W} | \Psi \rangle$ is evaluated for a transformed many-particle wave function $\hat{R}(\vec{\gamma})|\Psi\rangle$, for which each Slater determinant $|\vec{\sigma}\rangle$ is multiplied by individual phase factor $e^{i\gamma_{\vec{\sigma}}}$. Then, the interaction energy is averaged over the phases $\gamma_{\vec{\sigma}} \in [0, 2\pi[$ of each Slater determinant independently.

The transformation $\hat{R}(\vec{\gamma})$ of the many-particle wave functions, which multiplies each Slater determinant with an individual phase factor $e^{i\gamma_{\vec{\sigma}}}$ with real-valued angle $\gamma_{\vec{\sigma}}$, is

$$\hat{R}(\vec{\gamma}) = \sum_{\vec{\sigma}} |\vec{\sigma}\rangle e^{i\gamma_{\vec{\sigma}}} \langle \vec{\sigma}| \tag{F.146}$$

There is one angle $\gamma_{\vec{\sigma}}$ for every Slater determinant in Fock space. That is, $\vec{\gamma}$ is a vector in Fock space, not in the one-particle Hilbert space.

This average yields

$$\begin{aligned}
\left\langle \langle \Psi | \hat{W} | \Psi \rangle \right\rangle_{\vec{\gamma}} &= \left(\prod_{\vec{\sigma}} \int_0^{2\pi} \frac{d\gamma_{\vec{\sigma}}}{2\pi} \right) \langle \Psi | \hat{R}^\dagger(\vec{\gamma}) \hat{W} \hat{R}(\vec{\gamma}) | \Psi \rangle \\
&\overset{|\Psi\rangle = \sum_{\vec{\sigma}} |\vec{\sigma}\rangle c_{\vec{\sigma}}}{=} \left(\prod_{\vec{\sigma}} \int_0^{2\pi} \frac{d\gamma_{\vec{\sigma}}}{2\pi} \right) \sum_{\vec{\sigma}',\vec{\sigma}''} c^*_{\vec{\sigma}'} \langle \vec{\sigma}' | \hat{W} | \vec{\sigma}'' \rangle c_{\vec{\sigma}''} e^{i(\gamma_{\vec{\sigma}''} - \gamma_{\vec{\sigma}'})} \\
&= \sum_{\vec{\sigma}',\vec{\sigma}''} c^*_{\vec{\sigma}'} \langle \vec{\sigma}' | \hat{W} | \vec{\sigma}'' \rangle c_{\vec{\sigma}''} \underbrace{\int_0^{2\pi} \frac{d\gamma_{\vec{\sigma}'}}{2\pi} \int_0^{2\pi} \frac{d\gamma_{\vec{\sigma}''}}{2\pi} e^{i(\gamma_{\vec{\sigma}''} - \gamma_{\vec{\sigma}'})}}_{\delta_{\vec{\sigma}',\vec{\sigma}''}} \\
&= \sum_{\vec{\sigma}} \underbrace{c^*_{\vec{\sigma}} c_{\vec{\sigma}}}_{P_{\vec{\sigma}}} \langle \vec{\sigma} | \hat{W} | \vec{\sigma} \rangle
\end{aligned} \tag{F.147}$$

The random(average)-phase approximation used here converts a correlated many-particle wave function into a statistical ensemble of Slater determinants $|\vec{\sigma}\rangle$ with probabilities $P_{\vec{\sigma}} = |c_{\vec{\sigma}}|^2$. In other words, it removes the entanglement term from Eq. F.137.

The derivation can easily be generalized to ensembles $\{|\Psi_q\rangle, \bar{P}_q\}$ of many-particle wave functions $|\Psi_q\rangle = \sum_{\vec{\sigma}} |\vec{\sigma}\rangle c_{\vec{\sigma},q}$, rather than a single many-particle wave function used in this proof. In this case the probabilities of the Slater determinants are $P_{\vec{\sigma}} = \sum_q \bar{P}_q c^*_{\vec{\sigma},q} c^*_{\vec{\sigma}}$.

Let me alert you to a common mistake: It is important to understand, which phases are averaged. In the derivation above, we have first chosen a one-particle basisset. This choice defines the set of

[11] This random(average)-phase approximation is probably unrelated to the random(average)-phase approximation (APA), which leads to the screened interaction between electrons.

Slater determinants. It is the phases between the Slater determinants, rather than those of the one-particle orbitals that is averaged over.[12]

The choice of the one-particle basisset, which, in turn, determines the set of Slater determinants, and thus, whether the random(average)-phase approximation is a good or a poor approximation.

F.7 Spectral function in the Hartree-Fock approximation

F.7.1 Spectral function of Hartree-Fock at finite temperatures

In this section, I calculating the exact spectral function for the thermal ensemble from the thermal Hartree-Fock approximation. For a single Slater determinant, the one-particle spectral function exhibits delta peaks at the eigenvalues of the Fock operator.

At finite temperatures, considered here, the excitations experience thermal fluctuations, which leads to a thermal broadening of the spectral bands.

Let me start with the expression for the one-particle spectral function from the Lehmann representation.

$$\hat{\mathcal{A}}(\epsilon) \overset{\text{Eq. 9.32}}{=} \sum_{m,n} |\varphi_m\rangle \Bigg(\sum_{\vec{\sigma},\vec{\sigma'}} \Big(P_{\vec{\sigma}} + P_{\vec{\sigma'}} \Big) \langle \vec{\sigma} | \hat{a}_m | \vec{\sigma'} \rangle \langle \vec{\sigma'} | \hat{a}_n^\dagger | \vec{\sigma} \rangle \delta(\epsilon - (E_{\vec{\sigma'}} - E_{\vec{\sigma}}) \Bigg) \langle \varphi_n | \tag{F.148}$$

We will use the microstates $|\vec{\sigma}\rangle$ and probabilities $P_{\vec{\sigma}} = \frac{1}{Z} \mathrm{e}^{-\beta(\epsilon_n^{\text{eff}} - \mu)}$ from the thermal Hartree-Fock approximation, where ϵ_n^{eff} are the eigenvalues of the Fock operator for the ensemble.

The excitation energies are obtained from the total energies $E_{\vec{\sigma}}$ of the individual microstates.

$$\begin{aligned} E_{\vec{\sigma}} &= \langle \vec{\sigma} | \hat{h} + \hat{W} | \vec{\sigma} \rangle \\ &= \sum_n \sigma_n \langle \varphi_n | \hat{h} | \varphi_n \rangle + \frac{1}{2} \sum_{m,n=1}^{\infty} \sigma_m \sigma_n \Big(\langle \varphi_m, \varphi_n | \hat{W} | \varphi_m, \varphi_n \rangle - \langle \varphi_m, \varphi_n | \hat{W} | \varphi_n, \varphi_m \rangle \Big) \end{aligned} \tag{F.149}$$

The energy to add a particle in state $|\varphi_n\rangle$ to $|\vec{\sigma}\rangle$ is

$$\begin{aligned} \Delta E &= \langle \varphi_n | \hat{h} | \varphi_n \rangle + \sum_m^{\infty} \sigma_m \Big(\langle \varphi_m, \varphi_n | \hat{W} | \varphi_m, \varphi_n \rangle - \langle \varphi_m, \varphi_n | \hat{W} | \varphi_n, \varphi_m \rangle \Big) \\ &= \underbrace{\langle \varphi_n | \hat{h} + \hat{V}_H + \hat{V}_X | \varphi_n \rangle}_{\epsilon_n^{\text{eff}}} + \sum_m^{\infty} (\sigma_m - f_m) \Big(\langle \varphi_m, \varphi_n | \hat{W} | \varphi_m, \varphi_n \rangle - \langle \varphi_m, \varphi_n | \hat{W} | \varphi_n, \varphi_m \rangle \Big) \end{aligned} \tag{F.150}$$

It does not matter whether the sum over m includes n or not, because the corresponding matrix element for $m = n$ is zero. The energy ϵ_n^{eff} is the corresponding eigenstate of the Fock operator $\hat{h}^{\text{eff}} = \hat{h} + \hat{V}_H + \hat{V}_X$, which acts as an effective Hamiltonian.

While the first term ϵ_n^{eff} is the same for all microstates the ensemble, the second term describes thermal fluctuations, which differ from microstate to microstate. These fluctuations are low-energy excitations, which are thermally accessible.

[12] A similar random(average)-phase approximation can be used to arrive at the Boltzmann equation. There, however, the phases of one-particle orbitals are averaged, which is a much more severe approximation than the one done here.

The resulting spectral function is

$$\begin{aligned}
\mathcal{A}(\epsilon) &\overset{\text{Eq. 9.32}}{=} \sum_{m,n} |\varphi_n\rangle \Bigg\{ \sum_{\vec{\sigma},\vec{\sigma}'} \underbrace{\frac{\left(\mathrm{e}^{-\beta\sum_j \sigma_j(\epsilon_j-\mu)} + \mathrm{e}^{-\beta\sum_j \sigma'_j(\epsilon_j-\mu)}\right)}{\sum_{\vec{\sigma}''} \mathrm{e}^{-\beta\sum_j \sigma''_j(\epsilon_j-\mu)}}}_{P_{\vec{\sigma}}+P_{\vec{\sigma}'}} \underbrace{\delta_{\sigma_n,0}\delta_{\sigma'_n,1} \prod_{m;m\neq n} \delta_{\sigma_m,\sigma'_m}}_{\langle\vec{\sigma}|\hat{a}_m|\vec{\sigma}'\rangle\langle\vec{\sigma}'|\hat{a}_n^\dagger|\vec{\sigma}\rangle} \\
&\quad \times\delta\Bigg(\epsilon - \epsilon_n^{\text{eff}} - \sum_m^\infty (\sigma_m - f_m)\Big(\langle\varphi_m,\varphi_n|\hat{W}|\varphi_m,\varphi_n\rangle - \langle\varphi_m,\varphi_n|\hat{W}|\varphi_n,\varphi_m\rangle\Big)\Bigg)\Bigg\}\langle\varphi_n| \\
&= \sum_n |\varphi_n\rangle \Bigg\{ \frac{1}{\sum_{\vec{\sigma}'} \mathrm{e}^{-\beta\sum_j \sigma'_j(\epsilon_j-\mu)}} \sum_{\vec{\sigma}} \delta_{\sigma_n,0} \mathrm{e}^{-\beta\sum_j \sigma_j(\epsilon_j-\mu)} \Big(1 + \mathrm{e}^{-\beta(\epsilon_n^{eff}-\mu)}\Big) \\
&\quad \times\delta\Bigg(\epsilon - \epsilon_n^{\text{eff}} - \sum_m^\infty (\sigma_m - f_m)\Big(\langle\varphi_m,\varphi_n|\hat{W}|\varphi_m,\varphi_n\rangle - \langle\varphi_m,\varphi_n|\hat{W}|\varphi_n,\varphi_m\rangle\Big)\Bigg)\Bigg\}\langle\varphi_n| \\
&= \sum_n |\varphi_n\rangle \Bigg\{ \sum_{\vec{\sigma}} \delta_{\sigma_n,0} \frac{\mathrm{e}^{-\beta\sum_j \sigma_j(\epsilon_j-\mu)}}{\sum_{\vec{\sigma}'} \delta_{\sigma'_n,0} \mathrm{e}^{-\beta\sum_j \sigma'_j(\epsilon_j-\mu)}} \\
&\quad \times\delta\Bigg(\epsilon - \epsilon_n^{\text{eff}} - \sum_m^\infty (\sigma_m - f_m)\Big(\langle\varphi_m,\varphi_n|\hat{W}|\varphi_m,\varphi_n\rangle - \langle\varphi_m,\varphi_n|\hat{W}|\varphi_n,\varphi_m\rangle\Big)\Bigg)\Bigg\}\langle\varphi_n|
\end{aligned} \tag{F.151}$$

We see that each natural orbital contributes a large number of δ-peaks to the density of states. In other words, the density of states is broadened. The broadening is due to the potential fluctuations induced by the fluctuations of the occupation of other orbitals. These fluctuations are absent for orbitals with integer occupations $f_n = 0$ or $f_n = 1$.

If only one Slater determinant contributes to the ensemble (at $T = 0$) this thermal broadening is absent. If the ground state is, for example, doubly degenerate, the spectral function is the average of the two Slater determinants in the ground state ensemble.

Because the broadening is hard to calculate, the mean-field approximation is also done for the spectral function.

$$\hat{\mathcal{A}}^{mf}(\epsilon) = \sum_n |\varphi_n\rangle \delta\big(\epsilon - \epsilon_n^{\text{eff}}\big) \langle\varphi_n| \tag{F.152}$$

F.7.2 Spectral function beyond the mean-field spectral function

The discussion above rested on the mean-field approximation, where all particles experience the same potential.

In the spirit of section F.6.2, we explore the spectrum of an ensemble of Slater determinants built from the natural orbitals. This goes beyond the mean-field approximation, and it is consistent with the random(averaged)-phase approximation.

The one-particle energies $\epsilon_{n,\vec{\sigma}} = \langle\varphi_n|\hat{h} + \hat{V}_{H,\vec{\sigma}} + \hat{V}_{X,\vec{\sigma}}|\varphi_n\rangle$ depend on the specific Slater determinant in the ensemble, because each Slater determinant produces its own Hartree and exchange potential. The spectral function of the ensemble is

$$\hat{\mathcal{A}}(\epsilon) = \sum_{\vec{\sigma}} P_{\vec{\sigma}} \sum_n |\varphi_n\rangle \delta(\epsilon - \epsilon_{n,\vec{\sigma}}) \langle\varphi_n| = \sum_n |\varphi_n\rangle \Big\{ \sum_{\vec{\sigma}} P_{\vec{\sigma}} \delta(\epsilon - \epsilon_{n,\vec{\sigma}}) \Big\} \langle\varphi_n| \tag{F.153}$$

For each natural orbital $|\varphi_n\rangle$, I obtain a multitude of contributions at different energies $\epsilon_{n,\vec{\sigma}}$ with different weights $P_{\vec{\sigma}}$.

In the mean-field approximation the contributions for one natural orbital collapse into a single, average energy level at

$$\epsilon_n^{mf} = \sum_{\vec{\sigma}} P_{\vec{\sigma}} \epsilon_{n,\vec{\sigma}} \tag{F.154}$$

that is, the spectral function in the mean-field approximation is

$$\hat{\mathcal{A}}^{mf}(\epsilon) = \sum_n |\varphi_n\rangle \delta(\epsilon - \epsilon_n^{mf}) \langle\varphi_n| \tag{F.155}$$

The total weight and the mean energy of each natural orbital remains unchanged

$$\begin{aligned} \int d\epsilon\, \langle\varphi_n|\hat{\mathcal{A}}(\epsilon)|\varphi_n\rangle &= \int d\epsilon\, \langle\varphi_n|\hat{\mathcal{A}}^{mf}(\epsilon)|\varphi_n\rangle = 1 \\ \int d\epsilon\, \langle\varphi_n|\hat{\mathcal{A}}(\epsilon)|\varphi_n\rangle\, \epsilon &= \int d\epsilon\, \langle\varphi_n|\hat{\mathcal{A}}^{mf}(\epsilon)|\varphi_n\rangle\, \epsilon = \sum_{\vec{\sigma}} P_{\vec{\sigma}} \epsilon_{n,\vec{\sigma}} = \epsilon_n^{mf} \end{aligned} \tag{F.156}$$

When we adjust the ensemble, keeping the natural orbitals unchanged for the sake of simplicity, we find that the energy levels in the mean-field approximation shift when electrons are added or removed. The weight of each excitation energy remains unchanged.

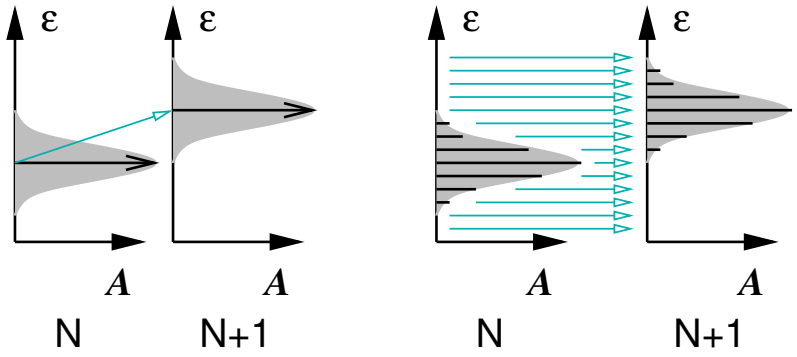

Fig. F.5: Scheme to demonstrate the a spectral function $\mathcal{A}_n(\epsilon, \vec{k})$ of a single band $\epsilon_n(\vec{k})$ for a specific k-point $\vec{k}$ in the mean-field approximation (left) in comparison to the spectral function obtained from a complete many-particle description (right). In the mean-field approximation the spectral function for a specific k-point and band index is a delta-function centered at the one-particle energy $\epsilon_n(\vec{k})$ as shown on the left. As a parameter such as the particle number N is changed, the delta function shifts with the one-particle energy, but it maintains its total weight. The true spectral function consists of a large, possibly continuous, set of peaks at the many-particle total-energy differences. For weak interactions they can be combined approximately into a Lorentzian of finite width. As the electron number N, or any other parameter, is changed, it is the weight of the individual peaks that change, while the positions of the many-particle energy differences remains fixed. Caution: The individual bands are not regular as in the graph, and the positions of the individual peaks are not strictly fixed.

Beyond the mean-field approximation, the energy levels $\epsilon_{n,\vec{\sigma}}$ remain unchanged, but the individual weights adjust with the changed ensemble as sketched in Fig. F.5. This consideration provides a first glimpse on the definition of the spectral function for general many-particle states and their ensemble in section 9.3

F.8 Post Hartree-Fock methods: Quantum chemistry

Editor: Sketch here the main ideas of post-Hartree-Fock methods of quantum chemistry. It may include configuration interaction (CI), complete active space (CAS) CI, Multireference, coupled cluster (CC) and possibly Møller-Plesset (MP) perturbation theory.

F.8.1 Coupled cluster:

Coupled-cluster theory is a quantum chemical method, which overcomes the problem of size inconsistency in the configuration interaction methods. It has been invented in the context of nuclear physics by Fritz Coester and Herman Kümmel in the early 1960s.[13] [14]

Use a unitary transformation $\hat{U}$ in Fock space to represent a general many-particle wave function $|\Phi\rangle$ in terms of some reference wave function $|\bar{\Phi}\rangle$.

The Fock-space can be spanned either by variation of the reference wave function or by variation of the transformation operator. This allows one to restrict the reference wave functions, for example, to Slater determinants.

$$|\Phi_{\vec{\sigma}}\rangle = \hat{U}|\bar{\Phi}\rangle = \mathrm{e}^{\frac{i}{\hbar}\hat{A}}|\bar{\Phi}\rangle = \mathrm{e}^{\frac{i}{\hbar}\left(\sum_{\alpha,\beta} a_{\alpha,\beta}\hat{c}^\dagger_\alpha\hat{c}_\beta + \sum_{\alpha,\beta,\gamma,\delta} b_{\alpha,\beta,\gamma,\delta}\hat{c}^\dagger_\alpha\hat{c}^\dagger_\beta\hat{c}_\gamma\hat{c}_\delta + \ldots\right)}|\bar{\Phi}\rangle \tag{F.157}$$

A unitary operator can be expressed in terms of an exponential of a hermitean operator $\hat{A}$. It makes sense to choose the operator as particle-number conserving, which implies that each term in $\hat{A}$ has the same number of creation and annihilation operators.

The parameters $a_{\alpha,\beta}$, $b_{\alpha,\beta,\gamma,\delta}$ are considered as variational parameters for the total energy, alongside with some reference wave function.

The total energy can be obtained by minimizing

$$\begin{aligned} E &= \min_{|\Phi\rangle} \operatorname*{stat}_{\Lambda}\Big\{\langle\Phi|\hat{H}|\Phi\rangle - \Lambda\Big(\langle\Phi|\Phi\rangle - 1\Big)\Big\} \\ &= \min_{|\bar{\Phi}\rangle,\hat{A}} \operatorname*{stat}_{\Lambda}\Big\{\langle\bar{\Phi}|\mathrm{e}^{-i\hat{A}}\hat{H}\mathrm{e}^{i\hat{A}}|\bar{\Phi}\rangle - \Lambda\Big(\langle\bar{\Phi}|\underbrace{\mathrm{e}^{-i\hat{A}}\mathrm{e}^{i\hat{A}}}_{=\hat{1}\text{ if }\hat{A}=\hat{A}^\dagger}|\bar{\Phi}\rangle - 1\Big)\Big\} \\ &= \min_{|\bar{\Phi}\rangle,\hat{A}(\hat{A}=\hat{A}^\dagger)} \operatorname*{stat}_{\Lambda}\Big\{\langle\bar{\Phi}|\mathrm{e}^{-i\hat{A}}\hat{H}\mathrm{e}^{i\hat{A}}|\bar{\Phi}\rangle - \Lambda\Big(\langle\bar{\Phi}|\bar{\Phi}\rangle - 1\Big)\Big\} \end{aligned} \tag{F.158}$$

Rather than using the stationary condition with respect to the operator $\hat{A}$, the stationary condition with respect to the reference wave function is used

$$\mathrm{e}^{-i\hat{A}}\hat{H}\mathrm{e}^{i\hat{A}}|\bar{\Phi}\rangle = |\bar{\Phi}\rangle\Lambda \tag{F.159}$$

This strategy is permitted, as long as the same portion of Fock space is spanned by the variation of $\hat{A}$ and the variation of the reference wave function.

This equation is solved by introducing a basis of Slater determinants $|\vec{\sigma}\rangle$.

$$\langle\vec{\sigma}|\mathrm{e}^{-i\hat{A}}\hat{H}\mathrm{e}^{i\hat{A}}|\bar{\Phi}\rangle = \langle\vec{\sigma}|\bar{\Phi}\rangle\Lambda \tag{F.160}$$

where the basis of Slater determinants $\langle\vec{\sigma}|$ must be sufficiently large to determine all parameters of the transformation operator, respectively of $\hat{A}$. It is convenient to select the Slater determinants such that the reference wave function is one of them.

[13] see [118] and references

[14] See also Sinanoglu[119] who introduced a variational formulation which is considered a predecessor of coupled cluster theory. This may be close to what I am using here.

Appendix G

Density-functional theory

Density-functional theory[29, 30] is an extremely powerful technique. It is based on an exact theorem that the ground-state energy is determined solely by the density alone.

The theorem says

- that all ground-state properties are unique functionals of the electron density and
- that the electron density can be obtained from a one-particle Schrödinger equation in an effective potential.

Density-functional theory maps the interacting electron system onto a system of non-interacting electrons in an effective potential. The effective potential depends in turn on the electron distribution and describes the interacting between the electrons in an effective way.

G.1 Existence of a density functional for the energy

Density-functional theory says that all ground-state properties can be expressed, at least in principle, as functionals of the charge density alone.

This statement is nontrivial, because the wave function contains far more information than the density. The statement also provides a dramatic simplification as the density, in contrast to the wave function, can be handled on a computer: The density is a function in three dimensions, while the wave function is a function in 3^N dimensions.

The original proof of existence for density functionals goes back to Hohenberg and Kohn[120]. Later, Levy[121, 122] and Lieb[123] have given a recipe how the density functional can actually be constructed . This proof contains the proof of existence. For this reason, I will not present the original proof of Hohenberg and Kohn, but show the one by Levy.

G.1.1 The many-particle Hamiltonian

Let us start with a Hamilton operator

$$\hat{H}_\lambda = \hat{T} + \hat{V}_{ext} + \lambda \hat{W} \ , \tag{G.1}$$

where the kinetic energy is

$$\hat{T} = \int d^4x \ \hat{\psi}^\dagger(\vec{x}) \frac{-\hbar^2}{2m_e} \vec{\nabla}^2 \hat{\psi}(\vec{x}) = \sum_{\alpha,\beta} \underbrace{\langle \chi_\alpha | \frac{\hat{\vec{p}}^2}{2m_e} | \chi_\beta \rangle}_{t_{\alpha,\beta}} \hat{c}_\alpha^\dagger \hat{c}_\beta \tag{G.2}$$

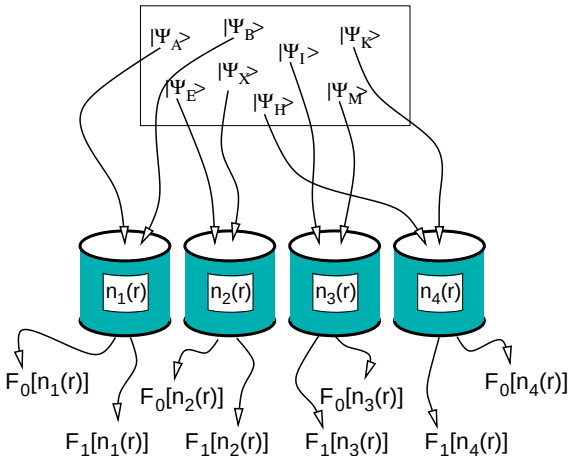

Fig. G.1: Sketch of Levy's derivation of a density functional.

The external potential operator describes the Coulomb potential of the nuclei

$$\hat{V} = \int d^4x \; v_{ext}(\vec{r}) \underbrace{\hat{\psi}^\dagger(\vec{x})\hat{\psi}(\vec{x})}_{\hat{n}(\vec{x})} = \sum_{\alpha,\beta} \underbrace{\langle \chi_\alpha | \hat{v}_{ext} | \chi_\beta \rangle}_{v_{\alpha,\beta}} \hat{c}^\dagger_\alpha \hat{c}_\beta \tag{G.3}$$

The interaction operator is

$$\begin{aligned} \hat{W} &\overset{\text{Eq. 3.75}}{=} \frac{1}{2} \int d^4x \int d^4x' \; \hat{\psi}^\dagger(\vec{x})\hat{\psi}^\dagger(\vec{x'}) \frac{e^2}{4\pi\epsilon_0 |\vec{r} - \vec{r'}|} \hat{\psi}(\vec{x'})\hat{\psi}(\vec{x}) \\ &= \frac{1}{2} \sum_{\alpha,\beta,\gamma,\delta} \underbrace{\int d^4x \int d^4x' \; \frac{e^2 \chi^*_\alpha(\vec{x})\chi^*_\beta(\vec{x'})\chi_\gamma(\vec{x'})\chi_\delta(\vec{x})}{4\pi\epsilon_0 |\vec{r} - \vec{r'}|}}_{U_{\alpha,\beta,\delta,\gamma}} \hat{c}^\dagger_\alpha \hat{c}^\dagger_\beta \hat{c}_\gamma \hat{c}_\delta \end{aligned} \tag{G.4}$$

The **U-tensor** is defined with the arguments $\vec{x}$ and $\vec{x'}$ in the same order for the product wave function and its complex conjugate.

$$U_{\alpha,\beta,\gamma,\delta} \overset{\text{def}}{=} \int d^4x \int d^4x' \; \frac{e^2 \chi^*_\alpha(\vec{x})\chi^*_\beta(\vec{x'})\chi_\gamma(\vec{x})\chi_\delta(\vec{x'})}{4\pi\epsilon_0 |\vec{r} - \vec{r'}|} \tag{G.5}$$

We scaled the electron-electron interaction by a coupling parameter λ, which allows us later to switch the electron-electron interaction on an off. This is not required for the proof of Levy, but later-on, we will often refer also to Hamiltonians without or with scaled interaction.

G.1.2 The proof: constrained search

The idea of the proof is very simple:

1. Group all normalized, antisymmetric many-particle wave functions $\{|\Phi\rangle\}$ according to their density.[1] Each such subset $\mathcal{A}[n(\vec{r})]$ contains all wave functions in the **Fock space** $\mathcal{F}$ with the same density $n(r)$.

$$\mathcal{A}[n(\vec{r})] = \{|\Phi\rangle \in \mathcal{F} : \langle \Phi | \hat{n}(\vec{r}) | \Phi \rangle = n(\vec{r})\}$$

[1] the density is considered as function not as value at a specific point in space.

2. For each subset $\mathcal{A}[n(\vec{r})]$, that is for each density, we determine that wave function $\left|\Phi_\lambda^{(0)}[n(\vec{r})]\right\rangle$ that provides the lowest energy $\langle\Phi|\hat{H}_\lambda|\Phi\rangle$. The minimum of the total energy defines the total energy functional $E_\lambda[n(\vec{r})]$ of the electron density.

$$E_\lambda[n(\vec{r})] = \min_{|\Phi\rangle\in\mathcal{A}[n(\vec{r})]} \left\langle \Phi \left| \hat{H}_\lambda \right| \Phi \right\rangle = \left\langle \Phi_\lambda^{(0)}[n(\vec{r})] \left| \hat{H}_\lambda \right| \Phi_\lambda^{(0)}[n(\vec{r})] \right\rangle$$

3. The energy can be divided into **universal density functional** $F_\lambda[n(\vec{r})]$, which is a general property of the electron gas, and a system-specific term, that depends on the external potential.

$$E_\lambda[n(\vec{r})] = \underbrace{F_\lambda[n(\vec{r})]}_{\langle\Phi_\lambda^{(0)}[n]|\hat{T}+\lambda\hat{W}|\Phi_\lambda^{(0)}[n]\rangle} + \underbrace{\int d^3r\; n(\vec{r})v_{ext}(\vec{r})}_{\langle\Phi_\lambda^{(0)}[n]|\hat{V}|\Phi_\lambda^{(0)}[n]\rangle}$$

Because the energy related to the external potential only depends on the density, it is a constant within each group of a given density. Thus, we can directly determine the universal functional $F_\lambda[n(\vec{r})]$ as minimum of $\langle\Phi|\hat{T}+\lambda\hat{W}|\Phi\rangle$ for all wave functions with the specified density.

UNIVERSAL DENSITY FUNCTIONAL

$$F_\lambda[n(\vec{r})] \stackrel{\text{def}}{=} \min_{|\Phi\rangle\in\mathcal{A}[n(\vec{r})]} \langle\Phi|\hat{T}+\lambda\hat{W}|\Phi\rangle$$

4. To find the ground-state energy $E_\lambda^{(0)}$ of an electron gas with N electrons in a given external potential, we minimize the total energy functional with respect to the density under the constraint of a specified total number of electrons.

$$E_\lambda^{(0)} = \min_{n(\vec{r}):\int d^3r\; n(\vec{r})=N} \left\{ F_\lambda[n(\vec{r})] + \int d^3r\; n(\vec{r})v_{ext}(\vec{r}) \right\}$$

This minimization with respect to the density provides us with the ground-state density and the ground-state energy. If we have remembered the wave function $|\Phi^0[n(\vec{r})]\rangle$ that minimized the total energy within a group with given density $n(\vec{r})$, we can, in principle work our way back to the ground-state wave function, which contains all information about the electronic ground state.

This concludes the proof by Levy on the existence of a universal functional of the density, that allows one to determine the ground-state energy and, in principle, all other properties of the electronic ground state.

G.2 More explicit proof at finite temperature

The previous section shows the principle of Levy's constrained search algorithm with the minimum conceptual complication. In this section, we generalize the proof given above to finite temperature.

- This will make us familiar with a few thermodynamic relations, that will be used later again. Thus, it shows, that the limitation to ground states implies the generalization to ensembles in thermal equilibrium.
- The second motivation for repeating the proof is to make the steps for constrained minimization more explicit. These expression provide us then with the set of equations that specify the minimum.

G.2.1 Grand potential

Let us start with the grand potential for a system of electrons. The grand potential[2] $\Omega_{T,\mu}$ is the thermodynamic potential for a system in contact with a heat bath and a particle reservoir. The heat bath is characterized by the temperature T and the particle reservoir is characterized by the chemical potential μ.

The **grand potential** has the form

$$\Omega_{T,\mu} = \min_{|\Phi_j\rangle,P_j} \operatorname*{stat}_{\boldsymbol{\Lambda},\eta} \Bigg\{ \underbrace{k_B T \sum_j P_j \ln(P_j)}_{-TS} + \underbrace{\sum_j P_j \langle\Phi_j|\hat{H}-\mu\hat{N}|\Phi_j\rangle}_{E-\mu N} - \sum_{j,k} \Lambda_{j,k}\Big(\langle\Phi_k|\Phi_j\rangle - \delta_{k,j}\Big) - \eta\Big(\sum_j P_j - 1\Big)\Bigg\} \tag{G.6}$$

where $|\Phi_j\rangle$ are many-electron wave functions in the Fock space and the P_j are their probabilities. The set $\{P_j, |\Phi_j\rangle\}$ of many-particle wave functions and their probabilities describes a general **ensemble**. The ensemble is a **macrostate**, while a single many-particle wave function describes a **microstate**. The symbol "stat" specifies a stationary point of the expression, which may be a minimum, a maximum or a saddle point, while the symbol "min" is reserved for true minima.

The minimum condition with respect to the probabilities can readily be worked out as

$$P_j = \frac{1}{Z_{T,\mu}} \mathrm{e}^{-\beta\langle\Phi_j|\hat{H}-\mu\hat{N}|\Phi_j\rangle} \tag{G.7}$$

with the **partition function**

$$Z_{T,\mu} = \sum_j \mathrm{e}^{-\beta\langle\Phi_j|\hat{H}-\mu\hat{N}|\Phi_j\rangle} \tag{G.8}$$

Inserting these probabilities into the expression for the grand potential, we obtain

$$\Omega_{T,\mu} = \min_{|\Phi_j\rangle} \operatorname*{stat}_{\boldsymbol{\Lambda}} \Bigg\{ -k_B T \ln\Bigg[\sum_j \mathrm{e}^{-\beta\langle\Phi_j|\hat{H}-\mu\hat{N}|\Phi_j\rangle}\Bigg] - \sum_{j,k} \Lambda_{j,k}\Big(\langle\Phi_k|\Phi_j\rangle - \delta_{k,j}\Big)\Bigg\} \tag{G.9}$$

The minimization with respect to the many-particle wave functions $|\Phi_j\rangle$ can be performed by diagonalizing $\hat{H}-\mu\hat{N}$. When the wave functions $|\Phi_j\rangle$ obey

$$\hat{H}|\Phi_j\rangle = |\Phi_j\rangle E_j \qquad \text{and} \qquad \hat{N}|\Phi_j\rangle = |\Phi_j\rangle N_j \;, \tag{G.10}$$

the grand potential obtains the form

$$\Omega_{T,\mu} = -k_B T \ln\Bigg[\sum_j \langle\Phi_j|\mathrm{e}^{-\beta(\hat{H}-\mu\hat{N})}|\Phi_j\rangle\Bigg] = -k_B T \ln \mathrm{Tr}\Big[\mathrm{e}^{-\beta(\hat{H}-\mu\hat{N})}\Big] \tag{G.11}$$

G.2.2 Helmholtz potential

In many practical problems, the particle number is fixed rather than the chemical potential. An equilibrium ensemble with constant temperature and particle number is called the **canonical ensemble**. The thermodynamic potential for the canonical ensemble is the **Helmholtz potential** $A_{T,N}$. It describes a system in the presence of a heat-bath, but, in contrast to the grand potential, without a particle reservoir.

[2] The thermodynamic potential of a homogeneous system, that only depends on intrinsic variables does not exist, because it would either be eaten up or grow to infinity in the presence of the reservoirs. Here the situation is different, because there are still the atoms, which are not affected by adding or removing energy or electrons.

The Helmholtz potential is obtained from the grand potential by a **Legendre-Fenchel transform**

$$A_{T,N} = \operatorname*{stat}_{\mu} \Big[\Omega_{T,\mu} + \mu N \Big] \tag{G.12}$$

If the expression Eq. G.6 for the grand potential is inserted, we recognize that the stationary condition is part of a constraint condition imposed by the method of Lagrange multipliers. We obtain

$$\begin{aligned} A_{T,N} = \min_{|\Phi_j\rangle, P_j} \operatorname*{stat}_{\mathbf{\Lambda},\eta,\mu} \Bigg\{ & \underbrace{k_B T \sum_j P_j \ln(P_j)}_{-TS} + \underbrace{\sum_j P_j \langle \Phi_j | \hat{H} | \Phi_j \rangle}_{E} \\ & - \mu \Big(\sum_j P_j \langle \Phi_j | \hat{N} | \Phi_j \rangle - N \Big) - \sum_{j,k} \Lambda_{j,k} \Big(\langle \Phi_k | \Phi_j \rangle - \delta_{k,j} \Big) - \eta \Big(\sum_j P_j - 1 \Big) \Bigg\} \end{aligned} \tag{G.13}$$

The Helmholtz potential approaches the ground state energy in the low-temperature limit.

In the following discussion, I will often refer to the Helmholtz potential as the energy. I do this for pedagogical reasons. The rationale is that the Helmholtz potential is a generalization of the energy for finite temperatures. The difficulty other quantities such as the internal energy are also generalizations of the energy for finite temperatures.

G.2.3 Density as fundamental variable

The important observation is that the external potential only acts on the electron density

$$\sum_j P_j \langle \Phi_j | \hat{V} | \Phi_j \rangle = \int d^3 r \; v_{ext}(\vec{r}) n(\vec{r}) \tag{G.14}$$

The electron density of an ensemble is defined as

$$\begin{aligned} n(\vec{r}) &\stackrel{\text{def}}{=} \sum_\sigma \sum_j P_j \langle \Phi_j | \hat{\psi}^\dagger(\vec{x}) \hat{\psi}(\vec{x}) | \Phi_j \rangle \\ &= \sum_\sigma \sum_{\alpha,\beta} \sum_j P_j \langle \Phi_j | \hat{c}_\alpha^\dagger \hat{c}_\beta | \Phi_j \rangle \chi_\alpha^*(\vec{x}) \chi_\beta(\vec{x}) = \sum_{\alpha,\beta} \rho_{\alpha,\beta} \sum_\sigma \chi_\alpha^*(\vec{x}) \chi_\beta(\vec{x}) \end{aligned} \tag{G.15}$$

where

$$\rho_{\alpha,\beta} \stackrel{\text{def}}{=} \sum_j P_j \langle \Phi_j | \hat{c}_\alpha^\dagger \hat{c}_\beta | \Phi_j \rangle \tag{G.16}$$

is the **one-particle-reduced density matrix**..

G.2.4 Constrained search

The fact that the external potential acts only on the density suggests that we divide the minimization into two steps:

$$\begin{aligned}
\Omega_{T,\mu} &\overset{\text{Eq. G.6}}{=} \min_{|\Phi_j\rangle,P_j} \operatorname*{stat}_{\boldsymbol{\Lambda},\eta} \Bigg\{ \underbrace{k_B T \sum_j P_j \ln(P_j)}_{-TS} + \underbrace{\sum_j P_j \langle\Phi_j|\hat{H}-\mu\hat{N}|\Phi_j\rangle}_{E-\mu N} \\
&- \sum_{j,k} \Lambda_{j,k} \Big(\langle\Phi_k|\Phi_j\rangle - \delta_{k,j} \Big) - \eta \Big(\sum_j P_j - 1 \Big) \Bigg\} \\
&= \min_{n(\vec{r})} \Bigg\{ \min_{|\Phi_j\rangle,P_j} \operatorname*{stat}_{\boldsymbol{\Lambda},\eta,\gamma(\vec{r}} \Bigg\{ \underbrace{k_B T \sum_j P_j \ln(P_j)}_{-TS} + \underbrace{\sum_j P_j \langle\Phi_j|\hat{H}-\mu\hat{N}|\Phi_j\rangle}_{E-\mu N} \\
&+ \int d^3r\, \gamma(\vec{r}) \Bigg(\Big(\sum_j P_j \sum_\sigma \langle\Phi_j|\hat{\psi}^\dagger(\vec{x})\hat{\psi}(\vec{x})|\Phi_j\rangle \Big) - n(\vec{r}) \Bigg) \\
&- \sum_{j,k} \Lambda_{j,k} \Big(\langle\Phi_k|\Phi_j\rangle - \delta_{k,j} \Big) - \eta \Big(\sum_j P_j - 1 \Big) \Bigg\} \Bigg\} \\
&= \min_{n(\vec{r})} \Bigg\{ \int d^3r\, n(\vec{r}) v_{ext}(\vec{r}) + F_T^W[n(\vec{r})] - \mu \int d^3r\, n(\vec{r}) \Bigg\} \qquad \text{(G.17)}
\end{aligned}$$

with

UNIVERSAL DENSITY FUNCTIONAL

The quantity

$$\begin{aligned}
F_T^{\lambda\hat{W}}[n(\vec{r})] &\overset{\text{def}}{=} \min_{|\Phi_j\rangle,P_j} \operatorname*{stat}_{\boldsymbol{\Lambda},\eta,\gamma(\vec{r}} \Bigg\{ \underbrace{k_B T \sum_j P_j \ln(P_j)}_{-TS} + \sum_j P_j \langle\Phi_j|\hat{T}+\lambda\hat{W}|\Phi_j\rangle \\
&+ \int d^3r\, \gamma(\vec{r}) \Bigg(\Big(\sum_j P_j \sum_\sigma \langle\Phi_j|\hat{\psi}^\dagger(\vec{x})\hat{\psi}(\vec{x})|\Phi_j\rangle \Big) - n(\vec{r}) \Bigg) \\
&- \sum_{j,k} \Lambda_{j,k} \Big(\langle\Phi_k|\Phi_j\rangle - \delta_{k,j} \Big) - \eta \Big(\sum_j P_j - 1 \Big) \Bigg\} \qquad \text{(G.18)}
\end{aligned}$$

is the **universal density functional** . It is called universal, because it is an intrinsic property of the electron gas and independent of the external potential. This implies that the universal density functional is independent of the particular system.
The universal density functional depends on the mass of the particles, the temperature, the interaction $\lambda\hat{W}$ and the property that they are fermions.

G.2.5 Exchange and correlation energy

There have been attempts to approximate the density functional directly. However, this turned out to be difficult, because it was difficult to represent chemical bonding.

The way out has been to use the kinetic energy of a non-interacting electron gas.

The universal density functional can be determined for any interaction $\hat{W}$. Setting the interaction

to zero yields the kinetic energy functional

$$F_T^0[n(\vec{r})] \stackrel{\text{def}}{=} \min_{|\Phi_j\rangle, P_j} \operatorname*{stat}_{\mathbf{\Lambda},\eta,\gamma(\vec{r})} \Bigg\{ \underbrace{k_B T \sum_j P_j \ln(P_j)}_{-TS} + \sum_j P_j \langle \Phi_j | \hat{T} | \Phi_j \rangle + \int d^3r\, \gamma(\vec{r}) \Bigg(\Big(\sum_j P_j \sum_\sigma \langle \Phi_j | \hat{\psi}^\dagger(\vec{x}) \hat{\psi}(\vec{x}) | \Phi_j \rangle \Big) - n(\vec{r}) \Bigg) - \sum_{j,k} \Lambda_{j,k} \Big(\langle \Phi_k | \Phi_j \rangle - \delta_{k,j} \Big) - \eta \Big(\sum_j P_j - 1 \Big) \Bigg\} \tag{G.19}$$

For a given density the minima for the interacting and the non-interacting functionals differ. That is, the many-particle wave functions differ. Nevertheless, we may rewrite the grand potential in the form

$$\Omega_{T,\mu} = \min_{n(\vec{r})} \Bigg\{ F^0[n(\vec{r})] + \int d^3r\, n(\vec{r}) v_{ext}(\vec{r}) + E_H[n(\vec{r})] + \underbrace{\Big(F_T^W[n(\vec{r})] - F^0[n(\vec{r})] - E_H[n(\vec{r})] \Big)}_{E_{xc}[n(\vec{r})]} - \mu \int d^3r\, n(\vec{r}) \Bigg\} \tag{G.20}$$

where E_H is the Hartree energy defined in Eq. 2.37 on p. 58.

EXCHANGE AND CORRELATION ENERGY

Thus, the grand potential is

$$\Omega_{T,\mu} = \min_{n(\vec{r})} \Bigg\{ F^0[n(\vec{r})] + \int d^3r\, n(\vec{r}) v_{ext}(\vec{r}) + E_H[n(\vec{r})] + E_{xc}[n(\vec{r})] - \mu \int d^3r\, n(\vec{r}) \Bigg\} \tag{G.21}$$

with the **exchange-correlation functional**

$$E_{xc}[n(\vec{r})] \stackrel{\text{def}}{=} F_T^W[n(\vec{r})] - F^0[n(\vec{r})] - E_H[n(\vec{r})] \tag{G.22}$$

It turns out that it is much simpler to find good approximations for the exchange-correlation functional than for the universal density functional. This is the underlying reason for the success of density-functional theory.

G.2.6 Kinetic energy functional

The kinetic-energy functional

$$F_T^0[n(\vec{r})] = \operatorname*{stat}_{\gamma(\vec{r})} \Bigg\{ - \int d^3r\, \gamma(\vec{r}) n(\vec{r}) + \min_{|\Phi_j\rangle, P_j} \operatorname*{stat}_{\mathbf{\Lambda},\eta} \Bigg\{ k_B T \sum_j P_j \ln(P_j) + \sum_j P_j \langle \Phi_j | \Big[\hat{T} + \int d^4x\, \gamma(\vec{r}) \hat{\psi}^\dagger(\vec{x}) \hat{\psi}(\vec{x}) \Big] | \Phi_j \rangle - \sum_{j,k} \Lambda_{j,k} \Big(\langle \Phi_k | \Phi_j \rangle - \delta_{k,j} \Big) - \eta \Big(\sum_j P_j - 1 \Big) \Bigg\} \tag{G.23}$$

can be expressed in terms of one-particle wave functions $|\psi_n\rangle$, the so-called **natural orbitals**, and **occupations** f_n of a non-interacting electron gas in an external potential $\gamma(\vec{r})$. The concept of

natural orbitals and occupations will be described below in more detail.

$$F_T^0[n(\vec{r})] = \operatorname*{stat}_{\gamma(\vec{r})}\Bigg\{ -\int d^3r\, \gamma(\vec{r}) n(\vec{r}) + \min_{f_n\in[0,1],|\psi_n\rangle} \operatorname*{stat}_{\mathbf{\Lambda}}\Bigg\{ k_B T \sum_n \Big(f_n \ln(f_n) + (1-f_n)\ln(1-f_n)\Big) + \sum_n f_n \langle\psi_n| \frac{\hat{\vec{p}}^2}{2m_e} + \hat{\gamma}|\psi_n\rangle - \sum_{m,n} \Lambda_{n,m}\Big(\langle\psi_m|\psi_n\rangle - \delta_{m,n}\Big)\Bigg\}\Bigg\} \tag{G.24}$$

The ground state of the non-interacting system is a statistical average over Slater determinants in a basis of eigenstates of the one-particle Hamiltonian

$$\hat{h} = \int d^4x |\vec{x}\rangle \left[\frac{-\hbar^2}{2m_e}\vec{\nabla}^2 + \gamma(\vec{r})\right]\langle\vec{x}| \tag{G.25}$$

Because of this form the Lagrange multiplier in the kinetic energy functional is named effective potential $v_{eff}(\vec{r}) = \gamma(\vec{r})$.

Thus, we arrive at the final form for the grand potential as it is used in density-functional calculations

$$\begin{aligned}\Omega_{T,\mu} = \min_{n(\vec{r})}\Bigg\{ \min_{f_n\in[0,1],|\psi_n\rangle} \operatorname*{stat}_{\mathbf{\Lambda},\gamma(\vec{r})}\Bigg\{ &\underbrace{\sum_n f_n\langle\psi_n|\frac{\hat{\vec{p}}^2}{2m_e}|\psi_n\rangle}_{\text{non-interacting } E_{\text{kin}}} + \int d^3r\; n(\vec{r}) v_{ext}(\vec{r}) \\ &+ \underbrace{\frac{1}{2}\int d^3r \int d^3r'\; \frac{e^2 n(\vec{r}) n(\vec{r'})}{4\pi\epsilon_0|\vec{r}-\vec{r'}|}}_{\text{Hartree energy}} + E_{xc}[n(\vec{r})] \\ &+ \underbrace{k_B T \sum_n \Big(f_n\ln(f_n) + (1-f_n)\ln(1-f_n)\Big)}_{-TS;\; S=\text{entropy of non-interacting electrons}} \underbrace{-\mu\int d^3r\; n(\vec{r})}_{-\mu N}\Bigg\} \\ &+ \int d^4x\, \gamma(\vec{r})\Big(\sum_n f_n \psi_n^*(\vec{x})\psi_n(\vec{x}) - n(\vec{r})\Big) - \sum_{m,n}\Lambda_{n,m}\Big(\langle\psi_m|\psi_n\rangle - \delta_{m,n}\Big)\Bigg\}\end{aligned} \tag{G.26}$$

G.2.7 Self-consistent equations

The minimum and stationary conditions define a set of equations that need to be obeyed simultaneously. It is called the set of self-consistent equations. These self-consistent equations can be solved iteratively to find the ground state.

We start with the variation with respect to density $n(\vec{r})$, one-particle wave functions $|\psi_n\rangle$ and occupations f_n.

$$\begin{aligned}\frac{\partial\Omega}{\partial n(\vec{r})} &= v_{ext}(\vec{r}) + \underbrace{\int d^3r'\; \frac{e^2 n(\vec{r'})}{4\pi\epsilon_0|\vec{r}-\vec{r'}|}}_{v_H(\vec{r})} + \frac{\partial E_{xc}}{\partial n(\vec{r})} - \mu - \gamma(\vec{r}) \stackrel{!}{=} 0 \\ \frac{1}{f_n}\frac{\partial\Omega}{\partial\langle\psi_n|} &= \Big[\frac{\hat{\vec{p}}^2}{2m_e} + \gamma(\vec{r})\Big]|\psi_n\rangle - \sum_m |\psi_m\rangle\Lambda_{m,n} \stackrel{!}{=} 0 \\ \frac{\partial\Omega}{\partial f_n} &= \langle\psi_n|\left[\frac{\hat{\vec{p}}^2}{2m_e} + \gamma(\vec{r})\right]|\psi_n\rangle + k_B T\Big[\ln(f_n) - \ln(1-f_n)\Big] \stackrel{!}{=} 0\end{aligned} \tag{G.27}$$

From the first equation we obtain a definition for the **effective potential** for the non-interacting electrons.

$$v_{eff}(\vec{r}) \stackrel{\text{def}}{=} \gamma(\vec{r}) + \mu = v_{ext}(\vec{r}) + \underbrace{\int d^3r' \, \frac{e^2 n(\vec{r'})}{4\pi\epsilon_0 |\vec{r} - \vec{r'}|}}_{v_H(\vec{r})} + \frac{\partial E_{xc}}{\partial n(\vec{r})} \tag{G.28}$$

The middle equation, is kind of Schrödinger equation.

$$\Big[\frac{\hat{\vec{p}}^2}{2m_e} + v_{eff}(\vec{r})\Big]|\psi_n\rangle = \sum_m |\psi_m\rangle\Big(\Lambda_{m,n} - \mu\delta_{m,n}\Big) \tag{G.29}$$

The Lagrange multipliers is the Hamilton matrix shifted relative to the chemical potential

$$\Lambda_{m,n} = \langle\psi_m|\Big[\frac{\hat{\vec{p}}^2}{2m_e} + v_{eff}(\vec{r})\Big]|\psi_n\rangle - \mu\delta_{m,n} \tag{G.30}$$

From the last equation, we obtain the equilibrium occupations as the Fermi distribution function. The diagonal elements of $\Lambda_{m,n}$ act here as energies.

$$f_n = \frac{1}{1 + e^{\beta(\Lambda_{n,n} - \mu)}} \tag{G.31}$$

The relation between the density and the wave functions and occupations is obtained from the constraint equation, i.e. the variation with respect to $\gamma(\vec{r})$

$$n(\vec{r}) = \sum_n f_n \psi_n^*(\vec{x})\psi_n(\vec{x}) \tag{G.32}$$

If all occupations differ, the wave functions must be furthermore eigenstates of the effective Hamiltonian.[3]

$$\Big[\frac{\hat{\vec{p}}^2}{2m_e} + v_{eff}(\vec{r})\Big]|\psi_n\rangle = |\psi_n\rangle\epsilon_n \tag{G.33}$$

The energy eigenvalues are called **Kohn-Sham energies**.

SELF-CONSISTENT EQUATIONS OF DFT

$$v_{eff}(\vec{r}) = v_{ext}(\vec{r}) + \int d^3r' \, \frac{e^2 n(\vec{r'})}{4\pi\epsilon_0 |\vec{r} - \vec{r'}|} + \frac{\partial E_{xc}}{\partial n(\vec{r})} \tag{G.34}$$

$$\Big[\frac{\hat{\vec{p}}^2}{2m_e} + v_{eff}(\vec{r})\Big]|\psi_n\rangle = |\psi_n\rangle\epsilon_n \tag{G.35}$$

$$n(\vec{r}) = \sum_n f_n \psi_n^*(\vec{x})\psi_n(\vec{x}) \tag{G.36}$$

$$f_n = \frac{1}{1 + e^{\beta(\epsilon_n - \mu)}} \tag{G.37}$$

G.3 One-particle density matrices and two-particle densities

In order to get used with the terminology, let me introduce a number of definitions related to density matrices[124].

[3] Editor: This is not convincing yet! Show the energy variation under a unitary transform.

G.3.1 N-particle density matrix

The ensemble of many-particle states is described uniquely by von-Neumann's statistical **density operator**

$$\hat{\rho}^{(N)} = \sum_n |\Phi_n\rangle P_n \langle\Phi_n| \tag{G.38}$$

where $|\Phi_n\rangle$ are arbitrary many-particle states in the Fock space and P_n are their probabilities.

The ensemble expectation value of any operator $\hat{A}$ can be obtained as trace of the product

$$\langle A\rangle = \mathrm{Tr}\left[\hat{\rho}^{(N)}\hat{A}\right] = \sum_n P_n \langle\Phi_n|\hat{A}|\Phi_n\rangle \tag{G.39}$$

G.3.2 one-particle-reduced density matrix

From the N-particle density matrix we can form several **contractions** that are physically important, because they allow one to represent expectation values of one-particle operators and the Coulomb interaction in an elegant fashion.

For example, we do not need the full N-particle density matrix to determine the expectation value of a one-particle operator, if we know the so-called one-particle density matrix.

A one-particle operator has the form

$$\hat{A} = \sum_{\alpha,\beta} A_{\alpha,\beta}\hat{c}^\dagger_\alpha \hat{c}_\beta \tag{G.40}$$

Its expectation value is

$$\langle A\rangle = \sum_{\alpha,\beta} A_{\alpha,\beta}\mathrm{Tr}\left[\hat{\rho}^{(N)}\hat{c}^\dagger_\alpha\hat{c}_\beta\right] = \sum_{\alpha,\beta} A_{\alpha,\beta}\rho^{(1)}_{\beta,\alpha} = \mathrm{Tr}\left[\boldsymbol{A\rho}^{(1)}\right] \tag{G.41}$$

where

$$\rho^{(1)}_{\alpha,\beta} \stackrel{\mathrm{def}}{=} \mathrm{Tr}\left[\hat{\rho}^{(N)}\hat{c}^\dagger_\beta\hat{c}_\alpha\right] = \sum_n P_n\langle\Phi_n|\hat{c}^\dagger_\beta\hat{c}_\alpha|\Phi_n\rangle \tag{G.42}$$

is the **one-particle-reduced density matrix** . Note here that the indices are reversed!

real-space representation: In real space the one-particle-reduced density matrix has the form of a function with two arguments

$$\rho^{(1)}(\vec{x},\vec{x'}) = \sum_n P_n\langle\Phi_n|\hat{\psi}^\dagger(\vec{x'})\hat{\psi}(\vec{x})|\Phi_n\rangle \tag{G.43}$$

From the diagonal elements we obtain the electron density

$$n(\vec{r}) = \sum_\sigma \rho^{(1)}(\vec{x},\vec{x}) \tag{G.44}$$

Natural orbitals and occupations In order to deal with the one-particle-reduced density matrix, one usually refers its eigendecomposition:

The one-particle density operator is itself expressed as one-particle operator

$$\hat{\rho}^{(1)} = \sum_{\alpha,\beta}|\chi_\alpha\rangle\rho_{\alpha,\beta}\langle\chi_\beta| = \int d^4x \int d^4x' \; |\vec{x}\rangle\rho^{(1)}(\vec{x},\vec{x'})\langle\vec{x'}| \tag{G.45}$$

Diagonalization yields the natural orbitals and occupations.

$$\hat{\rho}^{(1)}|\psi_n\rangle = |\psi_n\rangle f_n \tag{G.46}$$

- **Natural orbitals** $|\psi_n\rangle$ are the eigenstates of the one-particle-reduced density matrix
- occupations f_n are the eigenvalues of the one-particle reduced density matrix.

The occupations for a fermionic system lie between zero and one, and those of a bosonic system is positive. The occupations add up to the particle number.

The expectation value of a one-particle operator can the be obtained as

$$\langle A\rangle = \sum_n f_n \langle\psi_n|\hat{A}|\psi_n\rangle \tag{G.47}$$

G.3.3 Two-particle density

The Coulomb interaction is

$$\hat{W} \overset{\text{Eq. 3.75}}{=} \frac{1}{2}\int d^4x \int d^4x'\ \hat{\psi}^\dagger(\vec{x})\hat{\psi}^\dagger(\vec{x'})\frac{e^2}{4\pi\epsilon_0|\vec{r}-\vec{r'}|}\hat{\psi}(\vec{x'})\hat{\psi}(\vec{x}) \tag{G.48}$$

Thus, the interaction energy can be expressed with the help of the two-particle density

$$n^{(2)}(\vec{r},\vec{r'}) = \sum_{\sigma,\sigma'}\sum_n P_n\langle\Phi_n|\hat{\psi}^\dagger(\vec{x})\hat{\psi}^\dagger(\vec{x'})\hat{\psi}(\vec{x'})\hat{\psi}(\vec{x})|\Phi_n\rangle \tag{G.49}$$

as

$$W = \frac{1}{2}\int d^3r \int d^3r'\ \frac{e^2 n^{(2)}(\vec{r},\vec{r'})}{4\pi\epsilon_0|\vec{r}-\vec{r'}|} \tag{G.50}$$

Two-particle density matrix and U-tensor In order to obtain the two-particle density from a representation of orbitals, we need the complete two-particle density matrix

$$\hat{\rho}^{(2)}_{\alpha,\beta;\delta,\gamma} = \sum_n P_n\langle\Phi_n|\hat{c}^\dagger_\alpha\hat{c}^\dagger_\beta\hat{c}_\delta\hat{c}_\gamma|\Phi_n\rangle \tag{G.51}$$

Then the interaction is

$$\hat{W} = \frac{1}{2}\sum_{\alpha,\beta,\gamma,\delta} U_{\alpha,\beta,\delta,\gamma}\hat{\rho}^{(2)}_{\alpha,\beta;\gamma,\delta} \tag{G.52}$$

with the U-tensor

$$U_{\alpha,\beta,\delta,\gamma} = \int d^4x \int d^4x'\ \frac{e^2\chi^*_\alpha(\vec{x})\chi^*_\beta(\vec{x'})\chi_\gamma(\vec{x'})\chi_\delta(\vec{x})}{4\pi\epsilon_0|\vec{r}-\vec{r'}|} \tag{G.53}$$

G.3.4 Pair-correlation function and hole function

Another quantity that is useful is the **pair-correlation function**

PAIR-CORRELATION FUNCTION

$$g(\vec{r},\vec{r}_0) = \frac{n^{(2)}(\vec{r},\vec{r}_0)}{n(\vec{r}_0)}$$

The pair-correlation function describes the probability to find an electron at position $\vec{r}$, given that there is one at $\vec{r}_0$. The pair-correlation function is the electron density seen by one electron that is

located at $\vec{r}_0$. Consider an N-electron system. Pick out one electron and determine the density of the remaining $N-1$ electrons.

Given that an electron will see at large distances nothing but the charge density itself, it makes sense to define a more short-ranged quantity, namely the **exchange-correlation hole function** $h(\vec{r},\vec{r}_0)$

HOLE FUNCTION

$$g(\vec{r},\vec{r}_0) = n(\vec{r}) + h(\vec{r},\vec{r}_0)$$

The physical picture of the hole function is that each electron "sees" the total density $n(\vec{r})$ and the density $h(\vec{r},\vec{r'})$ of "one missing electron". The density $h(\vec{r},\vec{r'})$ is like a hole in the total charge density due to the fact that the remaining electrons do not come near to the electron in question. Thus, the Coulomb repulsion between the electrons is reduced relative to the Hartree energy by the attraction of the electron to its exchange-correlation hole.

Accurate calculations of the exchange-correlation hole have been obtained by quantum Monte Carlo calculations[125].

The two-particle density can now be expressed by the density and the exchange-correlation hole function as

$$n^{(2)}(\vec{r},\vec{r}_0) = n(\vec{r}_0)\,[n(\vec{r}) + h(\vec{r},\vec{r}_0)]$$

Now, we can also rewrite the interaction energy in the form

$$E_{int} = \underbrace{\frac{1}{2}\int d^3r \int d^3r' \, \frac{e^2 n(\vec{r}) n(\vec{r'})}{4\pi\epsilon_0 |\vec{r}-\vec{r'}|}}_{E_H} + \underbrace{\int d^3r \; n(\vec{r}) \frac{1}{2}\int d^3r' \, \frac{e^2 h(\vec{r'},\vec{r})}{4\pi\epsilon_0|\vec{r}-\vec{r'}|}}_{U_{xc}} \tag{G.54}$$

U_{xc} is the **potential energy of exchange and correlation**. It differs from the exchange and correlation energy E_{xc}, because it does not contain the kinetic energy contribution to the correlation energy.

G.4 Adiabatic connection

We learned that one can reasonably estimate the exchange-correlation hole, and evaluate the potential energy of exchange and correlation. However, it is nearly hopeless to estimate the contribution of the kinetic energy to the correlation energy, needed to arrive at the exchange and correlation energy functional $E_{xc}[n(\vec{r})]$.

If there would be no cost to deform the exchange-correlation hole, the latter would simply adjust such that the electrostatic energy is optimized. One can easily estimate how the hole would look like: It would have the shape of a hard sphere centered at the reference electron. Its radius would be determined by the sum rule that says that there is exactly one positive charge in the exchange-correlation hole. The reason for this shape is that the electron would repel its neighbors as much as possible, in order to reduce its electrostatic interaction.

However as the exchange-correlation hole is deformed, there is a price to pay, namely that the kinetic energy goes up. In the extreme case of a hard-sphere like hole, the wave functions would have steps, that is infinite curvature. The kinetic energy is just a measure of the curvature of the wave function. Thus, the deformation of the hole costs kinetic energy. The final shape of the XC-hole is therefore a balance between electrostatic gain and kinetic energy cost.

The **adiabatic connection**[126, 127, 128] is a theorem that allows one to relate the net energy gain, including the kinetic energy cost, to the electrostatic energy gain only, but for variable strengths

of the interaction energy. While this theorem looks like mystery, it cannot be applied directly. Nevertheless it provides an important route that allows important approximations to be made. The theorem is demonstrated in the following:

In order to simplify the derivation we consider only a single many-particle wave function instead of an ensemble. The generalization can be done without difficulties.

We consider a given electron density for which the non-interacting functional $F_0[n(\vec{r})]$ is exactly known.

$$F_\lambda[n(\vec{r})] = \langle\Phi_\lambda|\hat{T} + \lambda\hat{W}|\Phi_\lambda\rangle + \int d^3r\ \mu_\lambda(\vec{r})\Big(\langle\Phi_\lambda|\hat{n}(\vec{r})|\Phi_\lambda\rangle - n(\vec{r})\Big) - E_\lambda\Big(\langle\Phi_\lambda|\Phi_\lambda\rangle - 1\Big)$$

where $|\Phi_\lambda\rangle$ is the many-electron wave function that minimizes F_λ under the constraint that the density of the wave function is equal to $n(\vec{r})$. The function $\mu_\lambda(\vec{r})$ represents the Lagrange parameters. The operator

$$\hat{n}(\vec{r}) \stackrel{\text{def}}{=} \sum_\sigma \hat{\psi}^\dagger(\vec{x})\hat{\psi}(\vec{x})$$

is the operator that extracts the electron density from the wave function.

The wave functions that minimize the functional obey the Schrödinger equation

$$\left[\hat{T} + \lambda\hat{W} + \int d^3r\ \mu_\lambda(\vec{r})\hat{n}(\vec{r}) - E_\lambda\right]|\Phi_\lambda\rangle = 0 \tag{G.55}$$

This means that as the interaction strength is increased, a local potential, $\mu_\lambda(\vec{r})$, is switched on that ensures that the electron density remains unchanged.

If we know the derivatives of the functional with respect to the interaction strength λ, and if we know the functional for the non-interacting electron gas, we can determine the functional for the interacting electron gas as

$$\begin{aligned} F_1[n(\vec{r})] &= F_0[n(\vec{r})] + \int_0^1 d\lambda\ \frac{dF_\lambda[n(\vec{r})]}{d\lambda} \\ &= \langle\Phi_0|\hat{T}|\Phi_0\rangle + \int_0^1 d\lambda\ \frac{dF_\lambda[n(\vec{r})]}{d\lambda} \end{aligned}$$

The first term is simply the kinetic energy of the non-interacting electron gas with the same density as the interacting system.

Now we can show that the derivative of the functional with respect to the interaction strength can be determined from the interaction energy alone. The proof rests on the **Hellmann-Feynman the-**

orem.

$$\begin{aligned}
\frac{dF_\lambda[n(\vec{r})]}{d\lambda} &= \frac{d}{d\lambda}\Big[\langle\Phi_\lambda|\hat{T}+\lambda\hat{W}|\Phi_\lambda\rangle \\
&\quad + \int d^3r\,\mu_\lambda(\vec{r})\Big(\langle\Phi_\lambda|\hat{n}(\vec{r})|\Phi_\lambda\rangle - n(\vec{r})\Big) - E_\lambda\Big(\langle\Phi_\lambda|\Phi_\lambda\rangle - 1\Big)\Big] \\
&= \langle\frac{d\Phi_\lambda}{d\lambda}|\hat{T}+\lambda\hat{W}|\Phi_\lambda\rangle + \langle\Phi_\lambda|\hat{W}|\Phi_\lambda\rangle + \langle\Phi_\lambda|\hat{T}+\lambda\hat{W}|\frac{d\Phi_\lambda}{d\lambda}\rangle \\
&\quad + \int d^3r\,\frac{d\mu_\lambda(\vec{r})}{d\lambda}\underbrace{\big(\langle\Phi_\lambda|\hat{n}(\vec{r})|\Phi_\lambda\rangle - n(\vec{r})\big)}_{=0} \\
&\quad + \int d^3r\,\mu_\lambda(\vec{r})\left(\langle\frac{d\Phi_\lambda}{d\lambda}|\hat{n}(\vec{r})|\Phi_\lambda\rangle + \langle\Phi_\lambda|\hat{n}(\vec{r})|\frac{d\Phi_\lambda}{d\lambda}\rangle\right) \\
&\quad - \frac{dE_\lambda}{d\lambda}\underbrace{\Big(\langle\Phi_\lambda|\Phi_\lambda\rangle - 1\Big)}_{=0} - E_\lambda\Big(\langle\frac{d\Phi_\lambda}{d\lambda}|\Phi_\lambda\rangle + \langle\Phi_\lambda|\frac{d\Phi_\lambda}{d\lambda}\rangle\Big) \\
&= \langle\Phi_\lambda|\hat{W}|\Phi_\lambda\rangle \\
&\quad + \langle\frac{d\Phi_\lambda}{d\lambda}|\underbrace{\Big[\hat{T}+\lambda\hat{W}+\int d^3r\,\mu_\lambda(\vec{r})\hat{n}(\vec{r}) - E_\lambda\Big]}_{=0}|\Phi_\lambda\rangle \\
&\quad + \underbrace{\langle\Phi_\lambda|\Big[\hat{T}+\lambda\hat{W}+\int d^3r\,\mu_\lambda(\vec{r})\hat{n}(\vec{r}) - E_\lambda\Big]}_{=0}|\frac{d\Phi_\lambda}{d\lambda}\rangle \\
&\overset{\text{Eq. } G.55}{=} \langle\Phi_\lambda|\hat{W}|\Phi_\lambda\rangle
\end{aligned}$$

Thus, we can express the functional for the finite interaction strength as

$$F_1[n(\vec{r})] = \langle\Phi_0|\hat{T}|\Phi_0\rangle + \underbrace{\int_0^1 d\lambda\,\langle\Phi_\lambda|\hat{W}|\Phi_\lambda\rangle}_{E_H[n(\vec{r})]+E_{xc}[n(\vec{r})]}$$

Thus, we have obtained an explicit expression for the exchange-correlation energy, that does not directly refer to the kinetic energy.

$$E_{xc}[n(\vec{r})] = \int_0^1 d\lambda\,\langle\Phi_\lambda|\hat{W}|\Phi_\lambda\rangle - \underbrace{\frac{1}{2}\int d^3r\int d^3r'\,\frac{e^2 n(\vec{r})n(\vec{r'})}{4\pi\epsilon_0|\vec{r}-\vec{r'}|}}_{E_H}$$

This expression has the problem that we still need the wave functions $|\Phi_\lambda\rangle$ for all possible values for the interaction strength.

The interaction energy can further be expressed by the exchange-correlation hole for a given value of the interaction, namely

$$\langle\Phi_\lambda|\hat{W}|\Phi_\lambda\rangle = \frac{1}{2}\int d^3r\int d^3r'\,\frac{e^2 n(\vec{r})n(\vec{r'})}{4\pi\epsilon_0|\vec{r}-\vec{r'}|} + \int d^3r\,n(\vec{r})\frac{1}{2}\int d^3r'\,\frac{e^2 h_\lambda(\vec{r},\vec{r'})}{4\pi\epsilon_0|\vec{r}-\vec{r'}|}$$

so that

$$E_{xc} = \int d^3r\,n(\vec{r})\underbrace{\int_0^1 d\lambda\,\frac{1}{2}\int d^3r'\,\frac{e^2 h_\lambda(\vec{r},\vec{r'})}{4\pi\epsilon_0|\vec{r}-\vec{r'}|}}_{=:\epsilon_{xc}} \tag{G.56}$$

The variable ϵ_{xc}, which itself is a functional of the density is the exchange-correlation energy per electron.

G.5 Ideas that guide the construction of density functionals

G.5.1 Screened interaction

It is possible[4] to reformulate the exchange-correlation energy by the exchange-only energy with a screened interaction. This is a form that reminds of the so-called **GW approximation**, where the self-energy is expressed by Green's-function times screened interaction.

$$E_{xc} \overset{\text{Eq. G.56}}{=} \frac{1}{2}\int d^3r \int d^3r'\; n(r)h_0(r,r') \underbrace{\int d\lambda \frac{h_\lambda(\vec{r},\vec{r'})}{h_0(\vec{r},\vec{r'})}\frac{e^2}{4\pi\epsilon_0|\vec{r}-\vec{r'}|}}_{v_{scr}(\vec{r}-\vec{r'})}$$

$$= \frac{1}{2}\sum_{ij}\int d^3r \int d^3r'\; \varphi_i^*(\vec{r})\varphi_j(\vec{r})v_{scr}(\vec{r}-\vec{r'})\varphi_j^*(\vec{r'})\varphi_i(\vec{r'})$$

where the screened interaction is defined as

$$v_{scr}(\vec{r}-\vec{r'}) \overset{\text{def}}{=} \int d\lambda\; \frac{h_\lambda(\vec{r},\vec{r'})}{h_0(\vec{r},\vec{r'})}\frac{e^2}{4\pi\epsilon_0|\vec{r}-\vec{r'}|}$$

Note that, in contrast to the GW approximation, our expression is exact, but, on the other hand, it is limited to the ground state.

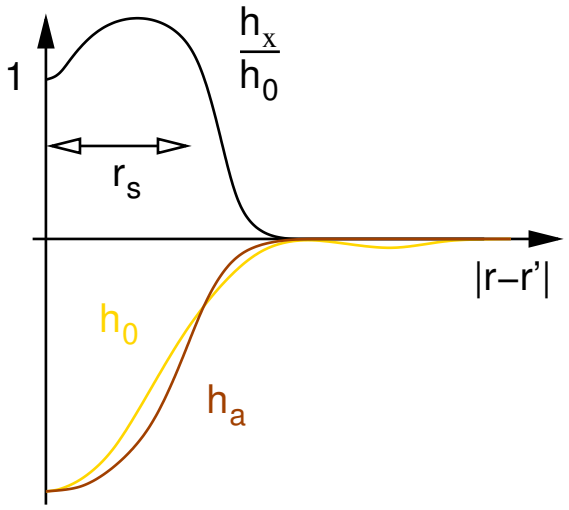

Fig. G.2: Schematic diagram of the effect of the screening of the interaction. The golden line h_0 is the hole function of the non-interacting reference system, while the red line h_λ is the hole function in presence of a scaled interaction. The ratio scales the Coulomb interaction in the exchange term. It suppresses the long-range tail of the interaction, and enhances the interaction for intermediate distances. r_s is the average electron radius $\frac{4\pi}{3}r_s^2 * n = 1$. ($h_a$ and h_x should be h_λ; Problem with the drawing program.)

Note also that the screened interaction in this formulation only enters the exchange term, but not the Hartree term. It also includes the kinetic energy correction.

The qualitative behavior can be understood easily:

- The hole function $h_\lambda(\vec{r},\vec{r'})$ for a finite interaction is generally more compact than the on obtained without interaction. Thus, the screened interaction v_{scr} is generally more short ranged than the unscreened interaction.

[4] This is an idea from the author, that has not been crosschecked properly. Therefore, some caution is required.

- The screened interaction for $\vec{r} = \vec{r'}$ is identical to the unscreened interaction, because the hole function cancels exactly the spin density, independent of the strength of the interaction.

- Due to the compression of the hole upon increasing interaction and because of the sum-rule that the hole integrates to exactly one positive charge, the interaction must be enhanced for intermediate distances.

- The screening will be more effective, if the price for the distortion of the wave function is low, that is for a low density. This implies that the unscreened interaction is a reasonable approximation in the high-density region around the atomic center, while the tail region of a molecule is better described by a more short-ranged interaction.

G.5.2 Hybrid functionals

The adiabatic connection scheme is exploited in the construction of so-called **hybrid functionals**. These density functionals describe the exchange-correlation energy as a mixture of the correct exchange, obtained as in the Hartree-Fock method and another local or gradient corrected functional.

The performance of the hybrid functionals is probably among the best. They have the disadvantage that they require that the Hartree-Fock exchange must be evaluated, which is computationally more challenging than the evaluation of the regular density functionals.

The idea behind the hybrid functionals is that the local functionals are appropriate if the interaction energy is very large. However if the interaction energy is small, the exchange hole is given by Hartree-Fock exchange.

If for example the kinetic energy dominates, the shape of the exchange-correlation hole cannot adjust, and we can approximate $h_\lambda(\vec{r}, \vec{r'}) \approx h_0(\vec{r}, \vec{r'})$ by the hole of the non-interacting electron gas. Thus, we obtain

$$\epsilon_{xc} \approx \frac{1}{2} \int d^3r' \, \frac{e^2 h_0(\vec{r}, \vec{r'})}{4\pi\epsilon_0 |\vec{r} - \vec{r'}|}$$

If the electrostatic interaction dominates over the kinetic energy then $h_1(\vec{r}, \vec{r'})$ would be a hard sphere, and therefore fairly local. Therefore, the hybrid functionals try to approximate the integral by a superposition of HF-exchange and a local density functional.

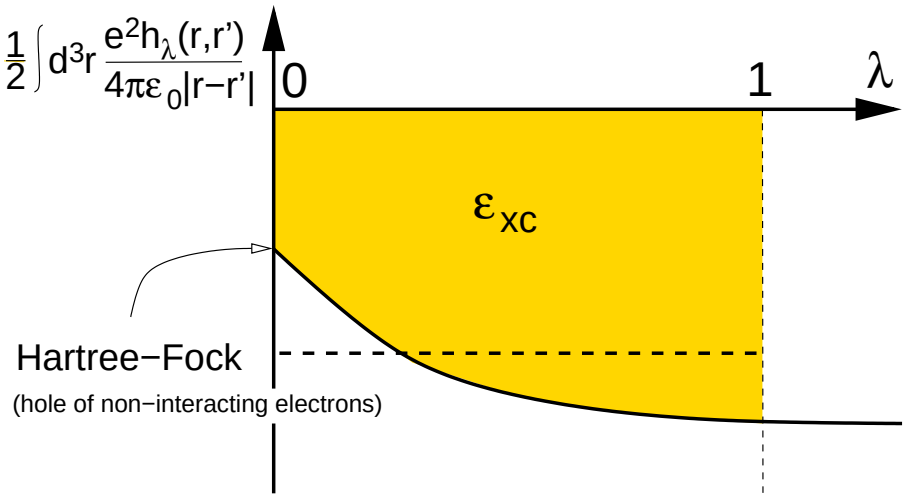

G.6 Scaling of with a fixed shape of the XC-hole function

Even before the invention of density-functional theory per se, the so-called X_α method has been introduced. Today, the X_α method has mostly historical value. The X_α method uses the expression for the exchange of a homogeneous electron gas instead of the exchange-correlation energy. However, the exchange energy has been scaled with a parameter, namely X_α, that has been adjusted to Hartree-Fock calculations. The results are shown in Fig. G.3.

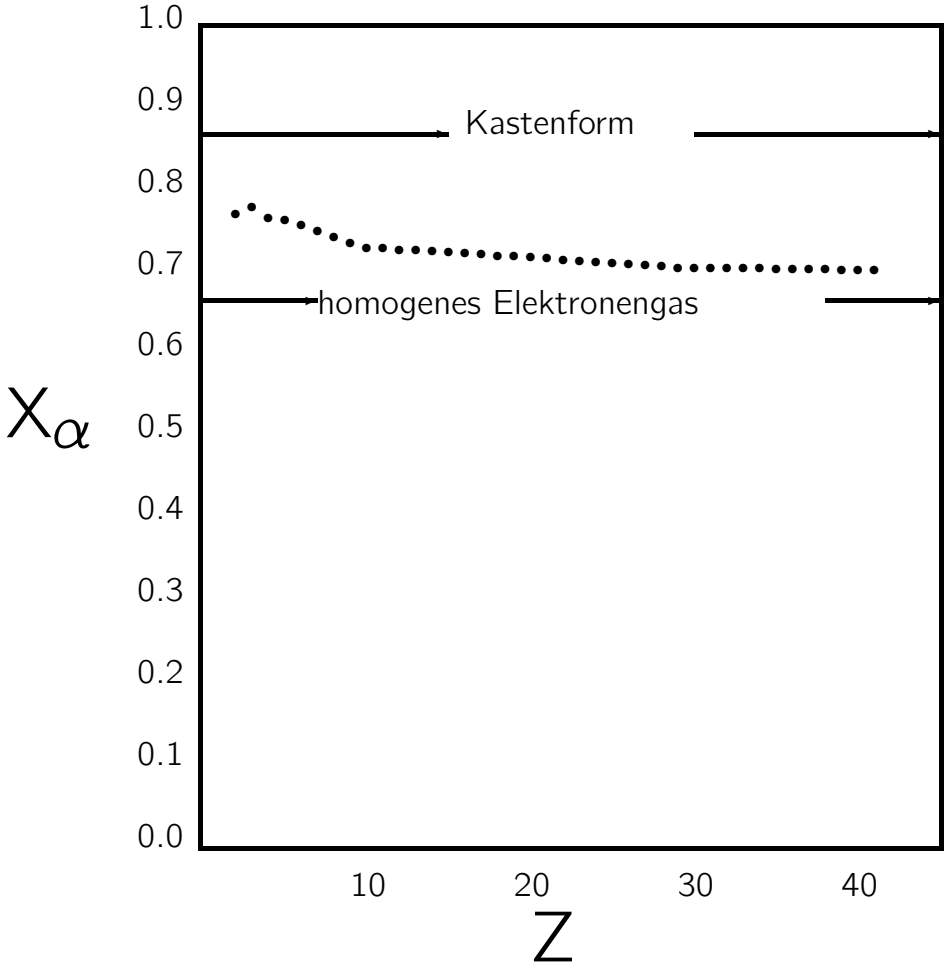

Fig. G.3: X_α value obtained by comparison of the atomic energy with exact Hartree-Fock calculations as function of atomic number of the atom.[129, 130]

The rationale behind the X_α-method is a dimensional argument. Choose a given shape for the exchange-correlation hole, but scale it according to the density and the electron sum rule. Then the exchange-correlation energy per electron always scales like $n^{\frac{1}{3}}$. Each shape corresponds to a pre-factor.

Consider a given shape described by a function $f(\vec{r})$ with

$$f(\vec{0}) = 1$$
$$\int d^3r\, f(\vec{r}) = 1$$

Now, we express the hole function by the function f by scaling its magnitude at the origin such that the amplitude of the hole cancels the electron density. Secondly, we stretch the function in space so that the sum rule, which says that the hole must integrate to -1, is fulfilled. These conditions yield

the model for the exchange-correlation hole.

$$h(\vec{r}_0, \vec{r}) = -n(\vec{r}_0) f(\frac{\vec{r} - \vec{r}_0}{n(\vec{r}_0)^{\frac{1}{3}}})$$

The corresponding exchange-correlation energy per electron is

$$\epsilon_{xc}(\vec{r}) = -\frac{1}{2} \int d^3r' \; \frac{e^2}{4\pi\epsilon_0 |\vec{r} - \vec{r'}|} f(\frac{\vec{r} - \vec{r'}}{n(\vec{r})^{\frac{1}{3}}})$$

If we introduce a variable transform

$$\vec{y} = \frac{\vec{r} - \vec{r'}}{n(\vec{r})^{\frac{1}{3}}}$$

we obtain

$$\epsilon_{xc}(\vec{r}) = -\frac{n(\vec{r})^{\frac{1}{3}}}{2} \int d^3y' \; \frac{e^2}{4\pi\epsilon_0 |\vec{y}|} f(\vec{y}) = -C n^{\frac{1}{3}}$$

where C is a constant that is entirely defined by the shape function $f(\vec{r})$.

In general, the X_α method yields larger band gaps than density-functional theory. The latter severely underestimates band gaps. This is in accord with the tendency of Hartree-Fock to overestimate band gaps. In contrast to Hartree-Fock, however, the X_α method is superior for the description of metals because it does not lead to a vanishing density of states at the Fermi level.

G.7 Local density functionals

The first true density functionals were constructed for the homogeneous electron gas, by extracting the exchange-correlation energy per electron ϵ_{xc} from a calculation of the interacting homogeneous electron gas.

A breakthrough came about when Ceperley and Alder[49] performed quantum Monte-Carlo calculations of the homogeneous electron gas as function of the density. Quantum Monte-Carlo calculations are computationally expensive, but provide the energy of an interacting electron gas in principle exactly, that is with the exceptions of numerical errors. These results have been parameterized by Perdew and Zunger[131] and combined with so-called RPA results for the high-density limit. **RPA** stands for **Random-Phase Approximation**[43], which is accurate in the high density limit.

These density functionals exhibit very good results for solids. Electron densities are nearly perfect. Bond distances are typically underestimated by 1-3 % and bond angles agree with experiment within few degrees. Binding energies, on the other hand, are strongly overestimated. The errors are in the range of electron volts and thus comparable to bond energies. Thus, these functionals have been useless for studying chemical reactions. However, the results for solid state processes such as diffusion have been very good. This has lead to a long-standing misunderstanding between solid state physicists and chemists about the usefulness of density-functional theory. The density functionals worked find for solids, which was what the physicists are interested in, while they were a disaster for the binding energies of molecules, the major interest of chemists. This difficulty has been overcome by the gradient corrected density functionals discussed later.

The overestimate of the binding energies covers up the lack of Van der Waals interactions. For example, the binding energy and the bond distances of Nobel gases are in very good agreement with experiment. However, the agreement is good for the wrong reason. The weak van der Waals interaction is not described properly in local density functionals, but the overbinding compensates for this fact.

For a long time it was surprising that the approximate density functionals work at all. They have been derived from a completely homogeneous electron gas and are applied to an electron density of

real materials, which are far from homogeneous. Jones and Gunnarsson gave one explanation, namely that density functionals observe an important sum rule, namely that the exchange-correlation hole integrates to minus one electron charge. Fig. G.4 compares the exchange hole of a free-electron gas with that of a nitrogen atom, demonstrating that despite their very different shape, their contributions to the exchange energy are similar.

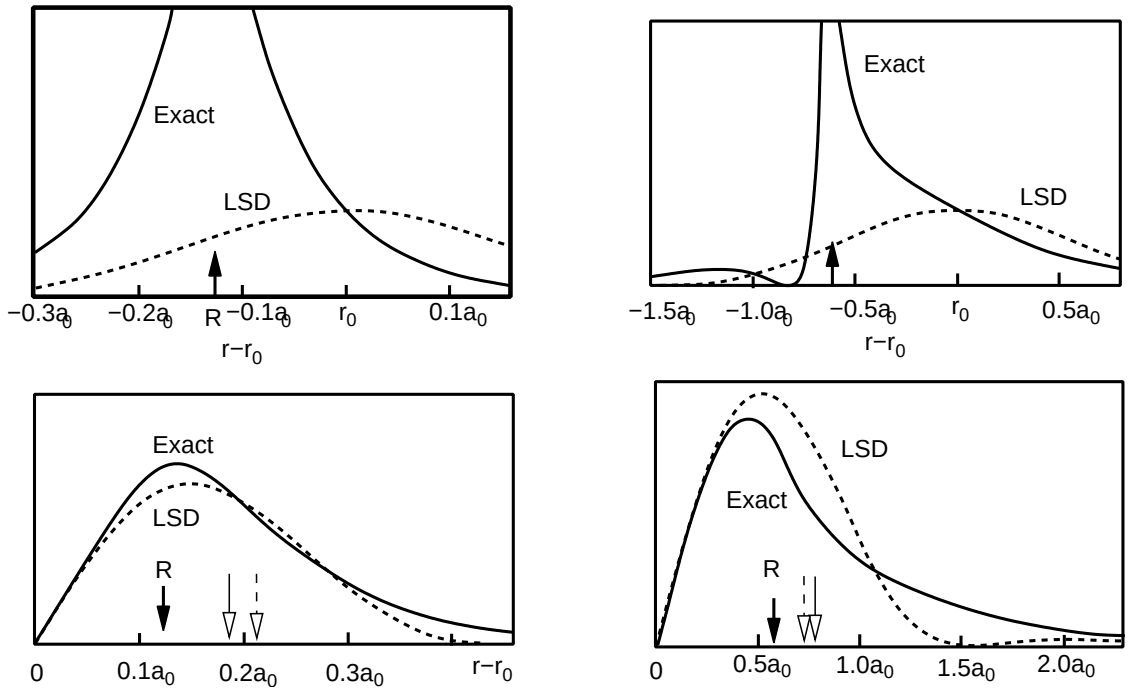

Fig. G.4: exchange-correlation hole of an electron in the nitrogen atom (full line) and in the local density-functional approximation (dashed) [132]. In the left row, the reference electron is located 0.13 a_0 from the nucleus and on the right it is located further, at 0.63 a_0. Even though the shape of the DFT-exchange hole deviates grossly from the correct exchange hole, the spherical averages shown in the bottom figures are similar, which is attributed to the particle sum rule, obeyed in the local density approximation (LDA). The arrows pointing down indicate the exact and the DFT result of $\left[\int d^3r \, \frac{|h(\vec{r},\vec{r}_0)|}{|\vec{r}-\vec{r}_0|}\right]^{-1}$. Similar results are available for neon[131].

G.8 Local spin-density approximation

In order to describe magnetic systems, or so-called open-shell molecules, one uses the local spin-density approximation, where the spin-dependent density $n(\vec{x}) = n(\vec{r},\sigma)$ is used instead of the total density $n(\vec{r}) = \sum_\sigma n(\vec{x})$. As a result, we obtain one-particle wave functions with spin-up and spin-down character and one obtains two effective potentials, one for the spin-up electrons and another for the spin-down electrons.

The difference between the effective potentials acts like a magnetic field, even though its origin is purely electrostatic, namely exchange and correlation also called the **exchange interaction**.

G.8.1 Non-collinear local spin-density approximation

While the local spin-density formalism only allows one-particle wave function to have either purely spin-up or purely spin-down character, the non-collinear formulation allows the wave functions to

have a mixed spin-up and spin-down character. As a result, the magnetization can not only vary in magnitude but also in direction.

G.9 Generalized gradient functionals

For a long time one has hoped to obtain better functionals by including also a dependence on the gradient of the density. The first attempts started from a model with a weakly oscillating electron density. The resulting functionals however were worse than the local functionals.

The reason for this failure was that when the expansion for slowly varying densities are extrapolated to strongly oscillating densities, the density of the exchange-correlation hole was overcompensating the total density.

Later, one realized that one should introduce a dimension-less scaled gradient defined as

$$s = \frac{r_s|\vec{\nabla} n|}{n}$$

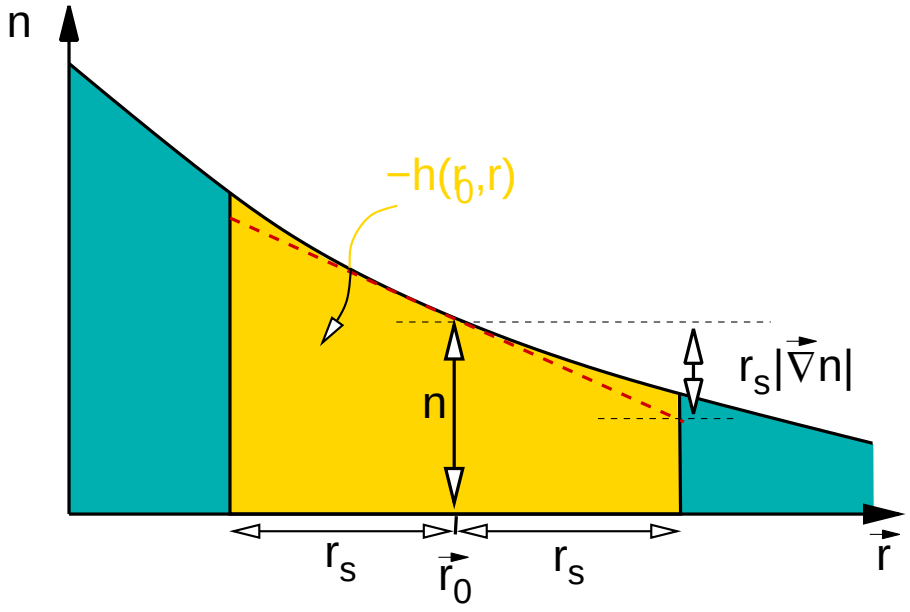

The scaled gradient allows one to switch off the gradient corrections in a physical sense, that is if the hole runs into the danger of producing a negative correlation function $g(\vec{x'}, \vec{x})$.

One way to construct the density is to use the results for slowly varying densities, which provides the parameter β.

$$\epsilon_{xc}(n,s) = \epsilon_{xc}^{hom}\left[1+\beta(n)s^2\right] \qquad \text{for} \qquad s << 1 \tag{G.57}$$

Surprisingly, the scaled gradient is largest in the tails of the wave functions, where the density falls off exponentially, that is

$$n(\vec{r}) \approx A\mathrm{e}^{-\lambda \vec{e}\vec{r}}$$

where $\vec{e}$ is the unit vector pointing into the direction in which the density falls off. Let us determine the scaled gradient for this density

$$s = \sqrt[3]{\frac{3}{4\pi}}\frac{A\lambda\exp(-\lambda\vec{e}\vec{r})}{A^{\frac{4}{3}}\lambda\exp(-\frac{4}{3}\lambda\vec{e}\vec{r})} = \sqrt[3]{\frac{3}{4\pi}}\lambda n^{-\frac{1}{3}} \to \infty$$

If we use only the gradient correction with the small-s expansion, the exchange-correlation energy per particle clearly becomes infinite.

However, in the tail region we can make use of other information. Consider an electron that is far outside of a molecule. It is clear that it "sees" a molecule with $N-1$ electrons. Thus, the hole is entirely localized on the molecule and the center of the hole is far from the reference electron. If the hole is at the molecule and the reference electron is far from it, we can estimate its interaction by

$$\epsilon_{xc} = \frac{1}{2r} \tag{G.58}$$

where r is the distance of the electron from the molecule.

Let me demonstrate the construction of such a gradient corrected functional using the example of Becke's gradient correction for exchange[133]. We make an ansatz for the exchange energy per electron as

$$\epsilon_{xc} = C n^{\frac{1}{3}} F(s) \tag{G.59}$$

where C is the pre-factor for the exchange energy. The function $F(s)$ is determined such that small gradient expansion, Eq. G.57, is reproduced, and that the exchange energy per electron in the tail region is correct.

To consider the tail region we require

$$\epsilon_{xc} \overset{\text{Eq. } G.59}{=} C n^{\frac{1}{3}} F(s) \overset{\text{Eq. } G.58}{=} \frac{1}{2r} \qquad \Rightarrow \qquad F(s) = \frac{1}{2C r n^{\frac{1}{3}}} \qquad \text{for} \quad s \to \infty$$

First we express the radius by the density and insert the result in Eq. G.60 to obtain an expression for $F(n(s))$.

$$\begin{aligned} n(r) = A\mathrm{e}^{-\lambda r} \qquad &\Rightarrow \qquad r(n) = -\frac{1}{\lambda}\ln\left[\frac{n}{A}\right] \\ \Rightarrow F(s) = \frac{1}{2C r n^{\frac{1}{3}}} &= \frac{-\lambda}{2C n^{\frac{1}{3}}\left(\ln[n] - \ln[A]\right)} \end{aligned}$$

Next we express the density by the scaled gradient and insert the result in the above equation to obtain an expression for $F(s)$.

$$\begin{aligned} s(n) &= \sqrt[3]{\frac{3}{4\pi}}\lambda n^{-\frac{1}{3}} \qquad \Rightarrow \qquad n(s) = \frac{3\lambda^3}{4\pi} s^{-3} \\ \Rightarrow F(s) &= \frac{-\lambda}{2C n^{\frac{1}{3}}\left(\ln[n] - \ln[A]\right)} \\ &= \frac{-\lambda}{2C\sqrt[3]{\frac{3\lambda^3}{4\pi}}\frac{1}{s}\left(\ln[\frac{3\lambda^3}{4\pi}s^{-3}] - \ln[A]\right)} \\ &= \frac{-s}{2C\sqrt[3]{\frac{3}{4\pi}}\left(\ln[\frac{3\lambda^3}{4\pi A^3}s^{-3}] - 3\ln[s]\right)} \\ &\overset{s\to\infty}{\approx} \frac{1}{6C}\sqrt[3]{\frac{4\pi}{3}}\,\frac{s^2}{s\ln[s]} \end{aligned}$$

This equation gives us the large gradient limit of $F(s)$.

In order to connect the low gradient limit with the large gradient limit we choose

$$F(s) = 1 + \frac{\beta s^2}{1 + 6C\beta s \sinh^{-1}(s)}$$

The result is shown in Fig. G.5.

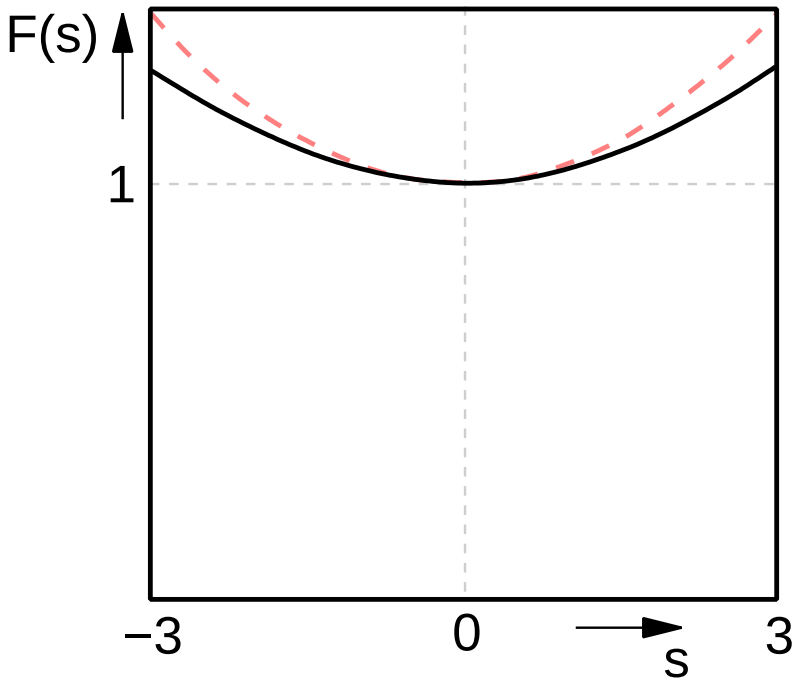

Fig. G.5: The function $F(s)$ from Becke's gradient corrected functional [133] for the exchange energy and from the small gradient expansion (dashed). Note that the gradient correction of Becke is smaller than the expansion for large gradients.

The gradient correction plays the role of a surface energy, as it contributes mostly in the tail region. While the exchange-correlation energy per electron falls off exponentially in the local functionals, it falls off as $\frac{1}{2r}$ in the gradient corrected functionals. This effect lowers the energy in the tail region of a molecule compared to the local functionals. If we break a bond, the surface area of a molecule increases, because the bond is transformed into a tail region. Thus, the gradient correction favors the dissociation of the bonds. As a consequence, gradient corrected functionals avoid the artificial overbinding of the local functionals. This argument also explains that local functionals perform fairly well in solids: If an atom diffuses, there is no additional surface created so that the gradient correction is minor.

Up to know there is an entire suite of different gradient corrected functionals. They are called **Generalized Gradient Approximations (GGA)** to differentiate them from the gradient expansions. The most common functionals are the Perdew-Wang-91-GGA, which has been superseded by the simpler Perdew-Burke-Ernzerhof functional. Both yield nearly identical results.

As shown in Fig. G.6, the performance of gradient corrected functionals is extremely good also for binding energies, which were unsatisfactory in the local density functionals. This has drawn also the chemists into the field of density-functional calculations.

G.10 Additional material

G.10.1 Relevance of the highest occupied Kohn-Sham orbital

According to Perdew[134, 135], the energy of the highest occupied Kohn Sham orbital is the ionization potential of the material.

This statement has been disputed by Kleinman[136].

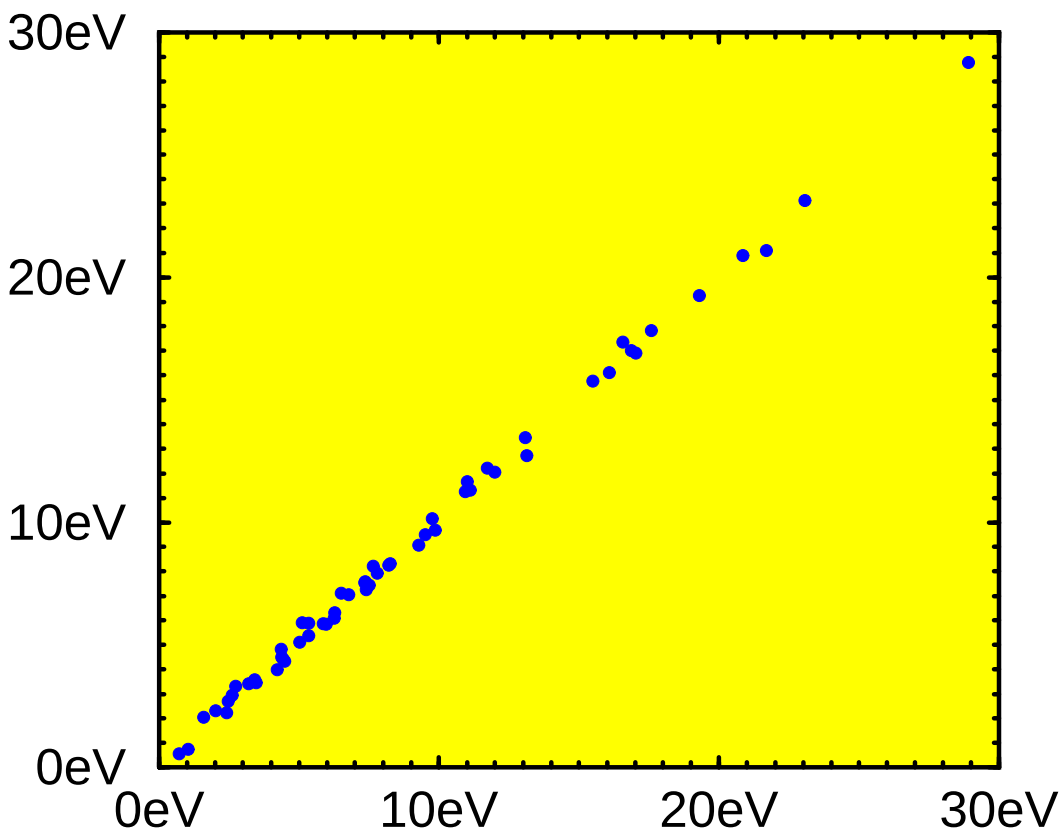

Fig. G.6: Accuracy of the atomization energies calculated with the Becke88-Perdew86 density functional compared to experiment.

G.10.2 Correlation inequality and lower bound of the exact density functional

G.11 Reliability of DFT

If we knew the exact density functional, we would be able to determine exactly

- the total energy
- the electron density and
- the energy of the highest occupied orbital

The argument that DFT predicts the highest occupied orbital, while the orbital energies of all other one-particle orbitals are, in principle, without physical meaning goes as follows: Far from the surface of a crystal the density of a one-particle orbital falls off as $e^{-\lambda z}$ where λ is related to the orbital energy by $\lambda = \frac{1}{\hbar}\sqrt{-2m_e\epsilon}$, where the orbital energy is measured relative to the vacuum level, that is $\lim_{z\to\infty} v_{eff}(\vec{r})$. For large distances the highest occupied orbital, which has the slowest decay, will dominate the electron density. Thus, if we would know the electron density very accurately far from a surface, we would be able to determine the dominant exponential decay constant and thus

the energy of the highest occupied orbital.[5] Thus, the energy of the highest occupied orbital can be determined from the density, which is an exact prediction of DFT.

Of course, even though exact DFT predicts these quantities accurately, it remains to be seen in each case if that also holds for the approximate functionals used in practice.

- Bond energies: Local functionals overestimate binding by often more than 1 eV. Energies are fairly good as long as the effective surface area of the system is not changed. This poor result is dramatically improved by the GGA's.
- Structures: bond lengths are underestimated in LDA by 0-2 %. They are overestimated by GGA's by 0-2 %.
- Dipole moments standard deviation 0.1 Debye[137]

G.12 Deficiencies of DFT

- **Missing Van der Waals interaction:** The van-der-Waals interaction is not included. Surprisingly the description of van der Waals bonds is nearly perfect with truly local density functionals. This however is an artifact of the tendency to overbinding in truly local density functionals on the one hand, and the lack of van der Waals interactions on the other. Since the overbinding of covalent bonds introduces errors in the range of 1 eV, it is generally not a good idea to use truly local density functionals instead of their gradient corrected counterparts.

  A density functional for the van der Waals interaction has been developed by Dion et al.[138]. It is named vdWDF (van-der-Waals density functional).
- **Band-gap Problem:** If we compare the spectrum of Kohn Sham states with optical absorption spectra we observe that the band gaps are too small. This is not a deficiency of density-functional theory, but an over-interpretation of the Kohn Sham spectrum. The excited states should not be calculated from the same potential as the ground state.
- **Reduced band width:** Band width of alkaline metals.
- **Mott insulators**
- **unstable negative ions**
- **Broken symmetry spin states:** singlet O_2 Molecule[139]
- **Transition states:**
- **High-energy spectrum:** The high energy part if the Kohn-Sham spectrum is too low compared to the measured optical spectrum[140]. The reason is that the exchange-correlation hole cannot follow the very fast electrons, while in the functionals we assume that full relaxation is always possible. Editor: It seems that the descrency[140] starts to grow above the plasma frequency.

[5] There is a caveat in the argument. Consider an insulator which may have surface states in the band gap. In that case the density would probe the highest occupied surface state, which may lie above the highest occupied bulk state.

Appendix H

Derivation of Slater-Condon rules

In this section, I derive the Slater-Condon rules[22, 50] spelled out in section 3.5 on p. 132.

The expectation values of Slater determinants[22] have been motivated earlier in the chapter 2 on the Hartree-Fock approximation in section 2.1.2 on p. 50 and section 2.1.4 on p. 55.

H.1 Maximum coincidence and orthonormality

An important ingredient to make the derivation of the Slater-Condon rule feasible is the concept of maximum coincidence:

Two Slater determinants, expressed in the same one-particle basisset, are in **maximum coincidence**, if all one-particle orbitals, which are present in both Slater determinants, are in the same position in both Slater determinants.

For example:

- the following determinants are in maximum coincidence with $|abcd\rangle$: $|efcd\rangle$, $|abcd\rangle$,$|aecd\rangle$.
- The determinants $|bacd\rangle$, $|eacd\rangle$ are not in maximum coincidence with $|abcd\rangle$. They can be brought into maximum coincidence by permuting one-particle orbitals, where each permutation contributes a factor (-1).

When two Slater-determinants $|\Phi\rangle$ and $|\Psi\rangle$ are in maximum coincidence, the distinct one-particle orbitals can be moved to the front without changing the matrix elements $\langle\Phi|\hat{A}|\Psi\rangle$ between the Slater determinants. This special form simplifies the bookkeeping in the arguments following below:

The other requirement for the derivation is that the one-particle orbitals are **orthonormal**. For non-orthonormal one-particle orbitals the expressions are considerably more complicated. When the expressions for non-orthonormal basis functions are needed, they can be obtained by transforming the expressions obtained with an orthonormal basisset.

H.2 Matrix elements with identical Slater determinants

The expectation values with a Slater determinant[22] make up the first set Slater-Condon rule Eq. 3.41.

H.2.1 Expectation value of a one-particle operator

First, we evaluate only the matrix element of the one-particle operator $\hat{h}_1$, that acts only on the coordinates of only one particle, namely the first. This result is then generalized for the other

particles and then summed up. Thus, we obtain the expectation value of the non-interacting part of the Hamiltonian.

To be concise, we write here the detailed expressions for the matrix elements of the one-particle Hamilton operator. The generalization to any other one-particle operator is straightforward. The expectation value with a one-particle orbital $|\varphi\rangle$ is

$$\begin{aligned}\langle\varphi|\hat{h}|\varphi\rangle &= \int d^4x \int d^4x' \; \langle\varphi|\vec{x}\rangle \quad \overbrace{\underbrace{\langle\vec{x}|\hat{h}|\vec{x'}\rangle}_{\delta(\vec{r}-\vec{r'})\delta_{\sigma,\sigma'}\left(-\frac{\hbar^2}{2m_e}\vec{\nabla}^2+v_{ext}(\vec{r})\right)}} \quad \langle\vec{x'}|\varphi\rangle \\ &= \sum_\sigma \int d^3r \; \varphi^*(\vec{r},\sigma)\left[\frac{-\hbar^2}{2m_e}\vec{\nabla}^2+v_{ext}(\vec{r})\right]\varphi(\vec{r},\sigma) \end{aligned} \tag{H.1}$$

The one-particle Hamiltonian $\hat{h}_j$ acting on the j-th particle in a many-particle wave function $|\Psi\rangle$ yields the expectation value

$$\langle\Psi|\hat{h}_j|\Psi\rangle = \int d^4x_1 \cdots \int d^4x_N \; \Psi^*(\vec{x}_1,\ldots,\vec{x}_N)\left(\frac{-\hbar^2}{2m_e}\vec{\nabla}_j^2+v_{ext}(\vec{r}_j)\right)\Psi(\vec{x}_1,\ldots,\vec{x}_N) \tag{H.2}$$

so that the matrix element for two product wave functions $|\varphi_1,\ldots,\varphi_N\rangle$ and $|\psi_1,\ldots,\psi_N\rangle$ is

$$\langle\varphi_1,\ldots,\varphi_N|\hat{h}_j|\psi_1,\ldots,\psi_N\rangle = \langle\varphi_1|\psi_1\rangle\cdots\langle\varphi_j|\hat{h}|\psi_j\rangle\cdots\langle\varphi_N|\psi_N\rangle \tag{H.3}$$

A Slater determinant $|\Psi\rangle$ has the form

$$\langle\vec{x}_1,\ldots,\vec{x}_N|\Psi\rangle \overset{\text{Eq. 1.88}}{=} \frac{1}{\sqrt{N!}}\sum_{i_1,\ldots,i_N=1}^{N}\epsilon_{i_1,\ldots,i_N}\langle\vec{x}_1|\varphi_{i_1}\rangle\cdots\langle\vec{x}_N|\varphi_{i_N}\rangle \tag{H.4}$$

Thus, the matrix element of a one-particle operator Eq. 2.5 is

$$\begin{aligned}\langle\Psi|\sum_{i=1}^{N}\hat{h}_i|\Psi\rangle &= N\langle\Psi|\hat{h}_1|\Psi\rangle \\ &\overset{\text{Eq. H.4}}{=} N\cdot\frac{1}{N!}\sum_{i_1,i_2,\ldots,i_N}^{N}\sum_{j_1,j_2,\ldots,j_N}^{N}\epsilon_{i_1,i_2,\ldots,i_N}\langle\varphi_{i_1},\ldots,\varphi_{i_N}|\hat{h}_1|\varphi_{j_1},\ldots,\varphi_{j_N}\rangle\epsilon_{j_1,j_2,\ldots,j_N} \\ &\overset{\text{Eq. H.3}}{=} N\frac{1}{N!}\sum_{i_1,i_2,\ldots,i_N}^{N}\sum_{j_1,j_2,\ldots,j_N}^{N}\epsilon_{i_1,i_2,\ldots,i_N}\epsilon_{j_1,j_2,\ldots,j_N}\langle\varphi_{i_1}|\hat{h}_1|\varphi_{j_1}\rangle\underbrace{\langle\varphi_{i_2}|\varphi_{j_2}\rangle}_{\delta_{i_2,j_2}}\cdots\underbrace{\langle\varphi_{i_N}|\varphi_{j_N}\rangle}_{\delta_{i_N,j_N}} \\ &= N\frac{1}{N!}\sum_{i_1,j_1=1}^{N}\langle\varphi_{i_1}|\hat{h}_1|\varphi_{j_1}\rangle\underbrace{\sum_{i_2,\ldots,i_N}^{N}\epsilon_{i_1,i_2,\ldots,i_N}\epsilon_{j_1,i_2,\ldots,i_N}}_{\delta_{i_1,j_1}(N-1)!} \\ &= \sum_{j=1}^{N}\langle\varphi_j|\hat{h}_1|\varphi_j\rangle\end{aligned}$$

In the last step, we exploited, that the sum over j_1 only contributes when $j_1 = i_1$: There is only one orbital left if all the orbitals but the first are determined. Thus, the first orbital must be the same for both Levi-Civita Symbols.

Finally, we obtain the expectation value of the one-particle Hamiltonian for a Slater determinant $|\Psi\rangle$ as

EXPECTATION VALUE OF A ONE-PARTICLE OPERATOR WITH A SLATER DETERMINANT

$$\langle\Psi|\sum_{i=1}^{N}\hat{h}_i|\Psi\rangle = \sum_{i=1}^{N}\langle\varphi_i|\hat{h}|\varphi_i\rangle \tag{H.5}$$

Here, $|\Psi\rangle$ is a N-particle Slater determinant built from the one-particle orbitals $|\varphi_i\rangle$, and $\sum_{i=1}^{N}\hat{h}_i$ is a one-particle operator.

This is Eq. 2.15 provided on p. 51 and it is the first of the Slater-Condon rules Eq. 3.41 provided on p. 134.

H.2.2 Expectation value of a two-particle operator

We proceed as for the expectation value of a one-particle operator and relate the interaction energy between all particles to the interaction between the first two electrons. This is allowed because of the indistinguishability of the electrons: The interaction between any two electrons is identical to any other pair. There are $\frac{N(N-1)}{2}$ ordered pairs and therefore the interaction energy is

$$\begin{aligned}
E_W &= \langle\Psi|\frac{1}{2}\sum_{i\neq j}^{N}\hat{W}_{i,j}|\Psi\rangle = \frac{N(N-1)}{2}\langle\Psi|\hat{W}_{1,2}|\Psi\rangle \\
&\overset{\text{Eq. } H.4}{=} \frac{N(N-1)}{2}\frac{1}{N!}\sum_{i_1,i_2,\ldots,i_N}^{N}\sum_{j_1,j_2,\ldots,j_N}^{N}\epsilon_{i_1,i_2,\ldots,i_N}\epsilon_{j_1,j_2,\ldots,j_N}\langle\varphi_{i_1},\ldots,\varphi_{i_N}|\hat{W}_{12}|\varphi_{j_1},\ldots,\varphi_{j_N}\rangle \\
&= \frac{1}{2\cdot(N-2)!}\sum_{i_1,i_2,\ldots,i_N}^{N}\sum_{j_1,j_2,\ldots,j_N}^{N}\epsilon_{i_1,i_2,\ldots,i_N}\epsilon_{j_1,j_2,\ldots,j_N}\langle\varphi_{i_1},\varphi_{i_2}|\hat{W}_{12}|\varphi_{j_1},\varphi_{j_2}\rangle\underbrace{\langle\varphi_{i_3}|\varphi_{j_3}\rangle}_{\delta_{i_3,j_3}}\cdots\underbrace{\langle\varphi_{i_N}|\varphi_{j_N}\rangle}_{\delta_{i_N,j_N}} \\
&= \frac{1}{2\cdot(N-2)!}\sum_{i_1,i_2,j_1,j_2}^{N}\langle\varphi_{i_1},\varphi_{i_2}|\hat{W}_{12}|\varphi_{j_1},\varphi_{j_2}\rangle\underbrace{\sum_{i_3,\ldots,i_N}^{N}\epsilon_{i_1,i_2,i_3\ldots,i_N}\epsilon_{j_1,j_2,i_3\ldots,i_N}}_{=\begin{cases}(N-2)!\,\epsilon_{i_1,i_2}\epsilon_{j_1,j_2} & \text{for } i_1,i_2\in\{j_1,j_2\}\\ 0 & \text{else}\end{cases}} \\
&= \frac{1}{2}\sum_{i_1,i_2}^{N}\sum_{j_1,j_2\in\{i_1,i_2\}}\langle\varphi_{i_1},\varphi_{i_2}|\hat{W}_{12}|\varphi_{j_1},\varphi_{j_2}\rangle\underbrace{\epsilon_{i_1,i_2}\epsilon_{j_1,j_2}}_{\delta_{i_1,j_1}\delta_{i_2,j_2}-\delta_{i_1,j_2}\delta_{i_1,j_2}} \\
&= \frac{1}{2}\sum_{i_1,i_2}^{N}\Big(\langle\varphi_{i_1},\varphi_{i_2}|\hat{W}_{12}|\varphi_{i_1},\varphi_{i_2}\rangle - \langle\varphi_{i_1},\varphi_{i_2}|\hat{W}_{12}|\varphi_{i_2},\varphi_{i_1}\rangle\Big)
\end{aligned} \tag{H.6}$$

In the last step, I exploited that the two interaction terms cancel when the indices i_1 and i_2 are identical. Therefore, they need not be excluded from the sum. The expression with the terms $i_1 = i_2$ is more convenient to discuss the physical implications, while the former is commonly used in the quantum chemical literature.

Thus, we obtain the expectation value of the interaction energy of a Slater determinant as

EXPECTATION VALUE OF THE INTERACTION WITH A SLATER DETERMINANT

$$\langle\Psi|\frac{1}{2}\sum_{i\neq j}^{N}\hat{W}_{i,j}|\Psi\rangle = \frac{1}{2}\sum_{i,j=1}^{N}\Big[\langle\varphi_i,\varphi_j|\hat{W}|\varphi_i,\varphi_j\rangle - \langle\varphi_i,\varphi_j|\hat{W}|\varphi_j,\varphi_i\rangle\Big] \tag{H.7}$$

The matrix elements used in the above equation Eq. H.7 are

$$\langle\varphi_a,\varphi_b|\hat{W}|\varphi_c,\varphi_d\rangle \stackrel{\text{def}}{=} \sum_{\sigma,\sigma'}\int d^3r\int d^3r'\;\varphi_a^*(\vec{r},\sigma)\varphi_b^*(\vec{r'},\sigma')\frac{e^2}{4\pi\epsilon_0|\vec{r}-\vec{r'}|}\varphi_c(\vec{r},\sigma)\varphi_d(\vec{r'},\sigma') \tag{H.8}$$

H.3 Slater determinants differing by one orbital

H.3.1 One-particle operator

The matrix element of a one-particle operator with Slater determinants differing by one orbital is obtained as follows:

First, we consider Slater determinants

$$\langle\vec{x}_1,\ldots,\vec{x}_N|\Psi\rangle = \frac{1}{\sqrt{N!}}\sum_{i_1,\ldots,i_N=1}^{N}\epsilon_{i_1,\ldots,i_N}\langle\vec{x}_1|\psi_{i_1}\rangle\cdots\langle\vec{x}_N|\psi_{i_N}\rangle \tag{H.9}$$

$$\langle\vec{x}_1,\ldots,\vec{x}_N|\Phi\rangle = \frac{1}{\sqrt{N!}}\sum_{j_1,\ldots j_N=1}^{N}\epsilon_{j_1,\ldots j_N}\langle\vec{x}_1|\varphi_{j_1}\rangle\cdots\langle\vec{x}_N|\varphi_{j_N}\rangle \tag{H.10}$$

that differ by exactly one one-particle orbital. Due to the form of **maximum coincidence** defined in section 3.5, we can place these two orbitals in the first position. Hence, $|\psi_1\rangle \neq |\varphi_1\rangle$, but $|\psi_i\rangle = |\varphi_i\rangle$ for $i \neq 1$. Thus,

$$\langle\psi_i|\varphi_j\rangle = \delta_{i,j}(1-\delta_{i,1}) \tag{H.11}$$

Now, we can work out the matrix element for the one-particle operator $\hat{A}_1$ acting on the first particle coordinate.

$$\begin{aligned}\langle\Psi|\hat{A}_1|\Phi\rangle &= \frac{1}{N!}\sum_{i_1,\ldots,i_N=1}^{N}\sum_{j_1,\ldots j_N=1}^{N}\epsilon_{i_1,i_2,\ldots,i_N}\epsilon_{j_1,j_2,\ldots,j_N}\langle\psi_{i_1}|\hat{A}|\varphi_{j_1}\rangle\underbrace{\langle\psi_{i_2}|\varphi_{j_2}\rangle}_{\delta_{i_2,j_2}(1-\delta_{i_2,1})}\cdots\underbrace{\langle\psi_{i_N}|\varphi_{j_N}\rangle}_{\delta_{i_N,j_N}(1-\delta_{i_N,1})}\\ &\stackrel{\text{Eq. }H.11}{=} \frac{1}{N!}\sum_{i_2\ldots,i_N=1}^{N}\sum_{i_1,j_1=1}^{N}\underbrace{\epsilon_{i_1,i_2,\ldots,i_N}\epsilon_{j_1,i_2,\ldots,i_N}(1-\delta_{i_2,1})\ldots(1-\delta_{i_N,1})}_{(B)}\langle\psi_{i_1}|\hat{A}|\varphi_{j_1}\rangle\end{aligned} \tag{H.12}$$

The Levi-Civita symbol $\epsilon_{i_1,\ldots,i_N}$ is non-zero only, when all its indices differ. Thus, the term denoted as (B), is non-zero only,

- if the indices $i_2,\ldots,i_N$ are all different and
- if the indices are from $i_2,\ldots,i_N \in \{2,\ldots,N\}$.

Hence the Levi-Civita symbols are nonzero only when $i_1 = j_1 = 1$. When these conditions are fulfilled the term (B) equals $B = 1$.

Thus, we obtain

$$\langle\Psi|\hat{A}_1|\Phi\rangle = \frac{1}{N!}\sum_{i_2\ldots,i_N=2}^{N}(\epsilon_{1,i_2,\ldots,i_N})^2\,\langle\psi_1|\hat{A}|\varphi_1\rangle \tag{H.13}$$

The Levi-Civita symbols contribute, if all indices are different, This happens $(N-1)!$ times, which corresponds to the number of permutations of the indices $2,\ldots,N$. Thus, we obtain

$$\langle\Psi|\hat{A}_1|\Phi\rangle = \frac{1}{N}\langle\psi_1|\hat{A}|\varphi_1\rangle \tag{H.14}$$

Since the operator has the form $\hat{A} = \sum_{i=1}^{N}\hat{A}_i$, and since all operators $\hat{A}_i$ contribute the same result, we obtain

$$\langle\Psi|\hat{A}|\Phi\rangle = \langle\psi_1|\hat{A}|\varphi_1\rangle. \tag{H.15}$$

which corresponds to the first line in the second Slater-Condon rule Eq. 3.42.

H.3.2 Two-particle operator

The matrix element of a two-particle operator with Slater determinants differing by one orbital is obtained as follows:

We consider the matrix element between two Slater determinants

$$\langle\vec{x}_1,\ldots,\vec{x}_N|\Psi\rangle = \frac{1}{\sqrt{N!}}\sum_{i_1,\ldots,i_N=1}^{N}\epsilon_{i_1,\ldots,i_N}\langle\vec{x}_1|\psi_{i_1}\rangle\cdots\langle\vec{x}_N|\psi_{i_N}\rangle \tag{H.16}$$

$$\langle\vec{x}_1,\ldots,\vec{x}_N|\Phi\rangle = \frac{1}{\sqrt{N!}}\sum_{j_1,\ldots,j_N=1}^{N}\epsilon_{j_1,\ldots,j_N}\langle\vec{x}_1|\varphi_{j_1}\rangle\cdots\langle\vec{x}_N|\varphi_{j_N}\rangle \tag{H.17}$$

Because only the first orbital of the two Slater determinants $|\Psi\rangle$ and $|\Phi\rangle$ differ, the overlap between the one-particle orbitals has the result

$$\langle\psi_i|\varphi_j\rangle = \delta_{ij}(1-\delta_{i,1}) \tag{H.18}$$

we obtained already earlier in Eq. H.11

Note, that the Slater determinants are chosen in **maximum coincidence**, defined in section 3.5: the two orbitals that are present in only one of the two Slater determinants stand at the same position, namely the first and second. That is, $|\psi_1\rangle$ and $|\psi_2\rangle$ differ from all $|\phi_j\rangle$ for $j\in\{1,\ldots,N\}$, and $|\phi_1\rangle$ and $|\phi_2\rangle$ differ from all $|\psi_j\rangle$ for $j\in\{1,\ldots,N\}$. The orbitals which are identical for both Slater determinants are in the same position, i.e. $|\phi_j\rangle = |\psi_j\rangle$ for $j\in\{3,\ldots,N\}$.

Now, we can work out the matrix element of the interaction operator $\hat{W}_{1,2}$ that acts exclusively on the first two particle coordinates. If the interaction would act onto any other orbital, at least one of the orbitals in the first position would be connected with another one by an overlap matrix element. This overlap matrix element vanishes because the orbitals in the first position are orthogonal to all other orbitals involved.

Later, we will see that the result is the same for each pair of coordinates, so that the sum over

pairs is done easily at the end of the calculation.

$$\begin{aligned}
\langle\Psi|\hat{W}_{1,2}|\Phi\rangle &= \frac{1}{N!}\sum_{i_1,\ldots,i_N=1}^{N}\sum_{j_1,\ldots,j_N=1}^{N}\epsilon_{i_1,i_2,\ldots,i_N}\epsilon_{j_1,j_2,\ldots,j_N} \\
&\quad\cdot\langle\psi_{i_1}\psi_{i_2}|\hat{W}_{1,2}|\varphi_{j_1}\varphi_{j_2}\rangle\underbrace{\langle\psi_{i_3}|\varphi_{j_3}\rangle}_{\delta_{i_3,j_3}(1-\delta_{i_3,1})}\cdots\underbrace{\langle\psi_{i_N}|\varphi_{j_N}\rangle}_{\delta_{i_N,j_N}(1-\delta_{i_N,1})} \\
&= \frac{1}{N!}\sum_{i_3,\ldots,i_N=1}^{N}\sum_{i_1,i_2,j_1,j_2=1}^{N}\underbrace{\epsilon_{i_1,i_2,i_3,\ldots,i_N}\epsilon_{j_1,j_2,i_3,\ldots,i_N}(1-\delta_{i_3,1})\ldots(1-\delta_{i_N,1})}_{(B)}\langle\psi_{i_1}\psi_{i_2}|\hat{W}_{1,2}|\varphi_{j_1}\varphi_{j_2}\rangle \\
&= \frac{1}{N!}\sum_{i_3,\ldots,i_N=2}^{N}\sum_{n=2}^{N}\sum_{i_1,i_2,j_1,j_2\in\{1,n\}}\epsilon_{i_1,i_2,i_3,\ldots,i_N}\epsilon_{j_1,j_2,i_3,\ldots,i_N}\langle\psi_{i_1}\psi_{i_2}|\hat{W}_{1,2}|\varphi_{j_1}\varphi_{j_2}\rangle \\
&= \frac{1}{N!}\sum_{n=2}^{N}\sum_{i_1,i_2,j_1,j_2\in\{1,n\}}\langle\psi_{i_1}\psi_{i_2}|\hat{W}_{1,2}|\varphi_{j_1}\varphi_{j_2}\rangle\sum_{i_3,\ldots,i_N=2}^{N}\epsilon_{i_1,i_2,i_3,\ldots,i_N}\epsilon_{j_1,j_2,i_3,\ldots,i_N}
\end{aligned} \tag{H.19}$$

The factor (B) is nonzero, if the indices $i_3,\ldots,i_N$ are different from each other and if they are element of $\{2,\ldots,N\}$. We exploit that for each set $i_3,\ldots,i_N$ in the sum, there is one pair of numbers $\{1,\ldots,N\}$, which has not been used. One number is 1, and the other we call n. The second number n is selected by adding the sum, while we exploit that the only nozero term in that sum is the one from the elements not covered already, which differs from 1.

The only nonzero contributions for $i_1,i_2,j_1,j_2\in\{1,n\}$ with $n\in\{2,\ldots,N\}$ are

$$\begin{aligned}
\sum_{i_3,\ldots,i_N=2}^{N}\epsilon_{i_1,i_2,i_3,\ldots,i_N}\epsilon_{j_1,j_2,i_3,\ldots,i_N} &= (N-2)(N-3)\cdots 1\begin{cases}+1 & \text{for } i_1=j_1 \text{ and } i_2=j_2\\ -1 & \text{for } i_1=j_2 \text{ and } i_2=j_1\\ 0 & \text{else}\end{cases} \\
&= (N-2)!\left(\delta_{i_1,j_1}\delta_{i_2,j_2}-\delta_{i_1,j_2}\delta_{i_2,j_1}\right)
\end{aligned} \tag{H.20}$$

Thus, we obtain

$$\begin{aligned}
\langle\Psi|\hat{W}_{1,2}|\Phi\rangle &= \frac{(N-2)!}{N!}\sum_{n=2}^{N}\Big(\langle\psi_1\psi_n|\hat{W}|\varphi_1\varphi_n\rangle-\langle\psi_1\psi_n|\hat{W}|\varphi_n\varphi_1\rangle-\langle\psi_n\psi_1|\hat{W}|\varphi_1\varphi_n\rangle+\langle\psi_n\psi_1|\hat{W}|\varphi_n\varphi_1\rangle\Big) \\
&= \frac{2}{N(N-1)}\sum_{n=2}^{N}\Big(\langle\psi_1\psi_n|\hat{W}|\varphi_1\varphi_n\rangle-\langle\psi_1\psi_n|\hat{W}|\varphi_n\varphi_1\rangle\Big)
\end{aligned} \tag{H.21}$$

In the last line, we exploited that the simultaneous interchange of the two orbitals in the bra and those in the ket do not change the matrix element of the interaction.

Since the operator has the form $\hat{W}=\frac{1}{2}\sum_{i\neq j}^{N}\hat{W}_{i,j}$. Each pair contributes the same result. As there are $N(N-1)$ distinct pairs in the double-sum, we obtain

$$\langle\Psi|\hat{W}|\Phi\rangle=\sum_{n=1}^{N}\left(\langle\psi_1\psi_n|\hat{W}_{1,2}|\varphi_1\varphi_n\rangle-\langle\psi_1\psi_n|\hat{W}_{1,2}|\varphi_n\varphi_1\rangle\right) \tag{H.22}$$

This result corresponds to the Slater-Condon rule Eq. 3.43. The sum runs now over all terms because the element with $n=1$ cancels anyway.

H.4 Slater determinants differing by two orbitals

H.4.1 One-particle operator

The matrix element of a one-particle operator with Slater determinants differing by two orbitals is

$$\begin{aligned}\langle\Psi|\hat{A}_1|\Phi\rangle = \frac{1}{N!}\sum_{i_1,\ldots,i_N=1}^{N}\sum_{j_1,\ldots j_N=1}^{N}\epsilon_{i_1,i_2,\ldots,i_N}\epsilon_{j_1,j_2,\ldots j_N}\\ \cdot\langle\psi_{i_1}|\hat{A}|\varphi_{j_1}\rangle\underbrace{\langle\psi_{i_2}|\varphi_{j_2}\rangle}_{\delta_{i_2,j_2}(1-\delta_{i_2,1})(1-\delta_{i_2,2})}\cdots\underbrace{\langle\psi_{i_N}|\varphi_{j_N}\rangle}_{\delta_{i_N,j_N}(1-\delta_{i_N,1})(1-\delta_{i_N,2})} = 0\end{aligned} \tag{H.23}$$

It is evident that this matrix element vanishes, because in each term there is at least one scalar product between to orbitals that differ in the two Slater determinants.

This result corresponds to the first line in the third Slater-Condon rule Eq. 3.44.

H.4.2 Two-particle operator

The matrix element of a two-particle operator with Slater determinants differing by two orbitals is

$$\begin{aligned}\langle\Psi|\hat{W}_{x_1,x_2}|\Phi\rangle &= \frac{1}{N!}\sum_{i_1,\ldots,i_N}\sum_{j_1,\ldots j_N}\epsilon_{i_1,i_2,\ldots,i_N}\epsilon_{j_1,j_2,\ldots j_N}\\ &\quad\cdot\langle\psi_{i_1}\psi_{i_2}|\hat{W}|\varphi_{j_1}\varphi_{j_2}\rangle\underbrace{\langle\psi_{i_3}|\varphi_{j_3}\rangle}_{\delta_{i_3,j_3}(1-\delta_{i_3,1})(1-\delta_{i_3,2})}\cdots\underbrace{\langle\psi_{i_N}|\varphi_{j_N}\rangle}_{\delta_{i_N,j_N}(1-\delta_{i_N,1})(1-\delta_{i_N,2})}\\ &= \frac{1}{N!}\sum_{i_1,i_2=1}^{2}\sum_{j_1,j_2=1}^{2}\langle\psi_{i_1}\psi_{i_2}|\hat{W}|\varphi_{j_1}\varphi_{j_2}\rangle\sum_{i_3,\ldots,i_N}\epsilon_{i_1,i_2,i_3\ldots,i_N}\epsilon_{j_1,j_2,i_3\ldots,i_N}\\ &= \frac{1}{N!}\sum_{i_1,i_2=1}^{2}\sum_{j_1,j_2=1}^{2}\langle\psi_{i_1}\psi_{i_2}|\hat{W}|\varphi_{j_1}\varphi_{j_2}\rangle(N-2)!\,(\delta_{i_1,j_1}\delta_{i_2,j_2}-\delta_{i_1,j_2}\delta_{i_2,j_1})\\ &= \frac{2}{N(N-1)}\left(\langle\psi_1\psi_2|\hat{W}|\varphi_1\varphi_2\rangle-\langle\psi_1\psi_2|\hat{W}|\varphi_2\varphi_1\rangle\right)\end{aligned} \tag{H.24}$$

With the interaction $\hat{W} = \frac{1}{2}\sum_{i\neq j}^{N}\hat{W}_{i,j}$ we obtain with $\langle\Psi|W_{i,j}|\Phi\rangle = \langle\Psi|W_{1,2}|\Phi\rangle$

$$\langle\Psi|\hat{W}|\Phi\rangle = \langle\psi_1\psi_2|\hat{W}|\varphi_1\varphi_2\rangle-\langle\psi_1\psi_2|\hat{W}|\varphi_2\varphi_1\rangle \tag{H.25}$$

This result corresponds to the second line in the third Slater-Condon rule Eq. 3.45.

H.5 Slater determinants differing by more than two orbitals

The matrix elements of one- and two-particle operators between two Slater determinants differing by more than two orbitals vanish. The argument is analogous to that about in Section H.4.1

Appendix I

One- and two-particle operators expressed by field operators

Here, we will explicitly derive the form of one- and two-particle operators by field operators as given by Eqs. 3.49 and 3.50 on p. 135.

OPERATORS EXPRESSED BY ANNIHILATION AND CREATION OPERATORS

A one-particle operator has the form

$$\hat{A} = \sum_{i,j} A_{i,j} \hat{c}_i^\dagger \hat{c}_j \tag{I.1}$$

and a two-particle operator has the form

$$\hat{W} = \frac{1}{2} \sum_{i,j,k,l} W_{i,j,k,l} \hat{c}_i^\dagger \hat{c}_j^\dagger \hat{c}_l \hat{c}_k \tag{I.2}$$

Note the reversed order of the annihilators relative to the indices!

Our approach will be to work out the matrix elements of a product of creation and annihilation operators between Slater determinants. Then the result will be compared with the Slater-Condon rules Eqs. 3.41 -3.44 on p. 134

Our argument is restricted to Slater determinants constructed from the zero state by a product of creation operators in a unique basis of one-particle orbitals. Thus, these states are eigenstates of the occupation-number operator

$$\hat{n}_k \stackrel{\text{def}}{=} \hat{c}_k^\dagger \hat{c}_k \tag{I.3}$$

That is, we consider here only states that obey

$$\hat{n}_k |\Phi\rangle = |\Phi\rangle n_k \tag{I.4}$$

As the occupation-number eigenstates for a complete orthonormal basis of one-particle eigenstates form a complete basis in the Fock space, we will obtain general matrix elements using the rules determined here.

I.1 Matrix elements between identical Slater determinants

One-particle operator

Let us determine the matrix element of a one-particle operator between two identical Slater determinants $|\Phi\rangle$.

In the first step, we use $\langle\Phi|\hat{c}_i^\dagger\hat{c}_j|\Phi\rangle = 0$ for $i \neq j$: Applied to a Slater determinant, $\hat{c}_i^\dagger\hat{c}_j$ with $i \neq j$ produces a different Slater determinant that is orthogonal to the original one. Thus, only the diagonal terms contribute.

$$\langle\Phi|\hat{c}_j^\dagger\hat{c}_k|\Phi\rangle = \delta_{j,k}\langle\Phi|\underbrace{\hat{n}_j}_{\hat{c}_j^\dagger\hat{c}_j}|\Phi\rangle \overset{\text{Eq. I.4}}{=} \delta_{j,k}n_j$$

$$\Rightarrow \langle\Phi|\sum_{j,k}A_{j,k}\hat{c}_j^\dagger\hat{c}_k|\Phi\rangle = \sum_{j=1}^{\infty}n_jA_{j,j} \overset{\text{Eq. 3.51}}{=} \sum_{j=1}^{\infty}n_j\langle\varphi_j|\hat{A}|\varphi_j\rangle \tag{I.5}$$

where $|\varphi_j\rangle = \hat{c}_j^\dagger|\mathcal{O}\rangle$ are the one-particle states related to the creation operators. $|\mathcal{O}\rangle$ is the vacuum state.

Eq. I.5 is identical to the first Slater-Condon rule for one-particle operators Eq. 3.41 on p.134. Thus,

$$\langle\Phi|\sum_{j,k}A_{j,k}\hat{c}_j^\dagger\hat{c}_k|\Phi\rangle \overset{\text{Eq. I.5}}{=} \sum_{j=1}^{\infty}n_j\langle\varphi_j|\hat{A}|\varphi_j\rangle \overset{\text{Eq. 3.41}}{=} \langle\Phi|\hat{A}|\Phi\rangle \tag{I.6}$$

In Eq. I.5, we sum over all one-particle basis functions and the occupation numbers n_i select those that are present in the Slater determinant. In Eq. 3.41, the sum goes directly over the one-orbitals in the determinant.

Thus, we have shown that the operator $\sum_{i,j}A_{i,j}\hat{c}_i^\dagger\hat{c}_j$ has the same matrix elements as the operator $\hat{A}$, if both wave functions are identical Slater determinants.

Two-particle operator

To work out the expressions for a two-particle operator, we use a similar argument. Unless the operator $\hat{c}_i^\dagger\hat{c}_j^\dagger\hat{c}_k\hat{c}_l$ creates all orbitals that it destroys, the resulting Slater determinant will differ from and be orthogonal to the original Slater determinant. There are just two possibilities that contribute to a nonzero value, namely

- case 1: $i = k$ and $j = l$.

$$\hat{c}_i^\dagger\hat{c}_j^\dagger\hat{c}_i\hat{c}_j \overset{[\hat{c}_i^\dagger,\hat{c}_j]_+=\delta_{i,j}}{=} \hat{c}_i^\dagger\delta_{i,j}\hat{c}_j - \hat{c}_i^\dagger\hat{c}_i\hat{c}_j^\dagger\hat{c}_j = \delta_{i,j}\hat{n}_i - \hat{n}_i\hat{n}_j$$

- case 2: $i = l$ and $j = k$

$$\hat{c}_i^\dagger\hat{c}_j^\dagger\hat{c}_j\hat{c}_i \overset{[\hat{c}_j,\hat{c}_j]_+=0}{=} -\hat{c}_i^\dagger\hat{c}_j^\dagger\hat{c}_i\hat{c}_j \overset{[\hat{c}_i^\dagger,\hat{c}_j]_+=\delta_{i,j}}{=} -\hat{c}_i^\dagger\delta_{i,j}\hat{c}_j + \hat{c}_i^\dagger\hat{c}_i\hat{c}_j^\dagger\hat{c}_j = -\delta_{i,j}\hat{n}_i + \hat{n}_i\hat{n}_j$$

- All other cases vanish because the creators and annihilators do not match.

Thus, we obtain

$$\begin{aligned}\langle\Phi|\hat{c}_i^\dagger\hat{c}_j^\dagger\hat{c}_k\hat{c}_l|\Phi\rangle &= \delta_{i,k}\delta_{j,l}\Big(\delta_{i,j}n_i - n_in_j\Big) + \delta_{i,l}\delta_{j,k}\Big(-\delta_{i,j}n_i + n_in_j\Big)\\ &= \underbrace{\delta_{i,k}\delta_{j,l}\delta_{i,j}n_i}_{a} - \underbrace{\delta_{i,k}\delta_{j,l}n_in_j}_{b} - \underbrace{\delta_{i,l}\delta_{j,k}\delta_{i,j}n_i}_{c} + \underbrace{\delta_{i,l}\delta_{j,k}n_in_j}_{d}\\ &\overset{a=c}{=} \underbrace{\delta_{i,l}\delta_{j,k}n_in_j}_{d} - \underbrace{\delta_{i,k}\delta_{j,l}n_in_j}_{b}\end{aligned}$$

which yields

$$\Rightarrow \langle\Phi| \sum_{i,j,k,l} W_{i,j,k,l} \hat{c}_i^\dagger \hat{c}_j^\dagger \hat{c}_l \hat{c}_k |\Phi\rangle = \sum_{i,j} n_i n_j \left[W_{i,j,i,j} - W_{i,j,j,i}\right]$$

Note, that we interchanged the two annihilators which changes the sign of the expression.

Let us compare this result again with that of the first Slater-Condon rule Eq. 3.41 on p. 134.

I.2 Matrix elements between Slater determinants differing by one orbital

We construct pairs of N-particle Slater determinants that differ by a single orbital from a common $(N-1)$-particle Slater determinant $|\Phi\rangle$ by creating two different one-particle orbitals (one for each). We obtain $\hat{c}_a^\dagger|\Phi\rangle$ and $\hat{c}_b^\dagger|\Phi\rangle$. They differ by exactly one one-particle orbital since $a \neq b$ and they are automatically in **maximum coincidence**. Remember, that the bra related to $\hat{c}_a^\dagger|\Phi\rangle$ is $\langle\hat{c}_a^\dagger\Phi| = \langle\Phi|\hat{c}_a$.

One-particle operators

Let us construct the matrix element of a one-particle operator $\hat{A} = \sum_{j,k} A_{j,k} \hat{c}_j^\dagger \hat{c}_k$ between two Slater determinants $|\Phi_a\rangle \stackrel{\text{def}}{=} \hat{c}_a^\dagger|\Phi\rangle$ and $|\Phi_b\rangle \stackrel{\text{def}}{=} \hat{c}_b^\dagger|\Phi\rangle$ differing by two distinct one-particle orbitals $|\psi_a\rangle$ and $|\psi_b\rangle$, i.e. $a \neq b$.

$$\langle\Phi|\hat{c}_a \hat{c}_j^\dagger \hat{c}_k \hat{c}_b^\dagger|\Phi\rangle \stackrel{a\neq b}{=} \delta_{a,j}(1-n_j)\delta_{k,b}(1-n_b)$$

$$\Rightarrow \langle\Phi|\hat{c}_a \left(\sum_{j,k} A_{j,k} \hat{c}_j^\dagger \hat{c}_k\right) \hat{c}_b^\dagger|\Phi\rangle = \sum_{j,k} A_{j,k}\delta_{a,i}(1-n_i)\delta_{j,b}(1-n_b) = A_{a,b}(1-n_a)(1-n_b)$$

where $n_j = \langle\Phi|\hat{c}_j^\dagger \hat{c}_j|\Phi\rangle$. This result can be compared to the Slater-Condon rule Eq. 3.43 on p. 134. The role of $(1-n_a)$ and $(1-n_b)$ is to test if the corresponding one-particle orbitals are already occupied in $|\Phi\rangle$. If one of the orbitals a or b is already present in $|\Phi\rangle$, the creation operators[1] $c_a^\dagger$ or $c_b^\dagger$ would turn this state into a zero state, for which the matrix element vanishes.

Two-particle operator

For the interaction matrix elements between two Slater determinants $|\Phi_a\rangle \stackrel{\text{def}}{=} \hat{c}_a^\dagger|\Phi\rangle$ and $|\Phi_b\rangle \stackrel{\text{def}}{=} \hat{c}_b^\dagger|\Phi\rangle$ differing by two distinct one-particle orbitals $|\psi_a\rangle$ and $|\psi_b\rangle$, i.e. $a \neq b$, we need to determine matrix elements of the type

$$\langle\Phi_a|\hat{c}_i^\dagger \hat{c}_j^\dagger \hat{c}_k \hat{c}_l|\Phi_b\rangle = \langle\Phi|\hat{c}_a \hat{c}_i^\dagger \hat{c}_j^\dagger \hat{c}_k \hat{c}_l \hat{c}_b^\dagger|\Phi\rangle\,. \tag{I.7}$$

For this matrix element to be non-zero, each annihilator must be paired with a creator of the same orbital.

The matrix element can be evaluated with brute force by commutating all operators so that the creation operators stand to the left of all annihilation operators. Once the matrix elements have this form, they are readily evaluated.

Here, however, we try to be more economical:

1. Let us pair the annihilator $\hat{c}_a$ with one of the creation operators. There are two possibilities: $i = a$ and $j = a$. The possibility $b = a$ has been excluded, because this is the case of two identical Slater determinants, which has been investigated in the previous section. The case $i = j$ does not contribute because the two creation operators stand next to each other and $\hat{c}_j^\dagger \hat{c}_j^\dagger = \hat{0}$.

[1] $\langle\hat{c}_a^\dagger\Phi| = \langle\Phi|\hat{c}_a$

2. For each of the two possibilities there are two cases $b = k$ and $b = l$ where the creator $\hat{c}_b$ is paired with one of the annihilators. As before the cases $a = b$ and $k = l$ do not contribute.

Thus, there are four sets of indices with nonzero value, namely

$$\begin{aligned}
\langle\Phi|\hat{c}_a\hat{c}_i^\dagger\hat{c}_j^\dagger\hat{c}_k\hat{c}_l\hat{c}_b^\dagger|\Phi\rangle &= \Big(\delta_{a,i}\Big(\delta_{b,k}\delta_{j,l}+\delta_{b,l}\delta_{j,k}\Big)+\delta_{a,j}\Big(\delta_{b,k}\delta_{i,l}+\delta_{b,l}\delta_{i,k}\Big)\Big)\langle\Phi|\hat{c}_a\hat{c}_i^\dagger\hat{c}_j^\dagger\hat{c}_k\hat{c}_l\hat{c}_b^\dagger|\Phi\rangle \\
&= \delta_{a,i}\delta_{b,k}\delta_{j,l}\langle\Phi|\hat{c}_a\hat{c}_a^\dagger\hat{c}_j^\dagger\hat{c}_b\hat{c}_j\hat{c}_b^\dagger|\Phi\rangle + \delta_{a,i}\delta_{b,l}\delta_{j,k}\langle\Phi|\hat{c}_a\hat{c}_a^\dagger\hat{c}_j^\dagger\hat{c}_j\hat{c}_b\hat{c}_b^\dagger|\Phi\rangle \\
&+ \delta_{a,j}\delta_{b,k}\delta_{i,l}\langle\Phi|\hat{c}_a\hat{c}_i^\dagger\hat{c}_a^\dagger\hat{c}_b\hat{c}_i\hat{c}_b^\dagger|\Phi\rangle + \delta_{a,j}\delta_{b,l}\delta_{i,k}\langle\Phi|\hat{c}_a\hat{c}_i^\dagger\hat{c}_a^\dagger\hat{c}_i\hat{c}_b\hat{c}_b^\dagger|\Phi\rangle \\
&= -\delta_{a,i}\delta_{b,k}\delta_{j,l}\langle\Phi|\hat{c}_a\hat{c}_a^\dagger\left(\hat{c}_j^\dagger\hat{c}_j\right)\hat{c}_b\hat{c}_b^\dagger|\Phi\rangle + \delta_{a,i}\delta_{b,l}\delta_{j,k}\langle\Phi|\hat{c}_a\hat{c}_a^\dagger\left(\hat{c}_j^\dagger\hat{c}_j\right)\hat{c}_b\hat{c}_b^\dagger|\Phi\rangle \\
&\quad +\delta_{a,j}\delta_{b,k}\delta_{i,l}\langle\Phi|\hat{c}_a\hat{c}_a^\dagger\left(\hat{c}_i^\dagger\hat{c}_i\right)\hat{c}_b\hat{c}_b^\dagger|\Phi\rangle - \delta_{a,j}\delta_{b,l}\delta_{i,k}\langle\Phi|\hat{c}_a\hat{c}_a^\dagger\left(\hat{c}_i^\dagger\hat{c}_i\right)\hat{c}_b\hat{c}_b^\dagger|\Phi\rangle \\
&= -\delta_{a,i}\delta_{b,k}\delta_{j,l}(1-n_a)(1-n_b)n_j \quad + \quad \delta_{a,i}\delta_{b,l}\delta_{j,k}(1-n_a)(1-n_b)n_j \\
&\quad +\delta_{a,j}\delta_{b,k}\delta_{i,l}(1-n_a)(1-n_b)n_i \quad - \quad \delta_{a,j}\delta_{b,l}\delta_{i,k}(1-n_a)(1-n_b)n_i \qquad \text{(I.8)}
\end{aligned}$$

In the last step, I exploited that our Slater determinant $|\Phi\rangle$ is an eigenstate of the occupation-number operators

$$\begin{aligned}
\hat{c}_i^\dagger\hat{c}_i|\Phi\rangle &= |\Phi\rangle n_i \\
\hat{c}_i\hat{c}_i^\dagger|\Phi\rangle &= |\Phi\rangle(1-n_i) \qquad \text{(I.9)}
\end{aligned}$$

where n_i are the eigenvalues, which are the occupations of the orbital in $|\Phi\rangle$.

Thus, we obtain

$$\begin{aligned}
\langle\Phi|\hat{c}_a\hat{W}\hat{c}_b^\dagger|\Phi\rangle &= \langle\Phi|\hat{c}_a\left(\frac{1}{2}\sum_{i,j,k,l}W_{i,j,k,l}\hat{c}_i^\dagger\hat{c}_j^\dagger\hat{c}_l\hat{c}_k\right)\hat{c}_b^\dagger|\Phi\rangle \\
&= -\frac{1}{2}\sum_{i,j,k,l}W_{i,j,k,l}\langle\Phi|\hat{c}_a\hat{c}_i^\dagger\hat{c}_j^\dagger\hat{c}_k\hat{c}_l\hat{c}_b^\dagger|\Phi\rangle \\
&= -\frac{1}{2}\sum_j\Big(W_{a,j,j,b}(1-n_a)n_j(1-n_b) - W_{a,j,b,j}(1-n_a)n_j(1-n_b) \\
&\quad -W_{j,a,j,b}(1-n_a)n_j(1-n_b) + W_{j,a,b,j}(1-n_a)n_j(1-n_b)\Big) \\
&= -(1-n_a)(1-n_b)\frac{1}{2}\sum_j n_j\Big(W_{a,j,j,b} - W_{a,j,b,j} - W_{j,a,j,b} + W_{j,a,b,j}\Big) \qquad \text{(I.10)}
\end{aligned}$$

Because of the special form of the interaction $W(\vec{x},\vec{x'}) = W(\vec{x'},\vec{x})$, the terms can be combined pairwise, so that the number of independent terms is reduced from four to two. The definition of the matrix elements Eq. 3.51 from p. 135 is

$$W_{i,j,k,l} \overset{\text{Eq. 3.51}}{\overset{\text{def}}{=}} \int d^4x \int d^4x'\ \varphi_i^*(\vec{x})\varphi_j^*(\vec{x'})W(\vec{x},\vec{x'})\varphi_k(\vec{x})\varphi_l(\vec{x'})\,. \qquad \text{(I.11)}$$

With of $W(\vec{x},\vec{x'}) = W(\vec{x'},\vec{x})$, the interaction $W_{i,j,k,l}$ is symmetric under interchanging simultaneously the first two and the last two indices. Thus, $W_{a,j,j,b} = W_{j,a,b,j}$ and $W_{a,j,b,j} = W_{j,a,j,b}$ and The property $W(\vec{x},\vec{x'}) = W(\vec{x'},\vec{x})$ is an expression of Newton's third law *"actio=reactio"*.

$$\begin{aligned}
\langle\Phi|\hat{c}_a\hat{W}\hat{c}_b^\dagger|\Phi\rangle &= -(1-n_a)(1-n_b)\frac{1}{2}\sum_j n_j\Big(W_{a,j,j,b} - W_{a,j,b,j}\Big) \\
&= (1-n_a)(1-n_b)\frac{1}{2}\sum_{j=1}^{\infty} n_j\Big(W_{a,j,b,j} - W_{a,j,j,b}\Big) \qquad \text{(I.12)}
\end{aligned}$$

The first term ensures, that the result vanishes, if $|\Phi\rangle$ already contains the orbital $|\varphi_a\rangle$ or the orbital $|\varphi_b\rangle$.

Eq. I.12 is the result of the second Slater-Condon rule Eq. 3.43 on p. 134.

I.3 Matrix elements between Slater determinants differing by two orbitals

The procedure is analogous to the above case. We construct the N-electron Slater determinants $\hat{c}_a^\dagger \hat{c}_b^\dagger |\Phi\rangle$ and $\hat{c}_c^\dagger \hat{c}_d^\dagger |\Phi\rangle$ from the same $N-2$ electron Slater determinant $|\Phi\rangle$. All four indices a, b, c, d are pairwise different.

Then we select those terms where all creators are paired with an annihilator of the same orbital. All other terms vanish. Note that the bra related to $\hat{c}_a^\dagger \hat{c}_b^\dagger |\Phi\rangle$ is $\langle\Phi|\hat{c}_b \hat{c}_a$, because $\left(\hat{c}_a^\dagger \hat{c}_b^\dagger\right)^\dagger = \hat{c}_b \hat{c}_a$.

For the one-particle operator, the matrix element vanishes consistent with the third Slater-Condon rule Eq. 3.45, because the one-particle operator can only match one annihilator.

For the two-particle operator, we obtain

$$
\begin{aligned}
& \langle\Phi|\hat{c}_b \hat{c}_a \left(\hat{c}_i^\dagger \hat{c}_j^\dagger \hat{c}_k \hat{c}_l\right) \hat{c}_c^\dagger \hat{c}_d^\dagger |\Phi\rangle \\
= \;& \delta_{b,i}\delta_{a,j}\delta_{k,c}\delta_{l,d} \langle\Phi|\hat{c}_b \hat{c}_a \hat{c}_i^\dagger \hat{c}_j^\dagger \hat{c}_k \hat{c}_l \hat{c}_c^\dagger \hat{c}_d^\dagger |\Phi\rangle \\
+ \;& \delta_{b,i}\delta_{a,j}\delta_{k,d}\delta_{l,c} \langle\Phi|\hat{c}_b \hat{c}_a \hat{c}_i^\dagger \hat{c}_j^\dagger \hat{c}_k \hat{c}_l \hat{c}_c^\dagger \hat{c}_d^\dagger |\Phi\rangle \\
+ \;& \delta_{b,j}\delta_{a,i}\delta_{k,c}\delta_{l,d} \langle\Phi|\hat{c}_b \hat{c}_a \hat{c}_i^\dagger \hat{c}_j^\dagger \hat{c}_k \hat{c}_l \hat{c}_c^\dagger \hat{c}_d^\dagger |\Phi\rangle \\
+ \;& \delta_{b,j}\delta_{a,i}\delta_{k,d}\delta_{l,c} \langle\Phi|\hat{c}_b \hat{c}_a \hat{c}_i^\dagger \hat{c}_j^\dagger \hat{c}_k \hat{c}_l \hat{c}_c^\dagger \hat{c}_d^\dagger |\Phi\rangle \\
\hline
= \;& \delta_{b,i}\delta_{a,j}\delta_{k,c}\delta_{l,d} \langle\Phi|\hat{c}_b \hat{c}_a \hat{c}_b^\dagger \hat{c}_a^\dagger \hat{c}_c \hat{c}_d \hat{c}_c^\dagger \hat{c}_d^\dagger |\Phi\rangle \\
+ \;& \delta_{b,i}\delta_{a,j}\delta_{k,d}\delta_{l,c} \langle\Phi|\hat{c}_b \hat{c}_a \hat{c}_b^\dagger \hat{c}_a^\dagger \hat{c}_d \hat{c}_c \hat{c}_c^\dagger \hat{c}_d^\dagger |\Phi\rangle \\
+ \;& \delta_{b,j}\delta_{a,i}\delta_{k,c}\delta_{l,d} \langle\Phi|\hat{c}_b \hat{c}_a \hat{c}_a^\dagger \hat{c}_b^\dagger \hat{c}_c \hat{c}_d \hat{c}_c^\dagger \hat{c}_d^\dagger |\Phi\rangle \\
+ \;& \delta_{b,j}\delta_{a,i}\delta_{k,d}\delta_{l,c} \langle\Phi|\hat{c}_b \hat{c}_a \hat{c}_a^\dagger \hat{c}_b^\dagger \hat{c}_d \hat{c}_c \hat{c}_c^\dagger \hat{c}_d^\dagger |\Phi\rangle \\
\hline
\overset{c\neq d; a\neq b}{=} \;& \delta_{b,i}\delta_{a,j}\delta_{k,c}\delta_{l,d} \langle\Phi|\hat{c}_b \hat{c}_b^\dagger \hat{c}_a \hat{c}_a^\dagger \hat{c}_c \hat{c}_c^\dagger \hat{c}_d \hat{c}_d^\dagger |\Phi\rangle \\
- \;& \delta_{b,i}\delta_{a,j}\delta_{k,d}\delta_{l,c} \langle\Phi|\hat{c}_a \hat{c}_a^\dagger \hat{c}_b \hat{c}_b^\dagger \hat{c}_d \hat{c}_d^\dagger \hat{c}_c \hat{c}_c^\dagger |\Phi\rangle \\
- \;& \delta_{b,j}\delta_{a,i}\delta_{k,c}\delta_{l,d} \langle\Phi|\hat{c}_a \hat{c}_a^\dagger \hat{c}_b \hat{c}_b^\dagger \hat{c}_c \hat{c}_c^\dagger \hat{c}_d \hat{c}_d^\dagger |\Phi\rangle \\
+ \;& \delta_{b,j}\delta_{a,i}\delta_{k,d}\delta_{l,c} \langle\Phi|\hat{c}_a \hat{c}_a^\dagger \hat{c}_b \hat{c}_b^\dagger \hat{c}_d \hat{c}_d^\dagger \hat{c}_c \hat{c}_c^\dagger |\Phi\rangle \\
\hline
= \;& \delta_{b,i}\delta_{a,j}\delta_{k,c}\delta_{l,d}(1-n_d)(1-n_c)(1-n_a)(1-n_b) \\
- \;& \delta_{b,i}\delta_{a,j}\delta_{k,d}\delta_{l,c}(1-n_d)(1-n_c)(1-n_a)(1-n_b) \\
- \;& \delta_{b,j}\delta_{a,i}\delta_{k,c}\delta_{l,d}(1-n_d)(1-n_c)(1-n_a)(1-n_b) \\
+ \;& \delta_{b,j}\delta_{a,i}\delta_{k,d}\delta_{l,c}(1-n_d)(1-n_c)(1-n_a)(1-n_b)
\end{aligned}
$$

Thus, we obtain

$$
\begin{aligned}
& \langle\Phi|\hat{c}_b \hat{c}_a \left(\frac{1}{2}\sum_{i,j,k,l} W_{i,j,k,l} \hat{c}_i^\dagger \hat{c}_j^\dagger \hat{c}_l \hat{c}_k\right) \hat{c}_c^\dagger \hat{c}_d^\dagger |\Phi\rangle \\
= \;& -\frac{1}{2}\sum_{i,j,k,l} W_{i,j,k,l} \langle\Phi|\hat{c}_b \hat{c}_a \left(\hat{c}_i^\dagger \hat{c}_j^\dagger \hat{c}_k \hat{c}_l\right) \hat{c}_c^\dagger \hat{c}_d^\dagger |\Phi\rangle \\
= \;& -\frac{1}{2}\Big(W_{b,a,c,d} - W_{b,a,d,c} - W_{a,b,c,d} + W_{a,b,d,c}\Big) \\
& \cdot(1-n_d)(1-n_c)(1-n_a)(1-n_b)
\end{aligned}
$$

Now we exploit that a joint interchange of the first two indices and the last two indices does not change the matrix element, that is $W_{i,j,k,l} = W_{j,i,l.k}$. This is allowed because the interaction is inversion symmetric, that is $V(\vec{x}, \vec{x'}) = V(\vec{x}, \vec{x'})$, which is a special property of the Coulomb interaction.

$$\begin{aligned}
&\langle\Phi|\hat{c}_b\hat{c}_a\left(\frac{1}{2}\sum_{i,j,k,l} W_{i,j,k,l}\hat{c}_i^\dagger\hat{c}_j^\dagger\hat{c}_l\hat{c}_k\right)\hat{c}_c^\dagger\hat{c}_d^\dagger|\Phi\rangle \\
&= -\Big(W_{a,b,d,c} - W_{a,b,c,d}\Big)(1-n_d)(1-n_c)(1-n_a)(1-n_b) \\
&= +\Big(W_{a,b,c,d} - W_{a,b,d,c}\Big)(1-n_d)(1-n_c)(1-n_a)(1-n_b)
\end{aligned}$$

This result corresponds directly to the third Slater-Condon rule Eq. 3.45 on p. 134.

Appendix J

Addenda to the Equation of motion for the Green's function

This chapter, I will derive the second equation of motion for the Green's function, which changes the second time argument of the Greens function. The derivation is analogous to that for the equation of motion for the first time argument presented in section 8.1 on p. 253.

The second equation is required, for example, for the arguments (Eq. 3b in [87]) by Kadanoff and Baym.[86, 87] Editor: The connection of the equation of motion with respect to the second time argument with the left-hand equation in Baym needs to be shown here.

$$i\hbar\partial_t \hat{c}^{+}_{H,\zeta}(t) = \hat{\mathcal{U}}(0,t)\left[\hat{c}^{\dagger}_{S,\zeta}, \hat{H}\right]_{-} \hat{\mathcal{U}}(t,0) \tag{J.1}$$

In order to continue, we need the commutator of the creation operator in the Schrödinger picture with the Hamiltonian. For the sake of simplicity, we drop the explicit subscript S denoting the Schrodinger picture. It is implicitly assumed.

$$\hat{H} = \sum_{\alpha,\beta} h_{\alpha,\beta}\hat{c}^{\dagger}_{\alpha}\hat{c}_{\beta} + \frac{1}{2}\sum_{\alpha,\beta,\gamma,\delta} W_{\alpha,\beta,\delta,\gamma}\hat{c}^{\dagger}_{\alpha}\hat{c}^{\dagger}_{\beta}\hat{c}_{\gamma}\hat{c}_{\delta} \tag{J.2}$$

We begin with the one-particle operator

$$\left[\hat{c}^{\dagger}_{\zeta}, \sum_{\alpha,\beta} h_{\alpha,\beta}\hat{c}^{\dagger}_{\alpha}\hat{c}_{\beta}\right]_{-} = \sum_{\alpha,\beta} h_{\alpha,\beta}\left(\underbrace{\hat{c}^{\dagger}_{\zeta}\hat{c}^{\dagger}_{\alpha}}_{-\hat{c}^{\dagger}_{\alpha}\hat{c}^{\dagger}_{\zeta}}\hat{c}_{\beta} - \hat{c}^{\dagger}_{\alpha}\underbrace{\hat{c}_{\beta}\hat{c}^{\dagger}_{\zeta}}_{\delta_{\beta,\zeta}-\hat{c}^{\dagger}_{\zeta}\hat{c}_{\beta}}\right) = \sum_{\alpha,\beta} h_{\alpha,\beta}\hat{c}^{\dagger}_{\alpha}\delta_{\beta,\zeta} = \sum_{\beta} h_{\alpha,\zeta}\hat{c}^{\dagger}_{\alpha} \tag{J.3}$$

and continue with the interaction

$$
\begin{aligned}
\left[\hat{c}_\zeta^\dagger, \frac{1}{2}\sum_{\alpha,\beta,\gamma,\delta} W_{\alpha,\beta,\delta,\gamma}\hat{c}_\alpha^\dagger\hat{c}_\beta^\dagger\hat{c}_\gamma\hat{c}_\delta\right]_- &= \frac{1}{2}\sum_{\alpha,\beta,\gamma,\delta} W_{\alpha,\beta,\delta,\gamma}\Big(\underbrace{\hat{c}_\zeta^\dagger\hat{c}_\alpha^\dagger\hat{c}_\beta^\dagger}_{\hat{c}_\alpha^\dagger\hat{c}_\beta^\dagger\hat{c}_\zeta^\dagger}\hat{c}_\gamma\hat{c}_\delta - \hat{c}_\alpha^\dagger\hat{c}_\beta^\dagger\hat{c}_\gamma\hat{c}_\delta\hat{c}_\zeta^\dagger\Big) \\
&= \frac{1}{2}\sum_{\alpha,\beta,\gamma,\delta} W_{\alpha,\beta,\delta,\gamma}\hat{c}_\alpha^\dagger\hat{c}_\beta^\dagger\Big(\underbrace{\hat{c}_\zeta^\dagger\hat{c}_\gamma}_{\delta_{\zeta,\gamma}-\hat{c}_\gamma\hat{c}_\zeta^\dagger}\hat{c}_\delta - \hat{c}_\gamma\underbrace{\hat{c}_\delta\hat{c}_\zeta^\dagger}_{\delta_{\delta,\zeta}-\hat{c}_\zeta^\dagger\hat{c}_\delta}\Big) \\
&= \frac{1}{2}\sum_{\alpha,\beta,\gamma,\delta} W_{\alpha,\beta,\delta,\gamma}\hat{c}_\alpha^\dagger\hat{c}_\beta^\dagger\Big(\delta_{\zeta,\gamma}\hat{c}_\delta - \hat{c}_\gamma\delta_{\delta,\zeta}\Big) \\
&= \frac{1}{2}\sum_{\alpha,\beta,\delta} W_{\alpha,\beta,\delta,\zeta}\hat{c}_\alpha^\dagger\hat{c}_\beta^\dagger\hat{c}_\delta - \frac{1}{2}\sum_{\alpha,\beta,\gamma}\underbrace{W_{\alpha,\beta,\zeta,\gamma}}_{W_{\beta,\alpha,\gamma,\zeta}}\underbrace{\hat{c}_\alpha^\dagger\hat{c}_\beta^\dagger}_{-\hat{c}_\beta^\dagger\hat{c}_\alpha^\dagger}\hat{c}_\gamma \\
&= \frac{1}{2}\sum_{\alpha,\beta,\delta} W_{\alpha,\beta,\delta,\zeta}\hat{c}_\alpha^\dagger\hat{c}_\beta^\dagger\hat{c}_\delta + \frac{1}{2}\sum_{\alpha,\beta,\gamma} W_{\beta,\alpha,\gamma,\zeta}\hat{c}_\beta^\dagger\hat{c}_\alpha^\dagger\hat{c}_\gamma \\
&= \frac{1}{2}\sum_{\alpha,\beta,\delta} W_{\alpha,\beta,\delta,\zeta}\hat{c}_\alpha^\dagger\hat{c}_\beta^\dagger\hat{c}_\delta + \overbrace{\frac{1}{2}\sum_{\alpha,\beta,\delta} W_{\alpha,\beta,\delta,\zeta}\hat{c}_\alpha^\dagger\hat{c}_\beta^\dagger\hat{c}_\delta}^{\alpha\leftrightarrow\beta,\gamma\leftrightarrow\delta} \qquad \text{(J.4)} \\
&= \sum_{\alpha,\beta,\delta} W_{\alpha,\beta,\delta,\zeta}\hat{c}_\alpha^\dagger\hat{c}_\beta^\dagger\hat{c}_\delta \qquad \text{(J.5)}
\end{aligned}
$$

We exploited that a simultaneous interchange of the first two and, at the same time, the last two arguments leaves the value of the interaction matrix elements unchanged, i.e. $W_{\alpha,\beta,\gamma,\delta} = W_{\beta,\alpha,\delta,\gamma}$. This symmetry follows from the form of the interaction matrix elements defined in Eq. 3.51 on p. 135. Editor: This argument refers to the Coulomb interaction. What about the most general definition as $W(t) = \hat{H}(t) - \hat{h}$?

With the results Eqs. J.3, J.5, we can return to Eq. J.1 and evaluate the time derivative of the annihilator in the Heisenberg picture as

$$
\begin{aligned}
i\hbar\partial_t\hat{c}_{H,\zeta}^+(t) &= \hat{\mathcal{U}}(0,t)\left[\hat{c}_{S,\zeta}^\dagger, \hat{H}\right]_-\hat{\mathcal{U}}(t,0) \\
&\overset{Eqs.\ J.3,J.5}{=} \hat{\mathcal{U}}(0,t)\left(\sum_\alpha h_{\alpha,\zeta}\hat{c}_{S,\alpha}^\dagger + \sum_{\alpha,\beta,\delta} W_{\alpha,\beta,\delta,\zeta}\hat{c}_{S,\alpha}^\dagger\hat{c}_{S,\beta}^\dagger\hat{c}_{S,\delta}\right)\hat{\mathcal{U}}(t,0) \\
&= \sum_\alpha h_{\alpha,\zeta}\hat{c}_{H,\alpha}^+(t) + \sum_{\alpha,\beta,\delta} W_{\alpha,\beta,\delta,\zeta}\hat{c}_{H,\alpha}^+(t)\hat{c}_{H,\beta}^+(t)\hat{c}_{H,\delta}(t) \qquad \text{(J.6)}
\end{aligned}
$$

Now, we can evaluate the time derivative of the Green's function Eq. 7.16. We use the short-hand

notation $\Big\langle \dots \Big\rangle_{T,\mu} \stackrel{\text{def}}{=} \mathrm{Tr}\{\hat{\rho}^{(W)}_{T,\mu} \dots\}$.

$$
\begin{aligned}
& i\hbar\partial_{t'} G^{\mathcal{C}}_{\alpha,\beta}(t,t') \\
\stackrel{\text{Eq. 7.16}}{=}\ & i\hbar\partial_{t'}\left[\frac{\theta(t-t')}{i\hbar}\Big\langle \hat{c}_{H,\alpha}(t)\hat{c}^{+}_{H,\beta}(t')\Big\rangle_{T,\mu} - \frac{\theta(t'-t)}{i\hbar}\Big\langle \hat{c}^{+}_{H,\beta}(t')\hat{c}_{H,\alpha}(t)\Big\rangle_{T,\mu}\right] \\
=\ & -\delta(t-t')\Big\langle \hat{c}_{H,\alpha}(t)\hat{c}^{+}_{H,\beta}(t')\Big\rangle_{T,\mu} - \delta(t'-t)\Big\langle \hat{c}^{+}_{H,\beta}(t')\hat{c}_{H,\alpha}(t)\Big\rangle_{T,\mu} \\
+\ & \frac{\theta(t-t')}{i\hbar}\Big\langle \hat{c}_{H,\alpha}(t)\Big(i\hbar\partial_{t'}\hat{c}^{+}_{H,\beta}(t')\Big)\Big\rangle_{T,\mu} - \frac{\theta(t'-t)}{i\hbar}\Big\langle \Big(i\hbar\partial_{t'}\hat{c}^{+}_{H,\beta}(t')\Big)\hat{c}_{H,\alpha}(t)\Big\rangle_{T,\mu} \\
\stackrel{\text{Eq. J.6}}{=}\ & -\delta(t-t')\Big\langle \Big[\hat{c}_{H,\alpha}(t),\hat{c}^{+}_{H,\beta}(t')\Big]_{+}\Big\rangle_{T,\mu} \\
+\ & \frac{\theta(t-t')}{i\hbar}\Big\langle \hat{c}_{H,\alpha}(t)\Big(\sum_a h_{a,\beta}\hat{c}^{+}_{H,a}(t') + \sum_{a,b,d} W_{a,b,d,\beta}\hat{c}^{+}_{H,a}(t')\hat{c}^{+}_{H,b}(t')\hat{c}_{H,d}(t')\Big)\Big\rangle_{T,\mu} \\
-\ & \frac{\theta(t'-t)}{i\hbar}\Big\langle \Big(\sum_a h_{a,\beta}\hat{c}^{+}_{H,a}(t') + \sum_{a,b,d} W_{a,b,d,\beta}\hat{c}^{+}_{H,a}(t')\hat{c}^{+}_{H,b}(t')\hat{c}_{H,d}(t')\Big)\hat{c}_{H,\alpha}(t)\Big\rangle_{T,\mu} \\
=\ & -\delta(t-t')\Big\langle \Big[\hat{c}_{H,\alpha}(t),\hat{c}^{+}_{H,\beta}(t')\Big]_{+}\Big\rangle_{T,\mu} \\
+\ & \sum_a h_{a,\beta}\left(\frac{\theta(t-t')}{i\hbar}\Big\langle \hat{c}_{H,\alpha}(t)\hat{c}^{+}_{H,a}(t')\Big\rangle_{T,\mu} - \frac{\theta(t'-t)}{i\hbar}\Big\langle \hat{c}^{+}_{H,a}(t')\hat{c}_{H,\alpha}(t)\Big\rangle_{T,\mu}\right) \\
+\ & \sum_{a,b,d} W_{a,b,d,\beta}\left(\frac{\theta(t-t')}{i\hbar}\Big\langle \hat{c}_{H,\alpha}(t)\hat{c}^{+}_{H,a}(t')\hat{c}^{+}_{H,b}(t')\hat{c}_{H,d}(t')\Big\rangle_{T,\mu} - \frac{\theta(t'-t)}{i\hbar}\Big\langle \hat{c}^{+}_{H,a}(t')\hat{c}^{+}_{H,b}(t')\hat{c}_{H,d}(t')\hat{c}_{H,\alpha}(t)\Big\rangle_{T,\mu}\right) \\
\stackrel{\text{Eq. 8.7}}{=}\ & -\delta(t-t')\delta_{\alpha,\beta} + \sum_a h_{a,\beta}G_{\alpha,a}(t,t') \\
+\ & \sum_{a,b,d} W_{a,b,d,\beta}\underbrace{\left(\frac{\theta(t-t')}{i\hbar}\Big\langle \hat{c}_{H,\alpha}(t)\overbrace{\hat{c}^{+}_{H,a}(t')\hat{c}^{+}_{H,b}(t')\hat{c}_{H,d}(t')}^{A}\Big\rangle_{T,\mu} - \frac{\theta(t'-t)}{i\hbar}\Big\langle \overbrace{\hat{c}^{+}_{H,a}(t')\hat{c}^{+}_{H,b}(t')\hat{c}_{H,d}(t')}^{A}\hat{c}_{H,\alpha}(t)\Big\rangle_{T,\mu}\right)}_{\frac{1}{i\hbar}\Big\langle \mathcal{T}_{\mathcal{C}}\hat{c}_{H,\alpha}(t)\hat{c}^{+}_{H,a}(t')\hat{c}^{+}_{H,b}(t')\hat{c}_{H,d}(t')\Big\rangle_{T,\mu}}
\end{aligned}
\tag{J.7}
$$

Eq. J.7 can be brought into a form similar to the defining equation of the Green's function for non-interacting systems is

EQUATION OF MOTION FOR THE INTERACTING GREEN'S FUNCTION

$$
\sum_\gamma\Big(\delta_{\alpha,\gamma}i\hbar\partial_{t'} - h_{\alpha,\gamma}\Big)G^{\mathcal{C}}_{\gamma,\beta}(t,t') =
$$

$$
= -\delta(t-t')\delta_{\alpha,\beta} + \sum_\gamma\sum_{b,d}\overbrace{\frac{1}{i\hbar}\mathrm{Tr}\Big\{\hat{\rho}^{(W)}_{T,\mu}\mathcal{T}_{\mathcal{C}}\hat{c}_{H,\alpha}(t)\hat{c}^{+}_{H,\gamma}(t')\underbrace{\hat{c}^{+}_{H,b}(t')\hat{c}_{H,d}(t')}_{\sim\text{density operator}}\Big\}}^{}W_{\gamma,b,d,\beta} \tag{J.8}
$$

$$
= -\delta(t-t')\delta_{\alpha,\beta} + \sum_\gamma\frac{1}{i\hbar}\mathrm{Tr}\Big\{\hat{\rho}^{(W)}_{T,\mu}\mathcal{T}_{\mathcal{C}}\hat{c}_{H,\alpha}(t)\hat{c}^{+}_{H,\gamma}(t')\underbrace{\sum_{b,d}W_{\gamma,b,d,\beta}\underbrace{\hat{c}^{+}_{H,b}(t')\hat{c}_{H,d}(t')}_{\sim\text{density operator}}}_{\hat{V}_{ee}(t')}\Big\} \tag{J.9}
$$

$\hat{V}_{ee}$ is the operator describing the Coulomb potential from the (other) electrons.

Appendix K

Derivation of Wick's theorem

Wick's theorem[57] is summarized in section 10.2.3 on p. 303. Here, I provide a derivation of Wick's theorem. What is shown here is the so-called "generalized Wick's theorem"[81], which has been adjusted to time-dependent non-interacting Hamiltonians. The generalized Wick's theorem is valid also for finite temperatures and it avoids the problems of "adiabatic switching on the interaction", which can be problematic if the interaction interchanges ground and excited states.

The gist of Wick's theorem is to map a many-particle expectation value (in Fock space) onto an expression with only one-particle expectation values (in one-particle Hilbert space).

One of the key ingredients for the proof is that the anticommutators between creation and annihilation operators in the interaction picture are numbers, namely the one-particle Green's functions of non-interacting electrons. These anticommutators are worked out in sections K.2 and K.3.

In the following, I will refer to the complex-valued time contour and its time-ordering operator Eq. 6.36. The propagator can be expressed by the time-ordered exponential $\mathcal{T}_\mathcal{C}$ along the contour Eq. 6.37.

One has to remember that the propagator on the complex time contour is, in general, not unitary, Eq. 6.39. Similarly, the creation and annihilation operators in the interaction picture are not hermitian conjugates of each other. The creation operator is therefore indicated as $\hat{a}^+_{l,n}(t)$ instead of $\hat{a}^\dagger_{l,n}(t)$, where the latter is the hermitian conjugate of the annihilator. This is specified in Eq. 6.41 on p. 236 for Heisenberg operators.

Editor: Remark: One aspect is worth considering: The perturbation expansion in requires that the chemical potential of the interacting system is the same as that of the non-interacting system. The number of electrons in thermal equilibrium may be very different with and without interaction. This implies that the perturbation expansion may proceed through states that are very different from the interacting system of interest. This can be avoided by a suitable time-dependence of the non-interacting Hamiltonian, also along the imaginary time axis. While I have no doubt that the required time-dependence of a global energy shift is permitted, one should carefully check if this is indeed so.

K.1 Field operators in the interaction picture for complex time

FIELD OPERATORS IN THE INTERACTION PICTURE

The creation and annihilation operators $\hat{c}^\dagger_{I,\alpha}(t)$, $\hat{c}_{I,\alpha}(t)$ in the interaction picture on a complex time contour $\mathcal{C}$ have the form below in terms of the corresponding creation and annihilation operators $\hat{c}^\dagger_{S,\alpha}$, $\hat{c}_{S,\alpha}$ in the Schrödinger picture.

$$\hat{c}^\dagger_{I,\alpha}(t) \overset{\text{Eq. } K.28}{=} \sum_\beta \hat{c}^\dagger_{S,\beta}\ \langle\chi_\beta|\hat{U}(0,t)|\pi_\alpha\rangle \tag{K.1}$$

$$\hat{c}_{I,\alpha}(t) \overset{\text{Eq. } K.29}{=} \sum_\beta \langle\pi_\alpha|\hat{U}(t,0)|\chi_\beta\rangle\ \hat{c}_{S,\beta} \tag{K.2}$$

The one-particle orbitals $|\chi_\alpha\rangle$ may be non-orthonormal with an overlap matrix $S_{\alpha,\beta} = \langle\chi_\alpha|\chi_\beta\rangle$. Each orbital has a corresponding projector function $\langle\pi_\alpha| = \sum_\beta S^{-1}_{\alpha,\beta}\langle\chi_\beta|$. The creation and annihilation operators defined for this basisset are $\hat{c}^\dagger_\alpha = \int d^4x\ \hat{\psi}^\dagger(\vec{x})\langle\vec{x}|\pi_\alpha\rangle$ and $\hat{c}_\alpha = \int d^4x\ \langle\pi_\alpha|\vec{x}\rangle\hat{\psi}(\vec{x})$.
The propagator $\hat{U}(t,0)$ satisfies the time-dependent Schrödinger equation along the contour $\Big[i\hbar\partial_t - \hat{h}(t)\Big]\hat{U}(t,0) = 0$ with the (non-interacting) one-particle Hamiltonian $\hat{h}(t)$. It furthermore satisfies the initial condition $\hat{U}(t,t) = \hat{1}$. The propagator can be written as time-ordered exponential.

$$\begin{aligned}\hat{U}(t,0) &= \mathcal{T}_\mathcal{C} \mathrm{e}^{-\frac{i}{\hbar}\int_0^t dt\ \hat{h}(t)} \\ \hat{U}(0,t) &= \hat{U}^{-1}(t,0)\end{aligned} \tag{K.3}$$

Note that the propagator is unitary only on the branch of the contour with real-valued time.

K.1.1 Proof for a time-dependent non-interacting Hamiltonian in the complex time plane

Time-dependent one-particle states

Let me choose a complete, orthonormal one-particle basisset $\{|\varphi_n\rangle\}$. The creation and annihilation operators $\hat{a}^\dagger_n$, $\hat{a}_n$ and the Slater determinants $|\vec{\sigma}\rangle$ shall be defined with respect to this basiset.

Starting from this basisset $\{|\varphi_n\rangle\}$ as initial states, I construct a set $\big\{|\varphi_n(t)\rangle\big\}$ of time-dependent one-particle states, which satisfy

$$i\hbar\partial_t|\varphi_n(t)\rangle = \hat{h}(t)|\varphi_n(t)\rangle \quad \text{with } |\varphi_n(0)\rangle = |\varphi_n\rangle \tag{K.4}$$

on the complex time contour $\mathcal{C}$. Because the propagator is not unitary, when the time contour deviates from the real-time axis, the orthonormality is not preserved in general. The time-dependent overlap matrix is

$$O_{m,n}(t) \overset{\text{def}}{=} \langle\varphi_m(t)|\varphi_n(t)\rangle \tag{K.5}$$

The states $|\varphi_n(t)\rangle$ are **not** eigenstates of the instantaneous Hamiltonian $\hat{h}(t)$, except for $t = 0$. The propagator Eq. 4.31 in the one-particle Hilbert space is then

$$\hat{U}(t,0) \overset{\text{Eq. } 4.31}{=} \sum_{m,n} |\varphi_m(t)\rangle\ \underbrace{O^{-1}_{m,n}(0)}_{\delta_{m,n}}\langle\varphi_n(0)| \overset{\text{Eq. } 4.40}{=} \mathcal{T}_\mathcal{C}\mathrm{e}^{-\frac{i}{\hbar}\int_0^t dt'\ \hat{h}(t')} \tag{K.6}$$

$\mathcal{T}_\mathcal{C}$ is the time-ordering operator along the contour in the complex time plane. Similarly, the time integral in Eq. K.6 is to be interpreted as a contour integral along $\mathcal{C}$.

The inverse overlap matrix present in Eq. 4.31 has been dropped in Eq. K.6, because the orbitals $|\varphi(t)\rangle$ are orthonormal at $t = 0$.

The backward transformation $\hat{U}(0,t) \overset{\text{def}}{=} \hat{U}^{-1}(t,0)$ is

$$\hat{U}(0,t) \overset{\text{Eq. 4.31}}{=} \sum_{m,n} |\varphi_m(0)\rangle\, O^{-1}_{m,n}(t) \langle\varphi_n(t)| \tag{K.7}$$

Thus, the matrix elements of the propagator are

$$\begin{aligned} U_{m,n}(t,0) &\overset{\text{def}}{=} \langle\varphi_m(0)|\hat{U}(t,0)|\varphi_n(0)\rangle \overset{\text{Eq. K.6}}{=} \langle\varphi_m(0)|\varphi_n(t)\rangle \\ U_{m,n}(0,t) &\overset{\text{def}}{=} \langle\varphi_m(0)|\hat{U}(0,t)|\varphi_n(0)\rangle \overset{\text{Eq. K.7}}{=} \sum_j O^{-1}_{m,j}(t) \langle\varphi_j(t)|\varphi_n(0)\rangle \end{aligned} \tag{K.8}$$

The propagator $\hat{U}(t,0)$ acts in the one-particle Hilbert space and so does the Hamiltonian in the time-ordered exponential of Eq. K.6.[1]

Time-dependent many-particle states

From the time-dependent one-particle states $\big|\varphi_n(t)\big\rangle$, I can construct time-dependent Slater determinants in the form

$$\Phi(\vec{x}_1, \dots, \vec{x}_N, t) \overset{\text{Eq. 1.88}}{=} \frac{1}{\sqrt{N!}} \sum_{j_1,\dots j_N=1}^{N} \epsilon_{j_1,\dots j_N}\, \varphi_{j_1}(\vec{x}_1, t) \cdots \varphi_{j_N}(\vec{x}_N, t) \tag{K.9}$$

where the wave function corresponds to a Slater determinant with N electrons. The time-dependent wave function $|\Phi(t)\rangle$ is a Slater determinant of the time-dependent one-particle orbitals because it is propagated with the non-interacting Hamiltonian.

In this fashion, I construct a time-dependent basisset of Slater determinants $|\Phi_{\vec{\sigma}}(t)\rangle$, which satisfy

$$i\hbar\partial_t |\Phi_{\vec{\sigma}}(t)\rangle = \hat{h}(t)|\Phi_{\vec{\sigma}}(t)\rangle \qquad \text{and} \qquad |\Phi_{\vec{\sigma}}(0)\rangle = |\vec{\sigma}\rangle = \prod_{n=1}^{\infty} \big(\hat{a}_n^\dagger\big)^{\sigma_n} |\mathcal{O}\rangle \tag{K.10}$$

where $|\vec{\sigma}\rangle$ denotes the Slater determinants in the basis of $|\varphi_n(0)\rangle$.

The propagator in Fock space can then be written as

$$\begin{aligned} \hat{\mathcal{U}}^{(0)}(t,0) &= \sum_{\vec{\sigma},\vec{\sigma}'} \big|\Phi_{\vec{\sigma}}(t)\big\rangle \underbrace{\bar{O}^{-1}_{\vec{\sigma},\vec{\sigma}'}(0)}_{\delta_{\vec{\sigma},\vec{\sigma}'}} \big\langle\Phi_{\vec{\sigma}'}(0)\big| = \mathcal{T}_{\mathcal{C}} \mathrm{e}^{-\frac{i}{\hbar}\int_0^t dt'\, \hat{h}(t')} \\ \hat{\mathcal{U}}^{(0)}(0,t) &= \hat{\mathcal{U}}^{(0),-1}(t,0) = \sum_{\vec{\sigma},\vec{\sigma}'} \big|\Phi_{\vec{\sigma}}(0)\big\rangle \bar{O}^{-1}_{\vec{\sigma},\vec{\sigma}'}(t) \big\langle\Phi_{\vec{\sigma}'}(t)\big| \quad \text{with } \bar{O}_{\vec{\sigma},\vec{\sigma}'} = \big\langle\Phi_{\vec{\sigma}}(t)\big|\Phi_{\vec{\sigma}'}(t)\big\rangle \end{aligned} \tag{K.11}$$

The Hamiltonian in the time-ordered exponential is a one-particle-at-a-time operator in Fock space. The inverse overlap matrix (present in Eq. 4.31) has been dropped, because I required the basisset $|\varphi_n\rangle$ to be orthonormal at time $t = 0$. This, in turn, implies orthonormality, $\bar{O}_{\vec{\sigma},\vec{\sigma}'}(0) = \delta_{\vec{\sigma},\vec{\sigma}'}$, of the Slater determints in this basisset at $t = 0$.[2]

[1] The non-interacting Hamiltonian and the corresponding operator has the same symbols in the one-partcle Hilbert space and in the Fock space.

[2] This orthonormality is preserved along the real-valued time axis, but it does not hold for complex-valued time arguments.

Creation and annihilation operators

Let me define a set of creation and annihilation operators that construct the time-dependent orbitals $|\varphi_j(t)\rangle$. The creation operator $\hat{b}^+_{S,j}(t)$ shall be defined such that

$$|\varphi_j(t)\rangle = \hat{b}^+_{S,j}(t)|\mathcal{O}\rangle \tag{K.12}$$

I am using the symbol + rather than † to indicate that $\hat{b}^+_{I,j}(t)$ is not necessarily the hermitian conjugate of the corresponding annihilator, if the contour deviates from the real time axis.

The time evolution of the one-particle orbitals discussed in the section above satisfies

$$|\varphi_j(t)\rangle = \sum_k |\varphi_k(0)\rangle \underbrace{\langle\varphi_k(0)|\varphi_j(t)\rangle}_{U_{k,j}(t,0)} \overset{\text{Eq. } K.8}{=} \sum_k \underbrace{|\varphi_k(0)\rangle}_{\hat{a}^\dagger_{S,k}|\mathcal{O}\rangle} U_{k,j}(t,0) \tag{K.13}$$

The comparison of Eq. K.12 and Eq. K.13 suggests the following definition of $\hat{b}^\dagger_{S,k}(t)$

$$\hat{b}^+_{S,j}(t) \overset{\text{def}}{=} \sum_k \hat{a}^\dagger_{S,k} U_{k,j}(t,0) \tag{K.14}$$

$$\hat{b}_{S,j}(t) \overset{\text{def}}{=} \sum_k U_{j,k}(0,t)\hat{a}_{S,k} \tag{K.15}$$

The annihilator Eq. K.15 has been defined so that the equal-time anticommutator relation is conserved over time, which is verified as follows:

$$\begin{aligned}\left[\hat{b}^+_{S,m}(t), \hat{b}_{S,n}(t)\right]_+ &= \sum_{j,k} U_{j,m}(t,0)U_{n,k}(0,t)\left[\hat{a}^\dagger_{S,j}, \hat{a}_{S,k}\right]_+ = \sum_j U_{n,j}(0,t)U_{j,m}(t,0)\hat{1} \\ &= \delta_{m,n}\hat{1}\end{aligned} \tag{K.16}$$

The new creation operator $\hat{b}^+_{S,j}(t)$ can also be expressed by the (non-interacting) propagator in Fock space. Let me start with the identity in the one-particle Hilbert space.

$$\hat{b}^+_{S,j}(t)|\mathcal{O}\rangle \overset{\text{Eq. } K.12}{=} |\varphi_j(t)\rangle = \hat{\mathcal{U}}^{(0)}(t,0)\underbrace{\hat{a}_{S,j}|\mathcal{O}\rangle}_{|\varphi_j(0)\rangle} = \hat{\mathcal{U}}^{(0)}(t,0)\hat{a}_{S,j}\underbrace{\hat{\mathcal{U}}^{(0)}(0,t)|\mathcal{O}\rangle}_{=|\mathcal{O}\rangle} \tag{K.17}$$

This relation between $\hat{b}^+_{S,j}(t)$ and $\hat{a}^\dagger_{S,j}$ can be generalized from the one-particle Hilbert space to arbitrary Slater determinants: On the one hand, the time-dependent Slater determinants can be represented using the time-dependent one-particle orbitals via the definition of Eq. K.9.

$$|\Phi_{\vec{\sigma}}(t)\rangle \overset{\text{Eqs. K.9, K.12}}{=} \prod_{n=1}^{\infty}\left(\hat{b}^+_{S,n}(t)\right)^{\sigma_n}|\mathcal{O}\rangle \tag{K.18}$$

On the other hand, the time-dependent Slater determinants can be obtained by propagating the initial state $|\vec{\sigma}\rangle$.

$$|\Phi_{\vec{\sigma}}(t)\rangle = \hat{\mathcal{U}}^{(0)}(t,0)\underbrace{\prod_{n=1}^{\infty}\left(\hat{a}^\dagger_{S,n}\right)^{\sigma_n}|\mathcal{O}\rangle}_{=|\vec{\sigma}\rangle=|\Phi_{\vec{\sigma}}(t=0)\rangle} = \prod_{n=1}^{\infty}\left(\hat{\mathcal{U}}^{(0)}(t,0)\hat{a}^\dagger_{S,n}\hat{\mathcal{U}}^{(0)}(0,t)\right)^{\sigma_n}\underbrace{\hat{\mathcal{U}}^{(0)}(t,0)|\mathcal{O}\rangle}_{=|\mathcal{O}\rangle} \tag{K.19}$$

The comparison provides the identity

$$\hat{b}^+_{S,j}(t) = \hat{\mathcal{U}}^{(0)}(t,0)\hat{a}^\dagger_{S,j}\,\hat{\mathcal{U}}^{(0)}(0,t) \tag{K.20}$$

$$\hat{b}_{S,j}(t) = \hat{\mathcal{U}}^{(0)}(t,0)\hat{a}_{S,j}\,\hat{\mathcal{U}}^{(0)}(0,t) \tag{K.21}$$

Some caution is required: The operators $\hat{b}^{+}_{S,j}(t)$ and $\hat{b}_{S,j}(t)$ are Schrödinger operators and **not** the creation and annihilation operators in the interaction picture: the propagators in the equations above propagate in the opposite direction compared to the transformation Eq. 10.4 into the interaction picture. Rather, we can identify the *b*-operators in the interaction picture directly with the *a*-operators in the Schrödinger picture.

$$\hat{b}^{+}_{I,j}(t) \overset{\text{Eqs. 10.4, K.20}}{=} \hat{U}^{(0)}(0,t)\overbrace{\hat{U}^{(0)}(t,0)\hat{a}^{\dagger}_{S,j}\,\hat{U}^{(0)}(0,t)}^{\hat{b}^{\dagger}_{S,j}\quad\text{Eq. K.20}}\hat{U}^{(0)}(t,0) = \hat{a}^{\dagger}_{S,j} \tag{K.22}$$

$$\hat{b}_{I,j}(t) \overset{\text{Eqs. 10.4, K.21}}{=} \hat{U}^{(0)}(0,t)\overbrace{\hat{U}^{(0)}(t,0)\hat{a}_{S,j}\,\hat{U}^{(0)}(0,t)}^{\hat{b}_{S,j}\quad\text{Eq. K.21}}\hat{U}^{(0)}(t,0) = \hat{a}_{S,j} \tag{K.23}$$

Now we are ready to translate the creation and annihilation operators in the interaction picture to those in the Schrödinger picture.

- for the creation operator, I obtain

$$\begin{aligned}
\hat{a}^{+}_{I,n}(t) &\overset{\text{Eq. 10.4}}{=} \hat{U}^{(0)}(0,t)\hat{a}^{\dagger}_{S,n}\hat{U}^{(0)}(t,0) \\
&\overset{\text{Eq. K.14}}{=} \hat{U}^{(0)}(0,t)\overbrace{\sum_k \hat{b}^{+}_{S,k}(t)U_{k,n}(0,t)}^{\hat{a}^{\dagger}_{S,n}}\hat{U}^{(0)}(t,0) \\
&= \sum_k \underbrace{\hat{U}^{(0)}(0,t)\hat{b}^{+}_{S,k}(t)\hat{U}^{(0)}(t,0)}_{=\hat{b}^{+}_{I,k}(t)} U_{k,n}(0,t) \\
&\overset{\text{Eq. K.22}}{=} \sum_k \hat{a}^{\dagger}_{S,k}\, U_{k,n}(0,t)
\end{aligned} \tag{K.24}$$

- and for the annihilation operator, I obtain analogously

$$\begin{aligned}
\hat{a}_{I,n}(t) &\overset{\text{Eq. 10.4}}{=} \hat{U}^{(0)}(0,t)\hat{a}_{S,n}\hat{U}^{(0)}(t,0) \\
&\overset{\text{Eq. K.15}}{=} \hat{U}^{(0)}(0,t)\overbrace{\sum_k U_{n,k}(t,0)\hat{b}_{S,k}(t)}^{\hat{a}_{S,n}}\hat{U}^{(0)}(t,0) \\
&= \sum_k U_{n,k}(t,0)\underbrace{\hat{U}^{(0)}(0,t)\hat{b}_{S,k}(t)\hat{U}^{(0)}(t,0)}_{\hat{b}_{I,k}(t)} \\
&\overset{\text{Eq. K.23}}{=} \sum_k U_{n,k}(t,0)\hat{a}_{S,k}
\end{aligned} \tag{K.25}$$

Eqs. K.24 and K.25 are remarkable results: The field operators in the interaction picture can be represented as superpositions of field operators in the Schrödinger picture.

General (non-orthonormal) basissets

The derivation above used an orthonormal initial basisset. The restriction was not necessary, but has been chosen to keep things simple and move complications out of the picture.

Here, I transform the result to a general basisset of orbitals $|\chi_\alpha\rangle$, which shall be complete, but which need not be orthonormal. The overlap is $S_{\alpha,\beta} = \langle\chi_\alpha|\chi_\beta\rangle$. I am using projector functions $\langle\pi_\alpha|$, which satisfy the biorthogonality condition $\langle\pi_\alpha|\chi_\beta\rangle = \delta_{\alpha,\beta}$. The projector functions may be written as $\langle\pi_\alpha| = \sum_\beta S^{-1}_{\alpha,\beta}\langle\chi_\beta|$.

The creation and annihilation operators $\hat{c}_\alpha^\dagger$, $\hat{c}_\alpha$ of the non-orthonormal basisset $\{|\chi_\alpha\rangle\}$ are transformed onto those $\hat{a}_n^\dagger$, $\hat{a}_n$ of the orthonormal basisset $\{|\varphi_n\rangle\}$ as

$$\begin{aligned}\hat{c}_\alpha^\dagger &= \int d^4x\, \hat{\psi}^\dagger(\vec{x})\langle\vec{x}|\pi_\alpha\rangle = \sum_n \hat{a}_n^\dagger\langle\varphi_n|\pi_\alpha\rangle \\ \hat{c}_\alpha &= \int d^4x\, \langle\pi_\alpha|\vec{x}\rangle\hat{\psi}(\vec{x}) = \sum_n \langle\pi_\alpha|\varphi_n\rangle\hat{a}_n\end{aligned} \tag{K.26}$$

and vice versa

$$\begin{aligned}\hat{a}_n^\dagger &= \int d^4x\, \hat{\psi}^\dagger(\vec{x})\langle\vec{x}|\varphi_n\rangle = \sum_\alpha \hat{c}_\alpha^\dagger\langle\chi_\alpha|\varphi_n\rangle \\ \hat{a}_n &= \int d^4x\, \langle\varphi_n|\vec{x}\rangle\hat{\psi}(\vec{x}) = \sum_n \langle\varphi_n|\chi_\alpha\rangle\hat{c}_\alpha\end{aligned} \tag{K.27}$$

It is important to note that the anticommutator in the non-orthonormal basisset is the overlap of the projector functions!

$$\begin{aligned}\hat{c}_{l,\alpha}^\dagger &\overset{\text{Eq. K.26}}{=} \sum_n \hat{a}_{l,n}^+(t)\langle\varphi_n|\pi_\alpha\rangle \\ &\overset{\text{Eq. K.24}}{=} \sum_n \overbrace{\sum_k \hat{a}_{S,k}^\dagger \underbrace{U_{k,n}(0,t)}_{\langle\varphi_k|\hat{U}(0,t)|\varphi_n\rangle}}^{\hat{a}_{l,n}^+(t)} \langle\varphi_n|\pi_\alpha\rangle \\ &\overset{\text{Eq. K.27}}{=} \sum_{k,n} \overbrace{\sum_\beta \hat{c}_{S,\beta}^\dagger\langle\chi_\beta|\varphi_k\rangle}^{\hat{a}_{S,k}^\dagger}\langle\varphi_k|\hat{U}(0,t)|\varphi_n\rangle\langle\varphi_n|\pi_\alpha\rangle \\ &= \sum_\beta \hat{c}_{S,\beta}^\dagger\langle\chi_\beta|\hat{U}(0,t)|\pi_\alpha\rangle\end{aligned} \tag{K.28}$$

$$\begin{aligned}\hat{c}_{l,\alpha}(t) &\overset{\text{Eq. K.26}}{=} \sum_n \langle\pi_\alpha|\varphi_n\rangle\hat{a}_{l,n}(t) \\ &\overset{\text{Eq. K.25}}{=} \sum_n \langle\pi_\alpha|\varphi_n\rangle \overbrace{\sum_k \underbrace{U_{n,k}(t,0)}_{\langle\varphi_n|\hat{U}(t,0)|\varphi_n\rangle} \hat{a}_{S,k}}^{\hat{a}_{l,n}(t)} \\ &\overset{\text{Eq. K.27}}{=} \sum_{k,n} \langle\pi_\alpha|\varphi_n\rangle\langle\varphi_n|\hat{U}(t,0)|\varphi_k\rangle \overbrace{\sum_\beta \langle\varphi_k|\chi_\beta\rangle\hat{c}_{S,\beta}}^{\hat{a}_{S,k}} \\ &= \langle\pi_\alpha|\hat{U}(t,0)|\chi_\beta\rangle\hat{c}_{S,\beta}\end{aligned} \tag{K.29}$$

K.1.2 Sanity check: One-orbital model

The following is a minimal model for many-particle physics. Its one-particle Hilbert space has only a single one-particle orbital. Consequently the Fock space is spanned by only two Slater determinants, namely the vacuum state and the sole one-particle orbital. In this example we consider the time as complex-valued variable.

One-particle Hilbert space: Consider a one-particle Hilbert space with a single one-particle orbital $|\varphi\rangle$. Let me now also define the time-dependent one-particle orbital, which obeys the Schröedinger equation with the Hamiltonian

$$\hat{h} = |\varphi\rangle\bar{\epsilon}(t)\langle\varphi| \tag{K.30}$$

The Hamiltonian shall only depend on the real part of the time, i.e. $\hat{h}(t) = \hat{h}(t^*)$.

The Schrödinger equation is

$$\begin{aligned} i\hbar\left(\frac{dt}{ds}\right)^{-1}\partial_s\Big|\psi(t(s))\Big\rangle &= \hat{h}(t(s))\Big|\psi(t(s))\Big\rangle \\ \Leftrightarrow \qquad i\hbar\partial_t\Big|\psi(t)\Big\rangle &= \hat{h}(t)\Big|\psi(t)\Big\rangle \end{aligned} \tag{K.31}$$

The solution is

$$\begin{aligned} \Big|\psi(t(s))\Big\rangle &= \Big|\psi(t(0))\Big\rangle e^{-\frac{i}{\hbar}\int_0^s ds' \, \frac{dt}{ds}\bar{\epsilon}(t(s'))} \\ \Leftrightarrow \qquad \Big|\psi(t)\Big\rangle &= \Big|\psi(0)\Big\rangle e^{-\frac{i}{\hbar}\int_{\mathcal{C},0}^t dt' \, \bar{\epsilon}(t')} \end{aligned} \tag{K.32}$$

Let me choose a solution $|\varphi(t)\rangle$ to the Schrödinger equation with specific initial conditions $|\varphi(0)\rangle = |\varphi\rangle$ to define a time-dependent orbital

$$\Big|\varphi(t)\Big\rangle = \Big|\varphi\Big\rangle e^{-\frac{i}{\hbar}\int_{\mathcal{C},0}^t dt' \, \bar{\epsilon}(t)} \tag{K.33}$$

The time-dependent orbital is not normalized and the overlap is

$$\begin{aligned} O(t) = \langle\varphi(t)|\varphi(t)\rangle &= \left(e^{-\frac{i}{\hbar}\int_{\mathcal{C},0}^t dt' \, \bar{\epsilon}(t)}\right)^* \langle\varphi||\varphi\rangle e^{-\frac{i}{\hbar}\int_{\mathcal{C},0}^t dt' \, \bar{\epsilon}(t)} = |e^{-\frac{i}{\hbar}\int_{\mathcal{C},0}^t dt' \, \bar{\epsilon}(t)}| \\ &= \exp\left(\frac{1}{\hbar}\mathrm{Im}\left(\int_{\mathcal{C},0}^t dt' \, \bar{\epsilon}(t)\right)\right) \end{aligned} \tag{K.34}$$

The time-dependent orbital remains normalized as long as the time argumnent remains real valued. As the contour deviates from the real axis, the overlap changes.

The propagator in the one-particle Hilbert space is

$$\hat{U}(t,0) = |\varphi(t)\rangle \underbrace{O^{-1}(0)}_{=1}\langle\varphi(0)| = |\varphi\rangle e^{-\frac{i}{\hbar}\int_0^t dt' \, \bar{\epsilon}(t)}\langle\varphi| \tag{K.35}$$

The back transformation is the inverse of the forward propagator.

$$\begin{aligned} \hat{U}(0,t) &= |\varphi(0)\rangle O^{-1}(t)\langle\varphi(t)| \\ &= |\varphi(0)\rangle \frac{1}{\left(e^{-\frac{i}{\hbar}\int_0^t dt' \, \bar{\epsilon}(t')}\right)^\dagger \left(e^{-\frac{i}{\hbar}\int_0^t dt' \, \bar{\epsilon}(t')}\right)} \left(e^{-\frac{i}{\hbar}\int_0^t dt' \, \bar{\epsilon}(t')}\right)^\dagger \langle\varphi(0)| \\ &= |\varphi(0)\rangle e^{+\frac{i}{\hbar}\int_0^t dt' \, \bar{\epsilon}(t')}\langle\varphi(0)| \end{aligned} \tag{K.36}$$

Fock space: The Fock space of the one-orbital model contains only two states, the vacuum state $|\mathcal{O}\rangle$ and the one-particle orbital $|\varphi\rangle$. The occupation-number vector of a Slater determinants has only one element, namely $\sigma \in \{0,1\}$. Editor: In the following I am ignoring the time-dependence of the Hamiltonian.

The creation and annihilation operators are

$$\begin{aligned} \hat{a}^\dagger &= |\varphi\rangle\langle\mathcal{O}| \\ \hat{a} &= |\mathcal{O}\rangle\langle\varphi| \end{aligned} \tag{K.37}$$

The Hamiltonian in Fock space is

$$\hat{h} = \bar{\epsilon}\hat{a}^\dagger\hat{a} \tag{K.38}$$

and the Schrödinger equation is

$$i\hbar\partial_t|\Psi(t)\rangle = \hat{h}|\Psi(t)\rangle \tag{K.39}$$

It has the general solution

$$|\Psi(t)\rangle = \hat{\mathcal{U}}^{(0)}(t,0)|\Psi(0)\rangle = |\mathcal{O}\rangle\langle\mathcal{O}|\Psi(0)\rangle + |\varphi\rangle \mathrm{e}^{-\frac{i}{\hbar}\bar{\epsilon}t}\langle\varphi|\Psi(0)\rangle \tag{K.40}$$

Let me define the time-dependent Slater determinants by choosing the basis-states as initial values. The indices are $\vec{\sigma} \in \{0,1\} = \{\mathcal{O}, \varphi\}$.

$$\begin{aligned} |\Phi_0\rangle &= |\mathcal{O}\rangle \\ |\Phi_1\rangle &= |\varphi\rangle \underbrace{\mathrm{e}^{-\frac{i}{\hbar}\bar{\epsilon}t}}_{U(t,0)} \end{aligned} \tag{K.41}$$

where $\hat{U}(t,0) = |\varphi\rangle U(t,0)\langle\varphi|$ is the propagator in the one-particle Hilbert space.

When calculating the overlap matrix, we need to take into account that the time argument is complex-valued.

$$\bar{\boldsymbol{O}}(t) = \begin{pmatrix} \langle\Phi_0(t)|\Phi_0(t)\rangle & \langle\Phi_0(t)|\Phi_1(t)\rangle \\ \langle\Phi_1(t)|\Phi_0(t)\rangle & \langle\Phi_1(t)|\Phi_1(t)\rangle \end{pmatrix} = \begin{pmatrix} 1 & 0 \\ 0 & \mathrm{e}^{\frac{i}{\hbar}\bar{\epsilon}(t^*-t)} \end{pmatrix} \tag{K.42}$$

The $(1,1)$ overlap matrix element can be expressed by the propagator $\hat{U}^\dagger(t,0)$ in the one-particle Hilbert space as $\bar{O}_{1,1}(t) = \langle\varphi|\hat{U}^\dagger(t,0)\hat{U}(t,0)|\varphi\rangle$. Notice, that the propagator is not unitary, if the time is complex valued.

The propagator has the form

$$\hat{\mathcal{U}}^{(0)}(t,0) = \sum_{\vec{\sigma},\vec{\sigma'}} |\Phi_{\vec{\sigma}}(t)\rangle \bar{O}^{-1}_{\vec{\sigma},\vec{\sigma'}}(0)\langle\Phi_{\vec{\sigma}}(0)| = |\mathcal{O}\rangle\langle\mathcal{O}| + |\varphi\rangle \mathrm{e}^{-\frac{i}{\hbar}\bar{\epsilon}t}\langle\varphi| \tag{K.43}$$

Let me calculate the inverse transformation

$$\begin{aligned} \hat{\mathcal{U}}^{(0)}(0,t) &= \sum_{\vec{\sigma}} |\Phi_{\vec{\sigma}}(0)\rangle \bar{O}^{-1}_{\vec{\sigma},\vec{\sigma'}}(t)\langle\Phi_{\vec{\sigma'}}(t)| \\ &= |\mathcal{O}\rangle\langle\mathcal{O}| + |\varphi\rangle \underbrace{\mathrm{e}^{-\frac{i}{\hbar}\bar{\epsilon}(t^*-t)}}_{O^{-1}_{\varphi,\varphi}} \underbrace{\mathrm{e}^{+\frac{i}{\hbar}\bar{\epsilon}t^*}\langle\varphi|}_{\langle\varphi(t)|} \\ &= |\mathcal{O}\rangle\langle\mathcal{O}| + |\varphi\rangle \mathrm{e}^{+\frac{i}{\hbar}\bar{\epsilon}t}\langle\varphi| \end{aligned} \tag{K.44}$$

Notice that the inverse transformation is not simply the hermitian conjugate, if the time argument is complex-valued.

$$\mathcal{U}^\dagger(t,0) = \mathcal{U}(0,t)\bar{\boldsymbol{O}}(t) \tag{K.45}$$

Let me now turn to the creation and annihilation operators in the interaction picture

$$\begin{aligned} \hat{a}^+_I(t) &= \overbrace{\Big(|\mathcal{O}\rangle\langle\mathcal{O}| + |\varphi\rangle \mathrm{e}^{+\frac{i}{\hbar}\bar{\epsilon}t}\langle\varphi|\Big)}^{\hat{\mathcal{U}}(0,t)} \overbrace{|\varphi\rangle\langle\mathcal{O}|}^{\hat{a}^\dagger_S} \overbrace{\Big(|\mathcal{O}\rangle\langle\mathcal{O}| + |\varphi\rangle \mathrm{e}^{-\frac{i}{\hbar}\bar{\epsilon}t}\langle\varphi|\Big)}^{\hat{\mathcal{U}}(t,0)} \\ &= |\varphi\rangle \mathrm{e}^{+\frac{i}{\hbar}\bar{\epsilon}t}\langle\mathcal{O}| = \underbrace{\mathrm{e}^{+\frac{i}{\hbar}\bar{\epsilon}t}}_{U(0,t)} \hat{a}^\dagger_S \\ \hat{a}_I(t) &= \overbrace{\Big(|\mathcal{O}\rangle\langle\mathcal{O}| + |\varphi\rangle \mathrm{e}^{+\frac{i}{\hbar}\bar{\epsilon}t}\langle\varphi|\Big)}^{\hat{\mathcal{U}}(0,t)} \overbrace{|\mathcal{O}\rangle\langle\varphi|}^{\hat{a}_S} \overbrace{\Big(|\mathcal{O}\rangle\langle\mathcal{O}| + |\varphi\rangle \mathrm{e}^{-\frac{i}{\hbar}\bar{\epsilon}t}\langle\varphi|\Big)}^{\hat{\mathcal{U}}(t,0)} \\ &= |\varphi\rangle \mathrm{e}^{-\frac{i}{\hbar}\bar{\epsilon}t}\langle\mathcal{O}| = \hat{a}_S \underbrace{\mathrm{e}^{-\frac{i}{\hbar}\bar{\epsilon}t}}_{U(t,0)} \end{aligned} \tag{K.46}$$

In the interaction picture, the creation and annihilation operators are **not** complex conjugates of each other, unless the time argument is real valued.

The anticommutator of creation and annihilation operators at different times are

$$\left[\hat{a}_I^+(t), \hat{a}_I(t')\right]_+ = \left[\hat{a}_S^+, \hat{a}_S\right]_+ \underbrace{\mathrm{e}^{-\frac{i}{\hbar}\bar{\epsilon}(t'-t)}}_{=U(0,t)U(t',0)} \tag{K.47}$$

The commutator is readily obtained in this simple example. Let me, nevertheless, now work through the intermediate steps:

The new creation and annihilation operators are defined via the propagator $U(t,0) = \exp\left(-\frac{i}{\hbar}\int_0^t dt'\; h(t')\right)$ of the one-particle problem.

$$\begin{aligned}\hat{b}_S^+(t) &= \hat{a}_S^\dagger \underbrace{U(t,0)}_{\mathrm{e}^{-\frac{i}{\hbar}\bar{\epsilon}t}} \\ \hat{b}_S(t) &= \underbrace{U(0,t)}_{\mathrm{e}^{+\frac{i}{\hbar}\bar{\epsilon}t}} \hat{a}_S\end{aligned} \tag{K.48}$$

Let me verify the relation

$$\begin{aligned}\hat{b}_S^+(t) &= \overbrace{\left(|\mathcal{O}\rangle\langle\mathcal{O}| + |\varphi\rangle\mathrm{e}^{-\frac{i}{\hbar}\bar{\epsilon}t}\langle\varphi|\right)}^{\hat{\mathcal{U}}(t,0)} \overbrace{|\varphi\rangle\langle\mathcal{O}|}^{\hat{a}_S^\dagger} \overbrace{\left(|\mathcal{O}\rangle\langle\mathcal{O}| + |\varphi\rangle\mathrm{e}^{+\frac{i}{\hbar}\bar{\epsilon}t}\langle\varphi|\right)}^{\hat{\mathcal{U}}(0,t)} \\ &= |\varphi\rangle\mathrm{e}^{-\frac{i}{\hbar}\bar{\epsilon}t}\langle\mathcal{O}| = \hat{a}_S^\dagger \underbrace{\mathrm{e}^{-\frac{i}{\hbar}\bar{\epsilon}t}}_{U(t,0)} \\ \hat{b}_S(t) &= \overbrace{\left(|\mathcal{O}\rangle\langle\mathcal{O}| + |\varphi\rangle\mathrm{e}^{-\frac{i}{\hbar}\bar{\epsilon}t}\langle\varphi|\right)}^{\hat{\mathcal{U}}(t,0)} \overbrace{|\mathcal{O}\rangle\langle\varphi|}^{\hat{a}_S} \overbrace{\left(|\mathcal{O}\rangle\langle\mathcal{O}| + |\varphi\rangle\mathrm{e}^{+\frac{i}{\hbar}\bar{\epsilon}t}\langle\varphi|\right)}^{\hat{\mathcal{U}}(0,t)} \\ &= |\varphi\rangle\mathrm{e}^{+\frac{i}{\hbar}\bar{\epsilon}t}\langle\mathcal{O}| = \underbrace{\mathrm{e}^{+\frac{i}{\hbar}\bar{\epsilon}t}}_{U(0,t)} \hat{a}_S\end{aligned} \tag{K.49}$$

$$\begin{aligned}\hat{a}_I^+(t) &= \hat{\mathcal{U}}^{(0)}(0,t) \overbrace{\underbrace{\mathrm{e}^{+\frac{i}{\hbar}\bar{\epsilon}t}}_{U(0,t)} \hat{b}_S^+(t)}^{\hat{a}_S^\dagger} \hat{\mathcal{U}}^{(0)}(t,0) = \mathrm{e}^{+\frac{i}{\hbar}\bar{\epsilon}t}\hat{b}_I^+(t) = \underbrace{\mathrm{e}^{+\frac{i}{\hbar}\bar{\epsilon}t}}_{U(0.t)} \hat{a}_S^\dagger \\ \hat{a}_I(t) &= \hat{\mathcal{U}}^{(0)}(0,t) \overbrace{\hat{b}_S(t)\underbrace{\mathrm{e}^{-\frac{i}{\hbar}\bar{\epsilon}t}}_{U(t,0)}}^{\hat{a}_S} \hat{\mathcal{U}}^{(0)}(t,0) = \hat{b}_I(t)\mathrm{e}^{-\frac{i}{\hbar}\bar{\epsilon}t} = \hat{a}_S \underbrace{\mathrm{e}^{-\frac{i}{\hbar}\bar{\epsilon}t}}_{U(t,0)}\end{aligned} \tag{K.50}$$

K.2 Anticommutators of field operators in the interaction picture

For the proof of the generalized Wick theorem in section 10.2.3 on p. 303, we need the anticommutator between creation and annihilation operators in the interaction picture for a time-dependent non-interacting Hamiltonian. In the following, it is shown that the anticommutator is a number (respectively a unit operator in Fock space.) albeit with a value given by the propagator of the non-interacting Hamiltonian.

ANTICOMMUTATORS BETWEEN CREATION AND ANNIHILATION OPERATORS IN THE INTERACTION PICTURE

The anticommutators of the creation and annihilation operators in the interaction picture are given by the matrix elements of the propagator $\hat{U}(t, t')$ in the one-particle Hilbert space. In Fock space, the anticommutators are numbers, that is they are proportional to the identity operator in Fock space.

$$\left[\hat{c}_{I,\alpha}(t_2), \hat{c}^{+}_{I,\beta}(t_1)\right]_+ \overset{\text{Eq. K.55}}{=} \left\langle \pi_\alpha \middle| \hat{U}(t_2, t_1) \middle| \pi_\beta \right\rangle \hat{1} \tag{K.51}$$

$$\left[\hat{c}^{+}_{I,m}(t_1), \hat{c}^{+}_{I,n}(t_2)\right]_+ = \hat{0} \tag{K.52}$$

$$\left[\hat{c}_{I,m}(t_1), \hat{c}_{I,n}(t_2)\right]_+ = \hat{0} \tag{K.53}$$

The one-particle orbitals $|\chi_\alpha\rangle$ may be non-orthonormal with an overlap matrix $S_{\alpha,\beta} = \langle\chi_\alpha|\chi_\beta\rangle$. Each orbital has a corresponding projector function $\langle\pi_\alpha| = \sum_\beta S^{-1}_{\alpha,\beta}\langle\chi_\beta|$. The creation and annihilation operators defined for this basisset are $\hat{c}^\dagger_\alpha = \int d^4x\, \hat{\psi}^\dagger(\vec{x})\langle\vec{x}|\pi_\alpha\rangle$ and $\hat{c}_\alpha = \int d^4x\, \langle\pi_\alpha|\vec{x}\rangle\hat{\psi}(\vec{x})$. The propagator $\hat{U}(t, 0)$ satisfies the time-dependent Schrödinger equation along the contour $\Big[i\hbar\partial_t - \hat{h}(t)\Big]\hat{U}(t, 0) = 0$ with the (non-interacting) one-particle Hamiltonian $\hat{h}(t)$. It furthermore satisfies the initial condition $\hat{U}(t, t) = \hat{1}$. The propagator can be written as time-ordered exponential.

$$\begin{aligned}\hat{U}(t, 0) &= \mathcal{T}_C \mathrm{e}^{-\frac{i}{\hbar}\int_0^t dt\, \hat{h}(t)} \\ \hat{U}(0, t) &= \hat{U}^{-1}(t, 0)\end{aligned} \tag{K.54}$$

Note that the propagator is unitary only on the branch of the contour with real-valued time. [a]

[a] Caution is needed to not confuse $\hat{U}(t_2, t_1$ with the propagator $\hat{\mathcal{U}}^{(0)}(t_2, t_1)$ in Fock space. They differ by the space they act on: $\hat{U}(t_2, t_1)$ acts in the one-particle Hilbert space, while $\hat{\mathcal{U}}^{(0)}(t_2, t_1)$ acts in the Fock space.

The anticommutator relations in the interaction picture are used for Wick's theorem in section 10.2.3 on p. 303.

The proof of Eq. K.51 rests on the finding, that the creation and annihilation operators in the interaction pictures can be expressed in terms of their Schrödinger counterparts as shown in Eq. K.24 and Eq. K.2. The operator $\hat{U}(t, 0)$ is the propagator in the one-particle Hilbert space, which differs from the propagator $\hat{\mathcal{U}}^{(0)}(t, 0)$ in Fock space.

$$\begin{aligned}\left[\hat{c}_{I,\alpha}(t), \hat{c}^{+}_{I,\beta}(t')\right]_+ &\overset{\text{Eqs. K.1, K.2}}{=} \Big[\sum_\gamma \langle\pi_\alpha|\hat{U}(t, 0)|\chi_\gamma\rangle\hat{c}_{S,\gamma}, \sum_\delta \hat{c}^\dagger_{S,\delta}\langle\chi_\delta|\hat{U}(0, t')|\pi_\beta\rangle\Big]_+ \\ &= \sum_\gamma\sum_\delta \langle\pi_\alpha|\hat{U}(t, 0)|\chi_\gamma\rangle \underbrace{\left[\hat{c}_{S,\gamma}, \hat{c}^\dagger_{S,\delta}\right]_+}_{\substack{\langle\pi_\gamma|\pi_\delta\rangle \\ \text{Eq. B.8}}} \langle\chi_\delta|\hat{U}(0, t')|\pi_\beta\rangle \\ &= \langle\pi_\alpha|\hat{U}(t, 0)\underbrace{\sum_\gamma |\chi_\gamma\rangle\langle\pi_\gamma|}_{\hat{1}}\underbrace{\sum_\delta |\pi_\delta\rangle\langle\chi_\delta|}_{\hat{1}}\hat{U}(0, t')|\pi_\beta\rangle \\ &= \langle\pi_\alpha|\hat{U}(t, t')|\pi_\beta\rangle\end{aligned} \tag{K.55}$$

K.3 Commutating a field operator with the density matrix

For the proof of the generalized Wick theorem we need to interchange the order of a creation operator in the interaction picture with the von-Neumann density matrix of a non-interacting system.

$$\hat{c}^{+}_{l,\alpha}(t)\hat{\rho}^{(0)}_{T,\mu} \overset{\text{Eq. } K.69}{=} \sum_{\gamma} \hat{\rho}^{(0)}_{T,\mu}\hat{c}^{+}_{l,\gamma}(t)\left\langle \chi_\gamma \middle| \hat{U}(t,0)\mathrm{e}^{\beta(\hat{h}-\mu\hat{1})}\hat{U}(0,t)\middle|\pi_\alpha\right\rangle \tag{K.56}$$

$$\hat{c}_{l,\alpha}(t)\hat{\rho}^{(0)}_{T,\mu} \overset{\text{Eq. } K.70}{=} \sum_{\gamma} \left\langle \pi_\alpha \middle| \hat{U}(t,0)\mathrm{e}^{-\beta(\hat{h}-\mu\hat{1})}\hat{U}(0,t)\middle|\chi_\gamma\right\rangle \hat{\rho}^{(0)}_{T,\mu}\hat{c}_{l,\gamma}(t) \tag{K.57}$$

where $\hat{U}(t,0)$ is the propagator in one-particle Hilbert space. $\hat{\rho}^{(0)}_{T,\mu}$ is the thermal von-Neumann density matrix of the non-interacting system in the grand canonical ensemble.

Editor: Can this can be shown also for a non-thermal ensemble?

Editor: Is the proof also possible directly in a non-orthonormal basisset?

Assumption: The non-interacting Hamiltonian depends only on the real part of the time. The non-interacting ensemble is determined for the Hamiltonian $\hat{h}(0)$ at time $t = 0$. In the following, I will drop the time argument of the Hamiltonian, when it is zero.

Let the basisset be the eigenstates of the non-interacting Hamiltonian $\hat{h}$. Let me denote the Slater determinants in this basisset in the occupation-number representation as $|\vec{\sigma}\rangle$.

$$\mathrm{e}^{-\beta(\hat{h}-\mu\hat{N})}|\vec{\sigma}\rangle = |\vec{\sigma}\rangle\mathrm{e}^{-\beta\sum_n \sigma_n(\epsilon_n-\mu)} \tag{K.58}$$

$$\Rightarrow \quad \begin{cases} \hat{a}^{\dagger}_{S,k}\mathrm{e}^{-\beta(\hat{h}-\mu\hat{N})}|\vec{\sigma}\rangle = \hat{a}^{\dagger}_{S,k}|\vec{\sigma}\rangle\mathrm{e}^{-\beta\sum_n \sigma_n(\epsilon_n-\mu)} \\ \mathrm{e}^{-\beta(\hat{h}-\mu\hat{N})}\hat{a}^{\dagger}_{S,k}|\vec{\sigma}\rangle = \hat{a}^{\dagger}_{S,k}|\vec{\sigma}\rangle\mathrm{e}^{-\beta\sum_n \sigma_n(\epsilon_n-\mu)}\mathrm{e}^{-\beta(\epsilon_k-\mu)} \end{cases} \tag{K.59}$$

$$\Rightarrow \quad \begin{cases} \hat{a}_{S,k}\mathrm{e}^{-\beta(\hat{h}-\mu\hat{N})}|\vec{\sigma}\rangle = \hat{a}_{S,k}|\vec{\sigma}\rangle\mathrm{e}^{-\beta\sum_n \sigma_n(\epsilon_n-\mu)} \\ \mathrm{e}^{-\beta(\hat{h}-\mu\hat{N})}\hat{a}_{S,k}|\vec{\sigma}\rangle = \hat{a}_{S,k}|\vec{\sigma}\rangle\mathrm{e}^{-\beta\sum_n \sigma_n(\epsilon_n-\mu)}\mathrm{e}^{+\beta(\epsilon_k-\mu)} \end{cases} \tag{K.60}$$

Combining the equations of each pair yields

$$\hat{a}^{\dagger}_{S,k}\mathrm{e}^{-\beta(\hat{h}-\mu\hat{N})} = \mathrm{e}^{-\beta(\hat{h}-\mu\hat{N})}\hat{a}^{\dagger}_{S,k}\mathrm{e}^{+\beta(\epsilon_k-\mu)} \tag{K.61}$$

$$\hat{a}_{S,k}\mathrm{e}^{-\beta(\hat{h}-\mu\hat{N})} = \mathrm{e}^{-\beta(\hat{h}-\mu\hat{N})}\hat{a}_{S,k}\mathrm{e}^{-\beta(\epsilon_k-\mu)} \tag{K.62}$$

Next I use Eqs. K.1 and K.2.

$$\hat{a}^{+}_{I,n}(t) \overset{\text{Eq. } K.1}{=} \sum_k \hat{a}^{\dagger}_{S,k}U_{k,n}(0,t) \tag{K.63}$$

$$\hat{a}_{I,n}(t) \overset{\text{Eq. } K.2}{=} \sum_k U_{n,k}(t,0)\hat{a}_{S,k} \tag{K.64}$$

to obtain

$$
\begin{aligned}
\hat{a}^{+}_{I,n}(t)\mathrm{e}^{-\beta(\hat{h}-\mu\hat{N})} &\overset{\text{Eq. } K.1}{=} \sum_k \hat{a}^{\dagger}_{S,k}\mathrm{e}^{-\beta(\hat{h}-\mu\hat{N})}U_{k,n}(0,t) \\
&\overset{\text{Eq. } K.61}{=} \sum_k \mathrm{e}^{-\beta(\hat{h}-\mu\hat{N})}\hat{a}^{\dagger}_{S,k}\mathrm{e}^{\beta(\epsilon_k-\mu)}U_{k,n}(0,t) \\
&= \sum_k \mathrm{e}^{-\beta(\hat{h}-\mu\hat{N})}\overbrace{\sum_p \hat{a}^{\dagger}_{S,p}\underbrace{\sum_q U_{p,q}(0,t)U_{q,k}(t,0)}_{\delta_{p,k}}}^{\hat{a}^{\dagger}_{S,k}}\mathrm{e}^{\beta(\epsilon_k-\mu)}U_{k,n}(0,t) \\
&= \mathrm{e}^{-\beta(\hat{h}-\mu\hat{N})}\sum_q \underbrace{\sum_p \hat{a}^{\dagger}_{S,p}U_{p,q}(0,t)}_{\hat{a}^{+}_{I,q}}\sum_k U_{q,k}(t,0)\mathrm{e}^{\beta(\epsilon_k-\mu)}U_{k,n}(0,t) \\
&\overset{\text{Eq. } K.1}{=} \mathrm{e}^{-\beta(\hat{h}-\mu\hat{N})}\sum_q \hat{a}^{+}_{I,q}\Big(\sum_k U_{q,k}(t,0)\mathrm{e}^{\beta(\epsilon_k-\mu)}U_{k,n}(0,t)\Big) \\
&\overset{\text{Eq. } K.1}{=} \mathrm{e}^{-\beta(\hat{h}-\mu\hat{N})}\sum_q \hat{a}^{+}_{I,q}\Big\langle\varphi_q\Big|\hat{U}(t,0)\mathrm{e}^{\beta(\hat{h}-\mu\hat{1})}\hat{U}(0,t)\Big|\varphi_n\Big\rangle \qquad \text{(K.65)} \\
\hat{a}_{I,n}(t)\mathrm{e}^{-\beta(\hat{h}-\mu\hat{N})} &\overset{\text{Eq. } K.2}{=} \sum_k U_{n,k}(t,0)\hat{a}_{S,k}\mathrm{e}^{-\beta(\hat{h}-\mu\hat{N})} \\
&\overset{\text{Eq. } K.62}{=} \sum_k U_{n,k}(t,0)\mathrm{e}^{-\beta(\hat{h}-\mu\hat{N})}\mathrm{e}^{-\beta(\epsilon_k-\mu)}\hat{a}_{S,k} \\
&= \mathrm{e}^{-\beta(\hat{h}-\mu\hat{N})}\sum_k U_{n,k}(t,0)\mathrm{e}^{-\beta(\epsilon_k-\mu)}\overbrace{\sum_p \underbrace{\sum_q U_{k,q}(0,t)U_{q,p}(t,0)}_{\delta_{k,p}}\hat{a}_{S,p}}^{\hat{a}_{S,k}} \\
&= \mathrm{e}^{-\beta(\hat{h}-\mu\hat{N})}\sum_k U_{n,k}(t,0)\mathrm{e}^{-\beta(\epsilon_k-\mu)}\sum_q U_{k,q}(0,t)\underbrace{\sum_p U_{q,p}(t,0)\hat{a}_{S,p}}_{\hat{a}_{I,q}(t)} \\
&\overset{\text{Eq. } K.2}{=} \mathrm{e}^{-\beta(\hat{h}-\mu\hat{N})}\sum_q \Big(\sum_k U_{n,k}(t,0)\mathrm{e}^{-\beta(\epsilon_k-\mu)}U_{k,q}(0,t)\Big)\hat{a}_{I,q}(t) \\
&= \mathrm{e}^{-\beta(\hat{h}-\mu\hat{N})}\sum_q \Big\langle\varphi_n\Big|\hat{U}(t,0)\mathrm{e}^{-\beta(\hat{h}-\mu\hat{1})}\hat{U}(0,t)\Big|\varphi_q\Big\rangle\hat{a}_{I,q}(t) \qquad \text{(K.66)}
\end{aligned}
$$

Normalizing the Boltzmann factors with the partition sum yields the density operator of the non-inteacting system

$$\hat{a}^{+}_{I,n}(t)\hat{\rho}^{(0)}_{T,\mu} = \sum_q \hat{\rho}^{(0)}_{T,\mu}\hat{a}^{+}_{I,q}\Big\langle\varphi_q\Big|\hat{U}(t,0)\mathrm{e}^{\beta(\hat{h}-\mu\hat{1})}\hat{U}(0,t)\Big|\varphi_n\Big\rangle \qquad \text{(K.67)}$$

$$\hat{a}_{I,n}(t)\hat{\rho}^{(0)}_{T,\mu} = \sum_q \Big\langle\varphi_n\Big|\hat{U}(t,0)\mathrm{e}^{-\beta(\hat{h}-\mu\hat{1})}\hat{U}(0,t)\Big|\varphi_q\Big\rangle\hat{\rho}^{(0)}_{T,\mu}\hat{a}_{I,q}(t) \qquad \text{(K.68)}$$

Transformation into a non-orthonormal basisset

Let me now transform from the orthonormal basisset $\{|\varphi_n\rangle\}$ with creation and annihilation operators $\hat{a}^{+}_{I,n}$ and $\hat{a}_{I,n}$ to a general non-orthonormal basisset $\{|\chi_\alpha\rangle\}$ with creation and annihilation operators

$\hat{c}^+_{l,\alpha}$ and $\hat{c}_{l,\alpha}$.

$$\begin{aligned}
\hat{c}^+_{l,\alpha}(t)\hat{\rho}^{(0)}_{T,\mu} &= \overbrace{\sum_n \hat{a}^+_{l,n}(t)\langle\varphi_n|\pi_\alpha\rangle}^{\hat{c}^+_{l,\alpha}(t)}\hat{\rho}^{(0)}_{T,\mu} \\
&\overset{\text{Eq. K.67}}{=} \sum_{n,q}\hat{\rho}^{(0)}_{T,\mu}\hat{a}^+_{l,q}\Big\langle\varphi_q\Big|\hat{U}(t,0)e^{\beta(\hat{h}-\mu\hat{1})}\hat{U}(0,t)\Big|\varphi_n\Big\rangle\langle\varphi_n|\pi_\alpha\rangle \\
&= \hat{\rho}^{(0)}_{T,\mu}\sum_{q,q'}\hat{a}^+_{l,q}\underbrace{\sum_\gamma\langle\varphi_q|\pi_\gamma\rangle\langle\chi_\gamma|\varphi_{q'}\rangle}_{\delta_{q,q'}}\Big\langle\varphi_{q'}\Big|\hat{U}(t,0)e^{\beta(\hat{h}-\mu\hat{1})}\hat{U}(0,t)|\pi_\alpha\rangle \\
&= \hat{\rho}^{(0)}_{T,\mu}\sum_\gamma\underbrace{\sum_q\hat{a}^+_{l,q}\langle\varphi_q|\pi_\gamma\rangle}_{\hat{c}^+_\gamma(t)}\langle\chi_\gamma|\underbrace{\sum_{q'}|\varphi_{q'}\rangle\Big\langle\varphi_{q'}\Big|}_{\hat{1}}\hat{U}(t,0)e^{\beta(\hat{h}-\mu\hat{1})}\hat{U}(0,t)|\pi_\alpha\rangle \\
&= \sum_\gamma\hat{\rho}^{(0)}_{T,\mu}\hat{c}^+_\gamma(t)\Big\langle\chi_\gamma\Big|\hat{U}(t,0)e^{\beta(\hat{h}-\mu\hat{1})}\hat{U}(0,t)\Big|\pi_\alpha\Big\rangle \qquad \text{(K.69)}
\end{aligned}$$

$$\begin{aligned}
\hat{c}_{l,\alpha}(t)\hat{\rho}^{(0)}_{T,\mu} &= \overbrace{\sum_n\langle\pi_\alpha\big|\varphi_n\rangle\hat{a}_{l,n}(t)}^{\hat{c}_{l,\alpha}(t)}\hat{\rho}^{(0)}_{T,\mu} \\
&\overset{\text{Eq. K.68}}{=} \sum_n\Big\langle\pi_\alpha\Big|\varphi_n\Big\rangle\sum_q\Big\langle\varphi_n\Big|\hat{U}(t,0)e^{-\beta(\hat{h}-\mu\hat{1})}\hat{U}(0,t)\Big|\varphi_q\Big\rangle\hat{\rho}^{(0)}_{T,\mu}\hat{a}_{l,q}(t) \\
&= \sum_q\Big\langle\pi_\alpha\Big|\underbrace{\sum_n|\varphi_n\rangle\langle\varphi_n|}_{\hat{1}}\hat{U}(t,0)e^{-\beta(\hat{h}-\mu\hat{1})}\hat{U}(0,t)\underbrace{\sum_\gamma|\chi_\gamma\rangle\langle\pi_\gamma|}_{\hat{1}}\Big|\varphi_q\Big\rangle\hat{\rho}^{(0)}_{T,\mu}\hat{a}_{l,q}(t) \\
&= \sum_\gamma\Big\langle\pi_\alpha\Big|\hat{U}(t,0)e^{-\beta(\hat{h}-\mu\hat{1})}\hat{U}(0,t)\Big|\chi_\gamma\Big\rangle\hat{\rho}^{(0)}_{T,\mu}\underbrace{\sum_q\langle\pi_\gamma|\varphi_q\rangle\hat{a}_{l,q}(t)}_{\hat{c}_\gamma} \\
&= \sum_\gamma\Big\langle\pi_\alpha\Big|\hat{U}(t,0)e^{-\beta(\hat{h}-\mu\hat{1})}\hat{U}(0,t)\Big|\chi_\gamma\Big\rangle\hat{\rho}^{(0)}_{T,\mu}\hat{c}_{l,\gamma}(t) \qquad \text{(K.70)}
\end{aligned}$$

K.4 Contract the trace

K.4.1 Single step of Wick's theorem

Consider the expectation value $Y = \mathrm{Tr}\Big\{\hat{A}_1\hat{A}_2\ldots\hat{A}_{2M}\hat{\rho}^{(0)}_{T,\mu}\Big\}$ of the time-ordered product of **fermionic** creation and annihilation operators $\hat{A}_j \in \{\hat{c}^+_{l,\alpha}(t), \hat{c}_{l,\alpha}(t)\}$ in the interaction picture as defined in Eq. 10.33.

Before beginning, let me collect the underlying assumptions and the definition of the symbols, so that we can look them up easily.

- The operators $\hat{A}_j$ are fermionic creation and annihilation operators in the interaction picture, i.e $\hat{A}_j \in \{\hat{c}^+_{l,\alpha}(t), \hat{c}_{l,\alpha}(t)\}$.
- The creation and annihilation operators are defined by a one-particle basisset $\{|\chi_\alpha\rangle\}$, i.e. $\hat{c}^\dagger_{S,\alpha}|\mathcal{O}\rangle = |\pi_\alpha\rangle$. which may be non-orthonormal. Each orbital $|\chi_\alpha\rangle$ has a projector function $\langle\pi_\alpha| = \sum_\beta S^{-1}_{\alpha,\beta}\langle\chi_\beta|$, where $S_{\alpha,\beta} = \langle\chi_\alpha|\chi_\beta\rangle$ is the overlap matrix.
- The number of creation and annihilation operators is equal. There are M annihilation operators and M creation operators in the product.

- The time of the operators is increasing from right to left, i.e. $t_1 \geq t_2 \geq \ldots \geq t_{2M}$.

- $\hat{U}(t_2, t_1)$ is the propagator in the one-particle Hilbert space by the time-dependent, non-interacting Hamiltonian $\hat{h}(t)$. That is $\big(\hat{1} i\hbar\partial_t - \hat{h}(t)\big)\hat{U}(t, t') = \hat{0}$ and $\hat{U}(t, t) = \hat{1}$.

- $\hat{\rho}^{(0)}_{T,\mu}$ is the von-Neumann density matrix for the non-interacting Hamiltonian $\hat{h}(t)$ at time $t = 0$, i.e. $\hat{\rho}^{(0)}_{T,\mu} = \frac{1}{Z^{(0)}_{T,\mu}} \mathrm{e}^{-\beta(\hat{h}(0) - \mu\hat{N})}$.

Remember, that the operators $\hat{A}_j$ and $\hat{\rho}^{(0)}_{T,\mu}$ act in the Fock space and $\hat{U}(t, t')$ and the one-particle-reduced density matrix $\hat{\rho}^{(1)(0)}_{T,\mu}$ act on the one-particle Hilbert space. The non-interacting Hamiltonian $\hat{h}(t)$ can be either, an operator in one-particle Hilbert space or a one-particle-at-a-time operator in Fock space.

Now, we are ready to begin with the derivation

$$\begin{aligned}
Y &\overset{\text{Eq. } 10.33}{=} \mathrm{Tr}\Big\{\hat{A}_1\hat{A}_2\ldots\hat{A}_{2M}\hat{\rho}^{(0)}_{T,\mu}\Big\} \\
&= \mathrm{Tr}\Big\{[\hat{A}_1, \hat{A}_2]_+\ldots\hat{A}_{2M}\hat{\rho}^{(0)}_{T,\mu}\Big\} - \mathrm{Tr}\Big\{\hat{A}_2\hat{A}_1\ldots\hat{A}_{2M}\hat{\rho}^{(0)}_{T,\mu}\Big\} \\
&= \mathrm{Tr}\Big\{[\hat{A}_1, \hat{A}_2]_+\ldots\hat{A}_{2M}\hat{\rho}^{(0)}_{T,\mu}\Big\} - \mathrm{Tr}\Big\{\hat{A}_2[\hat{A}_1, \hat{A}_3]_+\ldots\hat{A}_{2M}\hat{\rho}^{(0)}_{T,\mu}\Big\} \\
&\quad + \mathrm{Tr}\Big\{\hat{A}_2\hat{A}_3\hat{A}_1\hat{A}_4\ldots\hat{A}_{2M}\hat{\rho}^{(0)}_{T,\mu}\Big\} \\
&= \underbrace{\sum_{j=2}^{2M}(-1)^j \mathrm{Tr}\Big\{(\hat{A}_2\cdots\hat{A}_{j-1})[\hat{A}_1, \hat{A}_j]_+(\hat{A}_{j+1}\cdots\hat{A}_{2M})\hat{\rho}^{(0)}_{T,\mu}\Big\}}_{X} \\
&\quad - \underbrace{(-1)^{2M}}_{=+1} \mathrm{Tr}\Big\{\hat{A}_2\cdots\hat{A}_{2M}\Big(\hat{A}_1\hat{\rho}^{(0)}_{T,\mu}\Big)\Big\}
\end{aligned} \tag{K.71}$$

As shown in Eq. K.56 and Eq. K.57, the operator $A_1\hat{\rho}^{(0)}_{T,\mu}$ can be expressed as a superposition of terms $\hat{\rho}^{(0)}_{T,\mu}A_1$ with the order interchanged.

$$\hat{c}^+_{l,\alpha}(t)\hat{\rho}^{(0)}_{T,\mu} \overset{\text{Eq. } K.56}{=} \sum_\gamma \hat{\rho}^{(0)}_{T,\mu}\hat{c}^+_{l,\gamma}(t)\Big\langle\chi_\gamma\Big|\hat{U}(t,0)\mathrm{e}^{\beta(\hat{h}-\mu\hat{1})}\hat{U}(0,t)\Big|\pi_\alpha\Big\rangle \tag{K.72}$$

$$\hat{c}_{l,\alpha}(t)\hat{\rho}^{(0)}_{T,\mu} \overset{\text{Eq. } K.57}{=} \sum_\gamma \Big\langle\pi_\alpha\Big|\hat{U}(t,0)\mathrm{e}^{-\beta(\hat{h}-\mu\hat{1})}\hat{U}(0,t)\Big|\chi_\gamma\Big\rangle\hat{\rho}^{(0)}_{T,\mu}\hat{c}_{l,\gamma}(t) \tag{K.73}$$

Cyclic permutation in the trace will bring $\hat{A}_1$ to the front so that the trace has the same structure as Y. Thus, we arrive at a system of equations, which can be resolved for Y.

Notation: We need to distingish several cases, which I distinguish by attaching a superscript $\pm \in \{+, -\}$ and an orbital index α to the result $Y^\pm_\alpha$. The superscript is $\pm = +$ if $\hat{A}_1 = \hat{c}^+_{l,\alpha}(t)$ is a creation operator and it is $\pm = -$ if $\hat{A}_1 = \hat{c}_{l,\alpha}(t)$ is an annihilation operator. In a similar spirit, I will introduce a short-hand notation $X^\pm_\alpha$.

- for $\hat{A}_1 = \hat{c}^+_{l,\alpha}(t)$, I obtain Y^+_α

$$
\begin{aligned}
Y^+_\alpha &\overset{\text{def}}{=} \mathrm{Tr}\Big\{\overbrace{\hat{c}^+_{l,\alpha}(t)}^{\hat{A}_1}\hat{A}_2\ldots\hat{A}_{2M}\hat{\rho}^{(0)}_{T,\mu}\Big\} \\
&\overset{\text{Eq. } K.71}{=} \underbrace{\sum_{j=2}^{2M}(-1)^j\mathrm{Tr}\Big\{(\hat{A}_2\cdots\hat{A}_{j-1})[\hat{A}_1,\hat{A}_j]_+(\hat{A}_{j+1}\cdots\hat{A}_{2M})\hat{\rho}^{(0)}_{T,\mu}\Big\}}_{=:X^+_\alpha} \\
&\quad -\mathrm{Tr}\Big\{\hat{A}_2\cdots\hat{A}_{2M}\overbrace{\sum_\gamma\hat{\rho}^{(0)}_{T,\mu}\hat{c}^+_{l,\gamma}(t)\Big\langle\chi_\gamma\Big|\hat{U}(t,0)e^{\beta(\hat{h}-\mu\hat{1})}\hat{U}(0,t)\Big|\pi_\alpha\Big\rangle}^{\hat{A}_1\hat{\rho}^{(0)}_{T,\mu}\quad\text{Eq. K.56}}\Big\} \\
&= X^+_\alpha - \sum_\gamma\underbrace{\overbrace{\mathrm{Tr}\Big\{\hat{c}^+_{l,\gamma}(t)\hat{A}_2\cdots\hat{A}_{2M}\hat{\rho}^{(0)}_{T,\mu}\Big\}}^{\mathrm{Tr}\left\{\hat{A}_2\cdots\hat{A}_{2M}\hat{\rho}^{(0)}_{T,\mu}\hat{c}^+_{l,\gamma}(t)\right\}}}_{Y^+_\gamma}\Big\langle\chi_\gamma\Big|\hat{U}(t,0)e^{\beta(\hat{h}-\mu\hat{1})}\hat{U}(0,t)\Big|\pi_\alpha\Big\rangle \quad \text{(K.74)}
\end{aligned}
$$

This is a system of equations for the $\{Y^+_\gamma\}$. I bring all terms containing one of the $\{Y^+_\gamma\}$ to the left-hand side of the equation, and multiply both sides with the inverse of the prefactor.

$$
\begin{aligned}
&\Rightarrow \quad \sum_\gamma Y^+_\gamma\overbrace{\Big\langle\chi_\gamma\Big|\hat{U}(t,0)\Big(\hat{1}+e^{\beta(\hat{h}-\mu\hat{1})}\Big)\hat{U}(0,t)\Big|\pi_\alpha\Big\rangle}^{\delta_{\gamma,\alpha}+\left\langle\chi_\gamma\left|\hat{U}(t,0)e^{\beta(\hat{h}-\mu\hat{1})}\hat{U}(0,t)\right|\pi_\alpha\right\rangle} = X^+_\alpha \\
&\Rightarrow \quad Y^+_\gamma = \sum_\alpha X^+_\alpha\Big\langle\chi_\alpha\Big|\hat{U}(t,0)\Big(\hat{1}+e^{\beta(\hat{h}-\mu\hat{1})}\Big)^{-1}\hat{U}(0,t)\Big|\pi_\gamma\Big\rangle \\
&\overset{\alpha\to\gamma\to\alpha_1}{\Rightarrow} \quad Y^+_{\alpha_1} = \sum_\gamma X^+_\gamma\Big\langle\chi_\gamma\Big|\hat{U}(t_1,0)\Big(\hat{1}+e^{\beta(\hat{h}-\mu\hat{1})}\Big)^{-1}\hat{U}(0,t_1)\Big|\pi_{\alpha_1}\Big\rangle \qquad \text{(K.75)}
\end{aligned}
$$

Notation: In the last step, I renamed the indices (α_1 rather than α) so that I can distinguish the orbital indices α_j of several operators $\hat{A}_j$. Furthermore, I am denoting the time argument of $\hat{A}_j$ with t_j.

Let me now turn to X^+_γ. Let $\hat{A}_j = \hat{c}_{l,\alpha_j}(t_j)$ and $\hat{A}_1 = \hat{c}^+_{l,\alpha_1}(t_1)$. I will use Eqs. K.51, K.52 and K.53 from p. 570. The anticommutator of two creation operators vanishes also in the interaction picture, which is taken into account by limiting the sum to annihilators.

$$
\begin{aligned}
X^+_\gamma &\overset{\text{def}}{=} \sum_{\substack{j=2\\ \hat{A}_j=\text{annihilator}}}^{2M}(-1)^j\mathrm{Tr}\Big\{(\hat{A}_2\cdots\hat{A}_{j-1})\overbrace{[\hat{c}^+_{l,\gamma}(t_1),\hat{c}_{l,\alpha_j}(t_j)]_+}^{[\hat{A}_1,\hat{A}_j]_+}(\hat{A}_{j+1}\cdots\hat{A}_{2M})\hat{\rho}^{(0)}_{T,\mu}\Big\} \\
&\overset{\text{Eq. } K.51}{=} \sum_{\substack{j=2\\ \hat{A}_j=\text{annihilator}}}^{2M}(-1)^j\mathrm{Tr}\Big\{(\hat{A}_2\cdots\hat{A}_{j-1})\langle\pi_{\alpha_j}|\hat{U}(t_j,t_1)|\pi_\gamma\rangle(\hat{A}_{j+1}\cdots\hat{A}_{2M})\hat{\rho}^{(0)}_{T,\mu}\Big\}
\end{aligned}
\qquad \text{(K.76)}
$$

which yields

$$
\begin{aligned}
Y^{+}_{\alpha_1} &\overset{\text{Eq. } K.75}{=} \sum_{\gamma} \overbrace{\sum_{\substack{j=2 \\ \hat{A}_j=\text{annihilator}}}^{2M} (-1)^j \mathrm{Tr}\Big\{(\hat{A}_2\cdots\hat{A}_{j-1})(\hat{A}_{j+1}\cdots\hat{A}_{2M})\hat{\rho}^{(0)}_{T,\mu}\Big\}\Big\langle \pi_{\alpha_j}\Big|\hat{U}(t_j,t_1)\Big|\pi_\gamma\Big\rangle}^{X^{+}_{\gamma}} \\
&\qquad\qquad \times\Big\langle \chi_\gamma\Big|\hat{U}(t_1,0)\Big(\hat{1}+\mathrm{e}^{\beta(\hat{h}-\mu\hat{1})}\Big)^{-1}\hat{U}(0,t_1)\Big|\pi_{\alpha_1}\Big\rangle \\
&= \sum_{\substack{j=2 \\ \hat{A}_j=\text{annihilator}}}^{2M} (-1)^j \mathrm{Tr}\Big\{(\hat{A}_2\cdots\hat{A}_{j-1})(\hat{A}_{j+1}\cdots\hat{A}_{2M})\hat{\rho}^{(0)}_{T,\mu}\Big\} \\
&\qquad\qquad \times\Big\langle \pi_{\alpha_j}\Big|\hat{U}(t_j,0)\Big(\hat{1}+\mathrm{e}^{\beta(\hat{h}-\mu\hat{1})}\Big)^{-1}\hat{U}(0,t_1)\Big|\pi_{\alpha_1}\Big\rangle \qquad \text{(K.77)}
\end{aligned}
$$

We find that Y^{+}_{α} is expressed by a sum of terms, having a similar structure as $Y^{\pm}_{\alpha}$, albeit with less operators in the product. This indicates that the same rule can be applied iteratively to shrink the products in the trace and ultimately make them vanish. What we gain is that a complicated trace in Fock space is replaced by an expression of matrix elements in the one-particle Hilbert space, albeit a lengthy one.

The operator $\big(\hat{1}+\mathrm{e}^{\beta(\hat{h}-\mu\hat{1})}\big)^{-1}$ can be identified with one-particle-reduced density matrix $\hat{\rho}^{(1),(0)}_{T,\mu}$ in thermal equilibrium with the initial non-interacting Hamiltonian $\hat{h}(0)$

$$
\hat{\rho}^{(1)(0)}_{T,\mu} = f_{T,\mu}(\hat{h}(0)) = \Big(\hat{1}+\mathrm{e}^{\beta(\hat{h}-\mu\hat{1})}\Big)^{-1} \qquad \text{(K.78)}
$$

Here, $f_{T,\mu}(\epsilon) \overset{\text{def}}{=} (1+\mathrm{e}^{-\beta(\epsilon-\mu)})^{-1}$ is the Fermi distribution.

The prefactor in Eq. K.77 can be identified with the Green's function of the non-interacting Hamiltonian, which is given in Eq. 7.27 (p.247) as

$$
\hat{G}^{\mathcal{C},(0)}(t,t') \overset{\text{Eq. } 7.27}{=} \frac{1}{i\hbar}\hat{U}(t,0)\Big\{\underbrace{\theta_{\mathcal{C}}(t-t')\big(\hat{1}-\hat{\rho}^{(1)(0)}_{T,\mu}\big)}_{\text{electrons}} - \underbrace{\theta_{\mathcal{C}}(t'-t)\hat{\rho}^{(1)(0)}_{T,\mu}}_{\text{holes}}\Big\}\hat{U}(0,t') \qquad \text{(K.79)}
$$

The prefactor in Eq. K.77 can thus be rewritten as

$$
\begin{aligned}
\Big\langle \pi_{\alpha_j}\Big|\hat{U}(t_j,0)\Big(\hat{1}+\mathrm{e}^{\beta(\hat{h}-\mu\hat{1})}\Big)^{-1}\hat{U}(0,t_1)\Big|\pi_{\alpha_1}\Big\rangle &\overset{t_1\geq t_j}{=} \overbrace{\theta_{\mathcal{C}}(t_1-t_j)}^{=1 \text{ for } t_1\geq t_j}\Big\langle \pi_{\alpha_j}\Big|\hat{U}(t_j,0)\overbrace{\hat{\rho}^{(1)(0)}_{T,\mu}}^{\left(\hat{1}+\mathrm{e}^{\beta(\hat{h}-\mu\hat{1})}\right)^{-1}}\hat{U}(0,t_1)\Big|\pi_{\alpha_1}\Big\rangle \\
&\overset{\text{Eq. } 7.27}{=} -i\hbar\Big\langle \pi_{\alpha_j}\Big|\hat{G}^{\mathcal{C}(0)}(t_j,t_1)\Big|\pi_{\alpha_1}\Big\rangle \\
&= -i\hbar\, G^{\mathcal{C}(0)}_{\alpha_j,\alpha_1}(t_j,t_1) \qquad \text{(K.80)}
\end{aligned}
$$

The sign factor $(-1)^{j+1}$ in Eq. K.77 can be related to the number of permutations of the indices in the original time-ordered product to bring them into the order $(j,1,2,\ldots,j-1,j+1,\ldots,2M)$ of the final result. There are $j-1$ permutations to bring the index j to the front which gives the desired sign factor $(-1)^{j-1} = (-1)^{j+1}$. This allows one to rewrite the sign factor in the form

$$
(-1)^{j+1} = \epsilon_{j,1,2,\ldots j-1,j+1,\ldots,2M} \qquad \text{(K.81)}
$$

where $\epsilon_{j_1,\ldots,2M}$ is the fully antisymmetric tensor.

Thus, the final result for $Y^+_{\alpha_1}$ is

$$Y^+_{\alpha_1} = i\hbar \sum_{\substack{j=2 \\ \hat{A}_j=\text{annihilator}}}^{2M} \epsilon_{j,1,2,\ldots,j-1,j+1,\ldots,2M}\, \hat{G}^{\mathcal{C}(0)}_{\alpha_j,\alpha_1}(t_j,t_1)\mathrm{Tr}\Big\{(\hat{A}_2\cdots\hat{A}_{j-1})(\hat{A}_{j+1}\cdots\hat{A}_{2M})\hat{\rho}^{(0)}_{T,\mu}\Big\} \tag{K.82}$$

Before we continue, let me turn to the second case where $\hat{A}_1$ is an annihilator. The derivation for annihilators and creators is analogous.

- Let me now proceed with the case when $\hat{A}_1$ is an annihilator, that is for $\hat{A}_1 = \hat{c}_{l,\alpha}(t)$. Similar to the previous case, I am introducing the symbols Y^-_α and X^-_α

$$\begin{aligned}
Y^-_\alpha(t) &\overset{\text{def}}{=} \mathrm{Tr}\Big\{\overbrace{\hat{c}_{l,\alpha}(t)}^{\hat{A}_1}\hat{A}_2\ldots\hat{A}_{2M}\hat{\rho}^{(0)}_{T,\mu}\Big\} \\
&\overset{\text{Eq. }K.71}{=} \underbrace{\sum_{j=2}^{2M}(-1)^j\mathrm{Tr}\Big\{(\hat{A}_2\cdots\hat{A}_{j-1})[\hat{A}_1,\hat{A}_j]_+(\hat{A}_{j+1}\cdots\hat{A}_{2M})\hat{\rho}^{(0)}_{T,\mu}\Big\}}_{=:X^-_\alpha} \\
&\quad -\mathrm{Tr}\Big\{\hat{A}_2\cdots\hat{A}_{2M}\overbrace{\sum_\gamma\Big\langle\pi_\alpha\Big|\hat{U}(t,0)\mathrm{e}^{-\beta(\hat{h}-\mu\hat{1})}\hat{U}(0,t)\Big|\chi_\gamma\Big\rangle\hat{\rho}^{(0)}_{T,\mu}\hat{c}_{l,\gamma}(t)}^{\hat{A}_1\hat{\rho}^{(0)}_{T,\mu}\quad\text{Eq. K.57}}\Big\} \\
&= X^-_\alpha - \sum_q\Big\langle\pi_\alpha\Big|\hat{U}(t,0)\mathrm{e}^{-\beta(\hat{h}-\mu\hat{1})}\hat{U}(0,t)\Big|\chi_\gamma\Big\rangle\underbrace{\overbrace{\mathrm{Tr}\Big\{\hat{c}_{l,\gamma}(t)\hat{A}_2\cdots\hat{A}_{2M}\hat{\rho}^{(0)}_{T,\mu}\Big\}}^{\mathrm{Tr}\left\{\hat{A}_2\cdots\hat{A}_{2M}\hat{\rho}^{(0)}_{T,\mu}\hat{c}_{l,\gamma}(t)\right\}}}_{Y^-_\gamma}
\end{aligned} \tag{K.83}$$

This is a system of equations for $\{Y^-_\gamma\}$. I bring all terms containing one of the $\{Y^-_\gamma\}$ to the left hand side of the equation, and multiply both sides with the inverse of the prefactor.

$$\begin{aligned}
&\Rightarrow \quad \sum_\gamma\overbrace{\Big\langle\pi_\alpha\Big|\hat{U}(t,0)\Big(\hat{1}+\mathrm{e}^{-\beta(\hat{h}-\mu\hat{1})}\Big)\hat{U}(0,t)\Big|\chi_\gamma\Big\rangle}^{\delta_{\alpha,\gamma}+\left\langle\chi_\alpha\left|\hat{U}(t,0)\mathrm{e}^{-\beta(\hat{h}-\mu\hat{1})}\hat{U}(0,t)\right|\chi_\gamma\right\rangle}Y^-_\gamma = X^-_\alpha \\
&\Rightarrow \quad Y^-_\gamma = \sum_\alpha\Big\langle\pi_\gamma\Big|\hat{U}(t,0)\Big(\hat{1}+\mathrm{e}^{-\beta(\hat{h}-\mu\hat{1})}\Big)^{-1}\hat{U}(0,t)\Big|\chi_\alpha\Big\rangle X^-_\alpha \\
&\overset{\alpha\to\gamma\to\alpha_1}{\Rightarrow} \quad Y^-_{\alpha_1} = \sum_\gamma\Big\langle\pi_{\alpha_1}\Big|\hat{U}(t,0)\Big(\hat{1}+\mathrm{e}^{-\beta(\hat{h}-\mu\hat{1})}\Big)^{-1}\hat{U}(0,t)\Big|\chi_\gamma\Big\rangle X^-_\gamma
\end{aligned} \tag{K.84}$$

Let me now turn to X^-_γ. Let $\hat{A}_j = \hat{c}^+_{l,\alpha_j}(t_j)$ and $\hat{A}_1 = \hat{c}_{l,\alpha_1}(t_1)$. I will use Eqs. K.51, K.52 and K.53 from p. 570.

$$\begin{aligned}
X^-_\gamma &\overset{\text{def}}{=} \sum_{\substack{j=2 \\ \hat{A}_j=\text{creator}}}^{2M}(-1)^j\mathrm{Tr}\Big\{(\hat{A}_2\cdots\hat{A}_{j-1})\overbrace{[\hat{c}_{l,\gamma}(t_1),\hat{c}^+_{l,\alpha_j}(t_j)]_+}^{[\hat{A}_1,\hat{A}_j]_+}(\hat{A}_{j+1}\cdots\hat{A}_{2M})\hat{\rho}^{(0)}_{T,\mu}\Big\} \\
&\overset{\text{Eq. }K.51}{=} \sum_{\substack{j=2 \\ \hat{A}_j=\text{creator}}}^{2M}(-1)^j\mathrm{Tr}\Big\{(\hat{A}_2\cdots\hat{A}_{j-1})\overbrace{\langle\pi_\gamma|\hat{U}(t_1,t_j)|\pi_{\alpha_j}\rangle}^{[\hat{A}_1,\hat{A}_j]_+}(\hat{A}_{j+1}\cdots\hat{A}_{2M})\hat{\rho}^{(0)}_{T,\mu}\Big\}
\end{aligned} \tag{K.85}$$

which yields

$$Y^-_{\alpha_1} = \sum_\gamma \Big\langle \pi_{\alpha_1} \Big| \hat{U}(t_1,0)\Big(\hat{1}+\mathrm{e}^{-\beta(\hat{h}-\mu\hat{1})}\Big)^{-1}\hat{U}(0,t_1)\Big|\chi_\gamma\Big\rangle \overbrace{\times \sum_{\substack{j=2\\ \hat{A}_j=\text{creator}}}^{2M} (-1)^j \Big\langle \pi_\gamma\Big|\hat{U}(t_1,t_j)\Big|\pi_{\alpha_j}\Big\rangle \mathrm{Tr}\Big\{(\hat{A}_2\cdots\hat{A}_{j-1})(\hat{A}_{j+1}\cdots\hat{A}_{2M})\hat{\rho}^{(0)}_{T,\mu}\Big\}}^{X^-_\gamma}$$

$$= \sum_{\substack{j=2\\ \hat{A}_j=\text{creator}}}^{2M} (-1)^j \Big\langle \pi_{\alpha_1}\Big|\hat{U}(t_1,0)\Big(\hat{1}+\mathrm{e}^{-\beta(\hat{h}-\mu\hat{1})}\Big)^{-1}\hat{U}(0,t_j)\Big|\pi_{\alpha_j}\Big\rangle \times \mathrm{Tr}\Big\{(\hat{A}_2\cdots\hat{A}_{j-1})(\hat{A}_{j+1}\cdots\hat{A}_{2M})\hat{\rho}^{(0)}_{T,\mu}\Big\} \tag{K.86}$$

The term with the Boltzmann factor can be expressed by the thermal one-particle-reduced density matrix for the initial non-interacting Hamiltonian $\hat{h}(0)$.

$$\Big(\hat{1}+\mathrm{e}^{-\beta(\hat{h}(0)-\mu\hat{1})}\Big)^{-1} = \hat{1} - f_{T,\mu}(\hat{h}(0)) = \hat{1} - \hat{\rho}^{(1)(0)}_{T,\mu} \tag{K.87}$$

where $f_{T,\mu}(\epsilon)$ is the Fermi distribution.

The prefactor can then be expressed by the Green's function of the non-interacting system.

$$\begin{aligned}\Big\langle \pi_{\alpha_1}\Big|\hat{U}(t_1,0)\Big(\hat{1}+\mathrm{e}^{-\beta(\hat{h}-\mu\hat{1})}\Big)^{-1}\hat{U}(0,t_j)\Big|\pi_{\alpha_j}\Big\rangle &\overset{t_1\geqq t_j}{=} \overbrace{\theta_{\mathcal{C}}(t_1-t_j)}^{=1}\Big\langle \pi_{\alpha_1}\Big|\hat{U}(t_1,0)\overbrace{\Big(\hat{1}-\hat{\rho}^{(1)(0)}_{T,\mu}\Big)}^{\left(\hat{1}+\mathrm{e}^{-\beta(\hat{h}-\mu\hat{1})}\right)^{-1}}\hat{U}(0,t_j)\Big|\pi_{\alpha_j}\Big\rangle \\ &= i\hbar\Big\langle \pi_{\alpha_1}\Big|\hat{G}^{\mathcal{C}(0)}(t_1,t_j)\Big|\pi_{\alpha_j}\Big\rangle \\ &= i\hbar\, G^{\mathcal{C}(0)}_{\alpha_1,\alpha_j}(t_1,t_j)\end{aligned} \tag{K.88}$$

Let me relate the sign factor $(-1)^{j+1}$ to the number of permutations of the indices in the original time-ordered product to bring them into the order $(1,j,2,\ldots,j-1,j+1,\ldots,2M)$ of the final result.

$$(-1)^j = \epsilon_{1,j,2,\ldots j-1,j+1,\ldots,2M} \tag{K.89}$$

where $\epsilon_{j_1,\ldots,2M}$ is the fully antisymmetric tensor.

Thus, we obtain the final result for $Y^-_{n_1}$

$$Y^-_{\alpha_1} = i\hbar \sum_{\substack{j=2\\ \hat{A}_j=\text{creator}}}^{2M} \epsilon_{1,j,2,\ldots j-1,j+1,\ldots,2M}\, \hat{G}^{\mathcal{C}(0)}_{\alpha_1,\alpha_j}(t_1,t_j)\mathrm{Tr}\Big\{(\hat{A}_2\cdots\hat{A}_{j-1})(\hat{A}_{j+1}\cdots\hat{A}_{2M})\hat{\rho}^{(0)}_{T,\mu}\Big\} \tag{K.90}$$

Summary of one step of Wick's theorem:

Let me combine the two cases:

$$Y = i\hbar\sum_{j=2}^{2M}\mathrm{Tr}\Big\{(\hat{A}_2\cdots\hat{A}_{j-1})(\hat{A}_{j+1}\cdots\hat{A}_{2M})\hat{\rho}^{(0)}_{T,\mu}\Big\} \times \begin{cases}\epsilon_{j,1,2,\ldots j-1,j+1,\ldots,2M}\ \hat{G}^{\mathcal{C}(0)}_{\alpha_j,\alpha_1}(t_j,t_1) & \text{if } A_1 \text{ creator and } A_j \text{ annihilator}\\ \epsilon_{1,j,2,\ldots j-1,j+1,\ldots,2M}\ \hat{G}^{\mathcal{C}(0)}_{\alpha_1,\alpha_j}(t_1,t_j) & \text{if } A_j \text{ creator and } A_1 \text{ annihilator}\\ 0 & \text{else}\end{cases} \tag{K.91}$$

In words:

1. The first operator $\hat{A}_1$ is paired with all operators $\hat{A}_j$ of opposite type. That is, when $\hat{A}_1$ is a creation operator it is paired with all $\hat{A}_j$, that are annihilators, and vice versa.
2. Each pair is represented by a Green's function where the annihilator of the pair enters as the left and the creator as the right argument.
3. The order of the indices, after placing Green's function up front (or to the end), enters the fully antisymmetric tensor to determine the sign.
4. A factor $i\hbar$ is introduced.
5. The trace of operators contains two operators less, which made up the Green's function.
6. The product in the trace is still time ordered.

K.4.2 Sequence of Wick's iterations:

So far, we described a single step of Wick's theorem. This step is executed iteratively for the remaining products in the trace, until only $\mathrm{Tr}[\hat{\rho}^{(0)}_{T,\mu}]$ is left, which is a factor 1, that can be ignored.

After all rounds of Wick's theorem have been completed, the result has the form

$$\overbrace{\mathrm{Tr}\Big\{\hat{\rho}^{(0)}_{T,\mu}\hat{A}_1\cdots\hat{A}_{2M}\Big\}}^{Y} = (i\hbar)^M \sum_{\vec{P}\in\mathbb{X}} \epsilon_{P_1,\ldots,P_{2M}} \prod_{j=1}^{M} G^{\mathcal{C}(0)}_{\alpha_{P_{2j-1}},\alpha_{P_{2j}}}(t_{P_{2j-1}}, t_{P_{2j}}) \tag{K.92}$$

where the set $\mathbb{X}$ of vectors $\vec{P}$ needs to be specified.

The vectors $\vec{P}\in\mathbb{X}$ map the operator indices from the initial time order onto the operator sequence as they turn up after Wicks theorem. This order is also the time order of the time arguments in the final result.

Let me walk through the rounds of Wicks theorem:

1. In the first round of Wick's theorem, the first operator $\hat{A}_1$ in the trace is paired up with each operator of opposite type, that is creators are paired with annihilators and vice versa. Each pair is converted into a non-interacting Green's function. The result is a sum with M terms each containing one Green's function and a trace with $2M-2$ operators in the trace.
2. In the second round of Wick's theorem, the first of the remaining operators in the trace is paired up with all operators of opposite type. This divides each term of the first round further into $M-1$ terms. After the second round, the sum has $M(M-1)$ terms, each with a product of two Green's functions and a trace with $2M-4$ operators.
3. After the M-th round of Wick's theorem, the sum has $M!$ terms, each consisting of a product of M Green's functions. The trace contains only the von-Neumann density matrix, $\mathrm{Tr}\{\hat{\rho}^{(0)}_{T,\mu}\}=1$. This is the last round of Wick's theorem.

The final sum contains all complete pairings of operators with a partner of the opposite type. Each of the $M!$ complete pairings occurs exactly once in the sum.

Let refine the description of the set $\mathbb{X}$ further:

1. The components of the $2M$-dimensional vectors $\vec{P}\in\mathbb{X}$ are integers with $1\le P_j\le 2M$. There are M^M such vectors.
2. The fully antisymmetric tensor filters all vectors out that are not permutations of the initial sequence $(1,2,\ldots,2M)$ of operators. There are $(2M)!$ permutations of the initial operator sequence.

3. From the result Eq. K.91 of one round of Wicks theorem, we notice that the annihilation operators occur always as left arguments of a Green's function and the creation operators occur as the right argument. There are $(M!)^2$ vectors $\vec{P}$ with this property: there are $M!$ permutations of the creation operators among each other and $M!$ permutations of the annihilation operators.

4. Two vectors $\vec{P}$, which correspond to an interchange of two (or more) Green's functions in the product, describe the same pairing. To avoid double counting of the same pairing, only one of them can be an element of $\mathbb{X}$. In order to select exactly one vector describing the same pairing, let me require that the even indices, are in ascending order, that is, they maintain the order of creation operator in the initial operator product.

$$P_2 < P_4 < \ldots < P_{2M} \qquad \text{for } \vec{P} \in \mathbb{X} \tag{K.93}$$

Let me summarize this in different words: the indices of the creation operators in the order of the initial product determines the components of $\vec{P}$ with even index. That is, all elements of $\mathbb{X}$ have the same sequence of components P_{2j} with even index $2j$. The components of $\vec{P}$ with odd index refer to the indices of the annihilation operators. These M indices can occur in any order and consequently there are $M!$ terms in the set $\mathbb{X}$.

The selection of the vectors $\vec{P}$ is still a bit clumsy. Bear with me, it will get a little better below...

K.4.3 Wick's theorem for a product that is not time ordered

In the derivation of Wick's theorem, we required in Eq. 10.33 that the operators are already time ordered. This implies that the time ordering $\mathcal{T}_\mathcal{C}$ along the contour has already been performed.

When the time-ordering operator acts on a sequence of operators, it introduces a sign change for every permutation of neighboring fermionic operators. These sign due to the time ordering need to be added to the ones introduced by Wick's theorem.

All these sign changes can described by a fully antisymmetric tensor which monitors the permutations from the order in the operator product to the time-ordered product and further to the order of indices in the final product of Green's functions.

The vector $\vec{P}$ maps the indices in the final product to their arrangement of operators in the initial product before applying the time-ordering operator.

The result of the sequence has the form

$$\mathrm{Tr}\Big\{\hat{\rho}^{(0)}_{T,\mu}\mathcal{T}_\mathcal{C}\hat{A}_1\cdots\hat{A}_{2M}\Big\} \overset{\text{Eq. } K.92}{=} (i\hbar)^M \sum_{\vec{P}\in\mathbb{X}'} \epsilon_{P_1,\ldots,P_{2M}} \prod_{j=1}^{M} G^{\mathcal{C}(0)}_{\alpha_{P_{2j-1}},\alpha_{P_{2j}}}(t_{P_{2j-1}}, t_{P_{2j}}) \tag{K.94}$$

There is a subtle difference between the trace in the equation above and the product Y used earlier in Eq. K.92, namely, the time-ordering operator $\mathcal{T}_\mathcal{C}$ has been inserted. Consequently, the set $\mathbb{X}'$ differs from the set $\mathbb{X}$ used earlier in Eq. K.92, because the vectors map the final sequence of arguments to the initial order of operators, which have no time order.

In the equation above the product $\hat{A}_1\cdots\hat{A}_{2M}$ is **not time ordered**. The time order is established through the time-ordering operator, but then the order of the operators has already changed, i.e. the indices are no more ascending. Only this, rearranged, product of operators can be used in the expression Y for Wick's theorem.

The insertion of the time-ordering operator maintains the same structure of the result, because the sign changes due to rearrangement of the operators from the initial order to the time order are tracked by the fully antisymmetric tensor.

K.4.4 Alternating order of annihilation an creation operators

It is often convenient to bring the creation and annihilation operators under the time-ordering operator into a specific order, so that the annihilation operators alternate with creation operators.

$$\begin{aligned}\mathcal{T}_{\mathcal{C}}\hat{W}_I(t) &\overset{\text{Eq. } K.95}{=} \frac{1}{2}\sum_{i_1,o_1,i_2,o_2} W_{o_1,o_2,i_1,i_2}\mathcal{T}_{\mathcal{C}}\Big\{\hat{c}^+_{I,o_1}(t^+)\hat{c}^+_{I,o_2}(t^+)\hat{c}_{I,i_2}(t)\hat{c}_{I,i_1}(t)\Big\} \\ &= \frac{1}{2}\sum_{i_1,o_1,i_2,o_2} W_{o_1,o_2,i_1,i_2}\mathcal{T}_{\mathcal{C}}\Big\{\hat{c}_{I,i_1}(t)\hat{c}^+_{I,o_1}(t^+)\hat{c}_{I,i_2}(t)\hat{c}^+_{I,o_2}(t^+)\Big\} \qquad \text{(K.95)}\end{aligned}$$

There are no sign changes.

Inspection of the Green's function in Eq. 10.22 shows that this alternating order is consistent with the order of the operators in the Green's function.

$$\mathrm{Tr}\Big\{\hat{\rho}^{(0)}_{T,\mu}\mathcal{T}_{\mathcal{C}}\prod_{j=1}^{M}\hat{c}_{I,i_j}(t'_j)\hat{c}^\dagger_{I,o_j}(t^+_j)\Big\} \overset{\text{Eq. } K.94}{=} (i\hbar)^M\sum_{\vec{P}\in\mathbb{X}''}\epsilon_{P_1,\ldots,P_{2M}}\prod_{j=1}^{M}G^{\mathcal{C}(0)}_{i_j,o_j}(t'_{\mathcal{P}_j},t^+_j) \qquad \text{(K.96)}$$

The $\mathbb{X}''$ differs from the one used previously because it is the mapping for a different ordering of the initial operator product.

For this specific order of the initial operators, the $2M$-dimensional permutation vectors $\vec{P}$ can be expressed by a set of M-dimensional vectors $\vec{\mathcal{P}}$.

$$\vec{P} = (2\mathcal{P}_1 - 1,\, 2,\, 2\mathcal{P}_2 - 1\,, 4, \ldots, 2\mathcal{P}_M - 1,\, 2M) \qquad \text{(K.97)}$$

$$\epsilon_{\vec{P}} = \epsilon_{2\mathcal{P}_1-1,2,2\mathcal{P}_2-1,4,\ldots,2\mathcal{P}_M-1,2M} \overset{?}{=} \epsilon_{\mathcal{P}_1,\mathcal{P}_2,\ldots,\mathcal{P}_M} = \epsilon_{\vec{\mathcal{P}}} \qquad \text{(K.98)}$$

For a vector $\vec{\mathcal{P}} = (1, 2, \ldots, M)$ the two antisymmetric tensors are equal, i.e. $\epsilon_{\vec{P}} = 1 = \epsilon_{\vec{\mathcal{P}}}$.

Next, I need to show that the interchange of two neighboring components of the vector $\vec{\mathcal{P}}$ involves three interchanges of neighboring components in the corresponding vector $\vec{P}$. Let me demonstrate it for $M = 2$.

$$\begin{array}{ccc}(\mathcal{P}_1,\mathcal{P}_2) & \rightarrow & (\mathcal{P}_2,\mathcal{P}_1)\\ (P_{2P_1-1},2,P_{2P_2-1},4) \overset{\text{1st}}{\rightarrow} (2,P_{2P_1-1},P_{2P_2-1},4) & \overset{\text{2nd}}{\rightarrow} & (2,P_{2P_2-1},P_{2P_1-1},4) \overset{\text{3rd}}{\rightarrow} (P_{2P_2-1},2,P_{2P_1-1},4)\end{array} \qquad \text{(K.99)}$$

In both cases the permutation introduces a sign change. Thus, we have shown that $\epsilon_{\vec{P}} = \epsilon_{\vec{\mathcal{P}}}$ if the vector $\vec{P}$ is related to $\vec{\mathcal{P}}$ as described above.

With this choice, the result Eq. K.96 obtains the form

$$\mathrm{Tr}\Big\{\hat{\rho}^{(0)}_{T,\mu}\mathcal{T}_{\mathcal{C}}\prod_{j=1}^{M}\hat{c}_{I,i_j}(t'_j)\hat{c}^\dagger_{I,o_j}(t^+_j)\Big\} \overset{\text{Eq. } K.96}{=} (i\hbar)^M\sum_{\vec{\mathcal{P}}}\epsilon_{\mathcal{P}_1,\ldots,\mathcal{P}_M}\prod_{j=1}^{M}G^{\mathcal{C}(0)}_{i_{\mathcal{P}_j},o_j}(t'_{\mathcal{P}_j},t^+_j) \qquad \text{(K.100)}$$

The set of permutation vectors $\vec{\mathcal{P}}$ is much simpler than the set $\mathbb{X}$: It contains all M-dimensional integer vectors with elements between one and M. The fully antisymmetric tensor selects those vectors that are permutation vectors.

K.4.5 Final form of Wick's theorem

Let me now summarize the final form of Wick's theorem, as it given in Eq. 10.38 on p. 305 of the main text.

WICK'S THEOREM

$$\mathrm{Tr}\Big\{\hat{\rho}^{(0)}_{T,\mu}\mathcal{T}_{\mathcal{C}}\prod_{j=1}^{M}\hat{c}_{I,i_j}(t'_j)\hat{c}^{\dagger}_{I,o_j}(t^{+}_j)\Big\}\overset{\text{Eq. } K.100}{=}(i\hbar)^M\sum_{\vec{\mathcal{P}}}\epsilon_{\mathcal{P}_1,\ldots,\mathcal{P}_M}\prod_{j=1}^{M}G^{\mathcal{C}(0)}_{i_{\mathcal{P}_j},o_j}(t'_{\mathcal{P}_j},t^{+}_j) \tag{K.101}$$

The creation and annihilation operators $\hat{c}^{\dagger}_{I,o}$ and $\hat{c}_{I,i}$ are given in the interaction picture with respect to a time-depending, non-interacting Hamiltonian $\hat{h}(t)$. While the Hamiltonian $\hat{h}(t)$ depends only on the real part of the complex-valued time argument, it propagates the wave functions, along a contour $\mathcal{C}$ in the complex time plane.
The time argument t^{+}_j stands for a time, which is infinitesimally displaced forward along the contour relative to the time t_j.
The one-particle basisset defining the creation and annihilation operators may be non-orthonormal.
The density matrix $\hat{\rho}^{(0)}_{T,\mu}$ is the thermal von-Neumann density matrix for the non-interacting Hamiltonian $\hat{h}(t)$ at time $t=0$.
The sum is performed over all M-dimensional vectors with components $\mathcal{P}_j\in\{1,2,\ldots,M\}$. The fully antisymmetric tensor $\epsilon_{\mathcal{P}_1,\mathcal{P}_2,\ldots,\mathcal{P}_M}$ selects the permutation vectors with $\mathcal{P}_j\neq\mathcal{P}_k$.
The non-interacting contour-ordered Green's function $G^{\mathcal{C}(0)}_{i,o}(t',t)$ has been defined in Eq. 7.27 (p.247) as

$$G^{\mathcal{C},(0)}_{i,o}(t',t)\overset{\text{Eq. } 7.27}{=}\frac{1}{i\hbar}\Big\langle\pi_i\Big|\hat{U}(t',0)\Big\{\underbrace{\theta_{\mathcal{C}}(t-t')(\hat{1}-\hat{\rho}^{(1)(0)}_{T,\mu})}_{\text{electrons}}-\underbrace{\theta_{\mathcal{C}}(t'-t)\hat{\rho}^{(1)(0)}_{T,\mu}}_{\text{holes}}\Big\}\hat{U}(0,t)\Big|\pi_o\Big\rangle$$

K.4.6 Why is the time-ordered Green's function important?

As we introduced the Green's function for many particle systems, we have seen that several Green's function could have been defined by adding a solution of the homogeneous Schrödinger equation. As motivation for the time-ordered Green's function, I referred to Wick's theorem. In the derivation above, the contractions are, up to a factor, equal to the time-ordered Green's function and no other type of Green's function, which explains the importance of the time-ordered Green's function.

K.4.7 Non-interacting grand potential

Editor: This is not for the reader. It shall be merged with the main text. See also Eq. 10.70 on p. 319 and Eq. 10.28 on p. 302. There are probably some duplications.

The grand potential is obtained from

$$\begin{aligned}\Omega^{(0)}_{T,\mu}&=-k_BT\ln\mathrm{Tr}\left\{\mathrm{e}^{-\beta(\hat{h}-\mu\hat{N})}\right\}\\&=-k_BT\ln\sum_{\vec{\sigma}}\mathrm{e}^{-\beta\sum_j\sigma_j(\epsilon_j-\mu)}\\&=-k_BT\sum_j\ln\left(1+\mathrm{e}^{-\beta(\epsilon_j-\mu)}\right)\\&=-k_BT\ \mathrm{Tr}\left[\ln\left(\mathbf{1}+\mathrm{e}^{-\beta(\boldsymbol{h}-\mu\mathbf{1})}\right)\right]\end{aligned} \tag{K.102}$$

We can express the grand potential also in terms of the occupations of the one-particle orbitals.

$$\begin{aligned} f_n &= \left(1 + \mathrm{e}^{\beta(\epsilon_n - \mu)}\right)^{-1} \\ \mathrm{e}^{\beta(\epsilon_n-\mu)} &= \frac{1}{f_n} - 1 = \frac{1 - f_n}{f_n} \\ 1 + \mathrm{e}^{-\beta(\epsilon_n-\mu)} &= 1 + \frac{f_n}{1 - f_n} = \frac{1}{1 - f_n} \end{aligned} \tag{K.103}$$

Thus, we obtain

$$\begin{aligned} \Omega^{(0)}_{T,\mu} &= +k_B T \sum_n \ln(1 - f_n) \\ &= +k_B T \,\mathrm{Tr}\ln(\hat{1} - \hat{\rho}^{(1)}) \\ &= +k_B T \,\mathrm{Tr}\ln\left(\hat{1} + i\hbar\hat{G}^{(0)}(t, t^+)\right) \\ &= +k_B T \,\mathrm{Tr}\ln\left(-i\hbar\hat{G}^{(0)}(t^+, t)\right) \end{aligned} \tag{K.104}$$

$$d\Omega^{(0)}_{T,\mu} = -k_B T \,\mathrm{Tr}\left[\left(\mathbf{1} + \mathrm{e}^{-\beta(\boldsymbol{h}-\mu\mathbf{1})}\right)^{-1}\left(-\beta\mathrm{e}^{-\beta(\boldsymbol{h}-\mu\mathbf{1})}\right) d\boldsymbol{h}\right] = \mathrm{Tr}\left[\left(1 + \mathrm{e}^{\beta(\boldsymbol{h}-\mu\mathbf{1})}\right)^{-1} d\boldsymbol{h}\right] \tag{K.105}$$

Appendix L

Code for the construction of Feynman diagrams

While it is important to understand the underpinnings of Feynman diagrams, many of the operations can be performed on the computer. This chapter contains a FORTRAN code that sets up the permutation vectors defining the Feynman diagrams to a specified order. The code determines the linked, topologically inequivalent diagrams together with their symmetry factor and the sign.

L.1 Procedure to exclude disconnected diagrams

The linked-cluster theorem Eq. 11.17 reduces the set of all closed diagrams to the subset of linked clusters. The disconnected diagrams, which need to be sorted out, are easily identified from the drawn diagram itself. Disconnected diagrams can also be identified on the basis of a permutation vector as mentioned in section 11.4 on p. 335. Here, I am sketching a systematic and efficient procedure, which can be used either by hand and which can be put on the computer.

The procedure to discard the disconnected diagrams passes through all vertices of a linked cluster in the diagram and identifies the vertices, which belong to it. If a vertex of the diagram is left over, the diagram is disconnected.

The procedure makes use of the permutation vector $\vec{\mathcal{P}}$ of the diagram. Let the set $\mathbb{B}$ be the linked cluster connected to the first vertex. We maintain an array, which keeps track, which vertices have already been identified as member of $\mathbb{B}$. The array has one entry for each vertex with value true or false

1. We start with the first vertex and complete the Fermi loop that passes through it. This is done by repeating the following two steps until a vertex is encountered that is already marked as member of $\mathbb{B}$.
   (a) The current vertex v_j is marked as member of $\mathbb{B}$
   (b) One proceeds to vertex with number $v_k = \mathcal{P}_j$
   (c) If this vertex has already been marked as member of $\mathbb{B}$, the Fermi loop has been completed and one proceeds to the next step (2) of the procedure described below. If not, one continues with (1.a) to follow along the Fermi loop as sketched above.
2. From the current vertex v_j, one proceeds through the vertices in ascending order of their numbers until a vertex is encountered that is not yet marked as member of $\mathbb{B}$.
3. If, on the one hand, the partner of the odd-even vertex pair containing the current vertex has not been marked as member of $\mathbb{B}$, the diagram at hand is disconnected and not a linked cluster. Thus, the procedure is complete and can be ended.

The reason that one can take the decision to identify a disconnected diagram already at this point, is that each Fermi loop is identified beginning at the vertex having the lowest index.

4. If, on the other hand, the partner of the odd-even vertex pair has already been marked as member of $\mathbb{B}$, the current vertex is connected to $\mathbb{B}$ by an interaction line. Thus, the current member is also part of $\mathbb{B}$. Therefore, one proceeds with step (1.a) to identify the Fermi loop passing through the current vertex.

5. When we arrive at the last vertex, all vertices belong to the same linked cluster $\mathbb{B}$ and the diagram is kept in the set of linked diagrams $\mathbb{L}$.

This procedure identifies a diagram as linked or disconnected in one pass. It can easily be put on the computer. The code is provided in the appendix L on p. 585. The implementation does not implement the procedure as described above, but follows it in spirit.

L.2 Installation:

Prerequisites are a FORTRAN compiler such as gfortran.

1. Download the code as "diagrams.f90". Be aware of special non-printing symbols when grabbing it from a pdf file.

2. Compile the code with `gfortran -o diagrams.x diagrams.f90`

3. Run the code as `diagrams.x`. You will be asked to provide the order of the diagrams to be calculated.

L.3 Example:

In order to obtain the result for the third order in the interaction execute the following on the command line of a UNIX system.

```
gfortran -o diagrams.x diagrams.f90; echo 3 | diagrams.x > out.dat
```

The resulting file `out.dat` is given below in section L.6.3.

Each line represents a linked Feynman diagram. The first column is the symmetry factor multiplied by the sign of the diagram. Denoted with `p=` is the permutation vector $\vec{\mathcal{P}}$. In order to draw the diagram,

1. start drawing n interaction lines, where n is the order of the diagram.

2. label the vertices so that each interaction line has one odd-numbered vertex and the next higher even-numbered vertex.

3. For each component p_j of the $2n$-dimensional permutation vector draw a bare Green's function line from vertex V_j to vertex V_{p_j}.

L.4 Code Description

- The subroutine **permutationvectors** sets up all $(2n)!$ permutation vectors with length $2n$, where n is the order of the diagrams. It implements the method is described in section 11.2.1 on p. 329.

- The subroutine **loops** determines the sign factor of the diagrams and it identifies disconnected diagrams. If the diagram is not a linked-cluster, the sign factor is set to zero. The routine follows in spirit the method described in section L.1 on p. 585. Editor: This routine does not exploit the description section L.1 in full: It searches for odd-even pairs from the beginning, rather than from the start of the most recent Fermi loop. It does not stop the search at the first possibility to detect a disconnected cluster, but only at the end.

- The subroutine **vertexmaps** sets up all $n!2^n$ transformations of permutation vectors, that result in a topologically equivalent diagram. A specific transformation is represented by a vector $\vec{M}$ with the same length $2n$ of the permutation vector.

$$\mathcal{P}'_{M_j} = M_{\mathcal{P}_j} \tag{L.1}$$

- The subroutine **symmetryfactor** determines the symmetry factor `sofd` of a specific diagram and it selects one specific diagram from a set of topologically equivalent diagrams. Internally, all topologically equivalent diagrams of the current diagram are created using the transformations set up in routine vertexmaps. A sequence for all diagrams is defined. If any of the transformed permutation vectors has a lower value in the sequence, the current diagram is omitted by exiting the routine after setting the symmetry factor `sofd` to zero. If the current diagram is one to be considered, the symmetry factor is determined by identifying the number of mere deformations among all transformations. The symmetry factor is provided as $S(D) =$`sofd`.

L.5 Source code:

The code `diagrams.f90` can be downloaded from the ΦSX Website `phisx.org`. For the sake of completeness it is included below.

```
      program main
!     ************************************************************************
!     ** determines the permutation vectors defining the topologically       **
!     ** inequivalent, linked feynman diagrams of the specified order        **
!     **                                                                     **
!     ** provide the order of the diagram from standard input (integer)      **
!     **                                                                     **
!     ** interaction lines connect odd numbered vertices with the next higher**
!     ** even numbered index. the j-th component p_j of the permutation      **
!     ** specifies a green's function from vertex j to vertex p_j.           **
!     **                                                                     **
!     ** the value of a diagram is given in                                  **
!     **   p.Bloechl, PhiSX Advanced Solid-State Theory                      **
!     **   http://www2.pt.tu-clausthal.de/atp/phisx.html                     **
!     **                                                                     **
!     ************************************************************************
!     ** COPYRIGHT (C) 2017 PETER BLOECHL, (MODIFIED M.I.T. LICENSE)         **
!     **                                                                     **
!     ** PERMISSION IS HEREBY GRANTED, FREE OF CHARGE, TO ANY PERSON         **
!     ** OBTAINING A COPY OF THIS SOFTWARE (THE "SOFTWARE"), TO DEAL IN THE  **
!     ** SOFTWARE WITHOUT RESTRICTION, INCLUDING WITHOUT LIMITATION THE      **
!     ** RIGHTS TO USE, COPY, MODIFY, MERGE, PUBLISH, DISTRIBUTE, SUBLICENSE,**
!     ** AND/OR SELL COPIES OF THE SOFTWARE, AND TO PERMIT PERSONS TO WHOM   **
!     ** THE SOFTWARE IS FURNISHED TO DO SO, SUBJECT TO THE FOLLOWING        **
!     ** CONDITIONS:                                                         **
```

```
!      **                                                                  **
!      ** THE ABOVE COPYRIGHT NOTICE AND THIS PERMISSION NOTICE SHALL BE   **
!      ** INCLUDED IN ALL COPIES OR SUBSTANTIAL PORTIONS OF THE SOFTWARE.  **
!      ** THE SOFTWARE IS PROVIDED "AS IS", WITHOUT WARRANTY OF ANY KIND,  **
!      ** EXPRESS OR IMPLIED, INCLUDING BUT NOT LIMITED TO THE WARRANTIES OF **
!      ** MERCHANTABILITY, FITNESS FOR A PARTICULAR PURPOSE AND            **
!      ** NONINFRINGEMENT. IN NO EVENT SHALL THE AUTHORS OR COPYRIGHT HOLDERS **
!      ** BE LIABLE FOR ANY CLAIM, DAMAGES OR OTHER LIABILITY, WHETHER IN AN **
!      ** ACTION OF CONTRACT, TORT OR OTHERWISE, ARISING FROM, OUT OF OR IN  **
!      ** CONNECTION WITH THE SOFTWARE OR THE USE OR OTHER DEALINGS IN THE   **
!      ** SOFTWARE.                                                        **
!      **                                                                  **
!      ** THIS LICENSE APPLIES ONLY TO THE SECTION OF FORTRAN CODE THAT    **
!      ** CONTAINS THIS LICENSE. IT DOES NOT APPLY TO THE PHISX LECTURE NOTES **
!      ** THAT MAY CONTAIN THE SOFTWARE.                                   **
!      **********************************************************************
       implicit none
       integer(4)             :: order     !order in the interaction
       integer(4)             :: len       !length of permutation vector
       integer(4)             :: nvecx     !X#(permutation vectors)
       integer(4)             :: nmapx
       integer(4),allocatable :: pvec(:,:) !(len,nvecx) permutation vector
       integer(4),allocatable :: map(:,:)  !(len,nmapx)
       integer(4),allocatable :: sofd(:)   !(nvecx) symmetry factor*sign
       integer(4),allocatable :: sgn(:)    !(nvecx)
       integer(4)             :: nvec      !#(permutation vectors)
       integer(4)             :: nmap
       integer(4)             :: i,j
       real(8)                :: svar
!      **********************************************************************
       write(*,fmt='("provide the order of the diagrams (integer):")')
       read(*,fmt=*)order
       write(*,fmt='(40(".",t1,"order of the diagrams",t40,i15)')order
       len=2*order
!
!      ======================================================================
!      == allocate array for permutation vector                            ==
!      == a permutation vector has the length len=2*order                  ==
!      == the number of permutation vectors in this order is factorial(len)  ==
!      ======================================================================
       nvecx=1
       do i=1,len
         nvecx=nvecx*i
       enddo
       allocate(pvec(len,nvecx))
       allocate(sgn(nvecx))
       allocate(sofd(nvecx))

!      ======================================================================
!      == determine all permutation vectors                                ==
!      ======================================================================
       call permutationvectors(len,nvecx,nvec,pvec)
       write(*,fmt='(40(".",t1,"nr. of all diagrams (=n!)",t40,i15)')nvec
!
```

```
!      ========================================================================
!      == count the number of loops (sign of the diagram)                    ==
!      == identify unlinked diagrams (sgn=0)                                 ==
!      ========================================================================
       do i=1,nvec
         call loops(len,pvec(:,i),sgn(i))
       enddo
!
!      ========================================================================
!      == remove unlinked diagrams                                           ==
!      ========================================================================
       j=0
       do i=1,nvec
         if(sgn(i).eq.0) cycle
         j=j+1
         pvec(:,j)=pvec(:,i)
         sgn(j)=sgn(i)
!         write(*,fmt='("(",20i4,")",i10)')pvec(:,j),sgn(j)
       enddo
       nvec=j
       write(*,fmt='(40(".",t1,"nr. of linked diagrams",t40,i15)')nvec
!
!      ========================================================================
!      == determine symmetry factor (sofd=0 for duplicates)                  ==
!      == sign is integrated into the symmetry factor                        ==
!      ========================================================================
       nmapx=1
       do i=1,order
         nmapx=nmapx*2*i
       enddo
       allocate(map(len,nmapx))
       call vertexmaps(len,nmapx,nmap,map)
       do i=1,nvec
         call symmetryfactor(len,pvec(:,i),nmap,map,sofd(i))
         sofd(i)=sofd(i)*sgn(i)
       enddo
       deallocate(map)
!
!      ========================================================================
!      == remove topologically equivalent diagrams                           ==
!      ========================================================================
       j=0
       do i=1,nvec
         if(sofd(i).eq.0) cycle
         j=j+1
         pvec(:,j)=pvec(:,i)
         sofd(j)=sofd(i)
         sgn(j)=sgn(i)
       enddo
       nvec=j
       write(*,fmt='(40(".",t1,"nr. of top. distinct diagrams",t40,i15)')nvec
!
!      ========================================================================
!      == test sum rule                                                      ==
```

```
!       ========================================================================
        svar=sum(1.d0/abs(sofd(:nvec)))
        do i=1,len/2
          svar=svar*2.d0*real(i,kind=8)
        enddo
        write(*,fmt='(40(".",t1,"sum-rule test 2^n * n! * S(D) ",t40,f15.1)')svar
        write(*,fmt='(40(".",t1,"...must reproduce number of linked diagrams")')
!
!       ========================================================================
!       == print resulting permutation vectors and symmetry factors            ==
!       ========================================================================
        write(*,*)
        write(*,fmt='("sign, symmetry factor and permutation vectors:")')
        do i=1,nvec
          write(*,fmt='(i8,"  sign*sofd=",i8," p=",20i4)') &
      &         i,sofd(i),pvec(:,i)
        enddo
        stop
        end
!
!       ..1.........2.........3.........4.........5.........6.........7.........8
        subroutine vertexmaps(len,nmapx,nmap,map)
!       ************************************************************************
!       ** determine the mappings of vertices that produce topologically       **
!       ** equivalent diagrams.                                                 **
!       ** the map array contains all permutations of the vertices among each  **
!       ** other.
!       ************************************************************************
        implicit none
        integer(4),intent(in) :: len    ! #(green's functions)
        integer(4),intent(in) :: nmapx
        integer(4),intent(out):: nmap
        integer(4),intent(out):: map(len,nmapx)
        integer(4),allocatable:: pvec(:,:)
        integer(4)            :: nvecx
        integer(4)            :: nvec
        integer(4)            :: nmap2,imap,jmap,ivec,i,j
!       ************************************************************************
        if(mod(len,2).eq.1) then
          stop 'argument len must be even'
        end if
!
!       == allocate dimension of map array ===================================
        nvecx=1
        do i=1,len/2
          nvecx=nvecx*i
        enddo
        allocate(pvec(len/2,nvecx))
        call permutationvectors(len/2,nvecx,nvec,pvec)
!
!       == construct all permutation of vertices
        nmap=0
        do ivec=1,nvec
          nmap=nmap+1
```

```
        do i=1,len/2
          map(2*i-1,nmap)=2*pvec(i,ivec)-1
          map(2*i  ,nmap)=2*pvec(i,ivec)
        enddo
        nmap2=nmap
        jmap=nmap
        do j=1,len/2
          do imap=nmap,nmap2
            jmap=jmap+1
            map(:,jmap)=map(:,imap)
            map(2*j-1,jmap)=map(2*j,imap)
            map(2*j,jmap)=map(2*j-1,imap)
          enddo
          nmap2=jmap
        enddo
        nmap=nmap2
      enddo
      return
      end
!
!     ..1.........2.........3.........4.........5.........6.........7.........8
      subroutine symmetryfactor(len,pvec,nmap,map,sofd)
!     ******************************************************************
!     ** determine symmetry factor                                    **
!     ** a zero value for the symmetry factor is set if a topologically **
!     ** equivalent diagram has already been considered.              **
!     **                                                              **
!     ** The symmetry factor Sofd is the ratio of mere deformations among **
!     ** all n!2^n diagrams obtained by remapping the vertices.       **
!     **                                                              **
!     ** for each diagram there are n!2^n diagrams that give the same value. **
!     ** These diagrams are obtained by remapping the vertices. These **
!     ** these mappings (1) permutate the interaction lines and       **
!     ** (2) they interchange the two vertices of one interaction.    **
!     **                                                              **
!     ** A deformation is characterized by the same permutation vector and **
!     ** is thus the identical diagram. Hence it must not be counted. **
!     **                                                              **
!     ** each diagram is converted into a value obtained from the permutation**
!     ** vector. Only those diagrams are retained, for which the      **
!     ** topologically equivalent partners have a higher number than the **
!     ** diagram itself. This singles out one diagram from each class of **
!     ** topologically distinct diagrams.                             **
!     **                                                              **
!     ******************************************************************
      implicit none
      integer(4),intent(in) :: len         ! #(green's function in the diagram)
      integer(4),intent(in) :: pvec(len)   ! permutation vector
      integer(4),intent(in) :: nmap
      integer(4),intent(in) :: map(len,nmap)
      integer(4),intent(out):: sofd        ! symmetry factor
      integer(4)            :: imap,i
      integer(4)            :: ndef        ! #(deformations)
      integer(4)            :: ovec(len)
```

```
      logical(4)            :: tident
      integer(4)            :: order
      integer(4)            :: ndistinct
!     ************************************************************************
      order=len/2
!
!     ========================================================================
!     == initial checks                                                     ==
!     ========================================================================
!     == check that len is even. It is the number of green's functions and  ==
!     == that number is twice the number of interaction lines               ==
      if(mod(len,2).eq.1) then
        stop 'argument len must be even'
      end if
!
!     ========================================================================
!     == loop over all mappings
!     ========================================================================
      do imap=1,nmap
!       == remap vertices ====================================================
        do i=1,len
          ovec(map(i,imap))=map(pvec(i),imap)
        enddo
!
!       ======================================================================
!       == exclude all diagrams that map onto another one with a smaller count=
!       ======================================================================
        tident=.true.
        do i=1,len
          if(ovec(i).ne.pvec(i)) then
            if(tident.and.ovec(i).lt.pvec(i)) then
              sofd=0 ! is already counted by another pvec
              return
            end if
            exit
          end if
        enddo
      enddo

!     ========================================================================
!     == count mere deformations                                            ==
!     ========================================================================
      ndef=0
      do imap=1,nmap
        do i=1,len
          ovec(map(i,imap))=map(pvec(i),imap)
        enddo
        tident=.true.
        do i=1,len
          if(ovec(i).ne.pvec(i)) then
            tident=.false.
            exit
          end if
        enddo
```

```
        if(tident)ndef=ndef+1
      enddo
!
!     ========================================================================
!     == calculate symmetry factor                                          ==
!     ========================================================================
!     == the diagram has ndef deformations. the number of topologically     ==
!     == equivalent diagrams which are not mere deformations is             ==
!     == ndistinct=nmap/ndef.                                               ==
!     == the inverse of symmetry factor is the number of                    ==
!     == topologically equivalent, which are not mere deformations,         ==
!     == divided by the factor n!2^n.                                       ==
!     == Hence, 1/sofd=ndistinct/nmap=1/ndef                                ==
!     ========================================================================
      ndistinct=nmap/ndef
      sofd=ndef !=nmap/ndistinct
      return
      end
!
!     ..1.........2.........3.........4.........5.........6.........7.........8
      subroutine loops(len,pvec,sgn)
!     ************************************************************************
!     **  sgn=1 for an even number of green's function loops                **
!     **  sgn=-1 for an odd number of green's function loops                **
!     **  sgn=0 for a diagram which is not a linked cluster                 **
!     **                                                                    **
!     ** the sign theorem links the sign of a diagram to the number of      **
!     ** loops formed by Green's functions.                                 **
!     **                                                                    **
!     ** the code follows green's function lines and marks each vertex      **
!     ** visited by a loop number. If an un-marked vertex (iloop=0) is      **
!     ** encountered, the code searches for interaction lines, of which one **
!     ** vertex has been visited and the other not. At such an interaction  **
!     ** the loop index in increased, and loop search  at the unmarked vertex**
!     ** is initiated.                                                      **
!     **                                                                    **
!     ** if interaction lines with two unmarked vertices are left over      **
!     ** the diagram consists of disconnected parts and sgn=0 is set.       **
!     ** otherwise the sign is determined from the the number of loops.     **
!     **                                                                    **
!     ************************************************************************
      implicit none
      integer(4),intent(in) :: len        ! #(greens functions)
      integer(4),intent(in) :: pvec(len)  ! permutation vector of diagram
      integer(4),intent(out):: sgn        ! sign or (zero for linked cluster)
      integer(4)            :: work(len)  ! holds loop indices for each vertex
      logical(4)            :: t1,t2
      integer(4)            :: iloop      ! loop index
      integer(4)            :: ip         ! vertex pointer
      integer(4)            :: i
!     ************************************************************************
      if(mod(len,2).eq.1) then
        write(*,*)'argument len must be even'
        stop 'in loops'
```

```
      end if
!
!     ========================================================================
!     == explore diagram for fermi loops                                    ==
!     ========================================================================
      work(:)=0
      iloop=1
      ip=1
      work(ip)=iloop
!
1000  continue
!
!     == walk around the first loop of greensfunctions and mark with loop nr.
      do
        ip=pvec(ip)
        if(work(ip).ne.0) exit ! end of Fermi loop encountered
        work(ip)=iloop
      enddo
!
!     == find interaction with one vertex that has been visited and another
!     == one that has not been visited.
      ip=0
      do i=1,len/2
        t1=work(2*i-1).eq.0
        t2=work(2*i).eq.0
        if(t1.eqv.t2) cycle  ! both are true or both are false.
!       -- set pointer to unmarked vertex ----------------------------------
        if(t1) then
          ip=2*i-1
        else
          ip=2*i
        end if
      enddo
!     == jump back to next fermi-loop search or exit
      if(ip.ne.0) then  ! vertex for fermi-loop search found
        iloop=iloop+1   ! increase loop index
        work(ip)=iloop  ! mark actual vertex
        goto 1000
      end if
!
!     ========================================================================
!     == calculate sgn                                                      ==
!     ========================================================================
      sgn=1
      if(mod(iloop,2).eq.1) sgn=-1
!
!     ========================================================================
!     == check if this is a linked diagram                                  ==
!     ========================================================================
      do i=1,len
        if(work(i).eq.0) then
          sgn=0
          exit
        end if
```

```
      enddo
!
      return
      end
!
!     ..1.........2.........3.........4.........5.........6.........7.........8
      subroutine permutationvectors(len,nvecx,nvec,pvec)
!     ************************************************************************
!     ** construct all len-factorial permutation vectors of length len       **
!     ** as described in section 11.1.1 "Construct all permutation vectors"  **
!     ** of P.Bloechl PhiSX Advanced Solid-State Theory                      **
!     ************************************************************************
      implicit none
      integer(4),intent(in)  :: len
      integer(4),intent(in)  :: nvecx           ! X#(permutation vectors)
      integer(4),intent(out) :: nvec            ! #(permutation vectors)
      integer(4),intent(out) :: pvec(len,nvecx) ! permutation vectors
      integer(4)             :: i,j,k,ip1,ip2,isvar
      integer(4)             :: work(len)
!     ************************************************************************
      isvar=1
      do i=1,len
        isvar=isvar*i
      enddo
      if(nvecx.lt.isvar) then
        stop 'nvecx too small (a)'
      end if
!
!     ========================================================================
!     ==  start the recursive construction with trivial vector (1,2,.., len) ==
!     ========================================================================
      nvec=1
      do i=1,len
        pvec(i,nvec)=i
      enddo
!
!     ========================================================================
!     == construct all other permutation vectors recusively
!     ========================================================================
      do
!
!       == find longest trailing descending sequence ===========================
!       == that is pvec(ip1) > pvec(ip1+1) > pvec(ip1+2) > ... ================
        j=len
        ip1=0
        do j=len,2,-1
          if(pvec(j-1,nvec).gt.pvec(j,nvec)) cycle
          ip1=j-1
          exit
        enddo
        if(ip1.eq.0) exit ! sequence is descending, exit
!
!       == prepare an entry for a new perturbation vector ====================
        nvec=nvec+1
```

```
          if(nvec.gt.nvecx) then
            stop 'nvec exceeds nvecx (b)'
          end if
!
!         == copy previous permutation vector as non-descending part ============
          pvec(:,nvec)=pvec(:,nvec-1)

!         -- ip1 is the start of the descending series. -------------------------
!         -- identify the smallest component of pvec in the descending sequence -
!         -- that is still larger than the first element of the descending ------
!         -- sequence. ----------------------------------------------------------
          ip2=ip1+1
          do k=ip1+1,len
            if(pvec(k,nvec).lt.pvec(ip1,nvec))exit
            ip2=k
          end do
!
!         -- replace first element of descending seqence ------------------------
          isvar=pvec(ip1,nvec)
          pvec(ip1,nvec)=pvec(ip2,nvec)
          pvec(ip2,nvec)=isvar
!
!         -- change descending sequence into an ascending one -------------------
          work(ip1+1:)=pvec(ip1+1:,nvec)
          do j=1,len-ip1
            pvec(ip1+j,nvec)=work(len+1-j)
          enddo
        enddo
        return
        end
```

L.6 Low-order diagrams with symmetry factor and sign

L.6.1 First order

```
provide the order of the diagrams (integer):
order of the diagrams..................              1
nr. of all diagrams (=n!)..............              2
nr. of linked diagrams.................              2
nr. of top. distinct diagrams..........              2
sum-rule test..........................            2.0
...must reproduce number of linked diagrams

sign, symmetry factor and permutation vectors:
       1  sign*sofd=       2 p=   1   2
       2  sign*sofd=      -2 p=   2   1
```

- The vector $\mathcal{P}_1 = (1, 2)$ is the eyeglass diagram

- The vector $\mathcal{P}_2 = (2, 1)$ is the oyster diagram

L.6.2 Second order

```
provide the order of the diagrams (integer):
order of the diagrams.................              2
nr. of all diagrams (=n!).............             24
nr. of linked diagrams................             20
nr. of top. distinct diagrams.........              5
sum-rule test.........................           20.0
...must reproduce number of linked diagrams

sign, symmetry factor and permutation vectors:
       1  sign*sofd=      -2 p=   1   3   2   4
       2  sign*sofd=       1 p=   1   3   4   2
       3  sign*sofd=      -2 p=   2   3   4   1
       4  sign*sofd=       4 p=   3   4   1   2
       5  sign*sofd=      -4 p=   3   4   2   1
```

- The vector $\mathcal{P}_4 = (3, 4, 1, 2)$ is the double ring diagram
- The vector $\mathcal{P}_5 = (3, 4, 2, 1)$ is the double exchange diagram

L.6.3 Third order

```
provide the order of the diagrams (integer):
order of the diagrams.................              3
nr. of all diagrams (=n!).............            720
nr. of linked diagrams................            592
nr. of top. distinct diagrams.........             20
sum-rule test.........................          592.0
...must reproduce number of linked diagrams

sign, symmetry factor and permutation vectors:
       1  sign*sofd=       2 p=   1   3   2   5   4   6
       2  sign*sofd=      -1 p=   1   3   2   5   6   4
       3  sign*sofd=      -1 p=   1   3   4   5   2   6
       4  sign*sofd=       1 p=   1   3   4   5   6   2
       5  sign*sofd=      -2 p=   1   3   5   2   4   6
       6  sign*sofd=       1 p=   1   3   5   2   6   4
       7  sign*sofd=       3 p=   1   3   5   4   2   6
       8  sign*sofd=      -1 p=   1   3   5   6   2   4
       9  sign*sofd=       1 p=   1   3   5   6   4   2
      10  sign*sofd=       2 p=   2   3   1   5   6   4
      11  sign*sofd=      -3 p=   2   3   4   5   6   1
      12  sign*sofd=      -2 p=   2   3   5   1   6   4
      13  sign*sofd=       1 p=   2   3   5   6   1   4
      14  sign*sofd=      -1 p=   2   3   5   6   4   1
      15  sign*sofd=       6 p=   3   4   5   6   1   2
      16  sign*sofd=      -6 p=   3   4   5   6   2   1
      17  sign*sofd=      -6 p=   3   5   1   6   2   4
      18  sign*sofd=       2 p=   3   5   1   6   4   2
      19  sign*sofd=      -2 p=   3   5   2   6   4   1
      20  sign*sofd=       6 p=   3   5   6   2   4   1
```

- The vector $\mathcal{P}_{15} = (3, 4, 5, 6, 1, 2)$ is the particle-particle ladder diagram.

- The vector $\mathcal{P}_{16} = (3, 4, 5, 6, 2, 1)$ is the wheel diagram.
- The vector $\mathcal{P}_{17} = (3, 5, 1, 6, 2, 4)$ is the triple ring diagram
- The vector $\mathcal{P}_{20} = (3, 5, 6, 2, 4, 1)$ is the particle-hole ladder.

L.6.4 Fourth order

```
provide the order of the diagrams (integer):
order of the diagrams.................              4
nr. of all diagrams (=n!).............          40320
nr. of linked diagrams................          33888
nr. of top. distinct diagrams.........            107
sum-rule test.........................       33888.0
...must reproduce number of linked diagrams

sign, symmetry factor and permutation vectors:
       1  sign*sofd=      -2 p=   1   3   2   5   4   7   6   8
       2  sign*sofd=       1 p=   1   3   2   5   4   7   8   6
       3  sign*sofd=       1 p=   1   3   2   5   6   7   4   8
       4  sign*sofd=      -1 p=   1   3   2   5   6   7   8   4
       5  sign*sofd=       1 p=   1   3   2   5   7   4   6   8
       6  sign*sofd=      -1 p=   1   3   2   5   7   4   8   6
       7  sign*sofd=      -1 p=   1   3   2   5   7   6   4   8
       8  sign*sofd=       1 p=   1   3   2   5   7   6   8   4
       9  sign*sofd=       1 p=   1   3   2   5   7   8   4   6
      10  sign*sofd=      -1 p=   1   3   2   5   7   8   6   4
      11  sign*sofd=      -1 p=   1   3   4   5   2   7   8   6
      12  sign*sofd=      -1 p=   1   3   4   5   6   7   2   8
      13  sign*sofd=       1 p=   1   3   4   5   6   7   8   2
      14  sign*sofd=      -1 p=   1   3   4   5   7   2   6   8
      15  sign*sofd=       1 p=   1   3   4   5   7   2   8   6
      16  sign*sofd=       1 p=   1   3   4   5   7   6   2   8
      17  sign*sofd=      -2 p=   1   3   4   5   7   6   8   2
      18  sign*sofd=      -1 p=   1   3   4   5   7   8   2   6
      19  sign*sofd=       1 p=   1   3   4   5   7   8   6   2
      20  sign*sofd=      -1 p=   1   3   5   2   4   7   8   6
      21  sign*sofd=      -1 p=   1   3   5   2   6   7   4   8
      22  sign*sofd=       1 p=   1   3   5   2   6   7   8   4
      23  sign*sofd=      -2 p=   1   3   5   2   7   4   6   8
      24  sign*sofd=       1 p=   1   3   5   2   7   4   8   6
      25  sign*sofd=       1 p=   1   3   5   2   7   6   4   8
      26  sign*sofd=      -1 p=   1   3   5   2   7   8   4   6
      27  sign*sofd=       1 p=   1   3   5   2   7   8   6   4
      28  sign*sofd=       1 p=   1   3   5   4   2   7   8   6
      29  sign*sofd=      -1 p=   1   3   5   4   7   2   8   6
      30  sign*sofd=      -4 p=   1   3   5   4   7   6   2   8
      31  sign*sofd=       1 p=   1   3   5   4   7   8   2   6
      32  sign*sofd=      -1 p=   1   3   5   4   7   8   6   2
      33  sign*sofd=       2 p=   1   3   5   6   2   7   4   8
      34  sign*sofd=      -1 p=   1   3   5   6   2   7   8   4
      35  sign*sofd=       1 p=   1   3   5   6   4   7   8   2
      36  sign*sofd=      -2 p=   1   3   5   6   7   2   4   8
      37  sign*sofd=       1 p=   1   3   5   6   7   2   8   4
```

```
38  sign*sofd=      -1 p=   1   3   5   6   7   4   8   2
39  sign*sofd=      -1 p=   1   3   5   6   7   8   2   4
40  sign*sofd=       1 p=   1   3   5   6   7   8   4   2
41  sign*sofd=       2 p=   1   3   5   7   2   4   6   8
42  sign*sofd=      -1 p=   1   3   5   7   2   4   8   6
43  sign*sofd=       1 p=   1   3   5   7   2   8   4   6
44  sign*sofd=      -1 p=   1   3   5   7   2   8   6   4
45  sign*sofd=      -1 p=   1   3   5   7   4   2   6   8
46  sign*sofd=       1 p=   1   3   5   7   4   2   8   6
47  sign*sofd=      -1 p=   1   3   5   7   4   8   2   6
48  sign*sofd=       1 p=   1   3   5   7   4   8   6   2
49  sign*sofd=      -1 p=   1   3   5   7   6   2   8   4
50  sign*sofd=       1 p=   1   3   5   7   6   4   8   2
51  sign*sofd=       1 p=   1   3   5   7   6   8   2   4
52  sign*sofd=      -1 p=   1   3   5   7   6   8   4   2
53  sign*sofd=      -1 p=   1   3   5   7   8   2   4   6
54  sign*sofd=       1 p=   1   3   5   7   8   2   6   4
55  sign*sofd=       1 p=   1   3   5   7   8   4   2   6
56  sign*sofd=      -1 p=   1   3   5   7   8   4   6   2
57  sign*sofd=       2 p=   1   3   5   7   8   6   4   2
58  sign*sofd=      -2 p=   2   3   1   5   4   7   8   6
59  sign*sofd=       1 p=   2   3   1   5   6   7   8   4
60  sign*sofd=       1 p=   2   3   1   5   7   4   8   6
61  sign*sofd=      -1 p=   2   3   1   5   7   8   4   6
62  sign*sofd=       1 p=   2   3   1   5   7   8   6   4
63  sign*sofd=      -4 p=   2   3   4   5   6   7   8   1
64  sign*sofd=      -1 p=   2   3   4   5   7   1   8   6
65  sign*sofd=       1 p=   2   3   4   5   7   8   1   6
66  sign*sofd=      -1 p=   2   3   4   5   7   8   6   1
67  sign*sofd=      -2 p=   2   3   5   1   7   4   8   6
68  sign*sofd=       1 p=   2   3   5   1   7   8   4   6
69  sign*sofd=      -1 p=   2   3   5   1   7   8   6   4
70  sign*sofd=       2 p=   2   3   5   6   1   7   8   4
71  sign*sofd=      -2 p=   2   3   5   6   7   1   8   4
72  sign*sofd=       1 p=   2   3   5   6   7   8   1   4
73  sign*sofd=      -1 p=   2   3   5   6   7   8   4   1
74  sign*sofd=       2 p=   2   3   5   7   1   4   8   6
75  sign*sofd=      -1 p=   2   3   5   7   1   8   4   6
76  sign*sofd=       1 p=   2   3   5   7   1   8   6   4
77  sign*sofd=      -1 p=   2   3   5   7   4   1   8   6
78  sign*sofd=       1 p=   2   3   5   7   4   8   1   6
79  sign*sofd=      -1 p=   2   3   5   7   4   8   6   1
80  sign*sofd=       2 p=   2   3   5   7   6   8   4   1
81  sign*sofd=       1 p=   2   3   5   7   8   1   4   6
82  sign*sofd=      -1 p=   2   3   5   7   8   1   6   4
83  sign*sofd=      -1 p=   2   3   5   7   8   4   1   6
84  sign*sofd=       1 p=   2   3   5   7   8   4   6   1
85  sign*sofd=      -2 p=   3   4   1   5   7   8   2   6
86  sign*sofd=       1 p=   3   4   1   5   7   8   6   2
87  sign*sofd=      -2 p=   3   4   2   5   7   8   6   1
88  sign*sofd=       8 p=   3   4   5   6   7   8   1   2
89  sign*sofd=      -8 p=   3   4   5   6   7   8   2   1
90  sign*sofd=      -2 p=   3   4   5   7   1   8   2   6
91  sign*sofd=       1 p=   3   4   5   7   1   8   6   2
```

```
 92  sign*sofd=       2 p=   3   4   5   7   2   8   1   6
 93  sign*sofd=      -1 p=   3   4   5   7   2   8   6   1
 94  sign*sofd=      -2 p=   3   4   5   7   8   1   6   2
 95  sign*sofd=       2 p=   3   4   5   7   8   2   6   1
 96  sign*sofd=       8 p=   3   5   1   7   2   8   4   6
 97  sign*sofd=      -2 p=   3   5   1   7   2   8   6   4
 98  sign*sofd=      -4 p=   3   5   1   7   4   8   2   6
 99  sign*sofd=       1 p=   3   5   1   7   4   8   6   2
100  sign*sofd=       2 p=   3   5   1   7   8   2   6   4
101  sign*sofd=      -2 p=   3   5   1   7   8   4   6   2
102  sign*sofd=       4 p=   3   5   2   7   1   8   6   4
103  sign*sofd=      -1 p=   3   5   2   7   4   8   6   1
104  sign*sofd=      -2 p=   3   5   2   7   8   1   6   4
105  sign*sofd=       1 p=   3   5   2   7   8   4   6   1
106  sign*sofd=       8 p=   3   5   7   2   8   1   6   4
107  sign*sofd=      -4 p=   3   5   7   2   8   4   6   1
```

- The vector $\mathcal{P}_{88} = (3, 4, 5, 6, 7, 8, 1, 2)$ is the particle-particle ladder.
- The vector $\mathcal{P}_{89} = (3, 4, 5, 6, 7, 8, 2, 1)$ is the wheel.
- The vector $\mathcal{P}_{96} = (3, 5, 1, 7, 2, 8, 4, 6)$ is the quadruple ring diagram
- The vector $\mathcal{P}_{106} = (3, 5, 7, 2, 8, 1, 6, 4)$ is the particle-hole ladder.

Appendix M

Second-order perturbation theory

M.1 Perturbation theory

Let me do an error estimate based on second order perturbation theory in the off-site Hamilton matrix elements between pairs of Slater determinants.

I begin with the perturbation expansion by forming the derivatives of the Schrödinger equation with respect to a scale factor λ for the perturbation $\hat{W}$. The Hamiltonian has the form

$$\hat{H}(\lambda) = \hat{h} + \lambda\hat{W} \tag{M.1}$$

The perturbation expansion is obtained from the derivatives of the λ-dependent Schrödinger equation

$$\left(\hat{h} + \lambda\hat{W}\right)|\psi_n(\lambda)\rangle = |\psi_n(\lambda)\rangle E_n(\lambda)\ . \tag{M.2}$$

The derivatives are not taken at $\lambda = 0$ but at an arbitrary value of λ. This provides the next order by forming a first derivatives on the current order. The λ-dependent quantities are the energies $E_n(\lambda)$ and the wave functions $|\psi_n(\lambda)\rangle$. The λ-dependence is only made explicit where necessary. The first and second derivatives of the Schrödinger equation are

$$\left(\hat{h} + \lambda\hat{W}\right)\left|\frac{d\psi_n}{d\lambda}\right\rangle + \hat{W}|\psi_n(\lambda)\rangle \stackrel{\text{Eq. } M.2}{=} \left|\frac{d\psi_n}{d\lambda}\right\rangle E_n(\lambda) + \left|\psi_n(\lambda)\right\rangle\frac{dE_n}{d\lambda} \tag{M.3}$$

$$\left(\hat{h} + \lambda\hat{W}\right)\left|\frac{d^2\psi_n}{d\lambda^2}\right\rangle + 2\hat{W}\left|\frac{d\psi_n}{d\lambda}\right\rangle \stackrel{\text{Eq. } M.3}{=} \left|\frac{d^2\psi_n}{d\lambda^2}\right\rangle E_n(\lambda) + 2\left|\frac{d\psi_n}{d\lambda}\right\rangle\frac{dE_n}{d\lambda} + \left|\psi_n(\lambda)\right\rangle\frac{d^2E_n}{d\lambda^2} \tag{M.4}$$

In addition to the Schrödinger equation, I also need to satisfy the orthonormality.

$$\langle\psi_n(\lambda)|\psi_m(\lambda)\rangle = \delta_{m,n} \tag{M.5}$$

The first two derivatives are

$$\left\langle\frac{d\psi_n}{d\lambda}\middle|\psi_m\right\rangle + \left\langle\psi_m\middle|\frac{d\psi_n}{d\lambda}\right\rangle \stackrel{\text{Eq. } M.5}{=} 0 \tag{M.6}$$

$$\left\langle\frac{d^2\psi_n}{d\lambda^2}\middle|\psi_m\right\rangle + 2\left\langle\frac{d\psi_m}{d\lambda}\middle|\frac{d\psi_n}{d\lambda}\right\rangle + \left\langle\psi_m\middle|\frac{d^2\psi_n}{d\lambda^2}\right\rangle \stackrel{\text{Eq. } M.6}{=} 0 \tag{M.7}$$

First-order perturbation theory

First-order perturbation yields

$$\underbrace{\langle\psi_m|\Big(\hat{h}+\lambda\hat{W}\Big)}_{E_m\langle\psi_m|}\left|\frac{d\psi_n}{d\lambda}\right\rangle+\langle\psi_m|\hat{W}|\psi_n\rangle\overset{\text{Eq. M.5}}{=}\left\langle\psi_m\right|\frac{d\psi_n}{d\lambda}\Big\rangle E_n+\underbrace{\langle\psi_m|\psi_n\rangle}_{\delta_{m,n}}\frac{dE_n}{d\lambda}$$

$$\Rightarrow\qquad (E_m-E_n)\Big\langle\psi_m\left|\frac{d\psi_n}{d\lambda}\right\rangle \;=\; -\langle\psi_m|\hat{W}|\psi_n\rangle+\delta_{m,n}\frac{dE_n}{d\lambda} \tag{M.8}$$

For $m=n$, this yields the change of the eigenvalues and for $m\neq n$ it yields the first-order change of the eigenstates. The equation Eq. M.8 allow one to add of an arbitrary contribution of unperturbed $|\psi_n\rangle$ to the eigenstate.

This contribution is excluded by the normalization condition $\langle\psi_n(\lambda)|\psi_n(\lambda)\rangle=0$, Eq. M.6, which implies $\mathrm{Re}\big[\big\langle\psi_n\big|\frac{d|\psi_n\rangle}{d\lambda}\big]=0$. Only the real part is fixed. An arbitrary imaginary part may be added. This imaginary part follows from an arbitrary phase factor $\mathrm{e}^{i\varphi(\lambda)}$ multiplied with the wave function, which preserved the norm, but is contributes on additional imaginary term resulting from $\partial_\lambda \mathrm{e}^{i\varphi(\lambda)}=i\frac{\partial\varphi}{\partial\lambda}\mathrm{e}^{i\varphi(\lambda)}$

$$\begin{aligned}\frac{dE_n}{d\lambda}&=\langle\psi_n|\hat{W}|\psi_n\rangle\\ \left|\frac{d\psi_n}{d\lambda}\right\rangle&=\sum_{m;m\neq n}\frac{|\psi_m\rangle\langle\psi_m|}{E_n-E_m}\hat{W}|\psi_n\rangle+|\psi_n\rangle iC_1\end{aligned} \tag{M.9}$$

The real-valued factor C_1 can be chosen arbitrarily, because the norm-conservation determines only the real part of the prefactor of $|\psi_n\rangle$. (I have not extended this argument to degenerate states, where a λ-dependent unitary matrix can be used instead of the λ-dependent phase factor.)

Second-order perturbation theory

The second derivative yields

$$\begin{aligned}&\underbrace{\langle\psi_m|\Big(\hat{h}+\lambda\hat{W}\Big)}_{E_m\langle\psi_m|}\left|\frac{d^2\psi_n}{d\lambda^2}\right\rangle-\Big\langle\psi_m\left|\frac{d^2\psi_n}{d\lambda^2}\right\rangle E_n(\lambda)\\ &\qquad=-2\langle\psi_m|\hat{W}\left|\frac{d\psi_n}{d\lambda}\right\rangle+2\Big\langle\psi_m\left|\frac{d\psi_n}{d\lambda}\right\rangle\underbrace{\frac{dE_n}{d\lambda}}_{\langle\psi_n|\hat{W}|\psi_n\rangle}+\underbrace{\langle\psi_m|\psi_n\rangle}_{=\delta_{m,n}}\frac{d^2E_n}{d\lambda^2}\\ \Rightarrow\qquad &(E_m-E_n)\Big\langle\psi_m\left|\frac{d^2\psi_n}{d\lambda^2}\right\rangle=-2\langle\psi_m|\Big(\hat{W}-\langle\psi_n|\hat{W}|\psi_n\rangle\Big)\underbrace{\sum_{p\neq n}\frac{|\psi_p\rangle\langle\psi_p|}{E_n-E_p}\hat{W}|\psi_n\rangle}_{\left|\frac{d\psi_n}{d\lambda}\right\rangle}+\delta_{m,n}\frac{d^2E_n}{d\lambda^2}\end{aligned} \tag{M.10}$$

For $m=n$, I obtain

$$\frac{d^2E_n}{d\lambda^2}=-2\sum_{p\neq n}\frac{\langle\psi_m|\hat{W}|\psi_p\rangle\langle\psi_p|\hat{W}|\psi_n\rangle}{E_n-E_p} \tag{M.11}$$

For $m\neq n$, I obtain

$$\begin{aligned}\frac{1}{2}\Big\langle\psi_m\left|\frac{d^2\psi_n}{d\lambda^2}\right\rangle&=\frac{1}{E_n-E_m}\langle\psi_m|\Big(\hat{W}-\langle\psi_n|\hat{W}|\psi_n\rangle\Big)\sum_{p\neq n}\frac{|\psi_p\rangle\langle\psi_p|}{E_n-E_p}\hat{W}|\psi_n\rangle\\ &=-\frac{1}{E_m-E_n}\Big(\sum_{p\neq n}\frac{\langle\psi_m|\hat{W}|\psi_p\rangle\langle\psi_p|\hat{W}|\psi_n\rangle}{E_n-E_p}-\frac{\langle\psi_m|\hat{W}|\psi_n\rangle}{E_n-E_m}\langle\psi_n|\hat{W}|\psi_n\rangle\Big)\end{aligned} \tag{M.12}$$

The two equations above do not determine the change of the contribution of $|\psi_n\rangle$, which is obtained from the normalization condition $\langle\psi_n(\lambda)|\psi_n(\lambda)\rangle = 0$, which implies

$$\begin{aligned}\Big\langle\psi_n\Big|\frac{d^2\psi_n}{d\lambda^2}\Big\rangle + 2\Big\langle\frac{d\psi_n}{d\lambda}\Big|\frac{d\psi_n}{d\lambda}\Big\rangle + \Big\langle\frac{d^2\psi_n}{d\lambda^2}\Big|\psi_n\Big\rangle &= 0\\ \Big\langle\psi_n\Big|\frac{d^2\psi_n}{d\lambda^2}\Big\rangle = -\Big\langle\frac{d\psi_n}{d\lambda}\Big|\frac{d\psi_n}{d\lambda}\Big\rangle &= -\sum_{m;m\neq n}\frac{|\langle\psi_m|\hat{W}|\psi_n\rangle|^2}{(E_n-E_m)^2}\end{aligned} \tag{M.13}$$

$$\begin{aligned}\frac{1}{2}\Big|\frac{d^2\psi_n}{d\lambda^2}\Big\rangle &= +\sum_{m(\neq n)}|\psi_m\rangle\frac{1}{E_n-E_m}\Big(\sum_{p\neq n}\frac{\langle\psi_m|\hat{W}|\psi_p\rangle\langle\psi_p|\hat{W}|\psi_n\rangle}{E_n-E_p} - \frac{\langle\psi_m|\hat{W}|\psi_n\rangle}{E_n-E_m}\langle\psi_n|\hat{W}|\psi_n\rangle\Big)\\ &\quad - \frac{1}{2}|\psi_n\rangle\sum_{m;m\neq n}\frac{|\langle\psi_m|\hat{W}|\psi_n\rangle|^2}{(E_n-E_m)^2}\\ &= \sum_{m(\neq n)}|\psi_m\rangle\sum_{p\neq n}\frac{\langle\psi_m|\hat{W}|\psi_p\rangle\langle\psi_p|\hat{W}|\psi_n\rangle}{(E_n-E_p)(E_n-E_m)} - \sum_{m(\neq n)}|\psi_m\rangle\frac{\langle\psi_m|\hat{W}|\psi_n\rangle}{(E_n-E_m)^2}\langle\psi_n|\hat{W}|\psi_n\rangle\\ &\quad - |\psi_n\rangle\frac{1}{2}\sum_{m;m\neq n}\frac{|\langle\psi_m|\hat{W}|\psi_n\rangle|^2}{(E_n-E_m)^2} + |\psi_n\rangle iC_2\end{aligned} \tag{M.14}$$

The real-valued factor C_2 can be chosen arbitrarily, because the norm-conservation determines only the real value of the prefactor of $|\psi_n\rangle$. Important is that the phase factor is already included in the wave functions.

Energy and wave function in second-order perturbation theory

So far, we prepared the λ derivatives of energies and wave functions. From now on, we use the Taylor expansion at $\lambda = 0$.

$$E_n(\lambda) = E_n(0) + \lambda\,\frac{dE_n}{d\lambda}\Big|_{\lambda=0} + \frac{1}{2}\lambda^2\,\frac{d^2E_n}{d\lambda^2}\Big|_{\lambda=0} \tag{M.15}$$

In the following I indicate the unperturbed values with $\lambda = 0$ by a bar ontop of the symbol, i.e. $\bar{E}_n = E_n(\lambda = 0)$ and $|\bar{\psi}_n\rangle = |\psi_n(\lambda = 0)\rangle$. I obtain the energies up to second order in λ as

$$E_n(\lambda) = \langle\bar{\psi}_n|\Big(h + \lambda\hat{W}\Big)|\bar{\psi}_n\rangle + \lambda^2\sum_{m;m\neq n}\frac{|\langle\bar{\psi}_m|\hat{W}|\bar{\psi}_n\rangle|^2}{\bar{E}_n-\bar{E}_m} + O(\lambda^3) \tag{M.16}$$

and the eigenstates as

$$\begin{aligned}|\psi_n(\lambda)\rangle &= |\bar{\psi}_n\rangle + \Big(\sum_{m(\neq n)}\frac{|\bar{\psi}_m\rangle\langle\bar{\psi}_m|}{\bar{E}_n-\bar{E}_m}\Big)\hat{W}|\bar{\psi}_n\rangle - \underbrace{\Big(\sum_{m(\neq n)}\frac{|\bar{\psi}_m\rangle\langle\bar{\psi}_m|}{(\bar{E}_n-\bar{E}_m)^2}\Big)\hat{W}|\bar{\psi}_n\rangle\langle\bar{\psi}_n|\hat{W}|\bar{\psi}_n\rangle}_{\text{correction 1st order energy shift}}\\ &\quad \underbrace{- |\bar{\psi}_n\rangle\frac{1}{2}\sum_{m(\neq n)}\frac{|\langle\bar{\psi}_m|\hat{W}|\bar{\psi}_n\rangle|^2}{(\bar{E}_n-\bar{E}_m)^2}}_{\text{normalization 1st order}} + \underbrace{\Big(\sum_{m(\neq n)}\frac{|\bar{\psi}_m\rangle\langle\bar{\psi}_m|}{\bar{E}_n-\bar{E}_m}\Big)\hat{W}\Big(\sum_{p\neq n}\frac{|\bar{\psi}_p\rangle\langle\bar{\psi}_p|}{\bar{E}_n-\bar{E}_p}\Big)\hat{W}|\bar{\psi}_n\rangle}_{\text{true second order}} + O(\lambda^3)\end{aligned} \tag{M.17}$$

The wave function agrees with the socond order corrections on Wikipedia `https://en.wikipedia.org/wiki/Perturbation_theory_(quantum_mechanics)` retrieved June 24, 2022.

Second-order perturbation theory with Green's functions

Editor: This section with Green's function is unfinished! The equations are partly incorrect.

Let me use perturbation theory of energies and wave functions to construct the perturbed Green's functions. Here the discussion is limited to the one-particle Hilbert space, because the Green's function is an operator in the one-particle Hilbert space, and therefore also the perturbation $\hat{W}$ must be in the same space.

$$\hat{G}(\epsilon) = \sum_m \frac{|\psi_m\rangle\langle\psi_m|}{E - E_m} \tag{M.18}$$

In the summations for the perturbation theory the pole is always excluded. This can be achieved by going into the complex plane

$$\hat{G}(\epsilon) = \lim_{\eta\to 0+} \sum_m |\psi_m\rangle \frac{1}{E - E_m + i\eta}\langle\psi_m| \tag{M.19}$$

$$\hat{\bar{G}}(\epsilon) = \sum_m \frac{|\bar{\psi}_m\rangle\langle\bar{\psi}_m|}{E - \bar{E}_m} \tag{M.20}$$

Editor: In the following, the singularities of the Green's functions are not treated properly. In the perturbation expansion, the pole the singular term is removed.

$$E_n(\lambda) = \bar{E}_n + \lambda\langle\bar{\psi}_n|\hat{W}|\bar{\psi}_n\rangle + \lambda^2\langle\bar{\psi}_n|\hat{W}\hat{\bar{G}}(\bar{E}_n)\hat{W}|\bar{\psi}_n\rangle + O(\lambda^3) \tag{M.21}$$

In the following, I will use

$$\partial_\epsilon G(\epsilon) = \partial_\epsilon \sum_m \frac{|\psi_m\rangle\langle\psi_m|}{E - E_m} = -\sum_m \frac{|\psi_m\rangle\langle\psi_m|}{(E - E_m)^2} = -\hat{G}^2(\epsilon) \tag{M.22}$$

$$\begin{aligned}
|\psi_n(\lambda)\rangle = {} & |\bar{\psi}_n\rangle + \sum_{m;m\neq n} \frac{|\bar{\psi}_m\rangle\langle\bar{\psi}_m|}{\bar{E}_n - \bar{E}_m}\hat{W}|\bar{\psi}_n\rangle \\
& - \sum_{m(\neq n)} |\psi_m\rangle \frac{1}{\bar{E}_m - \bar{E}_n} \sum_{p\neq n} \frac{\langle\bar{\psi}_m|\hat{W}|\bar{\psi}_p\rangle\langle\bar{\psi}_p|\hat{W}|\bar{\psi}_n\rangle}{\bar{E}_n - \bar{E}_p} - \sum_{m(\neq n)} |\psi_m\rangle \frac{1}{\bar{E}_m - \bar{E}_n} \frac{\langle\bar{\psi}_m|\hat{W}|\bar{\psi}_n\rangle}{\bar{E}_n - \bar{E}_m}\langle\bar{\psi}_n|\hat{W}|\bar{\psi}_n\rangle \\
& - |\bar{\psi}_n\rangle \frac{1}{2} \sum_{m;m\neq n} \frac{|\langle\bar{\psi}_m|\hat{W}|\bar{\psi}_n\rangle|^2}{(\bar{E}_n - \bar{E}_m)^2} + O(\lambda^3) \\
= {} & |\bar{\psi}_n\rangle + \bar{G}(\bar{E}_n)\hat{W}|\bar{\psi}_n\rangle + \bar{G}(\bar{E}_n)\hat{W}\bar{G}(\bar{E}_n)\hat{W}|\bar{\psi}_n\rangle \underbrace{-\bar{G}^2(\bar{E}_n)\hat{W}|\bar{\psi}_n\rangle\langle\bar{\psi}_n|\hat{W}|\bar{\psi}_n\rangle}_{+(\partial_\lambda E_n)\partial_E \hat{\bar{G}}(E)\big|_{\bar{E}_n}\hat{W}|\psi_n\rangle} \\
& - |\bar{\psi}_n\rangle \frac{1}{2}\langle\bar{\psi}_n|\hat{W}\hat{G}^2(\bar{E}_n)\hat{W}|\bar{\psi}_n\rangle + O(\lambda^3) \\
= {} & |\bar{\psi}_n\rangle + \underbrace{\bar{G}(E_n(\lambda))\hat{W}|\psi_n\rangle}_{\bar{G}(\bar{E}_n)\hat{W}|\bar{\psi}_n\rangle + (\partial_\lambda E_n)\partial_E \hat{\bar{G}}(E)\big|_{\bar{E}_n}\hat{W}|\psi_n\rangle} + \bar{G}(\bar{E}_n)\hat{W}\bar{G}(\bar{E}_n)\hat{W}|\bar{\psi}_n\rangle \\
& - |\bar{\psi}_n\rangle \frac{1}{2}\langle\bar{\psi}_n|\hat{W}\hat{G}(\bar{E}_n)^2\hat{W}|\bar{\psi}_n\rangle + O(\lambda^3)
\end{aligned} \tag{M.23}$$

$$\begin{aligned}
\hat{G}^{-1}(E) &= \hat{\bar{G}}^{-1}(E) - \hat{W} \\
\Rightarrow \quad \hat{\bar{G}}(E) &= \hat{G}(E) - \hat{\bar{G}}(E)\hat{W}\hat{G}(E) \\
\Rightarrow \quad \hat{G}(E) &= \hat{\bar{G}}(E) + \hat{\bar{G}}(E)\hat{W}\hat{G}(E)
\end{aligned} \tag{M.24}$$

M.2 Ensembles of Slater determinants

In the chapter Eq. 2 on weakly interacting systems, I described an division Eq. 2.99 of the total energy of an interacting Hamiltonian into one contribution, which is the energy of an ensemble of Slater determinants, and a rest. The latter has been named the entanglement energy. Here, I use second-order approxmation theory to estimate the entanglement energy.

Let me divide the Hamiltonian $\hat{H} = \hat{h} + \hat{W}$ into a term diagonal in a basis of Slater determinants and the off-diagonal terms as in Eq. 2.99. The off-diagonal terms are then treated in second-order perturbation theory.

$$\hat{H}(\lambda) = \sum_{\vec{\sigma}} |\vec{\sigma}\rangle\langle\vec{\sigma}|\hat{H}|\vec{\sigma}\rangle\langle\vec{\sigma}| + \lambda \sum_{\vec{\sigma},\vec{\sigma'};\vec{\sigma}\neq\vec{\sigma'}} |\vec{\sigma}\rangle\langle\vec{\sigma}|\hat{H}|\vec{\sigma'}\rangle\langle\vec{\sigma'}| \tag{M.25}$$

The perturbation expansion depends on the one-particle basisset used to define the set of Slater determinants. If the Slater determinants are formed from the natural orbitals, the zero-th order contains the mean-field energy of the **thermal Hartree-Fock approximation** (THFA) and the energy due to **correlated occupation-number fluctuations** . The first order term is responsible for what I call the the **entanglement energy**.

The eigenvalues of $\hat{H}(\lambda)$ in second-order perturbation theory are

$$\begin{aligned} E_{\vec{\sigma}}(\lambda) &\overset{\text{def}}{=} \langle\Phi_{\vec{\sigma}}(\lambda)|\hat{H}(\lambda)|\Phi_{\vec{\sigma}}(\lambda)\rangle \\ &\overset{\text{Eq. } M.16}{=} \langle\vec{\sigma}|\hat{H}|\vec{\sigma}\rangle + \sum_{\vec{\sigma'};\vec{\sigma}\neq\vec{\sigma'}} \frac{|\langle\vec{\sigma}|\hat{H}|\vec{\sigma'}\rangle|^2}{\langle\vec{\sigma}|\hat{H}|\vec{\sigma}\rangle - \langle\vec{\sigma'}|\hat{H}|\vec{\sigma'}\rangle} + O(\lambda^3) \end{aligned} \tag{M.26}$$

The Hamiltonian in the equation above is the full Hamiltonian $\hat{H}(\lambda)$ including off-diagonal terms. The $|\Phi_{\vec{\sigma}}(\lambda)\rangle$ are the eigenstates of the perturbed Hamiltonian $\hat{H}(\lambda)$, that are connected through the perturbation expansion to the Slater determinant $|\vec{\sigma}\rangle$, i.e. $|\Phi_{\vec{\sigma}}(\lambda = 0)\rangle = |\vec{\sigma}\rangle$. The Slater determinants $|\vec{\sigma}\rangle$ are also the eigenstates of the unperturbed Hamiltonian $H(0) = \sum_{\vec{\sigma}} |\vec{\sigma}\rangle\langle\vec{\sigma}|\hat{H}|\vec{\sigma}\rangle\langle\vec{\sigma}|$ Similarly the eigenvalues $E_{\vec{\sigma}}(\lambda)$ inherit the label from the zeroth order solutions.

Let me now consider an ensemble $\{P_q, |\Phi_q(\lambda)\rangle\}$, with the λ-dependent eigenstates of the Hamiltonian as microstates $|\Phi_q\rangle$. The states are labeled according to the zero-th order Eigenstates so that $q = \vec{\sigma}$.

The goal is to determine the energy of the ensemble in second-order perturbation theory

$$E = \sum_q P_q E_q(\lambda) \qquad \text{with } \hat{H}(\lambda)|\Psi_q(\lambda)\rangle = |\Psi_q(\lambda)\rangle E_q(\lambda) \tag{M.27}$$

This yields

$$\begin{aligned} E[\{P_{\vec{\sigma}}\}] &= \sum_{\vec{\sigma}} P_{\vec{\sigma}} E_{\vec{\sigma}}(\lambda) = \sum_{\vec{\sigma}} P_{\vec{\sigma}} \langle\vec{\sigma}|\hat{H}|\vec{\sigma}\rangle + \sum_{\vec{\sigma},\vec{\sigma'};\vec{\sigma}\neq\vec{\sigma'}} P_{\vec{\sigma}} \frac{|\langle\vec{\sigma}|\hat{H}|\vec{\sigma'}\rangle|^2}{\langle\vec{\sigma}|\hat{H}|\vec{\sigma}\rangle - \langle\vec{\sigma'}|\hat{H}|\vec{\sigma'}\rangle} + O(\lambda^3) \\ &= \sum_{\vec{\sigma}} P_{\vec{\sigma}} \langle\vec{\sigma}|\hat{H}|\vec{\sigma}\rangle + \frac{1}{2} \sum_{\vec{\sigma},\vec{\sigma'};\vec{\sigma}\neq\vec{\sigma'}} \left(P_{\vec{\sigma}} - P_{\vec{\sigma'}}\right) \frac{|\langle\vec{\sigma}|\hat{H}|\vec{\sigma'}\rangle|^2}{\langle\vec{\sigma}|\hat{H}|\vec{\sigma}\rangle - \langle\vec{\sigma'}|\hat{H}|\vec{\sigma'}\rangle} + O(\lambda^3) \end{aligned} \tag{M.28}$$

Thus the correction to the ensemble energy from second order perturbation theory is

$$\Delta E = \sum_{\vec{\sigma}} P_{\vec{\sigma}} E_{\vec{\sigma}} - \sum_{\vec{\sigma}} P_{\vec{\sigma}} \langle\vec{\sigma}|\hat{H}|\vec{\sigma}\rangle = \frac{1}{2} \sum_{\vec{\sigma},\vec{\sigma'};\vec{\sigma}\neq\vec{\sigma'}} \left(P_{\vec{\sigma}} - P_{\vec{\sigma'}}\right) \frac{|\langle\vec{\sigma}|\hat{H}|\vec{\sigma'}\rangle|^2}{\langle\vec{\sigma}|\hat{H}|\vec{\sigma}\rangle - \langle\vec{\sigma'}|\hat{H}|\vec{\sigma'}\rangle} \tag{M.29}$$

When we use the probabilities as $P_\sigma = c_\sigma^* c_\sigma$ of a many-particle wave function $|\Phi\rangle = \sum_{\vec{\sigma}} |\vec{\sigma}\rangle c_{\vec{\sigma}}$, the entanglement energy is approximated as

Editor: Can one establish a reasonable link to Möller Plesset perturbation theory? [141]

Appendix N

Dictionary and Symbols

N.1 English-German Dictionary

caveat	Vorbehalt
coincidence	Übereinstimmung
convolution	Faltung
cross section	Wirkungsquerschnitt
esthetics	Ästetik
factorial	Fakultät (mathematische Operation)
faculty	Fakultät (akademische Verwaltungseinheit)
for the sake of ...	um ... willen (gen)
formidable	gewaltig, eindrucksvoll
full width at half maximum	Halbwertsbreite
propagator	Zeitentwicklungsoperator
commutate	kommutieren
rank	Rang
scattering amplitude	Streuamplitude
union	Vereinigung
without loss of generality	ohne Beschränkung der Allgemeinheit
wlog	oBdA (ohne Beschränkung der Allgemeinheit)
work function	Austrittsarbeit

N.2 Explanations

- caveat: Latin, a modifying or cautionary detail to be considered

N.3 Symbols

The list of symbols is not complete, nor is the usage of symbols unique. The list shall give a guidance.
Editor: The notes will not be completely consistent in the choice of symbols. Editor: Later, we may include also a reference to the equations defining the symbols.

Editor: The choice of symbols is a compromise between symbols that are (1) easily differentiated both in printed and hand-written form, that (2) exhibit similarity if there meaning is related, and (3) similarity to symbols commonly used in the literature.

N.4 Mathematical Symbols

- $\forall$ "for all".
- $[A,B]_- = [A,B] = AB - BA$: **commutator** of A and B. A and B may be matrices or operators.
- $[A,B]_+ = AB + BA$: **anti-commutator** of A and B. A and B may be matrices or operators.
- $\vec{a} \times \vec{b}$: **vector product** between two three dimensional vectors $\vec{a}$ and $\vec{b}$.

$$\vec{a} \times \vec{b} = \begin{pmatrix} a_y b_z - a_z b_y \\ a_z b_x - a_x b_z \\ a_x b_y - a_y b_x \end{pmatrix} \tag{N.1}$$

- $\vec{a} \otimes \vec{b}$: **outer product** or **dydadic product** of two vectors $\vec{a}$ and $\vec{b}$.

$$\left(\vec{a} \otimes \vec{b}\right)_{i,j} = a_i b_j \tag{N.2}$$

- $\det|\boldsymbol{A}|$: **determinant** of matrix $\boldsymbol{A}$
- $\mathrm{perm}|\boldsymbol{A}|$: **permanent** of matrix $\boldsymbol{A}$. The permanent is computed like the determinant with the exceptions that all terms are summed up without the sign changes for permutations.
- $\delta_{i,j}$: **Kronecker delta**

$$\delta_{i,j} = \begin{cases} 1 & \text{for } i = j \\ 0 & \text{else} \end{cases} \tag{N.3}$$

- $\delta(\vec{x})$: **Dirac's delta function** defined by

$$\forall_{f(x)} \int dx\, f(x)\delta(x) = f(0) \tag{N.4}$$

  which holds for all differentiable functions $f(x)$. The delta function of a vector is the product of the delta functions of its components.

- $\epsilon_{i_1,\ldots,i_N}$ **Levi-Civita Symbol** or **fully antisymmetric tensor**
- $\theta(x)$: **Heaviside step function**. A subscript defines a special region where the Heaviside is nonzero.
- $\mathrm{sgn}(x)$: sign function.
- $\mathrm{stat}_x F(x)$: value of the function $F(x)$ at its stationary point with respect to x. The stationary point may be a maximum, a minimum or a saddle point.
- $\mathrm{Tr}[\boldsymbol{A}]$: trace of a matrix A.
- $\sum_{x \in \mathbb{X}}$ sum over all elements x in the set $\mathbb{X}$.
- $\sum_{\sigma \in \{\uparrow,\downarrow\}}$ sum of the spin quantum number σ of a spin-$\frac{1}{2}$, which can assume values $\uparrow$ and $\downarrow$. The states are defined by the eigenvalue equations $\hat{S}_z|\uparrow\rangle = |\uparrow\rangle\left(+\frac{\hbar}{2}\right)$ and $\hat{S}_z|\downarrow\rangle = |\downarrow\rangle\left(-\frac{\hbar}{2}\right)$

N.5 Vectors, matrices, operators, functions, etc.

	typed	blackboard
vector	$\vec{a}$	$\vec{a}$
matrix	$\boldsymbol{A}$	$\underline{\underline{A}}$
state	$\|a\rangle$	$\|a\rangle$
operator	$\hat{A}$	$\hat{A}$

Vectors are indicated by a vector arrow such as $\vec{x}$. Matrices are made bold face such as $\boldsymbol{A}$. I have purposely combined two different notation, because this makes the difference optically more evident. I also used the psychological analogy of using an arrow for a one-dimensionally extended object, and "fat symbol" for a two-dimensionally extended object. On the blackboard, I use two underscores for matrices.

Functionals are indicated by an argument in brackets such as $F[y]$, where $y(x)$ is the function in the argument. If function arguments are mixed with normal arguments they are combined as in $F([y], x)$.

Commutators and anticommutators are indicated by brackets. The commutator has a minus sign as subscript or no subscript. An anticommutator always carries a plus sign as subscript.

- rather than using an integer counter for all summations $\sum_{i=1}^{N}$, I often use sums over sets of quantities such as $\sum_{\sigma\in\{\uparrow,\downarrow\}}$ for a sum over spin directions or $\{\sum_{\vec{t}}\}$ for a sum over all lattice translations. When the meaning is obvious, I drop the curly brackets as in $\sum_{\vec{t}}$. The curly brackets should not be dropped for a set of integers, because that would make the expression ambiguous.
- When the summation bounds or integration regions are dropped, "all values" of "the whole range" is implied.

N.6 Generic conventions

- Thermodynamic quantites have arguments related to reservoirs as subscripts.

N.7 Symbols of physical quantities

- t^+ variable t increased by an infinitesimally small, positive number. Useful for discontinuous functions.
- $\hat{c}^+_{H,\alpha}(t)$ creation operator for orbital α in the Heisenberg picture in the complex time plane. Equals $\hat{c}^\dagger_{H,\alpha}(t)$ on the real-time axis.
- $\hat{\rho}^{(1)}$ one-particle-reduced density matrix
- $\hat{\rho}^{(2)}$ two-particle-reduced density matrix
- $\hat{\rho}^{vN}_{T,\mu}$, $\hat{\rho}_{T,\mu}$ von-Neumann density matrix, many-particle density matrix
- $\hat{\rho}^{vN}_{T,\mu}$ von-Neumann density matrix, many-particle density matrix
- $\hat{\rho}^{vN,(0)}_{T,\mu}$, $\hat{\rho}^{(0)}_{T,\mu}$ many-particle density matrix or statistical operator specifically of the non-interacting system
- $\hat{\rho}^{vN,(W)}_{T,\mu}$, $\hat{\rho}^{(W)}_{T,\mu}$ many-particle density matrix or statistical operator specifically of the interacting system

- $Z_{T,\mu}$ partition function of the grand potential
- $Z^{(0)}_{T,\mu}$ partition function of the grand potential specifically for the non-interacting system
- $Z^{(W)}_{T,\mu}$ partition function of the grand potential specifically for the interacting system
- $\Omega_{T,\mu}$ grand potential
- $A_{T,N}$ Helmholtz potential
- $|\mathcal{O}\rangle$ vacuum state
- $|\varnothing\rangle$ zero state
- $\hat{c}^\dagger_\alpha$,$\hat{c}_\alpha$ creation and annihilation operators in a general basisset. Typically they refer local orbitals.
- $\hat{a}^\dagger_n$, $\hat{a}_n$ creation and annihilation operators in a basisset of one-particle eigenstates of the non-interacting Hamiltonian.
- $\hat{\psi}^\dagger(\vec{x})$, $\hat{\psi}(\vec{x})$ creation and annihilation operators in a real-space-and-spin basisset
- $\vec{x}$ composite vector containing a spatial coordinate $\vec{r}$ and a spin index σ.
- $|\vec{x}\rangle$ basis state of the real-space-and-spin representation. Eigenstate to position operator with eigenvalue $\vec{r}$ and of $\hat{S}_z$ with eigenvalue $\frac{\hbar}{2}\sigma$, where σ is the spin index.
- $|\chi_\alpha\rangle$ local orbital. Typically non-orthonormal. When they are orthonormal they can be Wannier orbitals.
- $\langle\pi_\alpha|$ projector function for the orbital $|\chi_\alpha\rangle$
- $|\varphi_j\rangle$: element of a orthonormal one-particle basisset. Often they are natural orbitals or the eigenstates of a one-particle Hamiltonian. Typically they are Bloch states.
- $\left\langle \hat{A} \right\rangle_{T,\mu} = \mathrm{Tr}\left[\hat{\rho}_{T,\mu}\hat{A}\right]$ thermal expectation value of the observable $\hat{A}$ in the grand ensemble.Editor: (legacy notation) Should be $A_{T,\mu}$.
- $\hat{W}$ interaction operator or generally perturbation of an unperturbed Hamilton operator
- $\hat{H}^{(0)}$ unperturbed Hamilton operator
- $\hat{h}$ unperturbed Hamilton operator (without interaction or time dependence)
- $\hat{H}^{(W)}$ Hamilton operator including the interaction or perturbation
- n, $n^{(1)}$ electron density
- E_H Hartree energy
- E_X exchange energy
- E_{xc} exchange-correlation energy
- T kinetic energy
- $\hat{G}(t,t')$ Green's function expressed as operator in the one-particle Hilbert space
- $\hat{D}(\epsilon)$ density of states expressed as operator in the one-particle Hilbert space
- $\hat{U}(t,t')$: propagator in the one-particle Hilbert space
- $\hat{\mathcal{U}}(t,t')$: propagator in the Fock space.

- $\hat{\Sigma}(t,t')$: usually the self energy. Also used for a general retarded potential.
- $\mathbb{A}_n$ set of all closed, labeled diagrams of order n in the interaction.
- $\mathbb{L}_n$ set of all closed, labeled, linked diagrams of order n in the interaction.
- $\mathbb{T}_n$ set of all closed, unlabeled (topologically inequivalent), linked diagrams of order n in the interaction.
- $\mathbb{S}_n$ set of all closed, unlabeled (topologically inequivalent), skeleton diagrams of order n in the interaction.
- $S(D)$ symmetry factor of an unlabeled diagram D

N.8 Comparison with Fetter Walecka

The Green's function G^{FW} in the Book of Fetter Walecka is related to our definition by

$$G = \frac{1}{\hbar} G^{FW}$$

see Eq. FW-7.1.

N.9 Greek Alphabet

A	α	alpha	N	ν	nu
B	β	beta	Ξ	ξ	ksi
Γ	γ	gamma	O	o,	omicron
Δ	δ	delta	Π	π, ϖ	pi
E	ϵ, ε	epsilon	P	ρ, ϱ	rho
Z	ζ	zeta	Σ	σ, ς	sigma
H	η	eta	T	τ	tau
Θ	θ, ϑ	theta	Υ	υ	upsilon
I	ι	iota	Φ	ϕ, φ	phi
K	κ	kappa	X	χ	chi
Λ	λ	lambda	Ψ	ϕ	phi
M	μ	mu	Ω	ω	omega

Appendix O

About the PhiSX Series

O.1 Philosophy of the PhiSX Series

In the ΦSX series, I tried to implement what I learned from the feedback given by the students which attended the courses and that relied on these books as background material.

The course should be **self-contained**. There should not be any statements "as shown easily..." if, this is not true. The reader should not need to rely on the author, but he should be able to convince himself, if what is said is true. I am trying to be as complete as possible in covering all material that is required. The basis is the mathematical knowledge. With few exceptions, the material is also developed in a sequence so that the material covered can be understood entirely from the knowledge covered earlier.

The derivations shall be **explicit**. The novice should be able to step through every single step of the derivation with reasonable effort. An advanced reader should be able to follow every step of the derivations even without paper and pencil.

All **units** are explicit. That is, formulas contain all fundamental variables, which can be inserted in any desirable unit system. Expressions are consistent with the SI system, even though I am quoting some final results in units, that are common in the field.

The equations that enter a specific step of a derivation are noted as **hyperlinks** ontop of the equation sign. The experience is that the novice does not immediately memorize all the material covered and that he is struggling with the math, so that he spends a lot of time finding the rationale behind a certain step. This time is saved by being explicit about it. The danger that the student gets dependent on these indications, is probably minor, as it requires some effort for the advanced reader to look up the assumptions, an effort he can save by memorizing the relevant material.

Important results and equations are highlighted by including them in **boxes**. This should facilitate the preparations for examinations.

Portraits of the key researchers and short biographical notes provide independent associations to the material. A student may not memorize a certain formula directly, but a portrait. From the portrait, he may associate the correct formula. The historical context provides furthermore an independent structure to organize the material.

The two first books are in german (That is the intended native language) in order to not add complications to the novice. After these first books, all material is in English. It is mandatory that the student masters this language. Most of the scientific literature is available only in English. English is currently the language of science, and science is absolutely dependent on international contacts.

I tried to include many graphs and figures. The student shall become used to use all his senses in particular the **visual sense**.

I have slightly modified the selection of the material commonly tought in most courses. Some topics, which I consider of mostly historical relevance I have removed. Others such as the Noether

theorem, I have added. Some, like chaos, stochastic processes, etc. I have not added yet.

Specific remarks for the "Advanced Solid-State Theory"

Editor: check these points for repetitions and eventually integrate into the general set of remarks if possible.

- Often, I provide **outlook** in the solutions to the exercises. This outlook does not aim at a comprehensive description, but rather to connect to prior knowledge or to provide a link to external sources for further reading.
- The exercises aim at treating **minimal models**. In the many-particle description of solids, model systems are often used to study and to describe certain physical effects.
- I took several measures to support students in keeping the **focus** in the learning process. These are (1) **boxes**, highlighting, the most relevant equations. (2) The **index** provides a list of relevant keywords. (3) The **introduction and summaries** of the chapters shall set the material into context.
- Overloaded terminology:
  - In the field the term **vacuum state** is used to denote the ground state such as the Fermi sea. While this use is correct in a world of electrons and holes, it still can be mistaken.
  - the non-interacting part of the Hamiltonian is often called the **kinetic energy**. This stems from the free-electron gas and is an illegal use.

O.2 About the Author

Prof. Dr. rer. nat Peter E. Blöchl studied physics at Karlsruhe University of Technology in Germany. Subsequently he joined the Max Planck Institutes for Materials Research and for Solid-State Research in Stuttgart, where he developed of electronic-structure methods related to the LMTO method and performed first-principles investigations of interfaces. He received his doctoral degree in 1989 from the University of Stuttgart.

Following his graduation, he joined the renowned T.J. Watson Research Center in Yorktown Heights, NY in the US on a World-Trade Fellowship. In 1990 he accepted an offer from the IBM Zurich Research Laboratory in Ruschlikon, Switzerland, which had just received two Nobel prices in Physics (For the Scanning Tunneling Microscope in 1986 and for the High-Temperature Superconductivity in 1987). He spent the summer term 1995 as visiting professor at the Vienna University of Technology in Austria, from where he was later awarded the habilitation in 1997. In 2000, he left the IBM Research Laboratory after a 10-year period and accepted an offer to be professor for theoretical physics at Clausthal University of Technology in Germany. Since 2003, Prof. Blöchl is member of the Braunschweigische Wissenschaftliche Gesellschaft (Academy of Sciences).

The main thrust of Prof. Blöchl's research is related to ab-initio simulations, that is, parameter-free simulation of materials processes and molecular reactions based on quantum mechanics. He developed the Projector Augmented Wave (PAW) method, one of the most widely used electronic structure methods to date. This work has been cited over 45,000 times.[1] It is among the 100 most cited scientific papers of all times and disciplines[2] , and it is among the 10 most-cited papers out of more than 500,000 published in the 120-year history of Physical Review. [3] Next to the research related to simulation methodology, his research covers a wide area from biochemistry, solid state chemistry to solid state physics and materials science. Prof. Blöchl contributed to 8 Patents and

[1] Researcher ID: B-3448-2012
[2] R. van Noorden, B. Maher and R. Nuzzo, Nature 514, 550 (2014)
[3] Oct. 15, 2014, search in the Physical Review Online Archive with criteria "a-z".

published about 100 research publications, among others in well-known Journals such as “Nature”. The work of Prof. Blöchl has been cited over 60,000 times, and he has an H-index of 44.[4]

[4]Researcher ID: B-3448-2012

Bibliography

[1] Peter E. Blöchl. ΦSX: Introduction to Solid State Theory. Blöchl, 2017. URL https://phisx.org/.

[2] G. Stefanucci and R. van Leeuwen. Nonequilibrium Many-Body theory of Quantum systems, volume 1. Cambridge University Press, 2013.

[3] A.L. Fetter and J.D. Walecka. Quantum Theory of Many-Particle Systems. McGraw-Hill, New York, 1971. ISBN 978-0-07-020653-3. URL http://store.doverpublications.com/0486428273.html.

[4] R.D. Mattuck. A Guide to Feynman Diagrams in the Many-Body Problem. McGraw-Hill, 1967.

[5] Peter Fulde. Electron Correlations in Molecules and Solids. Springer, 1995.

[6] J.W. Negele and H. Orland. Quantum Many-Particle Physics. Westview Press, 1988.

[7] W.-D. Schöne, C. Timm, and W.-D. Schotte. Theoretische festkörperphysik, teil 1. http://kolxo3.tiera.ru/_Papers/TU%20Wien%20Scripta/Physik/Festkoerperphysik/Theoretische_Festkoerperphysik_I_001(de)(189s).pdf, 2001.

[8] A. D. McNaught and A. Wilkinson, editors. IUPAC Compendium of Chemical Terminology. Blackwell Scientific Publications, Oxford, 2 edition, 1997. ISBN 0-9678550-9-8. doi: 10.1351/goldbook. URL https://doi.org/10.1351/goldbook.

[9] E.R. Cohen, T. Cvitas, J.G. Frey, B. Holmström, K. Kuchitsu, R. Marquardt, I. Mills, F. Pavese, M. Quack, J. Stohner, H.L. Strauss, M. Takami, and A.J. Thor, editors. Quantities, Units and Sumbols in Physical Chemistry, IUPAC Green Book. IUPAC and RSC Publishing, Cambridge, 3 edition, 2008. URL http://media.iupac.org/publications/books/gbook/IUPAC-GB3-2ndPrinting-Online-22apr2011.pdf.

[10] Wolfgang Walter. Einführung in die Theorie der Distributionen. BI-Wiss.Verl., 1994.

[11] G.H. Wannier. The structure of electronic excitation levels in insulating crystals. Phys. Rev., 52:191, 1937.

[12] P. E. Blöchl. Projector augmented-wave method. Phys. Rev. B, 50:17953–17979, Dec 1994. doi: 10.1103/PhysRevB.50.17953. URL http://link.aps.org/doi/10.1103/PhysRevB.50.17953.

[13] Peter E. Blöchl. ΦSX: Theoretische Physik I, Klassische Mechanik. Blöchl, 2015. URL https://phisx.org/.

[14] Peter E. Blöchl. ΦSX: Theoretical Physics III, Quantum Theory. Blöchl, 2015. URL https://phisx.org/.

[15] J. Hubbard. Electron correlations in narrow energy bands. Proc. R. Soc. Lond. A, 276:238, 1963. ISSN 0080-4630. doi: 10.1098/rspa.1963.0204.

[16] J. Kanamori. Electron correlation and ferromagnetism of transition metals. Prog. Theor. Phys., 30:275, 1963. doi: doi:10.1143/PTP.30.275. URL http://ptp.oxfordjournals.org/content/30/3/275.

[17] Martin C. Gutzwiller. Effect of correlation on the ferromagnetism of transition metals. Phys. Rev. Lett., 10(5):159, 1963. doi: 10.1103/PhysRevLett.10.159.

[18] Peter E. Blöchl. ΦSX: Quantum Mechanics of the Chemical Bond. Blöchl, 2015. URL https://phisx.org/.

[19] M.J. Rice and E.J. Mele. Elementary excitations of a linearly conjugated diatomic polymer. Phys. Rev. Lett., 49:1455, 1982.

[20] W.P. Su and J.R. Schrieffer. Soliton dynamics in polyacetylene. Proc. Natl. Acad. Sci. USA, 77:5626, 1980.

[21] Peter E. Blöchl. ΦSX: Theoretische Physik II, Elektrodynamik. Blöchl, 2015. URL https://phisx.org/.

[22] J.C. Slater. The theory of complex spectra. Phys. Rev., 34:1293, 1929.

[23] V. Fock. Näherungsmethode zur lösung des quantenmechanischen mehrkörperproblems. Zeitschr. Phys., 61:126, 1930.

[24] V. Fock. "selfconsistent field" mit austausch für natrium. Zeitschr. Phys., 62:795, 1930.

[25] P.W. Anderson. Concepts in Solids; Lectures on the Theory of Solids. W.A. Bejnamin, Inc, New York, 1963.

[26] Per-Olov Löwdin. Quantum theory of many-particle systems. i. physical interpretations by means of density matrices, natural spin-orbitals, and convergence problems in the method of configurational interaction. Phys. Rev., 97:1474, 1955. doi: 10.1103/PhysRev.97.1474. URL http://link.aps.org/doi/10.1103/PhysRev.97.1474.

[27] A.J. Coleman. Structure of fermion density matrices. Rev. Mod. Phys., 35:668, 1963. doi: 10.1103/RevModPhys.35.668. URL http://link.aps.org/doi/10.1103/RevModPhys.35.668.

[28] Mark S. Hybertsen and Steven G. Louie. Electron correlation in semiconductors and insulators: Band gaps and quasiparticle energies. Phys. Rev. B, 34:5390, 1986.

[29] Pierre Hohenberg and Walter Kohn. Inhomogeneous electron gas. Phys. Rev., 136:B864, 1964. doi: 10.1103/PhysRev.136.B864. URL http://link.aps.org/doi/10.1103/PhysRev.136.B864.

[30] Walter Kohn and Lu J. Sham. Self-consistent equations including exchange and correlation effects. Phys. Rev., 140:A1133, 1965. doi: 10.1103/PhysRev.140.A1133. URL http://link.aps.org/doi/10.1103/PhysRev.140.A1133.

[31] Kieron Burke, John P. Perdew, and Matthias Ernzerhof. Why semilocal functionals work: Accuracy of the on-top pair density and importance of system averaging. J. Chem. Phys., 109:3760, 1998.

[32] von Neumann. Mathematische Grundlagen der Qantenmechanik. Springer, Berlin, 1932.

[33] Peter E. Blöchl. ΦSX: Theoretical Physics IV, Statistical Physics. Blöchl, 2015. URL https://phisx.org/.

[34] J. von Neumann. Proof of the quasi-ergodic hypothesis. Proc. Natl. Acad. Sci. USA, 18:70, 1932.

[35] Calvin.C. Moore. Ergodic theorem, ergodic theory, and statistical mechanics. Proc. Natl. Acad. Sci. USA, 112:1907, 2015.

[36] C.E. Shannon. A mathematical theory of computation. Bell. Syst. Techn. J., 22:379, 1948.

[37] E.T. Jaynes. Information theory and statistical mechanics. Phys. Rev., 106:620, 1957.

[38] E.T. Jaynes. Information theory and statistical mechanics ii. Phys. Rev., 108:171, 1957.

[39] T.A. Kaplan and P.N. Argyres. Localized one-electron states in perfect crystals as a consequence of the thermal single-deteiniinant approximation. Phys. Rev. B, 1:2457, 1970.

[40] N. David Mermin. Stability of the thermal hartree-fock approximation. Ann. Phys., 21:99, 1963.

[41] Andrea Damascelli, Zahid Hussain, and Zhi-Xun Shen. Angle-resolved photoemission studies of the cuprate superconductors. Rev. Mod. Phys., 75:473–541, Apr 2003. doi: 10.1103/RevModPhys.75.473. URL https://link.aps.org/doi/10.1103/RevModPhys.75.473.

[42] R. Dronskowski and P.E. Blöchl. Crystal orbital Hamilton populations (COHP). Energy-resolved visualization of chemical bonding in solids based on density-functional calculations. J. Phys. Chem., 97:8617, 1993.

[43] David Bohm and David Pines. A collective description of electron interactions: Iii. coulomb interactions in a degenerate electron gas. Phys. Rev., 92:609, 1953.

[44] M. Gell-Mann and K.Brueckner. Correlation energy of an electron gas at high density. Phys. Rev., 106:364, 1957.

[45] Xinguo Ren, Patrick Rinke, Christian Joas, and Matthias Scheffler. Random-phase approximation and its applications in computational chemistry and materials science. J. Mater. Sci., 47: 7447, 2012. doi: https://doi.org/10.1007/s10853-012-6570-4.

[46] Fabio Carusoa and Feliciano Giustino. The gw plus cumulant method and plasmonic polarons: application to the homogeneous electron gas. Eur. Phys. J. B, 89:238, 2016. doi: https://doi.org/10.1140/epjb/e2016-70028-4.

[47] Johannes Lischner, G. K. Palsson, Derek Vigil-Fowler, S. Nemsak, J. Avila, M. C. Asensio, C. S. Fadley, and Steven G. Louie. Satellite band structure in silicon caused by electron-plasmon coupling. Phys. Rev. B, 91:295113, 2015. doi: 10.1103/PhysRevB.91.205113.

[48] S. Doniach and E.H. Sondheimer. Green's Functions for Solid State Physicists. The Benjamin/Cummings Publishing Company, INC, Reading, Massachusetts. Reprinted 1998 by Imperial college press, 1974.

[49] D.M. Ceperley and B.J. Alder. Ground state of the electron gas by a stochastic method. Phys. Rev. Lett., 45:566, 1980.

[50] E.U. Condon. The theory of complex spectra. Phys. Rev., 36:1121, 1930.

[51] Attila Szabo and Neil S. Ostlund. Modern Quantum Chemistry. McGraw-Hill, New York, 1989. ISBN 9780070627390. URL http://store.doverpublications.com/0486691861.html.

[52] G.D. Mahan. Many Particle Physics. Kluwer academic Publishers, 2000.

[53] Stephen Blundell. Magnetism in Condensed Matter. Oxford University Press, 2001.

[54] Malte Schüler, Erik G. C. P. van Loon, Mikhail I. Katsnelson, and Tim O. Wehling. Thermodynamics of the metal-insulator transition in the extended hubbard model. Scipost Phys., 6: 067, 2019.

[55] Y. Zhang and J. Callaway. Extended hubbard model in two dimensions. Phys. Rev. B, 39: 9397, 1989.

[56] F. J. Dyson. The radiation theories of tomonaga, schwinger, and feynman. Phys. Rev., 75: 486–502, Feb 1949. doi: 10.1103/PhysRev.75.486. URL https://link.aps.org/doi/10.1103/PhysRev.75.486.

[57] G.C. Wick. The evaluation of the collision matrix. Phys. Rev., 80:268, 1950.

[58] E.N. Economou. Green's Functions in Quantum Mechanics. Springer, 1979.

[59] P.W. Anderson. Localized magnetic states in metals. Phys. Rev., 124:41, 1961.

[60] U. Fano. Effects of configuration interaction on intensities and phase shifts. Phys. Rev., 124: 1866–1878, Dec 1961. doi: 10.1103/PhysRev.124.1866. URL https://link.aps.org/doi/10.1103/PhysRev.124.1866.

[61] N.G. van Kampen. Contribution to the quantum theory of light scattering. Dan. Mat. Fys. Medd., 26:3, 1951. URL https://www.lorentz.leidenuniv.nl/IL-publications/dissertations/sources/VanKampen_1952.pdf.

[62] Mariana M. Odashima, Beatriz G. Prado, and E. Vernek. Pedagogical introduction to equilibrium green's functions: condensed-matter examples with numerical implementations. Rev. Bras. Ensino de Fís, 39:e1303, 2017. doi: 10.1590/1806-9126-RBEF-2016-0087. URL https://doi.org/10.1590/1806-9126-RBEF-2016-0087.

[63] I.N. Bronstein and K.A. Semendjajew. Taschenbuch der Mathematik. BSB B.G. eubner Verlagsgesellschaft, Leipzig, 1983.

[64] Mathias Wagner. Expansions of non-equilibrium green's functions. Phys. Rev. B, 44: 6104, 1991. doi: 10.1103/PhysRevB.44.6104. URL https://link.aps.org/doi/10.1103/PhysRevB.44.6104.

[65] A. A. Abrikosow, L. P. Gorkov, and I. E. Dzyaloshinski. Methods of Quantum Field Theory in Statistical Physics. Prentice-Hall, Englewood Cliffs, NJ, 1964.

[66] P.C. Martin and J. Schwinger. Theory of many-particle systems. i. Phys. Rev., 115(6):1342–1373, Sep 1959. doi: 10.1103/PhysRev.115.1342.

[67] Robert van Leeuwen and Gianluca Stefanucci. Equilibrium and nonequilibrium many-body perturbation theory: a unified framework based on the martin-schwinger hierarchy. J. Phys.: Conf. Series, 427:012001, 2013. doi: 10.1088/1742-6596/427/1/012001.

[68] V. M. Galitskii and A. B. Migdal. Application of quantum field theory methods to the many body problem. In Sov. Phys. JETP Galitskii and Migdal [70], page 96.

[69] Walter Tarantino, Pina Romaniello, J. A. Berger, and Lucia Reining. Self-consistent dyson equation and self-energy functionals: An analysis and illustration on the example of the hubbard atom. Phys. Rev. B, 96:45124, 2017.

[70] V. M. Galitskii and A. B. Migdal. Application of quantum field theory methods to the many body problem. Sov. Phys. JETP, 7:96, 1958.

[71] V.M. Galitskii. The energy spectrum of a non-ideal fermi gas. Sov. Phys. JETP, 7:104, 1958.

[72] Ferdi Aryasetiawan. The GW approximation and vertex corrections, volume 1 of Advances in Condensed Matter Science, chapter 1, pages 1 – 96. Gordon and Breach Science Publishers, 2000. Booktitle "Strong Coulomb correlations in electronic structure calculations" Ed. V.I. Anisimov.

[73] J.D. Ortiz. Dyson-orbital concepts for description of electrons in molecules. J. Chem. Phys., 153:070902, 2020.

[74] J.F. Janak. Proof that $\partial e/\partial n_i = \epsilon_i$ in density functional theory. Phys. Rev. B, 18:7165, 1978.

[75] L. Hedin, B.I.Lundquist, and S. Lundquist. Beyond the one-electron approximation: Density of states for interacxting electrons. J. Res. Nat'l Bureau of Standards, 74a:417, 1970.

[76] G. Kotliar, S. Y. Savrasov, K. Haule, V. S. Oudovenko, O. Parcollet, and C. A. Marianetti. Electronic structure calculations with dynamical mean-field theory. Rev. Mod. Phys., 78:865–951, Aug 2006. doi: $10.1103/\mathrm{RevModPhys.78.865}$. URL `http://link.aps.org/doi/10.1103/RevModPhys.78.865`.

[77] Bengt I. Lundqvist). Single-particle spectrum of the degenerate electron gas i. the structure of the spectral weight function. Phys. Kondens. Materie, 6:193, 1967. doi: $10.1007/\mathrm{BF02422716}$.

[78] B.I. Lundqvist. Single-particle spectrum of the degenerate electron gas. Phys. Kondens. Materie, 7:117, 1968.

[79] F. Aryasetiawan, L. Hedin, and K. Karlsson. Multiple plasmon satellites in na and al spectral functions from ab initio cumulant expansion. Phys. Rev. Lett., 77:2268, 1996.

[80] C. Metz, Th. Tschentscher, , P. Suortti, A. S. Kheifets, D. R. Lun, T. Sattler, J. R. Schneider, and F. Bell. Three-dimensional electron momentum density of aluminum by $(\gamma, e\gamma)$ spectroscopy. Phys. Rev. B, 59:10512, 1999.

[81] T. Matsubara. A new approach to quantum-statistical physics. Prog. Theor. Phys., 14:351, 1955.

[82] M. Gaudin. Une démonstration simplifiié du théoréme de wick en mécanique statistique. Nucl. Phys., 15:89, 1960.

[83] Abdus Salam. Some speculations on the new resonances. Rev. Mod. Phys., 33:426, 1961.

[84] J. Goldstone. Derivation of the brueckner many-body theory. Proc. Roy. Soc. (London), A239: 267, 1957. doi: $\mathrm{doi:10.1098/rspa.1957.0037}$. URL `http://rspa.royalsocietypublishing.org/content/239/1217/267`.

[85] Claude Bloch and Cyrano de Dominicis. Un développement du potentiel de gibbs d'un systéme quantique composié d'un grand nombre de particules. Nucl. Phys., 7:459, 1958.

[86] Gordon Baym and Leo P. Kadanoff. Conservation laws and correlation functions. Phys. Rev., 124:287, 1961. doi: $10.1103/\mathrm{PhysRev.124.287}$. URL `http://link.aps.org/doi/10.1103/PhysRev.124.287`.

[87] G. Baym. Self-consistent approximations in many-body systems. Phys. Rev., 127:1391, 1962. doi: $10.1103/\mathrm{PhysRev.127.1391}$. URL `http://link.aps.org/doi/10.1103/PhysRev.127.1391`.

[88] J. M. Luttinger and J. C. Ward. Ground-state energy of a many-fermion system ii. Phys. Rev., 118:1417, 1960. doi: $10.1103/\mathrm{PhysRev.118.1417}$. URL `http://link.aps.org/doi/10.1103/PhysRev.118.1417`.

[89] Michael Potthoff. Self-energy-functional approach to systems of correlated electrons. Eur. Phys. J. B, 32:429, 2003. doi: $10.1140/\mathrm{epjb/e2003\text{-}00121\text{-}8}$. URL `http://link.springer.com/article/10.1140/epjb/e2003-00121-8`.

[90] Felix Hofmann, Martin Eckstein, Enrico Arrigoni, and Michael Potthoff. Nonequilibrium self-energy functional theory. Phys. Rev. B, 88:165124, 2013. doi: $10.1103/\mathrm{PhysRevB.88.165124}$.

[91] Lin Lina and Michael Lindseya. Variational structure of luttinger–ward formalism and bold diagrammatic expansion for euclidean lattice field theory. Proc. Natl. Acad. Sci. USA, 115: 2282, 2018.

[92] M. Potthoff. Non-perturbative construction of the luttinger-ward functional. Condens. Matter Phys., 9:557, 2006. doi: 10.5488/CMP.9.3.557. URL http://www.icmp.lviv.ua/journal/zbirnyk.47/011/abstract.html.

[93] R. Chitra and Gabriel Kotliar. Effective-action approach to strongly correlated fermion systems. Phys. Rev. B, 63:115110, Mar 2001. doi: 10.1103/PhysRevB.63.115110. URL http://link.aps.org/doi/10.1103/PhysRevB.63.115110.

[94] J. Campbell. Proc. Lond. Math. Soc., 1897.

[95] J. Campbell. Proc. Lond. Math. Soc., 1898.

[96] H. Baker. Proc.Lond. Math. Soc, 34, 1902. Baker-Campbell-Hausdorff theorem.

[97] H. Baker. Proc.Lond. Math. Soc, 35, 1903. Baker-Campbell-Hausdorff theorem.

[98] H. Baker. Proc.Lond. Math. Soc (Ser.2), 3:24, 1905. Baker-Campbell-Hausdorff theorem.

[99] F. Hausdorff. Die symbolische exponentialformel in der gruppentheorie. Ber. Verh. Sächs. Akad. Wiss. Leipzig, 58:19, 1906.

[100] W. Magnus. On the exponential solution of differential equations for a linear operator. Comm. Pure Appl. Math., 7:649, 1954.

[101] Sanwu Wang. Generalization of the thomas-reiche-kuhn and the bethe sum rules. Phys. Rev. A, 60:262–266, Jul 1999. doi: 10.1103/PhysRevA.60.262. URL http://link.aps.org/doi/10.1103/PhysRevA.60.262.

[102] Antoine Georges. The beauty of impurities: Two revivals of friedel's virtual bound-state concept. C.R. Physique, 17:430, 2016. doi: 10.1016/j.crhy.2015.12.005. URL http://dx.doi.org/10.1016/j.crhy.2015.12.005.

[103] A.A. Abrikosov. On the anomalous temperature dependence of the resistivity of non-magnetic metals with a weak concentration of magnetic impurities. Sov. Phys. JETP, 21:660, 1965.

[104] H. Suhl. Dispersion theory of the kondo effect. Phys. Rev., 138:A515–A523, Apr 1965. doi: 10.1103/PhysRev.138.A515. URL https://link.aps.org/doi/10.1103/PhysRev.138.A515.

[105] Klaas J.H. Giesbertz, Anna-Maija Uimonen, and Robert van Leeuwen. Approximate energy functionals for one-body reduced density matrix functional theory from many-body perturbation theory. Eur. Phys. J. B, 91:282, 2018.

[106] Peter Fulde, Joachim Keller, and Gertrud Zwicknagl. Theory of heavy fermion systems. Solid State Phys., 41:1, 1988. doi: 10.1016/S0081-1947(08)60378-1. URL https://doi.org/10.1016/S0081-1947(08)60378-1.

[107] Erich Runge and Gertrud Zwicknagel. Electronic structure calculations and strong correlations: A model study. Ann. Phys., 5:333, 1996. doi: 10.1002/andp.2065080404. URL https://doi.org/10.1002/andp.2065080404.

[108] Ebad Kamil, Robert Schade, Thomas Pruschke, and Peter E. Blöchl. Reduced density-matrix functionals applied to the hubbard dimer. Phys. Rev. B, 93:085141, Feb 2016. doi: 10.1103/PhysRevB.93.085141. URL http://link.aps.org/doi/10.1103/PhysRevB.93.085141.

[109] Peter M. W. Gill and John A. Pople. Exact exchange functional for the hydrogen atom. Phys. Rev. A, 47:2383–2385, Mar 1993. doi: 10.1103/PhysRevA.47.2383. URL https://link.aps.org/doi/10.1103/PhysRevA.47.2383.

[110] C.F. v. Weizsäcker. Zur theorie der kernmassen. Z. Phys., 96:431, 1935.

[111] A. Messiah. Quantum Mechanics. Dover, 2000.

[112] Fabien Tran, Peter Blaha, Karlheinz Schwarz, and Pavel Novák. Hybrid exchange-correlation energy functionals for strongly correlated electrons: Applications to transition-metal monoxides. Phys. Rev. B, 74:155108, 2006.

[113] Vladimir I. Anisimov, Jan Zaanen, and Ole K. Andersen. Band theory and mott insulators: Hubbard *U* instead of stoner *I*. Phys. Rev. B, 44:943–954, Jul 1991. doi: 10.1103/PhysRevB.44.943. URL http://link.aps.org/doi/10.1103/PhysRevB.44.943.

[114] T. Koopmans. über die zuordnung von wellenfunktionen und eigenwerten zu den einzelnen elektronen eines atoms. Physica, 1:104, 1934. doi: 10.1016/S0031-8914(34)90011-2.

[115] J. C. Phillips. Generalized koopmans' theorem. Phys. Rev., 123:420–424, Jul 1961. doi: 10.1103/PhysRev.123.420. URL https://link.aps.org/doi/10.1103/PhysRev.123.420.

[116] Roberto Car and Michele Parrinello. Unified approach for molecular dynamics and density-functional theory. Phys. Rev. Lett, 55:2471, 1985. doi: 10.1103/PhysRevLett.55.2471. URL http://link.aps.org/doi/10.1103/PhysRevLett.55.2471.

[117] L. Verlet. Computer "experiments" on classical fluids i. thermodynamical properties of lennard-jones molecules. Phys. Rev., 159:98, 1967.

[118] H. Kümmel, K.H. Lührmann, and J.G. Zabolitzky. Many-fermion theory in exp(*s*)- (or coupled cluster) form. Phys. Rep., 36C:1, 1978.

[119] Oktay Sinanoglu. Many-electron theory of atoms and molecules. Proc. Natl. Acad. Sci. USA, 47:1217, 1961. doi: 10.1073/pnas.47.8.1217. URL https://doi.org/10.1073/pnas.47.8.1217.

[120] Pierre Hohenberg and Walter Kohn. Inhomogeneous electron gas. Phys. Rev., 136:B864, 1964. doi: 10.1103/PhysRev.136.B864. URL http://link.aps.org/doi/10.1103/PhysRev.136.B864.

[121] Mel Levy. Universal variational functionals of electron densities, first order density matrixes and natural spin-orbitals and solution of the v-representability problem. Proc. Nat'l Acad. Sci. USA, 76:6062, 1979. URL http://www.pnas.org/content/76/12/6062.abstract.

[122] M. Levy. Electron densities in search of hamiltonians. Phys. Rev. A, 26:1200, 1982.

[123] Elliott H. Lieb. Density functionals for coulomb systems. Int. J. Quantum Chem., 24(3): 243–277, 1983. ISSN 1097-461X. doi: 10.1002/qua.560240302. URL http://dx.doi.org/10.1002/qua.560240302.

[124] R. McWeeny. Some recent advances in density matrix theory. Rev. Mod. Phys., 32:334, 1960.

[125] A. Puzder, M.Y. Chou, and R.Q. Hood. Exchange and correlation in the si atom: A quantum monte carlo study. Phys. Rev. A, 64:22501, 2001.

[126] J. Harris and R.O. Jones. The surface energy of a bounded electron gas. J. Phys. F: Met. Phys., 4:1170, 1974.

[127] David C. Langreth and John P. Perdew. The exchange-correlation energy of a metallic surface. Sol. St. Commun., 17:1425, 1975.

[128] Olle Gunnarsson and Bengt I. Lundquist. Exchange and correlation in atoms, molecules, and solids by the spin-density-functional formalism. Phys. Rev. B, 13:4274, 1976.

[129] K. Schwarz. Optimization of the statistical exchange parameter α for the free atoms h through nb. Phys. Rev. B, 5:2466, 1971.

[130] I. Lindgren and K. Schwarz. Analysis of the electronic exchange in atoms. Phys. Rev. A, 5: 542, 1972.

[131] J.P. Perdew and A. Zunger. Self interaction correction to density-functional approximations for many-electron systems. Phys. Rev. B, 23:5048, 1981.

[132] Robert O. Jones and Olle Gunnarsson. The density functional formalism, its applications and prospects. Rev. Mod. Phys., 61:689, 1989.

[133] A. D. Becke. Density-functional exchange energy with correct asymptotic behavior. Phys. Rev. A, 38:3098, 1988.

[134] John P. Perdew, Robert G. Parr, Mel Levy, and Jose L. Balduz. Density-functional theory for fractional particle number: Derivative discontinuities of the energy. Phys. Rev. Lett., 49: 1691–1694, Dec 1982. doi: http://dx.doi.org/10.1103/PhysRevLett.49.1691. URL `http://link.aps.org/doi/10.1103/PhysRevLett.49.1691`.

[135] Mel Levy, John P. Perdew, and Viraht Sahni. Exact differential equation for the density and ionization energy of a many-particle system. Phys. Rev. A, 30:2745–2748, Nov 1984. doi: 10.1103/PhysRevA.30.2745. URL `https://link.aps.org/doi/10.1103/PhysRevA.30.2745`.

[136] Leonard Kleinman. Reply to "comment on 'significance of the highest occupied kohn-sham eigenvalue' ". Phys. Rev. B, 56:16029–16030, Dec 1997. doi: 10.1103/PhysRevB.56.16029. URL `https://link.aps.org/doi/10.1103/PhysRevB.56.16029`.

[137] A. Klamt, V. Jonas, T. Bürger, and J.W. Lohrenz. Refinement and parameterization of cosmors. J. Phys. Chem. A, 102:5074, 1998.

[138] M. Dion, H. Rydberg, E. Schröder, D. C. Langreth, and B. I. Lundqvist. Van der waals density functional for general geometries. Phys. Rev. Lett, 92:246401, 2004.

[139] T. Ziegler, A. Rauk, and E.J. Baerends. On the calculation of multiplet energies by the hartree-fock-slater method. Theoret. Chim. Acta. (Berl.), 43:261, 1977.

[140] W. Speier, R. Zeller, and J. C. Fuggle. Studies of total density of states of metals up to 70 ev above E_F. Phys. Rev. B, 32:3597–3603, Sep 1985. doi: 10.1103/PhysRevB.32.3597. URL `https://link.aps.org/doi/10.1103/PhysRevB.32.3597`.

[141] Christian Møller and M.S. Plesset. Note on an approximation treatment for many-electron systems. Phys. Rev., 46:618, 1934. doi: 10.1103/PhysRev.46.618.

Index